http://researchcommons.waikato.ac.nz/

Research Commons at the University of Waikato

Copyright Statement:

The digital copy of this thesis is protected by the Copyright Act 1994 (New Zealand).

The thesis may be consulted by you, provided you comply with the provisions of the Act and the following conditions of use:

- Any use you make of these documents or images must be for research or private study purposes only, and you may not make them available to any other person.
- Authors control the copyright of their thesis. You will recognise the author's right to be identified as the author of the thesis, and due acknowledgement will be made to the author where appropriate.
- You will obtain the author's permission before publishing any material from the thesis.

SEDIMENT TRANSPORT AND TIDAL INLET HYDRAULICS

Volume 2: Figures and Tables

by
Kerry Peter Black

LIST OF FIGURES

1.1 Whangarei Harbour map (NZ5213, 1974)

1.2 Map of study region and numbered features

2.1 Underwater photography sites (Inner harbour)

2.2 Underwater photography sites (Port site)

2.3 Underwater photography sites (Mair Bank)

2.4 Underwater video tracks

2.5 Underwater video tracks (Entrance throat)

2.6 Diver verification of sediment "pathways"

2.7 Side-scan sonar survey (Inner Harbour)

2.8 Side-scan sonar survey (Mair Bank)

2.9 Median (D_{50}) grain sizes

2.10 Percentage of grain size distribution exceeding 1 phi ($P(1\phi)$)

2.11 Summary of the nature of the sea floor

2.12 Side-scan sonograph of ebb spit extending south-east of Snake Bank

2.13 Side-scan sonograph of shipping channel west of One Tree Point

2.14 Side-scan sonograph of sand waves and megaripples south-east of Busby Head

2.15 Side-scan sonograph of cuspate megaripples south-east of Busby Head

2.16 Side-scan sonograph of megaripple "fingers" on southern Mair Bank

2.17 Side-scan and depth sonograph of shell "sand waves"

2.18 Distribution of faunal zones after Bioresearches (1976)

2.19 Bedform wavelength against height

2.20 Distribution of megaripple wavelengths on the ebb spit extending south-east of Snake Bank

2.21 Distribution of megaripple wavelengths on the sub-tidal spit off Reotahi Bay

3.1 Sounding cross-section locations and comparisons of 1974 and 1981 isobaths (Inner Harbour)

3.2 Sounding cross-section locations and comparisons of 1974 and 1981 isobaths (Mair Bank)

3.3 Sounding cross-section L1H (One Tree to Reserve Points)

3.4 Sounding cross-section L2H (One Tree Pt. to old quarry)

3.5 Sounding cross-section L3H (Pt. Sinclair to McLeod Bay)

3.6 Sounding cross-section L4H (Port site to Darch Point)

3.7 Sounding cross-section L5H (NHB wharf to Reotahi Bay)

3.8 Sounding cross-section L6H (NHB wharf to Reotahi Bay)

3.9 Sounding cross-section L7H (Entrance throat)

3.10 Sounding cross-section L1M (Marginal channel, Marsden Point)

3.11 Sounding cross-section L2M (Marsden Pt, to Urquhart Bay)

3.12 Sounding cross-section L3M (Leading Light to Calliope Bank)

3.13 Sounding cross-section L4M (Marsden Pt. to McKenzie Bay)

3.14 Sounding cross-section L5M (Mair Bank to Calliope Bank)

3.15 Sounding cross-section L6M (2-3m contour, Central Mair Bank)

3.16 Bed level changes, inner harbour (1961 to 1981)

3.17 Bed level changes, Mair Bank (1959 to 1981)

3.18 Location of survey cross-sections at the port site and around Marsden Point, with string and wave probe sites

3.19 Inter-tidal zone surveys at the proposed port site (1-7)

3.20 Inter-tidal zone surveys at the proposed port site (8-14)

3.21 Inter-tidal zone surveys on Marsden Point (15-20)

3.22 Bed level changes on the inter-tidal port site as indicated by string surveys from 7-Jun-81 to 16-Aug-81 (S1.1-S1.5)

3.23 Bed level changes on the inter-tidal port site as indicated by string surveys from 7-Jun-81 to 16-Aug-81 (S2.1-S2.5)

3.24 Bed level changes on Marsden Point and the NZRC wharf pylons indicated by string surveys from 1-May-82 to 1-Feb-83

3.25 Plan of entrance throat cross-sections (NZ5213, 1981)

3.26 Entrance throat cross-sections 1-4 (NZ5213, 1981)

3.27 Entrance throat cross-sections 5-10 (NZ5213, 1981)

3.28 Maximum depth against cross-section width (Entrance throat)

3.29 Cross-section 7, present bathymetry and after port construction

4.1 Refraction of easterly waves in Bream Bay with 12s periods after Tonkin and Taylor (1981)

4.2 Refraction of north-easterly waves with 12s periods in Bream Bay after Tonkin and Taylor (1981)

4.3 Refraction of north-easterly waves with 12s periods in Bream Bay after Tonkin and Taylor (1981)

4.4 Refraction of north-easterly waves with 8s periods in Bream Bay after Tonkin and Taylor (1981)

4.5 Refraction of easterly waves (12s periods) over Mair Bank including wave heights and largest grain sizes which could be disturbed by 1m waves

4.6 Refraction of waves from 110° T over Mair Bank (12s periods)

4.7 Refraction of waves from 70° T over Mair Bank (12s periods)

4.8 Reverse ray tracking from central Mair Bank (12s periods)

4.9 Reverse ray tracking from the NZED Power Station (12s periods)

4.10 Wind velocity-direction-frequency for Marsden Point for the period January, 1969 to August, 1973 (Bioresearches, 1976)

4.11 Predictive JONSWAP wave spectra for Mair Bank

4.12 Reverse ray tracking from central Mair Bank (5s periods)

4.13 Cross-sectional profile of megaripple "fingers" on Mair Bank

4.14 Megaripple steepness against tractive force after Yalin and Karahan (1979)

4.15 Grain size distribution on megaripple "fingers" on Mair Bank

4.16 Wave potentials 15 and 30 days prior to 6 beach surveys on Marsden Point

5.1 Drogue design
5.2 General drogue tracking paths (Ebb)
5.3 General drogue tracking paths (Flood)
5.4 General drogue tracking velocities (Ebb)
5.5 General drogue tracking velocities (Flood)
5.6 Tidal record at Marsden Point, 8-Feb-82
5.7 Ebb full tidal cycle drogue paths
5.8 Ebb full tidal cycle drogue velocities
5.9 Brown plume boundaries in Bream Bay
5.10 Flood tull tidal cycle drogue paths
5.11 Water speeds at Post I on Mair Bank
5.12 Water speeds at Post II in the marginal channel off Marsden Point
5.13 Water speeds near the beach west of Post II
5.14 Water speeds on Marsden Point
5.15 Water speeds on upper Mair Bank
5.16 Residual flow at Marsden Point, and on Mair Bank
5.17 Aerial photograph of western Mair Bank
5.18 Aerial photograph of Mair Bank and Marsden Point
5.19 Aerial photograph of Mair Bank and Marsden Point
5.20 Sediment transport directions around upper Mair Bank
5.21 Maximum current directions around Snake Bank and Point Sinclair
5.22 Aerial photograph of Snake Bank
5.23 Aerial photograph of Snake Bank ebb shield
5.24 Schematic diagram of a flood-tidal delta after Boothroyd (1978)
5.25 Locations of Braystoke and Aanderaa current measurement sites
5.26 Typical vertical velocity profile record (18-Jan-81)
5.27 Histograms of ebb and flood 1m velocities
5.28 Velocity-time curves at 1m above the bed (Sites A to K)
5.29 Velocity-time curves at 1m above the bed (Sites M to A4)
5.30 Velocity-time curves at 1m above the bed (Sites B1 to D1)
5.31 Velocity-time curves at 1m above the bed (Sites D1 to S5)
5.32 Maximum speed against tidal range (NHB Aanderaa meter)
5.33 Maximum speed against tidal range over period (NHB Aanderaa meter)
5.34 Maximum speed against tidal range (BLACK Aanderaa meter)
5.35 Maximum speed against tidal range over period (BLACK Aanderaa meter)
5.36 Maximum speed against tidal range (OTP Aandreaa meter)
5.37 Maximum speed against tidal range over period (OTP Aanderaa meter)
5.38 Maximum speed against tidal range (SHOAL Aanderaa meter)
5.39 Maximum speed against tidal range over period (SHOAL Aanderaa meter)
5.40 Best fit curves of speed against tidal range
5.41 Tidal cycle residual mean vertically-averaged velocities

5.42 Tidal cycle residual lm velocities

5.43 Tidal cycle residual flow distances at lm above the bed

5.44 Residual velocity against Allen's (1980) Symmetry Index

6.1 Velocity gradient in turbulent boundary layers after Hinze (1959)

6.2 Comparison of UVDL and Hama boundary layer laws

6.3 Influence of non-simultaneity correction

6.4 Vertical velocity profiles in Whangarei Harbour

6.5 Histograms of ebb and flood Drag Coefficients

6.6 Friction velocity against lm velocity

6.7 Drag coefficient against friction velocity

6.8 Drag coefficient against velocity at lm

6.9 Distributions of ebb and flood correlation coefficients representing the goodness fit to the logarithmic boundary layer equations

6.10 Friction velocity against the correlation coefficient

6.11 Drag Statistic against the Drag Coefficient

6.12 Drag Statistics against the velocity ratio (u/u_1)

6.13 Velocity measurements at S1

6.14 Velocity measurements at S2

6.15 Velocity measurements at S3

6.16 Velocity measurements at S4

6.17 Velocity measurements at S5

6.18 Mean speed against time after high tide (S-series)

6.19 Correlation coefficient against time after high tide (S-series)

6.20 Friction velocity and velocity at lm against time after high tide (S-series)

6.21 Median Drag Coefficient against maximum lm speed (S-series)

6.22 Drag Coefficient against time after high tide (S-series)

6.23 Einstein and Barbarossa division of form drag and skin friction

6.24 Form drag friction coefficient

6.25 Engelund and Hansen and the Kishi and Kuroki effective Shields entrainment function

6.26 Comparison of skin friction velocity by the Engelund and Hansen and the Manning-Strickler methods

6.27 Friction factor against time after high tide (S-series)

6.28 Comparison of skin friction velocity by the Karman Prandtl and the Manning-Strickler methods

6.29 Comparison of skin friction velocity by the Engelund and Hansen and the Karman Prandtl methods

7.1 VUV sediment traps

7.2 Underwater video camera

7.3 Underwater video camera and frame

7.4 RNZN diving tender "Manawanui"

7.5 RNZN underwater photography team

7.6 NHB oil spill vessel, Maunu

7.7 Megaripples at S3

7.8 Megaripples at S4

7.9 Megaripples at S5

7.10 Megaripple advancing over semi-consolidated shell bed

7.11 Grain size distributions at S1

7.12 Grain size distributions at S3

7.13 Grain size distributions at S4

7.14 Grain size distributions at S5

7.15 Video observations of ripple advance and flow patterns

7.16 Sediment threshold and 1m speed at S1 (accelerating)

7.17 Sediment threshold and 1m speed at S1 (decelerating)

7.18 Sediment threshold and 1m speed at S2 (accelerating)

7.19 Sediment threshold and 1m speed at S1 (0.5 $m.s^{-1}$)

7.20 Correction factor for threshold over bedforms

7.21 Sediment threshold observations at Site T1

7.22 Sea bed photographs at threshold Site T2

7.23 Predicted Engelund and Hansen transport rate against the measured bedload rate

7.24 Bedload transport rate against friction velocity with the Yalin and Sternberg equations

7.25 Bedload transport rate against excess 1m velocity cubed with best fit curve

7.26 Bedload transport rate against the skin friction velocity with the Yalin bedload equation for plane beds (q = 3)

7.27 Bedload transport rate against the skin friction velocity with the Yalin bedload equation for plane beds (q = 1)

7.28 Vertically integrated suspended load against mean speed

7.29 Vertically integrated suspended load against friction velocity

7.30 Vertically integrated suspended load against 1m speed with best fit curve

7.31 Sediment concentration at 1m against the 1m speed

7.32 Predicted Engelund and Hansen transport rate against the measured total load

7.33 Bedload, suspended and total load against the 1m speed

7.34 Histogram of flood half tidal periods at Marsden Point

7.35 Histogram of ebb half tidal periods at Marsden Point

7.36 Histogram of flood tidal range at Marsden Point

7.37 Histogram of ebb tidal range at Marsden Point

7.38 Histogram of flood range over half period at Marsden Point

7.39 Histogram of ebb range over half period at Marsden Point

7.40 Histogram of flood and ebb tidal periods combined at Marsden Point

7.41 Histogram of flood and ebb tidal ranges combined at Marsden Point

7.42 Nett sediment fluxes at the proposed port site with side-scan sonar survey

8.1 Aerial photograph of proposed port site

8.2 Aerial photograph of proposed port site

8.3 Aerial photograph of proposed port site and Marsden Point

8.4 Fastest measured flow velocities at proposed port site

8.5 Measured velocities at the proposed port site

8.6 Resultant sediment trap catches in the inter-tidal zone at the proposed port site

8.7 Sediment trap catches during calibration experiments in the inter-tidal zone at the proposed port site

8.8 New sediment traps for the inter-tidal zone

8.9 Sediment trap catches during the June series

8.10 Sediment trap catches during the June series

8.11 Sediment trap catches during the June series

8.12 Average sediment trap catches and wind velocities for the June series

8.13 Average sediment trap catches and wind velocities for the August series

8.14 SUBTLE - System Utilising Both Tape and Logger Equipment - data acquisition system (photograph)

8.15 SUBTLE flow diagram

8.16 Capacitance type wave probe and transmitter (photograph)

8.17 Calibration of capacitance wave probe

8.18 Wave height probe deployed at Marsden Point (photograph)

8.19 Wind fetches for the wave probe at the proposed port site

8.20 Sea state at 5:52 on 15-Sep-83 at the proposed port site

8.21 Sea state at 23:52 on 14-Sep-83 at the proposed port site

8.22 Sea state at 11:52 on 15-Sep-83 at the proposed port site

8.23 Fourier spectrum for 5:52 on 15-Sep-83 with the JONSWAP spectrum

8.24 Theoretical wave height and period ratios against Beta after Black (1978)

8.25 Non-dimensional design frequency spectra after Lee and Black (1978)

8.26 Fourier and Zero up-crossing (ZUS) spectra at 5:52 on 15-Sep-83 at the proposed port site

9.1 Notation for one-dimensional, explicit, finite-difference scheme

9.2 Sloping wall cross-section schematisation

9.3 Influence of digital input time series

9.4 Dependence of friction factors on depth after Ramming and Kowalik (1980)

9.5 Dependence of friction factors on depth after Ramming and Kowalik (1980)

9.6 Sea levels in a 14,000m-long rectangular channel

9.7 Flow velocities in a 14,000m-long rectangular channel

9.8 Sea levels in a 40,000m-long rectangular channel

9.9 Locations of one-dimensional cross-sections (Whangarei Harbour)

9.10 One-dimensional cross-sections (Whangarei Harbour)

9.11 Basic graphs for hydraulic calculations after Smith-McNaught (1976)

9.12 Influence of the time step

9.13 Calibration run (14-Nov-81) with C = 60 $m^{\frac{1}{2}}.s^{-1}$

9.14 Calibration run (14-Nov-81) with z_o = 0.001m

9.15 Verification run (12-Nov-81) with z_o = 0.001m

9.16 Verification run (3-Dec-81) with z_o = 0.001m

9.17 Verification run (3-Dec-81) including a horizontal density gradient

9.18 Verification run (12-Nov-81) including a horizontal density gradient and wind

9.19 Verification run (14-Nov-81) including a horizontal density gradient and wind

9.20 Verification run (14-Nov-81) including a horizontal density gradient, wind and additional inflow

9.21 Examination of terms in the hydrodynamic equation (12-Nov-81)

9.22 Examination of terms in the hydrodynamic equation (3-Dec-81)

9.23 Average sea slope (3-Dec-81)

9.24 Average sea slope (12-Nov-81)

9.25 Average sea slope (14-Nov-81)

9.26 Average cross-section velocities (3-Dec-81)

9.27 Average cross-section velocities (12-Nov-81)

9.28 Average cross-section velocities (14-Nov-81)

9.29 B-series velocities across the entrance throat

10.1 Notation for the 2-dimensional, numerical hydrodynamic model scheme

10.2 Zig-zagging after Tee (1976)

10.3 Zig-zagging after DHI (1982)

10.4 Zig-zagging in 2DD at Whangarei Harbour

10.5 Cause of zig-zagging at land/sea boundaries

10.6 Velocities at a land/sea boundary

10.7 Whangarei Harbour at low tide showing integer codes for cell types

10.8 Approximation to Chezy's C

10.9 Steady state flow past a rectangular step 2000m long

10.10 Steady state flow past a rectangular step 400m long compared with S21

10.11 Steady state flow past a rectangular step with the convective momentum terms set to zero compared with S21

10.12 Steady state flow past a rectangular step with zero horizontal eddy diffusion compared with S21

10.13 Steady state flow past a rectangular step with high horizontal eddy diffusion compared with S21

10.14 Flow past a step with a non-slip boundary

10.15 Flow past a step with a free-slip boundary

10.16 Flow past a step with a 50%-slip boundary

10.17 Flow past a groyne compared with S21

10.18 Flow past a groyne with the convective momentum terms centred and compared with S21

10.19 Locations of the coarse and fine grid over Whangarei Harbour

10.20 Bathymetry of Whangarei Harbour for an overlay
10.21 Entrance throat and treatment of Passage Island
10.22 Calibration, A-series
10.23 Calibration, B-series
10.24 Calibration, C-series
10.25 Calibration, D-series
10.26 Verification, A-series
10.27 Verification, B-series
10.28 Verification, C-series
10.29 Verification, D-series
10.30 Calibration, NHB and BLACK Aanderaa meters
10.31 Calibration, OTP and SHOAL Aanderaa meters
10.32 Verification, NHB and BLACK Aanderaa meters
10.33 Verification, OTP and SHOAL Aanderaa meters
10.34 Flood drogue paths
10.35 Ebb drogue paths
10.36 Flow pattern for the calibration run (14-Nov-81)
10.37 Flow pattern for the verification run (3-Dec-81)
10.38 Entrance throat velocity-time curves (14-Nov-81)
10.39 Entrance throat velocity-time curves (3-Dec-81)
10.40 Tidal cycle residual velocities (14-Nov-81, $\Delta H = 2.6m$)
10.41 Tidal cycle residual velocities (3-Dec-81, $\Delta H = 1.6m$)
10.42 Side-scan sonar map of Whangarei Harbour for an overlay
10.43 Sediment transport loops in Whangarei Harbour
10.44 Residual distances (14-Dec-81, $\Delta H = 2.6m$)
10.45 Residual distances (3-Dec-81, $\Delta H = 1.6m$)
10.46 Residual distances (3-Dec-81, $\Delta H = 2.6m$)
10.47 Flood velocity differences for a wind of 10 $m.s^{-1}$ from 101° T
10.48 Ebb velocity differences for a wind of 10 $m.s^{-1}$ from 101° T
10.49 Flood velocity differences for a wind of 10 $m.s^{-1}$ from 236° T
10.50 Ebb velocity differences for a wind of 10 $m.s^{-1}$ from 236° T
10.51 Flood velocity differences for a wind of 10 $m.s^{-1}$ from 110° T
10.52 Ebb velocity differences for a wind of 10 $m.s^{-1}$ from 110° T
10.53 Residual tidal cycle velocities with a wind of 10 $m.s^{-1}$ from 110° T
10.54 Flood velocity differences after introduction of the Coriolis force
10.55 Ebb velocity differences after introduction of the Coriolis force
10.56 Flood percentage speed differences after introduction of the Coriolis force
10.57 Ebb percentage speed differences after introduction of the Coriolis force
10.58 Tidal cycle residual velocities with the Coriolis parameter set to zero

10.59 Peak flood with the convective momenta and Coriolis acceleration terms neglected

10.60 Peak ebb with the convective momenta and Coriolis acceleration terms neglected

10.61 Tidal cycle residuals with the convective momenta and Coriolis acceleration terms neglected

10.62 Peak flood in a levelled harbour of constant depth

10.63 Peak ebb in a levelled harbour of constant depth

10.64 Tidal cycle residual velocities for a levelled harbour of constant depth

10.65 Port layouts recommended by the DHI (1982)

10.66 Flood percentage speed changes after port construction (Neap tide with unchanged boundaries)

10.67 Ebb percentage speed changes after port construction (Neap tide with unchanged boundaries)

10.68 Flood percentage speed changes after port construction (Neap tide and updated boundaries)

10.69 Ebb percentage speed changes after port construction (Neap tide and updated boundaries)

10.70 Flow pattern after port construction (Spring tide)

10.71 Flow pattern after port construction (Neap tide)

10.72 Flood percentage speed changes after port construction (Spring)

10.73 Ebb percentage speed changes after port construction (Spring)

10.74 Flood velocity differences after port construction (Spring)

10.75 Ebb velocity differences after port construction (Spring)

10.76 Flood velocity differences after port construction (Neap)

10.77 Ebb velocity differences after port construction (Neap)

10.78 Flood percentage speed changes after port construction (DHI, 1982)

10.79 Ebb percentage speed changes after port construction (DHI, 1982)

10.80 Flood percentage speed changes after port construction with a 14m-deep dredge basin

10.81 Ebb percentage speed changes after port construction with a 14m-deep dredge basin

10.82 Flood velocity differences after port construction with a 14m-deep dredge basin

10.83 Ebb velocity differences after port construction with a 14m-deep dredge basin

10.84 Tidal cycle residual velocities after port construction (14-Nov-81, $\Delta H = 2.6m$)

10.85 Tidal cycle residual velocities after port construction (3-Dec-81, $\Delta H = 1.6m$)

10.86 Tidal cycle residual distances after port construction (14-Nov-81, $\Delta H = 2.6m$)

10.87 Tidal cycle residual distances after port construction (3-Dec-81, $\Delta H = 2.6m$)

11.1 Notation for the 2-dimensional sediment transport model scheme

11.2 Test rig initial condition (45° sandy zone)

11.3 Degeneration of a sandy zone with an unstable scheme

11.4 Round-off error test rig

11.5 Deterioration of a sandy zone in uni-directional flow

11.6 Introduction of sediment through an upstream boundary

11.7 Initial bathymetry for schematised inlet

11.8 Tauranga Entrance to Tauranga Harbour (NZ5411, 1975)

11.9 Peak flood in the schematised inlet (Initial bathymetry)

11.10 Peak ebb in the schematised inlet (Initial bathymetry)

11.11 Tidal cycle residuals in the schematised inlet (initial bathymetry) with overlay of residual transport and current after Davies-Colley and Healy (1978)

11.12 Nett sediment transport in Tauranga Harbour after Dahm (1983)

11.13 Nett sediment transport at the entrance to Tauranga Harbour after Dahm (1983)

11.14 Erosion/deposition pattern for the initial bathymetry

11.15 Bathymetry in the schematised inlet after 4 coupled iterations

11.16 Tidal cycle residual velocities in the schematised inlet after 4 coupled iterations

11.17 Erosion/deposition pattern in the schematised inlet after 4 coupled iterations

11.18 Bathymetry in the schematised inlet after 8 coupled iterations

11.19 Peak flood in the schematised inlet after 8 coupled iterations

11.20 Peak ebb in the schematised inlet after 8 coupled iterations

11.21 Tidal cycle residual velocities in the schematised inlet after 8 coupled iterations

11.22 Erosion/deposition pattern in the schematised inlet after 8 coupled iterations

11.23 Locations of underwater photograph sites at open boundaries

11.24 Photograph site locations and bed summary on the Marsden Point boundary

11.25 Photograph site locations and bed summary on the One Tree Point boundary

11.26 Stable harbour Availabilities from field data

11.27 Predicted annual volume changes for an all-sand harbour

11.28 Predicted annual bed level changes for an all-sand harbour

11.29 Annual volume changes for the stable harbour

11.30 Annual bed level changes for the stable harbour

11.31 Stable harbour obtained by iteration (Spring, 10 kg/m/tidal cycle cut-off)

11.32 Stable harbour obtained by iteration (Spring, 0.4 kg/m/tidal cycle cut-off)

11.33 Stable harbour obtained by iteration (Neap scaled to a Spring, 0.4 kg/m/tidal cycle cut-off)

11.34 Annual volume changes after port construction for an all-sand harbour

11.35 Annual bed level changes after port construction for an all-sand harbour

11.36 Stable cover with all sand in the proposed dredge basin

11.37 Annual volume changes after port construction for the stable harbour

11.38 Annual bed level changes after port construction for the stable harbour

11.39 Stable harbour after port construction obtained by iteration (Spring, 10 kg/m/tidal cycle cut-off)

11.40 Stable harbour after port construction obtained by iteration (Spring, 0.4 kg/m/tidal cycle cut-off)

11.41 Stable harbour after port construction obtained by iteration (Neap scaled to Spring, 0.4 kg/m/tidal cycle cut-off)

A1.1 Construction for sextant position fixing solution

A1.2 Construction for EDM equipment position fixing solution

A4.1 Circuit diagram for the SUTBLE frequency to voltage converter

A6.1 Rectangular trap effective width

A6.2 Circular trap effective width

LIST OF TABLES

1.1 Numbered landmarks and coordinates

2.1 Bedform classification after Harms et. al. (1975)

2.2 Megaripple wavelengths on the spit extending south-east of Snake Bank

2.3 Megaripple wavelengths off Reotahi Bay

3.1 Sounding line origins

3.2 Sounding line equations

3.3 Mair Bank volume changes after DHI (1982)

3.4 Characteristics of 10 entrance throat cross-sections

4.1 Predicted wave heights and periods at Mair Bank for south-east winds

4.2 Grain sizes on Mair Bank megaripple "fingers" and nearby

4.3 Wave potentials; onshore and offshore

5.1 General drogue experiments

5.2 Drogue positions and times; flood full-tidal cycle

5.3 Drogue positions and times; ebb full-tidal cycle

5.4 Drogue tracked mean water speeds in channels

5.5 Tides (24-Jul-81)

5.6 Coordinates of Mair Bank velocity measurement sites

5.7 Velocities around Snake Bank

5.8 Peak flow directions around Snake Bank

5.9 Braystoke site characteristics

5.10 Velocities at Aanderaa sites

5.11 Relationship of tide range to water speed

5.12 Braystoke site velocity statistics

5.13 Residual vectors at 1m above the bed (q = 1)

5.14 Residual vectors at 1m above the bed (q = 3)

6.1 Boundary layer velocity gradient

6.2 Braystoke site velocity profile analysis

6.3 Breakdown of velocity profile analysis into sand bed, shell bed, accelerating and decelerating components

6.4 Correlation coefficient to be exceeded for a profile to be logarithmic

6.5 Number of logarithmic profiles at the Braystoke sites

6.6 Drag Coefficient at the S-series sites

6.7 Friction factor at the S-series sites

7.1 Bedform geometry from underwater photographs

7.2 Grain sizes and average bedform heights and wavelengths at the S-series sites

7.3 Grain sizes at the S-series sites

7.4 Sediment threshold friction and 1m velocities

7.5 Roughness lengths and critical parameters at the S-series sites

7.6 Comparison of Sternberg's measured thresholds with the "new" threshold procedure

7.7 VUV trap catches for the S-series

7.8 Megaripple steepness, Engel and Lau (1981) correction and megaripple advance rates

7.9 Megaripple geometry at the S-series sites

7.10 Suspended sediment data

7.11 Tidal statistics for Marsden Point from June to December, 1981 inclusive

7.12 Sediment transport rates at the Braystoke sites

8.1 Velocity measurements on the inter-tidal zone at the proposed port site

8.2 Sediment trap catches (August series)

8.3 Average and resultant sediment trap catches (August series)

8.4 Overall sediment transport resultants for the August series

8.5 Wave heights and periods at Marsden Point

8.6 Wave heights and periods at Marsden Point

8.7 Ten largest wave events at Marsden Point

8.8 Wave heights recorded when winds exceeded 7 $m.s^{-1}$

8.9 Comparison of measured and predicted wave heights at Marsden Point

8.10 Zero up-crossing height and period ratios for 5 selected recording periods at Marsden Point

8.11 Sea level skewness and kurtosis at Marsden Point

9.1 Wind strengths at Marsden Point during modelling periods

9.2 Rainfall prior to modelled days

9.3 Tidal prisms for modelled days

9.4 Harbour volumes from Smith-McNaught (1976)

9.5 Mean speeds for the B-series

10.1 Bathymetry for the fine grid model

10.2 Tides for the calibration period (14-Nov-81)

10.3 Tides for the verification period (3-Dec-81)

10.4 Comparison of modelled and measured speeds at the Braystoke sites

10.5 Summary of model runs

11.1 Influence on the 1m speed of accounting for a measured boundary layer gradient change

11.2 Influence of z_o on u_1 and u_* obtained from $\bar{u}$

11.3 Bed grain sizes at RNZN sample sites after a textural analysis

A1.1 Sextant calibration

A1.2 Accuracy of coordinate conversions program

N.Z. 5213

DEPTHS IN METRES

RANGE OF LIGHTS IS NOMINAL RANGE

WARNING! CHANGES TO BUOYS AND CERTAIN SHORE MARKS

This chart will be affected by the introduction of IALA Maritime Buoyage System (Region A) (see NP 735 or MOT publication "System of Buoyage and Beaconage for New Zealand") scheduled for implementation in this area during 1992. The relevant amendments to this chart will be promulgated by Notice to Mariners or by inclusion in a new edition but this action may not be practicable until the changes to many of the aids concerned have taken place. For further information see New Zealand Notice to Mariners 177/81.

Refer to the New Zealand Nautical Almanac, Admiralty Sailing Directions (Pilot), List of Lights and other publications to supplement the information on this chart. For general information see The Mariners Handbook. For an explanation of chart symbols and abbreviations see NZ 200

NEW ZEALAND

NORTH ISLAND – EAST COAST

WHANGAREI HARBOUR

DEPTHS IN METRES

Depths in metres (under 20 in metres and decimetres) reduced to approximately MLWS.
Heights in metres. Underlined figures are drying heights above Chart Datum; all other heights are above MHWS.
Projection: Transverse Mercator. Positions are on Geodetic Datum 1949.
Authorities: New Zealand Surveys 1955 to 1961.
Soundings in upright figures from a smaller scale survey.

Figure 1.1(a): 1974 RNZN bathymetry map of Whangarei Harbour (NZ5213). Scale 1:50,000.

Tidal Levels referred to Datum of Soundings

Place	Heights in metres above Datum MHWS	MHWN	MLWN	MLWS	Datum and Remarks
Port Whangarei	3·0	2·6	0·9	0·5	5·182m below RNZN BM 8 No 1 1961 on the seaward nose the road on the West side of Port Whangarei Wharf.
Calliope Bay	2·6	2·2	0·6	0·3	4·986m below RNZN BM W No. 3 1961 in a concrete block at the Eastern end of Calliope jetty on a concrete slab.
Marsden Pt	2·6	2·3	0·7	0·4	4·818m below an iron bolt over bore of light standard above mentioned from landing steps of the Harbour Board Wharf on the core of the automatic tide gauge.

Tidal Streams referred to HW at AUCKLAND

Hrs	A Lat 35°31'·35 Long 174°31'·38 Direction	Rate (knots) Sp	Rate (knots) Mp	B Lat 35°50'·25 Long 174°30·48 Direction	Rate (knots) Sp	Rate (knots) Mp	C Lat 35°47'·98 Long 174°24'·98 Direction	Rate (knots) Sp	Rate (knots) Mp	Hrs
6	330°	0·3	0·3	084°	0·9	0·6	125°	0·1	0·1	6
5	339°	2·0	1·4	092°	0·7	0·6	338°	0·9	0·6	5
4	086°	2·2	1·5	090°	1·6	1·2	338°	1·3	1·0	4
3	088°	2·2	1·5	092°	1·6	1·2	338°	1·3	1·0	3
2	088°	1·9	1·4	088°	1·6	1·2	338°	0·8	0·6	2
1	088°	1·9	1·4	088°	1·6	1·2	338°	0·8	0·6	1
HW	317°	0·6	0·4	307°	0·3	0·2	272°	0·4	0·3	HW
1	174°	2·0	1·5	180°	1·4	0·9	131°	1·2	0·8	1
2	174°	2·0	1·5	172°	1·4	0·9	131°	1·2	0·8	2
3	183°	2·1	1·5	172°	2·0	1·4	129°	1·9	1·3	3
4	186°	2·1	1·5	180°	1·6	1·1	126°	1·7	1·1	4
5	186°	1·9	1·3	189°	1·6	1·1	126°	1·2	0·9	5
6	192°	0·4	0·3	183°	1·2	0·8	124°	0·2	0·1	6

Feet / Metres / Fms

Annual increase 3'

Variation 17° 59' E (1974)

Feet 1000 0 5000 10000 15000 20000 Feet

Metres 1000 500 0 1000 2000 3000 4000 5000 6000 Metres

Cables 10 5 0 1 2 3 Sea Miles

Longitude 174° 26' East from Greenwich

WHANGAREI HARBOUR

APPROACHES TO MARSDEN POINT

DEPTHS IN METRES

Projection: Transverse Mercator
Authorities: New Zealand Surveys 1959 to 1961
Soundings in upright figures from a smaller scale survey

Figure 1.1(b): 1974 RNZN bathymetry map of approaches to Whangarei Harbour (NZ5213). Scale 1:36,000.

Published at Auckland, January 1974, by the Hydrographic Office of the Royal New Zealand Navy, under the superintendence of Commander I.S. Monro, R.N.Z.N., Hydrographer

Crown Copyright 1975

DEPTHS IN METRES

N.Z. 5213

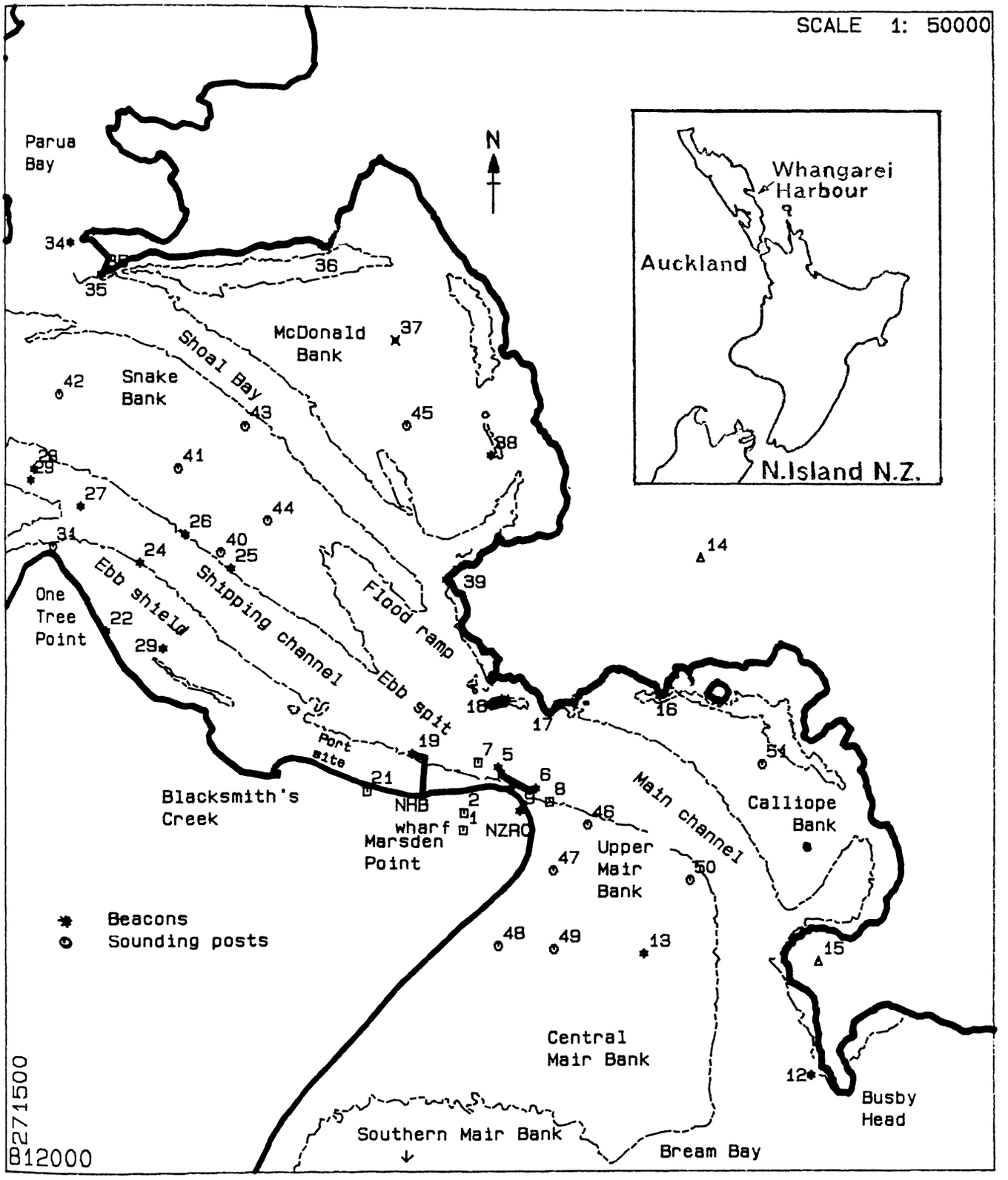

Figure 1.2: The study region in Whangarei Harbour, Mair Bank and Bream Bay. Numbered features are named in Table 1.1.

KEY

Bottom Facies as interpreted from underwater photography

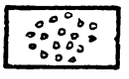

Predominant shelly lag gravel cover

P = Pink coralline algae encrustation

C = Clean shell

A = Algae growth on gravel

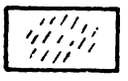

50% gravel and sand with no bedforms

T = active sand transport evident

H = hard packed

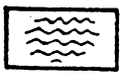

Dune bedforms

Ripple bedforms

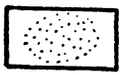

Flat sand bottom, usually fine sand

B = bioturbated

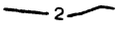

2 metre contour

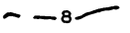

8 metre contour

solid lines join areas of similar facies.

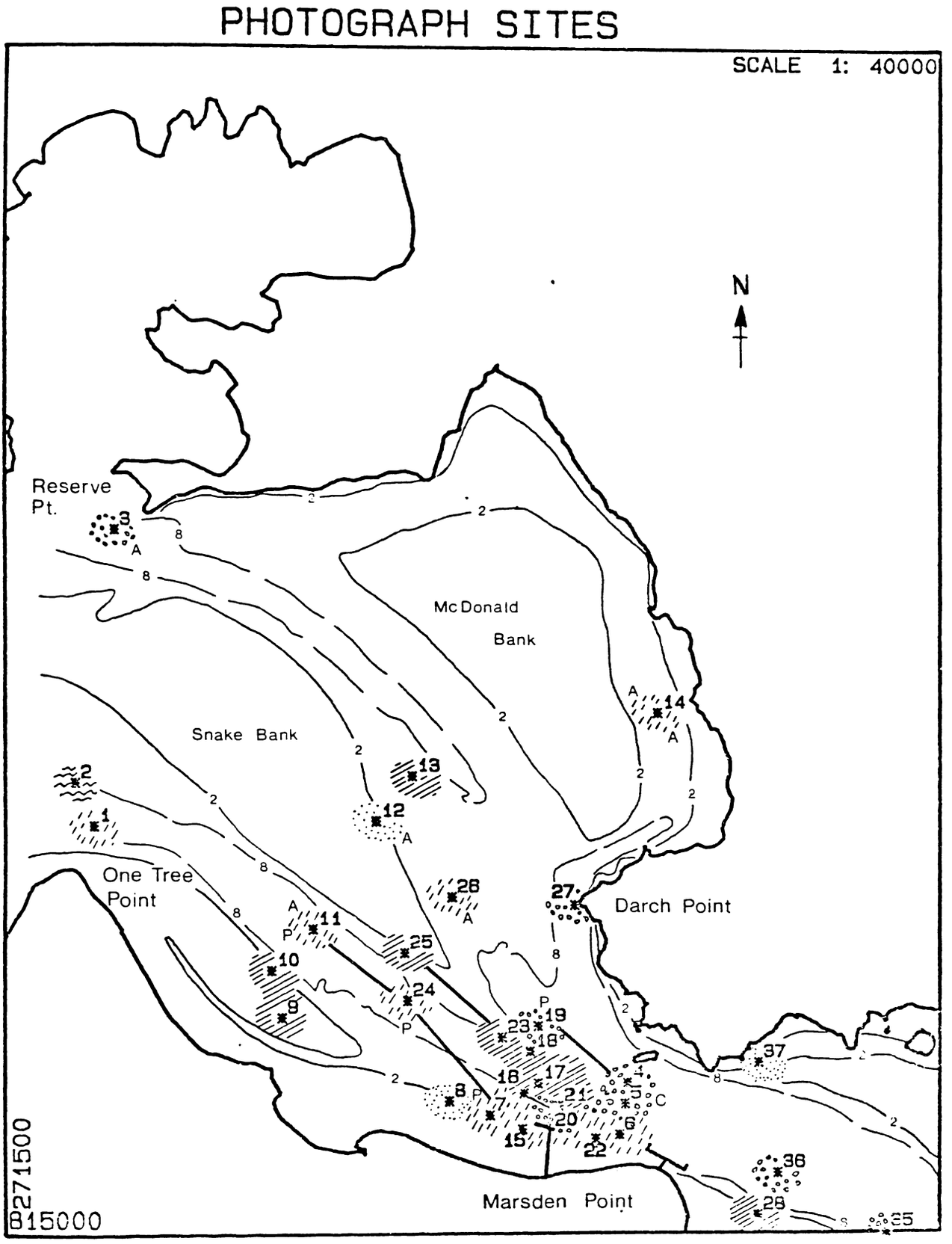

Figure 2.1: Underwater photography sites in Whangarei Harbour.

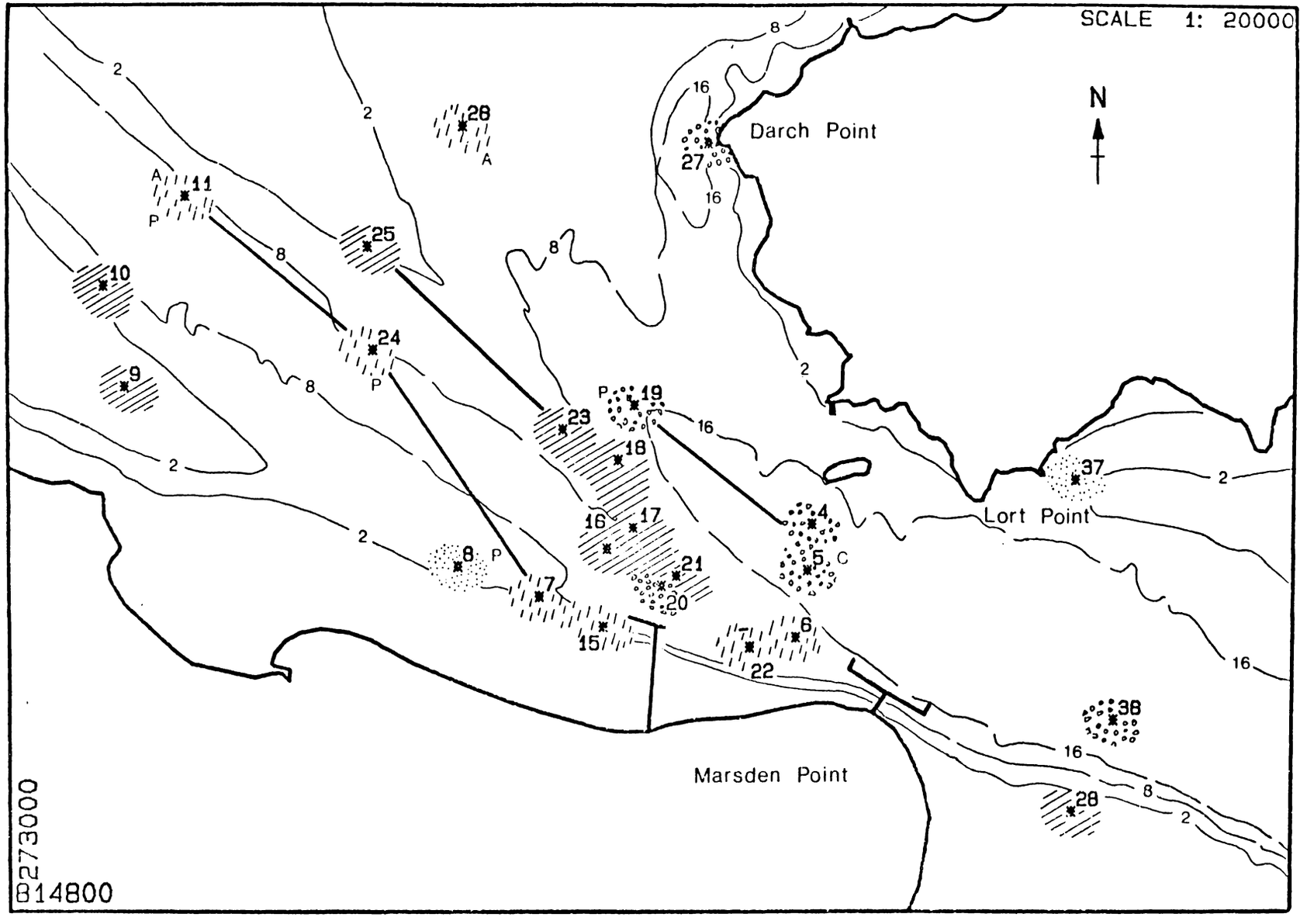

Figure 2.2: Enlargement of underwater photography survey results at the proposed timber port site (Marsden Point).

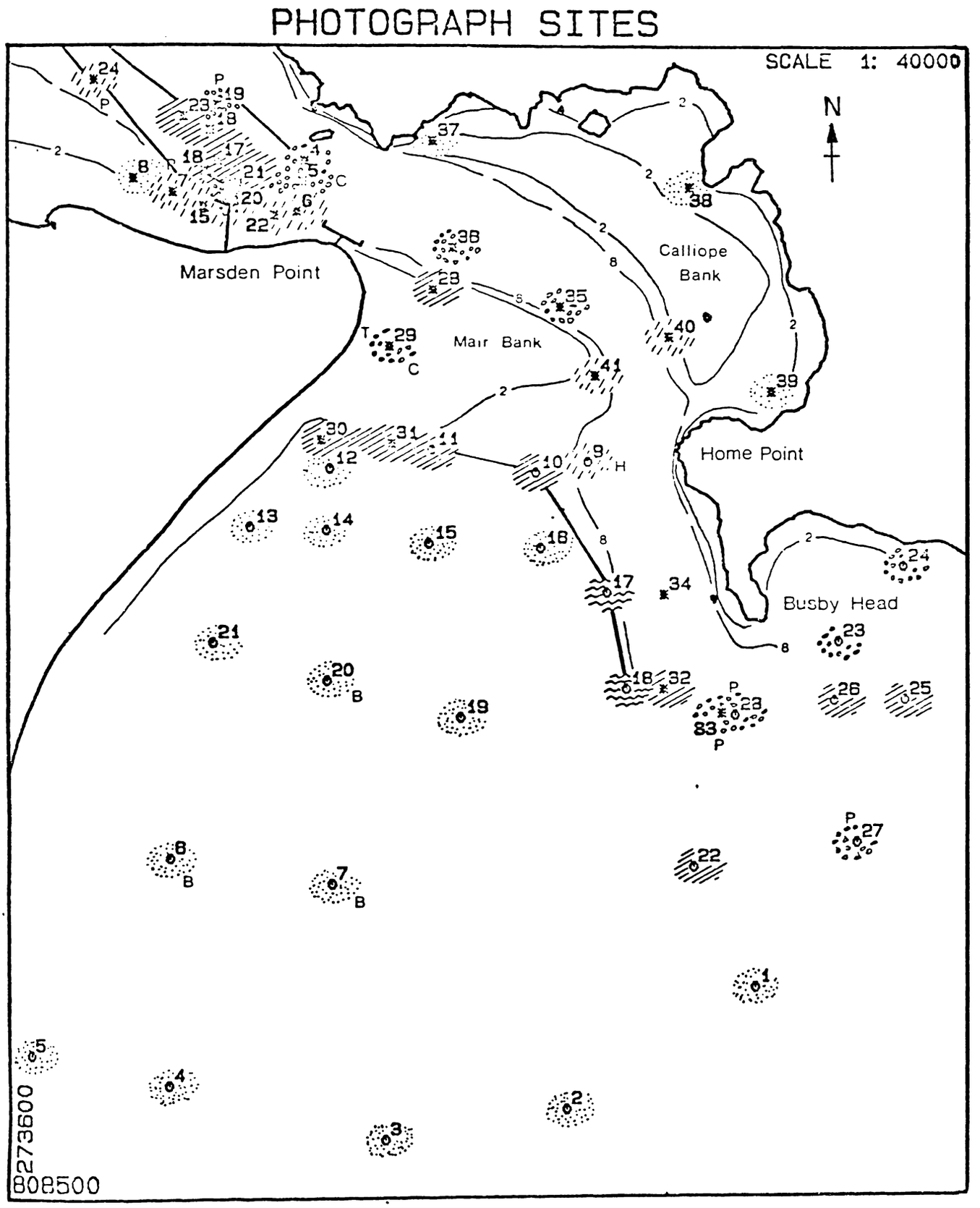

Figure 2.3: Underwater photography sites on Mair Bank and environs.
o NHB photographs
* RNZN photographs

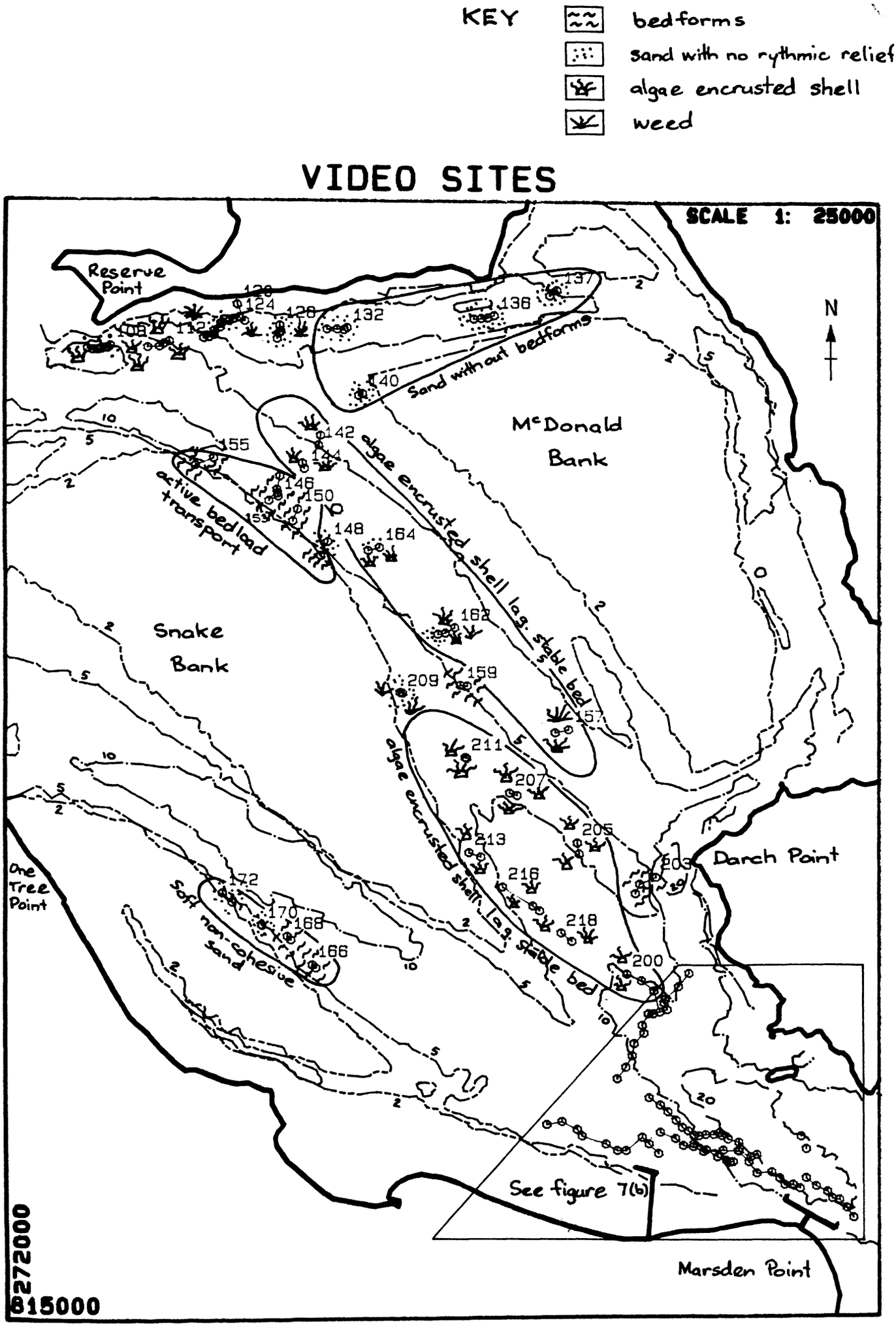

Figure 2.4: Underwater video tracks.

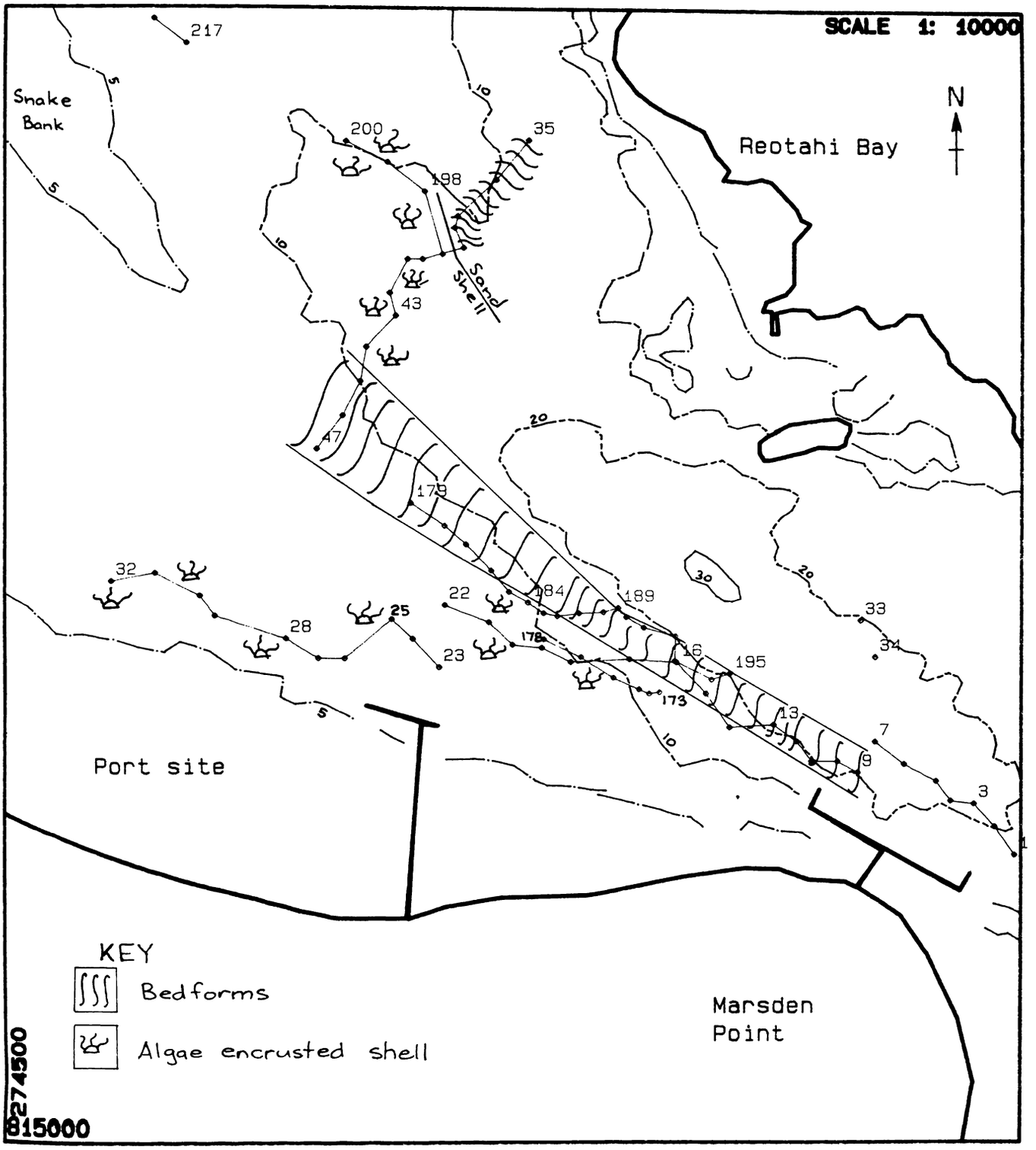

Figure 2.5: Underwater video tracks, with active megarippled regions. Boundaries shown are approximate in places as the bed was viewed along the video paths only.

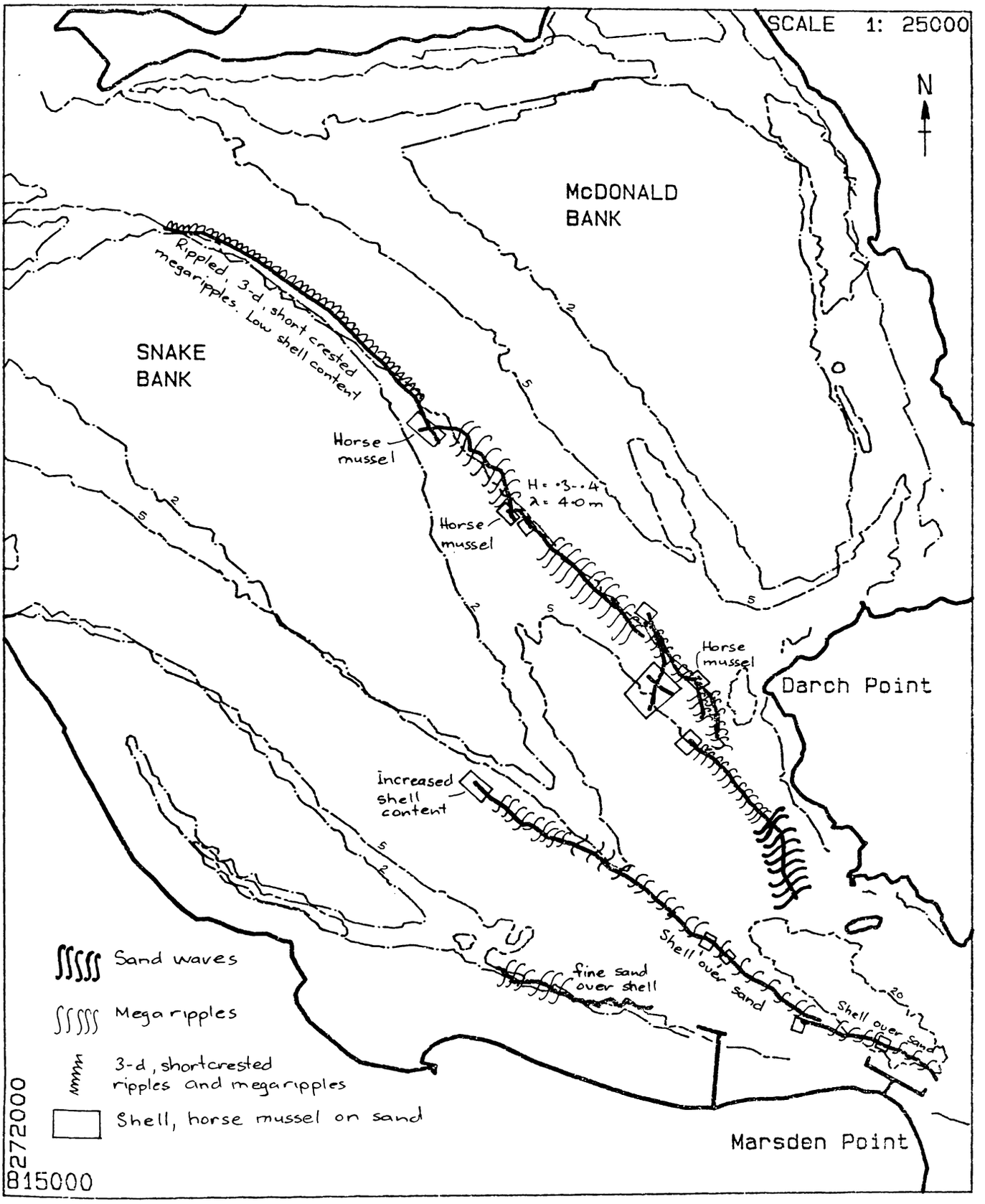

Figure 2.6: Diver verification of elongated sediment "pathways".

KEY

- Gravel
- Irregular features
- Distinct Irregular features
- Shell
- Megaripples
- Sandwaves
- Sandwaves with megaripples
- Algae
- Flat featureless or indistinct trace
- Photography site (N - Navy photo)

MUNRO WEST

rock intrusion

RESERVE POINT

McDONALD BANK

CALLIOPE BANK

SNAKE BANK

DARCH POINT

REOTAHI BAY

LORT POINT

HOME POINT

INSET

McKENZIE POINT

HIGH ISLAND

CASTLE ROCK

CALLIOPE BANK

PASSAGE ISLAND

MARSDEN POINT

PROPOSED TIMBER PORT SITE

MAIR BANK

ONE TREE POINT

POINT SINCLAIR

BLACKSMITH'S CREEK

SEE INSET

Notes. (1) The Mt Eden Geodetic metric coordinates are approximate. The map projection is Transverse Mercator

NORTHLAND HARBOUR BOARD

Figure 2.7: Side-scan sonar survey. Inner Harbour.

AMENDMENTS	DESIGN		APPROVED	DRAWING No
	DRAWN R.A. Aickin	2/83		
	CHECKED			
	SCALE 1:10 000		HARBOUR ENGINEER	SHEET No 1 A1

KEY

- Shell
- Megaripples, mr
- Cuspate megaripples
- Megaripple ribbons
- Sandwaves with megaripple
- Flat, featureless
- Limit of features on side-scan trace
- Photography site (N = Navy photo)
- gr Gravel

35° 52' 273 000 mE 174° 28' 812 000 mN

N

BREAM BAY BEACH

NAKELELE POINT

New Zealand Electricity Department Power Station

offshore bar

Bland signal no relief

Little bottom relief, some shelly gravel or discrete bedform

ripple bands with shadow

Featureless sand

Very light reflection from occasional lump (or bedform or gravel)

low irregular lumps & bedform (some gr or shell?)

Small discrete lumps, gr

no bedform

Featureless sand

Featureless but occasional bedform and gr

17° 30'

MAIR BANK

Sand ridges on flat sand

Sand - light gr

Sand waves on flat sand

Shell cover

linear sandwave field λ = 12 m h = 0.8 m

Light shelly gravel

Sand waves on flat sand

Sand waves on flat sand

Sand waves on flat sand

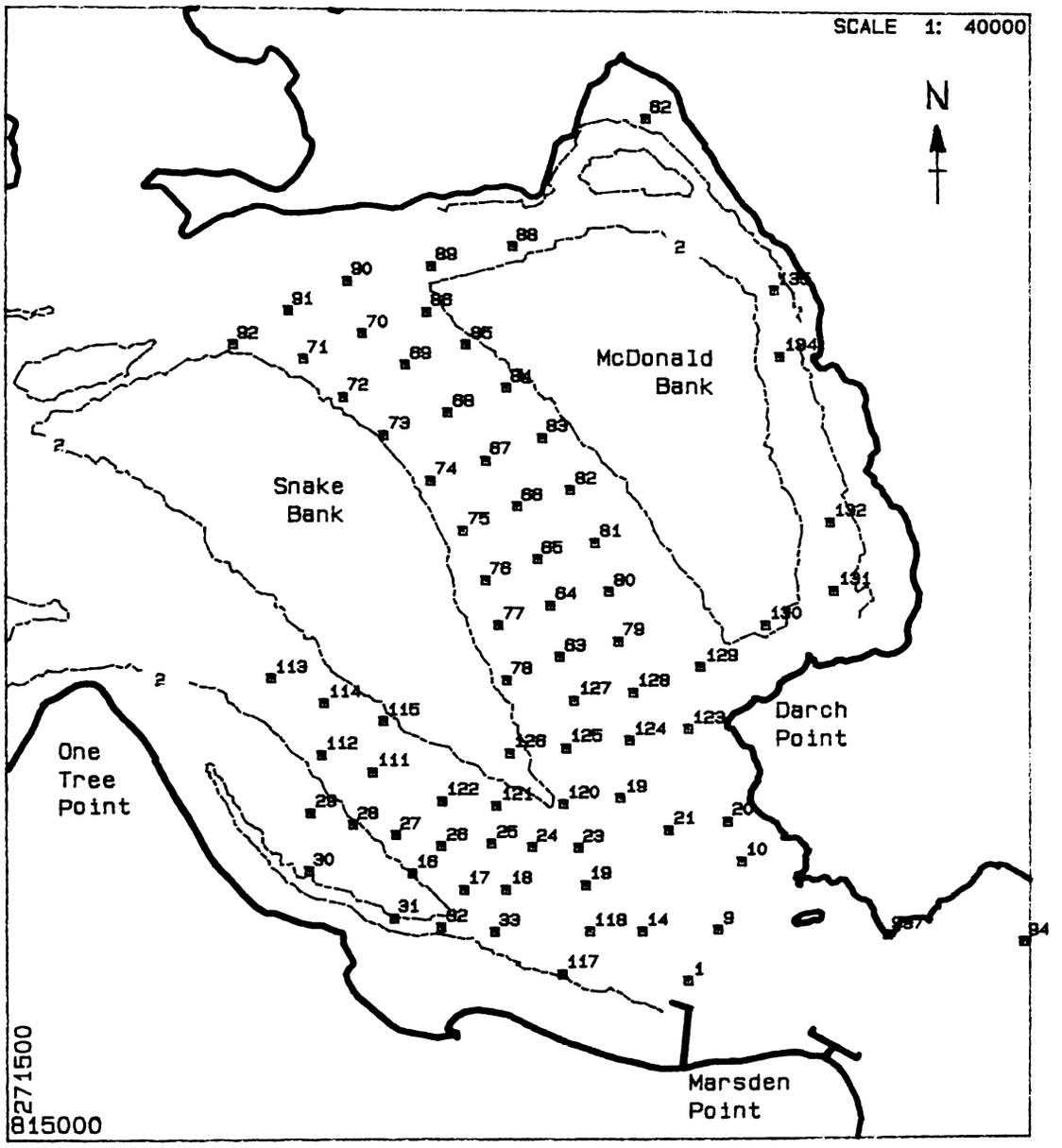

Figure 2.9(a): Locations of RNZN bed sediment sampling sites

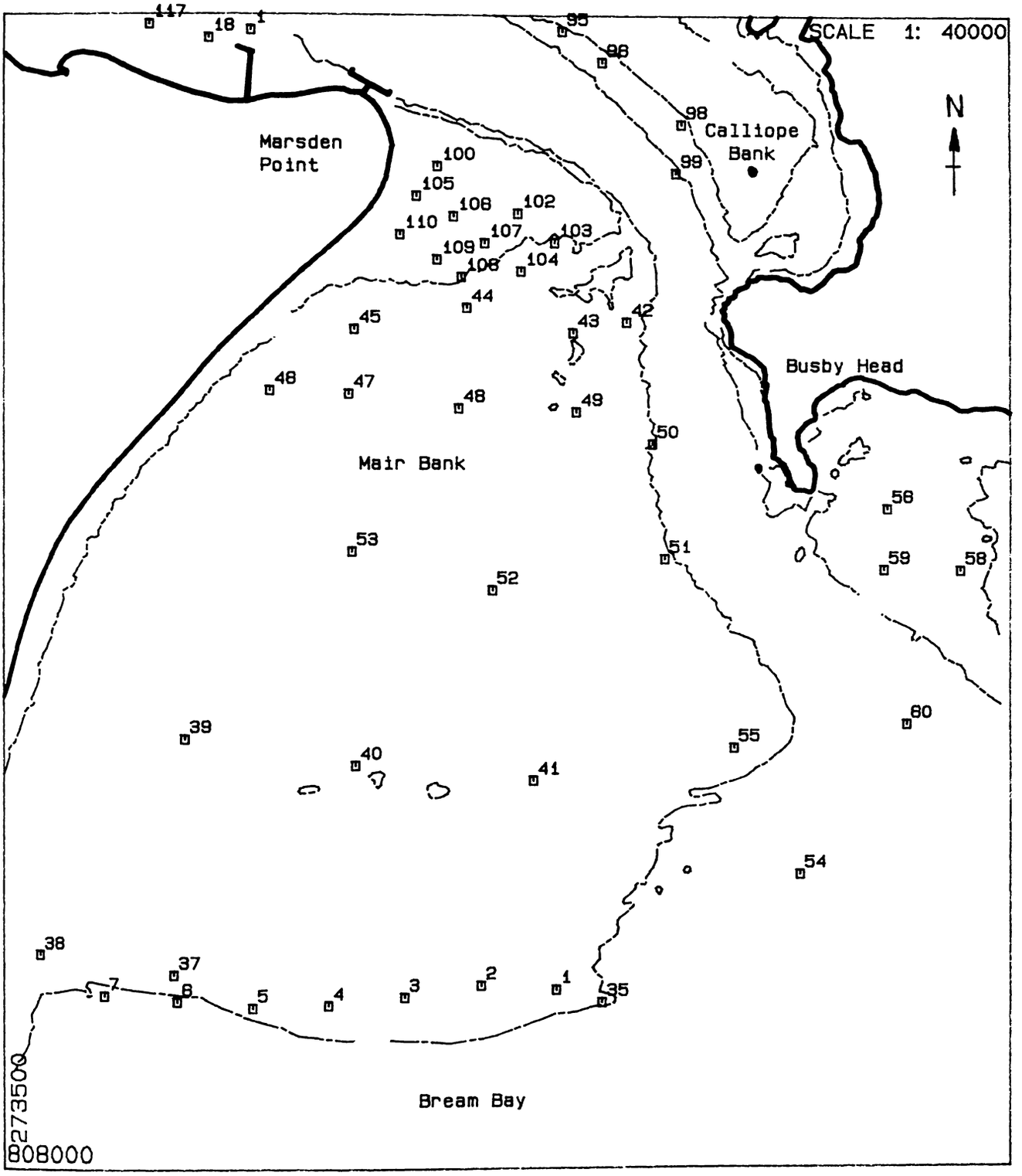

Figure 2.9(b): Locations of RNZN bed sediment sampling sites.

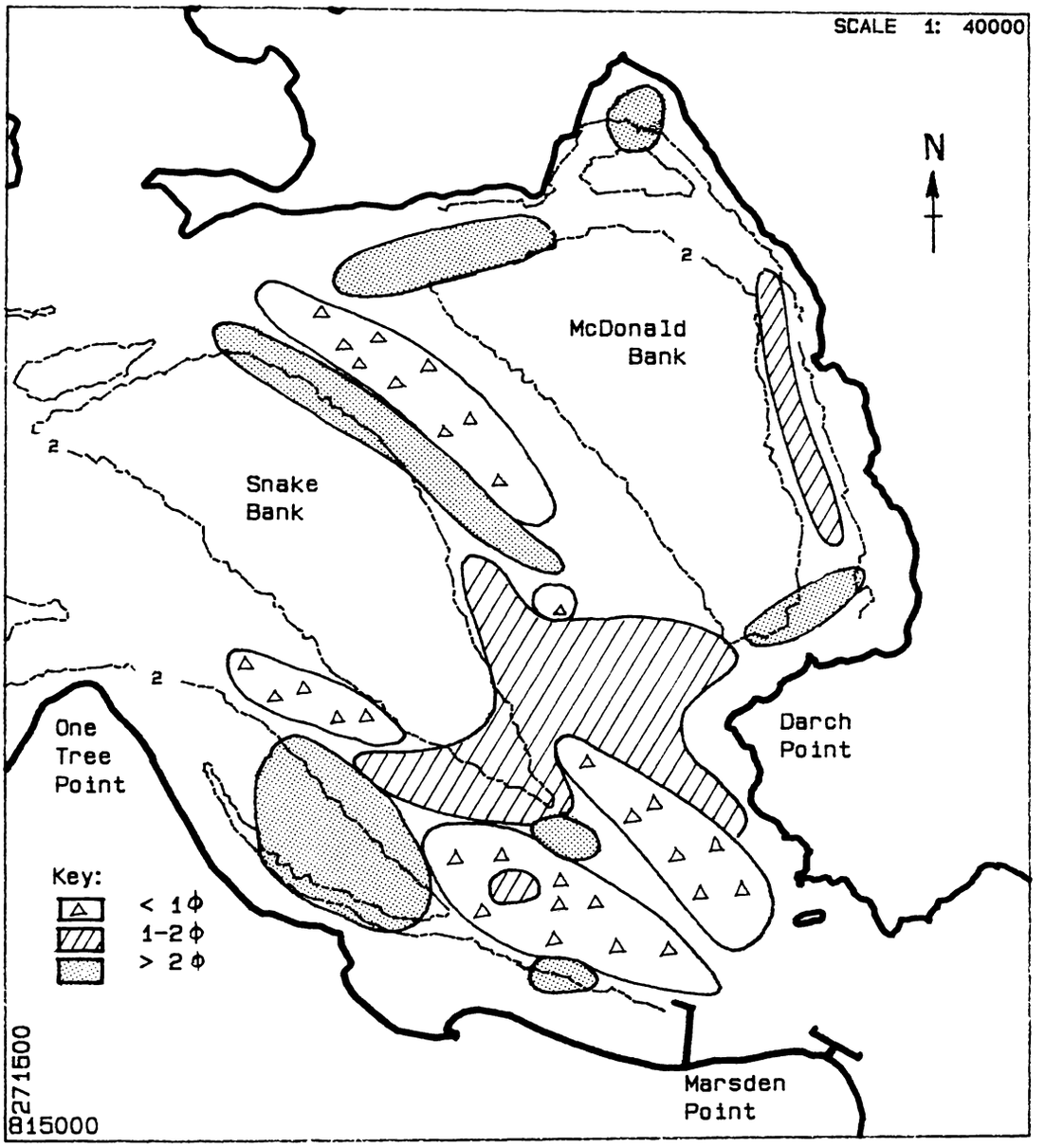

Figure 2.9(c): Contours of the median (D_{50}) grain size by weight after textural analysis of bed sediment samples

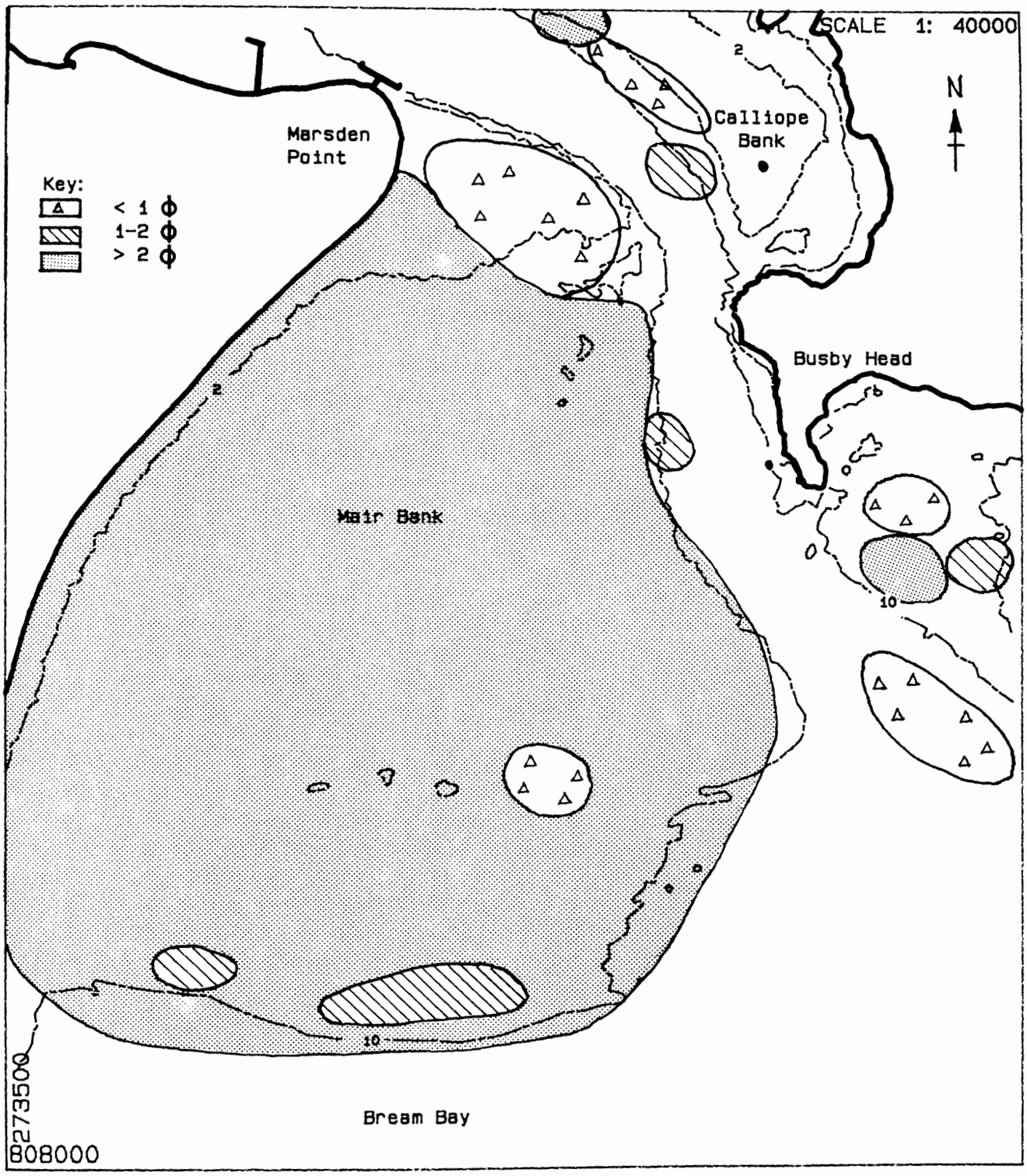

Figure 2.9(d): Contours of the median (D_{50}) grain size by weight after textural analysis of bed sediment samples

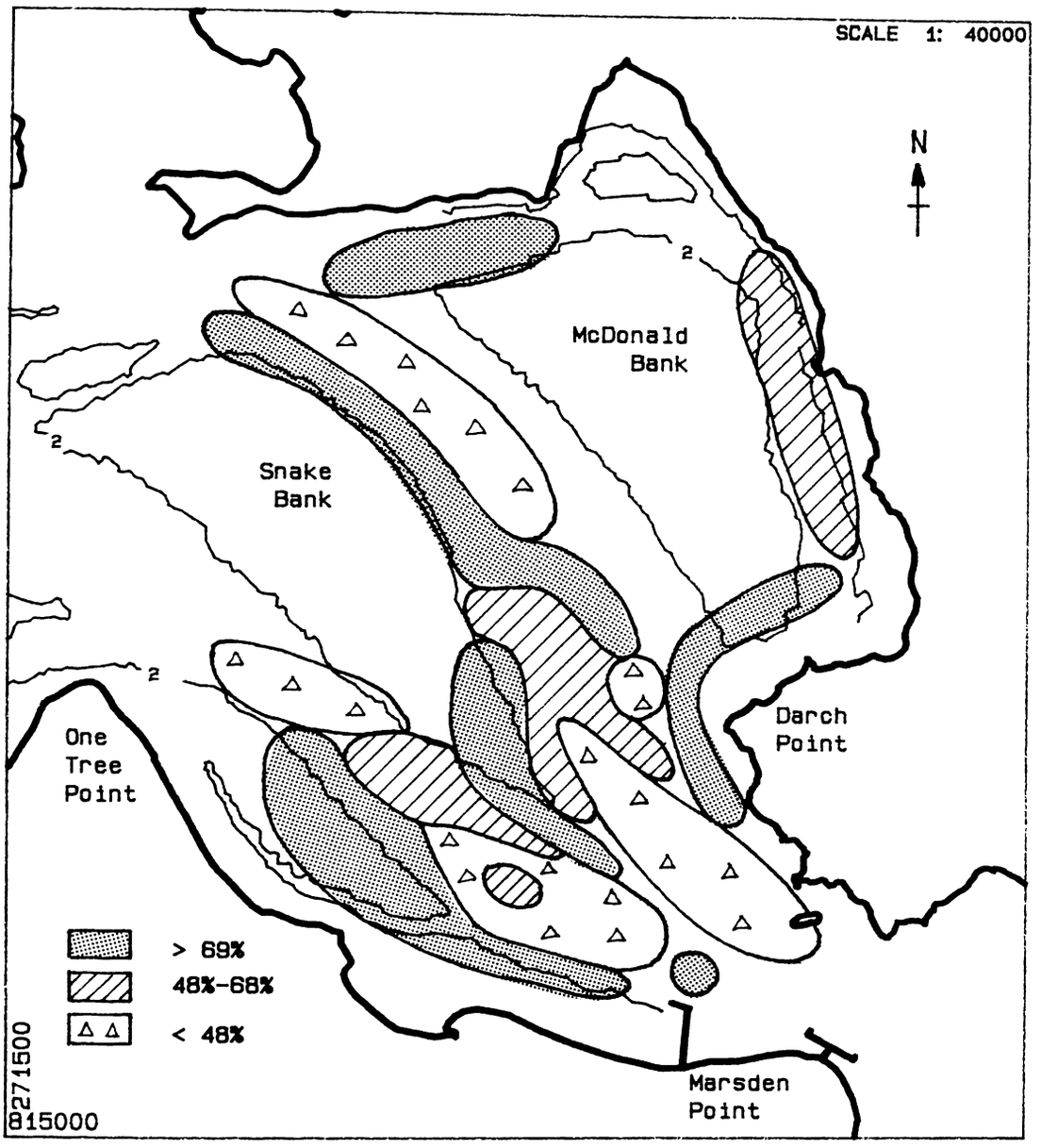

Figure 2.10(a): Contours of P(1ϕ), the percentage of weight with sizes greater than 1 phi, after textural analysis of bed sediment samples

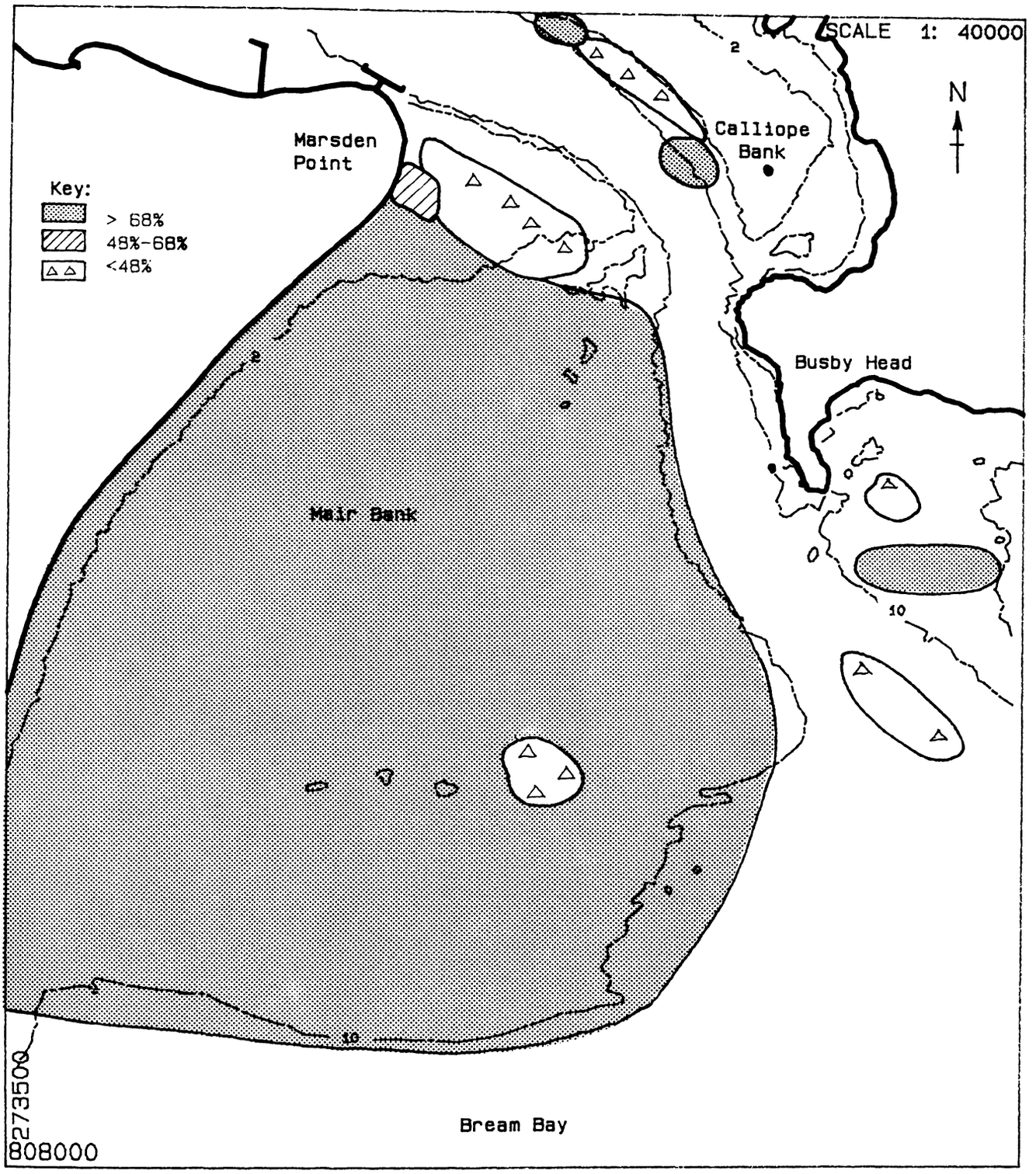

Figure 2.10(b): Contours of P(1ϕ), the percentage of weight with sizes greater than 1 phi after textural analysis of bed sediment samples.

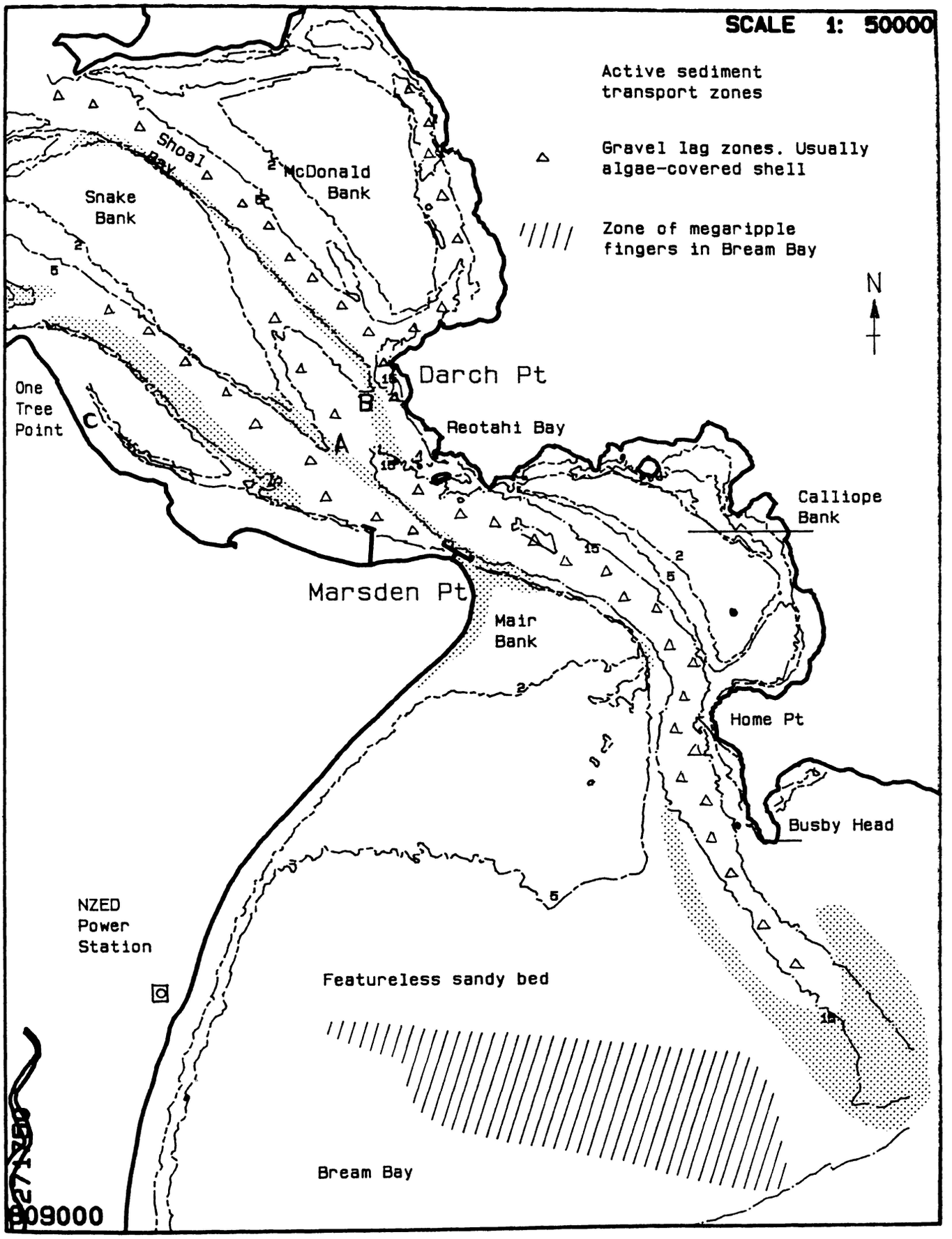

Figure 2.11: Summary of shelly and active sandy zones with location of megaripple bands in Bream Bay.

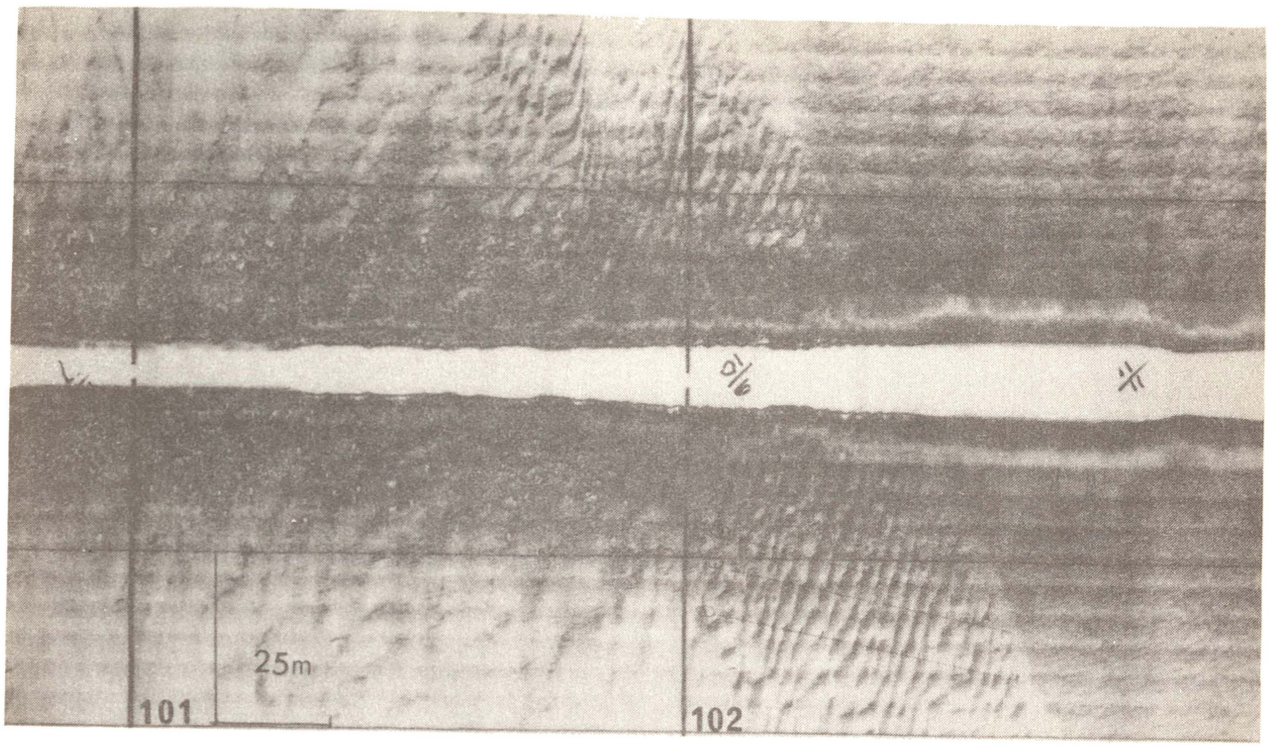

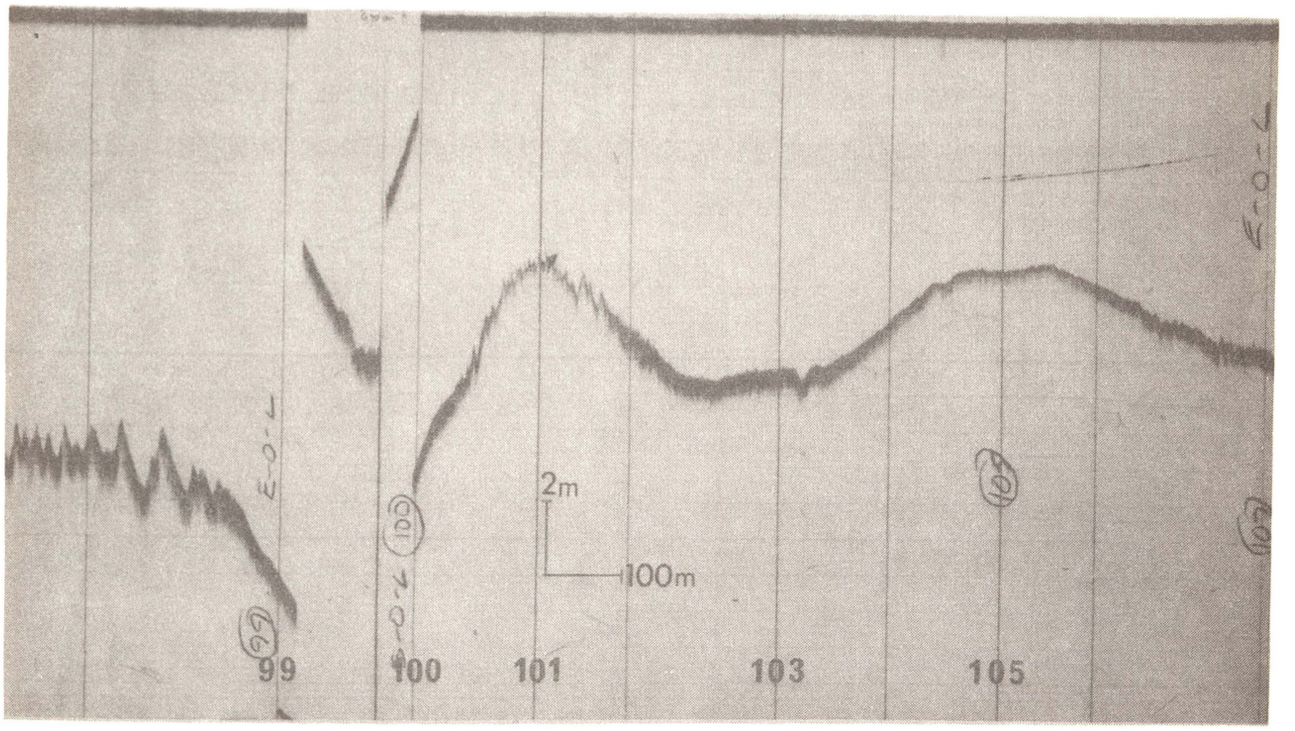

Figure 2.12: Side-scan sonar and depth sounder records at Fix 102 (Figure 2.7) showing the distinct megaripple and sand wave fields on the active south-east sub-tidal spit off Snake Bank.

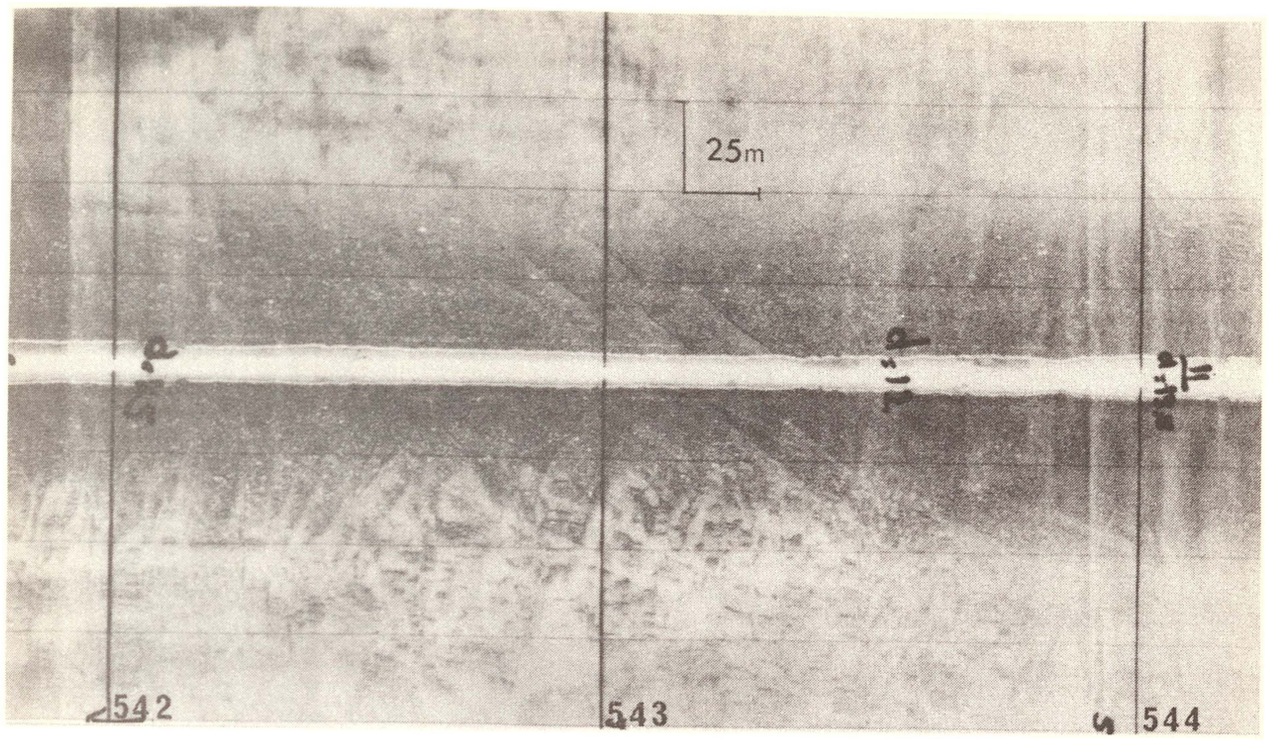

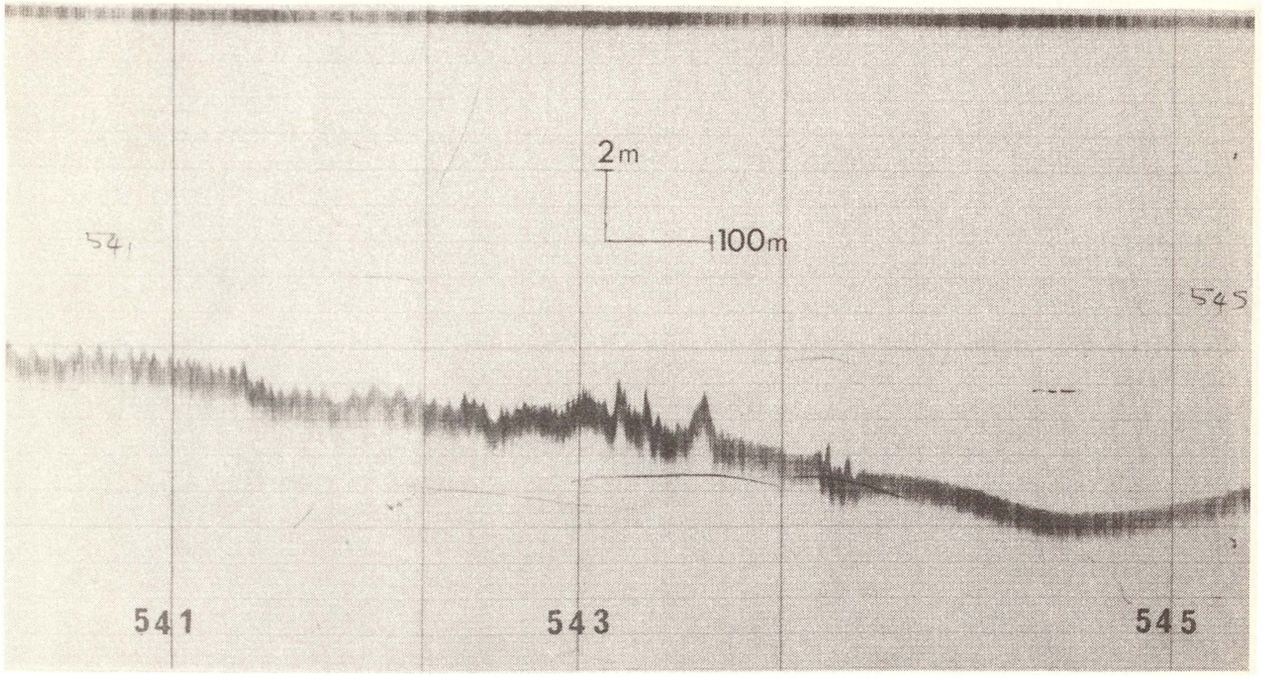

Figure 2.13: Side-scan sonar and depth sounder records at Fix 543 (Figure 2.7) showing the sandwaves on the southern side of the main shipping channel west of One Tree Point.

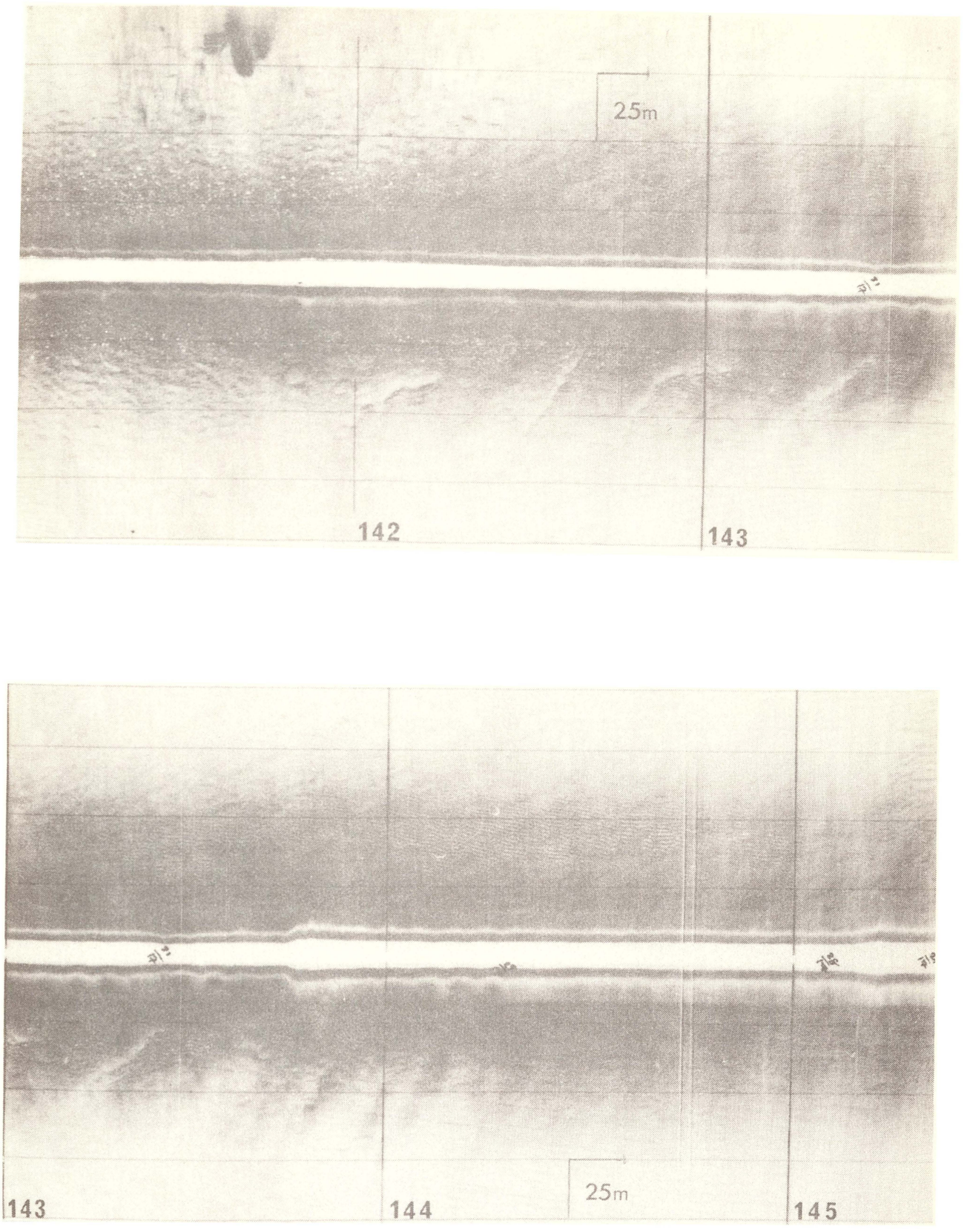

Figure 2.14: Side-scan sonar records at Fixes 142-145 (Figure 2.8) showing active megaripples south-east of Busby Head. Note also the sand waves with co-existant megaripples in the lower halves of the records.

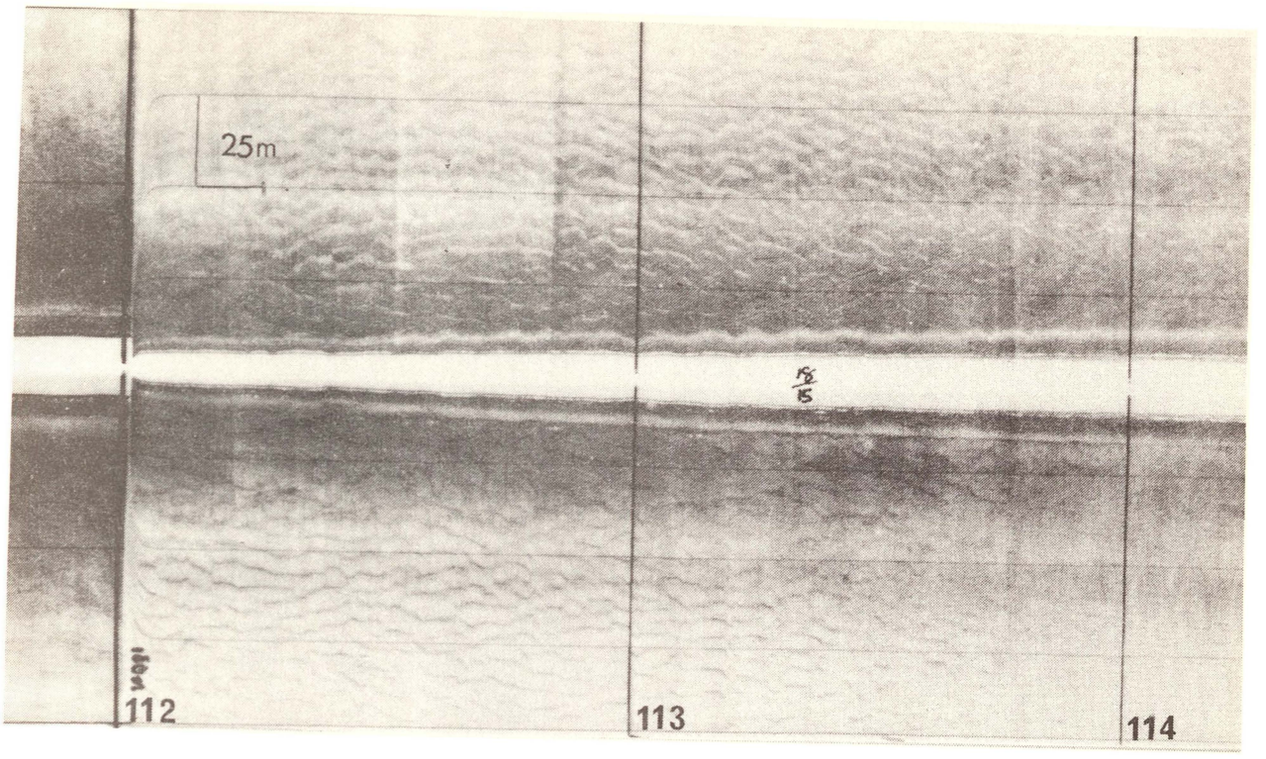

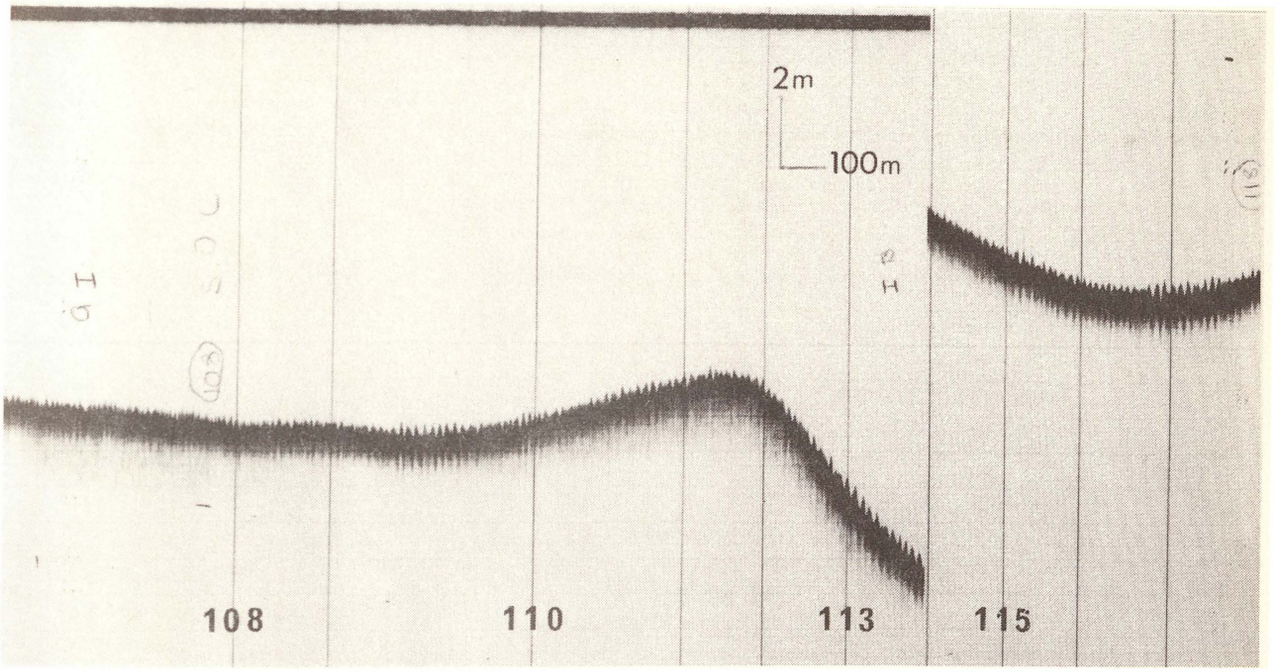

Figure 2.15: Side-scan sonar and depth sounder records at Fix 113 (Figure 2.8) showing active, cuspate megaripples south east of Busby Head.

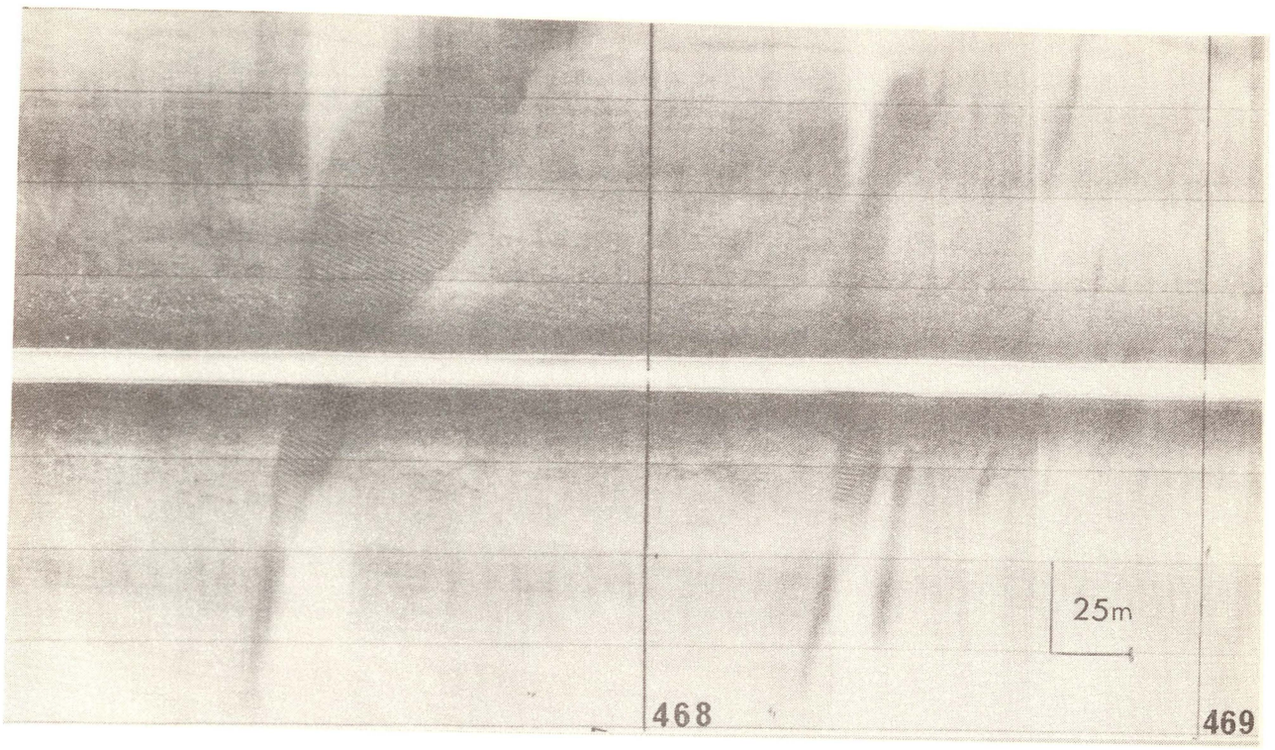

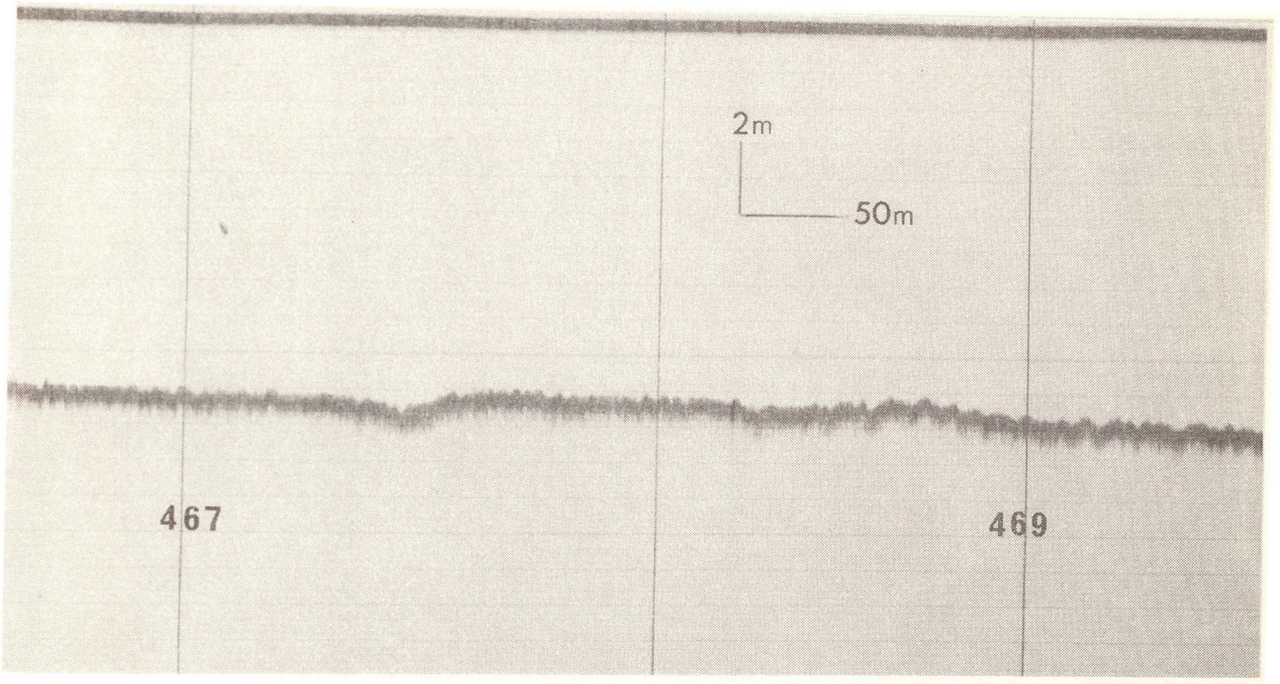

Figure 2.16: Side-scan sonar and depth sounder records at Fix 468 (Figure 2.8) showing confined bands of megaripple fingers in Bream Bay on the Mair Bank ebb-tidal delta.

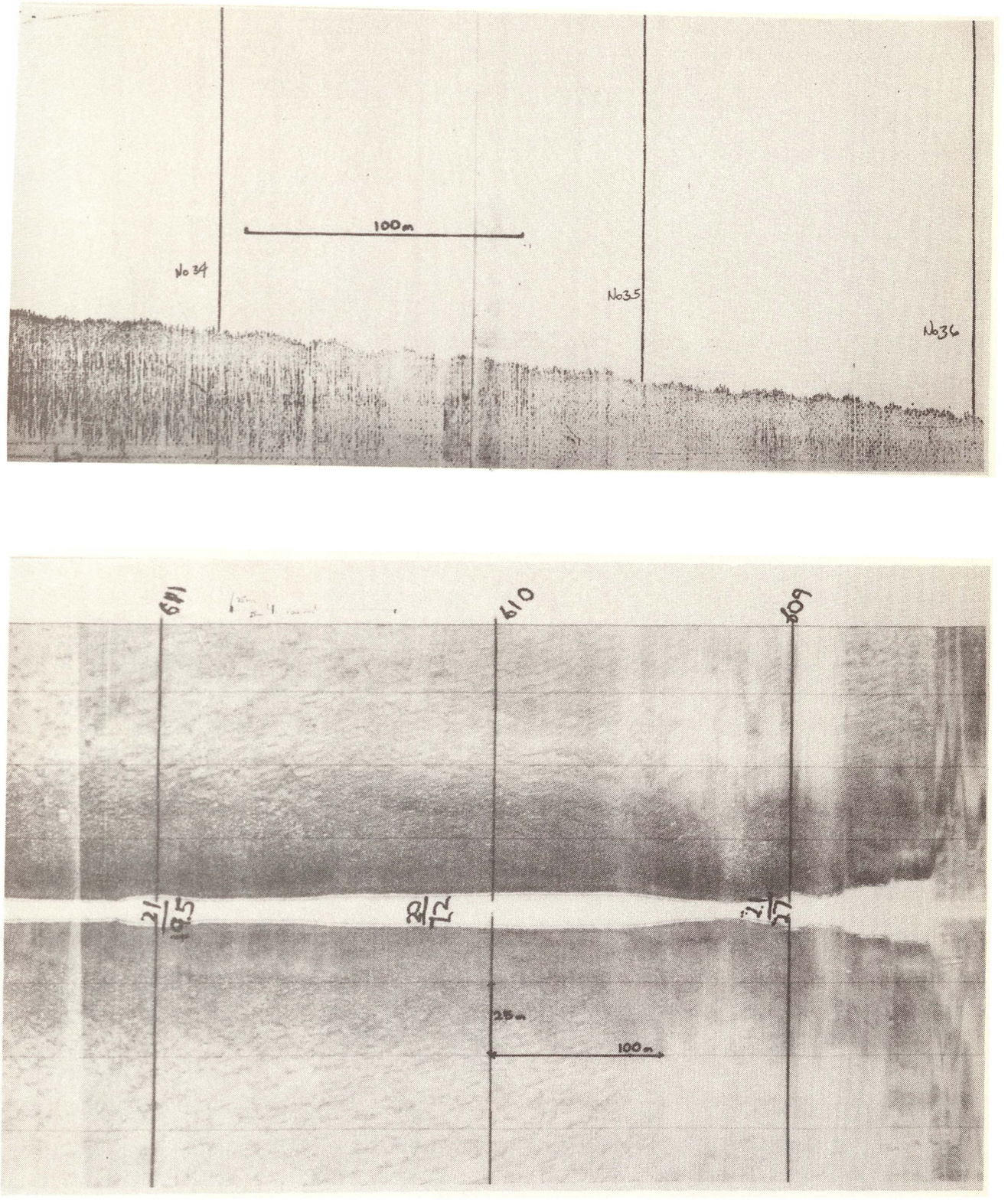

Figure 2.17: Side-scan sonar and depth sounder records at Fix 610 (Figure 2.7) showing shell "sand waves" in the main channel just outside the Harbour entrance throat.

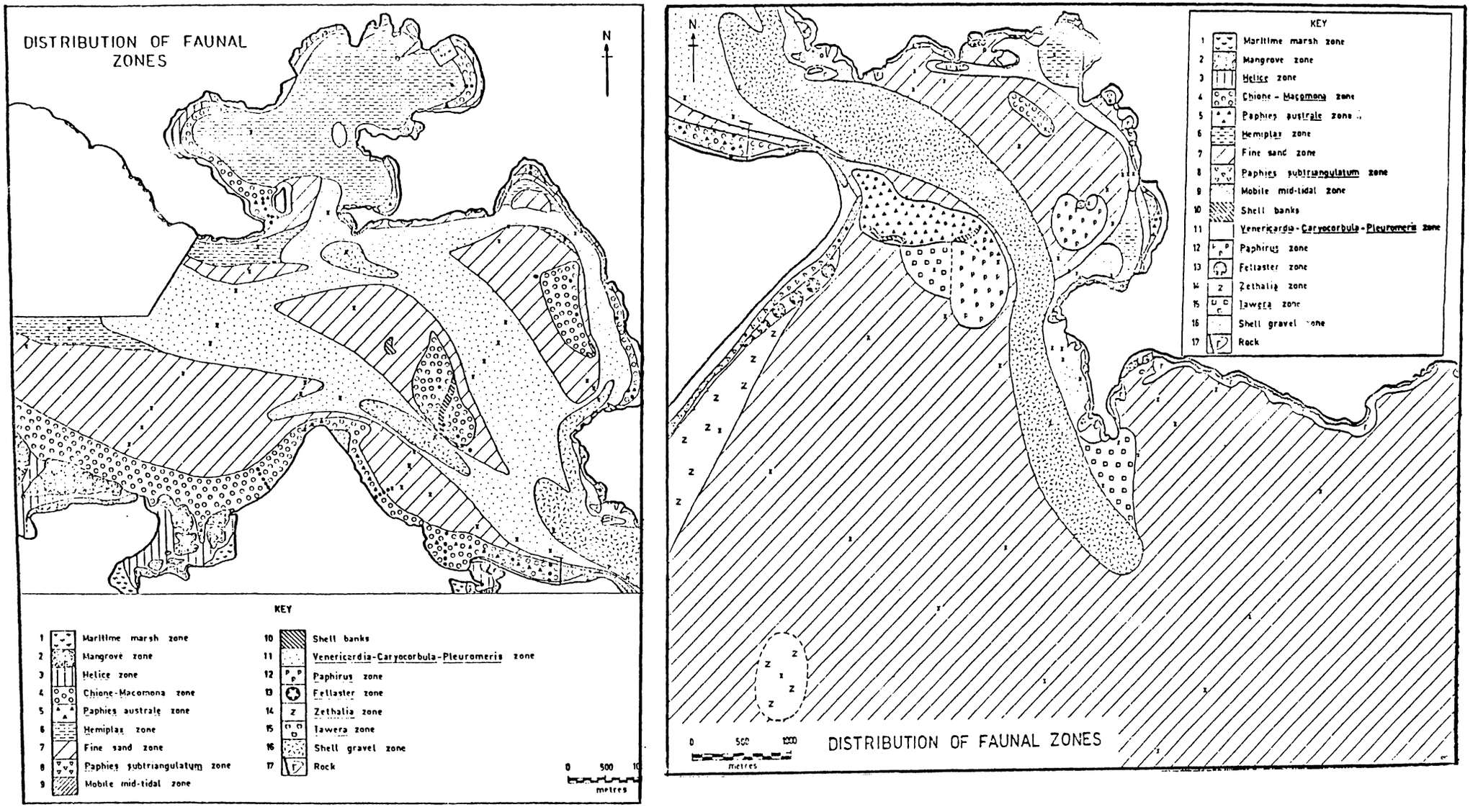

Figure 2.18: Distribution of faunal zones after Bioresearches (1976).

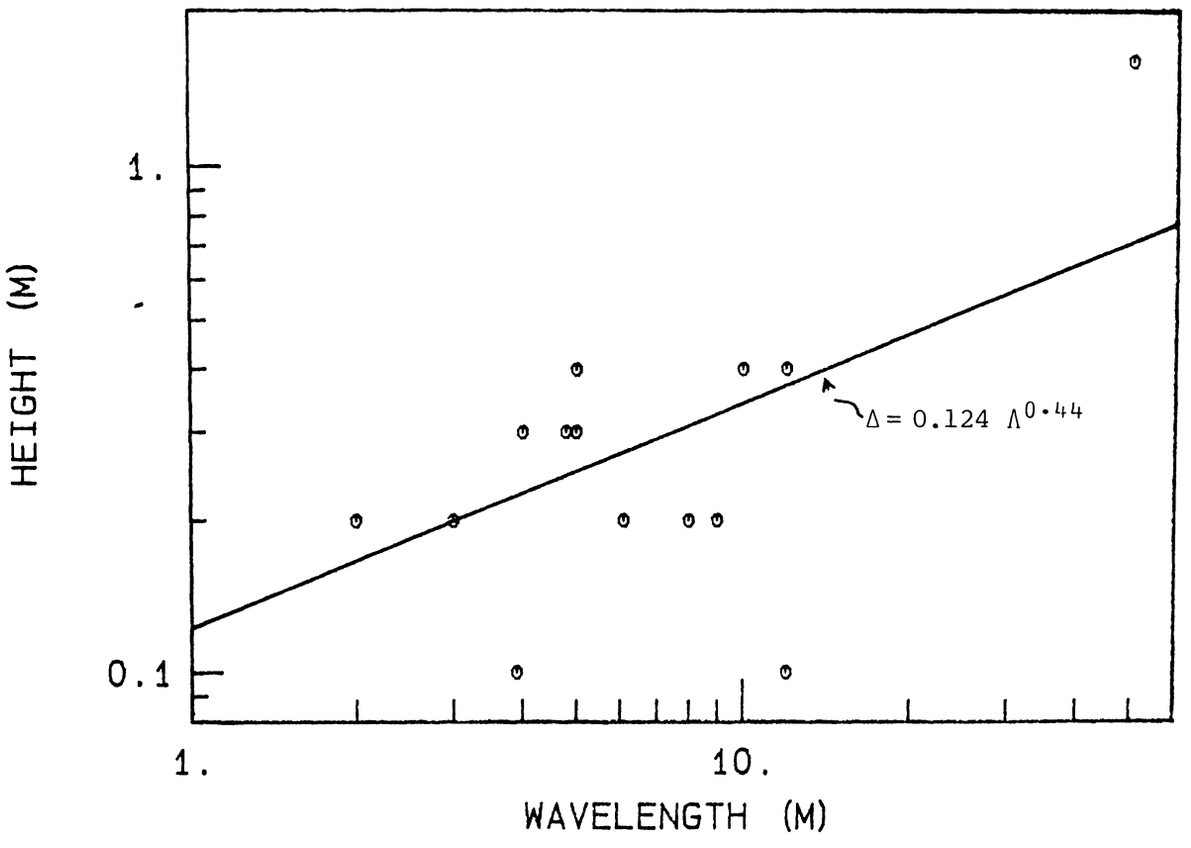

Figure 2.19: Average bedform height against average wavelength in Whangarei Harbour with empirical curve of Knight (1977).

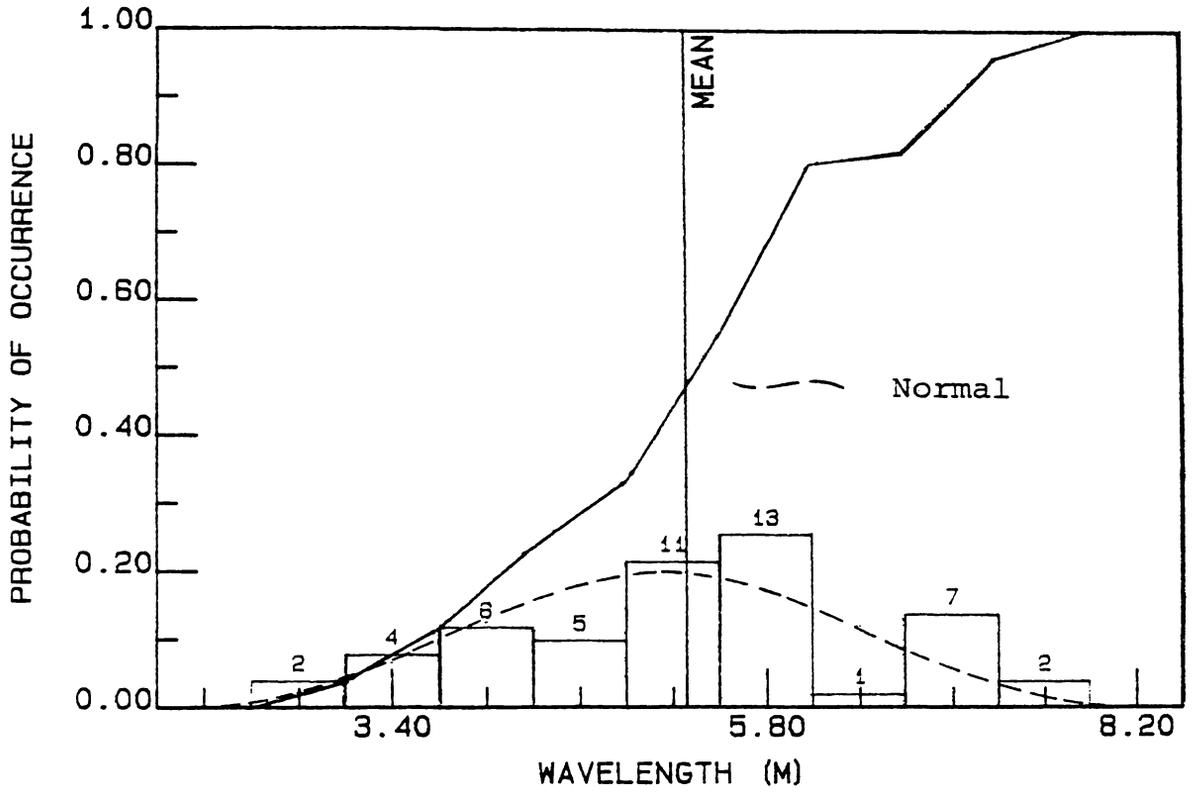

Figure 2.20: Distribution of megaripple wavelengths at Fix 102 with the Normal distribution .

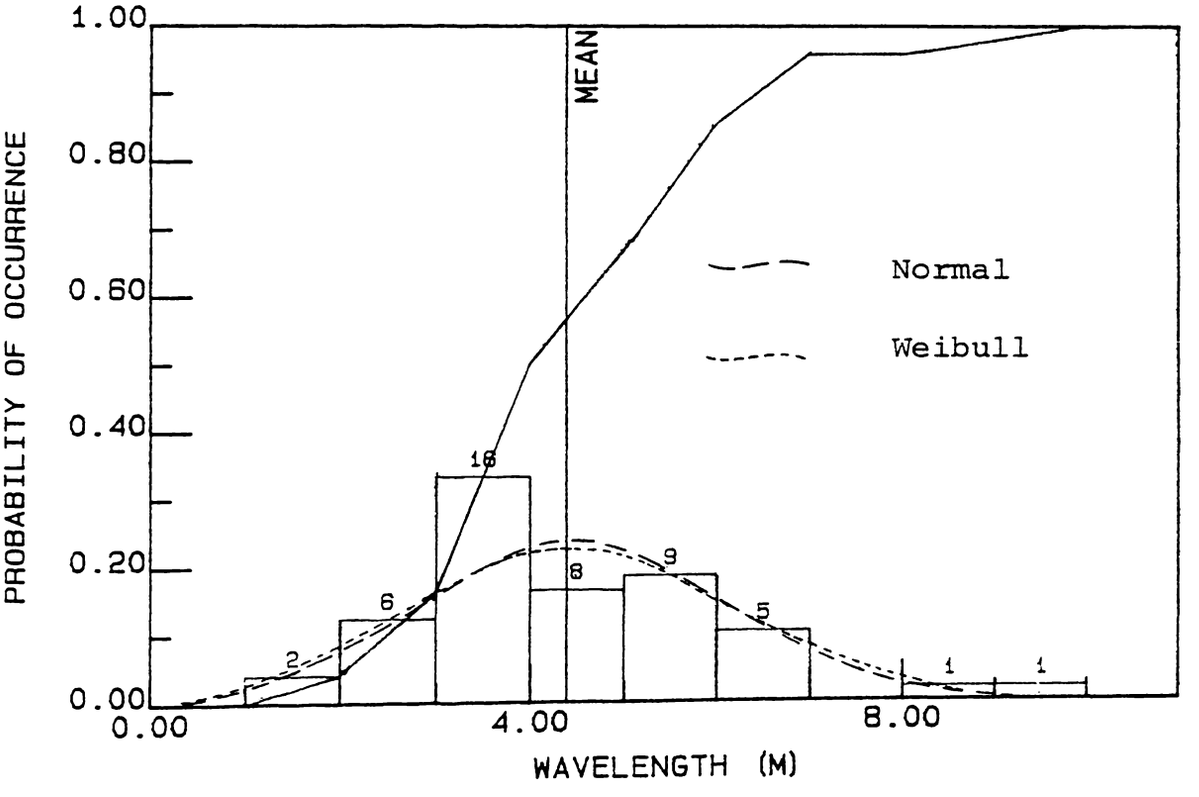

Figure 2.21: Distribution and megaripple wavelengths at Fix 589 with the Normal distribution and Weibull distributions.

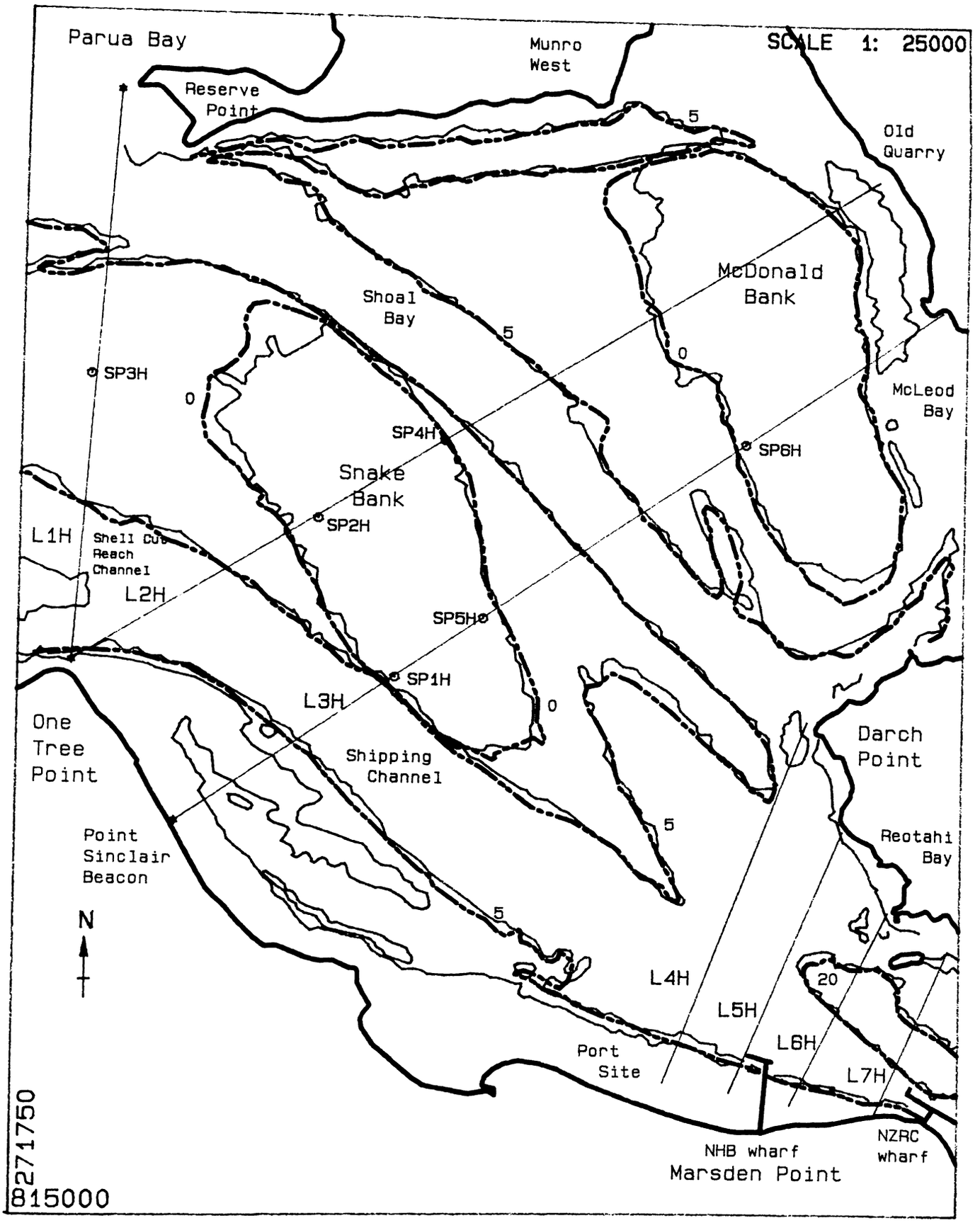

Figure 3.1: Lower harbour showing the writer's sounding cross-sections (L1H to L7H) and the sounding piles (SP1H to SP6H). Contours from 1974 (NZ5213) bathymetry (thick lines) and the 1981 RNZN bathymetric survey (thin lines) are shown for comparison.

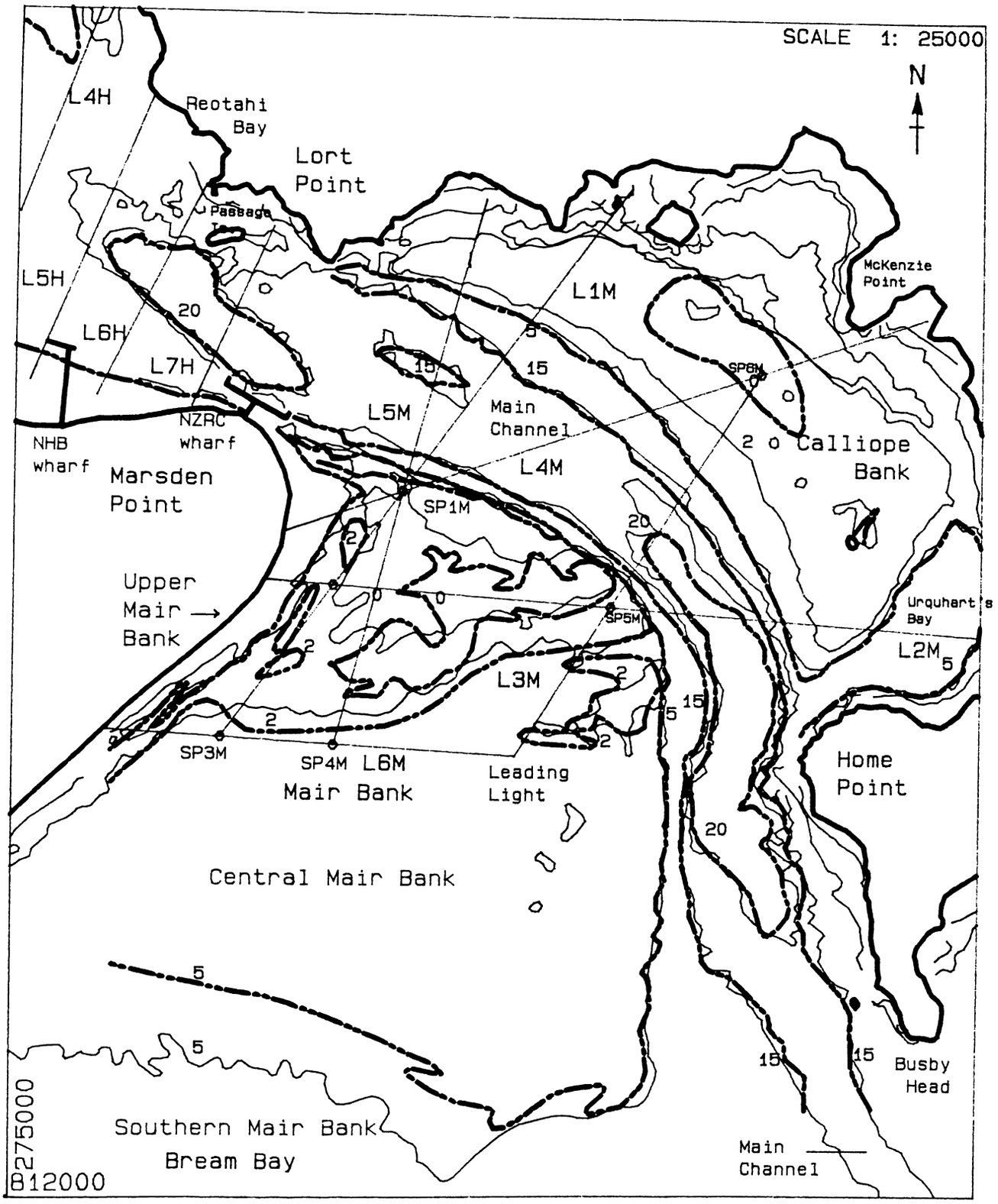

Figure 3.2: Mair Bank and environs, showing the writer's sounding cross-sections (L1M to L6M) and the sounding piles (SP1M to SP6M). Contours from the 1974 (NZ5213) bathymetry (thick lines) and the 1981 RNZN bathymetric survey (thin lines) are shown for comparison.

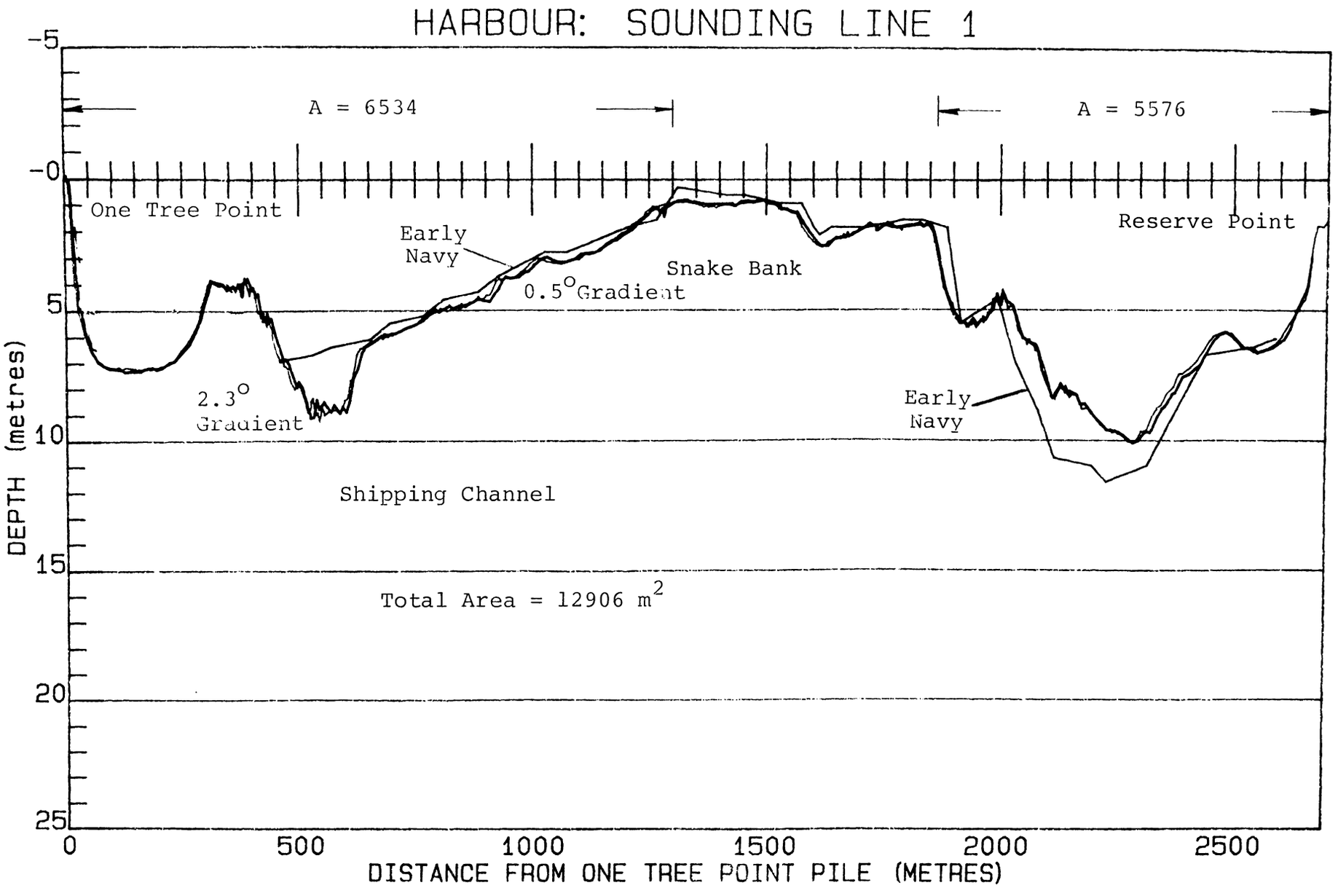

Figure 3.3: Sounding line LlH from One Tree Point to Reserve Point, compared with the 1961 RNZN survey. A is area below CD.

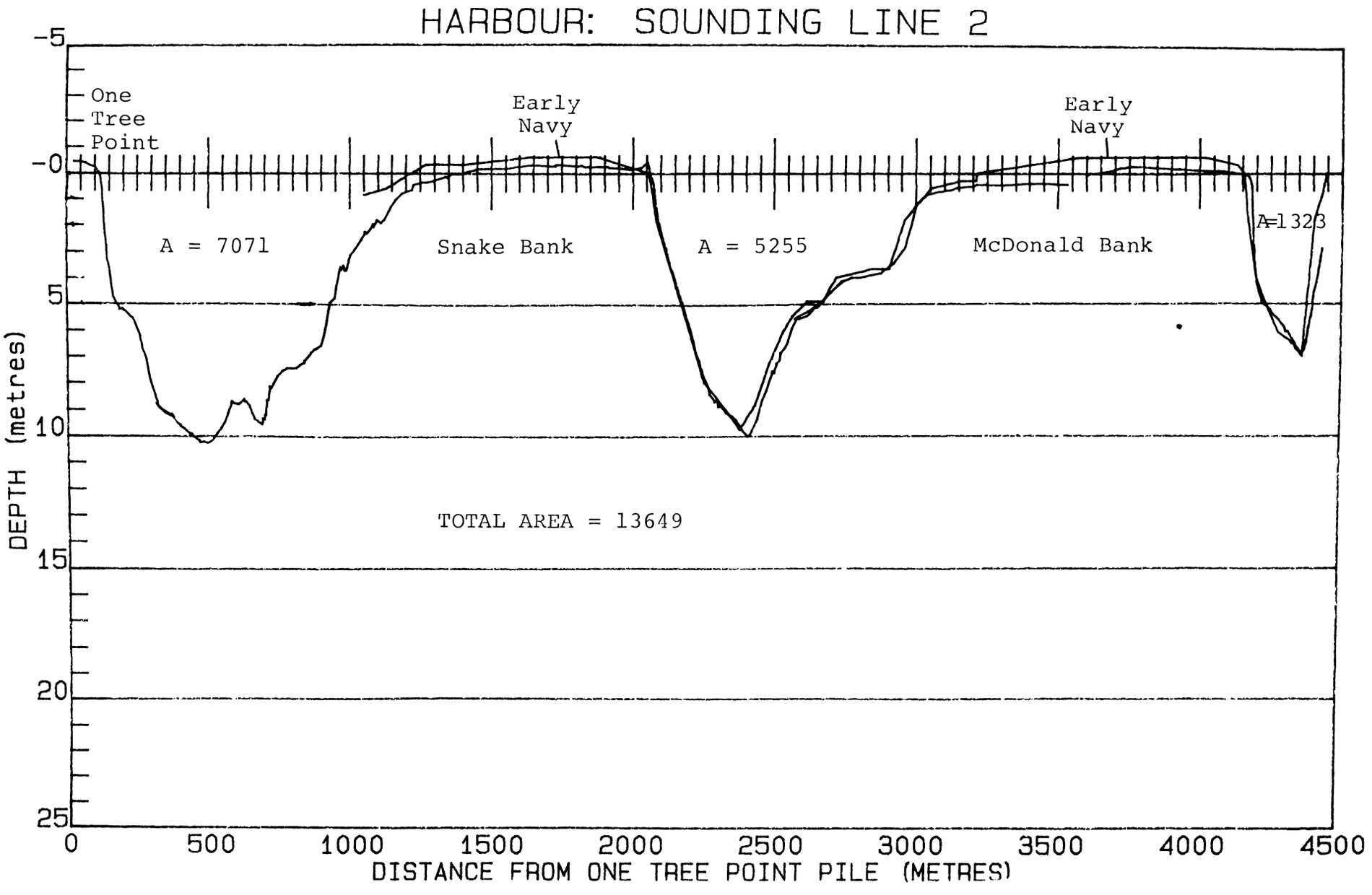

Figure 3.4: Sounding line L2H from One Tree Point to the old quarry, compared with the 1961 RNZN survey. A is area below CD.

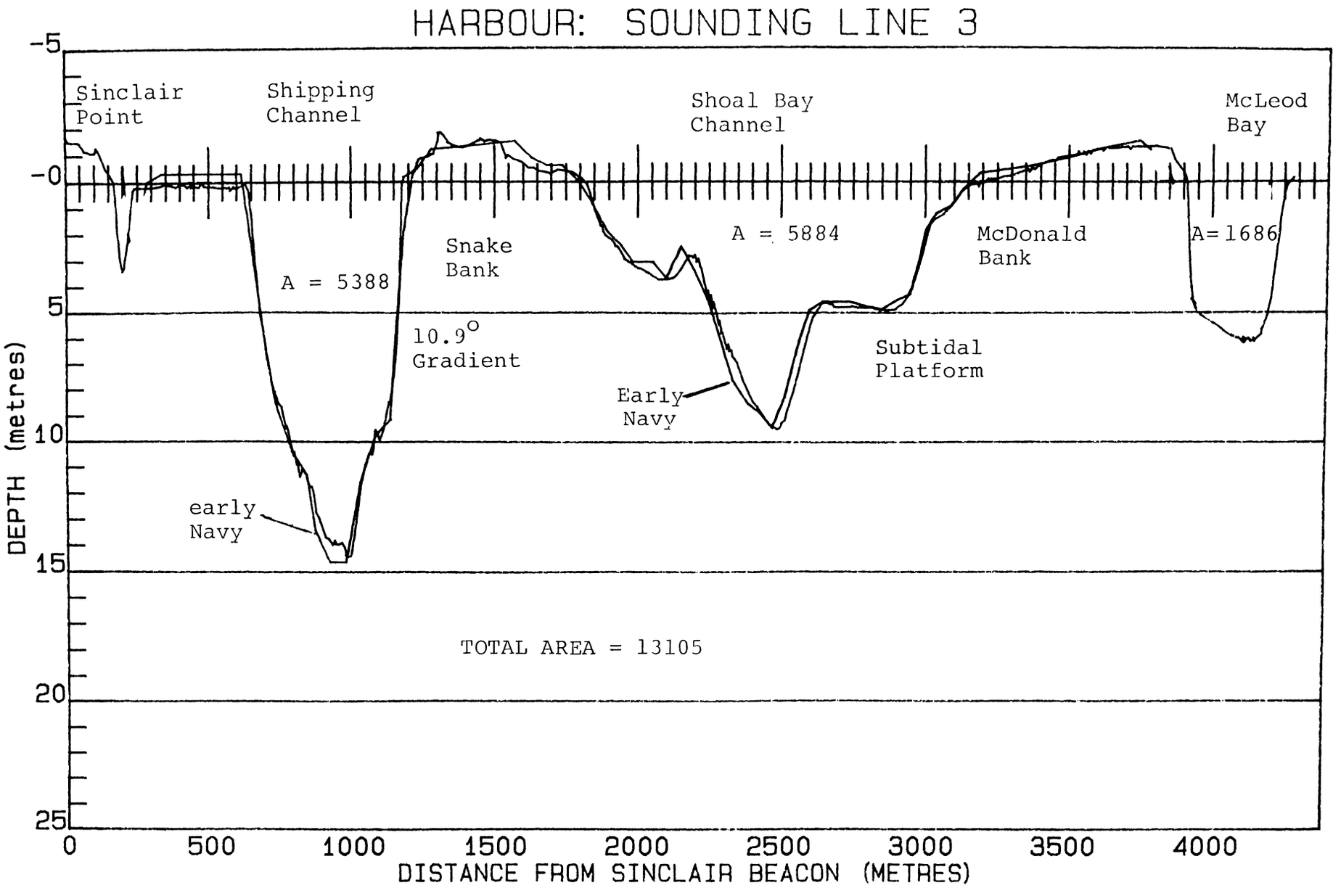

Figure 3.5: Sounding line L3H from Sinclair Beacon to McLeod Bay, compared with the 1961 RNZN survey. A is area below CD.

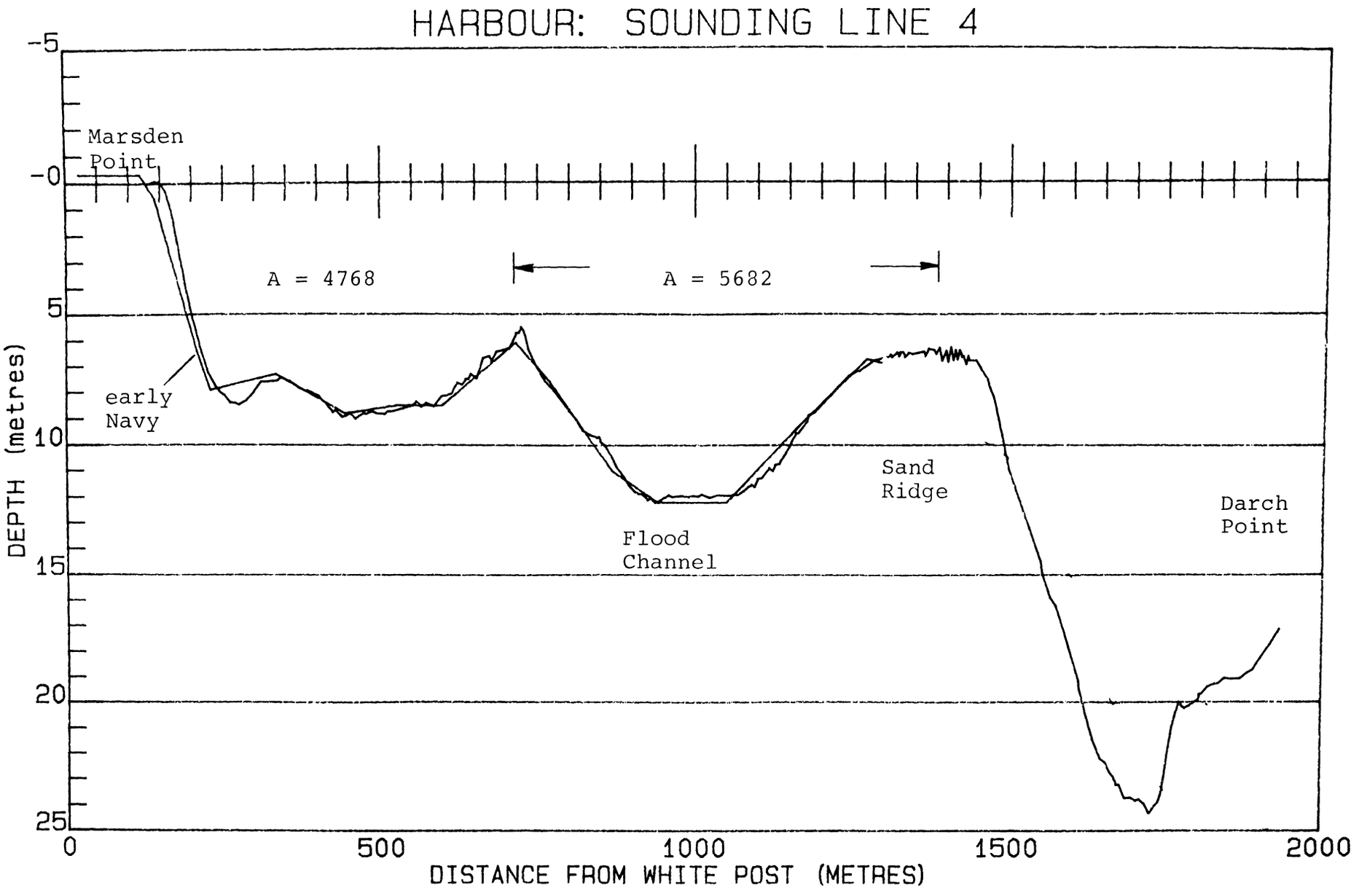

Figure 3.6: Sounding line L4H from the sand flat 450m west of NHB wharf to Darch Point, compared with the 1961 RNZN survey. A is area below CD.

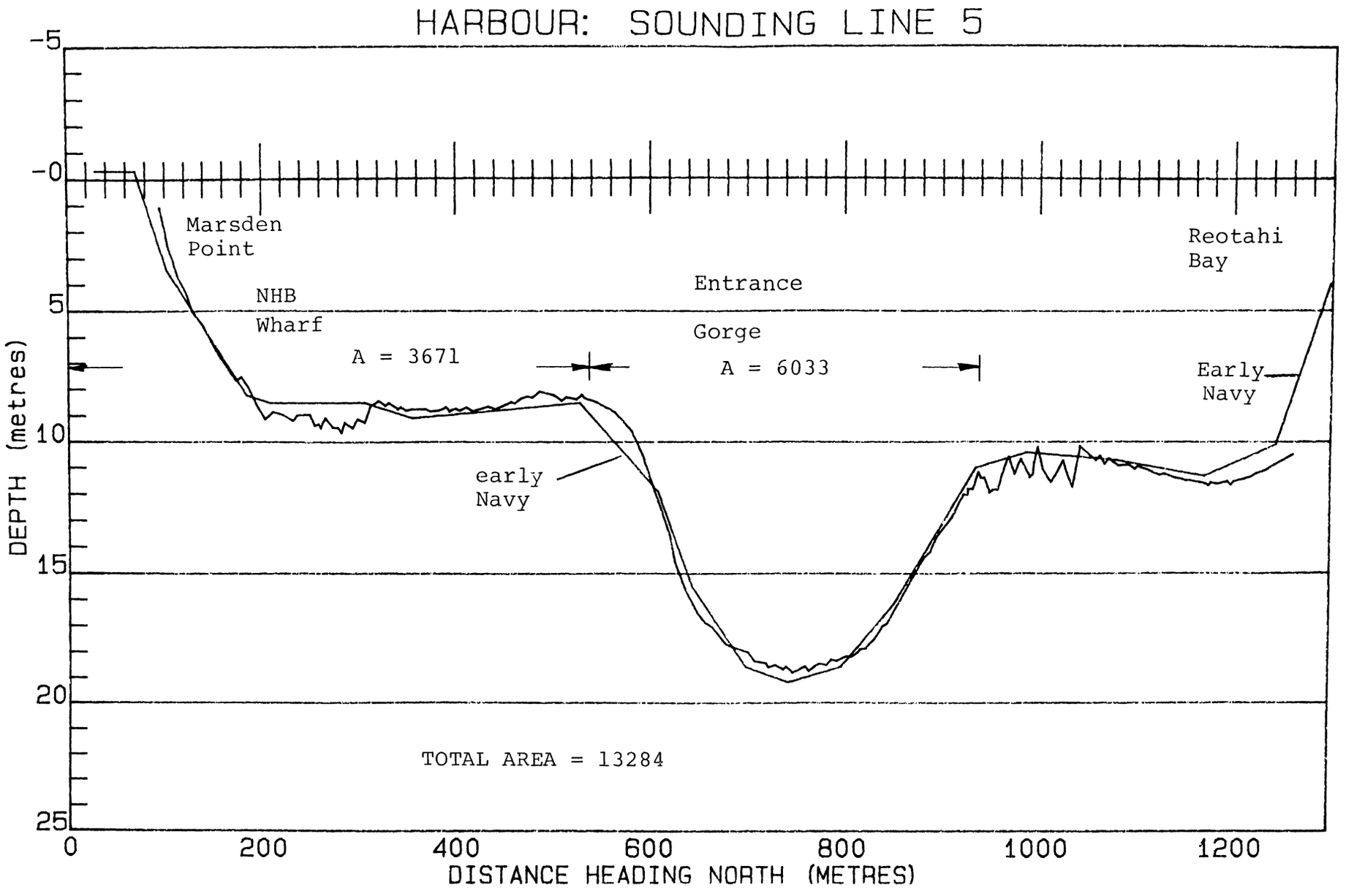

Figure 3.7: Sounding line L5H from western end of NHB wharf to Reotahi Bay, compared with 1961 RNZN survey. A is area below CD.

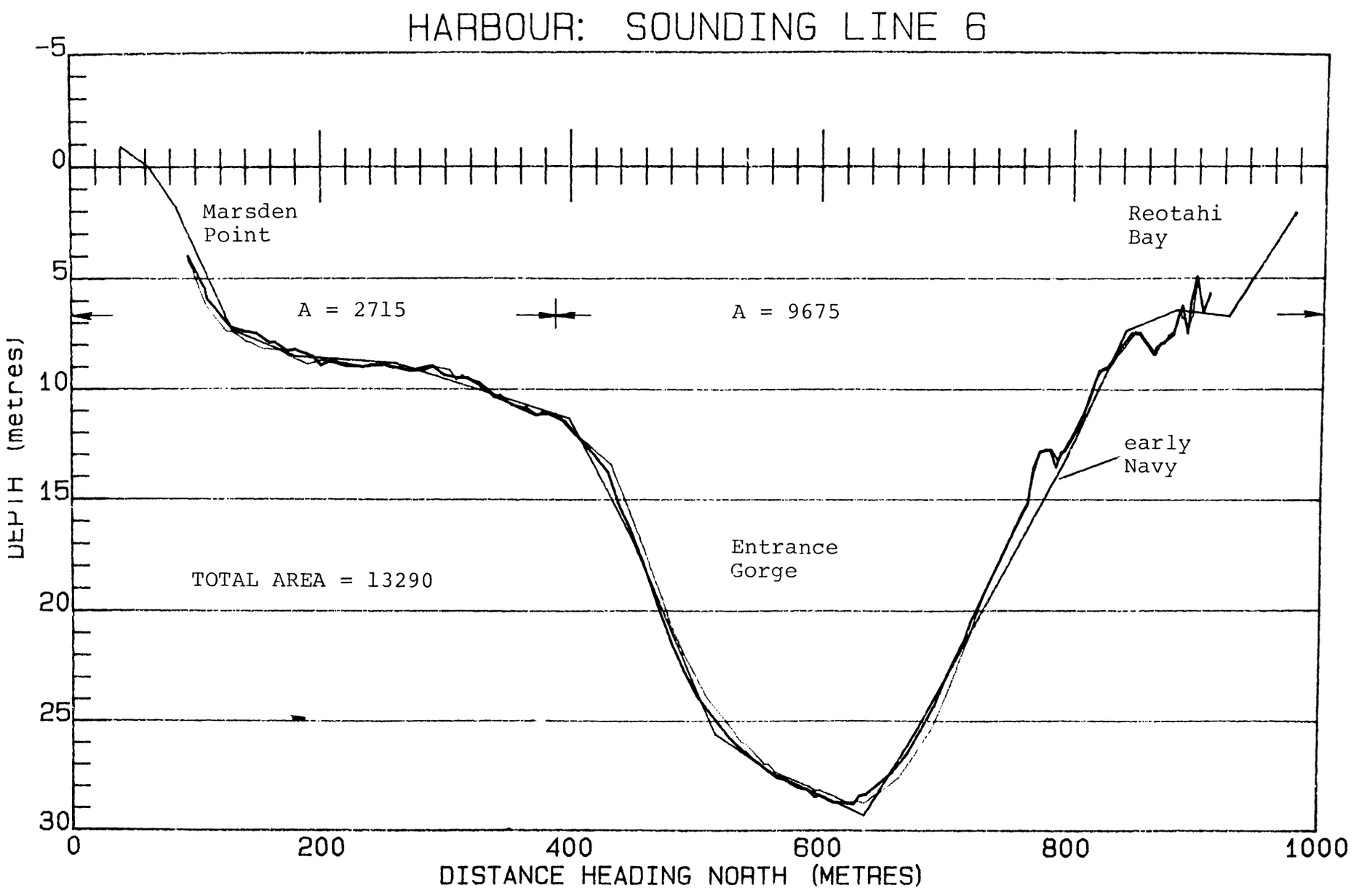

Figure 3.8: Sounding line L6H from eastern side of NHB wharf to Reotahi Bay, compared with 1961 RNZN survey. A is area below CD.

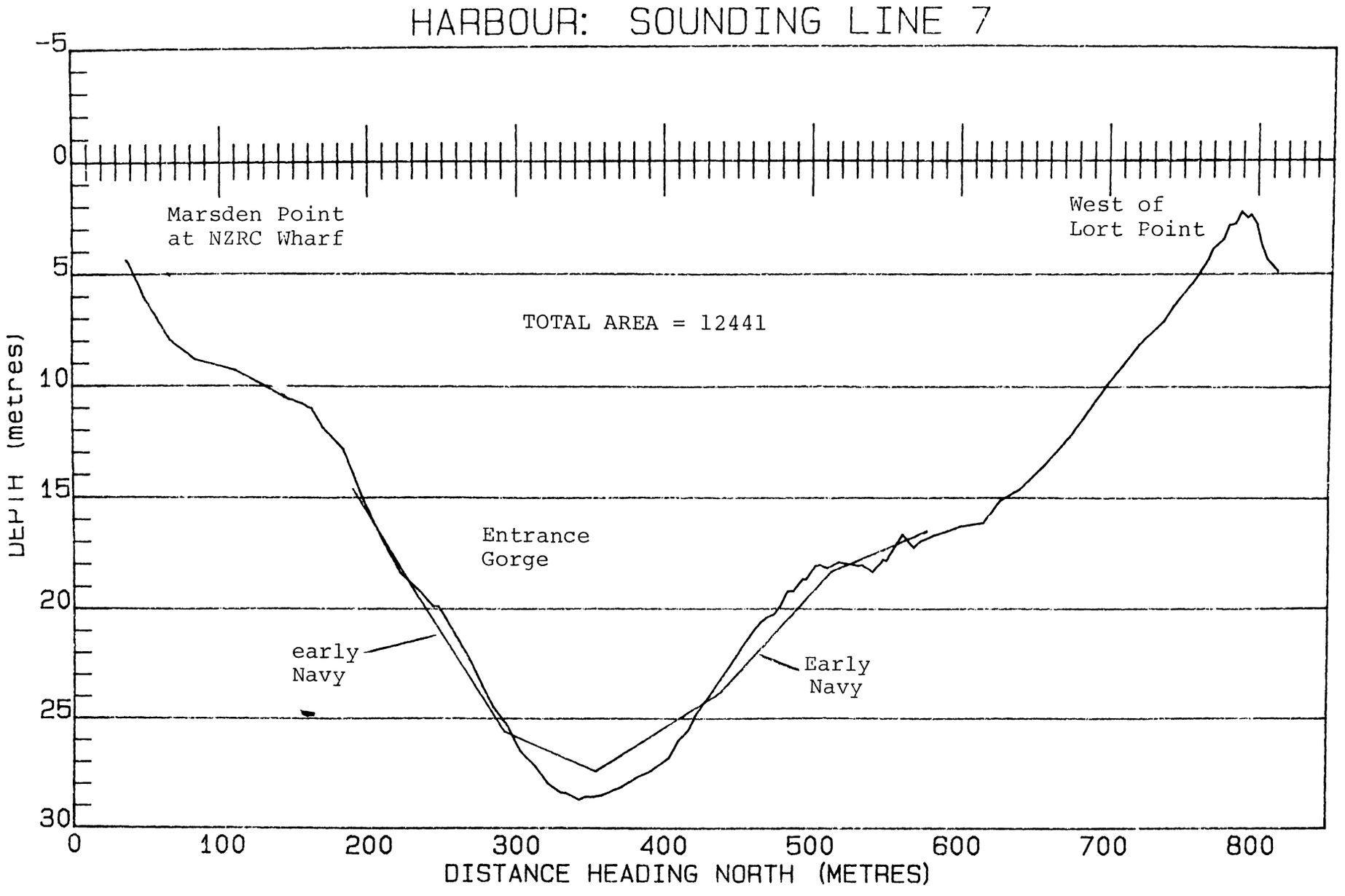

Figure 3.9: Sounding line L7H from west of NZRC wharf to east of Passage Island, compared with 1961 RNZN survey.

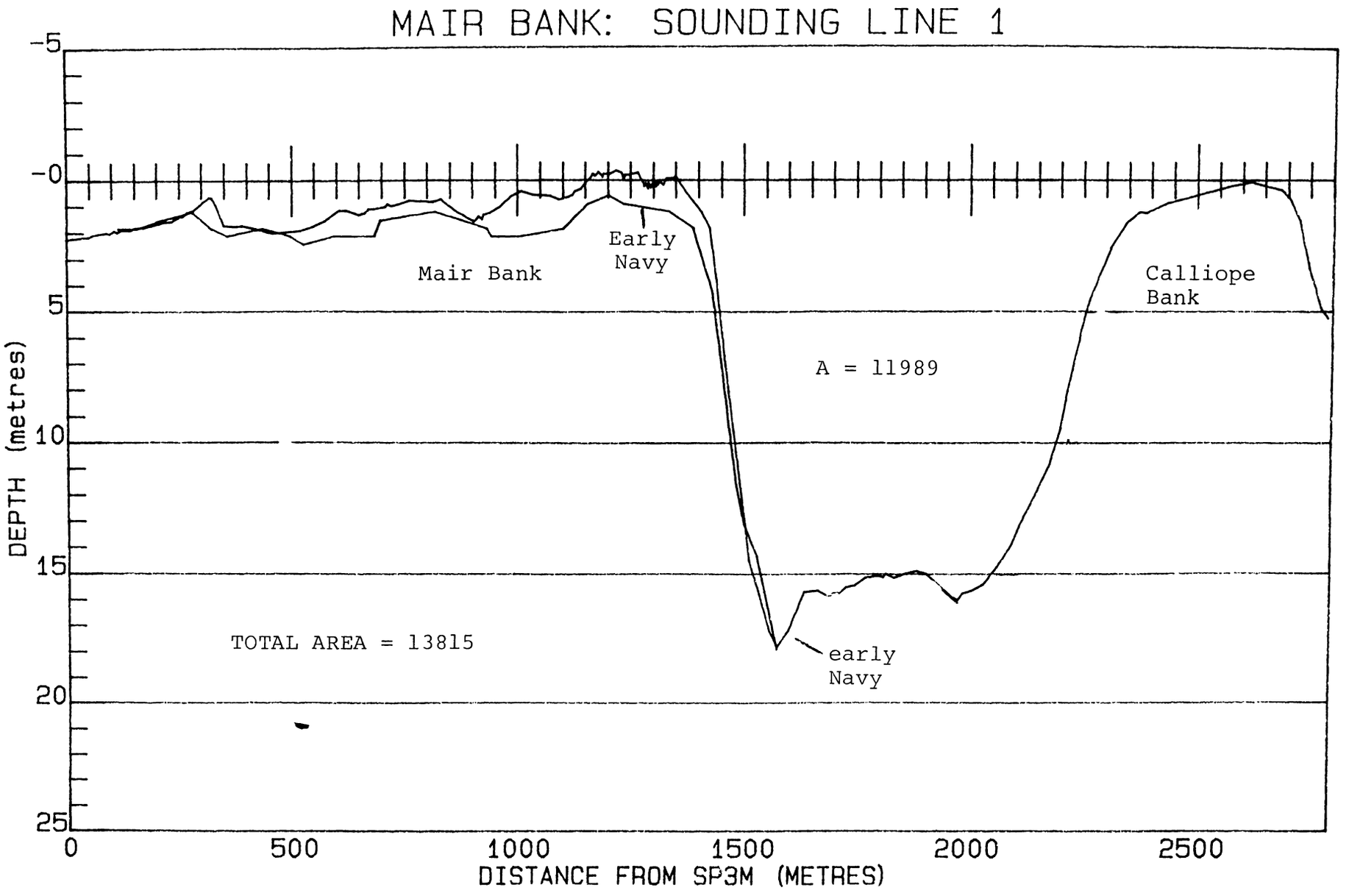

Figure 3.10: Sounding line L1M along distributary channel off Marsden Point, compared with 1959 RNZN survey. A is area below CD.

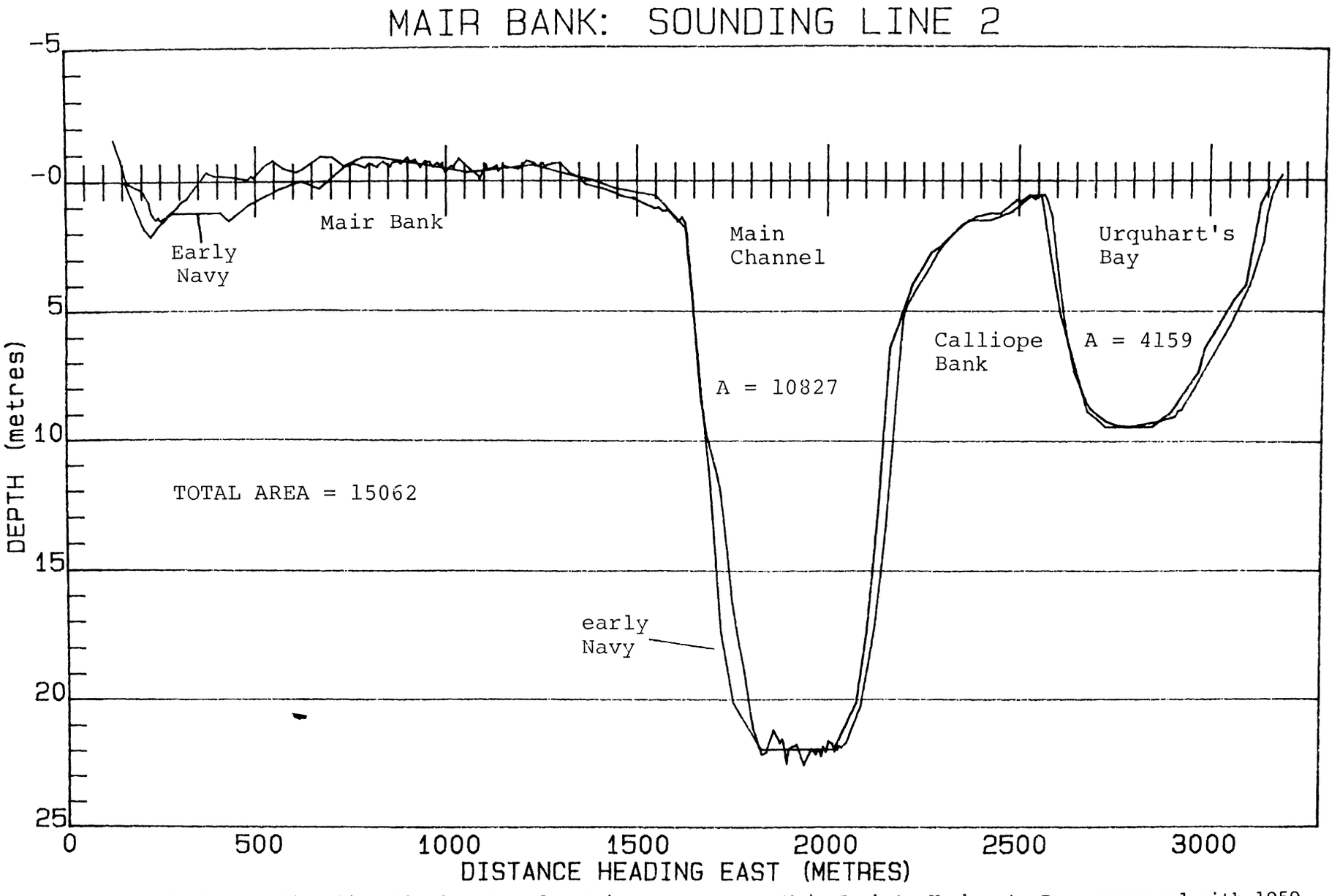

Figure 3.11: Sounding line L2M from Marsden Point east across Mair Bank to Urqhuart Bay, compared with 1959 RNZN survey. A is area below CD.

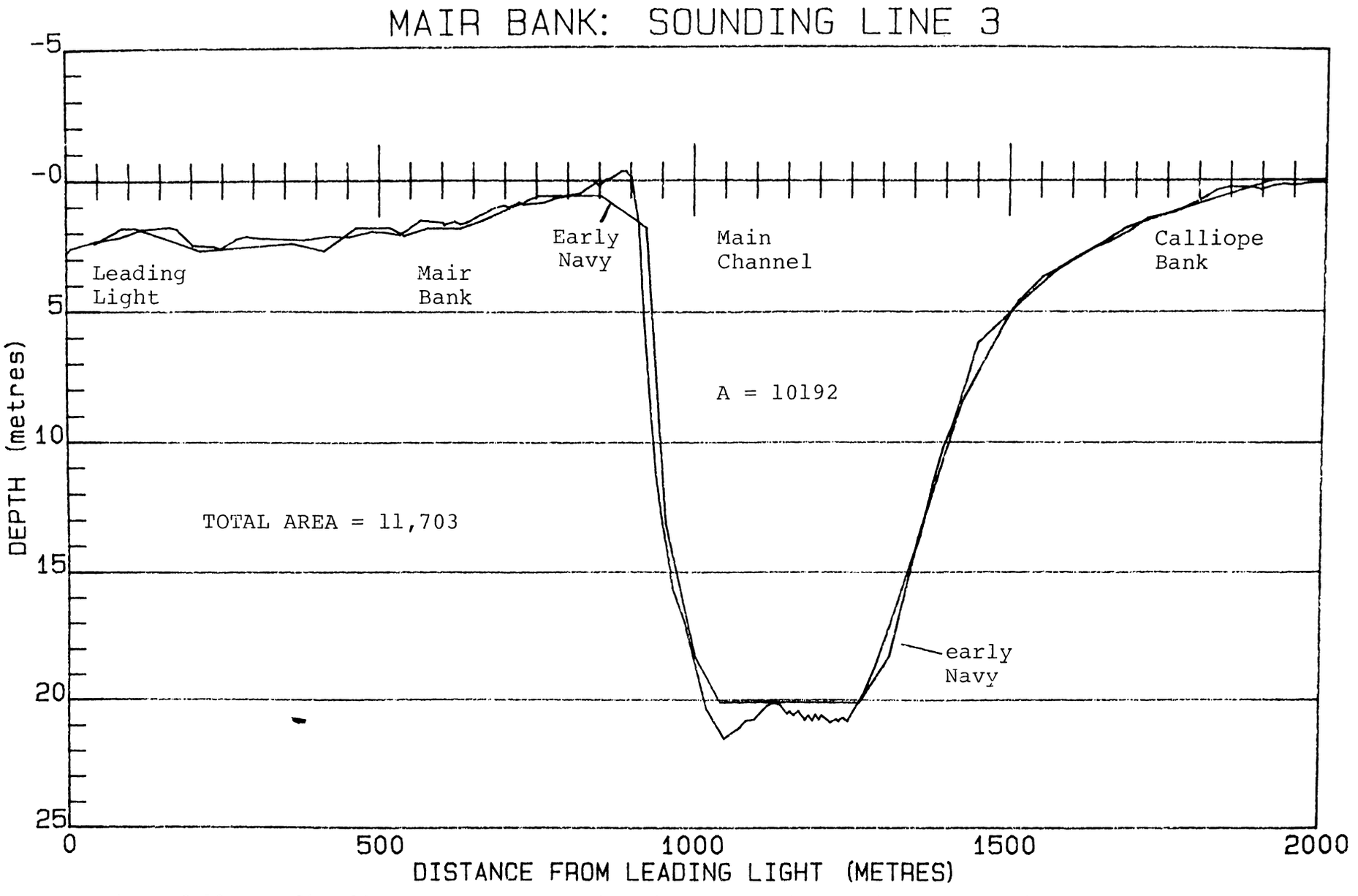

Figure 3.12: Sounding line L3M from the leading light to Calliope Bank, compared with 1959 RNZN survey. A is area below CD.

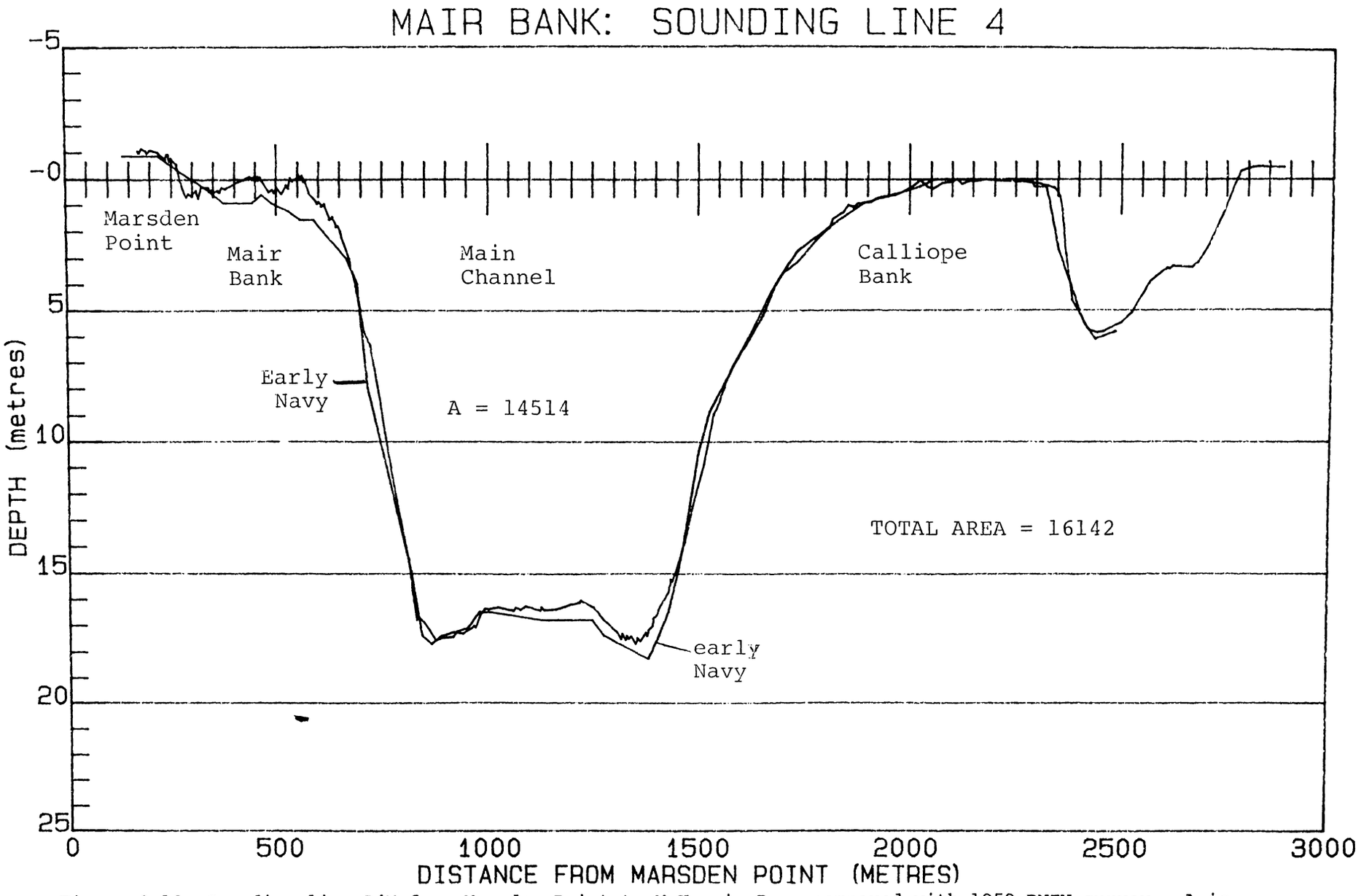

Figure 3.13: Sounding line L4M from Marsden Point to McKenzie Bay, compared with 1959 RNZN survey. A is area below CD.

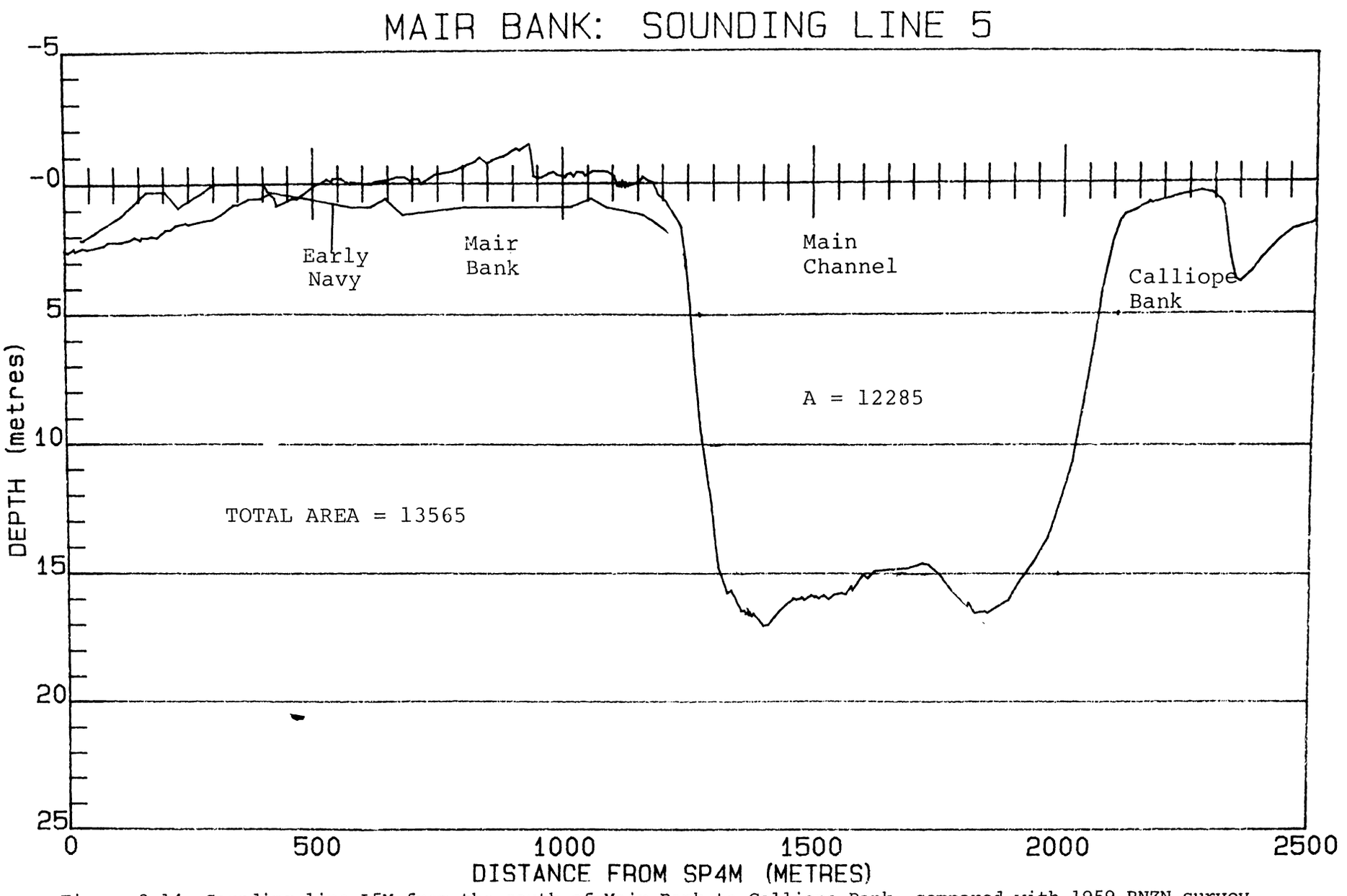

Figure 3.14: Sounding line L5M from the south of Mair Bank to Calliope Bank, compared with 1959 RNZN survey. A is area below CD.

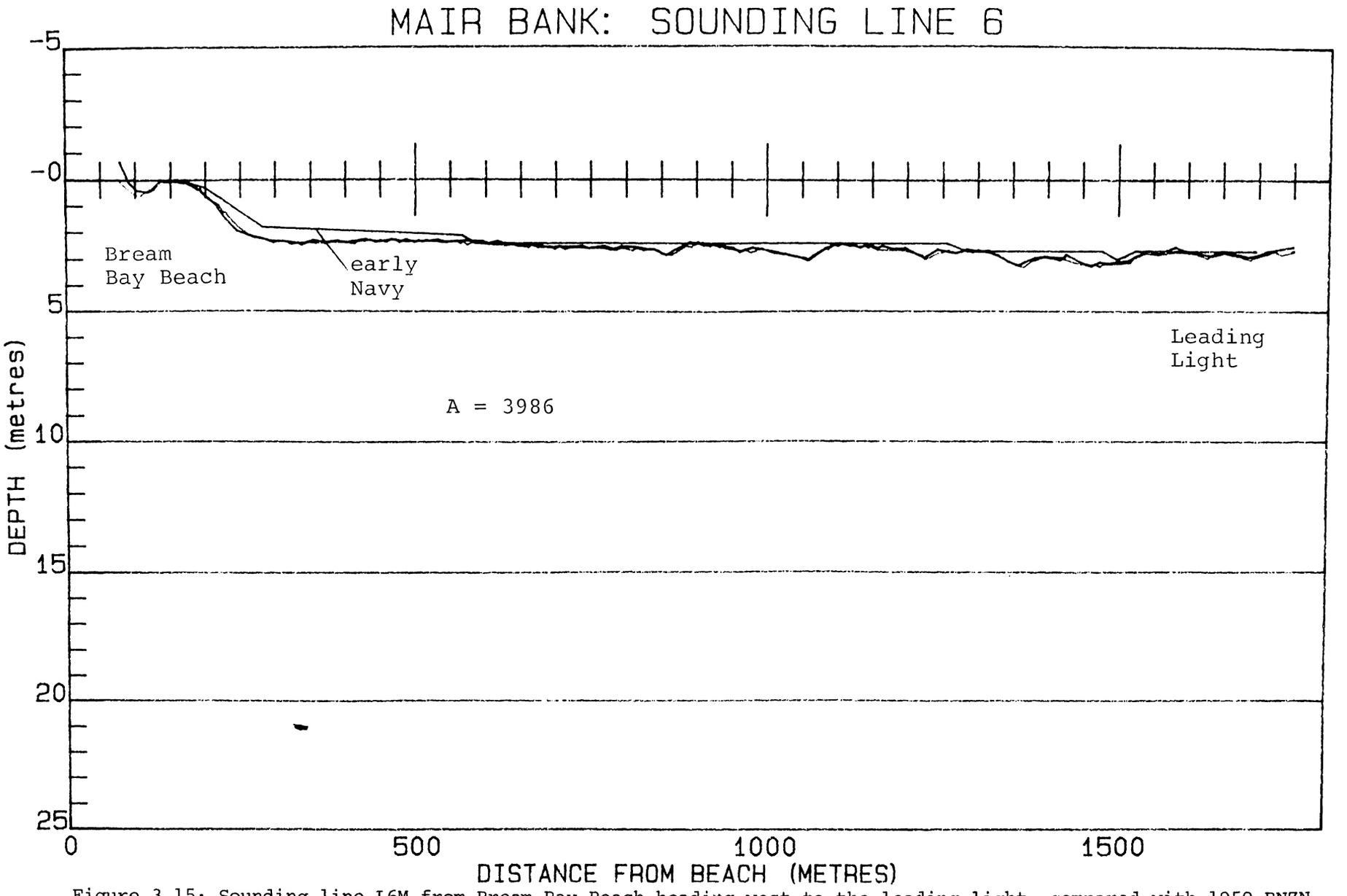

Figure 3.15: Sounding line L6M from Bream Bay Beach heading west to the leading light, compared with 1959 RNZN survey. A is area below CD.

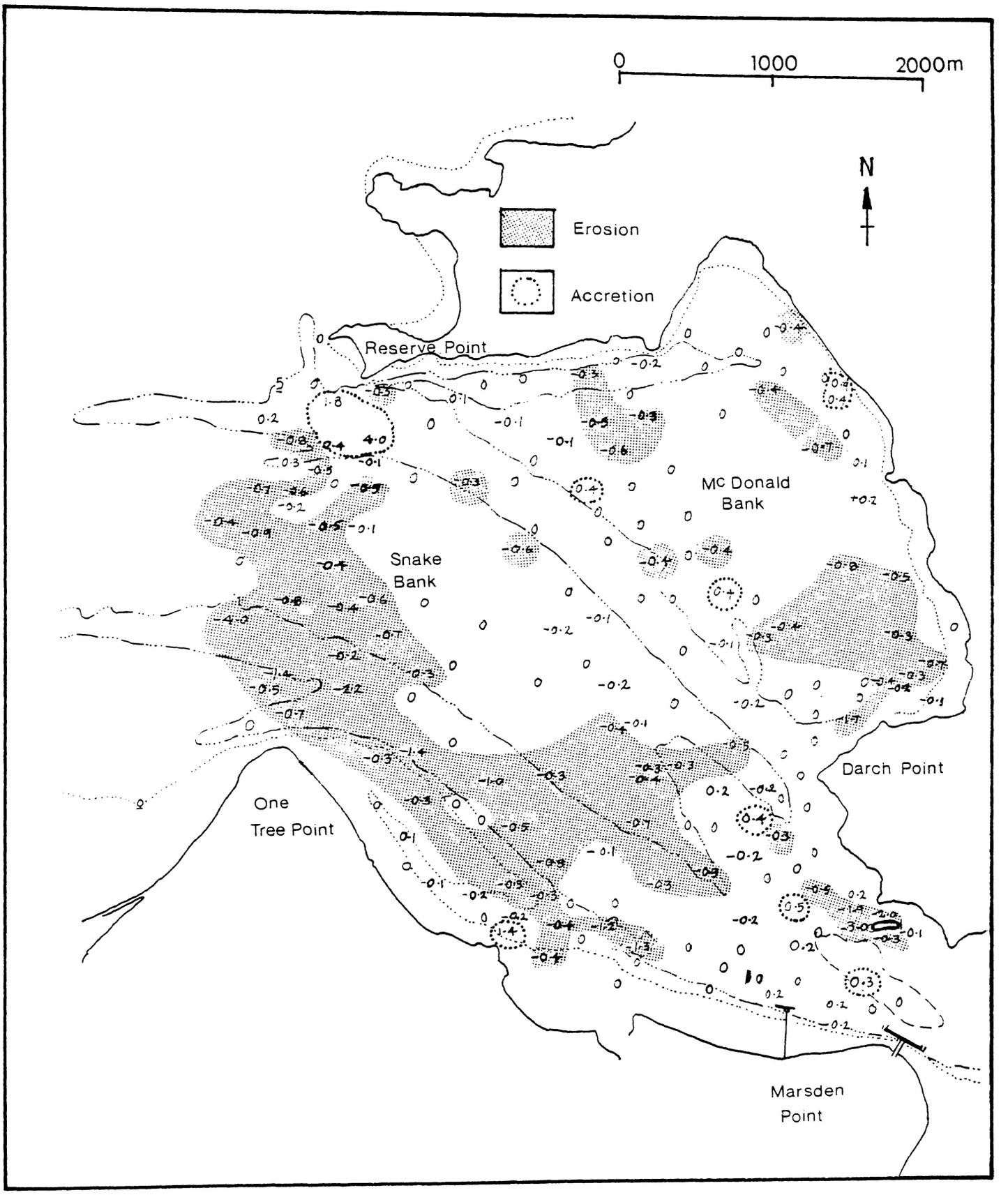

Figure 3.16: Lower harbour showing comparison of 1974 RNZN bathymetry chart (NZ5213) and the 1981 RNZN survey with depth changes in metres

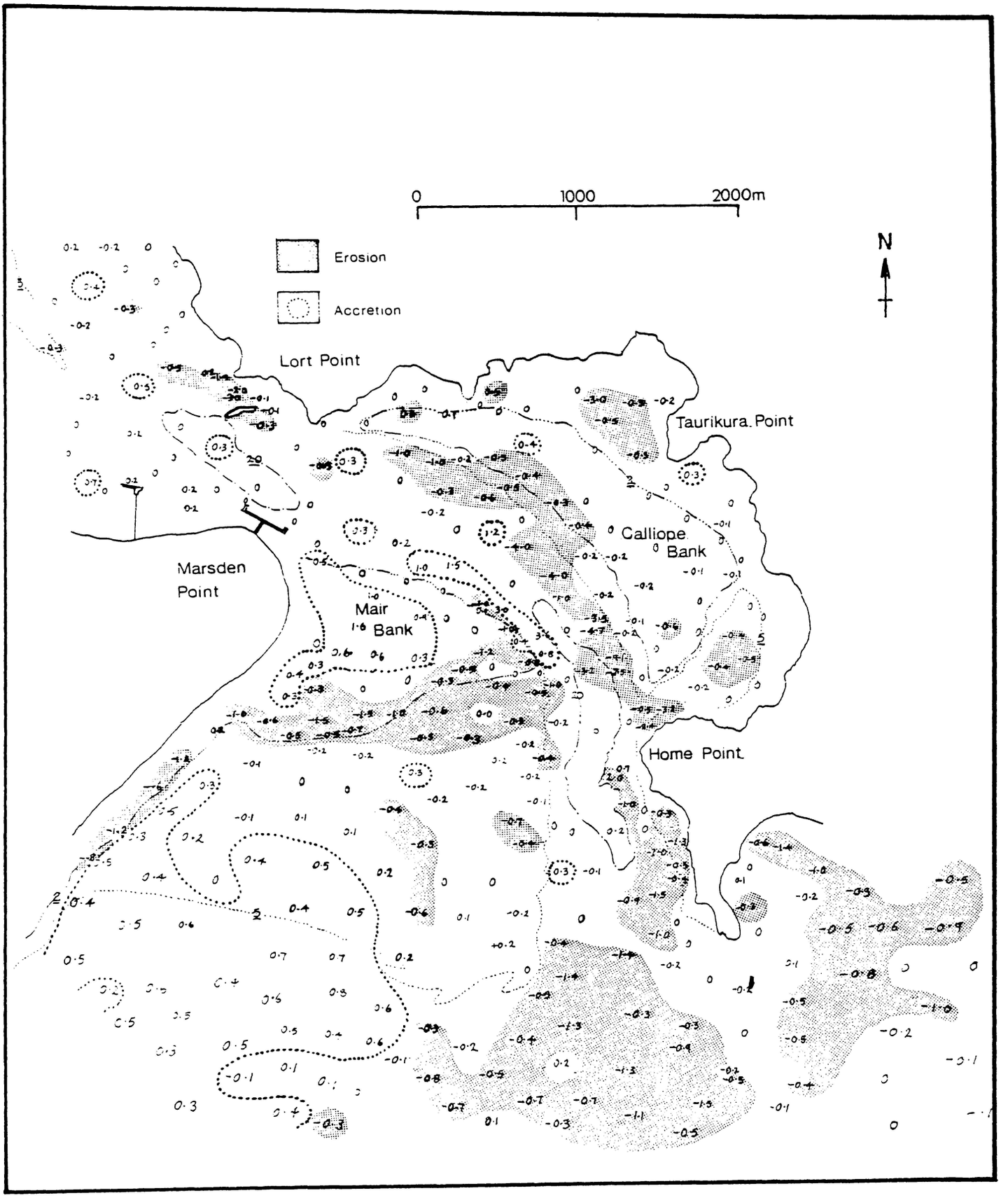

Figure 3.17: Mair Bank and environs showing comparison of 1974 RNZN bathymetry chart (NZ5213) and the 1981 RNZN survey with depth changes in metres

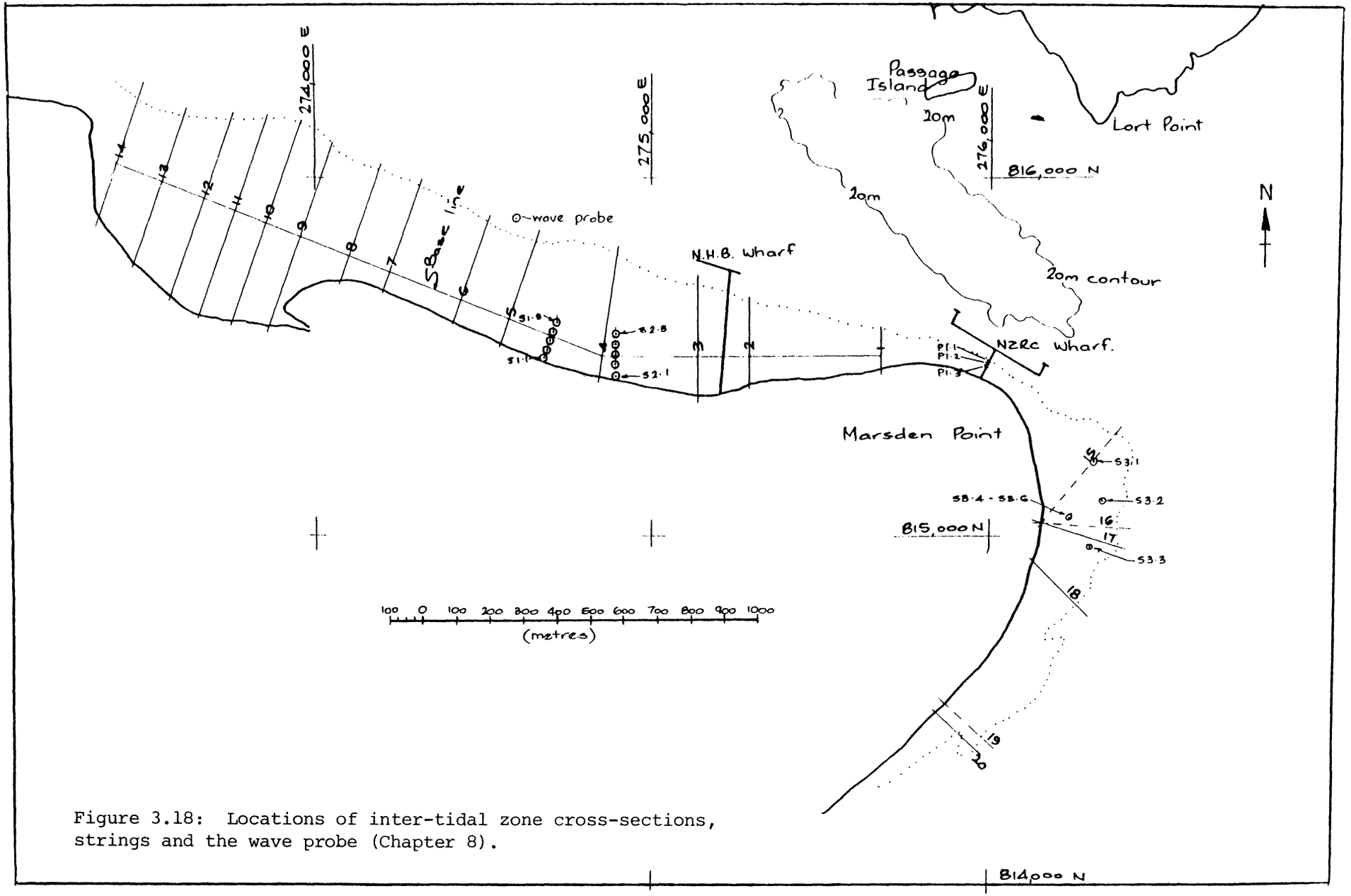

Figure 3.18: Locations of inter-tidal zone cross-sections, strings and the wave probe (Chapter 8).

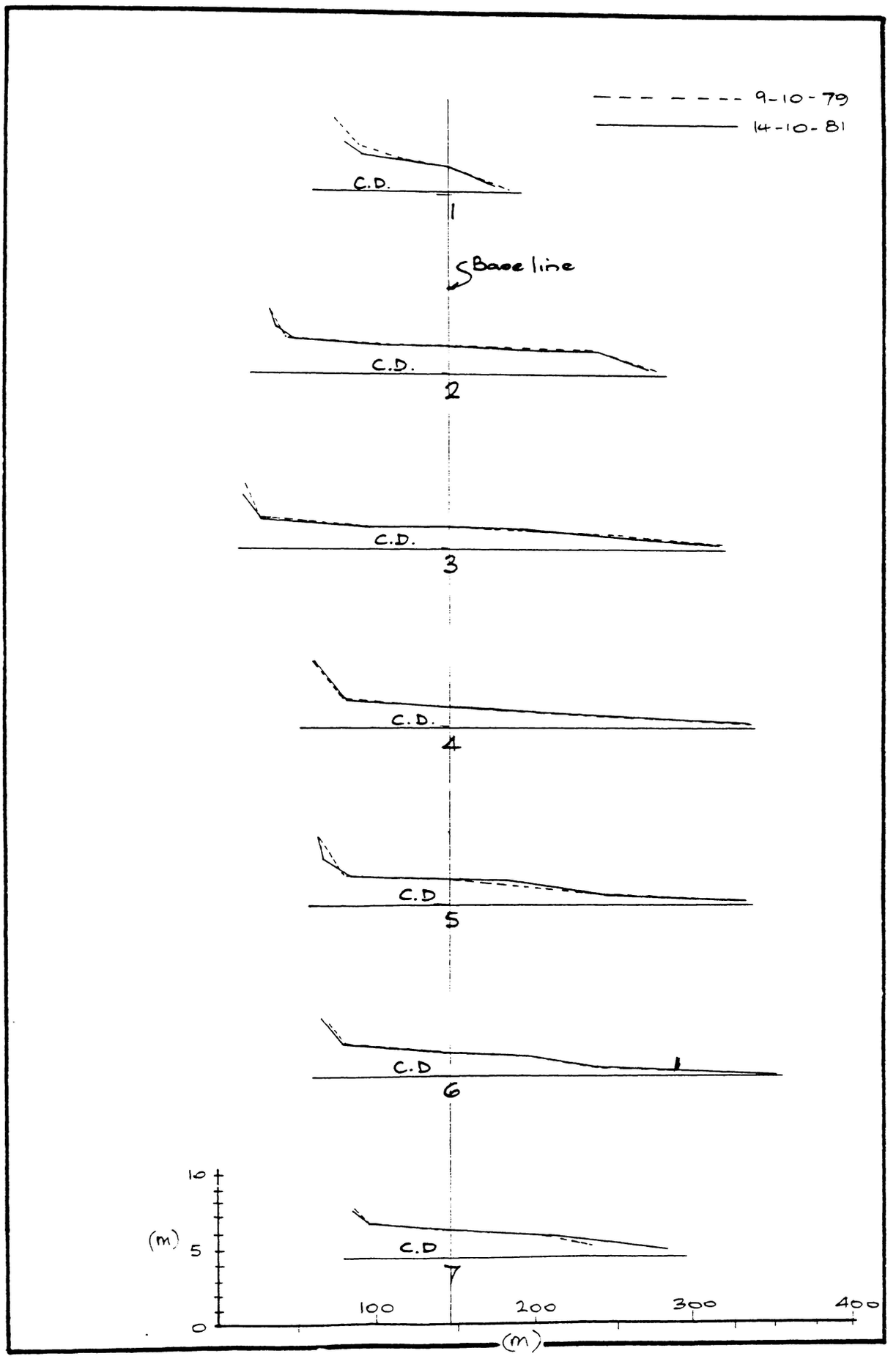

Figure 3.19: Repetitive surveys on 9-Oct-79 and 14-Oct-79 along the inter-tidal zone at the proposed timber port site (Marsden Point). Locations are shown in Figure 3.18.

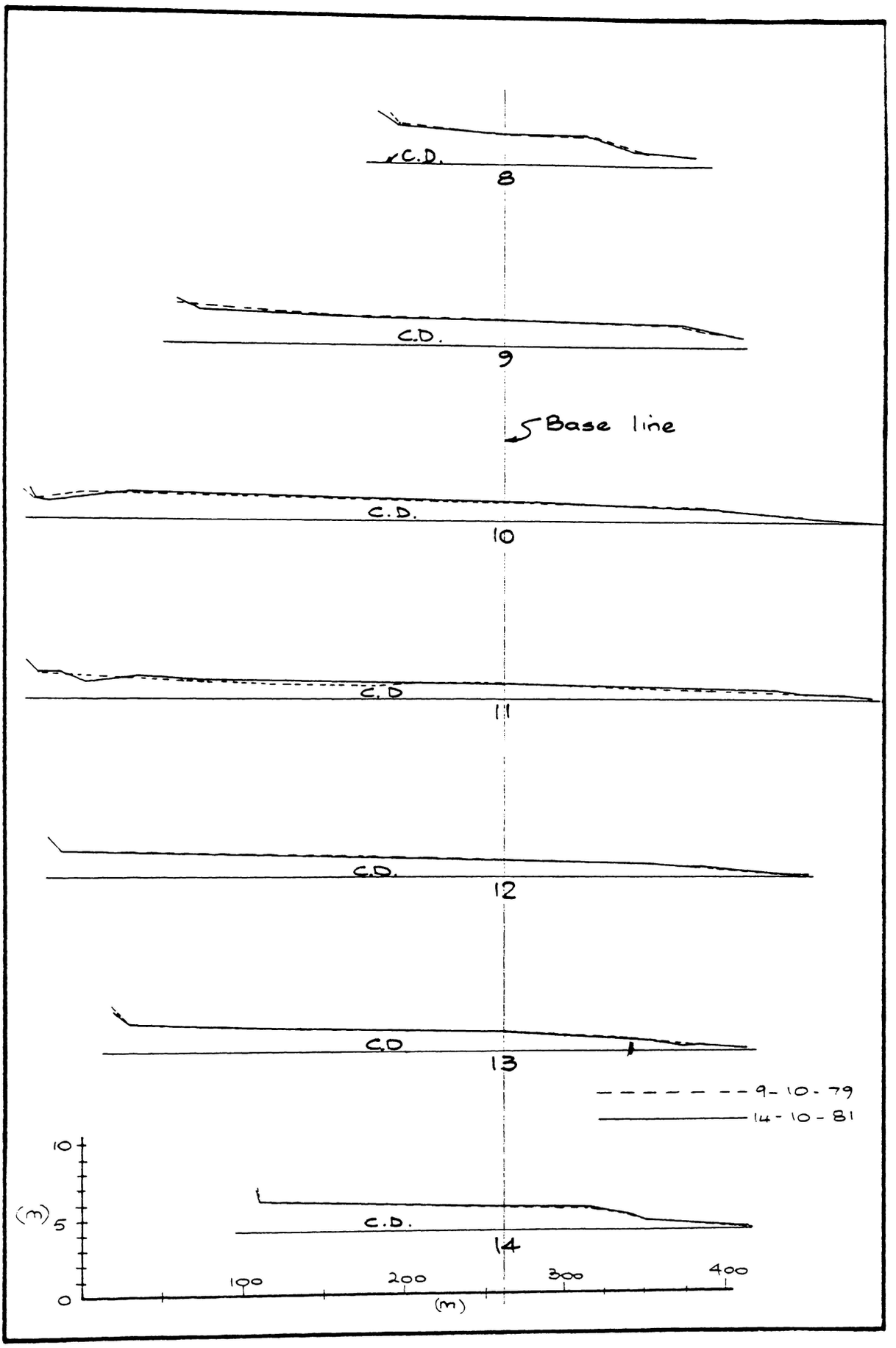

Figure 3.20: Repetitive surveys on 9-Oct-79 and 14-Oct-81 along the inter-tidal zone at the proposed timber port site (Marsden Point). Locations are shown in Figure 3.18.

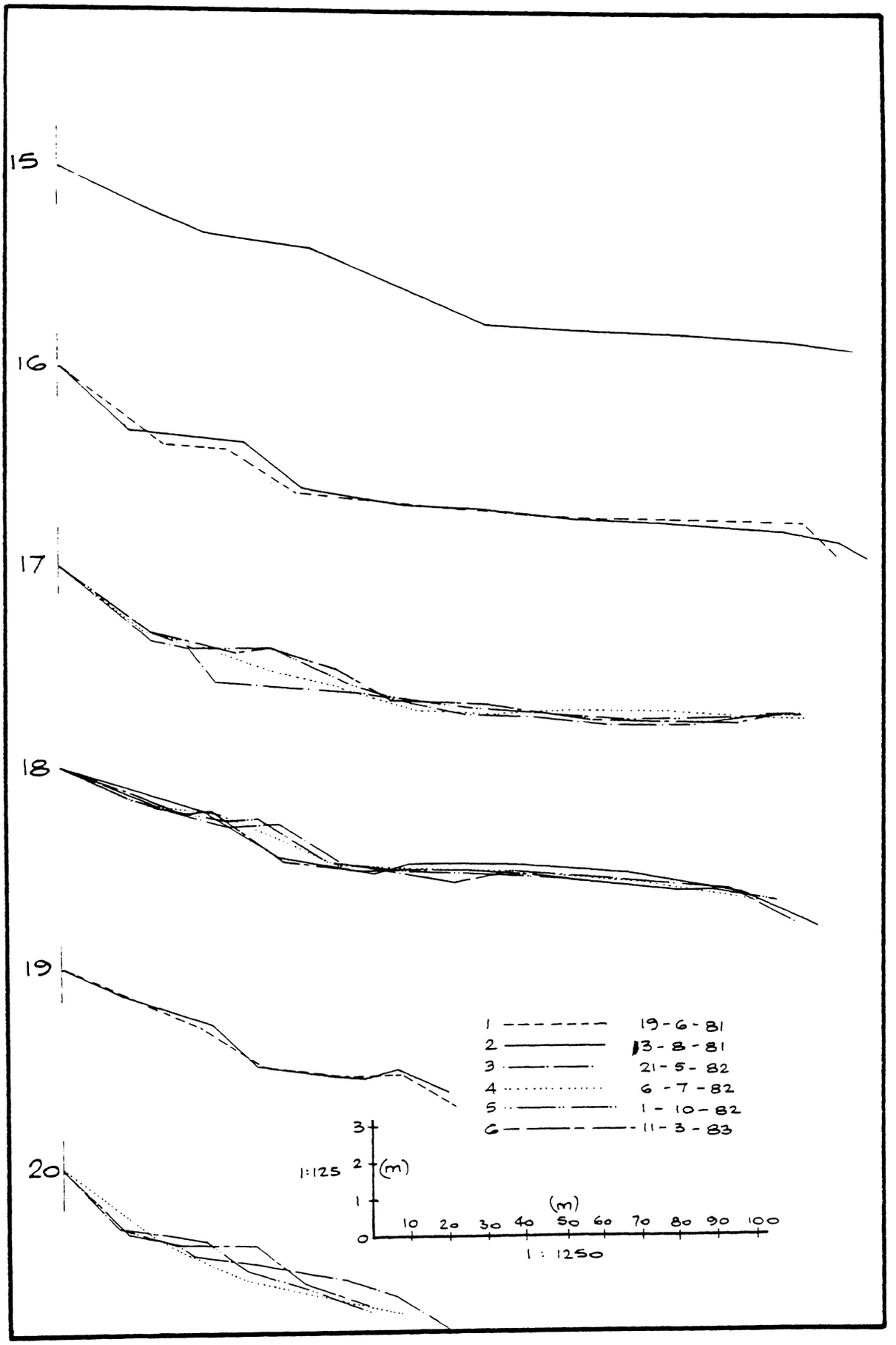

Figure 3.21: Repetitive surveys of Marsden Point in the period from 19-Jun-81 to 11-Mar-83. Locations are shown in Figure 3.18.

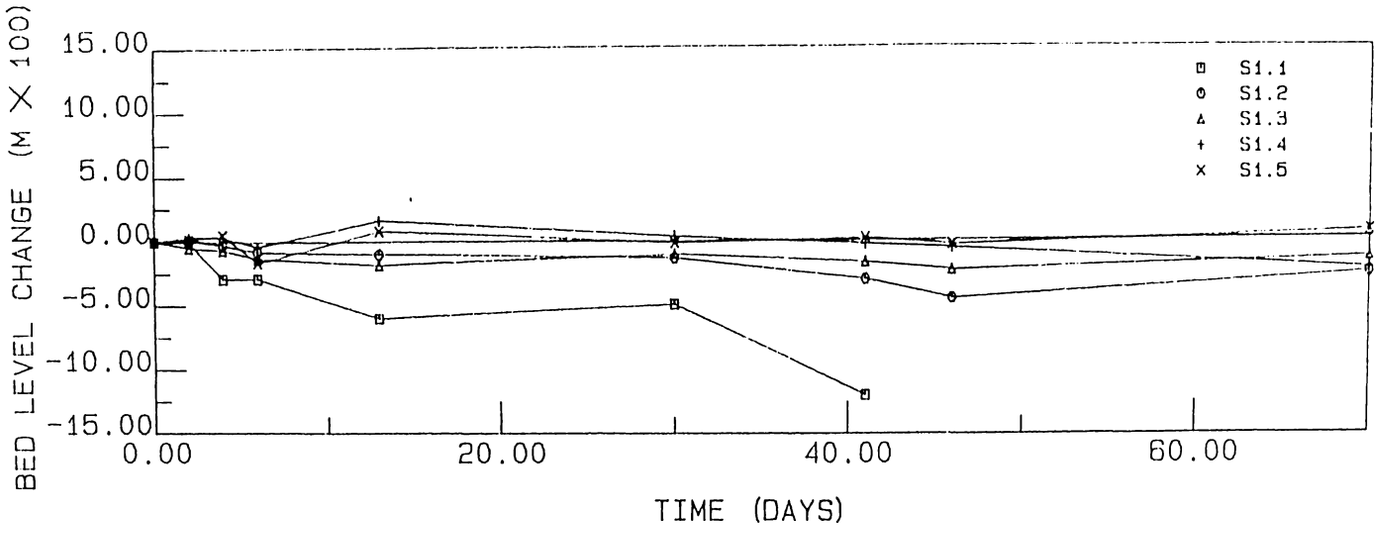

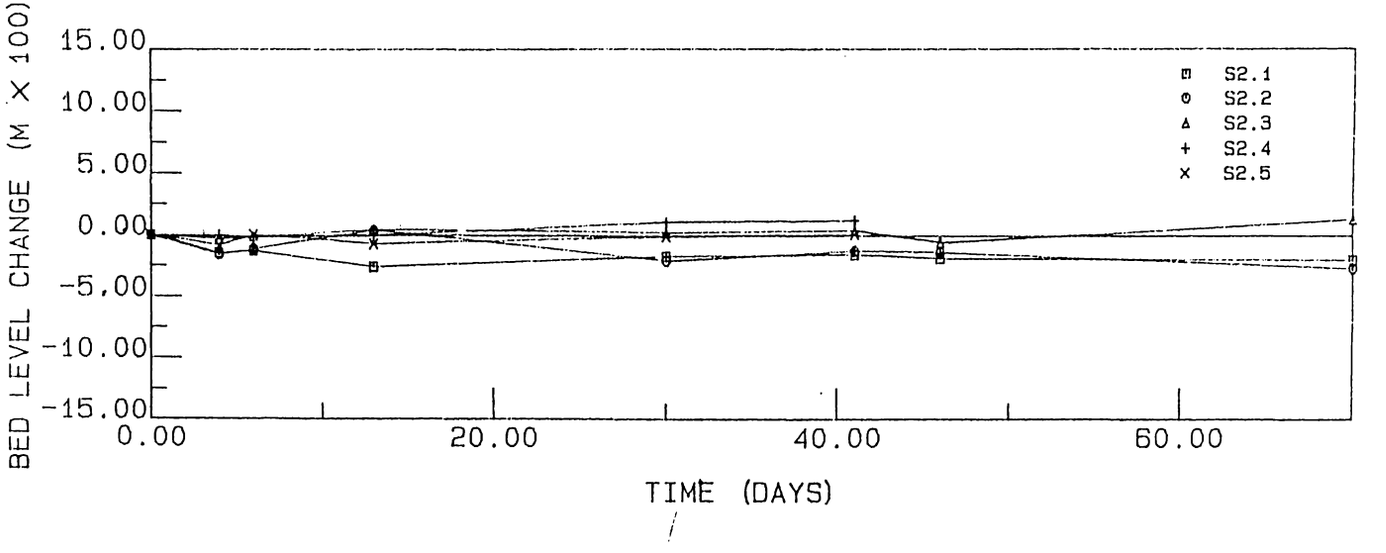

Figures 3.22 (upper) and 3.23: Bed level changes noted during string surveys of the inter-tidal zone at the proposed port site for the period from 7-Jun-81 to 16-Aug-81.

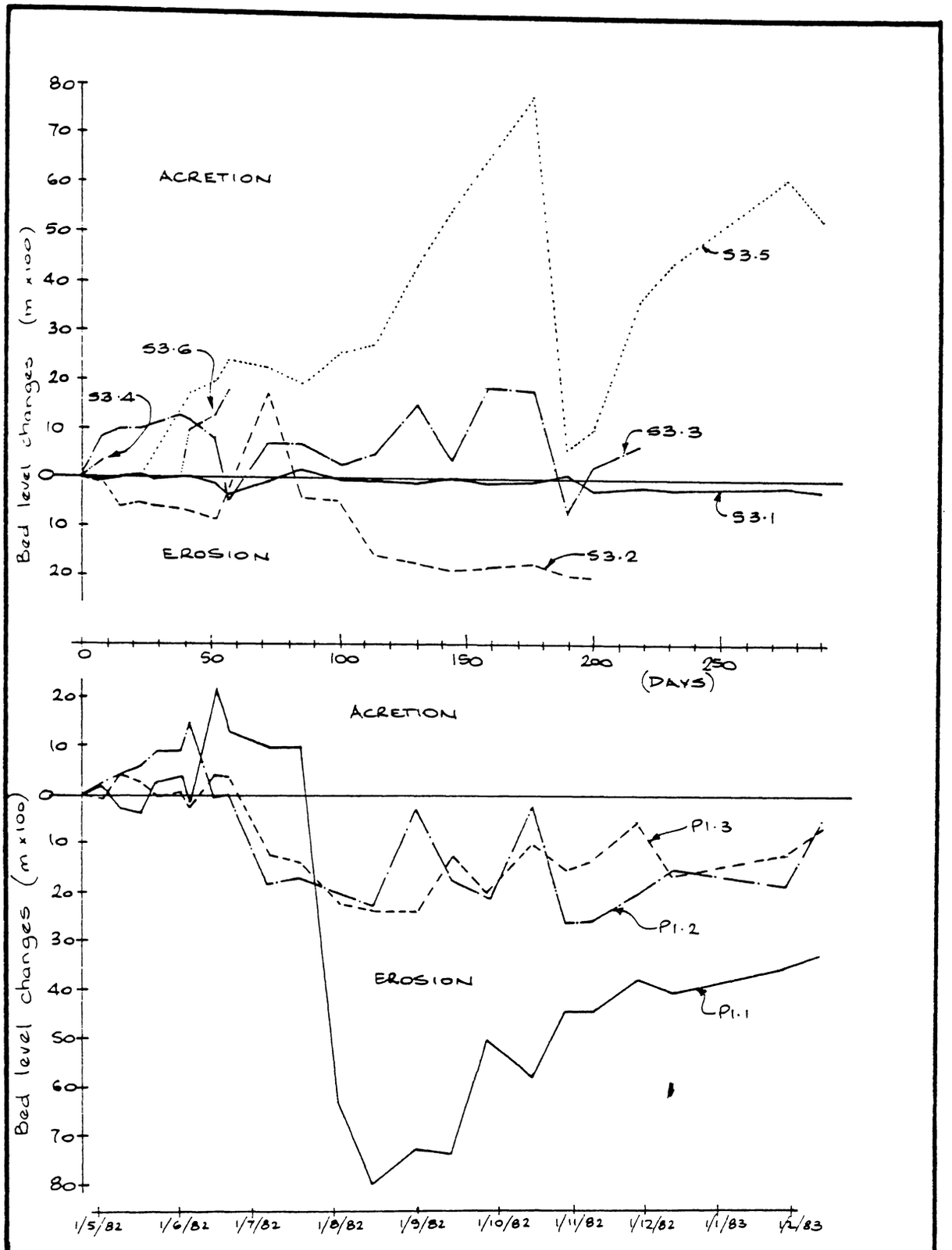

Figure 3.24: String surveys at Marsden Point (upper) and at the NZRC wharf pylons (lower) over the period from 1-May-82 to 1-Feb-83.

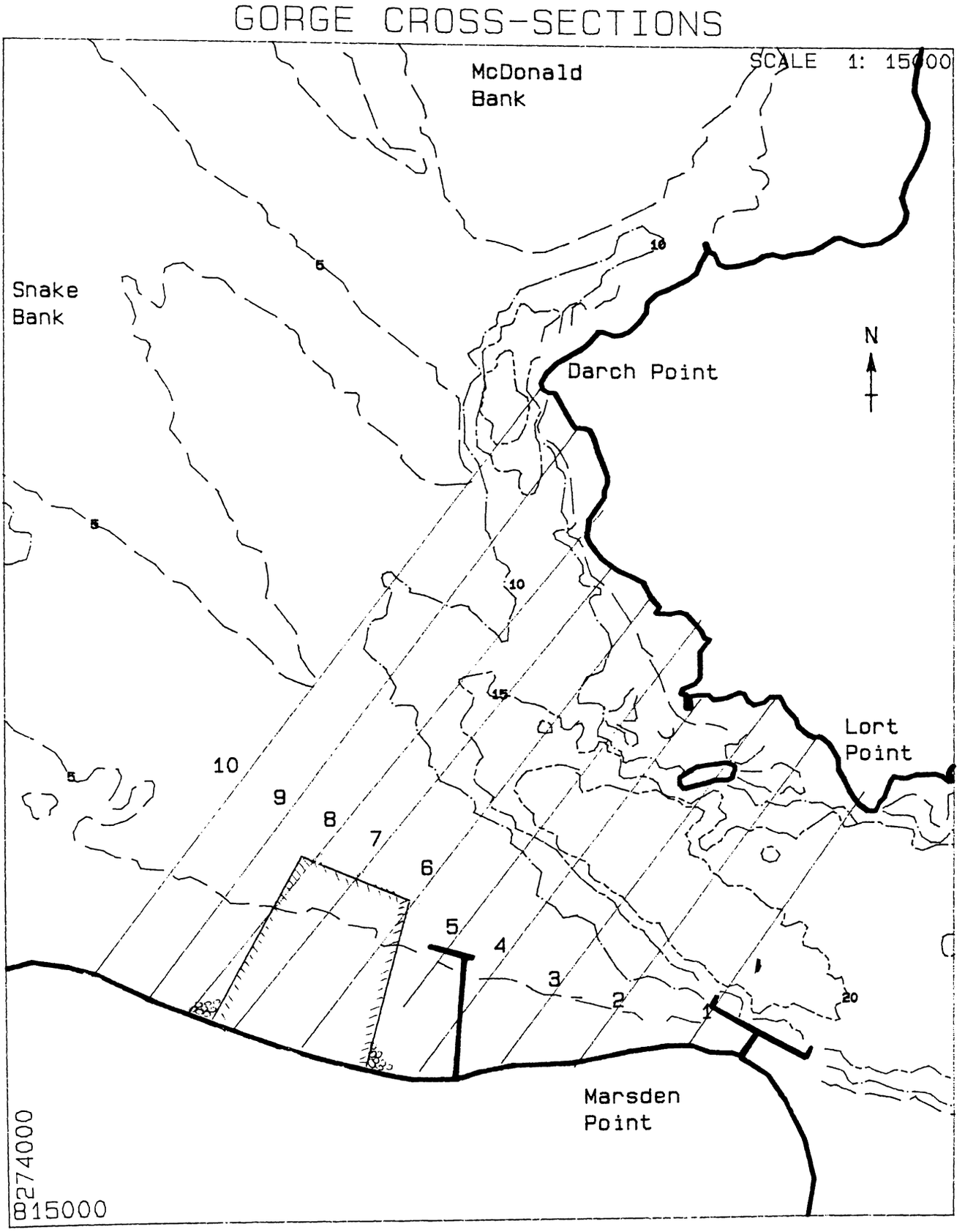

Figure 3.25: Locations of Digitised Cross-Sections from the 1981 Navy Bathymetric Survey.

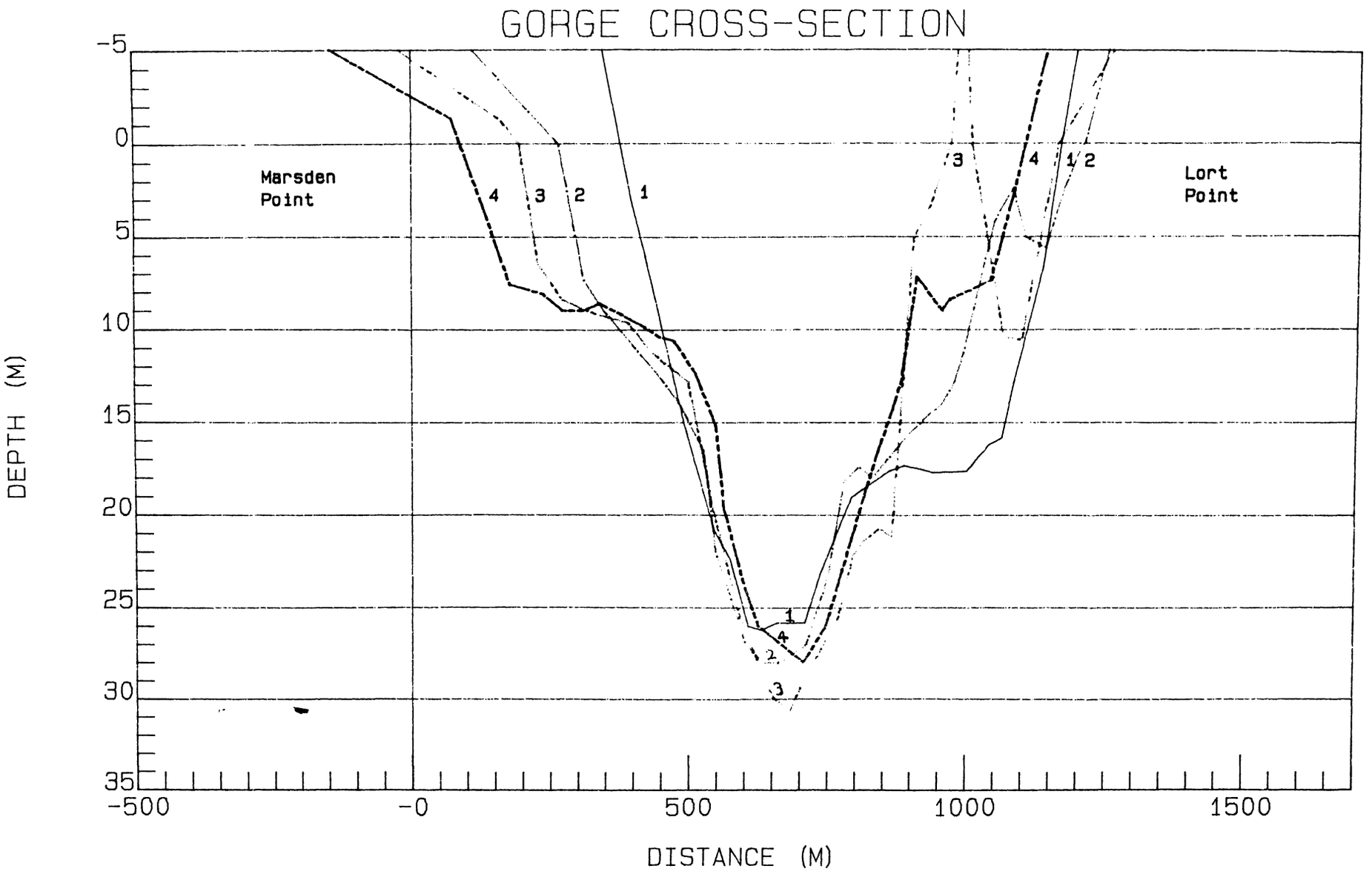

Figure 3.26: Entrance Gorge Cross-Sections (1-4) Digitised from the 1981 Navy Bathymetric Map.

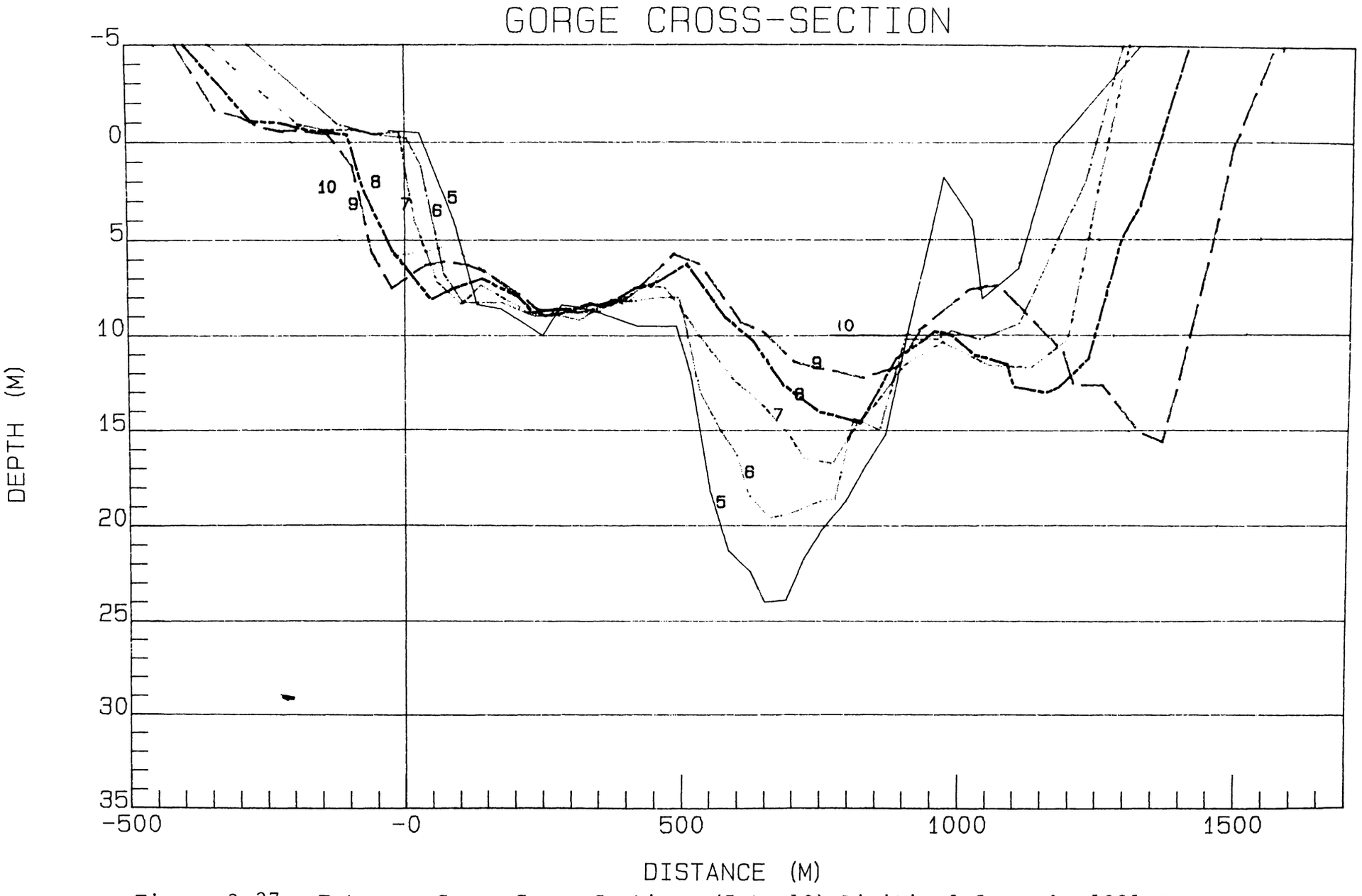

Figure 3.27: Entrance Gorge Cross-Sections (5 to 10) Digitised from the 1981 Navy Bathymetry Survey

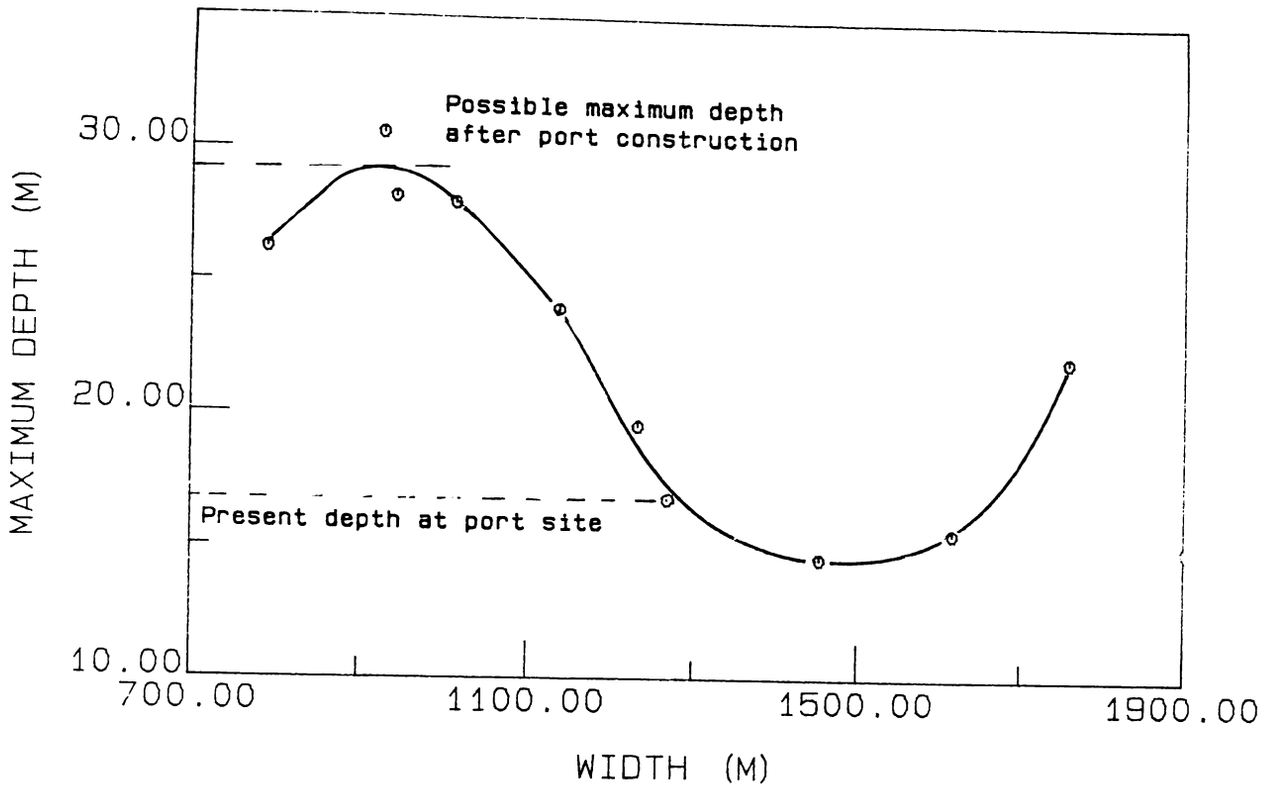

Figure 3.28: Maximum depth attained in the 10 cross-sections digitised from the 1981 RNZN bathymetric survey against the cross-section width at CD.

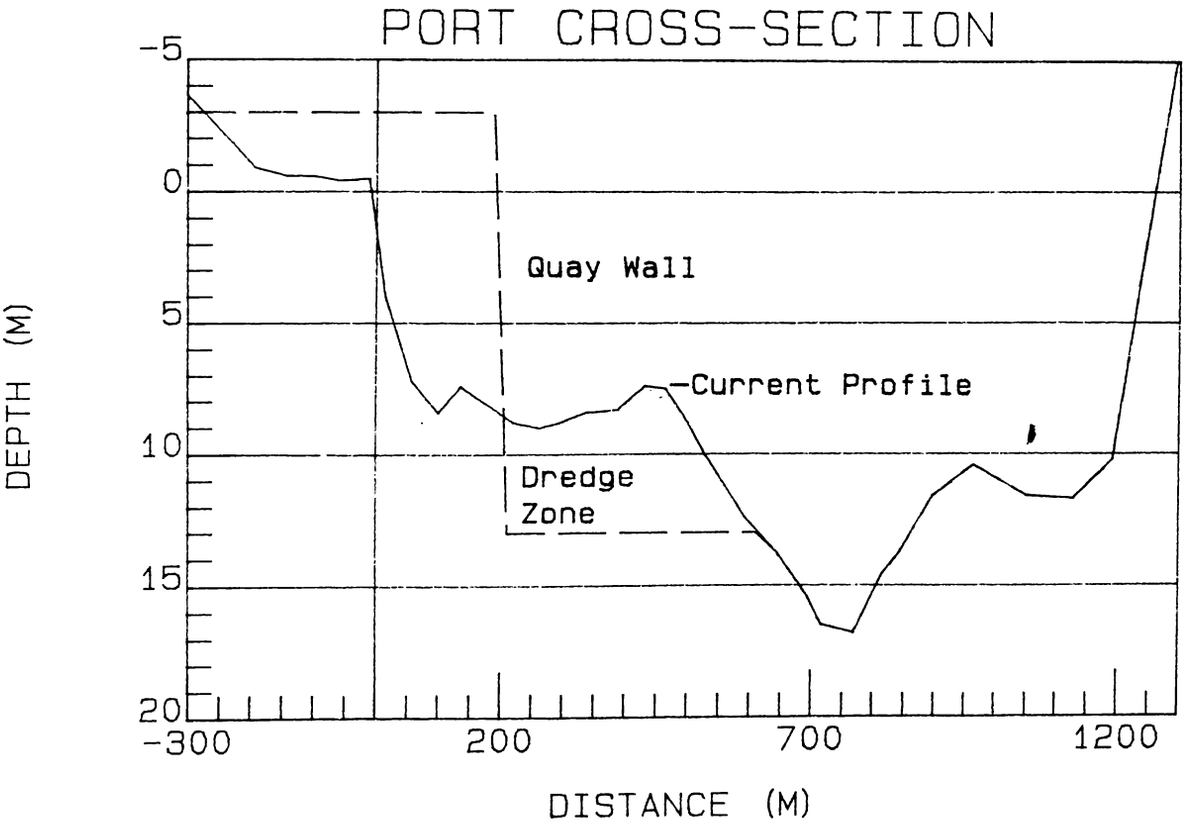

Figure 3.29: Cross-section 7, with the new profile after port construction and dredging.

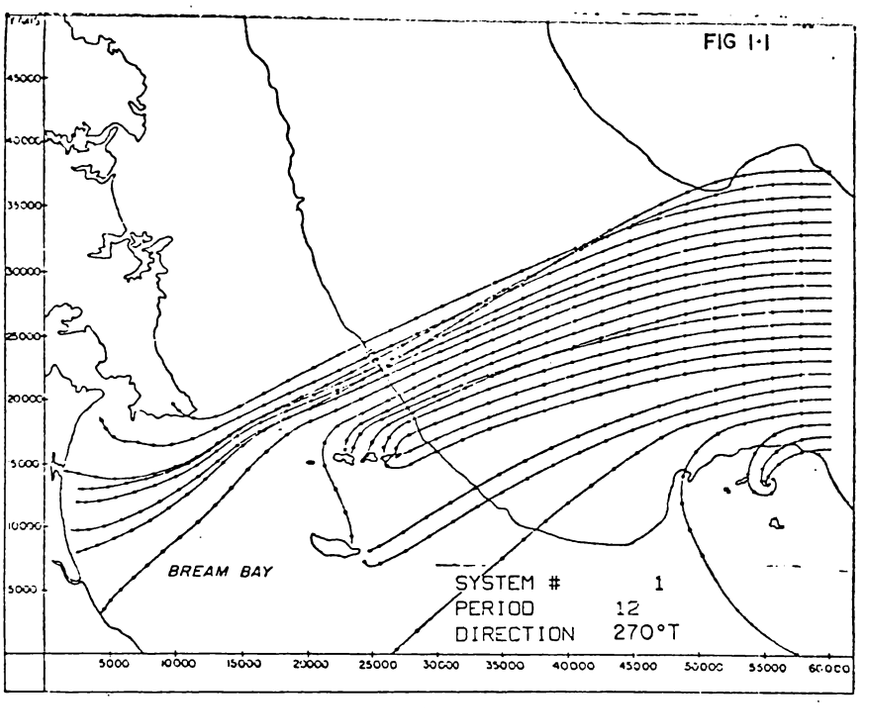

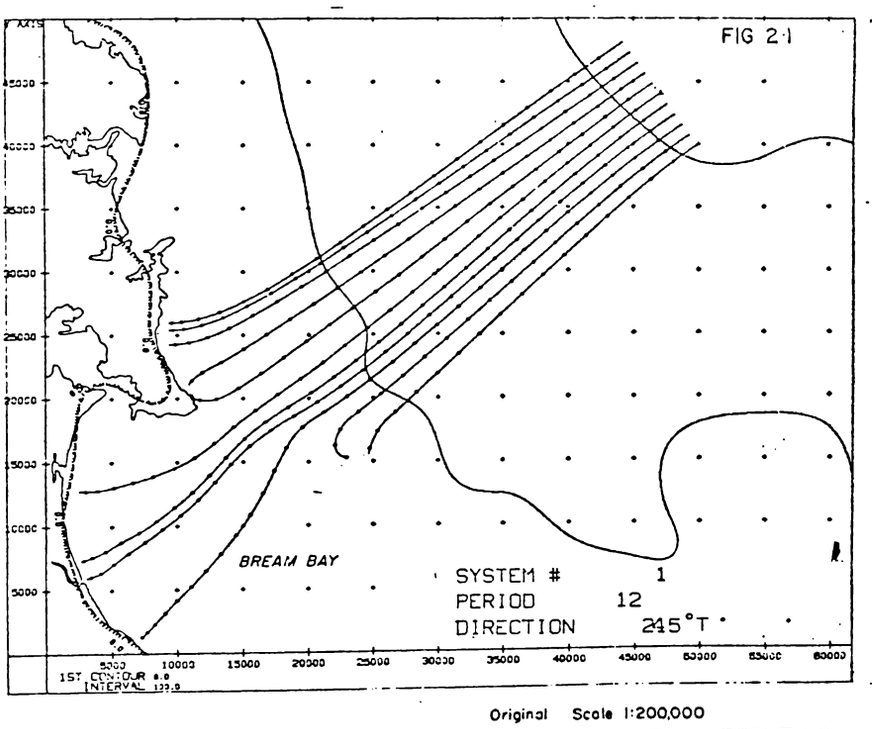

Figures 4.1 (upper) and 4.2: Wave refraction in Bream Bay by Christian (Tonkin and Taylor, 1981). Easterly (upper) and north-easterly waves with 12s periods (1:200,000).

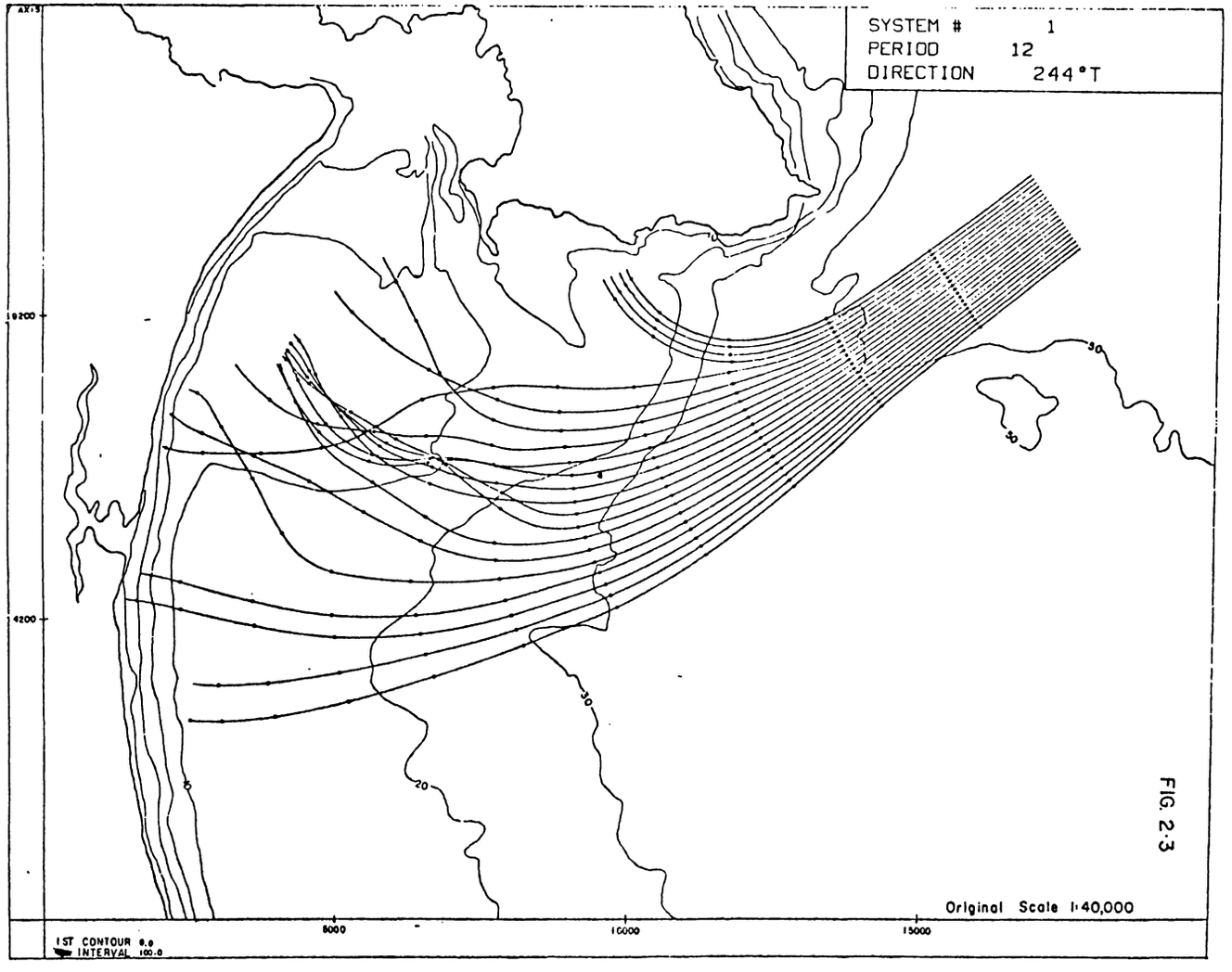

Figure 4.3: Wave refraction in Bream Bay by Christian (Tonkin and Taylor, 1981). North-easterly waves with 12s periods (1:40,000).

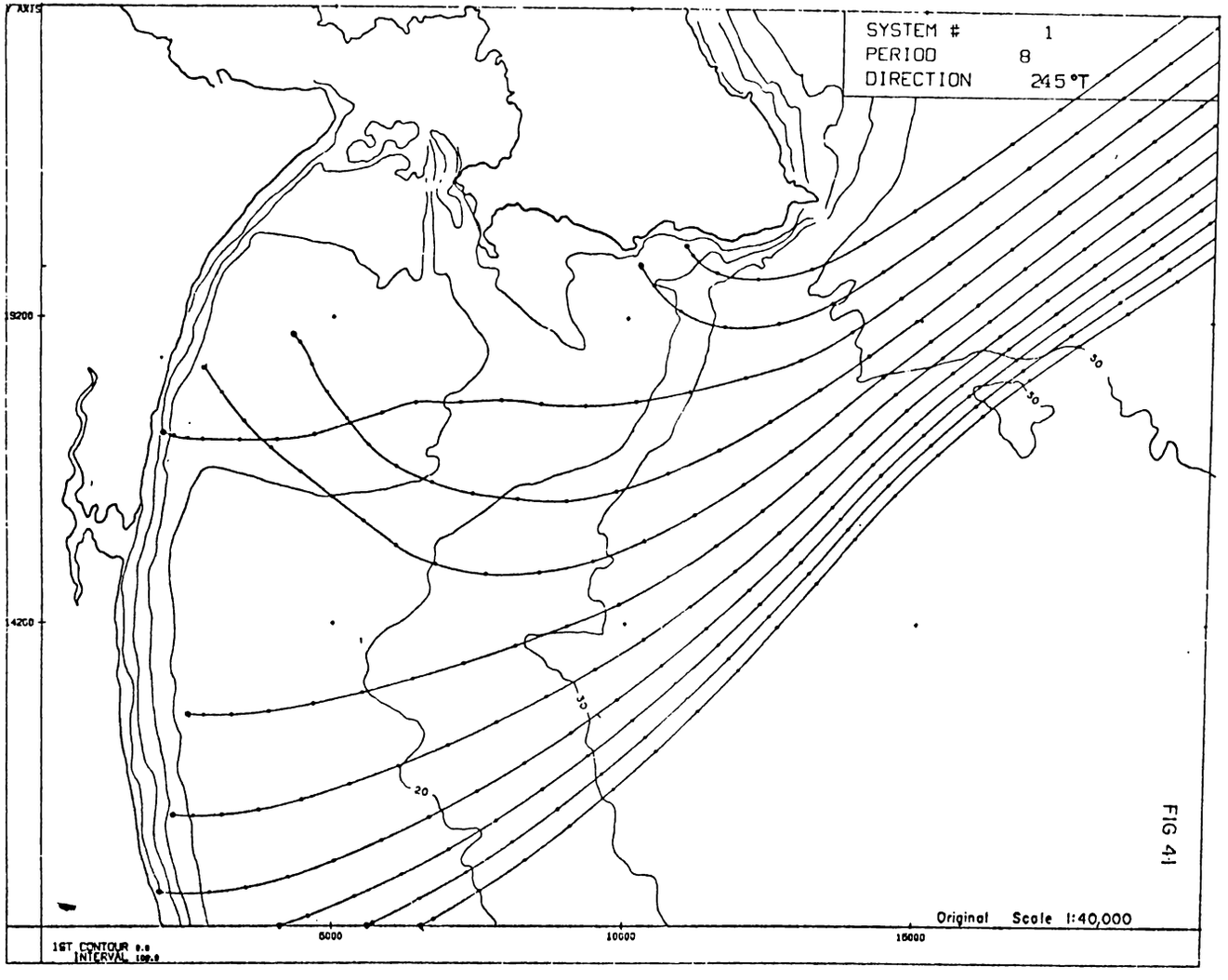

Figure 4.4: Wave refraction in Bream Bay by Christian (Tonkin and Taylor, 1981). North-easterly waves with 8s periods (1:40,000).

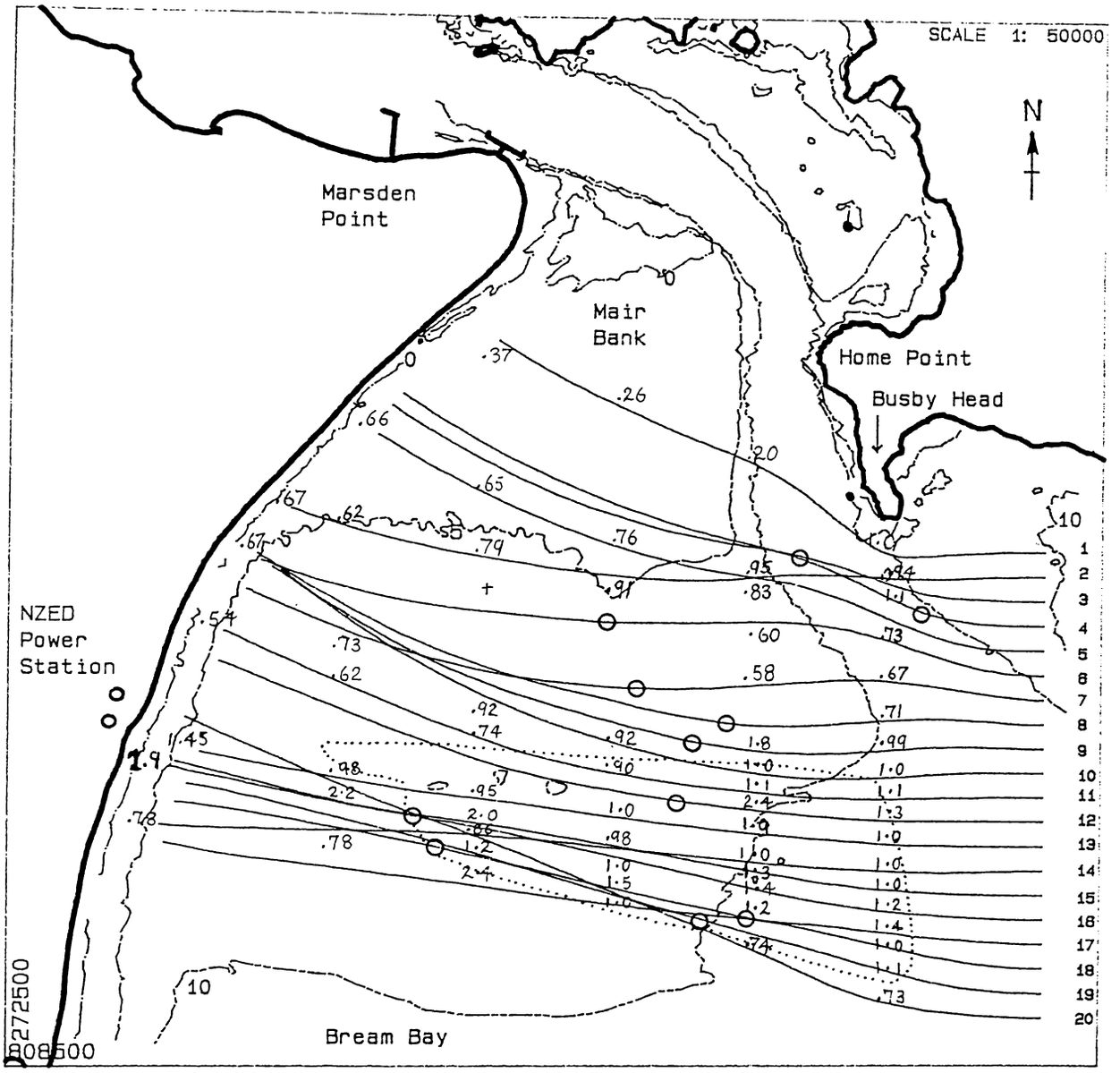

Figure 4.5(a): Refraction on the Mair Bank ebb-tidal delta for easterly waves with 12s periods. With an initial 1m height, the wave heights are shown along the rays at 1000m intervals. The circles show locations of caustics and the dotted region corresponds with the zone of megaripple fingers. Bathymetry was digitised on a 250m-square grid from the 1981 RNZN bathymetric survey (NZ5213). Tide level was 1.5m above Chart Datum.

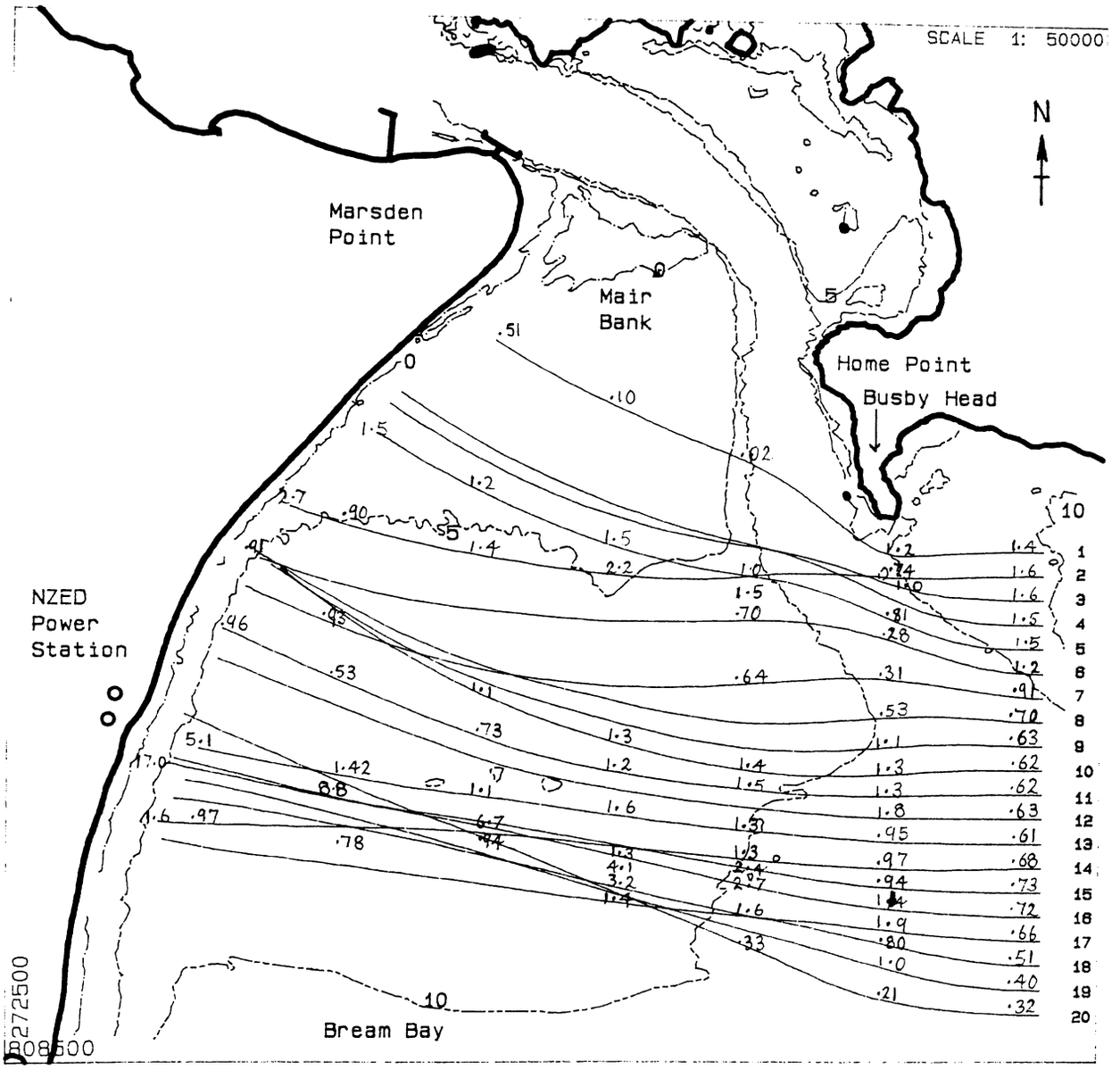

Figure 4.5(b): Refraction on the Mair Bank ebb-tidal delta for easterly waves with 12s periods. With an initial 1m height, the largest equivalent, sperical grain that the bed wave orbital velocities could move is shown. Grain sizes are in millimetres. Bathymetry was digitised on a 250m-square grid from the 1981 RNZN bathymetric survey (NZ5213). Tide level was 1.5m above Chart Datum.

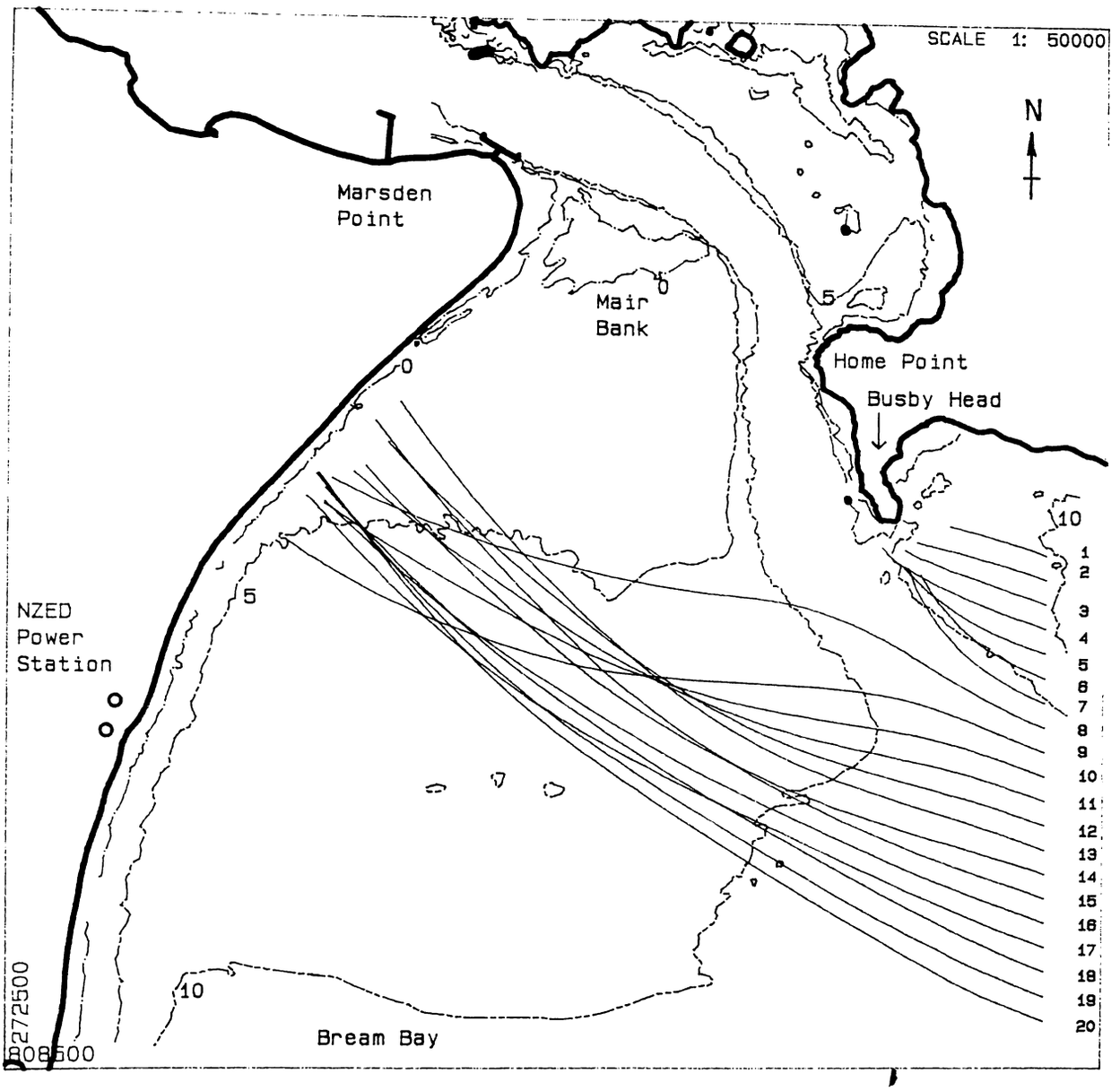

Figure 4.6: Refraction on the Mair Bank ebb-tidal delta for waves from 110° T with 12s periods. Bathymetry was digitised on a 250m-square grid from the 1981 RNZN bathymetric survey (NZ5213). Tide level was 1.5m above Chart Datum.

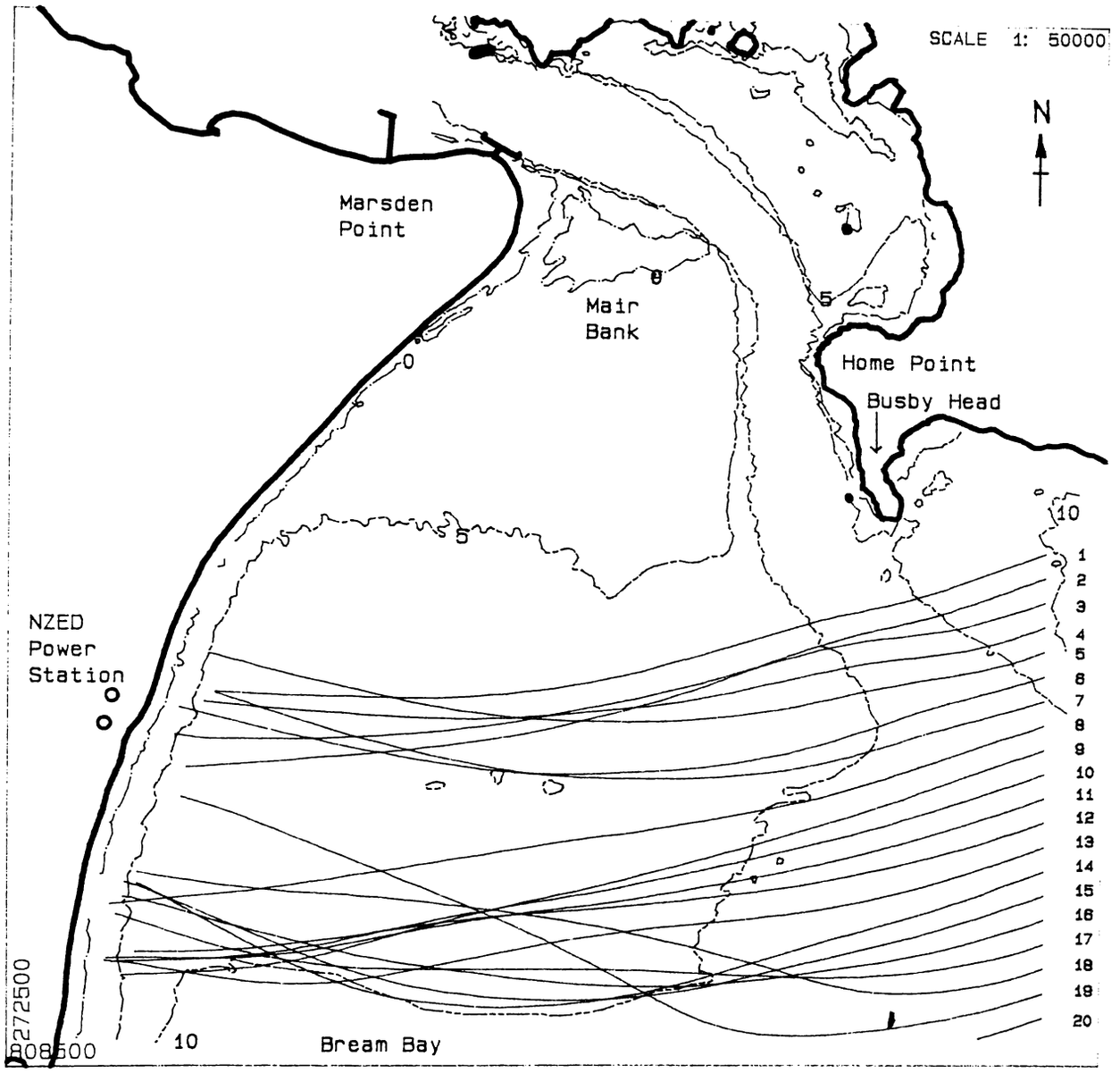

Figure 4.7: Refraction on the Mair Bank ebb-tidal delta for waves from 70° T with 12s periods. Bathymetry was digitised on a 250m-square grid from the 1981 RNZN bathymetric survey (NZ5213). Tide level was 1.5m above Chart Datum.

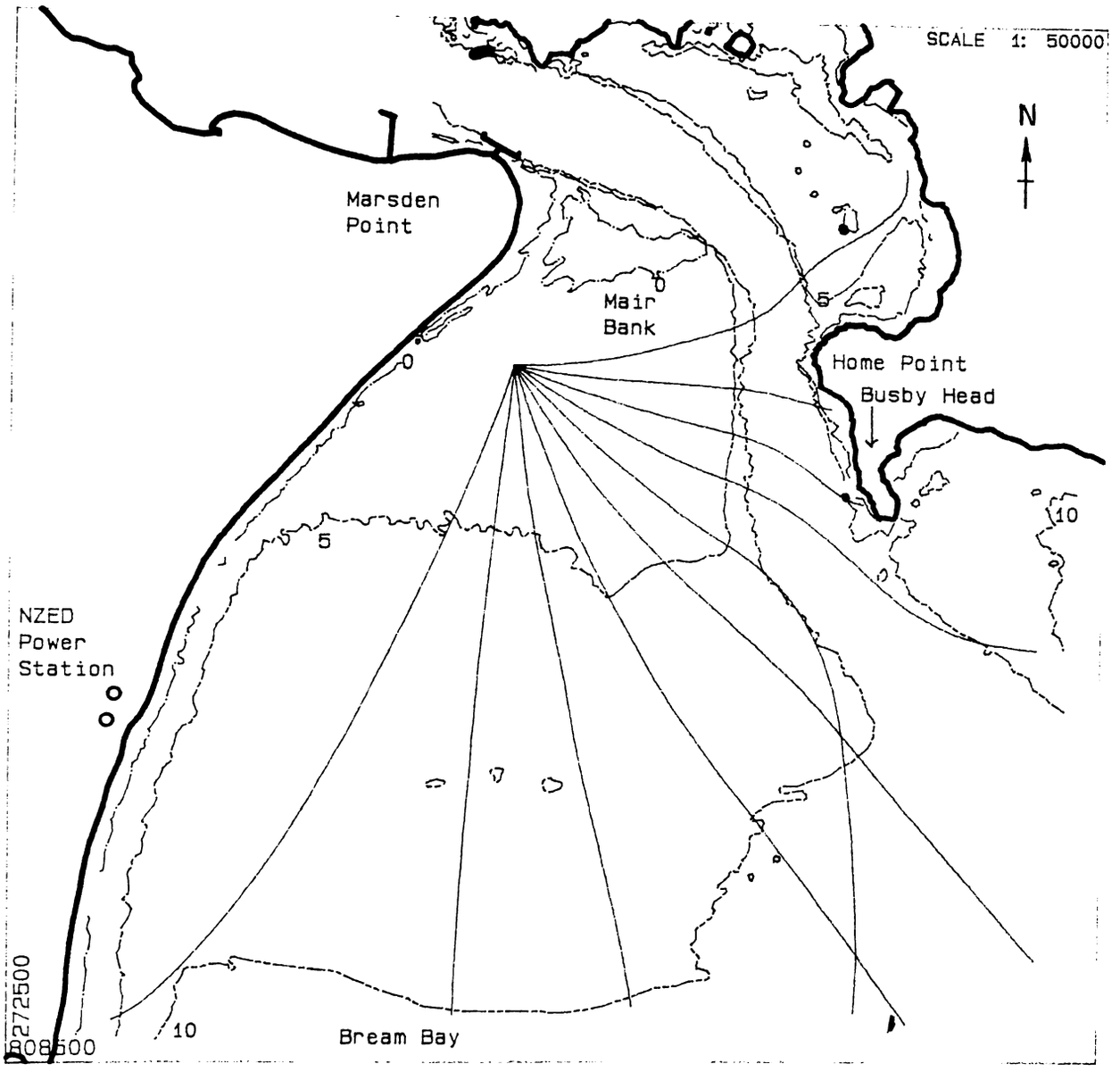

Figure 4.8: Reverse refraction ray tracking on Mair Bank ebb-tidal delta for waves with 12s periods. Bathymetry was digitised on a 250m-square grid from the 1981 RNZN bathymetric survey (NZ5213). Tide level was 1.5m above Chart Datum.

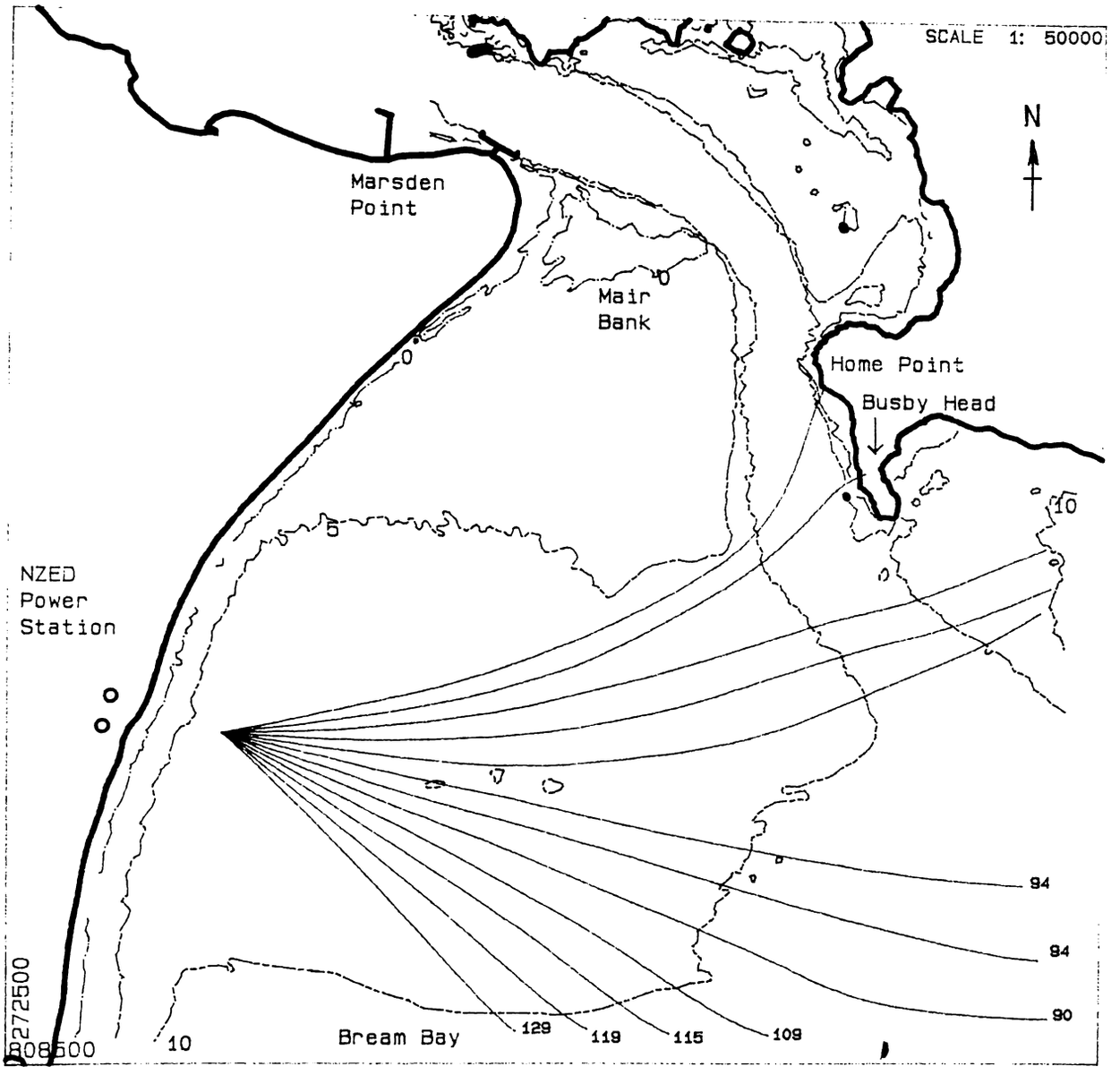

Figure 4.9: Reverse refraction ray tracking on Mair Bank ebb-tidal delta in front of the NZED power station, for waves with 12s periods. Bathymetry was digitised on a 250m-square grid from the 1981 RNZN bathymetric survey (NZ5213). Tide level was 1.5m above Chart Datum and numbers on the rays show the angle of wave orientation in degrees True at the edge of the grid.

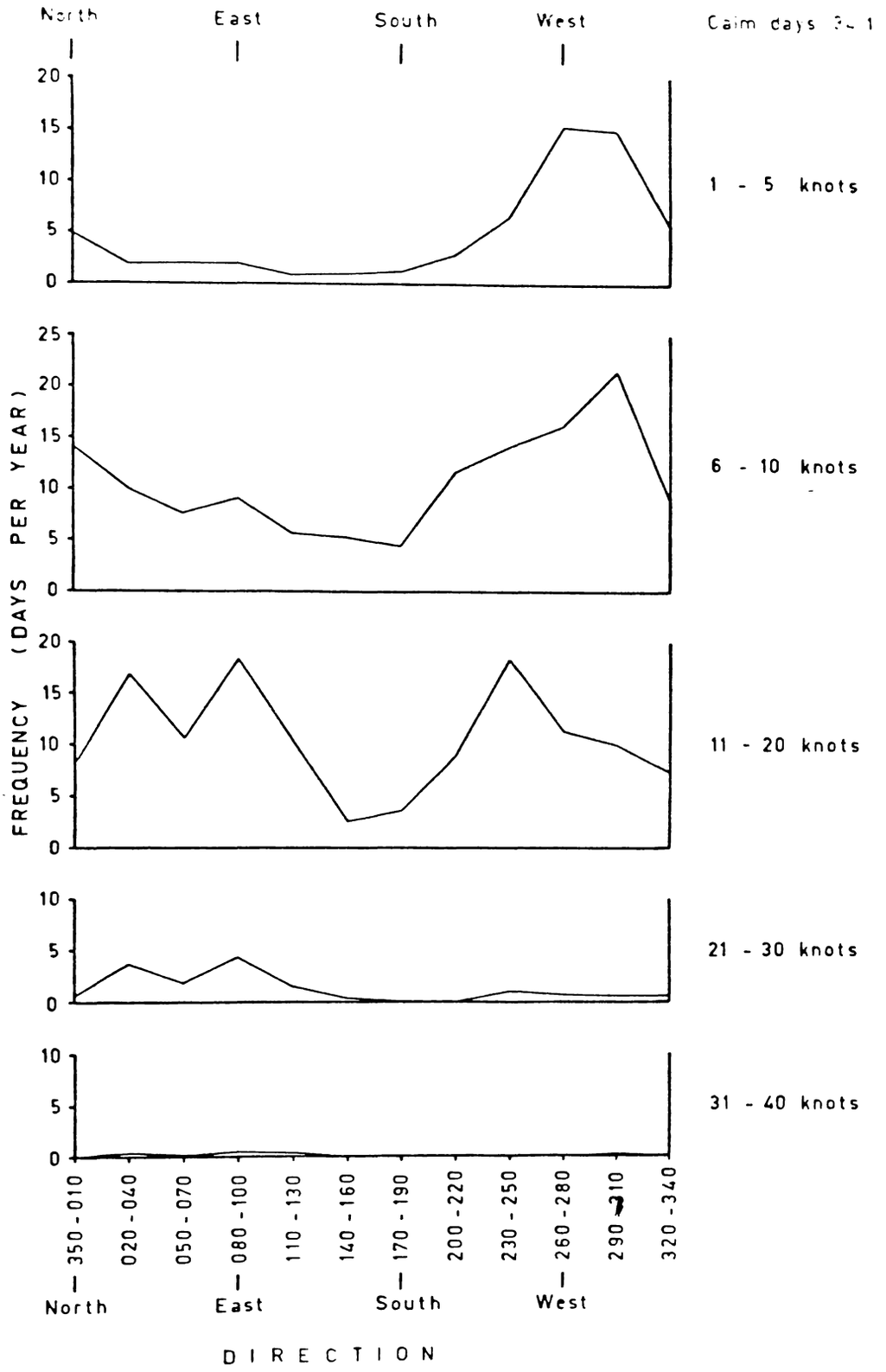

Figure 4.10: Wind velocity-direction-frequency for Marsden Point from the NHB anenometer for the period January, 1969 to August, 1973, (after Bioresearches, 1976b).

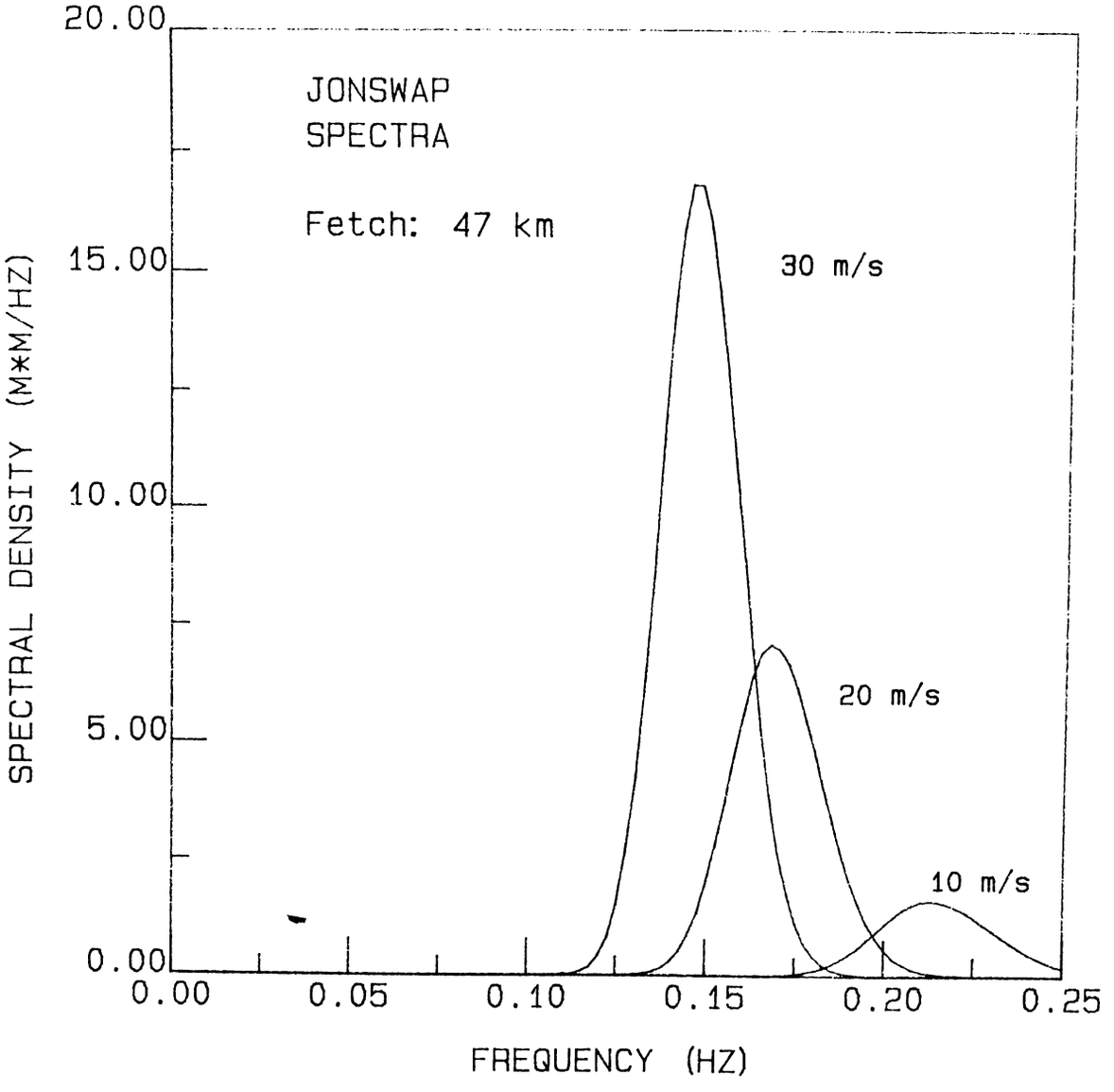

Figure 4.11: JONSWAP spectra for a fetch of 47km and wind speeds of 10, 20 and 30 $m.s^{-1}$.

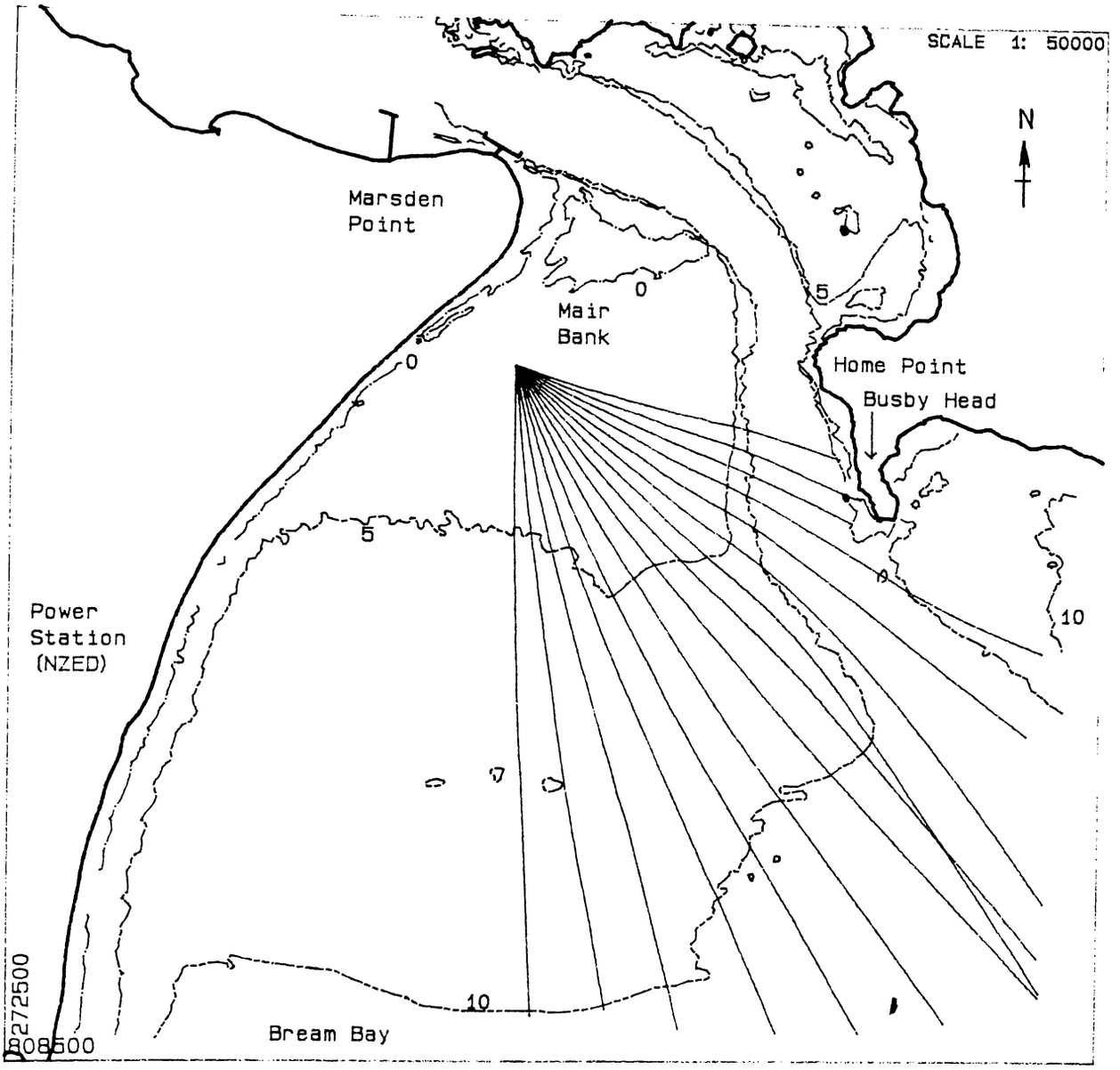

Figure 4.12: Reverse refraction ray tracking near Mair Bank for waves with 5s periods. Bathymetry was digitised on a 250m-square grid from the 1981 RNZN bathymetric survey (NZ5213). Tide level was 1.5m above Chart Datum.

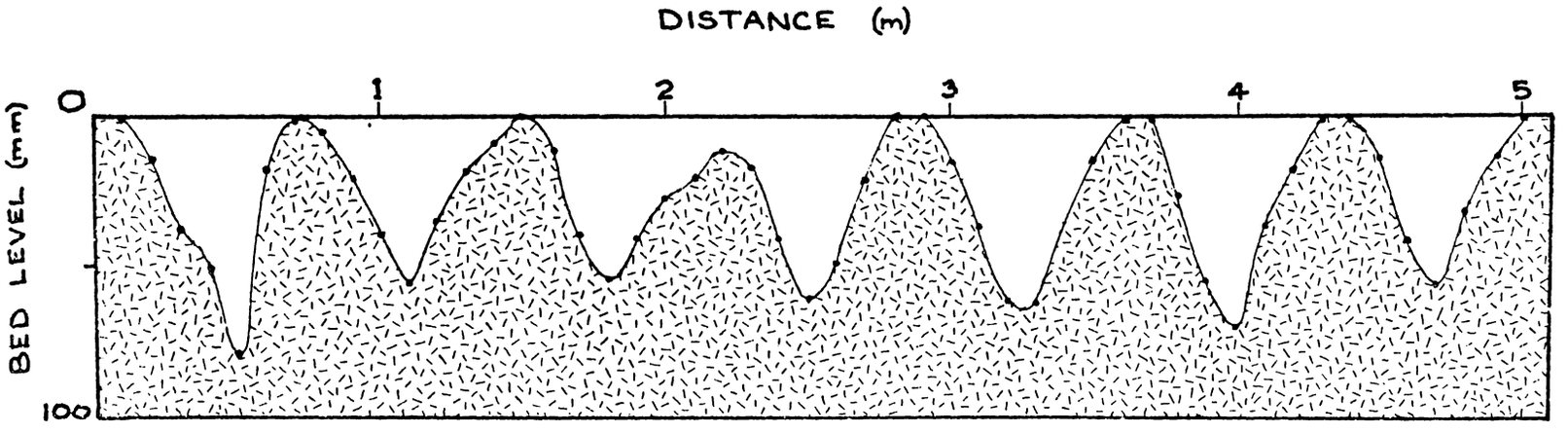

Figure 4.13: Cross-sectional profile of megaripple fingers measured by divers in Bream Bay on 27/5/82. Site location is shown on Figure 2.8.

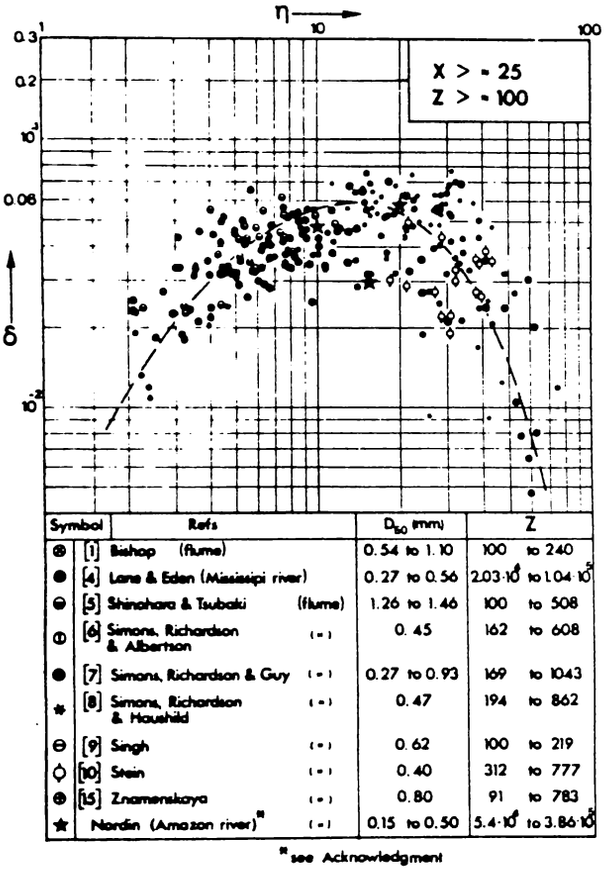

Figure 4.14: Variation of megaripple steepness ($\delta = \Delta/\Lambda$) with relative tractive force ($\eta = \tau_o/\tau_{ocr}$) for large values of $z = (d/D)$. Δ is the megaripple height; Λ is the wavelength; τ_o is the bed shear stress and τ_{ocr} the critical bed shear stress; d is the water depth and D is the grain size. After Yalin and Karahan (1979).

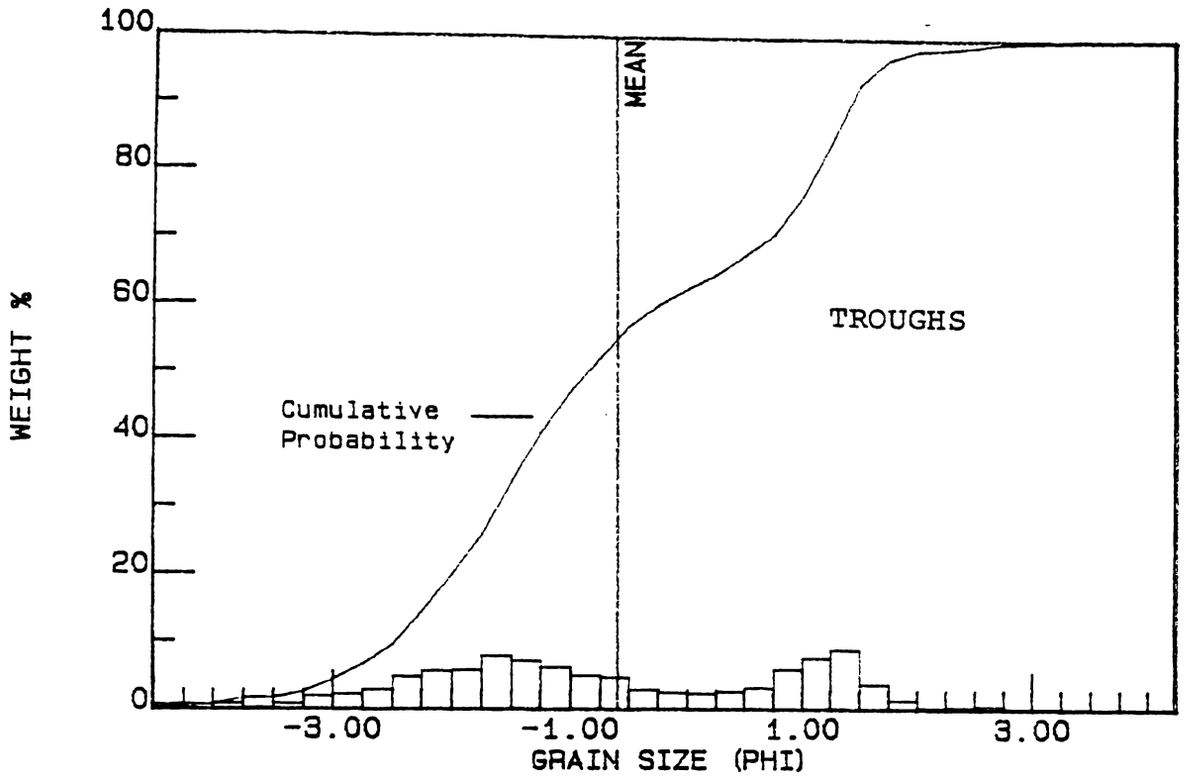

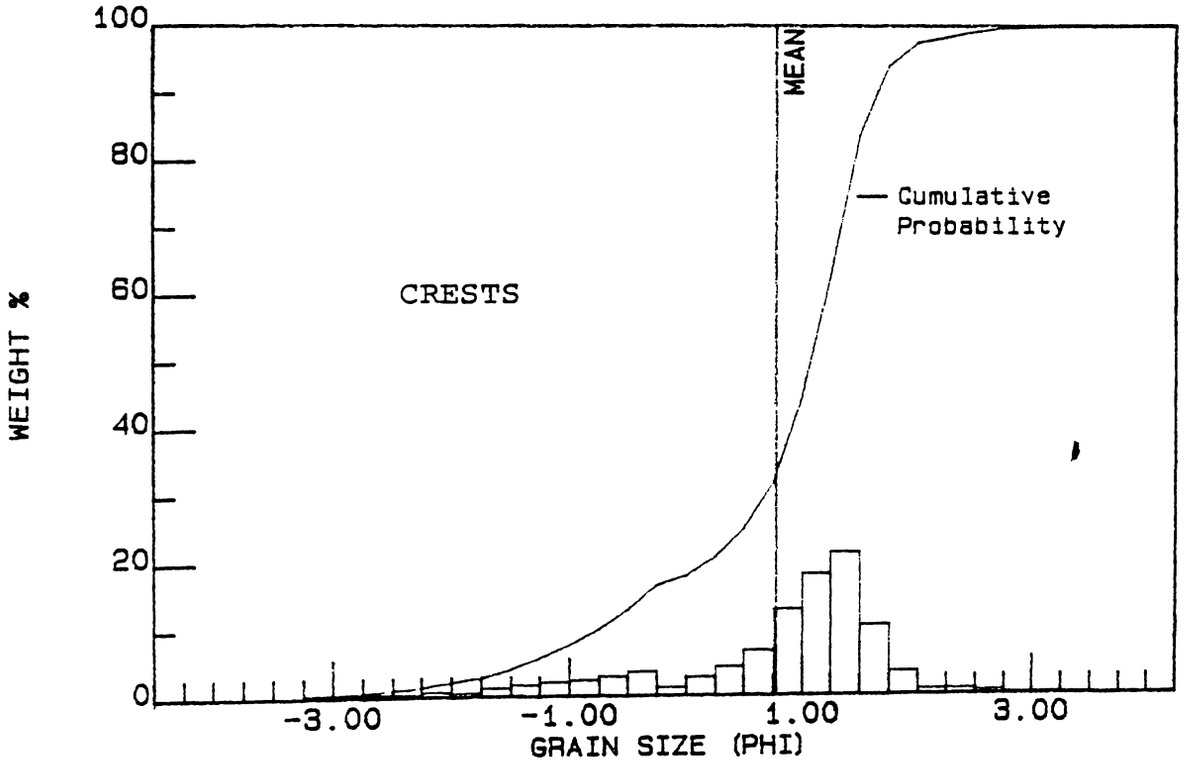

Figure 4.15: Grain size distributions from diver samples off the crest (lower) and trough of megaripple fingers in Bream Bay.

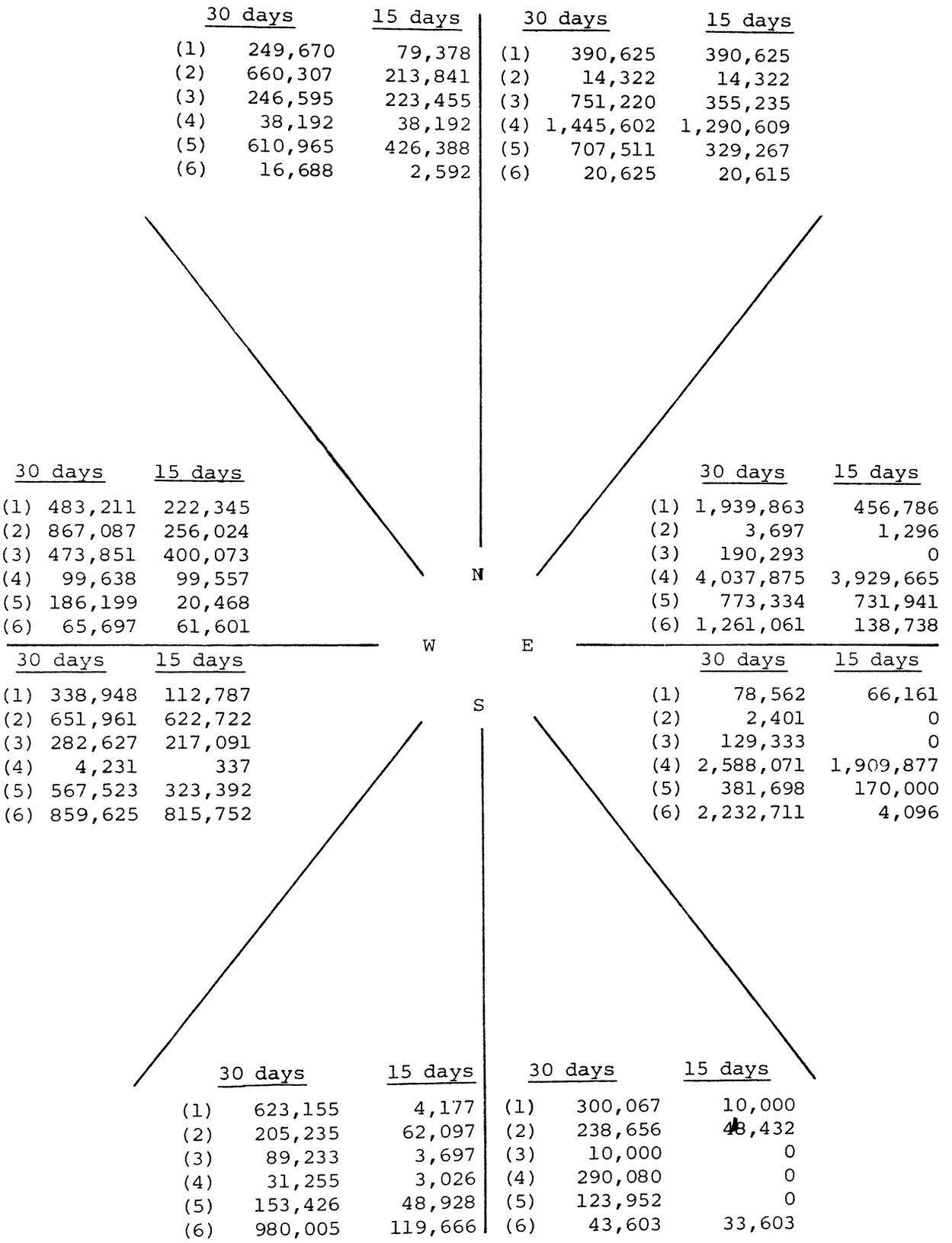

Figure 4.16: Wave potentials defined as the sum of the 6 hourly wind observations raised to the 4th power for each sector in the period 15 and 30 days prior to the beach surveys. Survey dates were: (1) 19/6/81, (2) 3/8/81, (3) 21/5/82, (4) 6/7/82, (5) 1/10/82 and (6) 11/3/83.

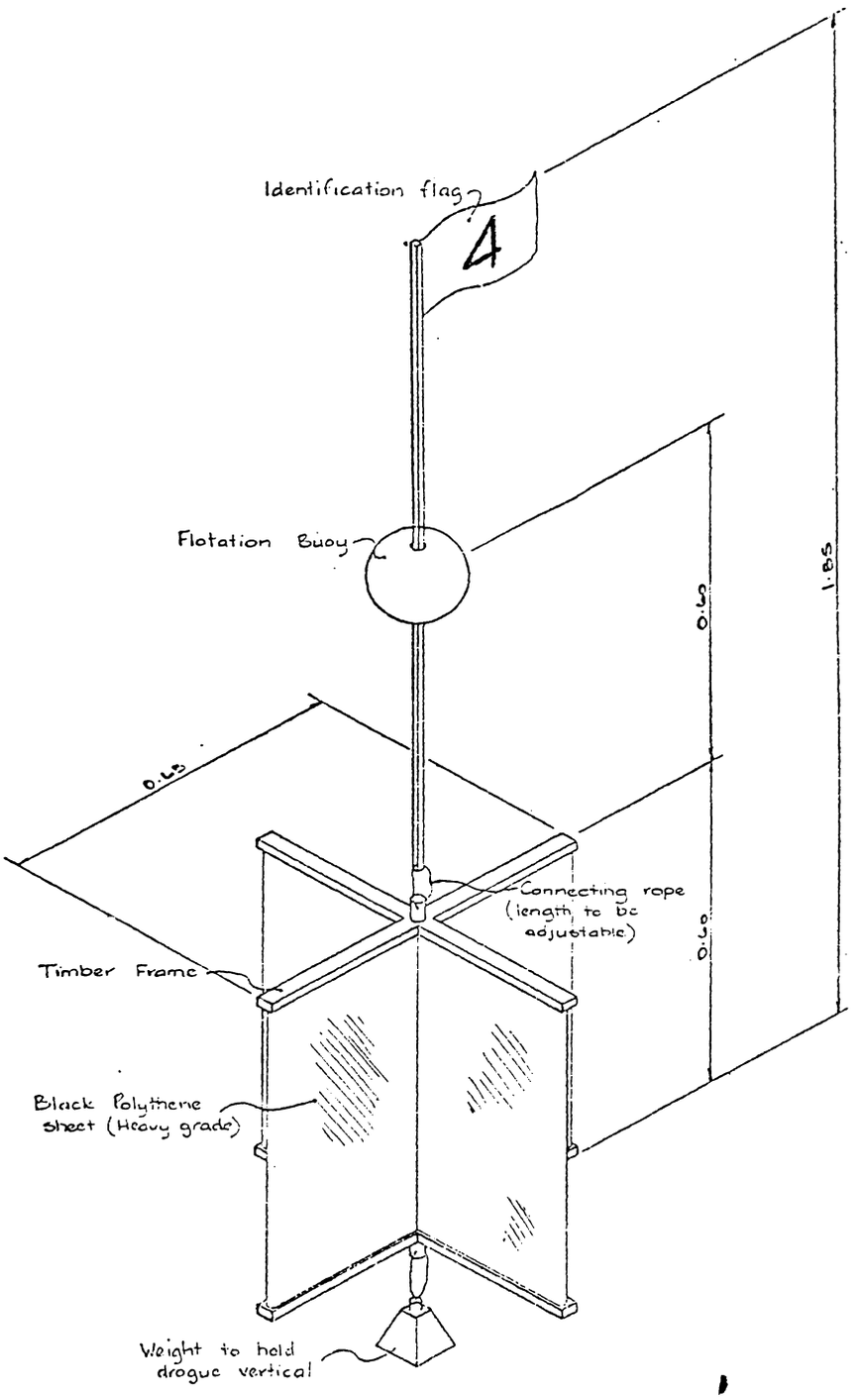

Figure 5.1: Schematic diagram showing drogue design.

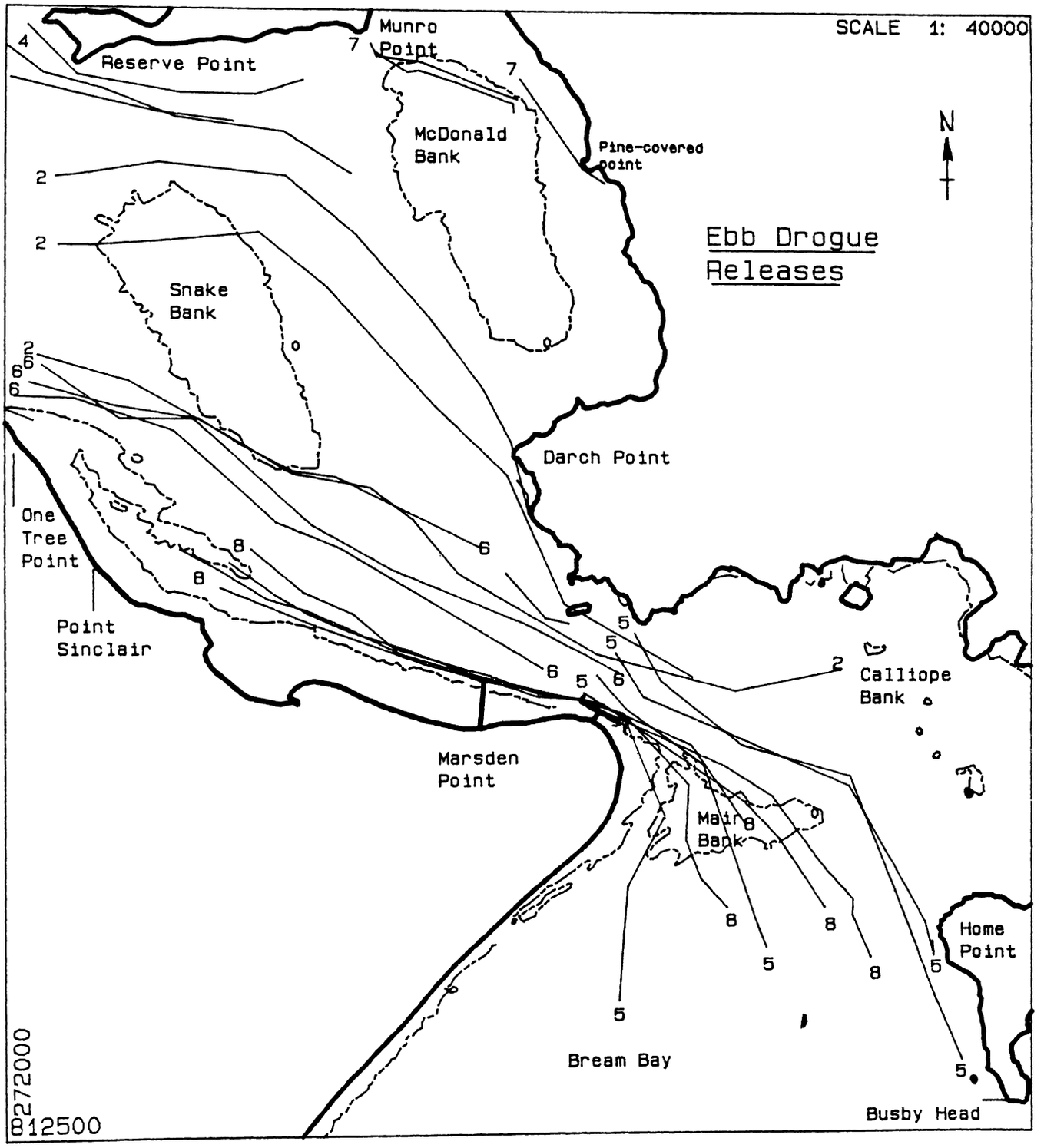

Figure 5.2: General tracking drogue paths during ebb tides. Experiment numbers shown correspond with statistics in Table 5.1.

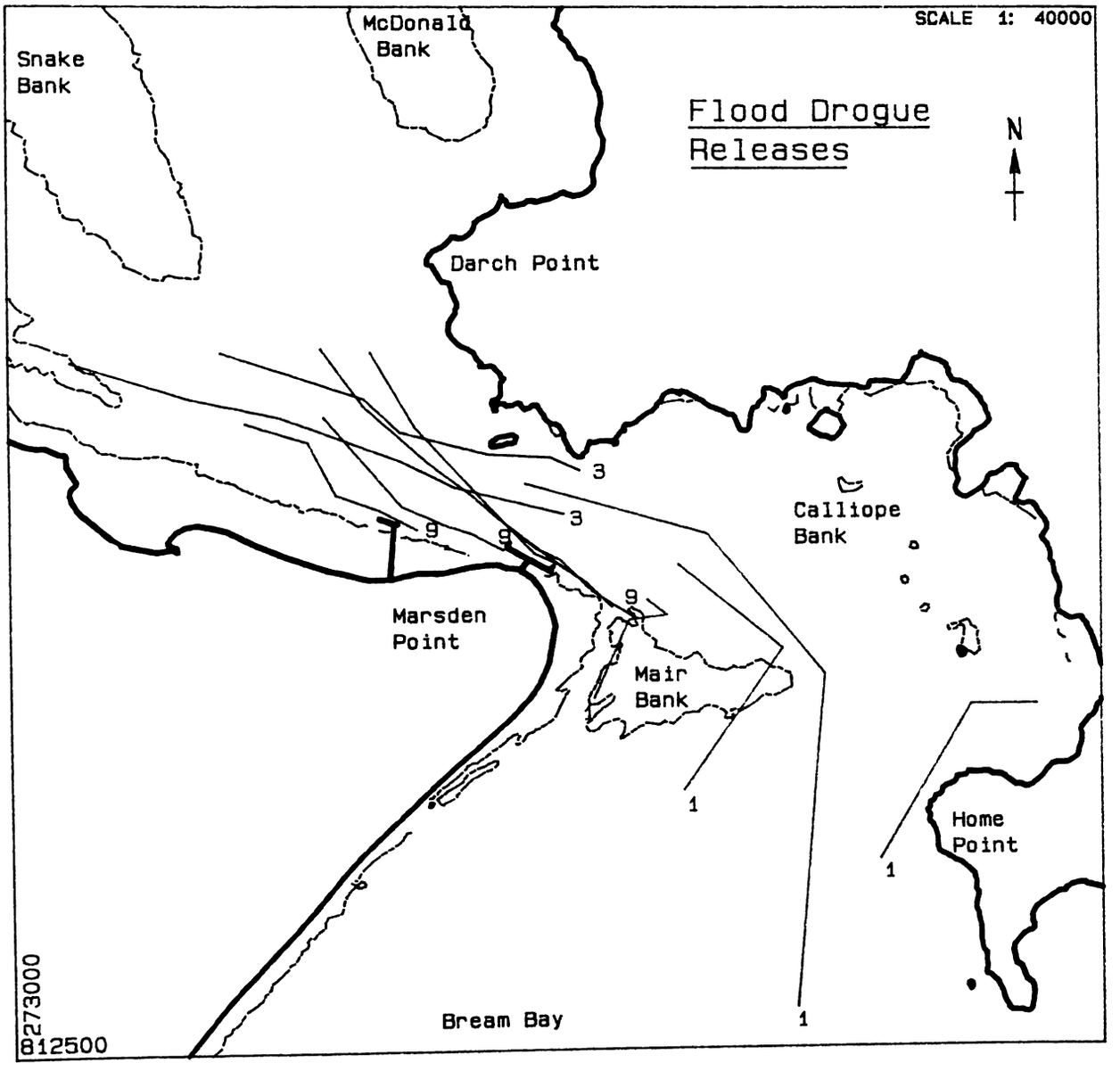

Figure 5.3: General tracking drogue paths during flood tides. Experiment numbers shown correspond with statistics in Table 5.1

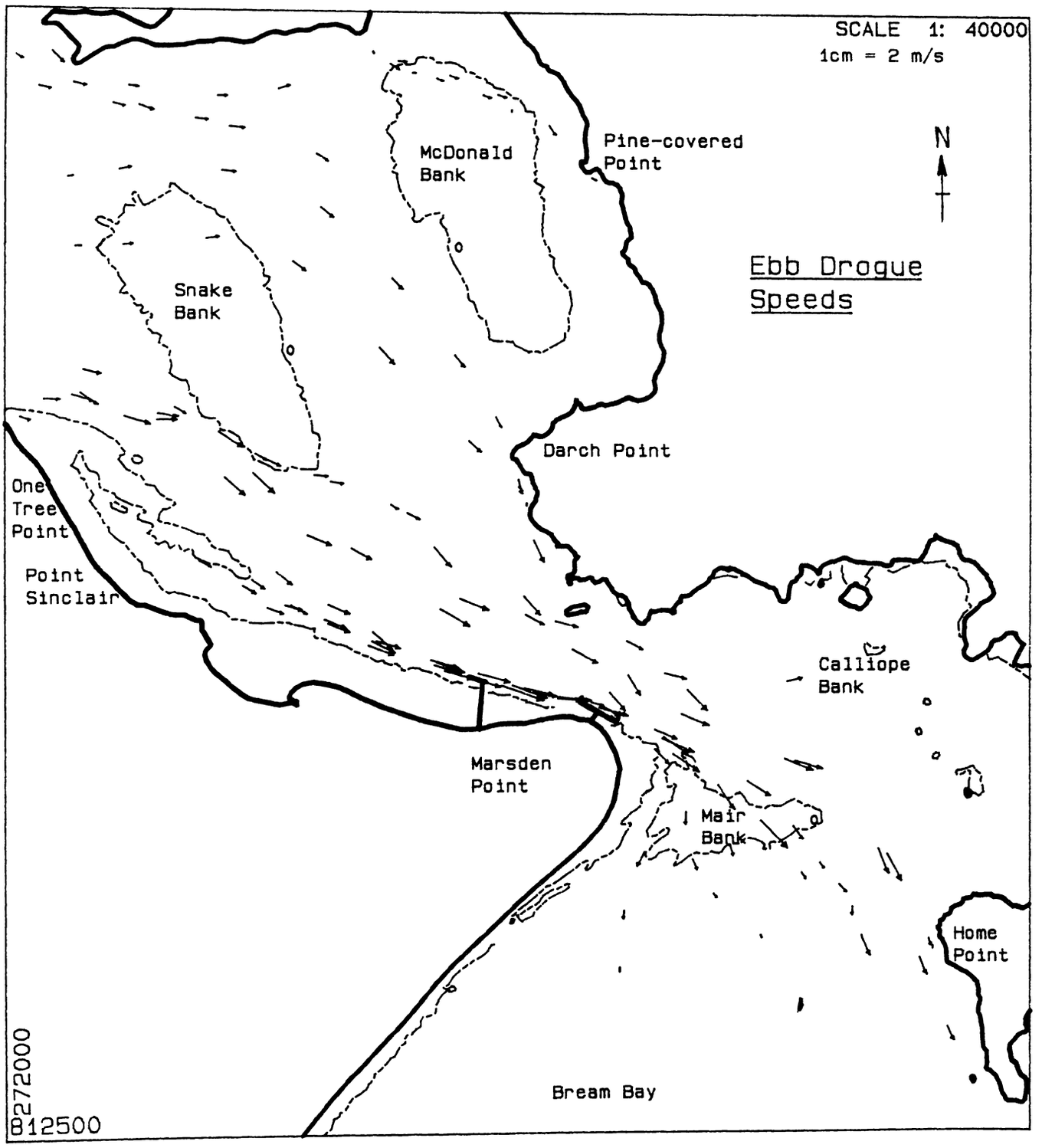

Figure 5.4: General tracking ebb drogue velocities corresponding with paths on Figure 5.2. The velocities are plotted with 1cm representing 2.0 $m.s^{-1}$.

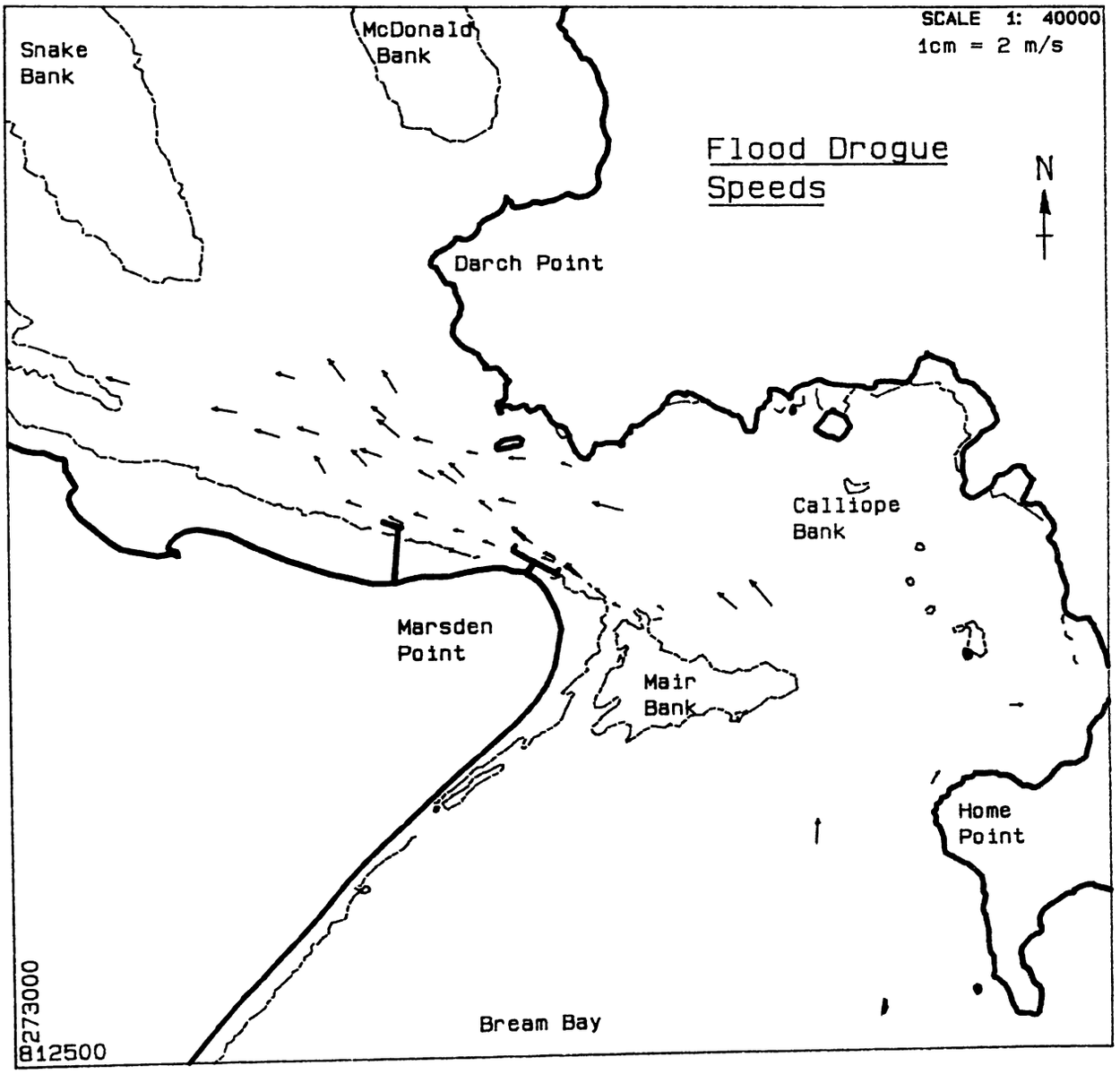

Figure 5.5: General tracking flood drogue velocities corresponding with paths on Figure 5.3. The velocities are plotted with 1cm representing 2 $m.s^{-1}$.

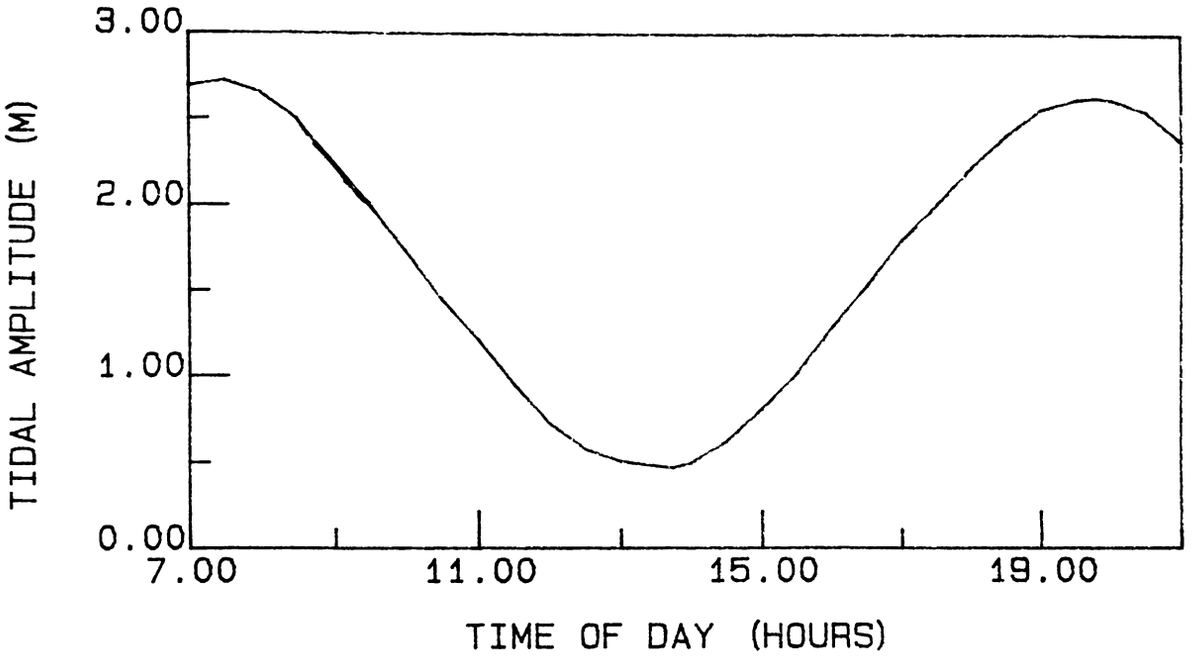

Figure 5.6: Tidal record from the Marsden Point gauge on the 8-Feb-82 during the ebb, full tidal cycle drogue experiment.

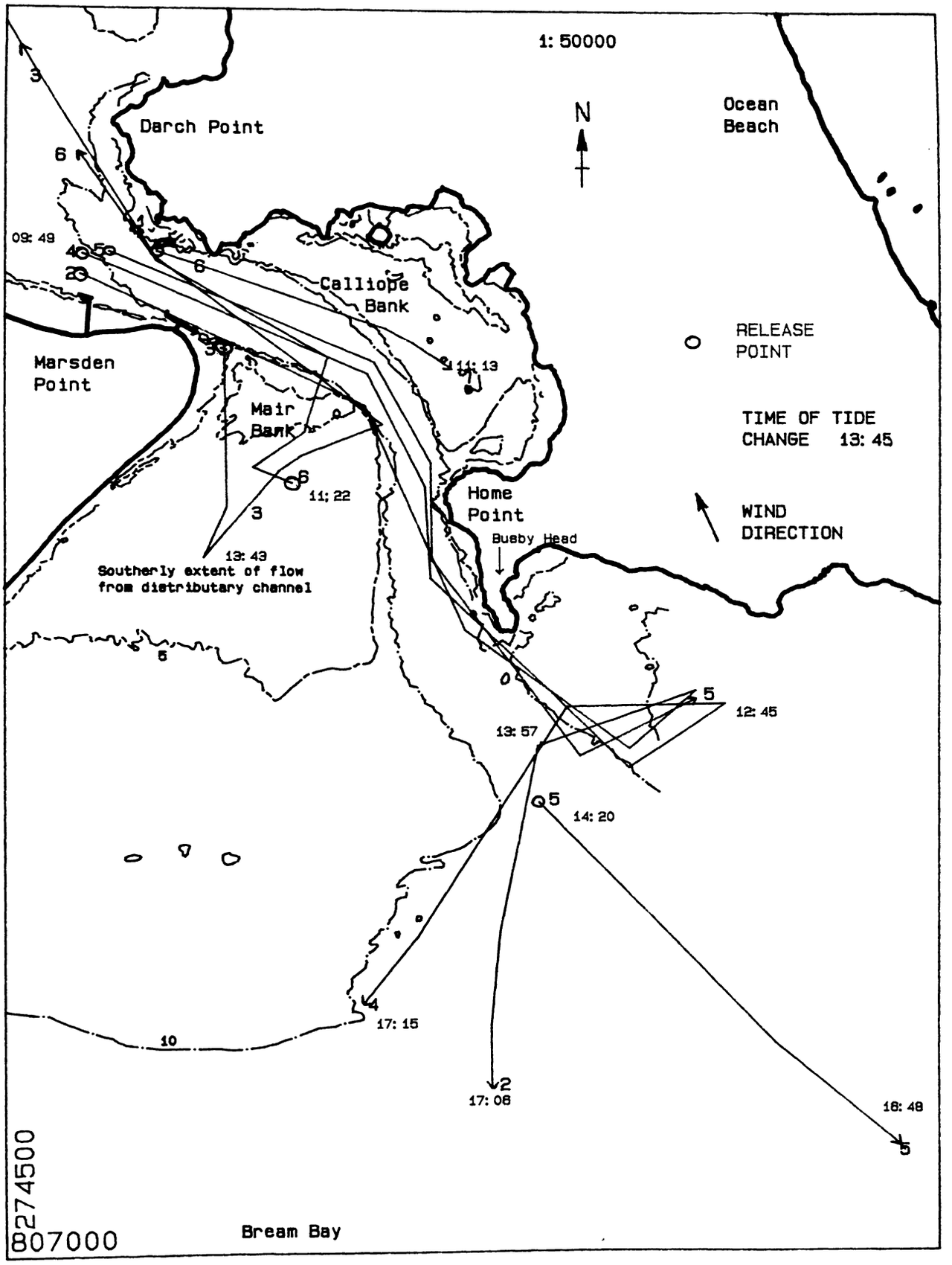

Figure 5.7: Drogue paths during the ebb, full tidal cycle tracking experiment. Release points and directions of travel are shown with representative times of day along the tracks.

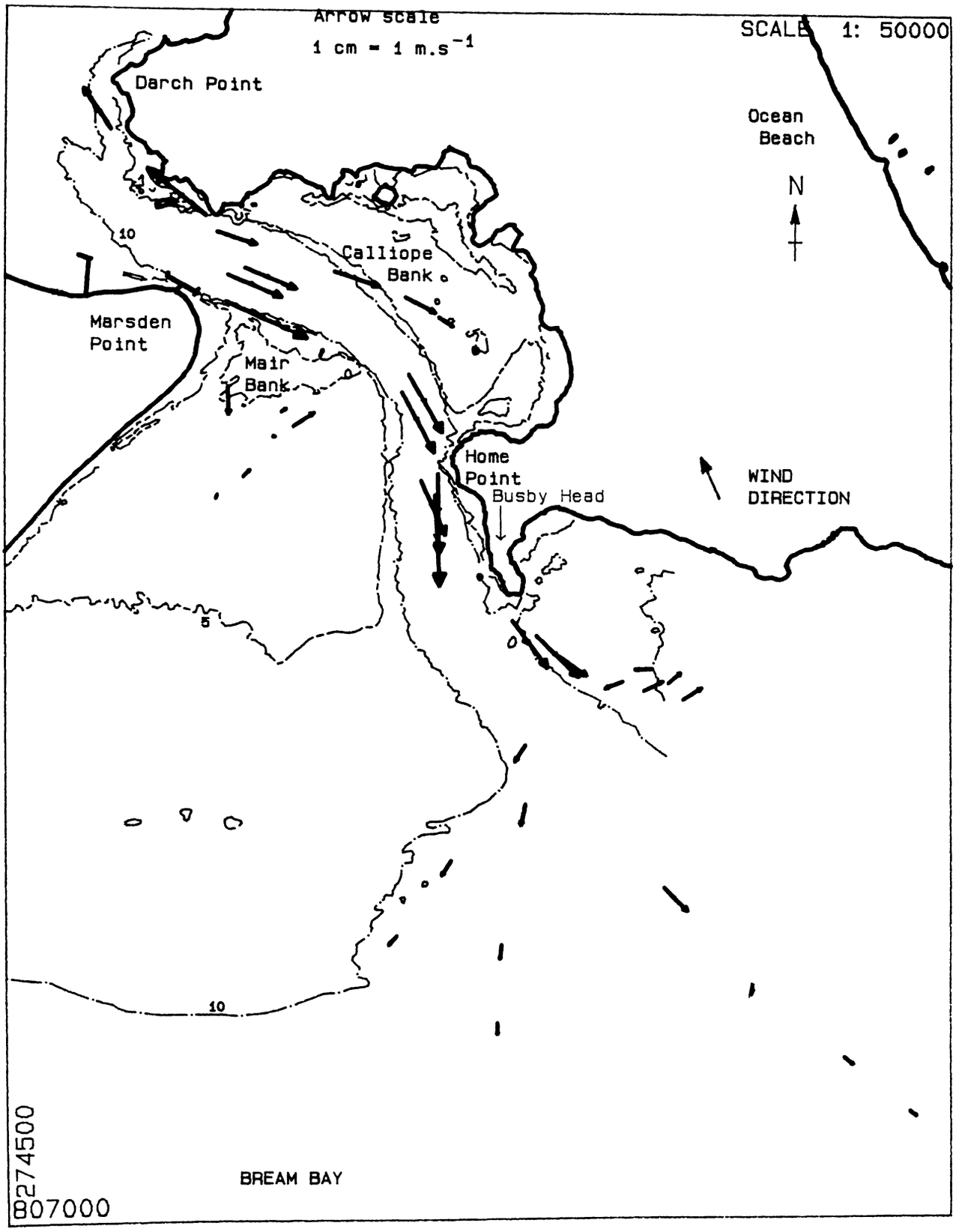

Figure 5.8: Drogue velocities during the ebb full tidal cycle tracking experiment corresponding with the paths in Figure 5.7. Velocities are plotted as 1cm representing 1 m.s^{-1}.

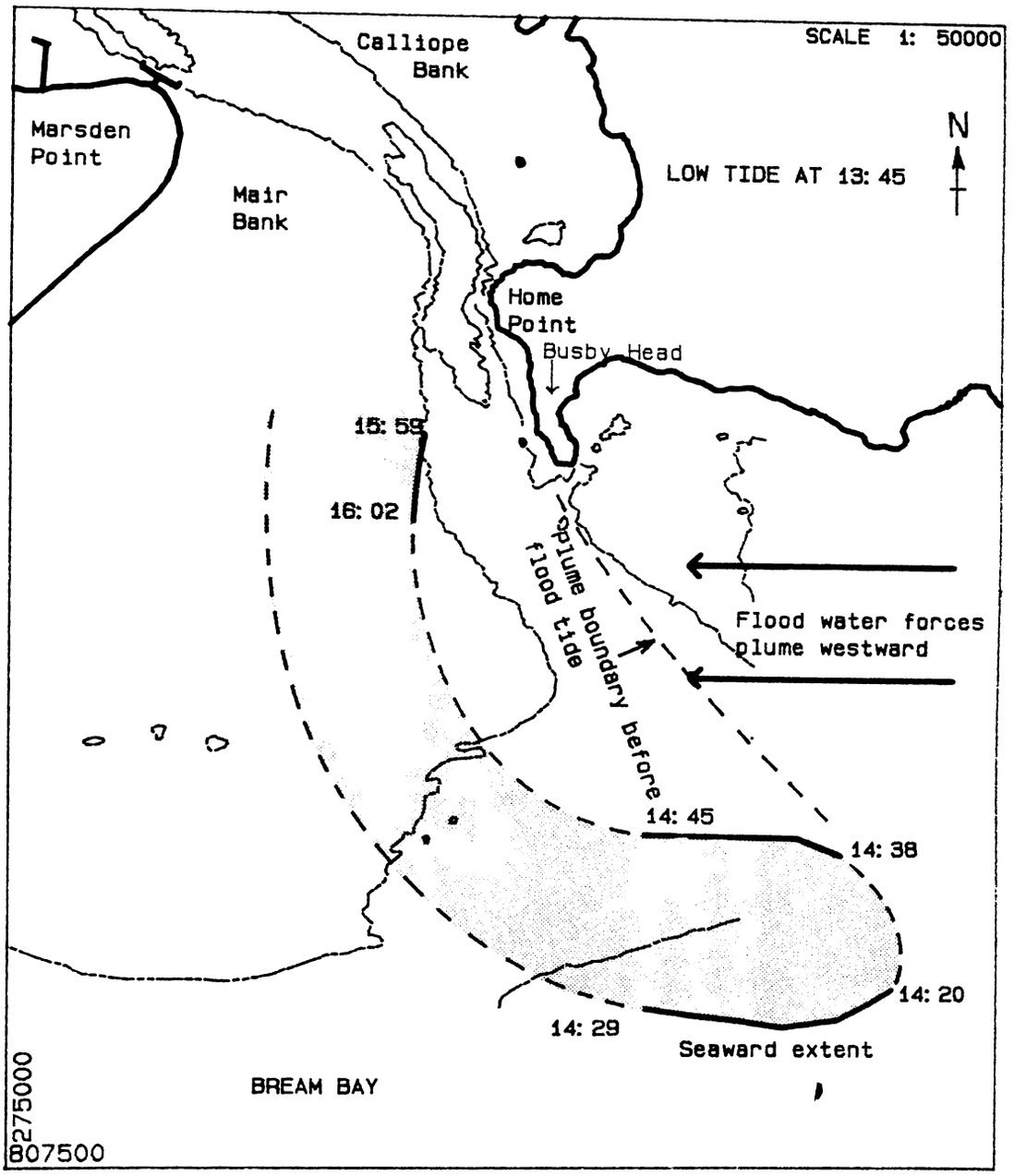

Figure 5.9: Locations of the Brown Plume boundaries marking the extension of the ebb jet into Bream Bay and its movement after low tide. Fix times are shown.

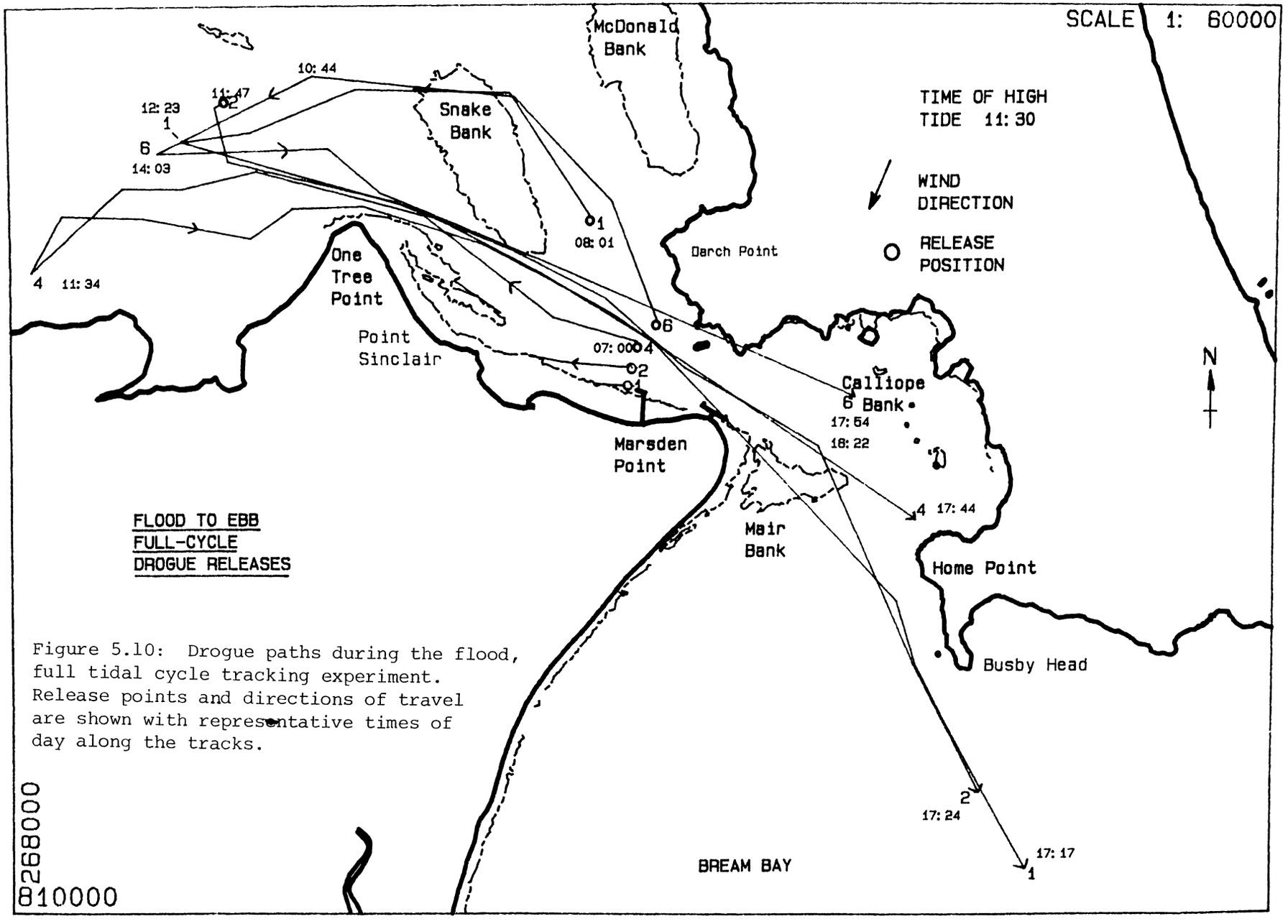

Figure 5.10: Drogue paths during the flood, full tidal cycle tracking experiment. Release points and directions of travel are shown with representative times of day along the tracks.

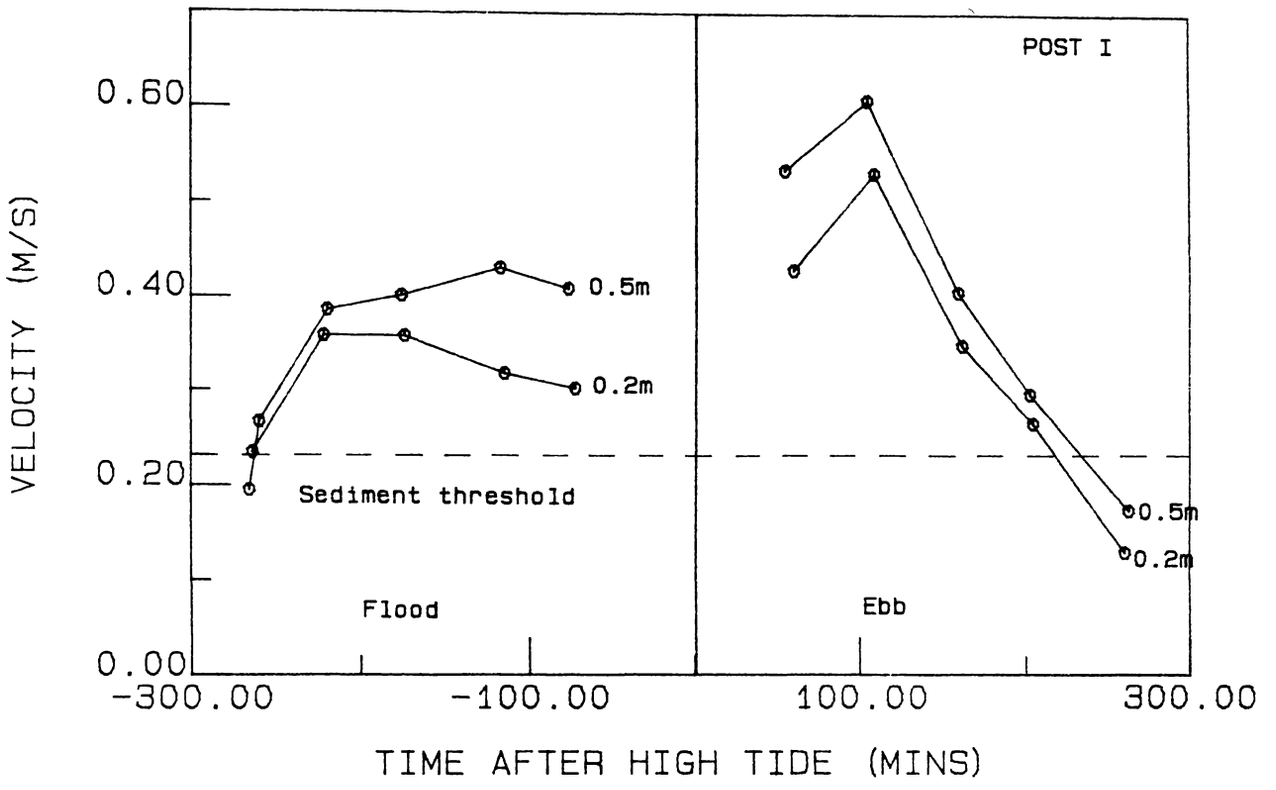

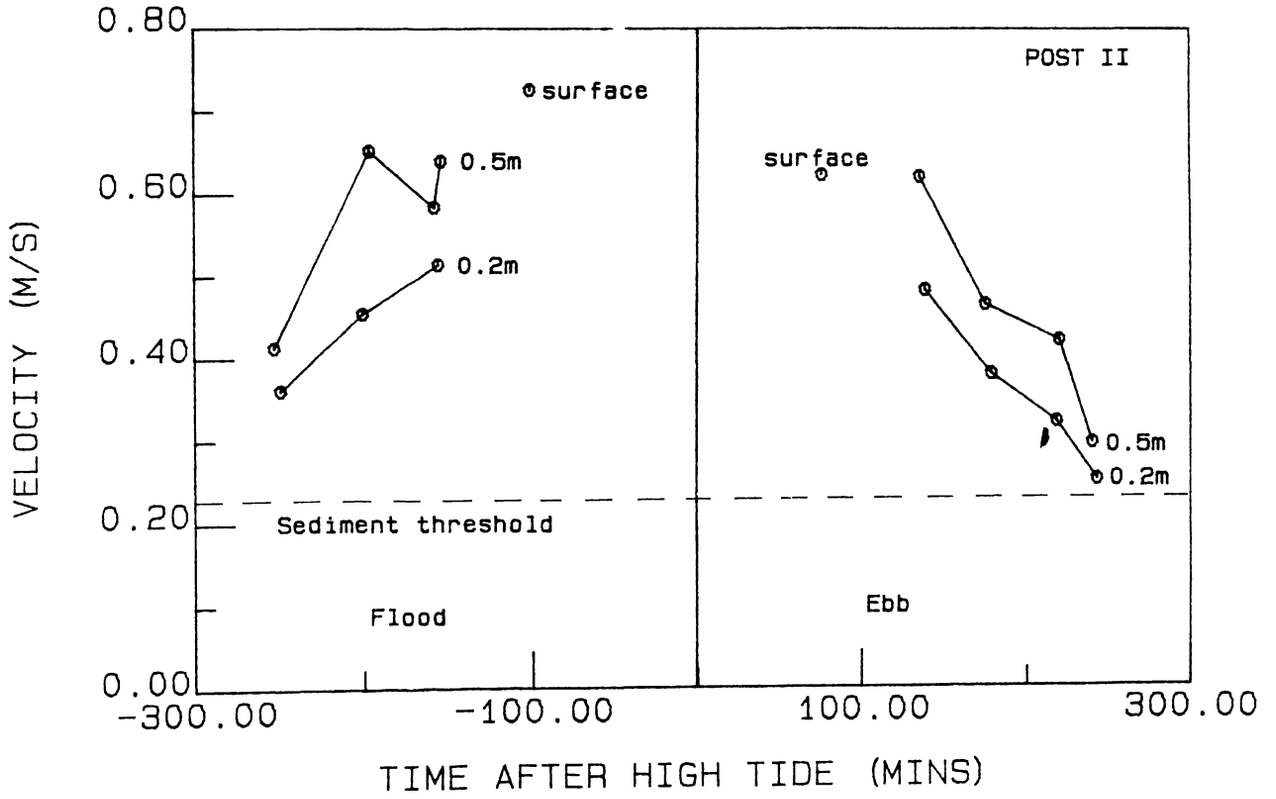

Figure 5.11 (upper) and 5.12: Water speeds measured with an Ott impellor-type meter 0.2m and 0.5m above the sea bed at Sounding Posts SP1M (upper) and SP2M on upper Mair Bank. Approximate, sandy, sediment threshold at 0.2m is shown.

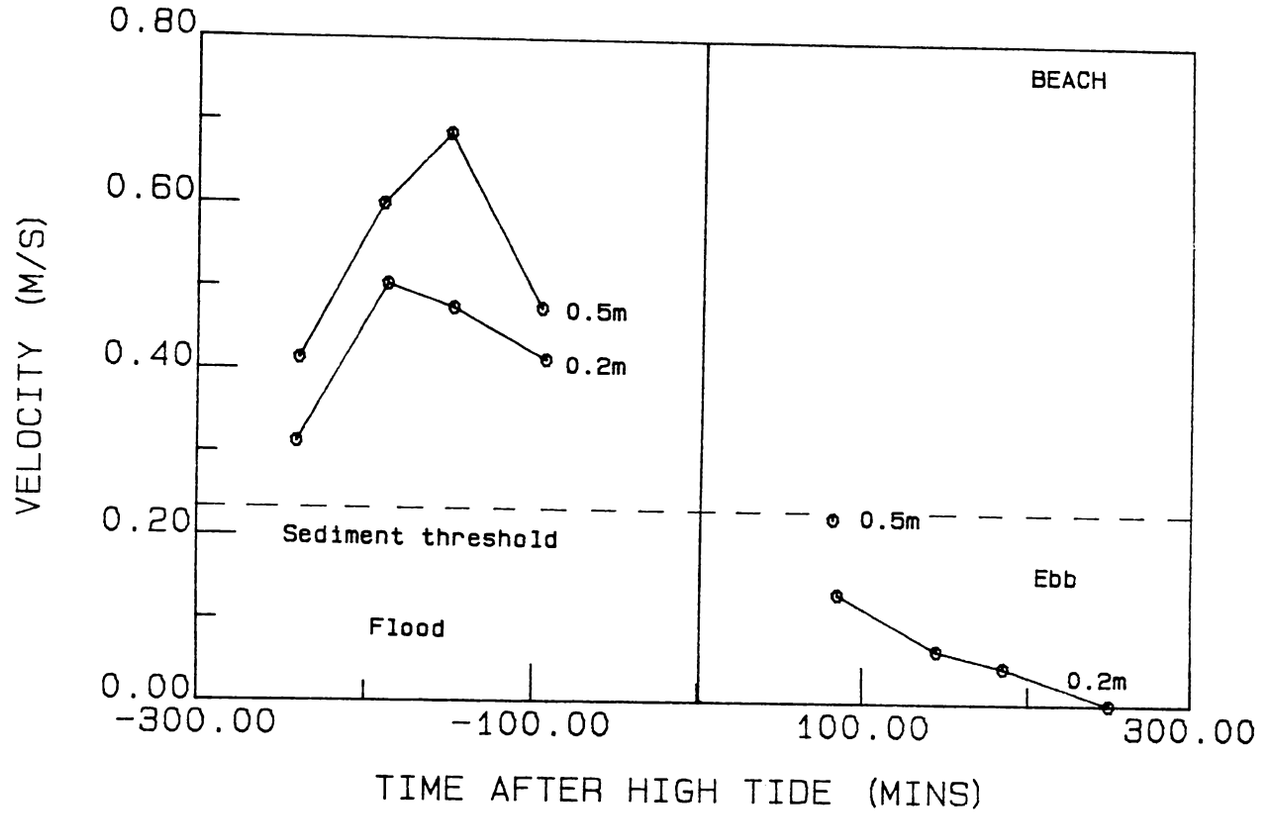

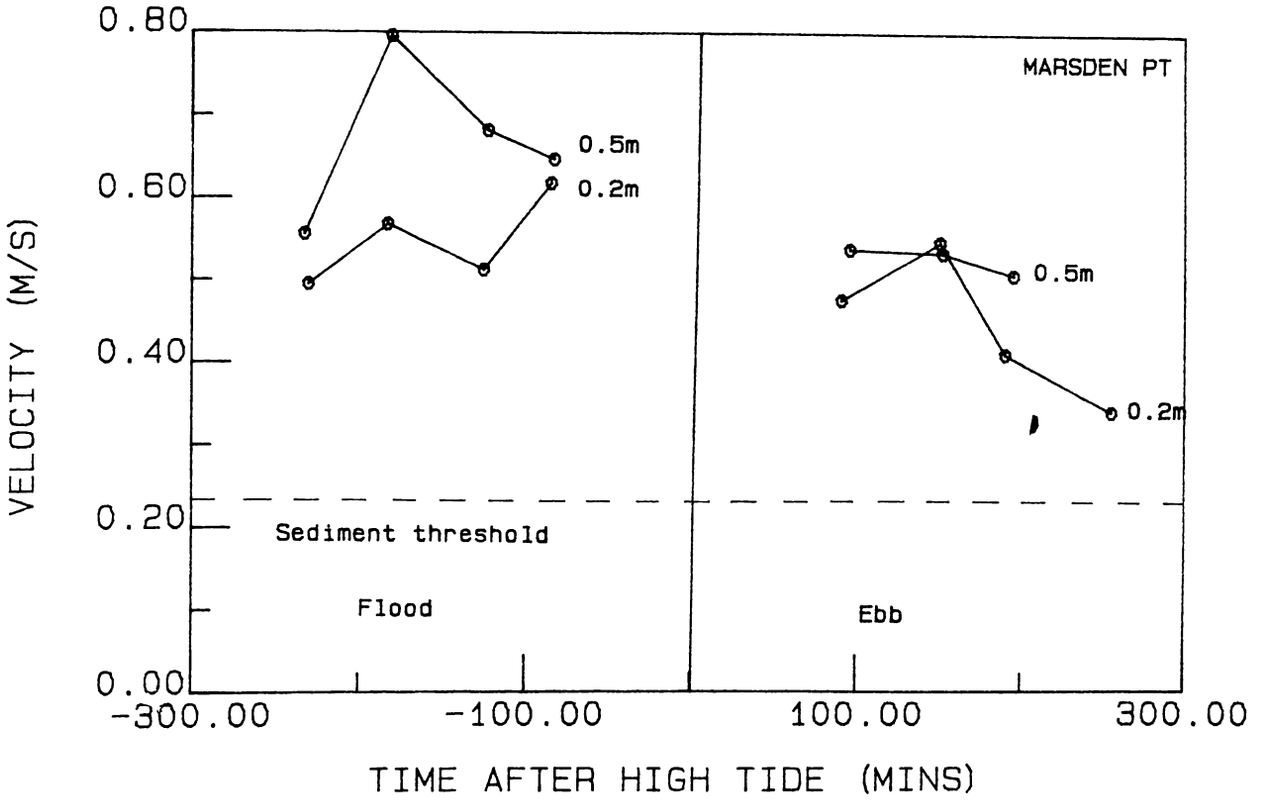

Figures 5.13 (upper) and 5.14: Water speeds measured with an Ott impellor-type meter 0.2m and 0.5m above the sea bed at 120m shoreward of SP12M (upper) and on Marsden Point. Approximate, sandy, sediment threshold at 0.2m is shown.

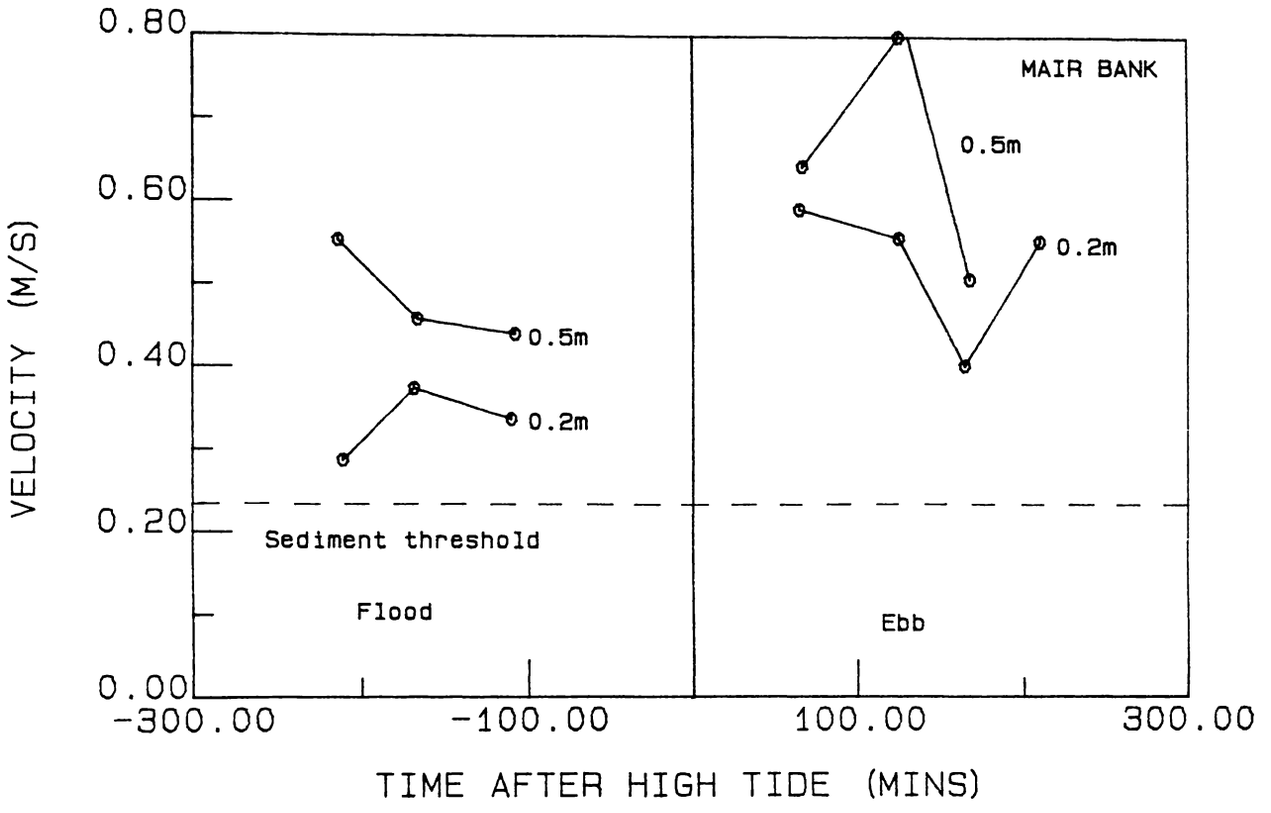

Figure 5.15: Water speeds measured with an Ott impellor-type meter 0.2m and 0.5m above the sea bed in the "middle" of upper Mair Bank. Approximate, sandy, sediment threshold at 0.2m is shown.

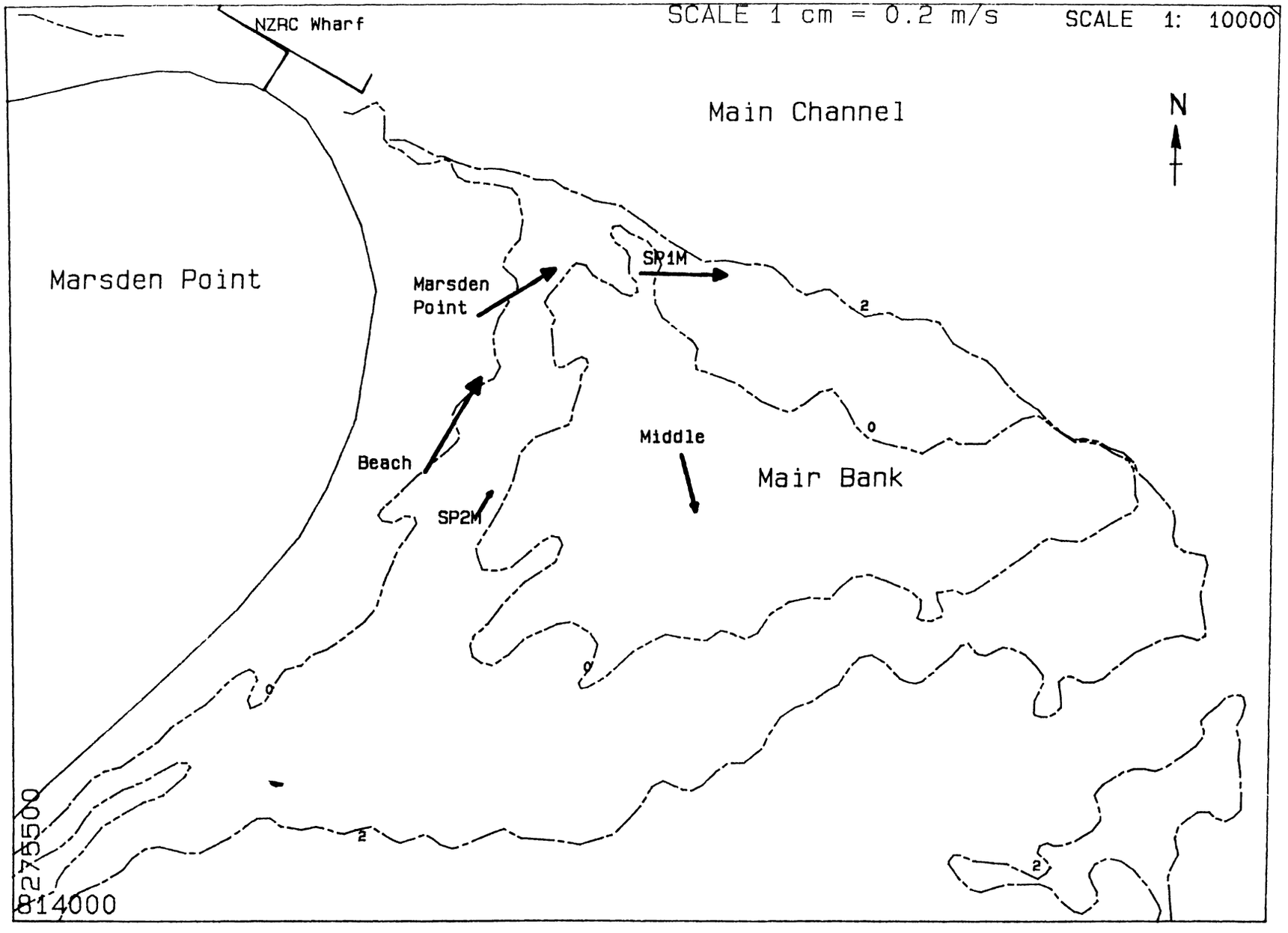

Figure 5.16: Ott current meter measurement sites on upper Mair Bank and Marsden Point with the residual velocities shown at the scale of 1cm representing 0.2 $m.s^{-1}$.

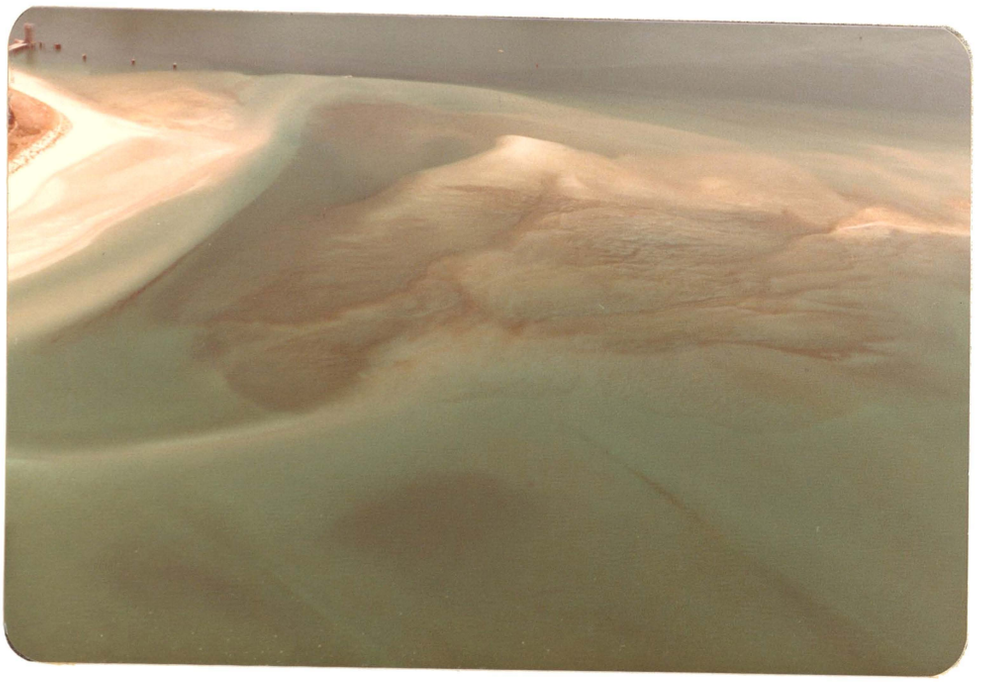

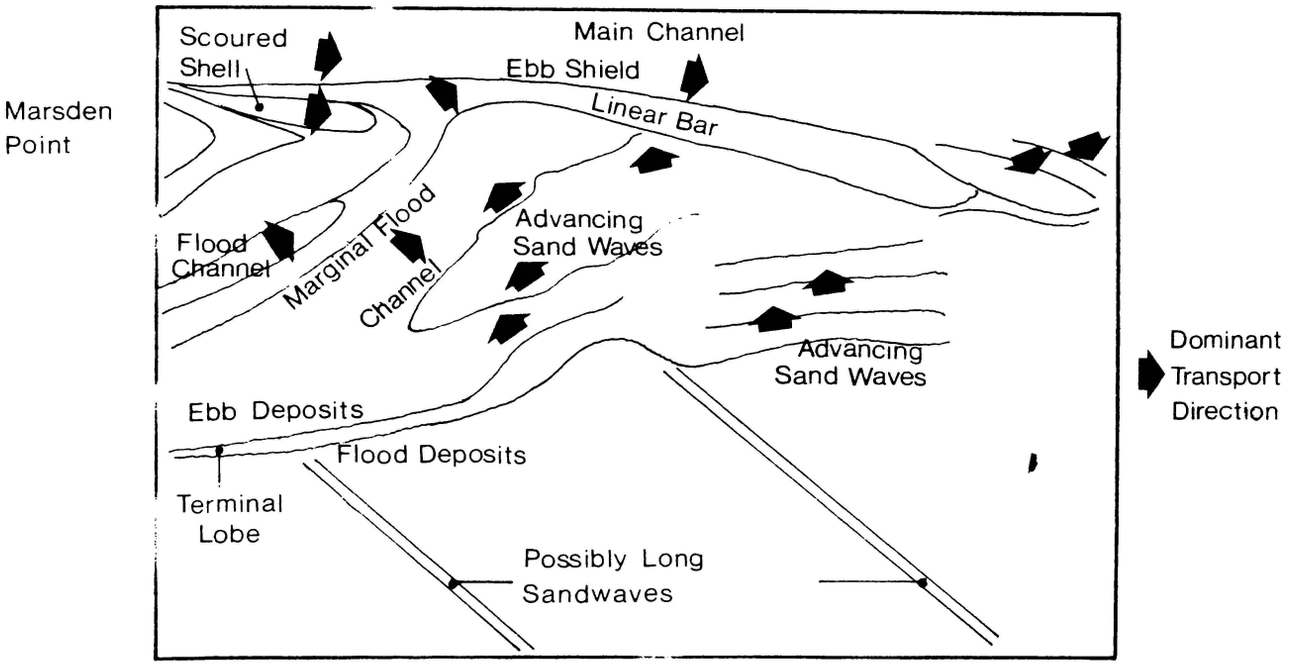

Figure 5.17: Aerial photograph and schematic diagram showing the upper Mair Bank ebb-tidal delta and Marsden Point. The nett sediment transport directions inferred from large-scale bedforms, and velocity measurements, are shown as bold arrows. Morphological features are identified.

Figure 5.18: Aerial photograph showing the upper Mair Bank ebb-tidal delta and Marsden Point with the NZRC refinery and wharf included. Calliope Bank is in the background.

Figure 5.19: Aerial photograph showing the upper Mair Bank ebb-tidal delta and Marsden Point looking from Bream Bay Beach.

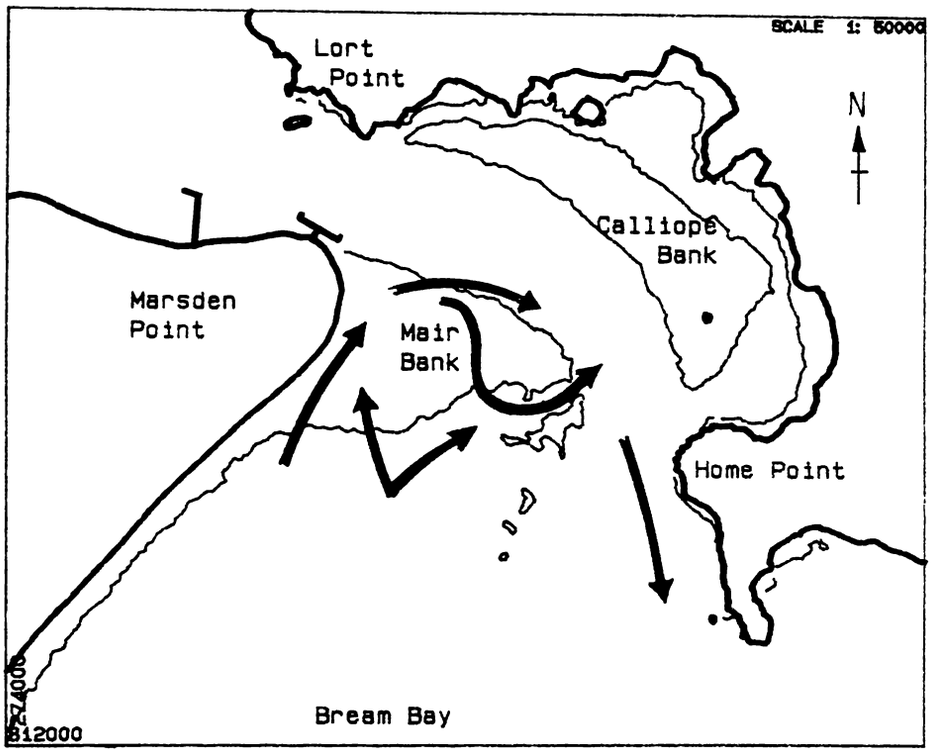

Figure 5.20: Schematisation of major sediment transport directions around upper Mair Bank ebb-tidal delta, inferred from Bank morphology, large-scale bedforms and velocity residuals.

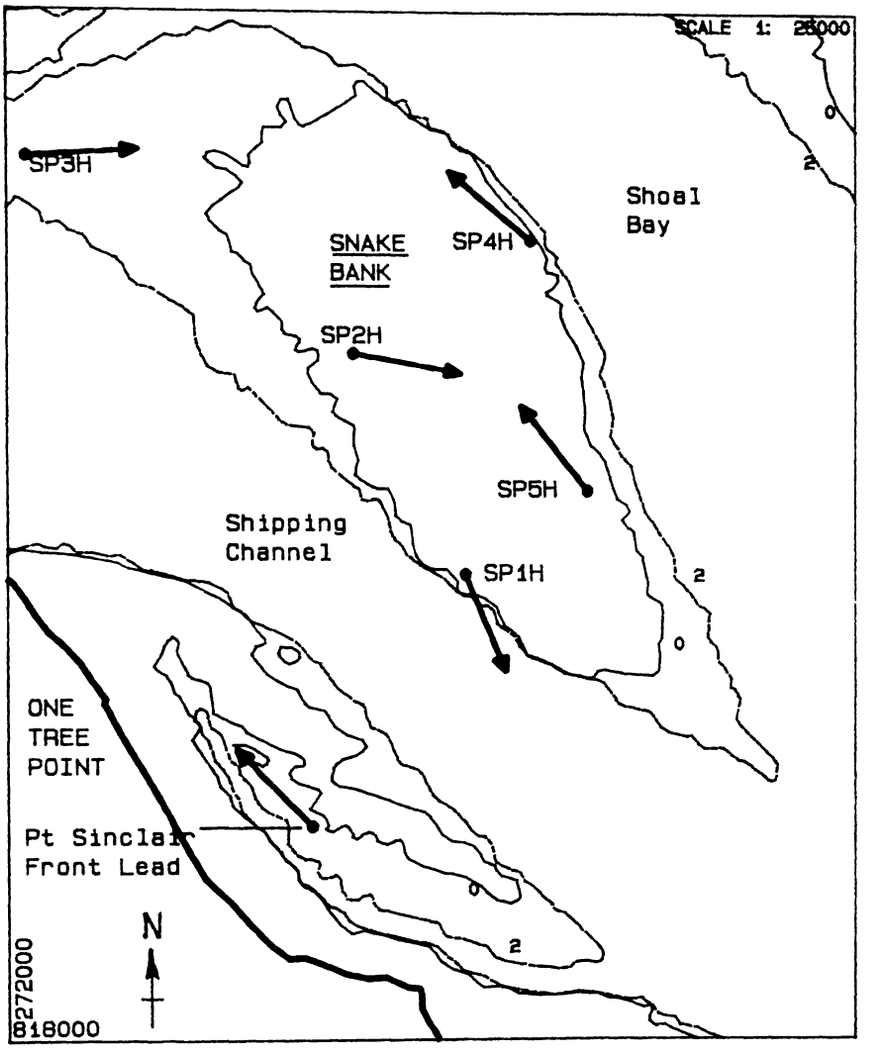

Figure 5.21: Snake Bank flood-tidal delta and the inter-tidal zone up to One Tree Point with Ott meter velocity measurement sites and the current direction at peak flow during the tidal cycle.

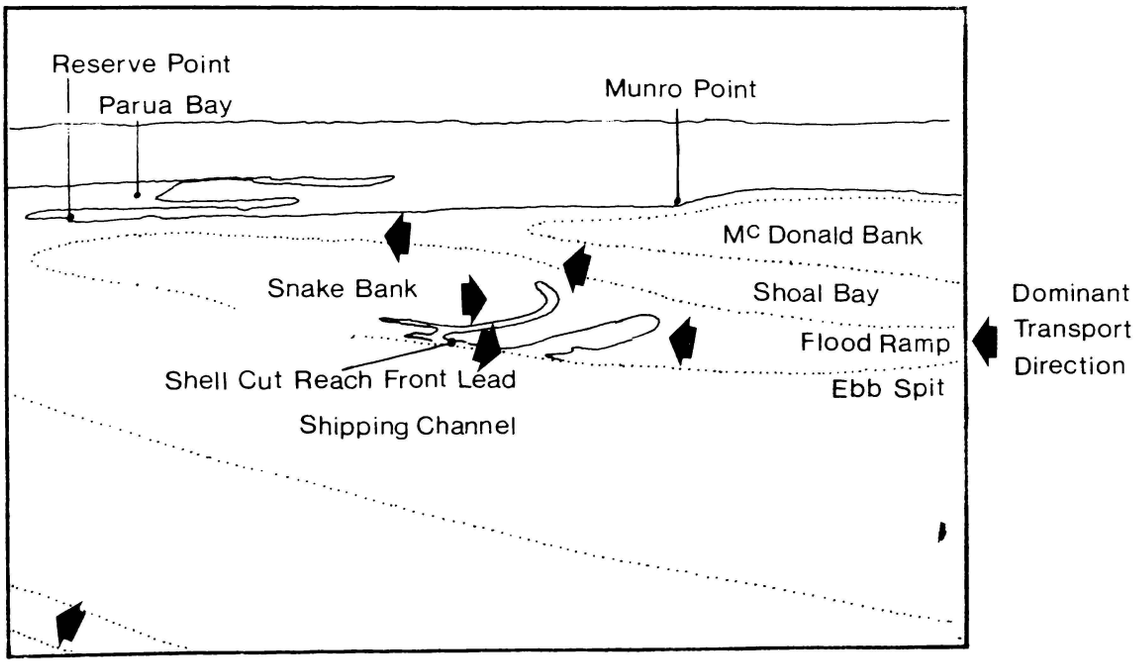

Figure 5.22: Aerial photograph of the Snake Bank flood-tidal delta. The accompanying schematic diagram shows the major morphological features and the dominant sedment transport directions represented by bold arrows and inferred from velocity measurements, large-scale bedforms and Bank morphology.

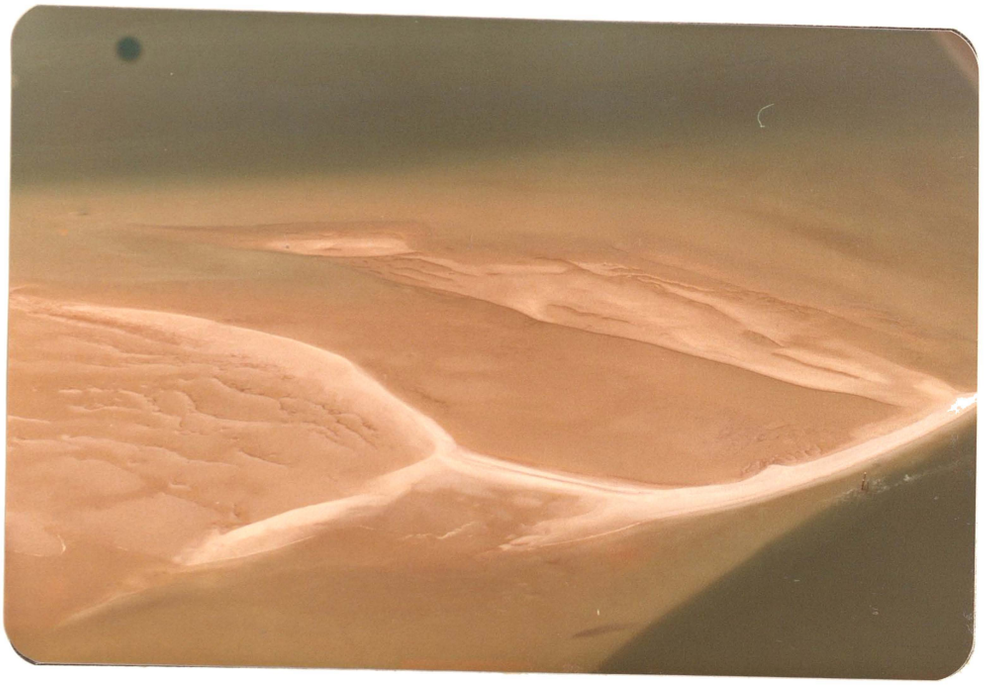

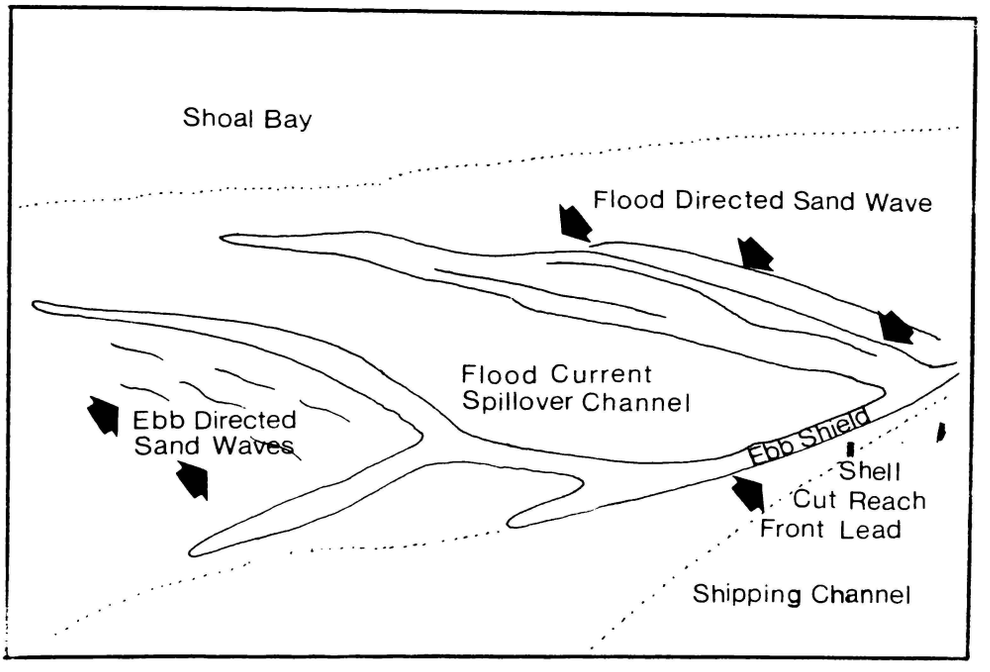

Figure 5.23: Aerial photograph of the Snake Bank ebb shield responsible for the Bank's name. The dominant sediment transport directions inferred from velocity measurements, large-scale bedforms and Bank morphology are shown on the accompanying schematic diagram as bold arrows.

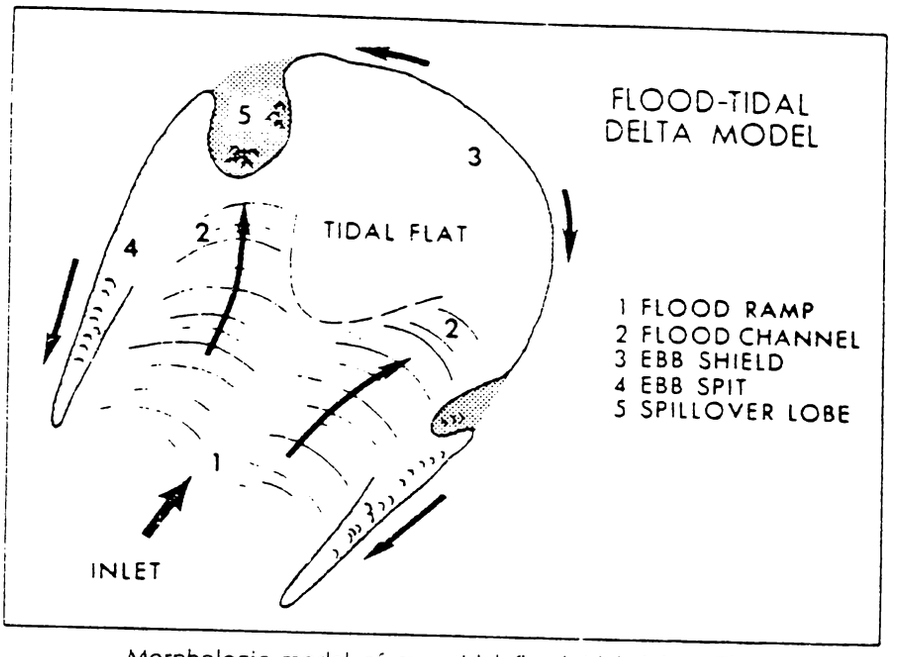

Morphologic model of mesotidal flood-tidal deltas. The arrows indicate the dominant direction of tidal-current flow (from Hayes and Kana, 1976).

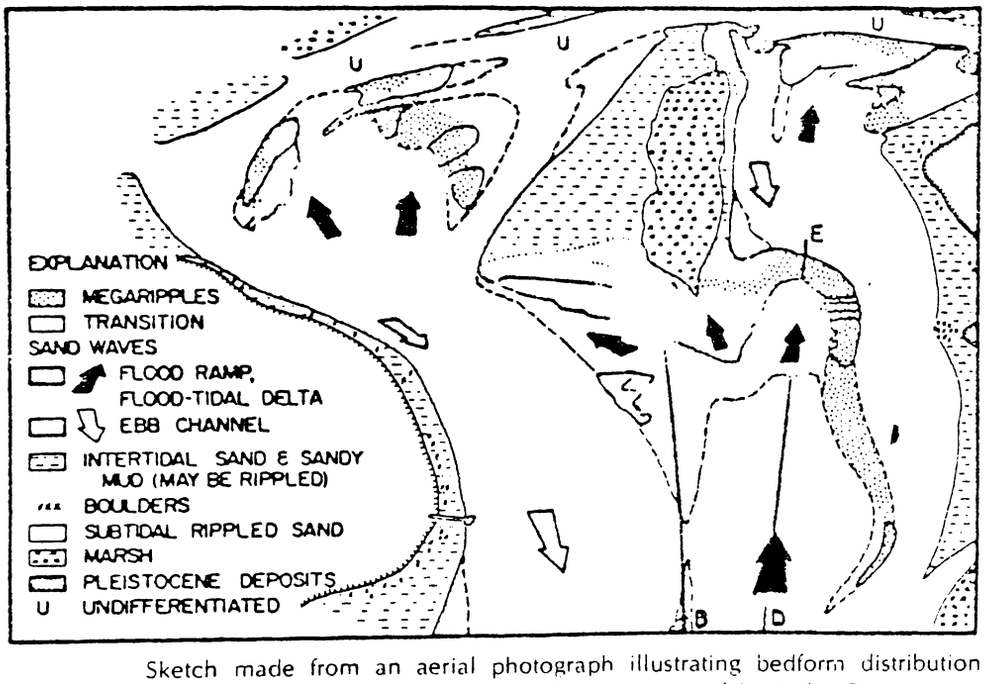

Sketch made from an aerial photograph illustrating bedform distribution patterns and other sub-environments of deposition in the vicinity of the Parker River estuary flood-tidal delta. Arrows indicate orientation of major bedforms and net direction of sediment transport. Bottom profile lines are also shown in Figure 20 (from Boothroyd and Hubbard, 1975).

Figure 5.24: Schematic diagram of a flood-tidal delta from Boothroyd (1978).

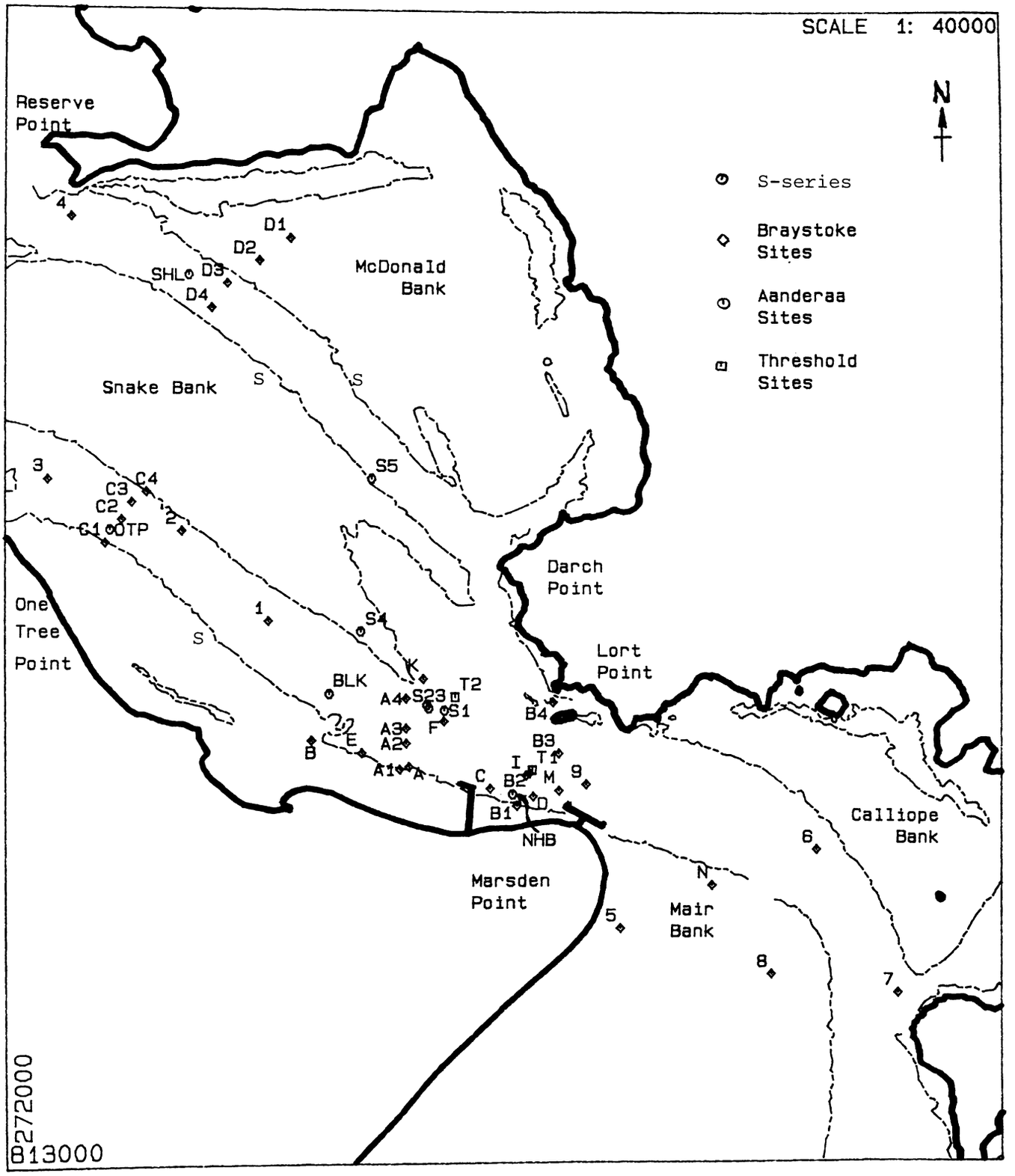

Figure 5.25: Locations of Braystoke vertical profile measurement sites, Aanderaa sites (NHB, BLK, OTP, SHL) and two sediment threshold sites (T1, T2) with the 5m isobath. Sites S2 and S3 are close together and are denoted by S23.

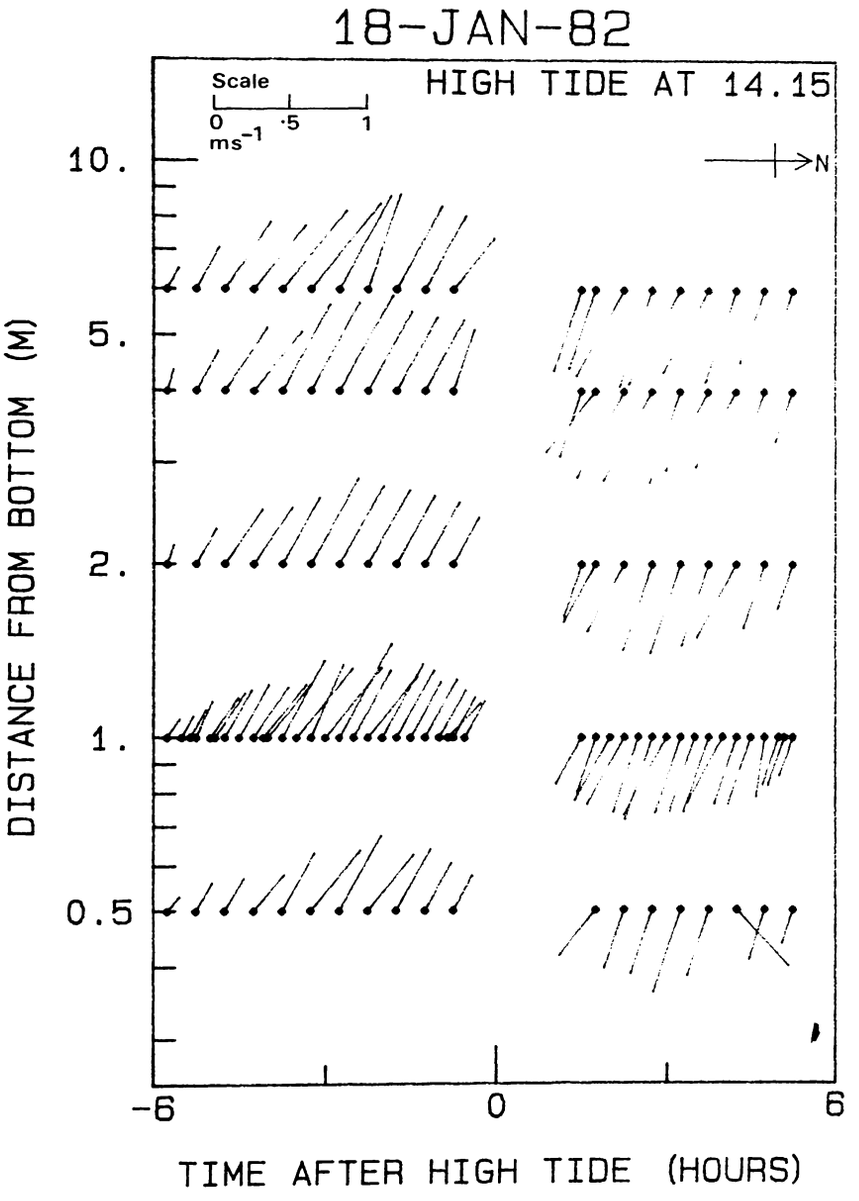

Figure 5.26: Typical velocity profile record made at Site S1 on 18-Jan-82. Speeds are plotted to the scale of 2cm representing 1 $m.s^{-1}$ and direction is plotted with true North to the right.

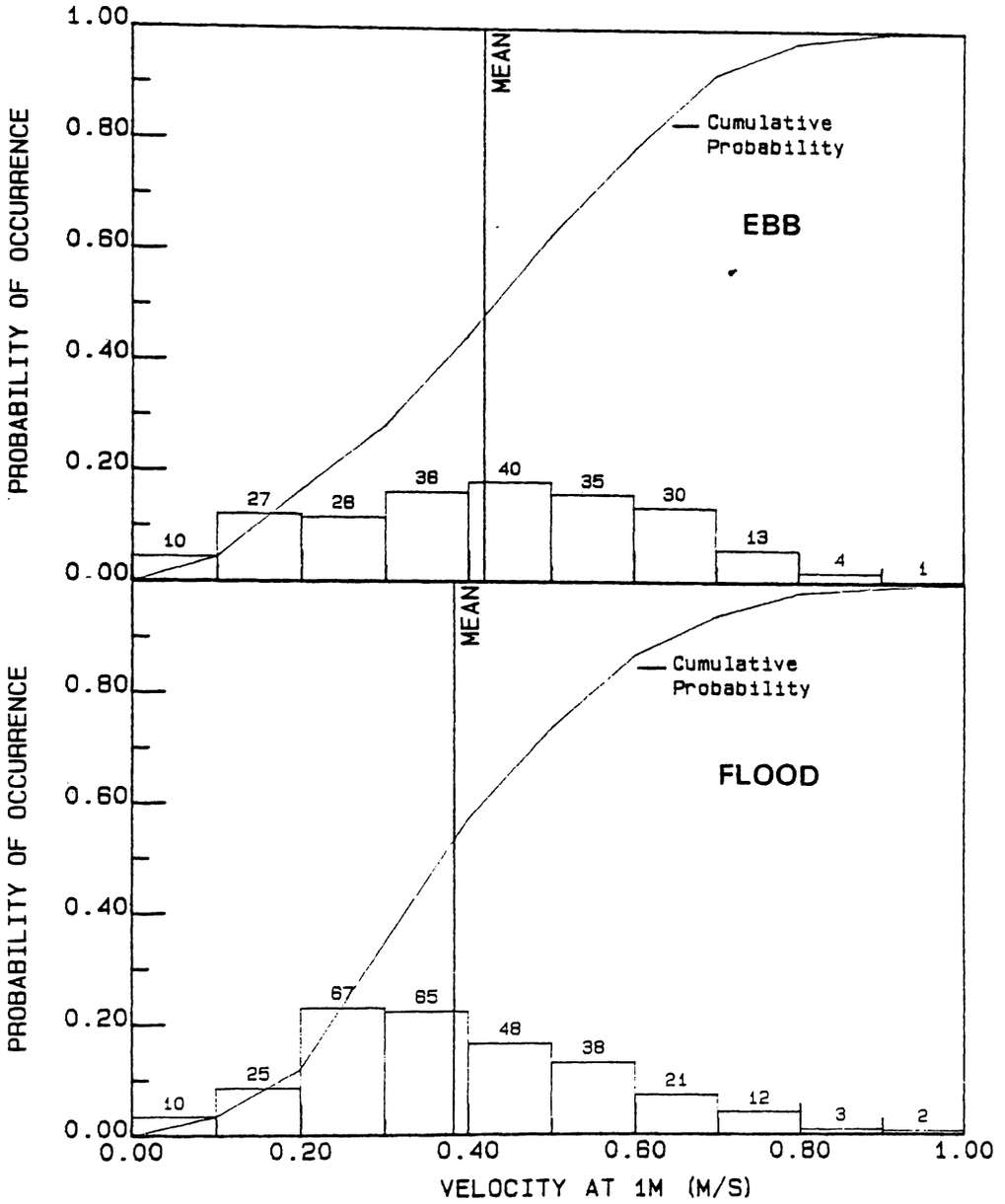

Figure 5.27: Distribution of ebb (upper) and flood velocities at 1m above the bed. Numbers above bars are the number of occurrences in each bin.

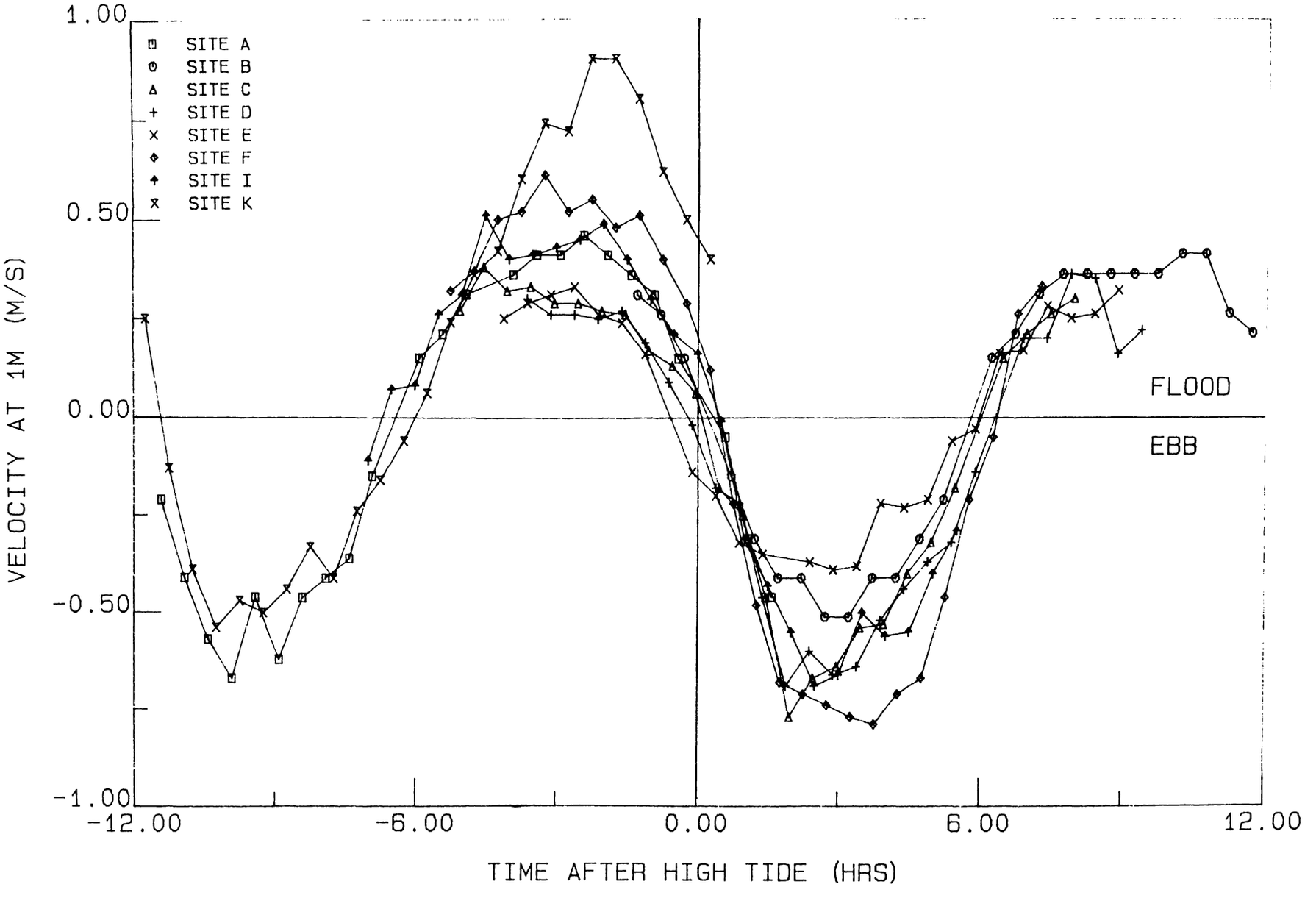

Figure 5.28: Velocity-time curve at 1m above the bed for Braystoke sites A to K.

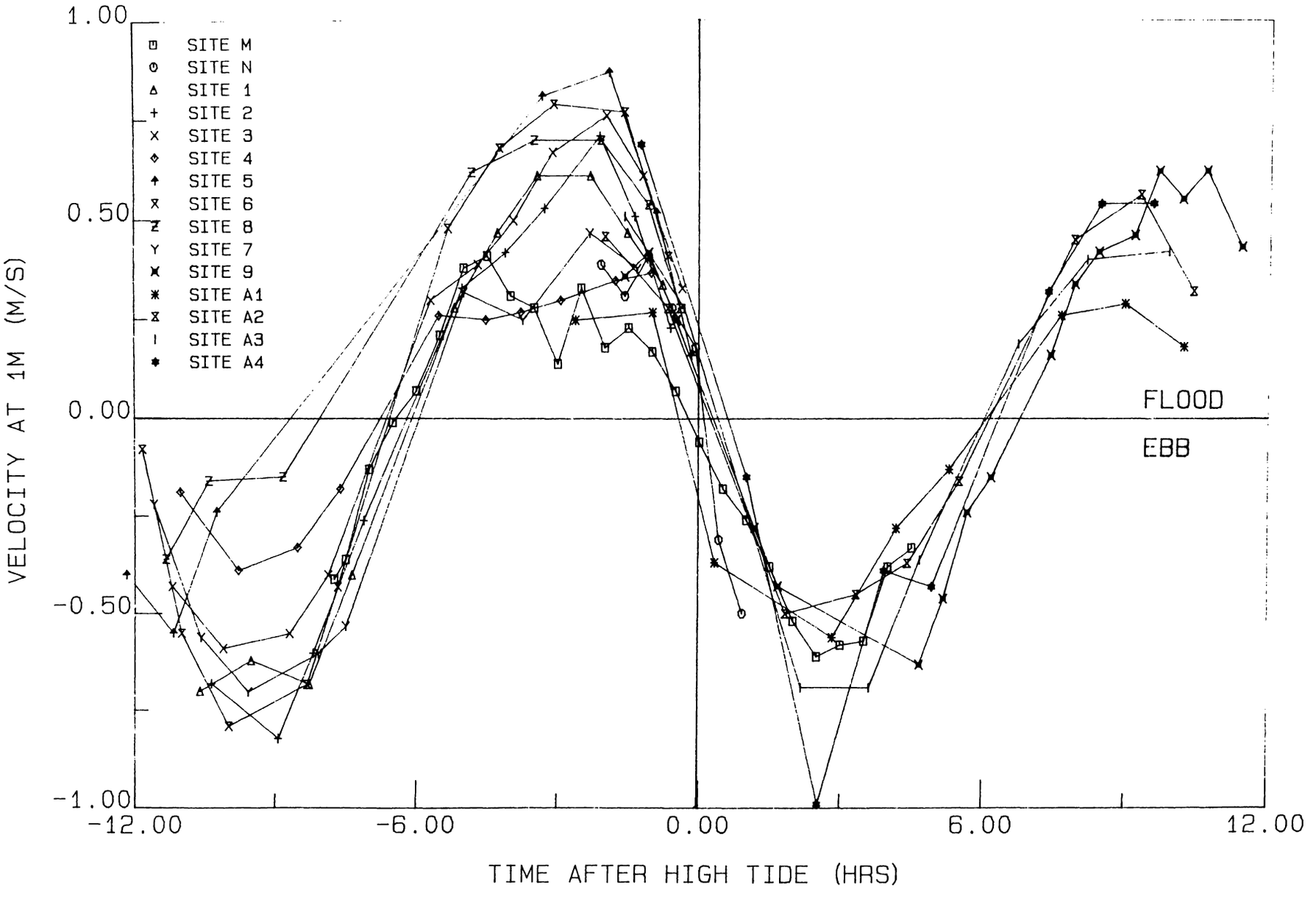

Figure 5.29: Velocity-time curves at 1m above the bed for Braystoke sites M to A4.

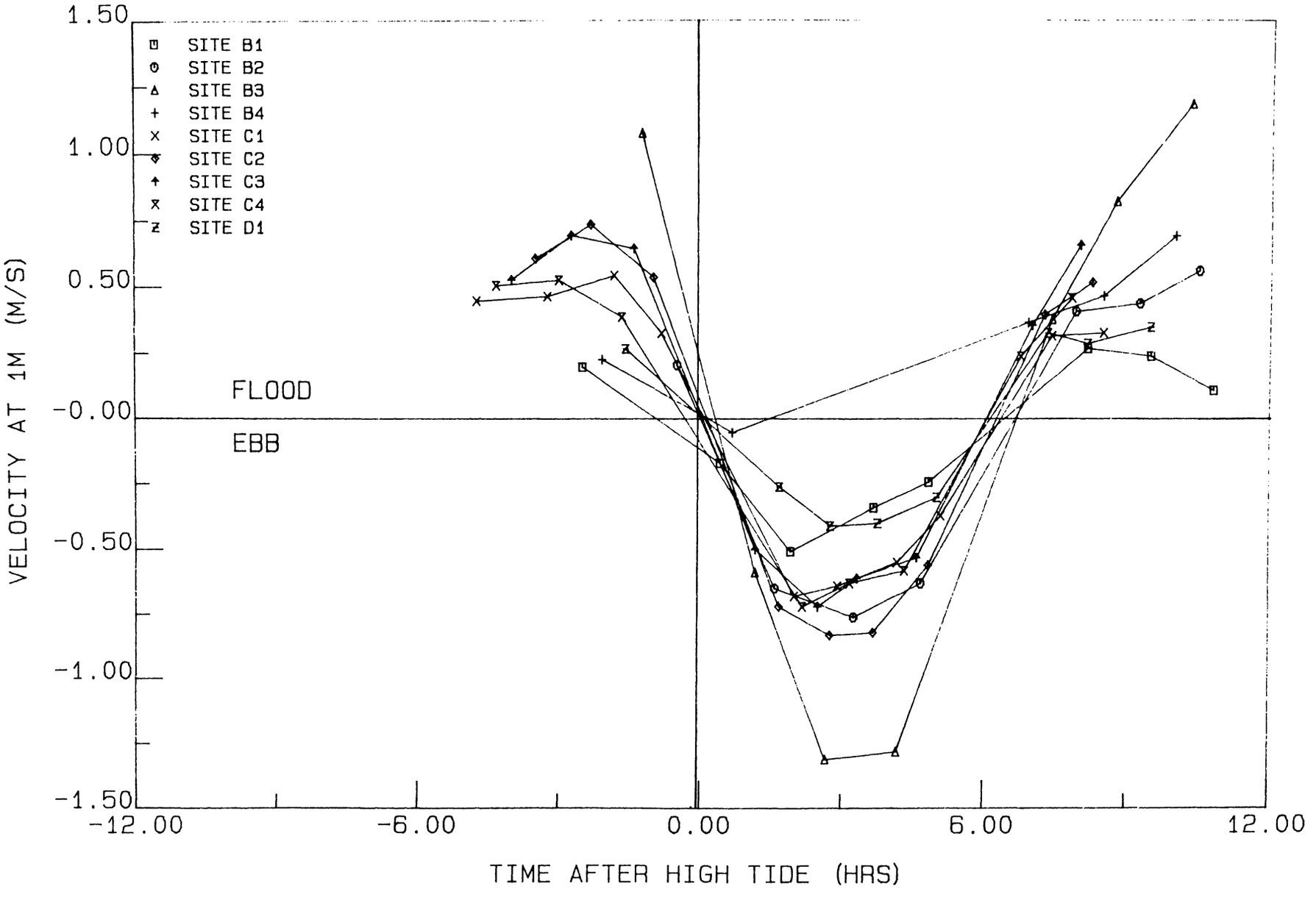

Figure 5.30: Velocity-time curves at 1m above the bed for Braystoke sites Bl to Dl.

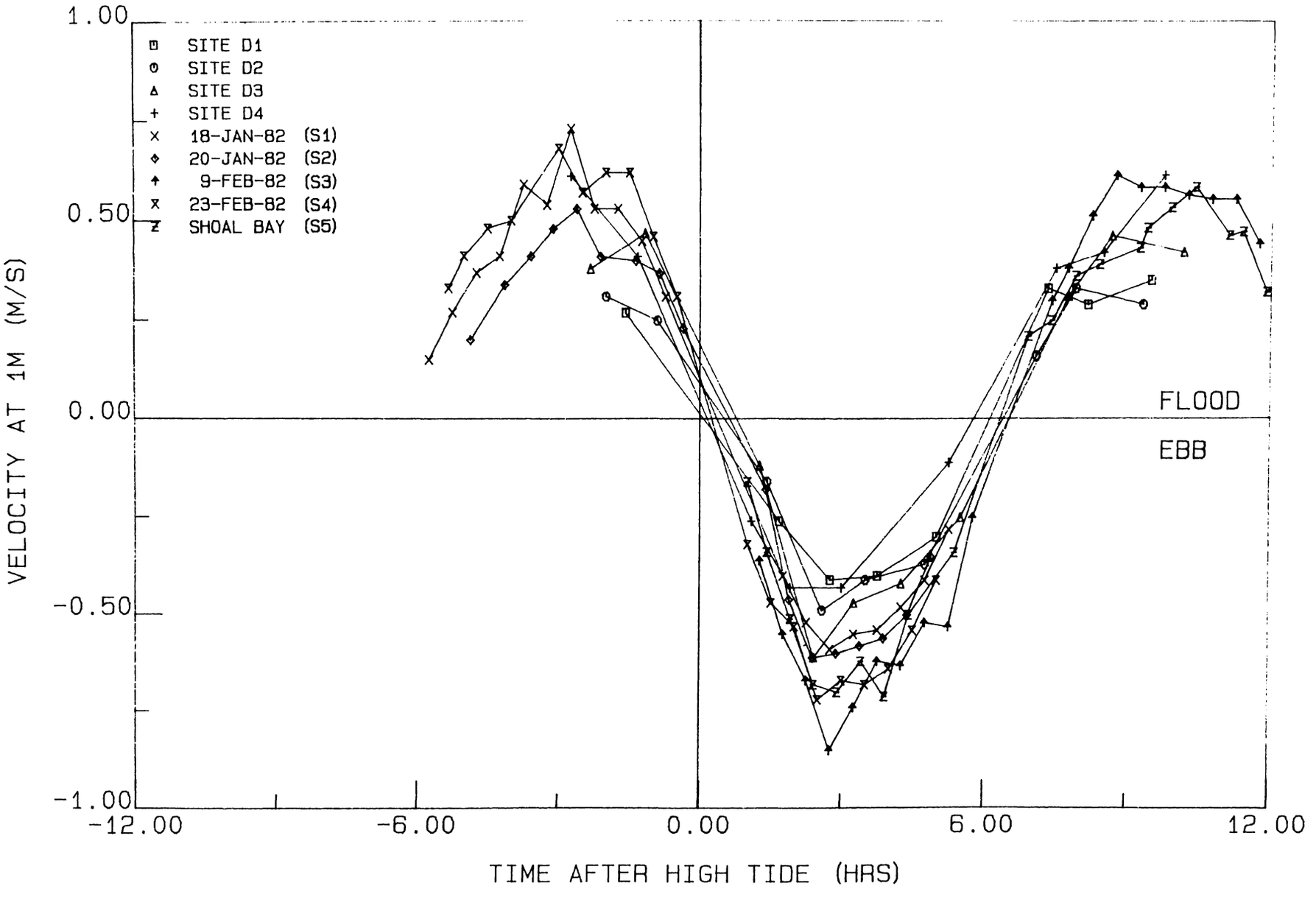

Figure 5.31: Velocity-time curves at 1m above the bed for Braystoke sites D1 to S5.

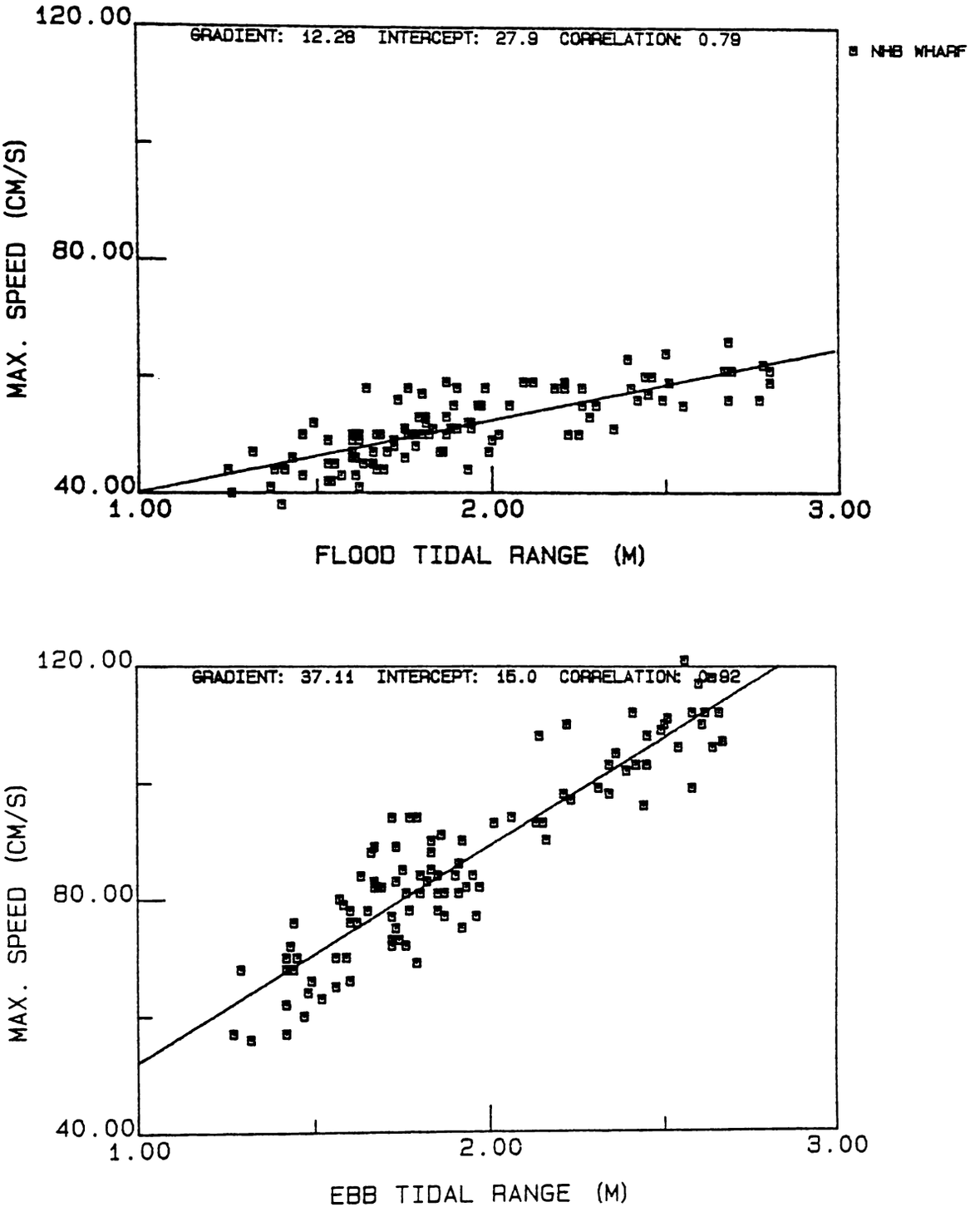

Figure 5.32: Maximum speed attained at the NHB Aanderaa current meter during each half cycle against the corresponding tidal range for flood (upper) and ebb half cycles respectively. Best fit linear curves are given.

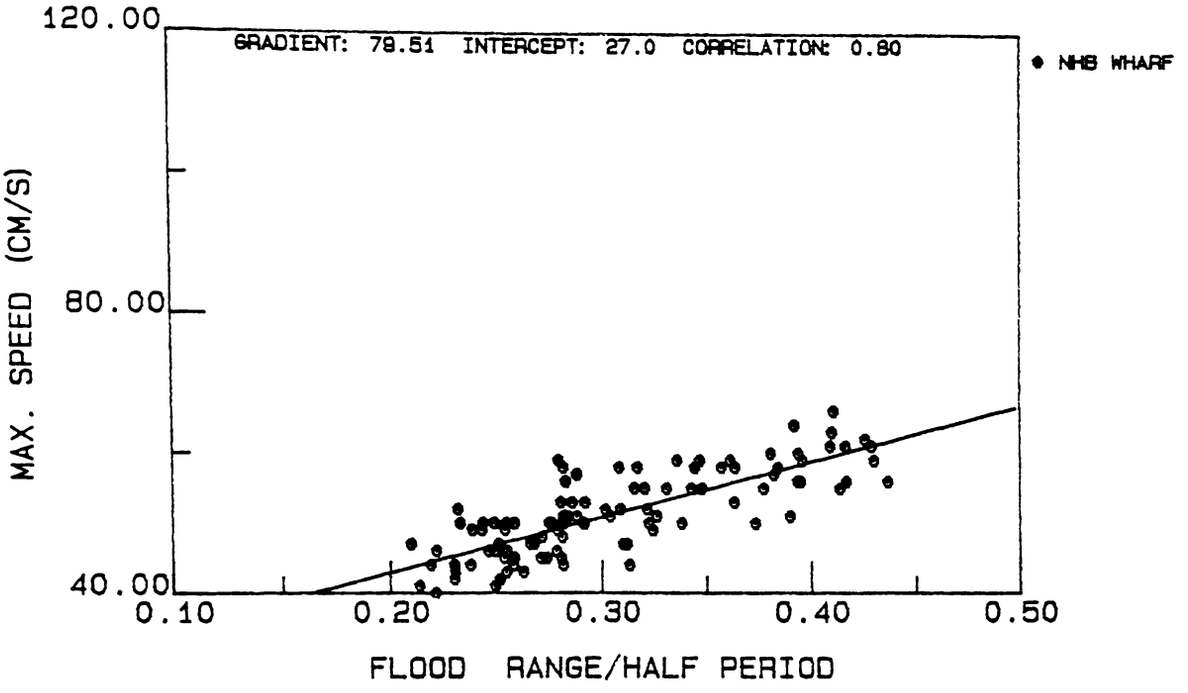

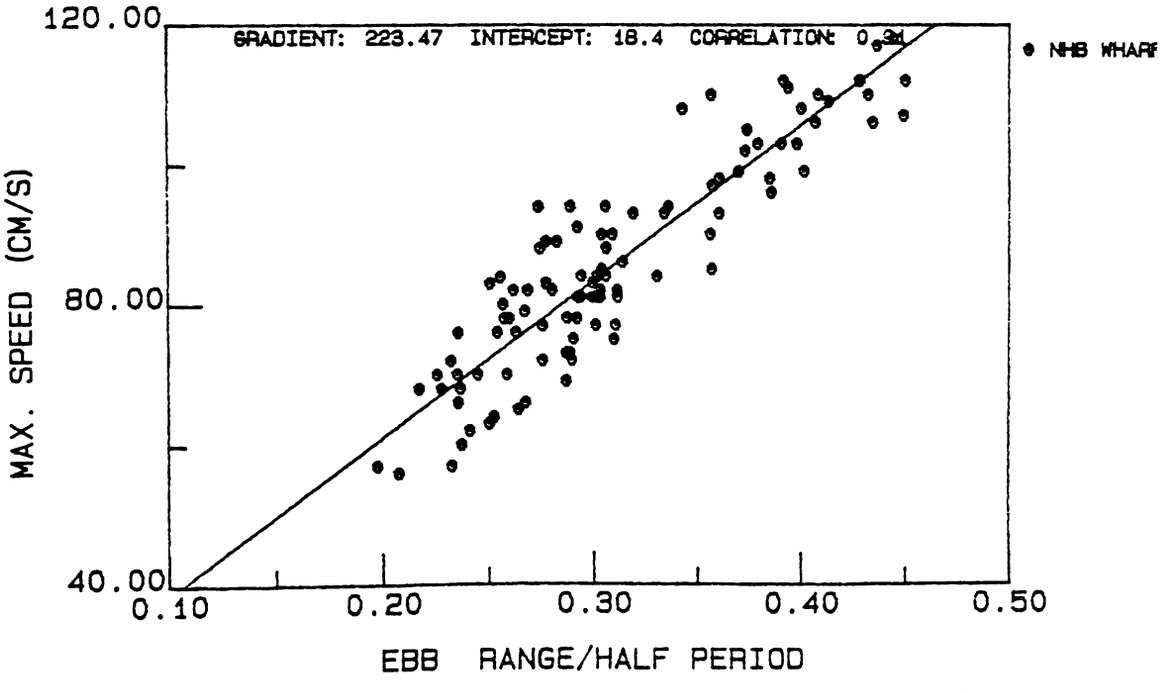

Figure 5.33: Maximum speed attained at the NHB Aanderaa current meter during each half cycle against the ratio of tidal range over the corresponding half tidal period for flood (upper) and ebb half cycles respectively. Best fit linear curves are given.

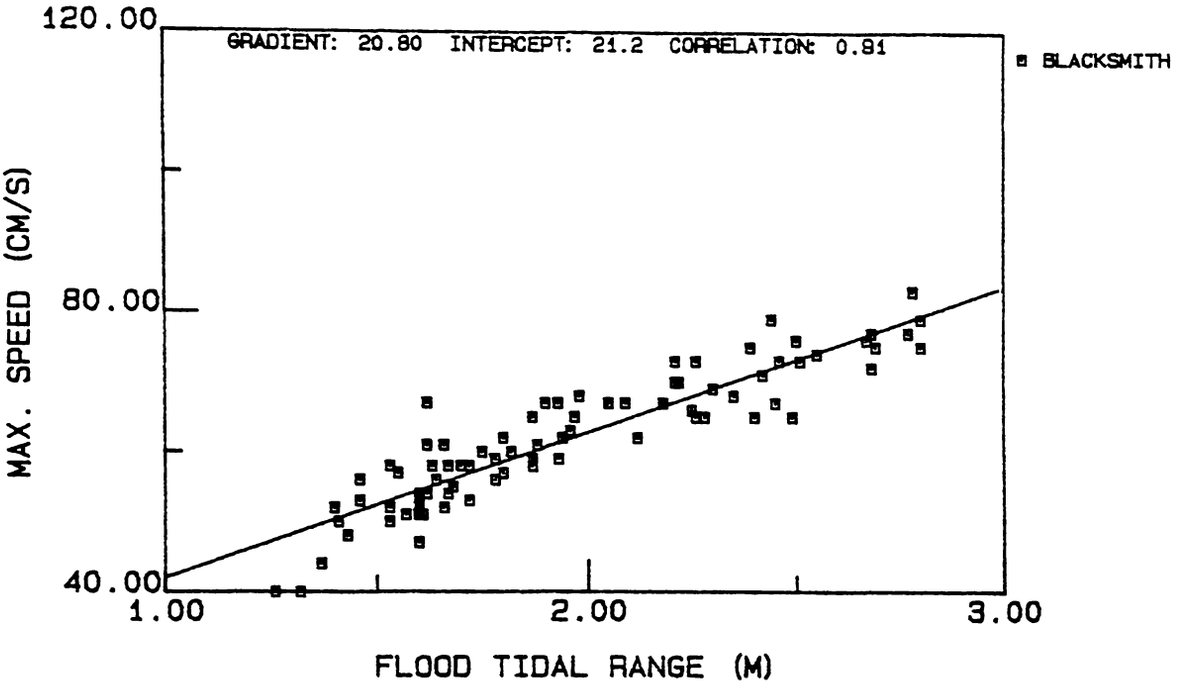

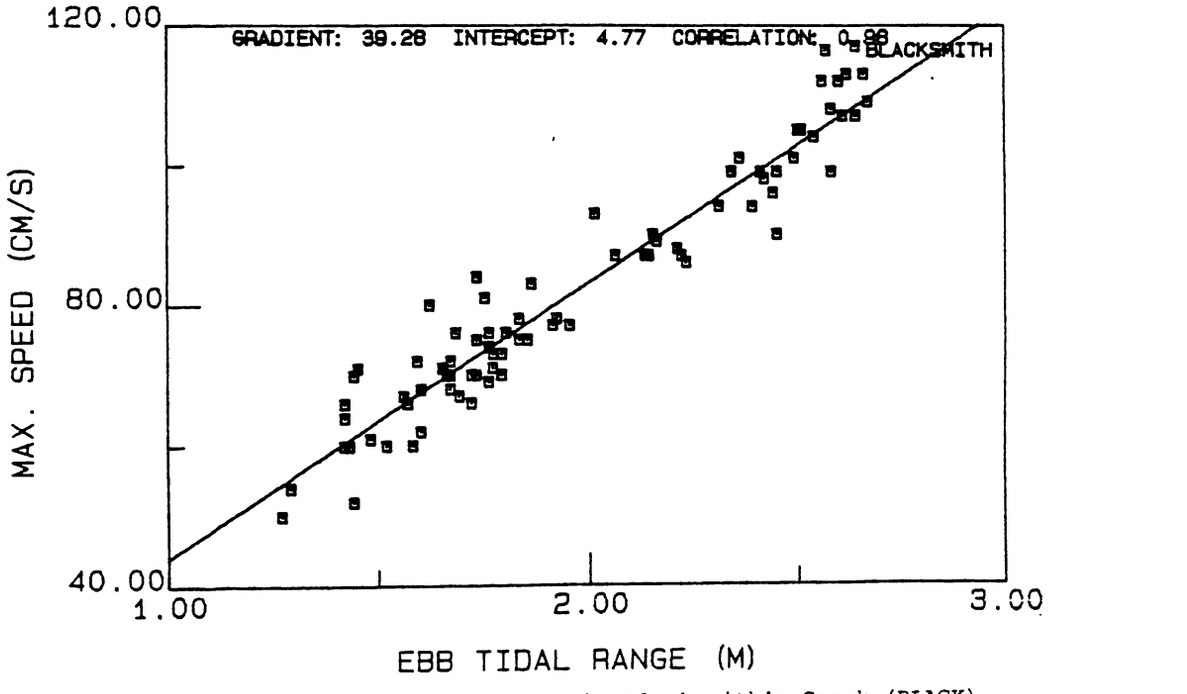

Figure 5.34: Maximum speed attained at the Blacksmith's Creek (BLACK) Aanderaa current meter during each half cycle against the corresponding tidal range for flood (upper) and ebb half cycles respectively. Best fit linear curves are given.

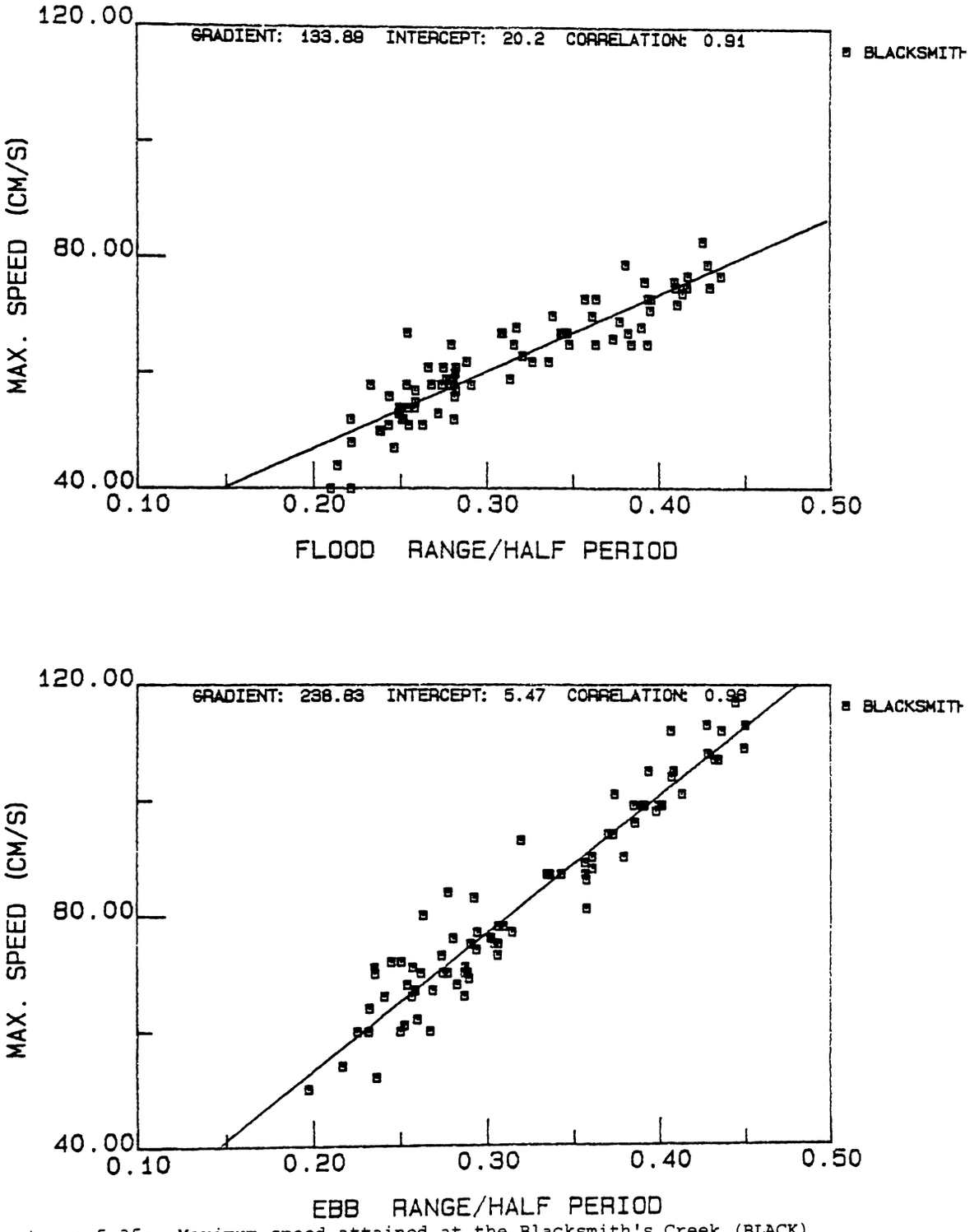

Figure 5.35: Maximum speed attained at the Blacksmith's Creek (BLACK) Aanderaa current meter during each half cycle against the ratio of tidal range over half tidal period for flood (upper) and ebb half cycles respectively. Best fit linear curves are given.

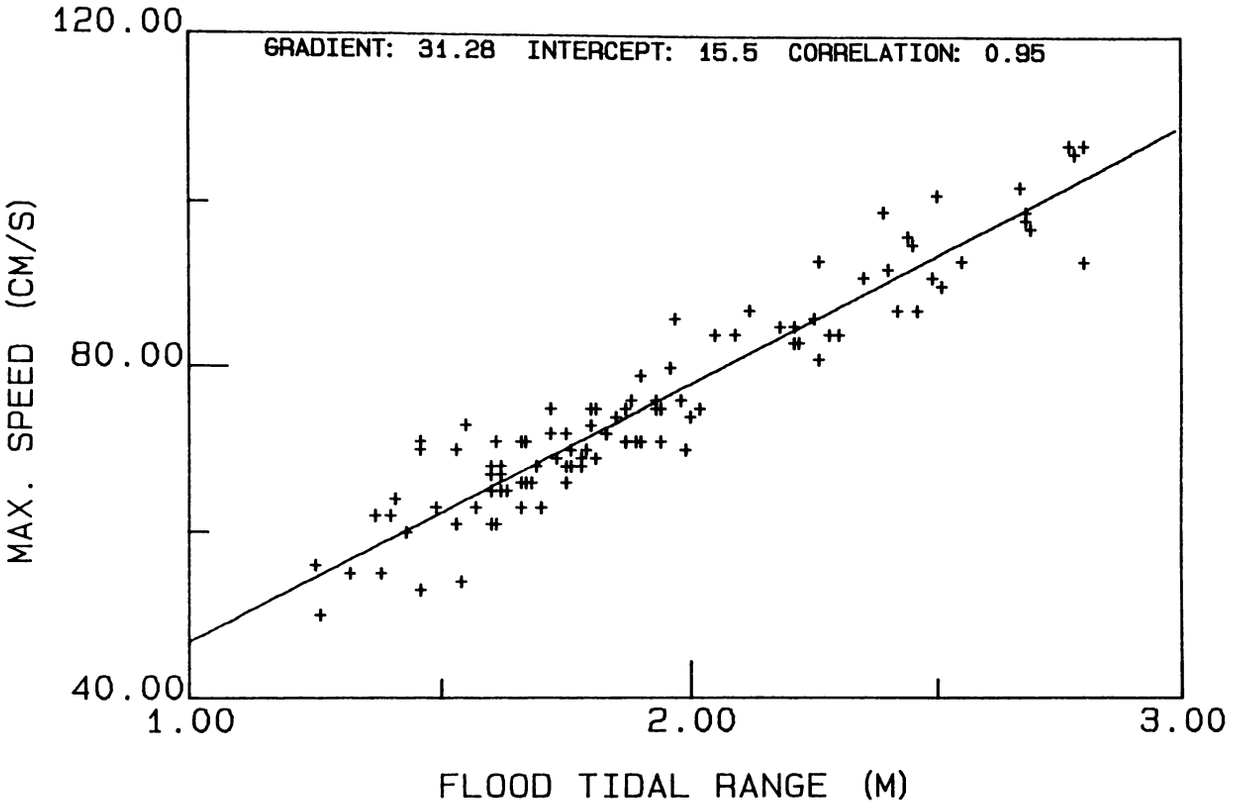

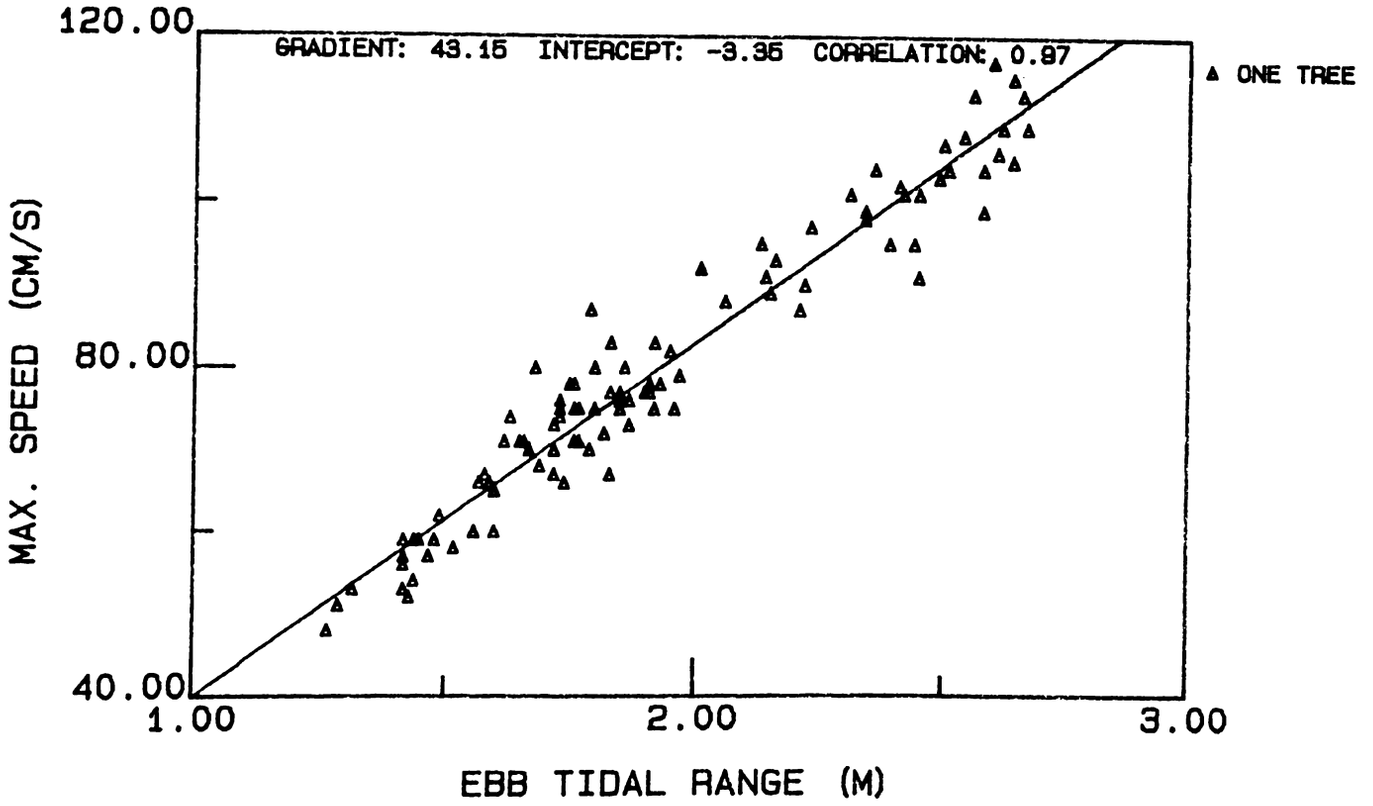

Figure 5.36: Maximum speed attained at the One Tree Point (OTP) Aanderaa current meter during each half cycle against the corresponding tidal range for flood (upper) and ebb half cycles respectively. Best fit inlear curves are given.

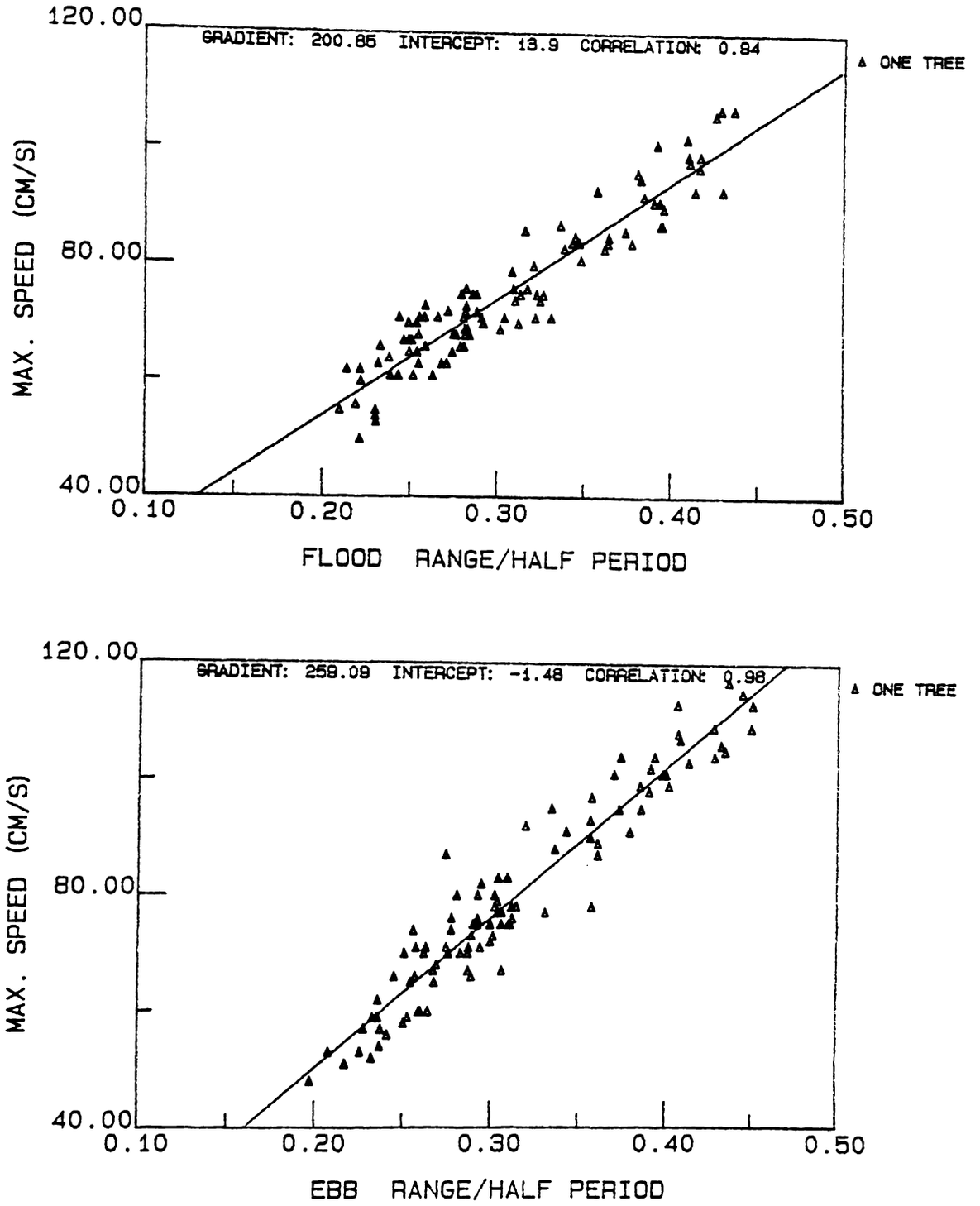

Figure 5.37: Maximum speed attained at the One Tree Point (OTP) Aanderaa current meter during each half cycle against the ratio of tidal range over half tidal period for flood (upper) and ebb half cycles respectively. Best fit linear curves are given.

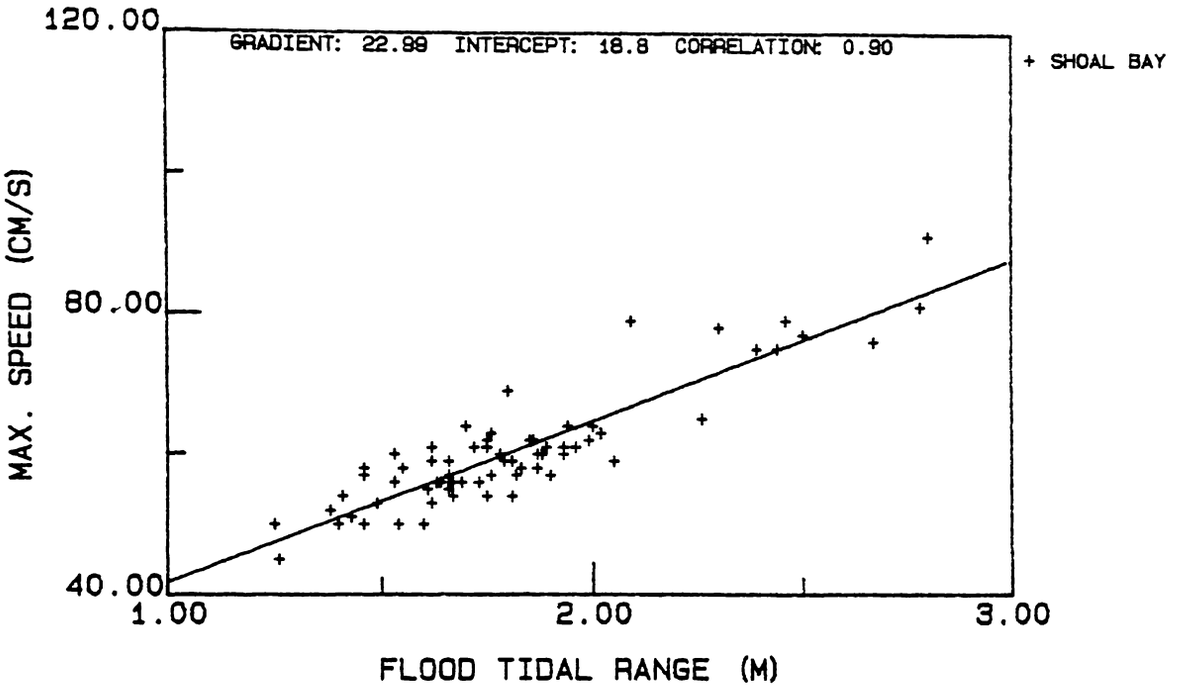

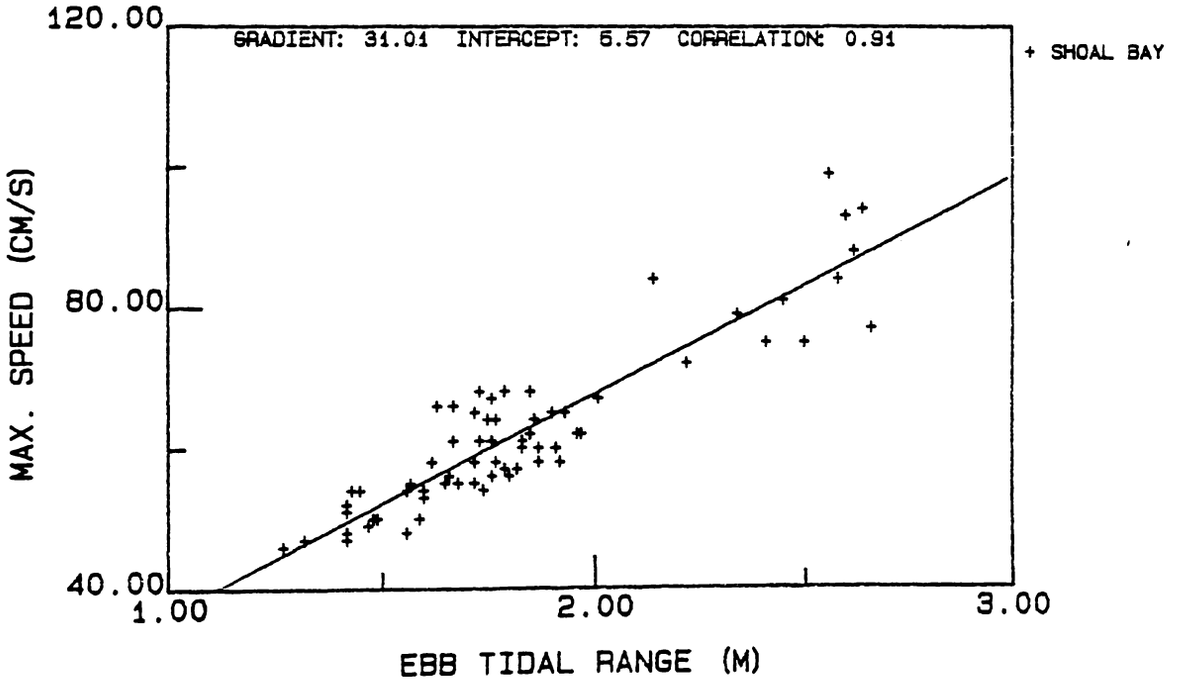

Figure 5.38: Maximum speed attained at the Shoal Bay (SHOAL) Aanderaa current meter during each half cycle against the corresponding tidal range for flood (upper) and ebb half cycles respectively. Best fit linear curves are given.

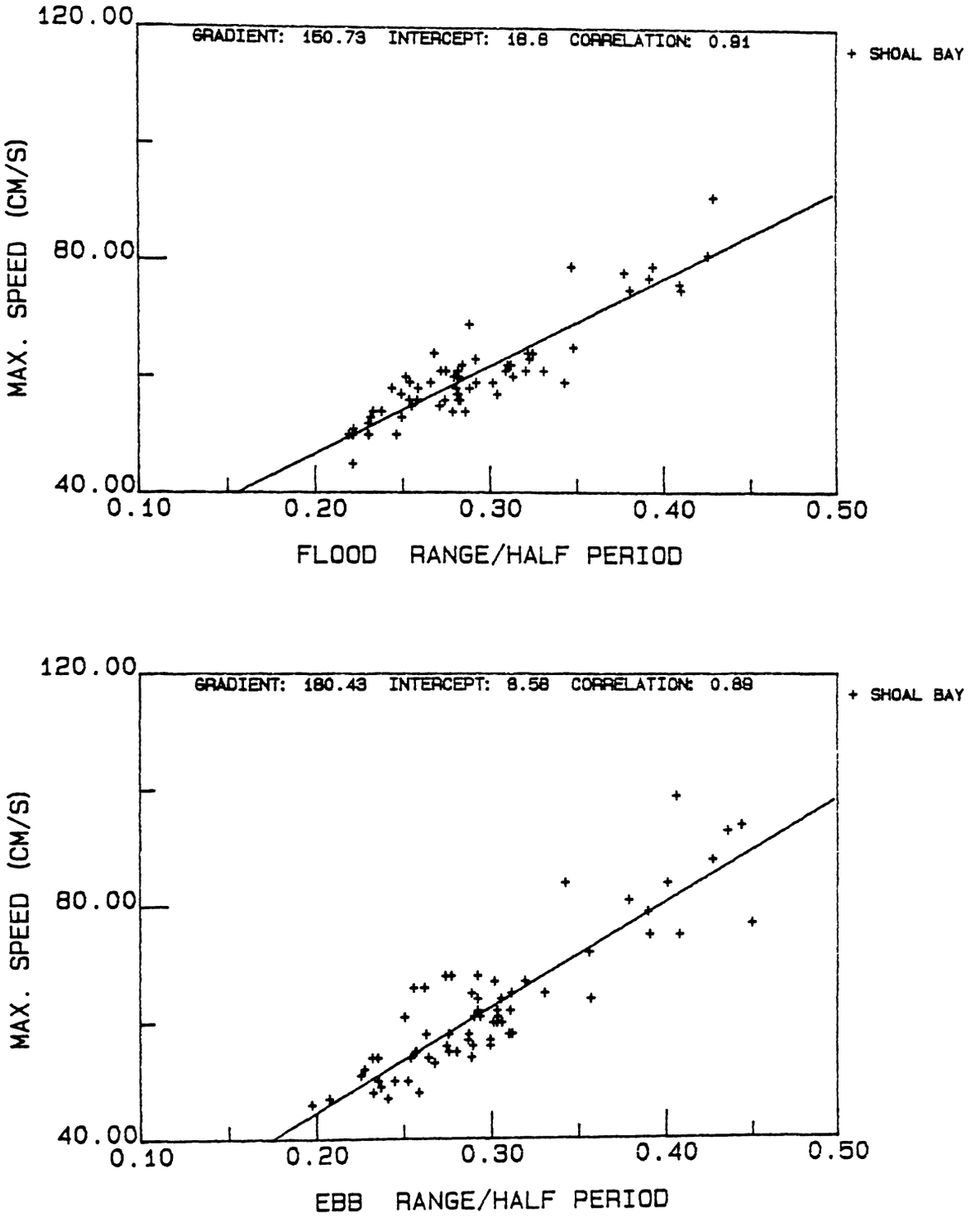

Figure 5.39: Maximum speed attained at the Shoal Bay (SHOAL) Aanderaa current meter during each half cycle against the ratio of tidal range over half tidal period for flood (upper) and ebb half cycles respectively. Best fit linear curves are given.

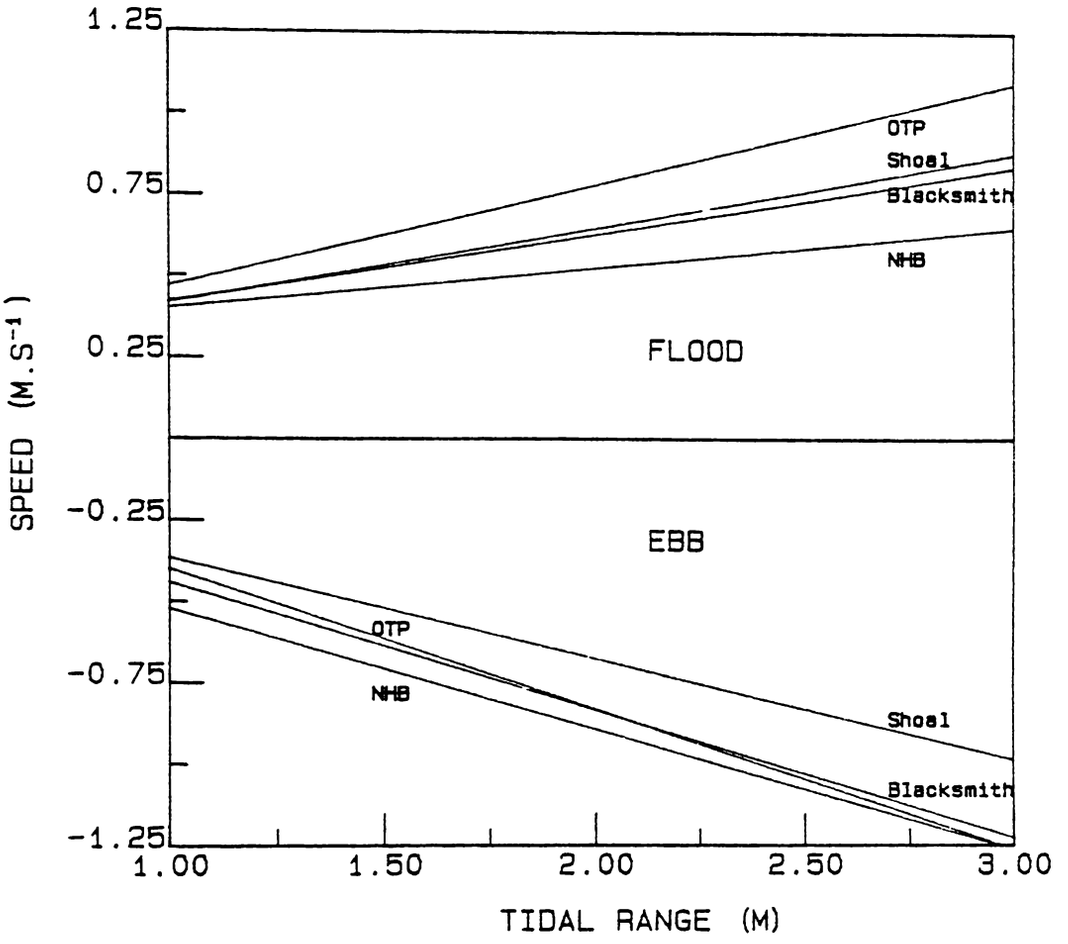

Figure 5.40: Best fit linear curves relating the maximum speed attained at the Aanderaa current meter sites during each ebb and flood half cycle to the corresponding tidal range.

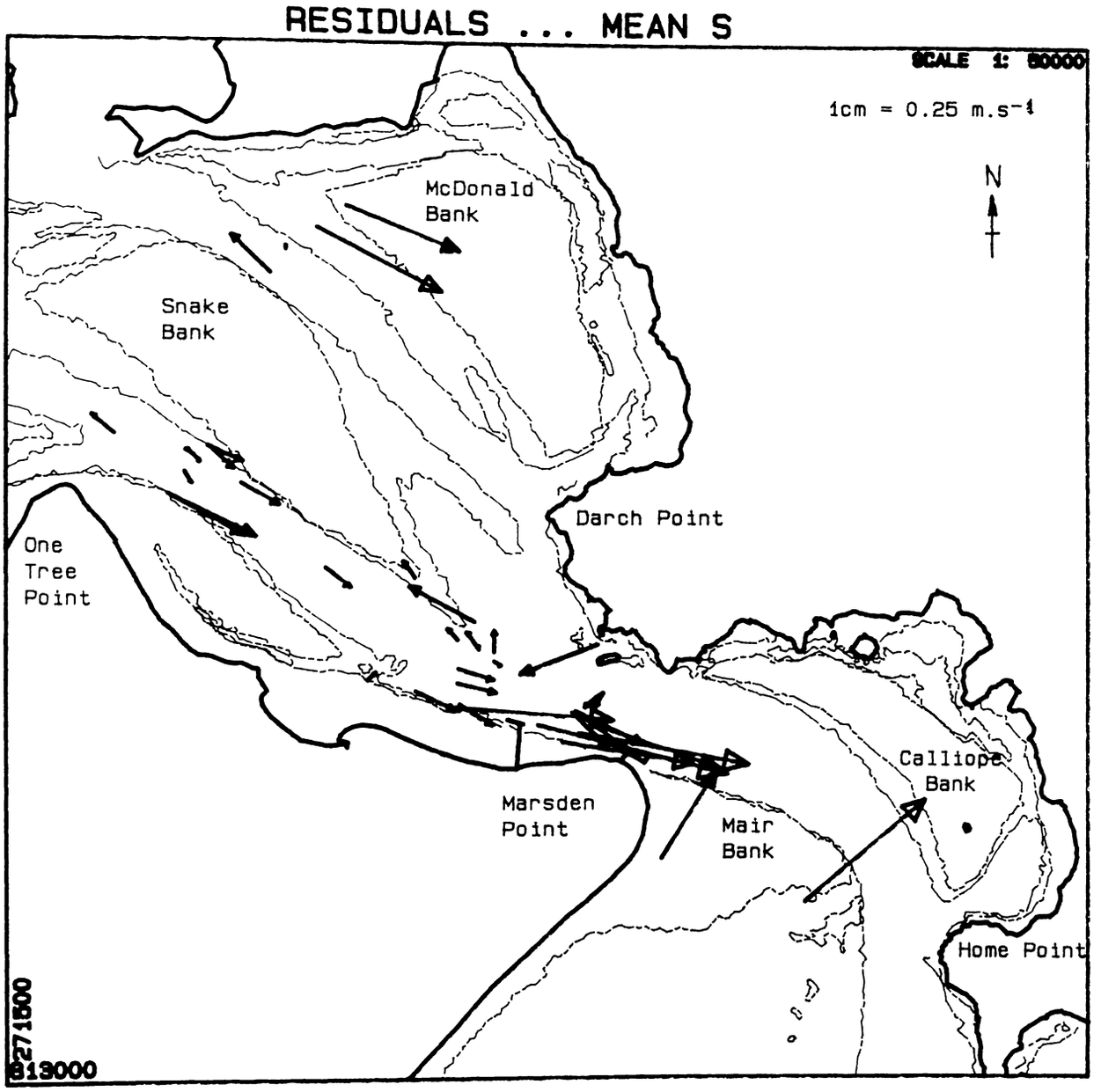

Figure 5.41: Tidal cycle residual mean vertically-averaged velocities for periods when the speed exceeded 0.4 $m.s^{-1}$ and power q=1. at the Braystoke sites. Velocities are plotted as 1=cm representing 0.25 $m.s^{-1}$.

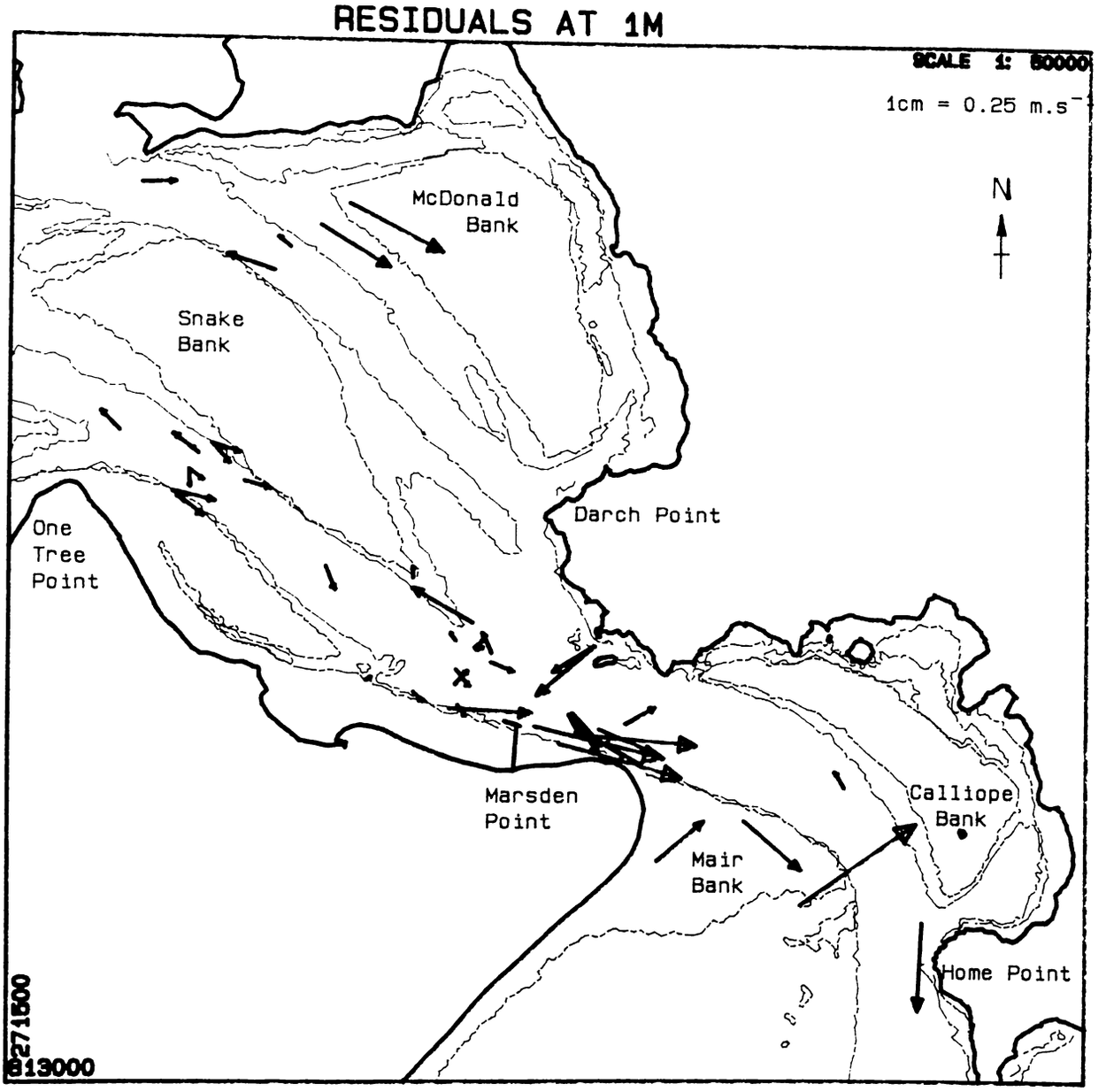

Figure 5.42: Tidal cycle residual velocities at 1m above the sea bed for periods when speed exceeded 0.33 $m.s^{-1}$ and power q=1 at the Braystoke sites. Velocities are plotted as 1=cm representing 0.25 $m.s^{-1}$.

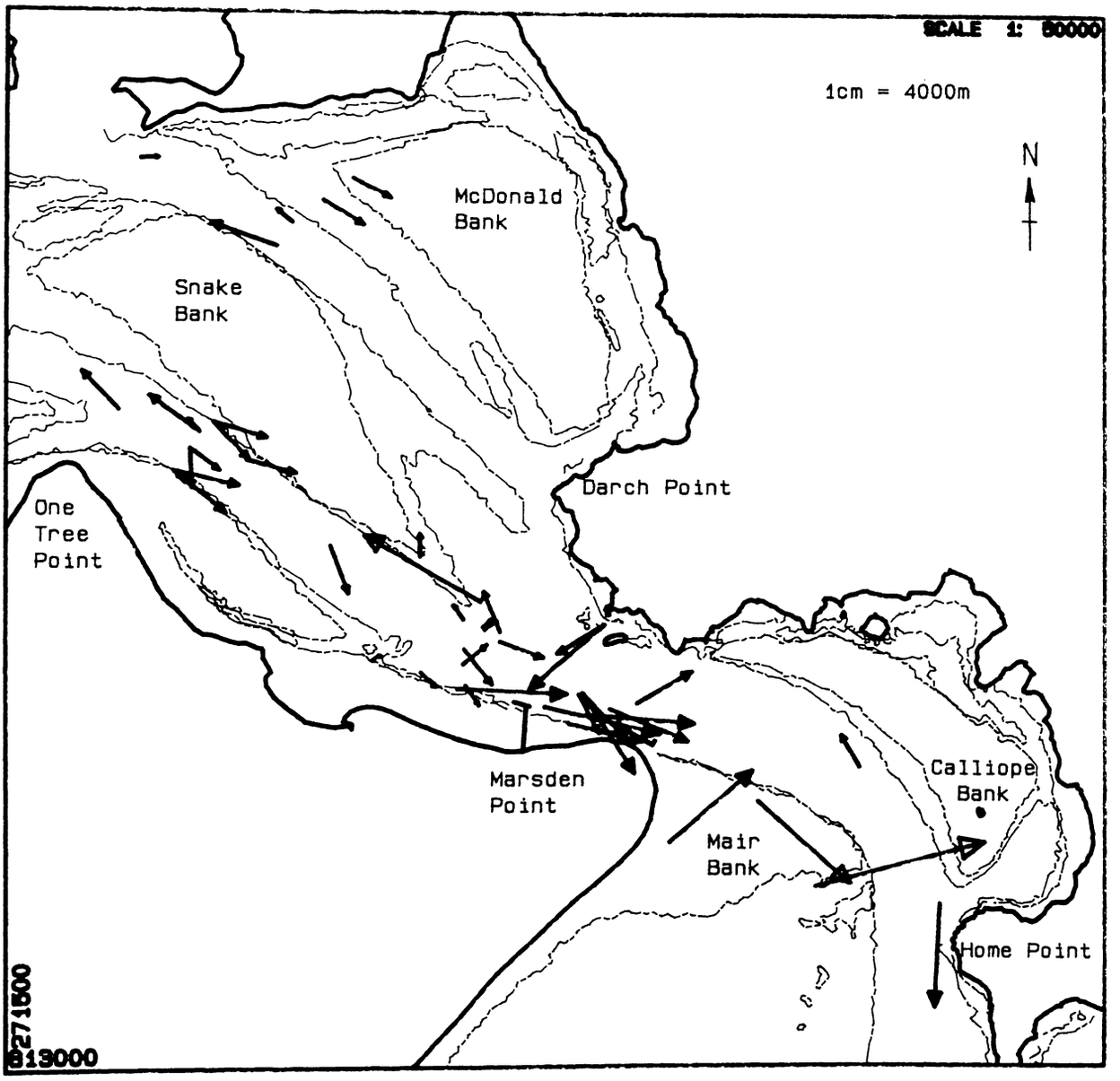

Figure 5.43: Tidal cycle residual distances at 1m above the sea bed for periods when the speed exceeded 0.33 $m.s^{-1}$ and power q=1 at the Braystoke sites. Distances are plotted as 1 cm representing 4000m.

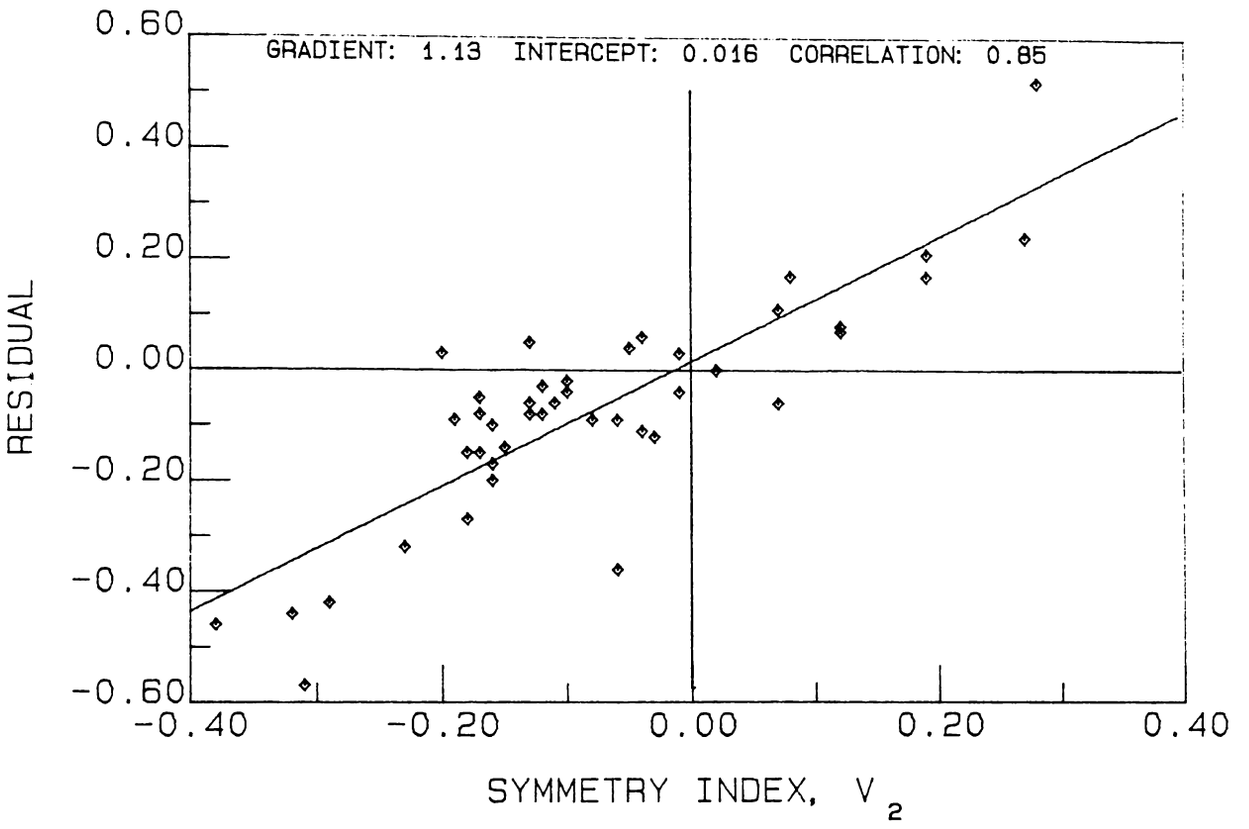

Figure 5.44: The residual velocity at 1m for periods when the velocity exceeded 0.33 $m.s^{-1}$ and power q=1, against Allen's (1980) Velocity Symmetry Index.

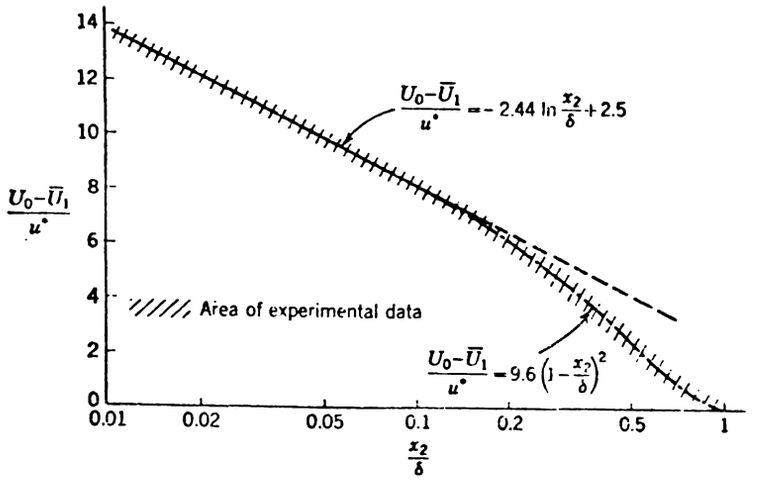

Figure 6.1: Logarithmic plot of velocity distributions in the outer part of turbulent boundary layers (Clauser, F.H., "Advances in Applied Mechanics", vol. 4, p. 1, New York, 1956), after Hinze (1959).

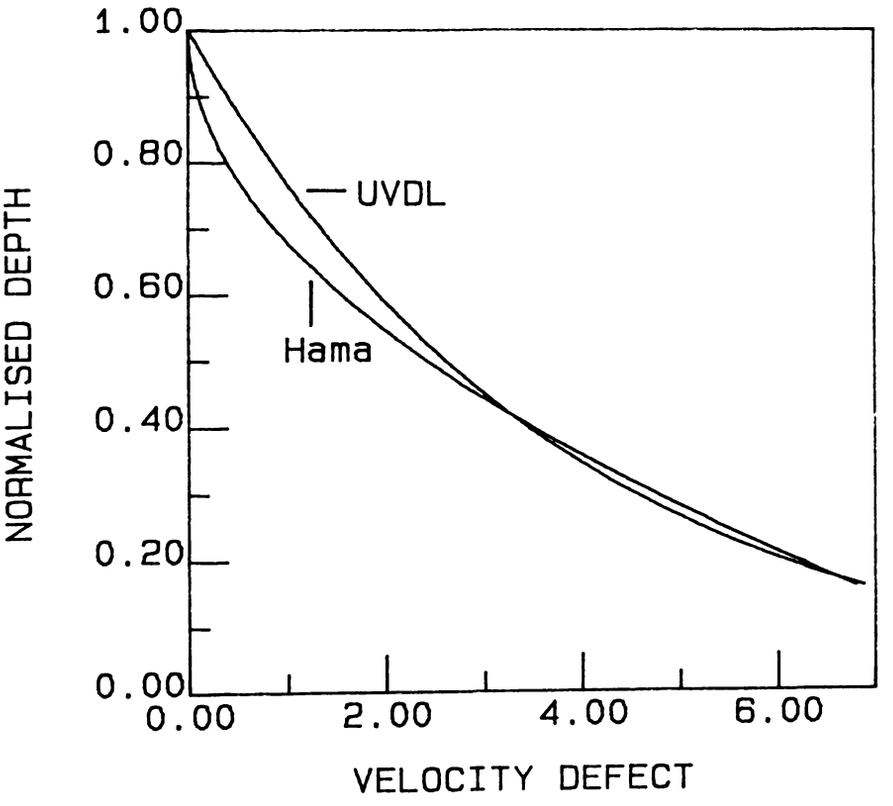

Figure 6.2: The Universal Velocity Defect Law and the Hama (1953) Defect Law, with the normalised depth (z/δ) against the velocity defect $[(U_\infty - u)/u_*]$.

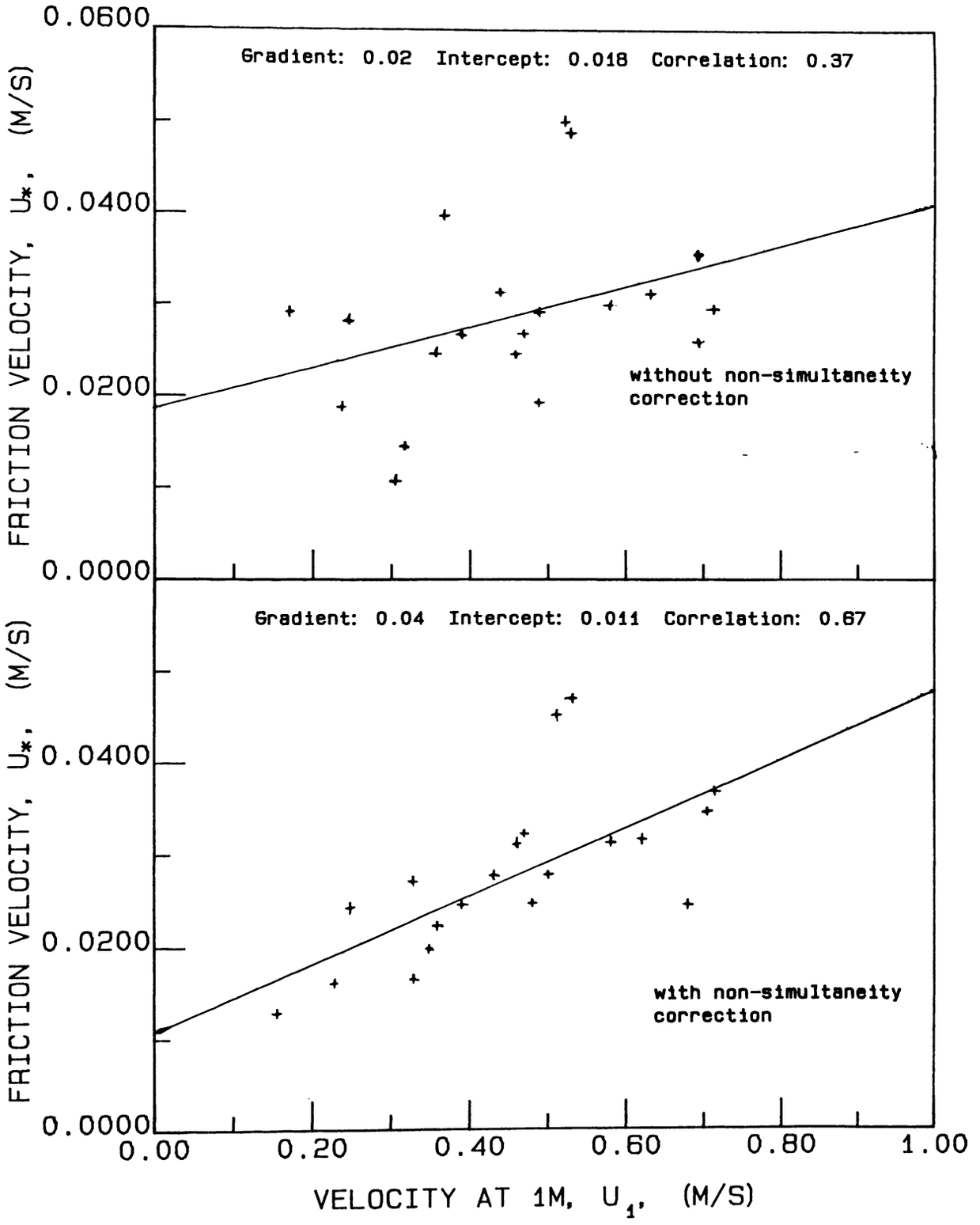

Figure 6.3: Relationship of friction velocity to 1m speed without (upper) and with the non-simultaneity correction.

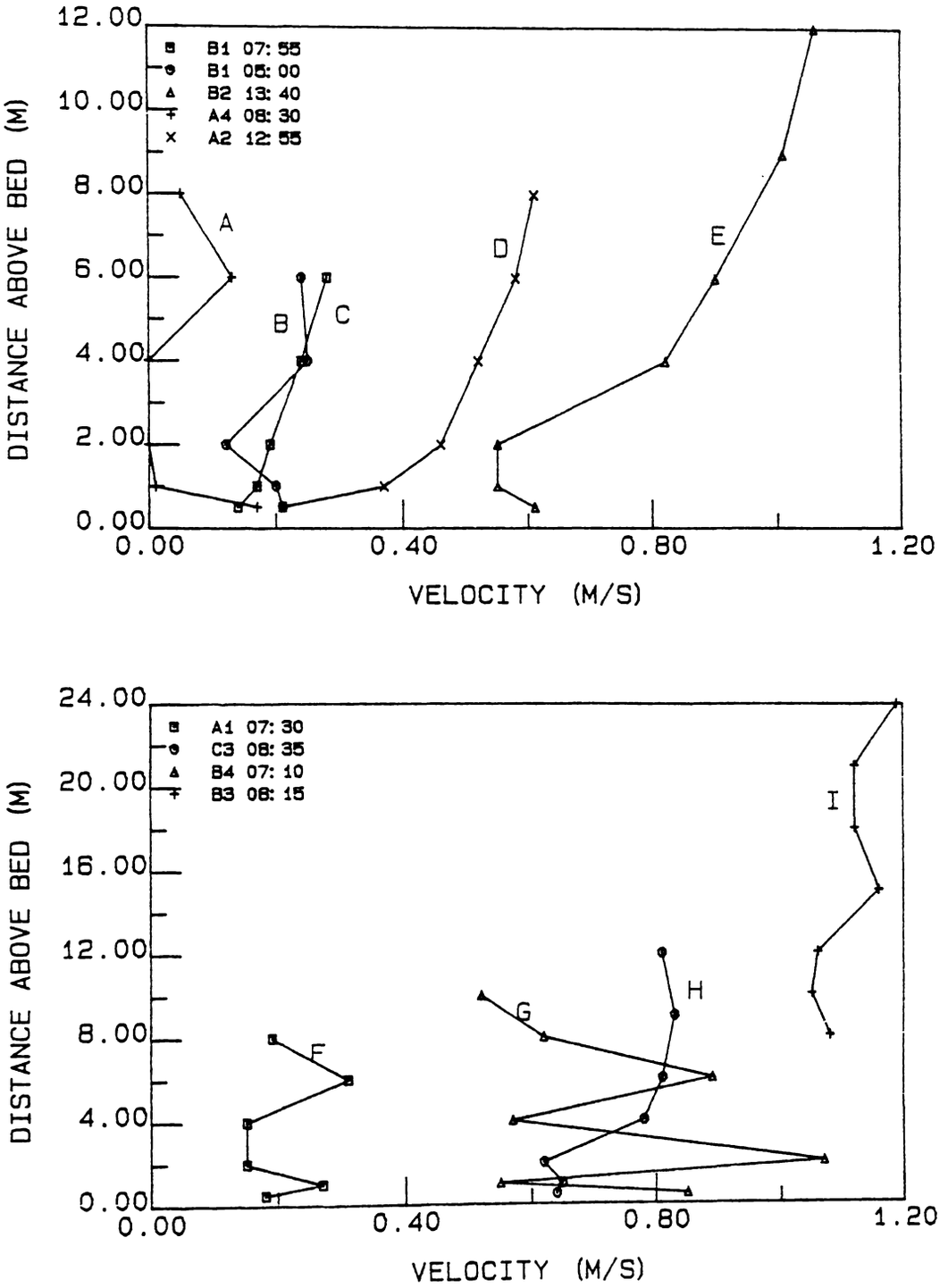

Figure 6.4: Examples of measured vertical velocity profiles in Whangarei Harbour.

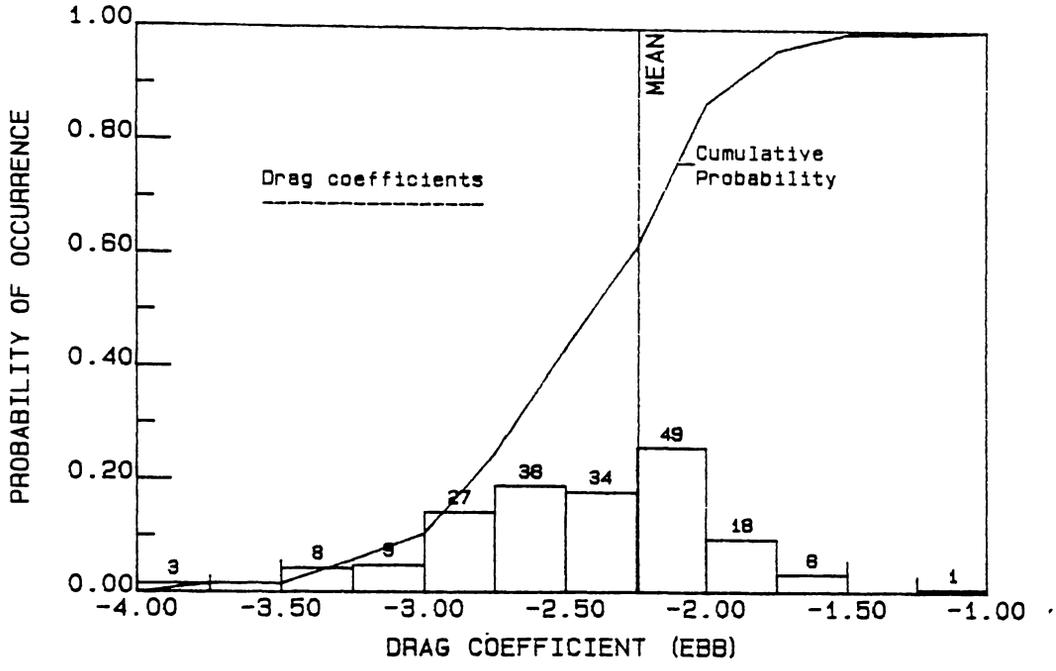

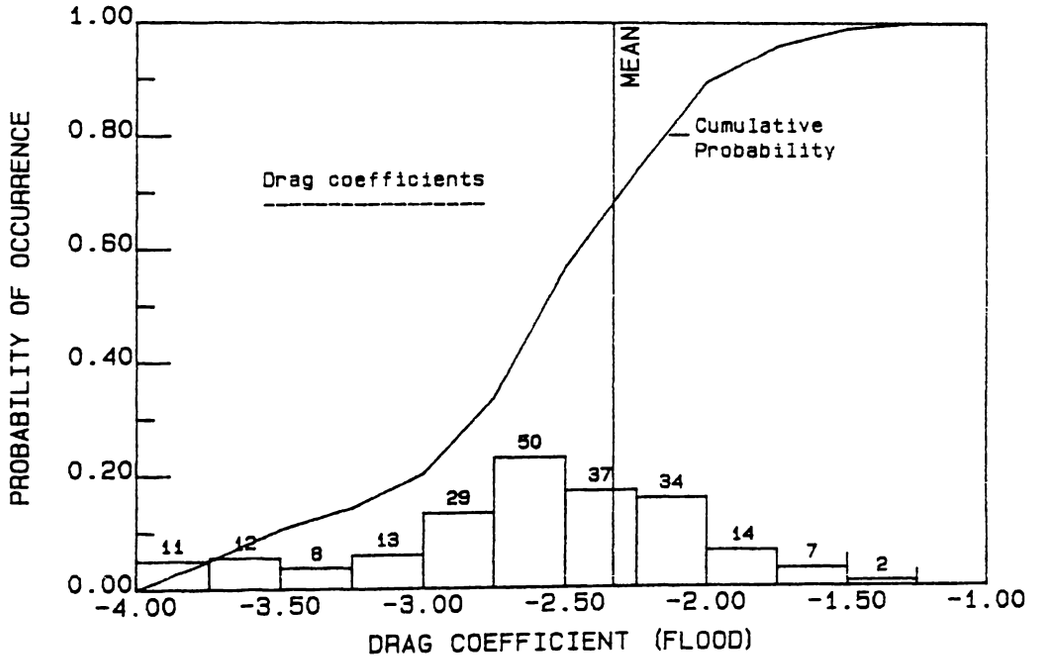

Figure 6.5: Ebb (upper) and flood distributions of the Drag Coefficient for $u_1 > 0.3$ m.s^{-1}. Numbers above bars are the number of occurrences in each bin.

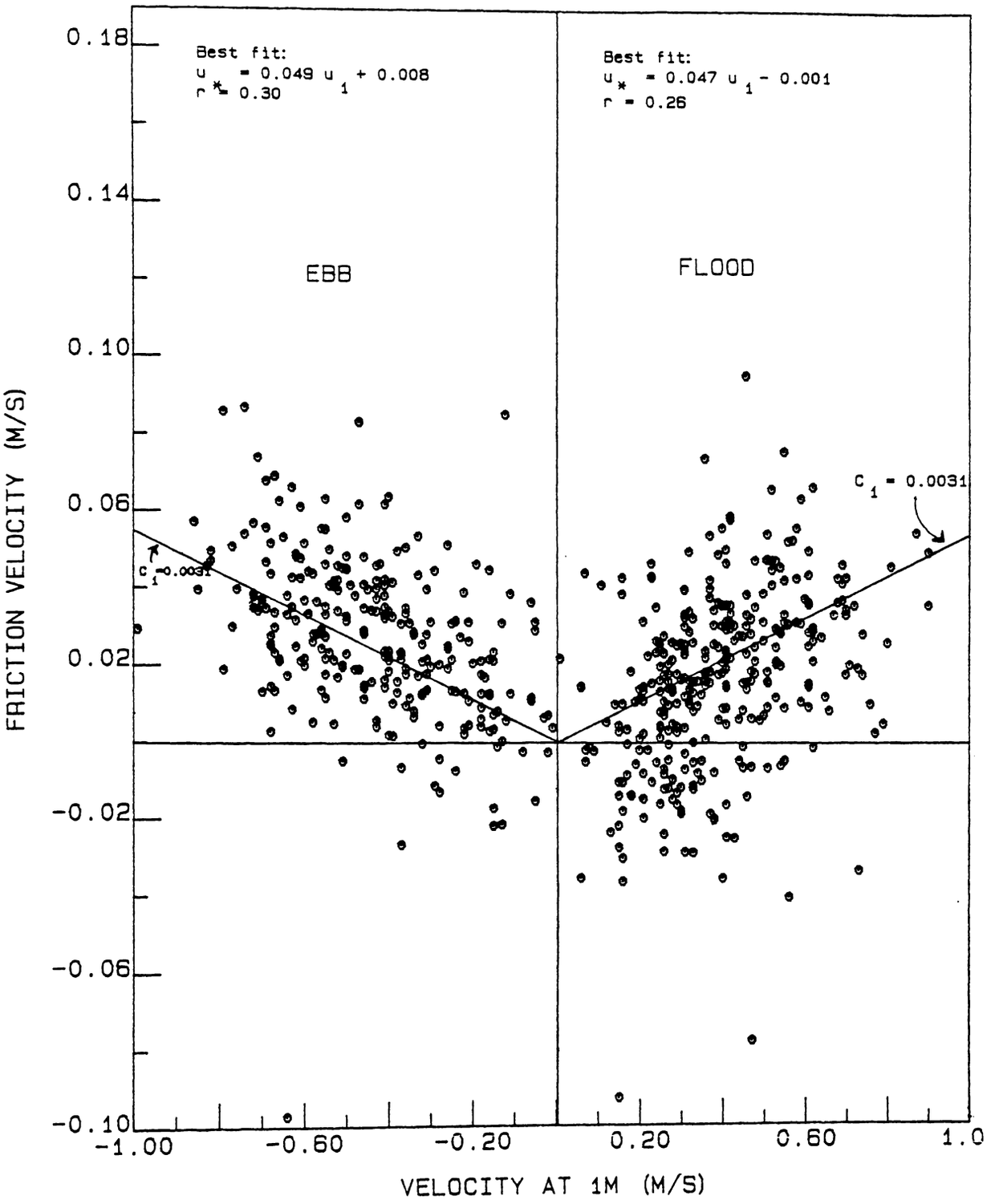

Figure 6.6: Friction velocity, u_*, against the 1m speed, u_1.

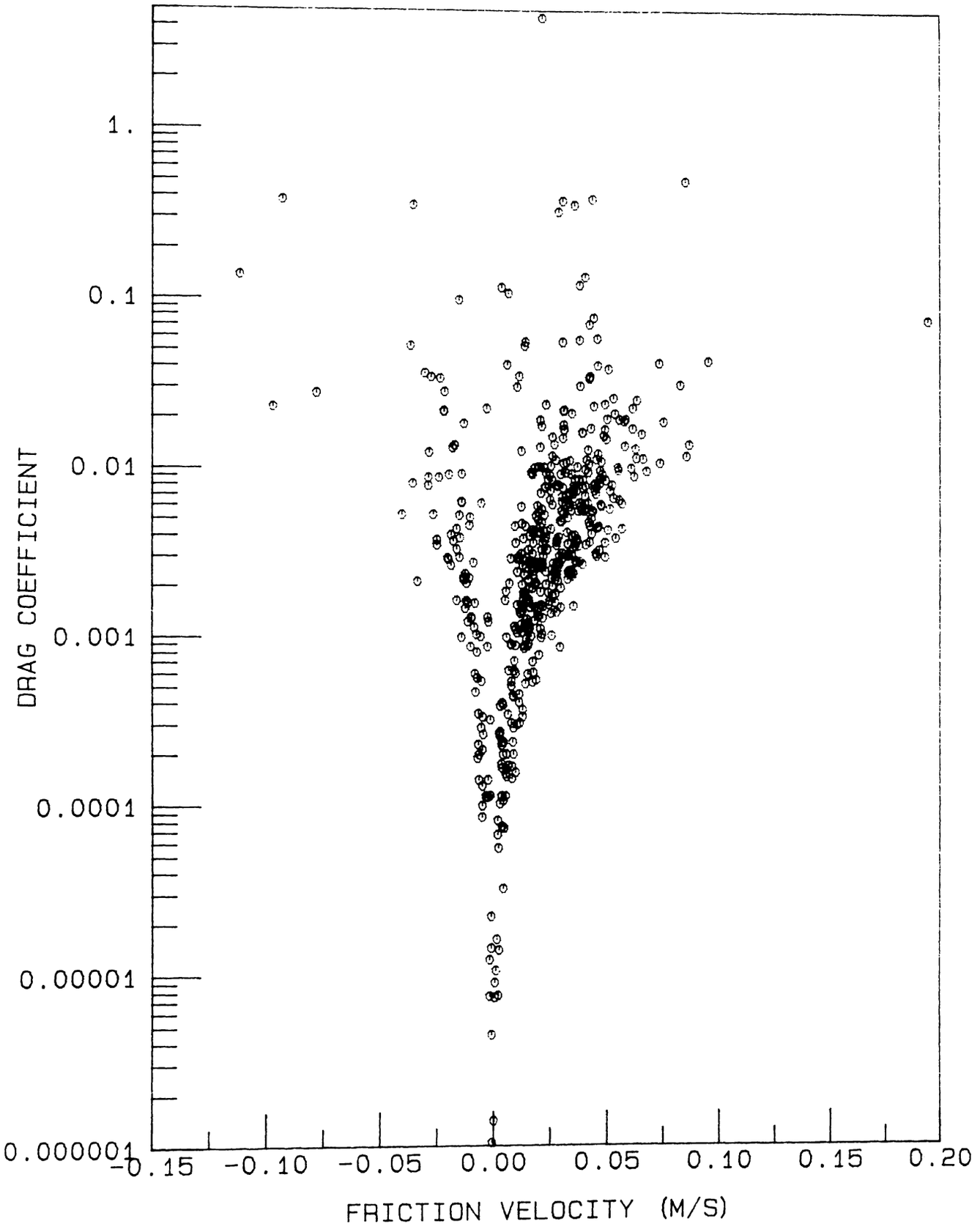

Figure 6.7: Drag Coefficient, C_1, against the friction felocity, u_*, for all sites combined and including those with $u_1<0.3$ m.s^{-1}.

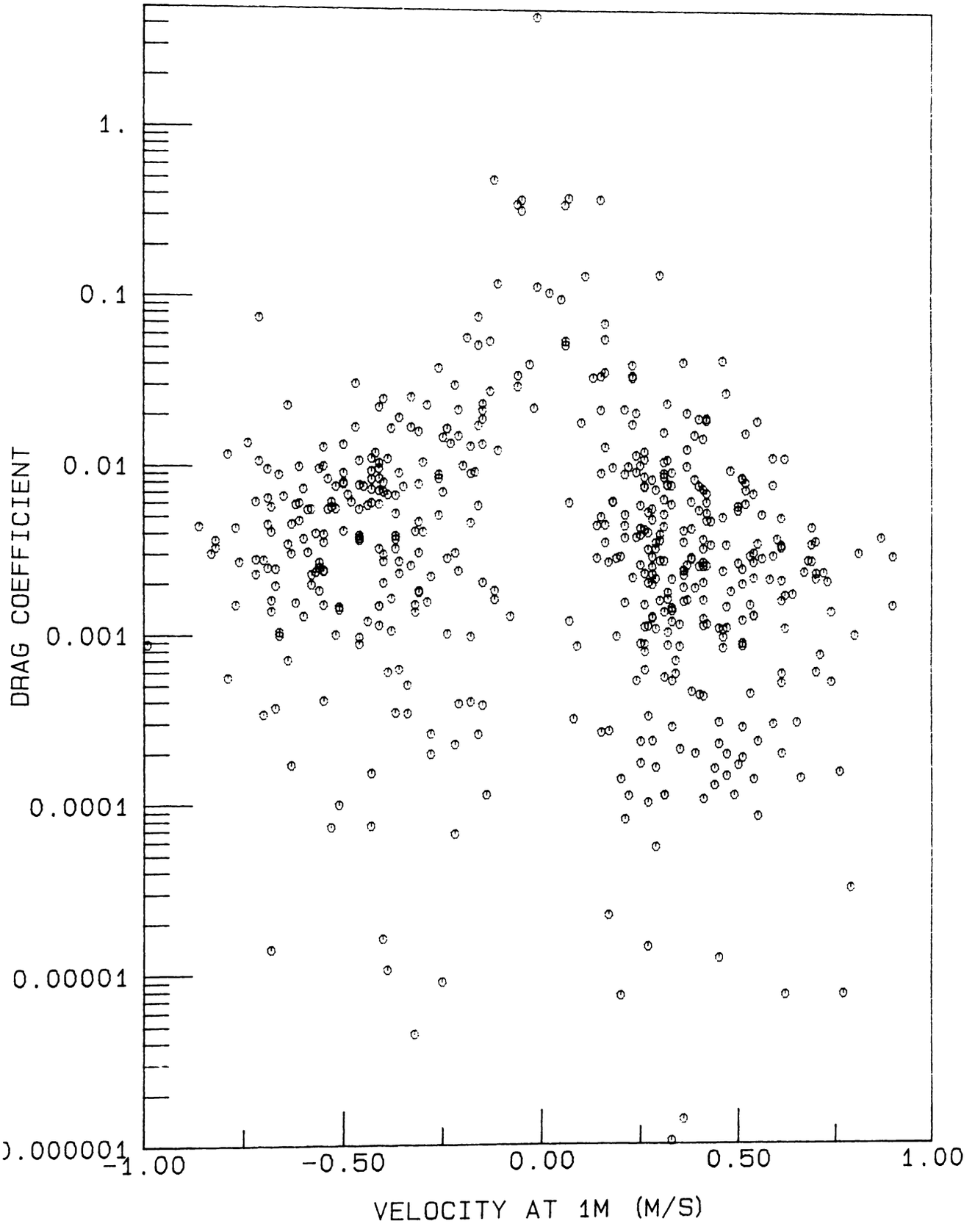

Figure 6.8: Drag Coefficient, C_1, against the 1m speed, u_1, for all sites combined, and including those with $u_1<0.3$ m.s^{-1}.

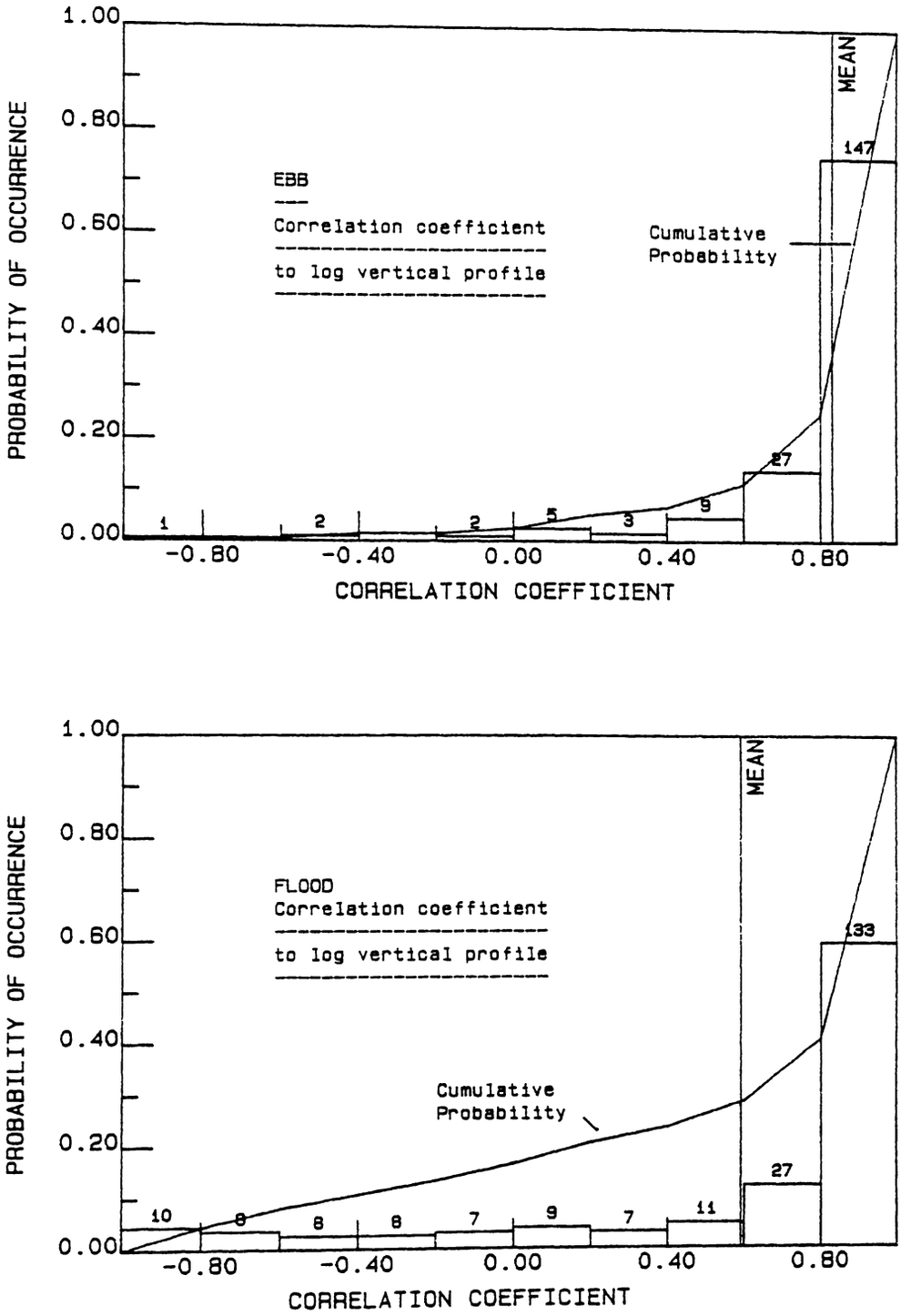

Figure 6.9: Distribution of the correlation coefficient representing the goodness of fit of the measured velocities to the logarithmic profile for the ebb (upper) and flood with all sites combined.

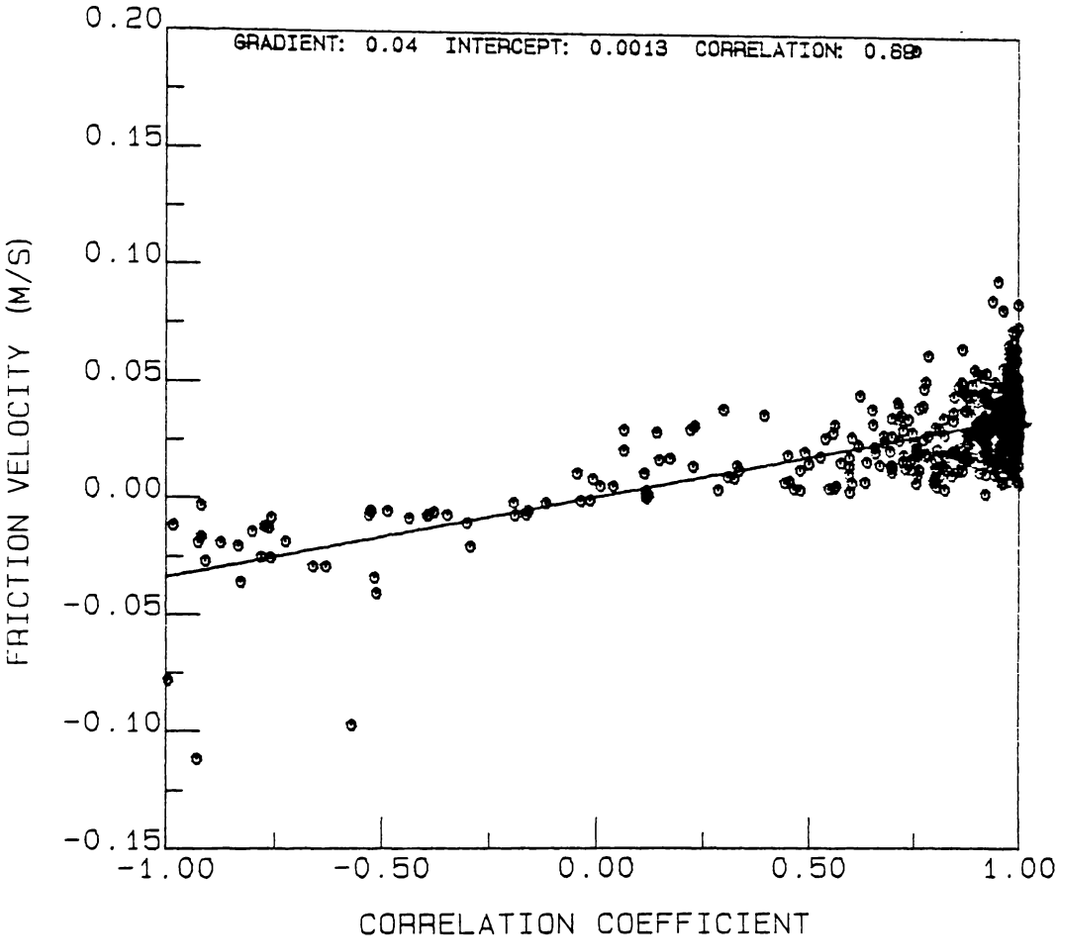

Figure 6.10: Friction velocity, u_*, against the correlation coefficient representing the goodness of fit to the logarithmic profile, r, for all sites combined.

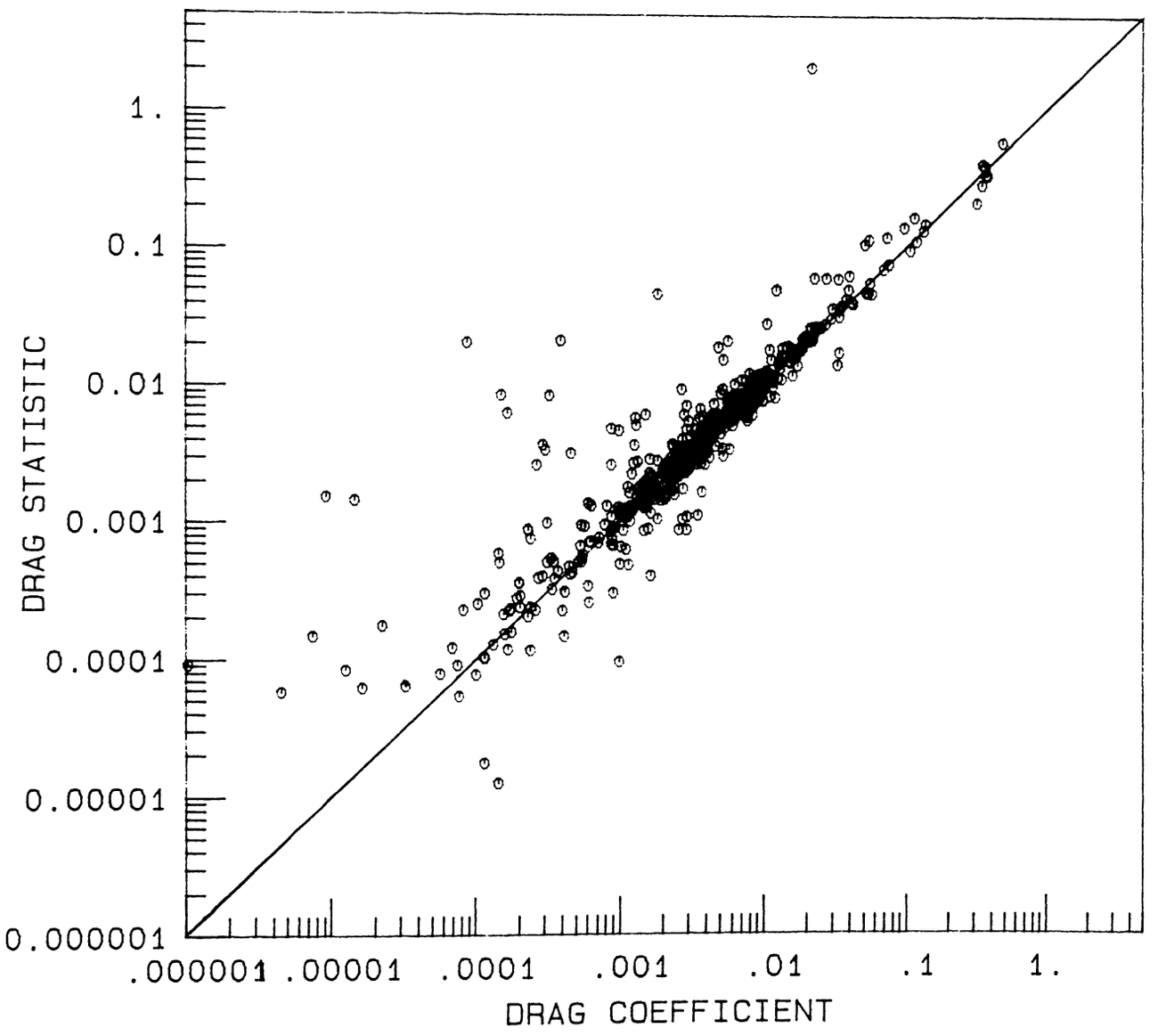

Figure 6.11: Drag Statistic, C_{DS}, against the Drag Coefficient, C_l, for all sites combined. Best fit linear curve had a correlation coefficient of 0.96.

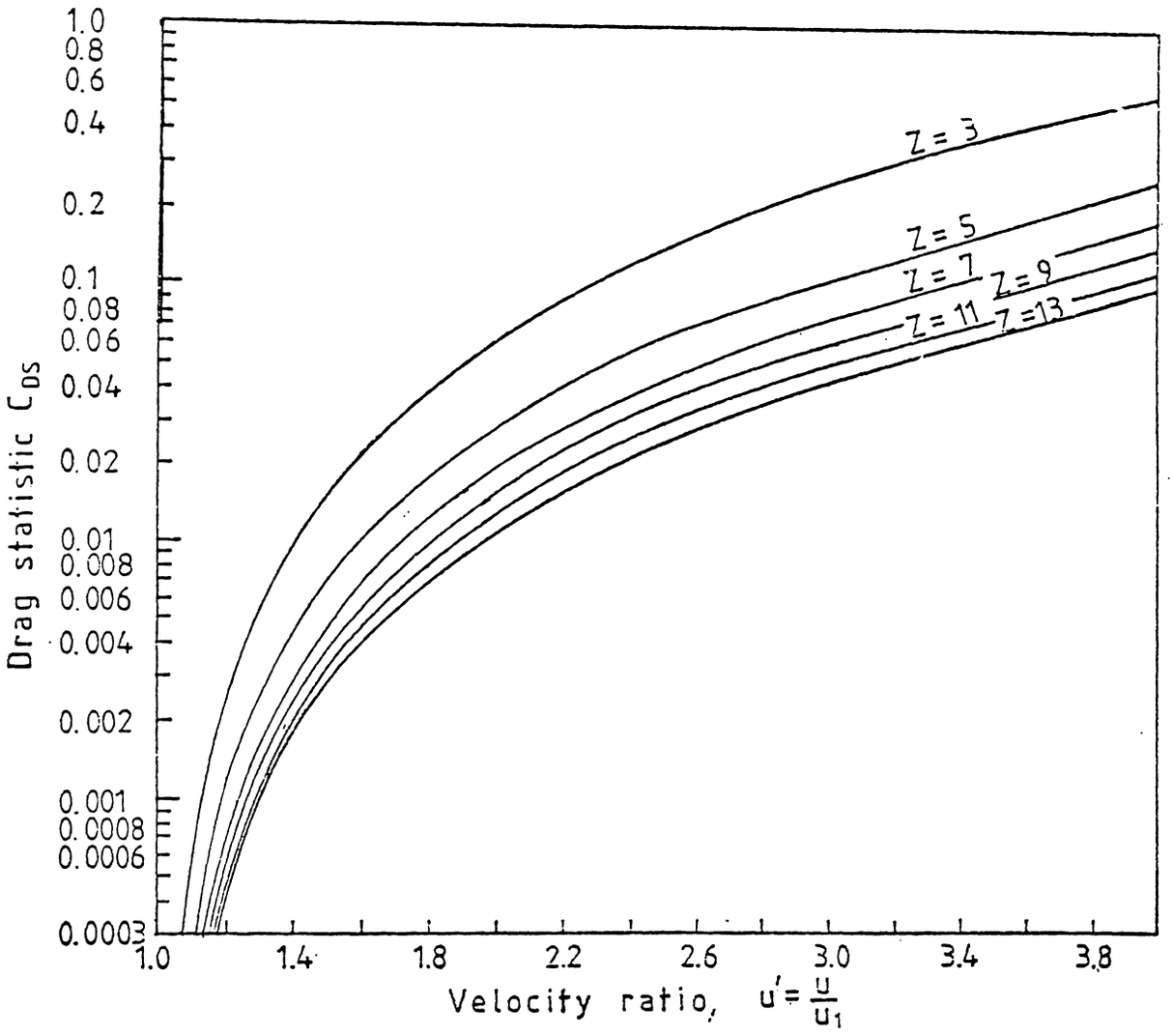

Figure 6.12: Family of curves to obtain the Drag Statistic C_{DS} against the velocity ratio, u/u_1 where u was measured z metres above the sea bed.

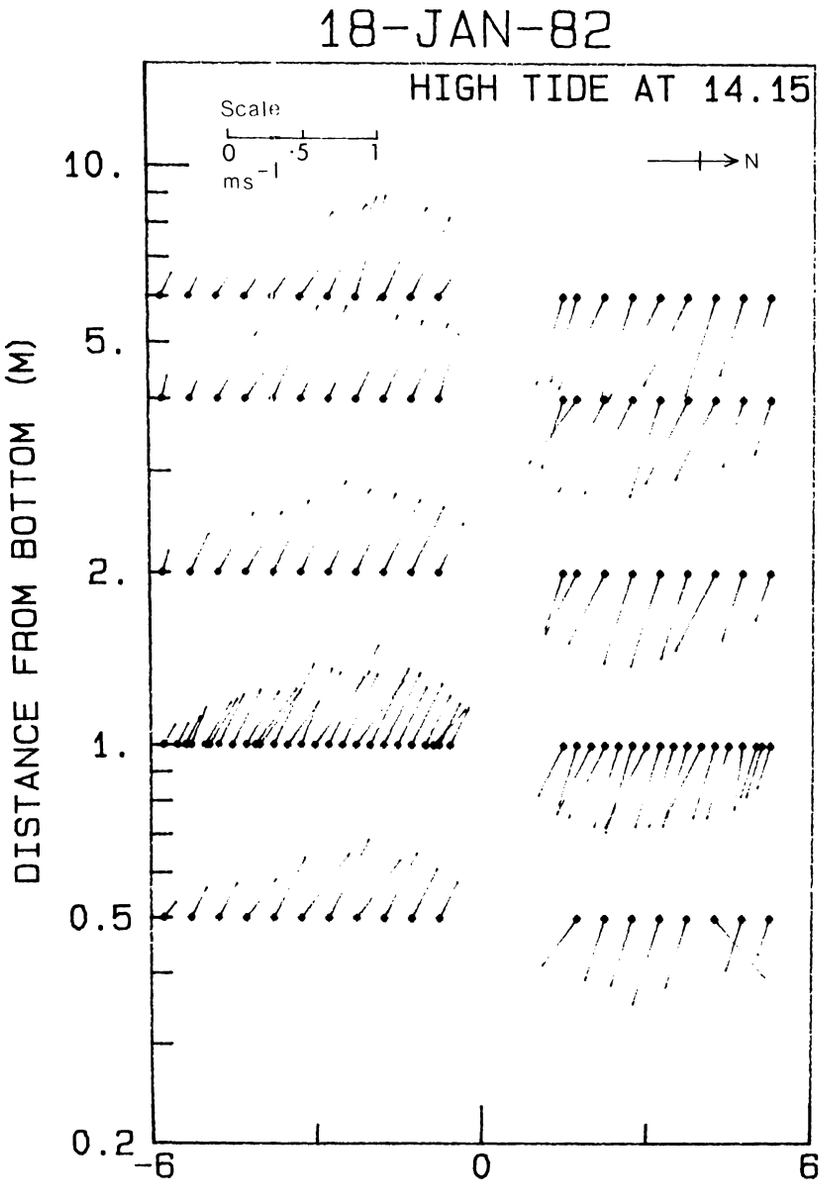

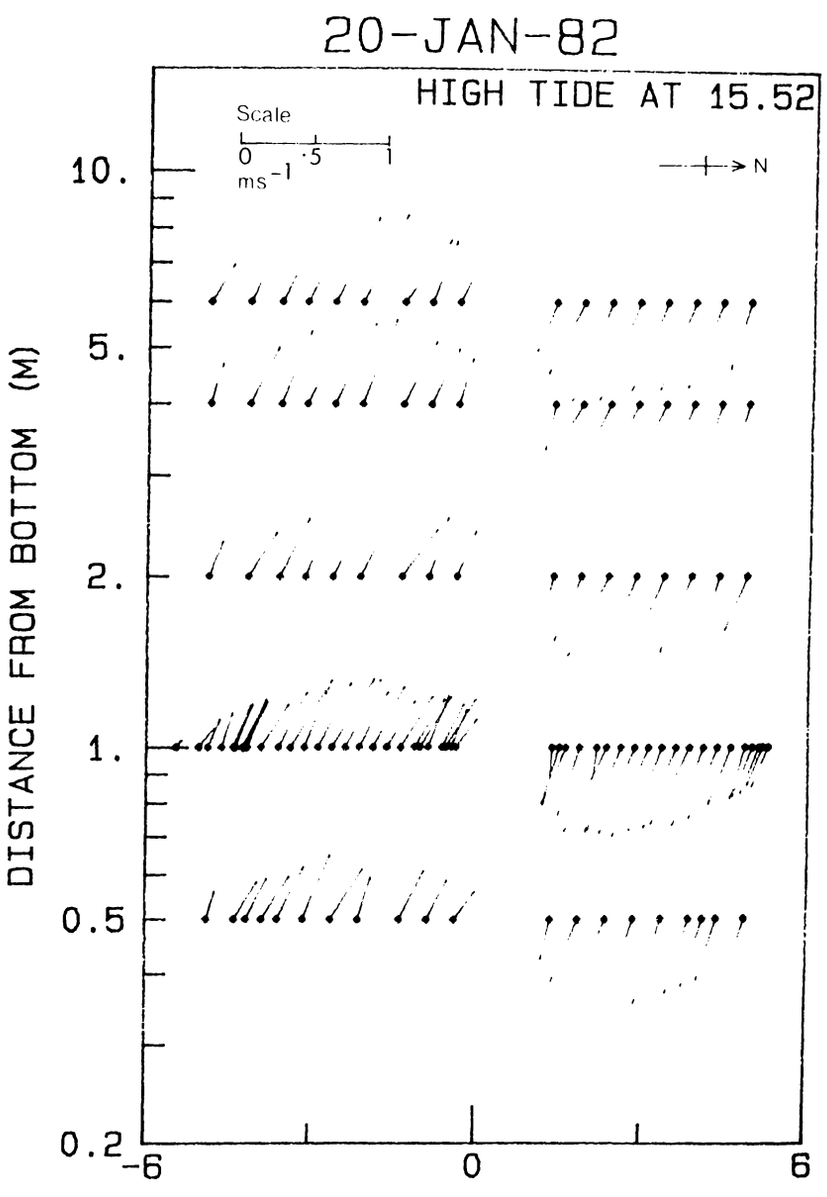

Figures 6.13 (left) and 6.14: Velocities measured during the S-series at S1 (18-Jan-82) and S2 (20-Jan-82) after correction for non-simultaneity. Velocities are plotted as 10mm representing 0.5 $m.s^{-1}$ with True North directed towards the right of the page.

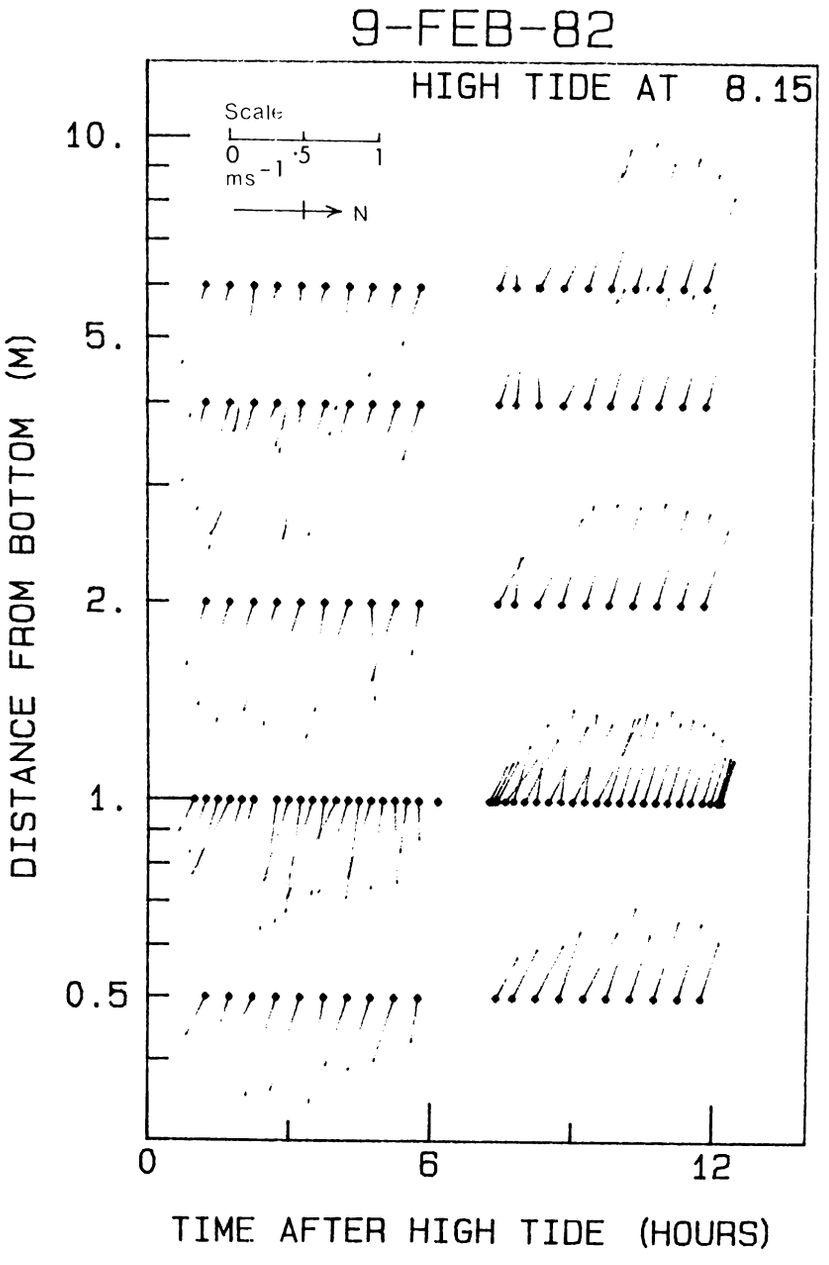

Figure 6.15: Velocities measured during the S-series at S3 (9-Feb-82) after correction for non-simultaneity. Velocities are plotted as 10mm representing 0.5 m.s^{-1} with True North directed towards the right of the page.

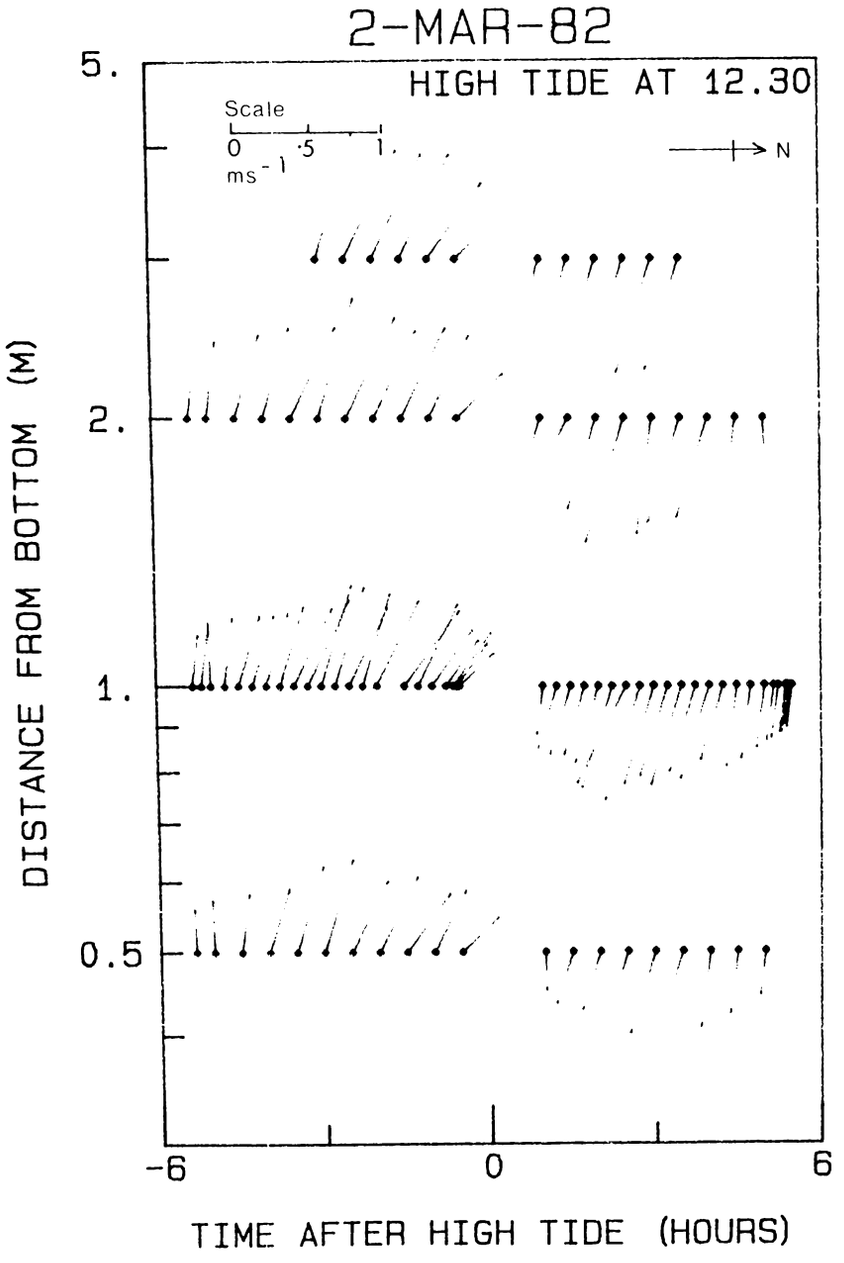

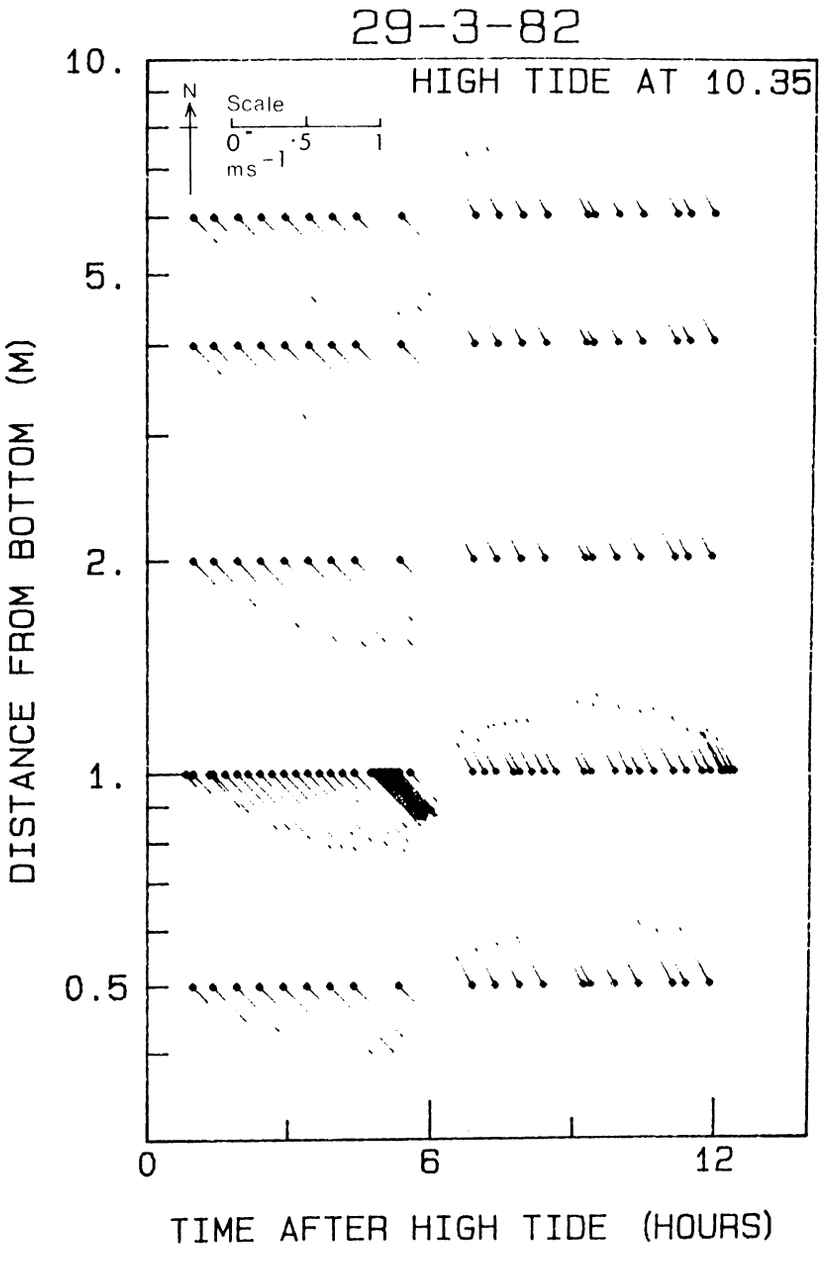

Figures 6.16 (left) and 6.17: Velocities measured during the S-series at S4 (2-Mar-82) and S5 (29-Mar-82) after correction for non-simultaneity. Velocities are plotted as 10mm representing 0.5 $m.s^{-1}$ and True North to the right at S4 and up the page at S5.

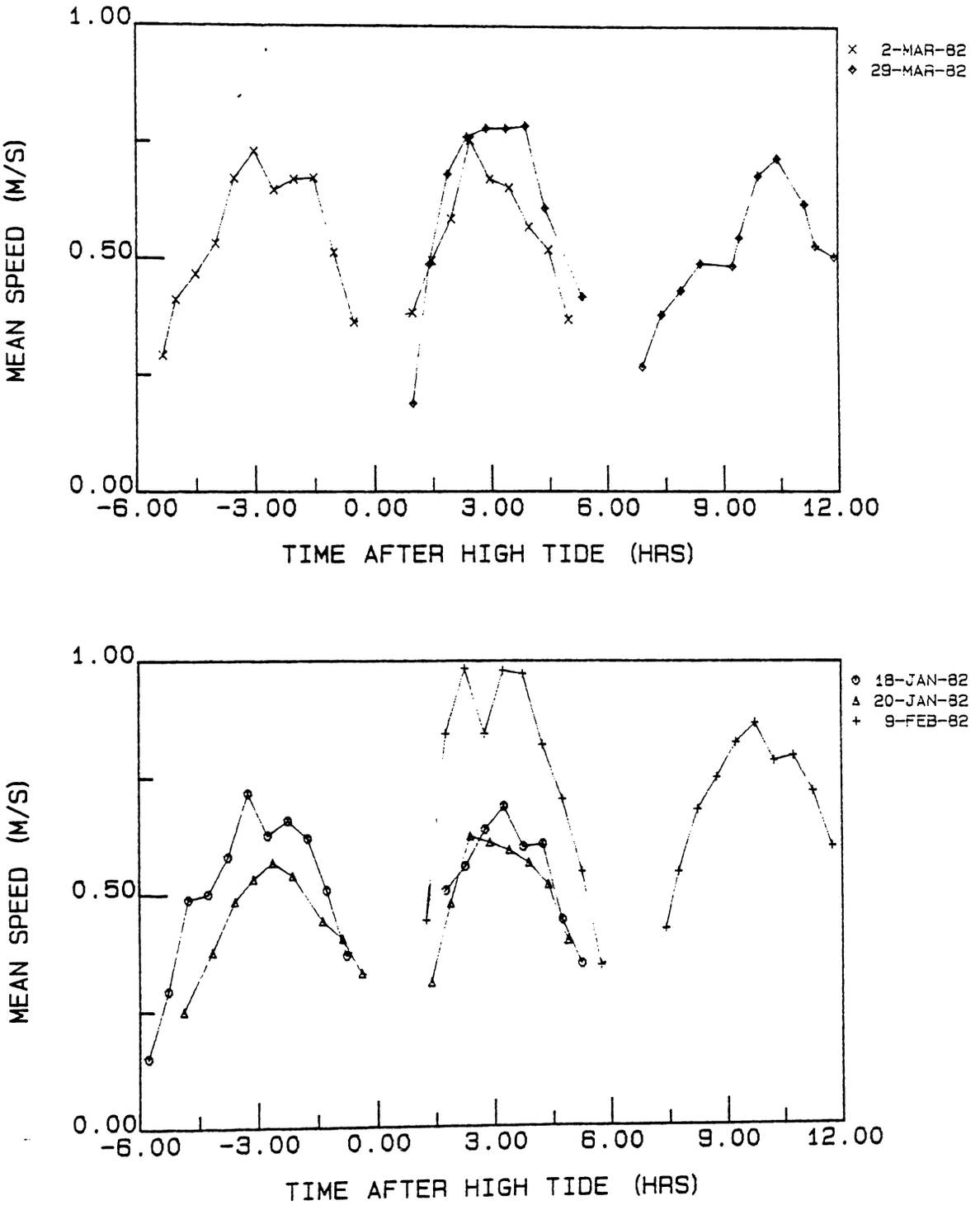

Figure 6.18: Mean vertically-averaged water speed during the S-series against time after high tide.

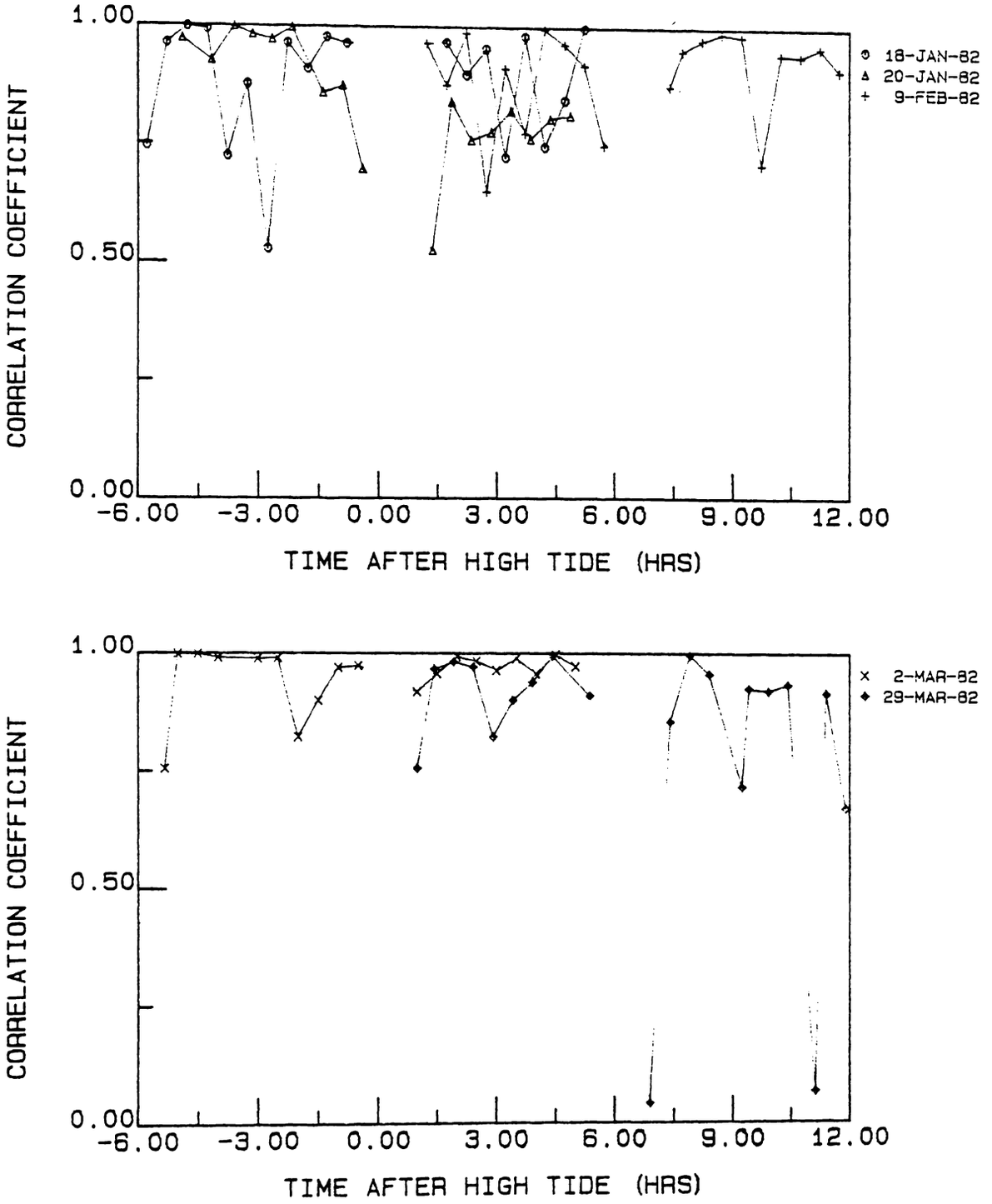

Figure 6.19: Correlation coefficients representing the goodness of fit of the measured water speeds to the logarithmic profile, r, against time after high tide during the S-series.

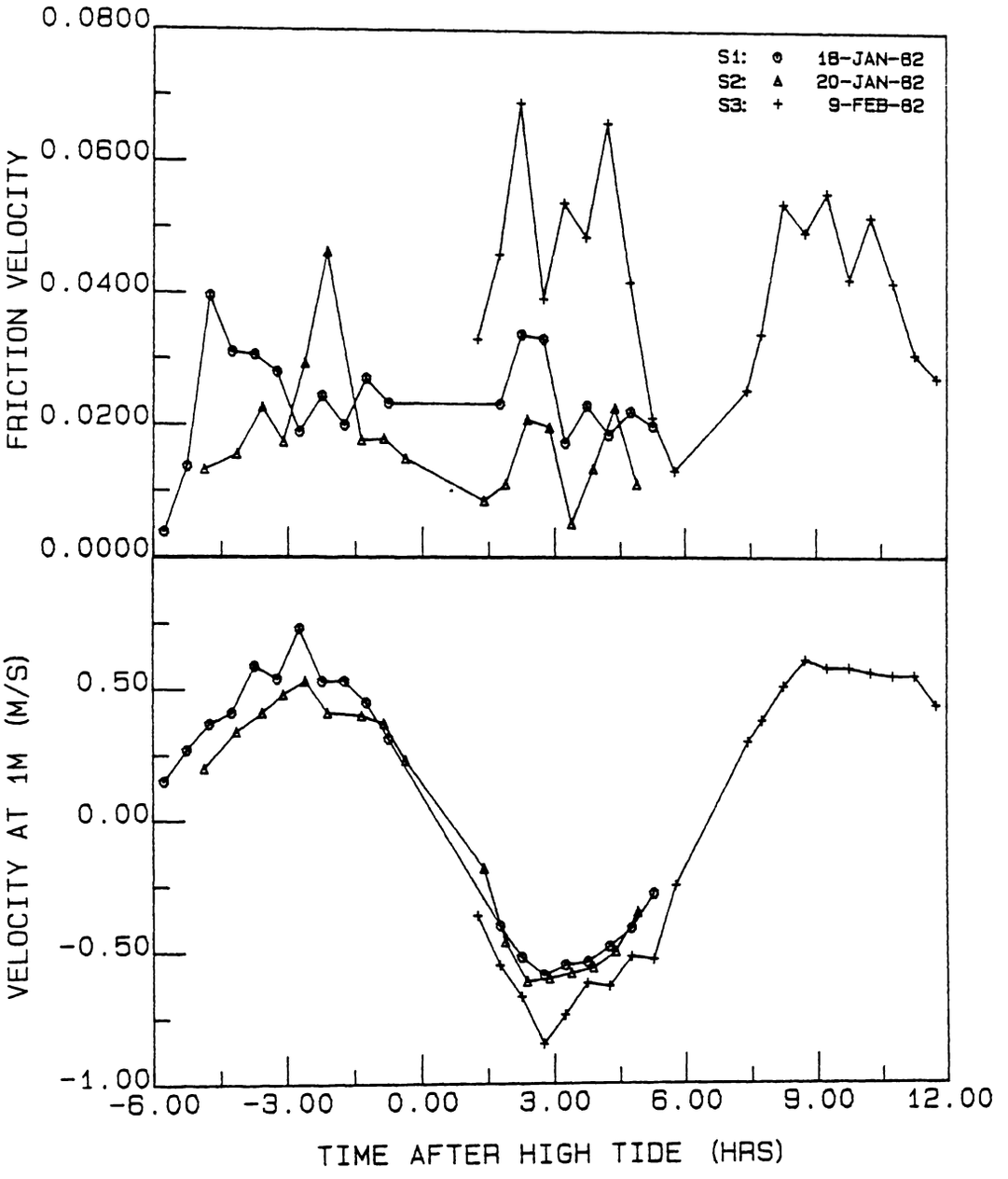

Figure 6.20(a): Friction velocity, $u*$, and velocity at 1m above the bed, u_1, against time after high tide for S1, S2 and S3.

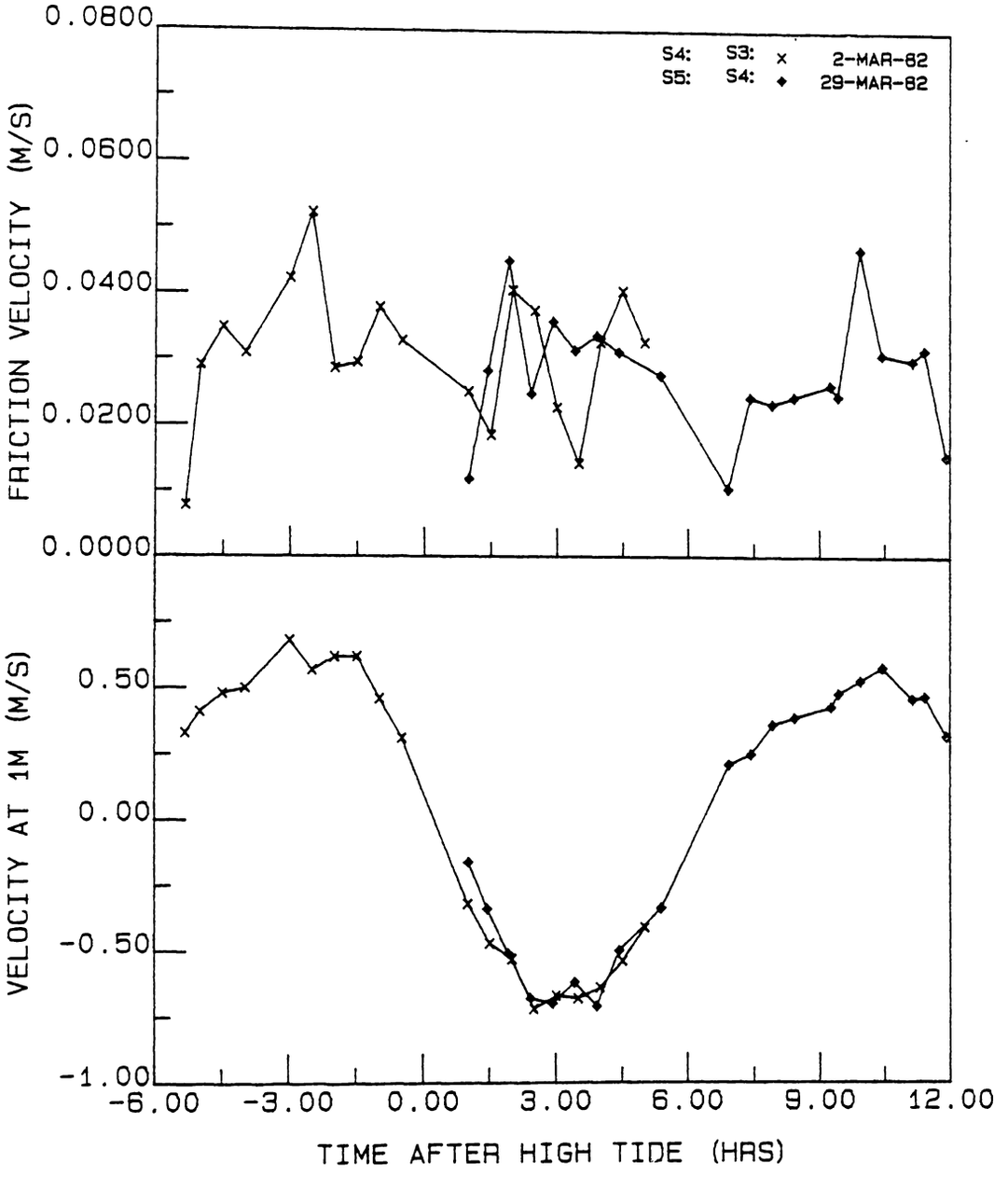

Figure 6.20(b): Friction velocity, u*, and velocity at 1m above the bed against time after high tide for S4 and S5.

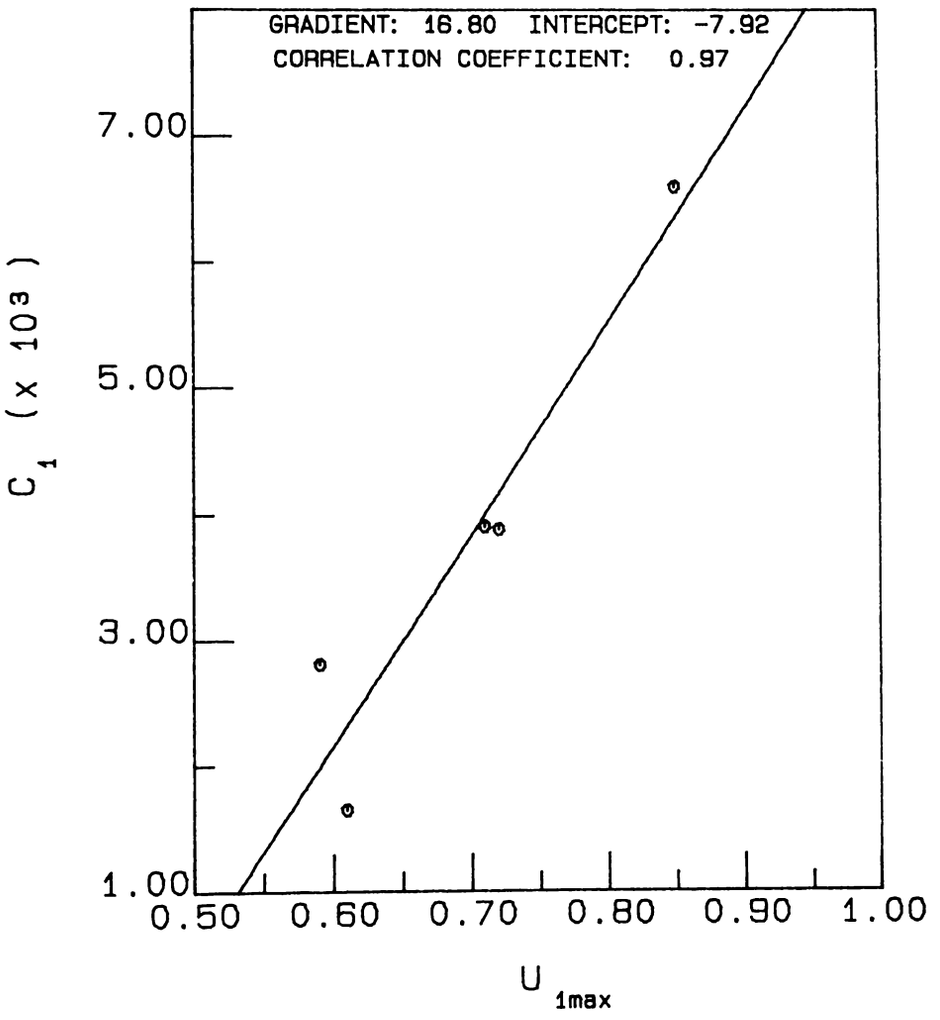

Figure 6.21: The median Drag Coefficient against the maximum recorded speed at 1m above the bed at the 5 S-series sediment transport experimental sites with best fit curve: $C_1 = (16.8\ u_{1max} - 7.92) \times 10^{-3}$.

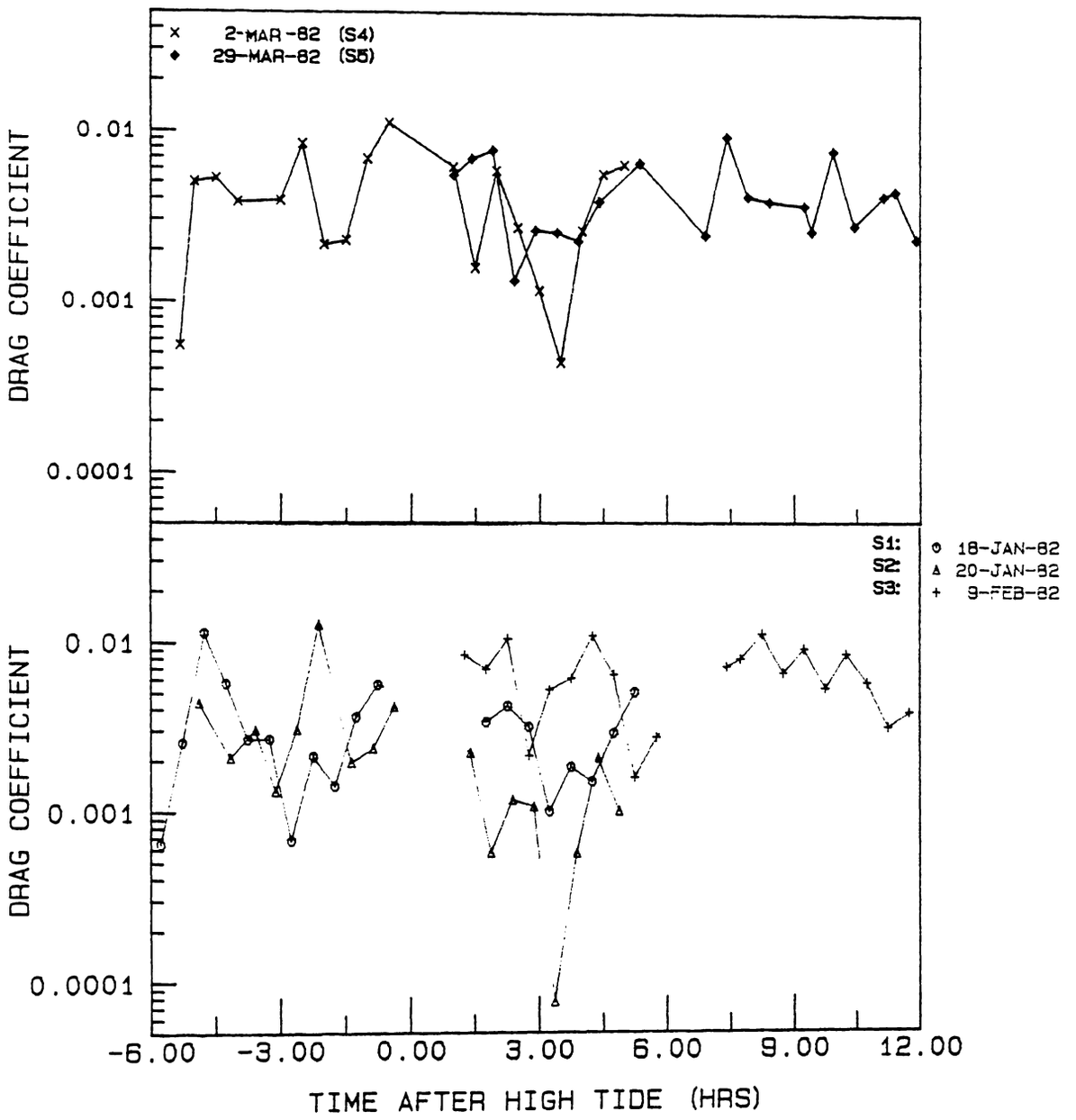

Figure 6.22: Drag coefficients during the S-series against time after high tide for S1, S2 and S3.

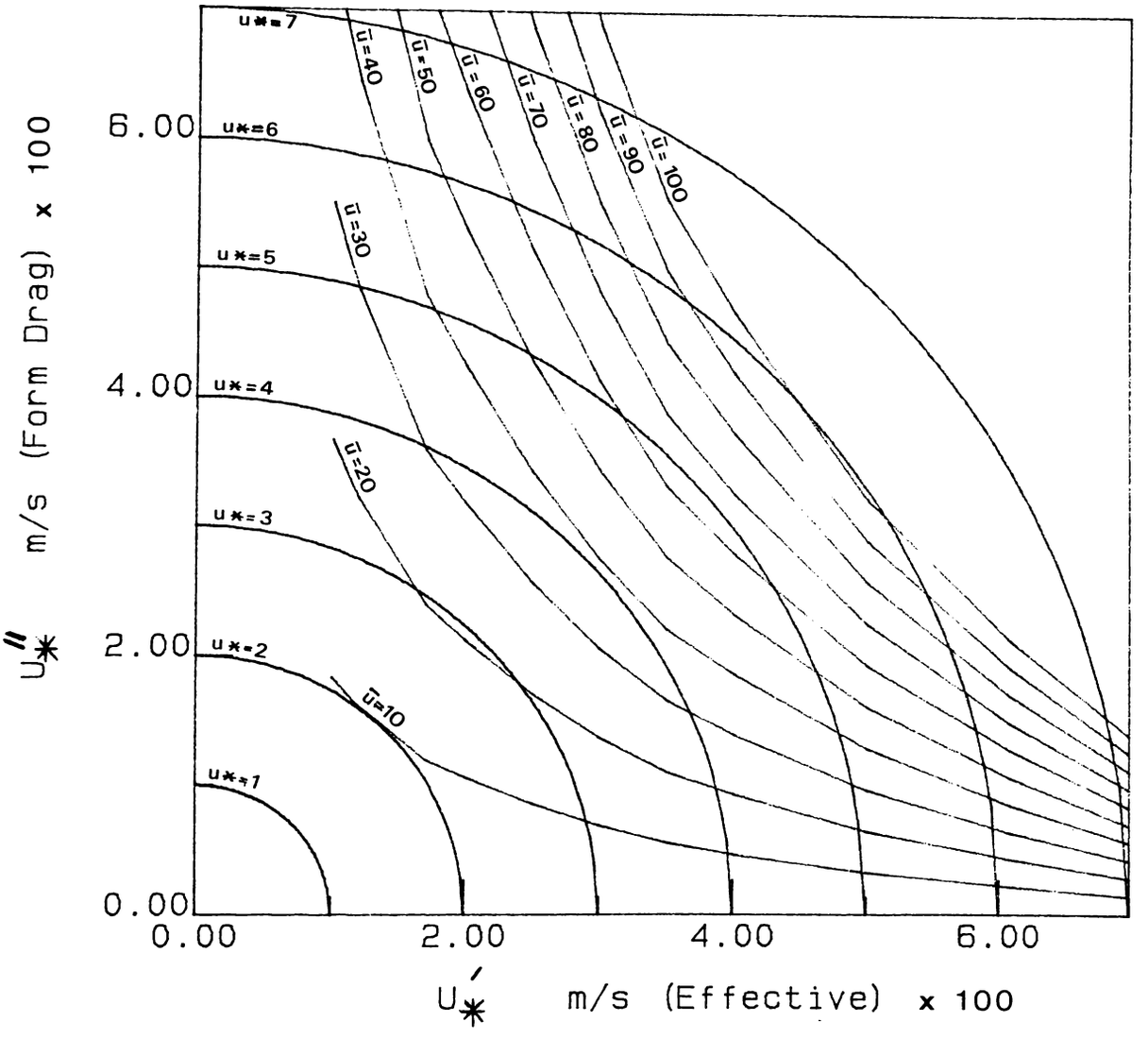

Figure 6.23: Einstein and Barbarossa division of form drag and skin friction velocities, given by the intersection of the mean ($\bar{u}$) and friction (u_*) velocity curves ($m.s^{-1}$ x 100) for D_{35} = 0.0002m, ρ_s = 2650 $kg.m^{-3}$, ρ = 1025 $kg.m^{-3}$.

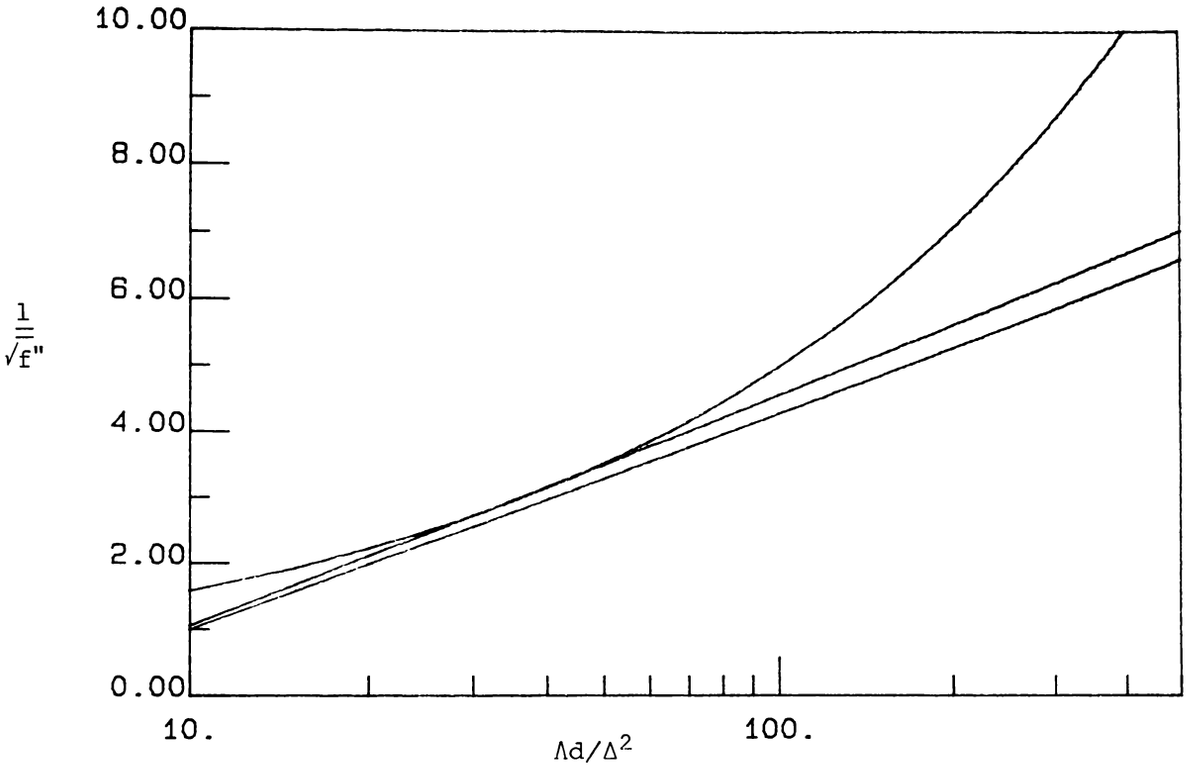

Figure 6.24: Comparison of the Engelund and Hansen, Pillai and Vanoni and Hwang equations for obtaining the Darch-Weisbach form drag friction coefficient (f") against the function $\Lambda d/\Delta^2$. Λ is bedform wavelength, Δ is bedform height and d is water depth.

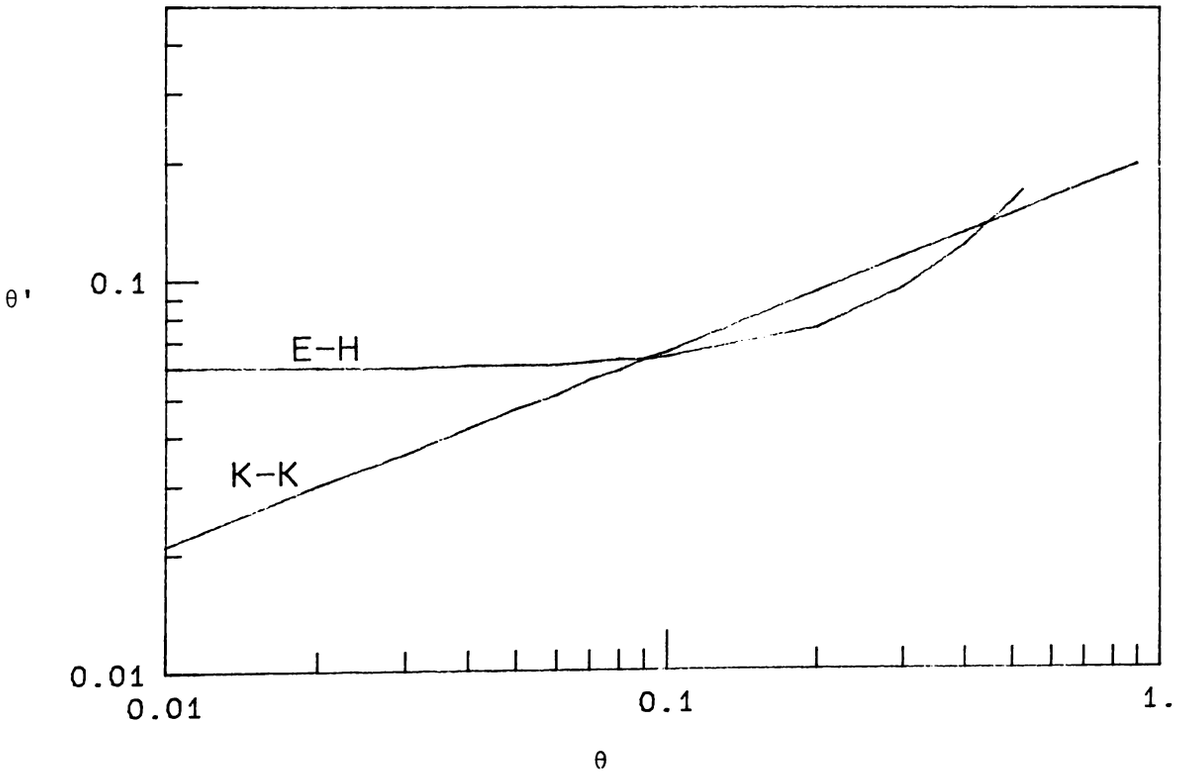

Figure 6.25: Comparison of Engelund and Hansen and Kishi and Kuroki equations for obtaining the skin friction velocity from the Shield's Entrainment Function, θ.

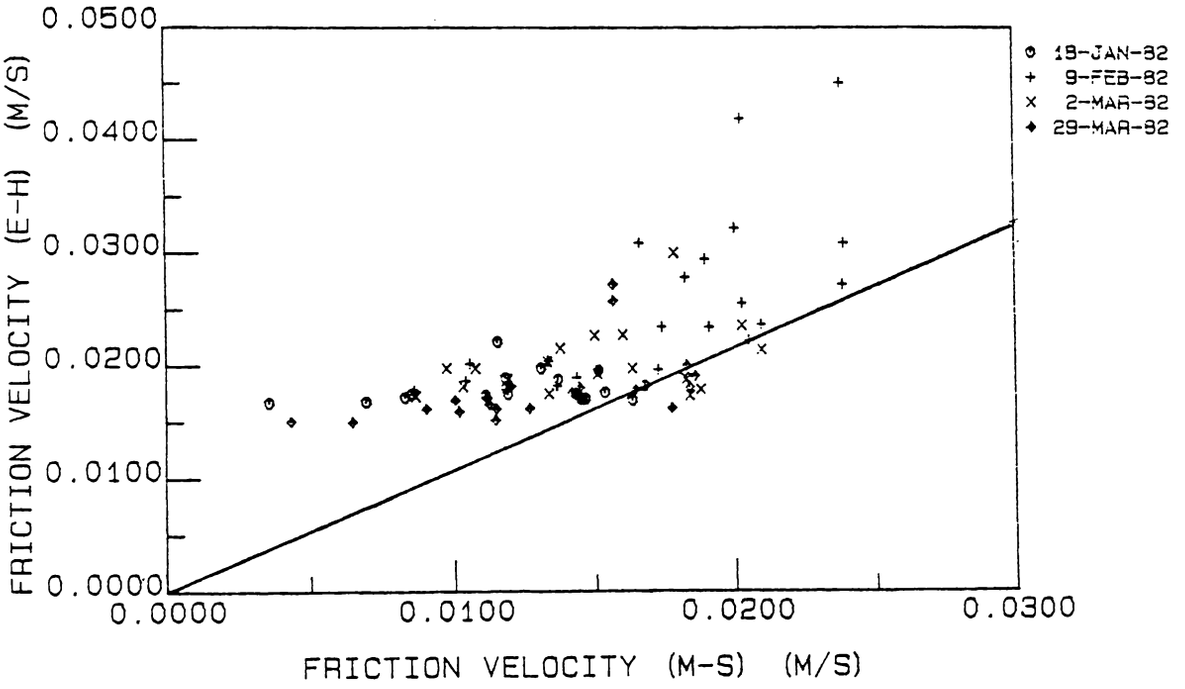

Figure 6.26: Skin friction velocity, u_*', obtained using the Engelund and Hansen formulation against u_*' using the Manning-Strickler equation, for the S-series over megaripples.

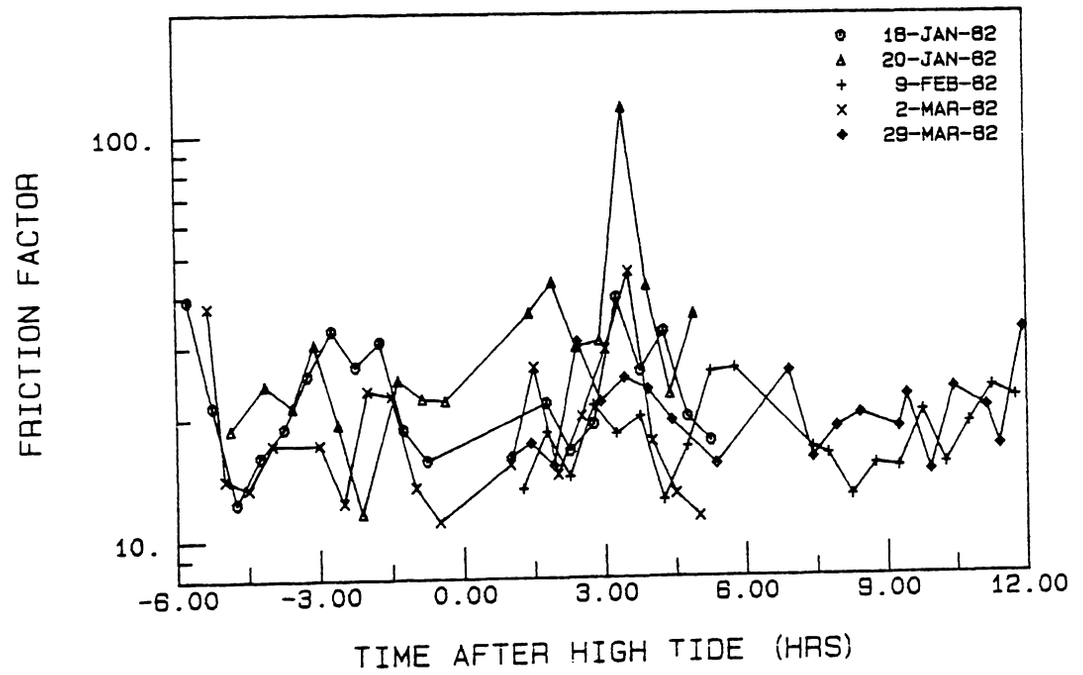

Figure 6.27: Friction factor, c, against the time after high tide for the S-series over megaripples.

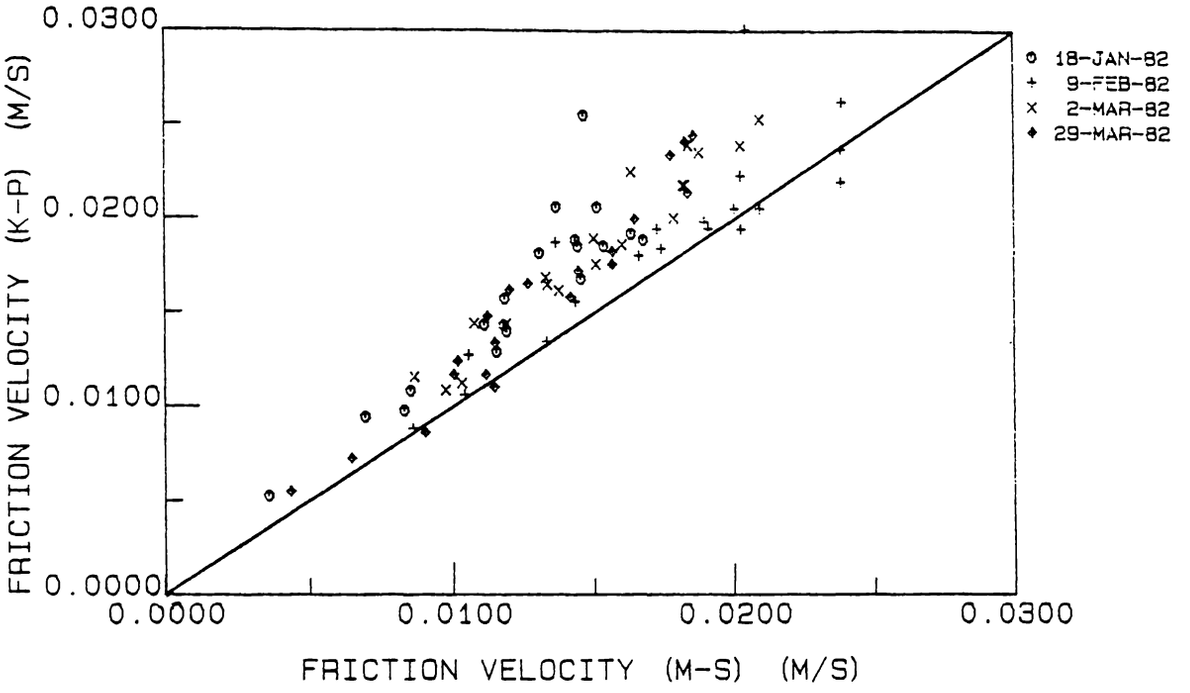

Figure 6.28: Skin friction velocity, u_*', obtained using the Karman-Prandtl equation against u_*', obtained using the Manning-Strickler equation.

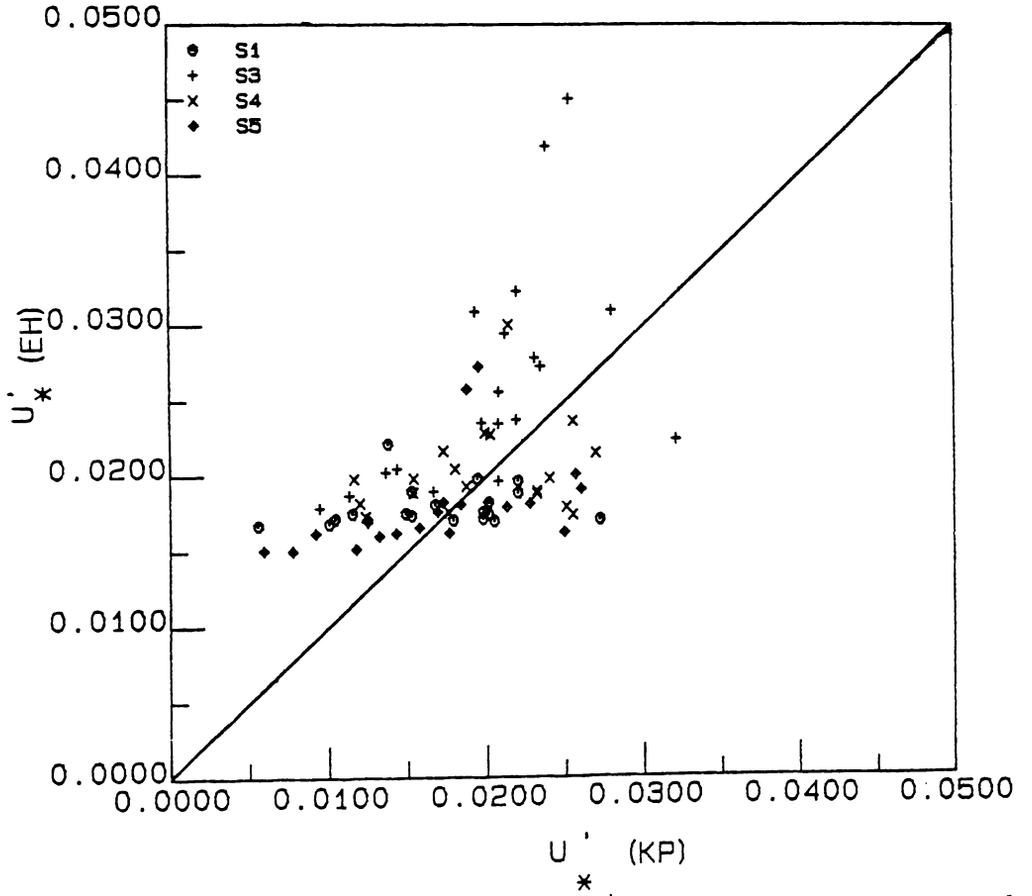

Figure 6.29: Skin friction velocity, u_*', obtained using the Engelund and Hansen formulation against u_*' obtained using the Karman Prandtl equation.

Figure 7.1: VUV-type sediment traps.

Figure 7.2: Underwater video camera with RNZN divers making adjustments to the lead weight tied below for scale.

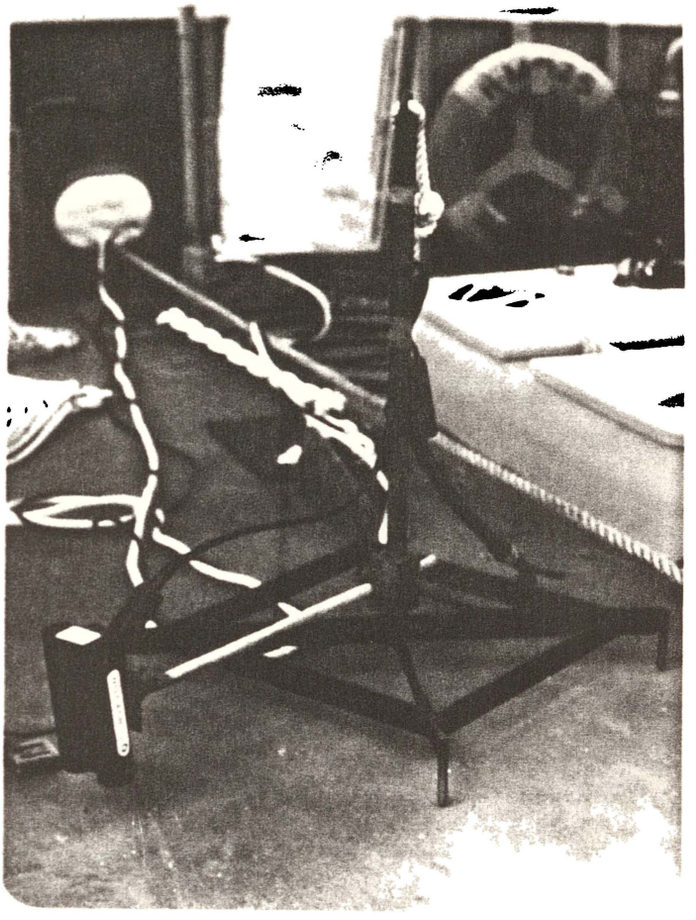

Figure 7.3: Underwater video camera and frame.

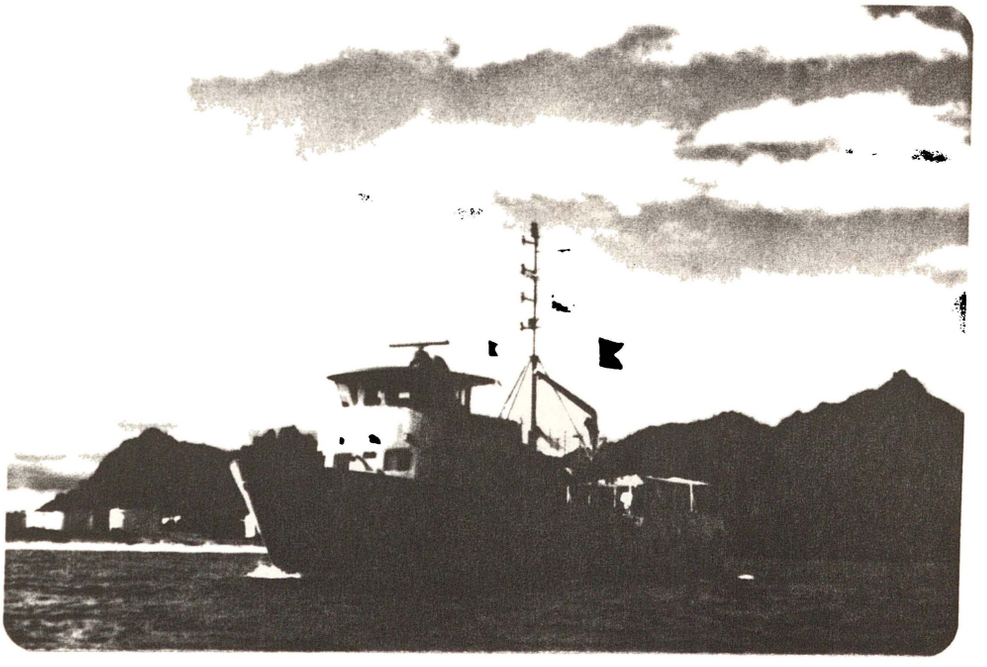

Figure 7.4: RNZN diving tender "Manawanui" in Bream Bay.

Figure 7.5: RNZN underwater photography diving team.

Figure 7.6: NHB oil spill vessel "Maunu".

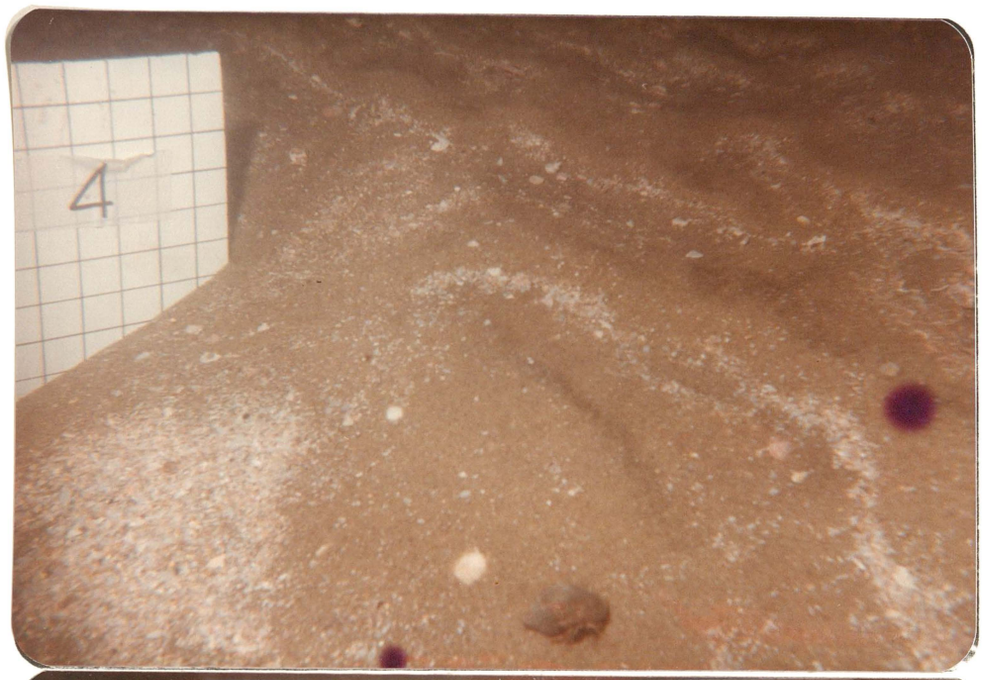

Figure 7.7(a): Megaripple crest and slipface at S3. Backboard has a 0.02m grid.

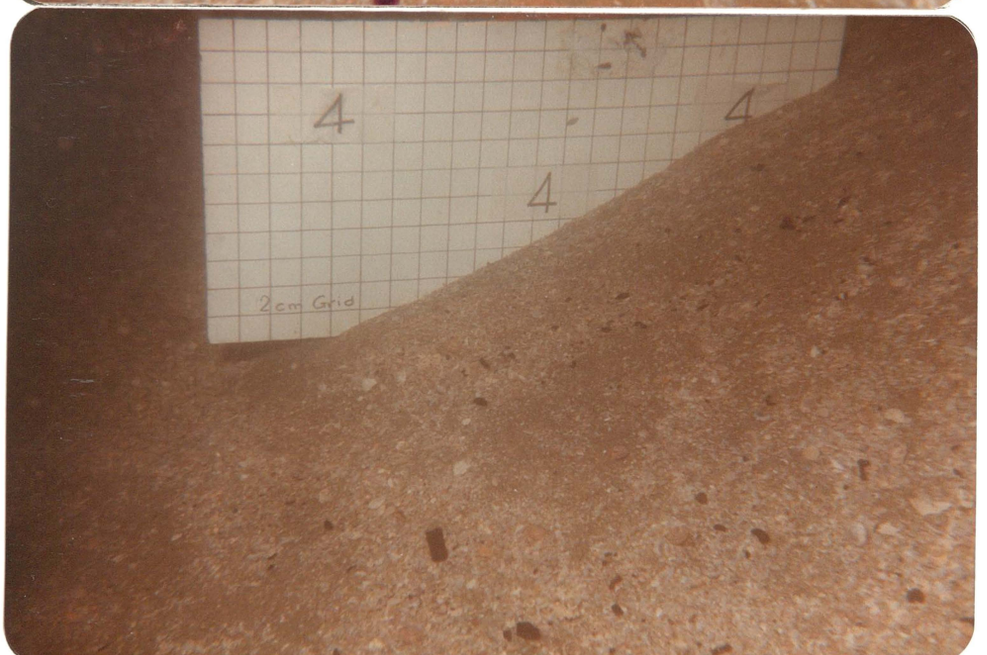

Figure 7.7(b): Megaripple slipface at S3. Backboard has a 0.02m grid.

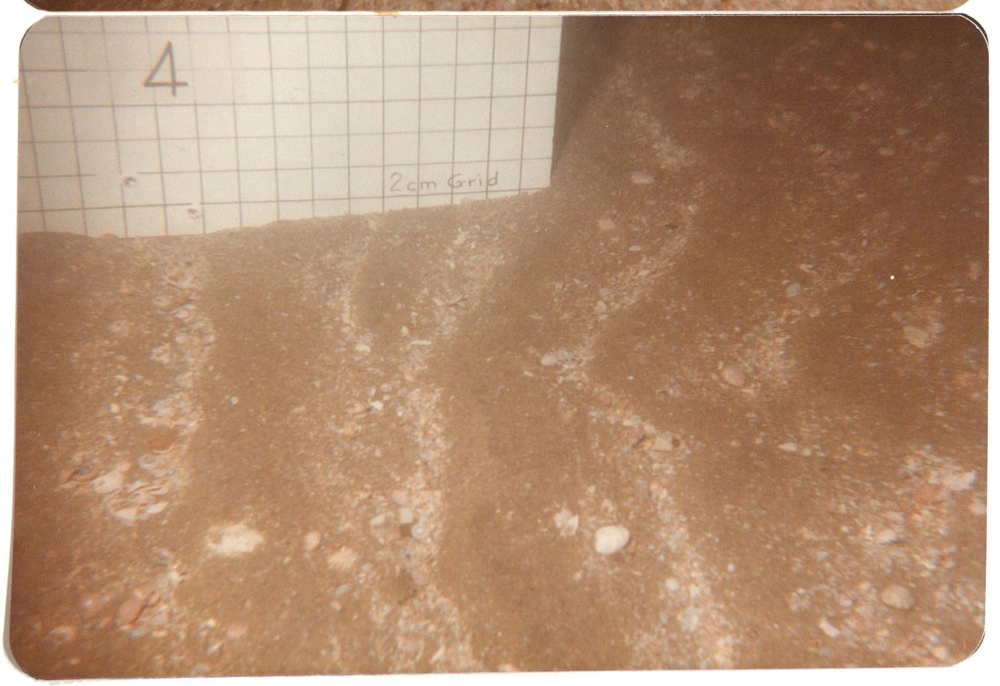

Figure 7.7(c): Ripples in a megaripple trough at S3. Backboard has a 0.02m grid.

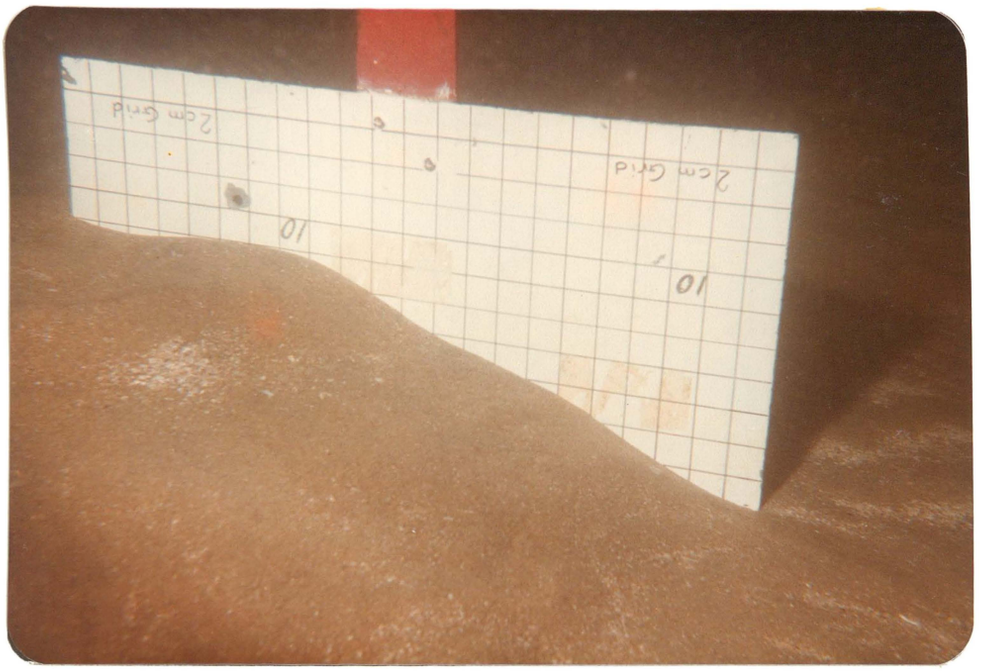

Figure 7.8(a): Megaripple slipface at S4. Backboard has a 0.02m grid.

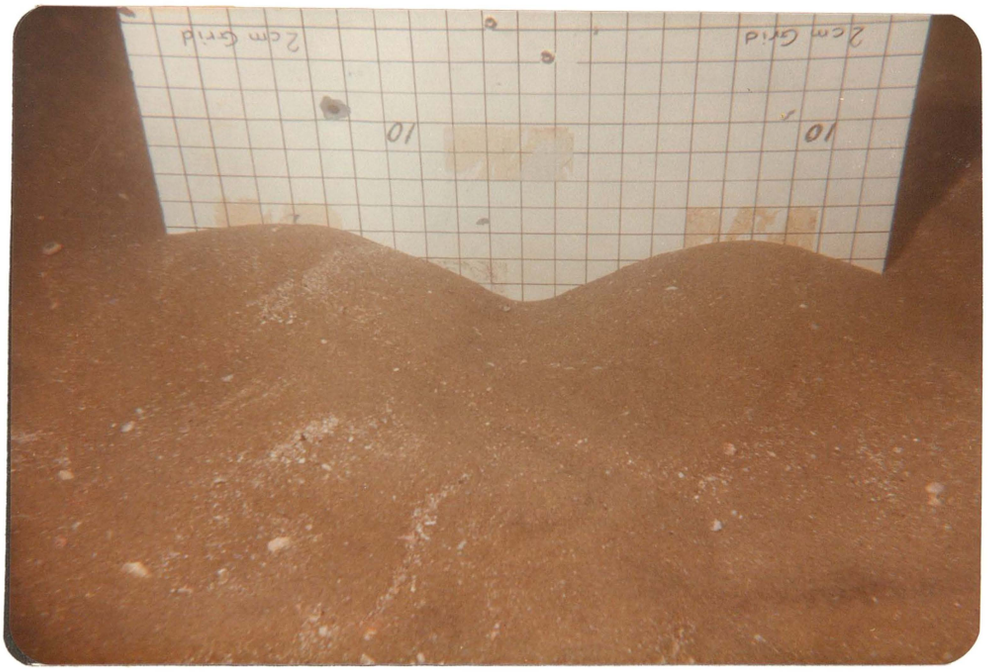

Figure 7.8(b): Ripples at S4. Backboard has a 0.02m grid.

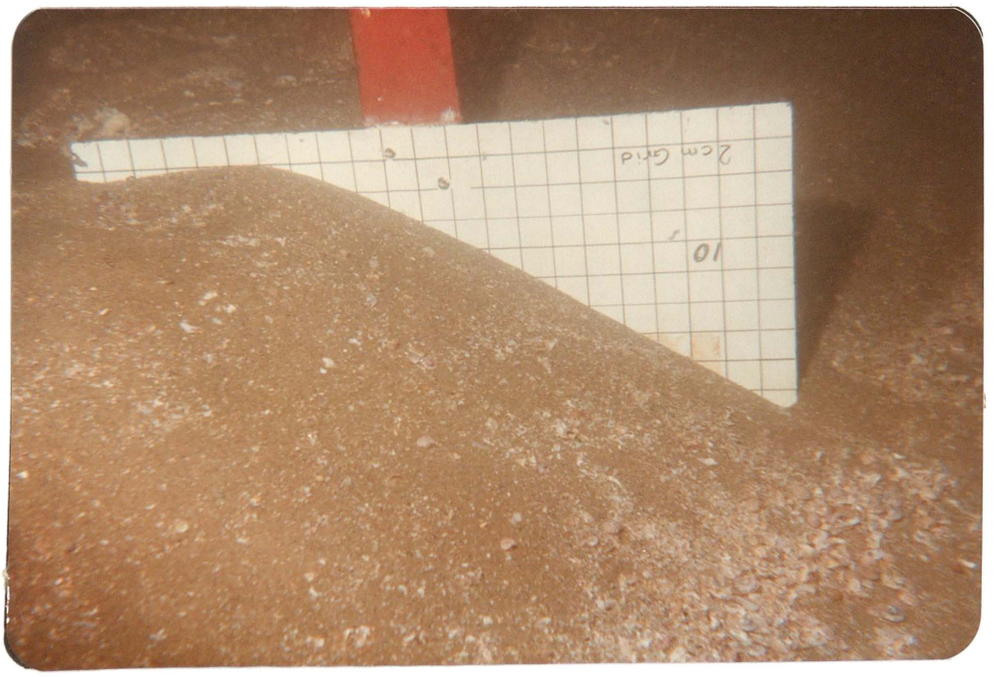

Figure 7.8(c): Megaripple slipface at S4. Backboard has a 0.02m grid.

Figure 7.8(d): Ripples in megaripple trough at S4. Backboard has a 0.02m grid.

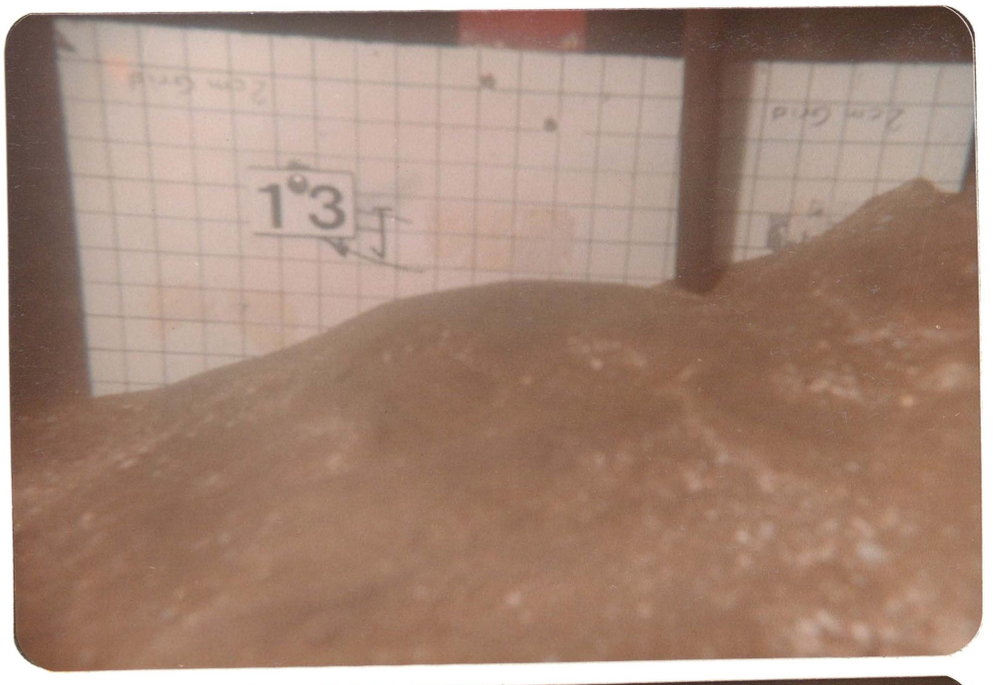

Figure 7.9(a): Megaripple slipface, and steel stake marking advance rate. Backboard has a 0.02m grid Site S5.

Figure 7.9(b): Megaripple slipface and steel stake marking advance rate. Backboard has a 0.02m grid Site S5.

Figure 7.10: Megaripple slipface advancing from left to right over a semi-consolidated bed of shell. Backboard has a 0.02m grid.

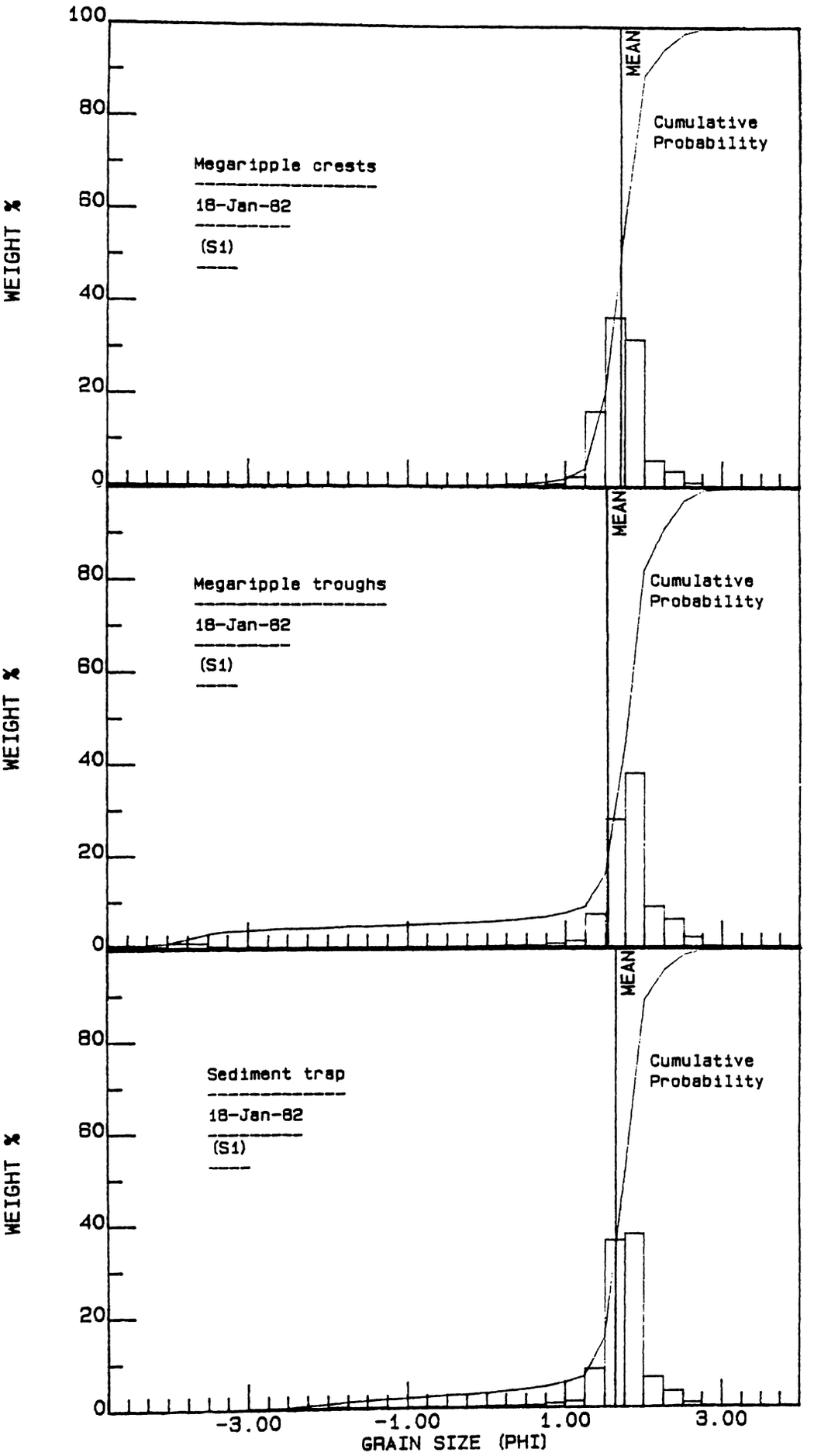

Figure 7.11: Grain size distributions at Site S1 (18-Jan-82).

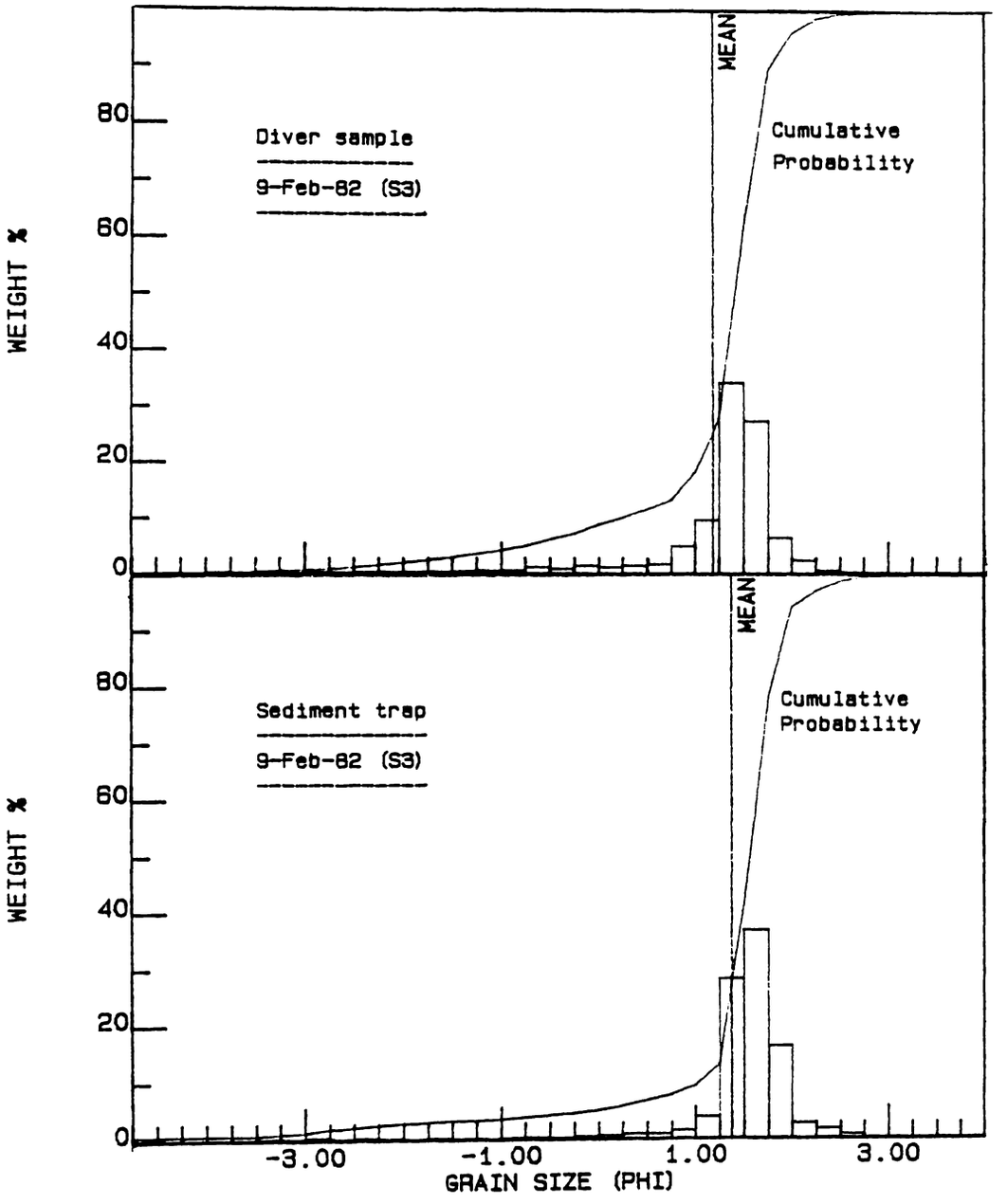

Figure 7.12: Grain size distributions at Site S3 (9-Feb-82).

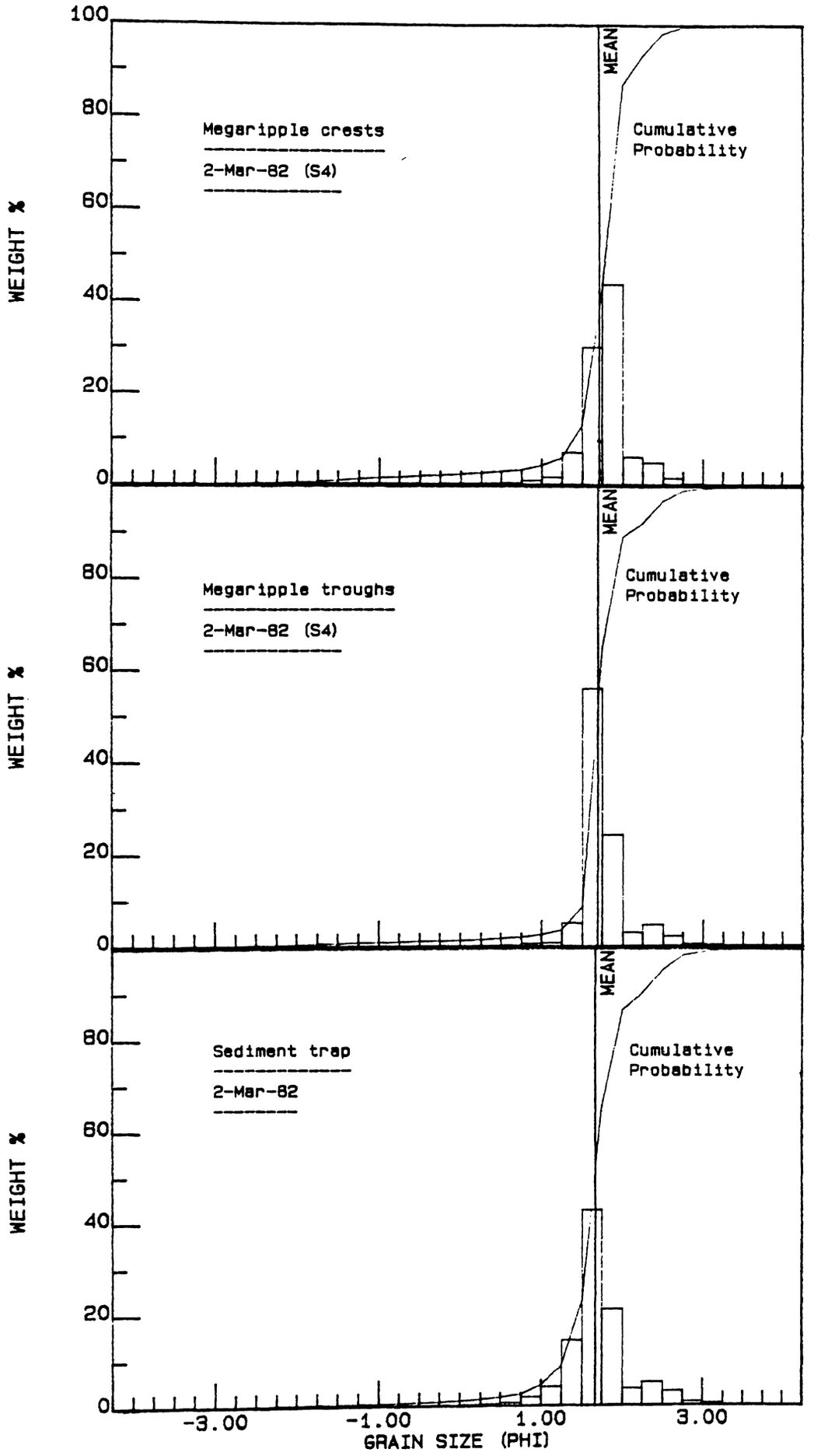

Figure 7.13: Grain size distributions at Site S4 (2-Mar-82).

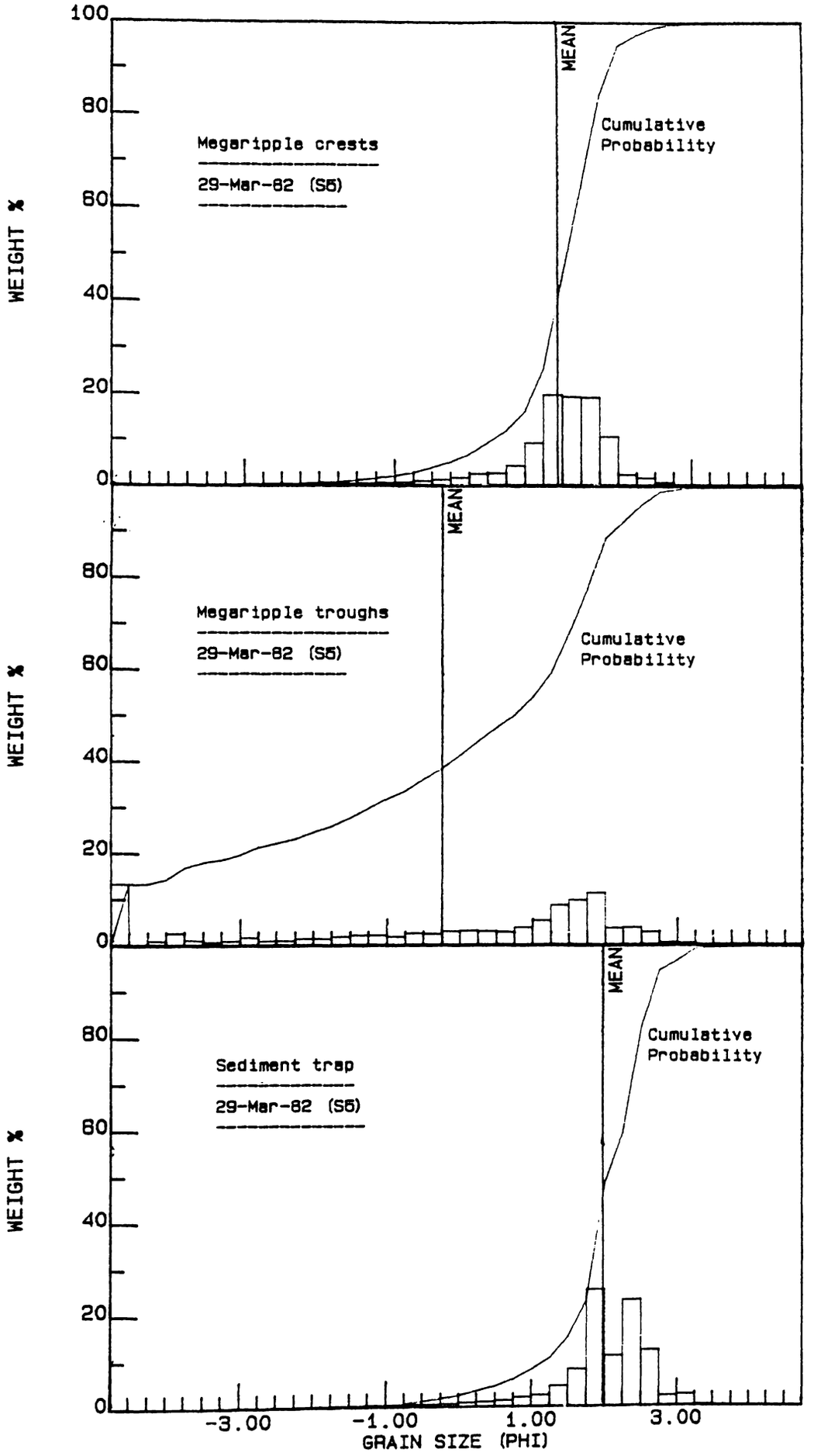

Figure 7.14: Grain size distributions at Site S5 (29-Mar-82).

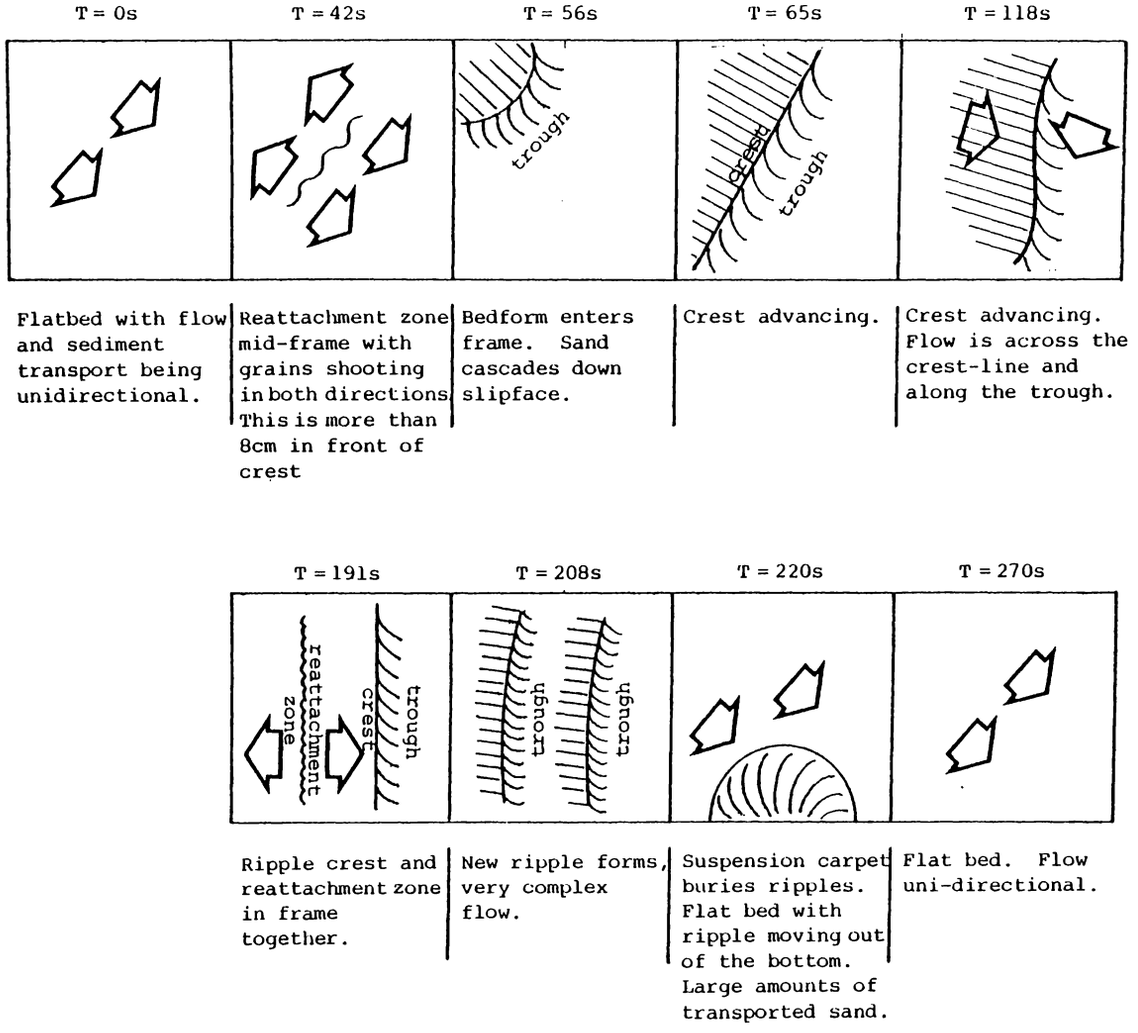

Figure 7.15: Ripple advance and flow patterns seen using an underwater video camera on Site S1 on 18-Jan-82 at 17.50. The velocity at 1m was 0.55 $m.s^{-1}$ and the width of the frame is approximately 0.16m. Heavy arrows show flow directions.

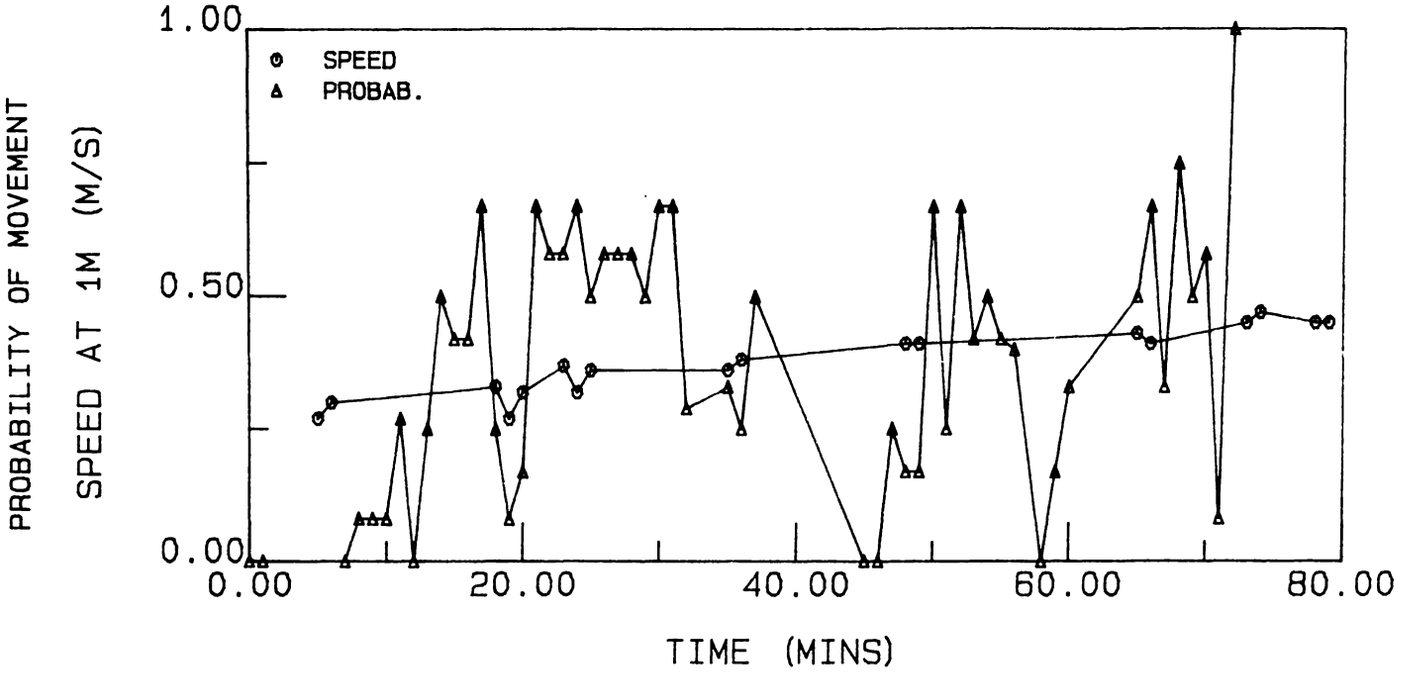

Figure 7.16: Sandy sediment threshold showing the probability that sand will move in a 1 minute interval with the speed at 1m, for 18-Jan-82 and based on analysis of video tapes.

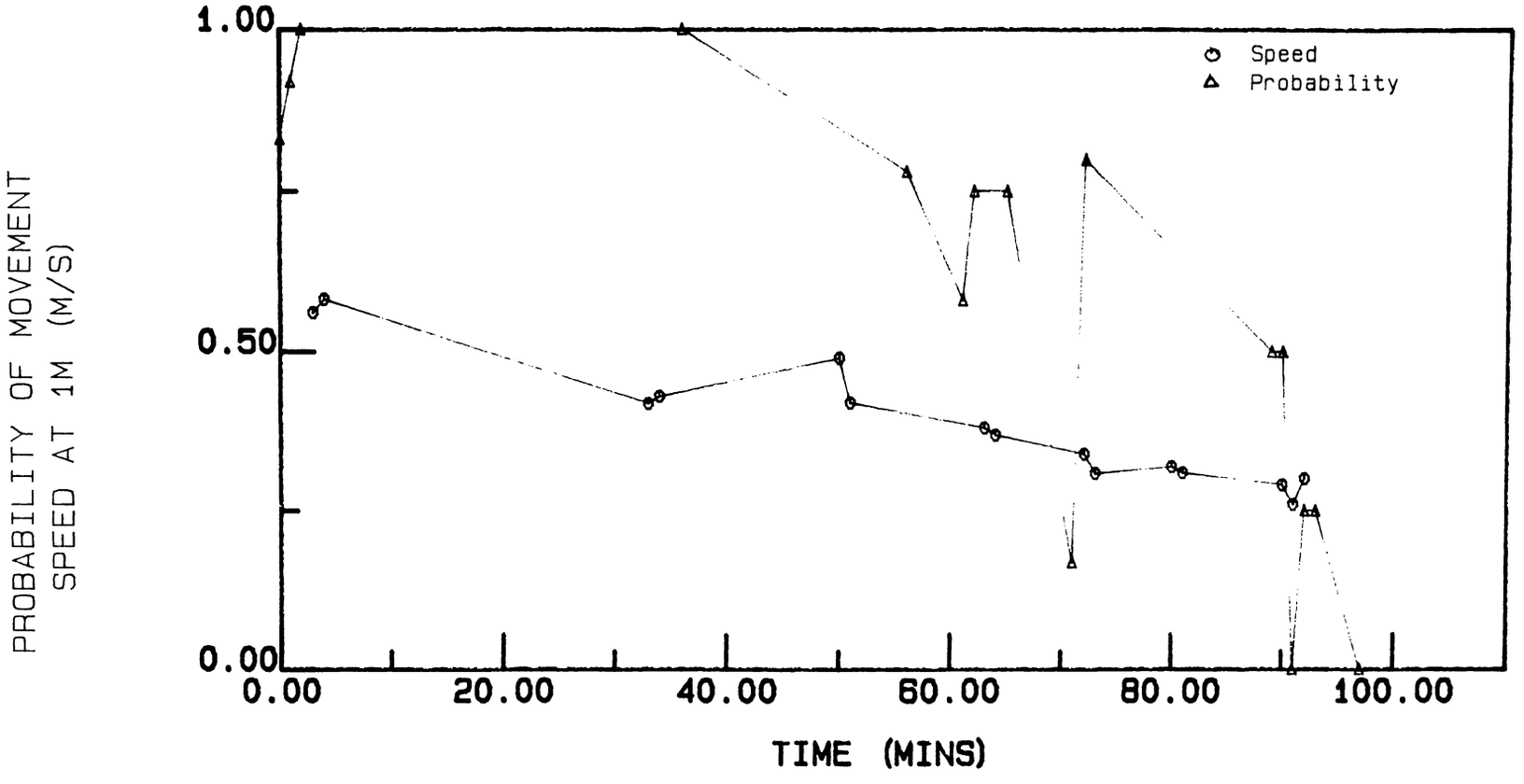

Figure 7.17: Sandy sediment threshold showing the probability that sand will be moving in a 1-minute interval with the speed at 1m for 18-Jan-82 (S1) and based on analysis of video tapes.

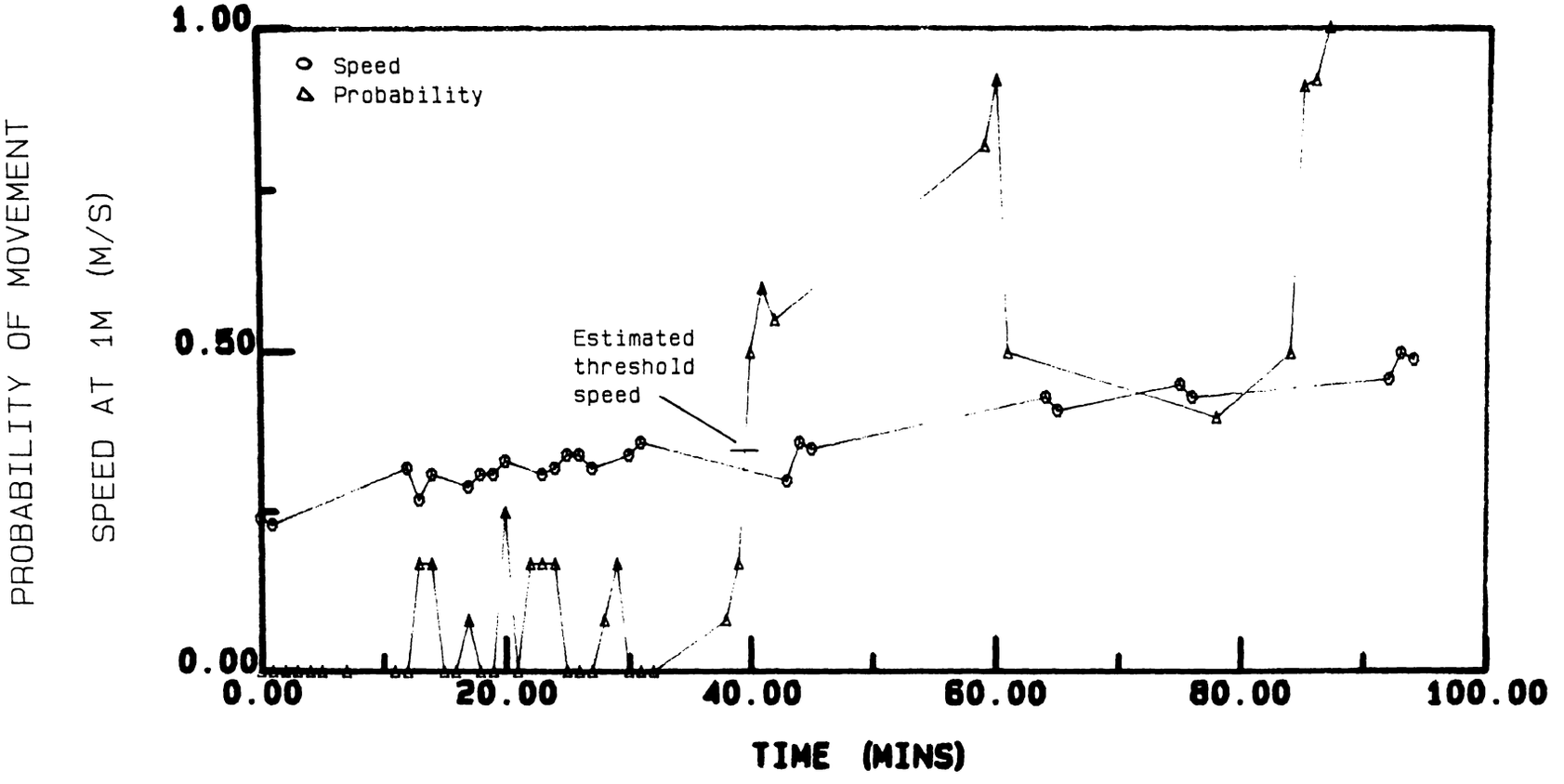

Figure 7.18: Sandy sediment threshold showing the probability that sand will be moving in a 1-minute interval with the speed at 1m for 20-Jan-82 (S2) and based on analysis of video tapes.

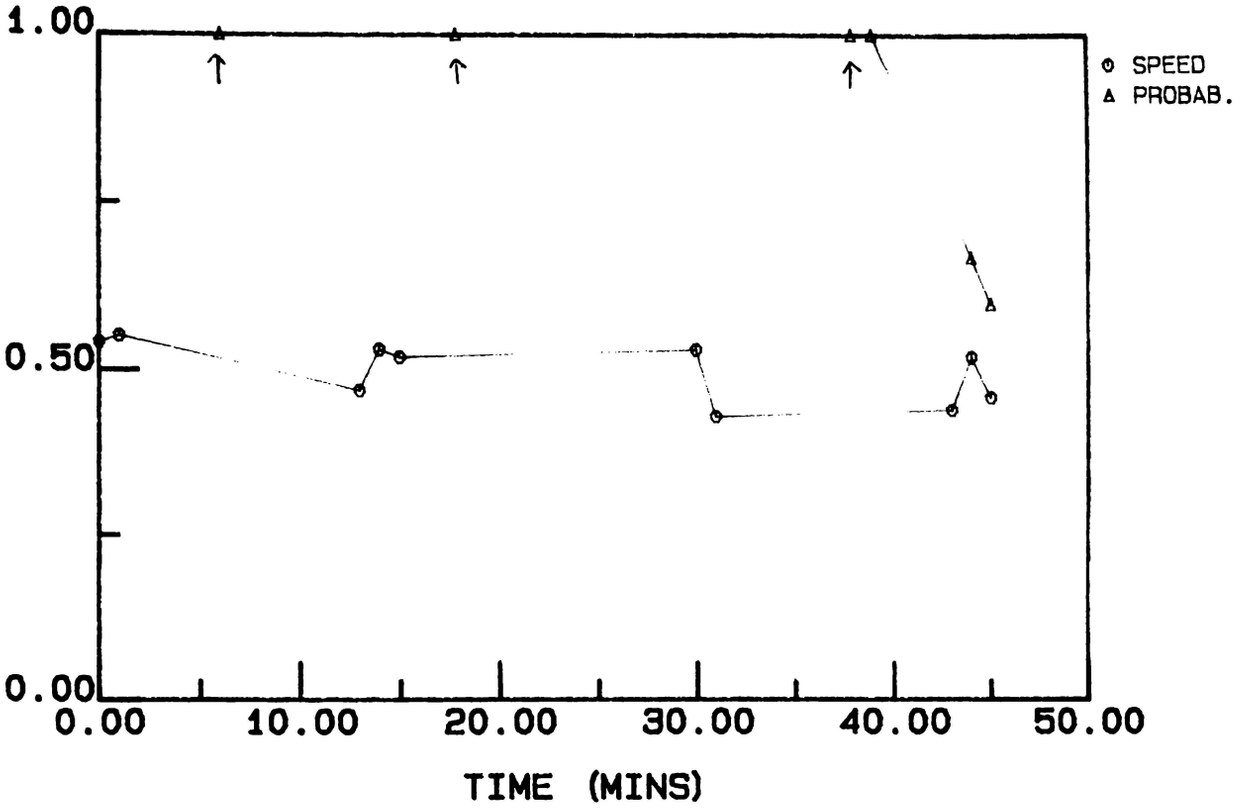

Figure 7.19: Sandy sediment threshold showing the probability that sand will be moving in a 1-minute interval with the 1m speed for 18-Jan-82 (S1) and based on analysis of video tapes. Note data along top axis shows constant bed movement.

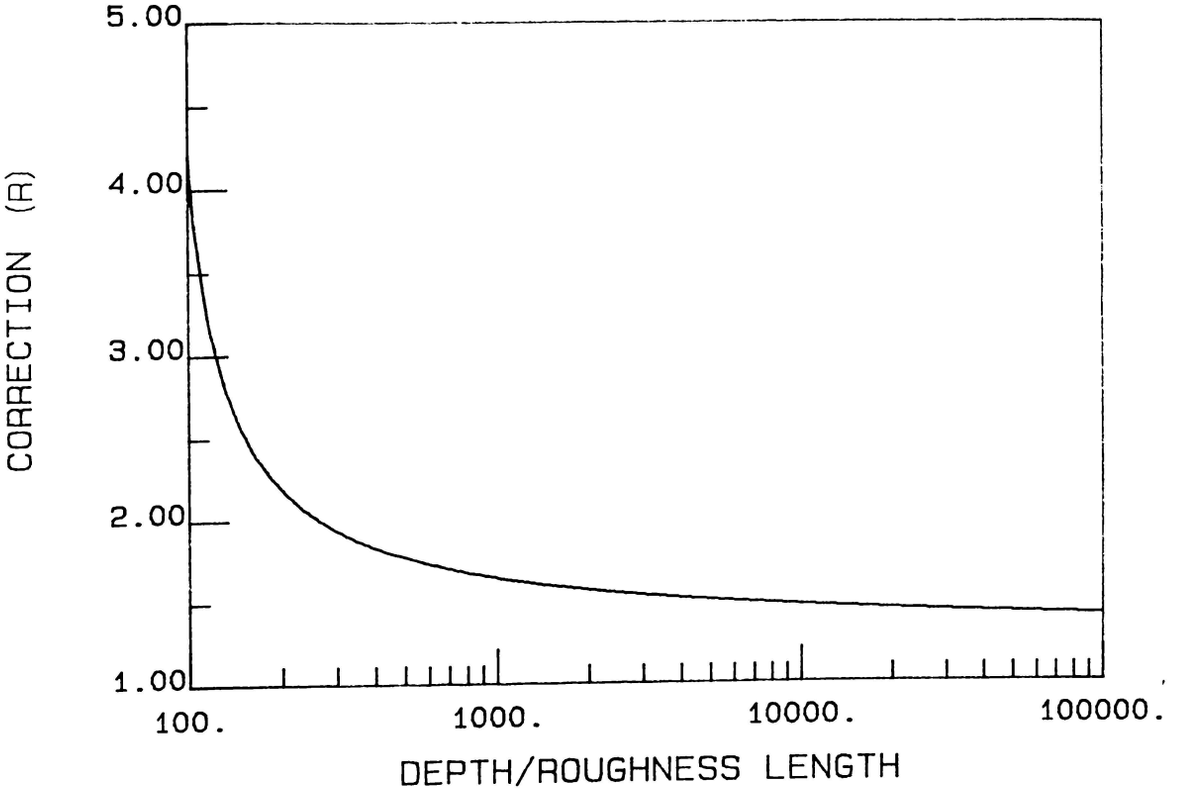

Figure 7.20: Correction factor, R, for determination of sediment threshold friction velocity over rippled and megarippled beds.

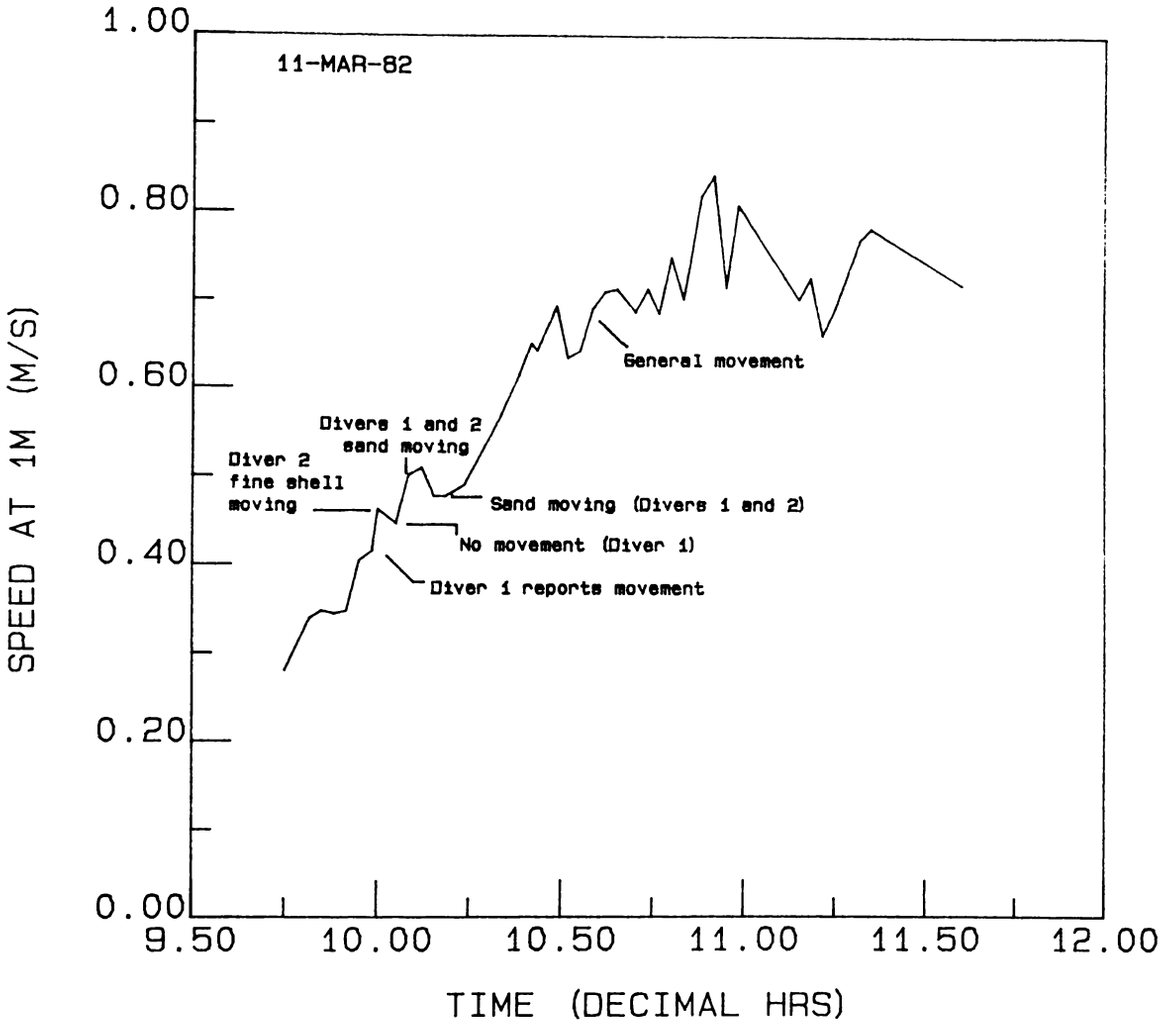

Figure 7.21: Summary of diver observations with the speed at 1m above the bed against the time of day at sediment threshold Site T1 on 11-Mar-82.

Figure 7.22(a): Shell/sand mixture at sediment threshold Site T2. Backboard has a 0.02m grid.

Figure 7.22(b): Aged total shell cover at sediment threshold Site T2. Backboard has a 0.02m grid.

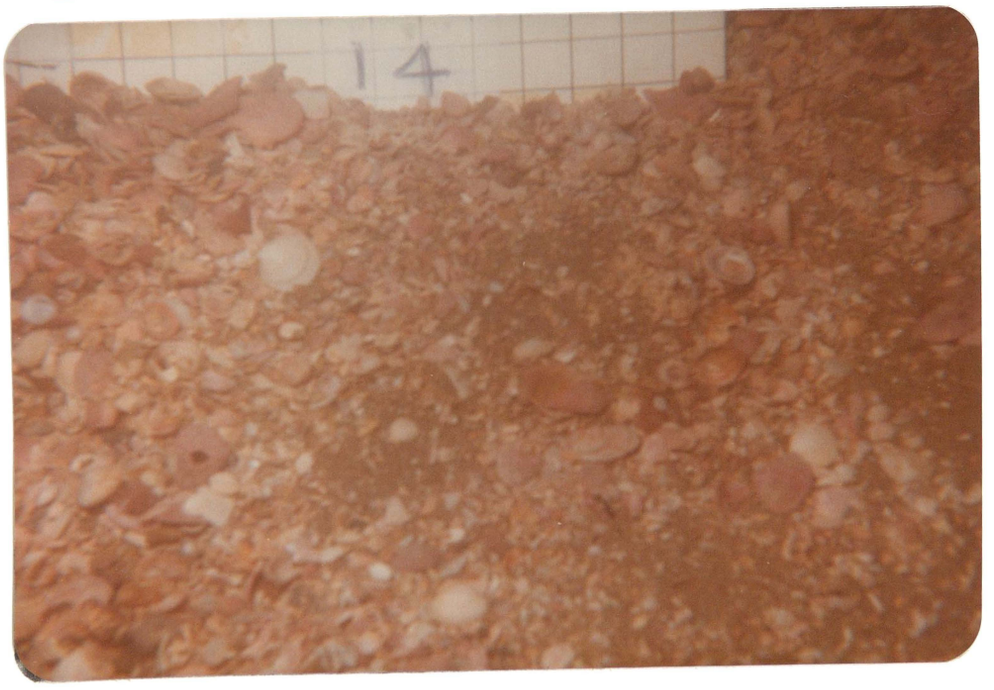

Figure 7.22(c): Distinct boundary between total shell and shell/sand beds at sediment threshold Site T2. Backboard has a 0.02m grid.

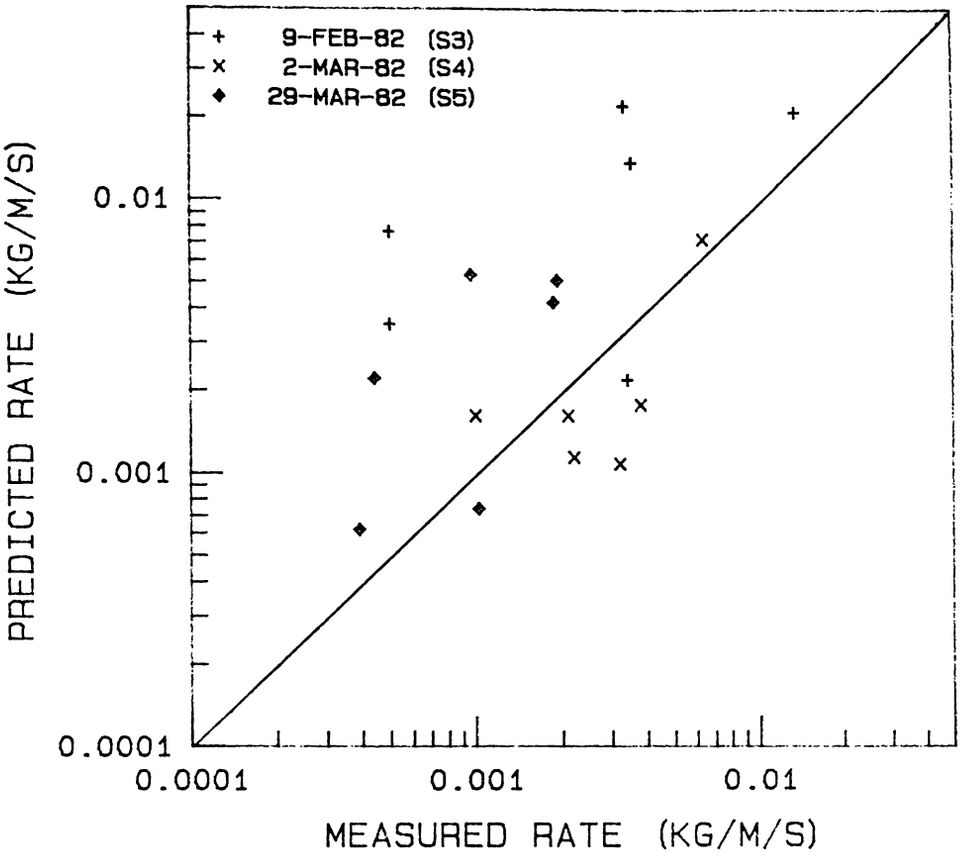

Figure 7.23: Transport rate according to the Engelund Hansen (1967) total load equation against the bedload trap measured rate.

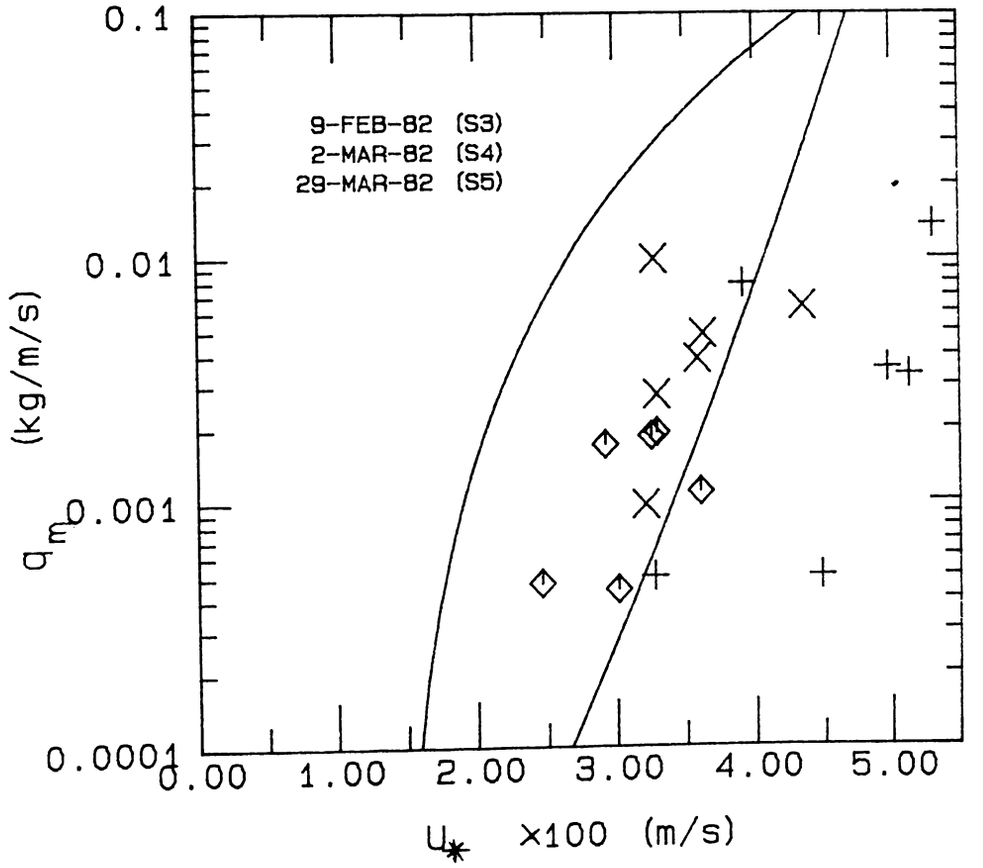

Figure 7.24: Measured bedload transport rate against the friction velocity, plotted with the Yalin and Sternberg bedload equations for D=0.0003m and u'_{*c} =0.014 m.s .

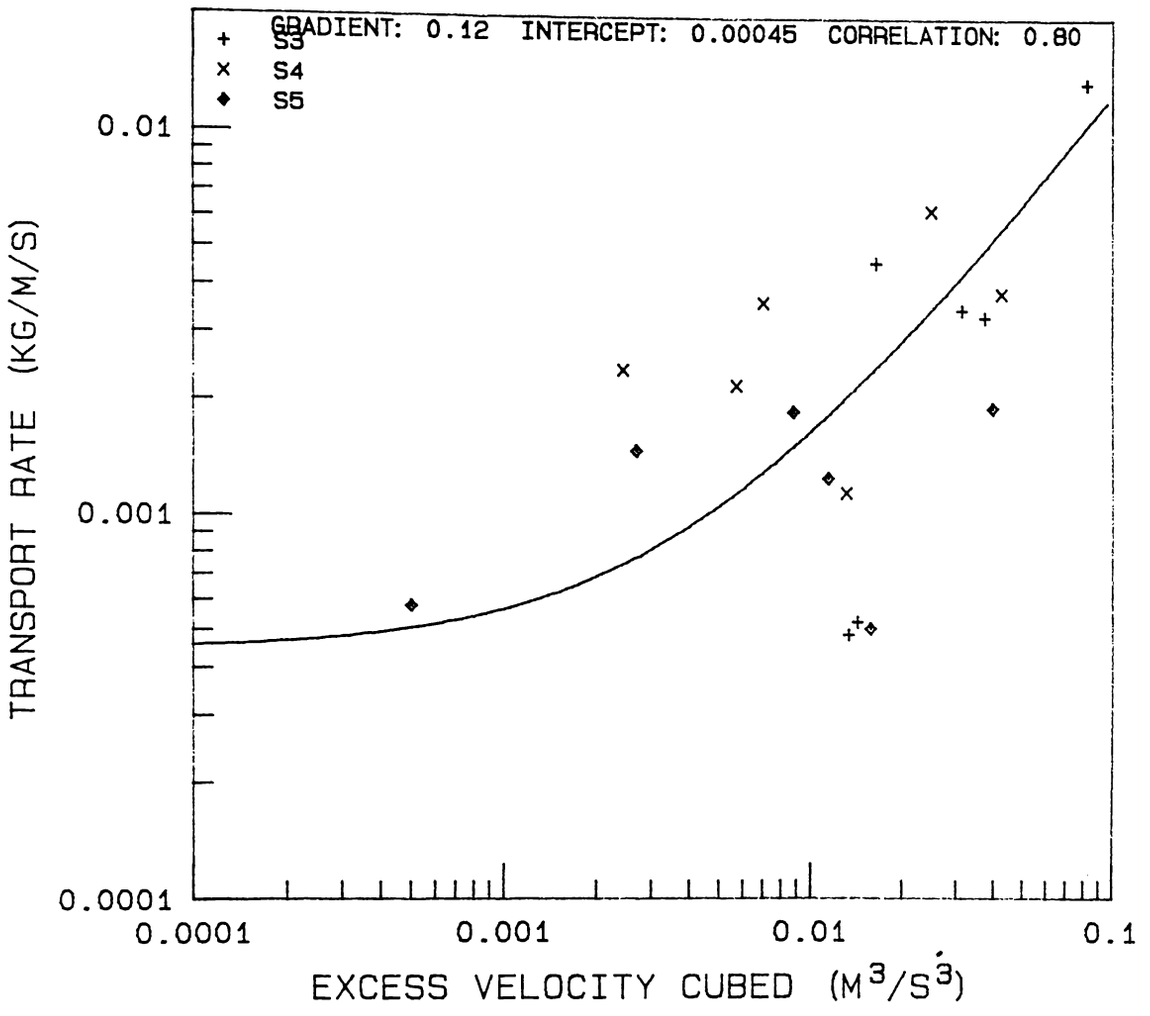

Figure 7.25: Measured bedload transport rate (q_m) against the cube of the excess velocity at lm $(u_l - u_{lcr})^3$, with the best fit linear equation.

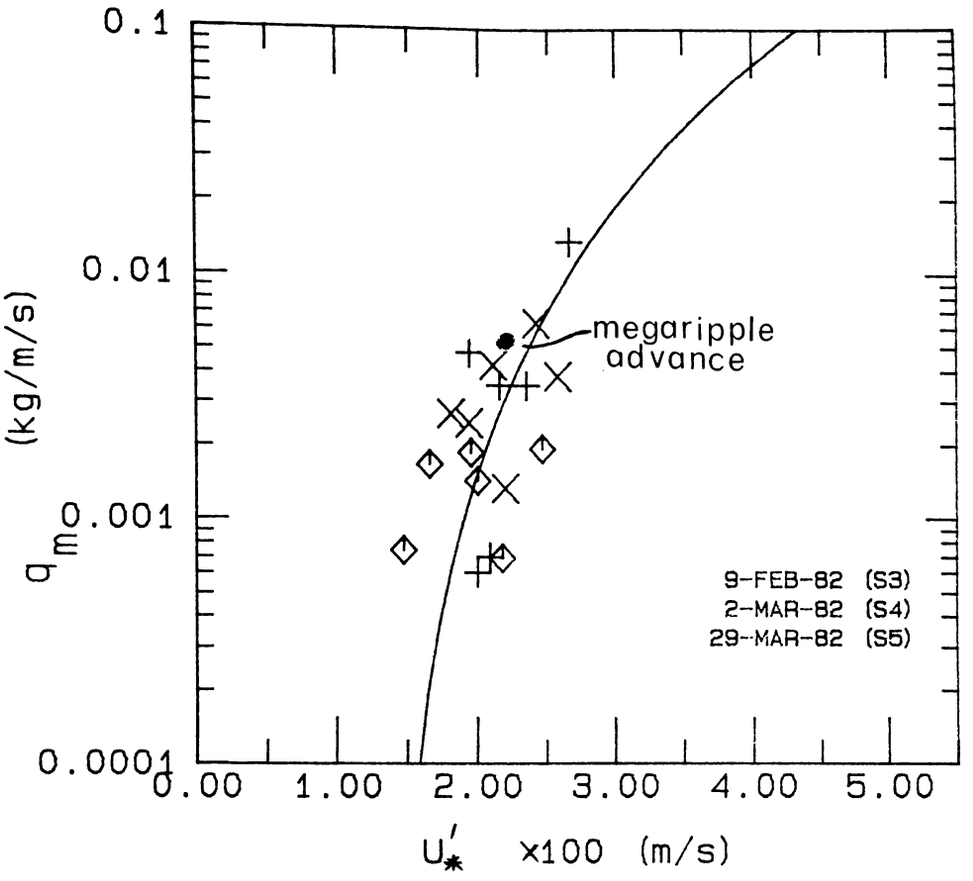

Figure 7.26: Measured bedload transport rate against the skin friction velocity, plotted with the Yalin bedload equation for D = 0.0003m and $u'_{*cr} = 0.014$ m.s^{-1}. The representative velocity was obtained with q = 3.

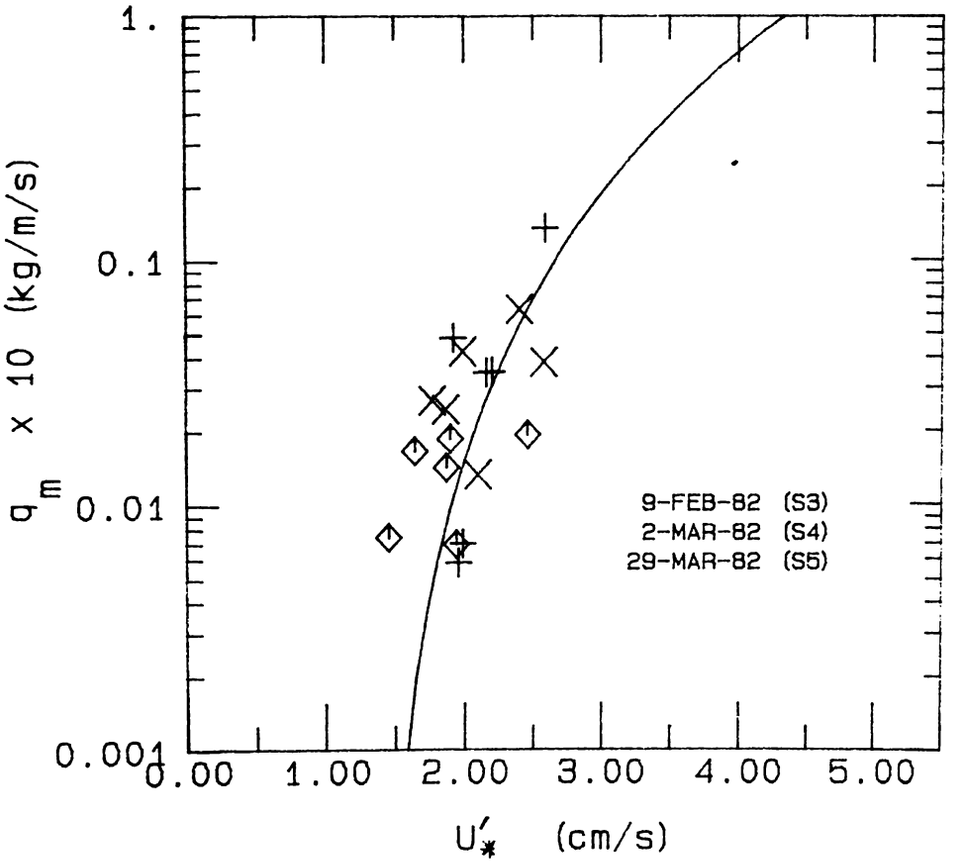

Figure 7.27: Measured bedload transport rates against the skin friction velocity, plotted with the Yalin bedload equation for D = 0.0003m and $U'_{*cr} = 0.014$ m.s^{-1}. The representative velocity was obtained with q = 1.

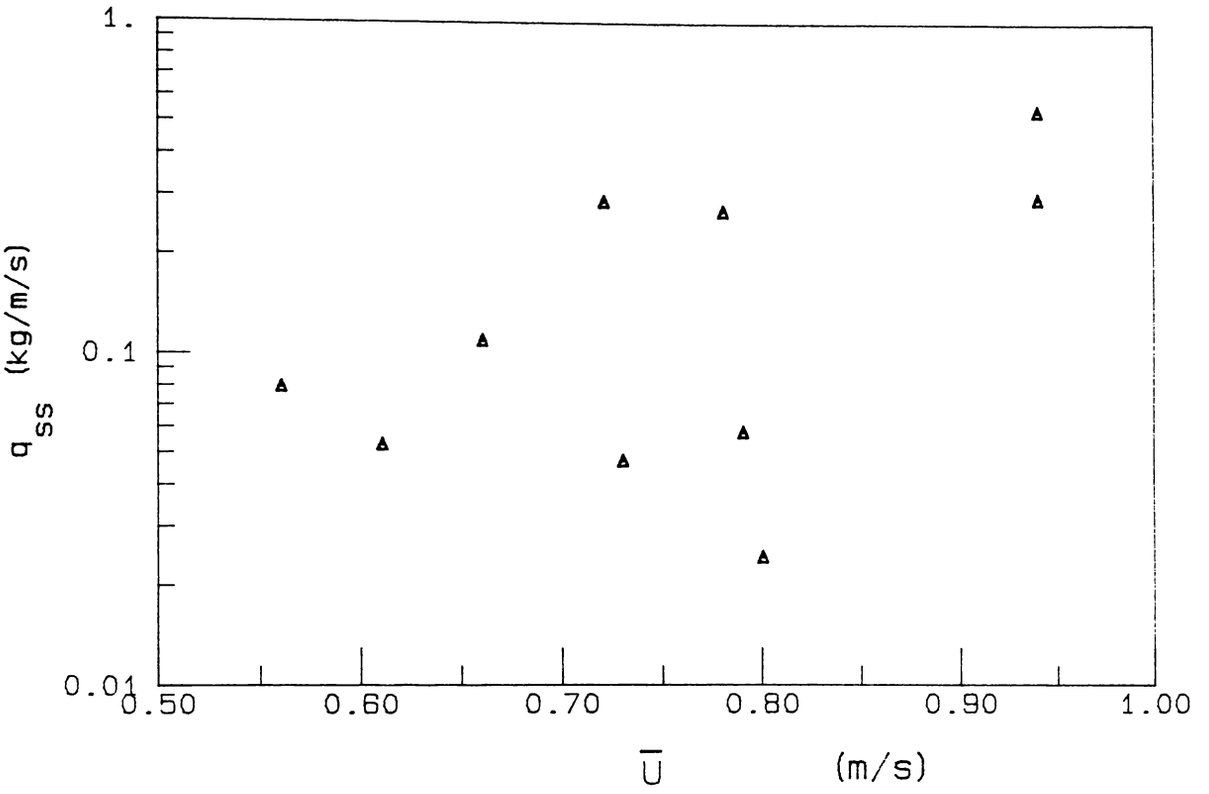

Figure 7.28: Suspended sediment mass transport rate (q_{ss},kg.m^{-1}.s^{-1}) against the mean velocity-averaged water velocity ($\bar{u}$), over megaripples at Sites S3-S5.

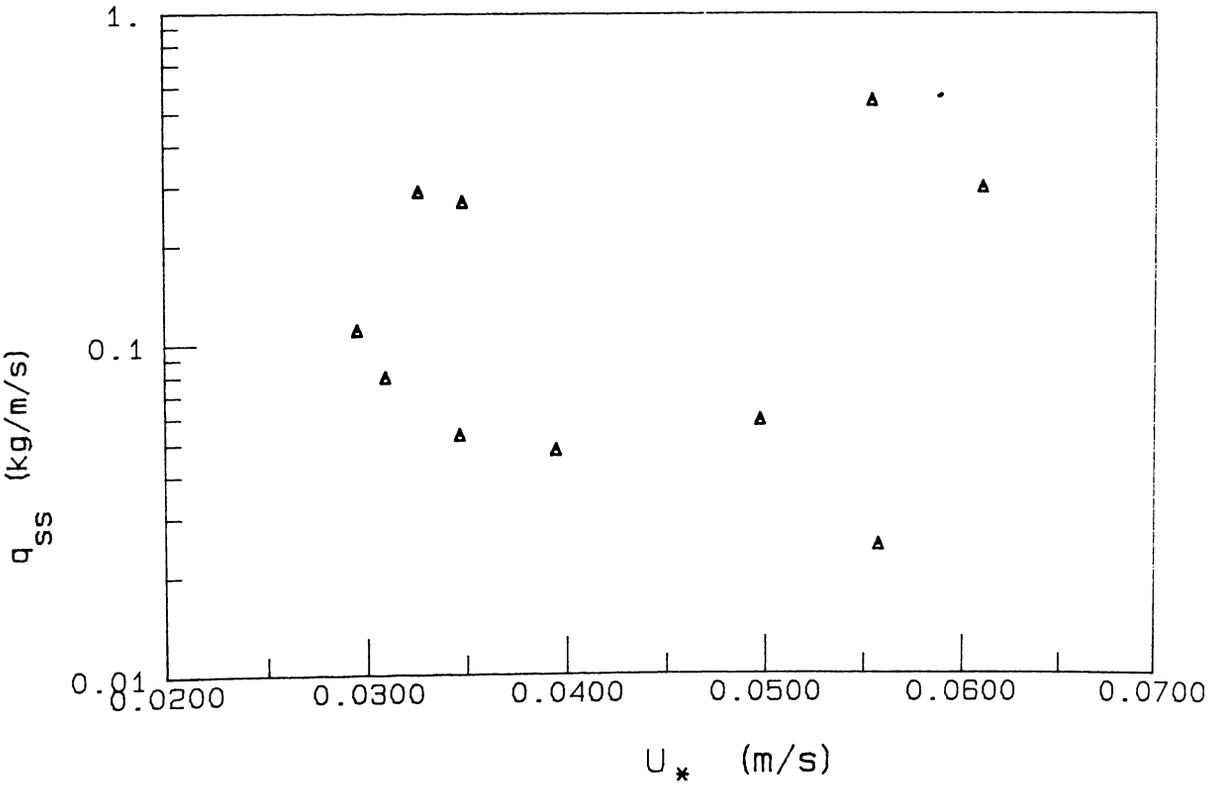

Figure 7.29: Suspended sediment mass transport rate (q_{ss} kg.m^{-1}.s^{-1}) against the friction velocity (u_*,m.s^{-1}), over megaripples at Sites S3-S5.

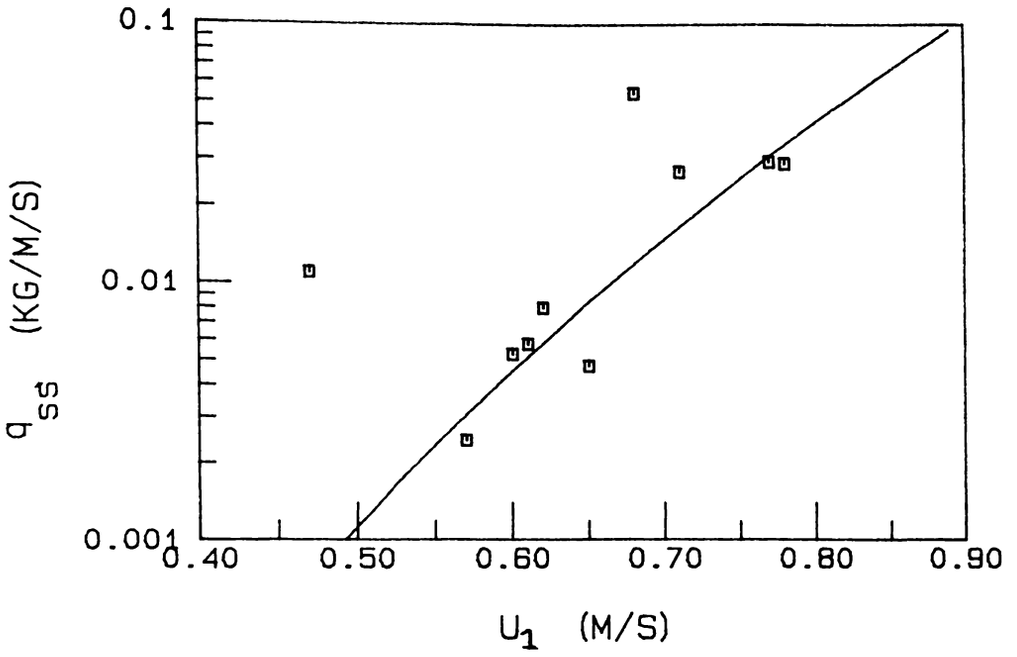

Figure 7.30: Suspended sediment mass transport rate against the speed at 1m with best fit curve.

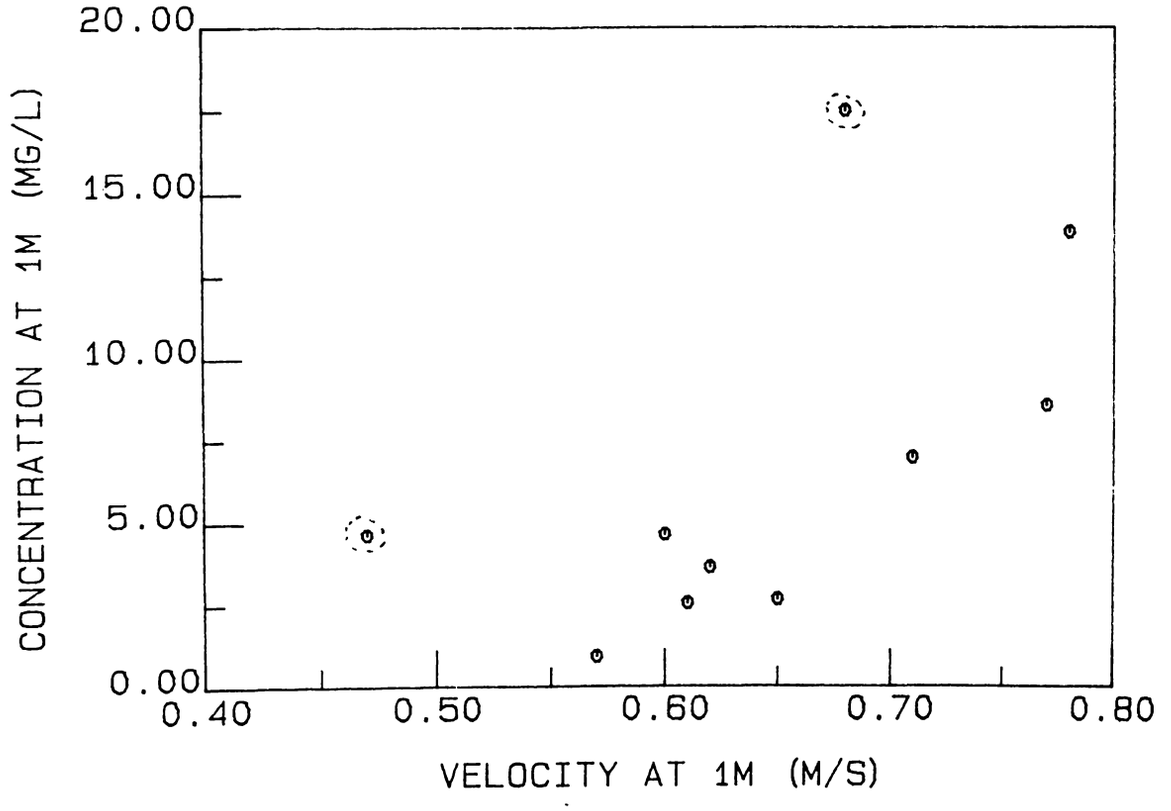

Figure 7.31: Suspended sandy sediment concentration at 1m above the bed against the 1m speed. Best fit curve, excluding the 2 data points circled is $C_1 = 56.5\ (u_1)^{6.3} \times 10^{-3}$, with correlation coefficient of 0.88.

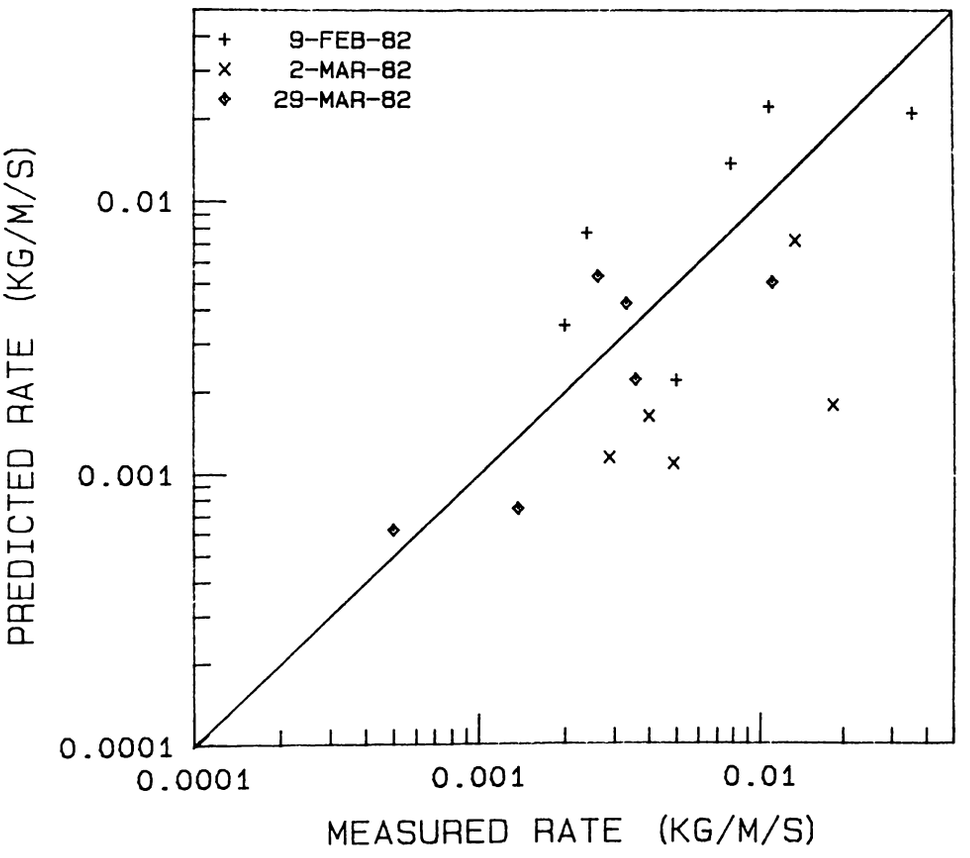

Figure 7.32: Predicted total load transport rate according to the Engelund Hansen equation against the measured total load transport rate.

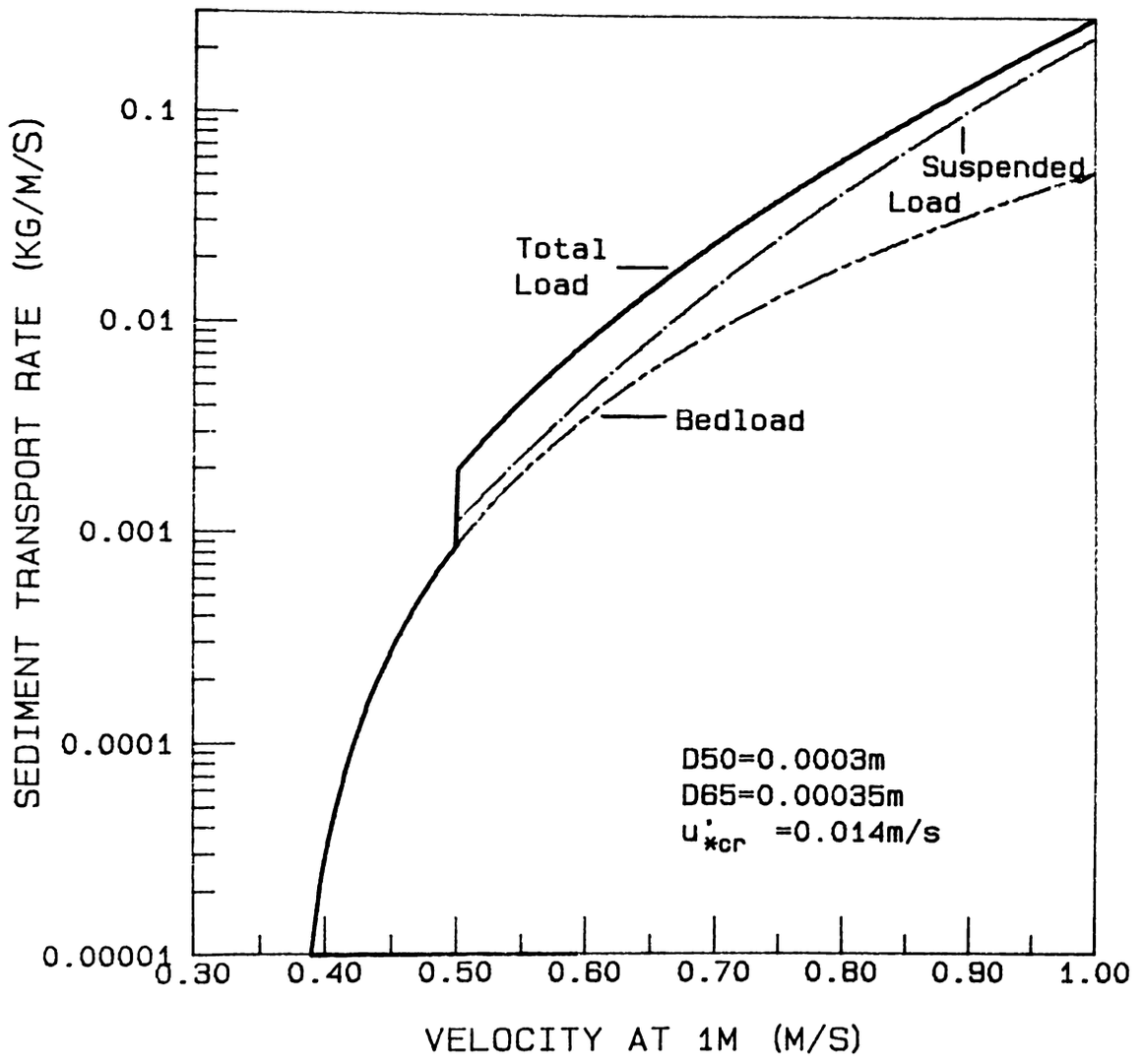

Figure 7.33: Bedload transport rate obtained with the procedure utilising the Yalin and Karman Prandtl equations; suspended load found empirically; and the total load against the speed at 1m above the bed for $D_{50} = 0.0003$m, $D_{65} = 0.00035$m and $u'_{*cr} = 0.014$ m.s^{-1}.

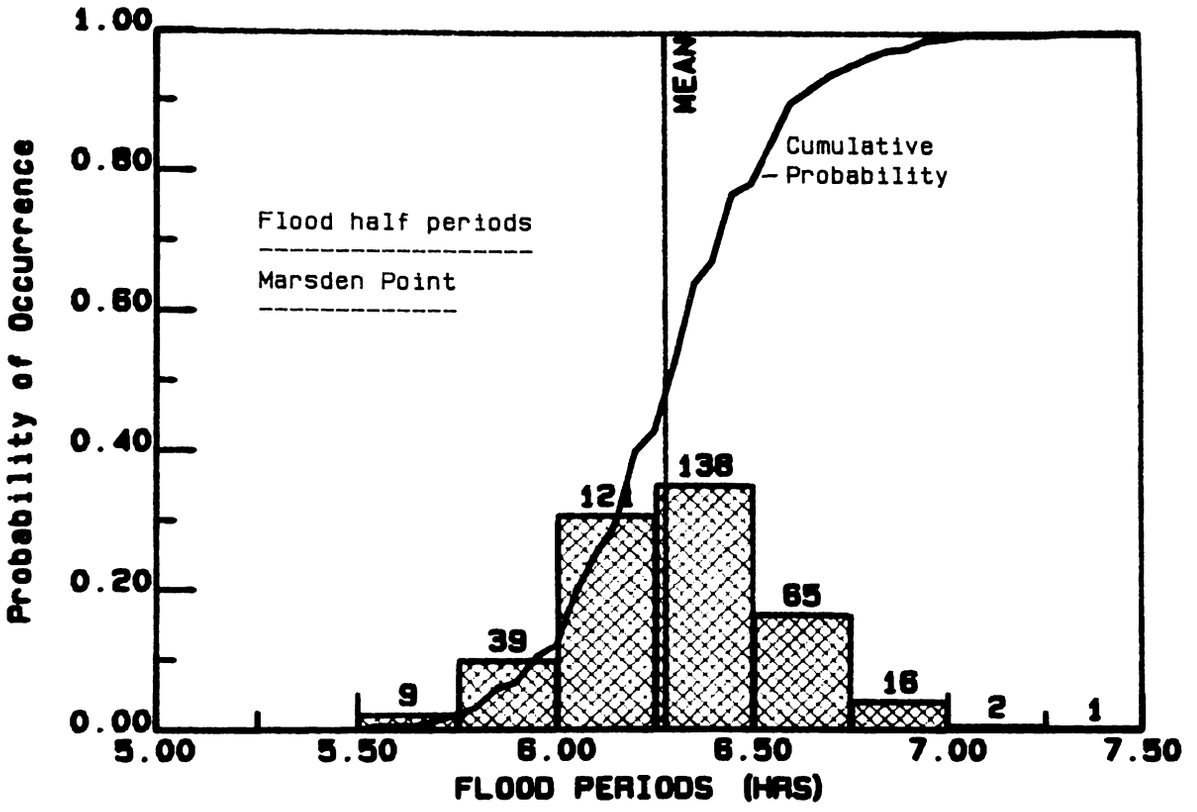

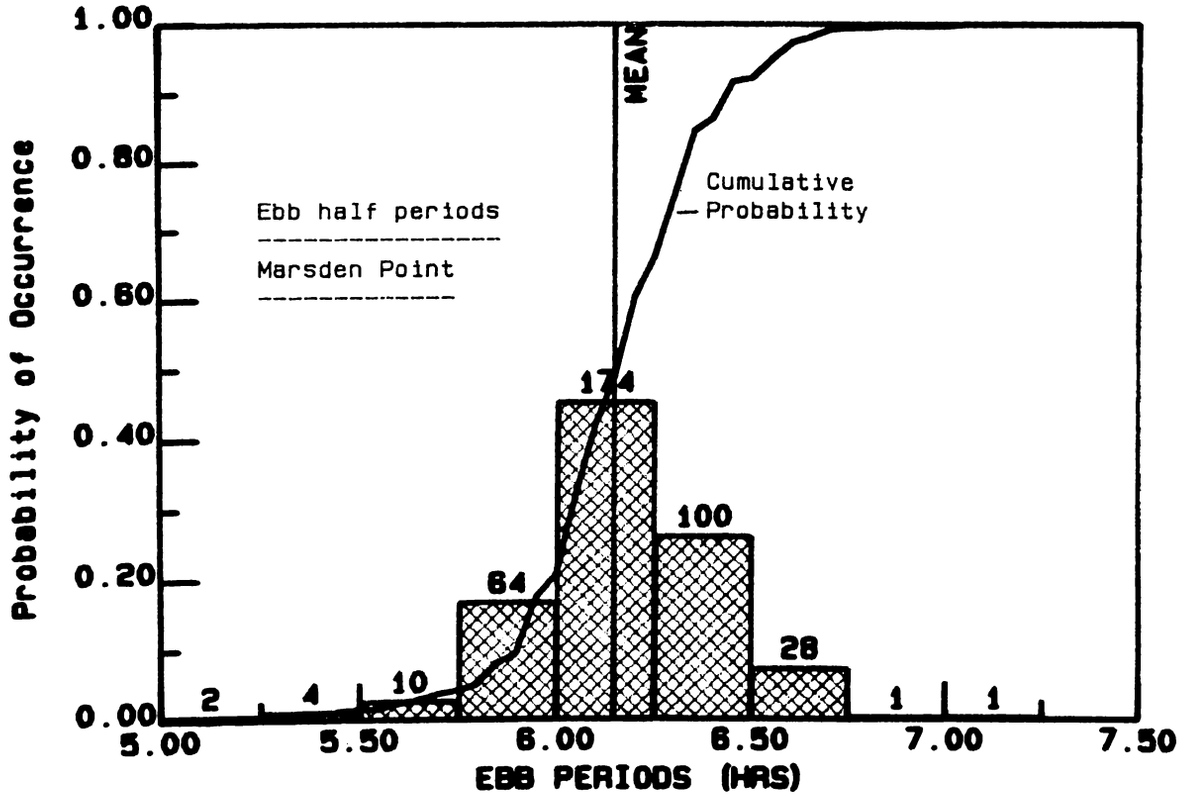

Figures 7.34 (upper) and 7.35: Histograms of flood (upper) and ebb half tidal periods ($T_{\frac{1}{2}}$) at Marsden Point wharf from June 1 to December 31, 1982.

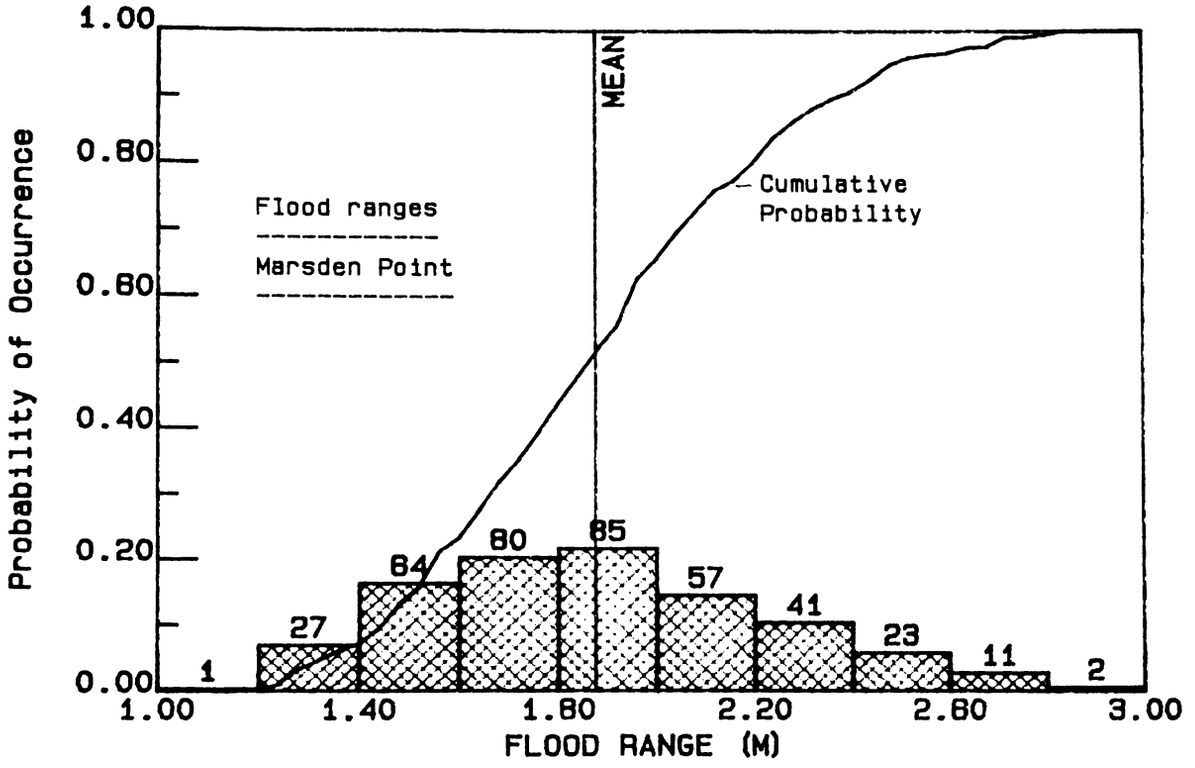

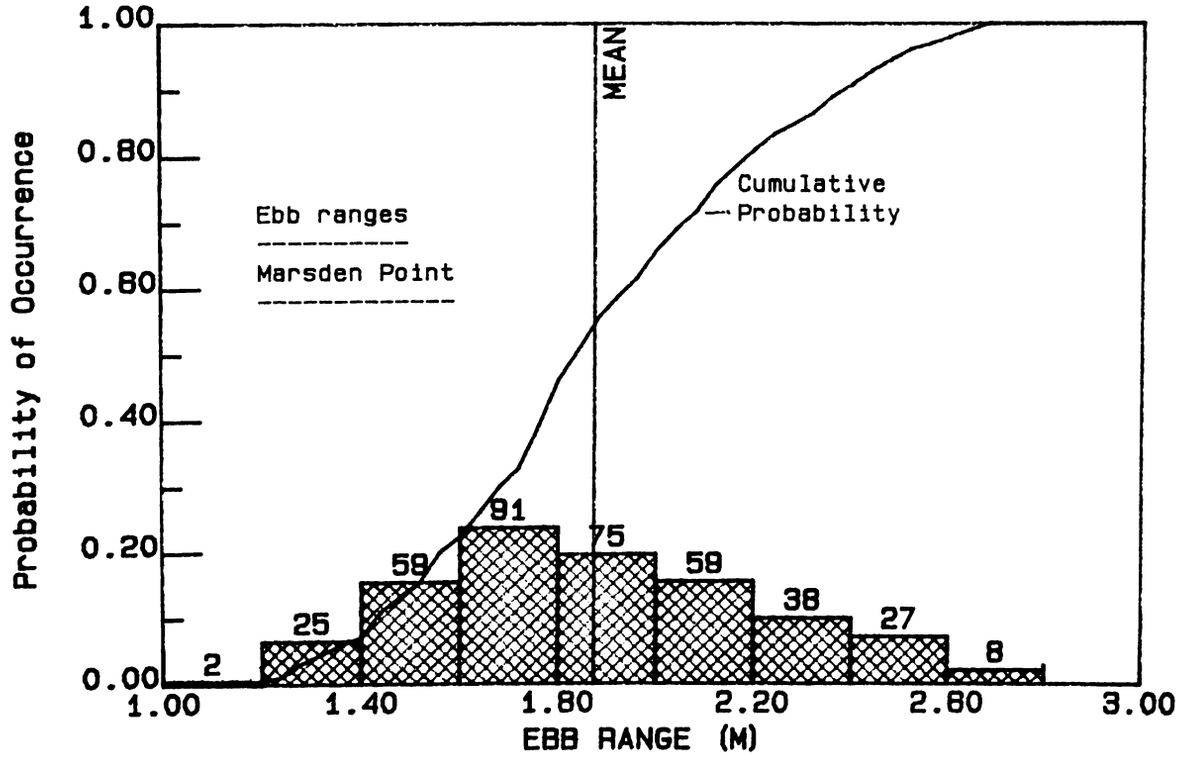

Figures 7.36 (upper) and 7.37: Histogram of flood (upper) and ebb tidal ranges (ΔH) at Marsden Point wharf from June 1 to December 31, 1982.

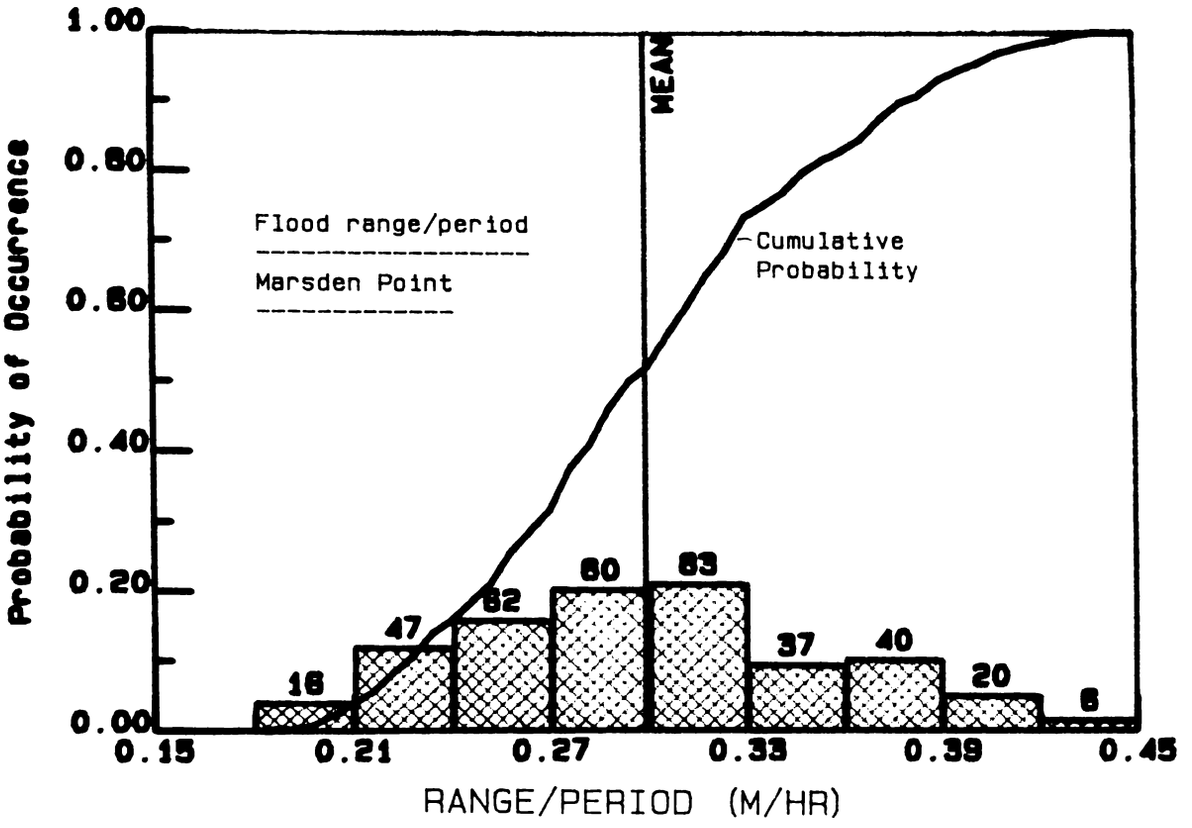

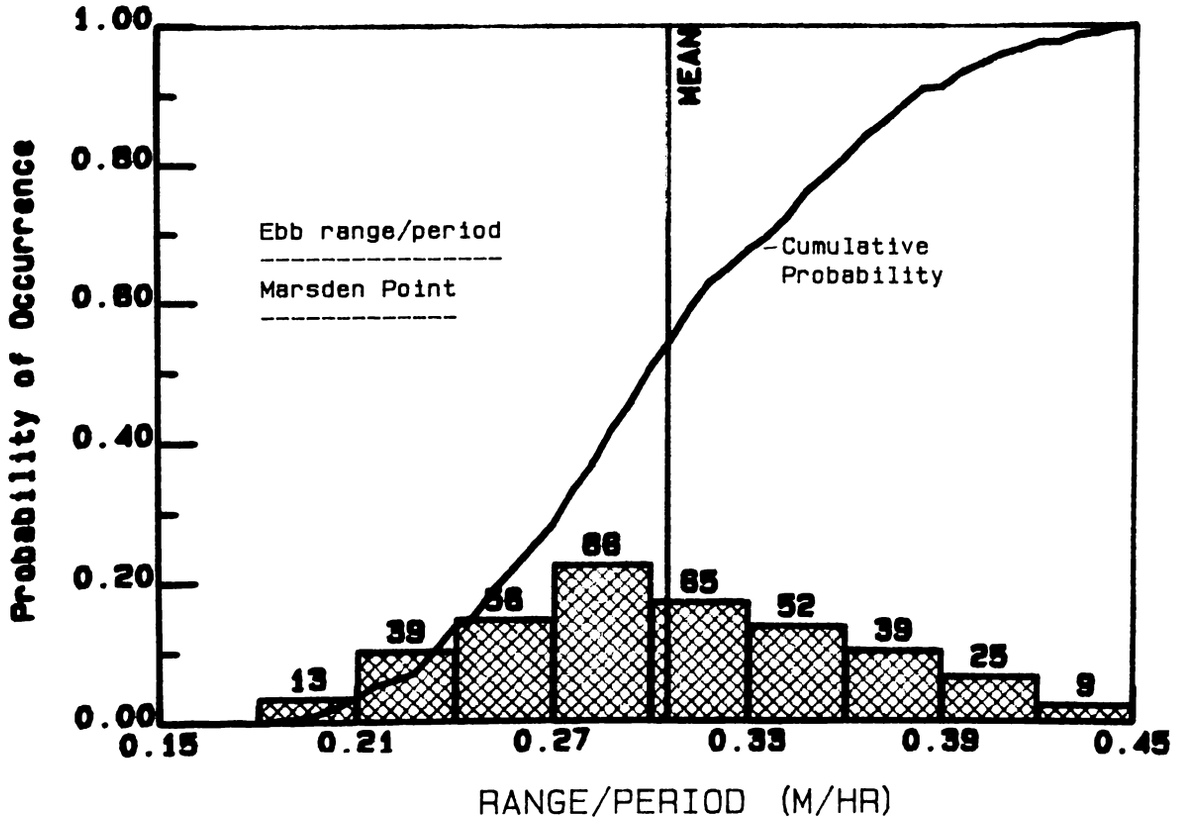

Figures 7.38 (upper) and 7.39: Histograms of flood (upper) and ebb ratios of tidal range over half tidal period ($\Delta H/T_{\frac{1}{2}}$), at Marsden Point wharf from June 1 to December 31, 1982.

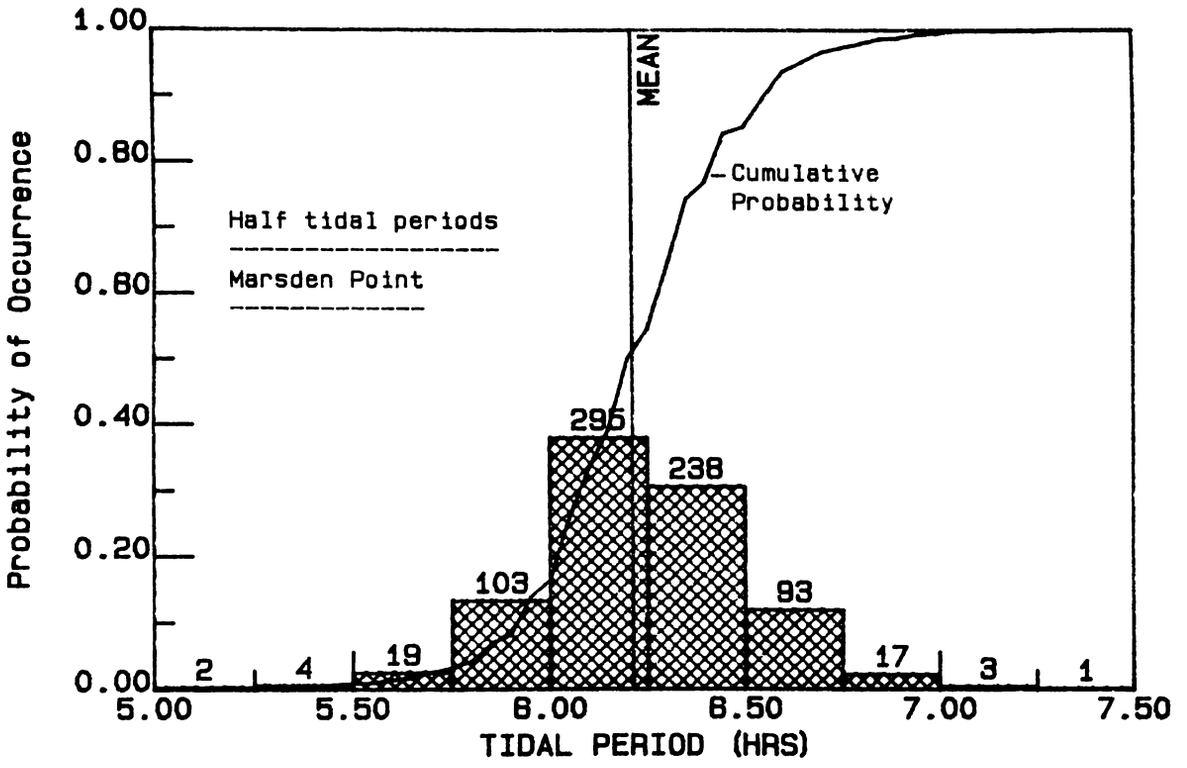

Figure 7.40: Histogram of half tidal periods ($T_{\frac{1}{2}}$) for ebb and flood tides combined at Marsden Point wharf from June 1 to December 31, 1982.

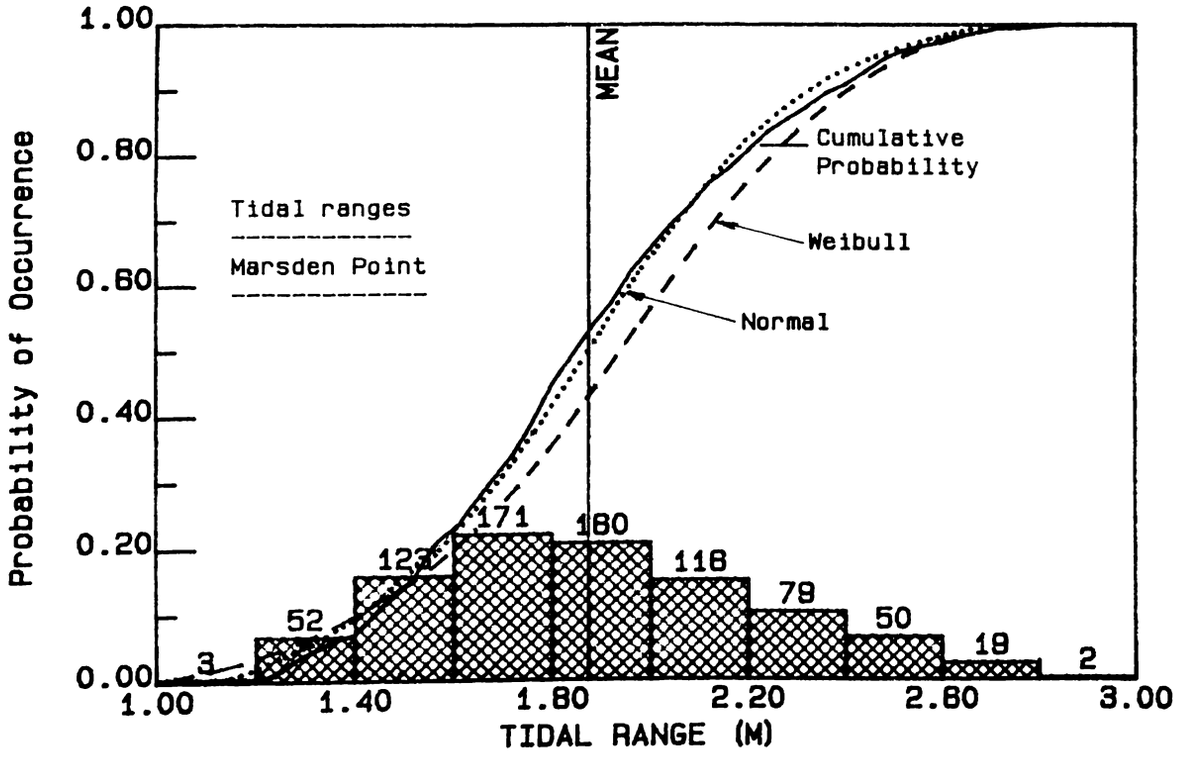

Figure 7.41: Histogram of tidal ranges (ΔH) for ebb and flood tides combined at Marsden Point wharf from June 1 to December 31, 1982. Best fit Weibull and Normal cumulative probability curves are also shown.

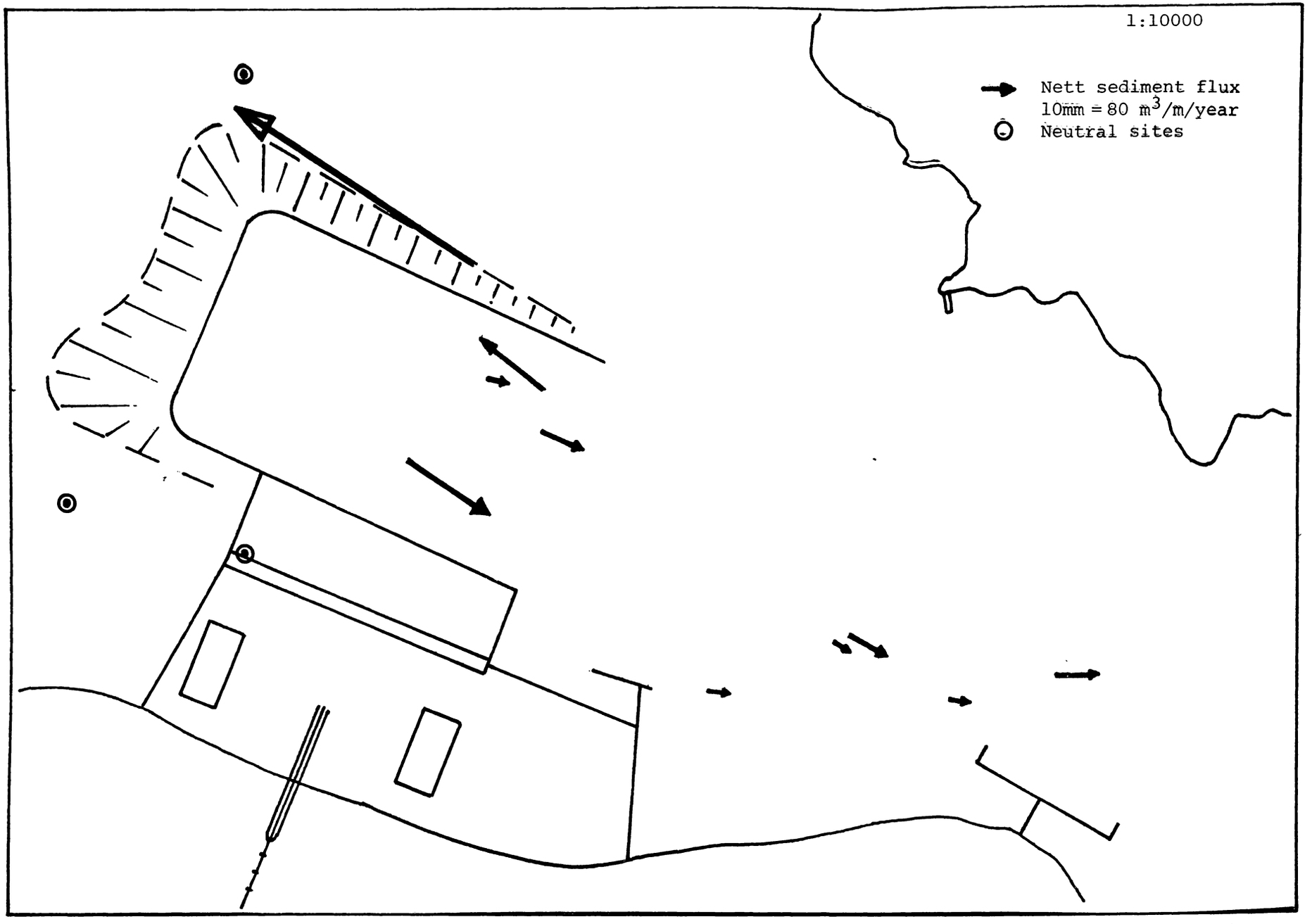

Figure 7.42: Nett sediment fluxes from Table 7.12 for the present bathymetry in the region of the proposed timber port. The side-scan sonar survey is also shown.

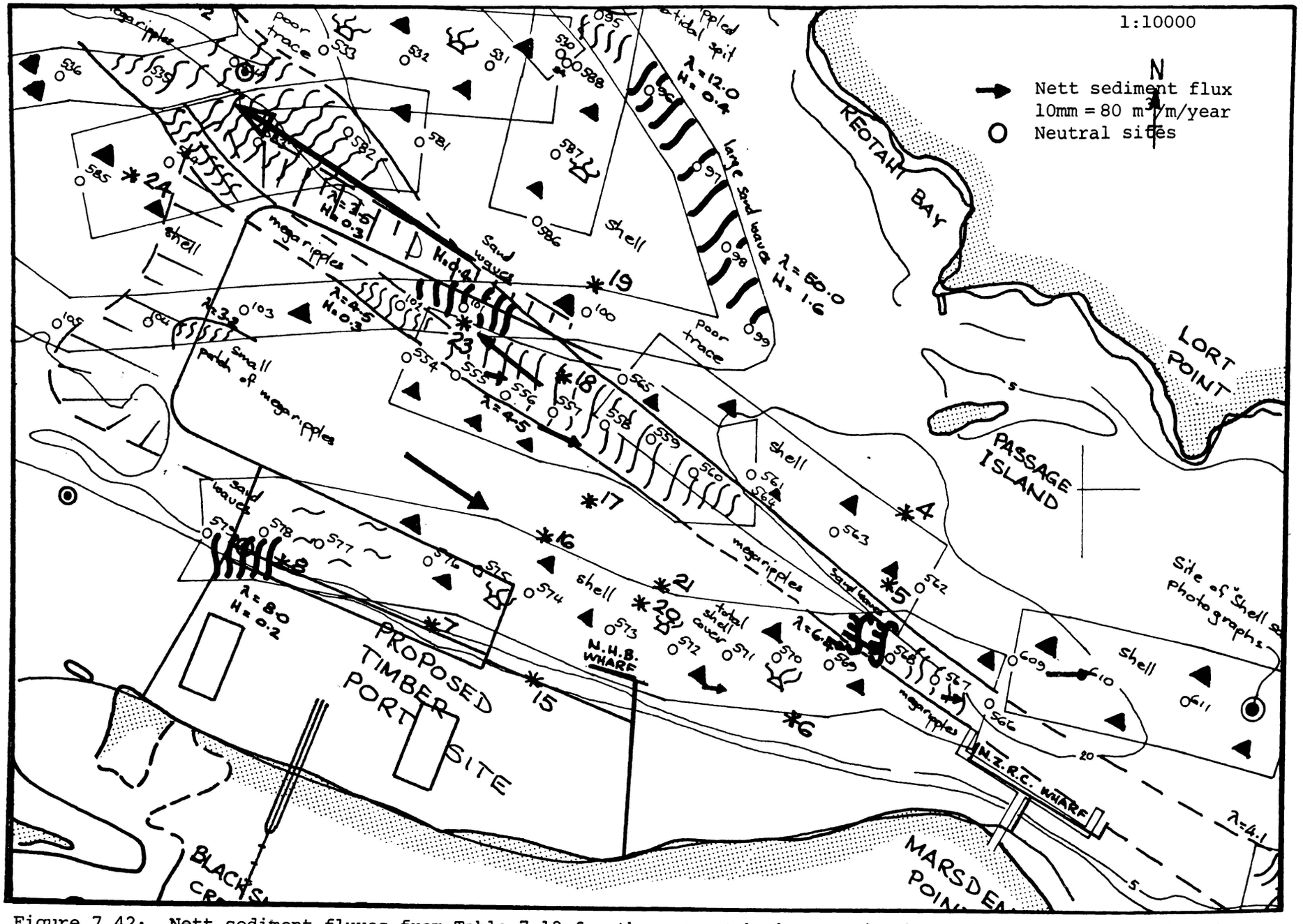

Figure 7.42: Nett sediment fluxes from Table 7.12 for the present bathymetry in the region of the proposed timber port. The side-scan sonar survey is also shown.

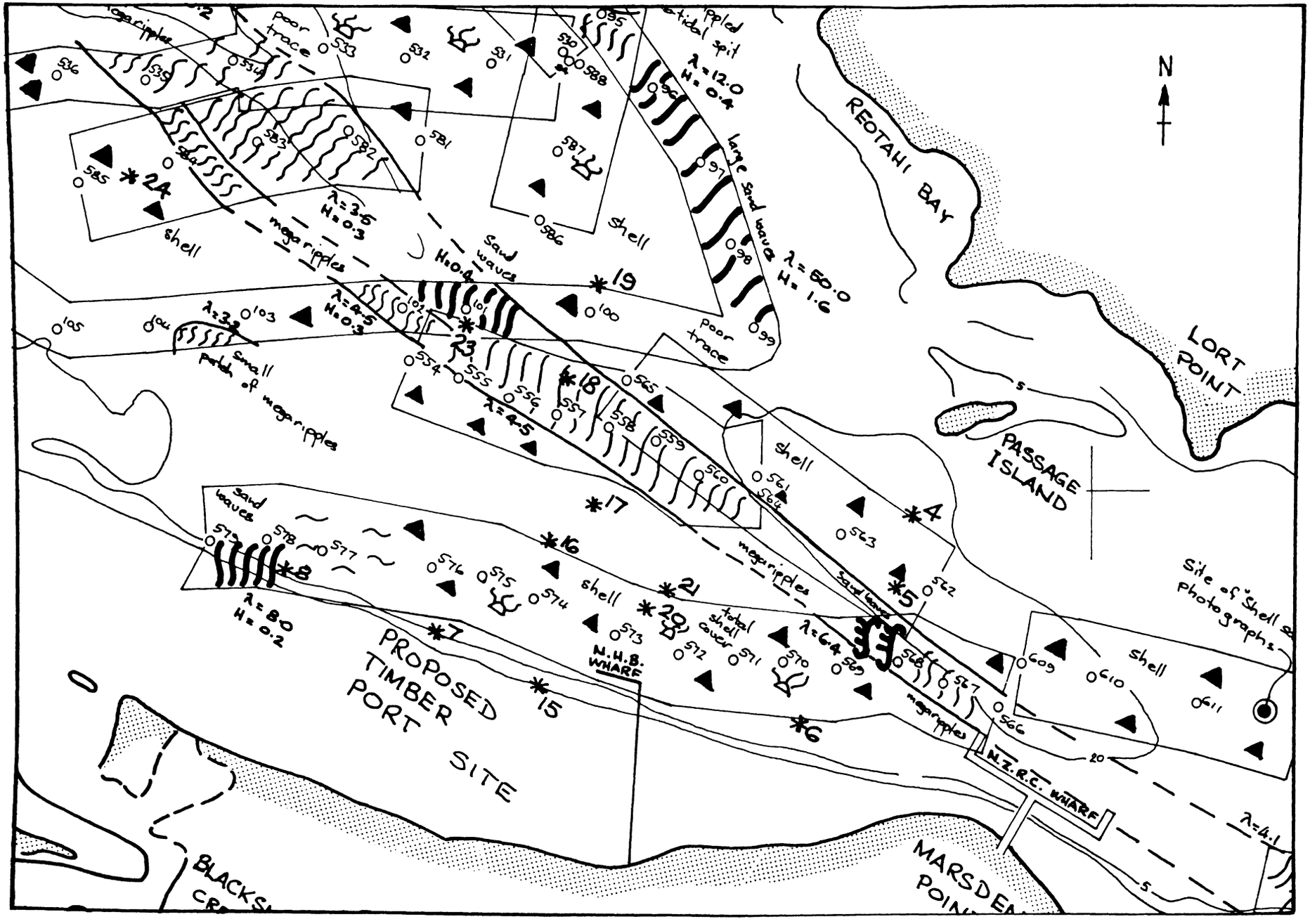
N
REOTAHI BAY
LORT POINT
PASSAGE ISLAND
PROPOSED TIMBER PORT SITE
N.H.B. WHARF
M.Z.R.C. WHARF
MARSDEN POINT
BLACKS
CR
shell
poor trace
large sand waves
sand waves
megaripples
small patch of megaripples
tidal shell cover
Site of "Shell" photographs
λ=12.0 H=0.4
λ=80.0 H=1.6
λ=3.6 H=0.3
λ=4.5 H=0.3
λ=3.9
λ=4.5
λ=8.0 H=0.2
λ=6.4
λ=4.1
H=0.4
20
5

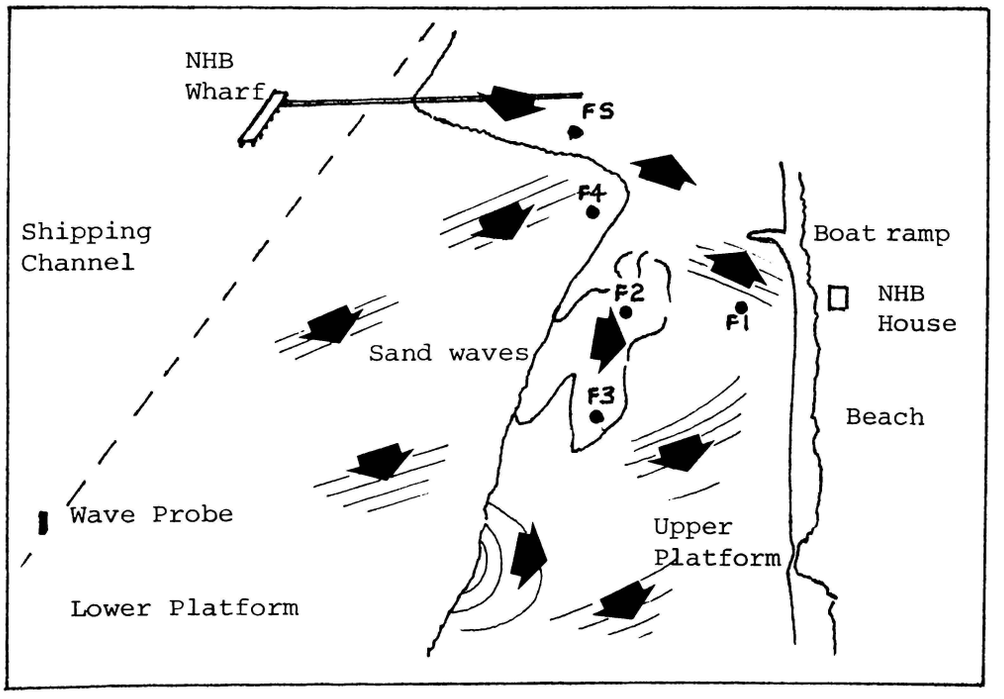

Figure 8.1: Schematic diagram of an aerial photograph showing the inter-tidal zone at the proposed port site. Sediment trapping sites and sediment transport directions inferred from the large-scale bedforms are shown. Note that the onshore arrows on the lower platform are opposed to the measured ebb current dominance. These are unsupported by any other field evidence.

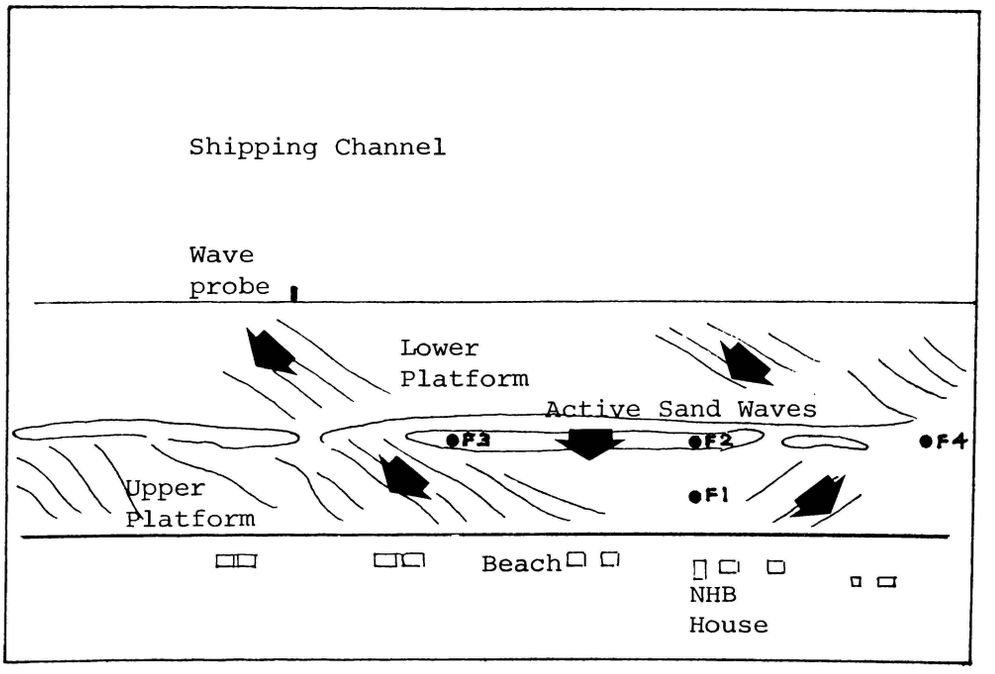

Figure 8.2: Schematic diagram of an aerial photograph showing the inter-tidal zone at the proposed port site. Sediment trapping sites and sediment transport direction inferred from the large-scale bedforms are shown.

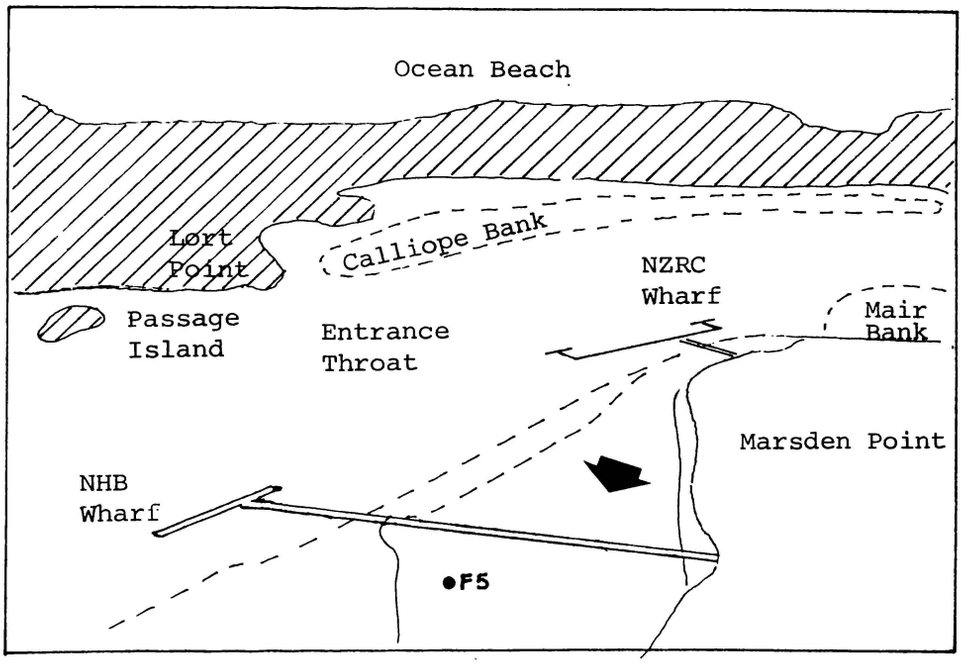

Figure 8.3: Schematic diagram showing sediment transport direction implied from the similarity of sediments on Marsden Point and between the wharves. The approximate location of Trapping Site F5 is shown.

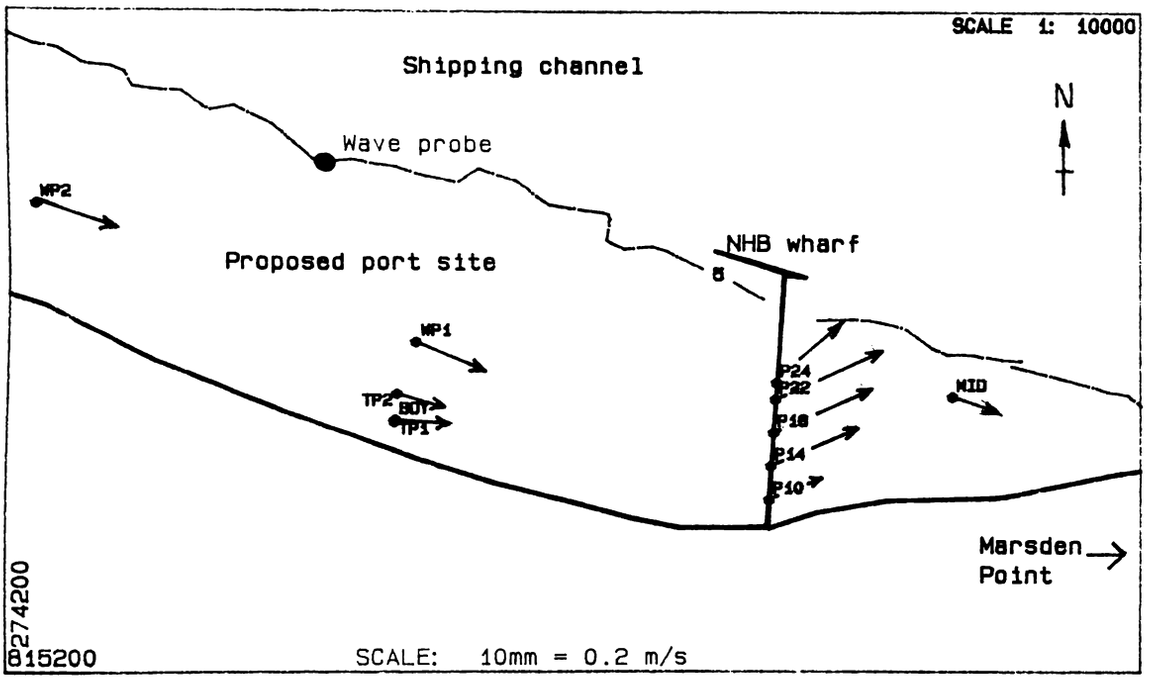

Figure 8.4: Water velocity measurement sites at the proposed port site. The arrows show the fastest velocity recorded at each location at 0.2m above the bed.

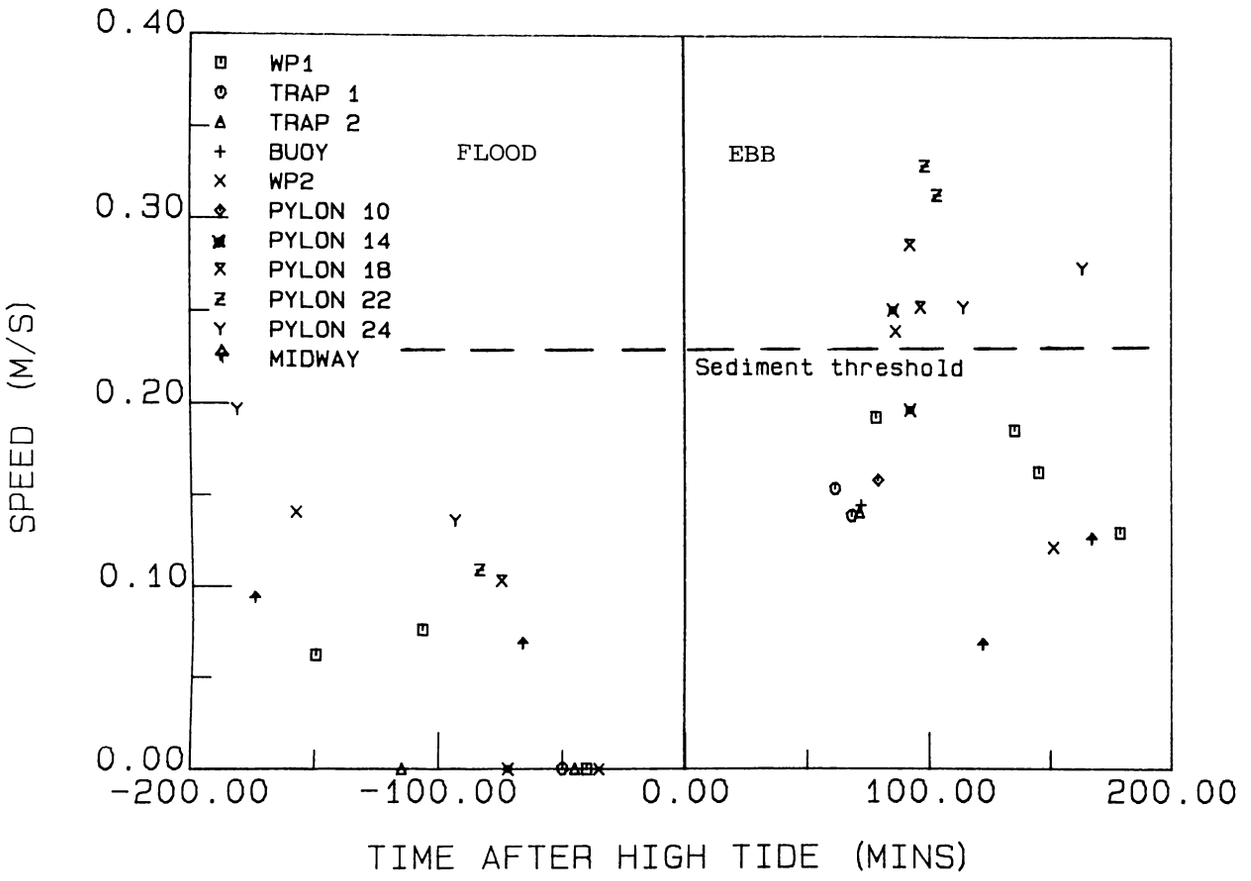

Figure 8.5: Water speeds at 0.2m above the bed measured with an Ott impellor-type meter on the sand flats at the proposed timber port site. The approximate sediment threshold speed is shown.

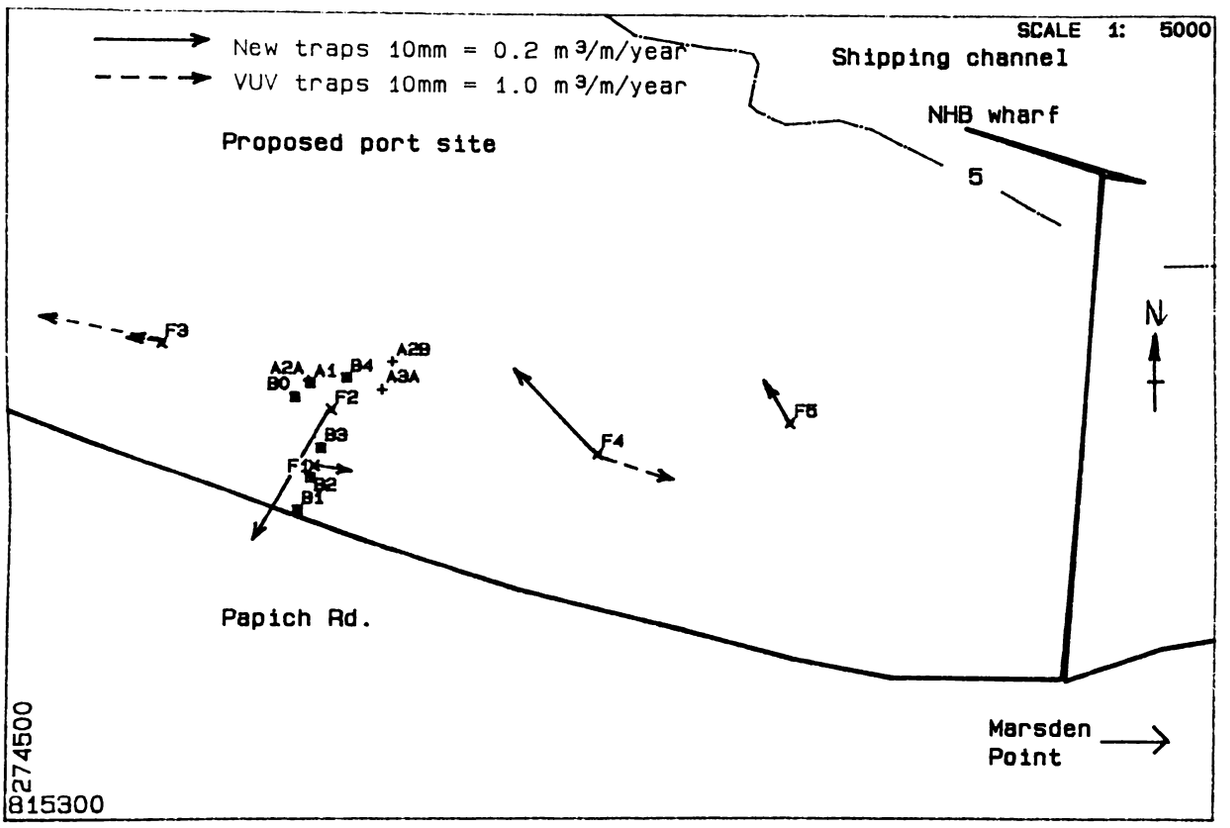

Figure 8.6: Sediment trapping sites on the inter-tidal zone at the proposed port site for the June and August series. Arrows show the resultant transport fluxes for the August series at the F series sites from Table 8.4.

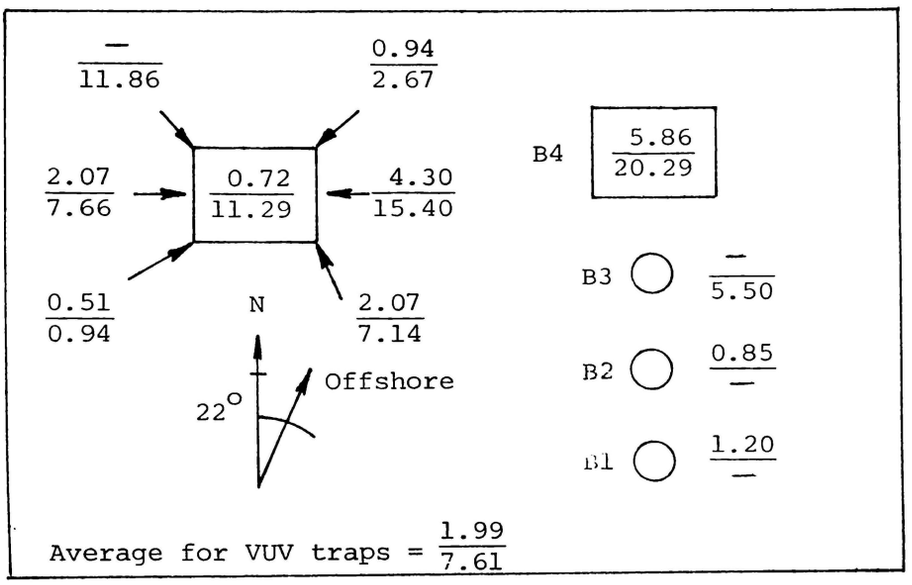

Figure 8.7: Schematic diagram showing scaled sediment trap catches (kg/m/tidal cycle) for two calibration experiments. Upper figures for the period 19:00 on 5-Jun-81 to 04:00 on 6-Jun-81. Lower figures for the next tidal cycle till 14:00 on 6-Jun-81.

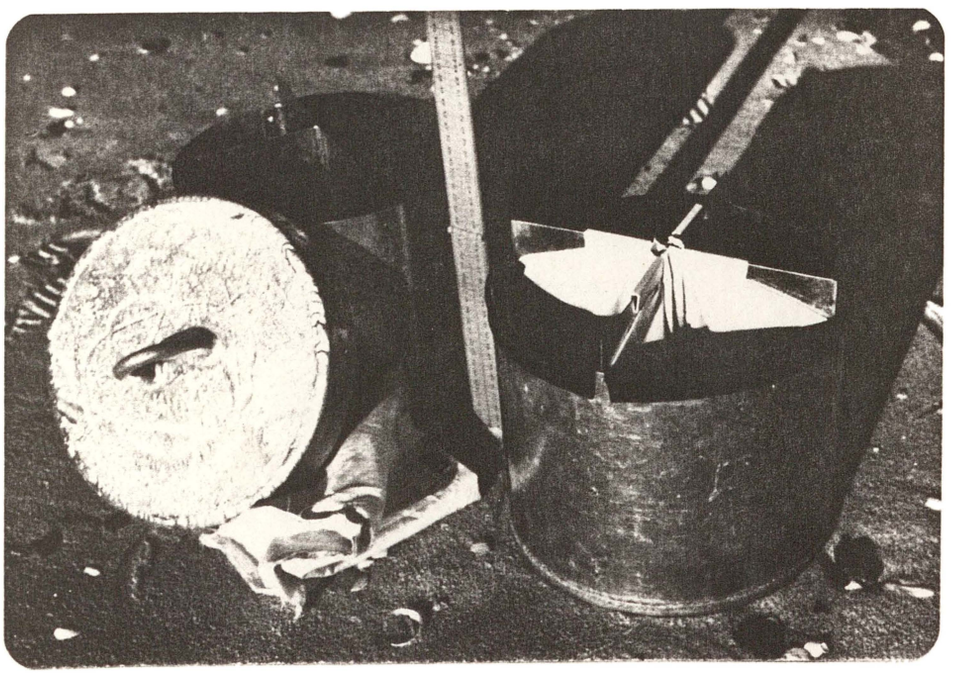

Figure 8.8: New sediment traps designed for the inter-tidal zone.

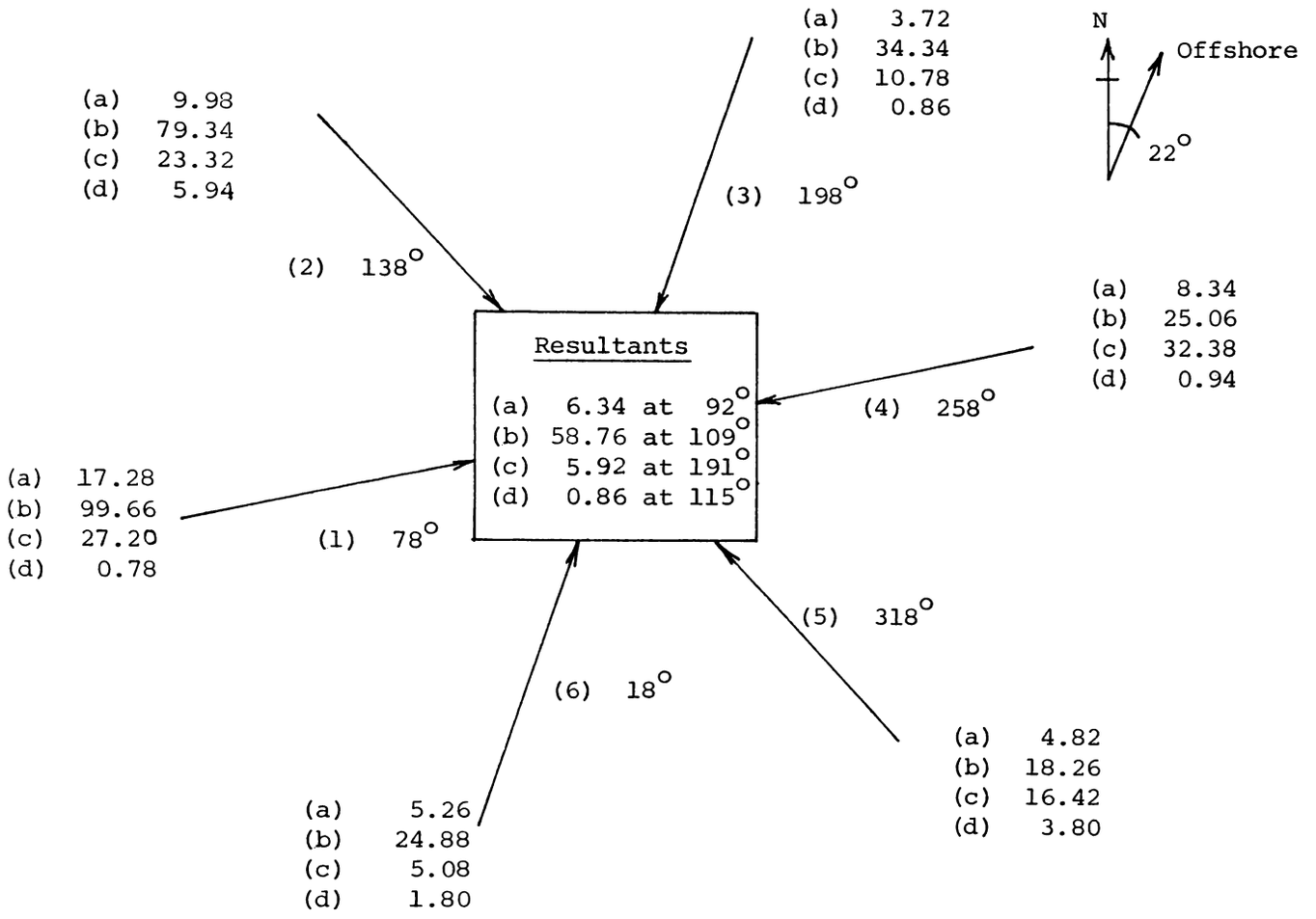

Figure 8.9: VUV corrected sediment trap catches in kg/m/tidal cycle for the periods (a) 0706 AM: 1930 on 6/6/81 to 06.00 on 7/6/81 (b) 0706 PM: until 16.00 on 7/6/81 (c) 0806 AM: until 06.00 on 8/6/81 (d) 0806 PM: until 18.00 on 8/6/81. Location A1 on a loosely-packed sandwave.

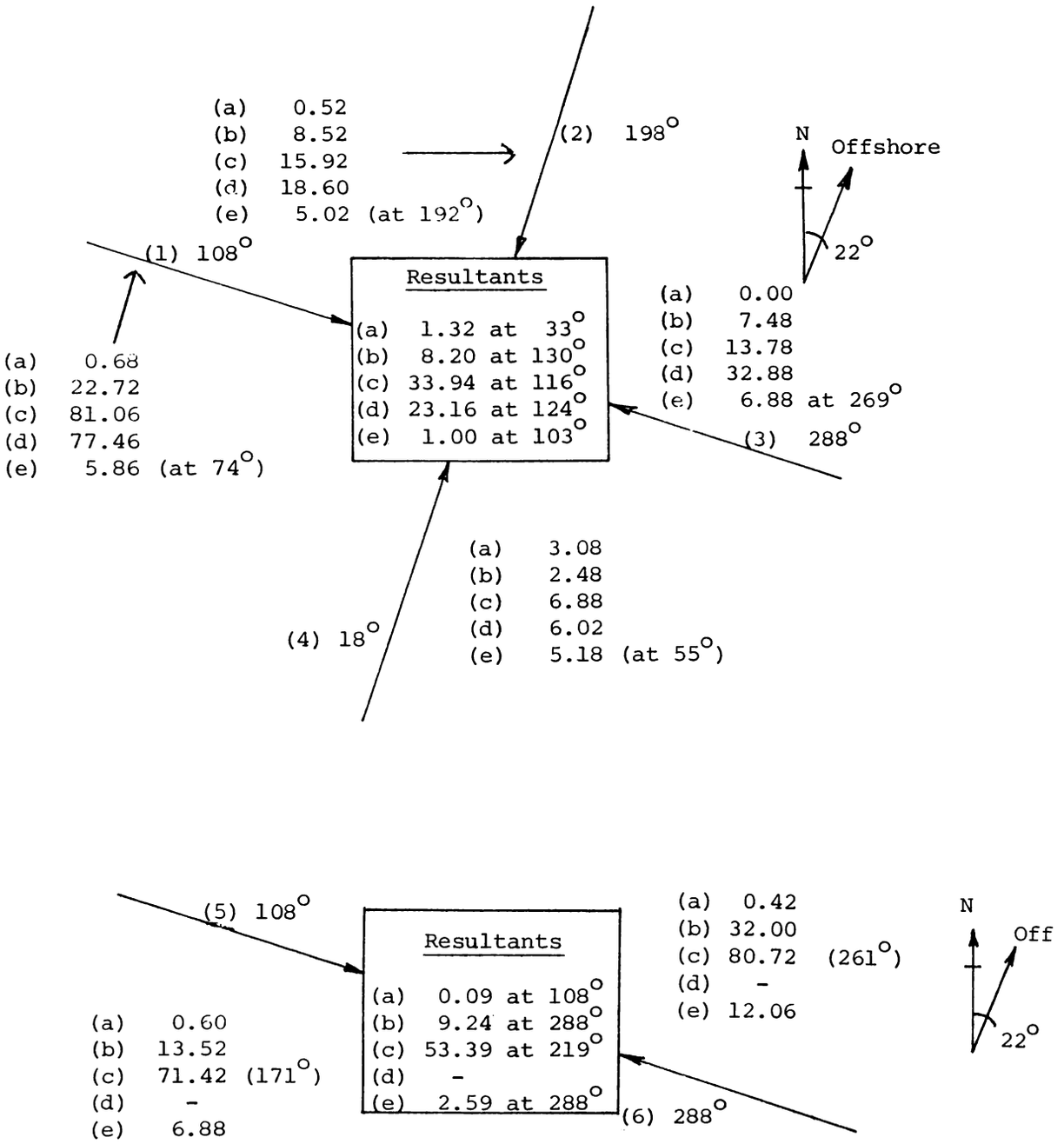

Figure 8.10: VUV corrected sediment trap catches in kg/m/tidal cycle for the periods (a) 0906 AM: 18.00 on 8/6/81 to 07.00 on 9/6/81 (b) 0906 PM: until 19.00 on the 9/6/81 (c) 1006 AM: until 08.00 on the 10/6/81 (d) 1006 PM: 08.00 until 14.00 on 10/6/81. Note this is for a flood half cycle only. Traps were retrieved at high tide except 5 and 6 (e) 1006 PM/2: until 22.00 on 10/6/81. Note this is for the ebb half cycle, except 5 and 6, which were deployed for a full cycle. Locations are A2A for the 4-trap array and A2B for the two-trap array.

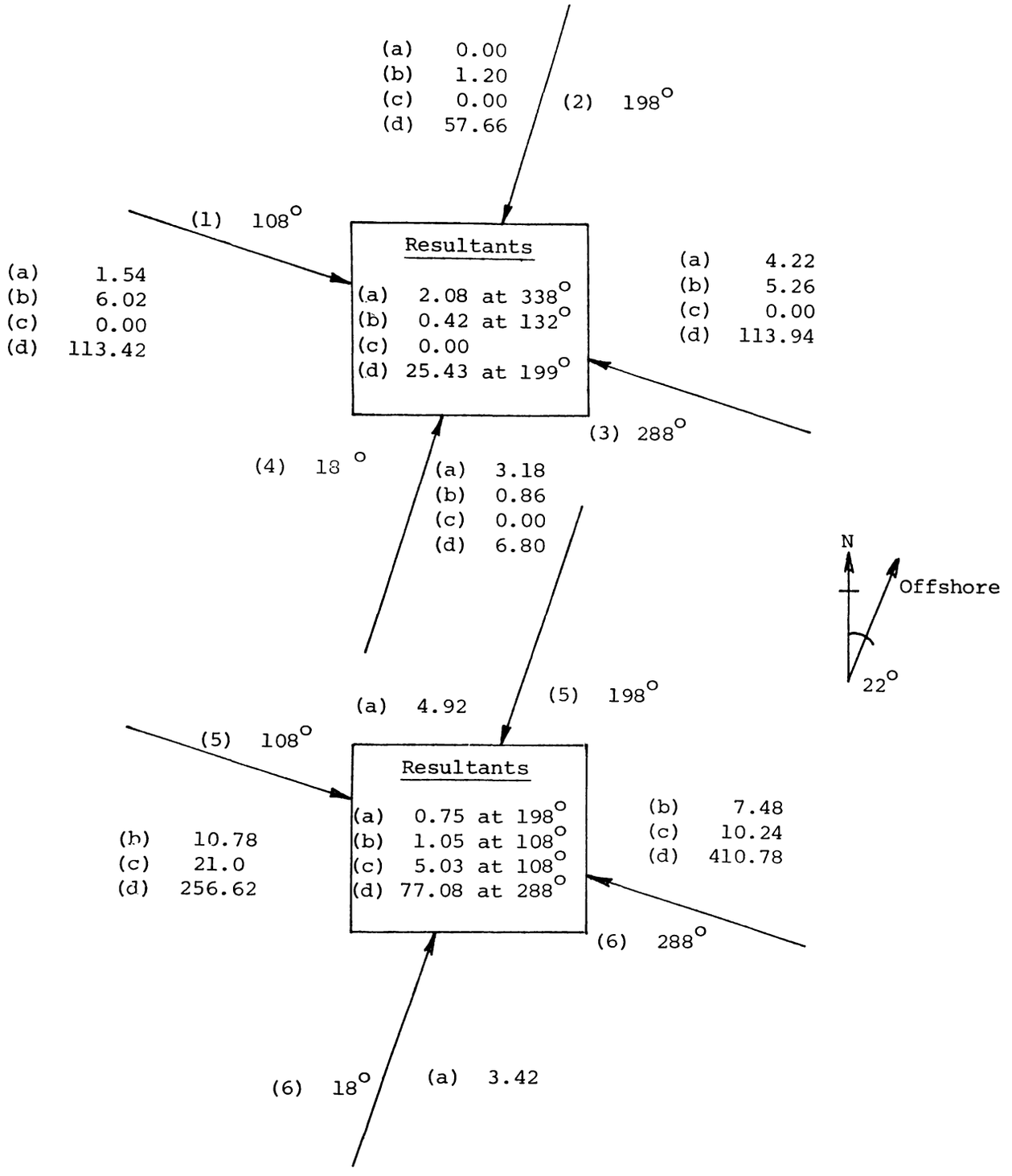

Figure 8.11: VUV corrected sediment trap catches in kg/m/tidal cycle for the periods (a) 1106 AM: 20.00 on 10/6/81 to 09.00 on the 11/6/81 (b) 1106 PM: until 21.00 on 11/6/81 (c) 1206 AM: until 09.00 on 12/6/81 (d) 1306 AM: until 10.00 on 13/6/81. Locations are A3A for the four trap array and A2B for the two-trap array.

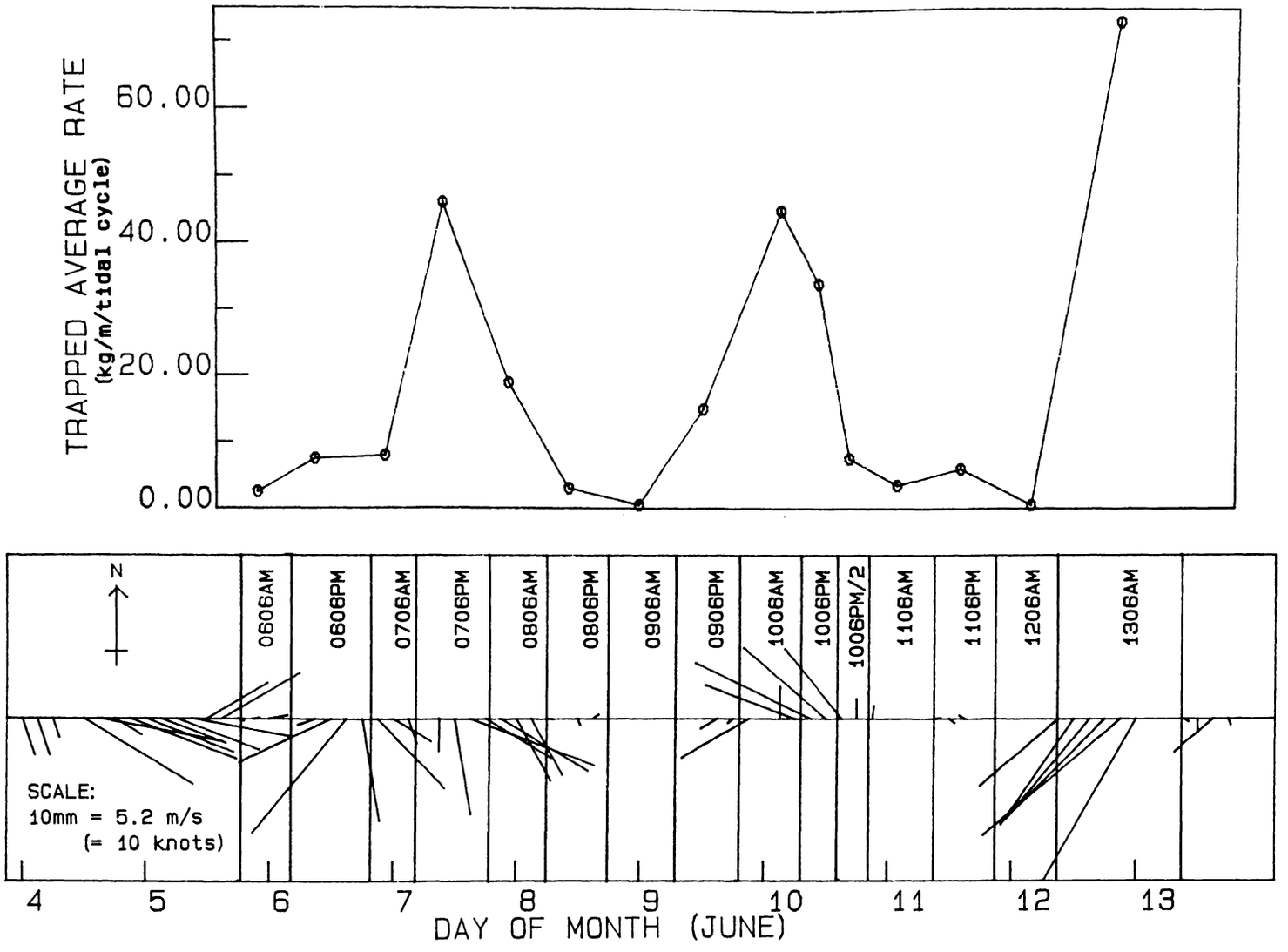

Figure 8.12: Wind velocities with the average sediment transport rates obtained using sediment traps for the June series.

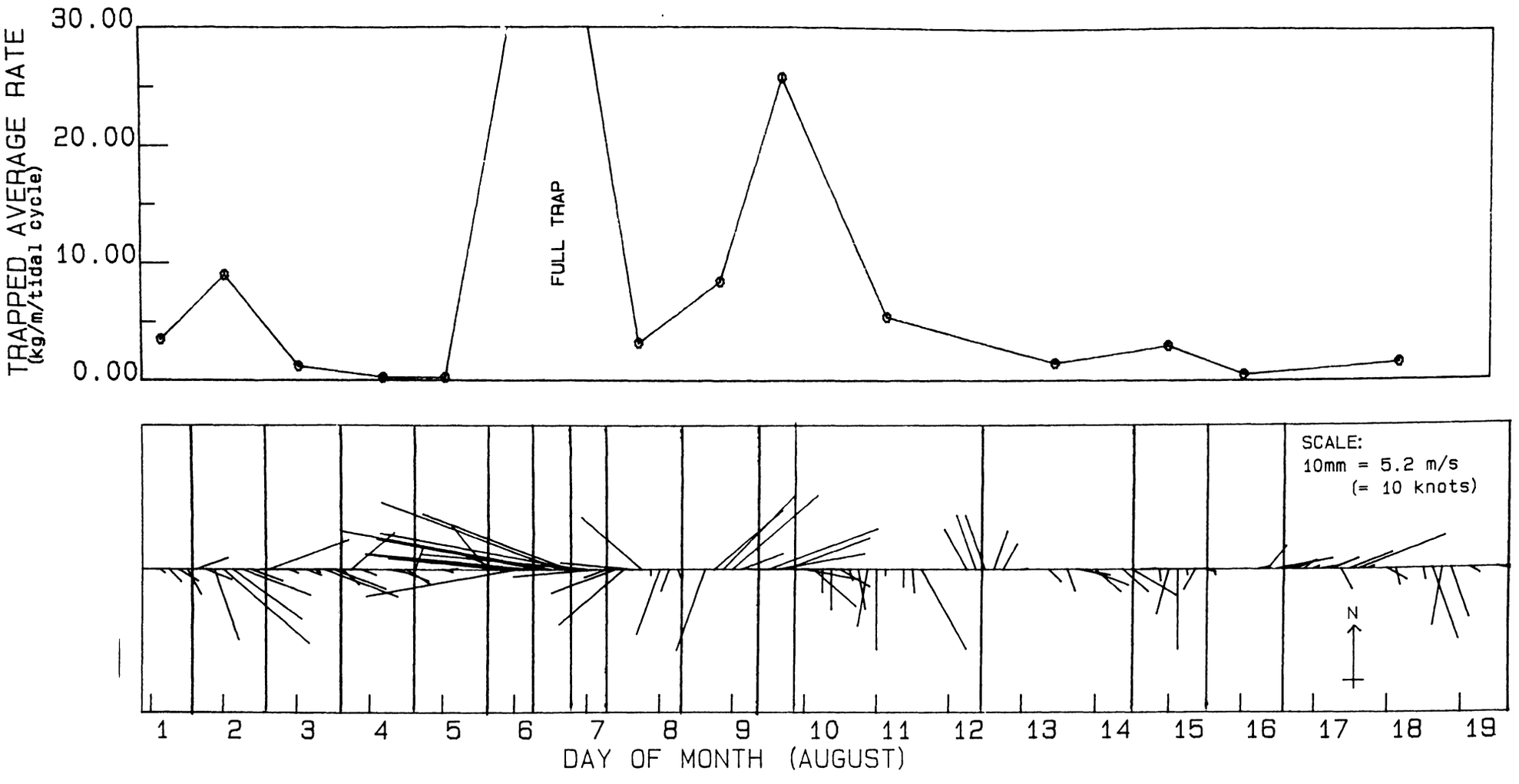

Figure 8.13: Wind velocities with the average sediment transport rates obtained using sediment traps for the August series.

Figure 8.14: SUBTLE, System Utilising Both Tape and Logger Equipment. From front anti-clockwise the components are: calculator for examination of solid state memories, cassette tape recorder, frequency to voltage converter, Tasman 32K mini data logger, timing unit. Also included are the wave probe transmitter and voltage scaling unit.

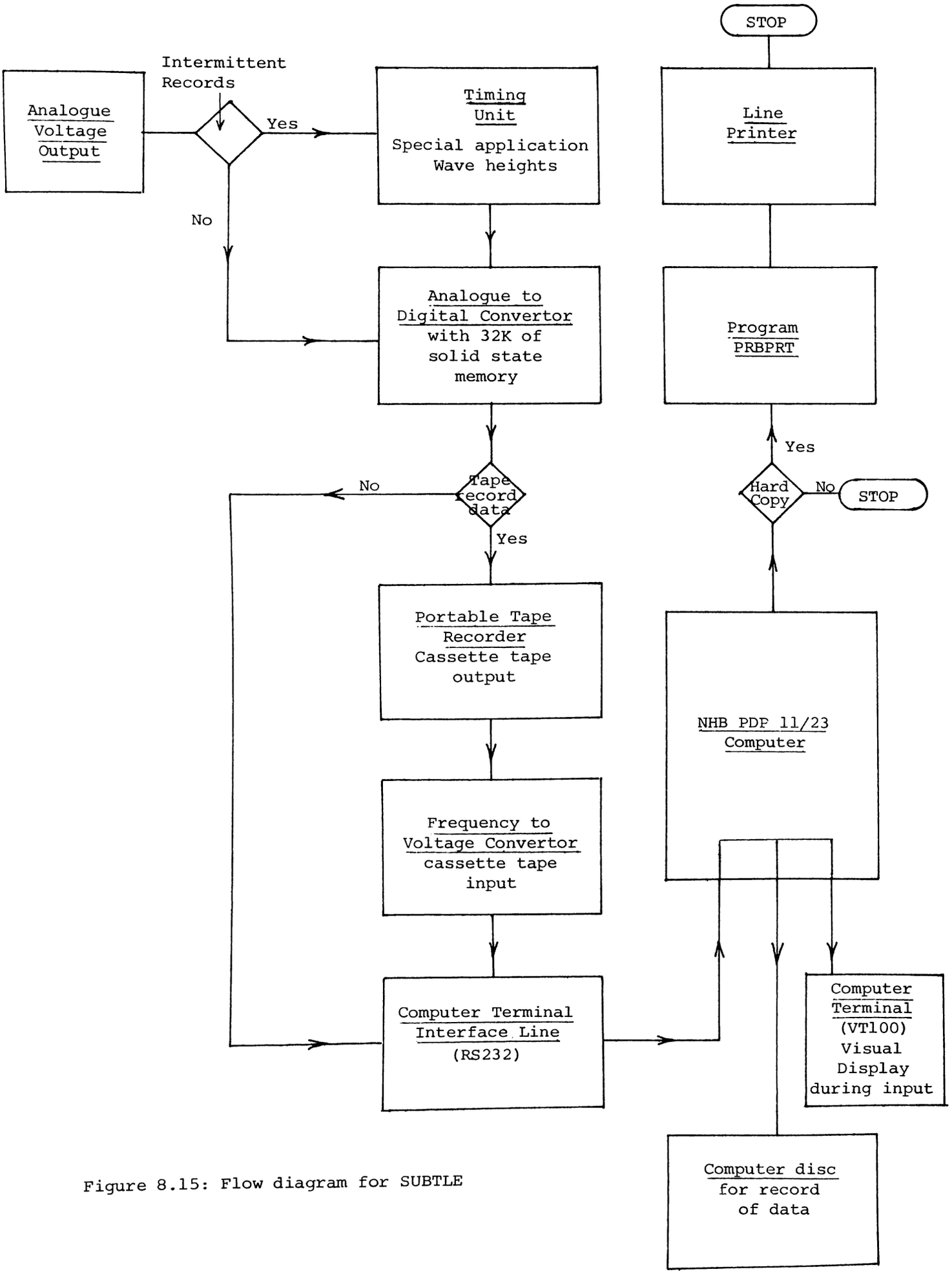

Figure 8.15: Flow diagram for SUBTLE

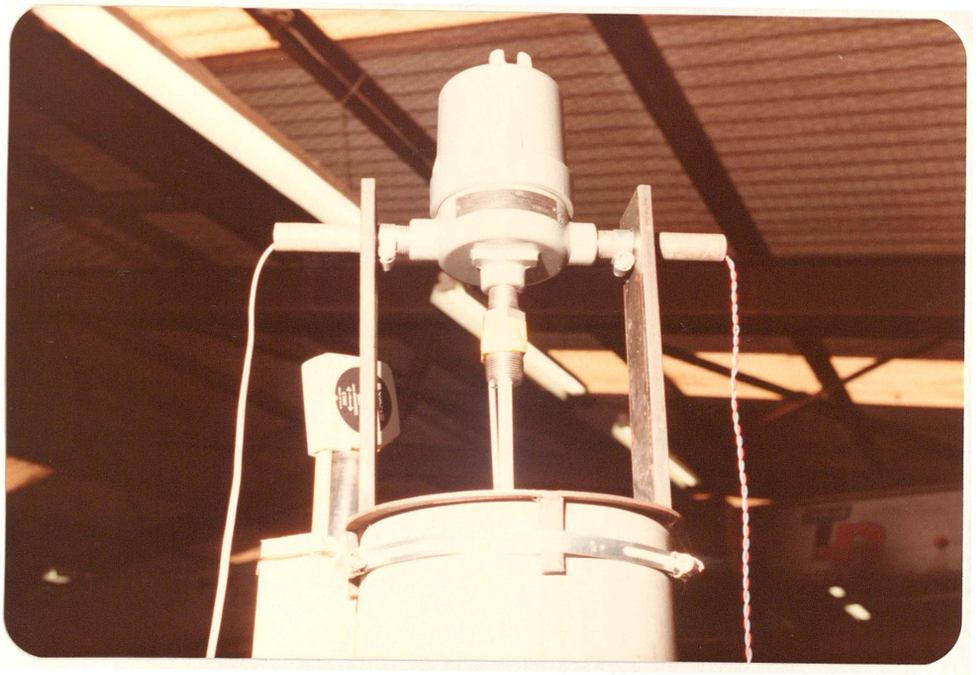

Figure 8.16: Capacitance-type wave probe and transmitter.

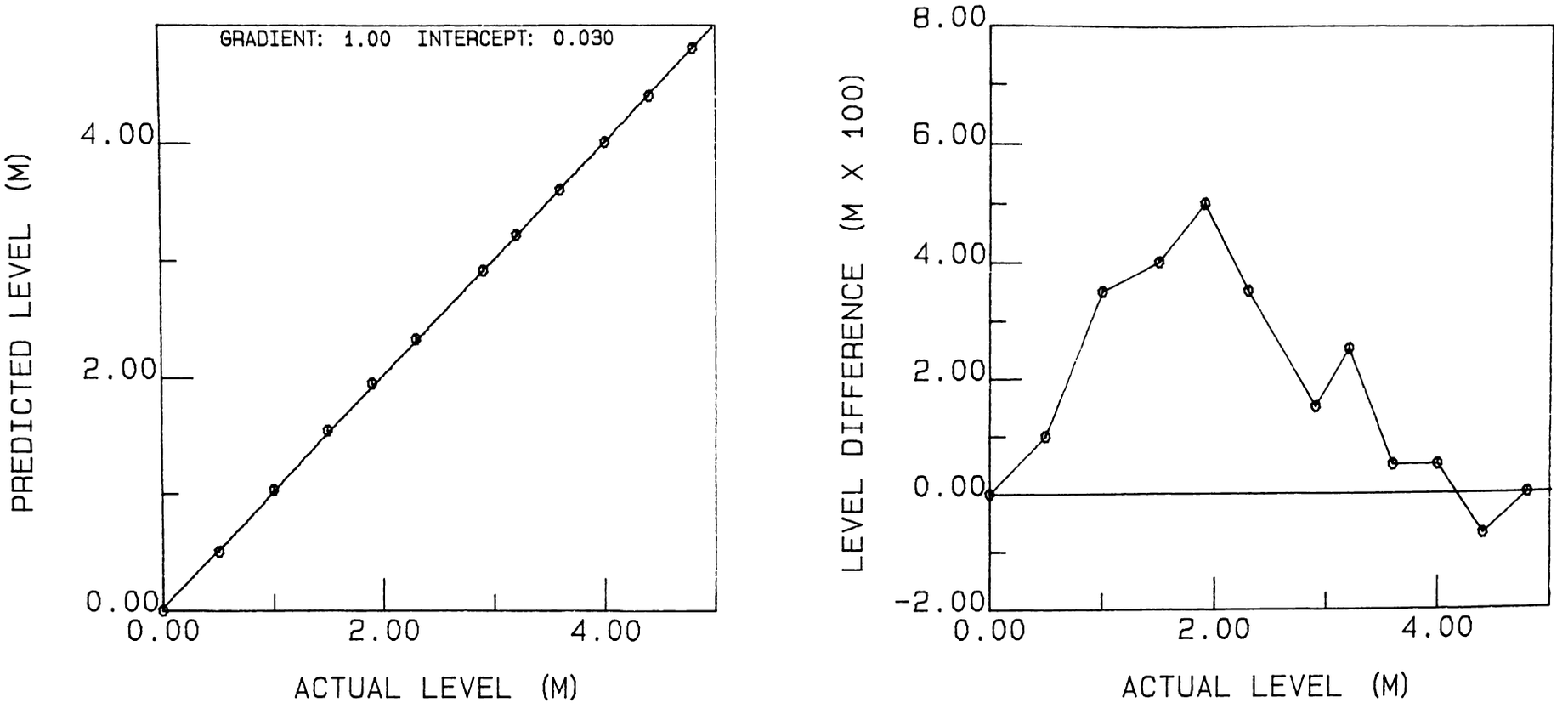

Figure 8.17: Wave probe calibration (28-Sep-82) made in the calibration tube at NHB Works Headquarters. The probe is linear to within 1% of its total span with the maximum deviation being 0.05m in a 4.8m length. The right-hand plot was incorporated into the computer program which converts voltages to sea levels.

Figure 8.18: Wave height capacitance probe deployed at Marsden Point on a metal frame attached to a 2-pile structure.

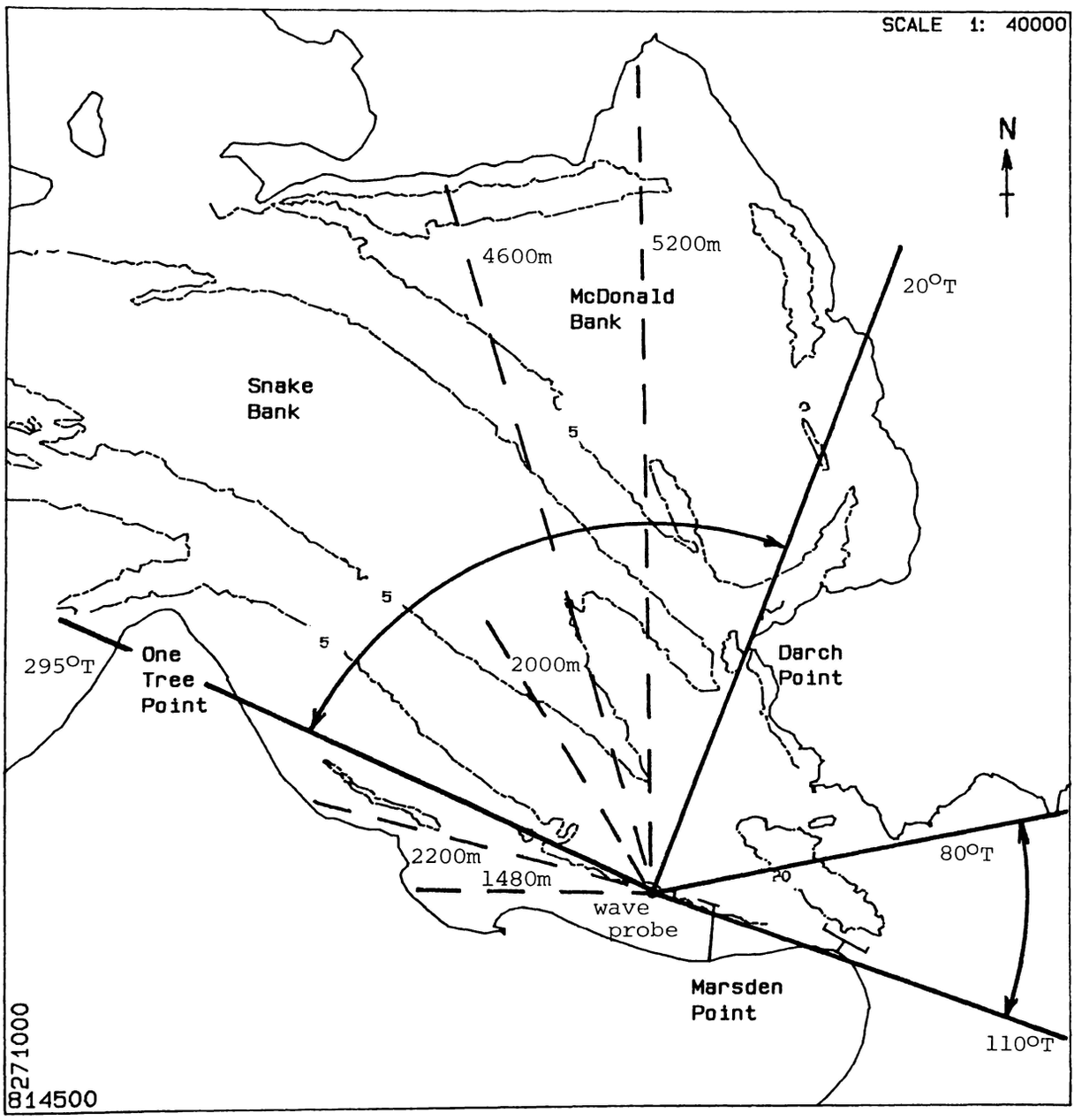

Figure 8.19: The wave probe is exposed to locally-generated surface wave attack through two major windows; 295° T to 20° T across Snake and McDonald Banks and 80° T to 110° T through the entrance throat. Also shown are the fetches for 5 cases chosen for comparison with semi-empirical wave generation formulae.

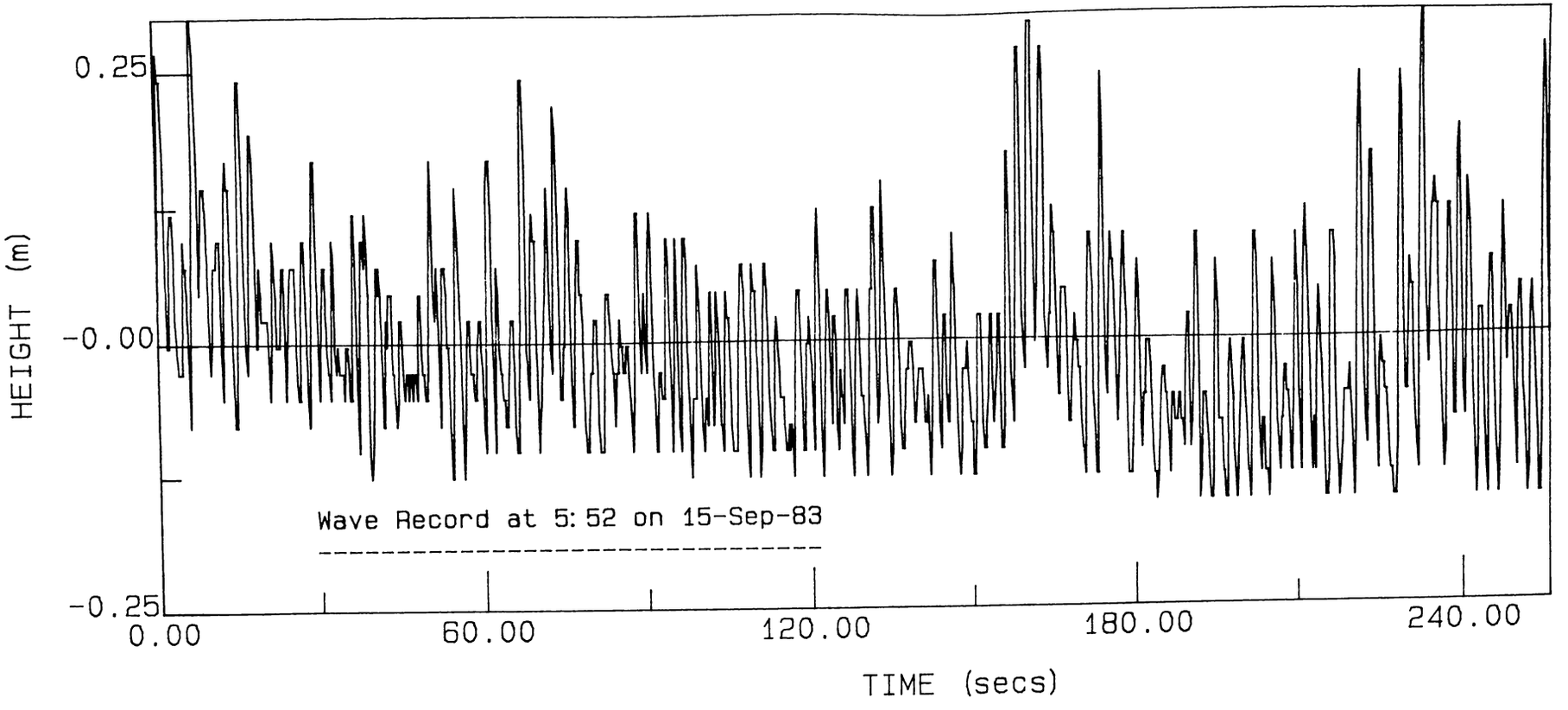

Figure 8.20: Sea level time series recorded at Marsden Point at 5:52 on 15-Sep-83 with the capacitance wave height probe. The wind strength was 14 $m.s^{-1}$ from 330° T.

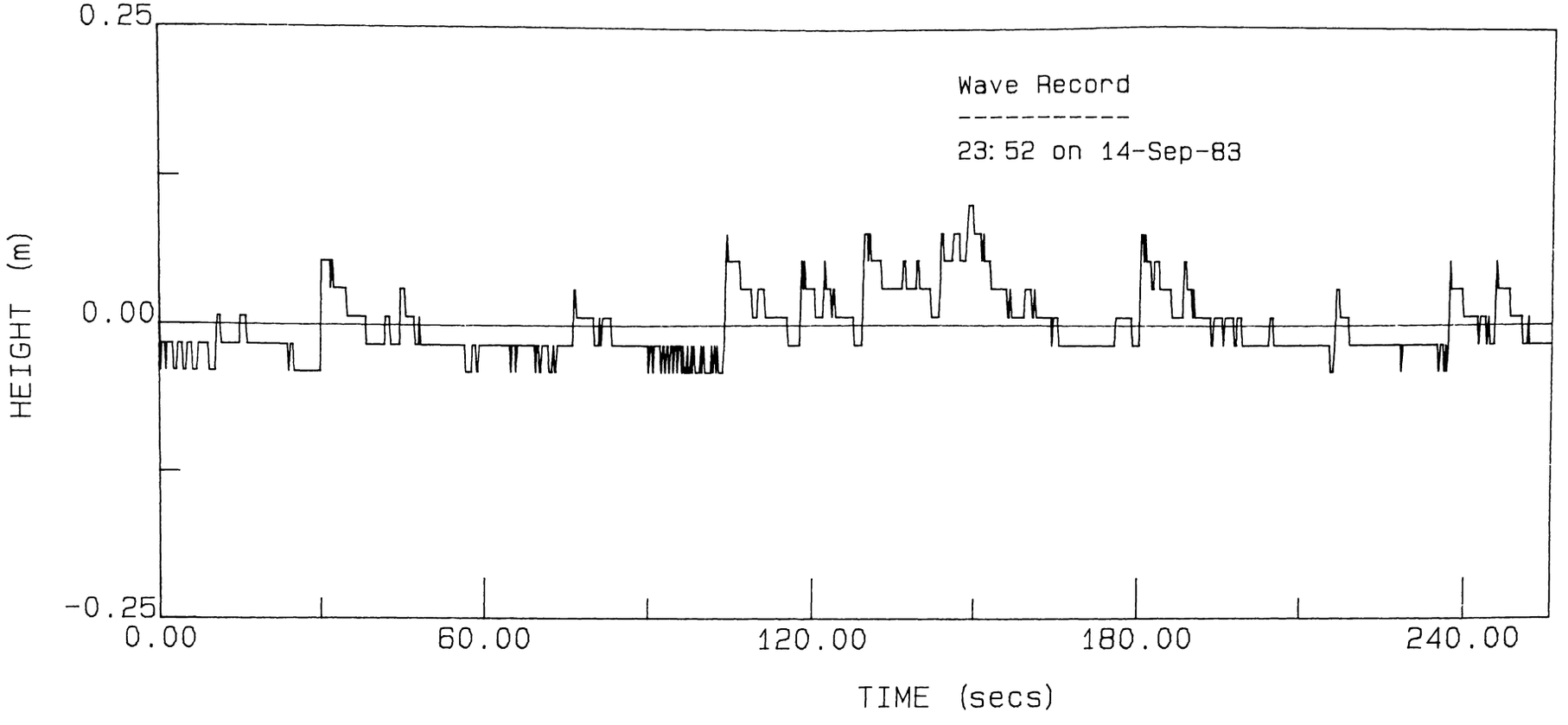

Figure 8.21: Sea level time series recorded at Marsden Point at 23:52 on 14-Sep-82 with the capacitance-type wave height probe. The wind strength was 8 $m.s^{-1}$ from 0^{o} T.

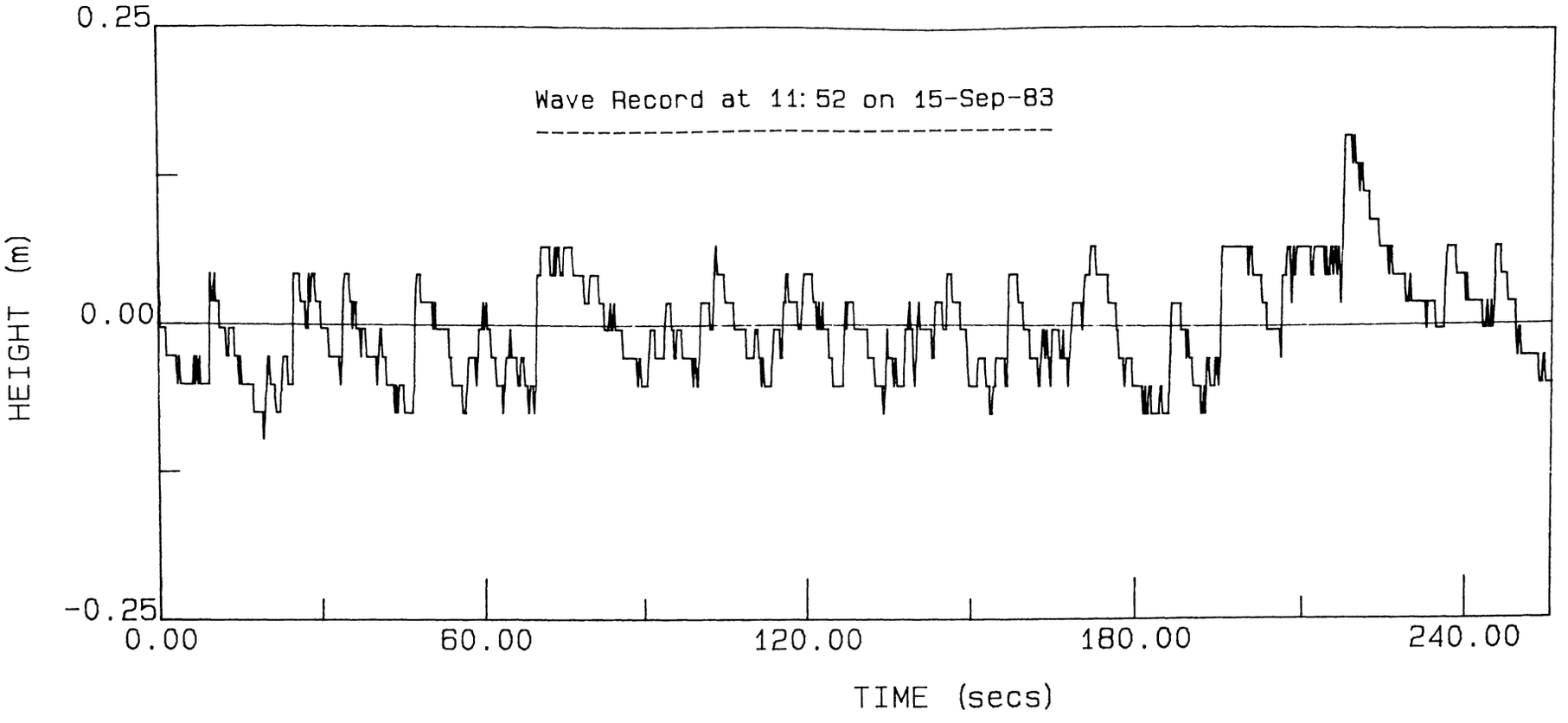

Figure 8.22: Sea level time series recorded at Marsden Point at 11:52 on 15-Sep-83 with the capacitance-type wave height probe. The wind strength was 10 $m.s^{-1}$ from 280° T.

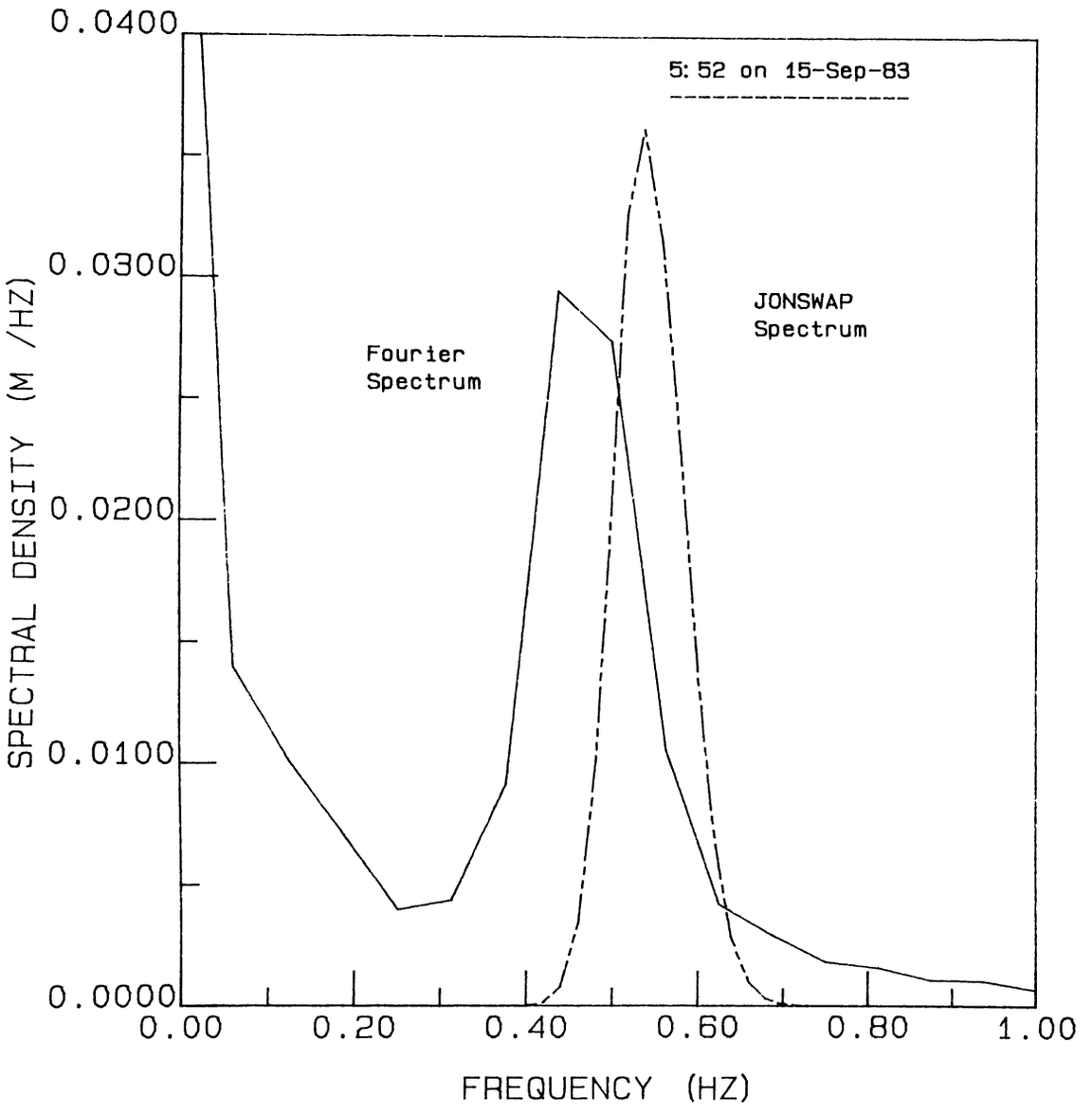

Figure 8.23: Fourier spectrum derived from sea levels measured at Marsden Point with a capacitance-type wave height probe at 5:52 on 15-Sep-83. The wind strength was 14 $m.s^{-1}$ from 330°T. This is compared with the JONSWAP spectrum for a fetch of 2000m and wind strength of 14 $m.s^{-1}$.

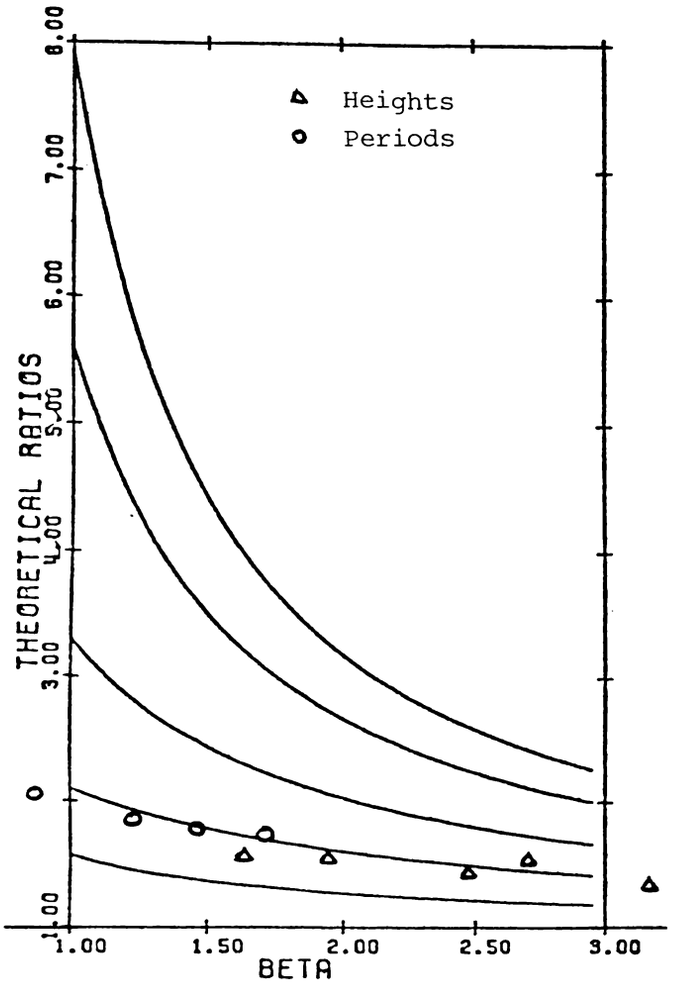

Figure 8.24: Theoretical ratios of wave height or wave period statistics for Weibull distributed data against the peakedness βeta (β). Data shown is the wave height and period ratios: $H_{z,1/3}/\bar{H}_z$ and $T_{z,1/3}/\bar{T}_z$ for the five test cases at Marsden Point from Table 8.10. Theoretical curves are from bottom to top: $X_{z,1/10}/X_{z,1/3}$, $X_{z,1/3}/\bar{X}_z$, $X_{z,1/10}/\bar{X}_z$, $X_{z,1/100}/\bar{X}_z$ and $X_{z,1/1000}/\bar{X}_z$, where X may be height or period. (after Black, 1978).

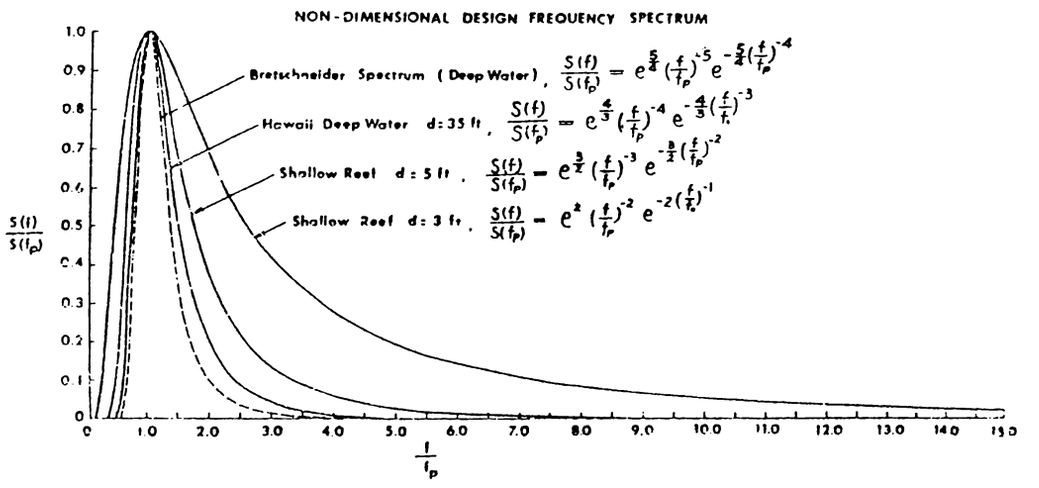

Figure 8.25: Non-dimensional design frequency spectra for a coral reef (after Lee and Black, 1978).

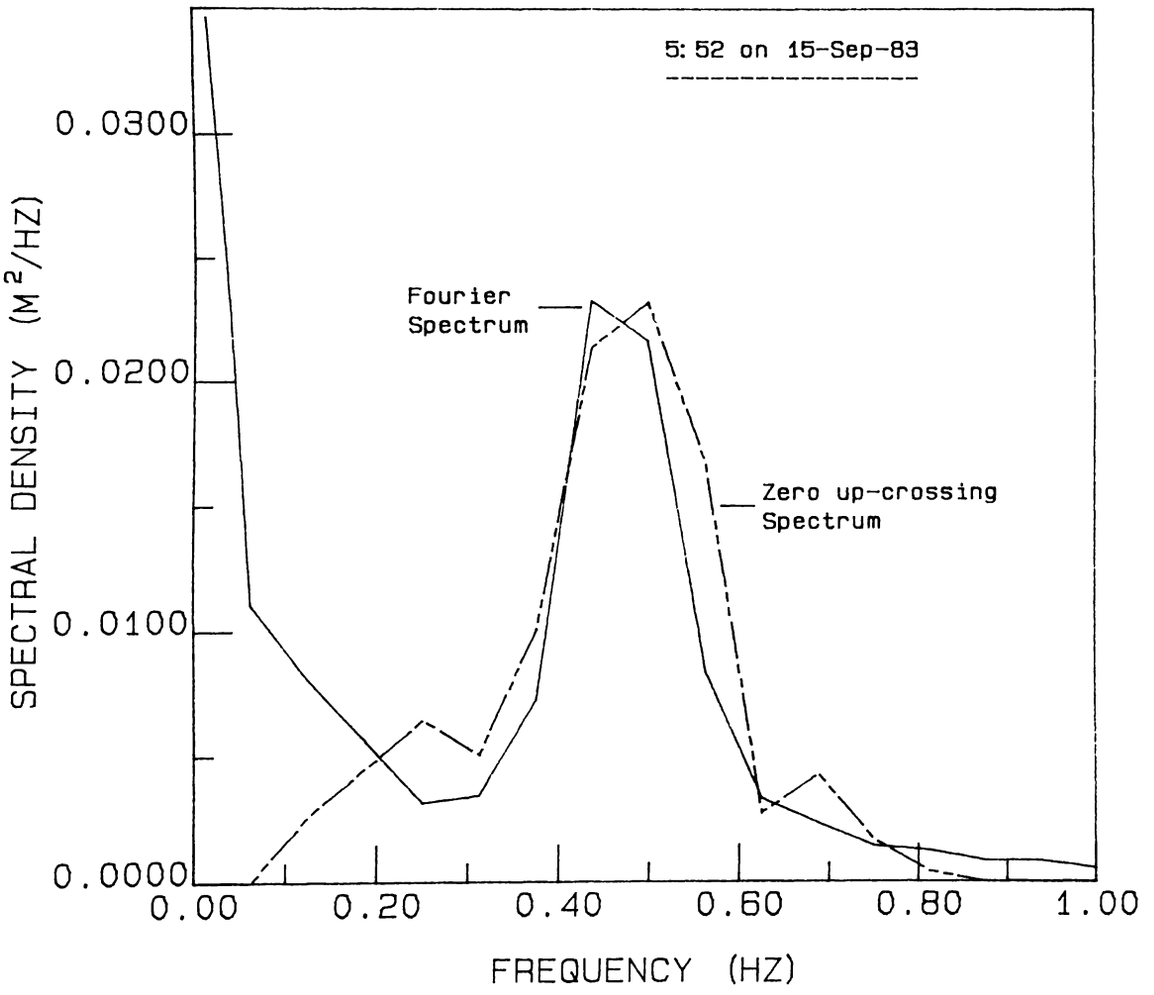

Figure 8.26: Fourier spectrum and the zero up-crossing spectrum derived from sea levels measured at Marsden Point with a capacitance-type wave height probe at 5:52 on 15-Sep-83. The wind strength was 14 $m.s^{-1}$ from 330° T. The 20% calibration correction for the capacitor has not been applied.

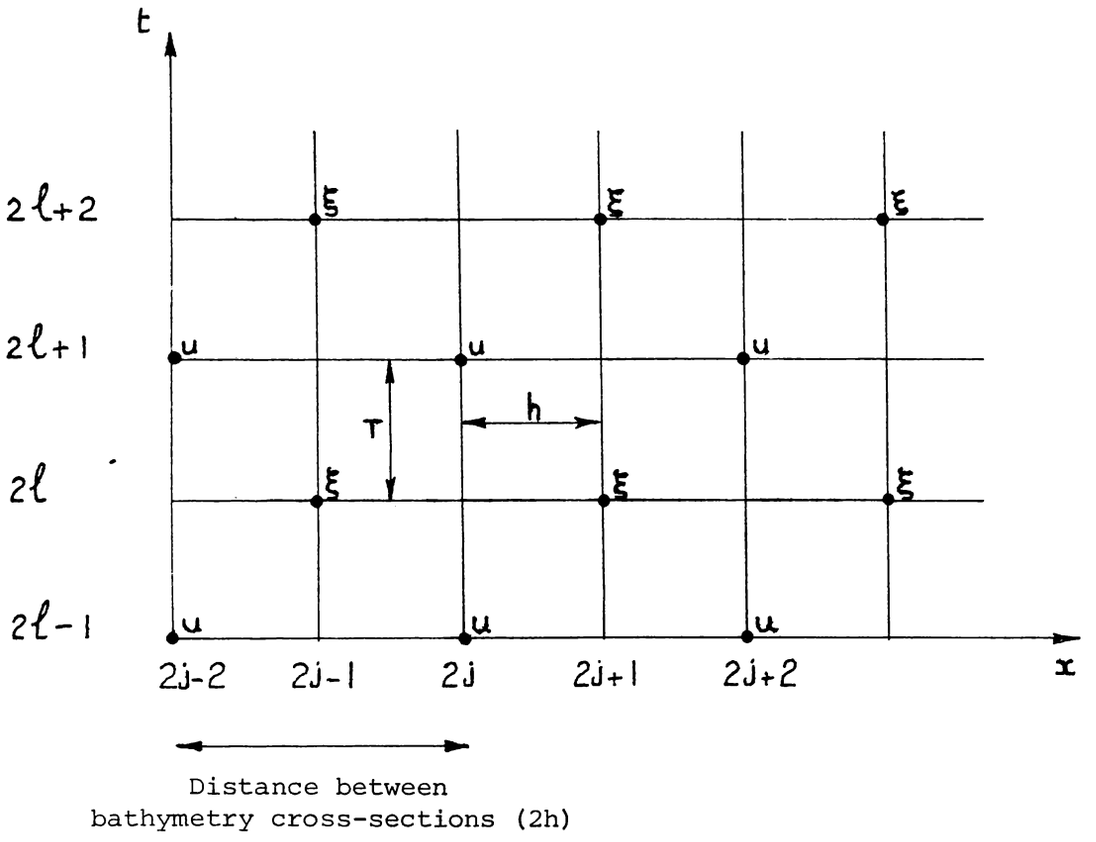

Figure 9.1: Notation for leap-frog, explicit, finite-difference scheme.

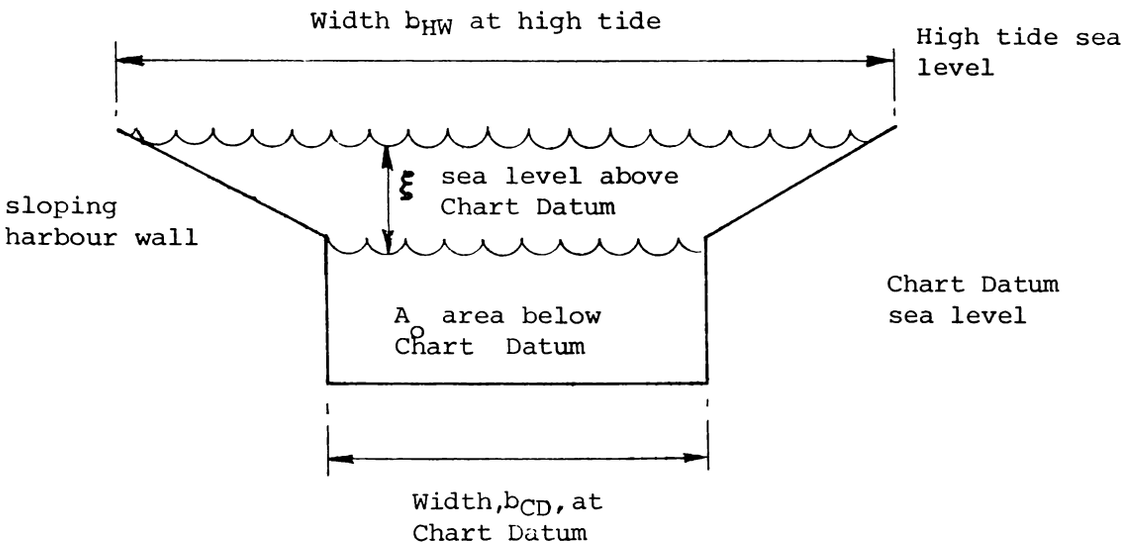

Figure 9.2: Harbour channel cross-section schematised as rectangular below Chart Datum and widening with sloping walls with increasing tide levels.

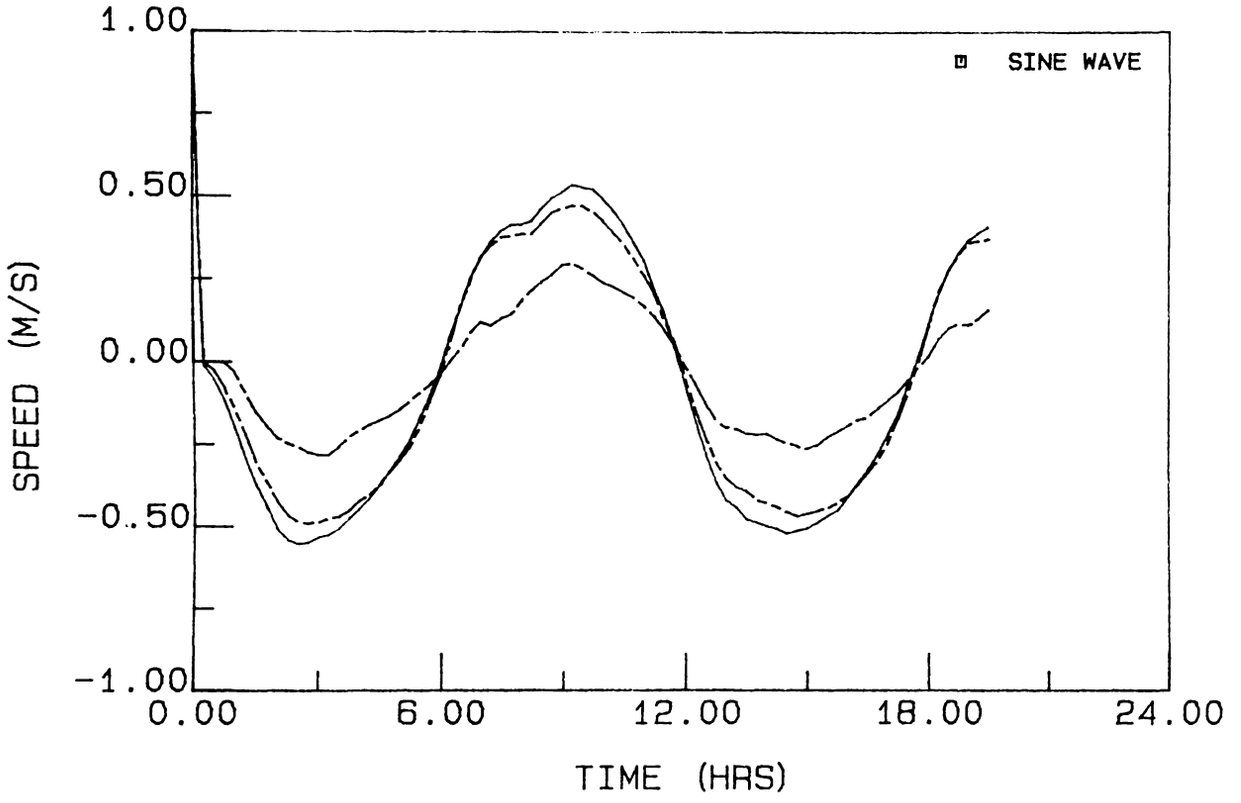

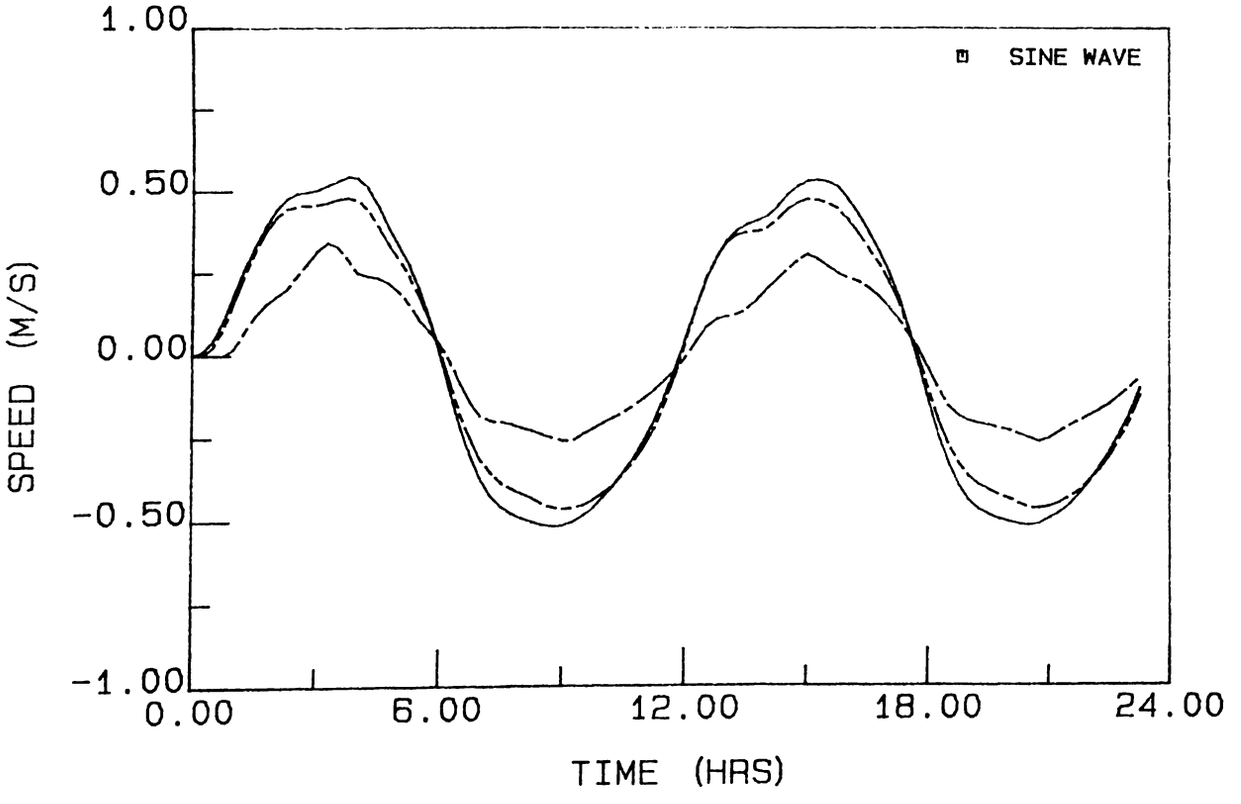

Figure 9.3: Velocity time profiles after parabolic interpolation of an input sine wave digitised to 15-minute intervals to describe the open boundary sea levels. For a 2m tidal range the upper diagram (9.3(a)) shows the result for 2 decimal place accuracy of the input data and the lower diagram (9.3(b)) corresponds with 3 decimal place accuracy.

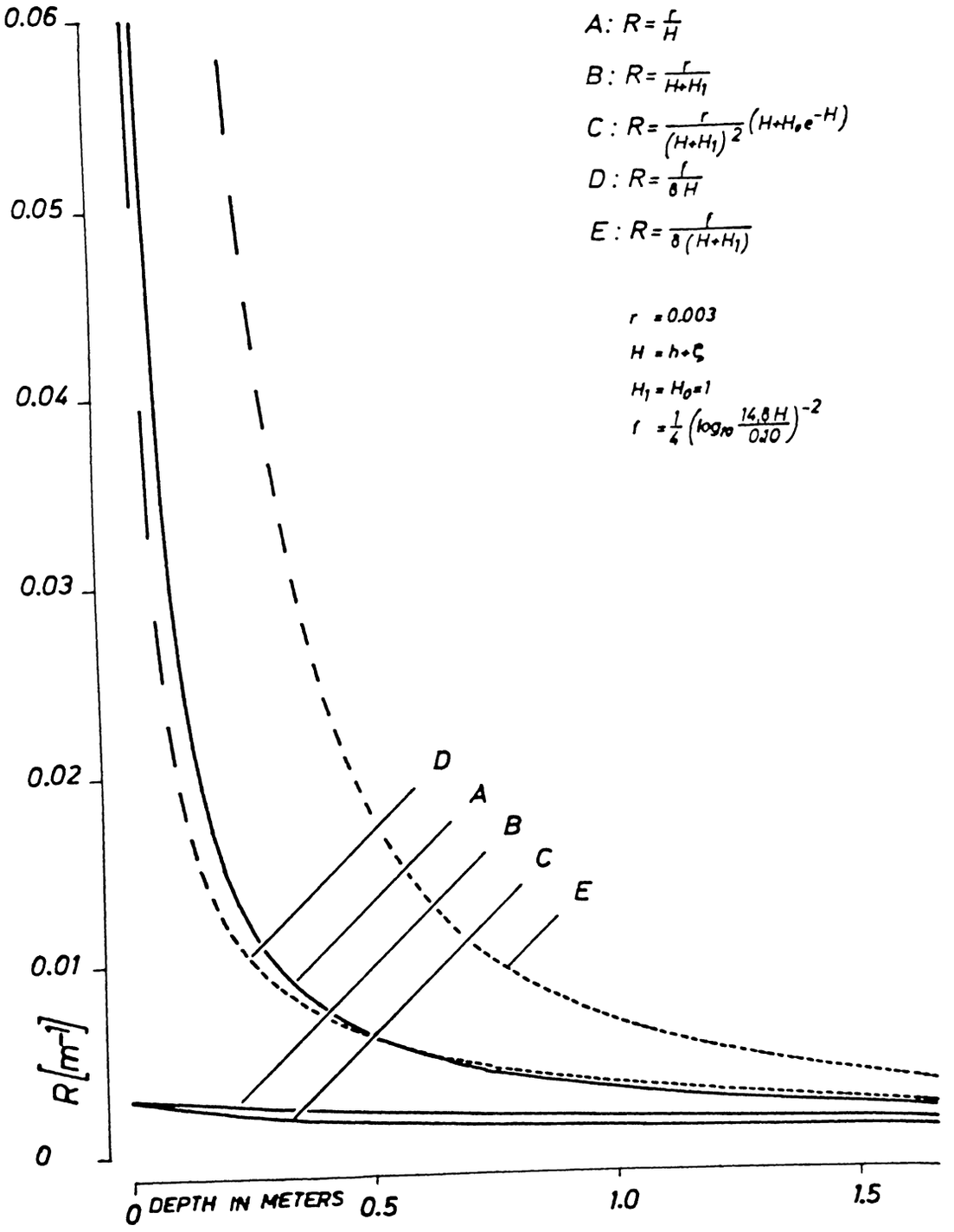

Figues 9.4: The dependence of different friction factors on depth after Ramming and Kowalik (1980, Figure 60).

$$A : R = \frac{r}{H}$$

$$B : R = \frac{r}{H+H_1}$$

$$C : R = \frac{r}{(H+H_1)^2}(H+H_0 e^{-H})$$

$$D : R = \frac{f}{8H}$$

$$E : R = \frac{f}{8(H+H_1)}$$

$$F : R = \frac{f}{8(H+H_1)^2}(H+H_0 e^{-H})$$

$$r = 0.003$$

$$H = h+\zeta$$

$$H_1 = H_0 = 1$$

$$f = \frac{1}{4}\left(\log_{10}\frac{14.8\,H}{0.10}\right)^{-2}$$

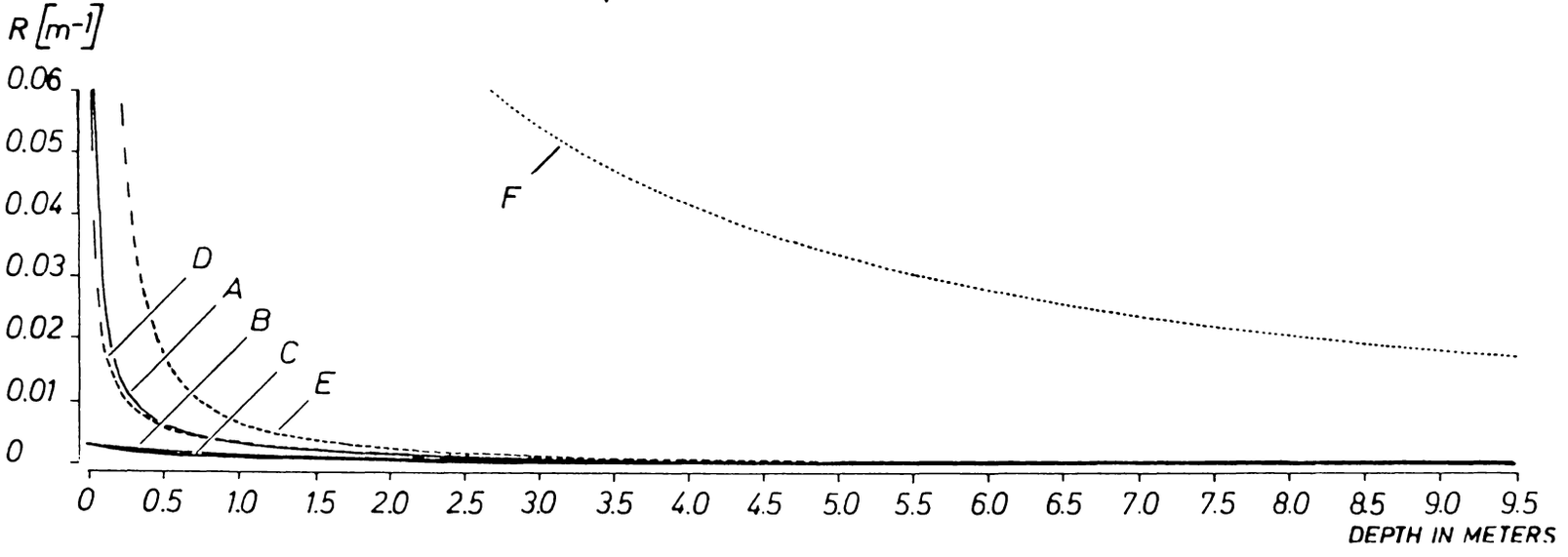

Figure 9.5: The dependence of different friction terms on depth after Ramming and Kowalik (1980, Figure 59).

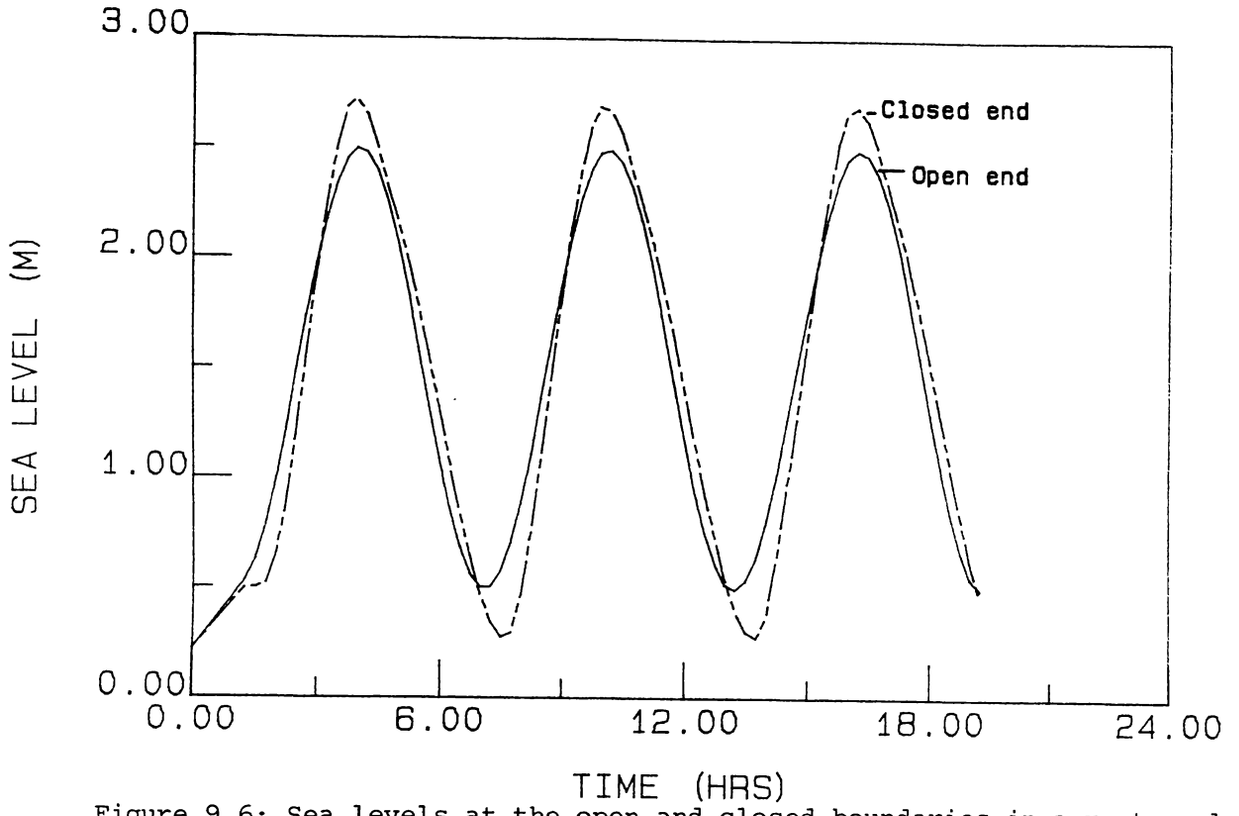

Figure 9.6: Sea levels at the open and closed boundaries in a rectangular channel 14,000m long, 1000m wide with mean depth of 4.5m and Chezy's C of 60 $m^{\frac{1}{2}}.s^{-1}$.

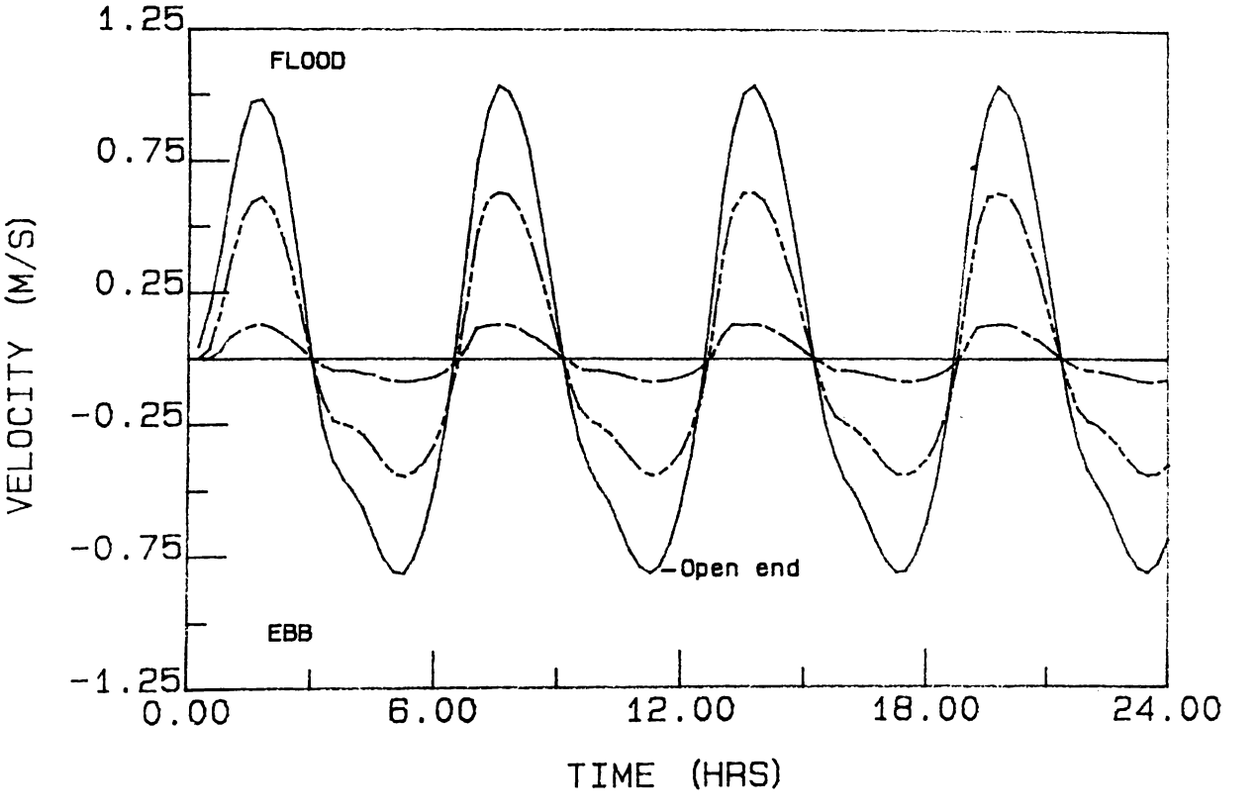

Figure 9.7: Mean cross-sectional flow velocities at the open end and at 7000m and 12600m from the open end in a rectangular channel 14,000m long, 1000m wide with mean depth of 4.5m and Chezy's C of 60 $m^{\frac{1}{2}}.s^{-1}$.

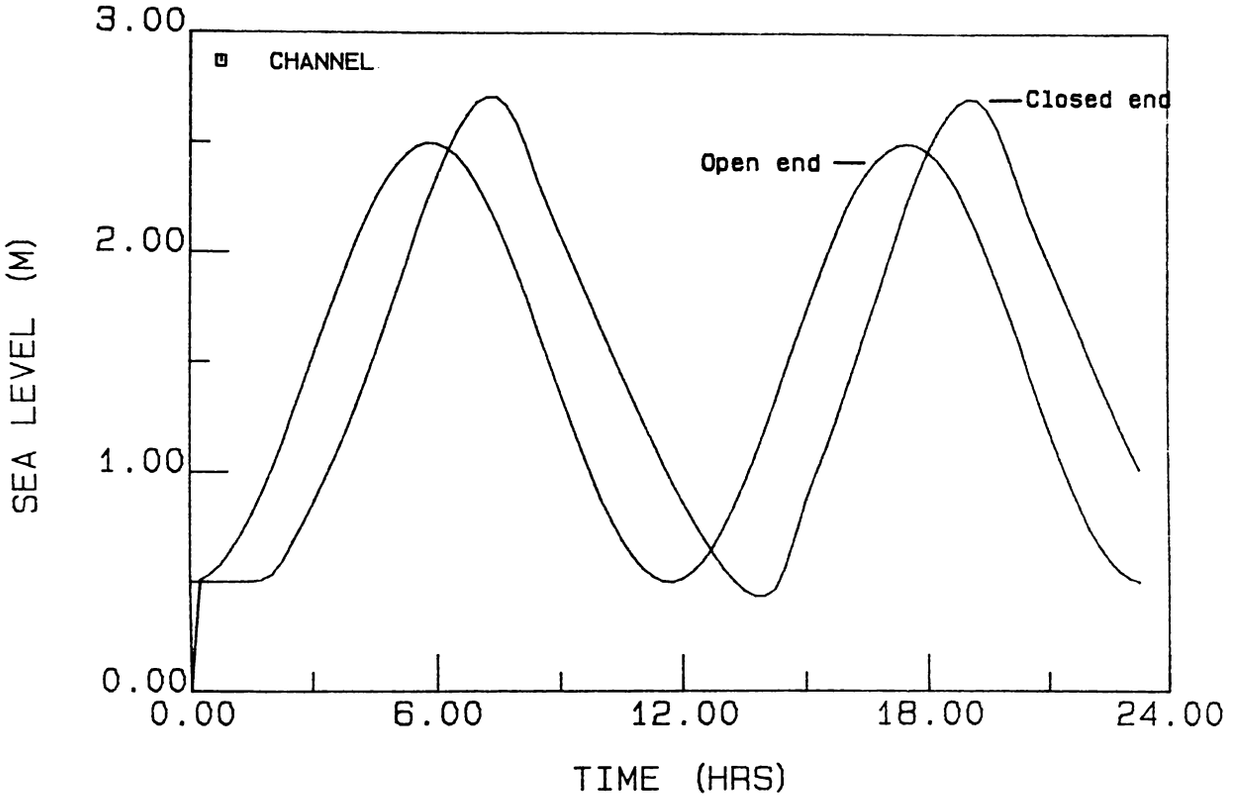

Figure 9.8: Sea levels at the open and closed boundaries in a rectangular channel 40,000m long, 1,000m wide with mean depth of 4.5m and Chezy's C of 60 $m^{\frac{1}{2}}.s^{-1}$.

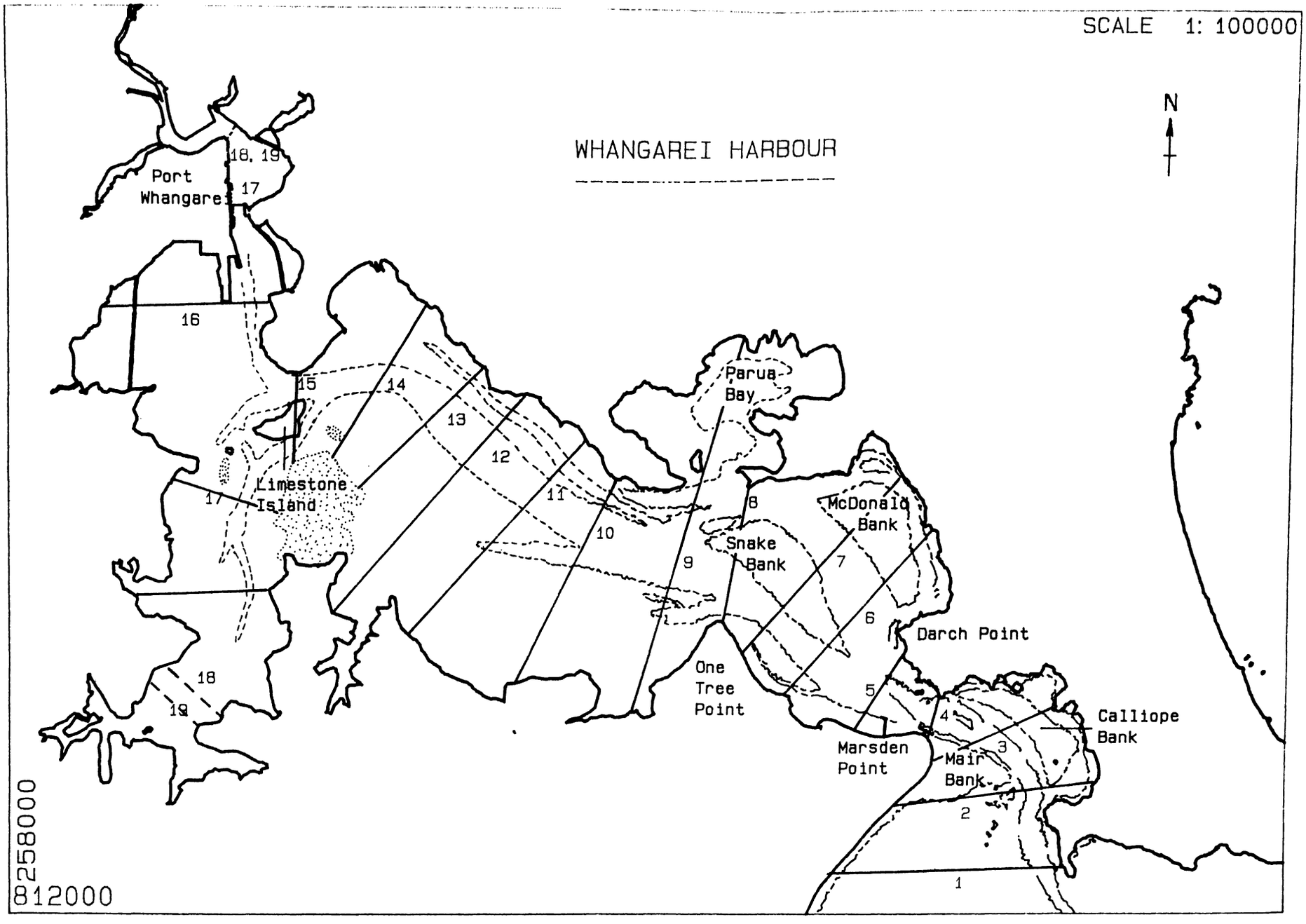

Figure 9.9: Whangarei Harbour showing the locations of the schematised cross-sections for the 1-dimensional model simulation.

	CD Width (m)	CD Area (m^2)	Gradient
1	2800	22,000	0
2	2400	18,000	0
3	1500	15,000	0
4	710	13,151	3
5	1400	13,151	100
6	3100	14,263	360
7	2240	11,395	850
8	2500	11,203	23
9	6000	15,600	600
10	2440	8,540	224
11	2340	6,786	544
12	1220	5,246	912
13	1060	4,876	776
14	1020	5,100	712
15	900	6,300	5
16	1125	6,750	550
17	1500	9,000	250
18	2000	2,000	250
19	4000	-800	250

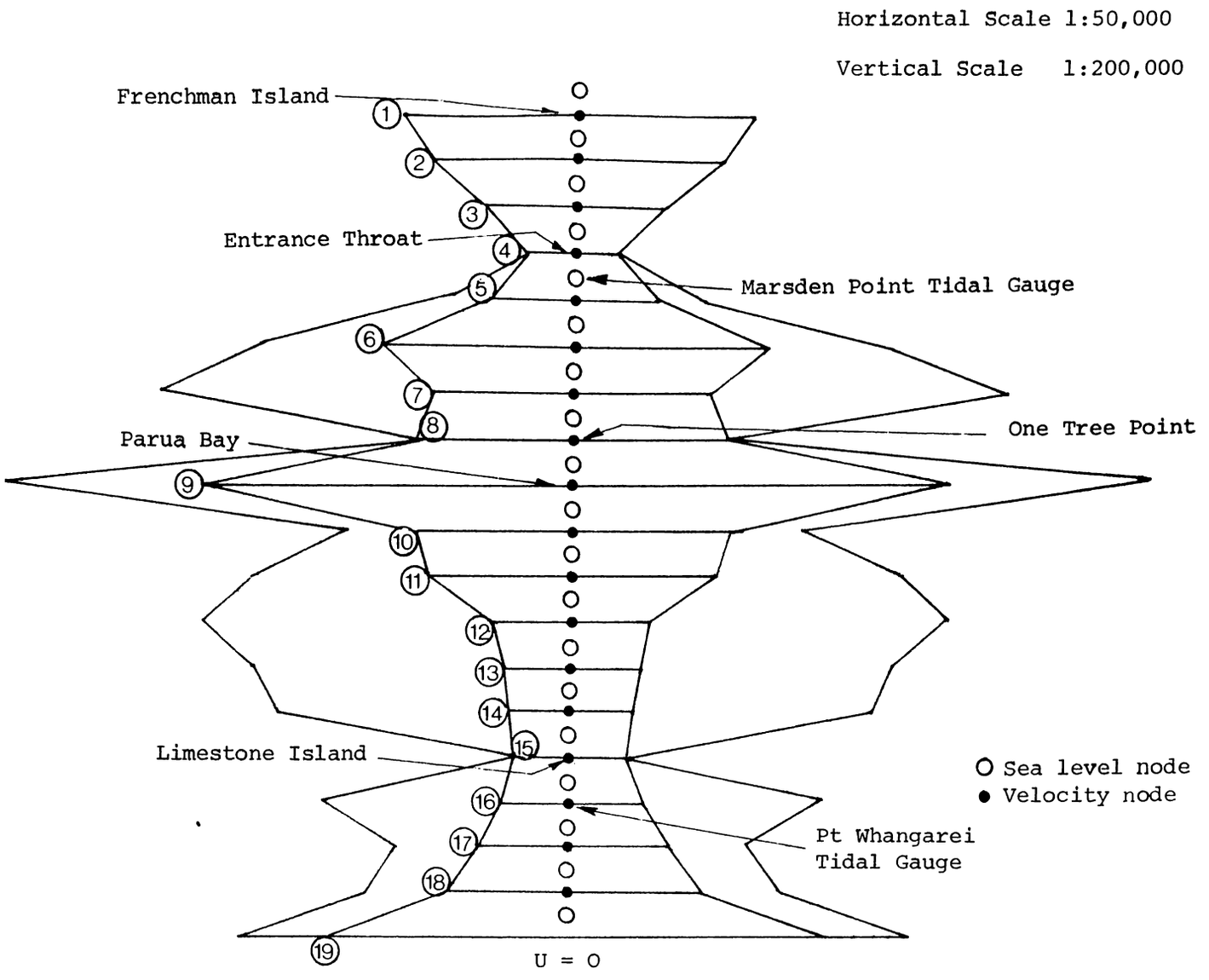

Figure 9.10: Whangarei Harbour one-dimensional schematisation showing the outline at Chart Datum and for a high tide of 2.6m above CD.

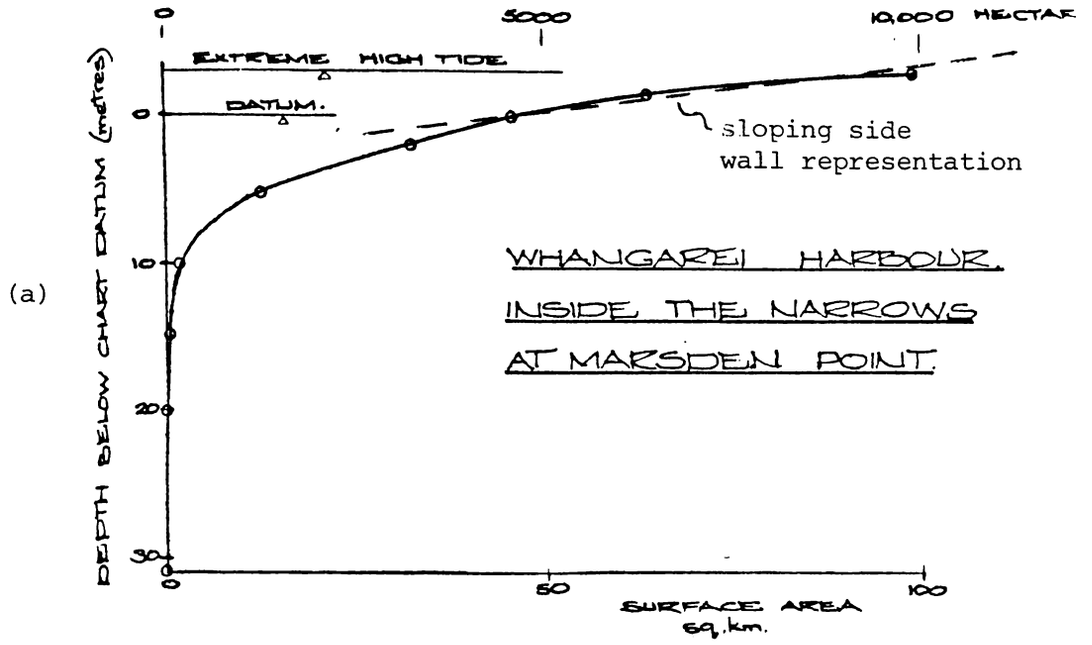

(a)

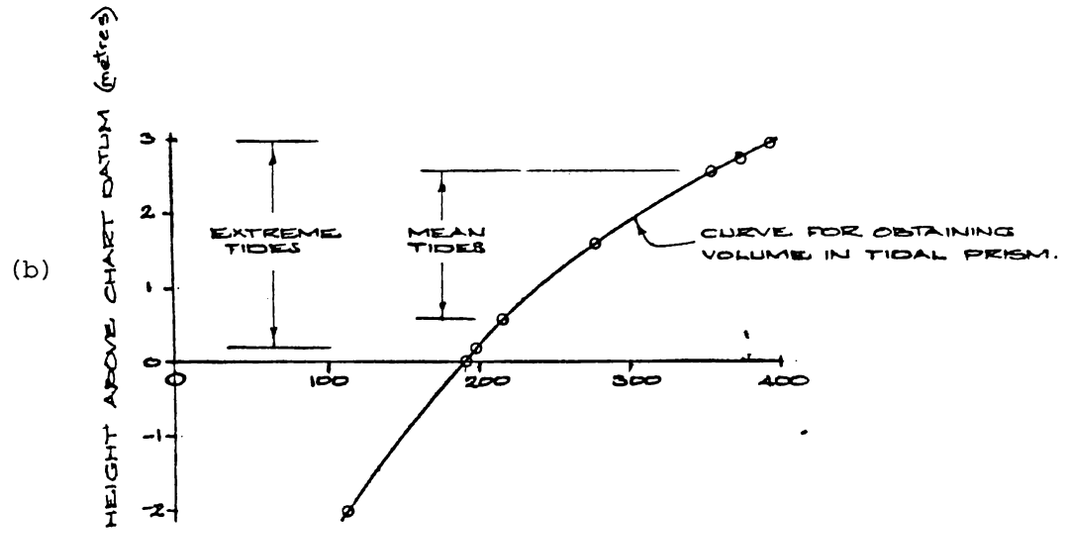

(b)

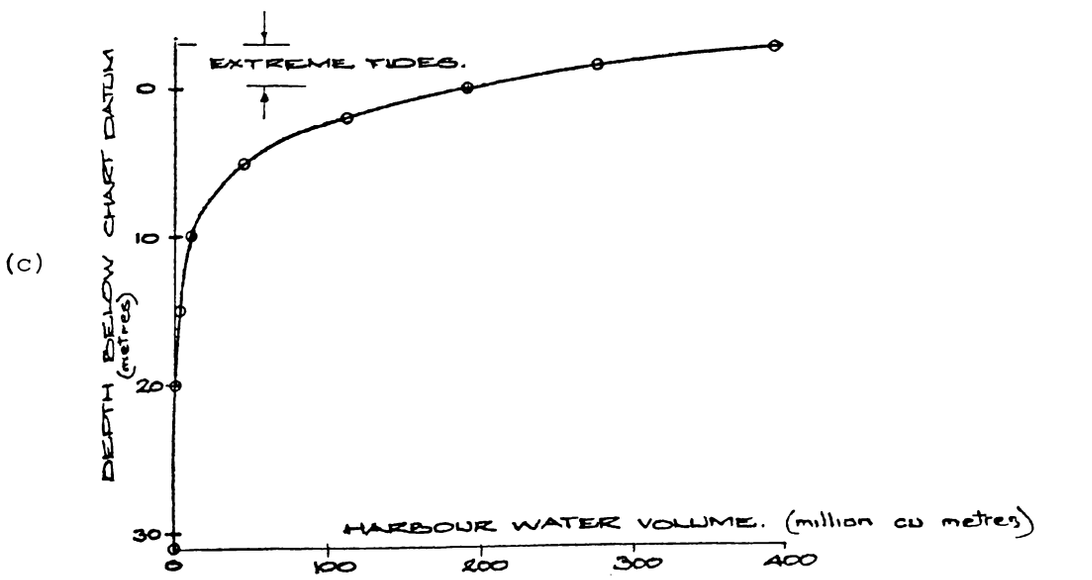

(c)

Figure 9.11: Basic graphs for hydraulic calculations after Smith-McNaught (1976). The sloping side wall schematisation is shown in case (a).

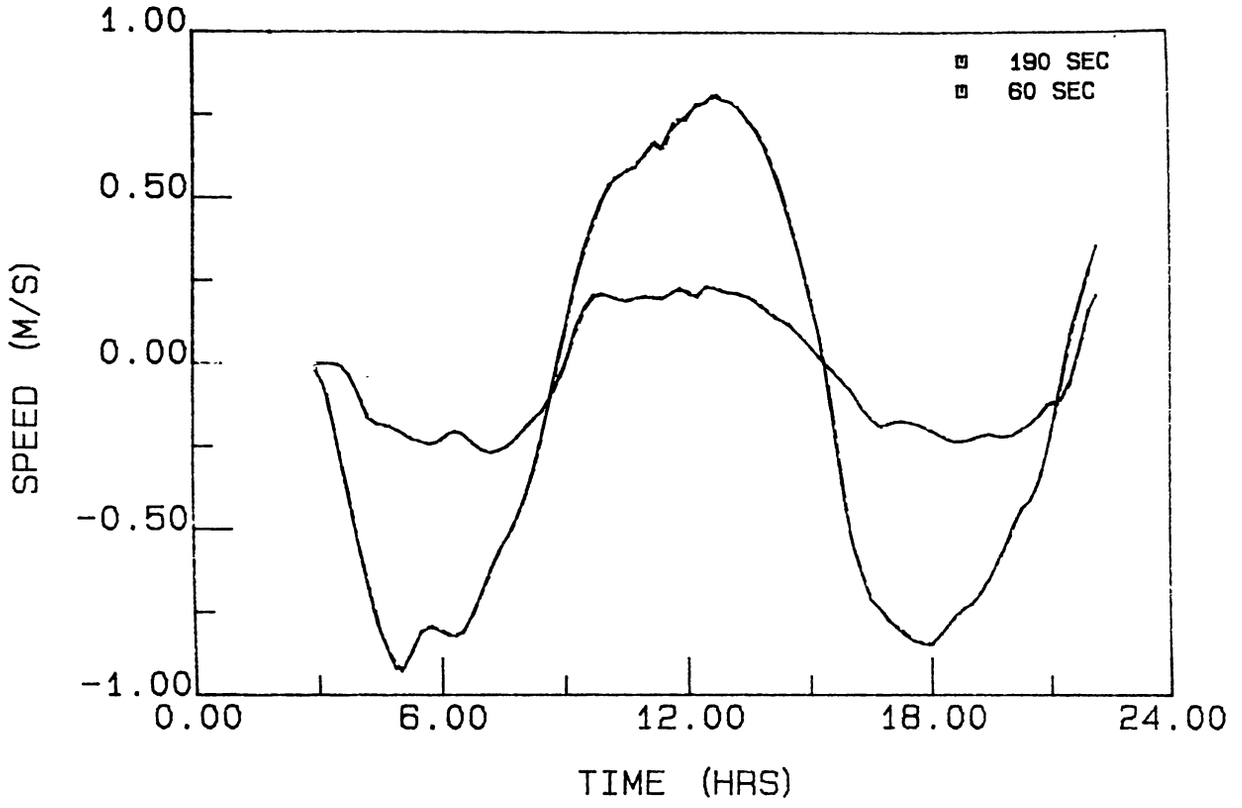

Figure 9.12: Comparisons of harbour modelled velocities at the open boundary with time steps of 95s and 30s (2T = 190,60).

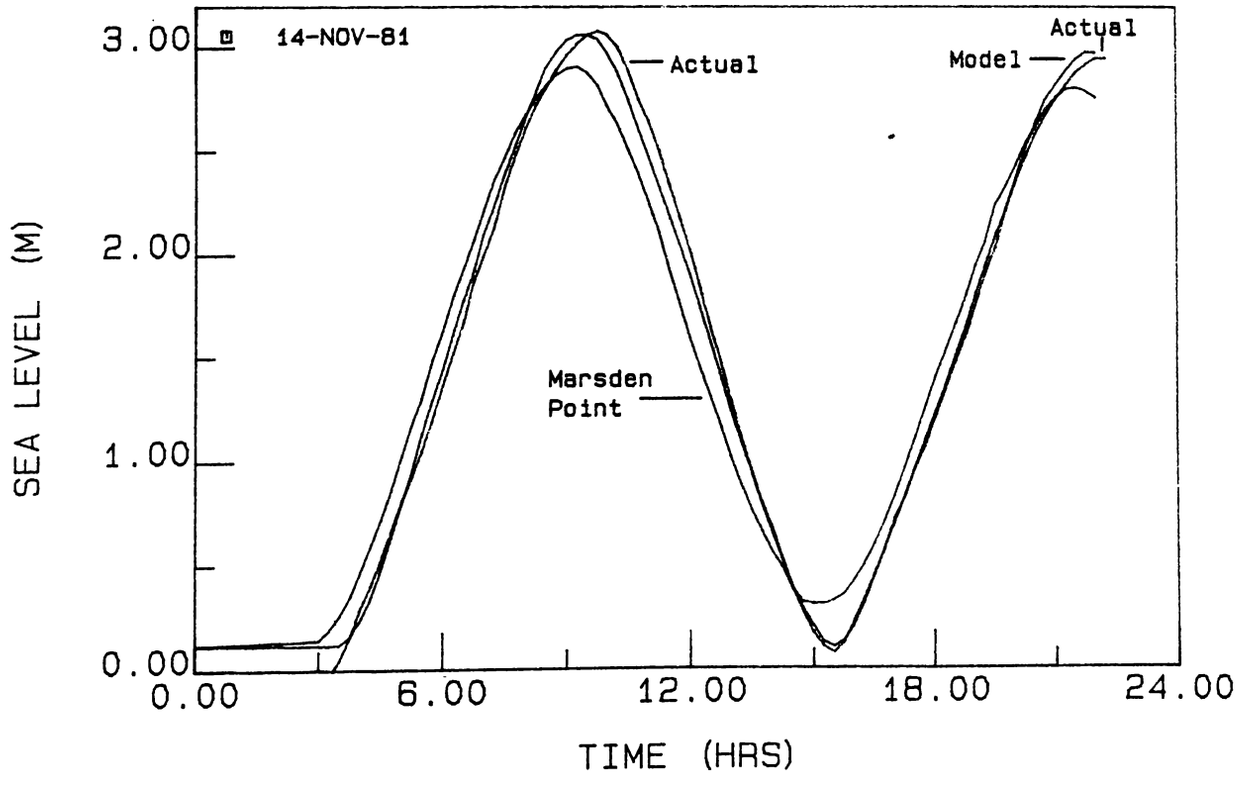

Figure 9.13: Calibration run for 14-Nov-81 with constant Chezy's C of 60 $m^{\frac{1}{2}}.s^{-1}$, comparing the modelled and actual tide levels at Port Whangarei.

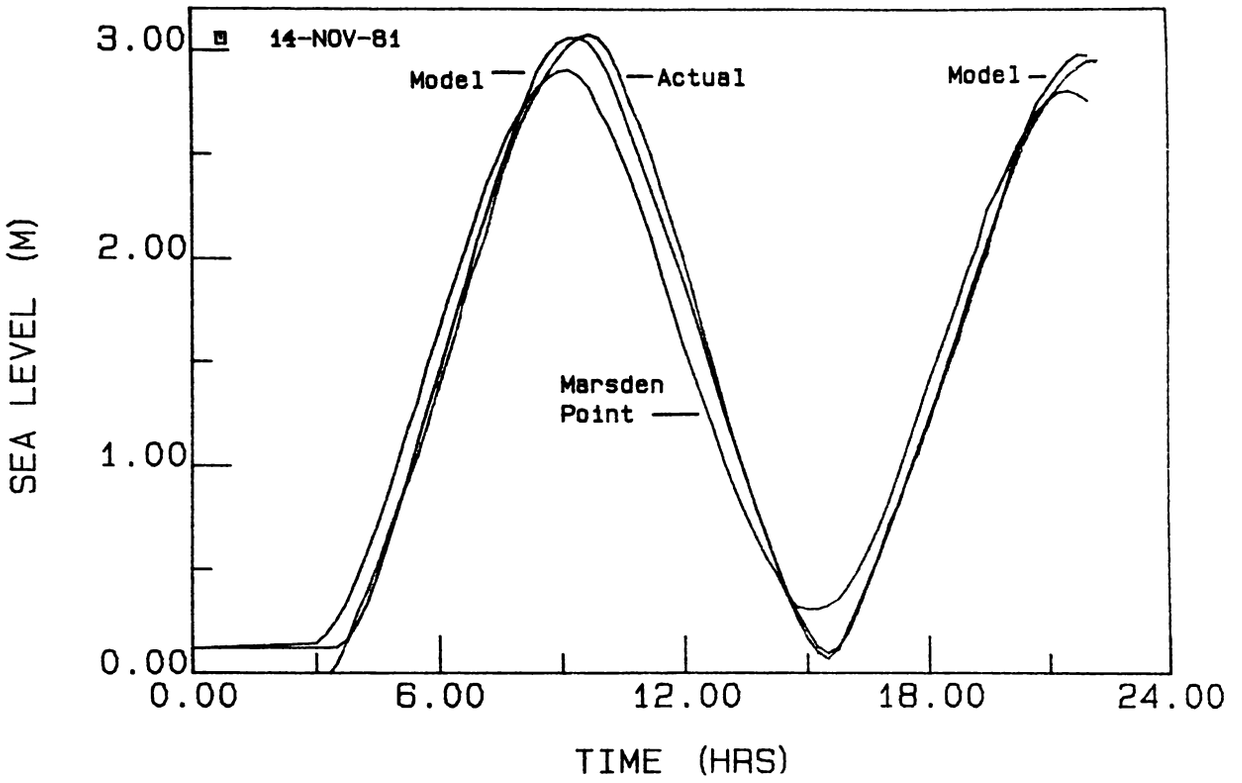

Figure 9.14: Calibration run for 14-Nov-81 with roughness length, z_o = 0.001m, comparing the modelled and actual tide levels at Port Whangarei.

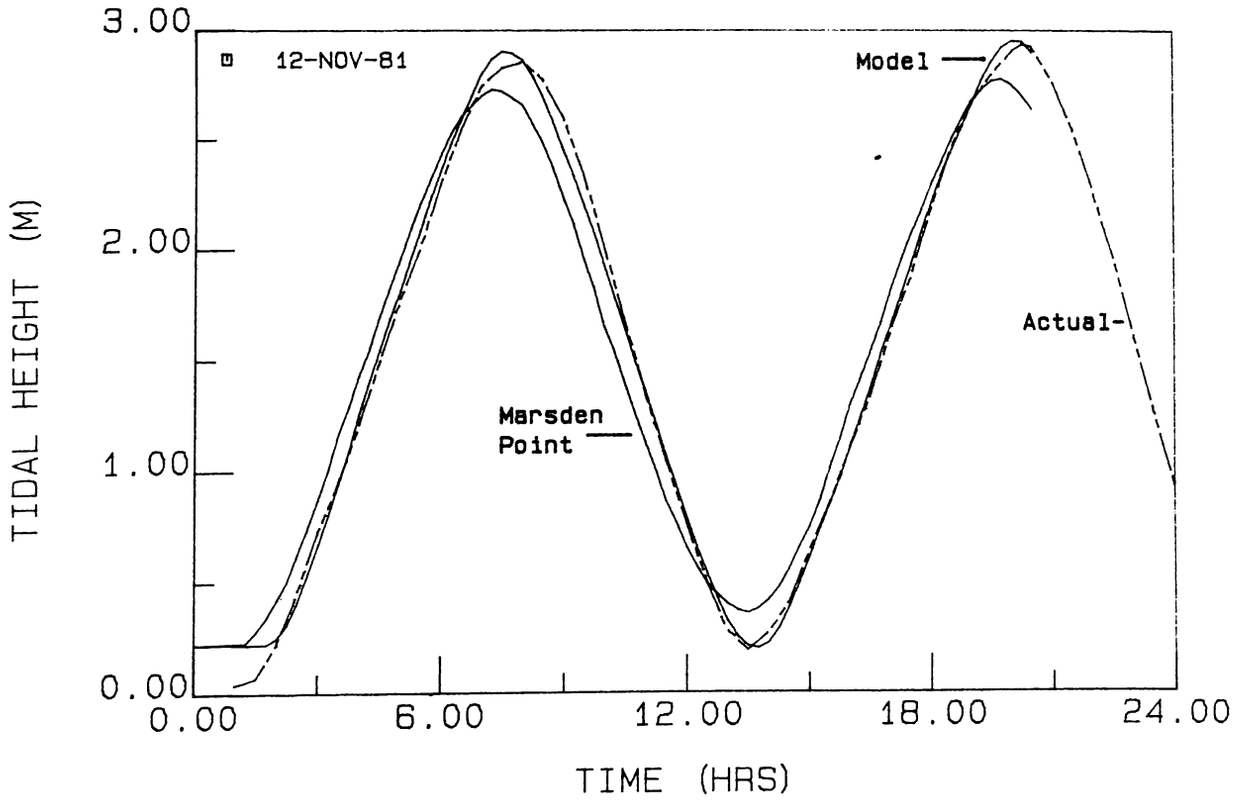

Figure 9.15: Verification run for 12-Nov-81 with roughness length, z_o = 0.001m, comparing the modelled and actual tide levels at Port Whangarei.

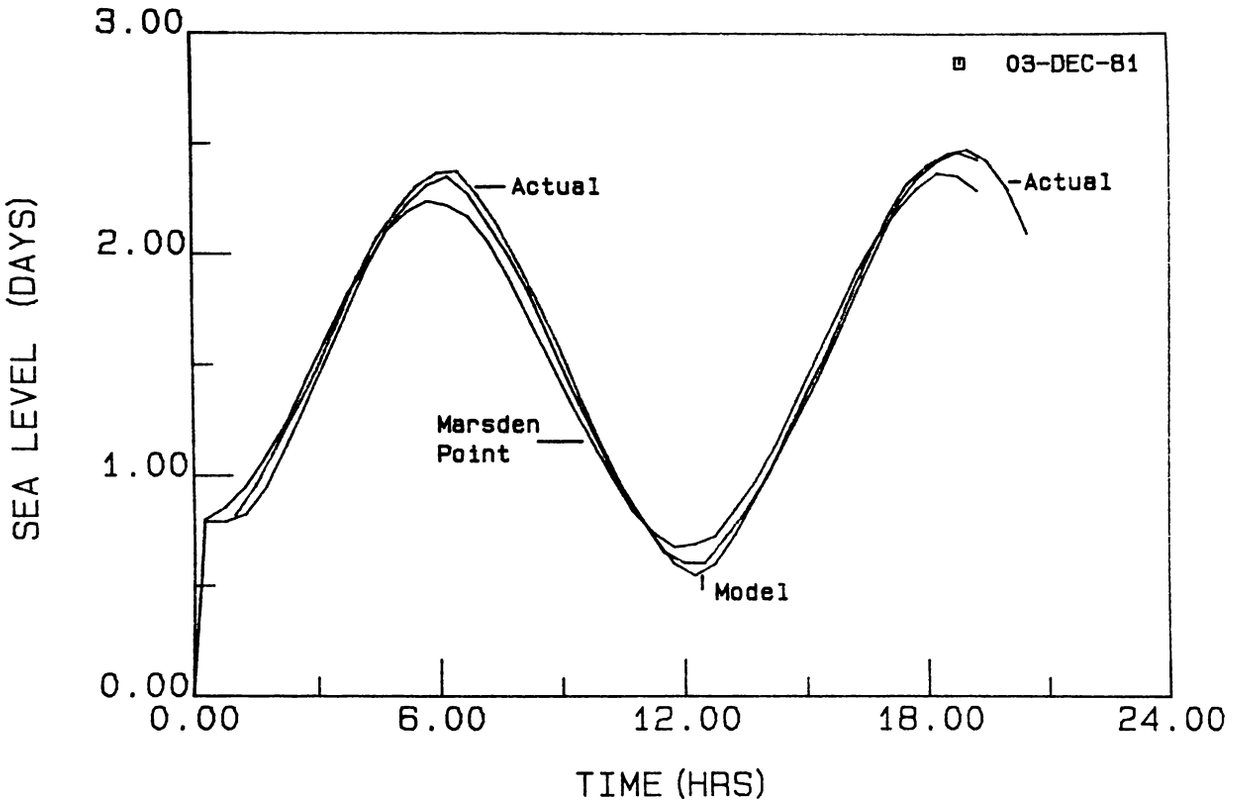

Figure 9.16: Verification run for 3-Dec-81 with roughness length, $z_o = 0.001m$, comparing modelled and actual tide levels at Port Whangarei.

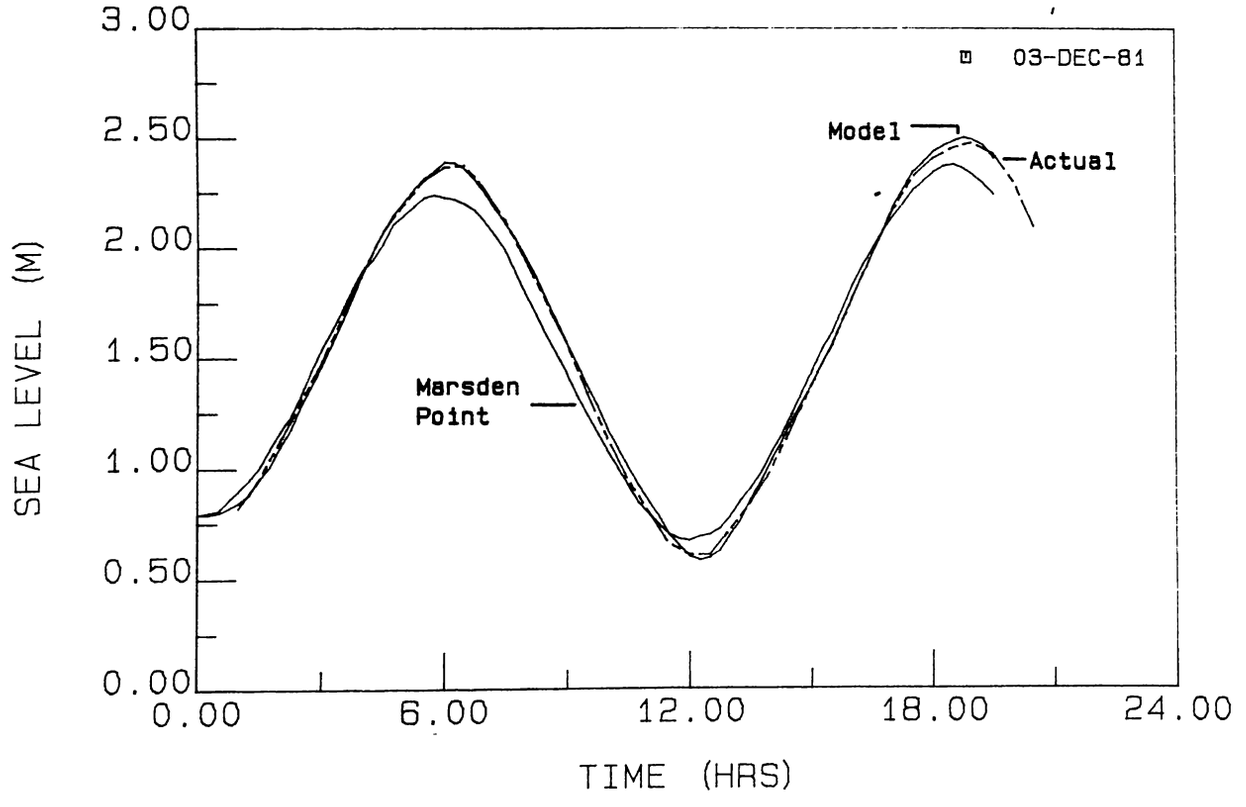

Figure 9.17: Verification run for 3-Dec-81 with roughness length, $z_o = 0.001m$ and longitudinal density gradient of $C_{den} = -5 \times 10^{-6}$, comparing the modelled and actual tide levels at Port Whangarei.

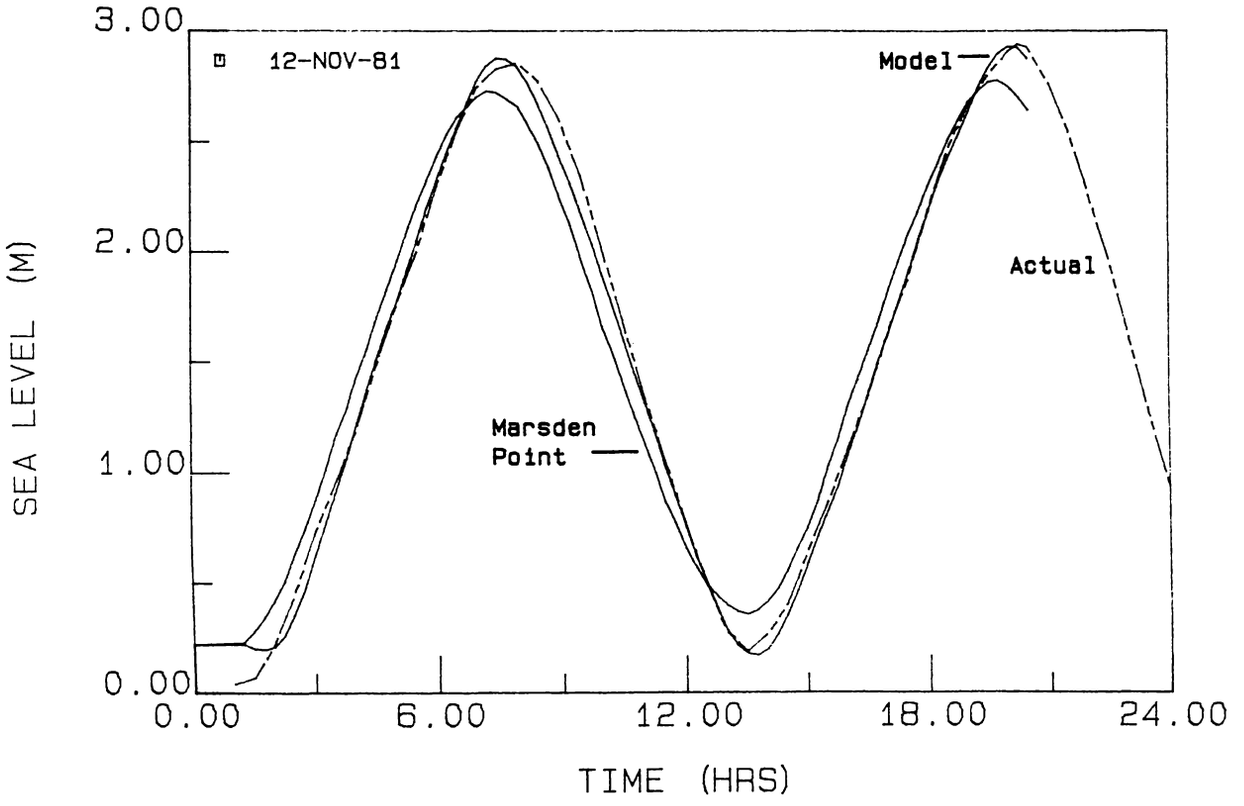

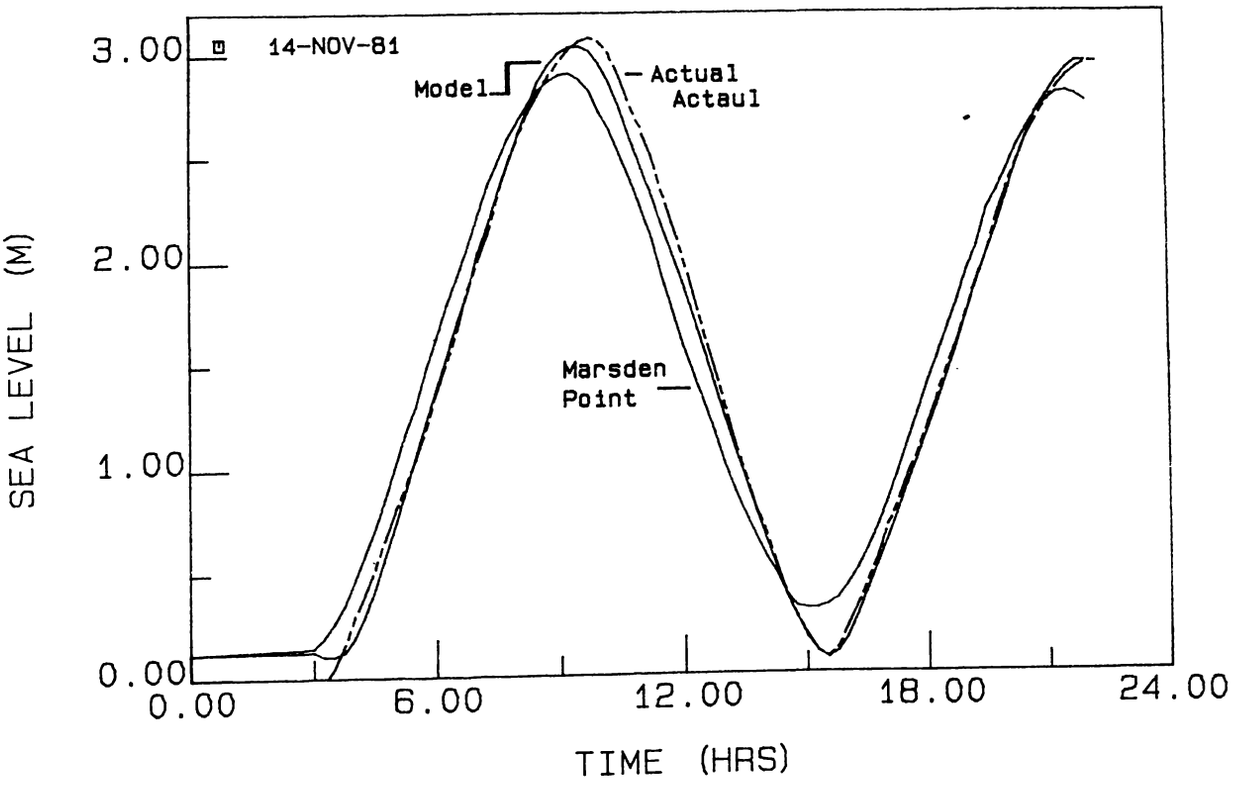

Figure 9.18: (upper) and 9.19: Verification run for 12-Nov-81 (upper) and 14-Nov-81 with roughness length $z_o = 0.001$m; longitudinal density gradient, $C_{den} = -5 \times 10^{-6}$; and wind of - 10 $m.s^{-1}$.

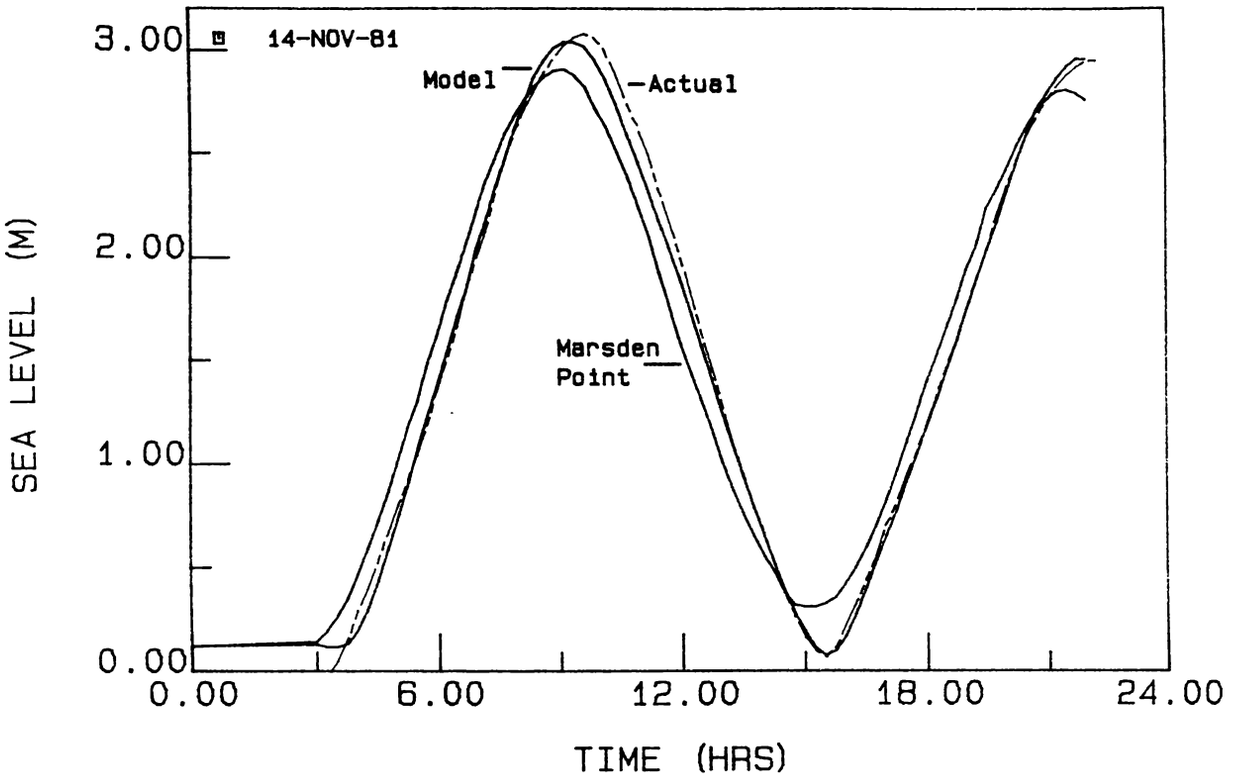

Figure 9.20: Verification run for 14-Nov-81 with roughness length, $z_o = 0.001m$; longitudinal density gradient, $C_{den} = -5 \times 10^{-6}$; wind of $-10\ m.s^{-1}$; and additional inflow of 100 cumecs at the closed end and 5 cumecs at each other node.

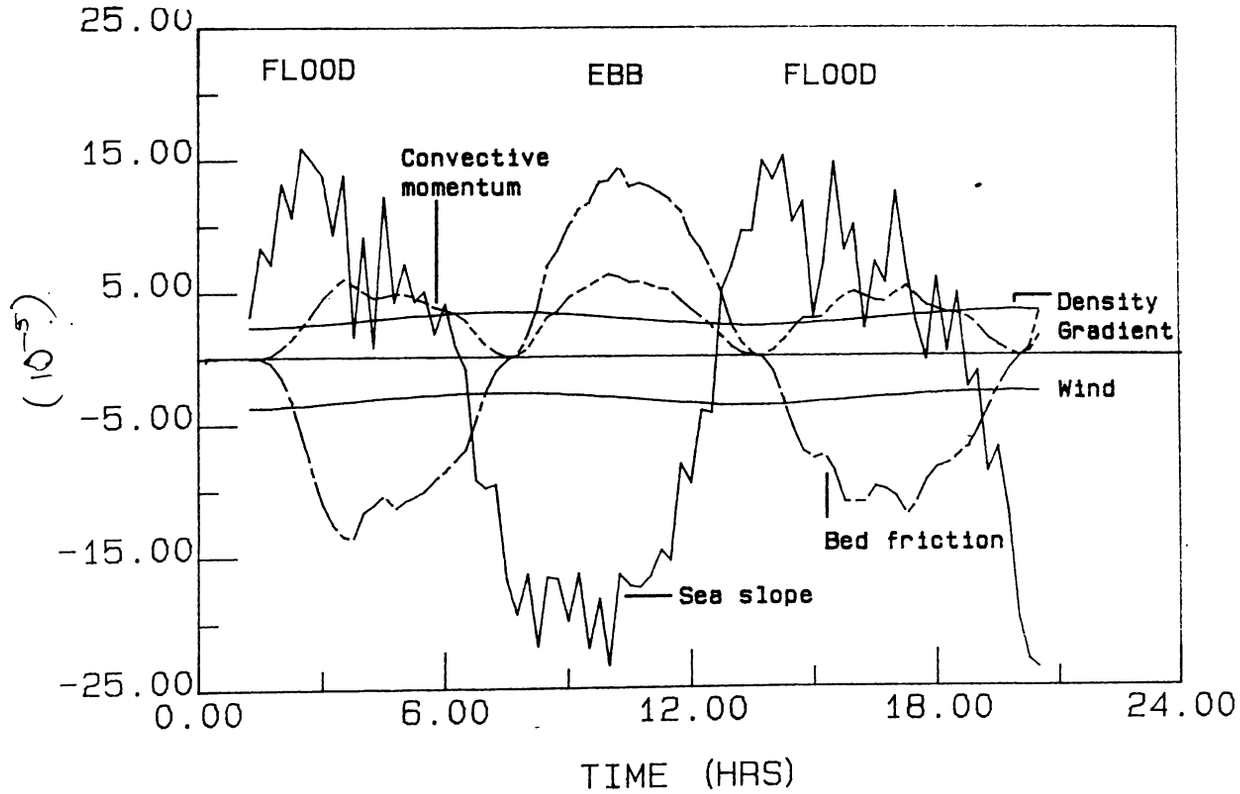

Figure 9.21: Examination of terms in the hydrodynamic equation for 12-Nov-81 at Section 8 (One Tree Point) with roughness length, $z_o = 0.001m$; longitudinal density gradient, $C_{den} = -5 \times 10^{-6}$; and wind of $-10\ m.s^{-1}$.

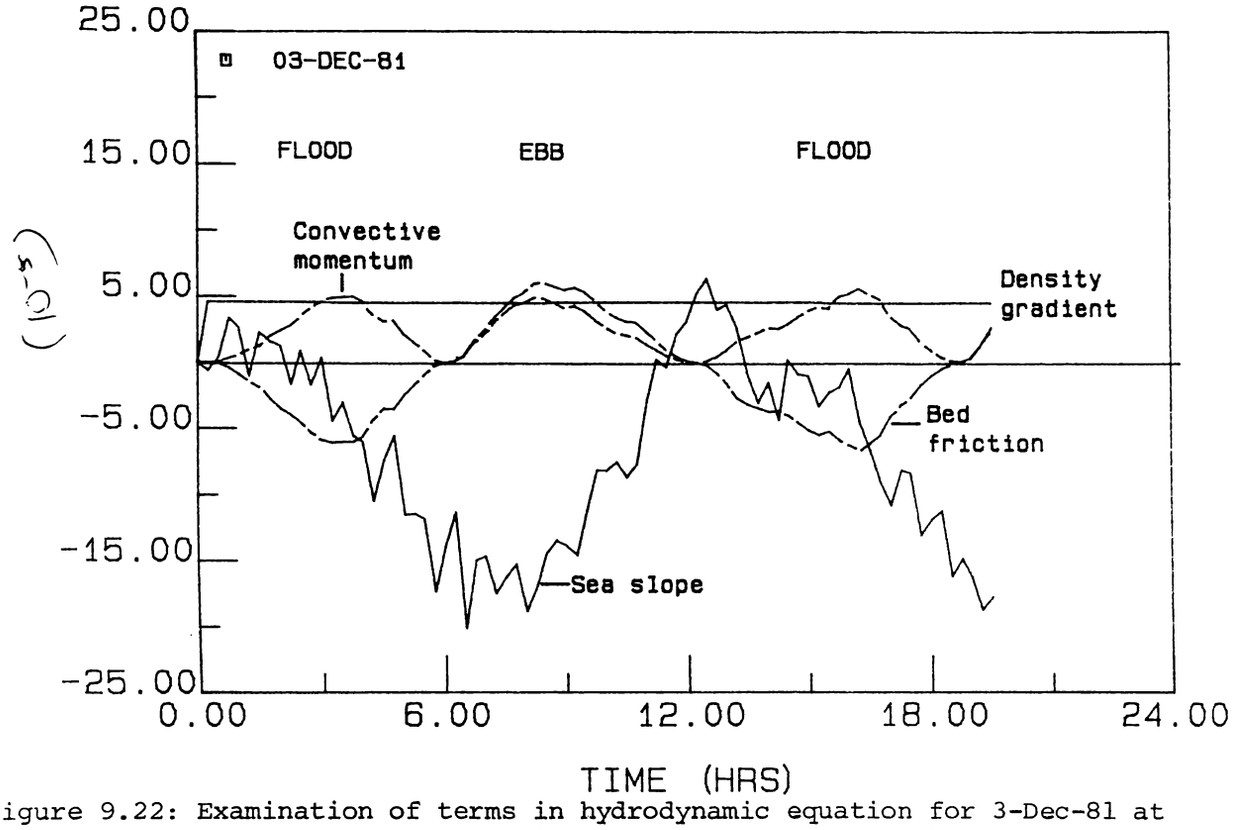

Figure 9.22: Examination of terms in hydrodynamic equation for 3-Dec-81 at Section 5 (open boundary at port site) with roughness length, $z_o = 0.001m$; and longitudinal density gradient, $C_{den} = -5 \times 10^{-6}$.

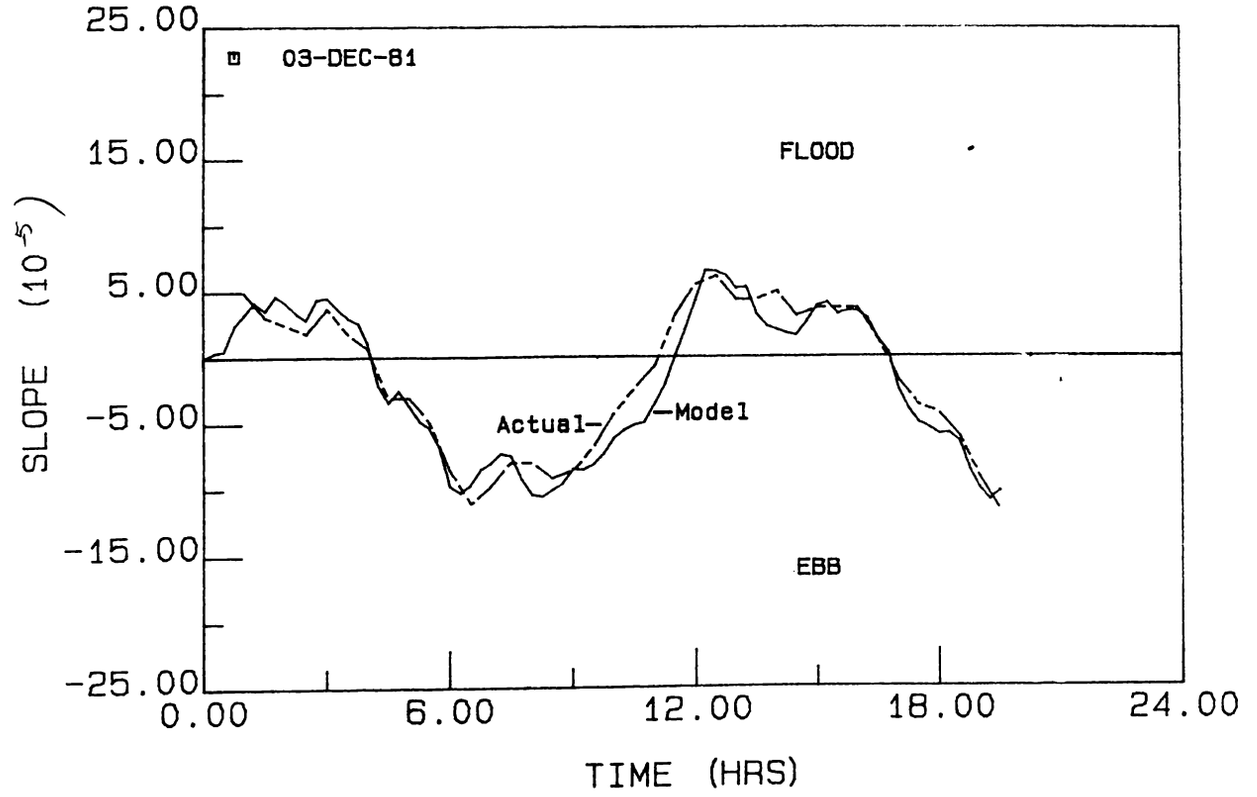

Figure 9.23: Average sea slope between Marsden Point and Port Whangarei for 3-Dec-81 comparing the modelled and actual cases. Roughness length of $z_o = 0.001m$ and longitudinal density gradient, $C_{den} = -5 \times 10^{-6}$.

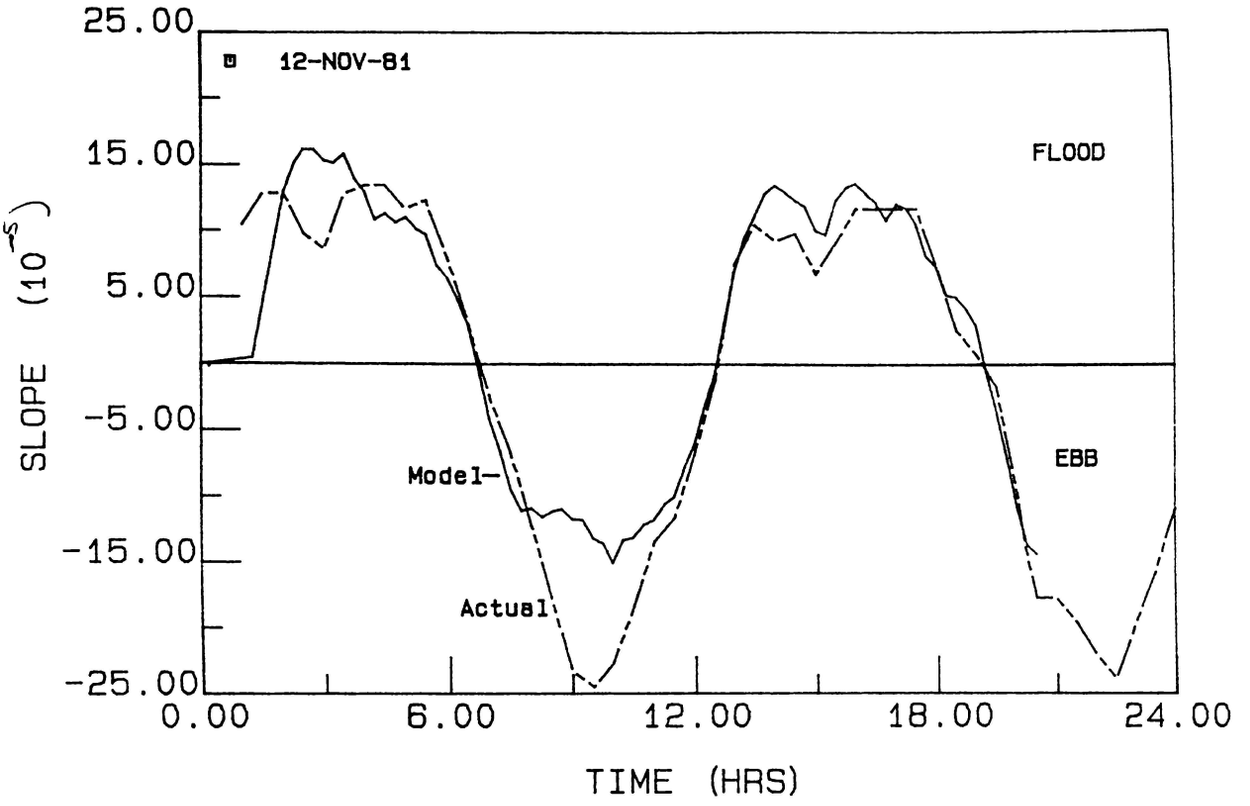

Figure 9.24: Average sea slope between Marsden Point and Port Whangarei for 12-Nov-81 comparing the modelled and actual cases. Roughness length, $z_o = 0.001m$; longitudinal density gradient, $C_{den} = -5 \times 10^{-6}$; and wind of $-10\ m.s^{-1}$.

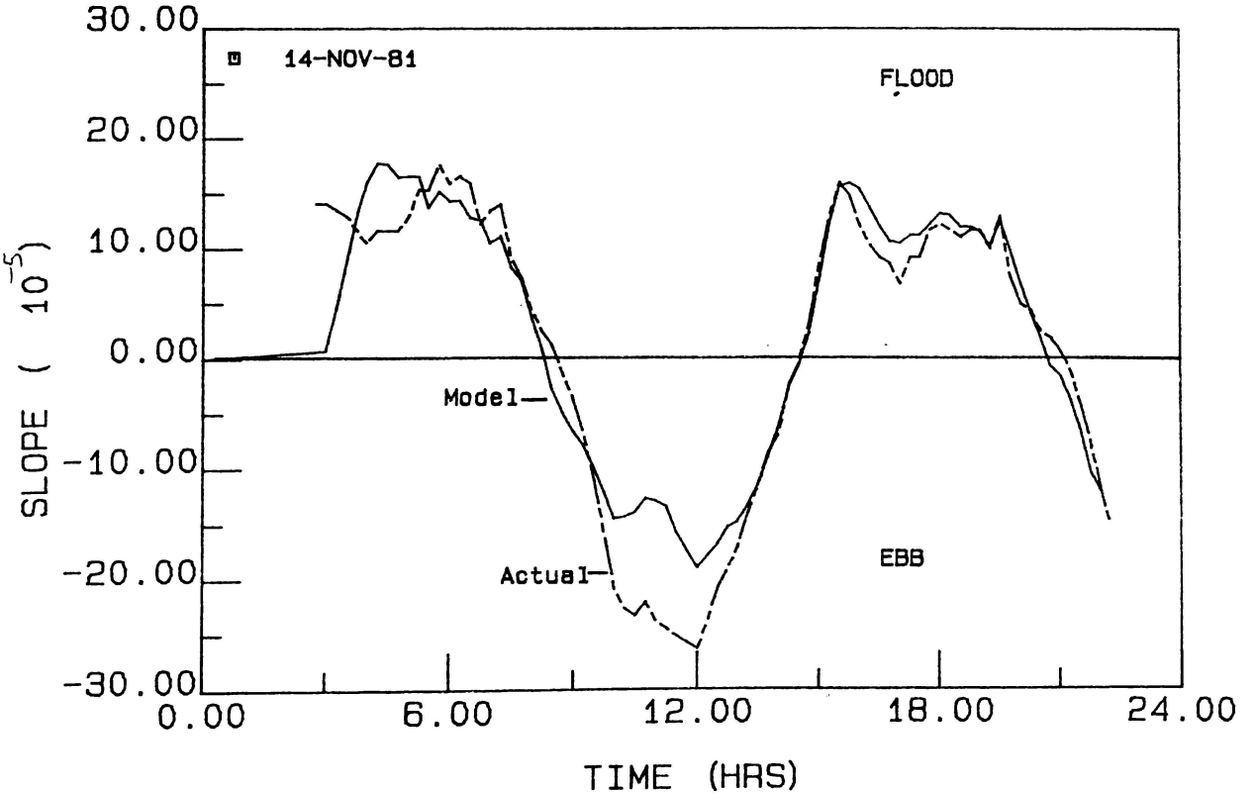

Figure 9.25: Average sea slope between Marsden Point and Port Whangarei for 14-Nov-81 comparing the modelled and actual cases. Roughness length, $z_o = 0.001m$; longitudinal density gradient, $C_{den} = -5 \times 10^{-6}$; wind of $-10\ m.s^{-1}$; and additional inflow of 100 cumecs at closed end and 5 cumecs at each other

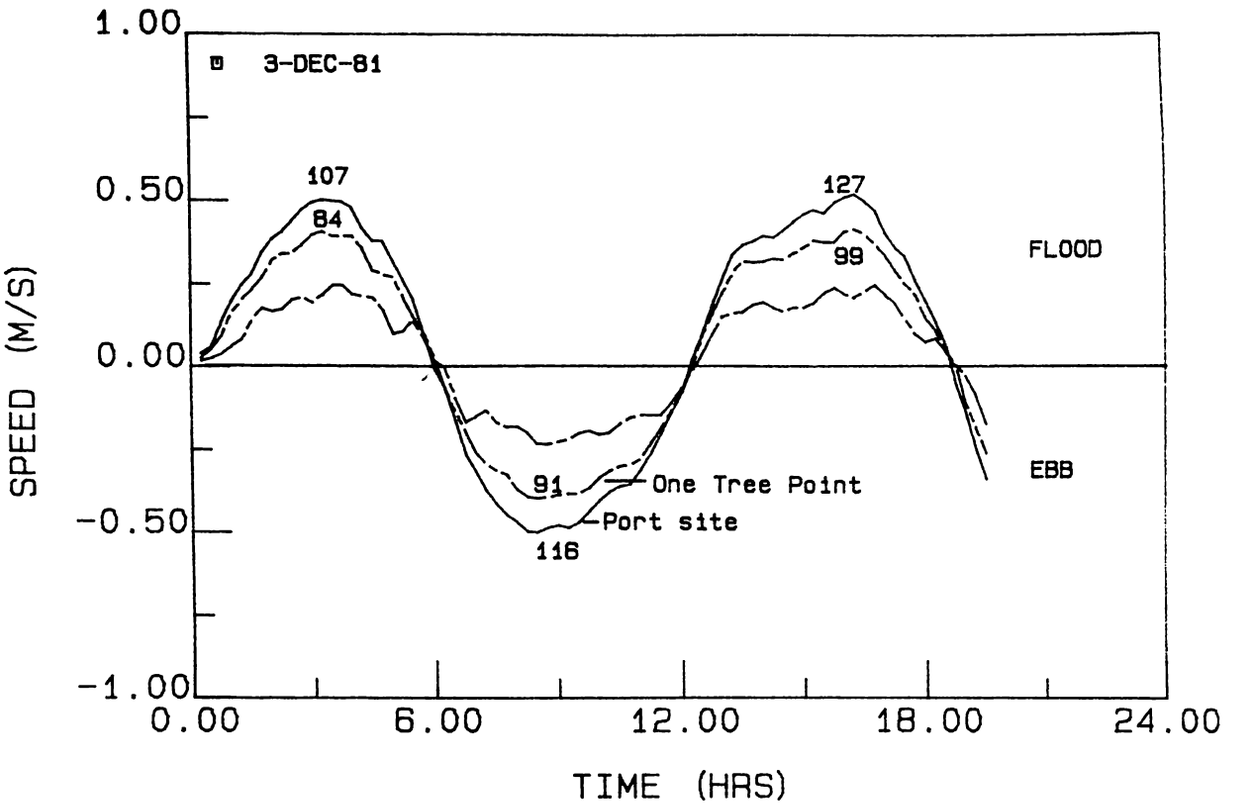

Figure 9.26: Average cross-section velocities ($m.s^{-1}$) at Section 5 (open boundary at port site), Section 8 (One Tree Point) and Section 15 (Limestone Island) for 3-Dec-81. Roughness length, $z_o = 0.001m$ and longitudinal density gradient, $C_{den} = -5 \times 10^{-6}$. Half tidal cycle prisms ($m^3 \times 10^6$) are given.

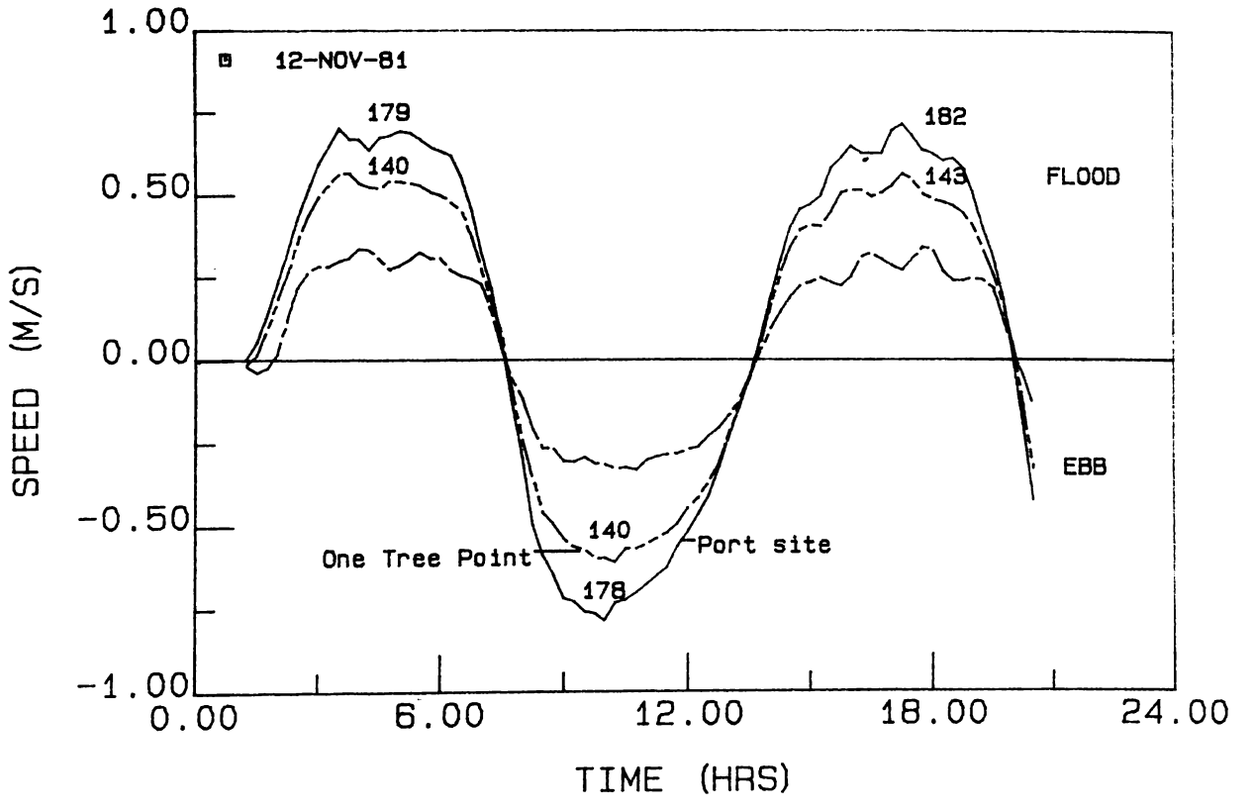

Figure 9.27: Average cross-section velocities ($m.s^{-1}$) at Section 5 (open boundary at port site), Section 8 (One Tree Point) and Section 15 (Limestone Island) for 12-Nov-81. Roughness length, $z_o = 0.001m$; longitudinal density gradient, $C_{den} = -5 \times 10^{-6}$; and wind of -10 $m.s^{-1}$. Half tidal cycle prisms ($m^3 \times 10^6$) are given.

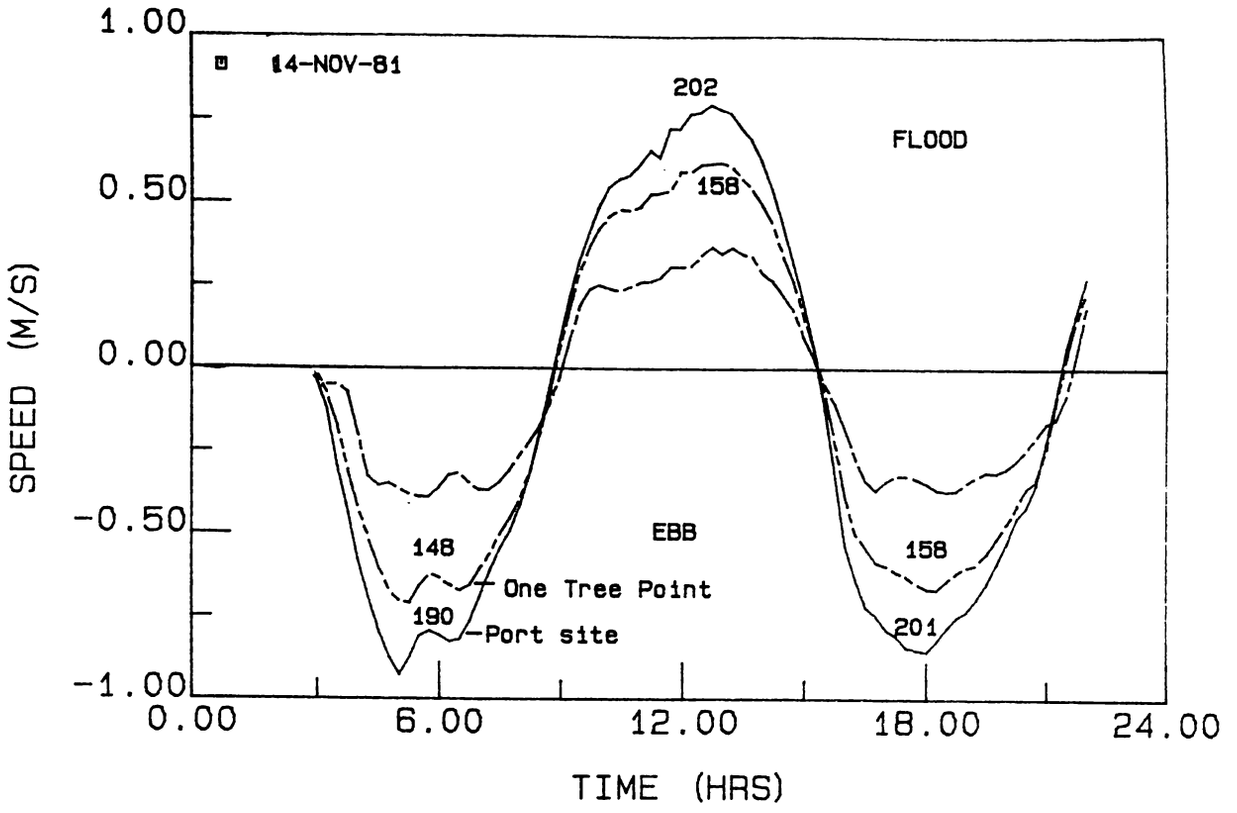

Figure 9.28: Average cross-section velocities ($m.s^{-1}$) at Section 5 (open boundary at port site) Section 8 (One Tree Point) and Section 15 (Limestone Island) for 14-Nov-81. Roughness length, $z_o = 0.001m$; longitudinal density gradient, $C_{den} = -5 \times 10^{-6}$; wind at -10 $m.s^{-1}$; and additional inflow of 100 cumecs at closed end and 5 cumecs at each other velocity node. Half tidal cycle prisms ($m^3 \times 10^6$) are given.

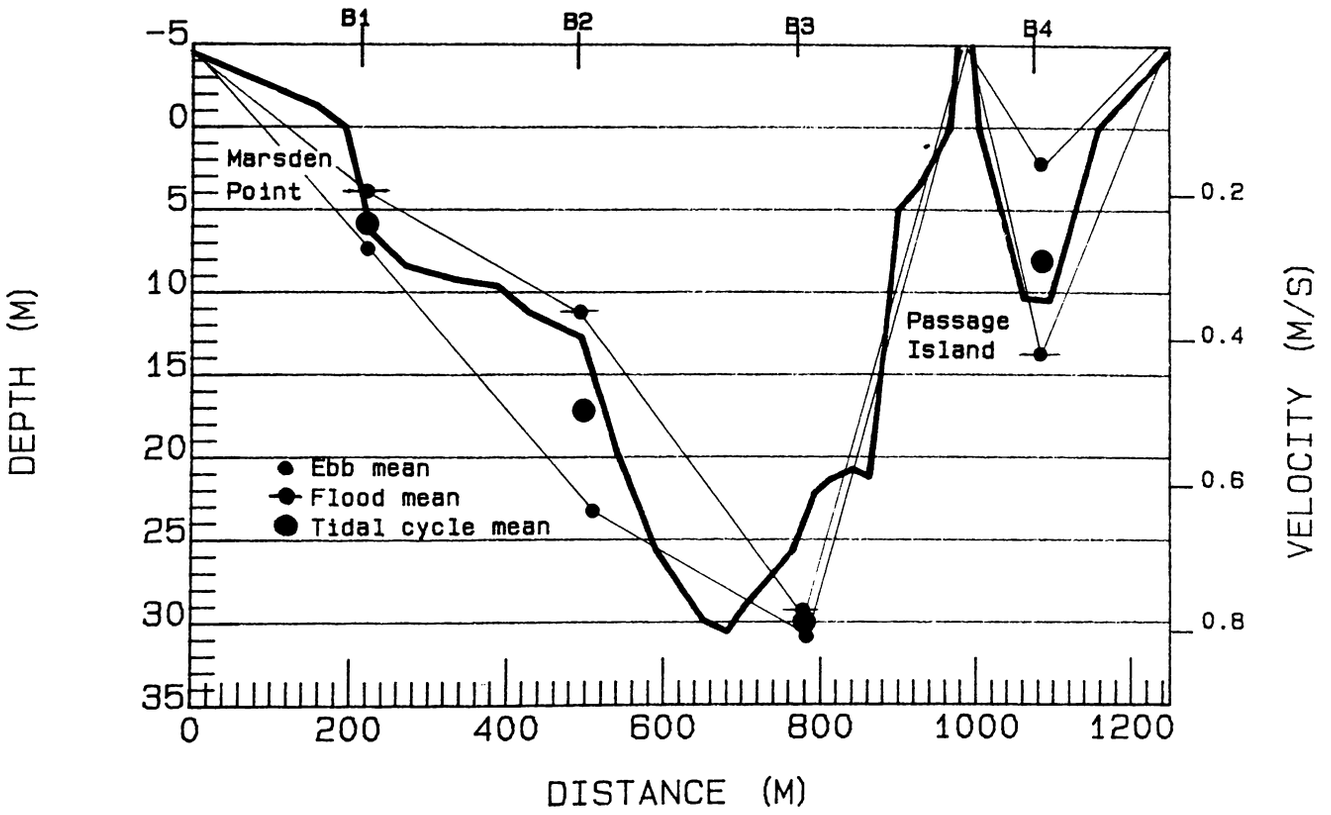

Figure 9.29: Entrance gorge cross-section with B-series half tidal cycle average velocities ($m.s^{-1}$) for 12-Nov-81.

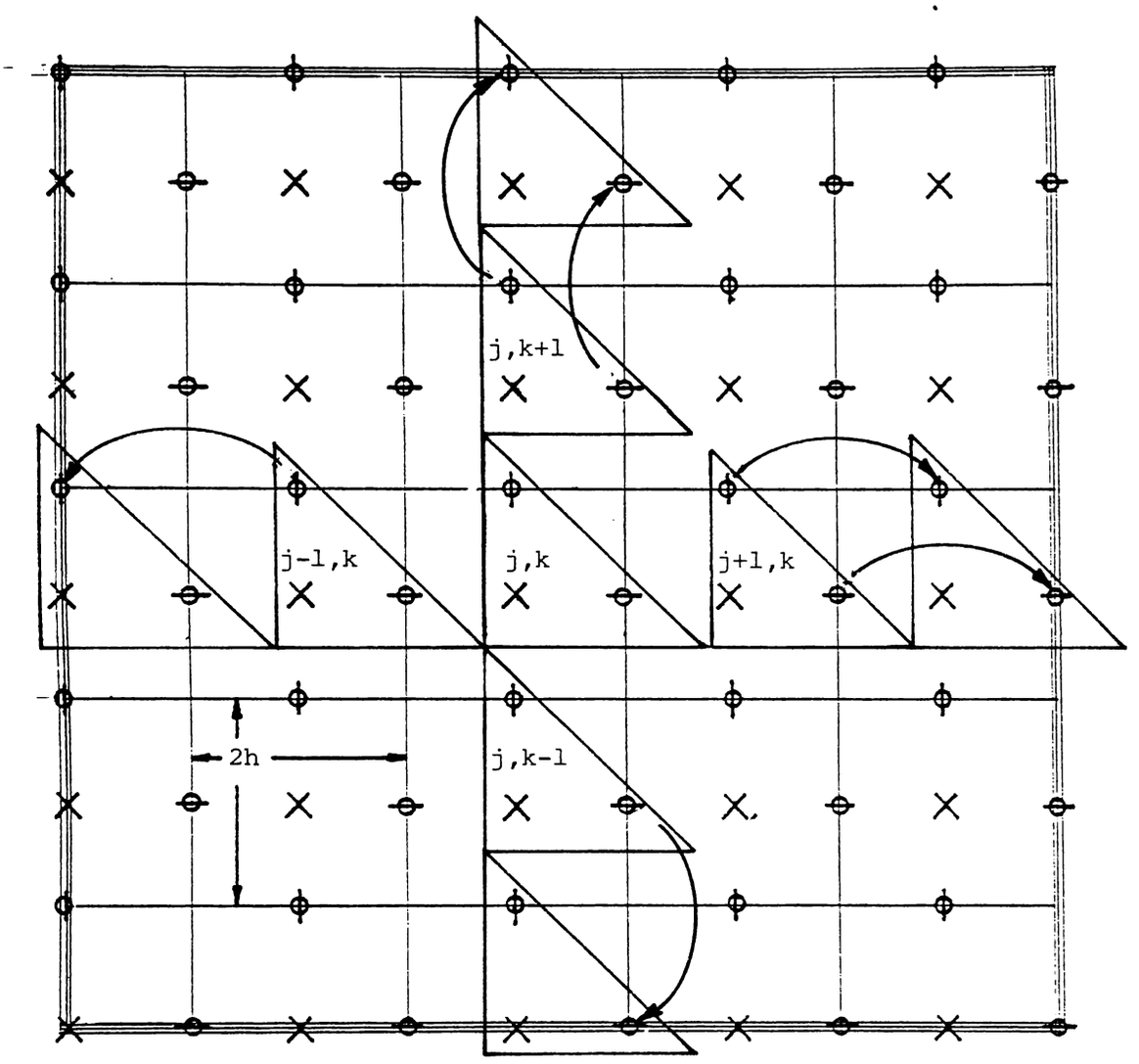

X sea level ($\xi_{j,k}$)

⊖ x-components of: depth below datum ($D_{Uj,k}$)
velocity ($U_{j,k}$)

ϕ y-components of: depth below datum ($D_{Vj,k}$)
velocity ($V_{j,k}$)

Figure 10.1: Grid defining the notation for the 1-dimensional, numerical model scheme. All nodes within the triangles have the subscript shown and parameters at these locations are listed above. Open boundaries are distinguished by an integer code from 4 to 7. The arrows relate applicable internal nodes used to set the values at corresponding boundary nodes for a given sea level. Other boundary velocities are derived with a simplified momentum balance equation.

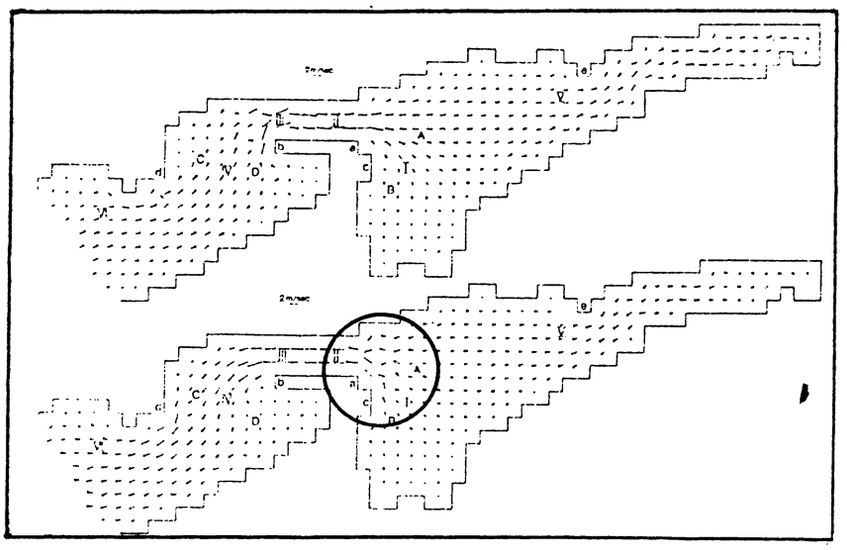

Figure 10.2: Example of zig-zagging in an explicit model published by Tee (1976).

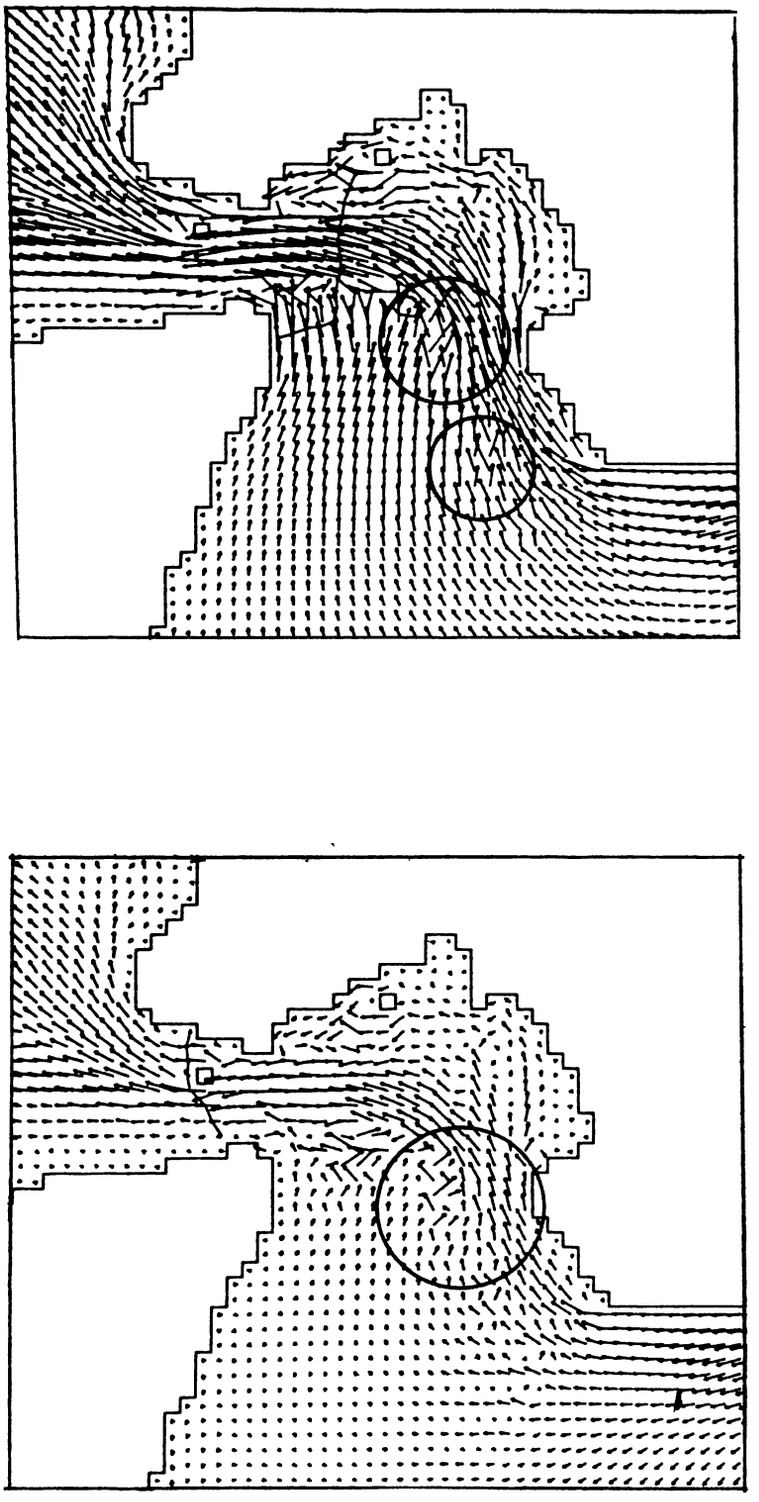

Figure 10.3 : Example of zig-zagging in the DHI (1982) simulation of Whangarei Harbour using the mixed-implicit model, S21. The zig-zagging has occurred on the steep channel flank at the entrance to Whangarei Harbour near Busby Head.

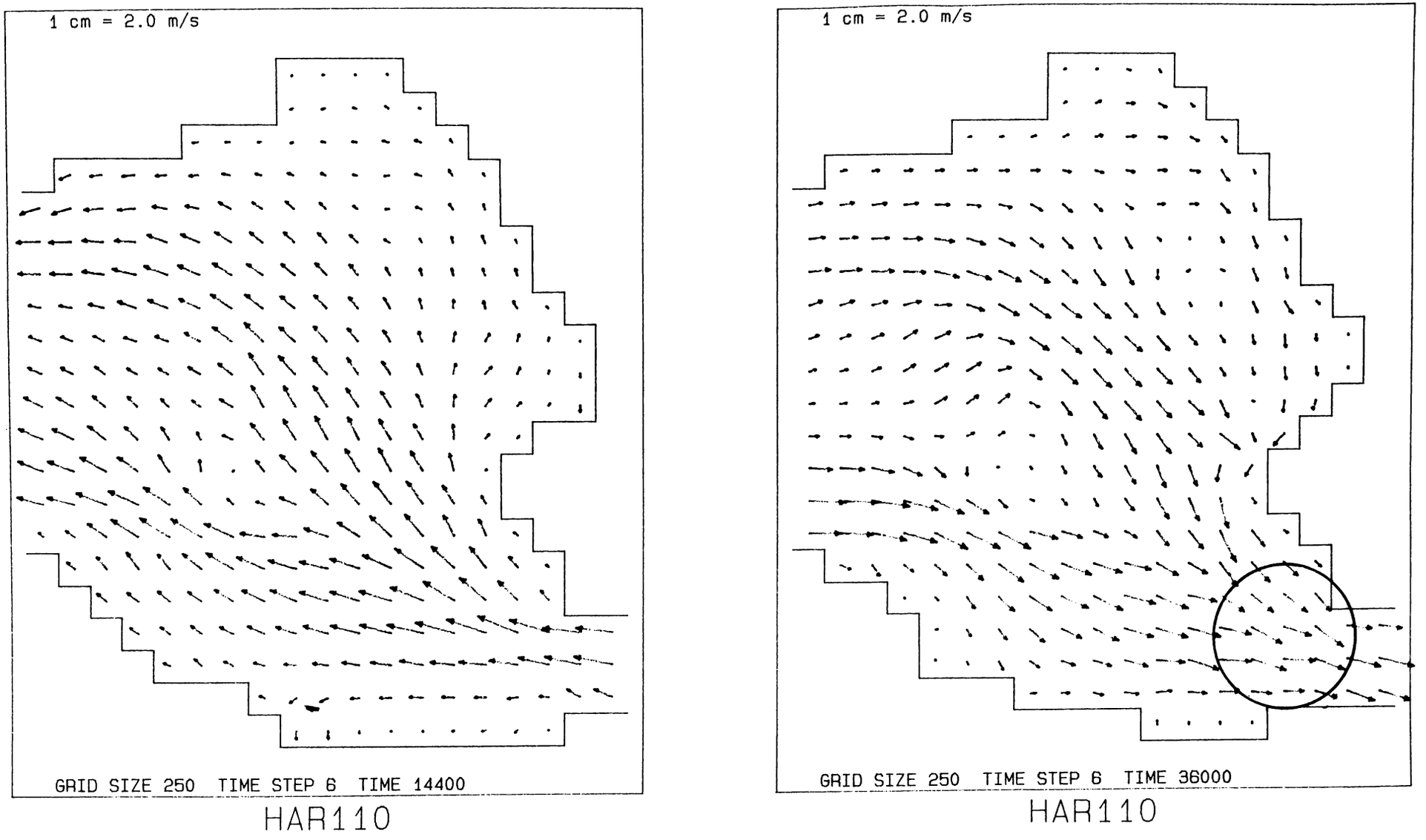

Figure 10.4: Zig-zagging evident in a simulation of Whangarei Harbour with 2DD. The phenomenon is caused by a poor approximation for the convective acceleration terms at the land/sea boundaries. Note that it only occurs in convergent flow during ebb tides at the entrance and propogates upstream.

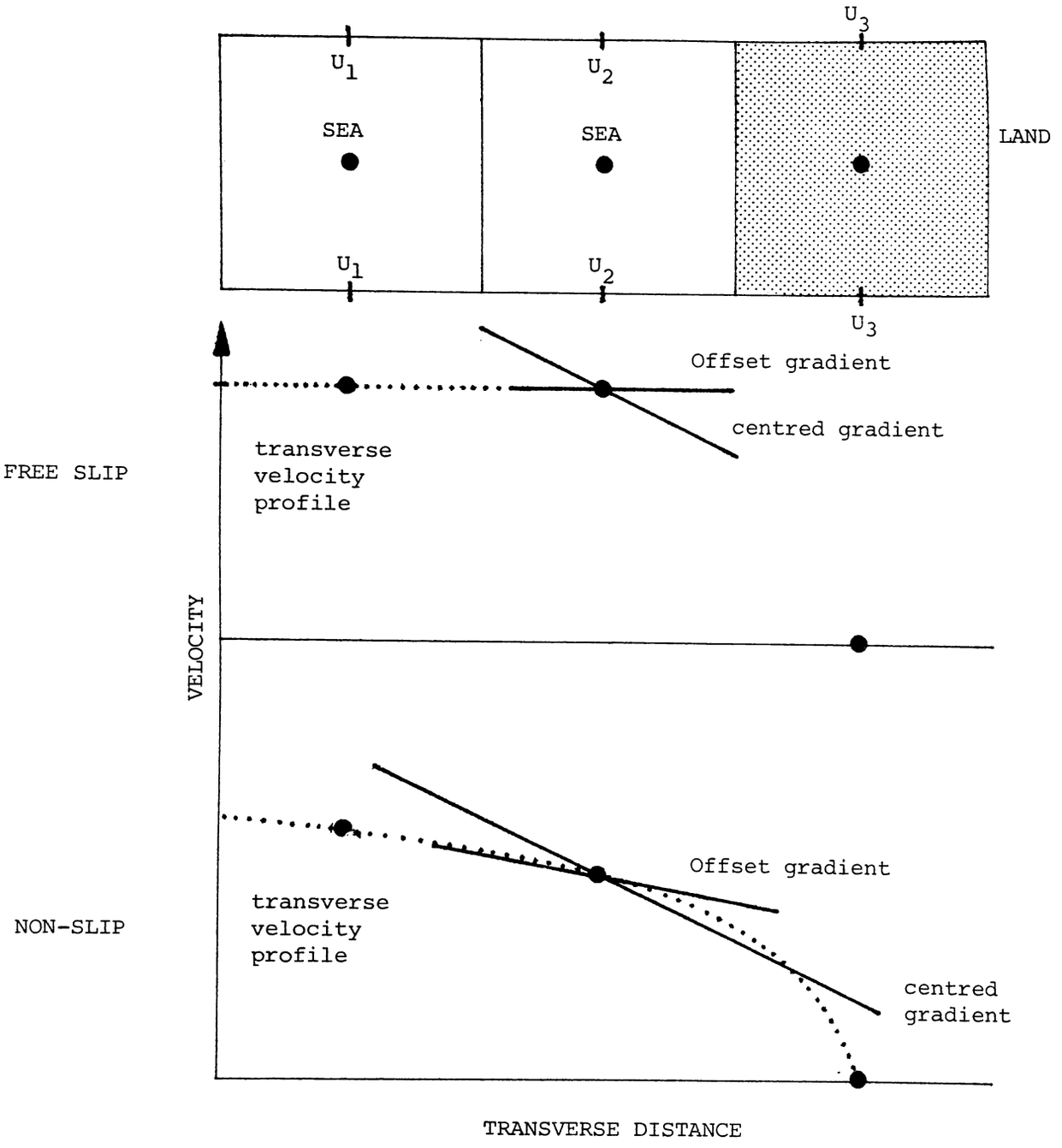

Figure 10.5 : Schematisation of the determination of the transverse velocity gradient at U_2 obtained using either a centred or offset derivative. Land speeds are always zero. At a free-slip land/sea boundary, the velocity gradient is approximately zero. By offsetting the derivative and using the two offshore speeds the finite difference approximation is accurate. However, the centred finite difference scheme provides a poor approximation to the gradient in the example shown. In the second case at a non-slip boundary, the deviation is not so large. However, for a typical transverse velocity profile where depths and velocities increase quickly away from the land, the gradient obtained using the offset derivative in the schematised diagram is still seen to be more accurate than the centred value.

In this special case where the velocity increases quickly offshore - as typically occurs in the entrance throat of tidal inlets - the offset derivative offers a better approximation to the transverse velocity gradient. Offsetting the derivative was found to eliminate zig-zagging.

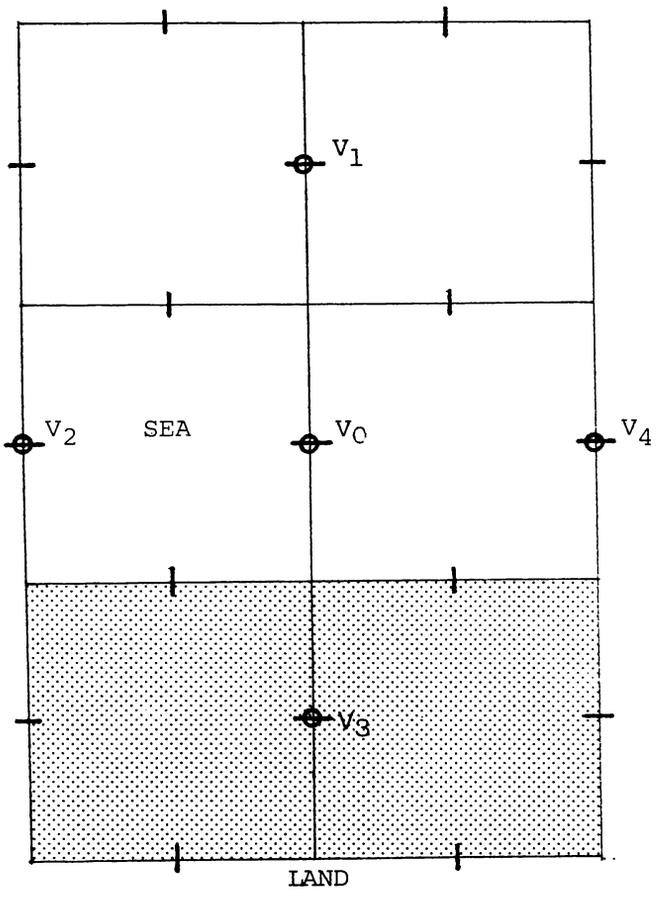

Figure 10.6: Velocities at a land/sea boundary. When V_3 is on land and set equal to zero, energy is absorbed from the flow by the eddy diffusion term and a horizontal boundary layer with a thickness of severall cell widths is established.

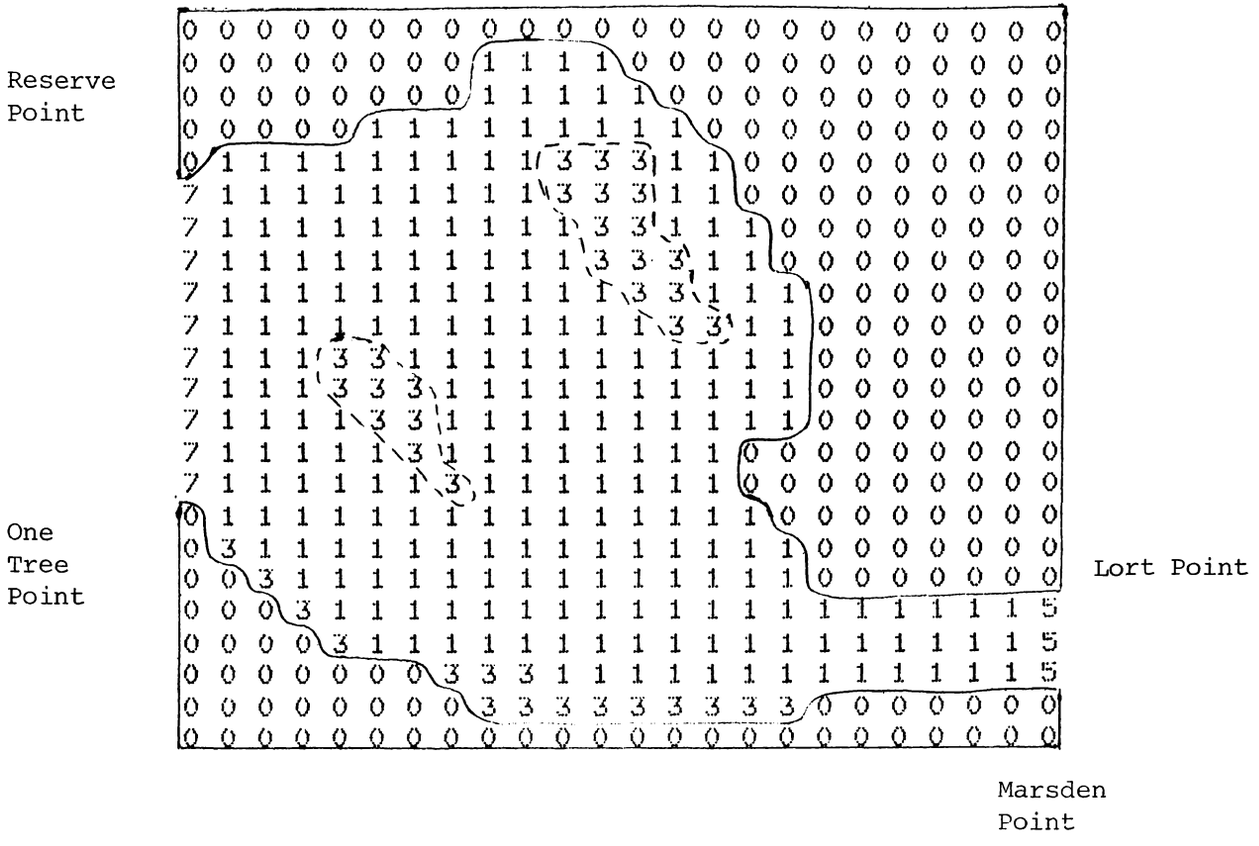

Figure 10.7: Whangarei Harbour at low tide represented in 2DD by an integer code. Type 0 cells represent land which cannot be flooded. Type 1 are flooded cells while Type 3, depicting Snake and McDonald Banks, are inter-tidal zones exposed by the low tide. Open boundary cells are coded as 5 (right hand) and 7 (left hand).

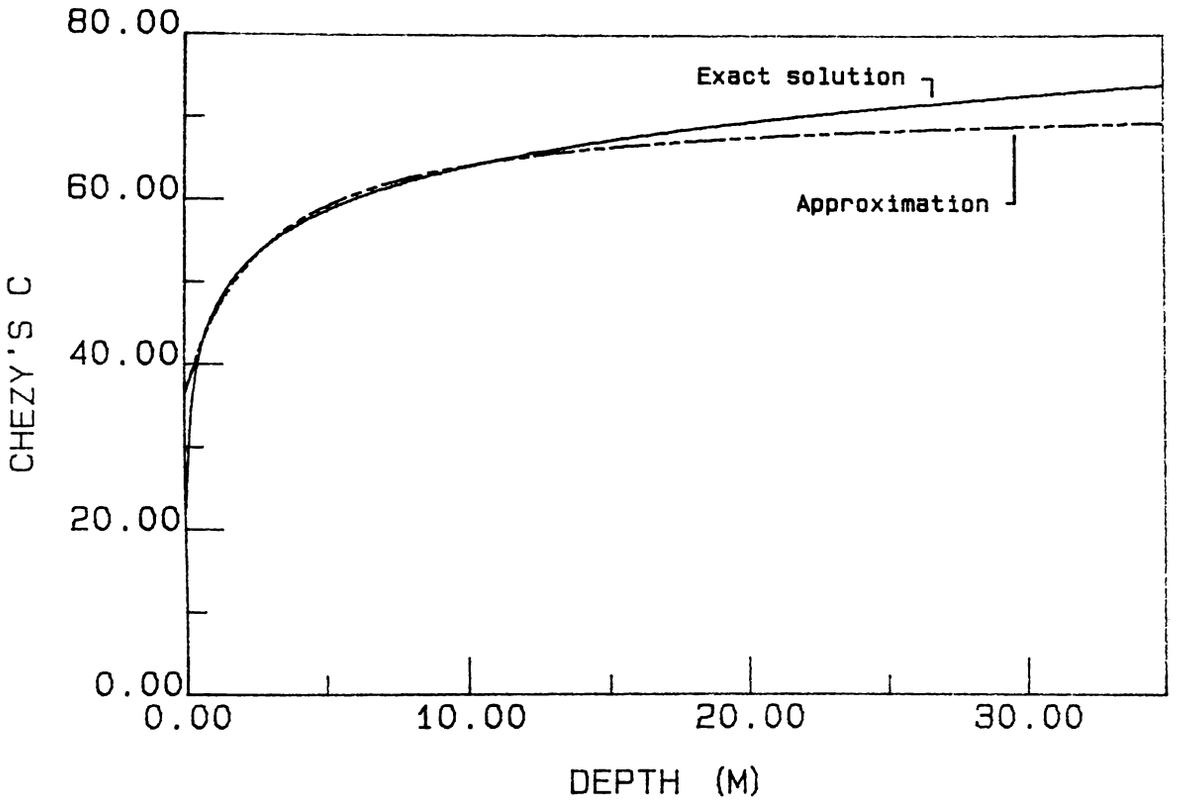

Figure 10.8: Comparison of the exact and approximate solution for Chezy's C with $z_o = 0.001$m in water depths up to 35m.

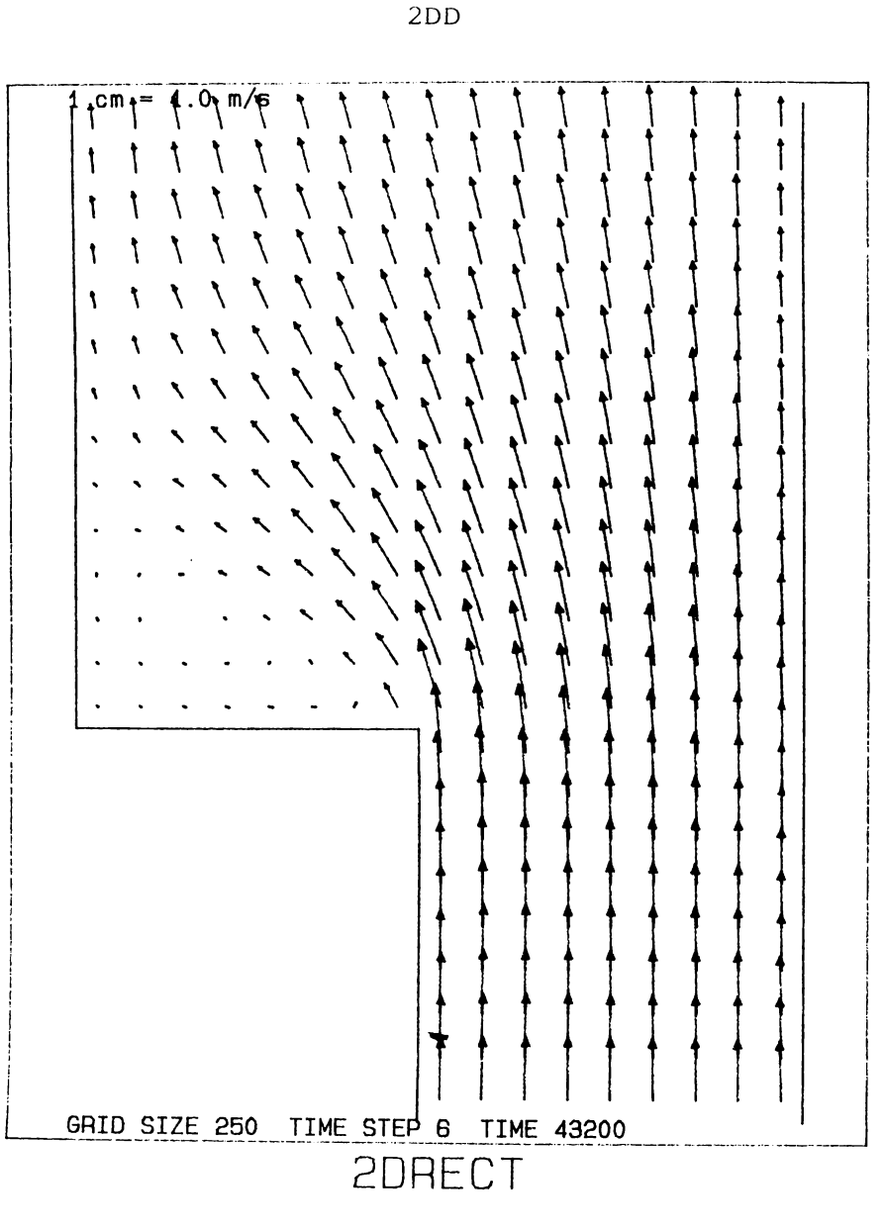

Figure 10.9: Steady-state flow past a rectangular step. The lee face is 2000m long and maximum flow speeds in the entrance channel are 0.8 $m.s^{-1}$. Other parameters are: depth, 5m; $A_H = 5\ m^2.s^{-1}$; Chezy's C, 60 $m^{\frac{1}{2}}.s^{-1}$; and a tide level difference at the open boundaries of 0.10m.

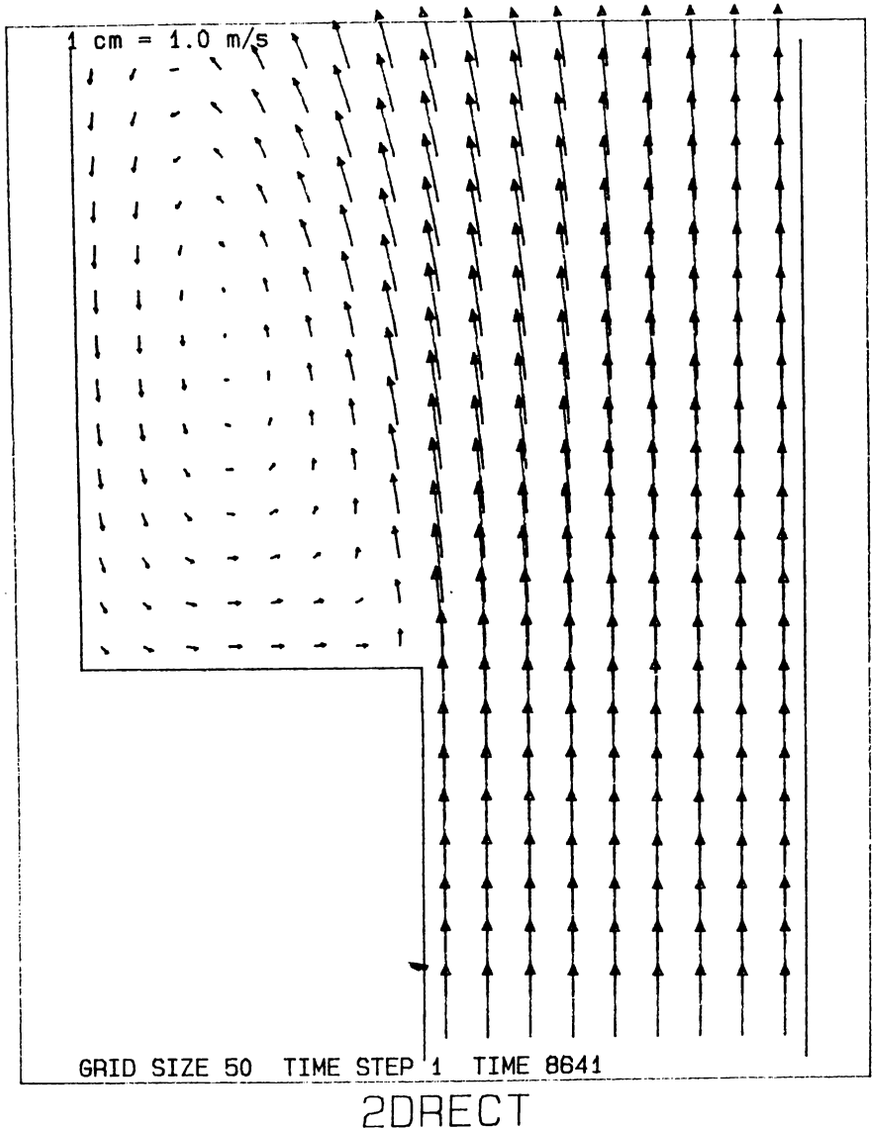

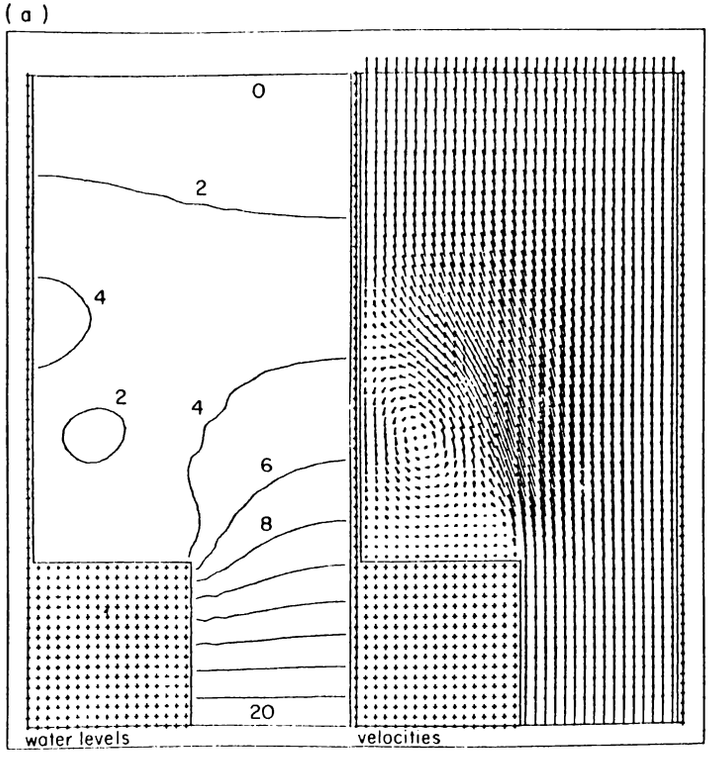

Figure 10.10: Steady-state flow past a rectangular step comparing 2DD and S21. In 2DD, the lee face is 400m long and speeds in the entrance channel are 0.9 $m.s^{-1}$. Other parameters are: depth, 5m; $A_H = 5\ m^2.s^{-1}$; Chezy's C, 60 $m^{\frac{1}{2}}.s^{-1}$; and a tide level difference at the open boundaries of 0.02m.

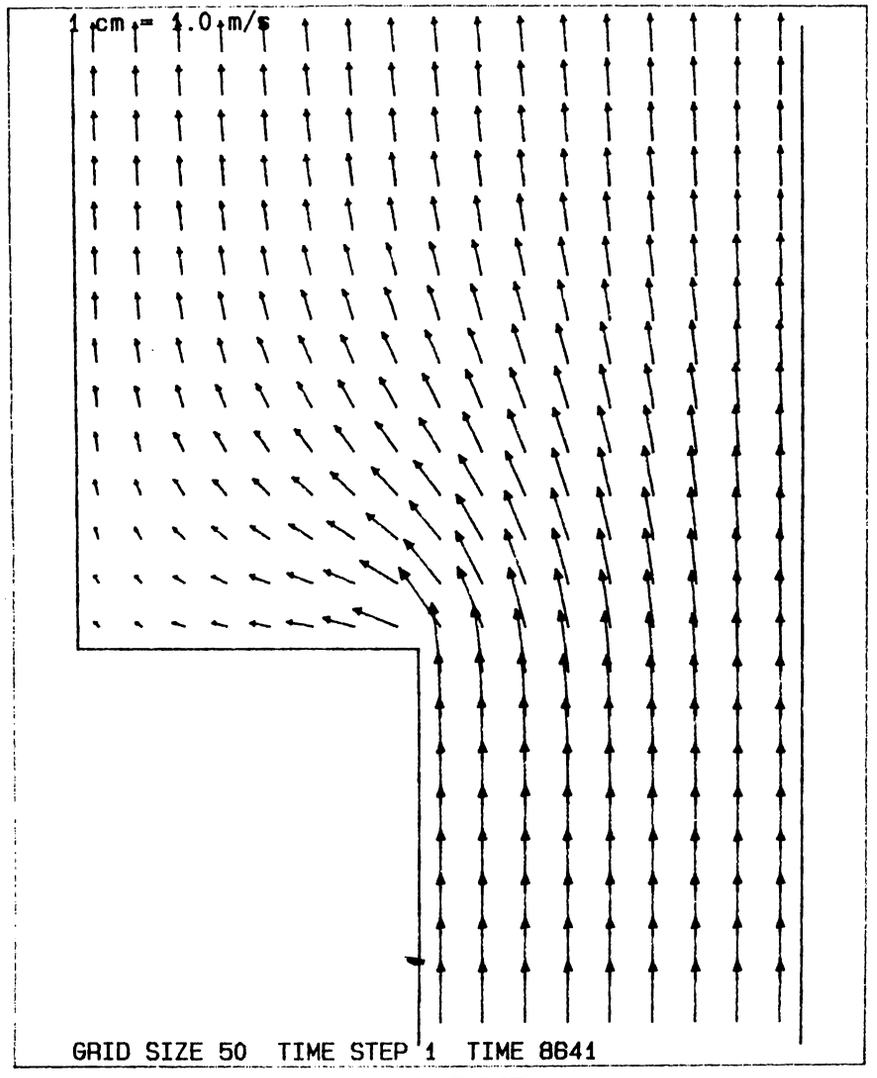

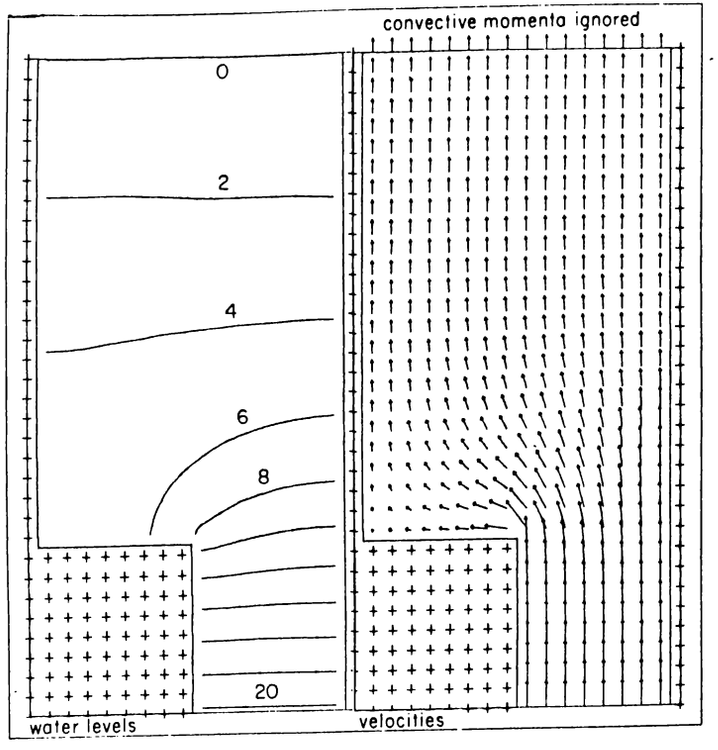

Figure 10.11: Steady-state flow past a rectangular step with the convective acceleration terms suppressed. The eddy circulation no longer occurs. S21 (right) shows a similar behaviour. In 2DD, the lee face is 400m long and speeds in the entrance channel are 0.74 $m.s^{-1}$. Other parameters are: depth, 5m; $A_H = 5\ m^2.s^{-1}$; Chezy's C, 60 $m^{\frac{1}{2}}.s^{-1}$; and a tide level difference at the open boundaries of 0.02m.

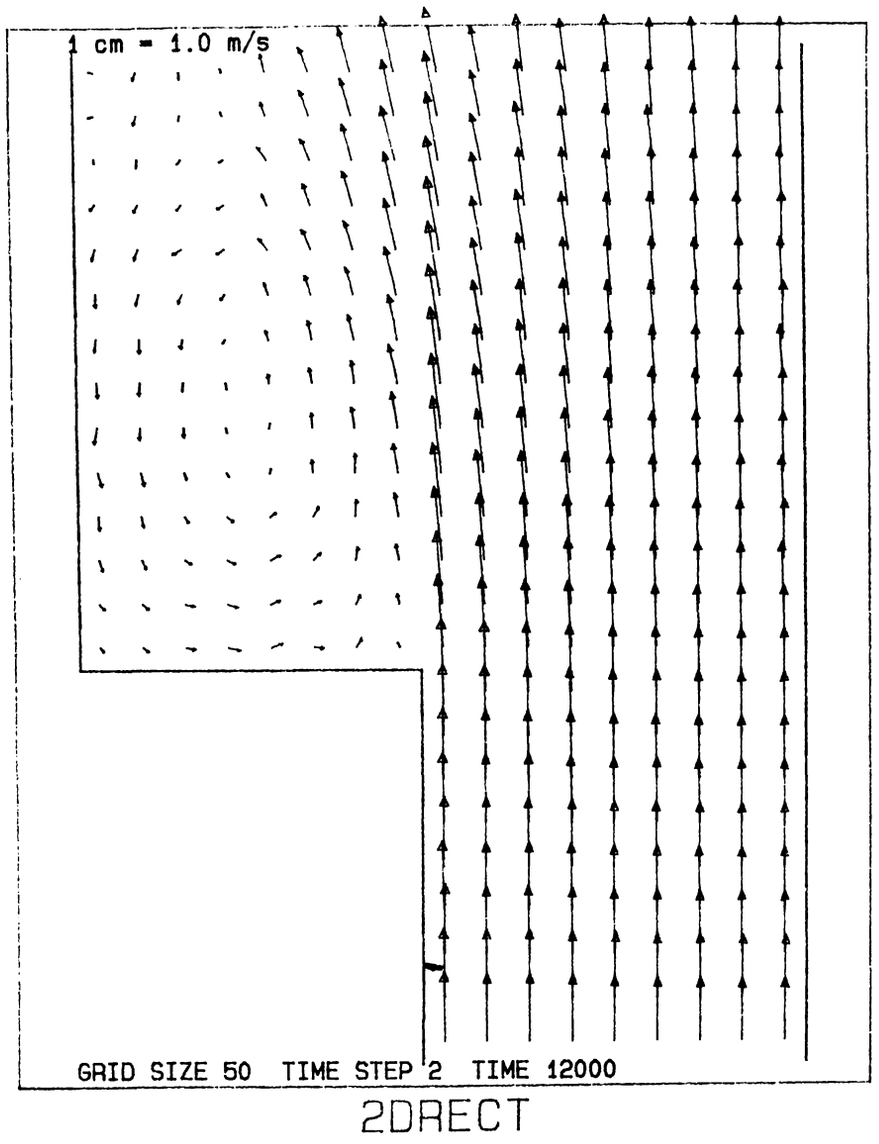

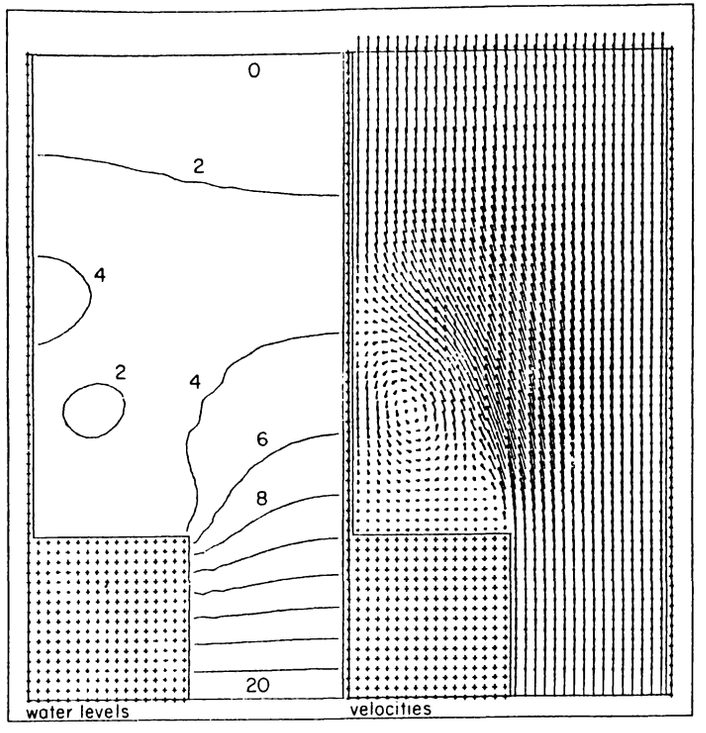

Figure 10.12: Steady-state flow past a rectangular step with the eddy diffusion coefficient set to zero. There are small instabilities and the eddy circulation is grossly reduced. S21 (right) is not as affected as 2DD by setting $A_H = 0$. In 2DD, the lee face is 400m long and speeds in the entrance channel are 0.82 $m.s^{-1}$. Other parameters are: depth, 5m; Chezy's C, 60 $m^{\frac{1}{2}}.s^{-1}$; and a tide level difference at the open boundaries of 0.02m.

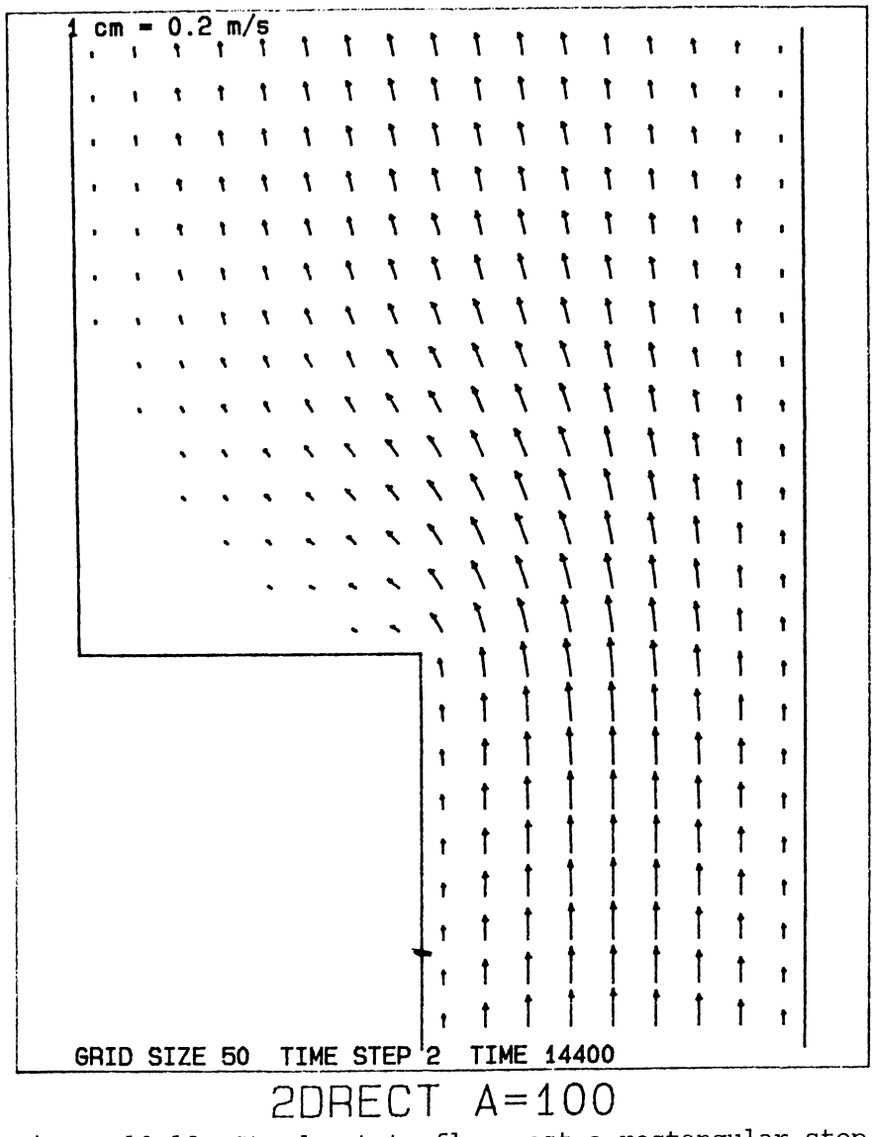

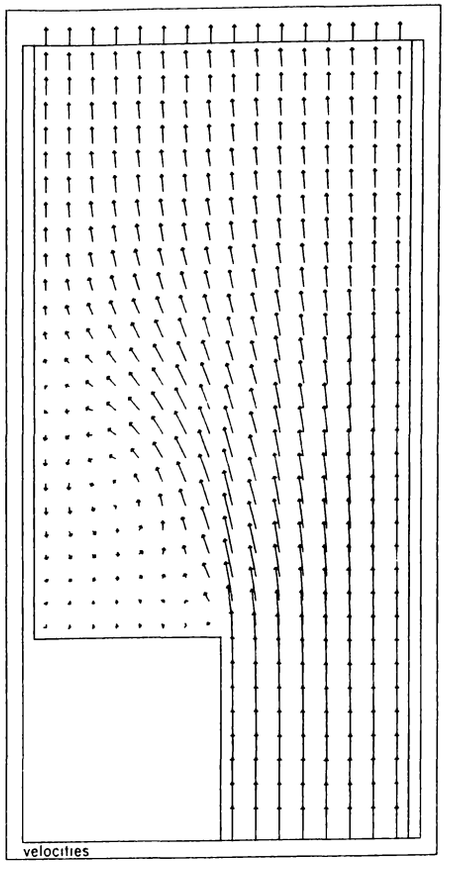

Figure 10.13: Steady-state flow past a rectangular step with the eddy diffusion coefficient set to 100 $m^2.s^{-1}$. The recirculating flow has been totally dampened. S21 (right) shows similar behaviour. In 2DD, the lee face is 400m long and speeds in the entrance channel are only 0.1 $m.s^{-1}$. Other parameters are: depth, 5m; Chezy's C, 60 $m^{\frac{1}{2}}.s^{-1}$, and a tide level difference at the open boundaries of 0.02m.

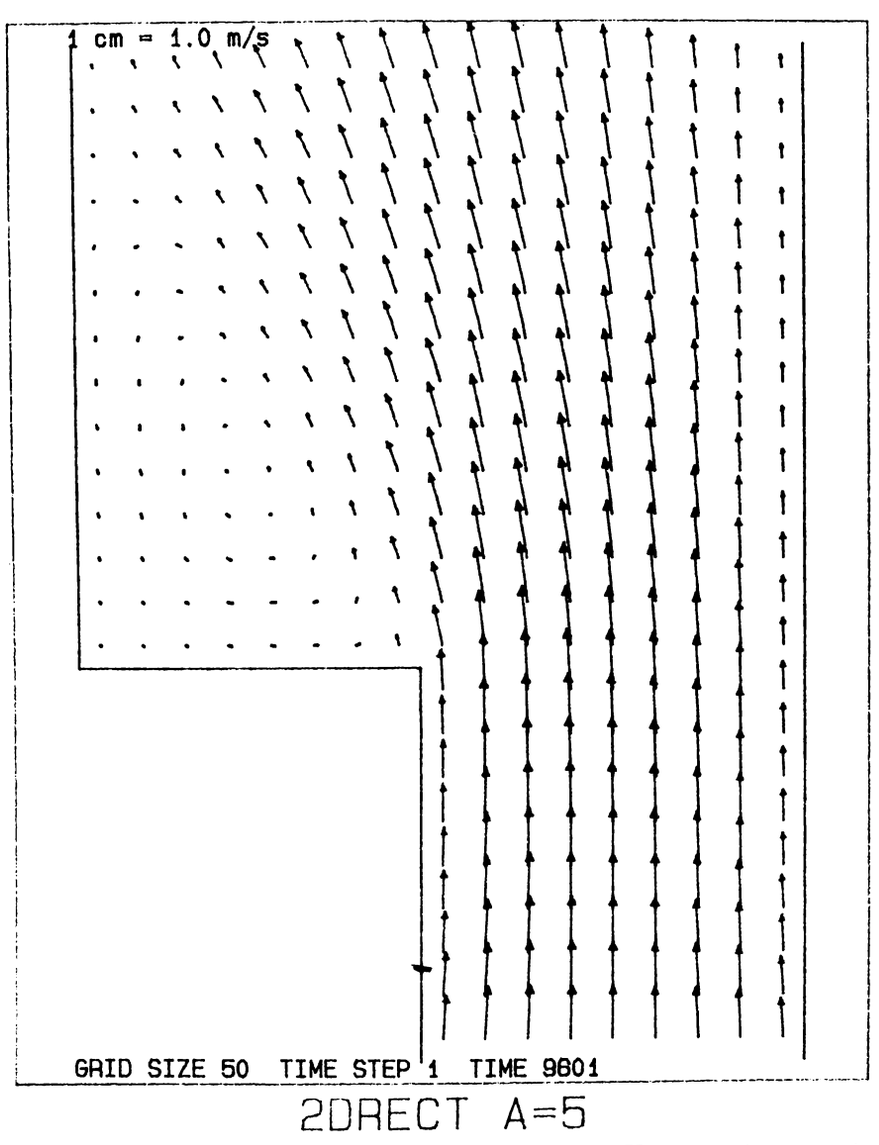

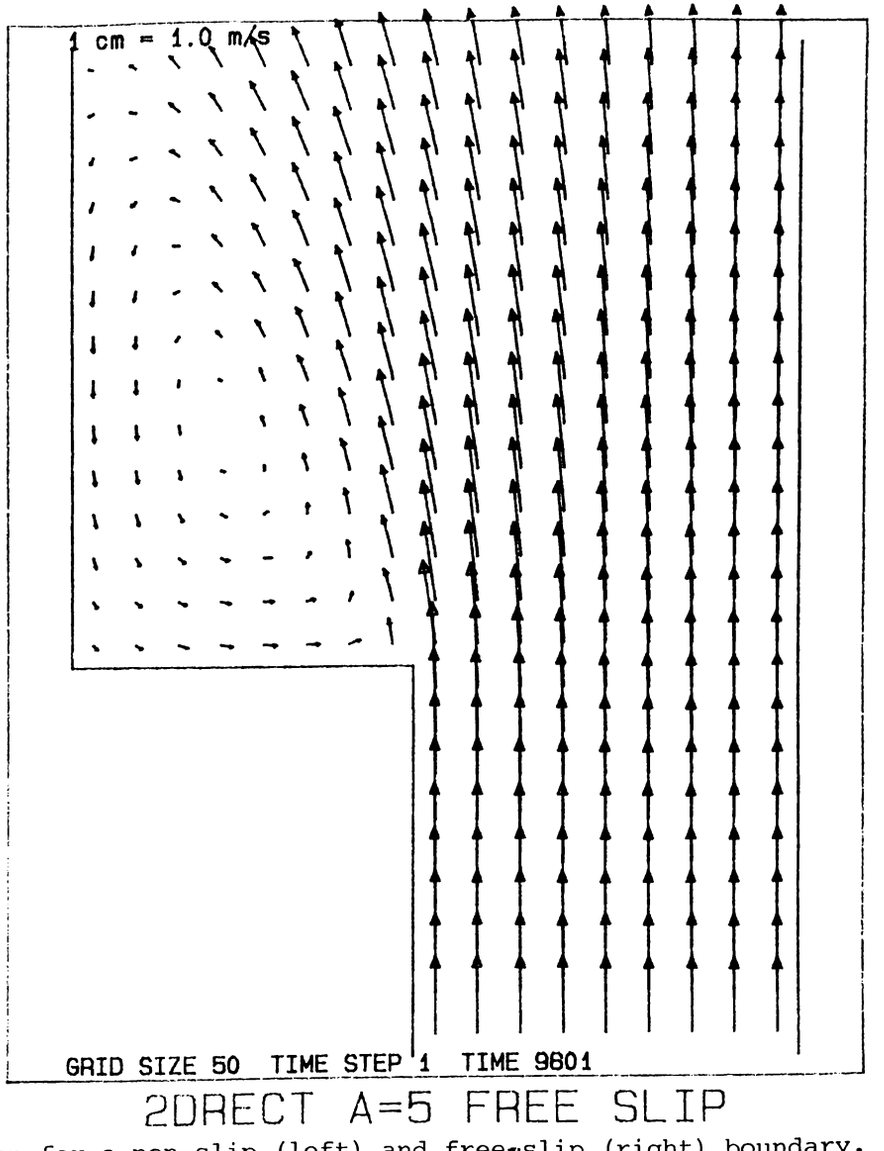

Figures 10.14 and 10.15: Steady-state flow past a rectangular step for a non-slip (left) and free-slip (right) boundary. The lee face is 400m long and speeds in the entrance channel are 0.55 $m.s^{-1}$ and 0.9 $m.s^{-1}$ respectively. Other parameters are: depth, 5m; Chezy's C, 60 $m^{\frac{1}{2}}.s^{-1}$; $A_H = 5\ m^2.s^{-1}$; and a tide level difference at the open boundaries of 0.02m.

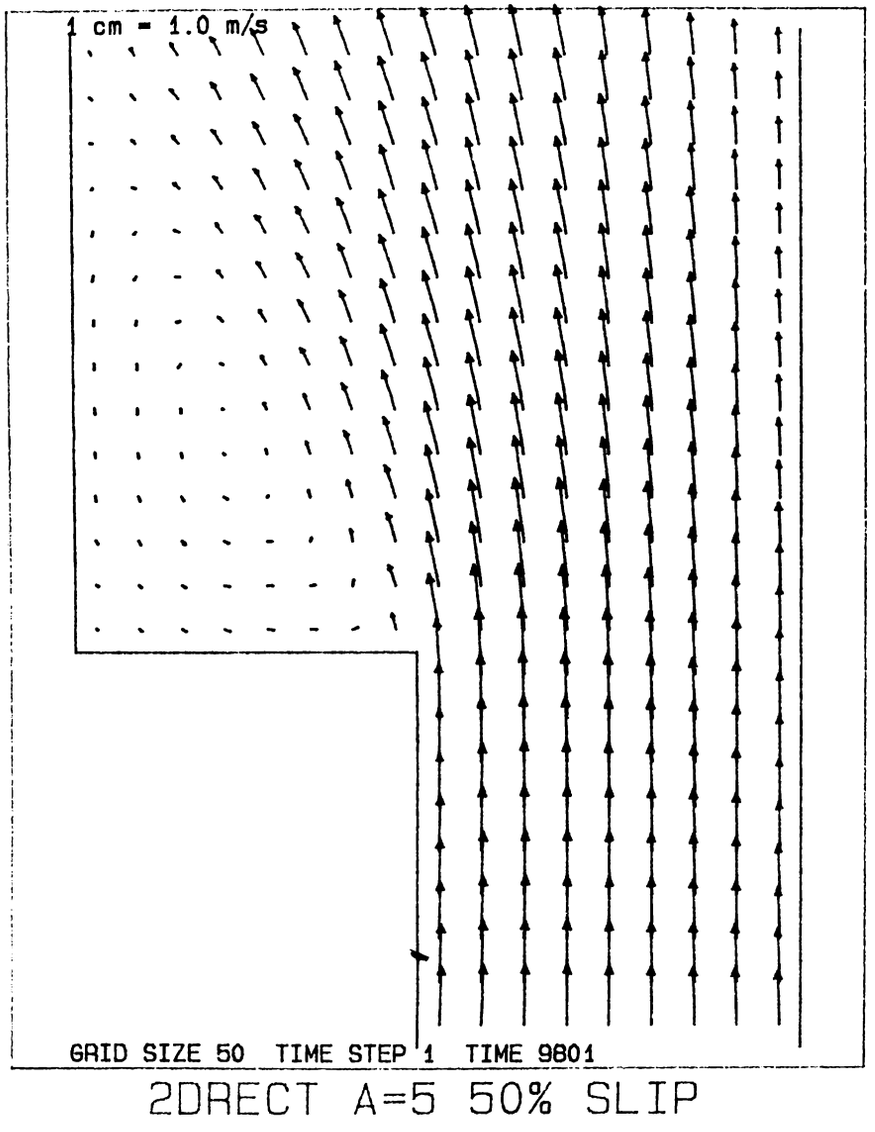

Figure 10.16: Steady-state flow past a rectangular step for a 50% slip boundary. The lee face is 400m long and speeds in the entrance are 0.62 $m.s^{-1}$. Other parameters are: depth, 5m; Chezy's C, 60 $m^{\frac{1}{2}}.s^{-1}$; A_H, 5 $m^2.s^{-1}$; and a tide level difference at the open boundaries of 0.02m.

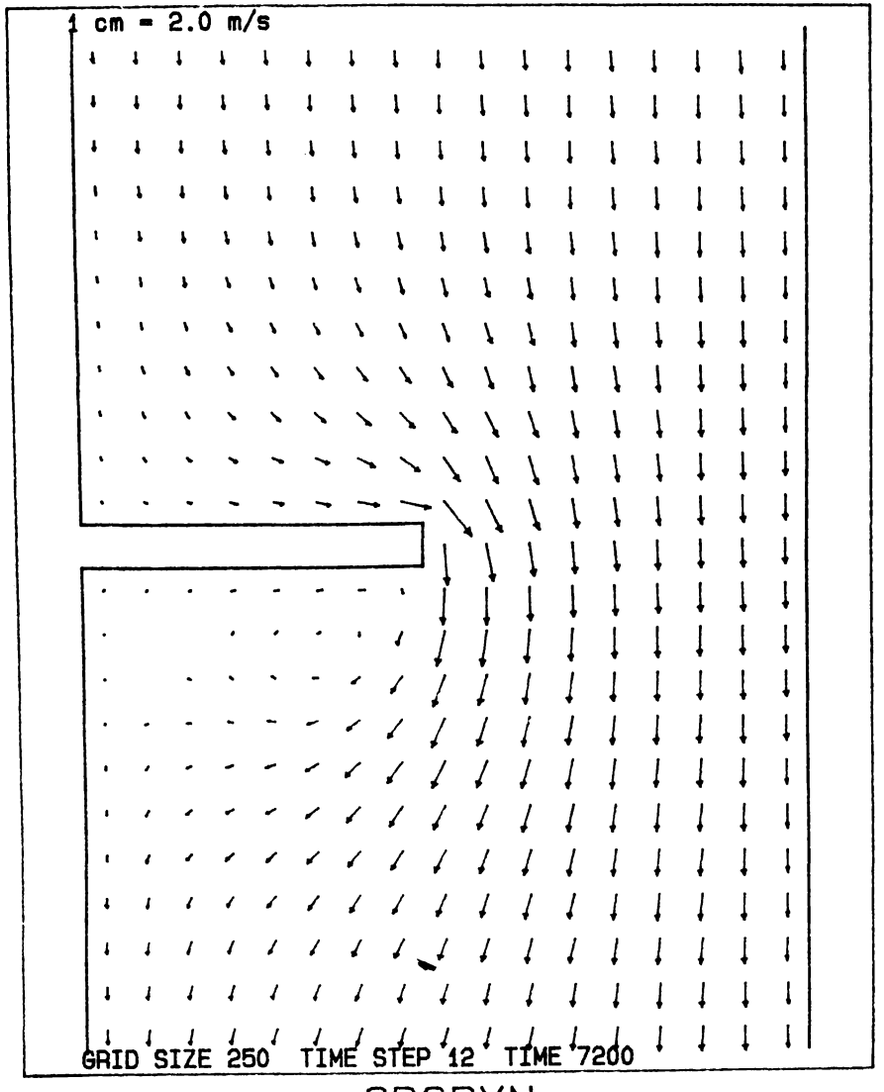

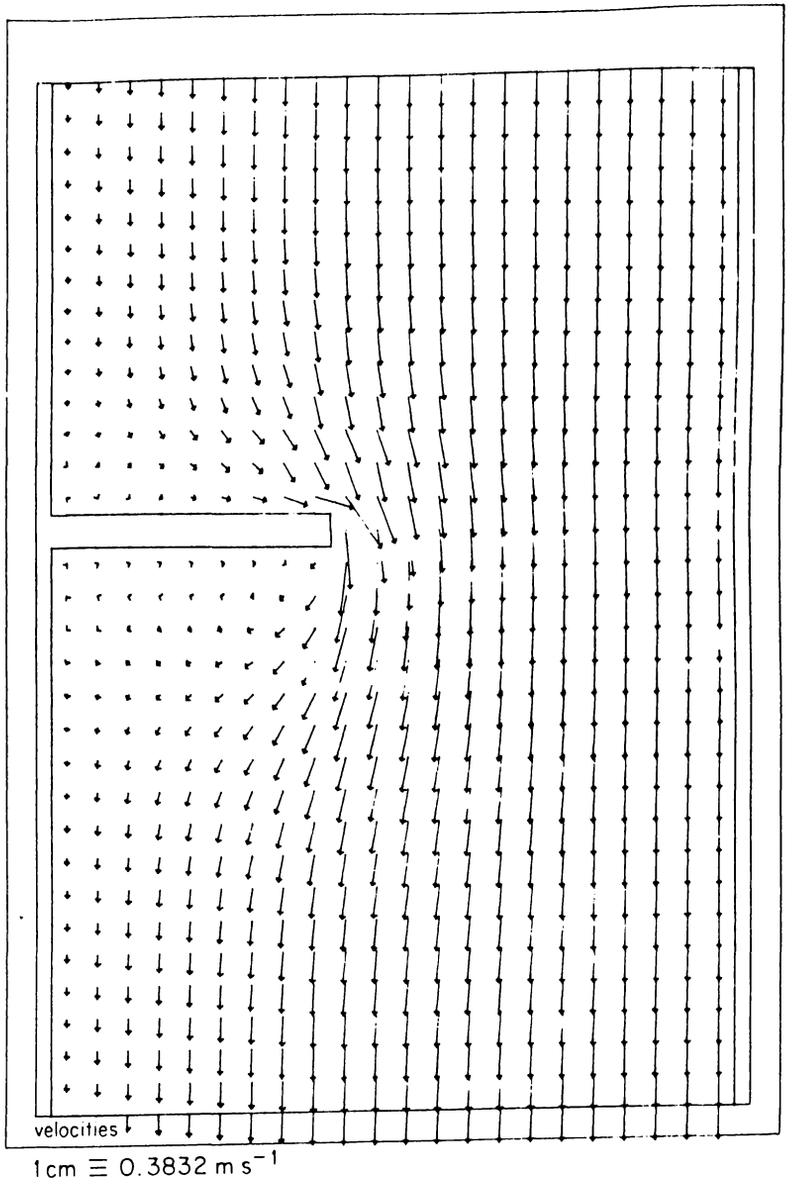

Figure 10.17: Steady-state flow around a groyne showing flow convergence at its toe and recirculation behind the structure. S21 (right) shows similar behaviour. The groyne is 2000m long and peak speeds are 1.1 $m.s^{-1}$. Other parameters are: depth 5m; Chezy's C, 60 $m^{\frac{1}{2}}.s^{-1}$; $A_H = 5\ m^2.s^{-1}$; and a tide level difference at the open boundaries of 0.10m.

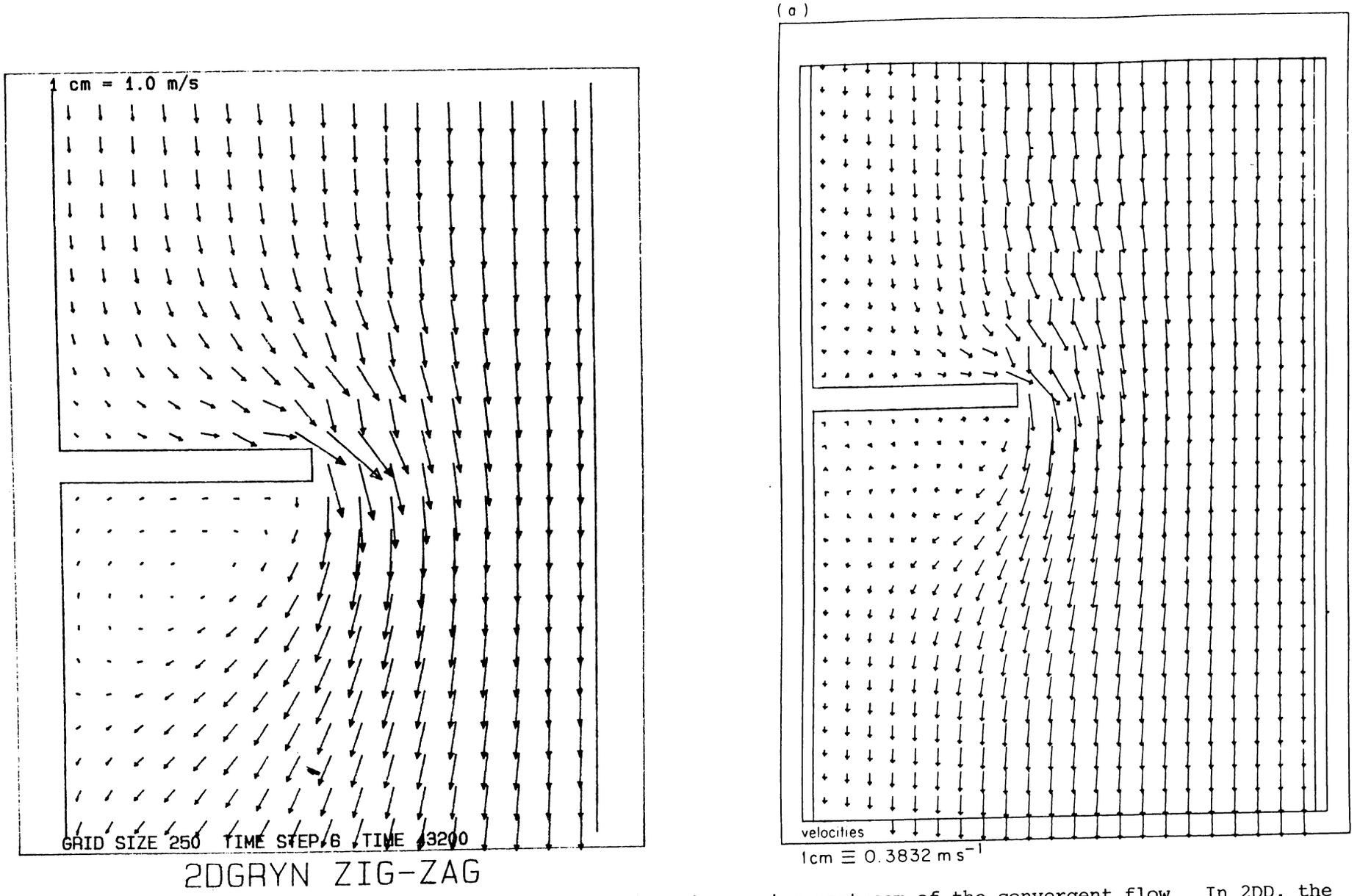

Figure 10.18: Steady-state flow around a groyne showing zig-zagging upstream of the convergent flow. In 2DD, the convective momenta terms were centred at the land/sea boundaries. In S21, (right) Abbott (1979) assigns the fault to "a second-order-accurate convective momentum approximation". Other parameters in the 2DD simulation are: depth, 5m; Chezy's C, 60 $m^{\frac{1}{2}}.s^{-1}$; $A_H = 5\ m^2.s^{-1}$; and a tide level difference at the open boundaries of 0.10m.

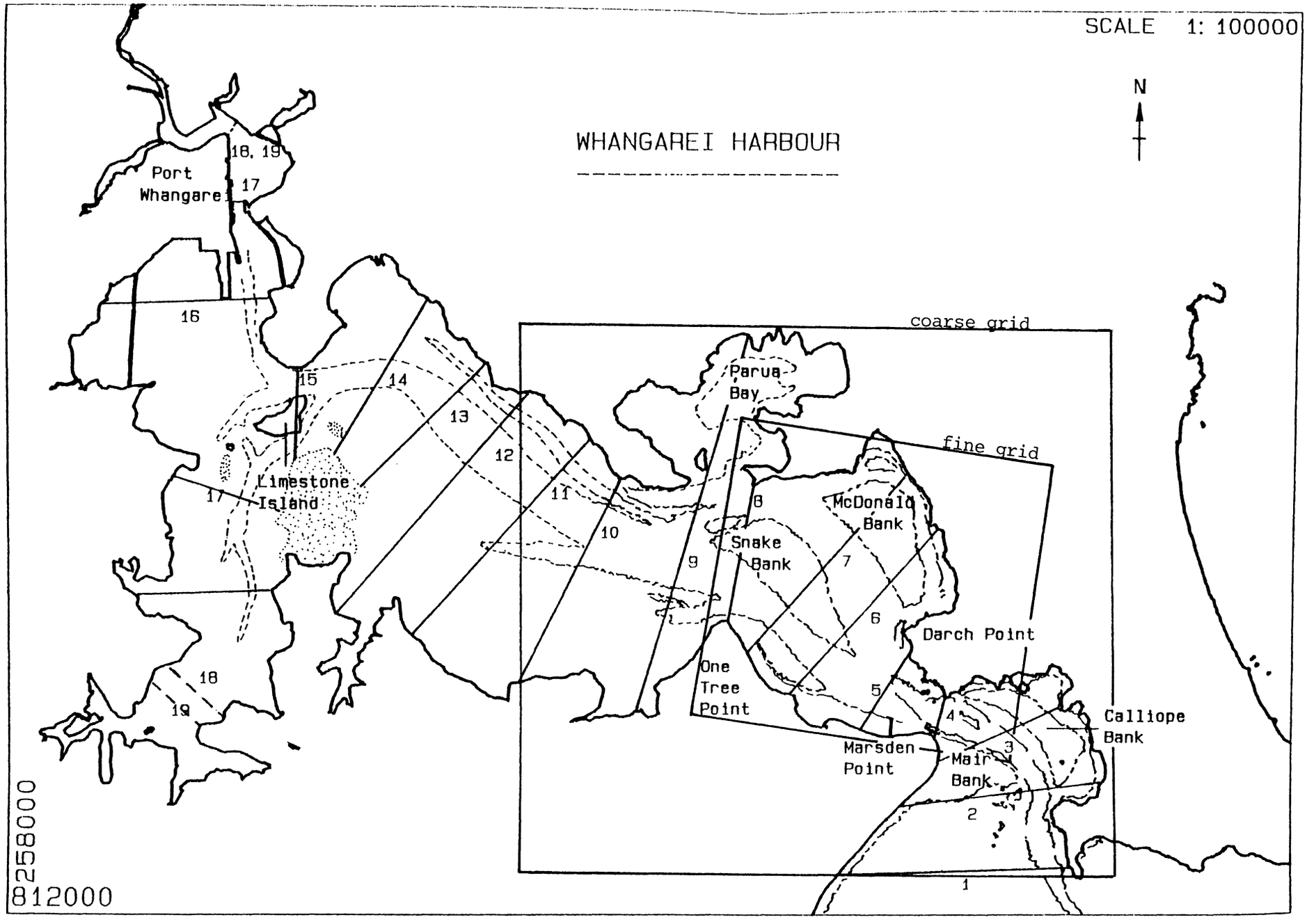

Figure 10.19: Whangarei Harbour showing the locations of the fine and coarse grids for the 2-dimensional, numerical model with the locations of the schematised cross-sections for the 1-dimensional model simulation.

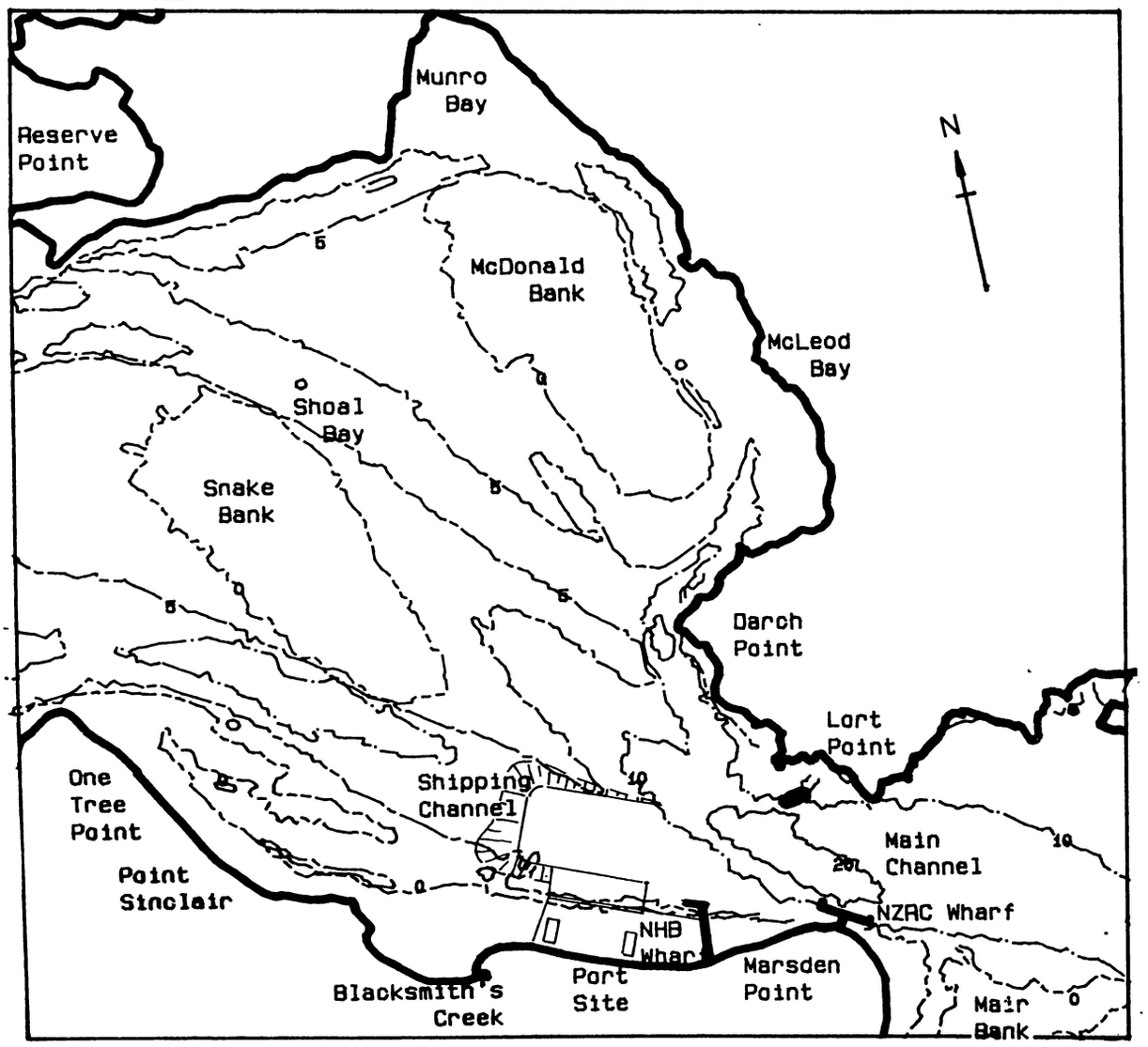

Figure 10.20: Bathymetry (NZ5213, 1981) for the fine grid model region at 1:40,000. The proposed port is shown with the present isobaths.

Figure 10.20: Bathymetry overlay

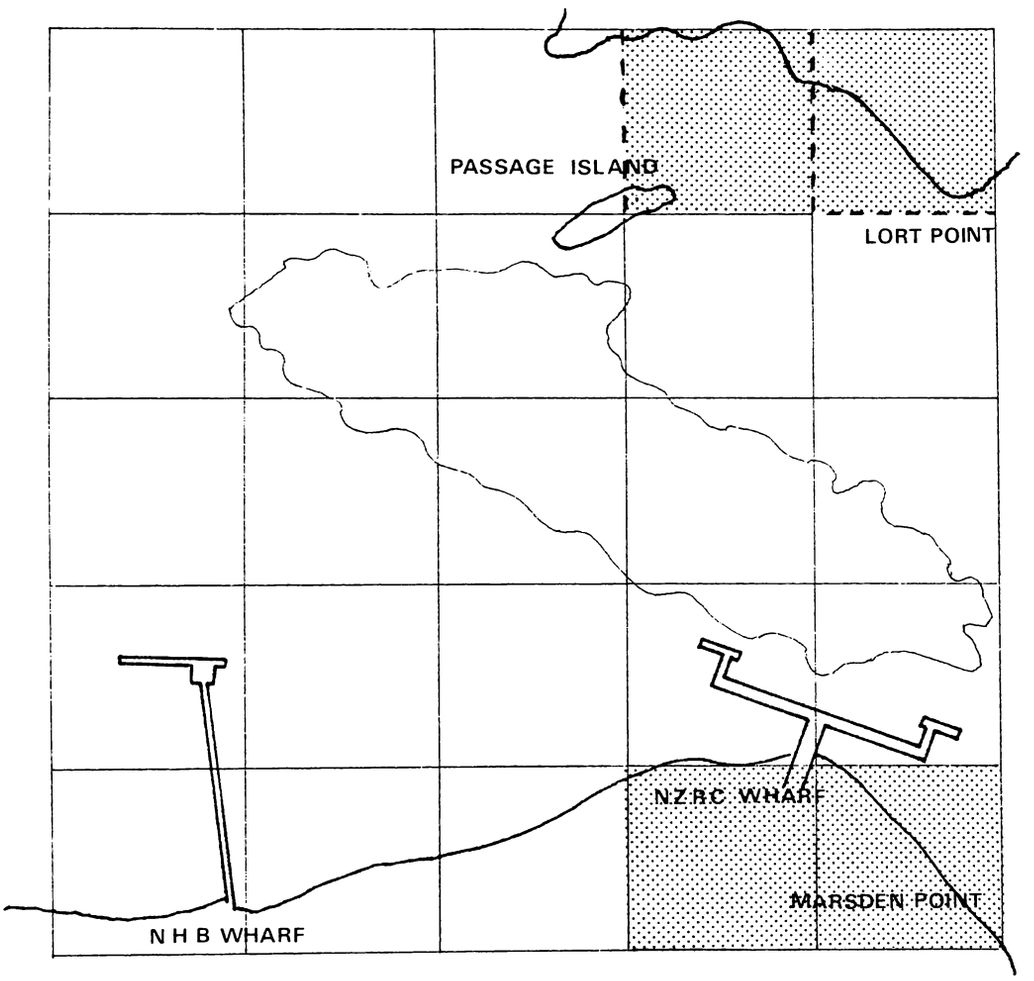

Figure 10.21: The entrance throat to Whangarei Harbour with the fine grid superimposed. Passage Island could be represented by either opening or closing the dashed sides of the adjacent shaded cells. Better representation was obtained with the cells closed.

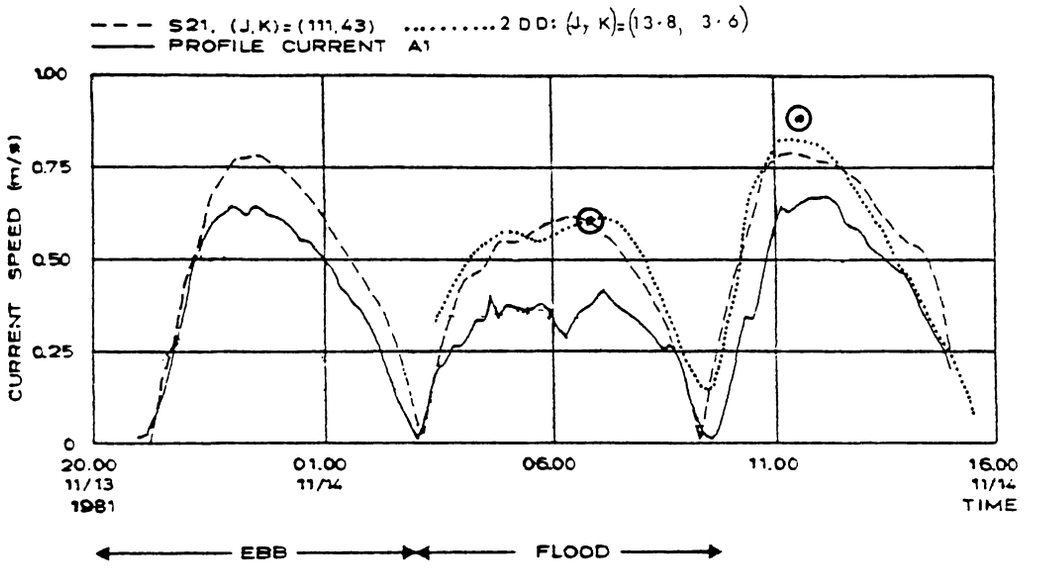

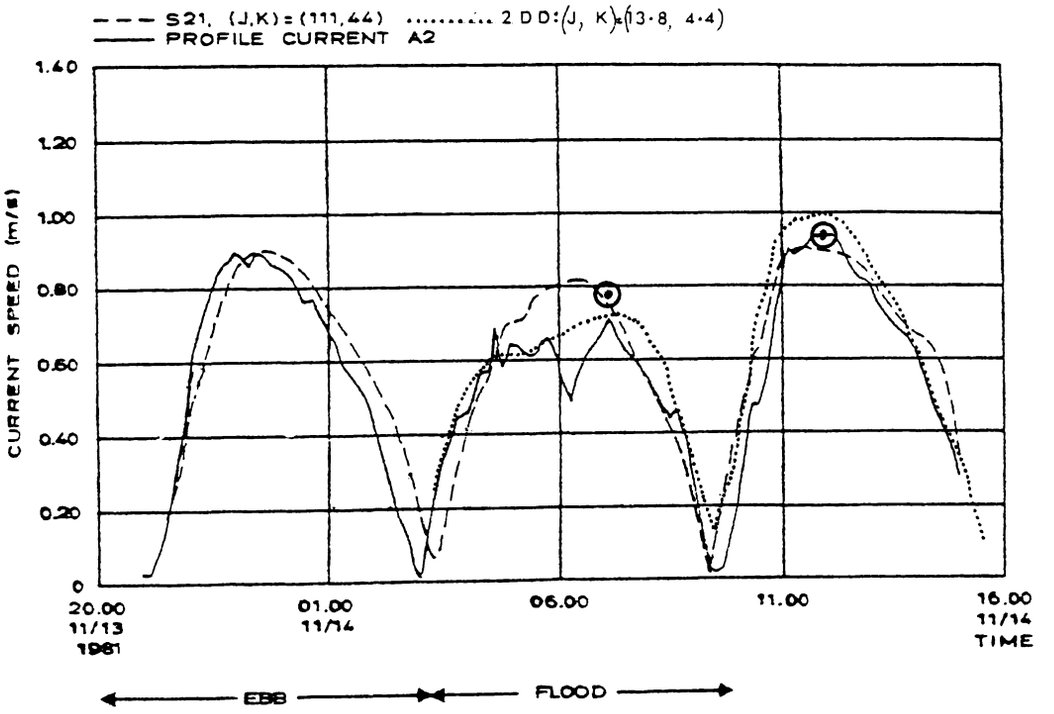

Figures 10.22 (1) and (2): Comparison of scaled measured velocities with those computed by 2DD and S21 (150m-grid) for the calibration period on 14-Nov-81. The maximum velocities attained at the vertical profile measurement sites scaled according to tidal range are shown.

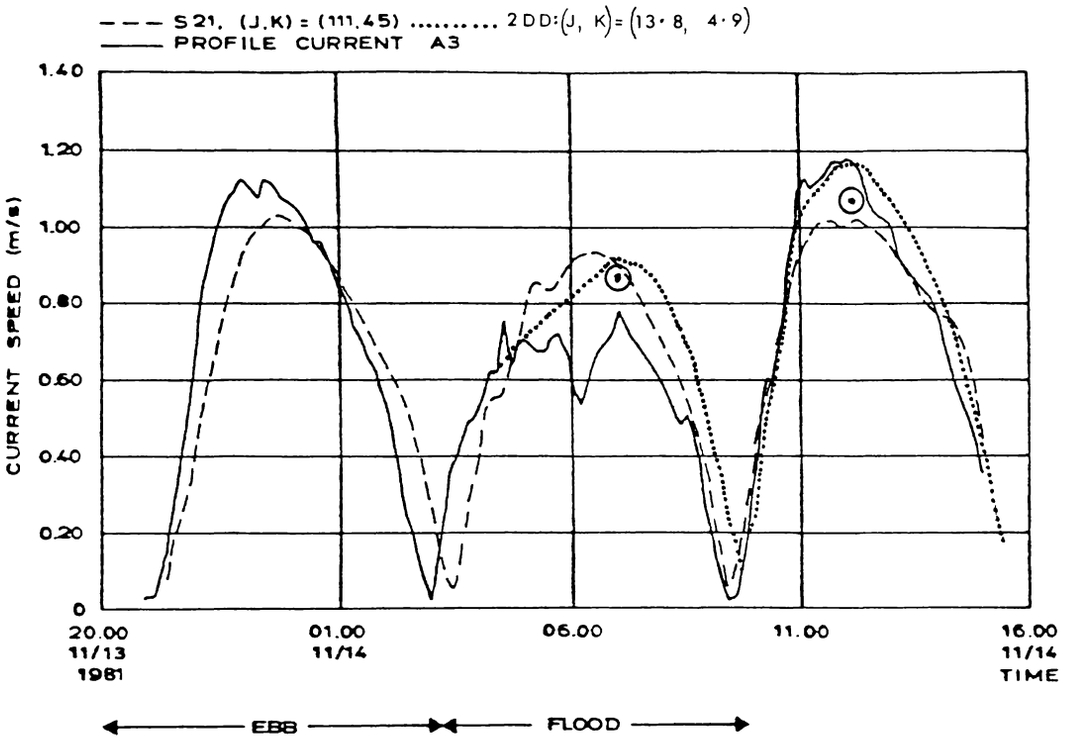

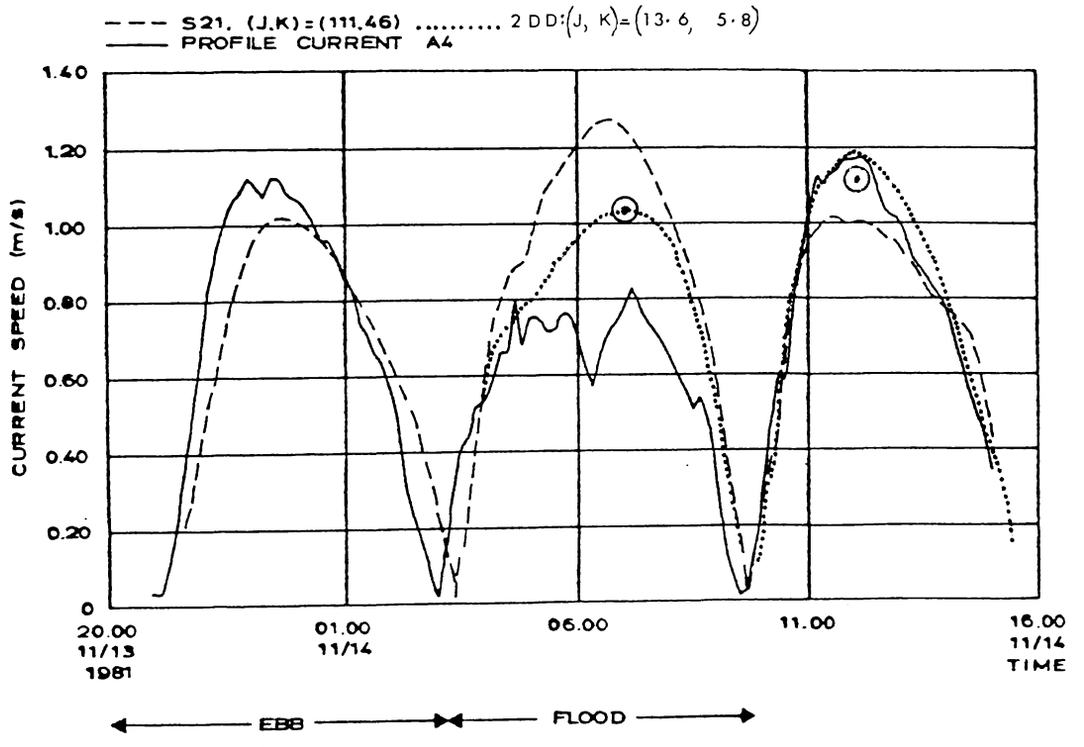

Figures 10.22 (3) and (4): Comparison of scaled measured velocities with those computed by 2DD and S21 (150m - grid) for the calibration period on 14-Nov-81. The maximum velocities attained at the vertical profile measurement sites scaled according to tidal range are shown.

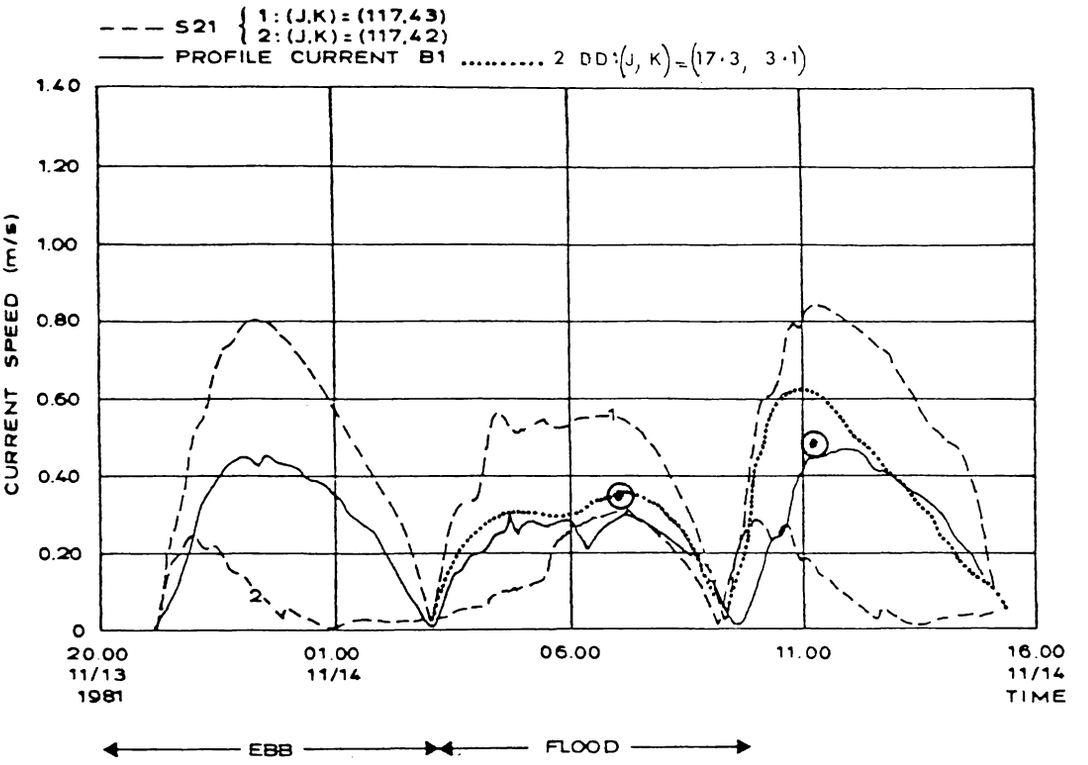

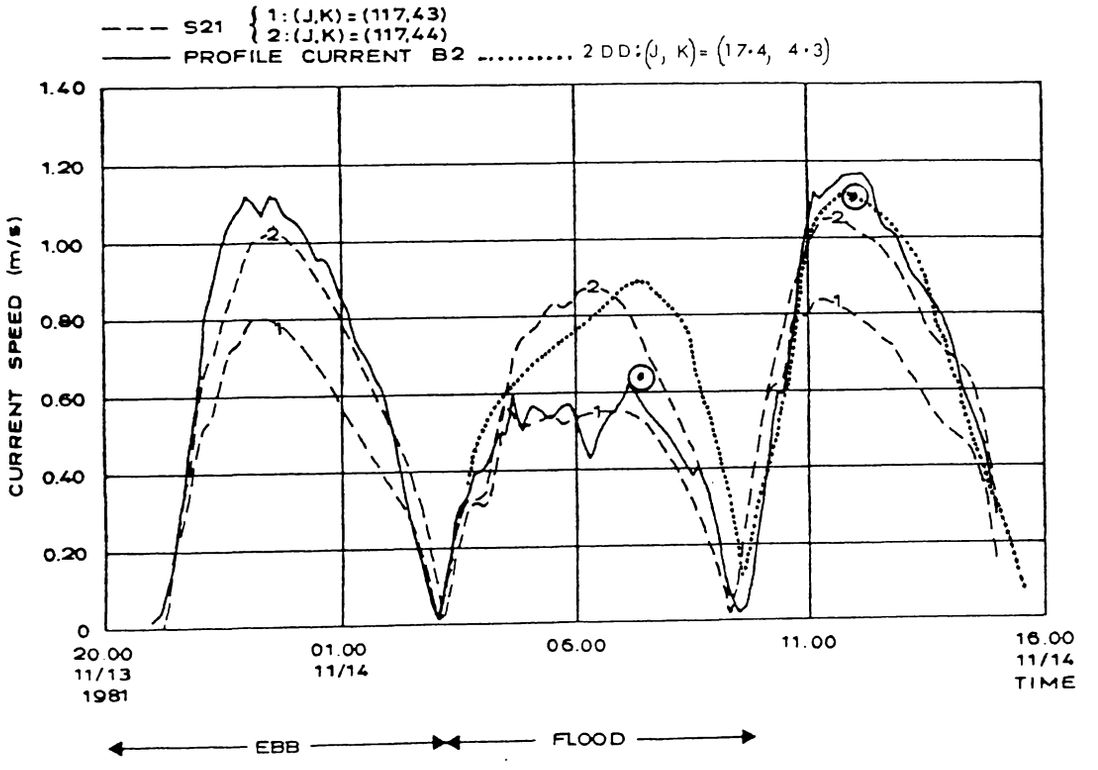

Figures 10.23 (1) and (2): Comparison of scaled measured velocities with those computed by 2DD and S21 (150m - grid) for the calibration period on 14-Nov-81. The maximum velocities attained at the vertical profile measurement sites scaled according to tidal range are shown.

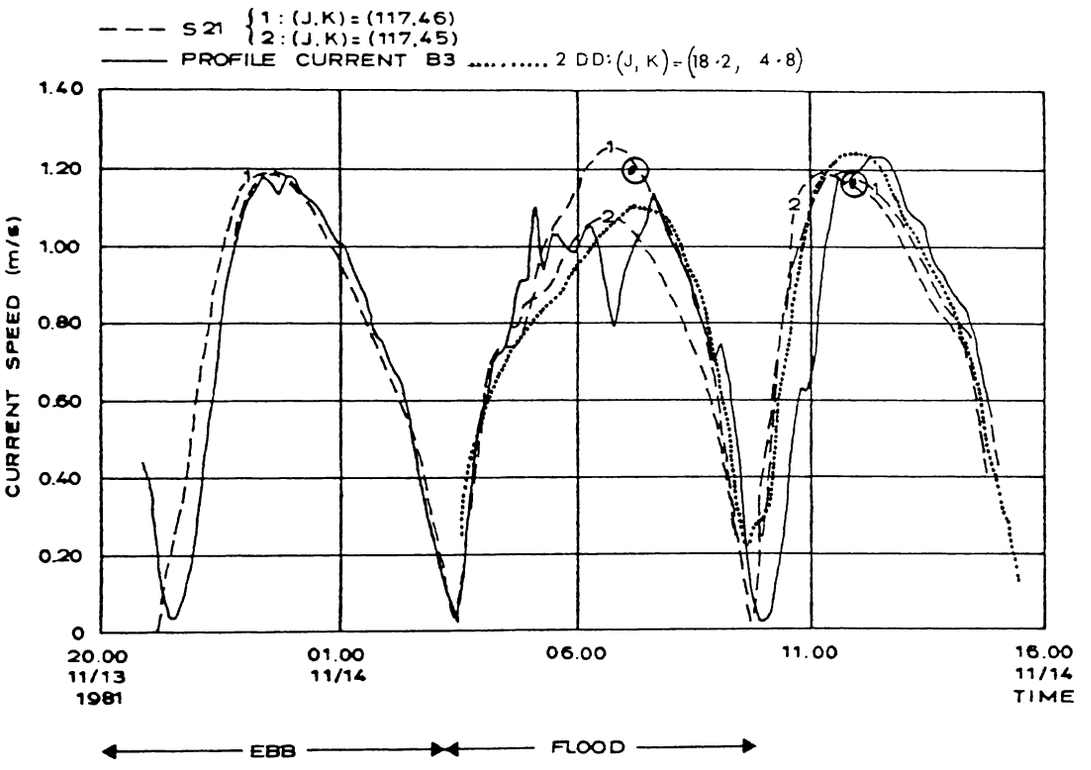

Figure 10.23 (3): Comparison of scaled measured velocities with those computed by 2DD and S21 (150m - grid) for the calibration period on 14-Nov-81. The maximum velocities attained at the vertical profile measurement sites scaled according to tidal range are shown.

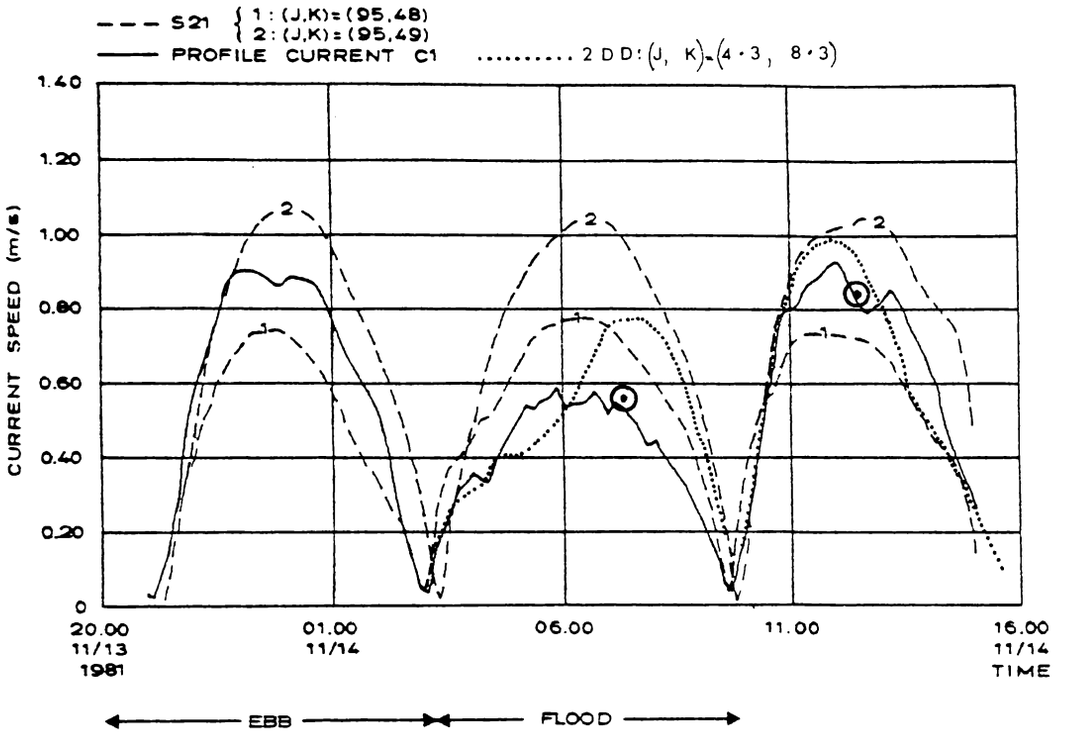

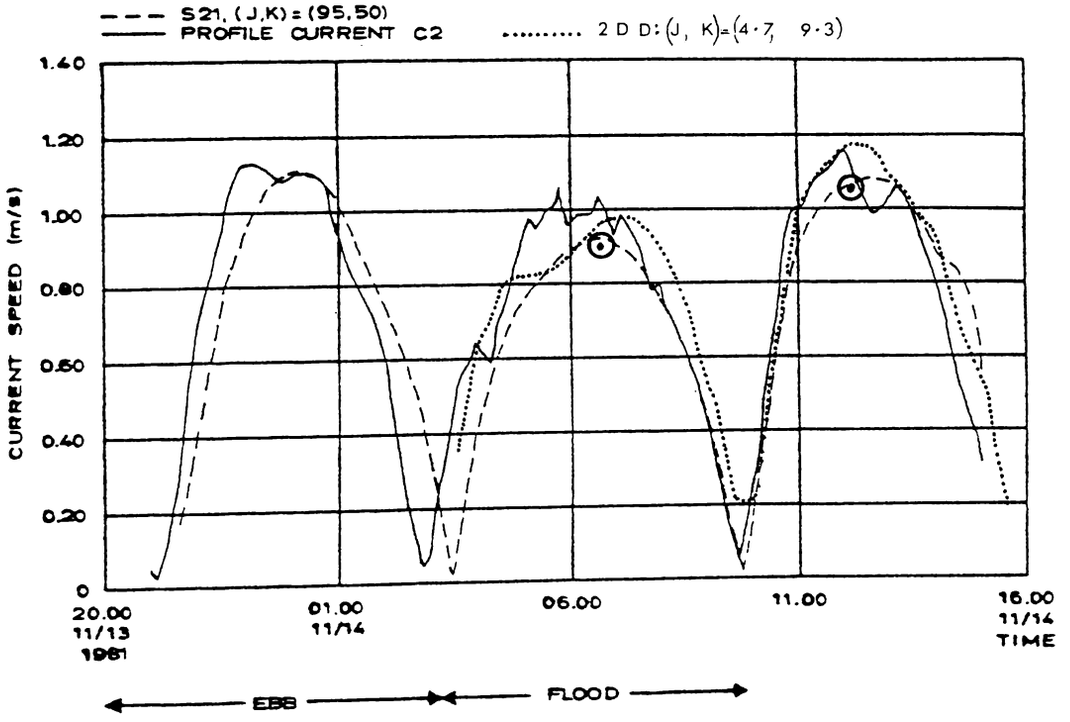

Figures 10.24 (1) and (2): Comparison of scaled measured velocities with those computed by 2DD and S21 (150m - grid) for the calibration period on 14-Nov-81. The maximum velocities attained at the vertical profile measurement sites scaled according to tidal range are shown.

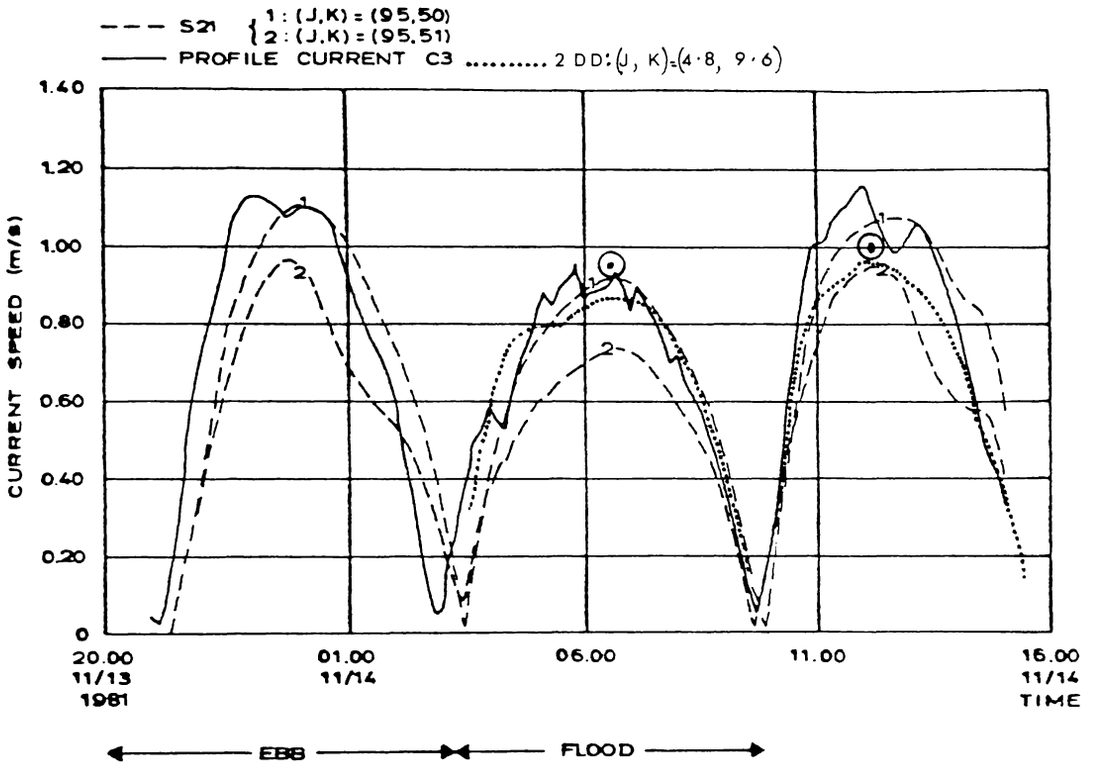

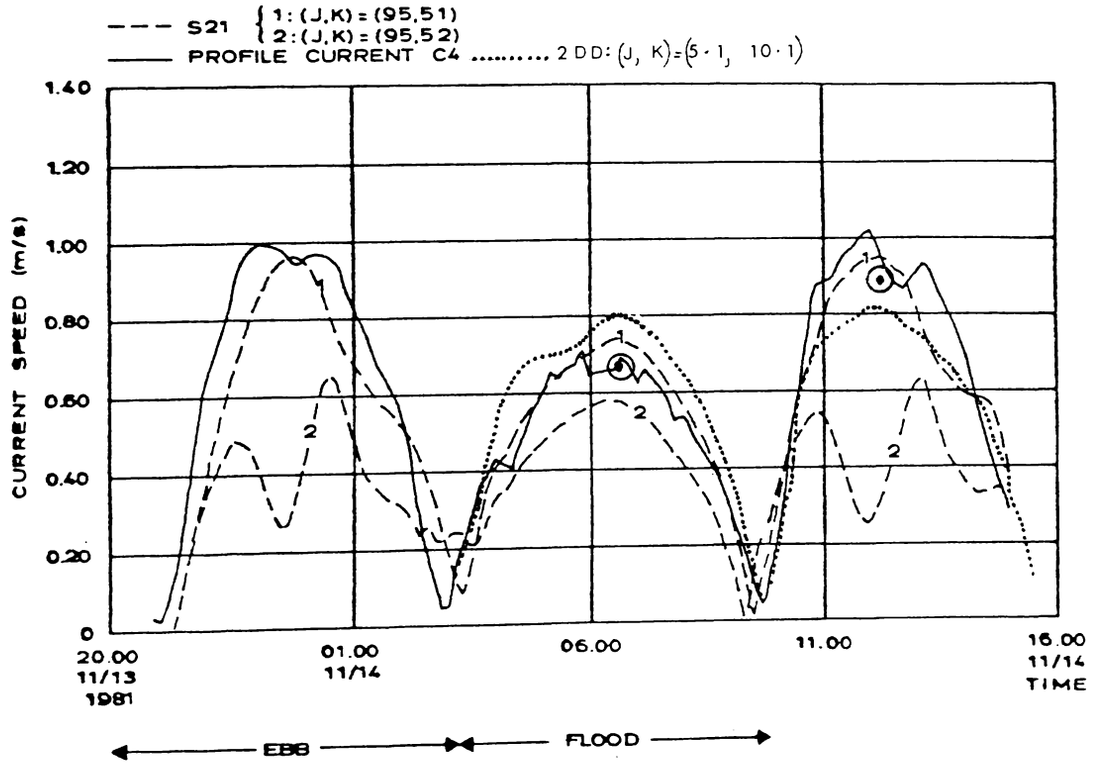

Figures 10.24 (3) and (4): Comparison of scaled measured velocities with those computed by 2DD and S21 (150m - grid) for the calibration period on 14-Nov-81. The maximum velocities attained at the vertical profile measurement sites scaled according to tidal range are shown.

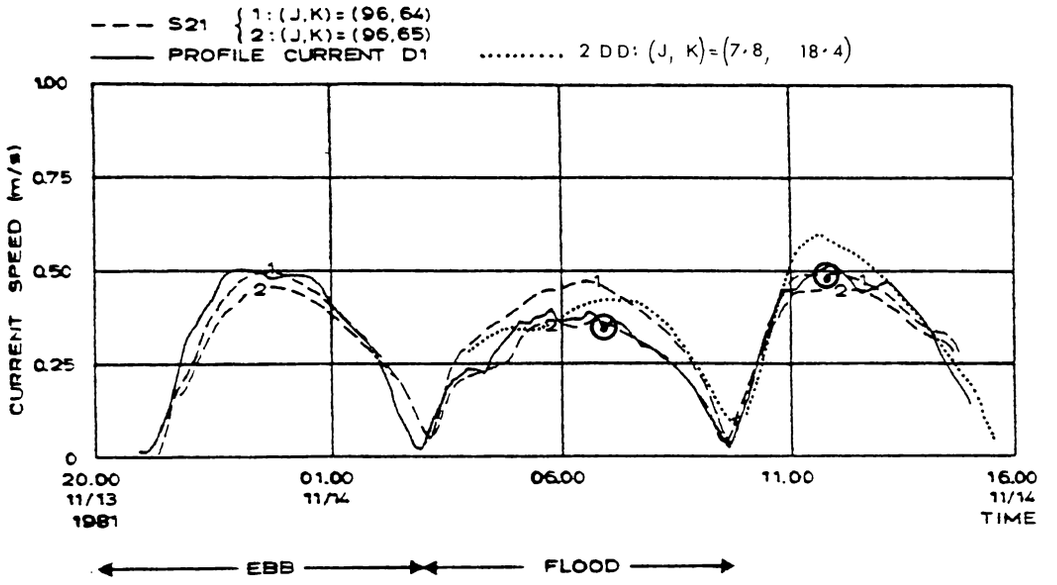

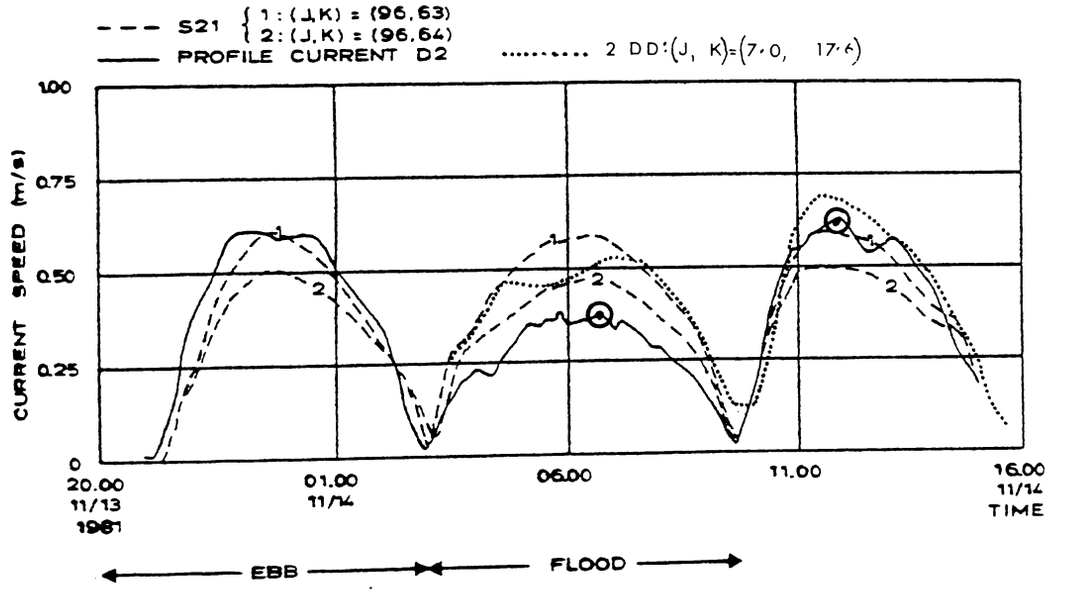

Figures 10.25 (1) and (2): Comparison of scaled measured velocities with those computed by 2DD and S21 (150m - grid) for the calibration period on 14-Nov-81. The maximum velocities attained at the vertical profile measurement sites scaled according to tidal range are shown.

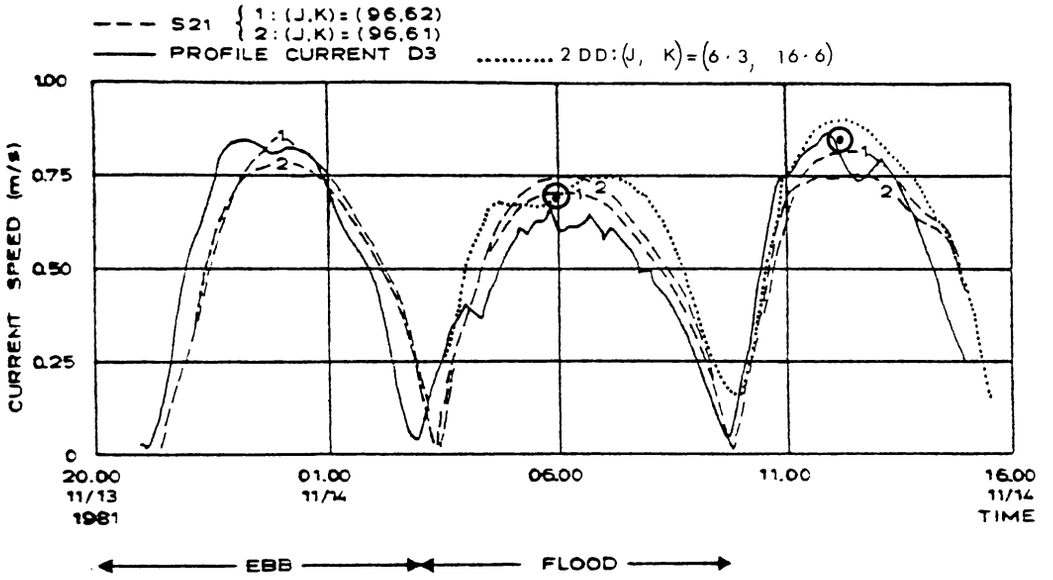

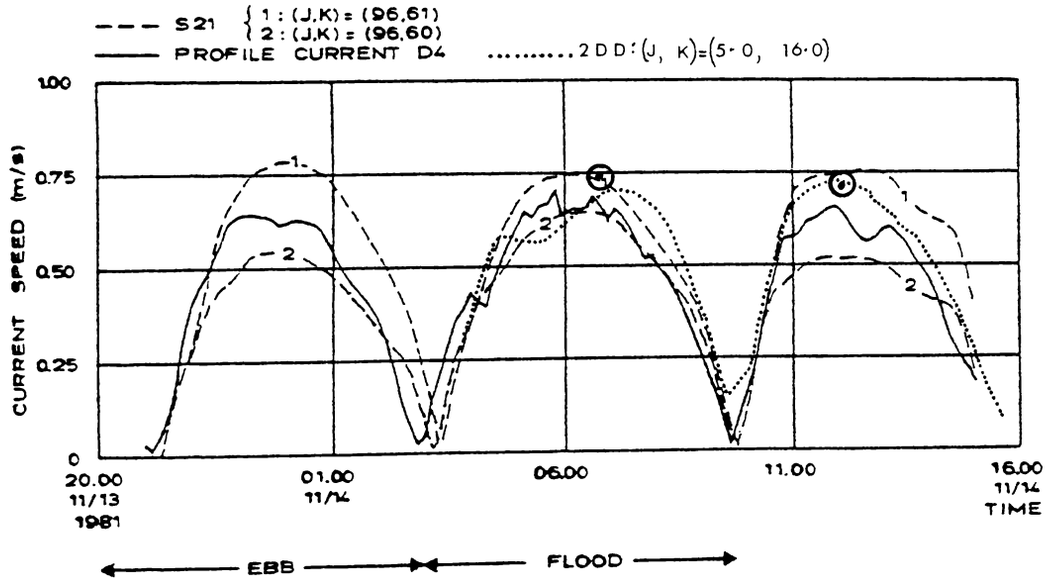

Figure 10.25 (3) and (4): Comparison of scaled measured velocities with those computed by 2DD and S21 (150m - grid) for the calibration period on 14-Nov-81. The maximum velocities attained at the vertical profile measurement sites scaled according to tidal range are shown.

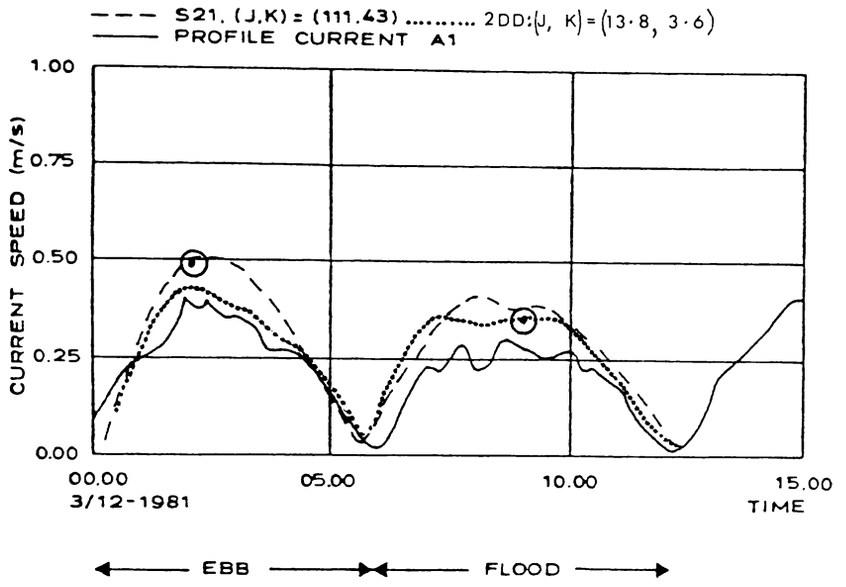

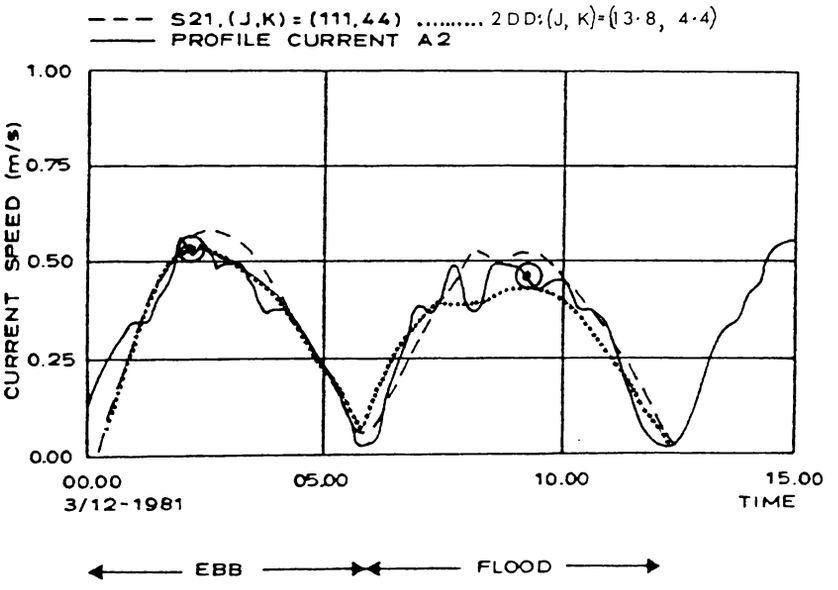

Figures 10.26(1) and (2): Comparison of scaled measured velocities with those computed by 2DD and S21 (150m - grid) for the verification period on 3-Dec-81. The maximum velocities attained at the vertical profile measurement sites scaled according to tidal range are shown.

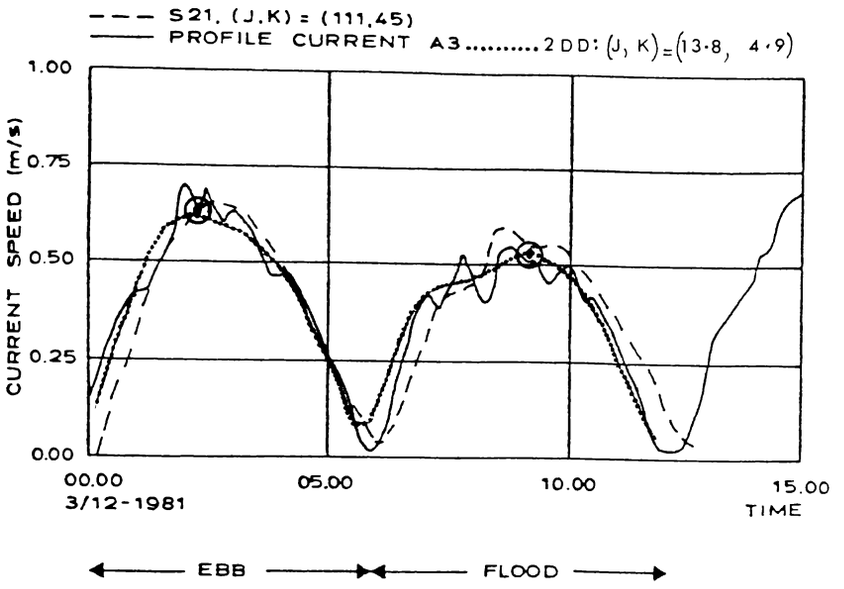

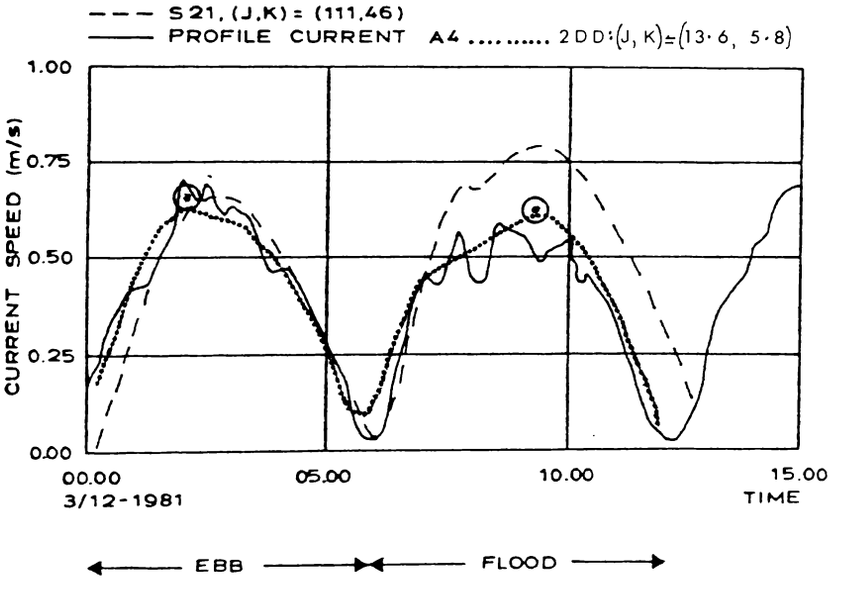

Figures 10.26 (3) and (4): Comparison of scaled measured velocities with those computed by 2DD and S21 (150m - grid) for the verification period on 3-Dec-81. The maximum velocities attained at the vertical profile measurement sites scaled according to tidal range are shown.

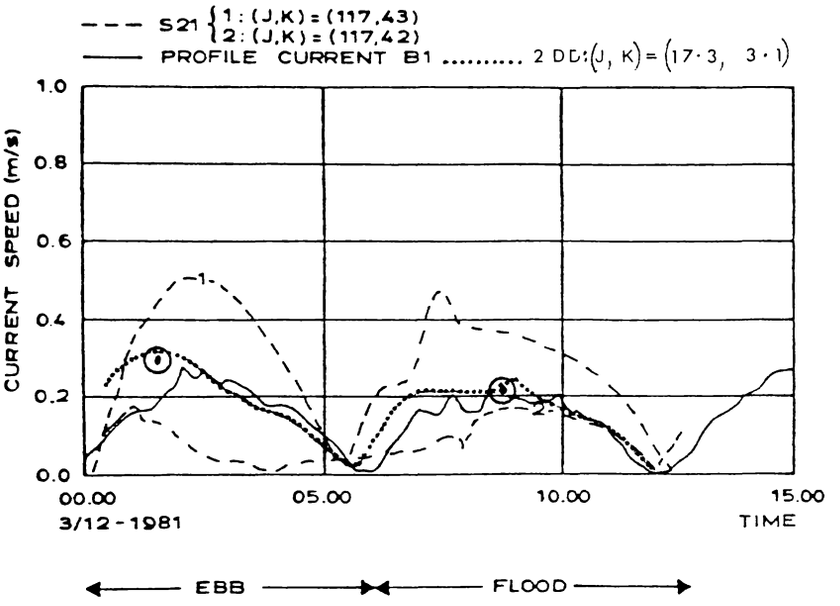

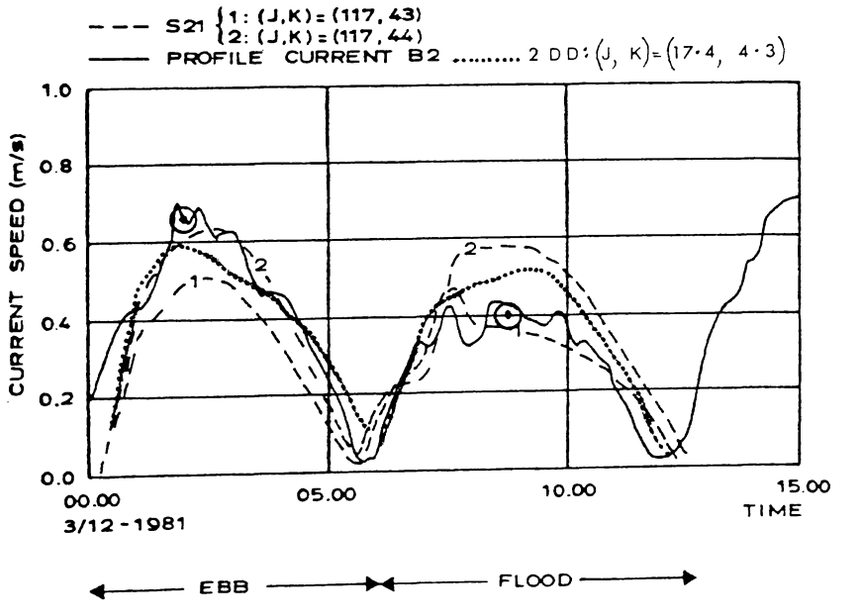

Figures 10.27(1) and (2): Comparison of scaled measured velocities with those computed by 2DD and S21 (150m - grid) for the verification period on 3-Dec-81. The maximum velocities attained at the vertical profile measurement sites scaled according to tidal range are shown.

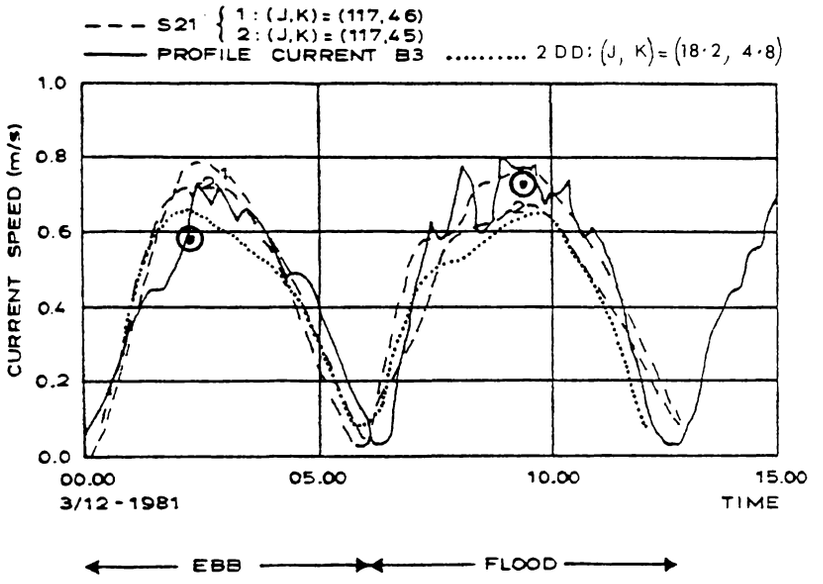

Figure 10.27 (3): Comparison of scaled measured velocities with those computed by 2DD and S21 (150m - grid) for the verification period on 3-Dec-81. The maximum velocities attained at the vertical profile measurement sites scaled according to tidal range are shown.

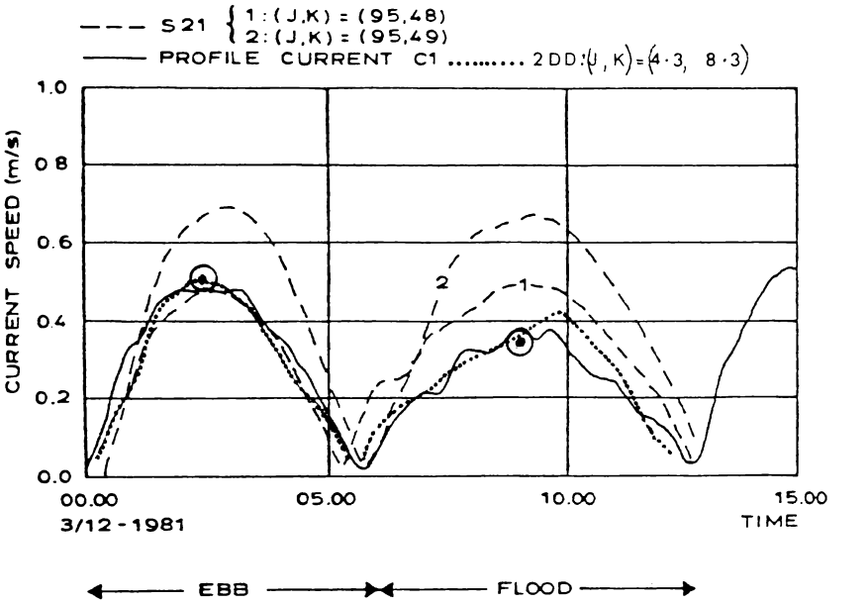

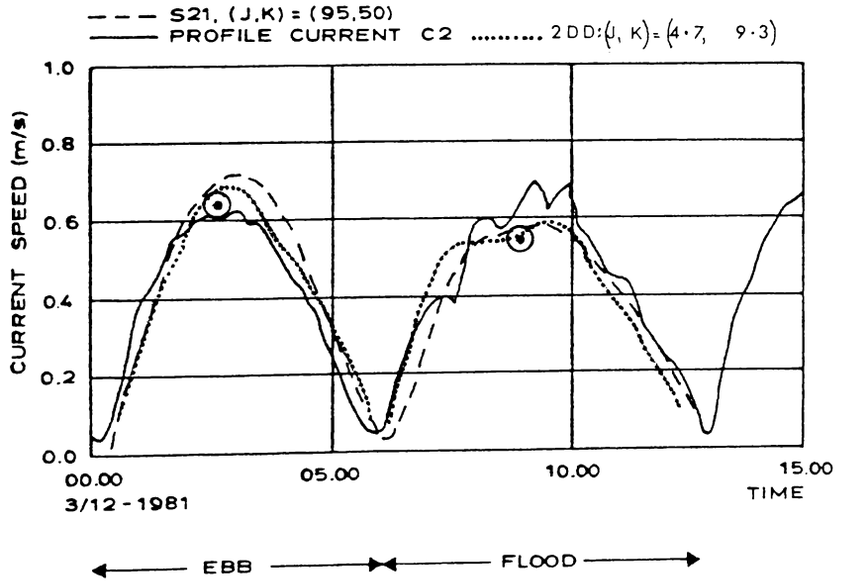

Figures 10.28 (1) and (2): Comparison of scaled measured velocities with those computed by 2DD and S21 (150m - grid) for the verification period on 3-Dec-81. The maximum velocities attained at the vertical profile measurement sites scaled according to tidal range are shown.

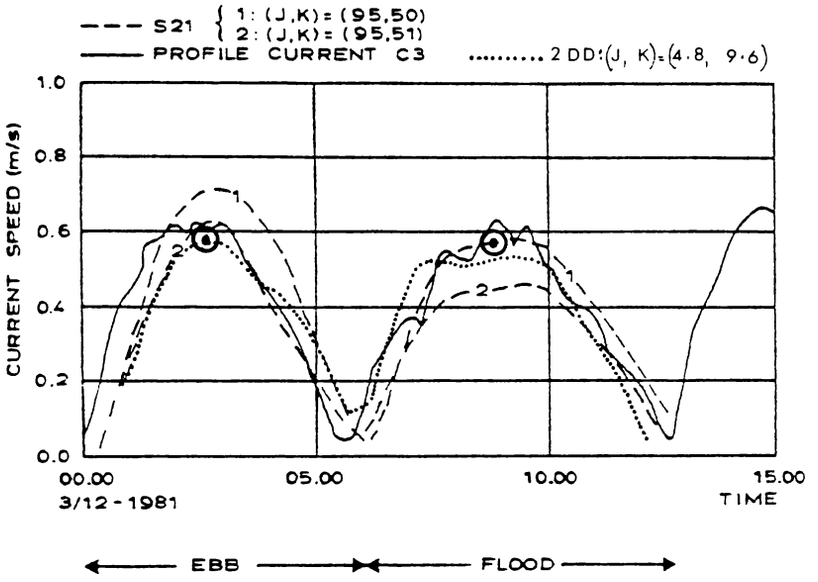

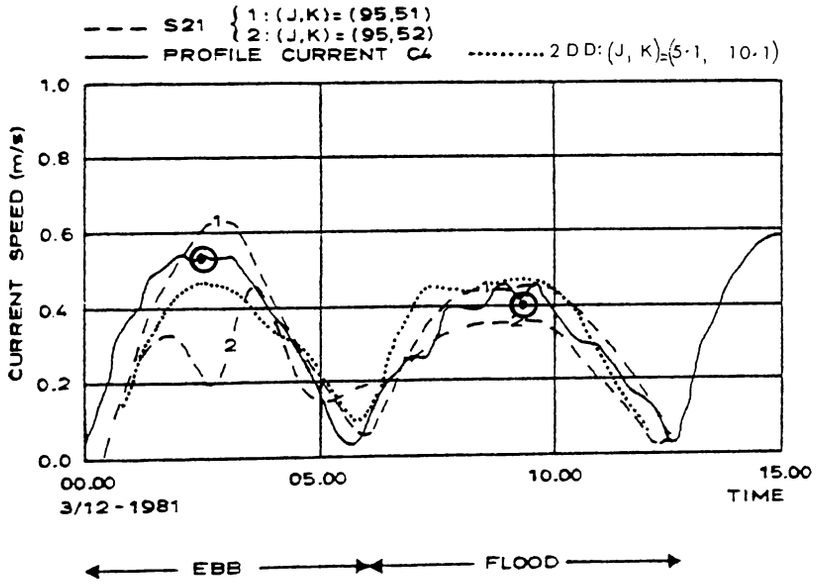

Figures 10.28 (3) and (4): Comparison of scaled measured velocities with those computed by 2DD and S21 (150m - grid) for the verification period on 3-Dec-81. The maximum velocities attained at the vertical profile measurement sites scaled according to tidal range are shown.

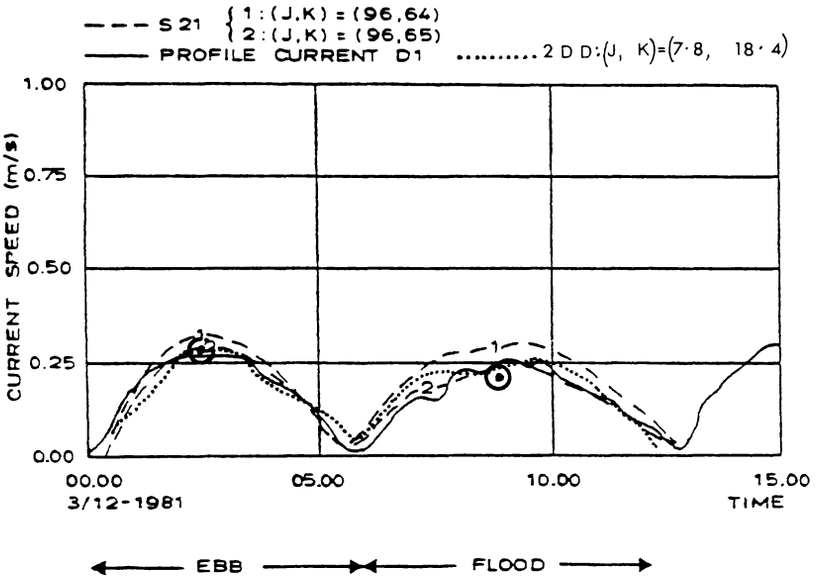

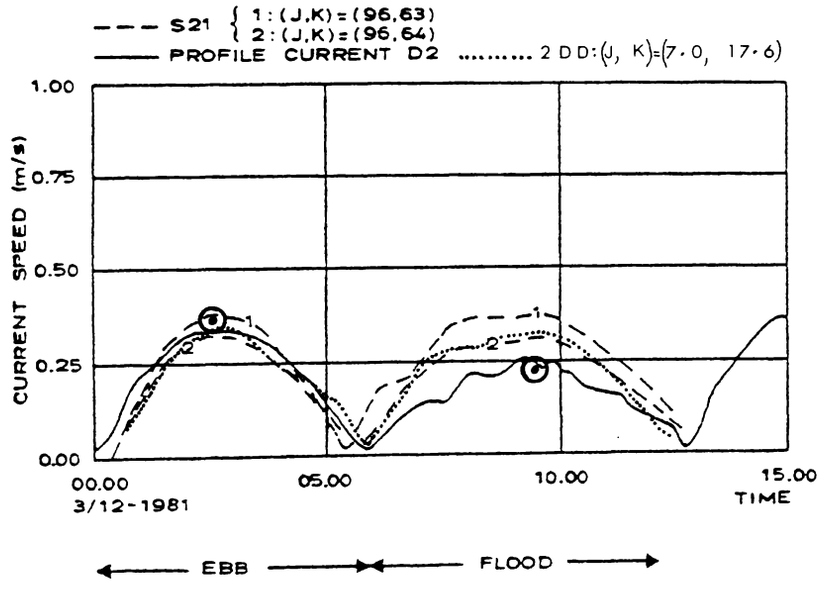

Figures 10.29 (1) and (2): Comparison of scaled measured velocities with those computed by 2DD and S21 (150m - grid) for the verification period on 3-Dec-81. The maximum velocities attained at the vertical profile measurement sites scaled according to tidal range are shown.

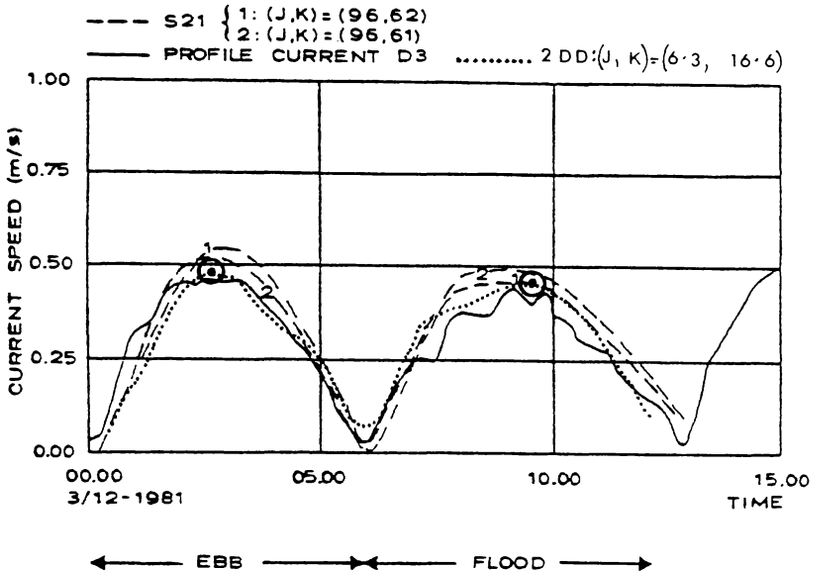

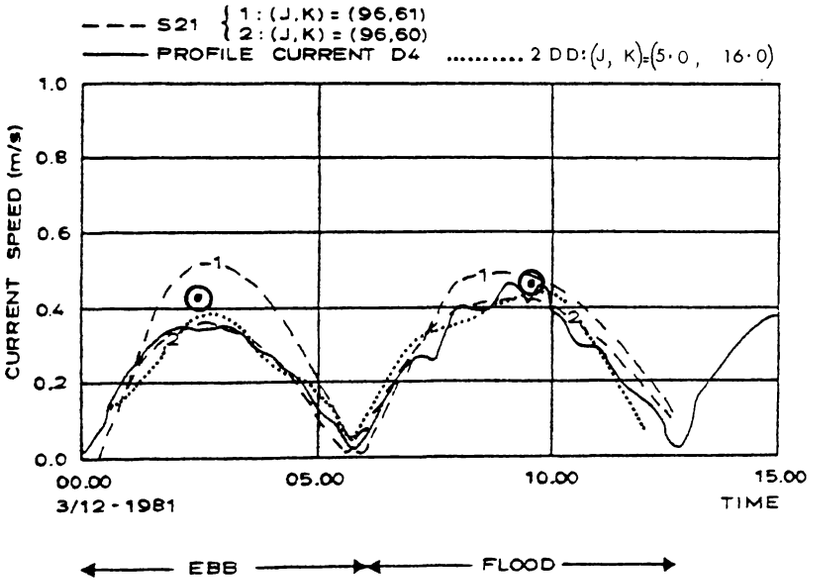

Figures 10.29 (3) and (4): Comparison of scaled measured velocities with those computed by 2DD and S21 (150m - grid) for the verification period on 3-Dec-81. The maximum velocities attained at the vertical profile measurement sites scaled according to tidal range are shown.

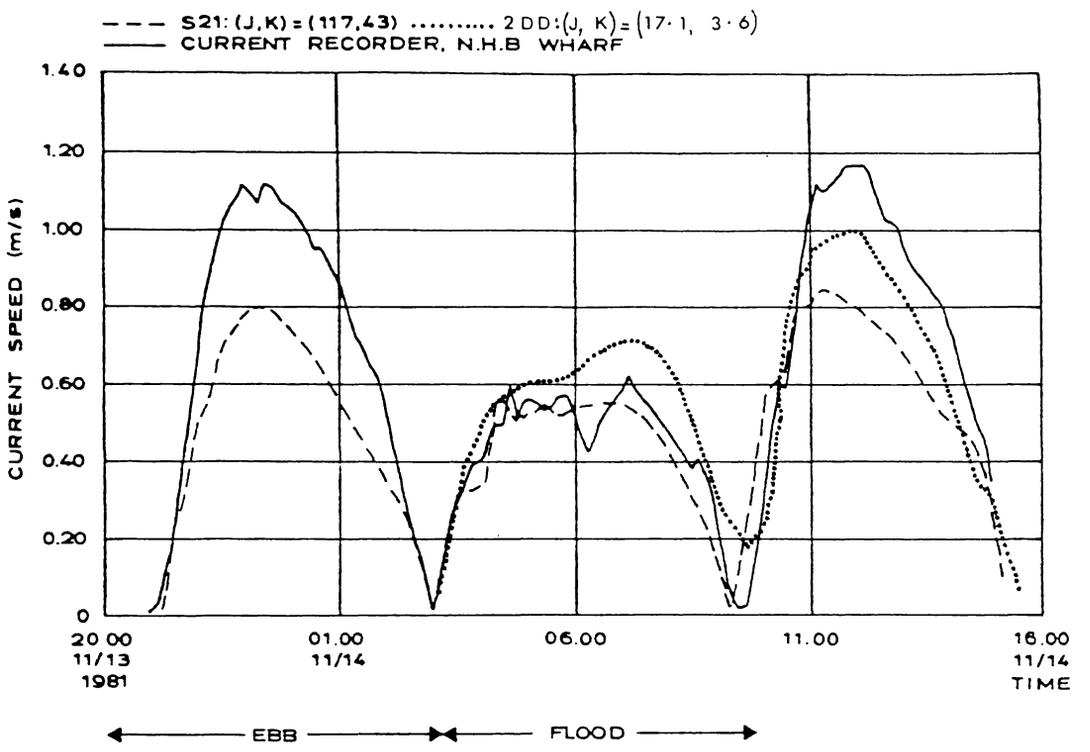

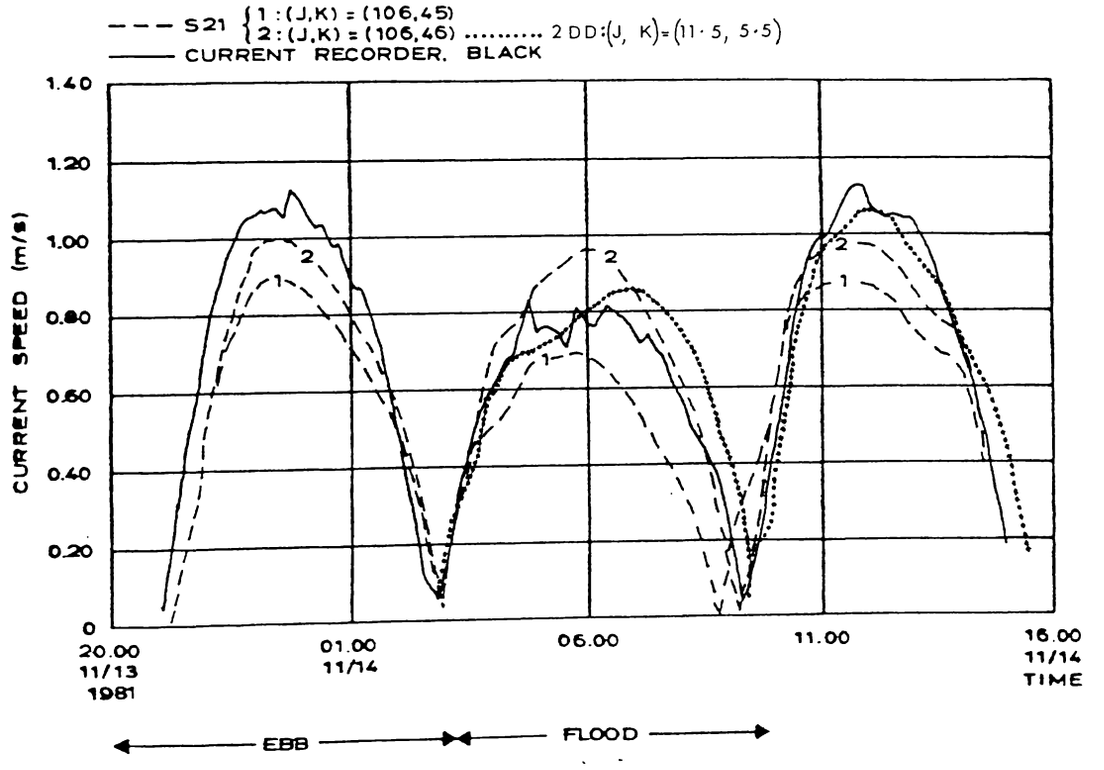

Figure 10.30: Comparison of velocities measured by an Aanderaa continuous-recording meter with those computed by 2DD and S21 (150m - grid) for the calibration period on 14-Nov-81.

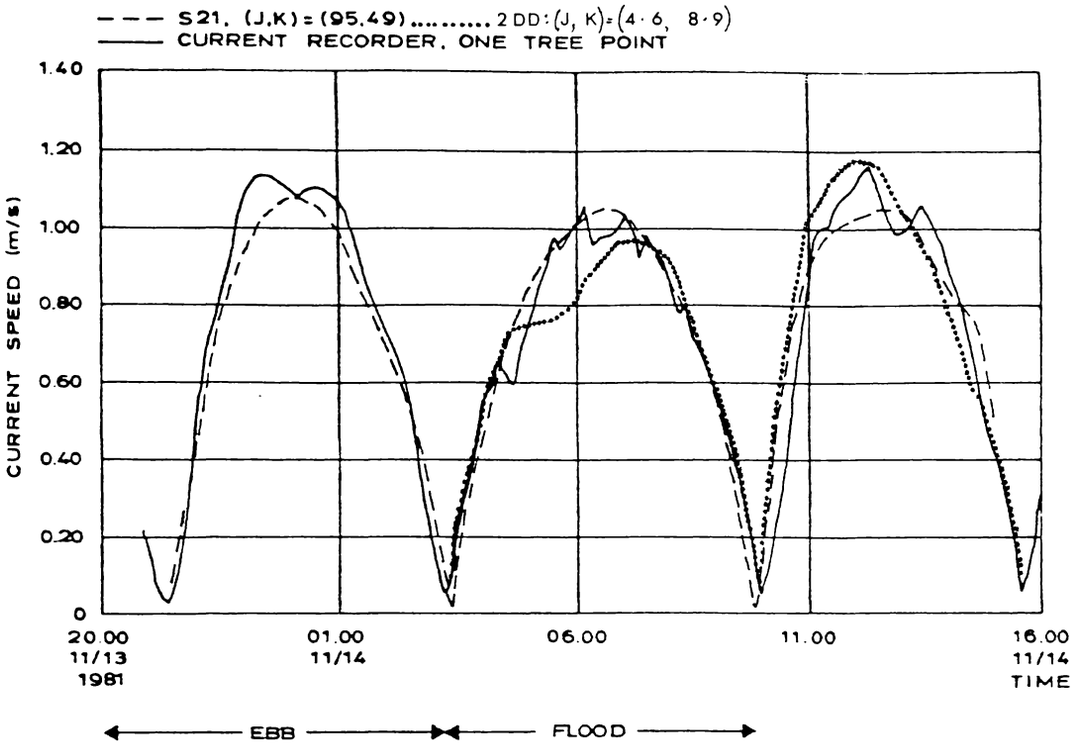

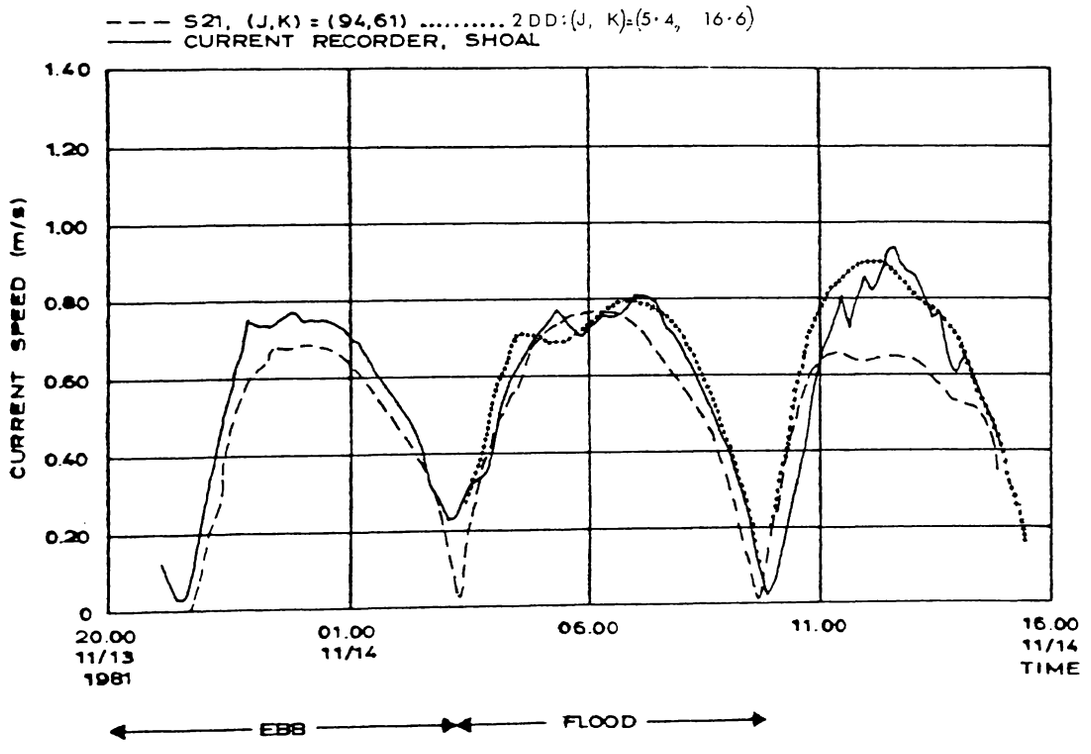

Figure 10.31: Comparison of velocities measured by an Aanderaa continuous-recording meter with those computed by 2DD and S21 (150m - grid) for the calibration period on 14-Nov-81.

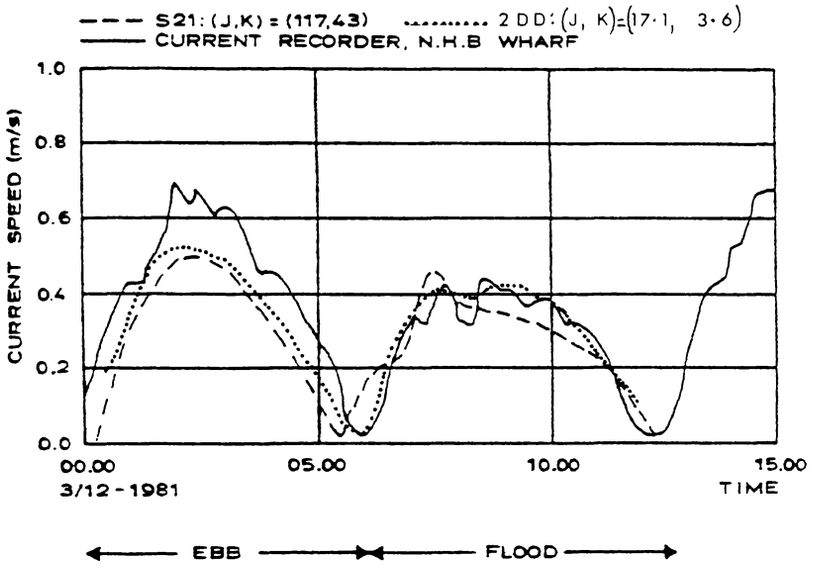

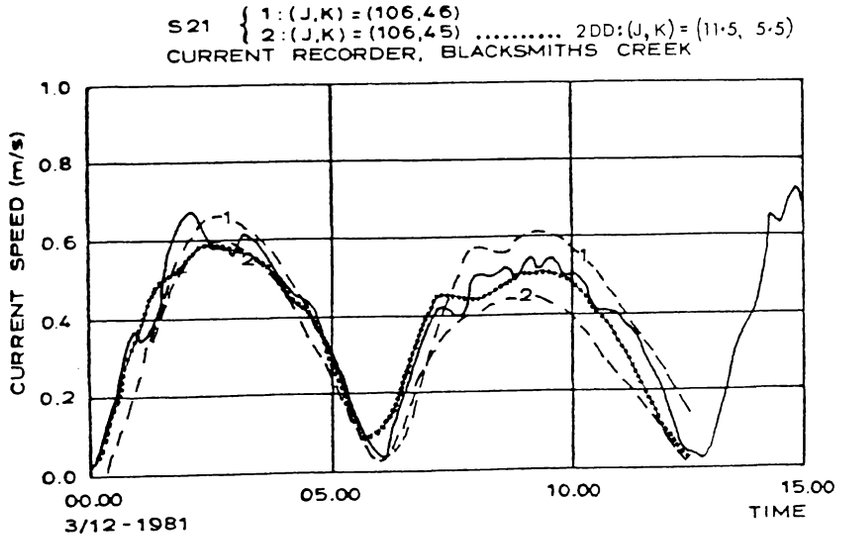

Figure 10.32: Comparison of velocities measured by an Aanderaa continuous-recording meter with those computed by 2DD and S21 (150m - grid) for the verification period on 3-Dec-81.

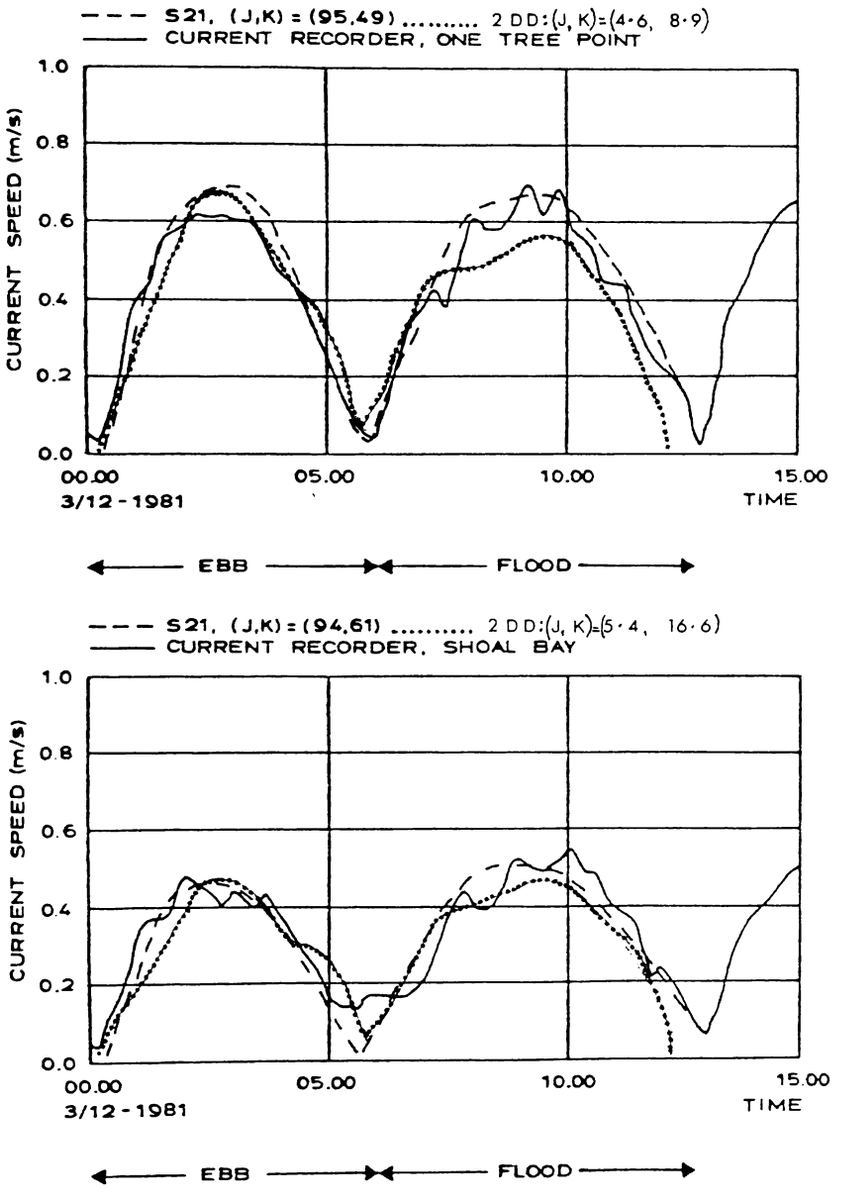

Figure 10.33: Comparison of velocities measured by an Aanderaa continuous-recording meter with those computed by 2DD and S21 (150m - grid) for the verification period on 3-Dec-81.

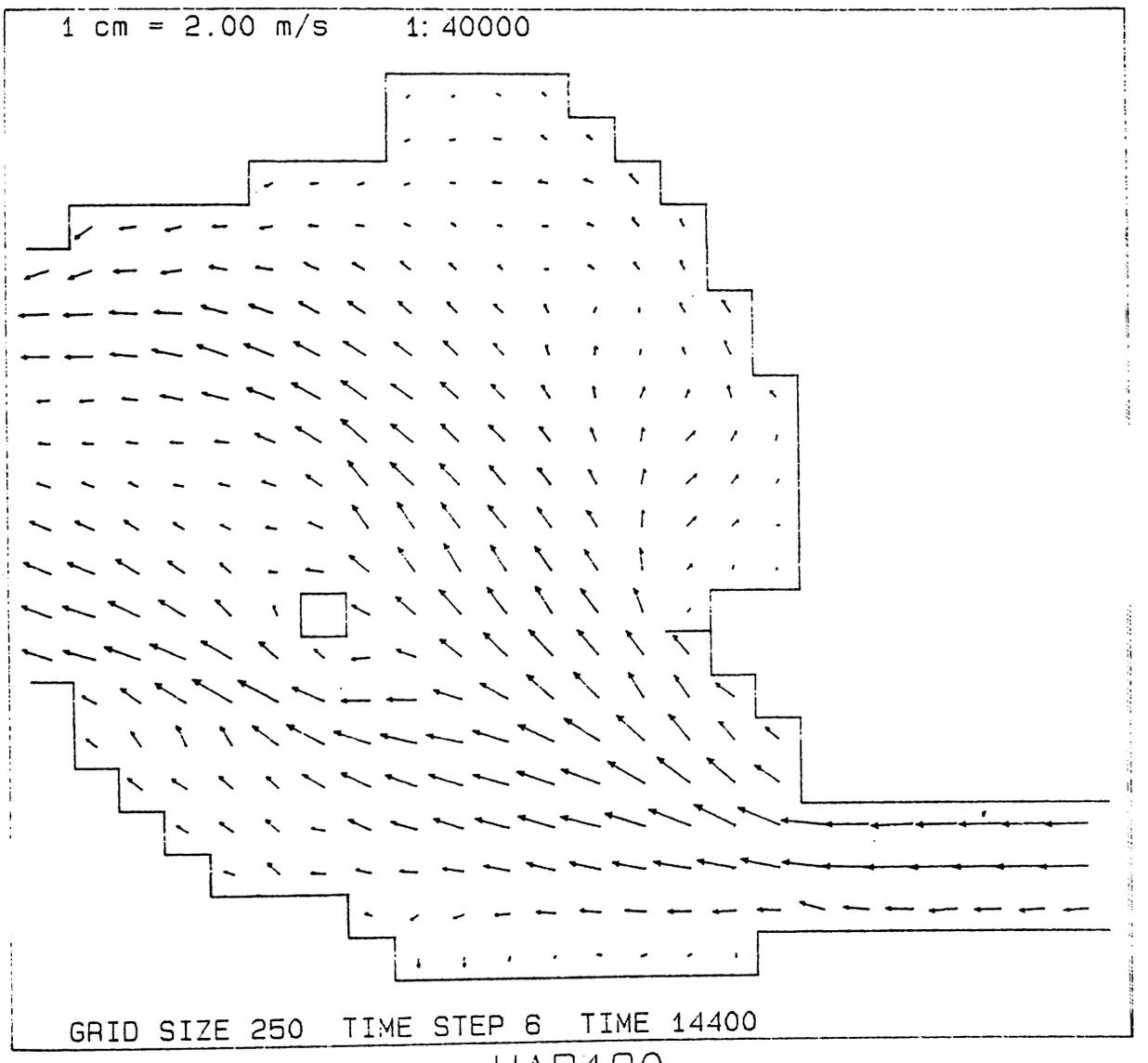

HAR190

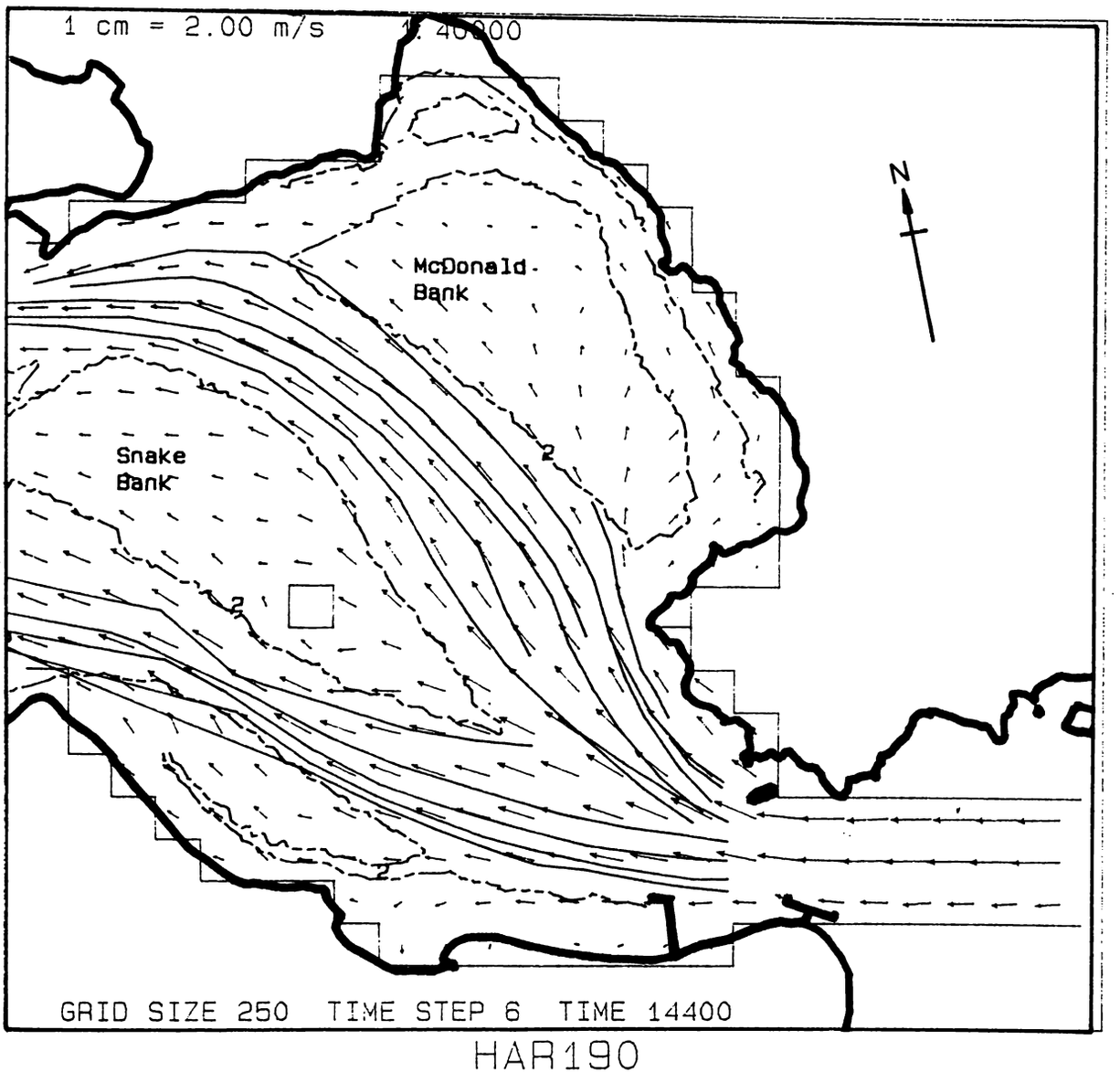

Figure 10.34: Drogue paths in Whangarei Harbour during flood tides.

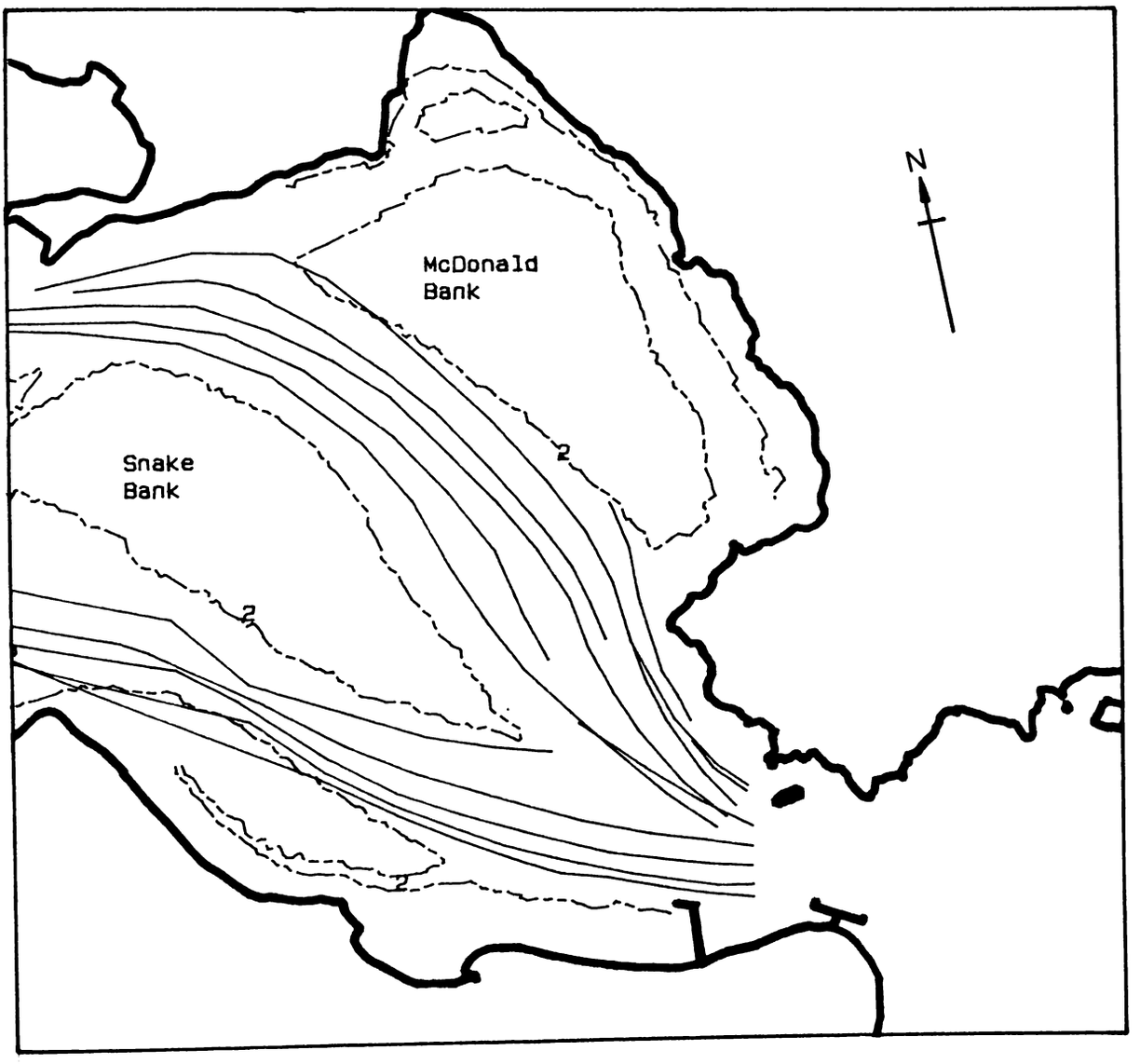

Figure 10.34: Drogue paths in Whangarei Harbour during flood tides.

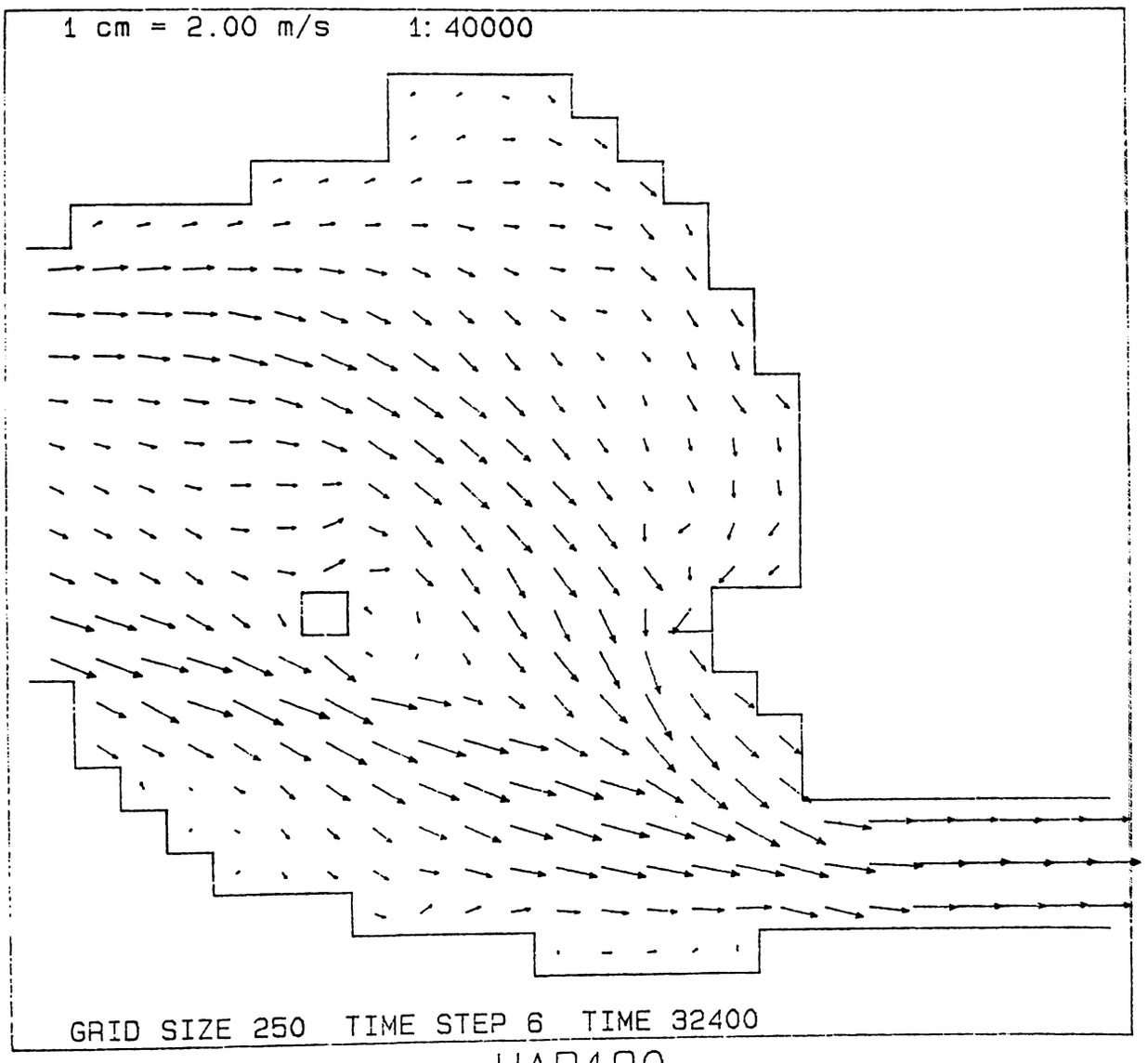

HAR190

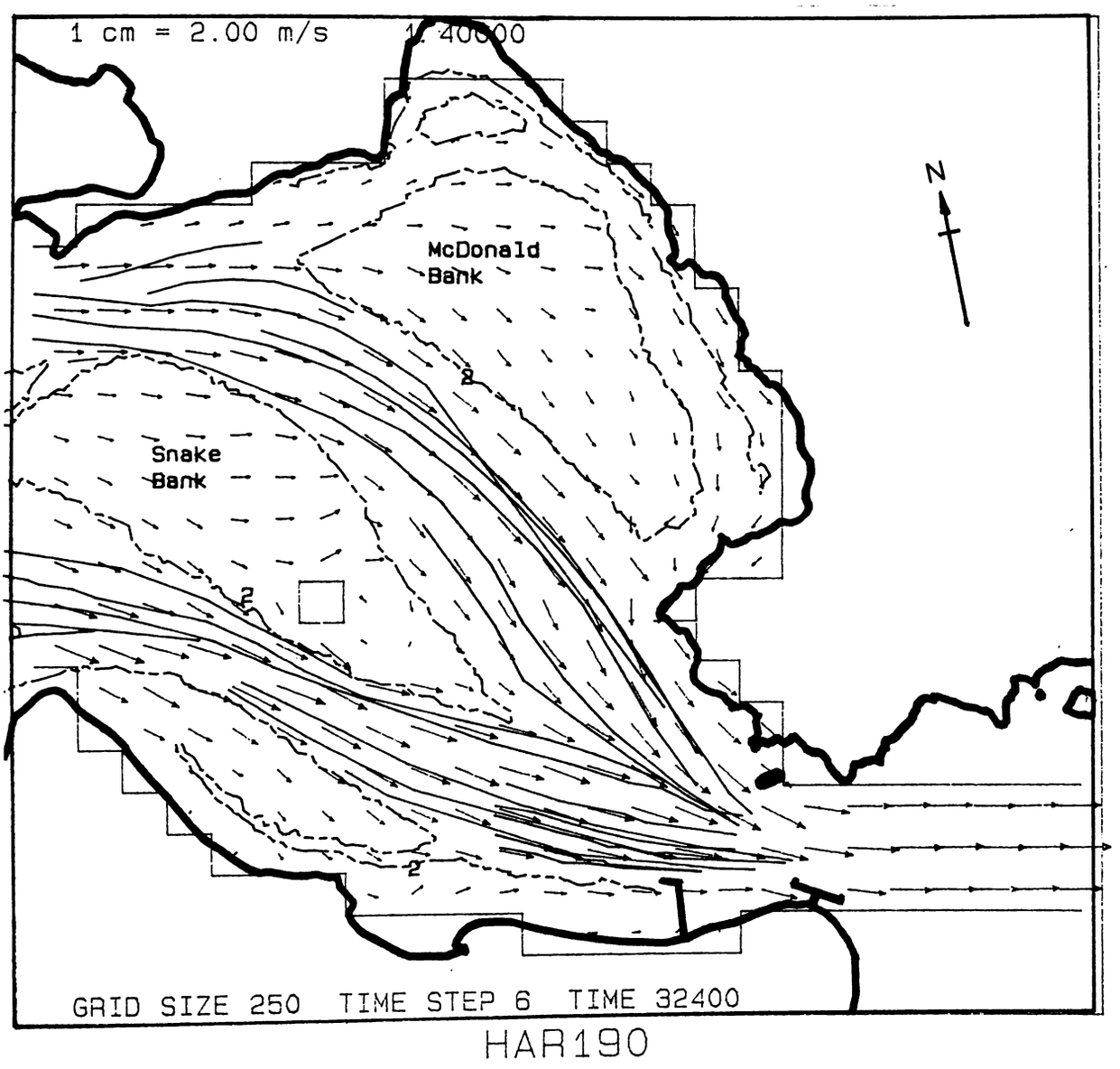

Figure 10.35: Drogue paths in Whangarei Harbour during ebb tides.

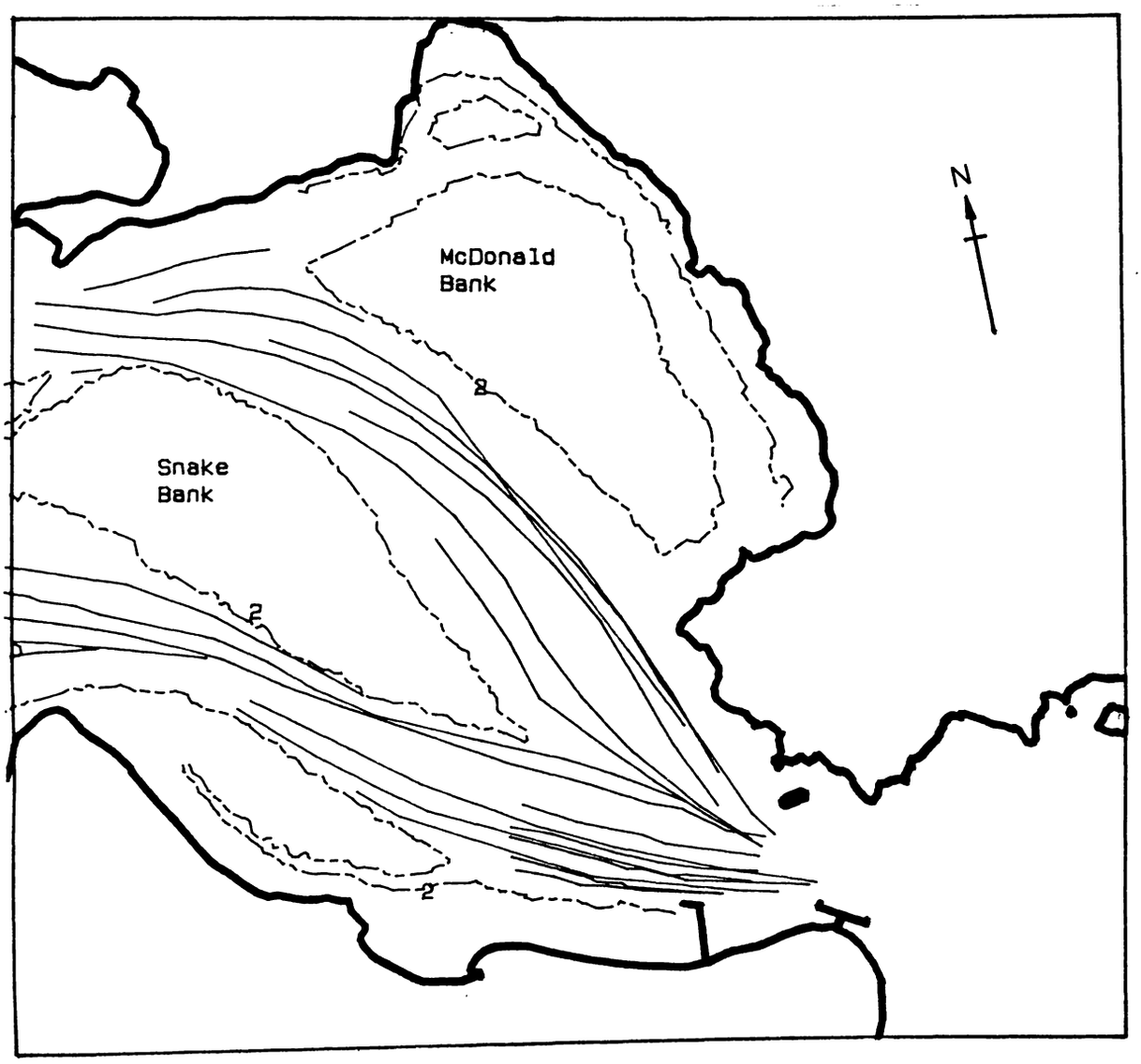

Figure 10.35: Drogue paths in Whangarei Harbour during ebb tides.

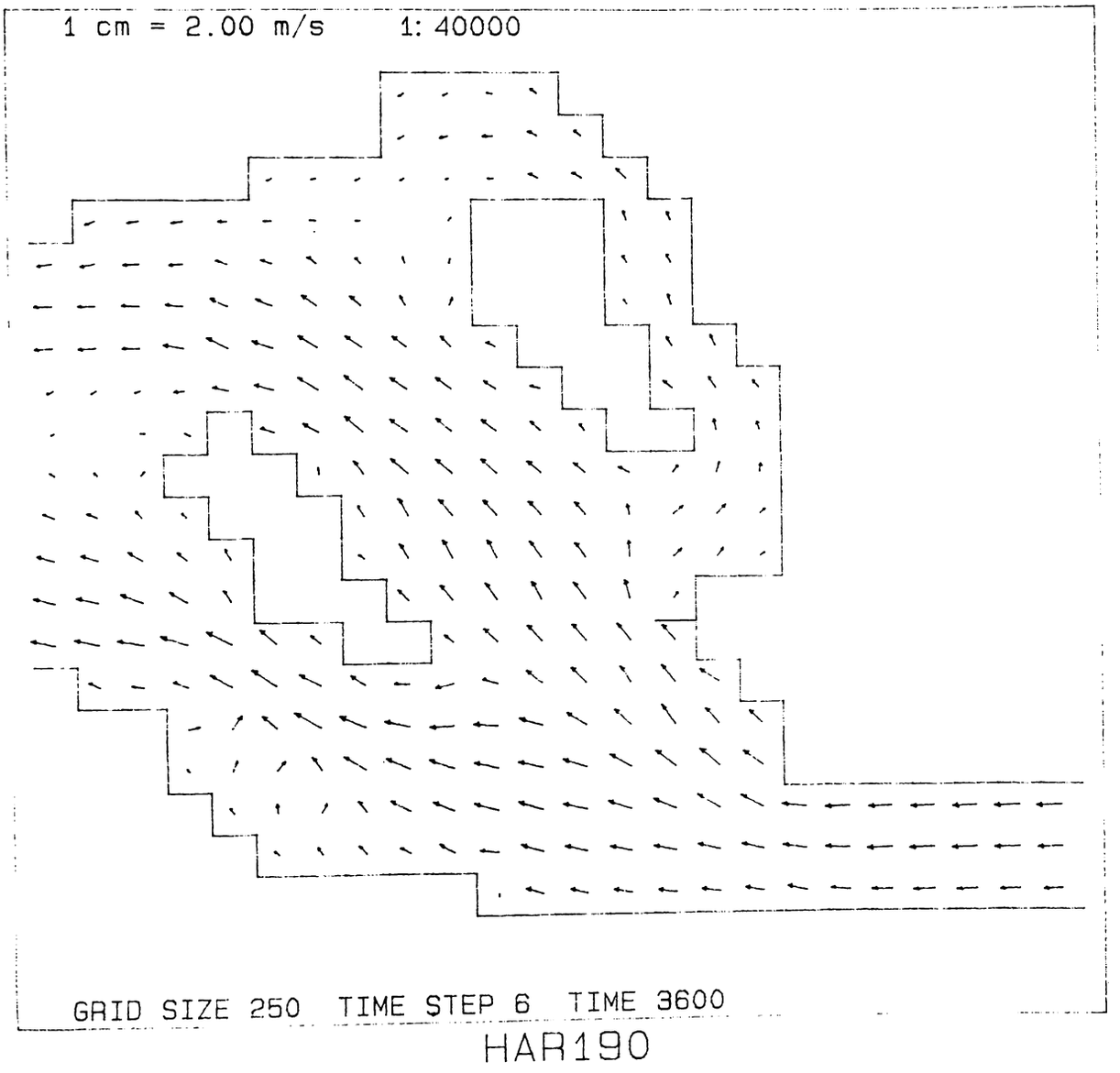

Figure 10.36(a): Flow pattern. Spring tide 1 hour after the low tide at 2:45 on 14-Dec-81.

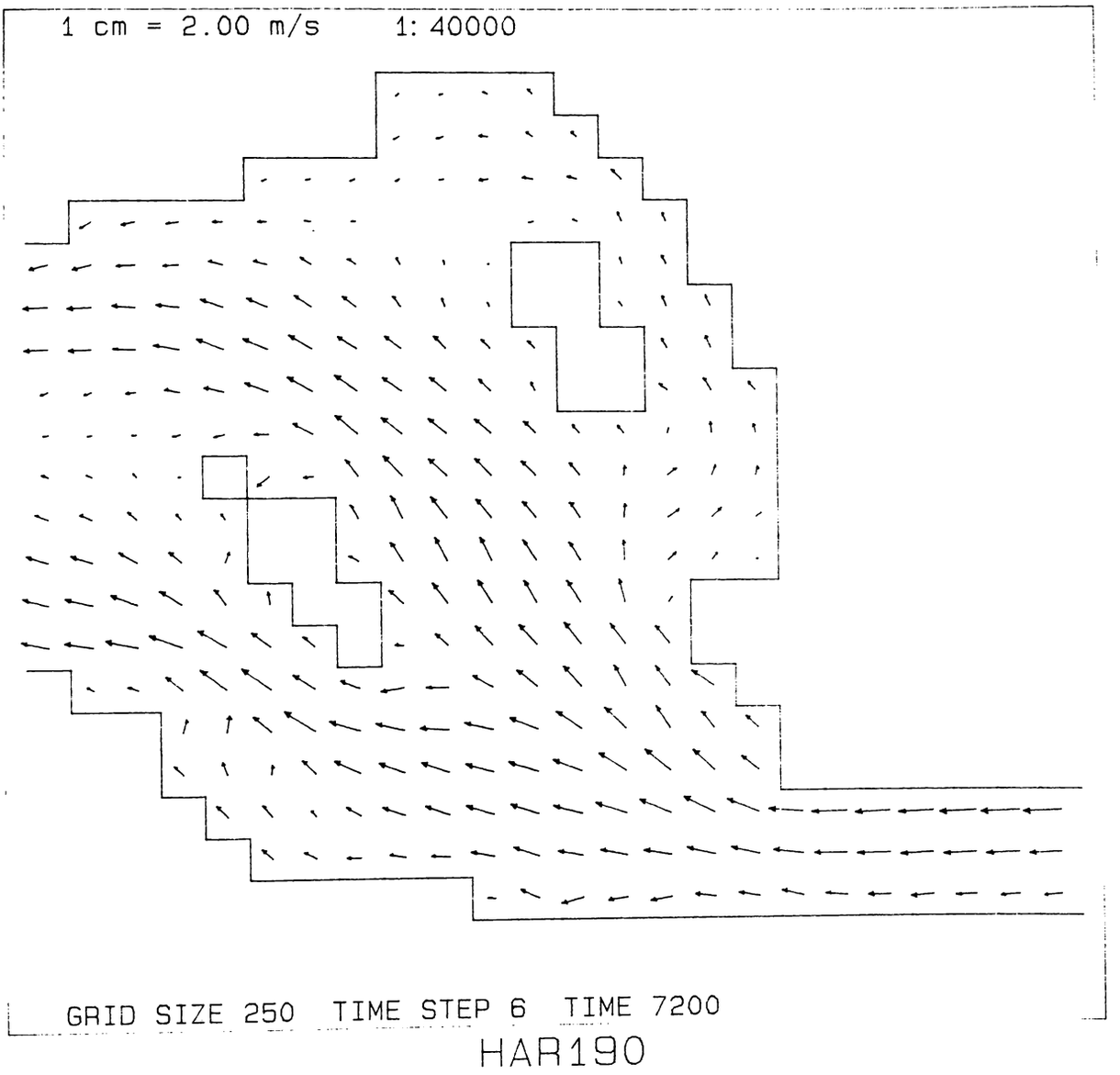

Figure 10.36(b): Flow pattern. Spring tide 2 hours after the low tide at 2:45 on 14-Dec-81.

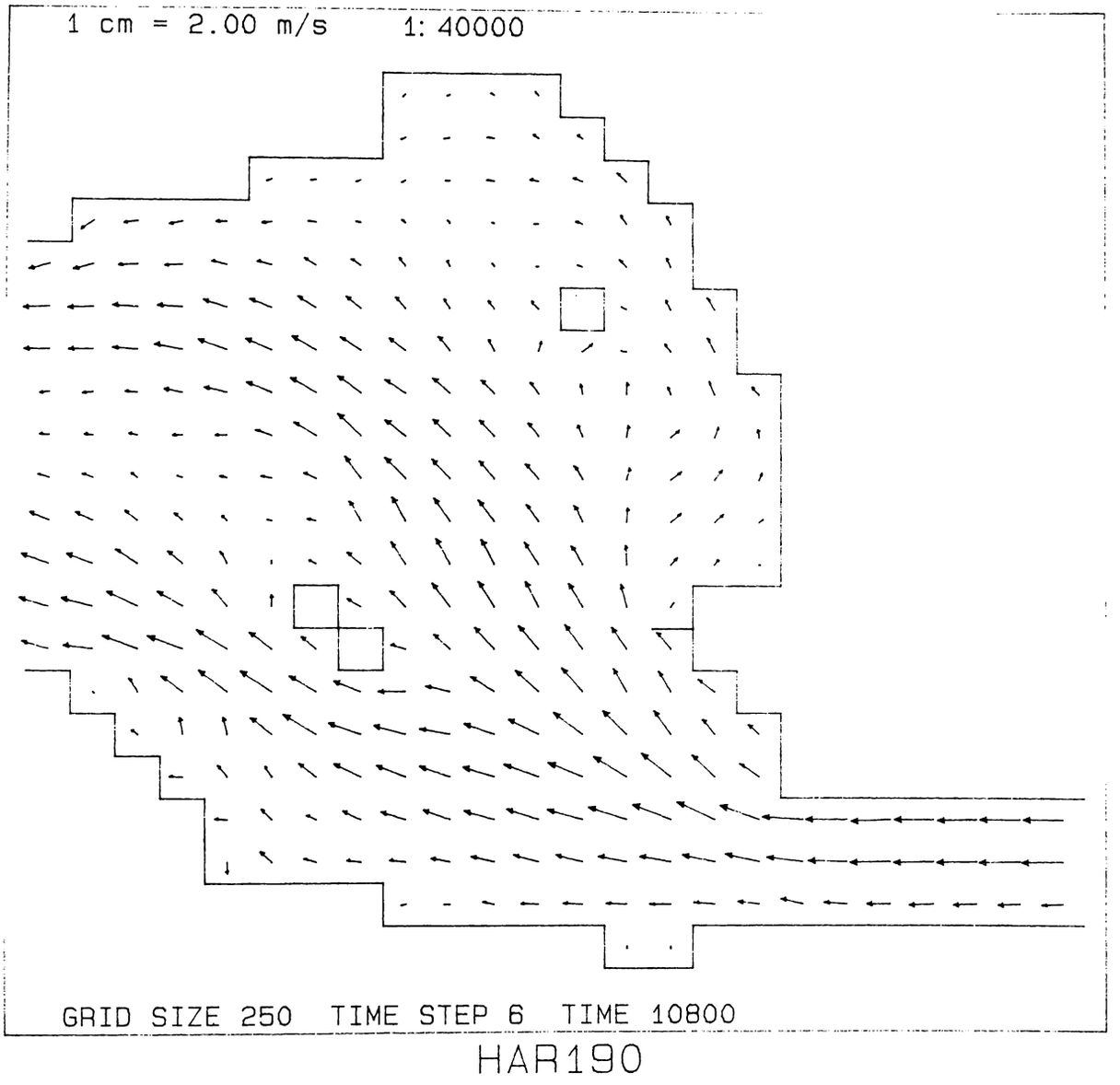

Figure 10.36(c): Flow pattern. Spring tide 3 hours after the low tide at 2:45 on 14-Dec-81.

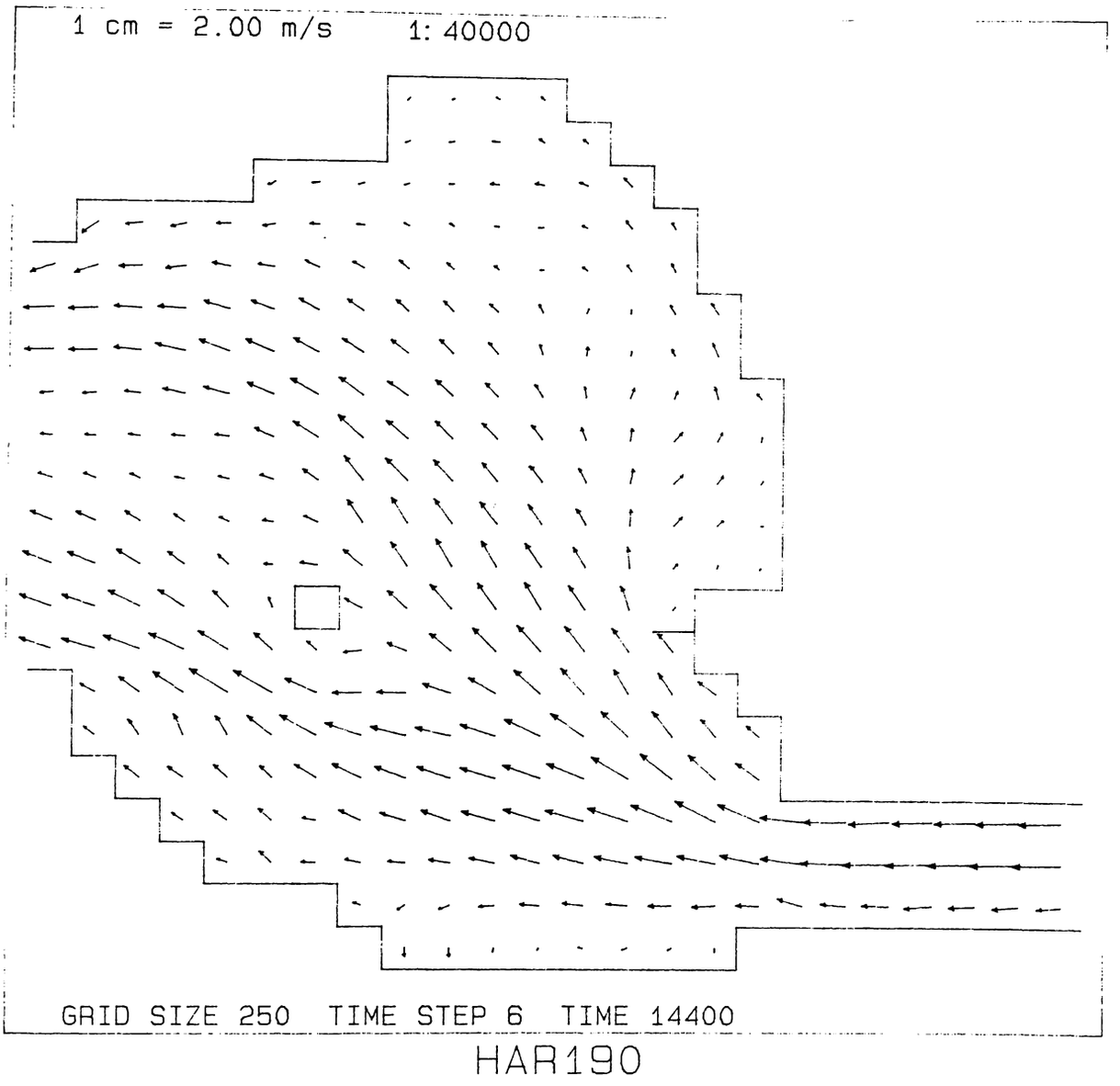

Figure 10.36(d): Flow pattern. Spring tide 4 hours after the low tide at 2:45 on 14-Dec-81.

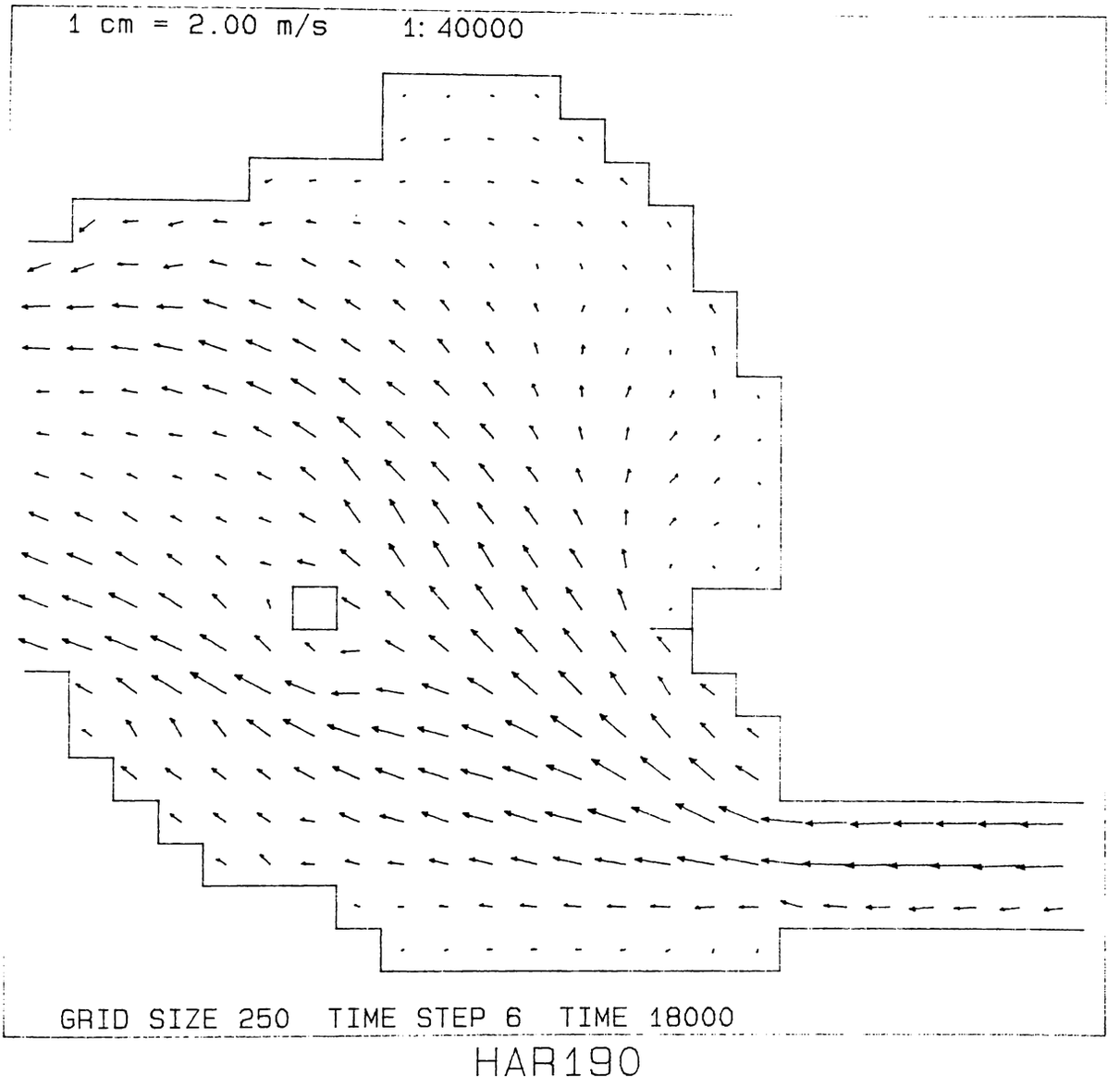

Figure 10.36(e): Flow pattern. Spring tide 5 hours after the low tide at 2:45 on 14-Dec-81.

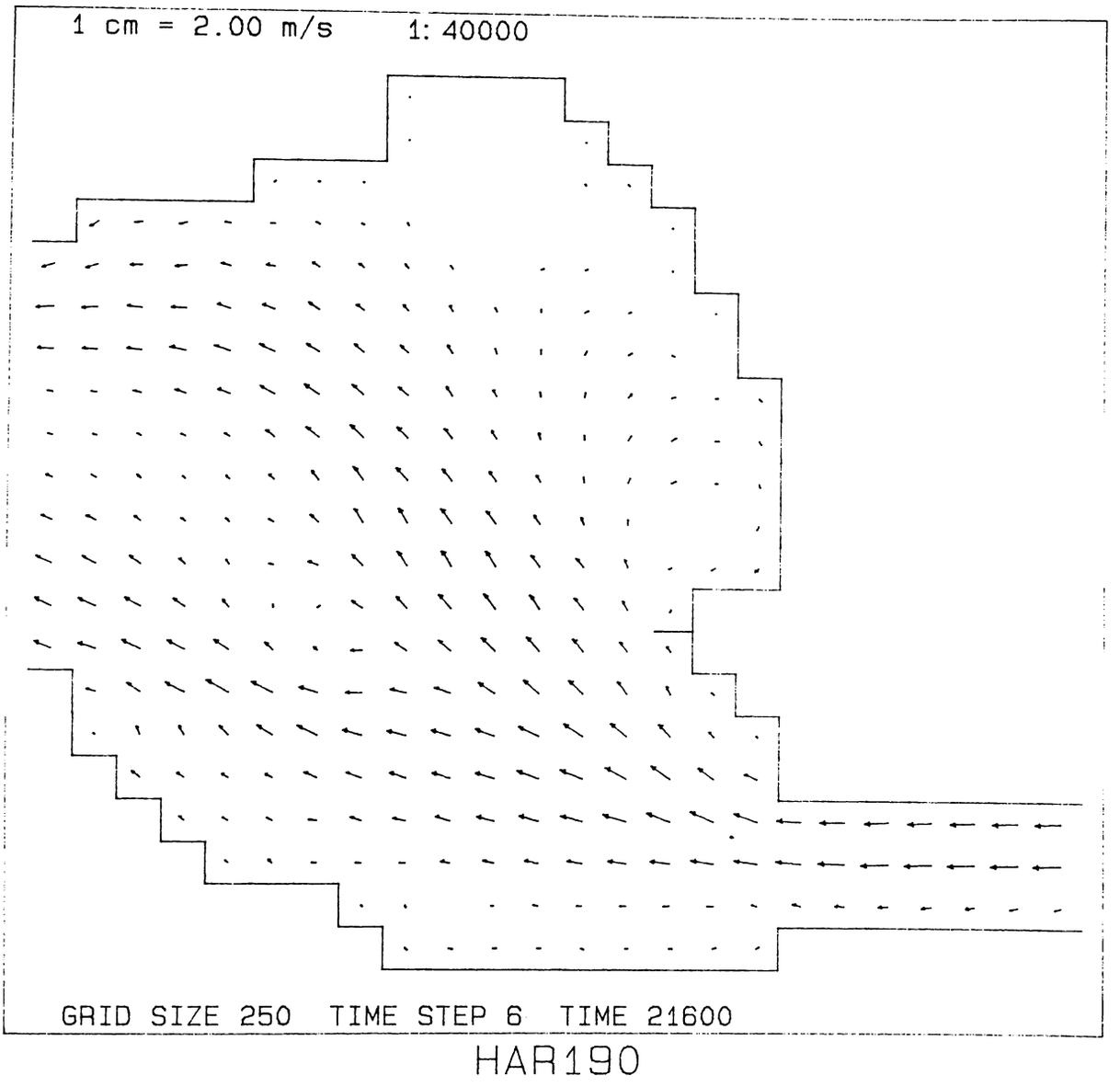

Figure 10.36(f): Flow pattern. Spring tide 6 hours after the low tide at 2:45 on 14-Dec-81.

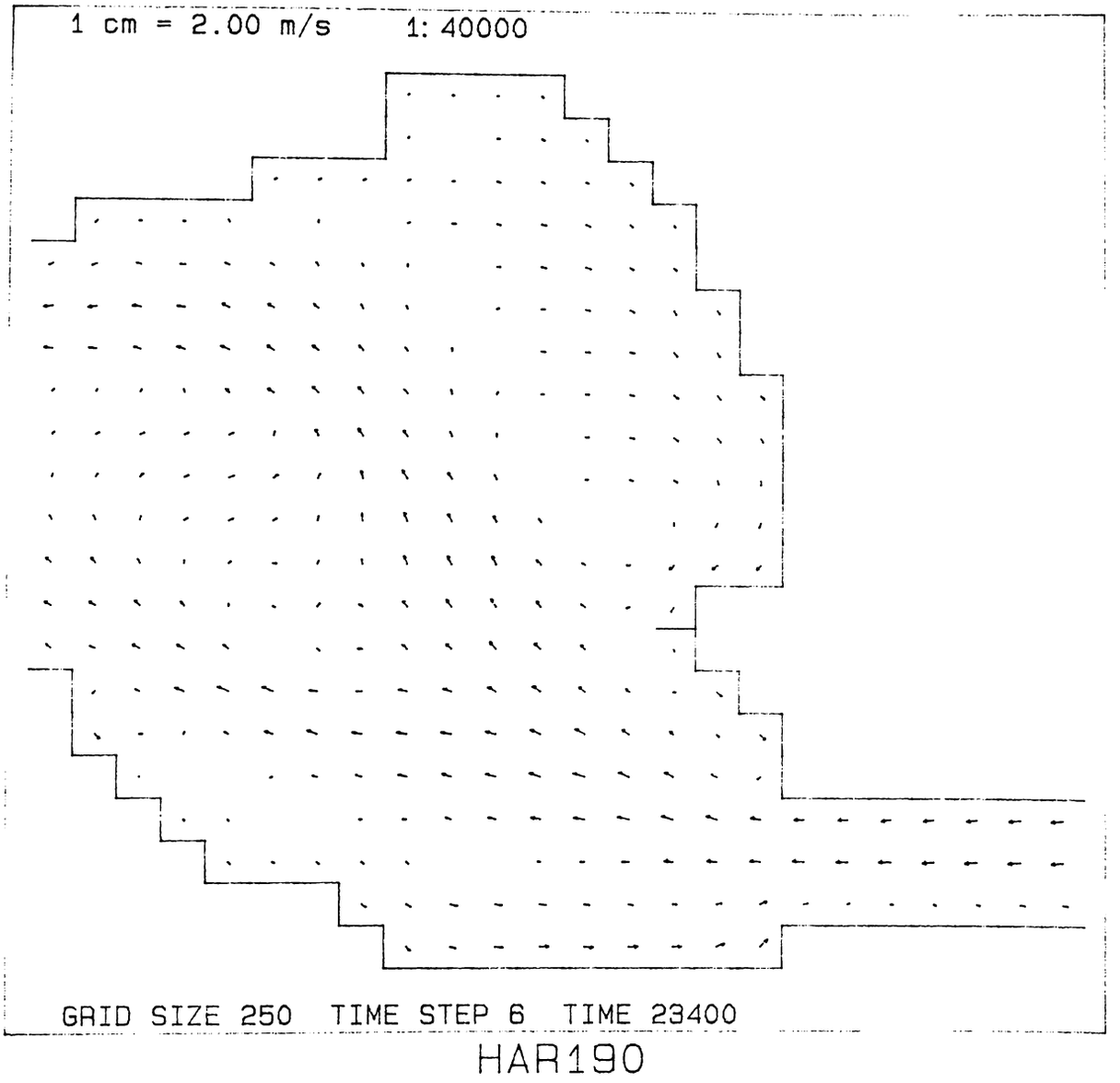

Figure 10.36(g): Flow pattern. Spring tide 6½ hours after the low tide at 2:45 on 14-Dec-81.

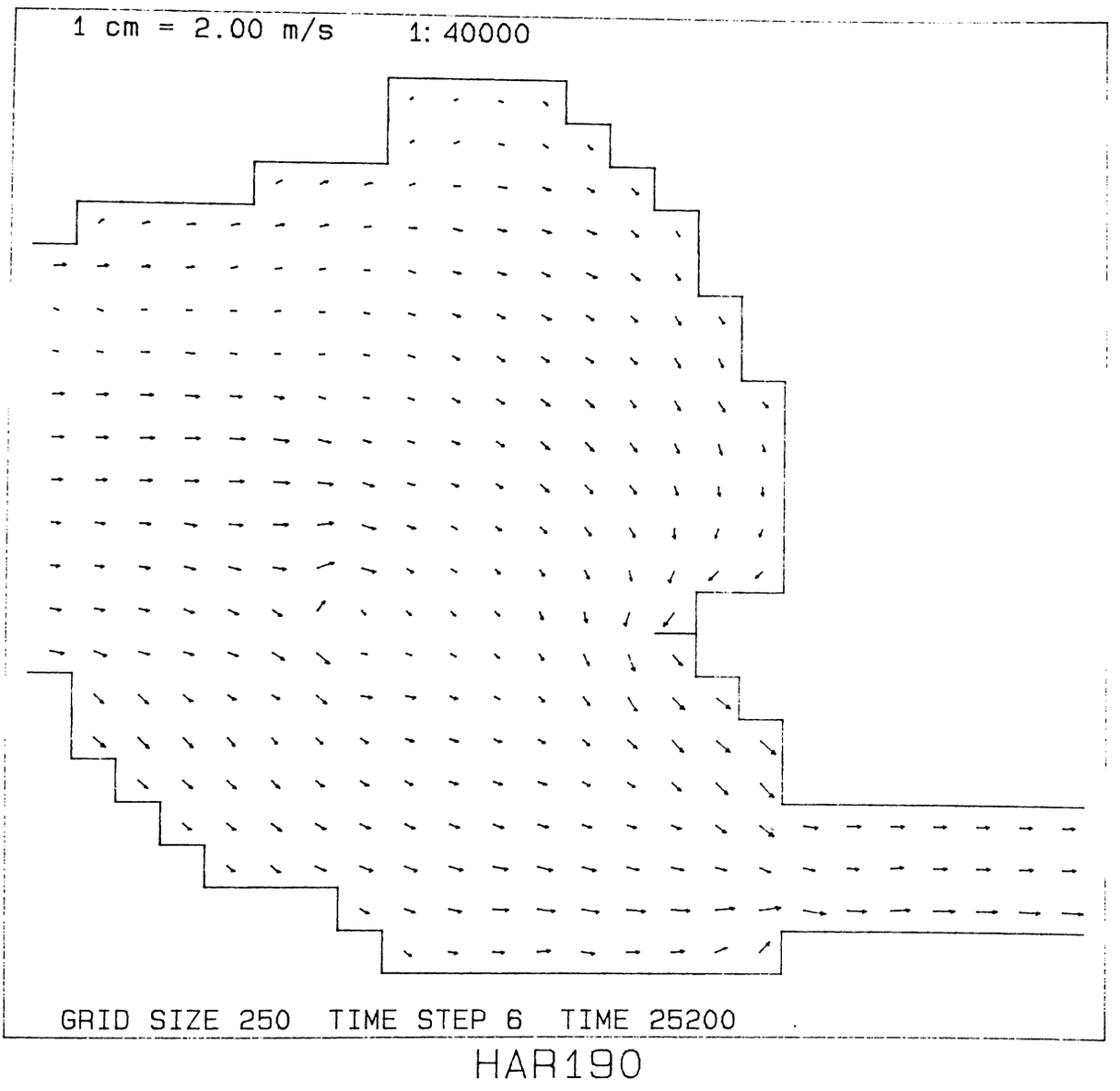

Figure 10.36(h): Flow pattern. Spring tide 7 hours after the low tide at 2:45 on 14-Dec-81.

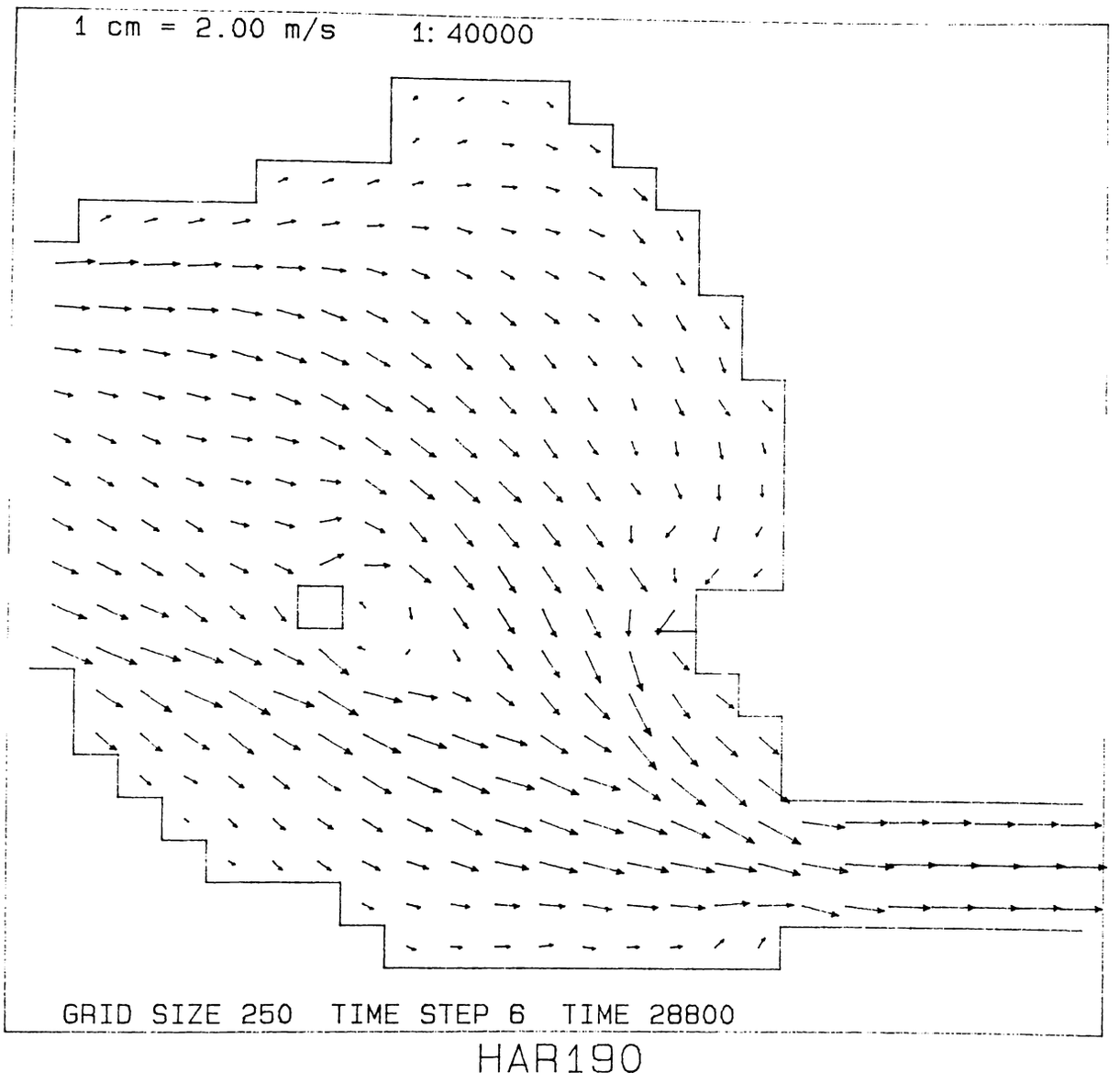

Figure 10.36(i): Flow pattern. Spring tide 8 hours after the low tide at 2:45 on 14-Dec-81.

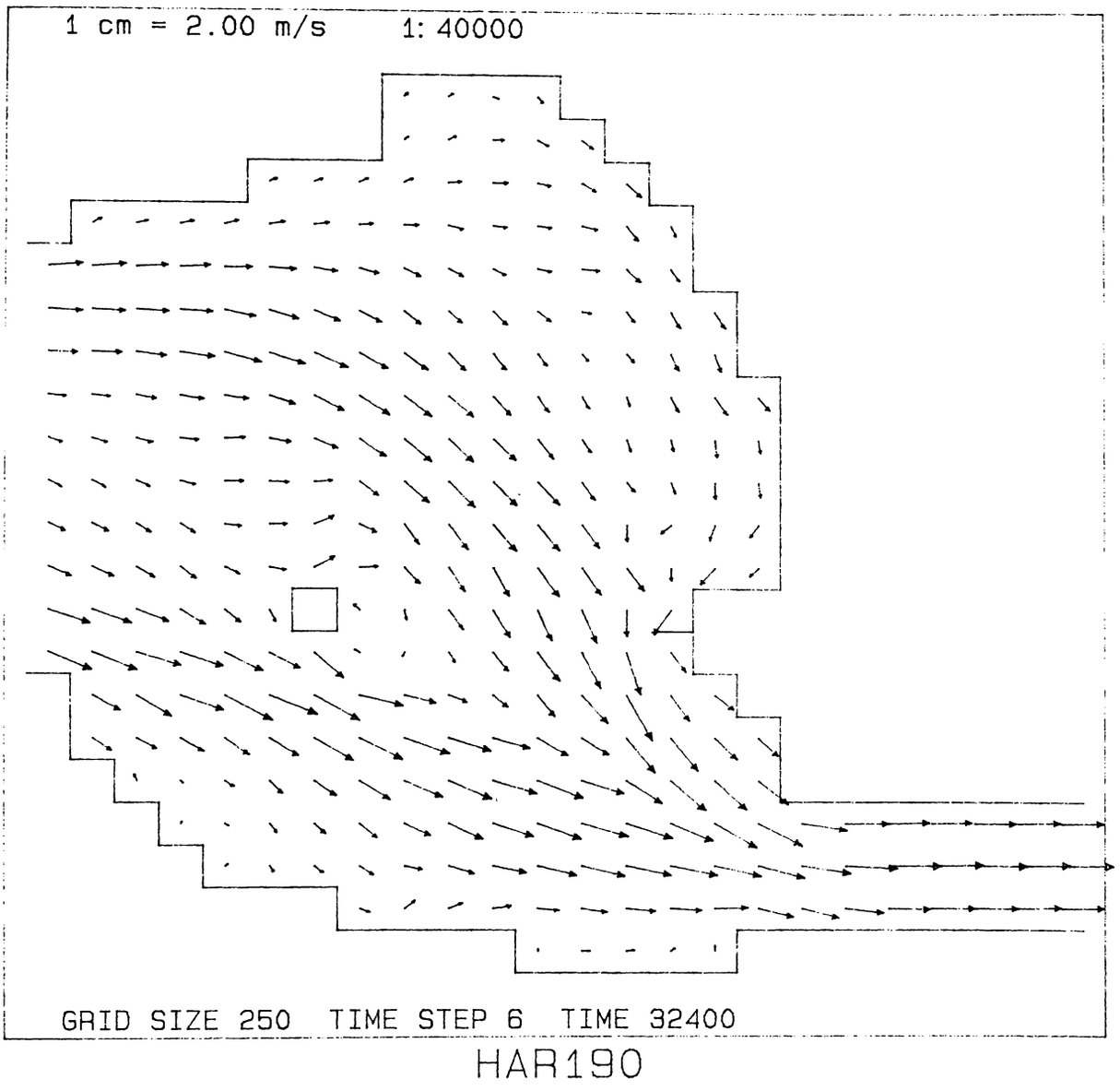

Figure 10.36(j): Flow pattern. Spring tide 9 hours after the low tide at 2:45 on 14-Dec-81.

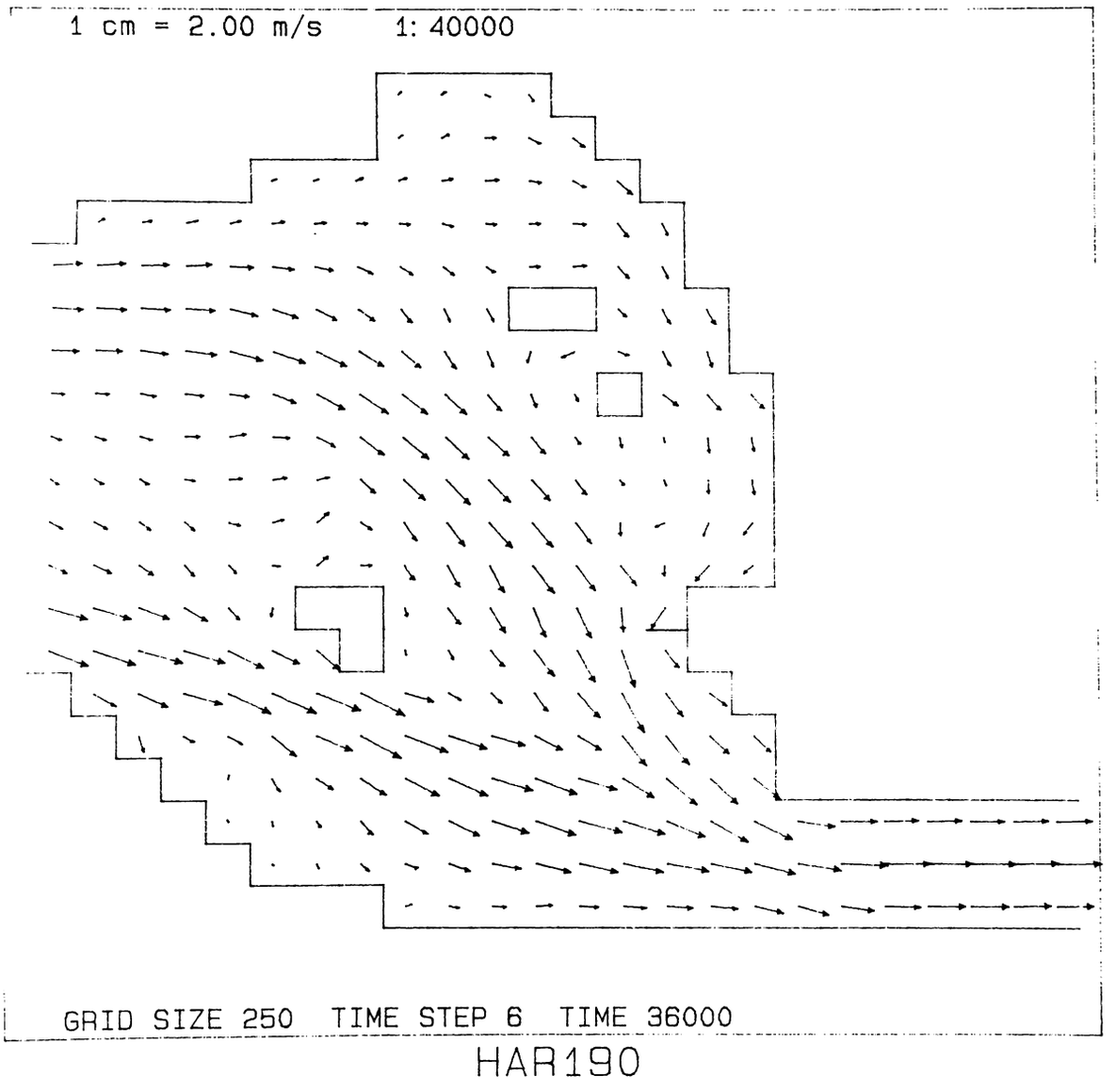

Figure 10.36(k): Flow pattern. Spring tide 10 hours after the low tide at 2:45 on 14-Dec-81.

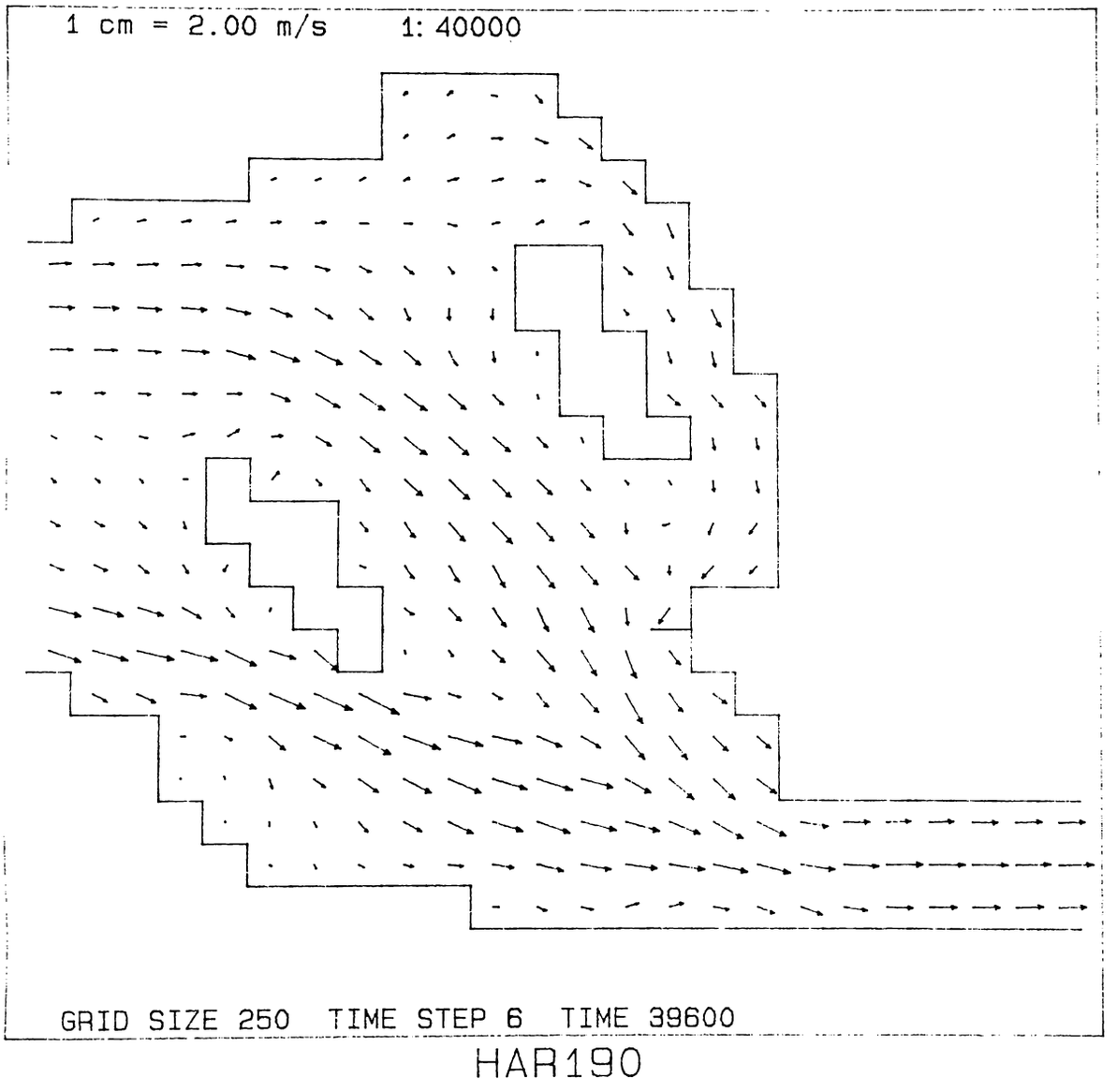

Figure 10.36(1): Flow pattern. Spring tide 11 hours after the low tide at 2:45 on 14-Dec-81.

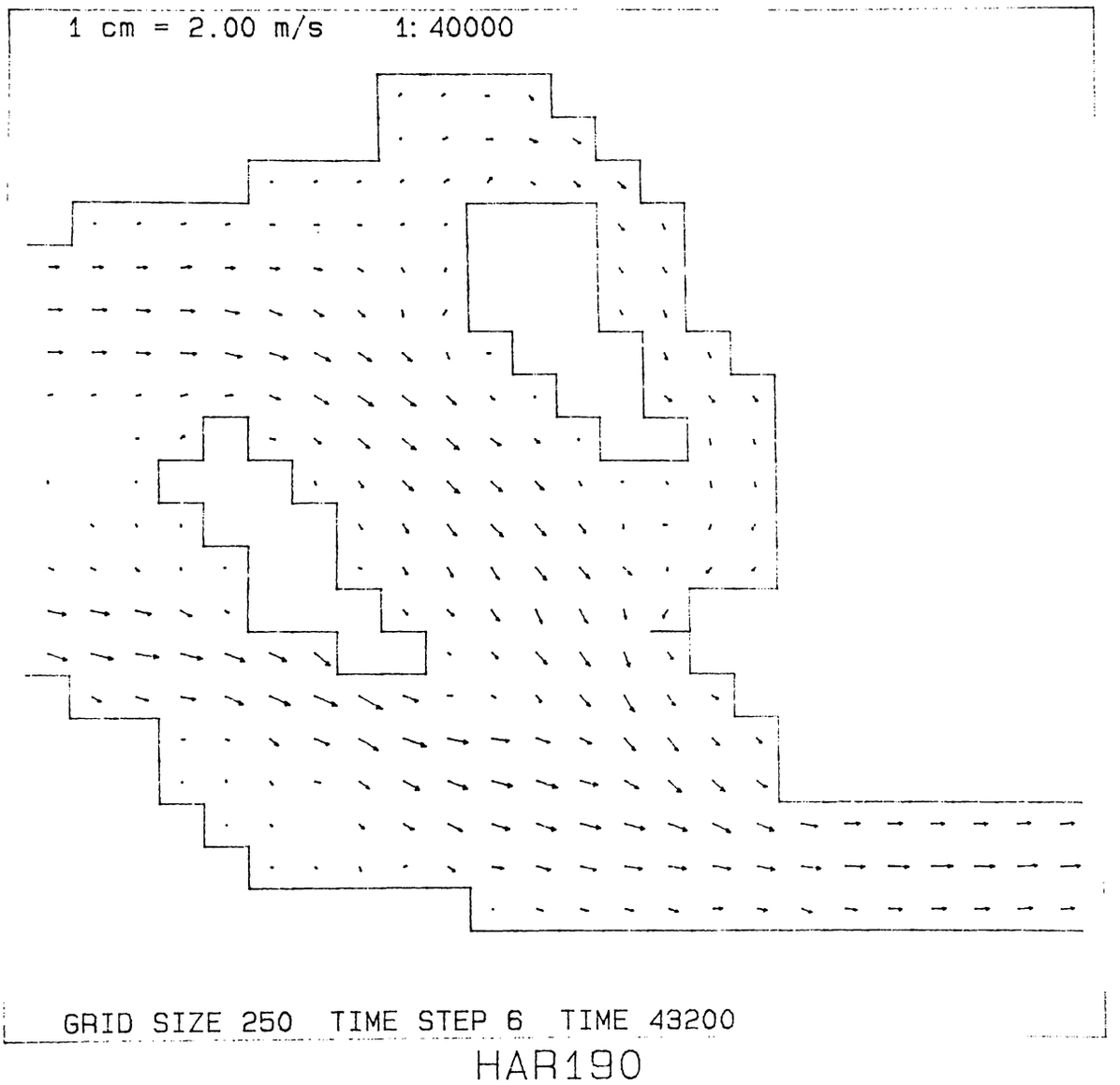

Figure 10.36(m): Flow pattern. Spring tide 12 hours after the low tide at 2:45 on 14-Dec-81.

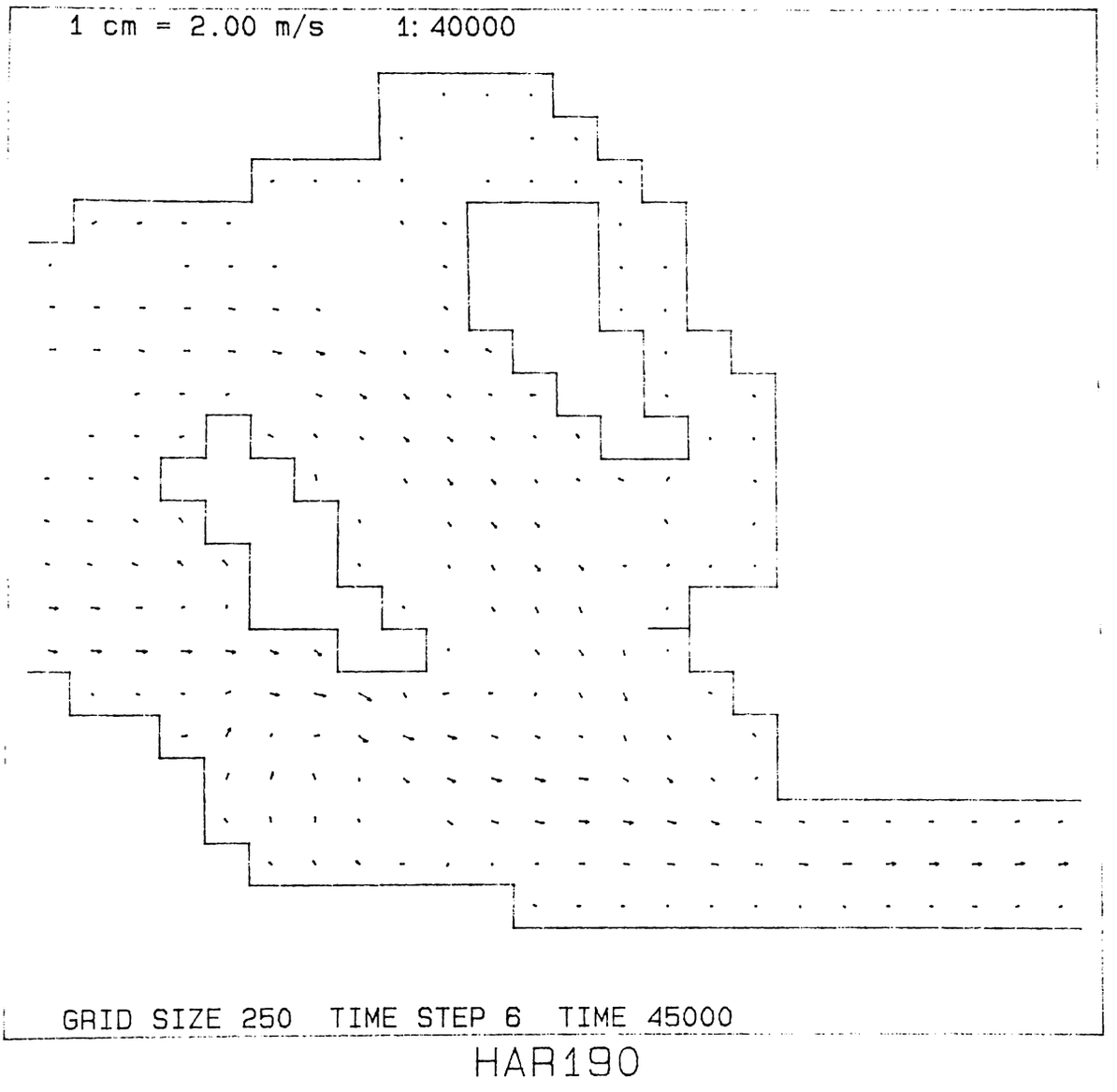

Figure 10.36(n): Flow pattern. Spring tide 13 hours after the low tide at 2:45 on 14-Dec-81.

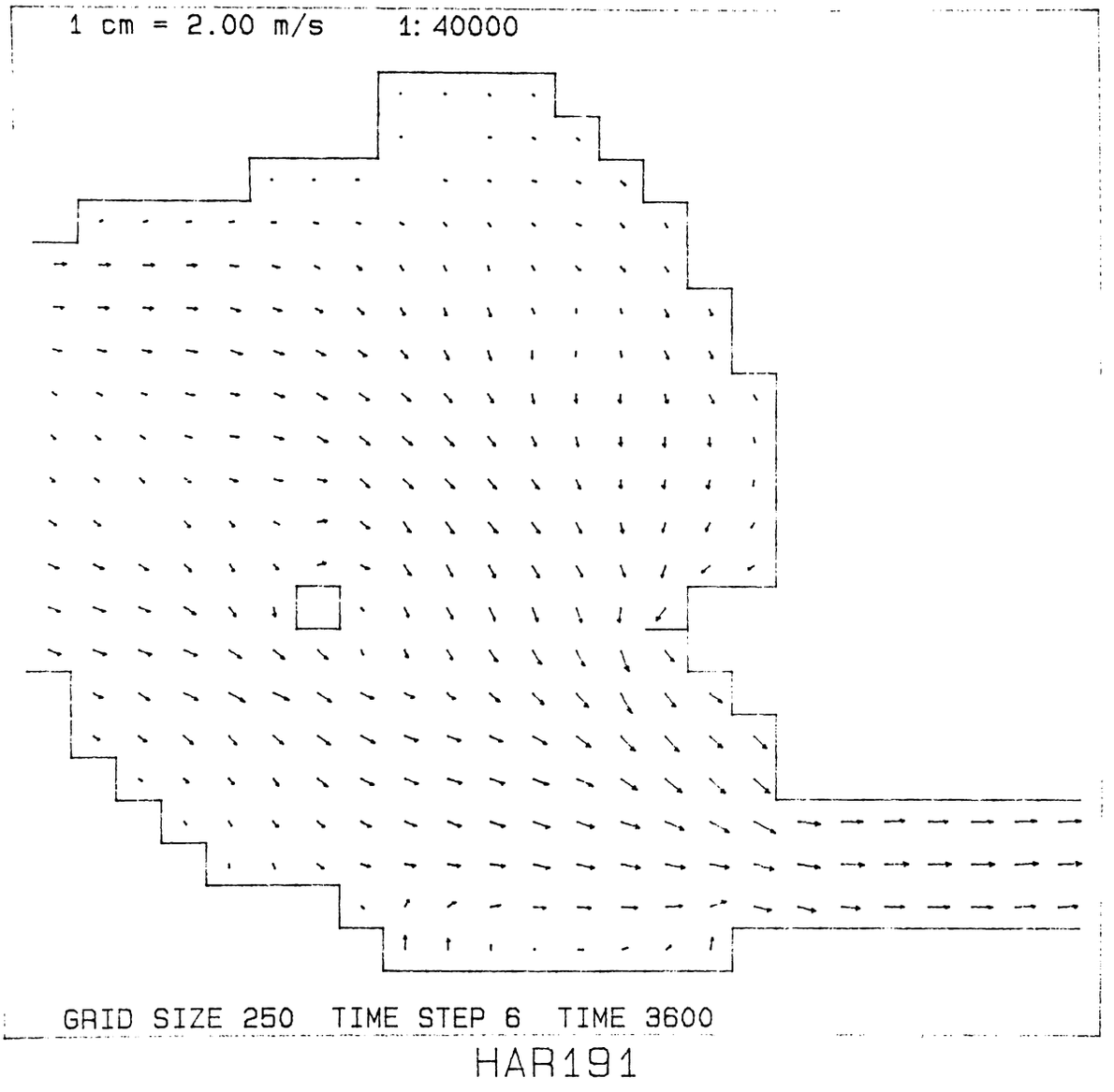

Figure 10.37(a): Flow pattern. Neap tide 1¾ hours after the high tide at 23:15 on 2-Dec-81.

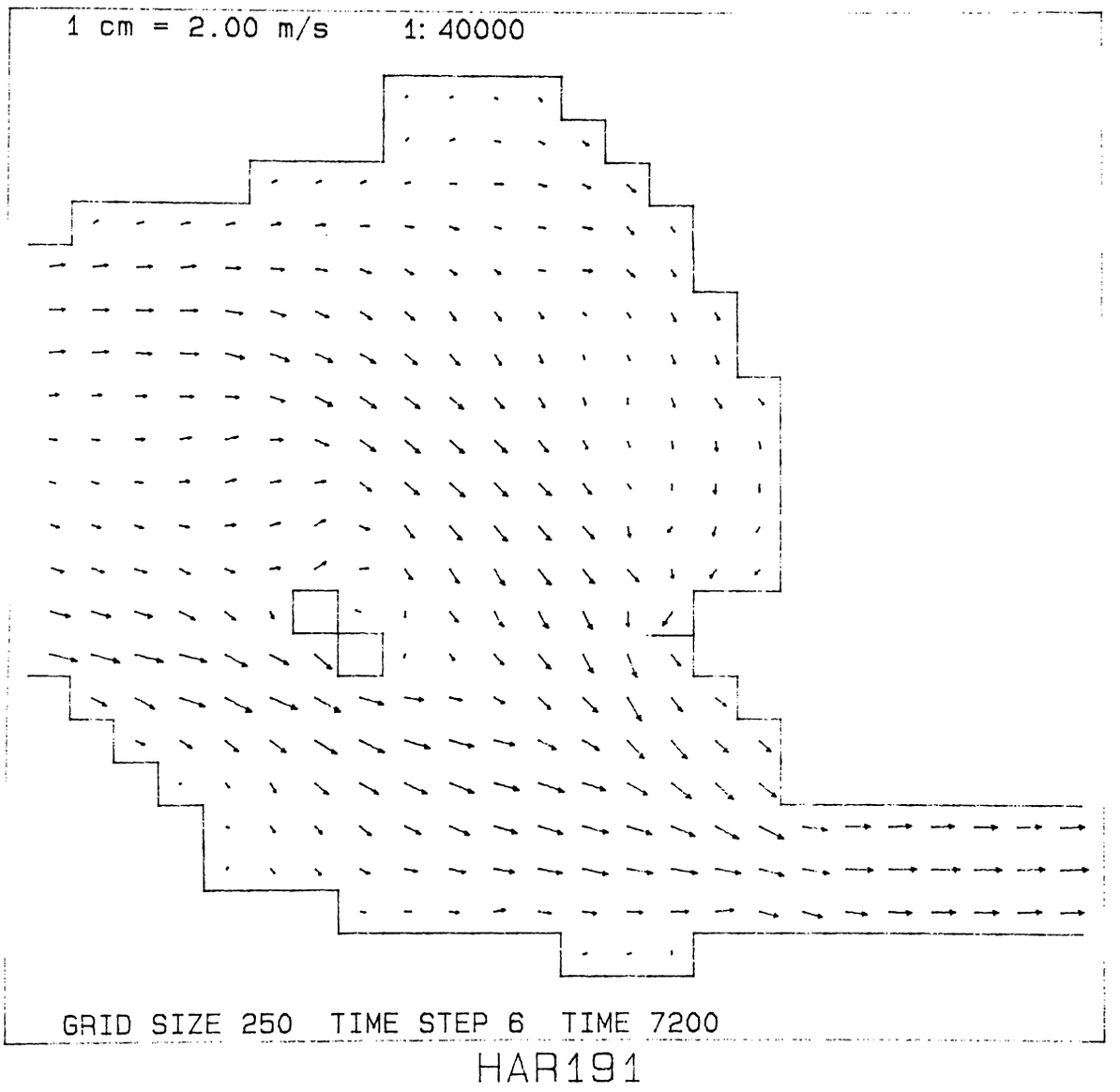

Figure 10.37(b): Flow pattern. Neap tide 2¾ hours after the high tide at 23:15 on 2-Dec-81.

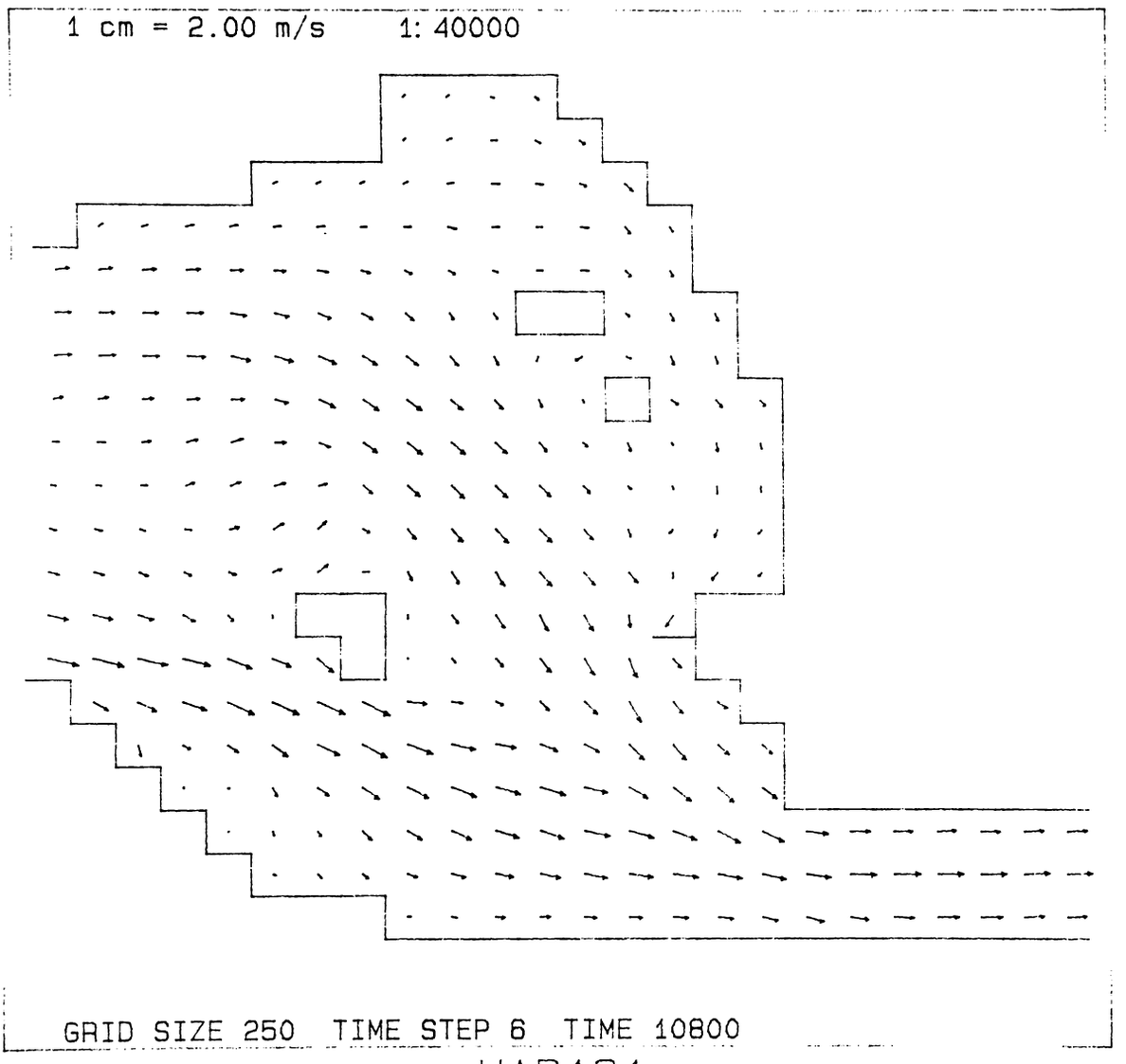

Figure 10.37(c): Flow pattern. Neap tide 3¾ hours after the high tide at 23:15 on 2-Dec-81.

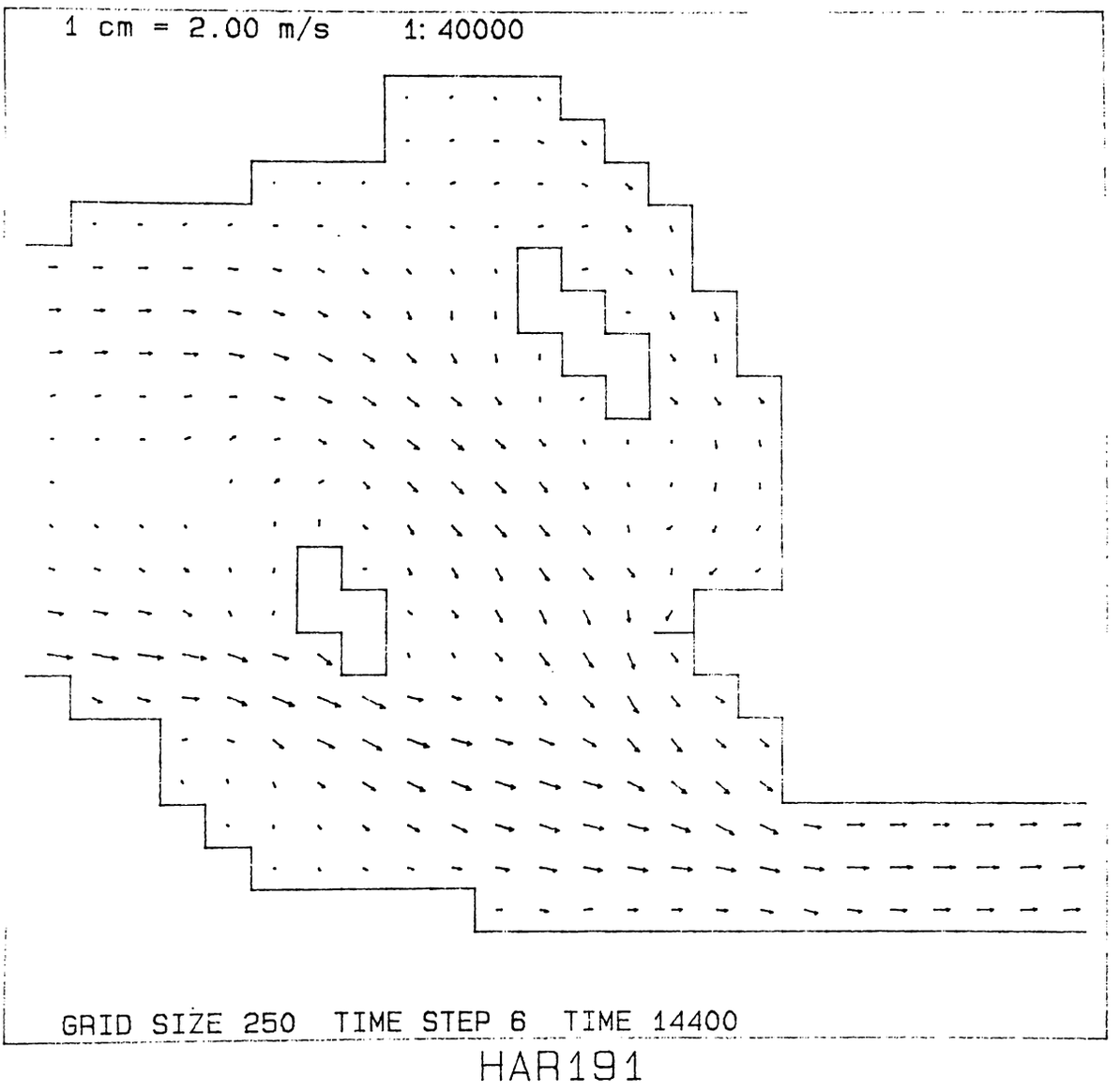

Figure 10.37(d): Flow pattern. Neap tide 4¾ hours after the high tide at 23:15 on 2-Dec-81.

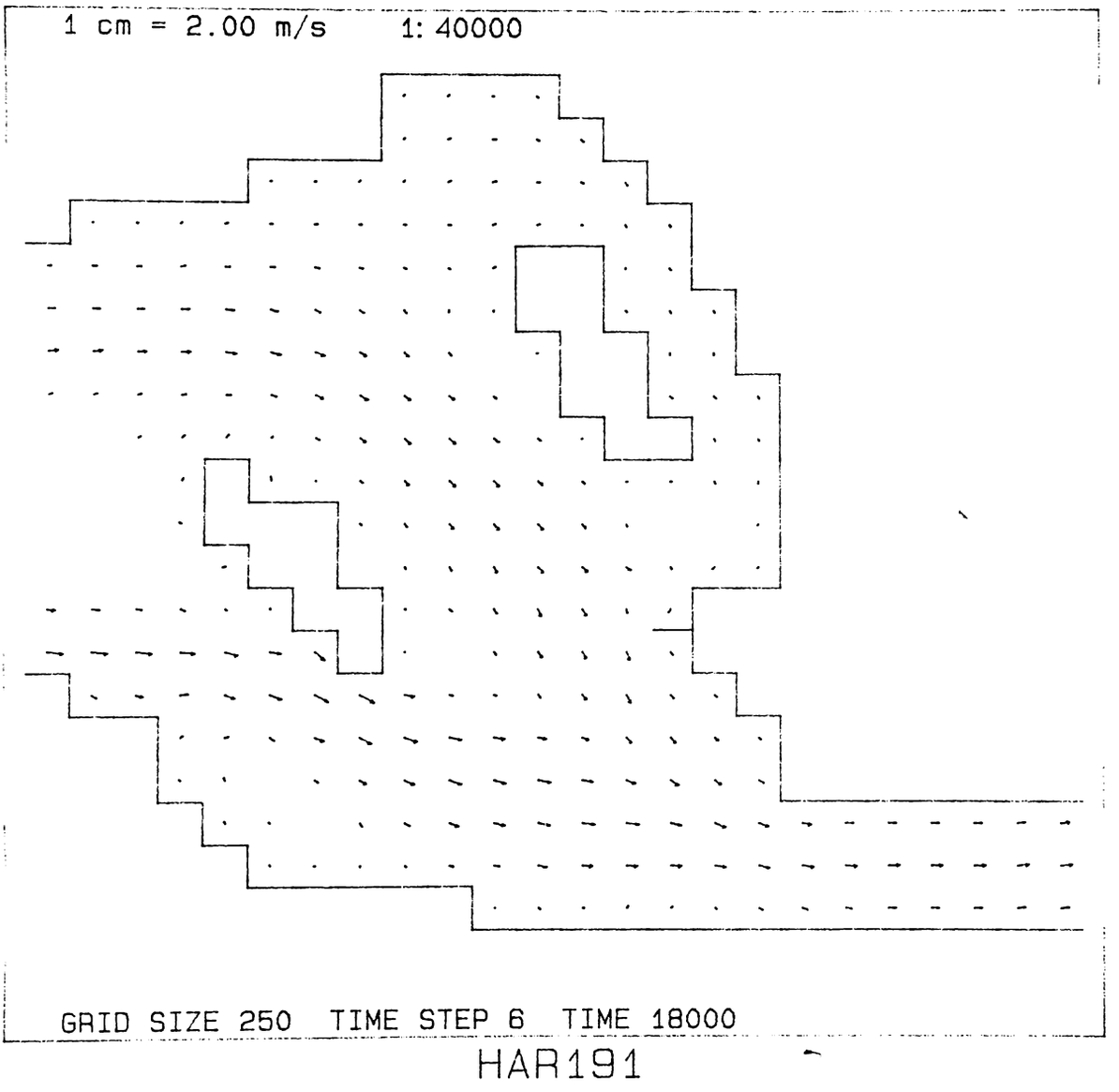

Figure 10.37(e): Flow pattern. Neap tide 5¾ hours after the high tide at 23:15 on 2-Dec-81.

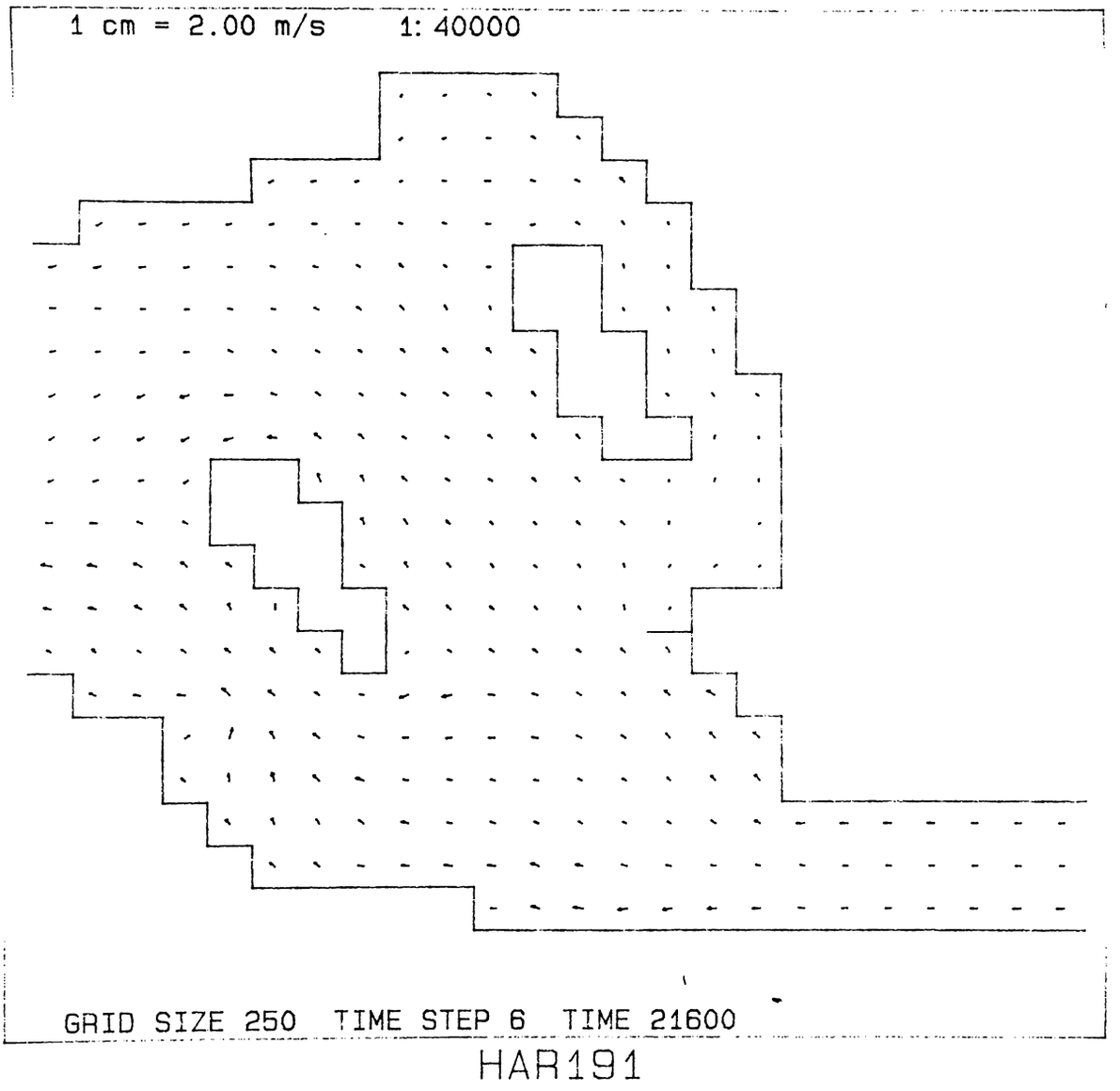

Figure 10.37(f): Flow pattern. Neap tide 6¾ hours after the high tide at 23:15 on 2-Dec-81.

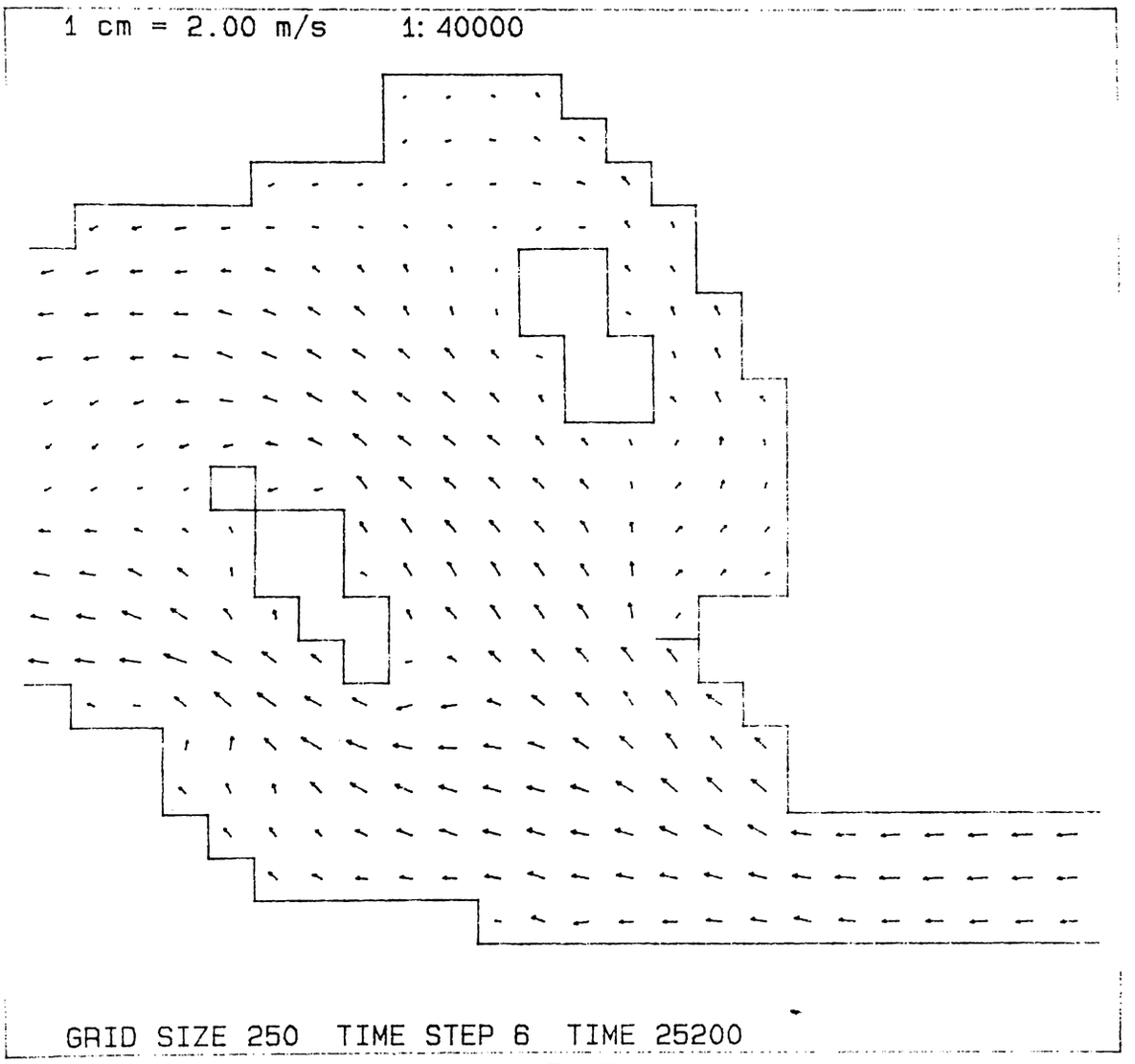

Figure 10.37(g): Flow pattern. Neap tide 7¾ hours after the high tide at 23:15 on 2-Dec-81.

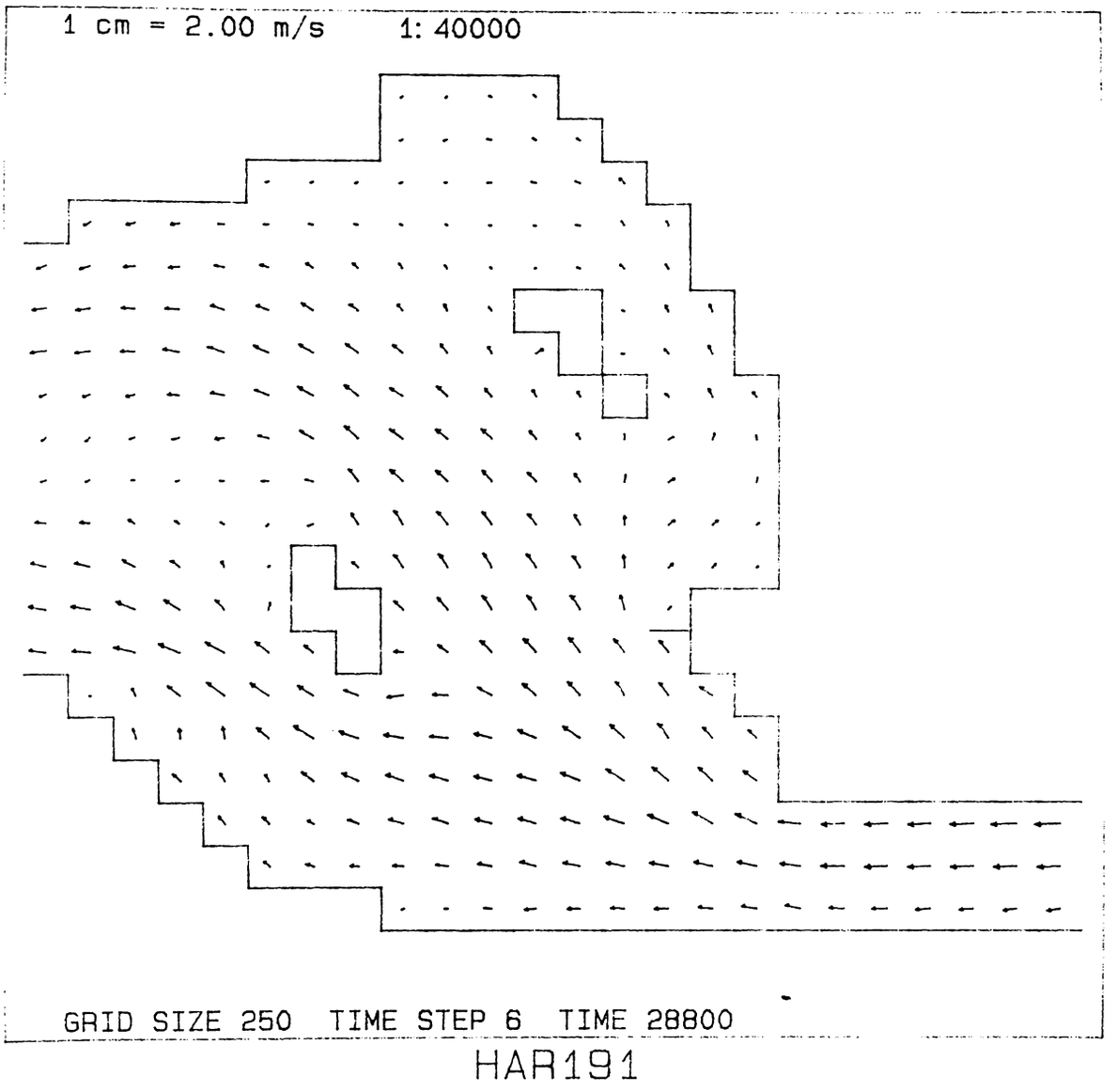

Figure 10.37(h): Flow pattern. Neap tide 8¾ hours after the high tide at 23:15 on 2-Dec-81.

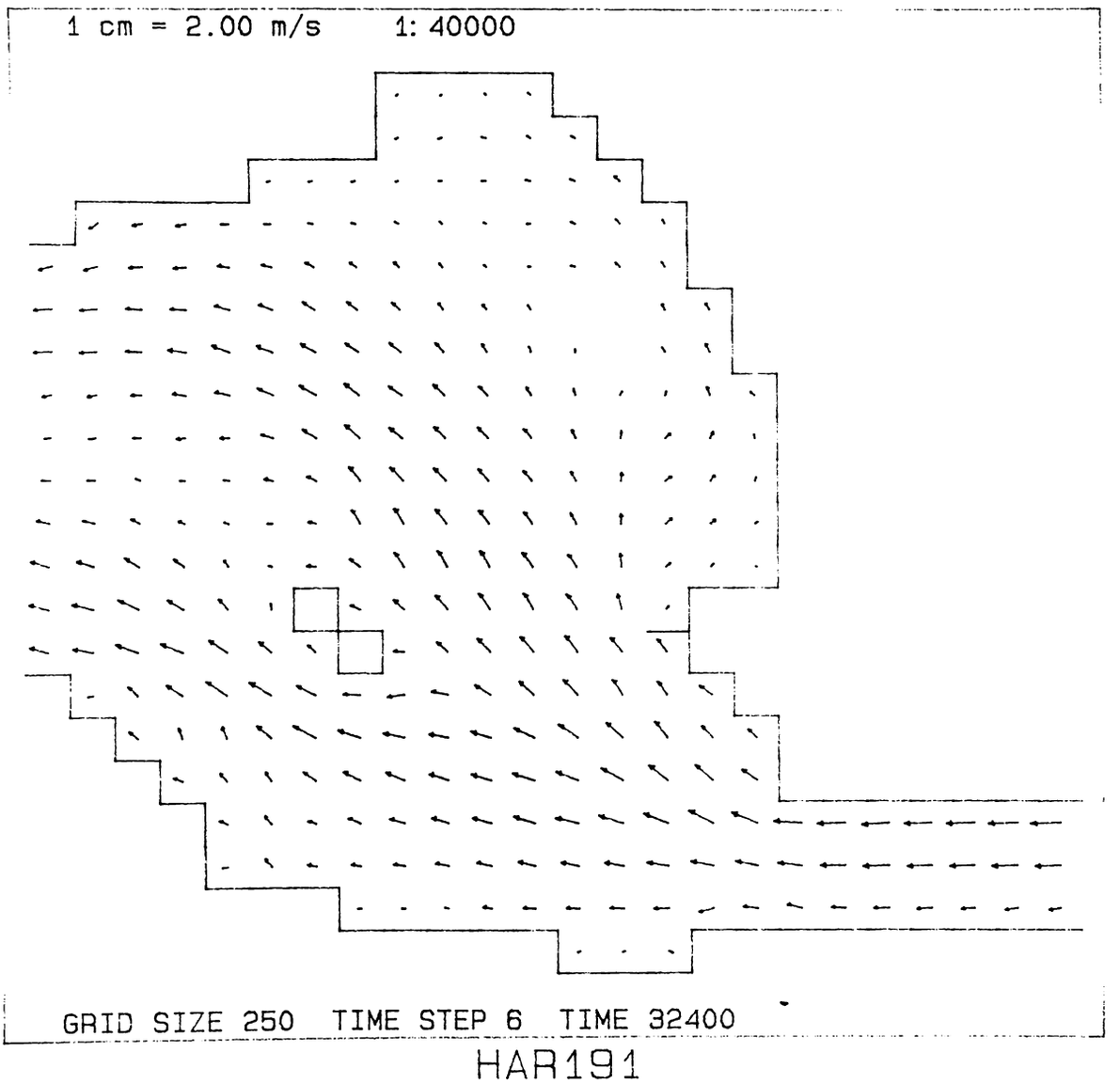

Figure 10.37(i): Flow pattern. Neap tide 9¾ hours after the high tide at 23:15 on 2-Dec-81.

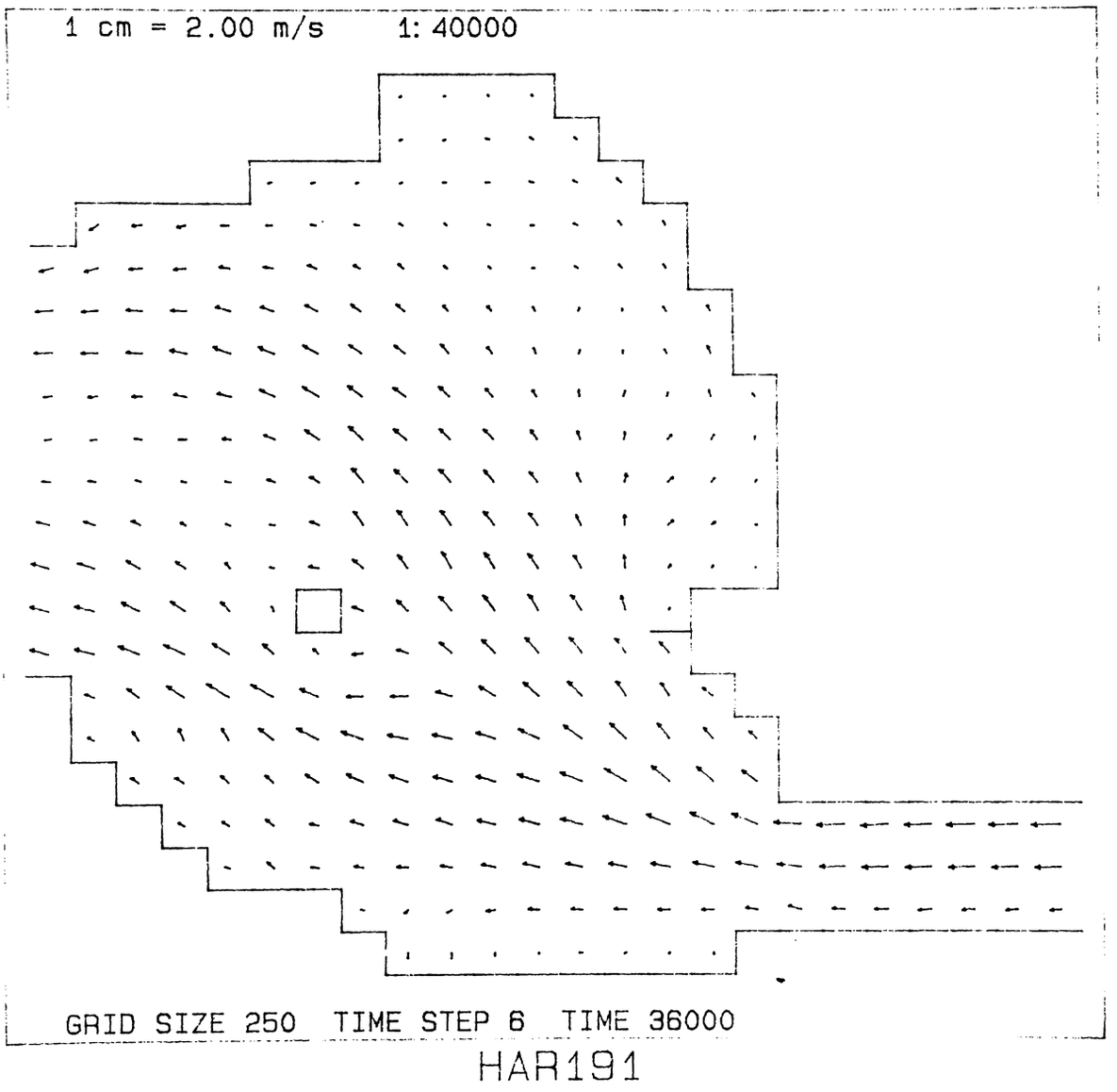

Figure 10.37(j): Flow pattern. Neap tide 10¾ hours after the high tide at 23:15 on 2-Dec-81.

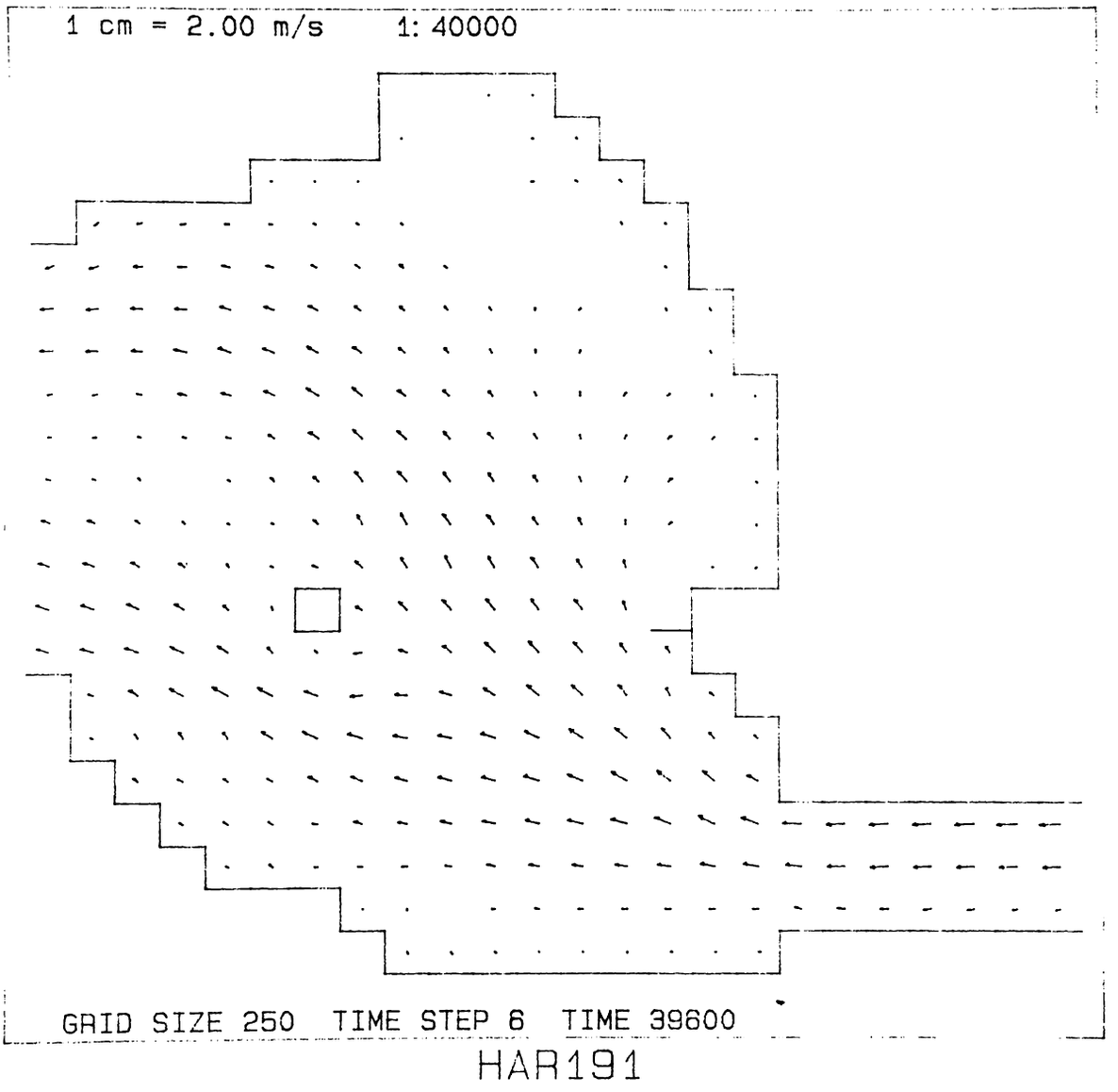

Figure 10.37(k): Flow pattern. Neap tide 11¾ hours after the high tide at 23:15 on 2-Dec-81.

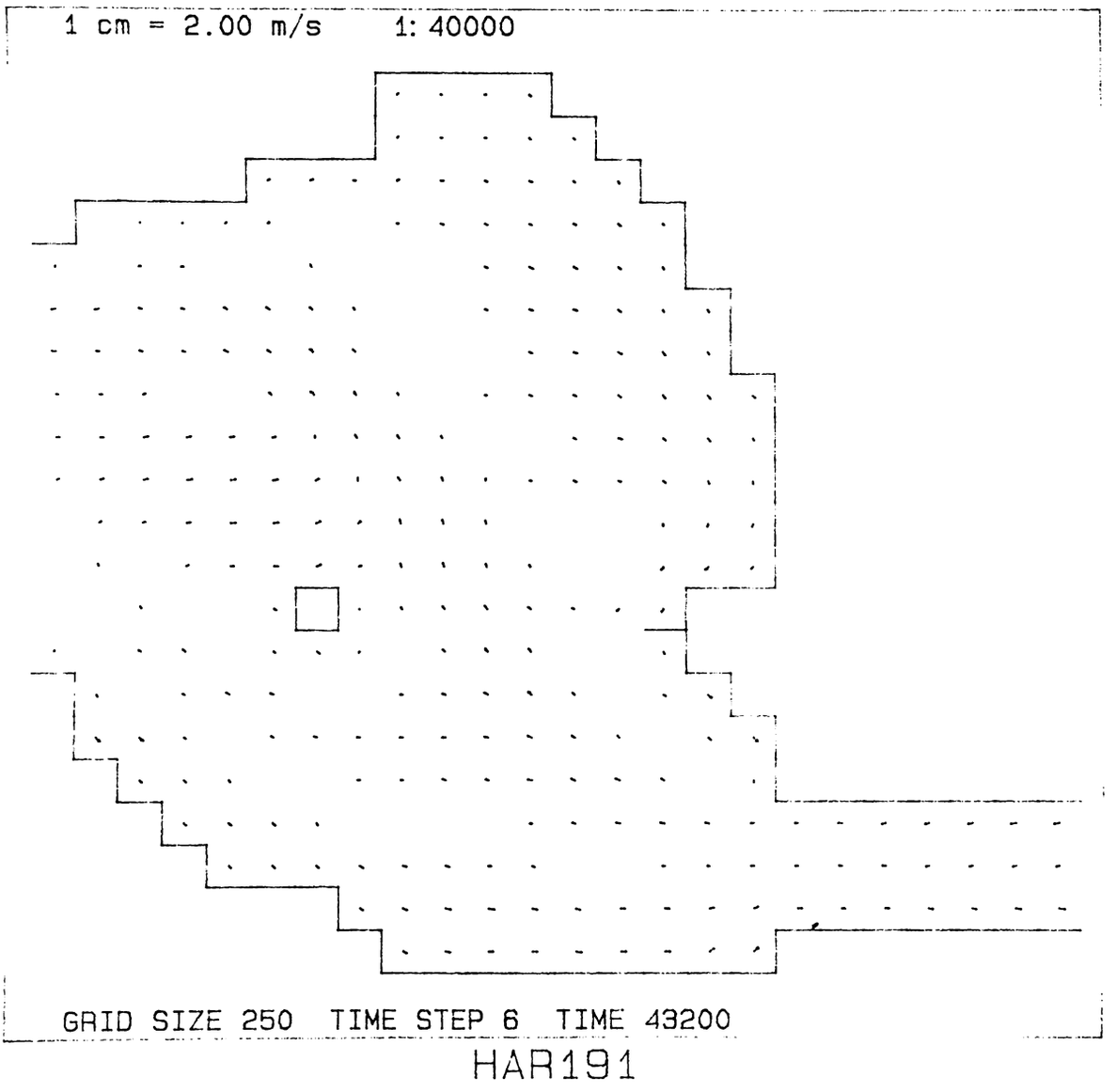

Figure 10.37(1): Flow pattern. Neap tide 12¾ hours after the high tide at 23:15 on 2-Dec-81.

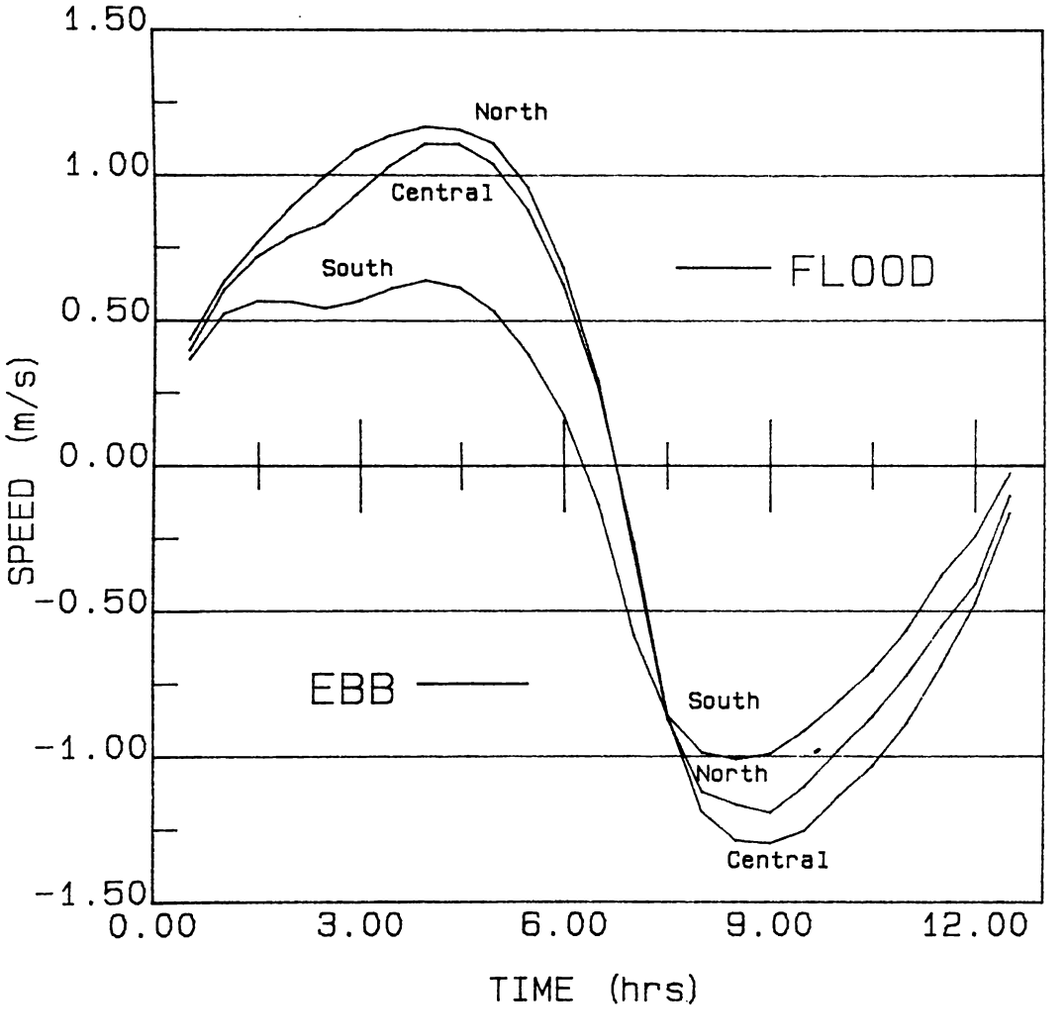

Figure 10.38: Velocity-time curves across the entrance throat at model nodes (J,K) = (18.5,3.5), (18.5,4.5), (18.5,5.5) for the Spring tide simulation of 14-Dec-81.

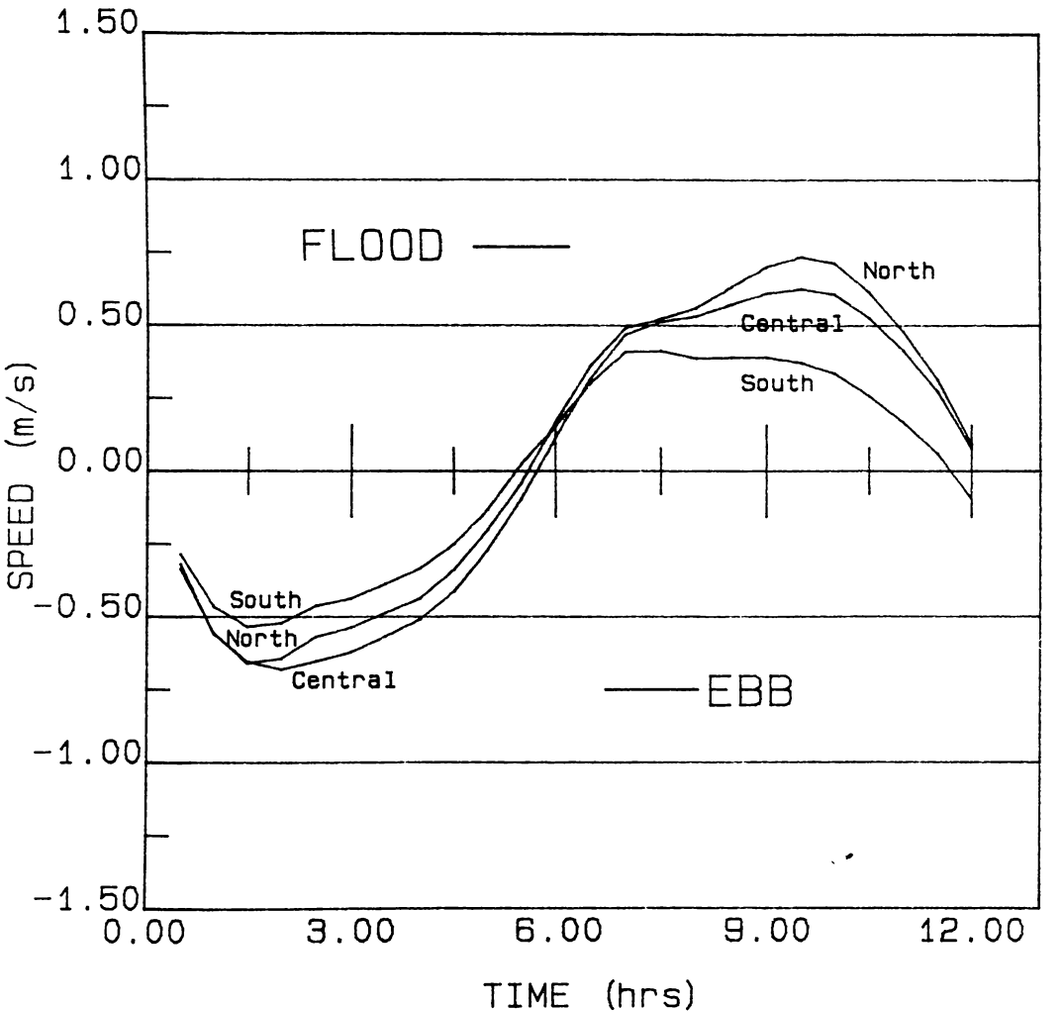

Figure 10.39: Velocity-time curves across the entrance throat at model nodes (J,K) = (18.5,3.5), (18.5,4.5), (18.5,5.5) for the Neap tide simulation of 3-Dec-81.

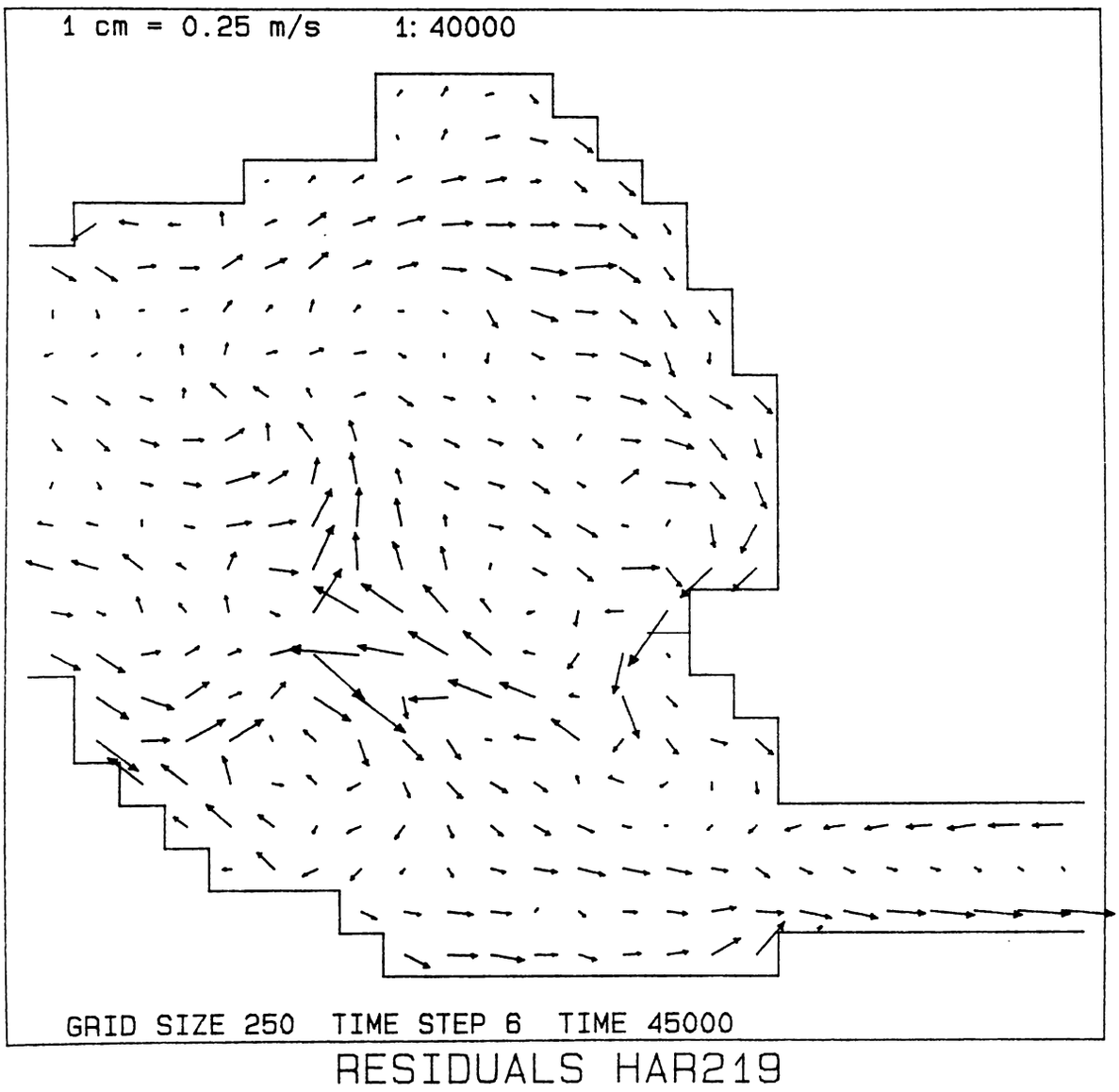

Figure 10.40: Tidal cycle residual velocities for the Spring tide simulation on 14-Dec-81 with ebb and flood velocities scaled to the common tidal range of 2.6m.

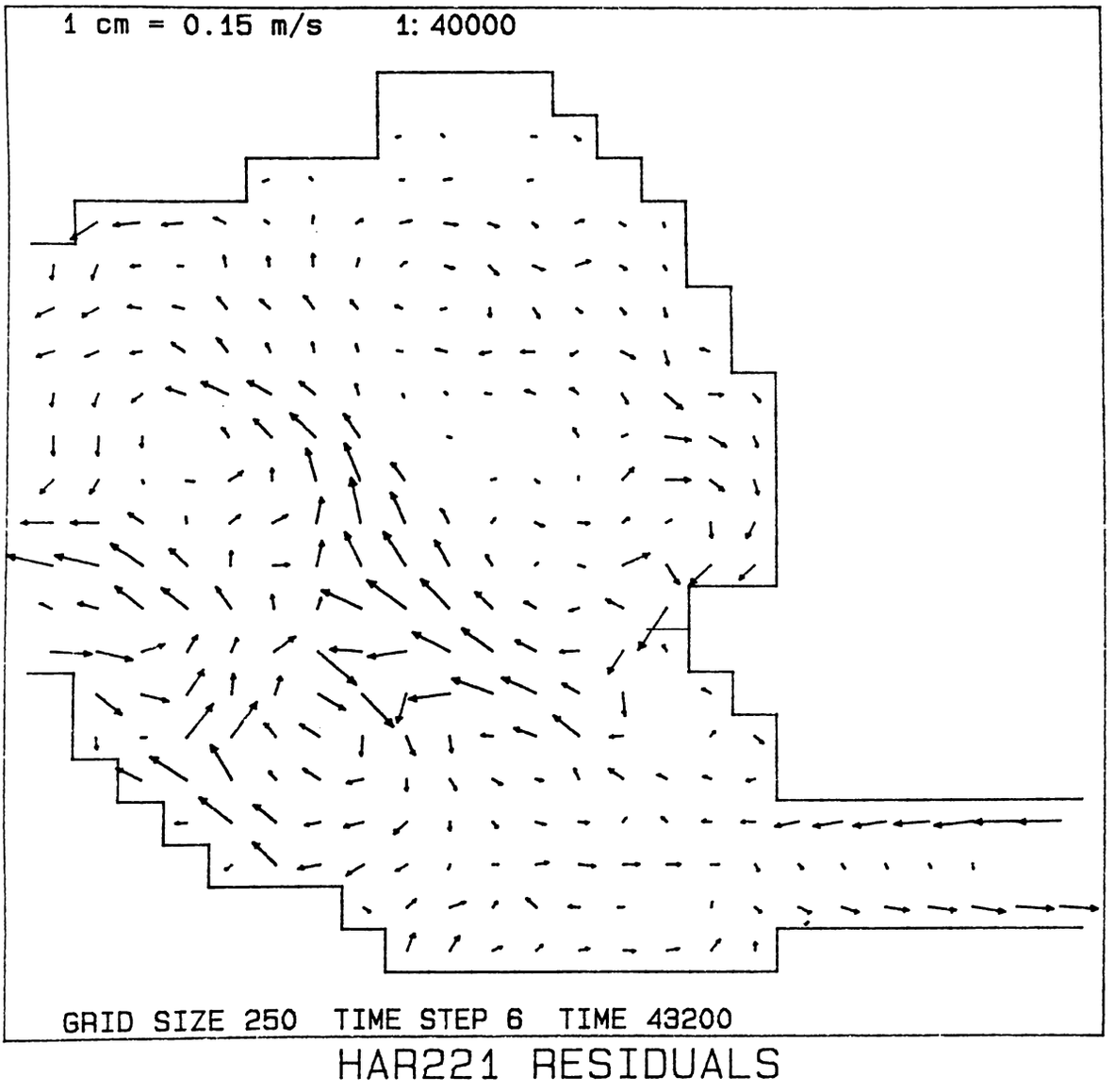

Figure 10.41: Tidal cycle residual velocities for the Neap tide simulation on 3-Dec-81 with ebb and flood velocities scaled to the common tidal range of 1.6m.

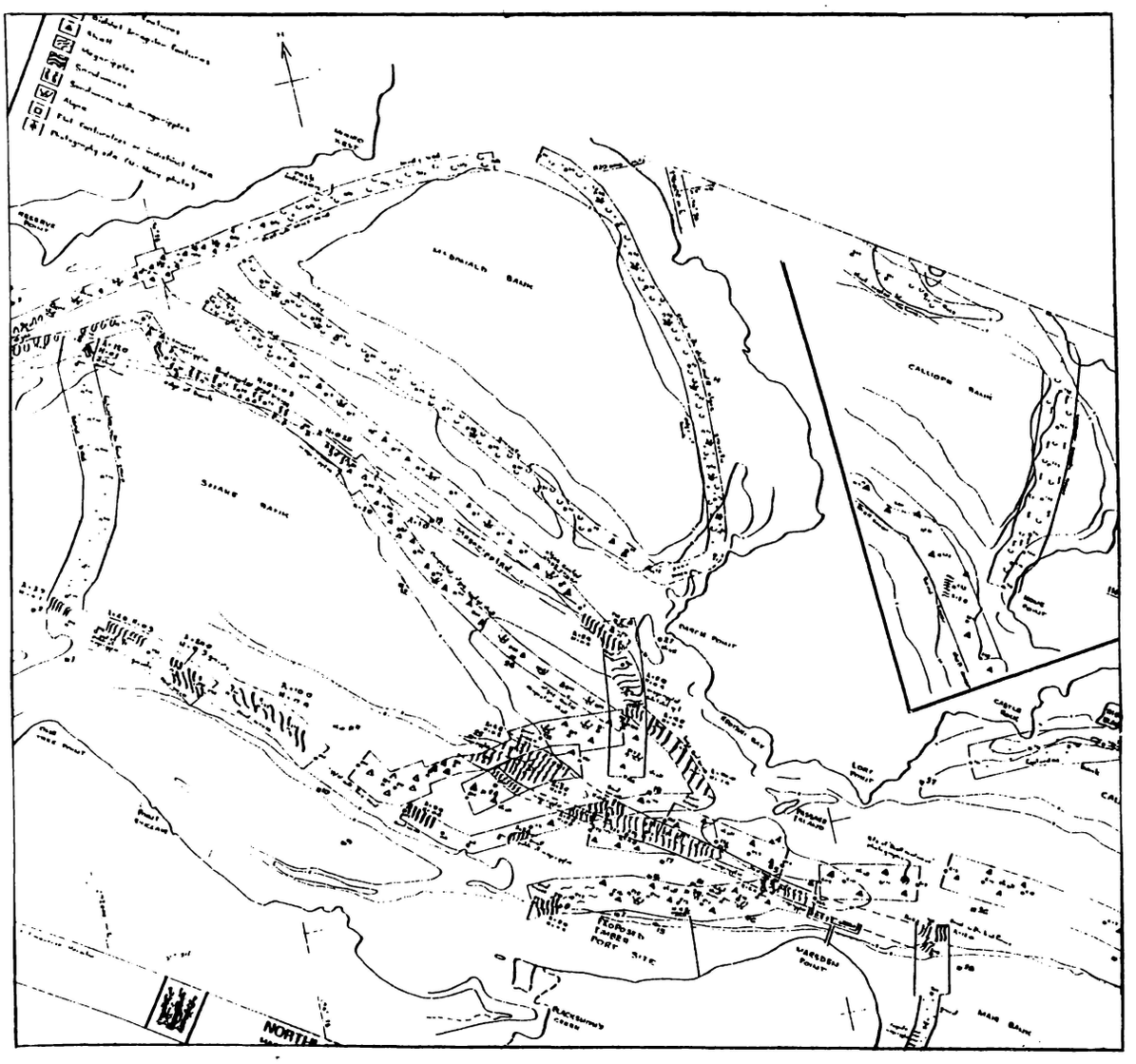

Figure 10.42: Side-scan sonar map of Whangarei Harbour (Figure 2.7) reduced to the scale of 1:40,000 to be used as an overlay.

Figure 10.42: Side-scan sonar overlay

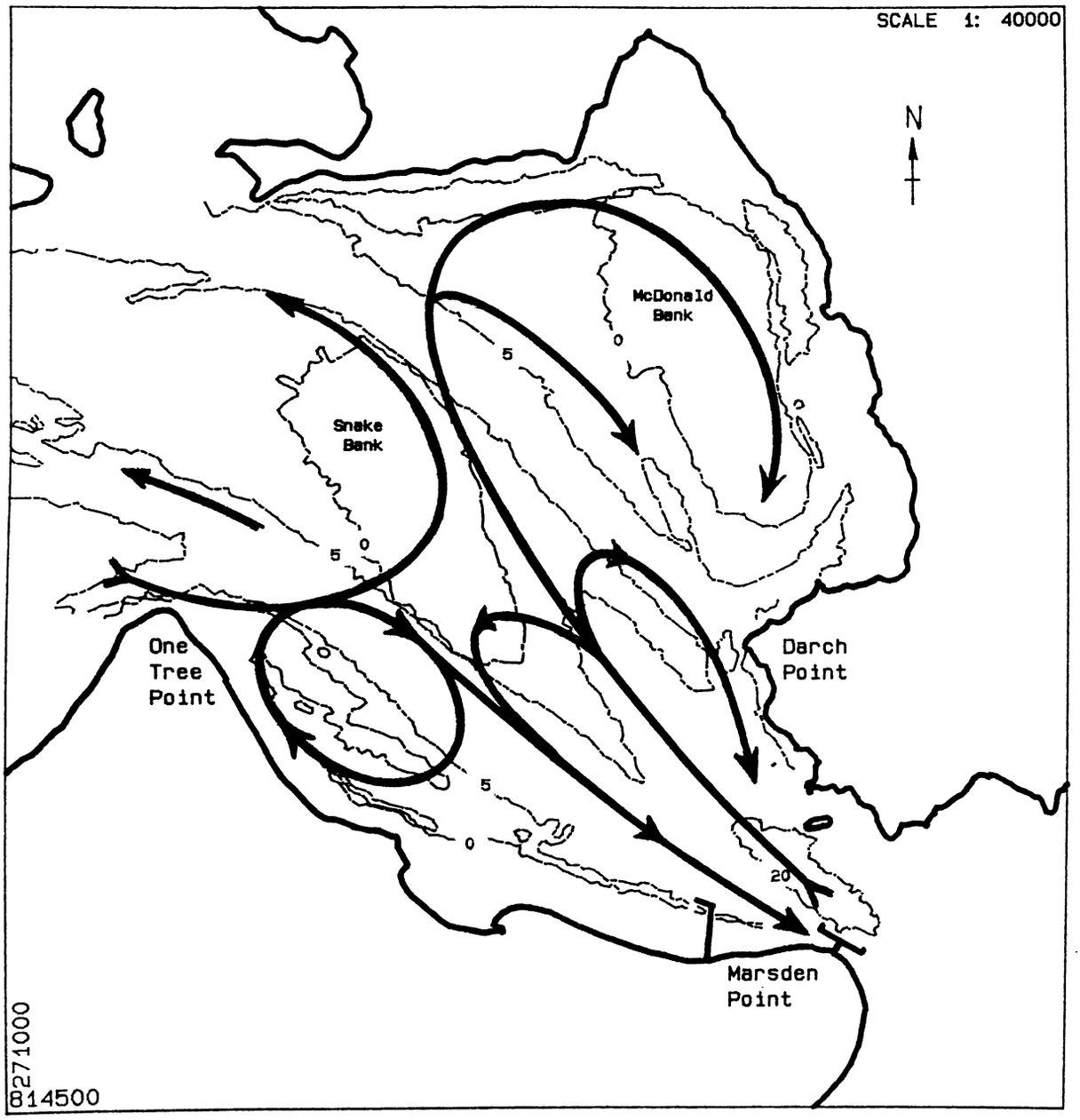

Figure 10.43: Schematic diagram showing sediment transport loops and pathways revealed by the residual velocities and distances from the 2-dimensional model of Whangarei Harbour in conjunction with field measurements.

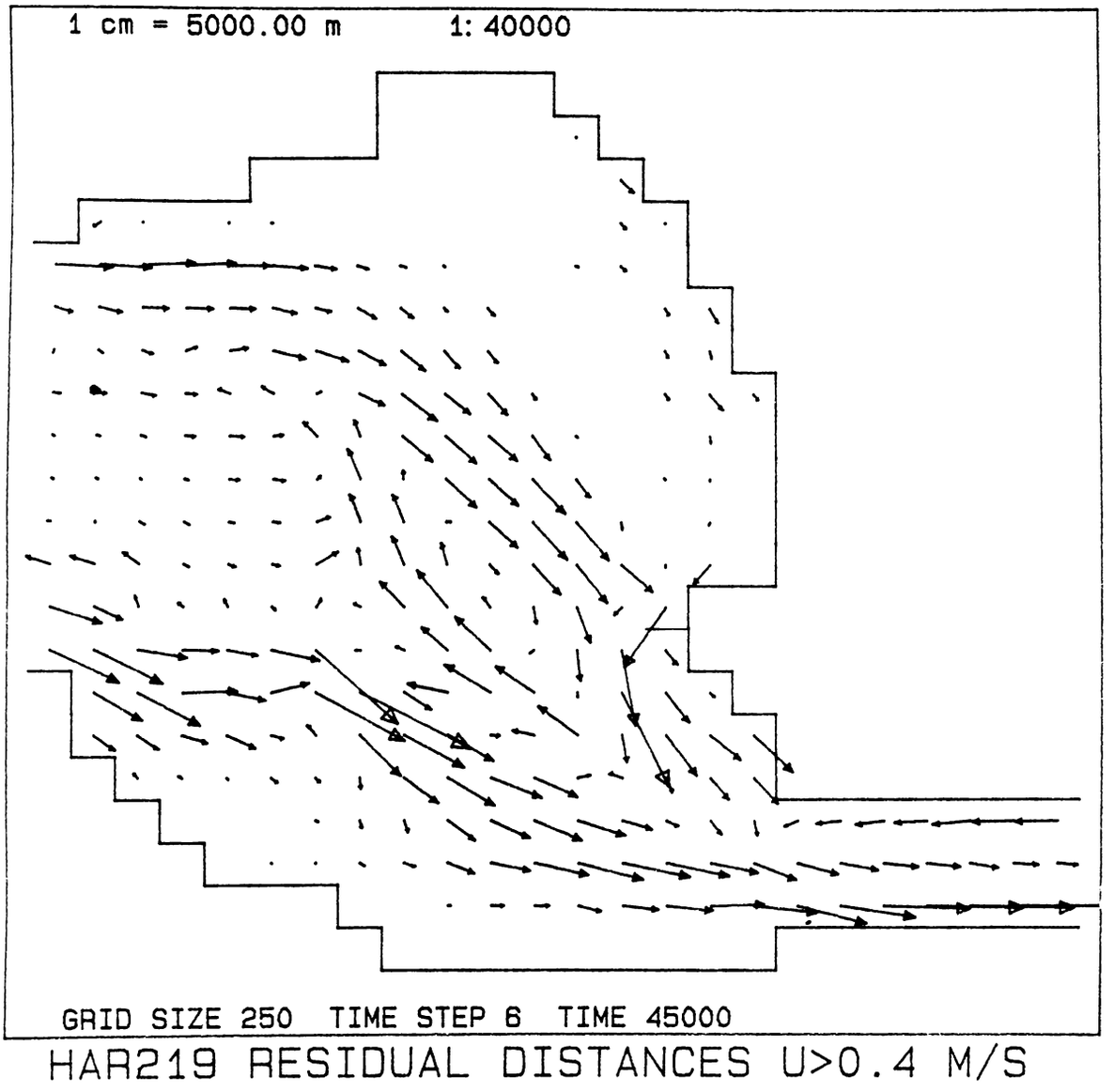

Figure 10.44: Tidal cycle residual distances for velocities greater than 0.4 $m.s^{-1}$. Spring tide simulation on 14-Dec-81 with ebb and flood velocities scaled to the common tidal range of 2.6m.

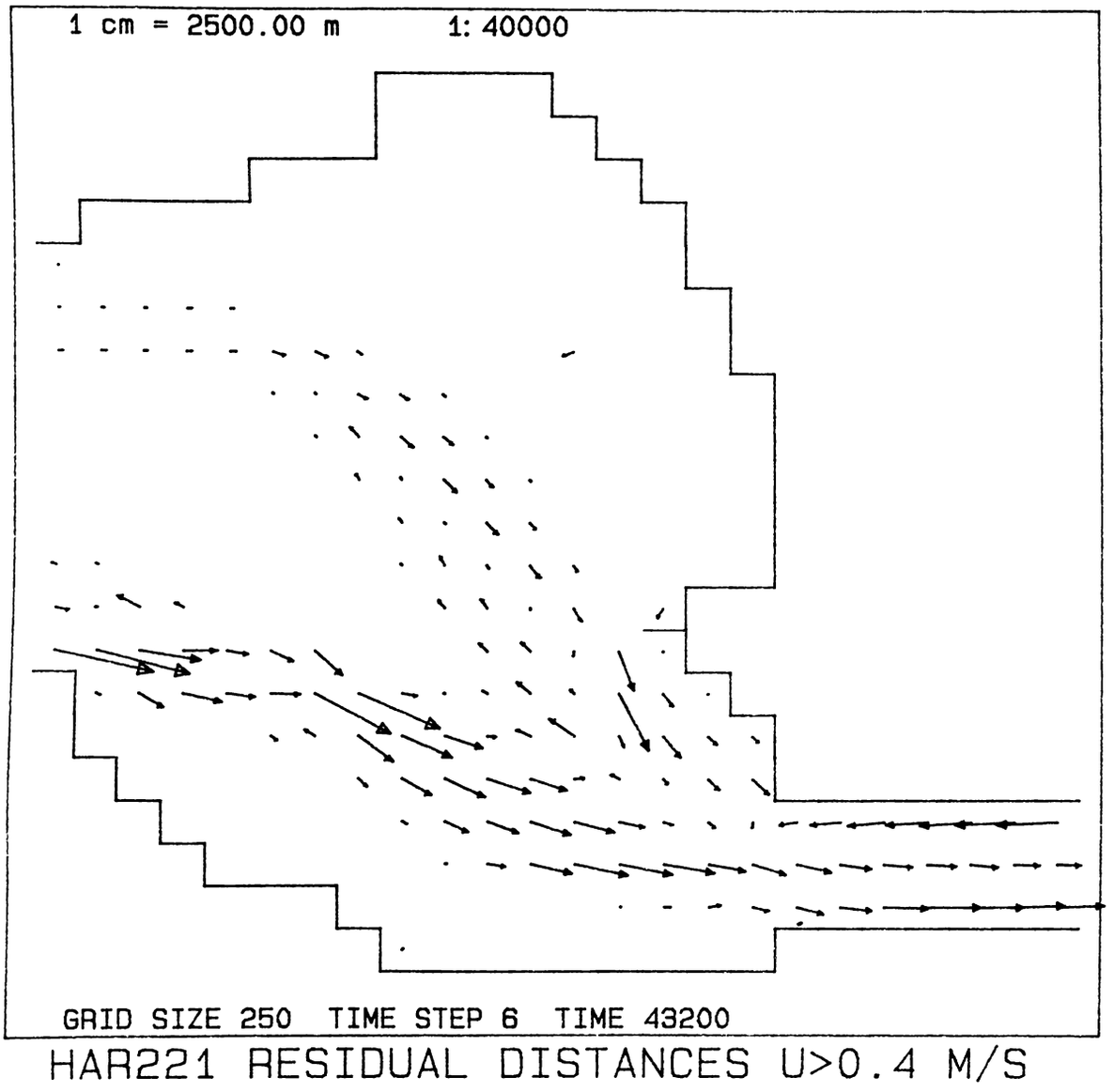

Figure 10.45: Tidal cycle residual distances for velocities greater than 0.4 $m.s^{-1}$. Neap tide simulation on 3-Dec-81 with ebb and flood velocities scaled to the common tidal range of 1.6m.

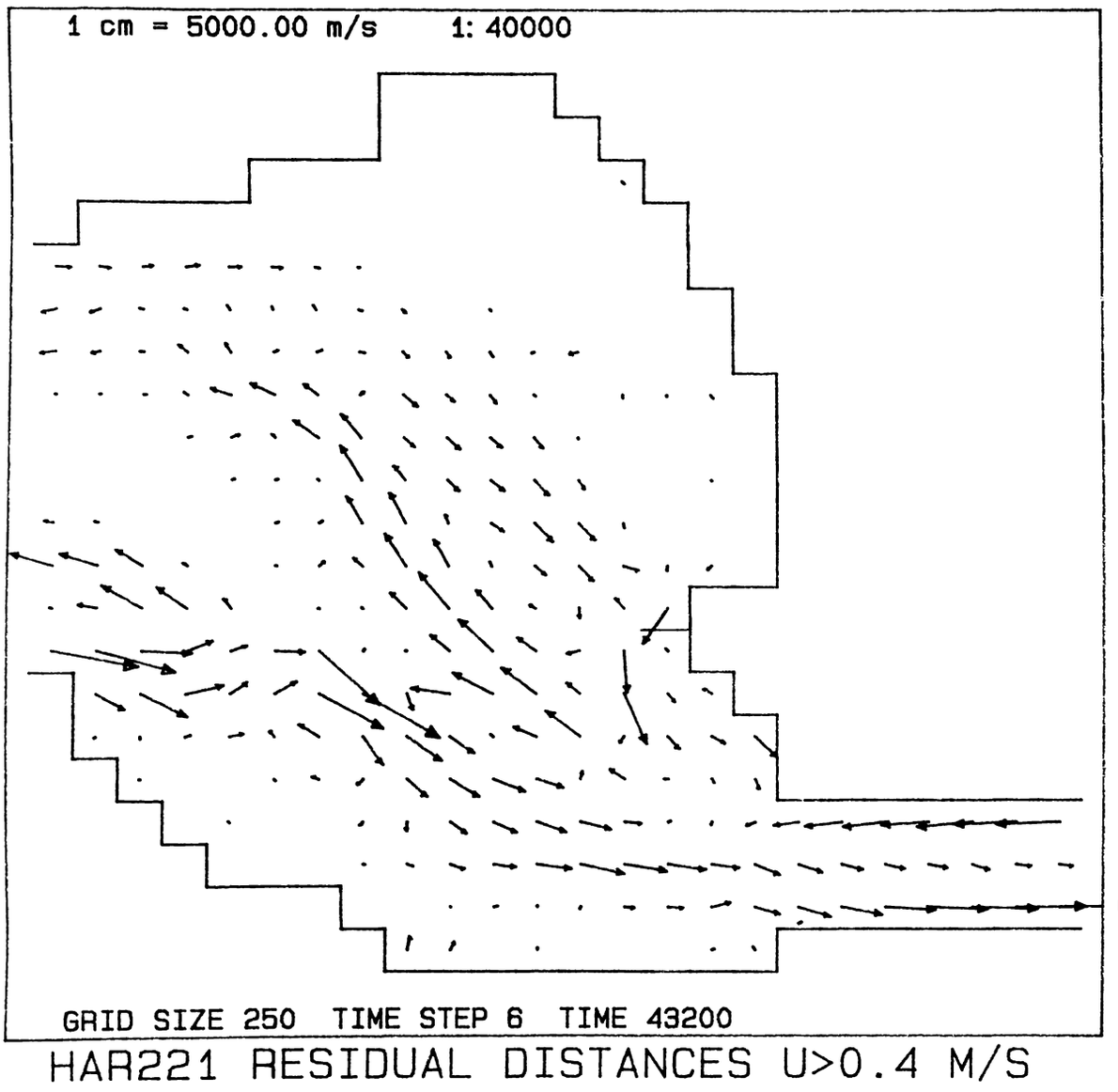

Figure 10.46: Tidal cycle residual distances for velocities greater than 0.4 $m.s^{-1}$. Neap tide simulation on 3-Dec-81 with ebb and flood velocities scaled to the common Spring tidal range of 2.6m.

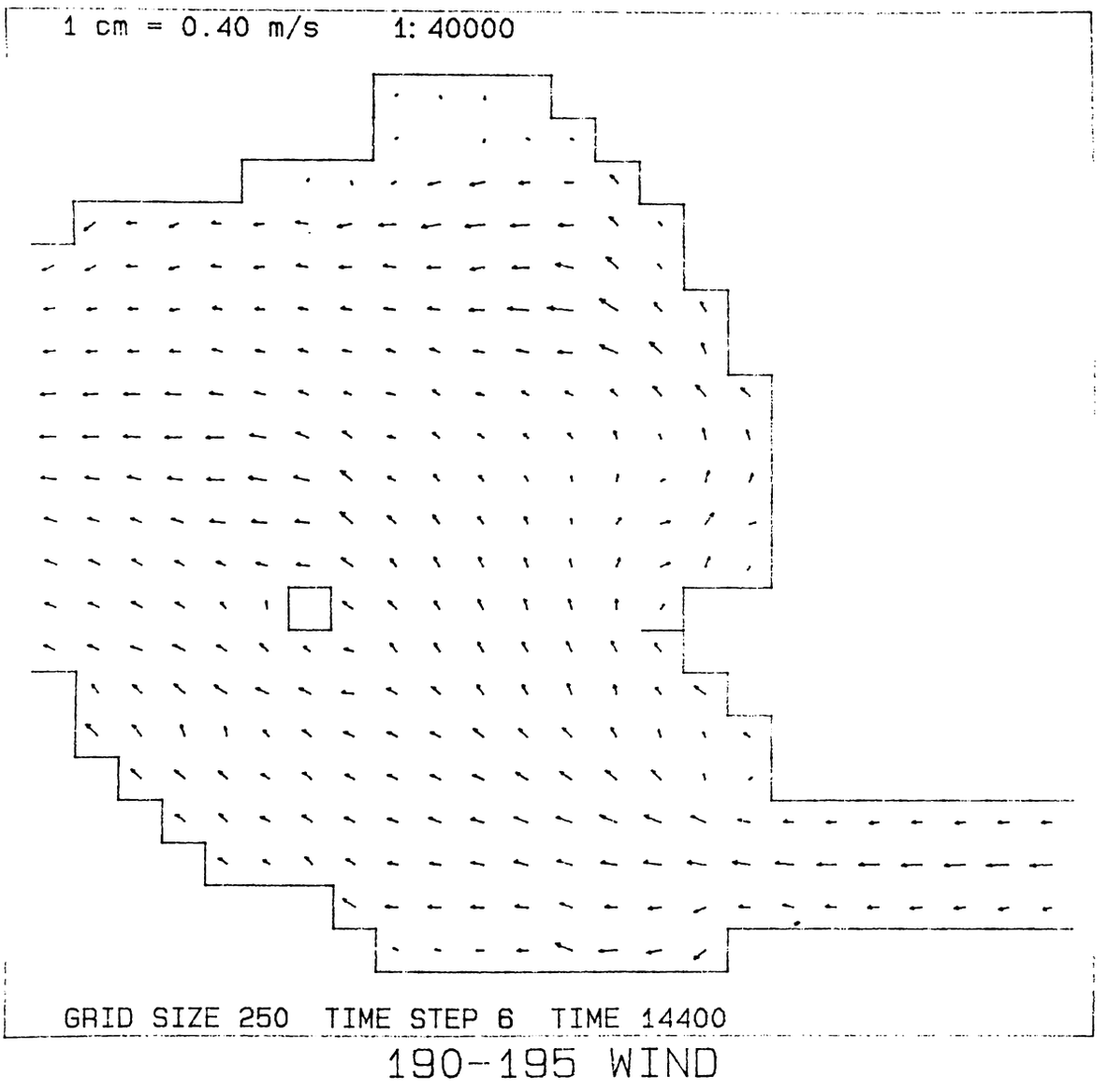

Figure 10.47: Vector velocity differences during the Spring flood tide after introduction of a 10 $m.s^{-1}$ wind from 101°T. Flood currents are faster with the supporting wind.

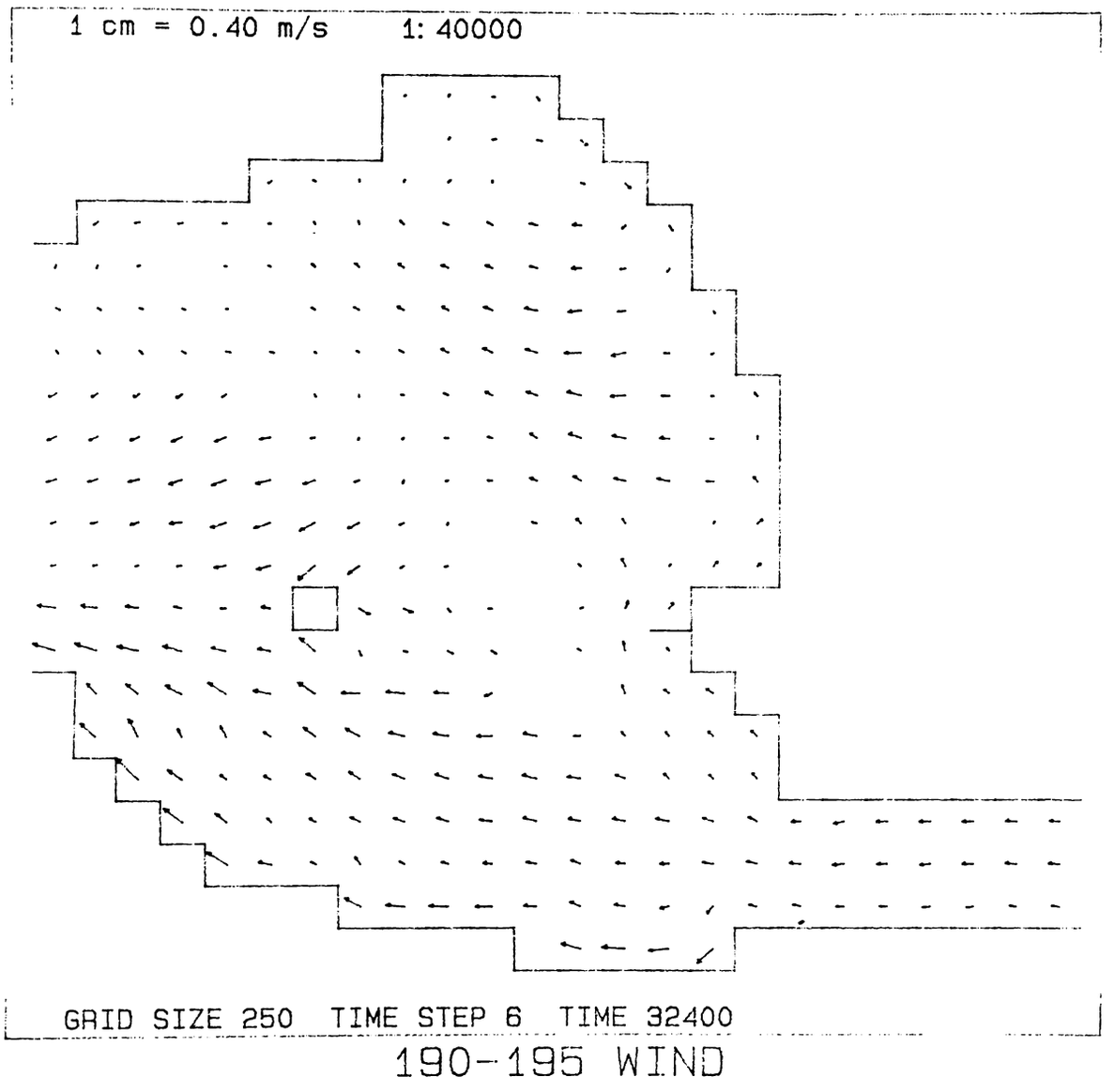

Figure 10.48: Vector velocity differences during the Spring ebb tide after introduction of a 10 $m.s^{-1}$ wind from 101° T. Ebb currents are slower with the opposing wind.

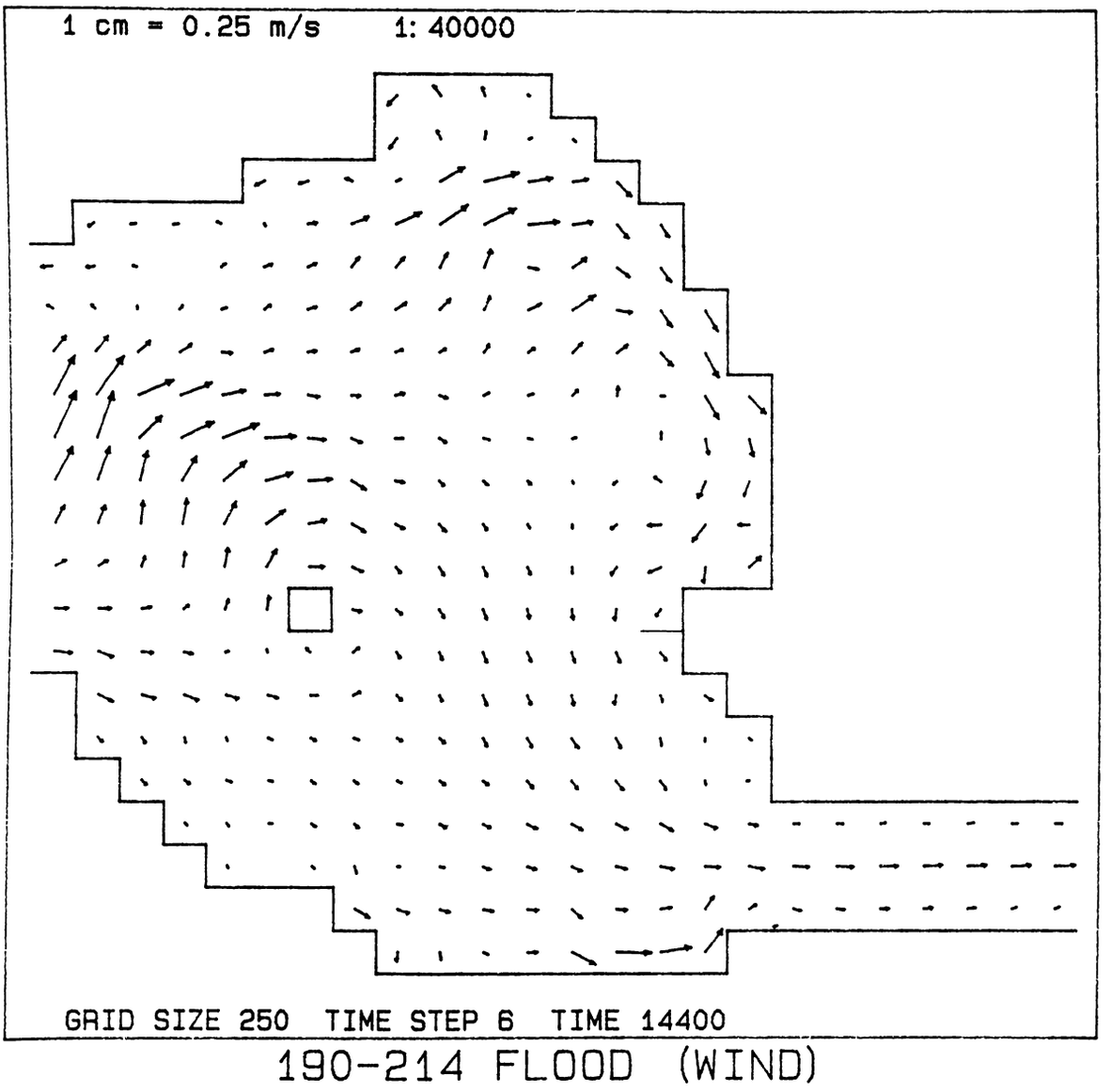

Figure 10.49: Vector velocity differences during the Spring flood tide after introduction of a 10 $m.s^{-1}$ wind from 236° T. The wind forces flow across Snake Bank and around McLeods Bay.

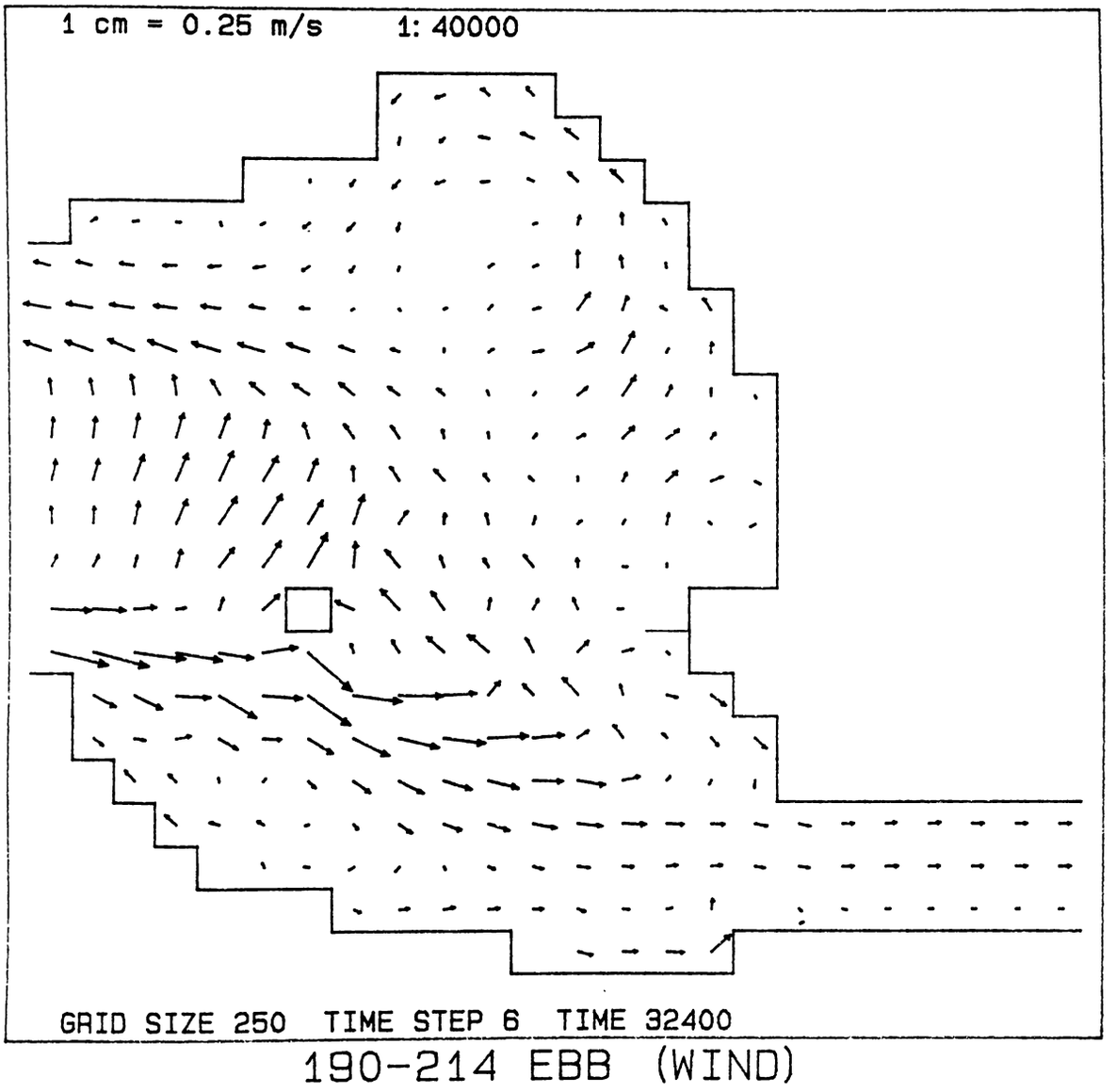

Figure 10.50: Vector velocity differences during the Spring ebb tide after introduction of a 10 $m.s^{-1}$ wind from 236° T. The wind forces flow across Snake Bank and accelerates currents in the shipping channel while retarding flow in Shoal Bay.

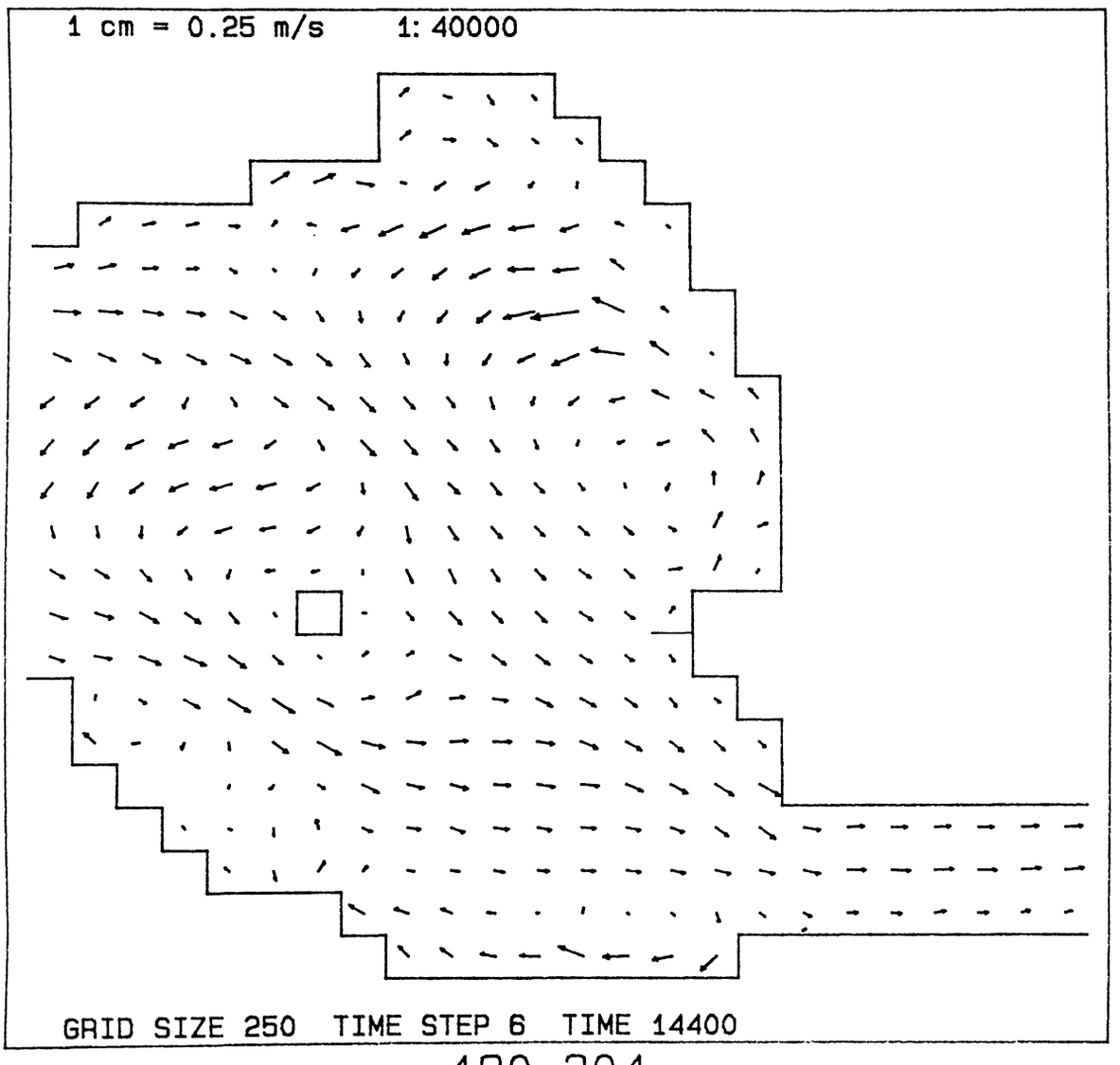

190-204

Figure 10.51: Vector velocity differences during the Spring flood tide after introduction of a 10 $m.s^{-1}$ wind from 110° T. Flow acceleration over the banks causes flood currents to diminish in the channels.

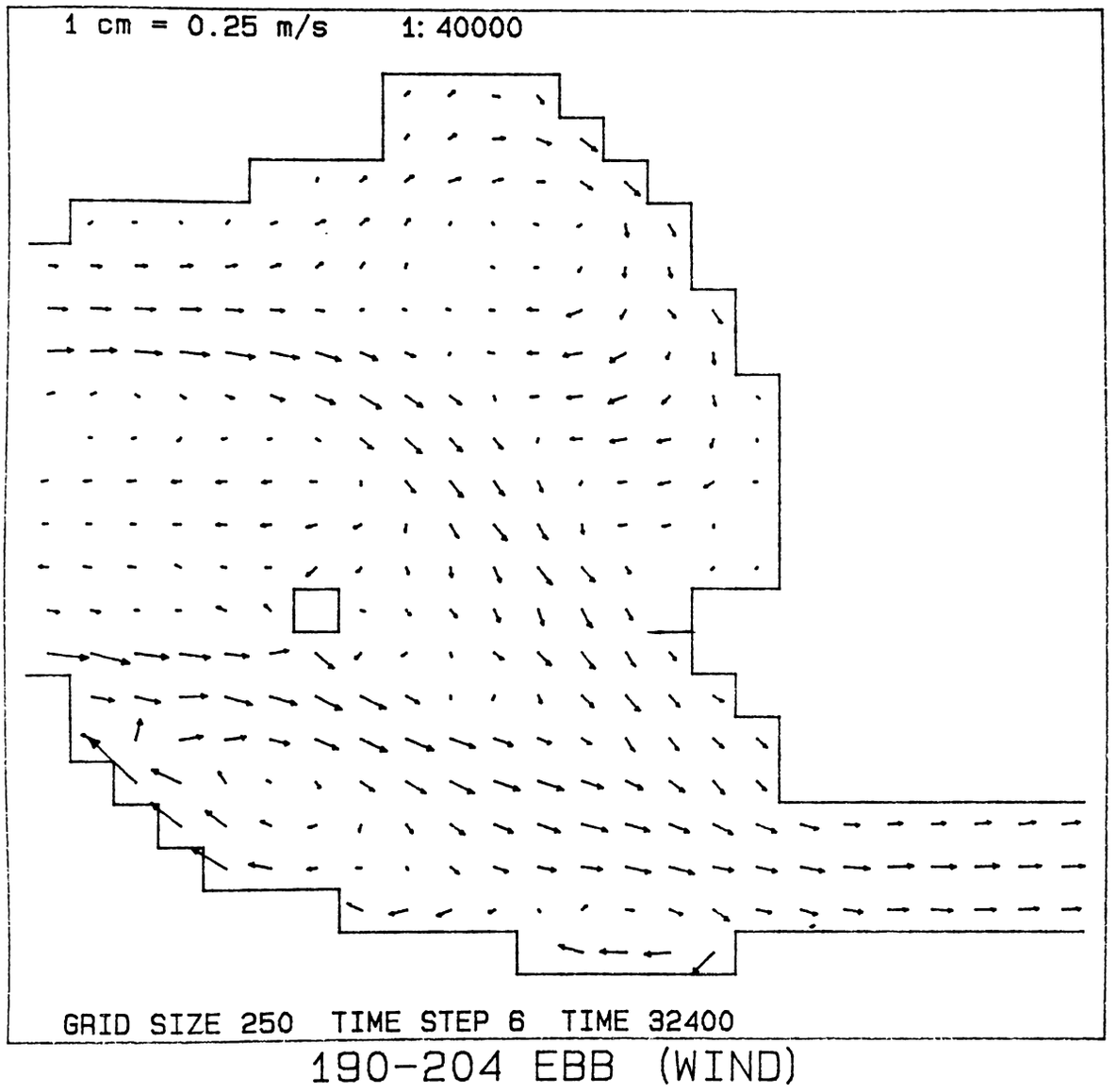

Figure 10.52: Vector velocity differences during the Spring ebb tide after introduction of a 10 $m.s^{-1}$ wind from 110° T. Flow retardation over the banks causes ebb currents to accelerate in the channels.

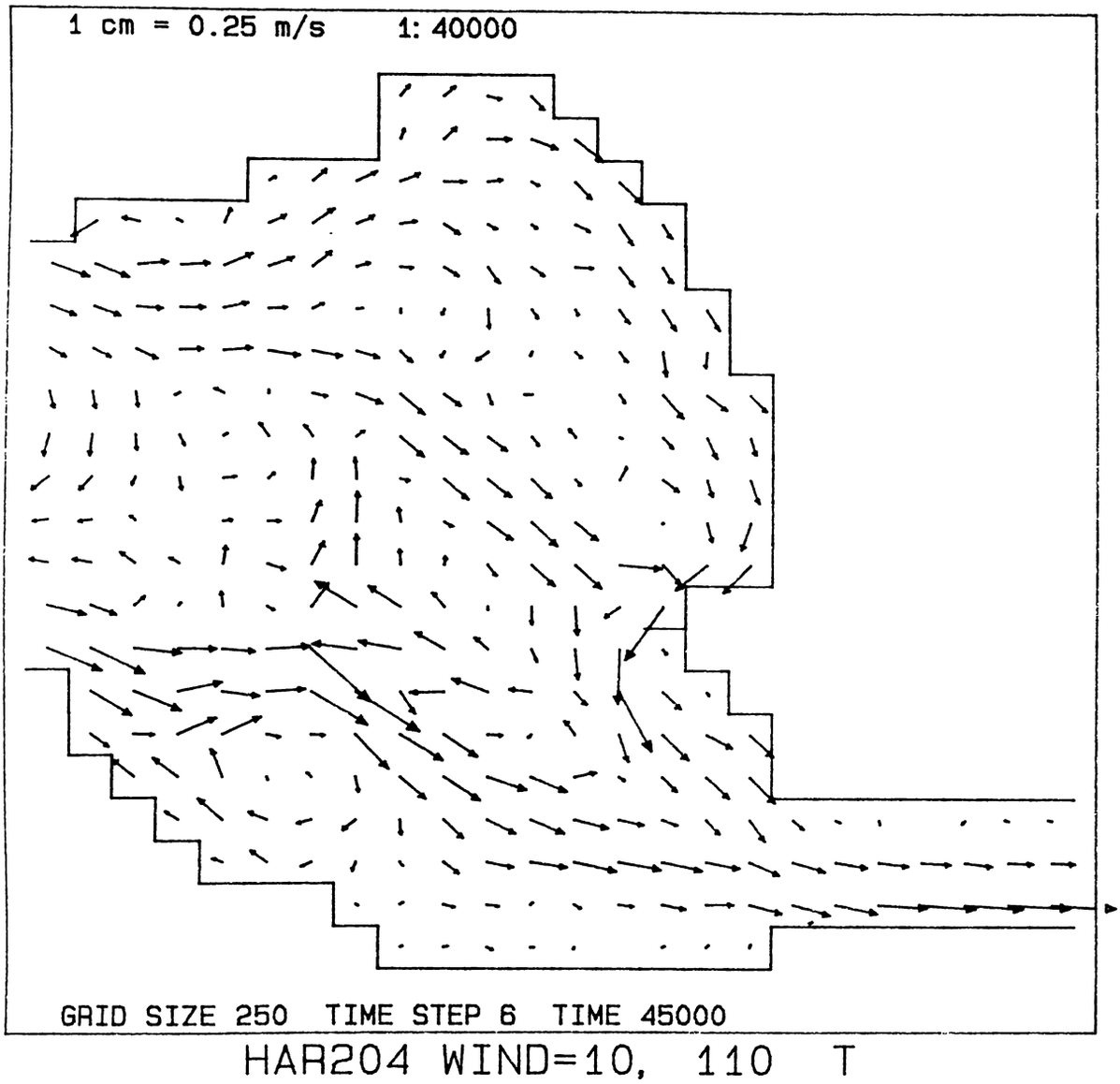

Figure 10.53: Residual velocities during the Spring tide after introduction of a 10 $m.s^{-1}$ wind from 110° T. Note the neutrality on the sand flat at the port site.

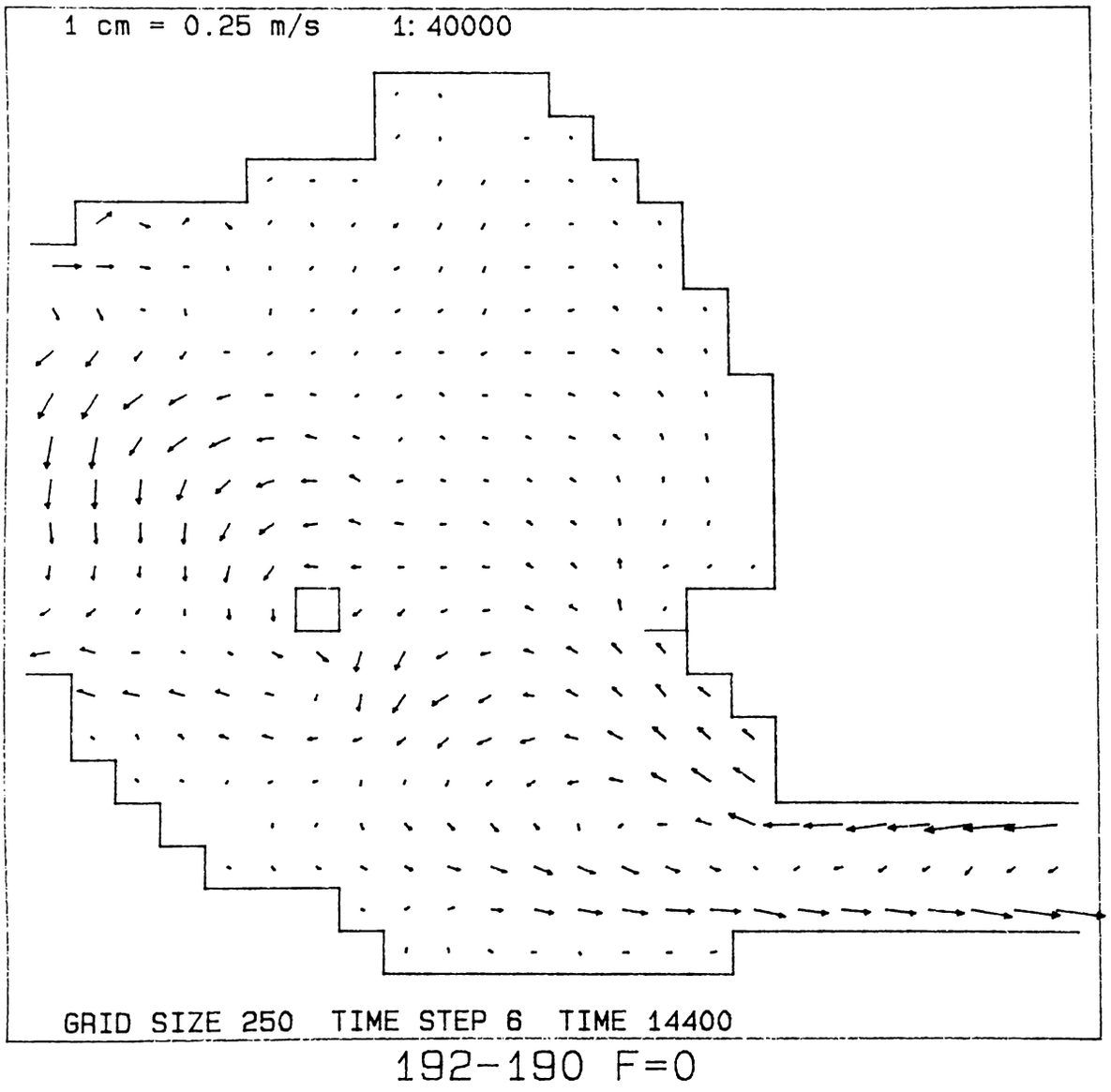

Figure 10.54: Vector velocity differences during the Spring flood tide, after introduction of the Coriolis force. Flow diverts to the left out of the Shoal Bay channel towards the shipping channel.

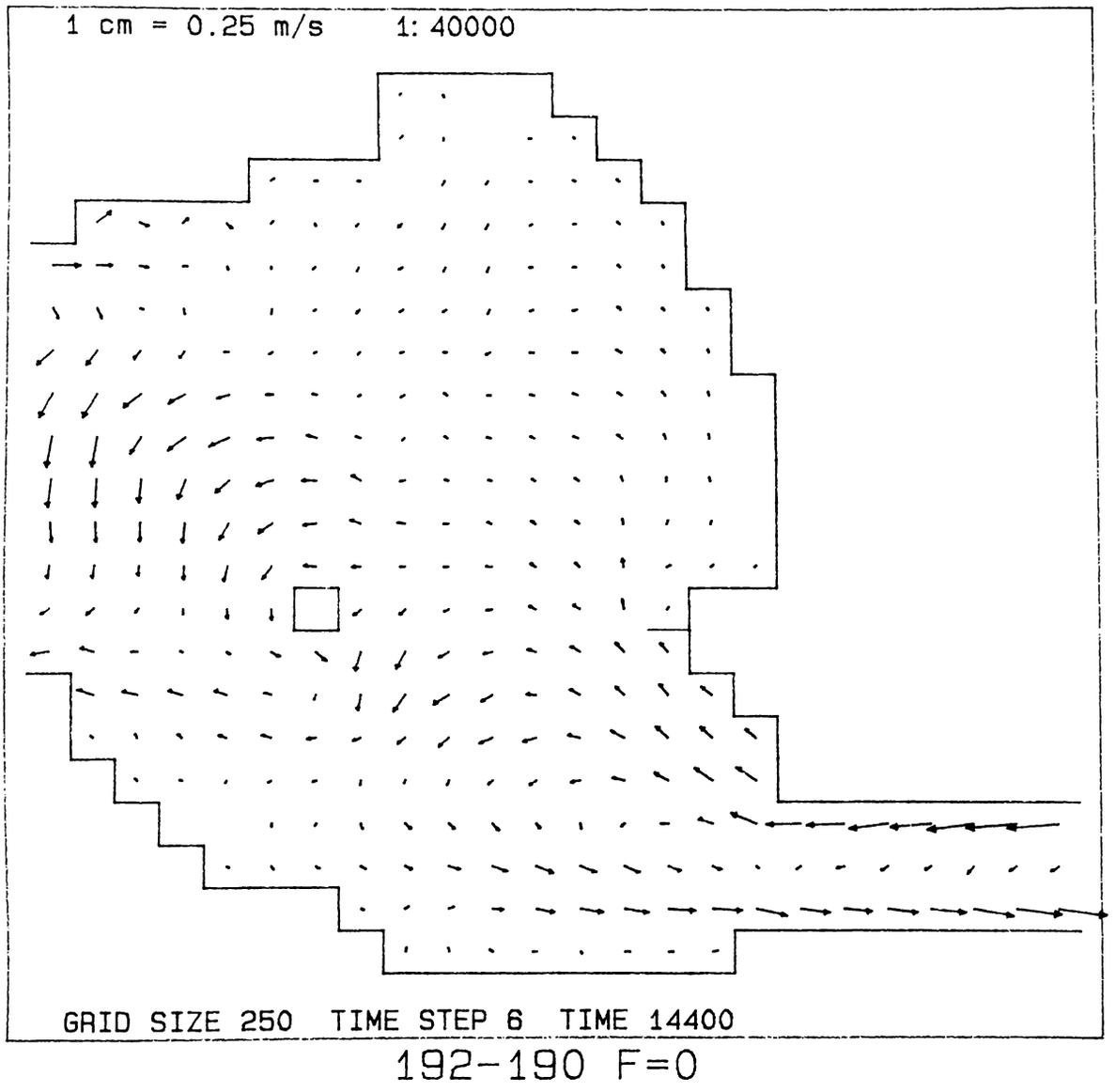

Figure 10.54: Vector velocity differences during the Spring flood tide, after introduction of the Coriolis force. Flow diverts to the left out of the Shoal Bay channel towards the shipping channel.

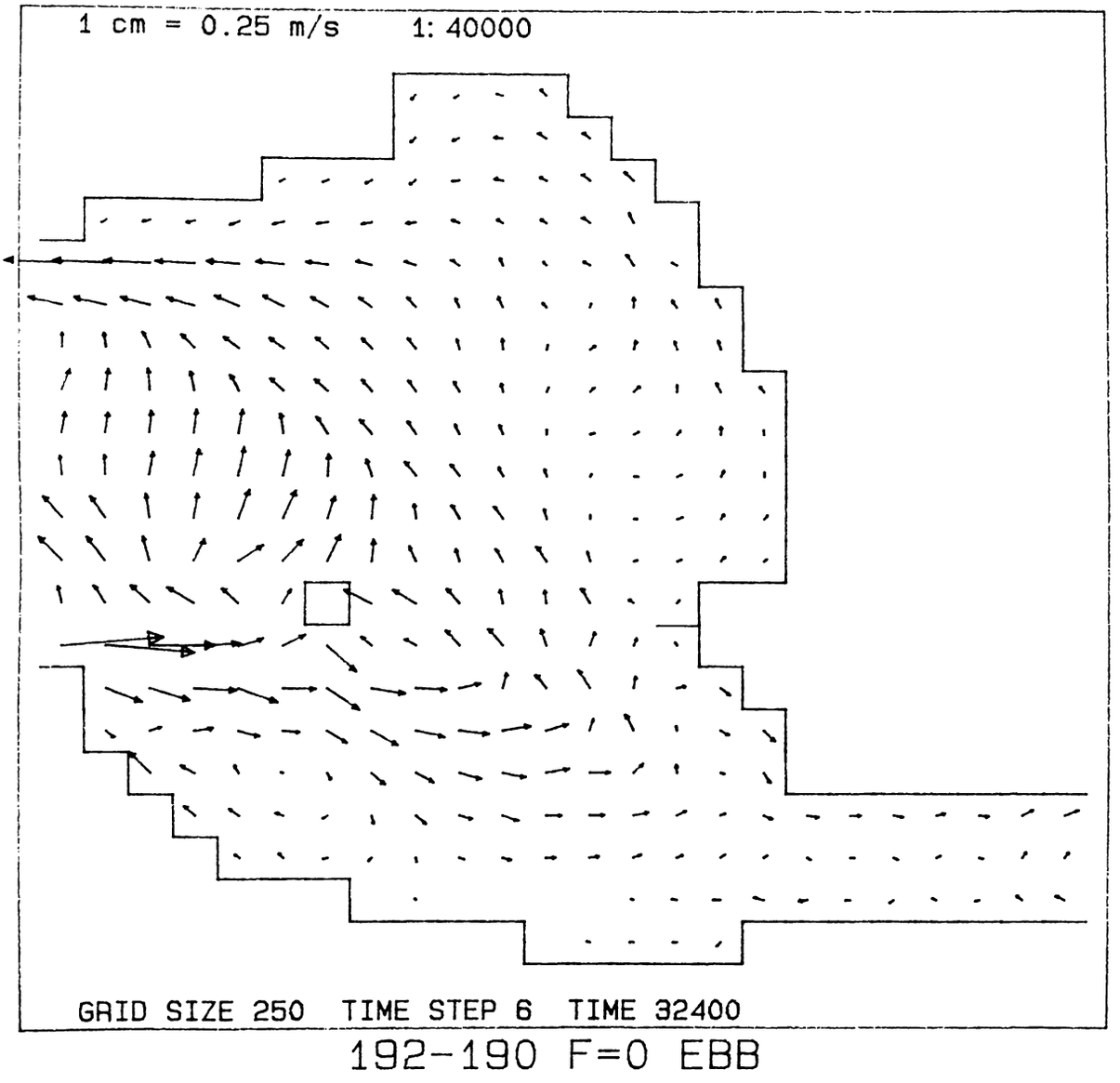

Figure 10.55: Vector velocity differences during the Spring ebb tide after introduction of the Coriolis force. Flow diverts to the left across Snake Bank into the Shoal Bay channel.

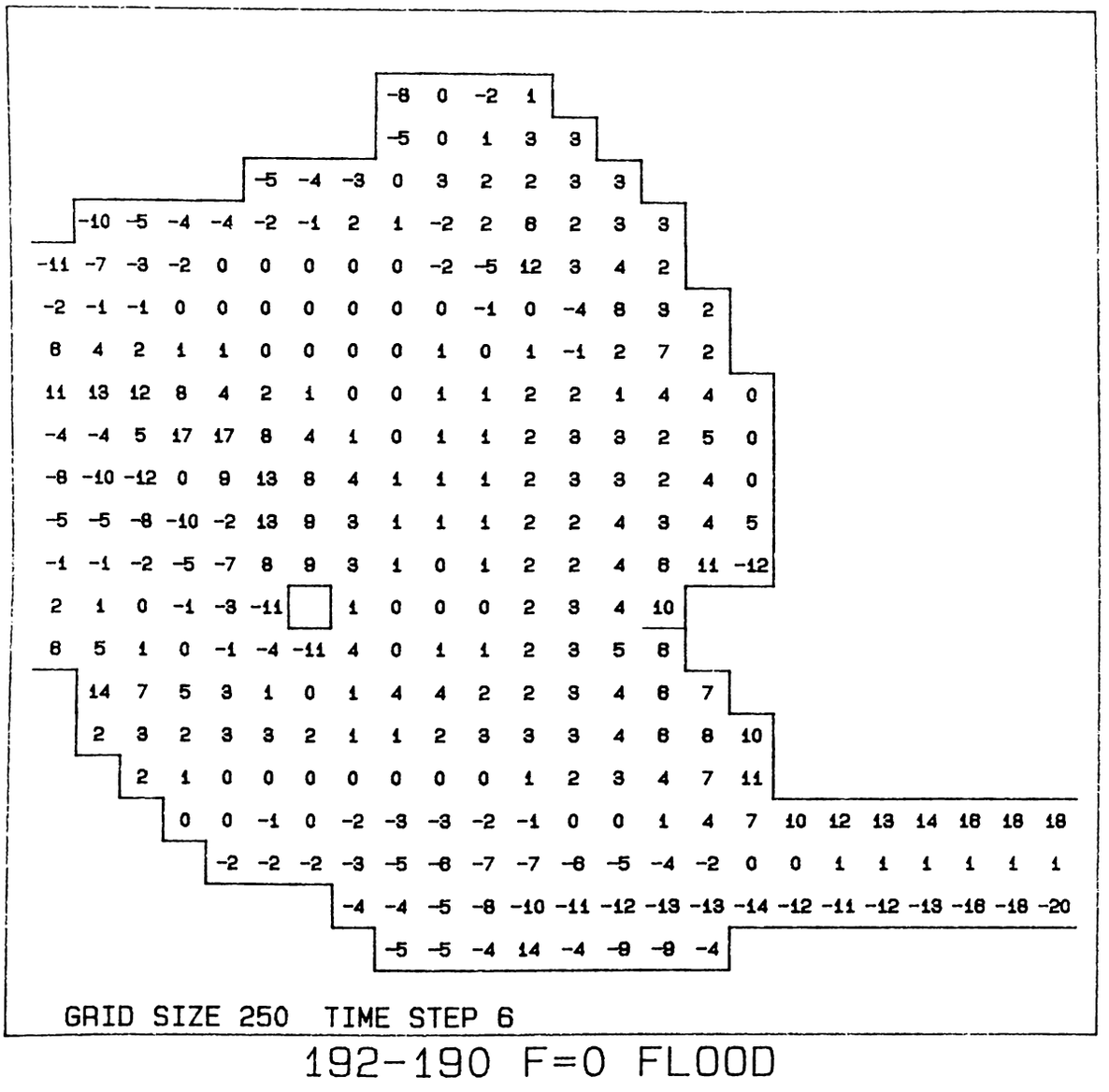

Figure 10.56: Percentage speed differences during the Spring flood tide after introduction of the Coriolis force.

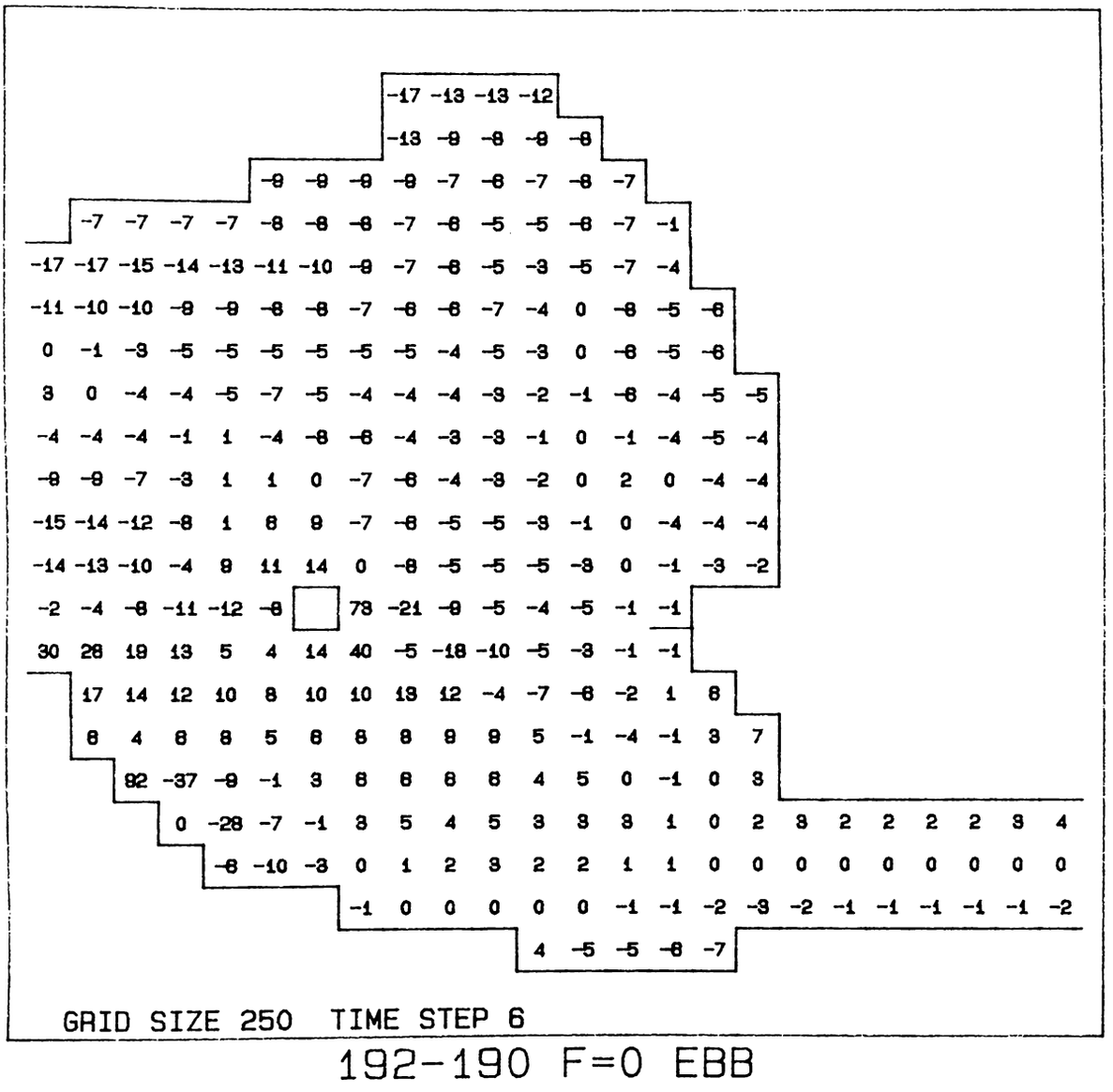

Figure 10.57: Percentage speed differences during the Spring ebb tide after introduction of the Coriolis force.

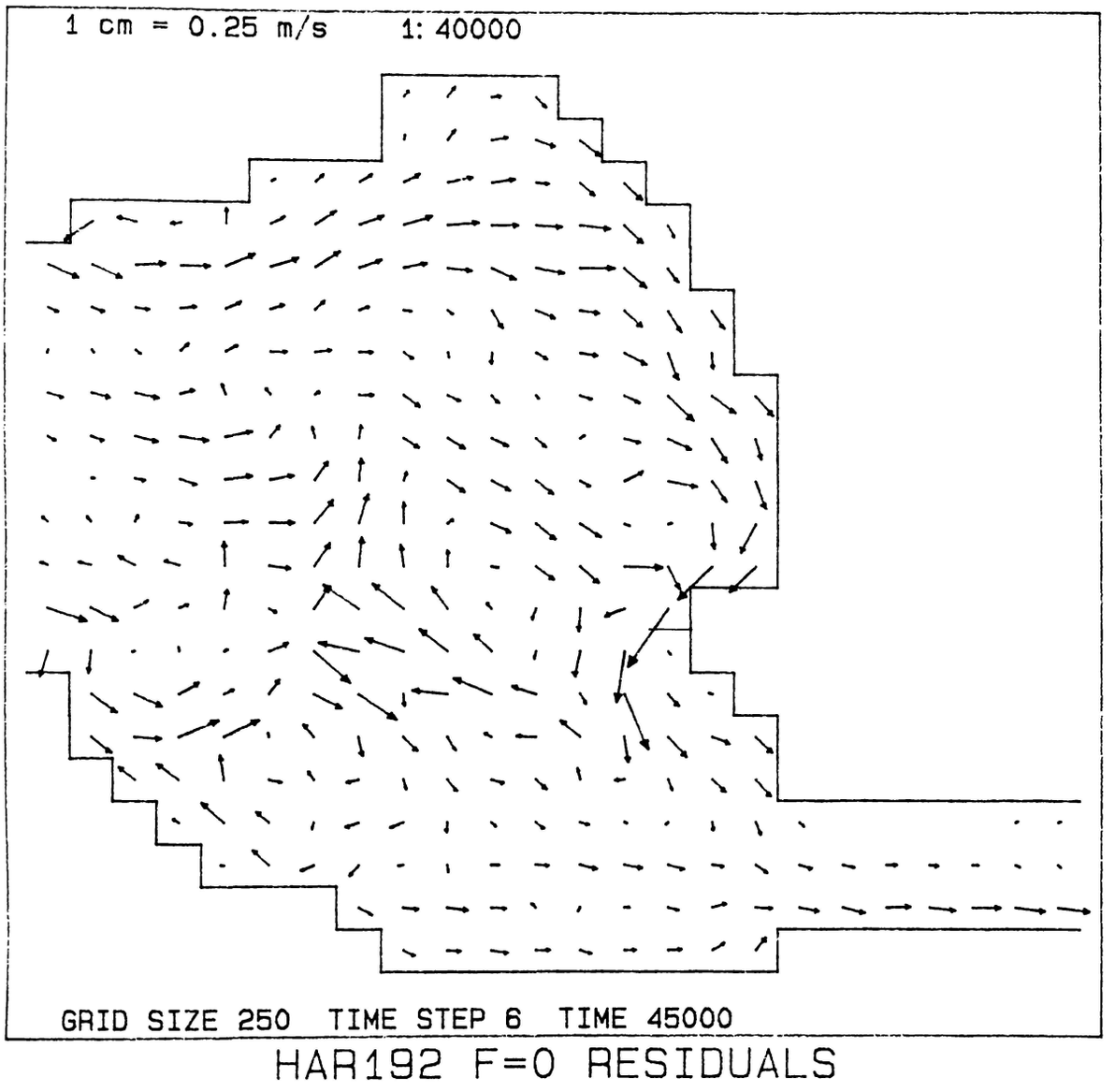

Figure 10.58: Tidal cycle residual velocities with the Coriolis parameter set to zero.

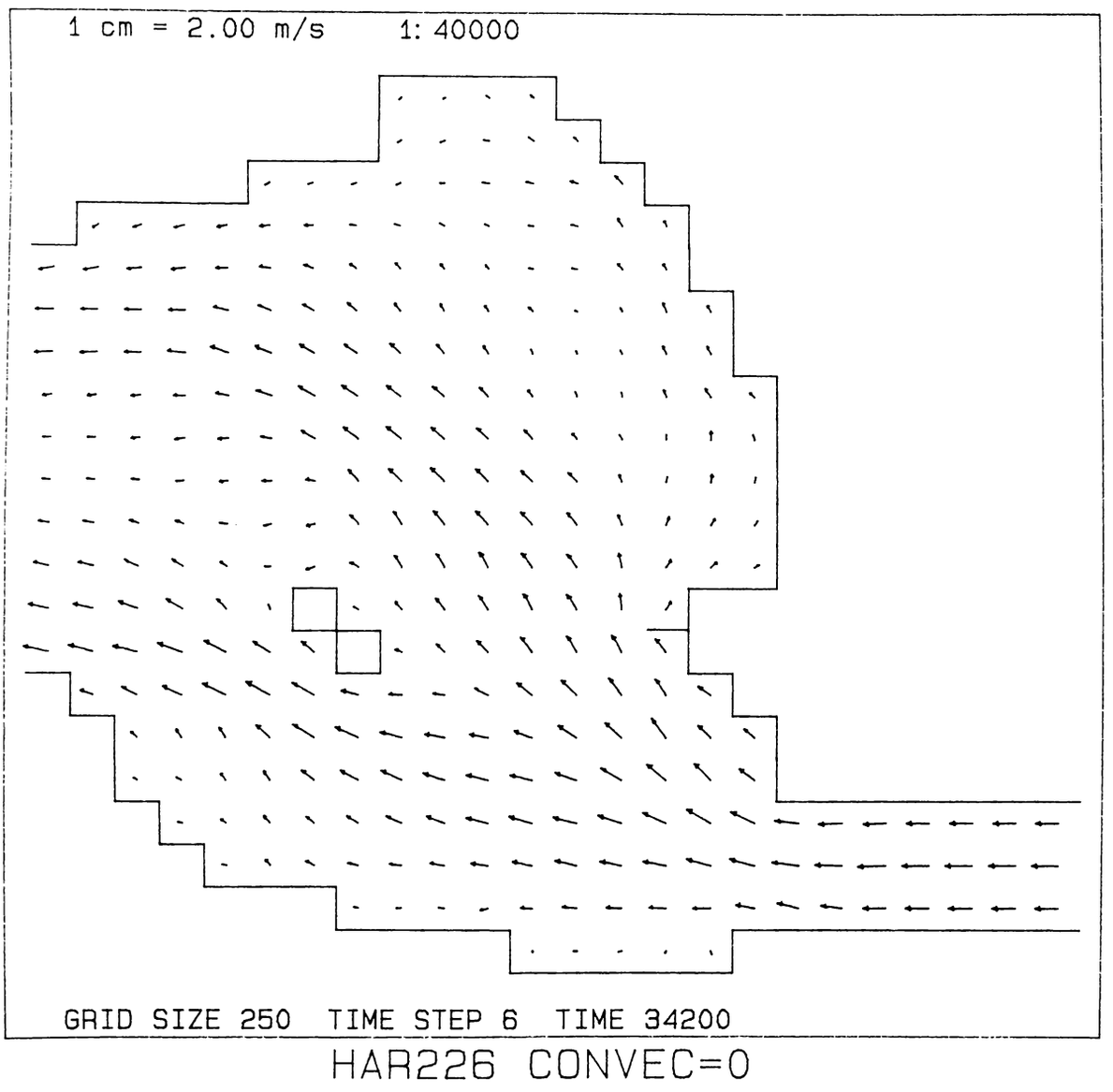

Figure 10.59: Neap tide simulation at peak flood with the convective momenta and Coriolis acceleration terms neglected.

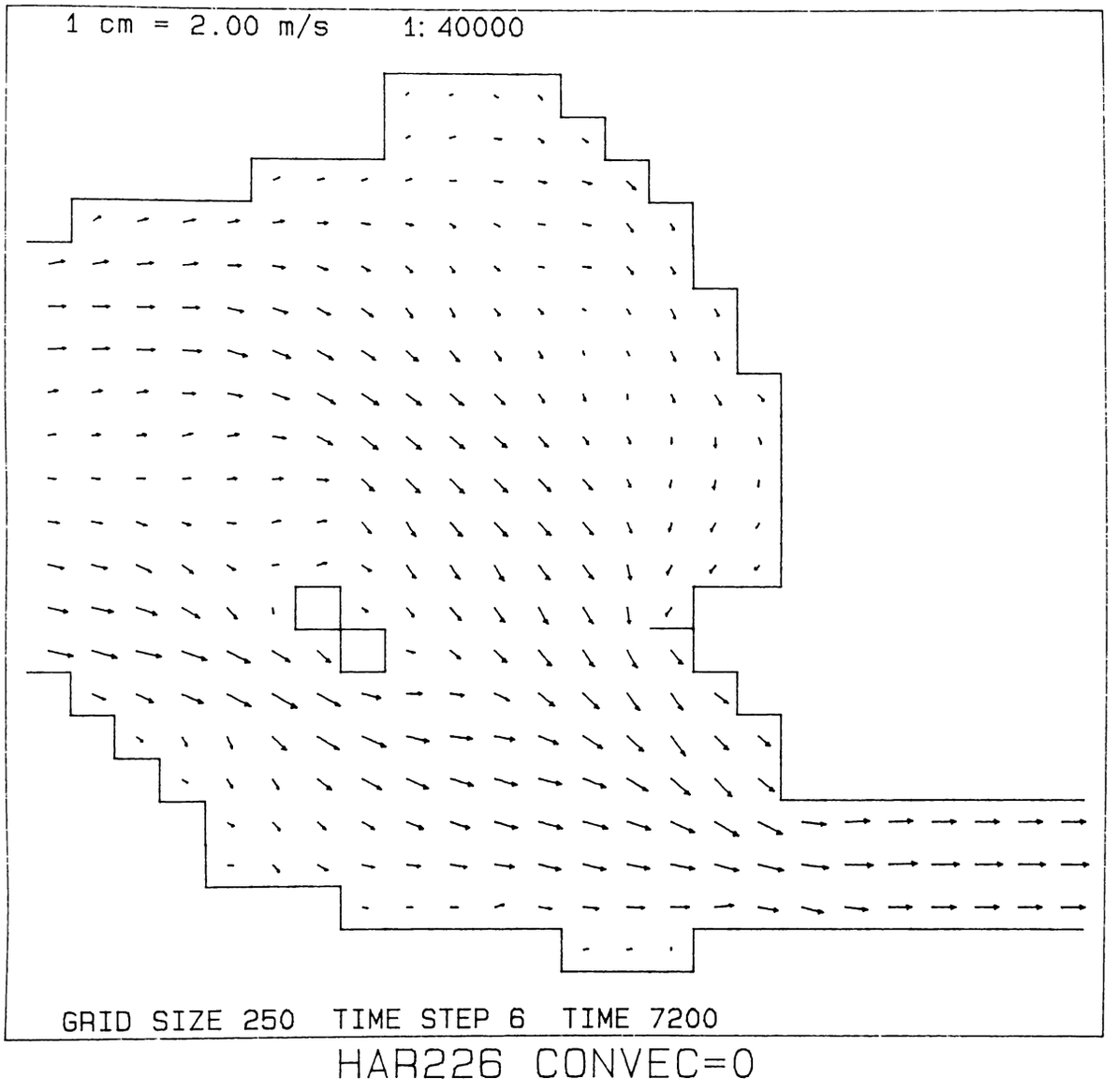

Figure 10.60: Neap tide simulation at peak ebb with the convective momenta and Coriolis acceleration terms neglected.

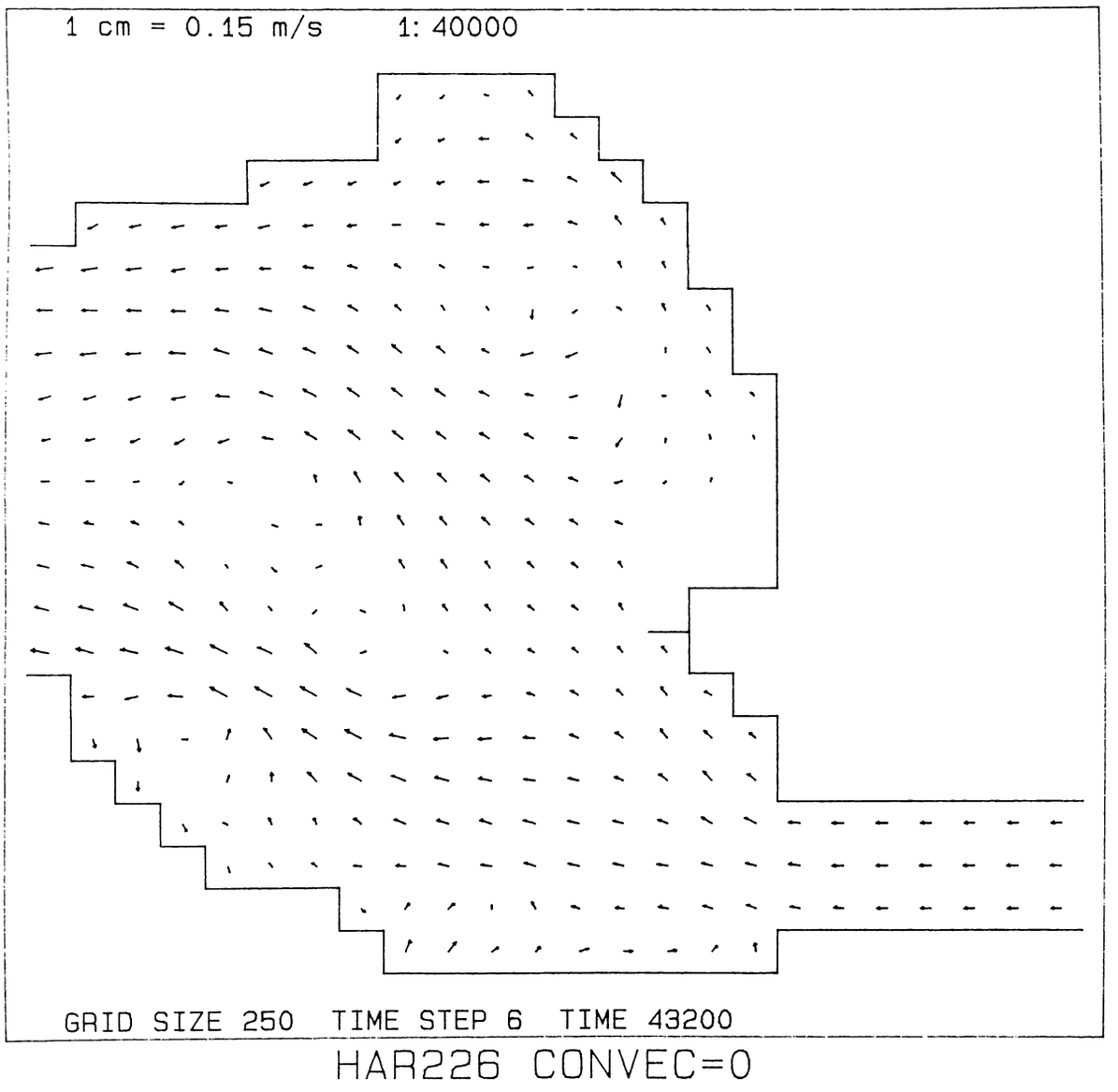

Figure 10.61: Tidal cycle residuals for the Neap tide simulation with the convective momenta and Coriolis acceleration terms neglected. Note that the complex residual circulation which typifies Whangarei Harbour is no longer evident.

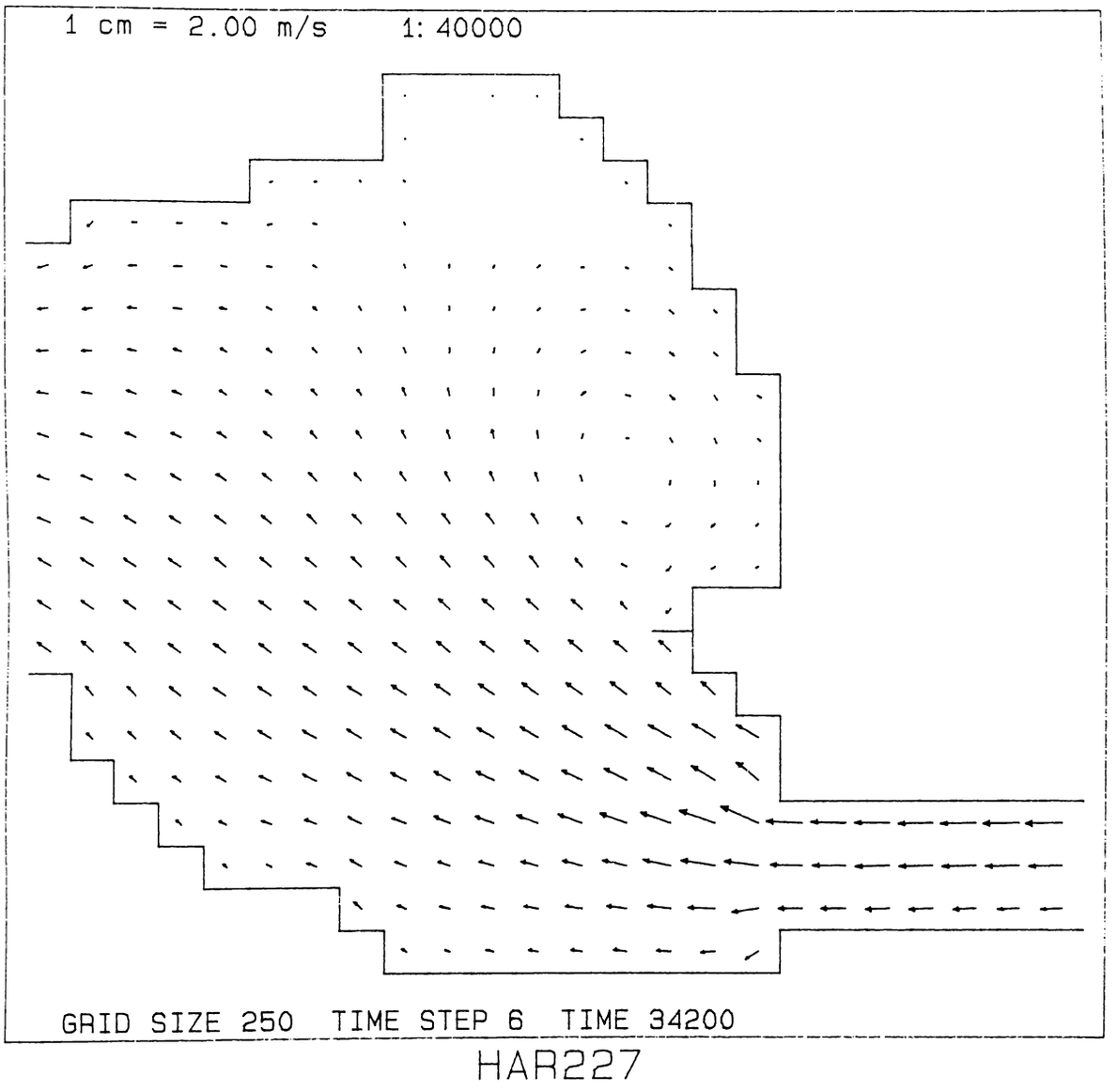

Figure 10.62: Peak flood in Whangarei Harbour with the bathymetry levelled. Depths were set to 5m except in the entrance throat which was set to 10m. Verification tide (3-Dec-81).

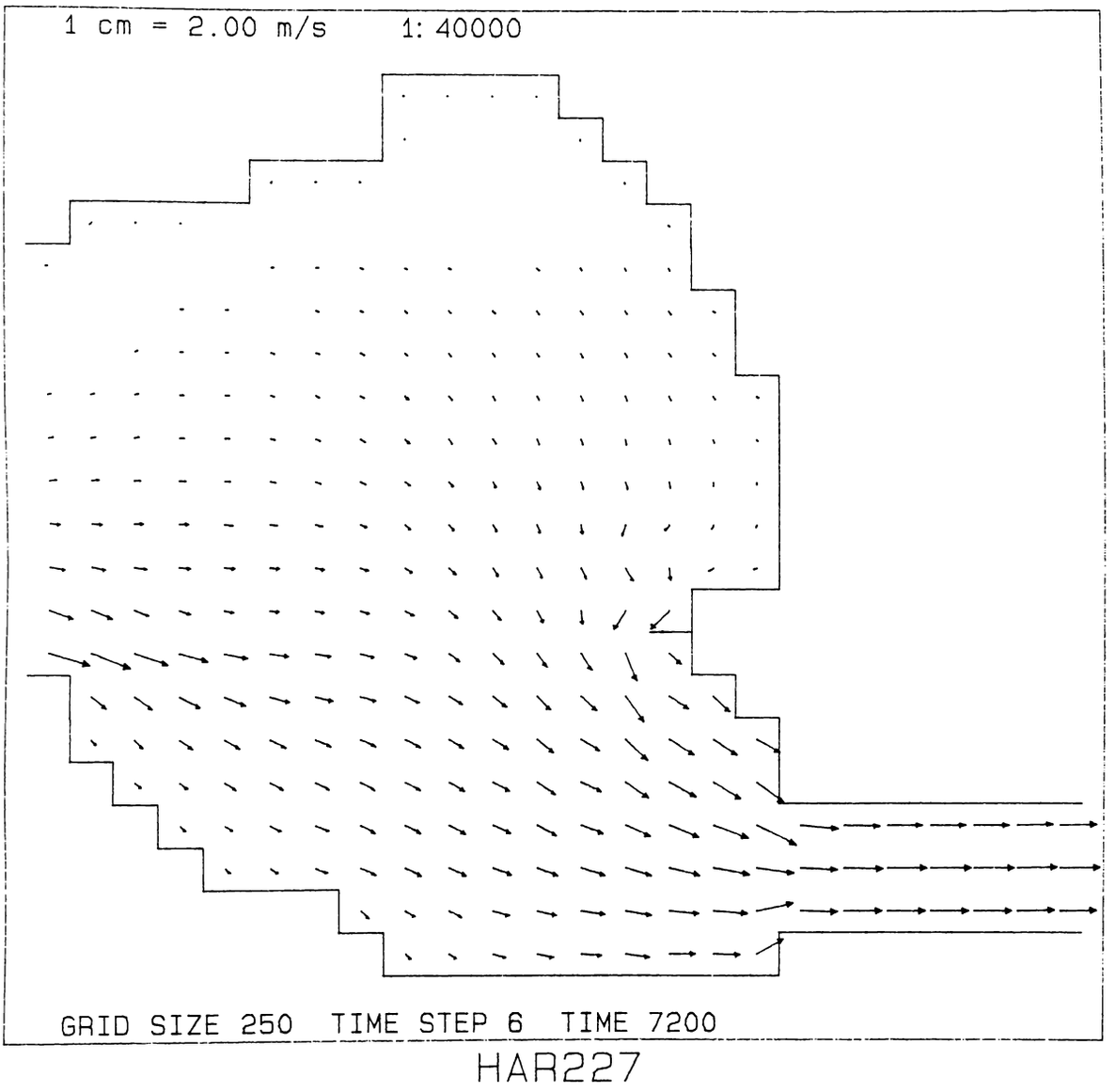

Figure 10.63: Peak ebb in Whangarei Harbour with the bathymetry levelled. Depths were set to 5m except in the entrance throat which was set to 10m. Verification tide (3-Dec-81).

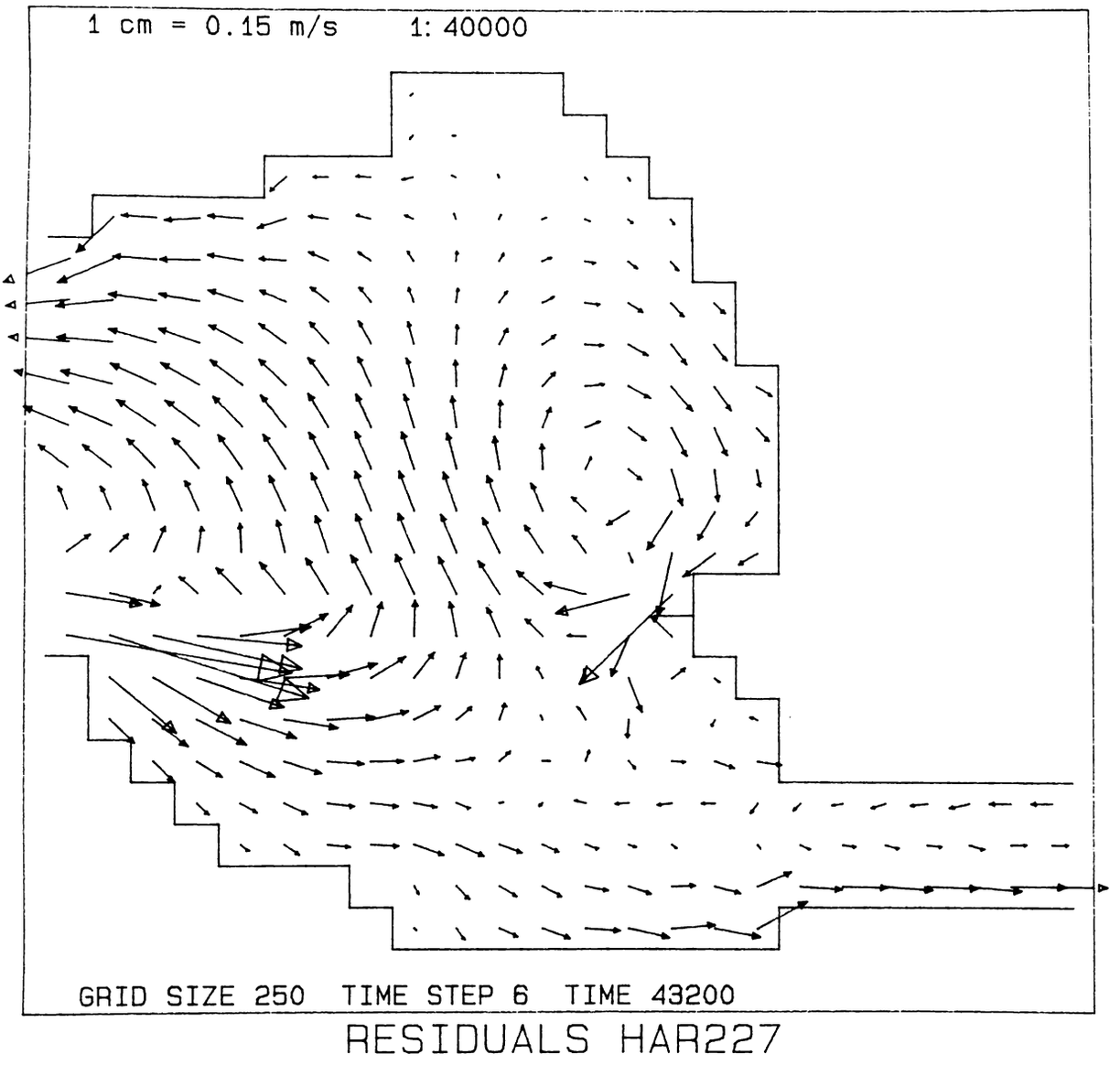

Figure 10.64: Tidal cycle residual velocities in Whangarei Harbour with the bathymetry levelled. Depths were set to 5m except in the entrance throat which was set to 10m. Verification tide (3-Dec-81).

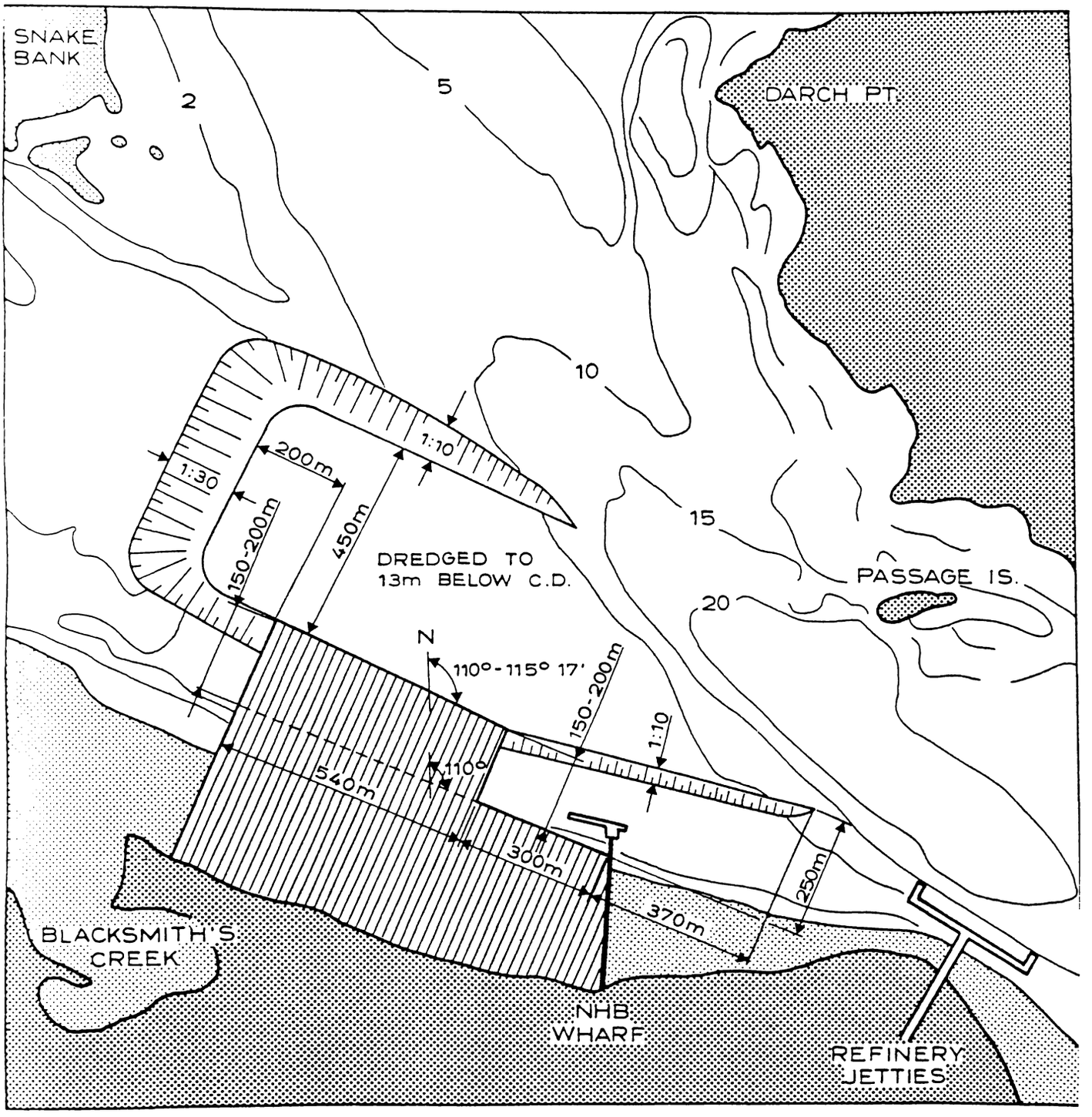

Figure 10.65: Port layouts recommended by the DHI (1982). Cases A7 and A3 are included in this range of designs.

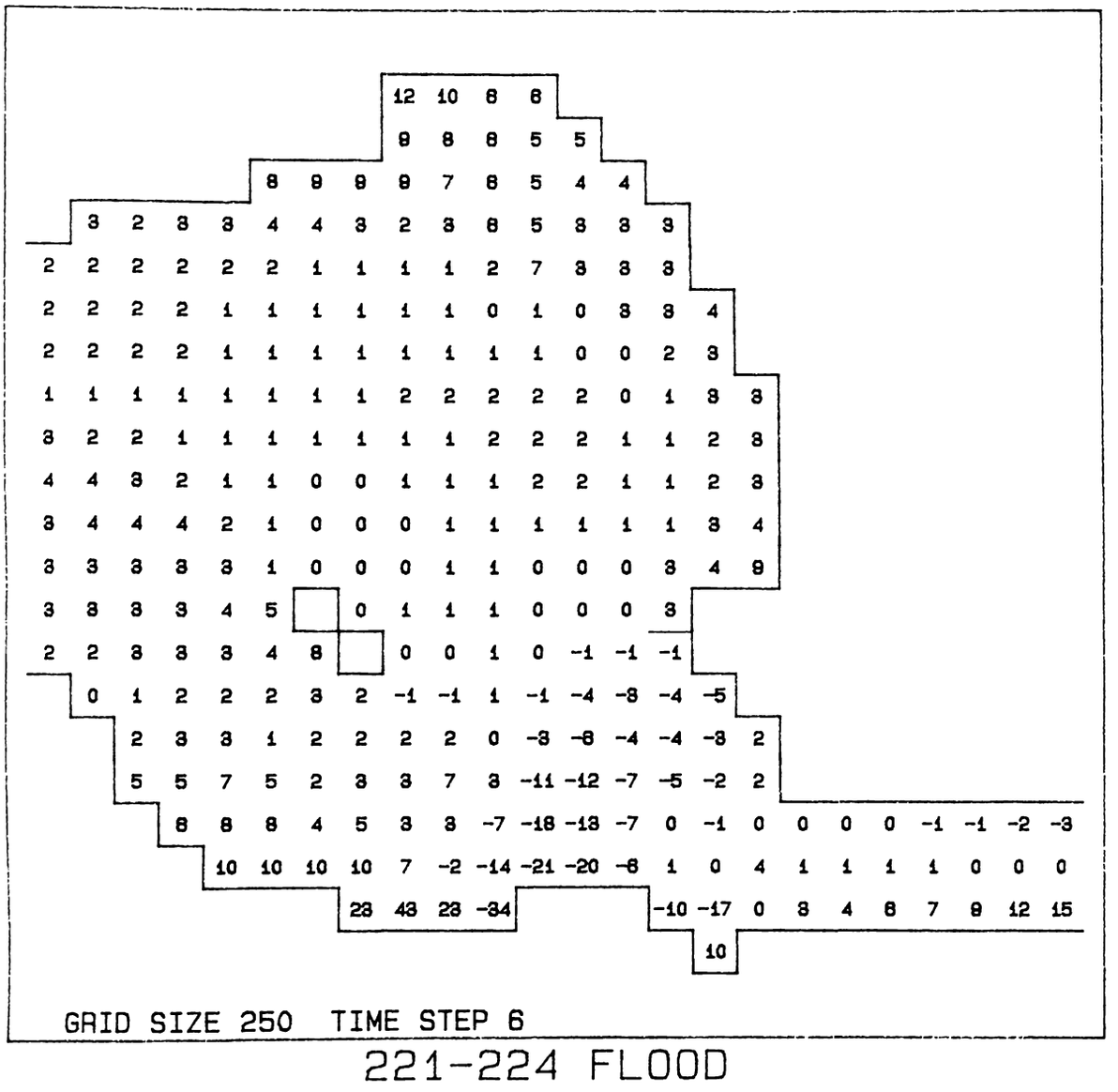

221-224 FLOOD

Figure 10.66: Percentage speed changes after introduction of the timber port during peak, Neap-tide, flood flow. The open boundary sea levels are unchanged from those for the present bathymetry.

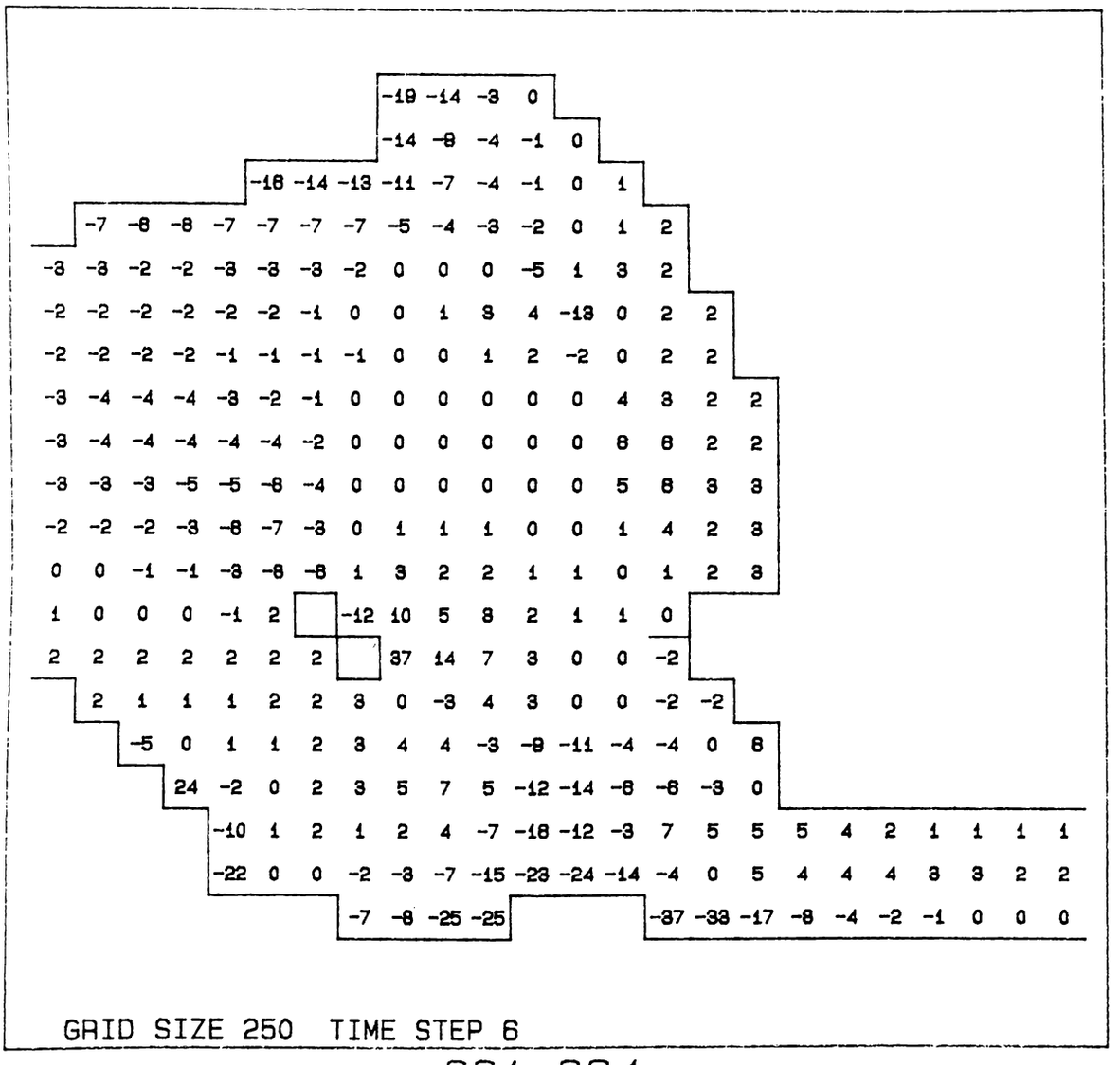

221-224

Figure 10.67: Percentage speed changes after introduction of the timber port during peak, Neap-tide, ebb flow. The open boundary sea levels are unchanged from those for the present bathymetry.

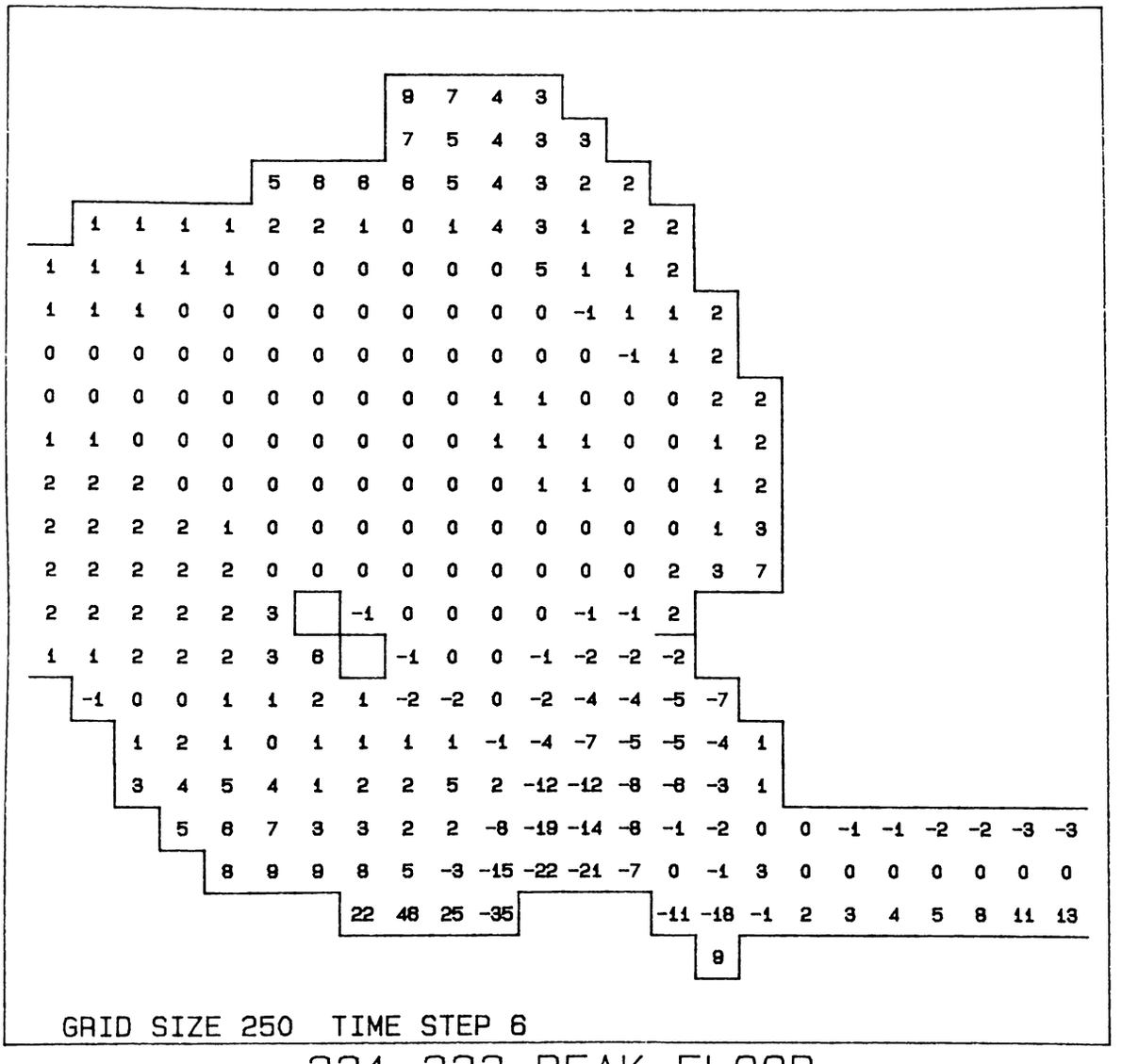

Figure 10.68: Percentage speed changes after introduction of the timber port during peak, Neap-tide, flood flow. The open boundary sea levels were generated in LINMOD with the port included.

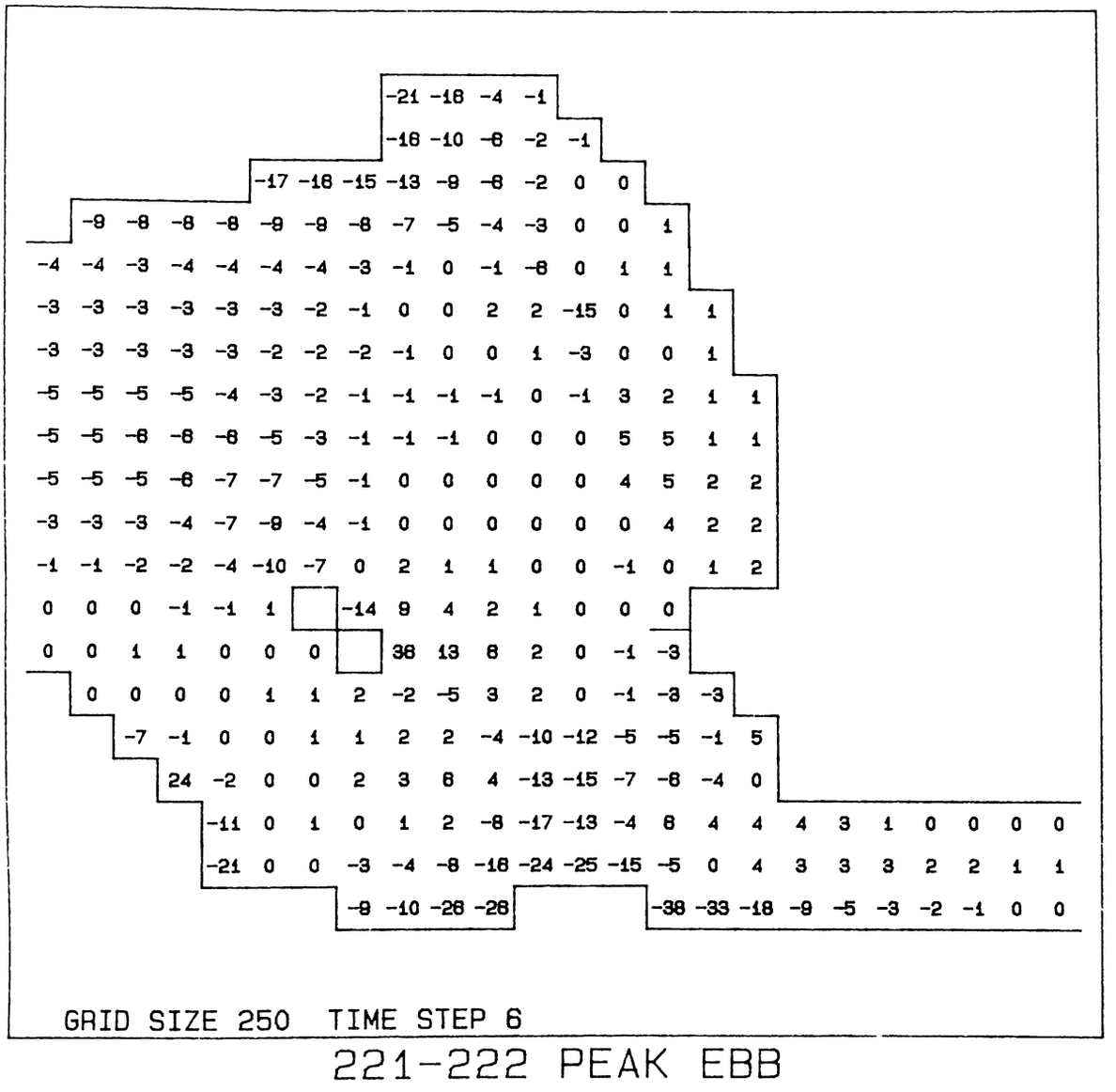

Figure 10.69: Percentage speed changes after introduction of the timber port during peak, Neap-tide, ebb flow. The open boundary sea levels were generated in LINMOD with the port included.

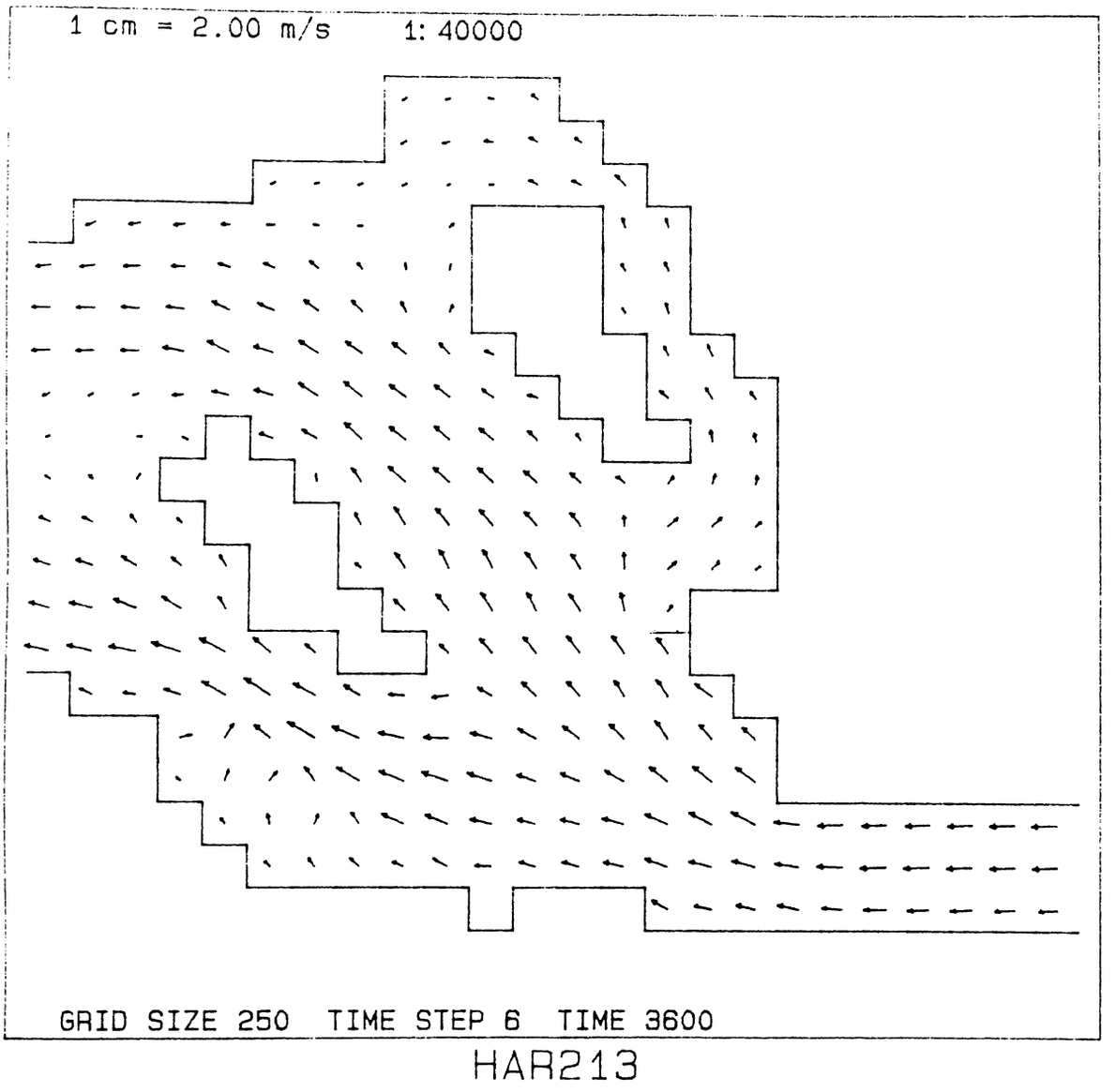

Figure 10.70(a): Flow pattern after port construction. Spring tide 1 hour after the low tide at 2:45 on 14-Dec-81.

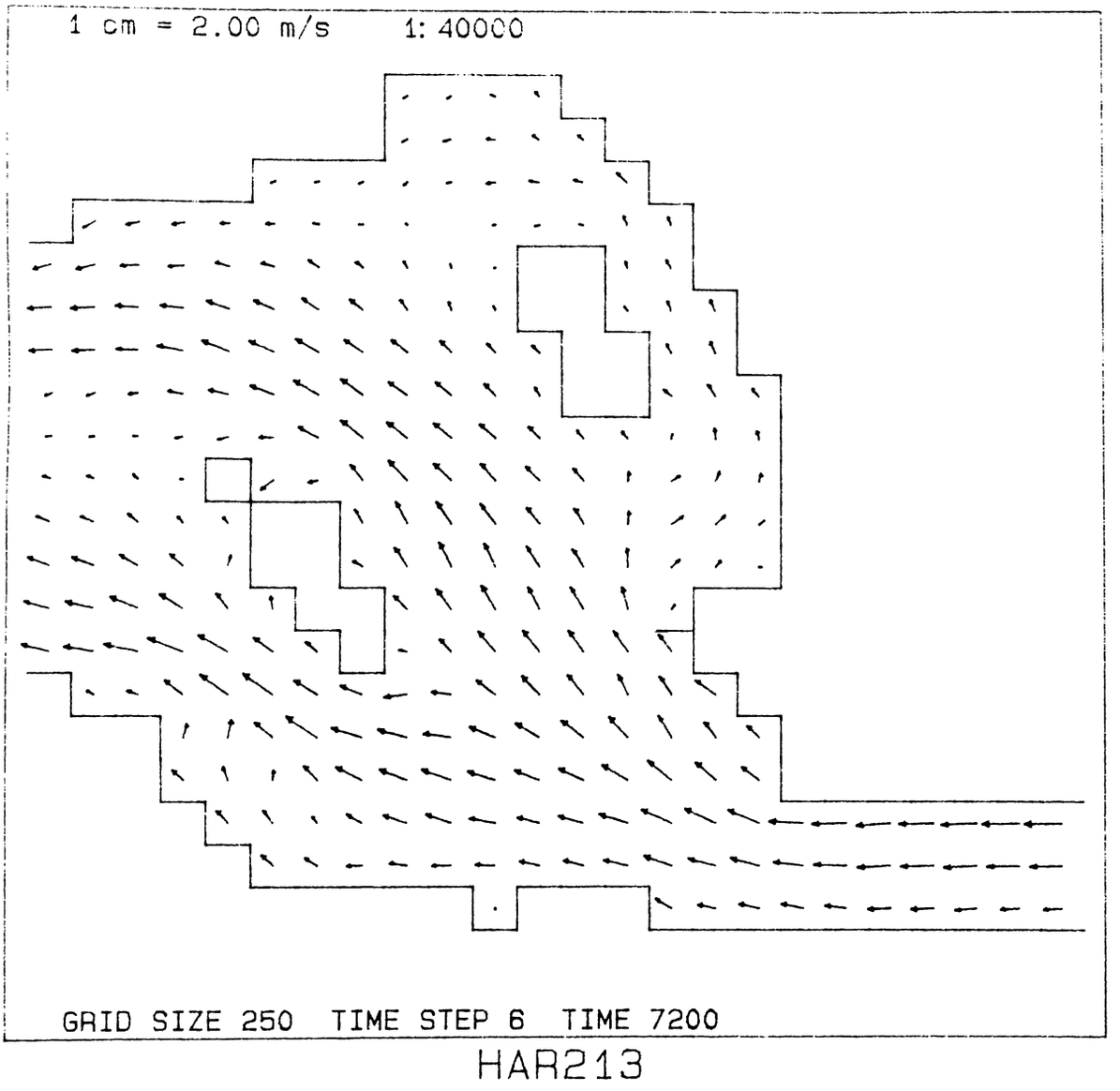

Figure 10.70(b): Flow pattern after port construction. Spring tide 2 hours after the low tide at 2:45 on 14-Dec-81.

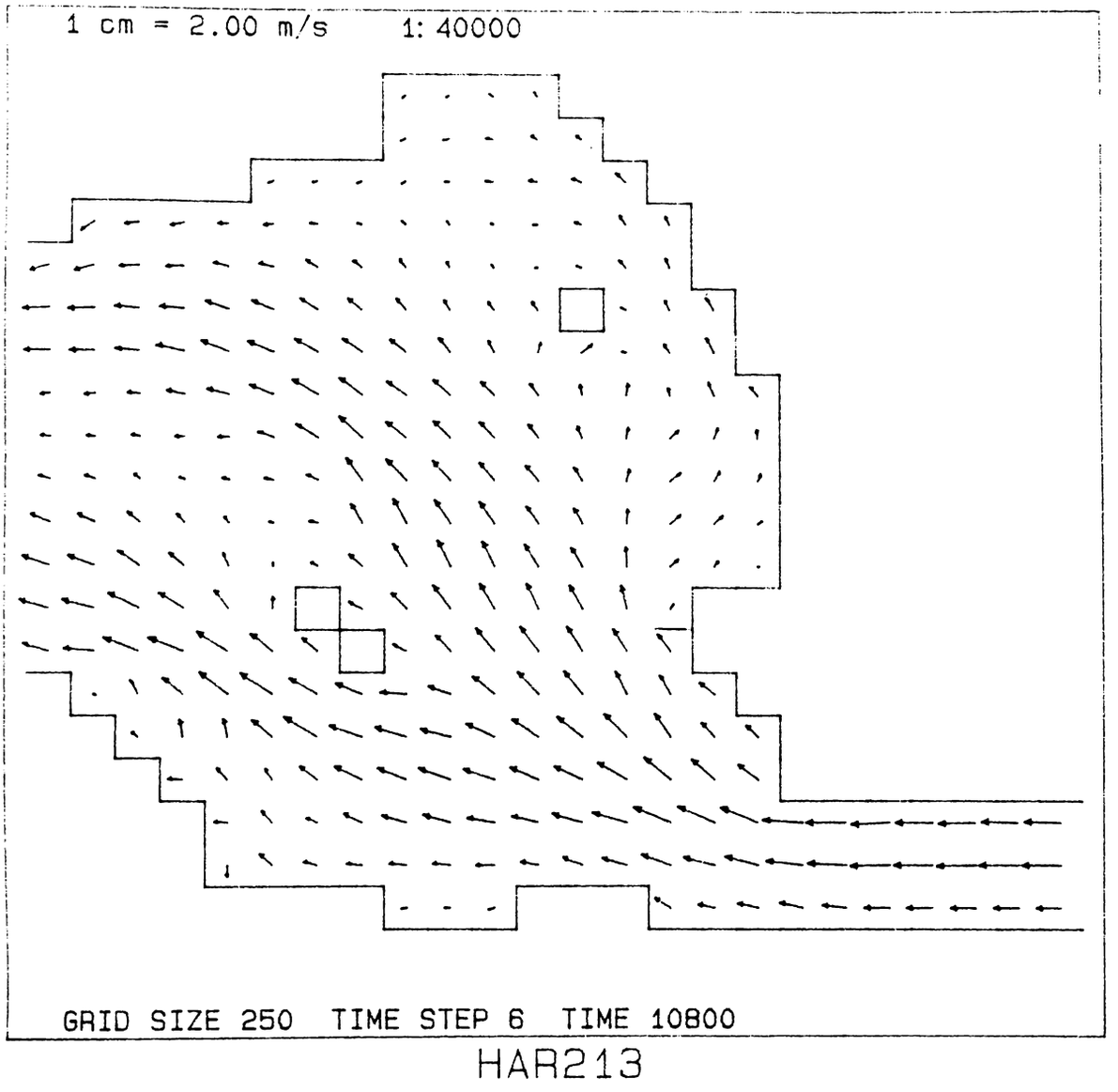

Figure 10.70(c): Flow pattern after port construction. Spring tide 3 hours after the low tide at 2:45 on 14-Dec-81.

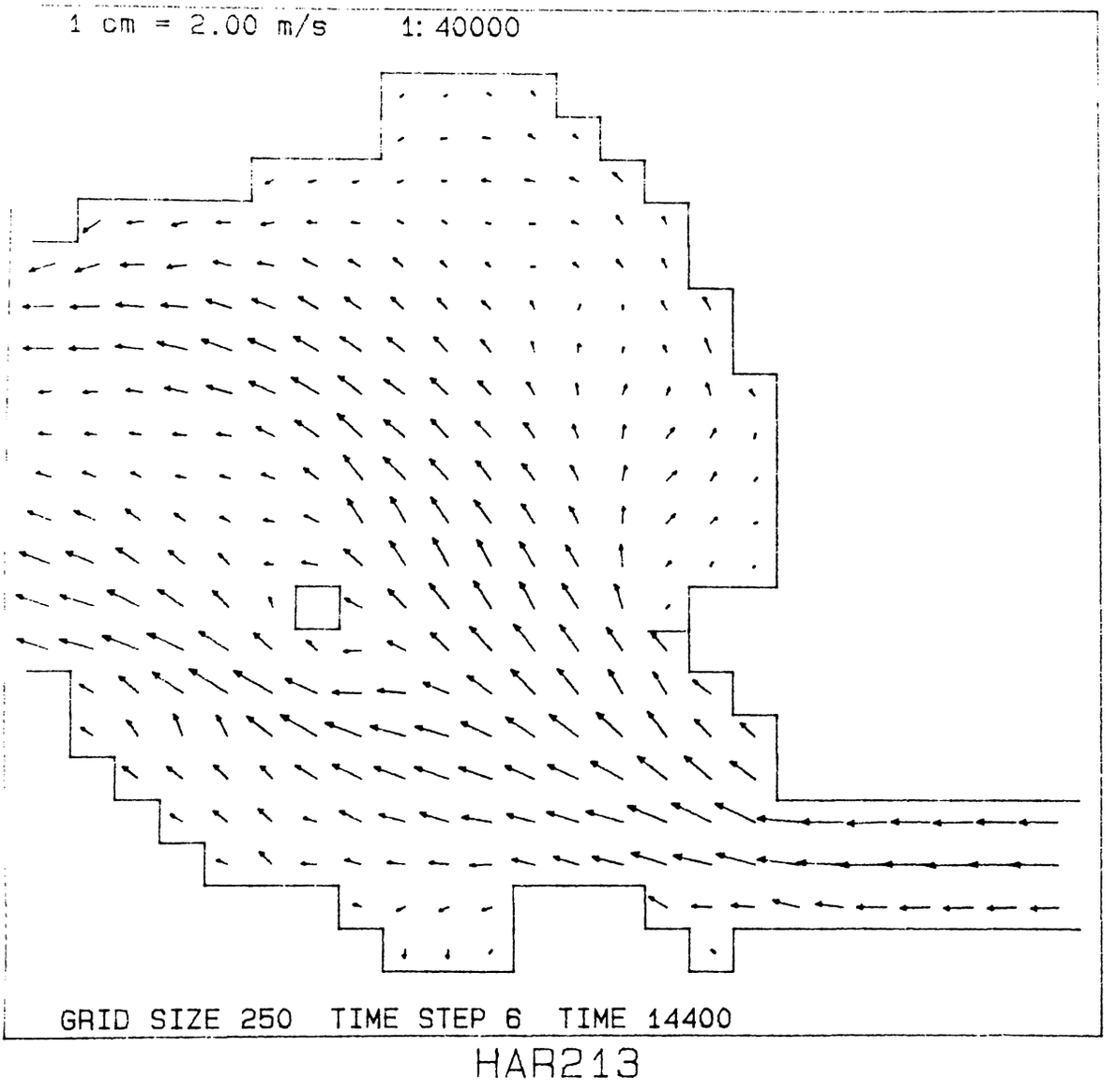

Figure 10.70(d): Flow pattern after port construction. Spring tide 4 hours after the low tide at 2:45 on 14-Dec-81.

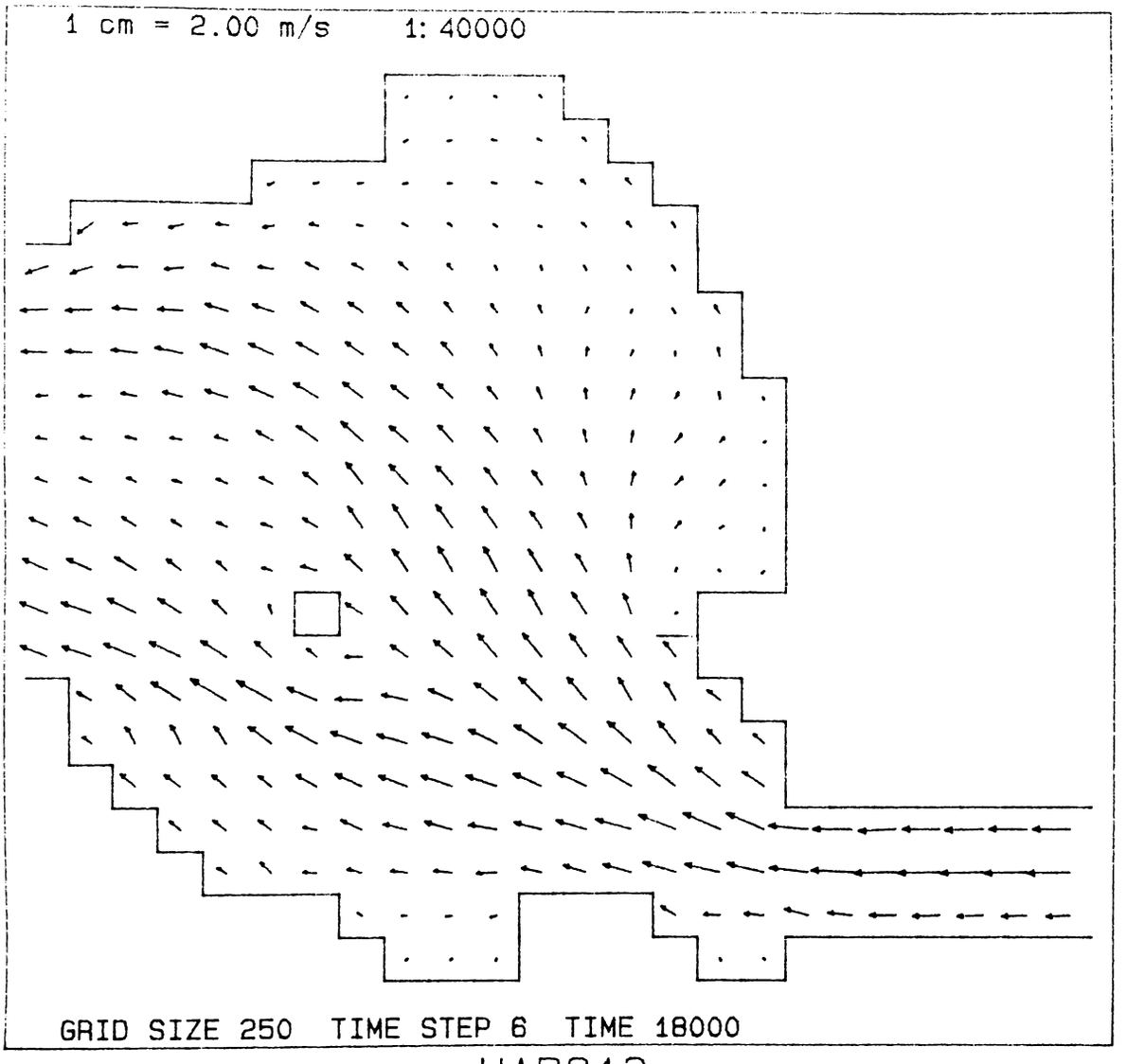

Figure 10.70(e): Flow pattern after port construction. Spring tide 5 hours after the low tide at 2:45 on 14-Dec-81.

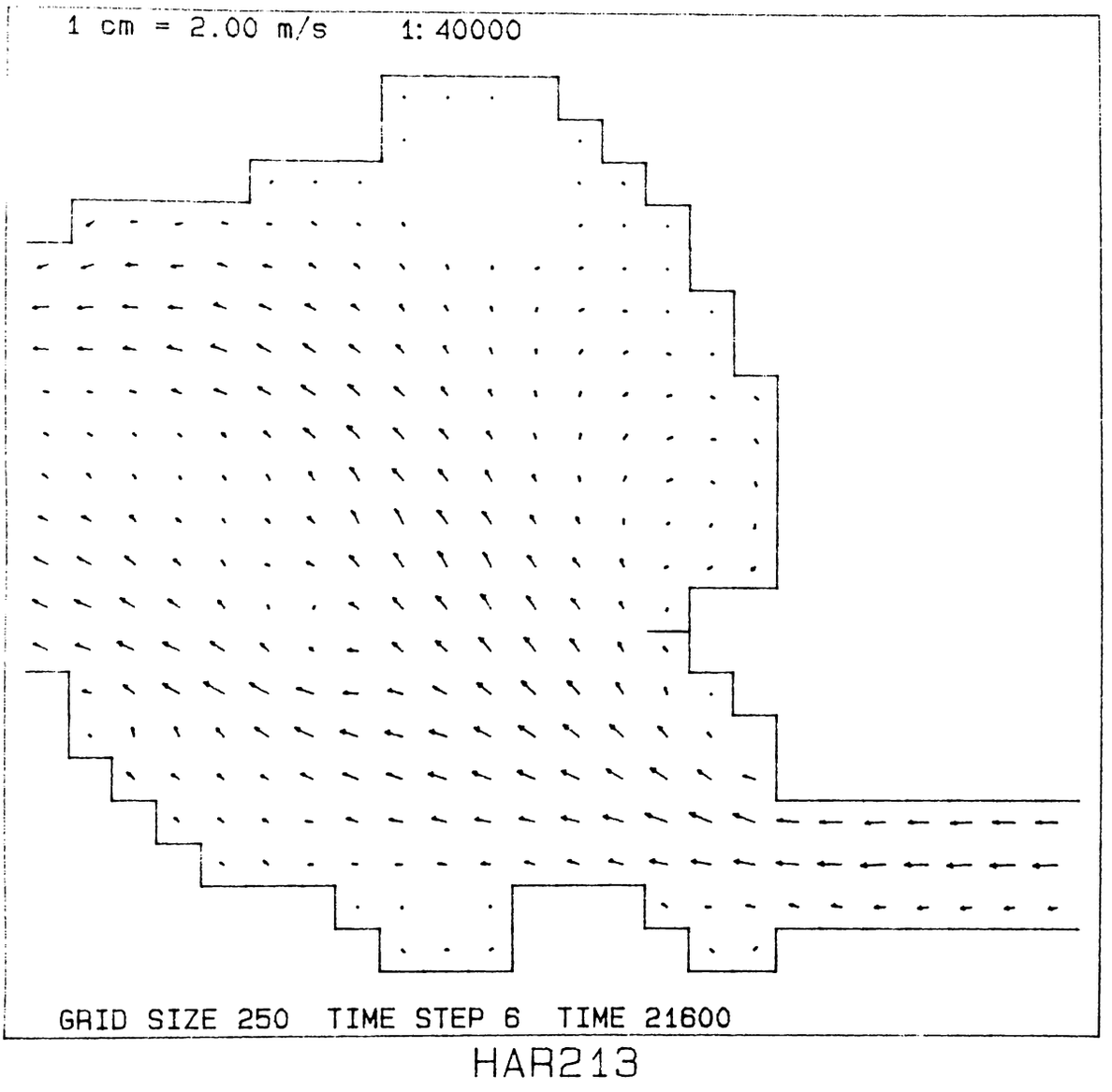

Figure 10.70(f): Flow pattern after port construction. Spring tide 6 hours after the low tide at 2:45 on 14-Dec-81.

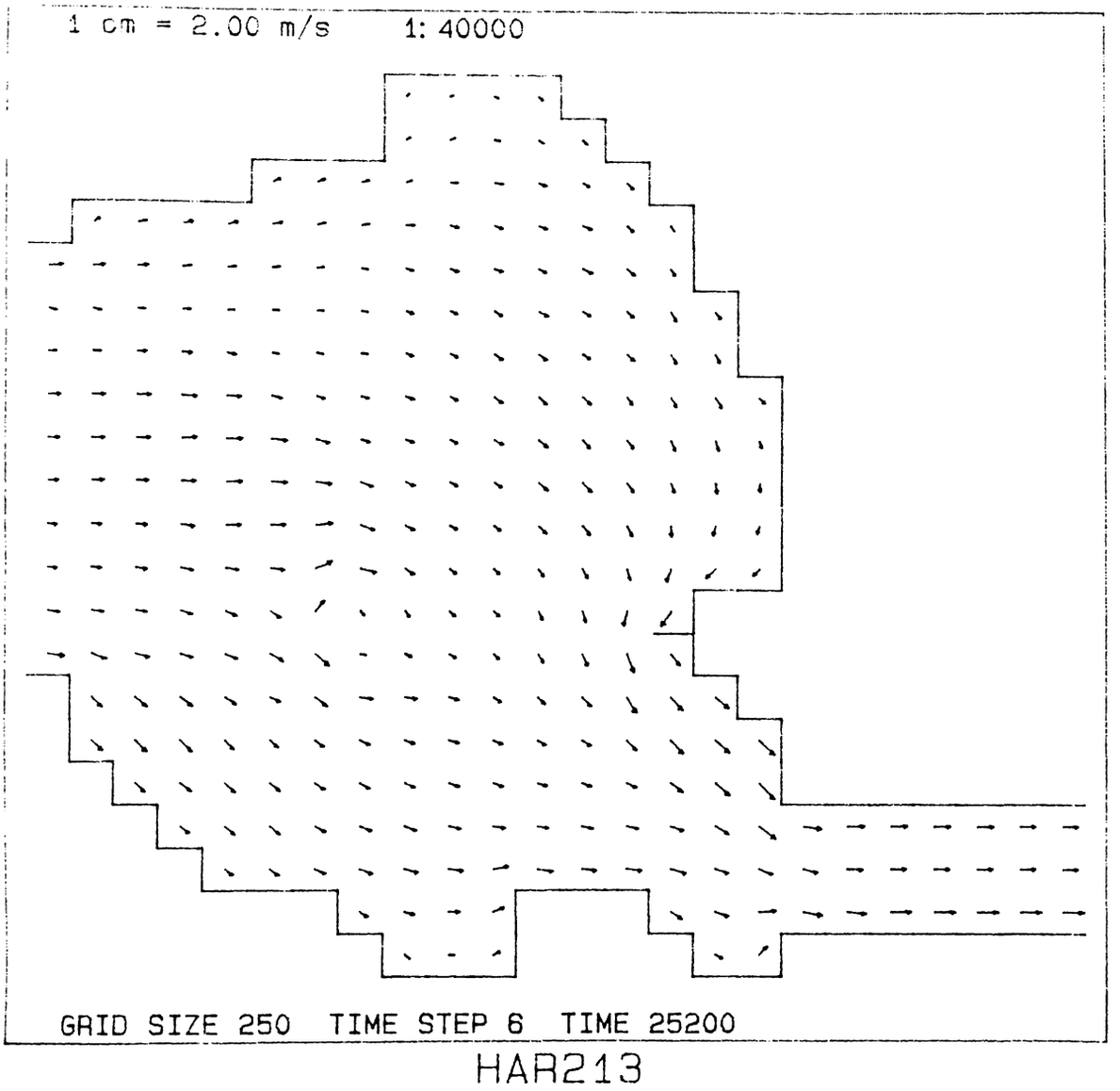

Figure 10.70(g): Flow pattern after port construction. Spring tide 7 hours after the low tide at 2:45 on 14-Dec-81.

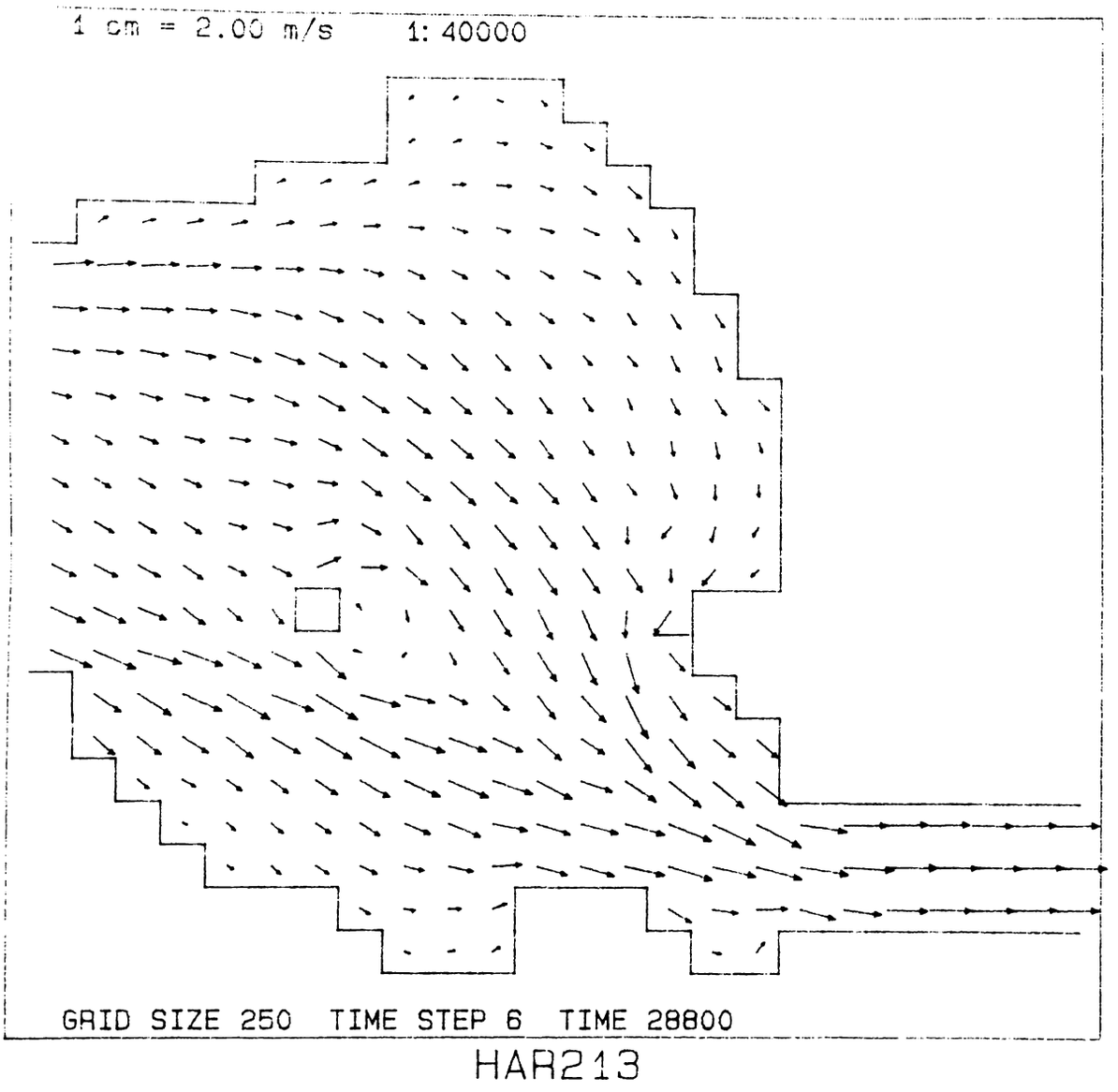

Figure 10.70(h): Flow pattern after port construction. Spring tide. 8 hours after low tide at 2:45 on 14-Dec-81.

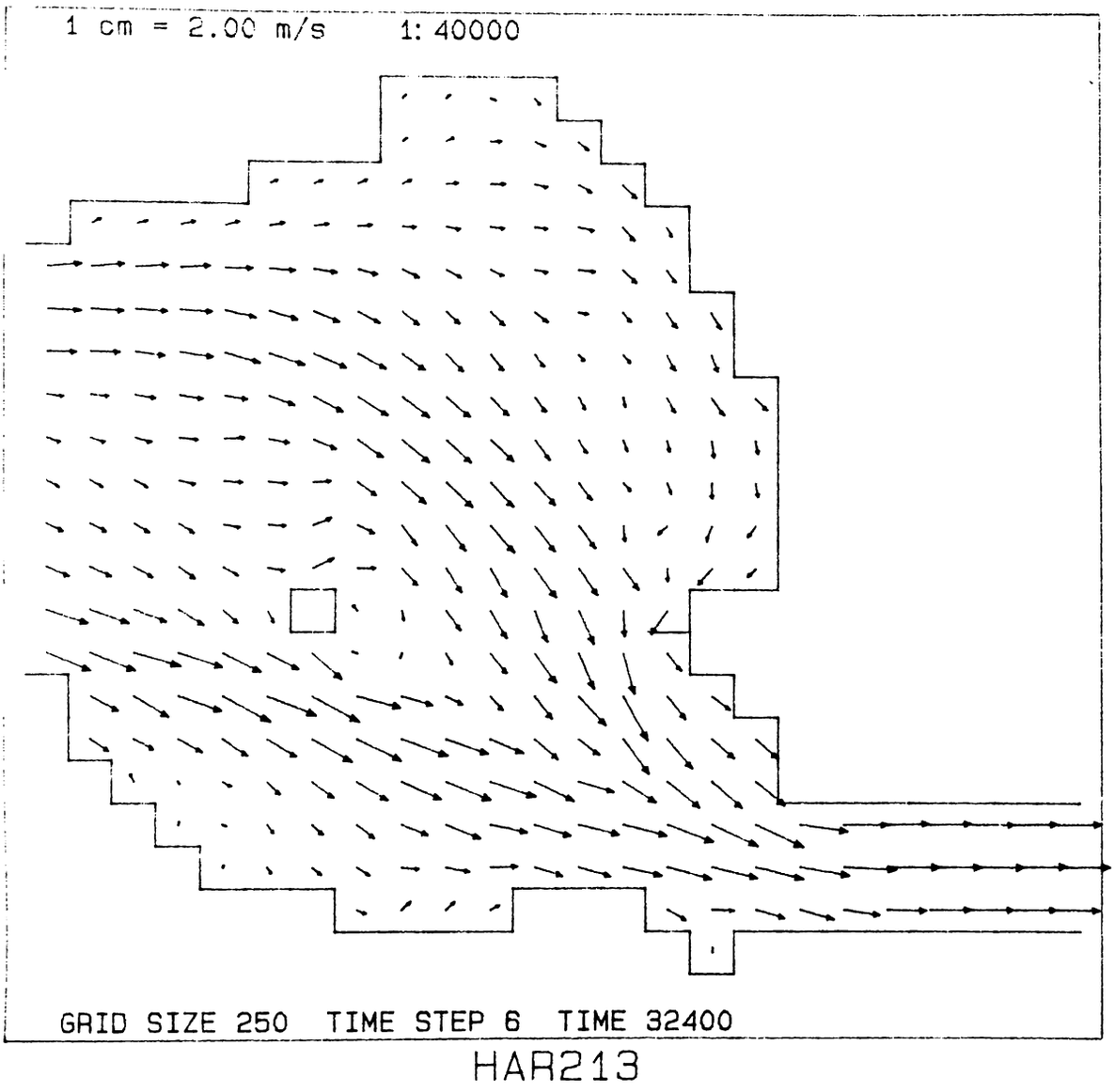

Figure 10.70(i): Flow pattern after port construction. Spring tide 9 hours after the low tide at 2:45 on 14-Dec-81.

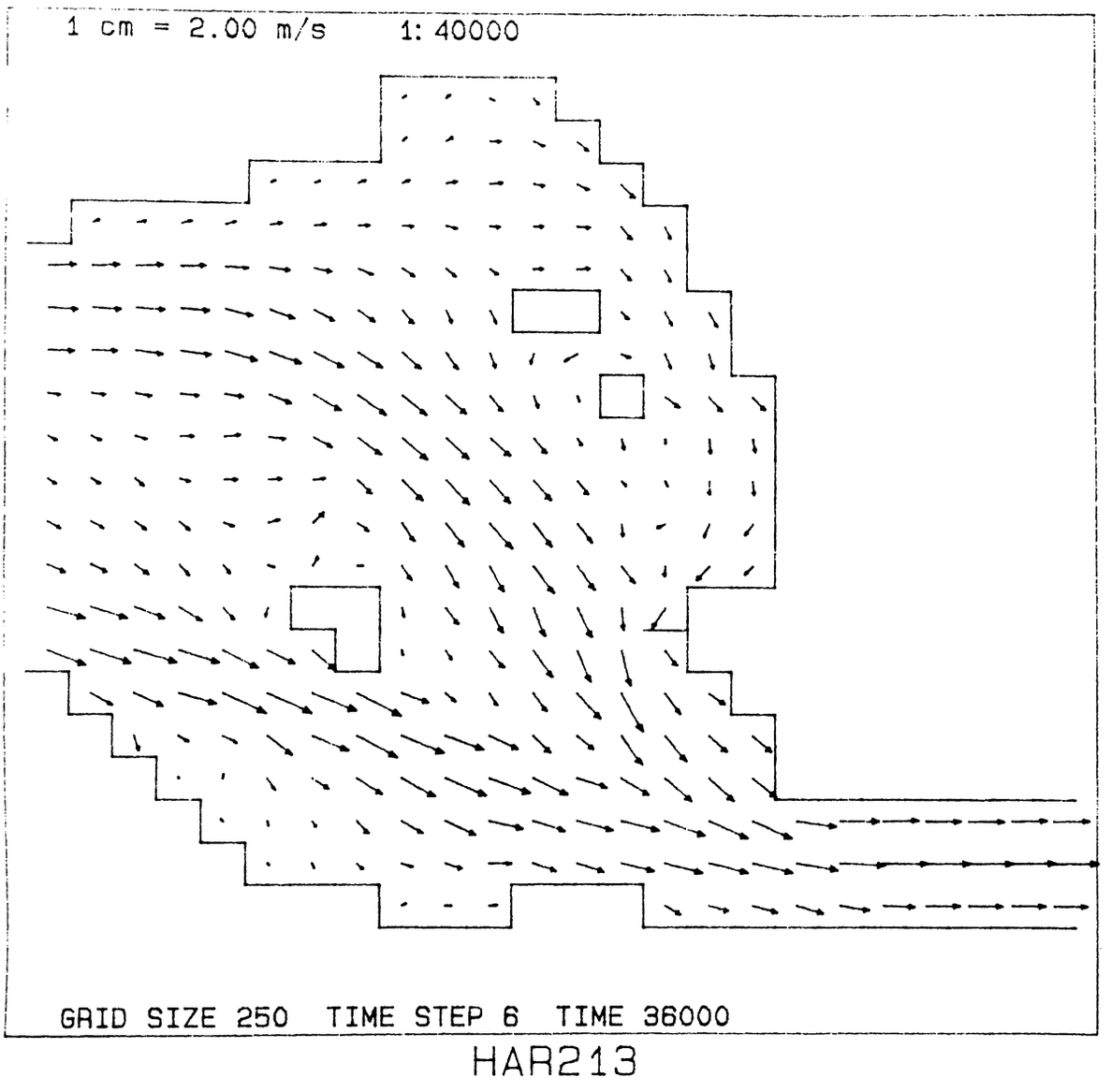

Figure 10.70(j): Flow pattern after port construction. Spring tide 10 hours after the low tide at 2:45 on 14-Dec-81.

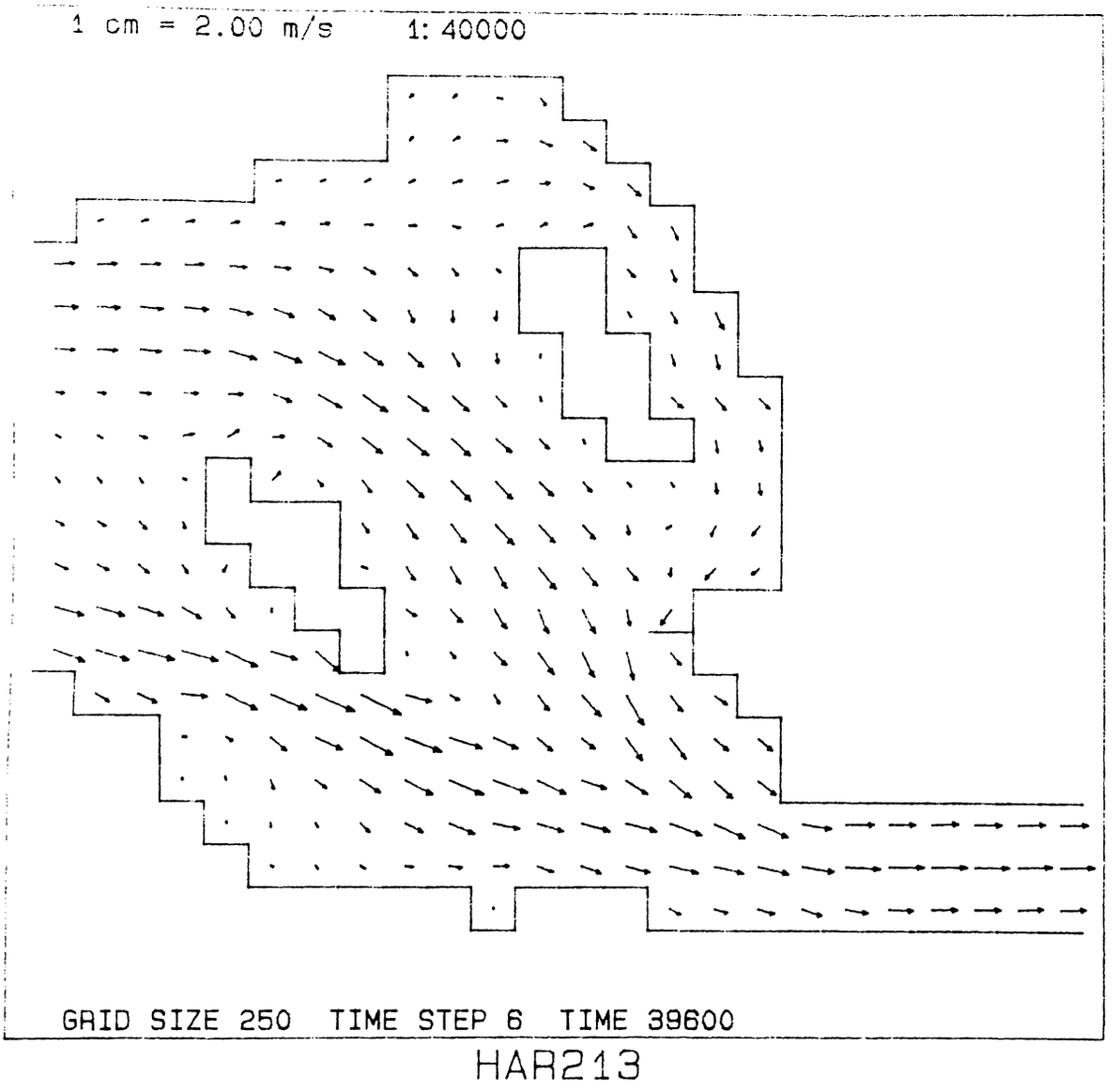

Figure 10.70(k): Flow pattern after port construction. Spring tide 11 hours after the low tide at 2:45 on 14-Dec-81.

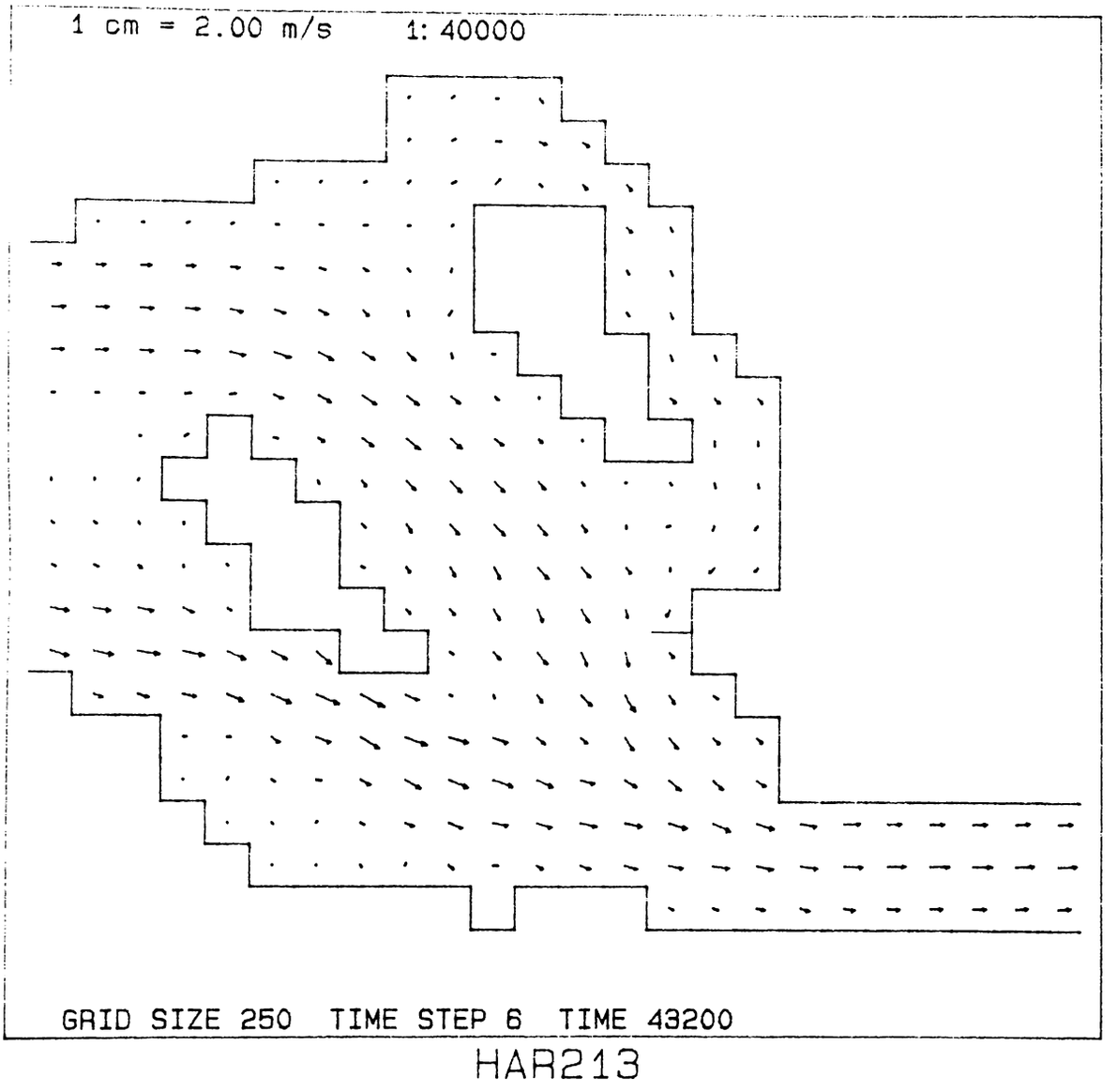

Figure 10.70(1): Flow pattern after port construction. Spring tide 12 hours after the low tide at 2:45 on 14-Dec-81.

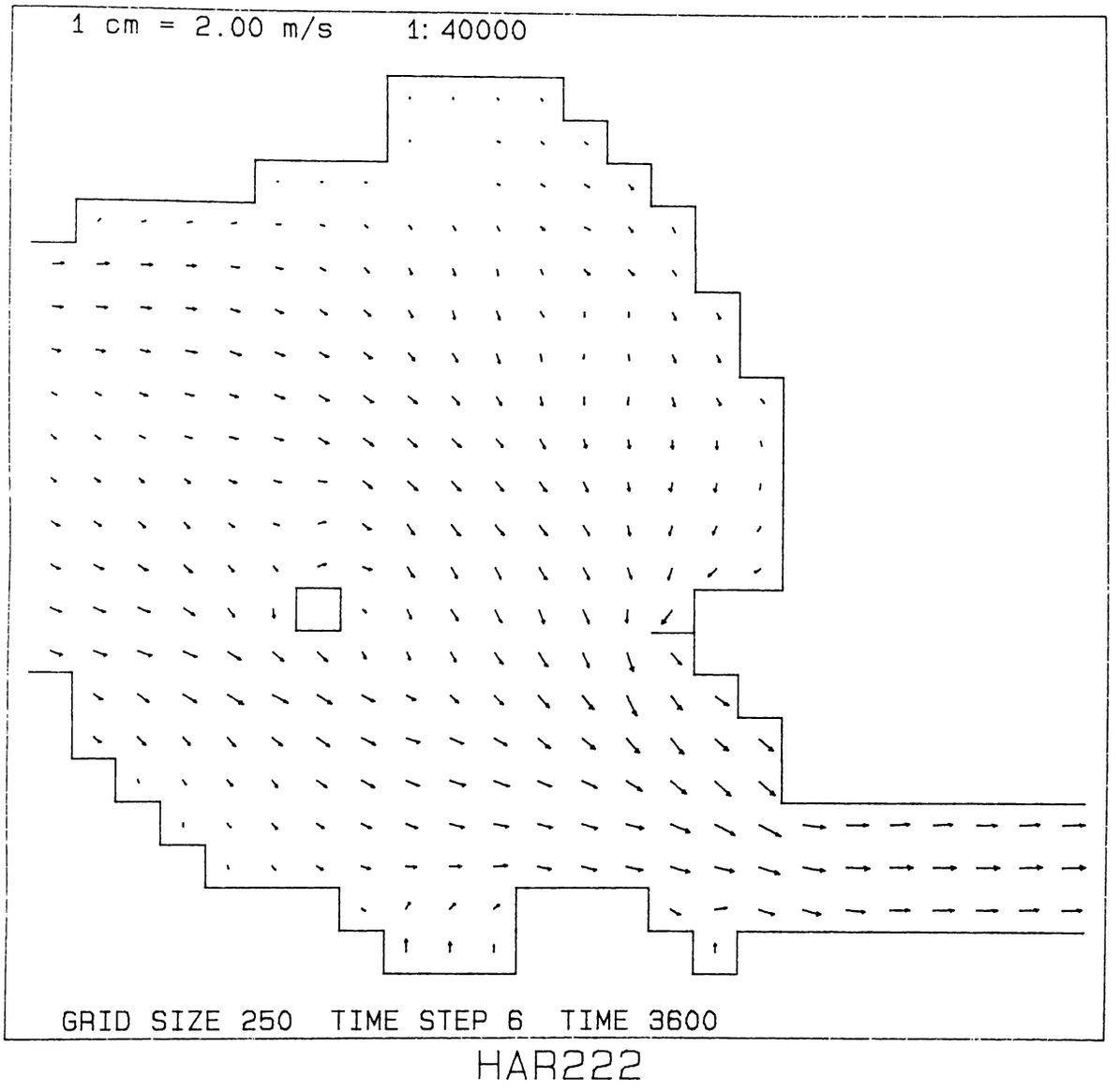

Figure 10.71(a): Flow pattern after port construction. Neap tide 1¾ hours after the high tide at 23:15 on 2-Dec-81.

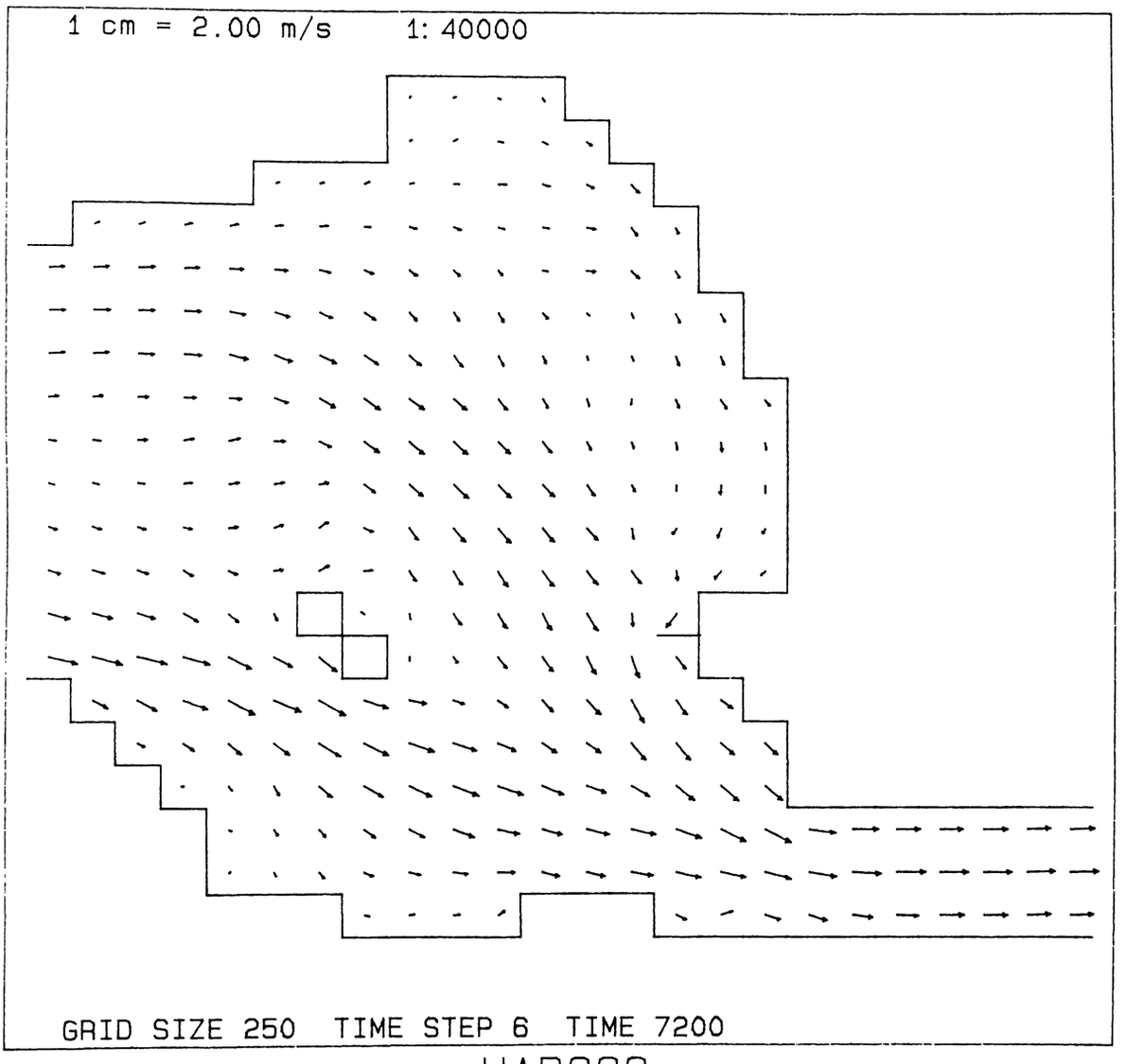

Figure 10.71(b): Flow pattern after port construction. Neap tide 2¾ hours after the high tide at 23:15 on 2-Dec-81.

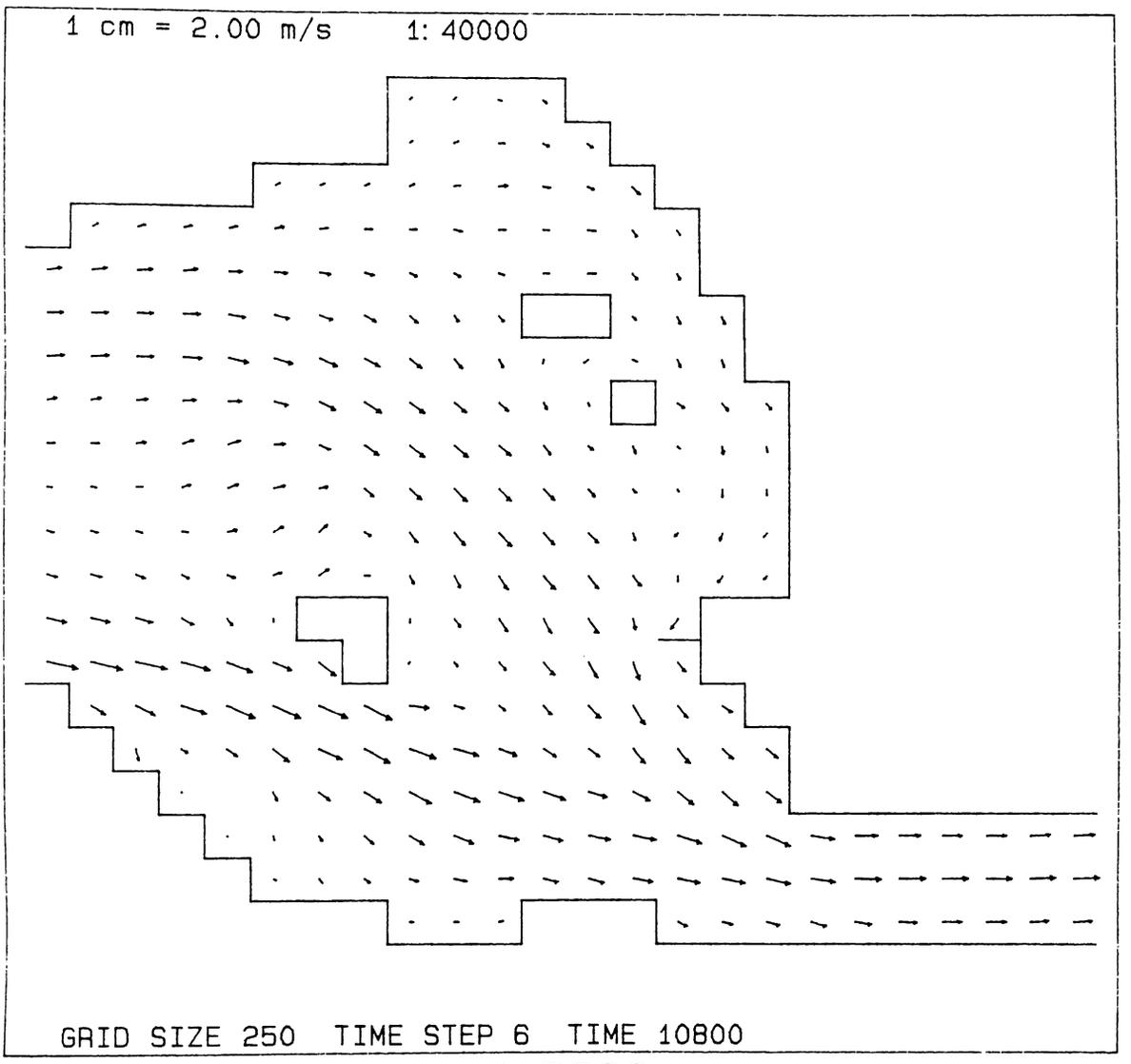

Figure 10.71(c): Flow pattern after port construction. Neap tide 3¾ hours after the high tide at 23:15 on 2-Dec-81.

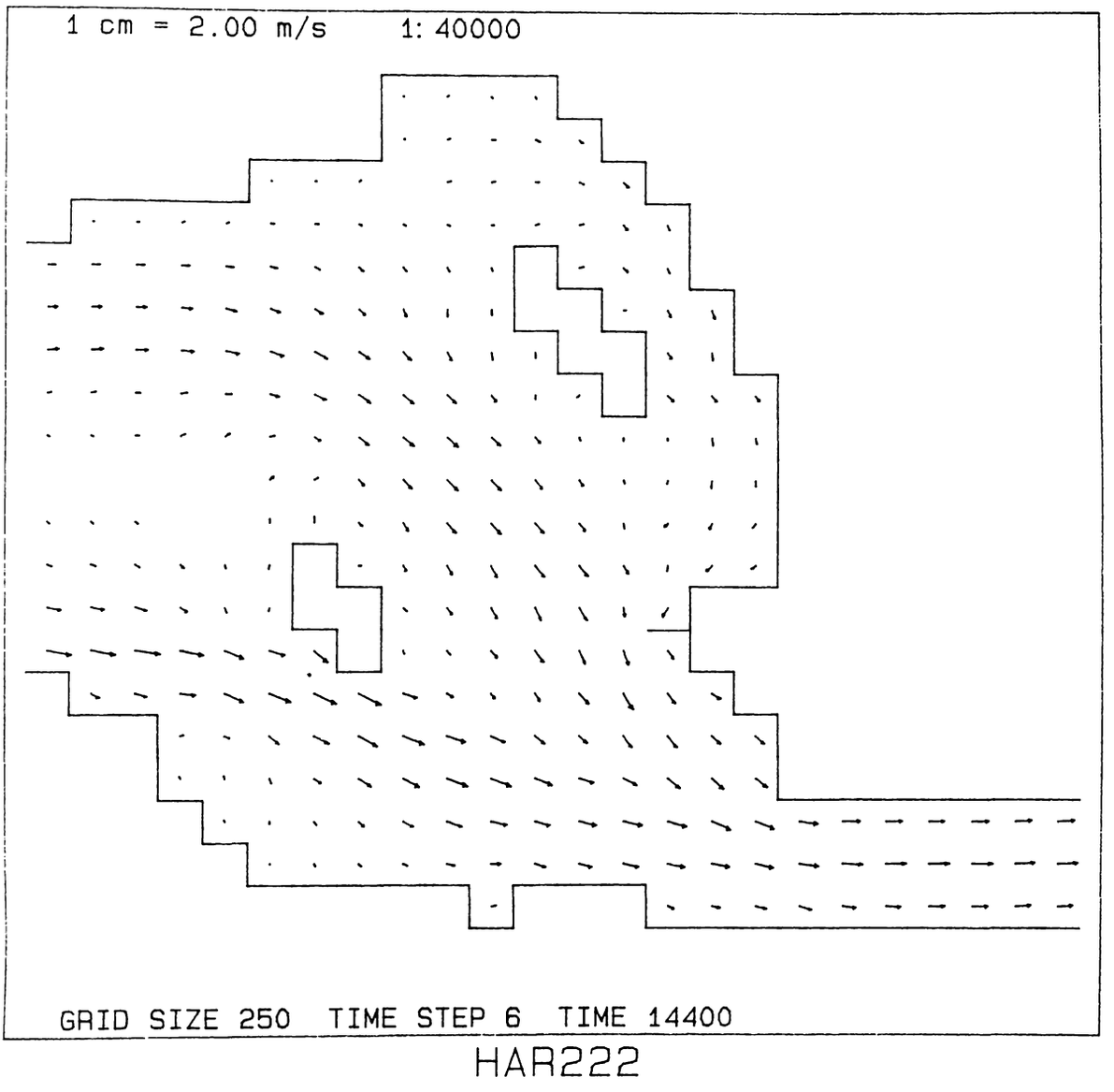

Figure 10.71(d): Flow pattern after port construction. Neap tide 4¾ hours after the high tide at 23:15 on 2-Dec-81.

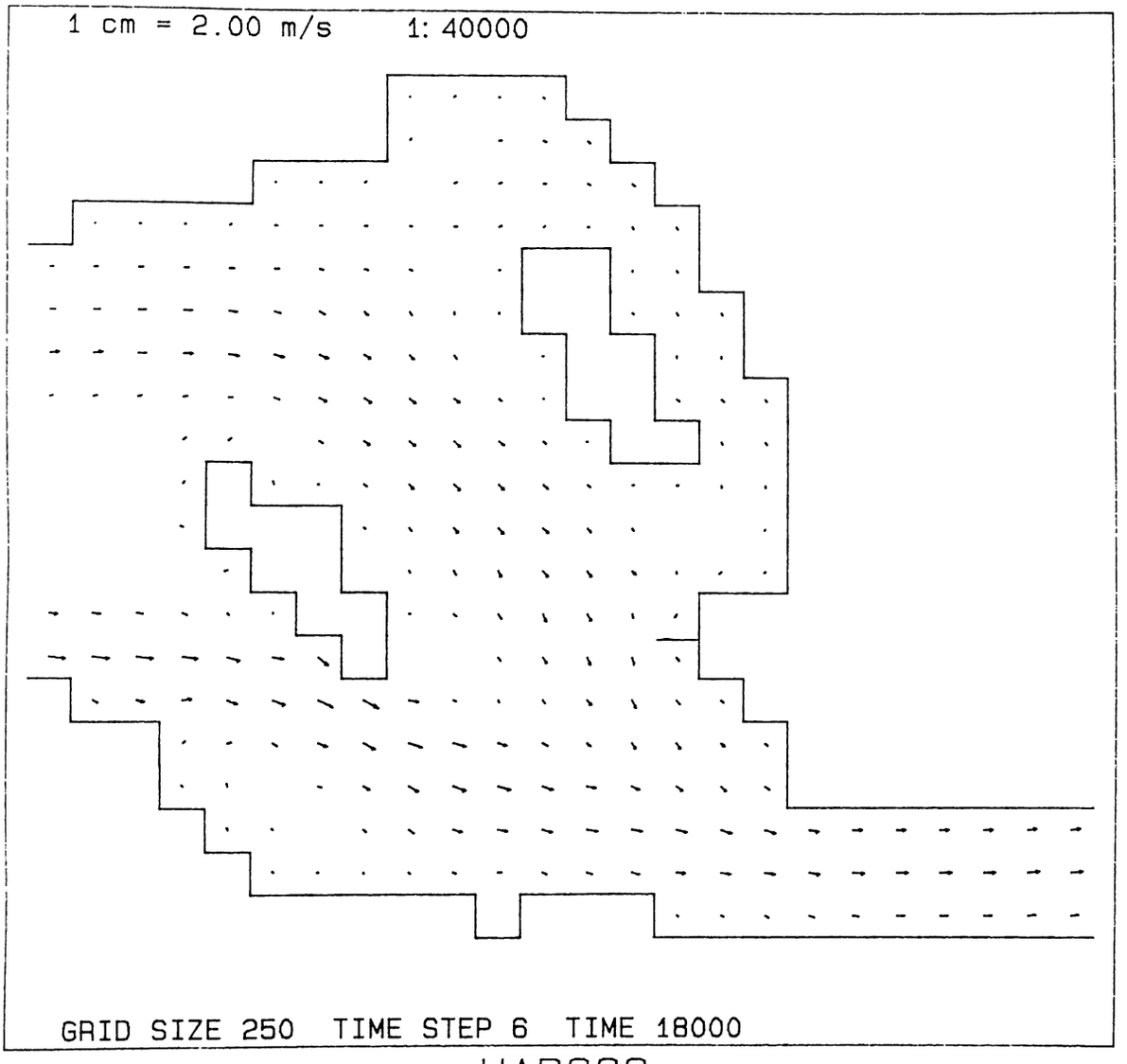

Figure 10.71(e): Flow pattern after port construction. Neap tide 5¾ hours after the high tide at 23:15 on 2-Dec-81.

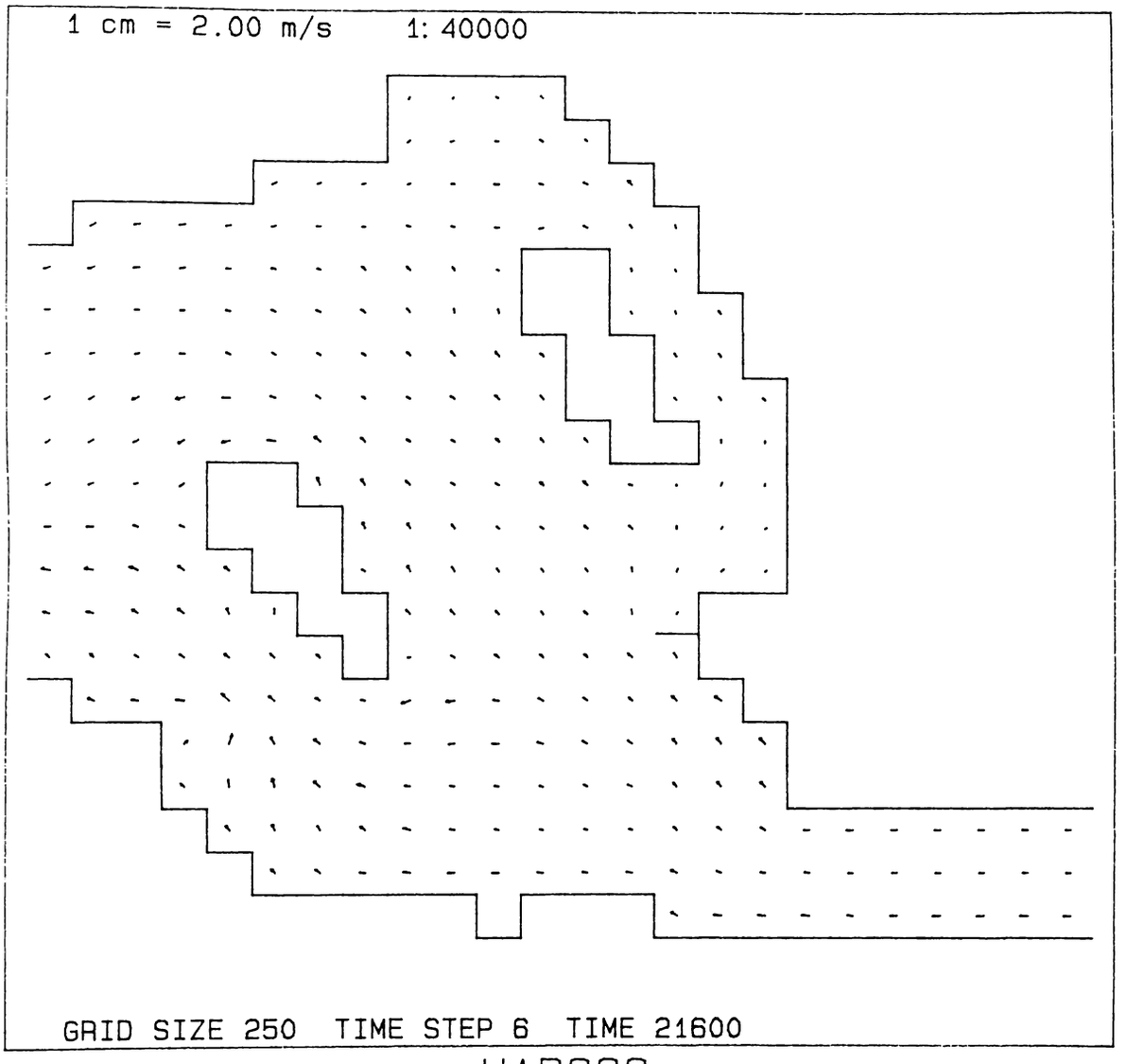

Figure 10.71(f): Flow pattern after port construction. Neap tide 6¾ hours after the high tide at 23:15 on 2-Dec-81.

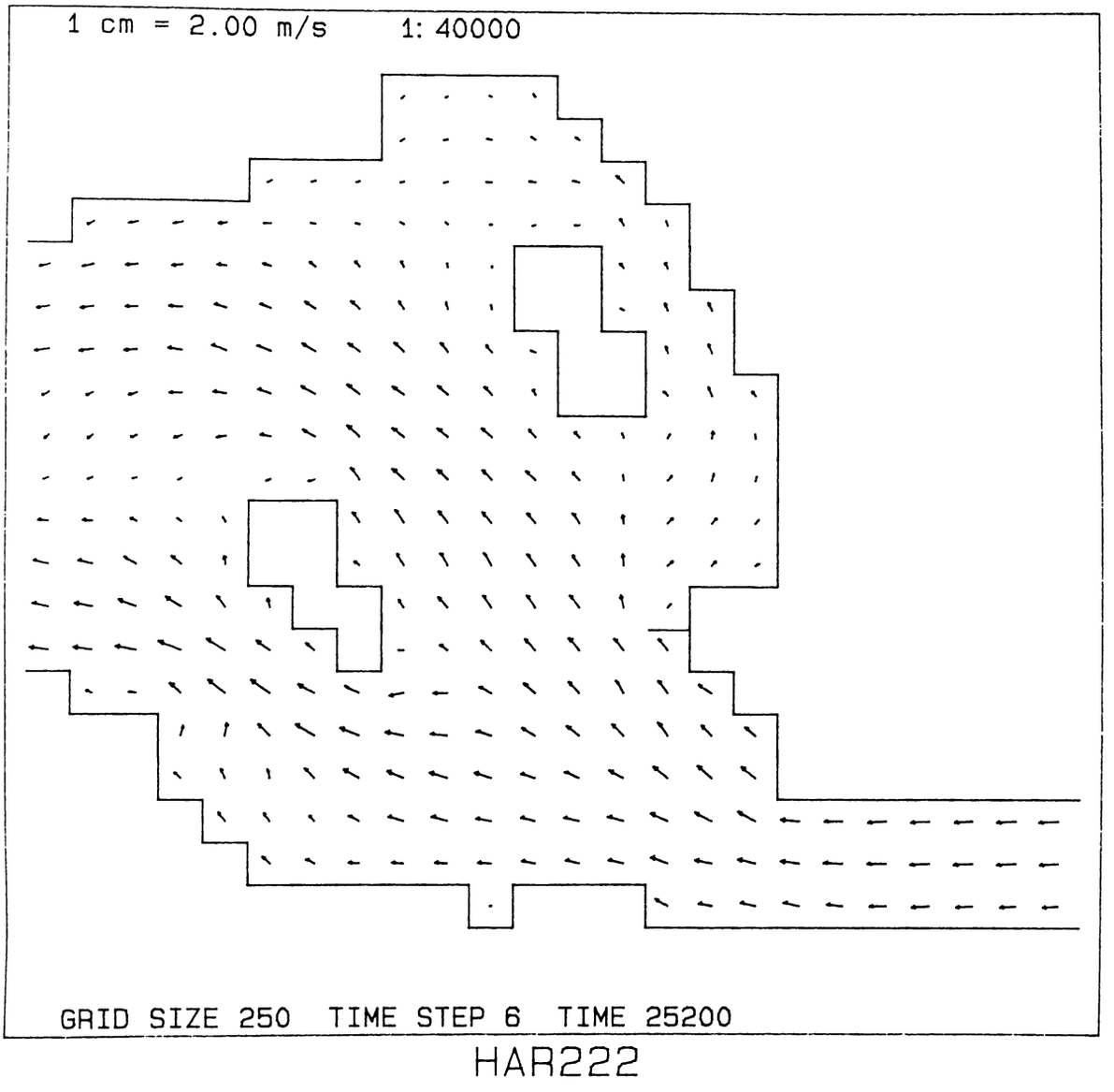

Figure 10.71(g): Flow pattern after port construction. Neap tide 7¾ hours after the high tide at 23:15 on 2-Dec-81.

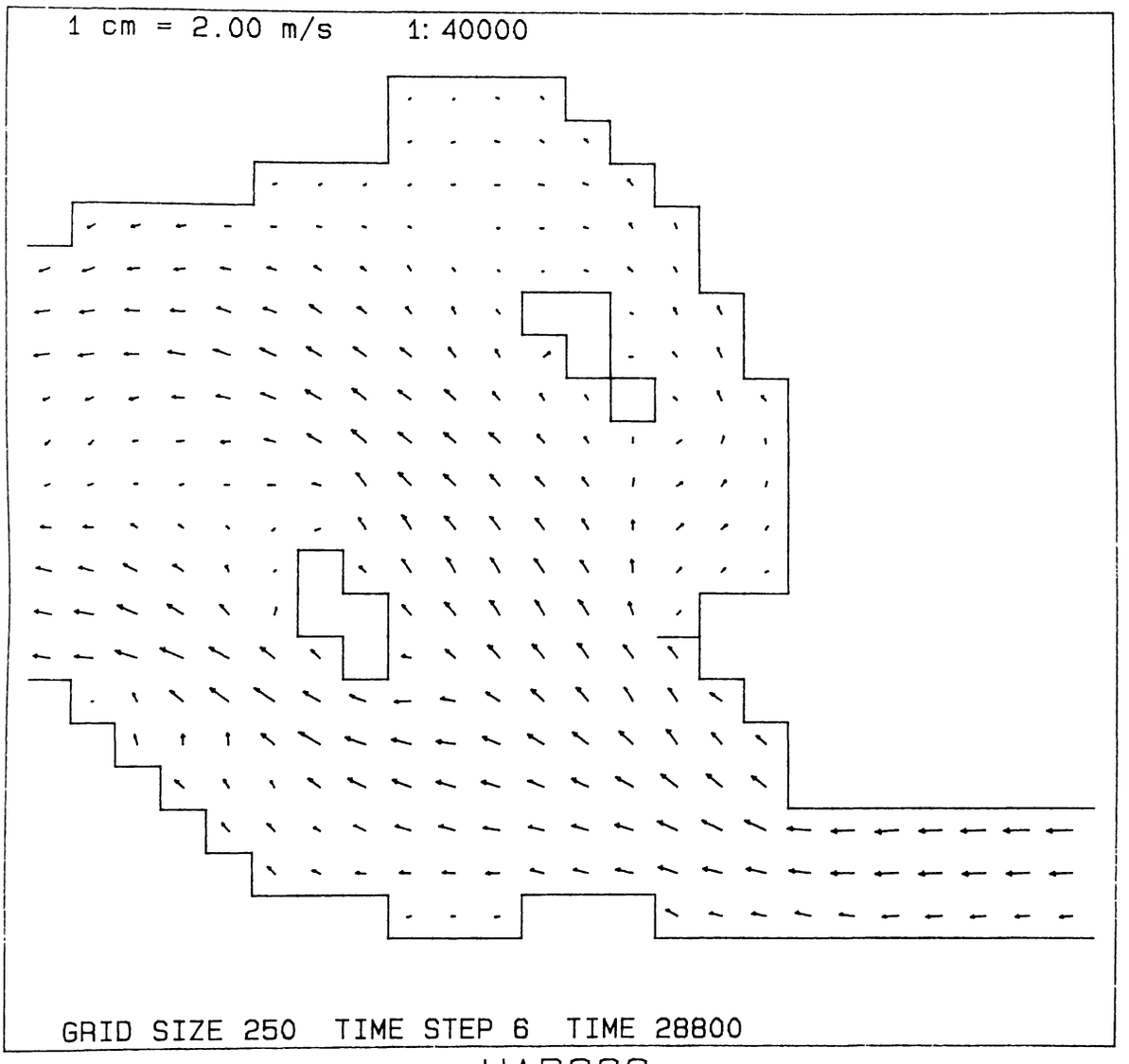

Figure 10.71(h): Flow pattern after port construction. Neap tide 8¾ hours after the high tide at 23:15 on 2-Dec-81.

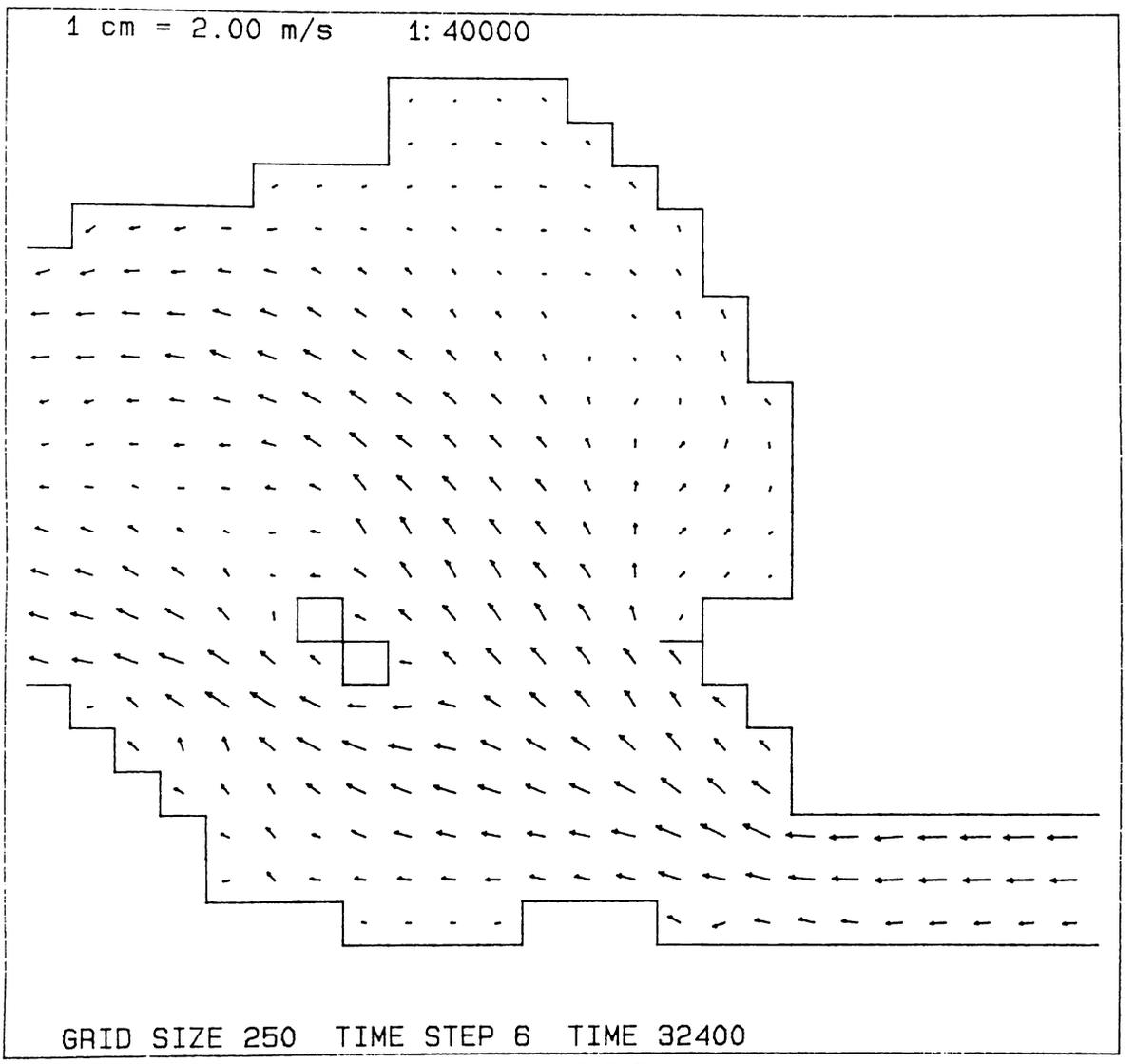

Figure 10.71(i): Flow pattern after port construction. Neap tide 9¾ hours after the high tide at 23:15 on 2-Dec-81.

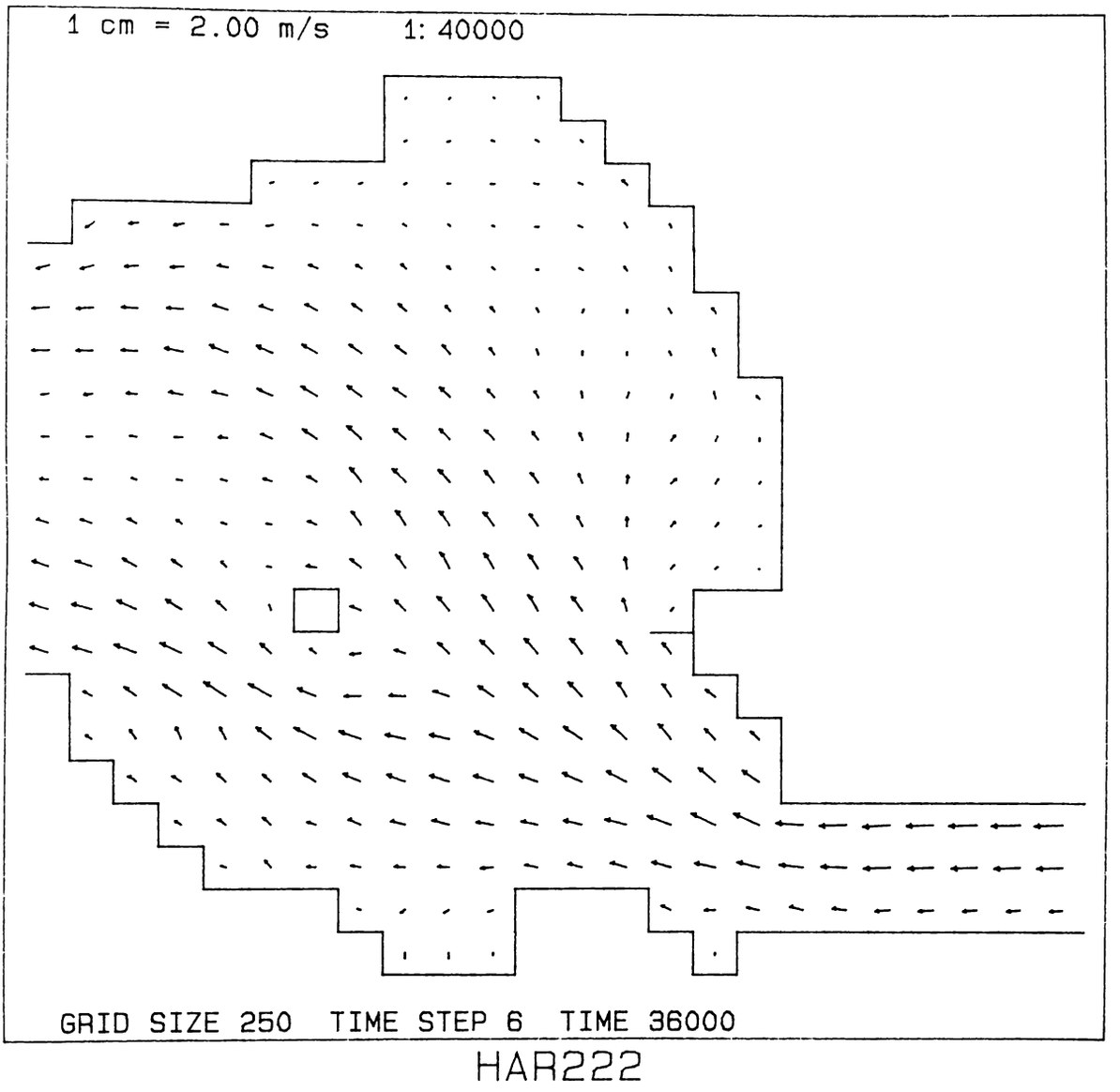

Figure 10.71(j): Flow pattern after port construction. Neap tide 10¾ hours after the high tide at 23:15 on 2-Dec-81.

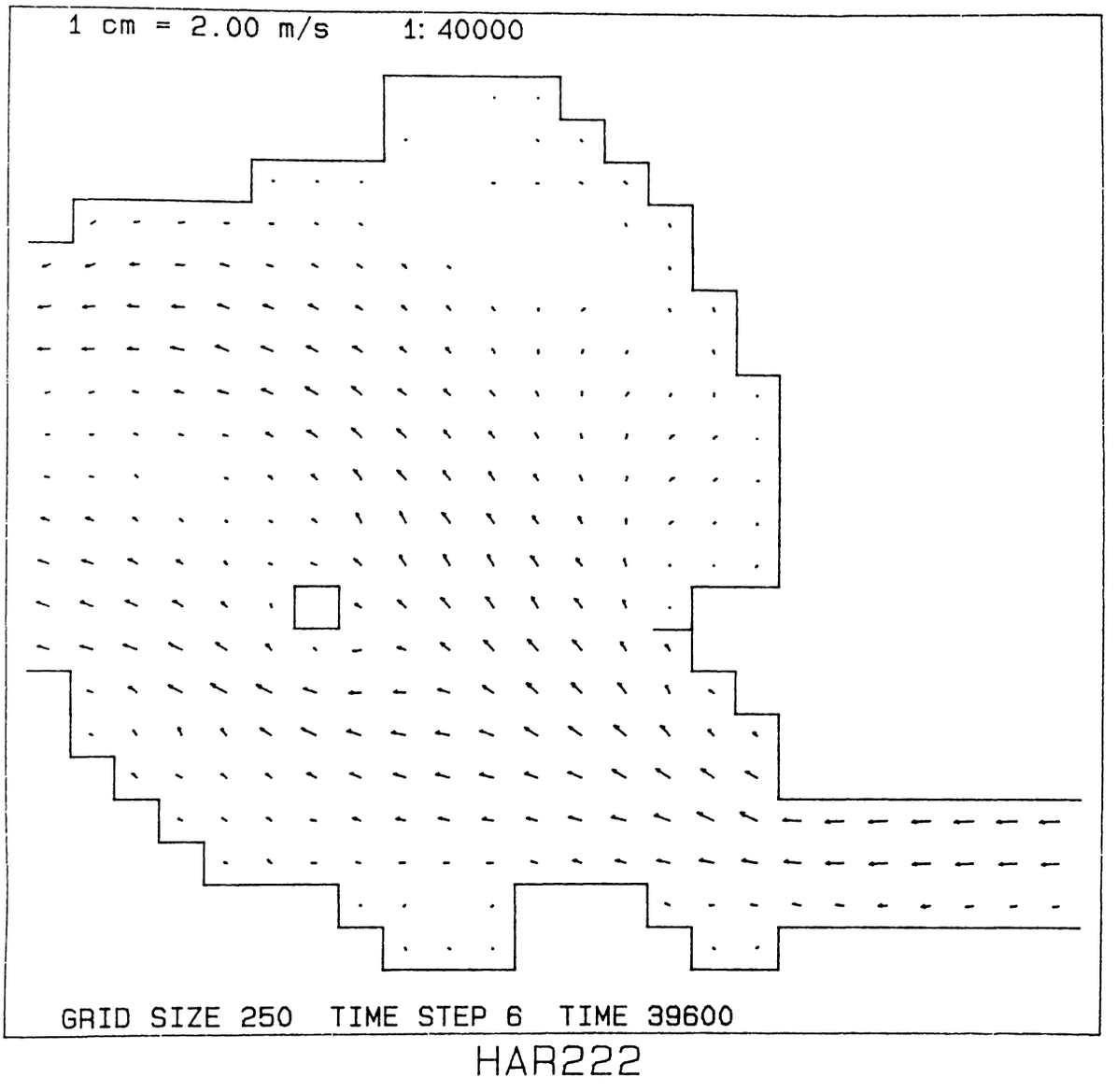

Figure 10.71(k): Flow pattern after port construction. Neap tide 11¾ hours after the high tide at 23:15 on 2-Dec-81.

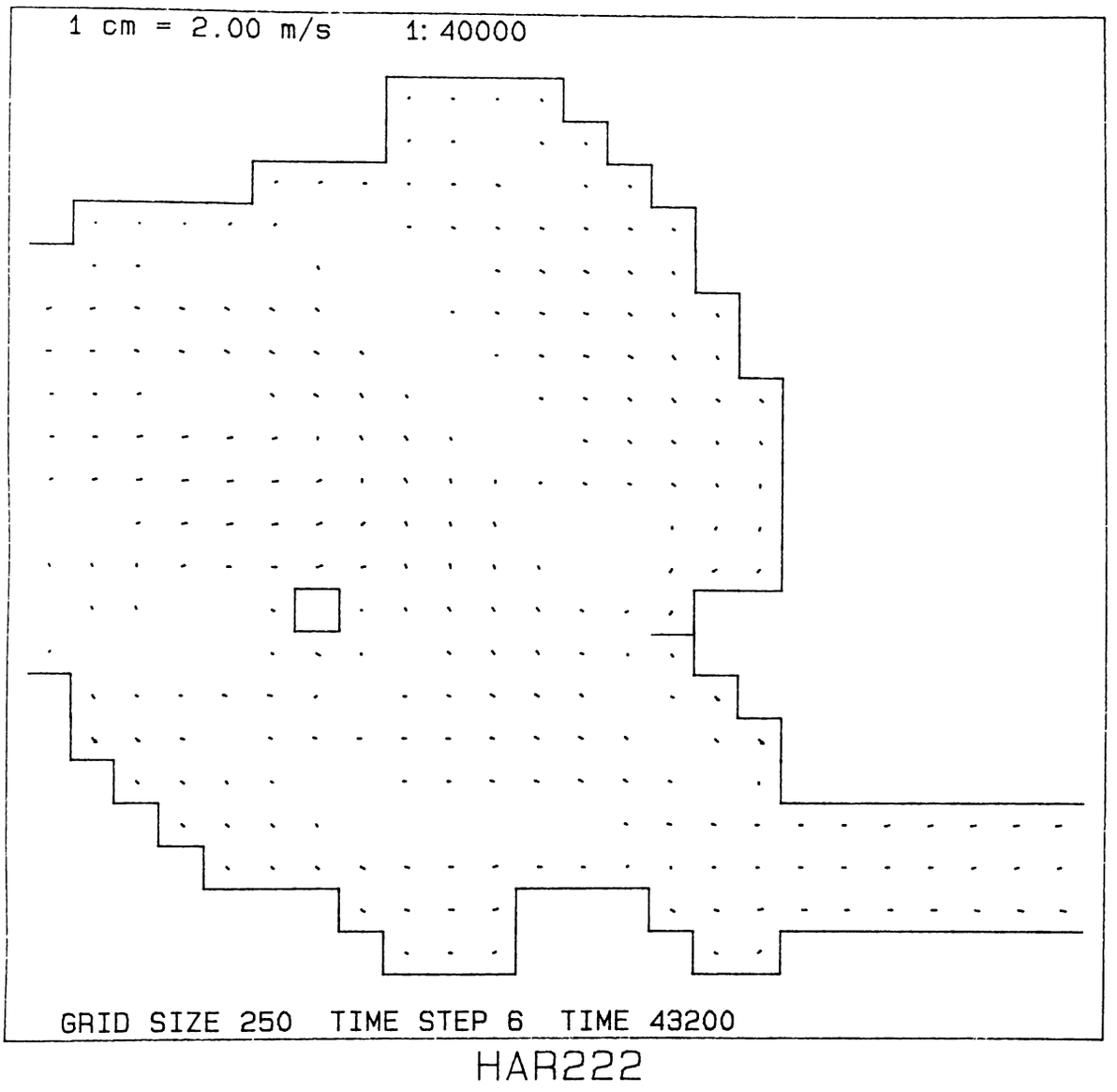

Figure 10.71(1): Flow pattern after port construction. Neap tide 12¾ hours after the high tide at 23:15 on 2-Dec-81.

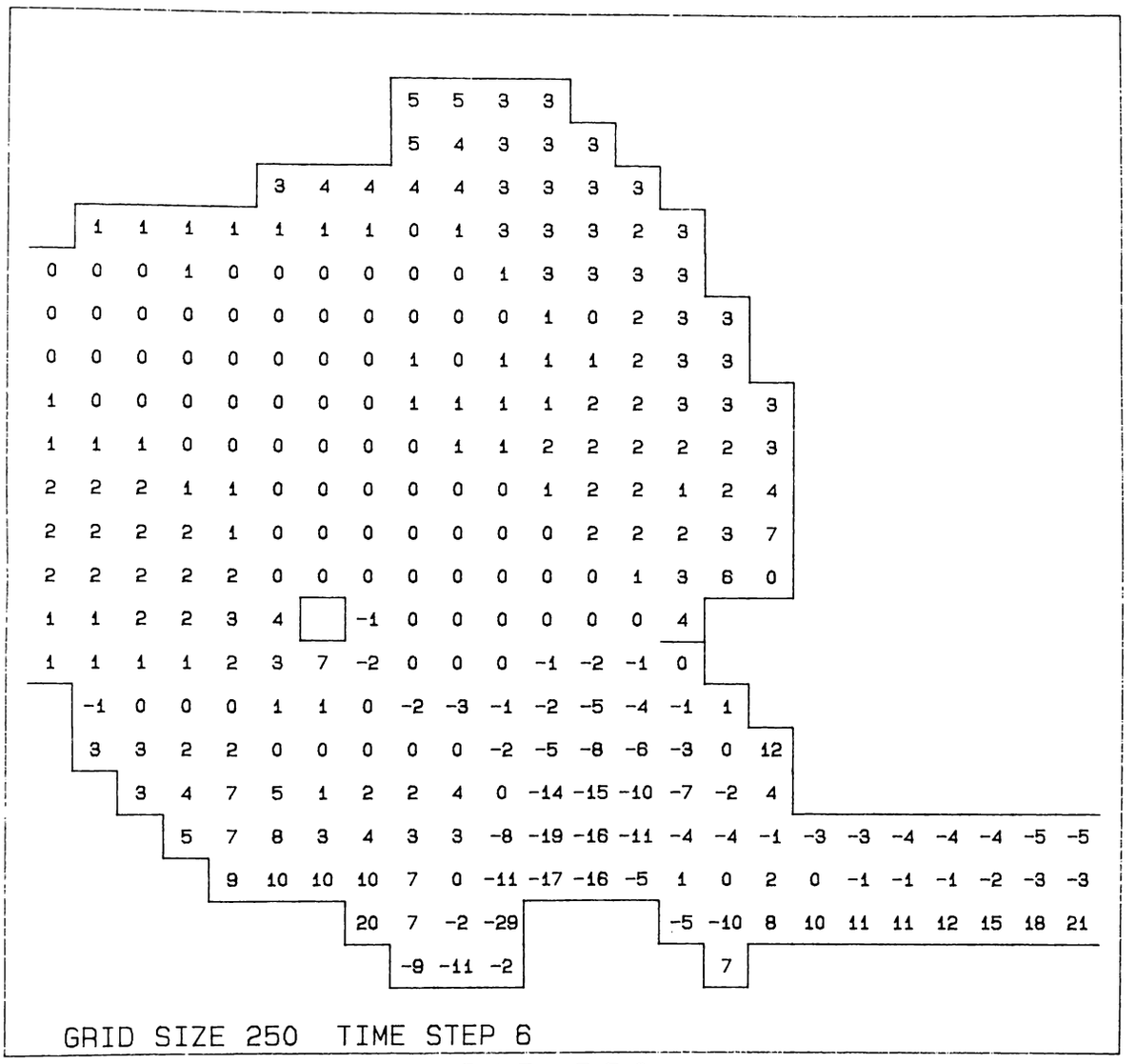

Figure 10.72: Percentage speed changes after introduction of the timber port during peak, Spring-tide, flood flow.

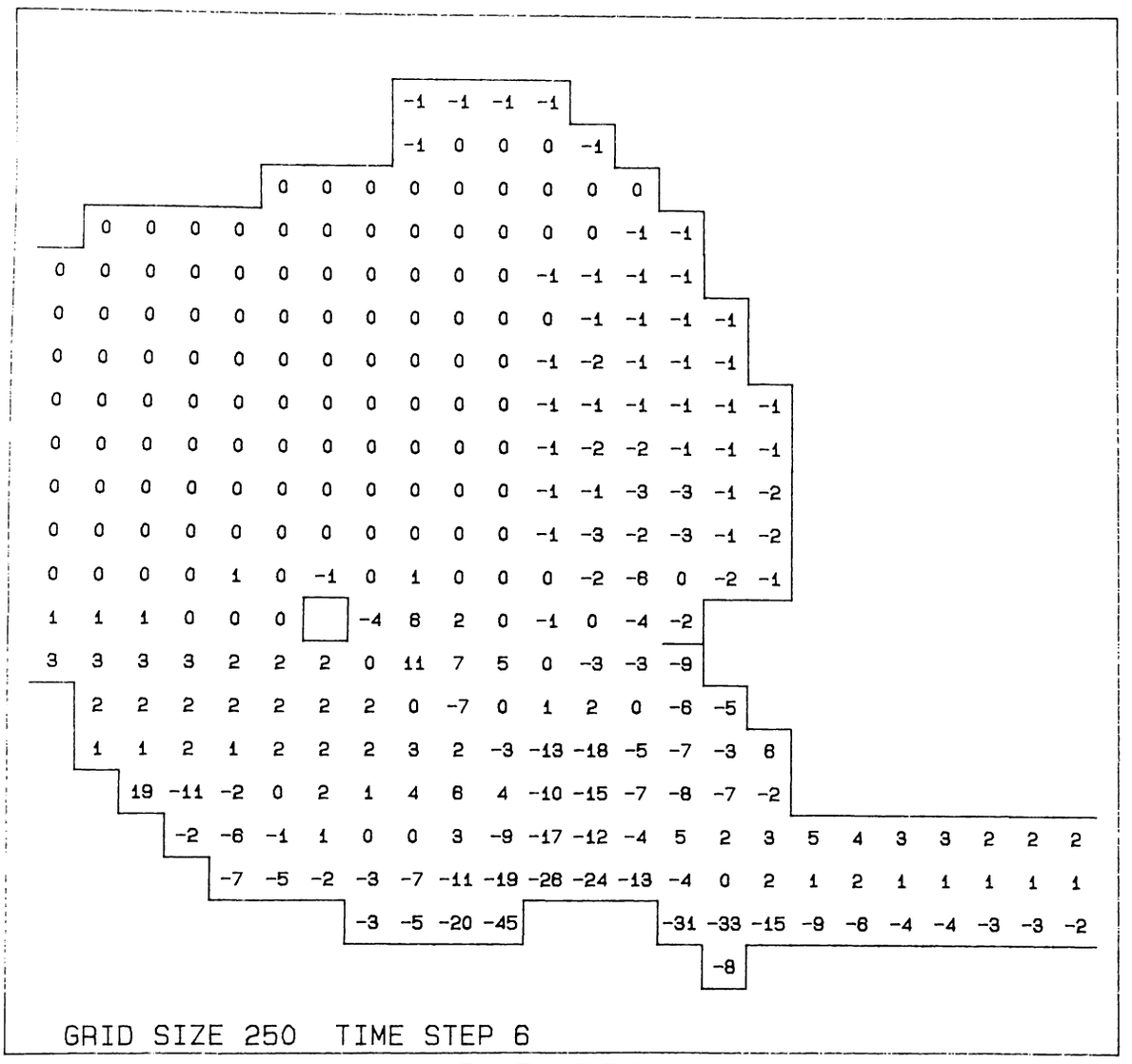

Figure 10.73: Percentage speed changes after introduction of the timber port during peak, Spring-tide, ebb flow.

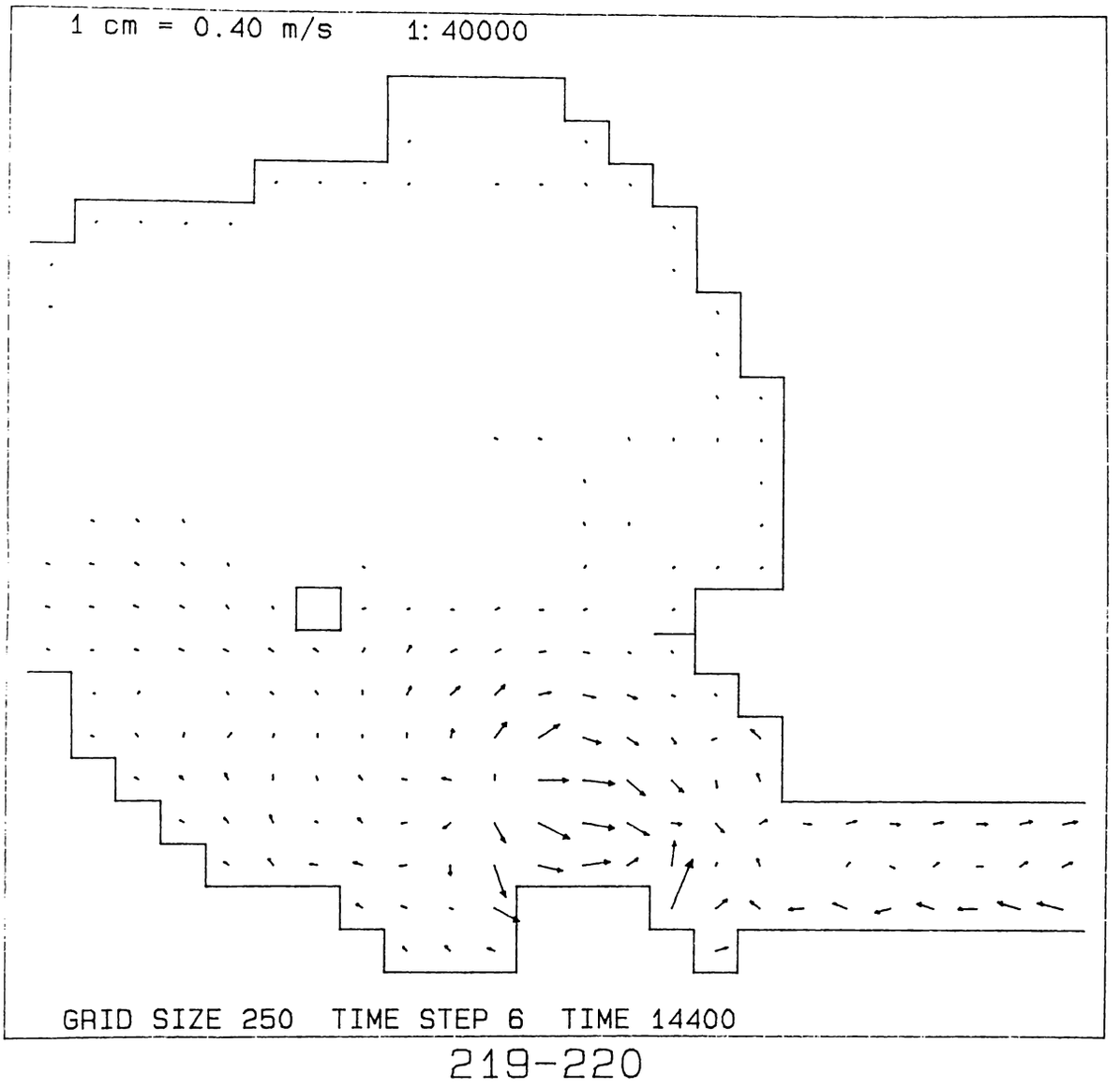

Figure 10.74: Vector velocity differences after introduction of the timber port during peak, Spring-tide, flood flow. Arrows pointing to the right (against the flow) reflect a decrease in velocity.

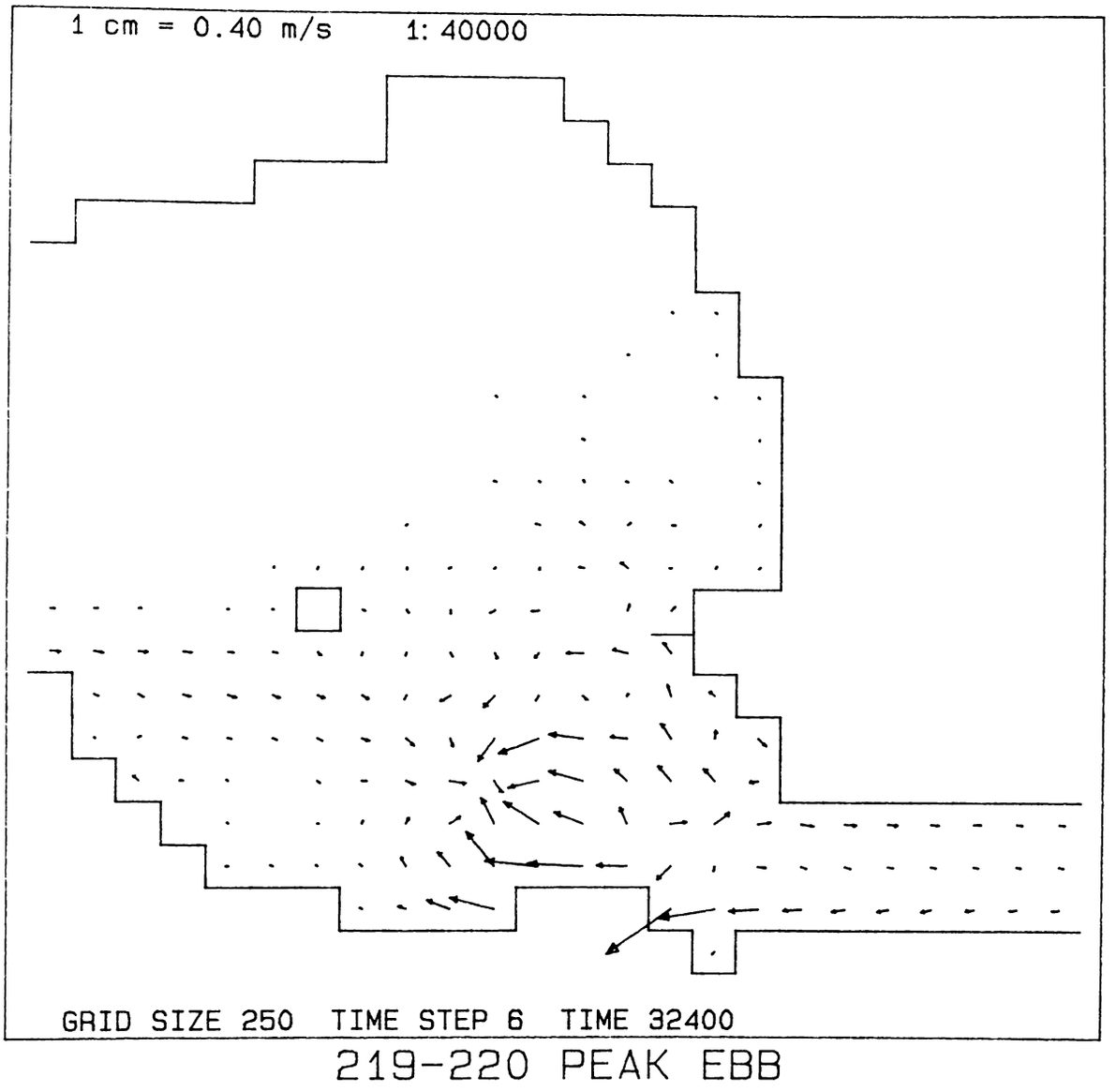

Figure 10.75: Vector velocity differences after introduction of the timber port during peak, Spring-tide, ebb flow. Arrows pointing to the left (against the flow) reflect a decrease in velocity.

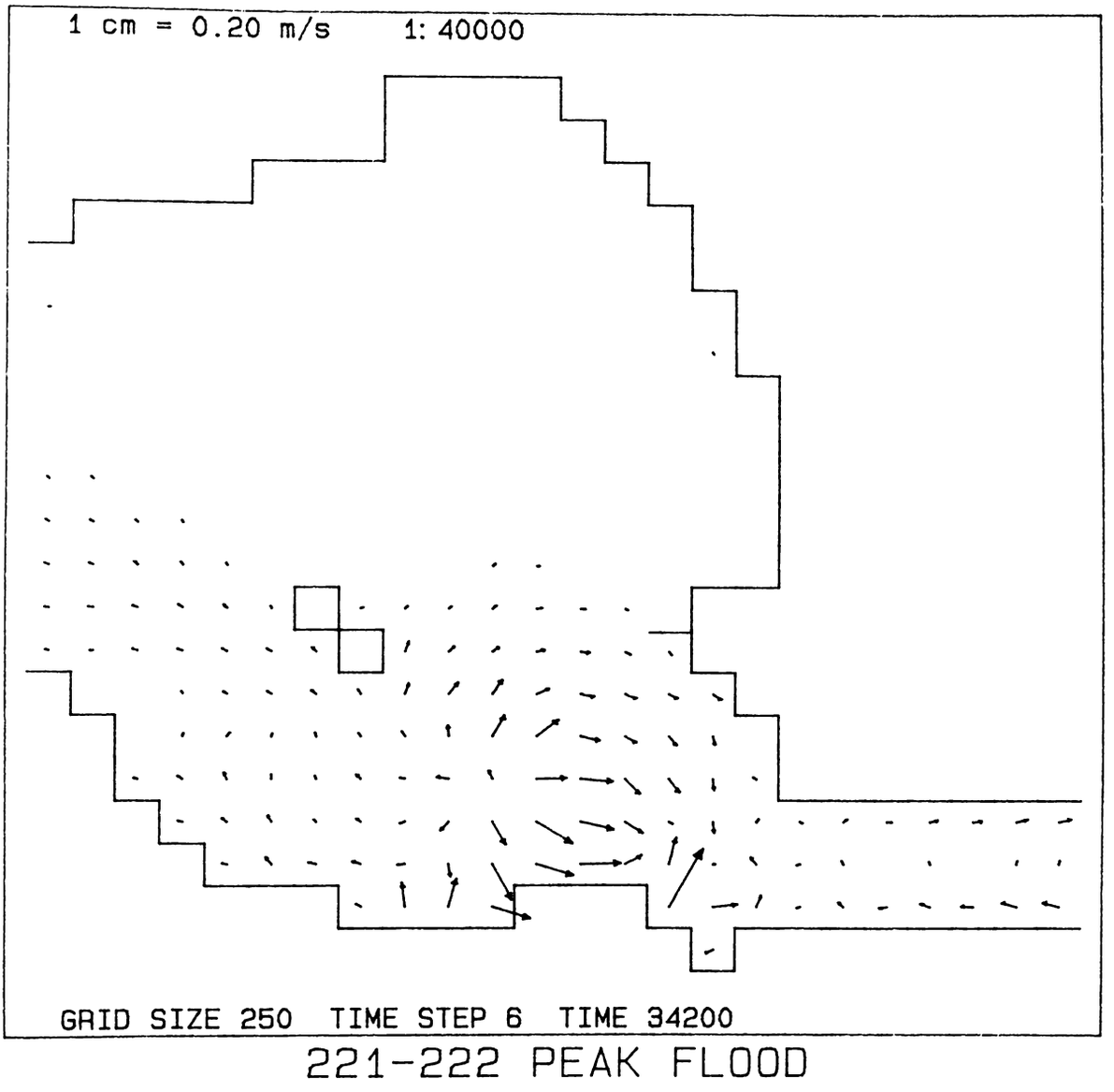

Figure 10.76: Vector velocity differences after introduction of the timber port during peak, Neap-tide, flood flow. Arrows pointing to the right (against the flow) reflect a decrease in velocity.

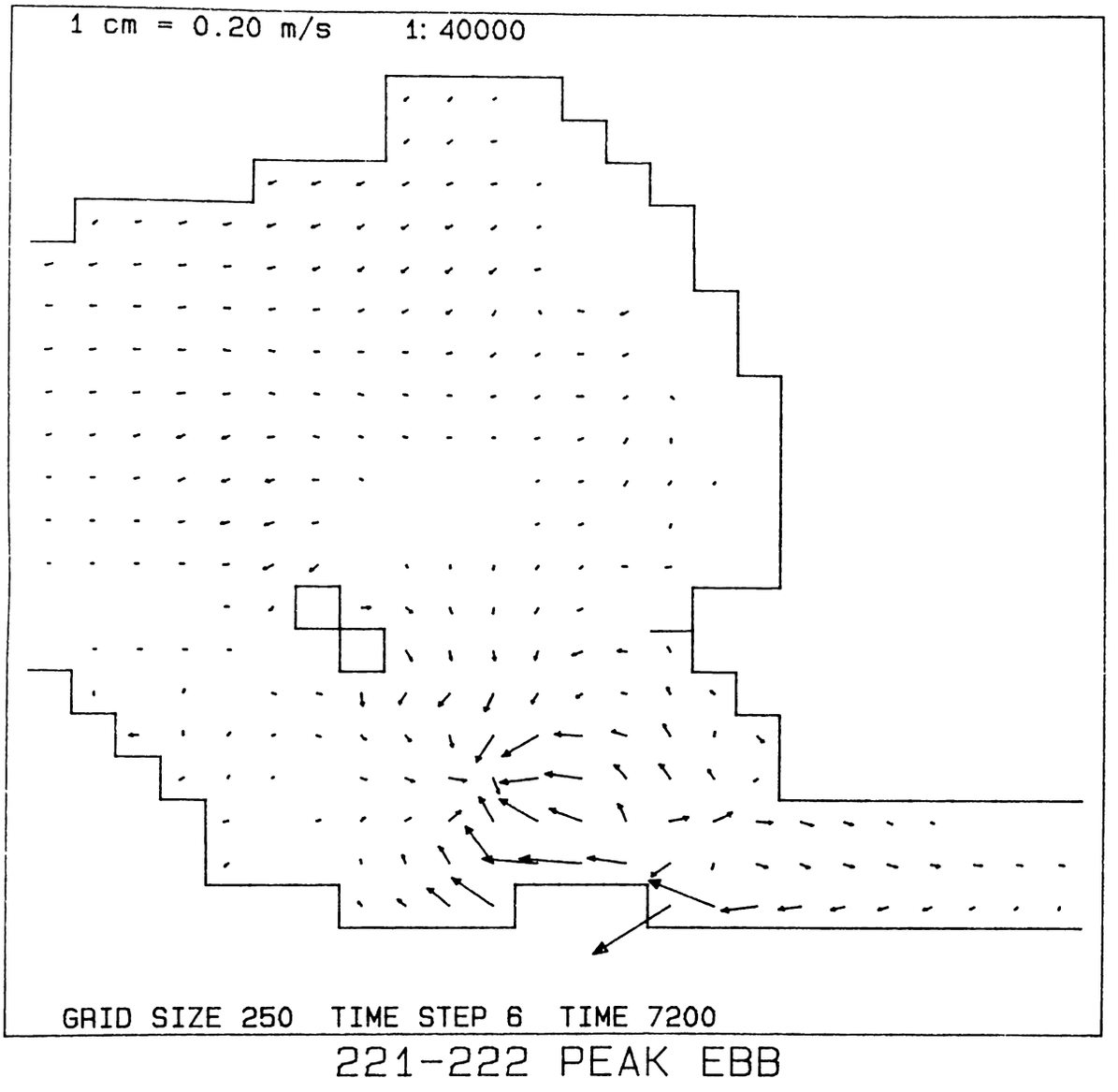

Figure 10.77: Vector velocity differences after introduction of the timber port during peak, Neap-tide, ebb flow. Arrows pointing to the left (against the flow) reflect a decrease in velocity.

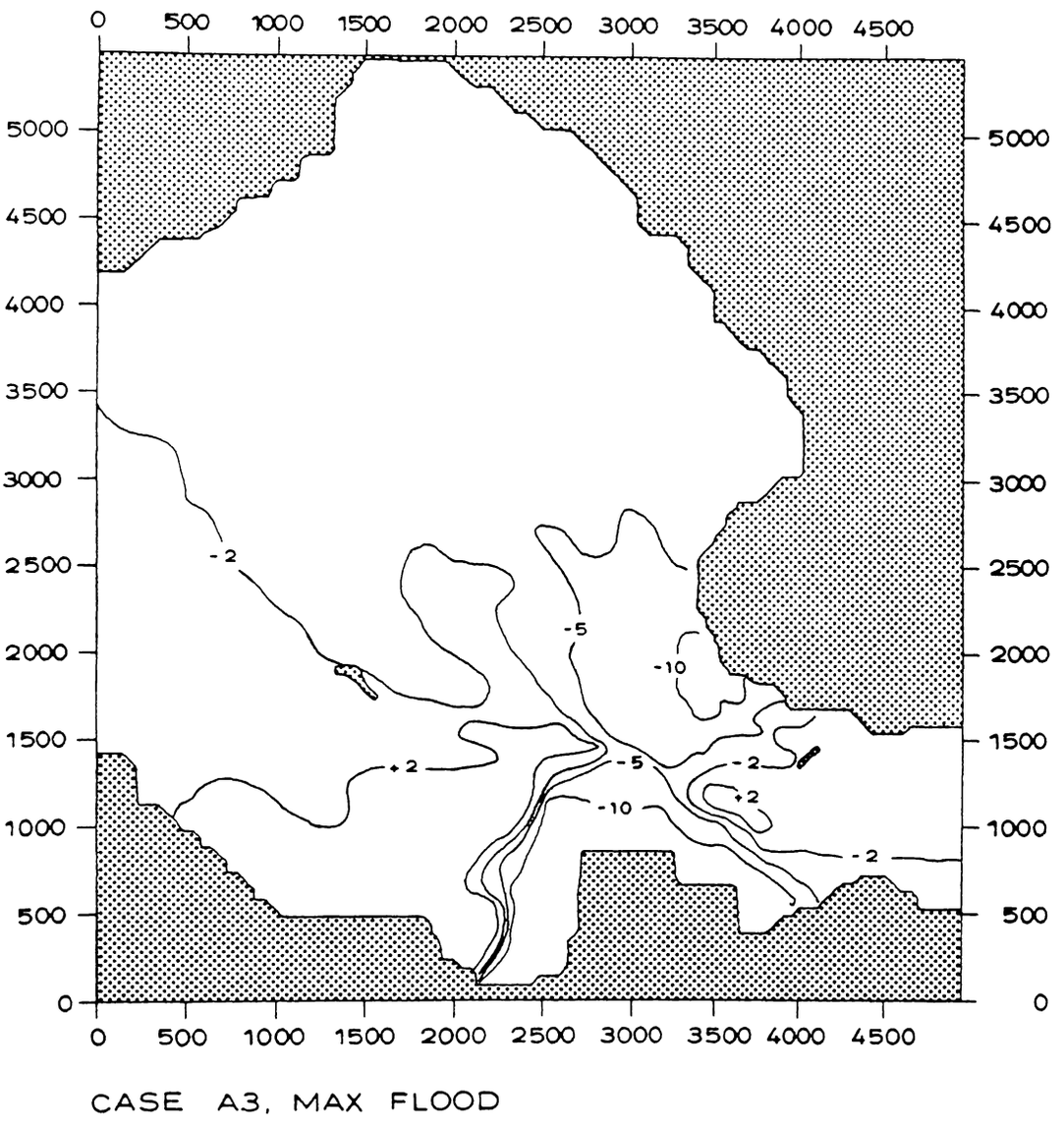

Figure 10.78: DHI (1982) model results showing the contours of percentage velocity changes after introduction of the timber port configuration A3. Peak flood during the Spring tide.

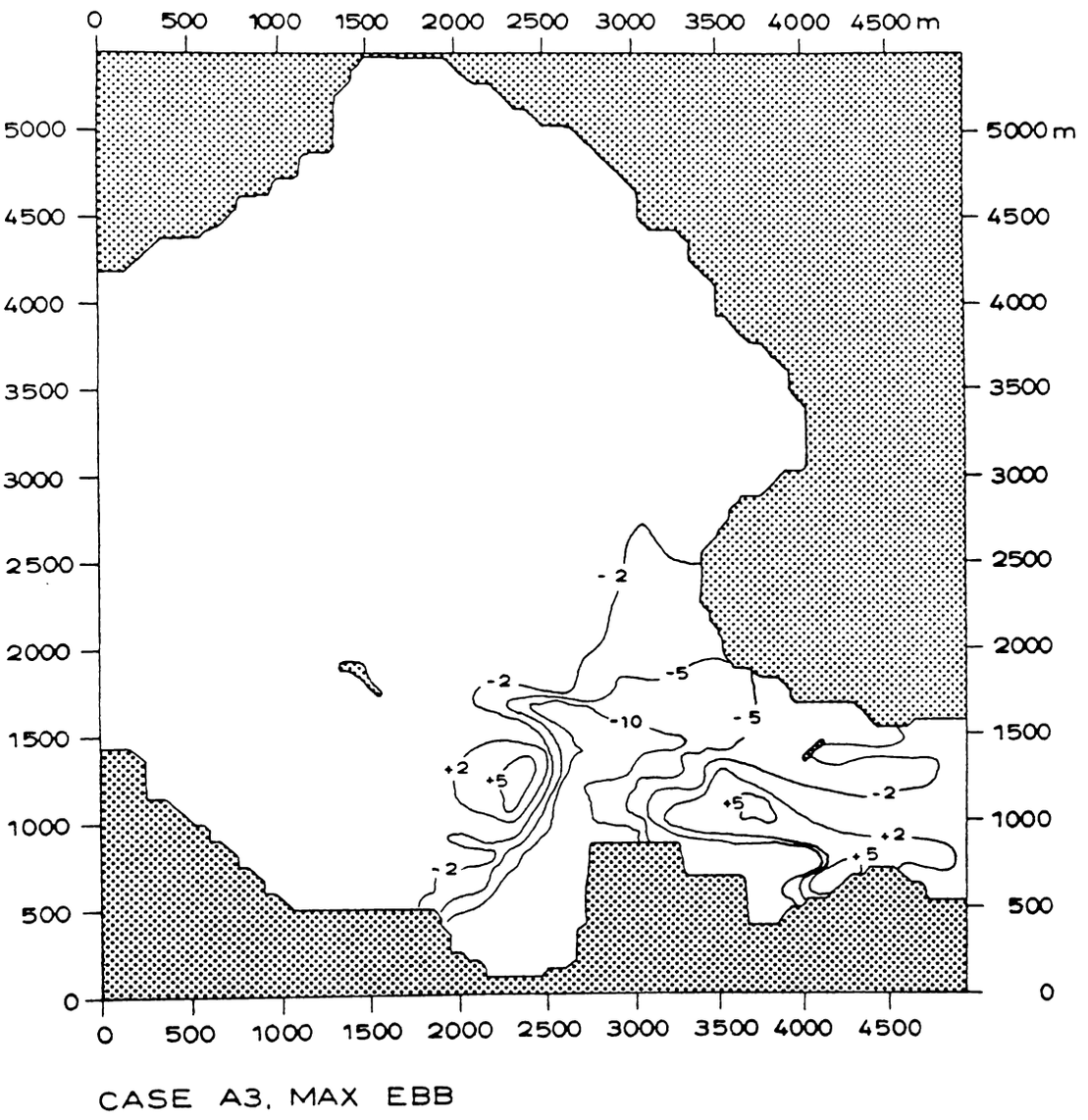

Figure 10.79: DHI (1982) model results showing the contours of percentage velocity changes after introduction of the timber port configuration A3. Peak ebb during the Spring tide.

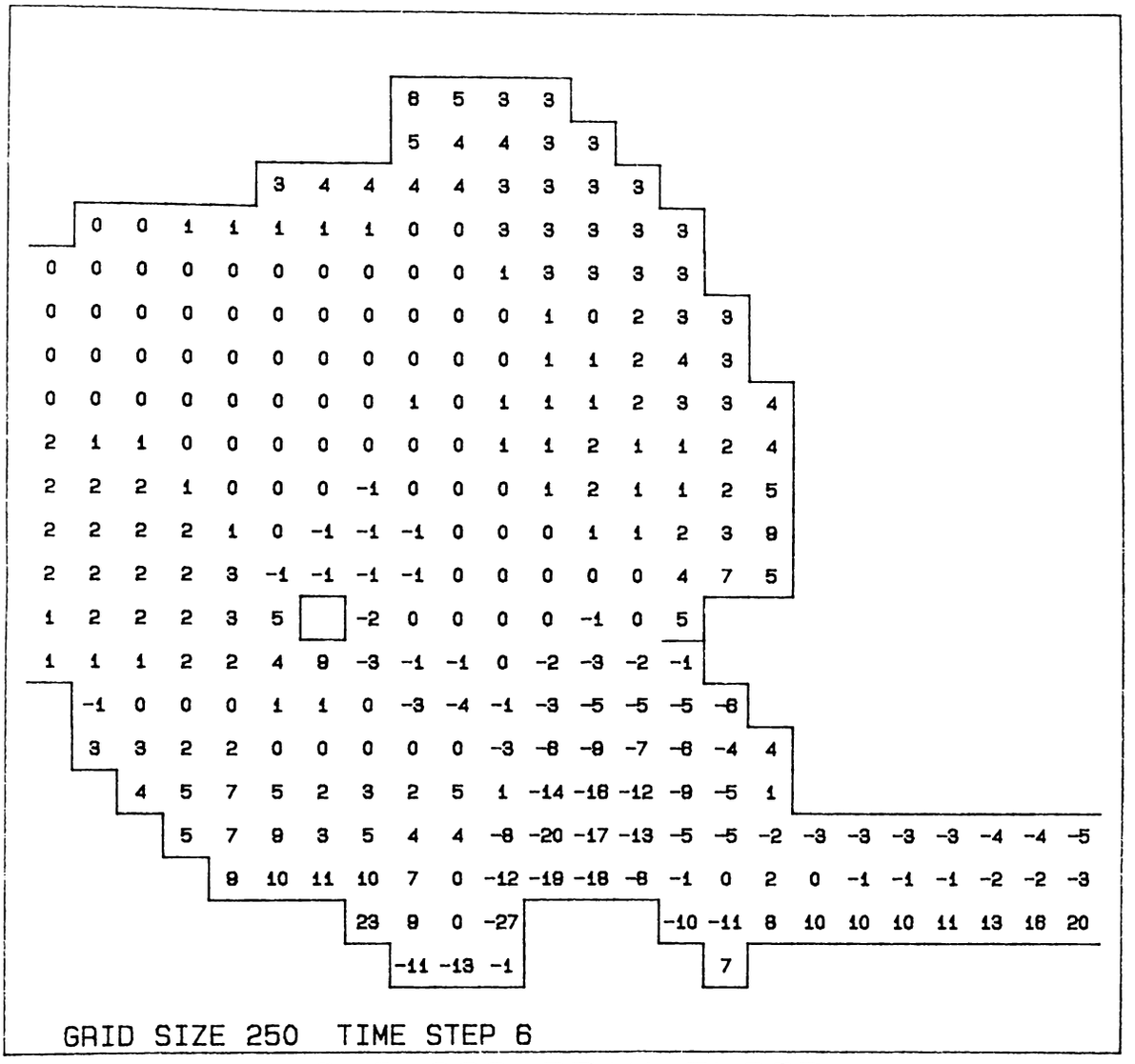

Figure 10.80: Percentage speed changes during peak, Spring-tide, flood flow after introduction of the timber port with the dredge zone being 14m deep.

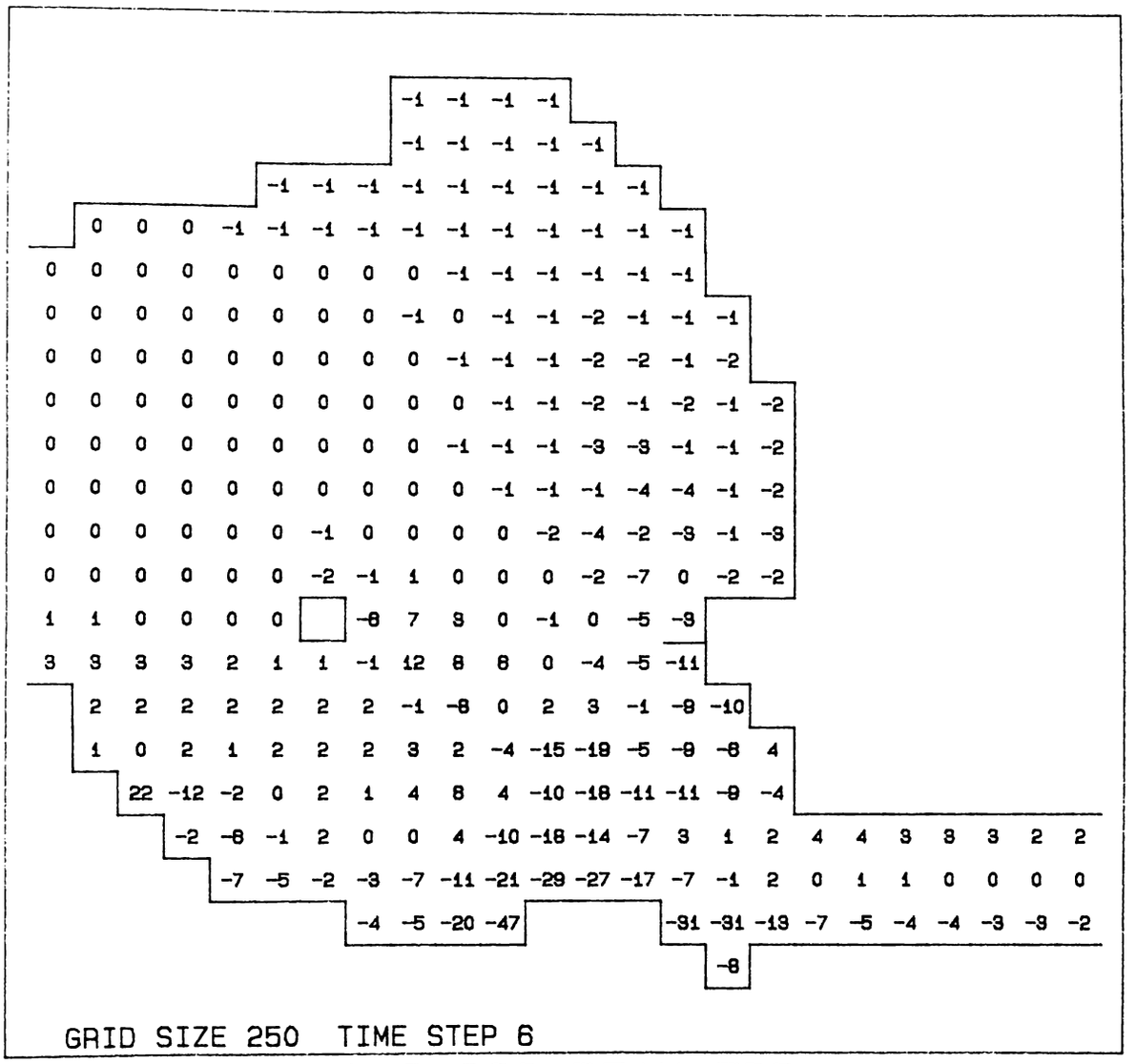

Figure 10.81: Percentage speed changes during peak, Spring-tide, ebb flow after introduction of the timber port with the dredge zone being 14m deep.

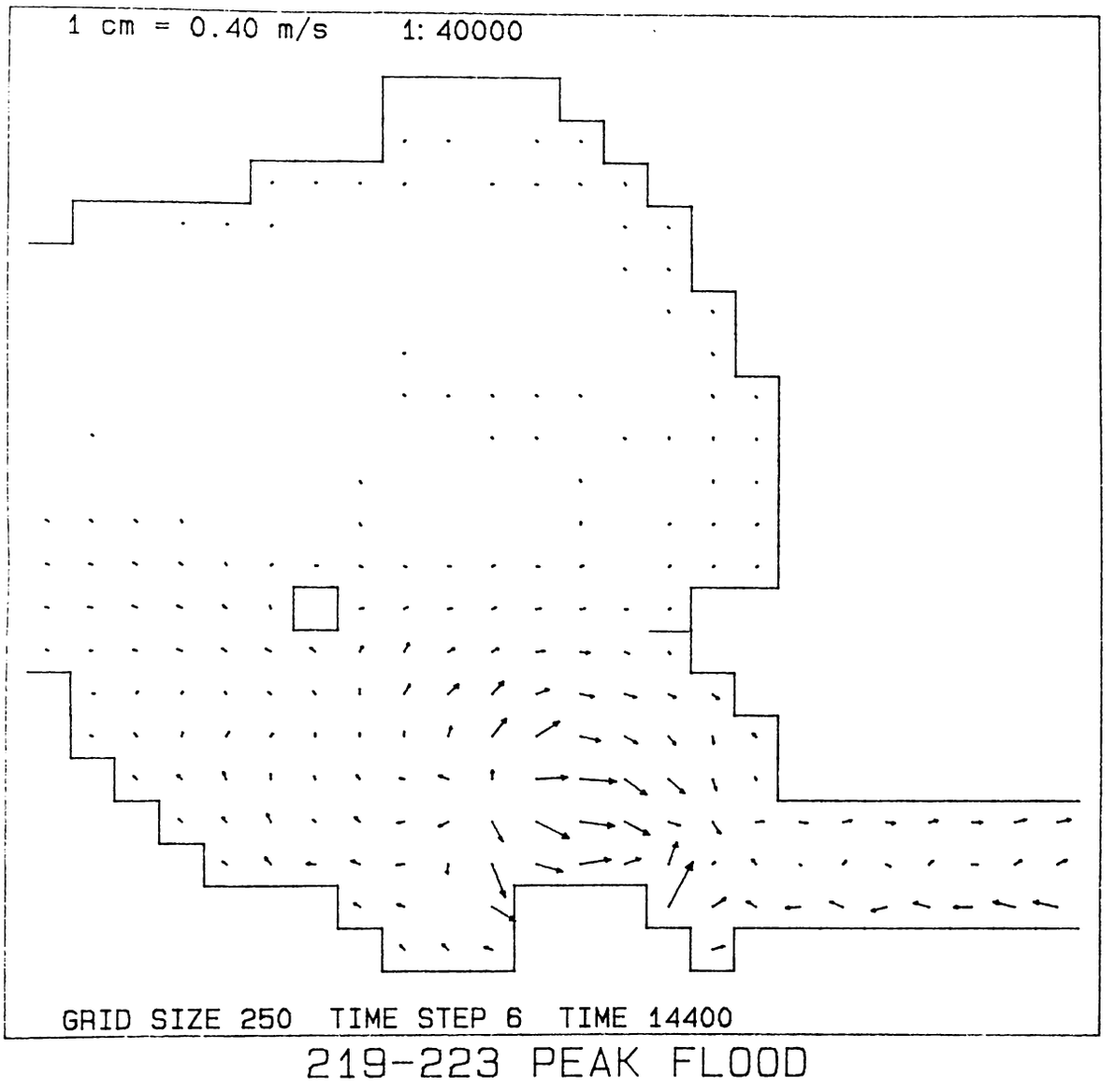

Figure 10.82: Vector velocity differences during peak, Spring-tide, flood flow after introduction of the timber port with the dredge zone being 14m deep.

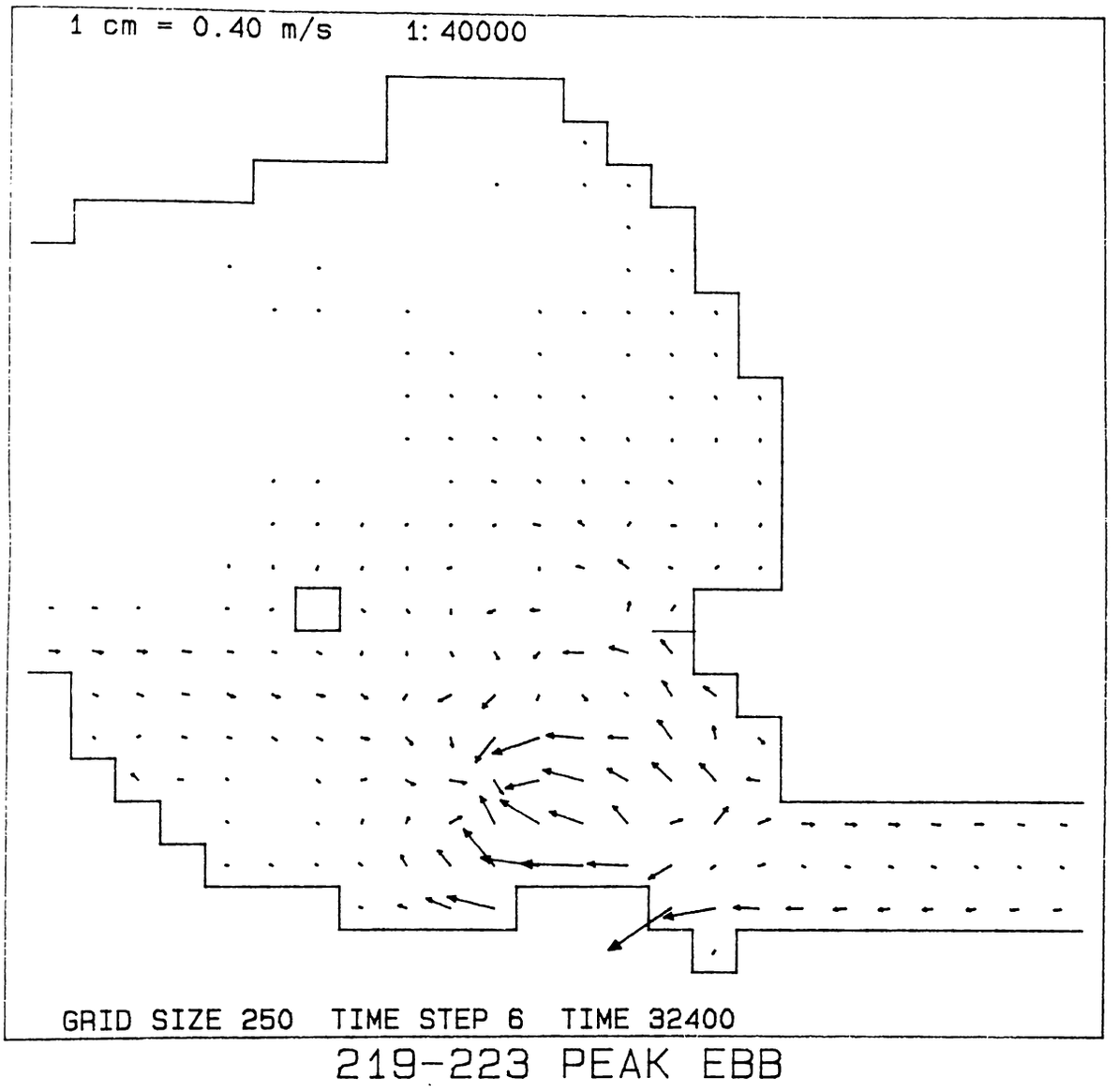

Figure 10.83: Vector velocity differences during peak, Spring-tide, ebb flow after introduction of the timber port with the dredge zone being 14m deep.

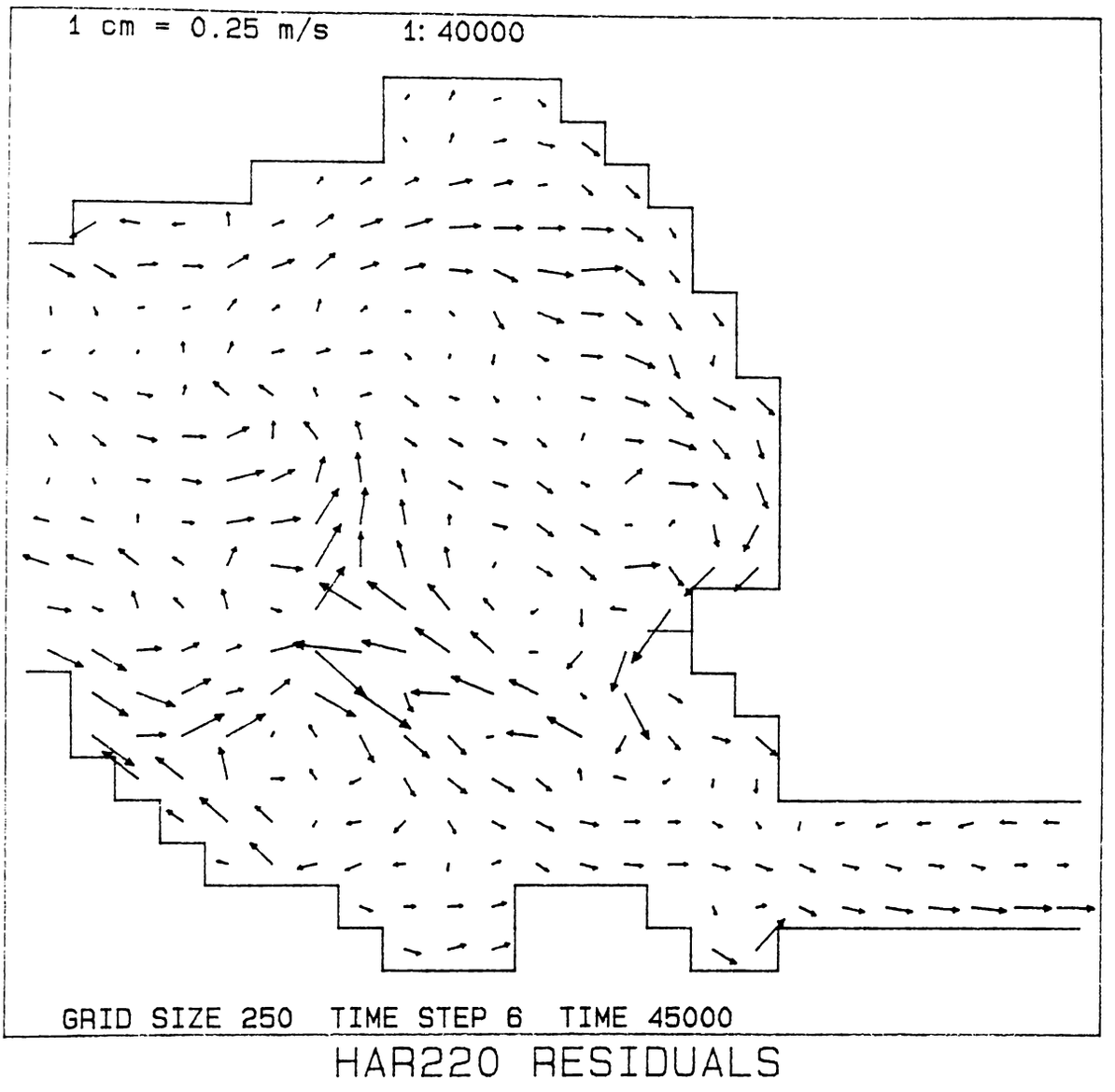

Figure 10.84: Tidal cycle residual velocities after introduction of the timber port for the Spring tide simulation. Ebb and flood velocities have been scaled to a common tidal range of 2.6m.

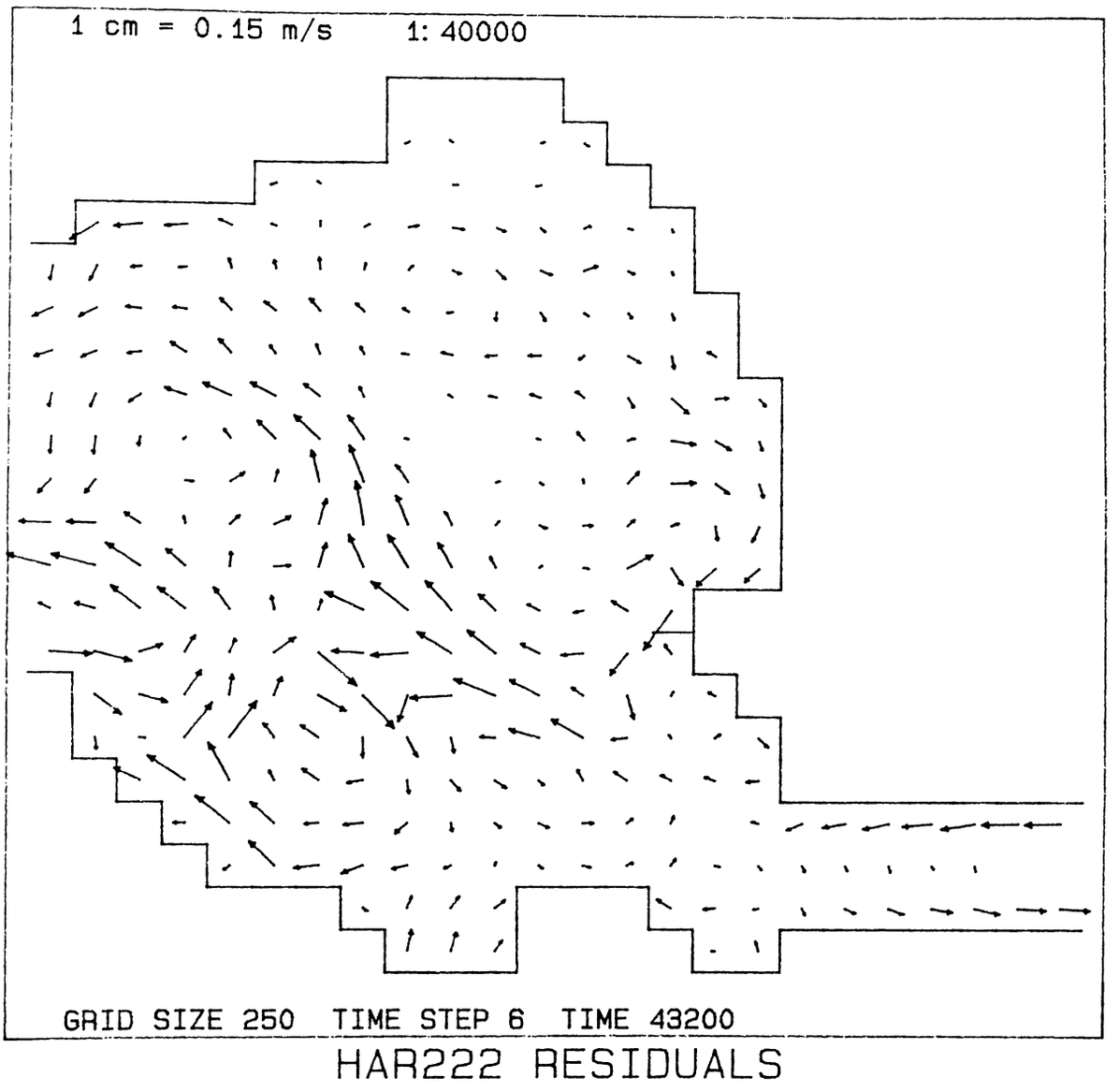

Figure 10.85: Tidal cycle residual velocities after introduction of the timber port for the Neap tide simulation. Ebb and flood velocities have been scaled to a common tidal range of 1.6m.

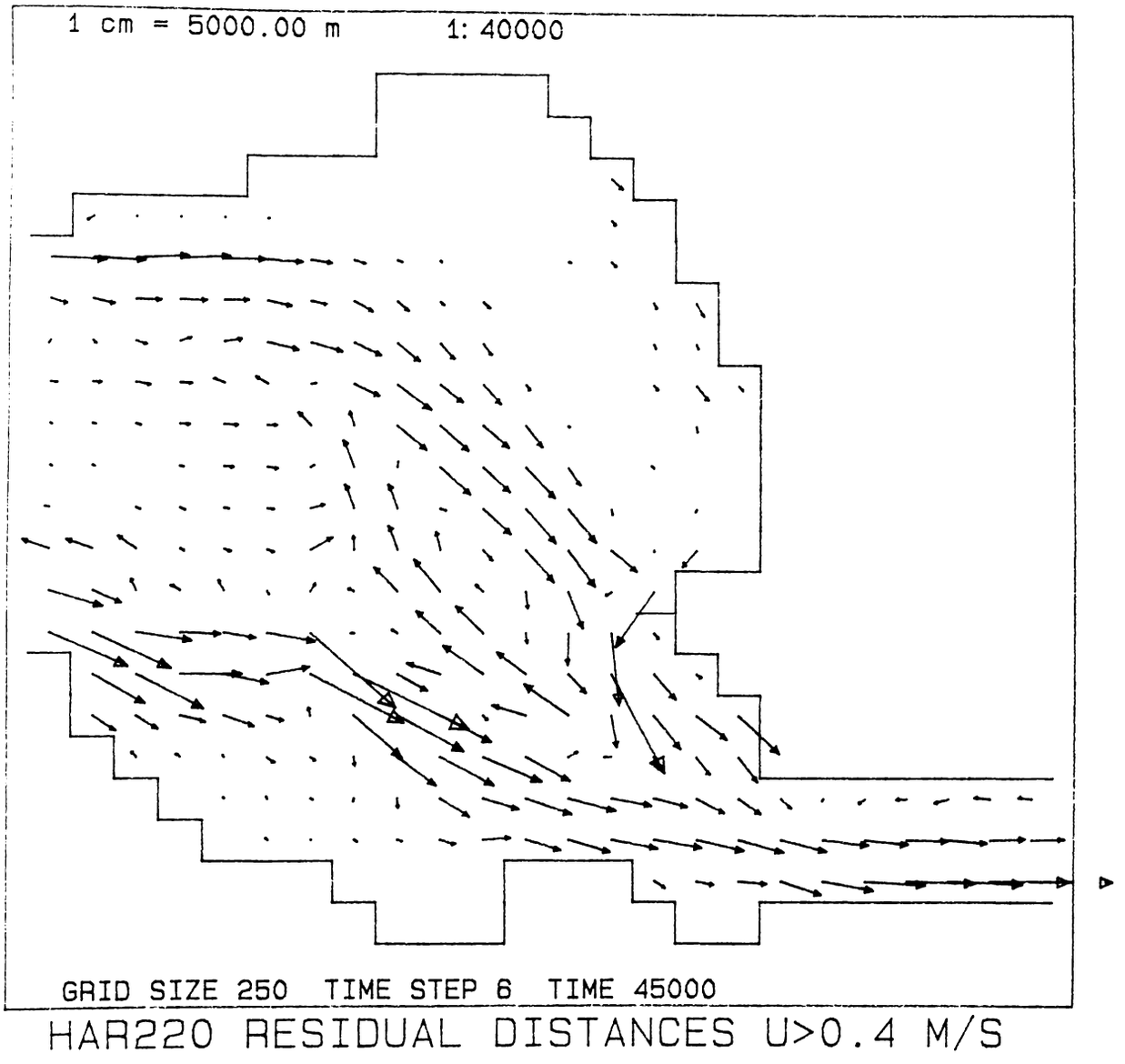

Figure 10.86: Tidal cycle residual distances for velocities exceeding 0.4 $m.s^{-1}$ after introduction of the timber port for the Spring tide simulation. Ebb and flood velocities have been scaled to a common tidal range of 2.6m.

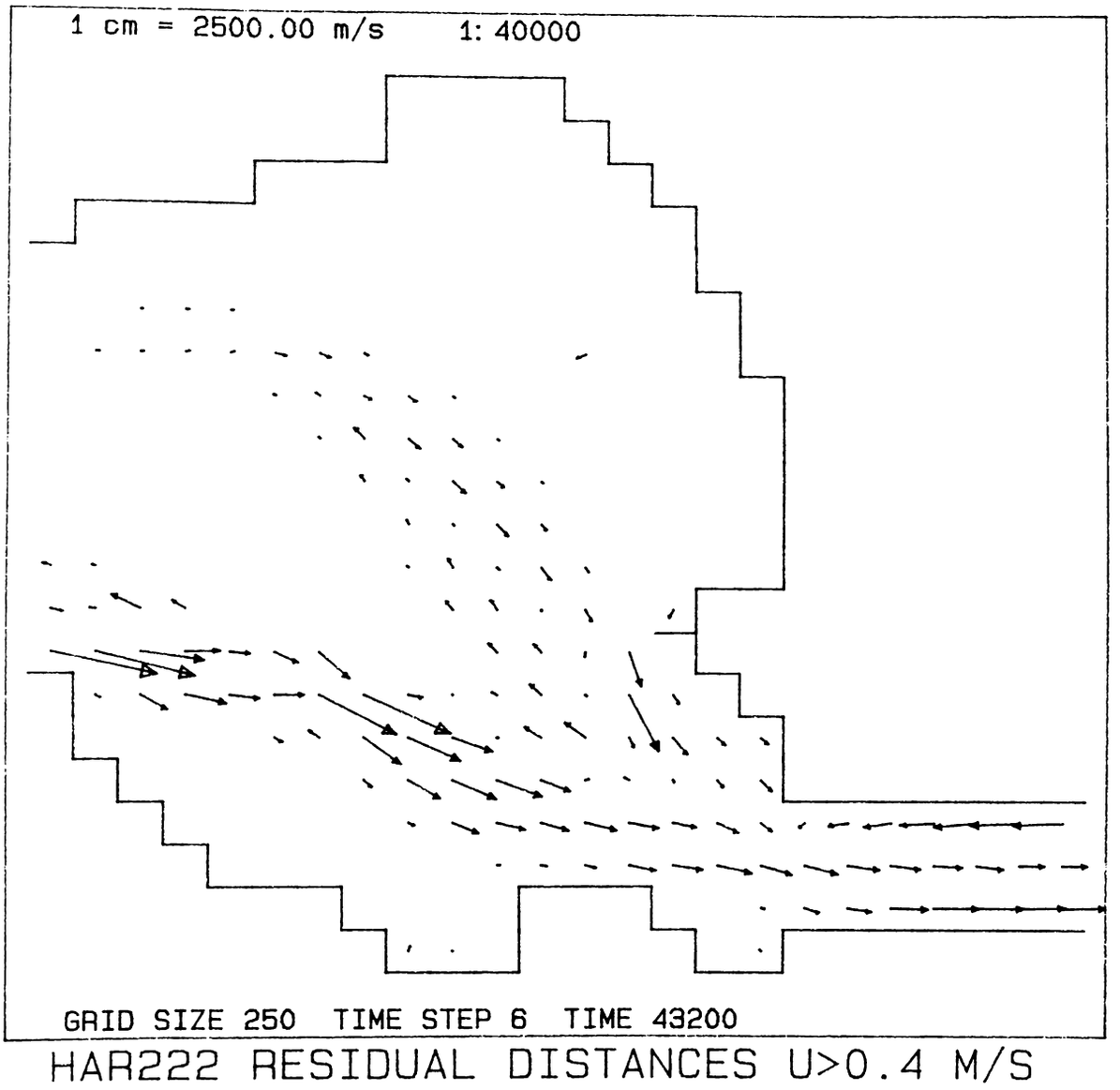

Figure 10.87: Tidal cycle residual distances for velocities exceeding 0.4 $m.s^{-1}$ after introduction of the timber port for the Neap tide simulation. Ebb and flood velocities have been scaled to a common tidal range of 2.6m.

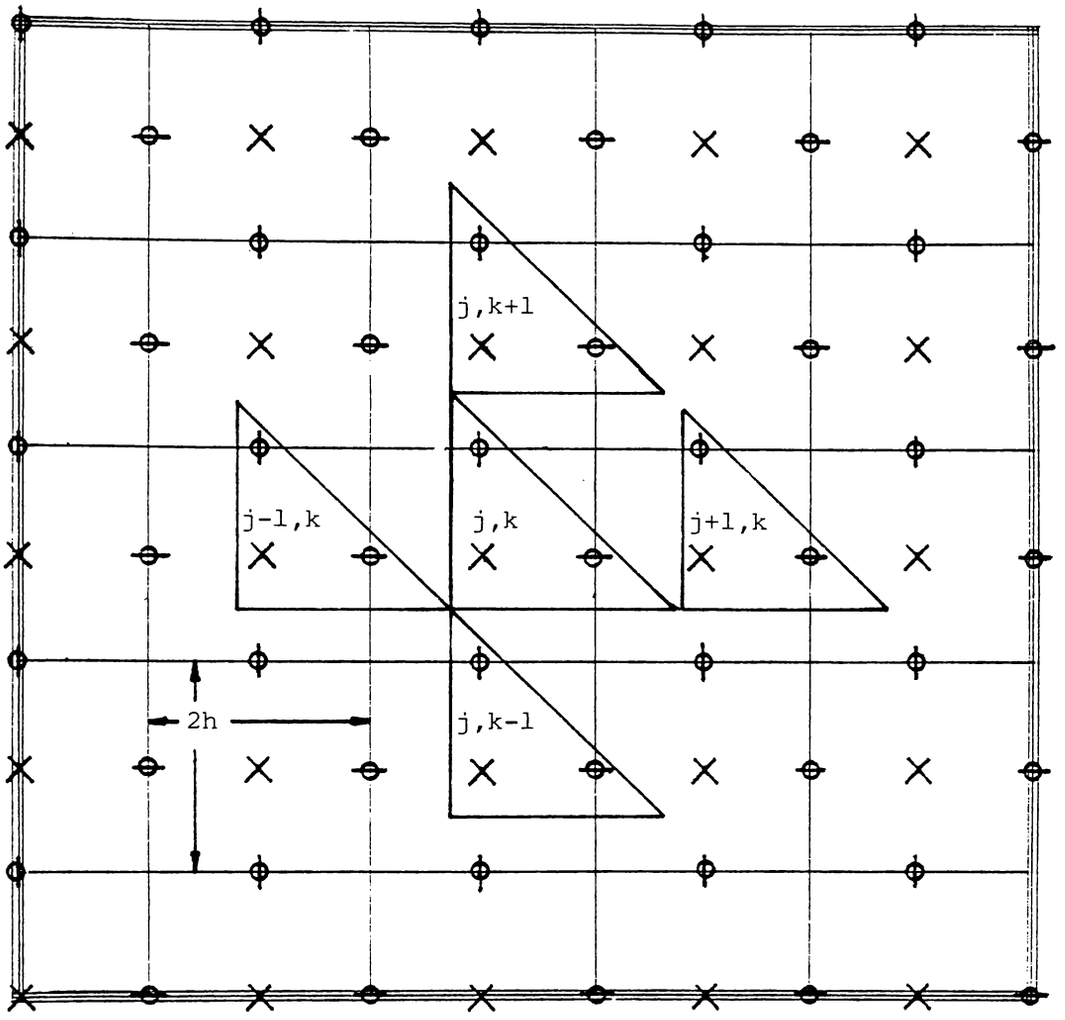

X velocity ($V_{j,k}$); sea level ($\xi_{j,k}$)
⊖ x-components of: depth below datum ($D_{Uj,k}$)
Availability ($A_{Uj,k}$)
Erodibility ($E_{Uj,k}$)
sediment flux ($q_{Uj,k}$)
ϕ y-components of: depth below datum ($D_{Vj,k}$)
Availability ($A_{Vj,k}$)
Erodibility ($E_{Vj,k}$)
sediment flux ($q_{Vj,k}$)

Figure 11.1: Grid defining the notation for the sediment transport model numerical scheme. The nodes within the triangles all have the same given subscript and parameters represented at these locations are listed above.

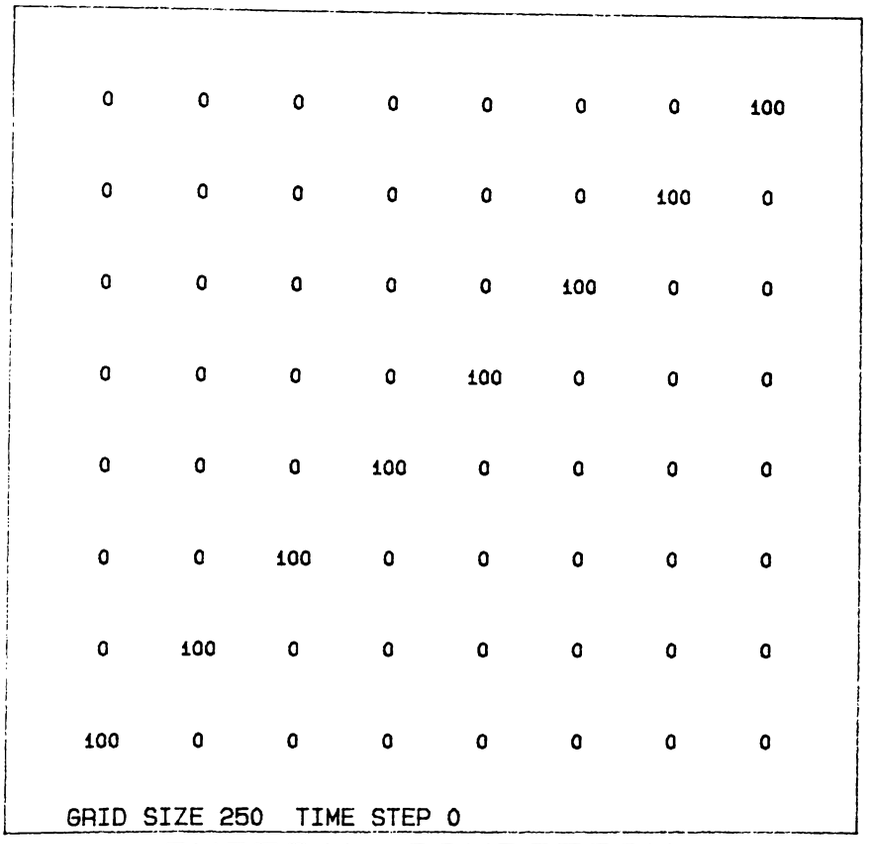

Figure 11.2: Availabilities in a test rig composed of a distended, non-cohesive sandy region (100% cover) entirely surrounded by a sand-free bed (0%). This is the initial condition for test rigs shown in Figures 11.4, 11.5 and 11.6.

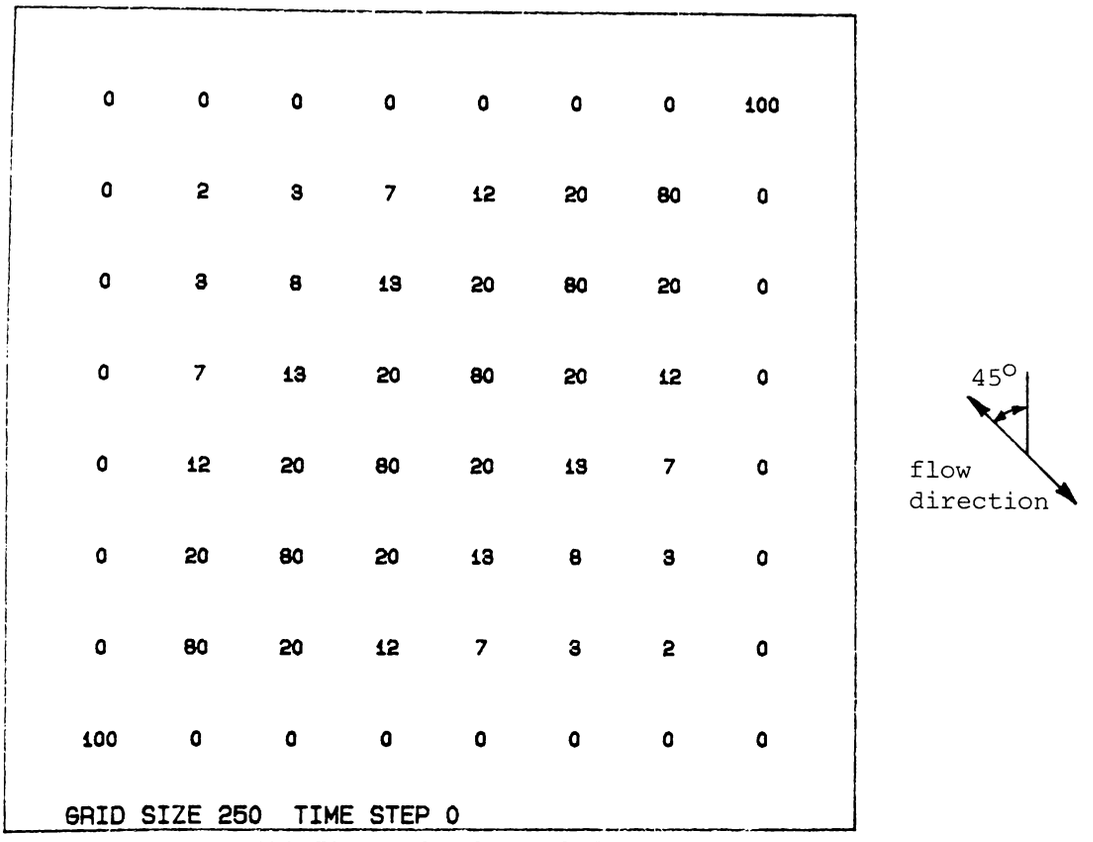

Figure 11.3(a): Deterioration of the initially sandy region (Figure 11.2) in transverse reversing, neutral flow after 20 iterations using an unstable scheme to represent the Availabilities.

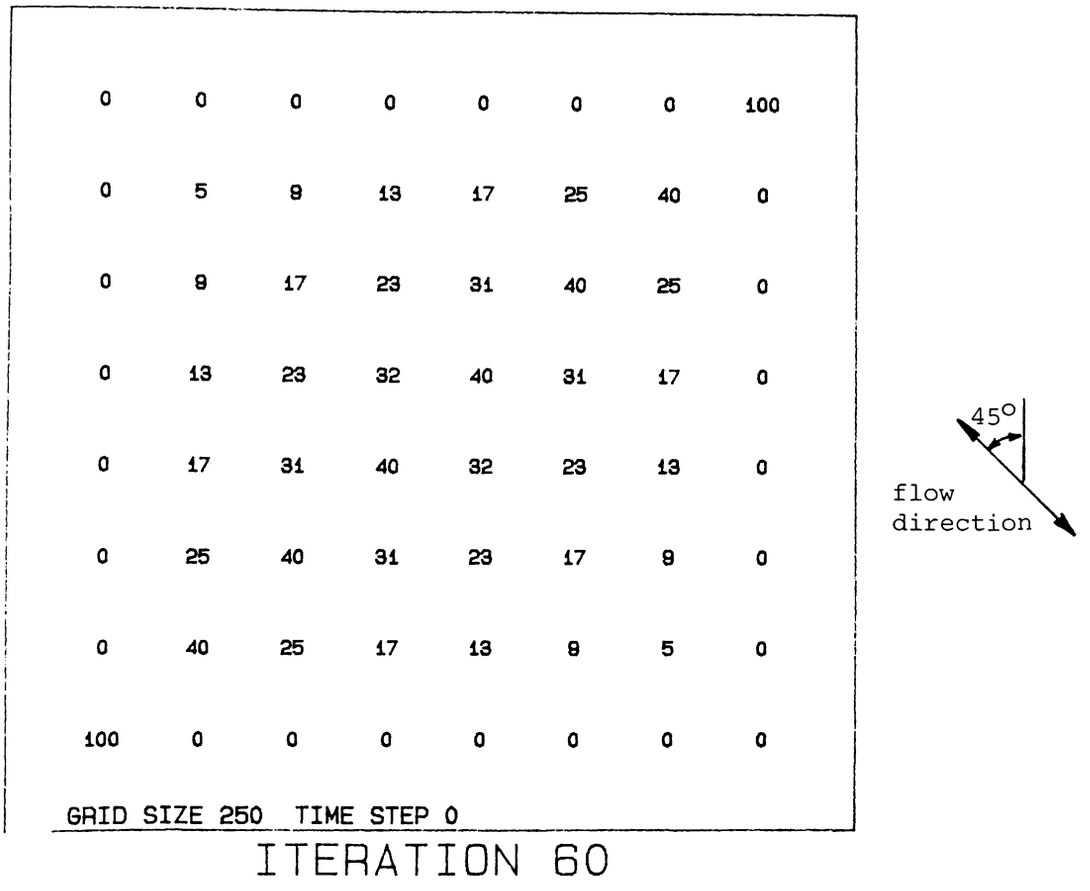

Figure 11.3(b): Deterioration of the initially sandy region (Figure 11.2) in transverse reversing neutral flow after 60 iterations with an unstable scheme to represent the Availabilities.

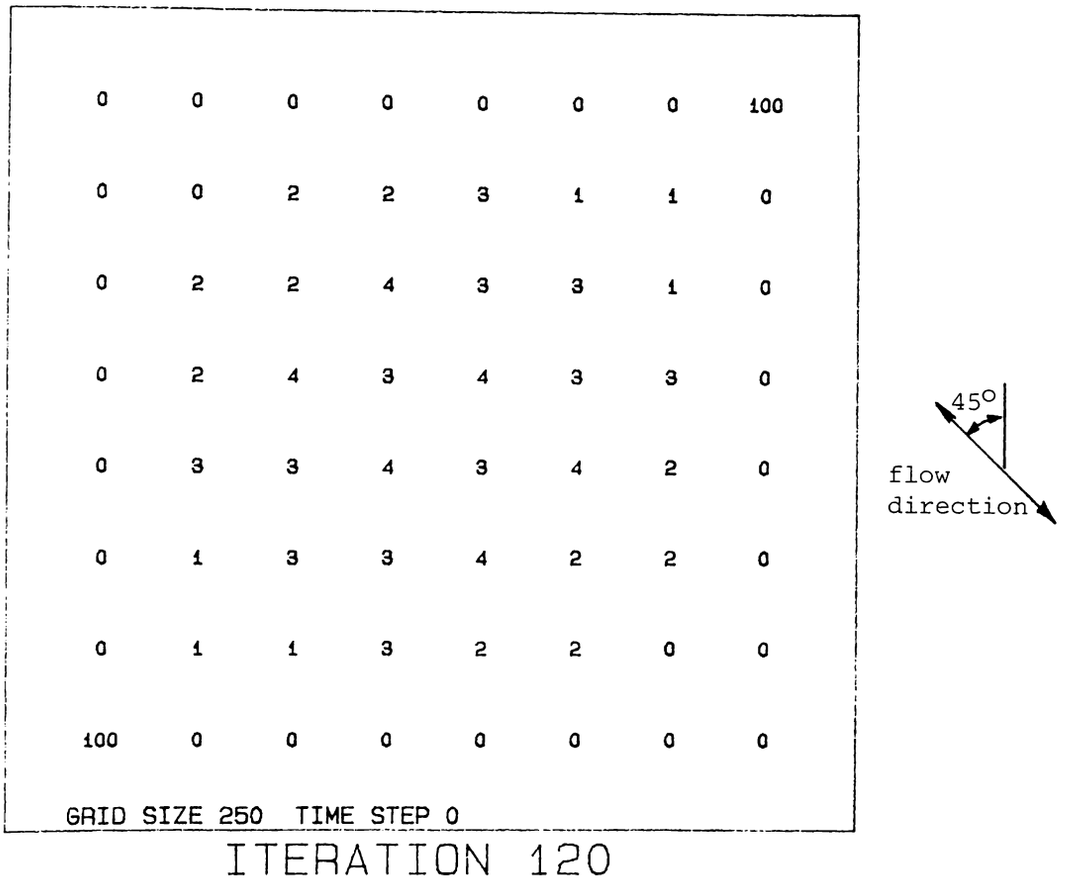

Figure 11.3(c): Availabilities after almost total deterioration of the initially sandy region (Figure 11.2) in transverse reversing neutral flow after 120 iterations with an unstable scheme to represent the Availabilities.

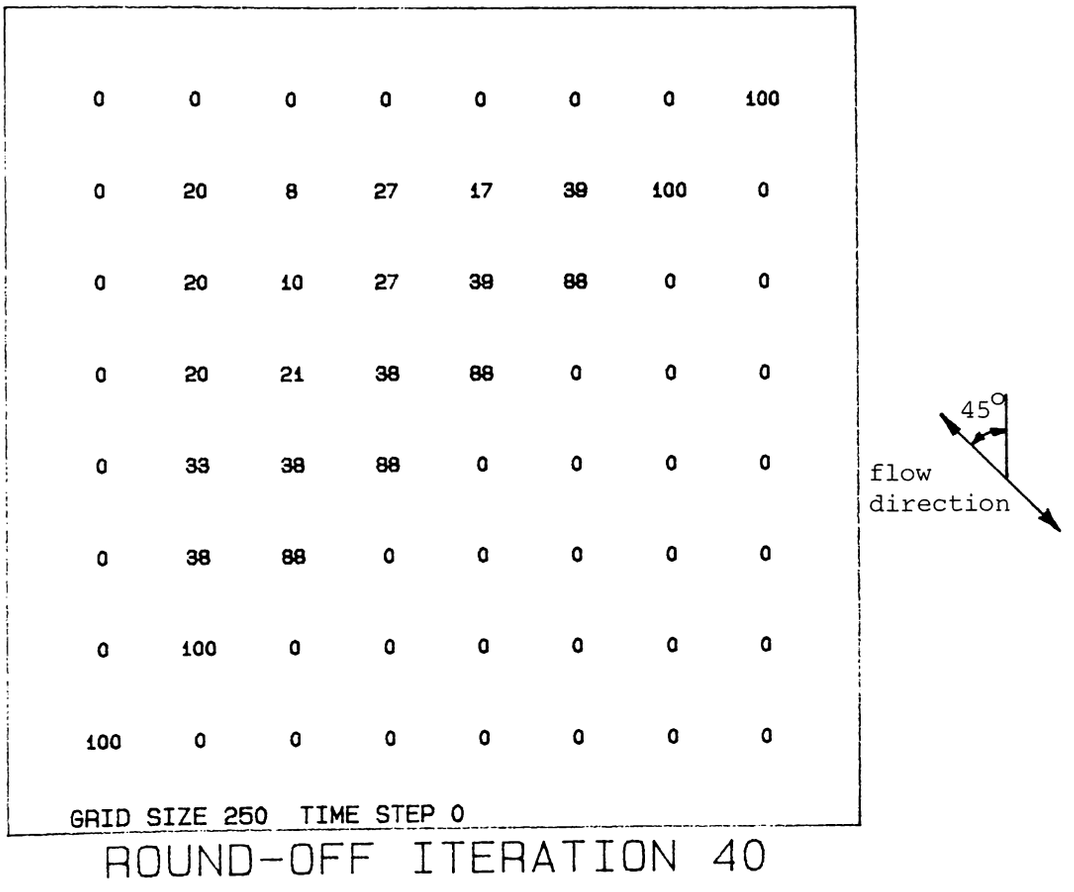

Figure 11.4(a): Deterioration of the distended, sandy region (Figure 11.2) after 40 iterations due to round-off error.

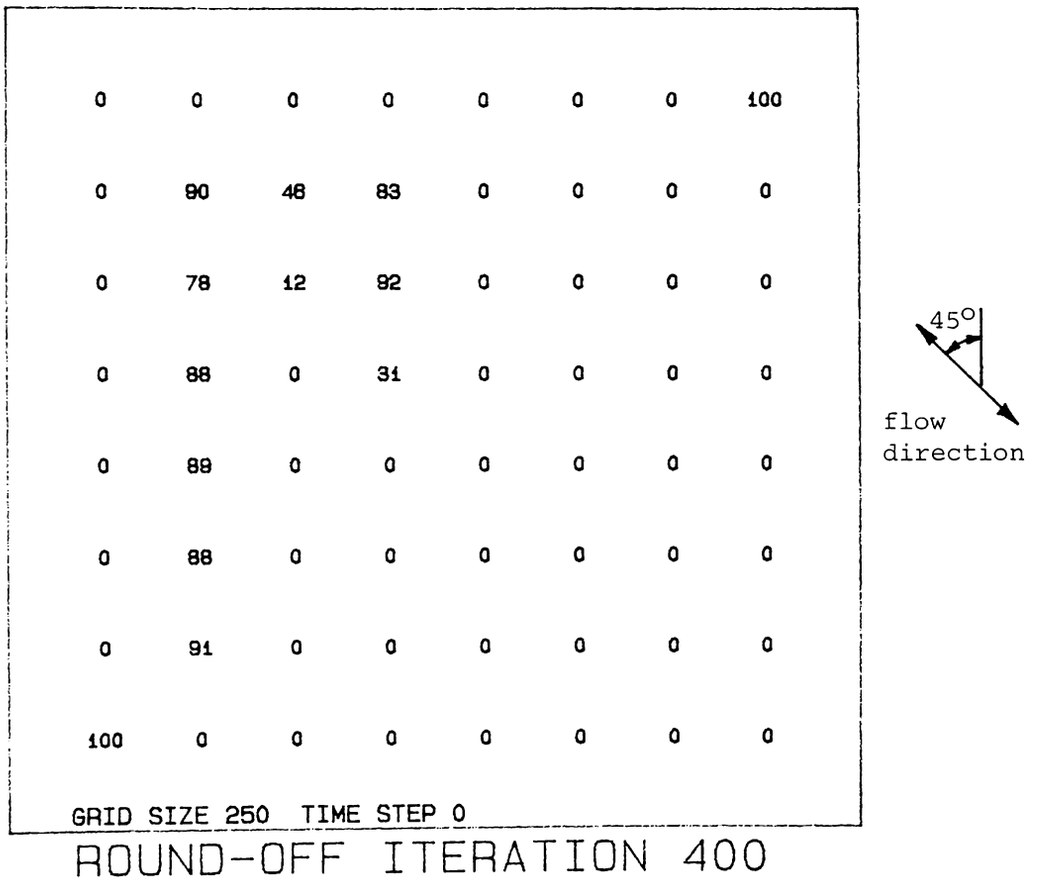

Figure 11.4(b); Stable configuration reached after deterioration of the distended sand region (Figure 11.2) due to round-off error.

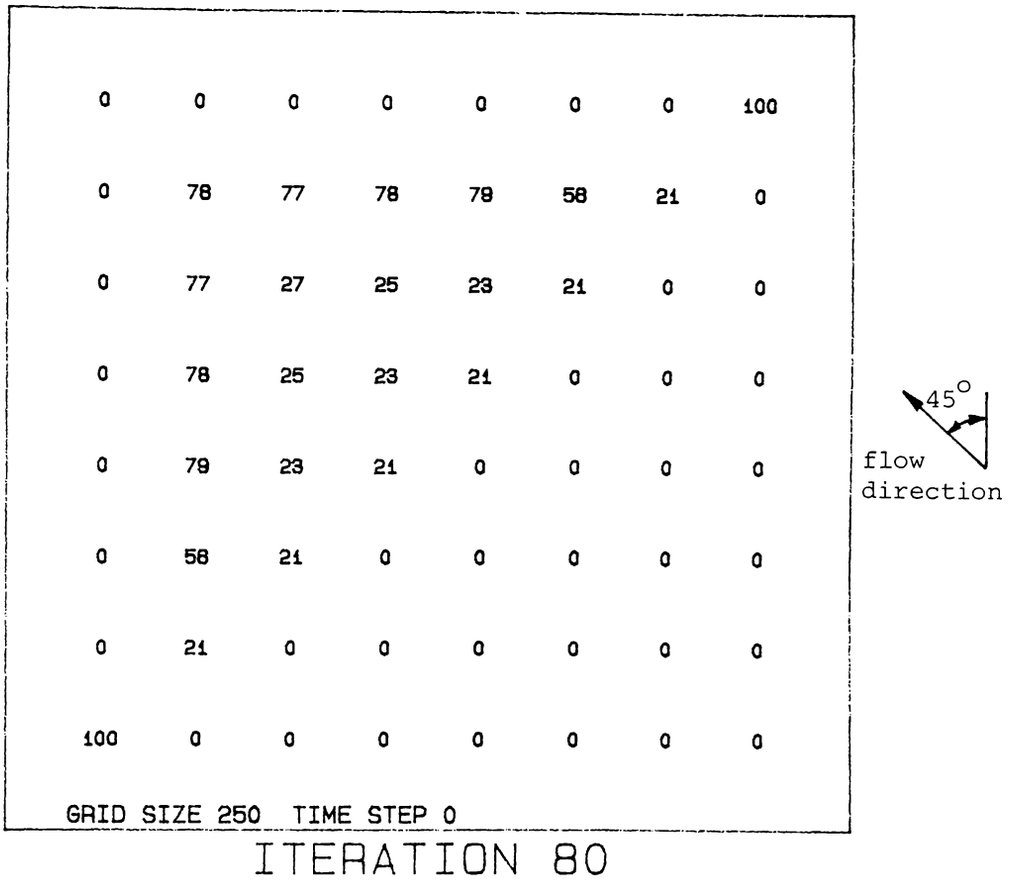

Figure 11.5(a): Dissipation of the distended sandy region (Figure 11.2) in transverse uni-directional flow after 80 iterations. Sediment is swept downstream from the sandy zone. Boundary Availabilities remain unchanged.

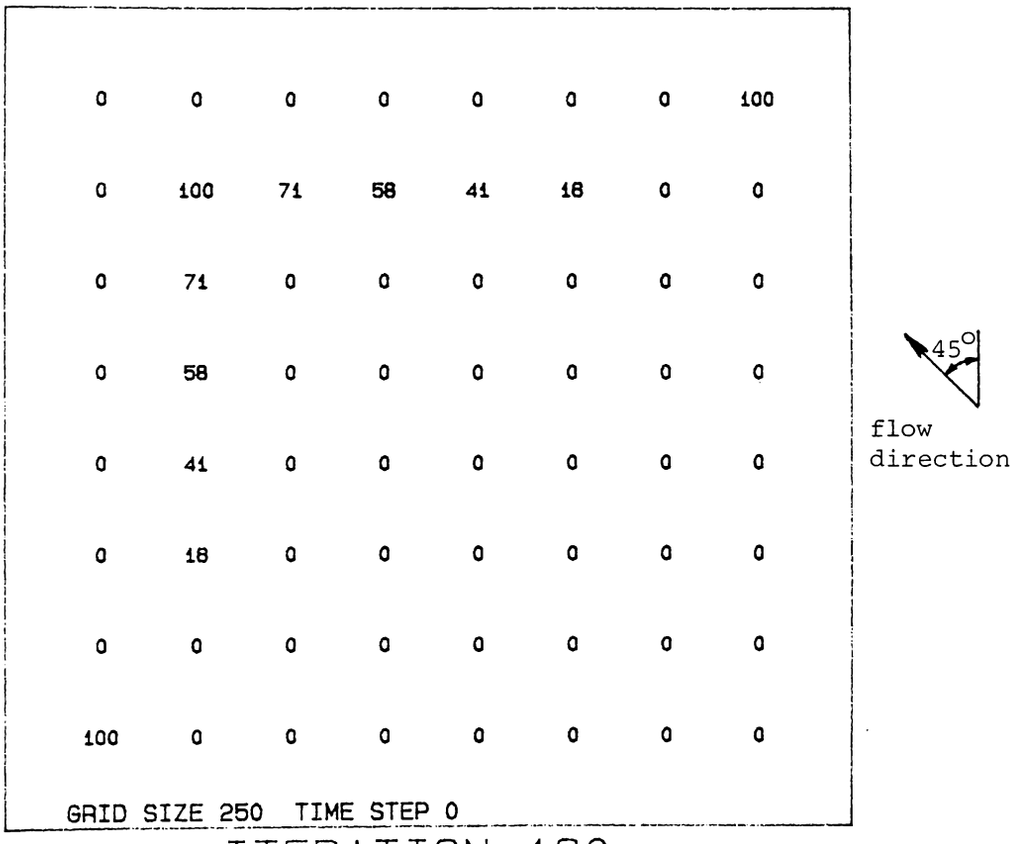

Figure 11.5(b): Dissipation of a distended sandy region (Figure 11.2) in transverse uni-directional flow after 120 iterations. Sediment is swept into the upper left corner. Boundary Availabilities remain unchanged.

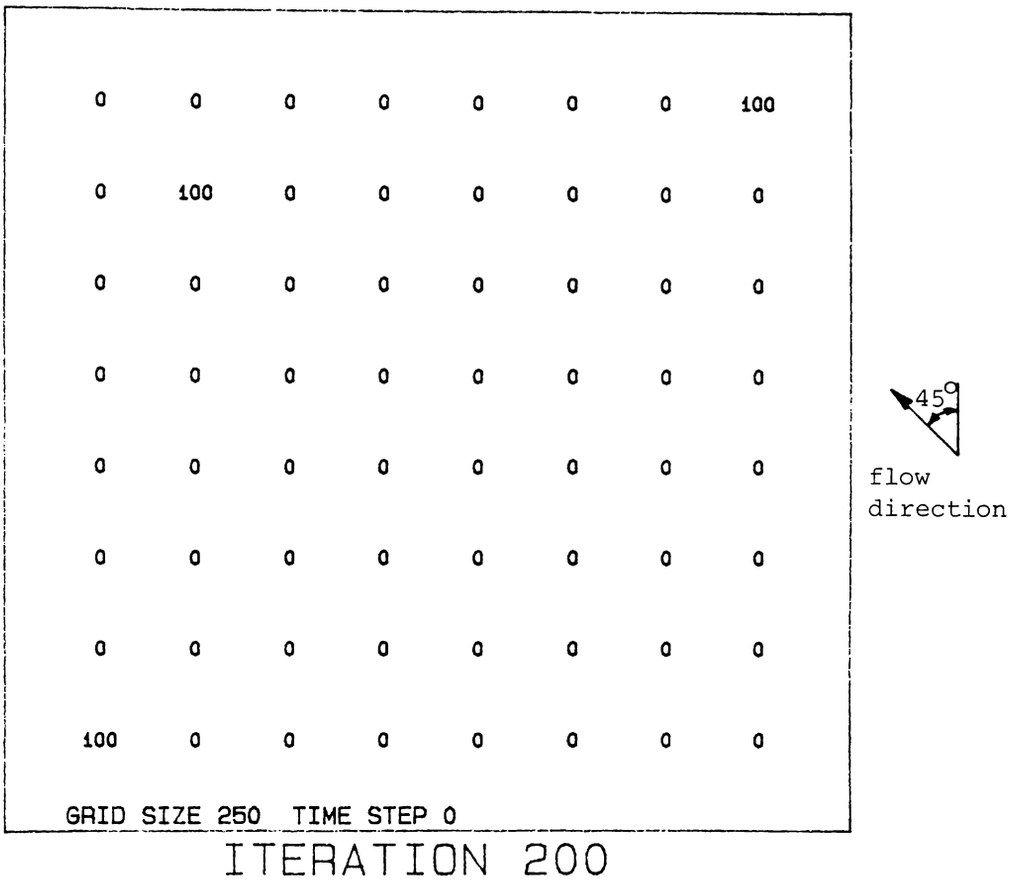

Figure 11.5(c): Dissipation of a distended sandy region in transverse uni-directional flow after 200 iterations. A stable configuration has been reached with sediment swept into the upper left corner. Boundary Availabilities remain unchanged.

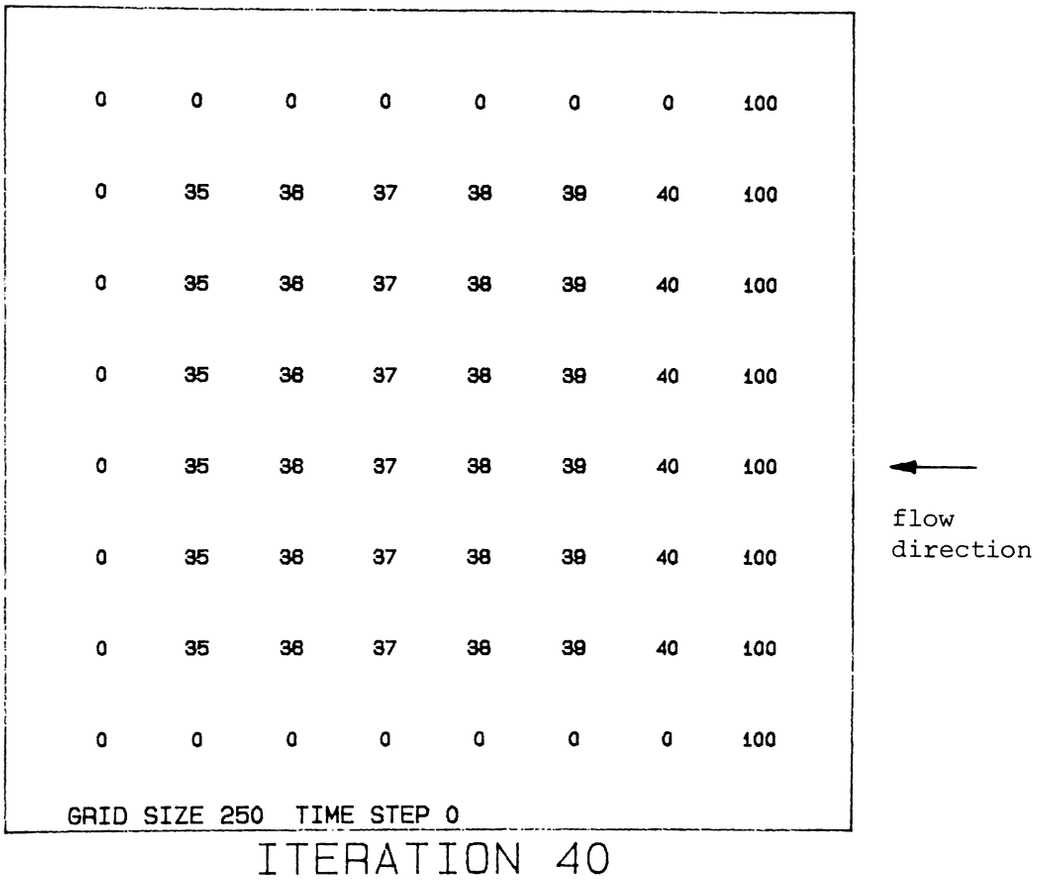

Figure 11.6(a): Availabilities after 40 iterations with a sandy region on the right-hand boundary under attack by a uni-directional current passing from right to left into the test rig. Boundary Availabilities remain unchanged.

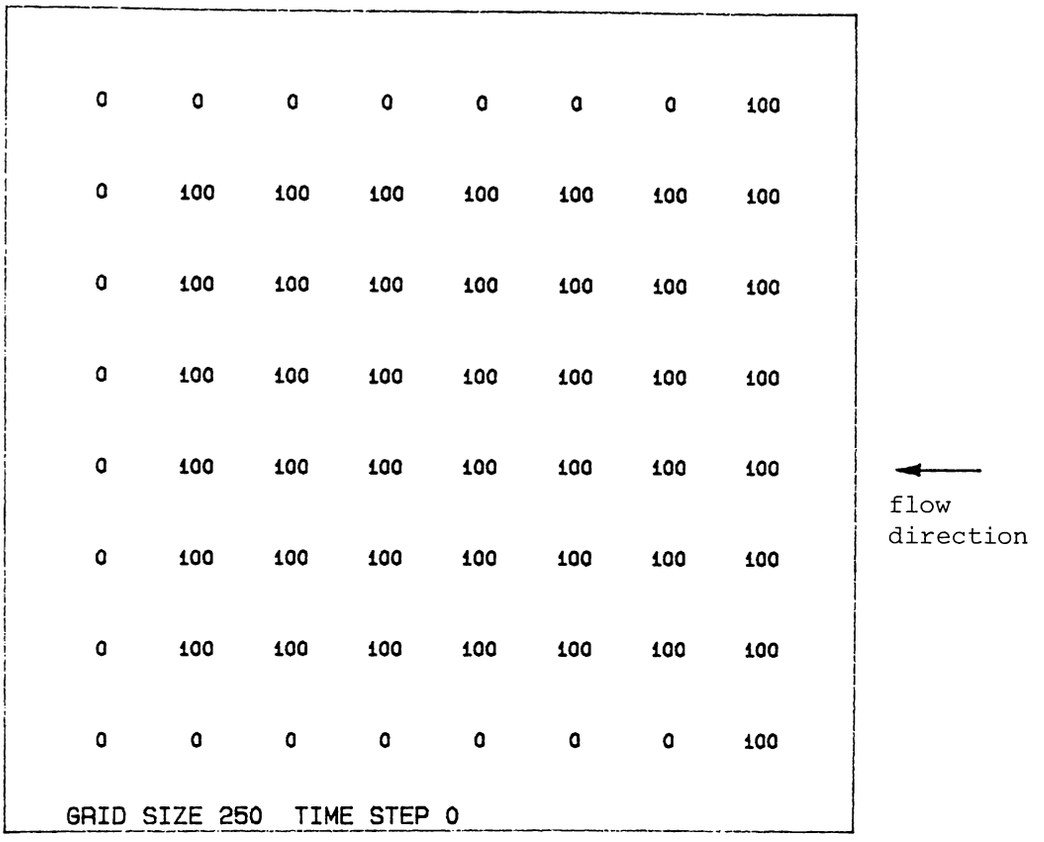

Figure 11.6(b): Availabilities after 120 iterations with a sandy region on the right-hand boundary under attack by a uni-directional current passing from right to left into the test rig. This configuration is stable. Boundary Availabilities remain unchanged.

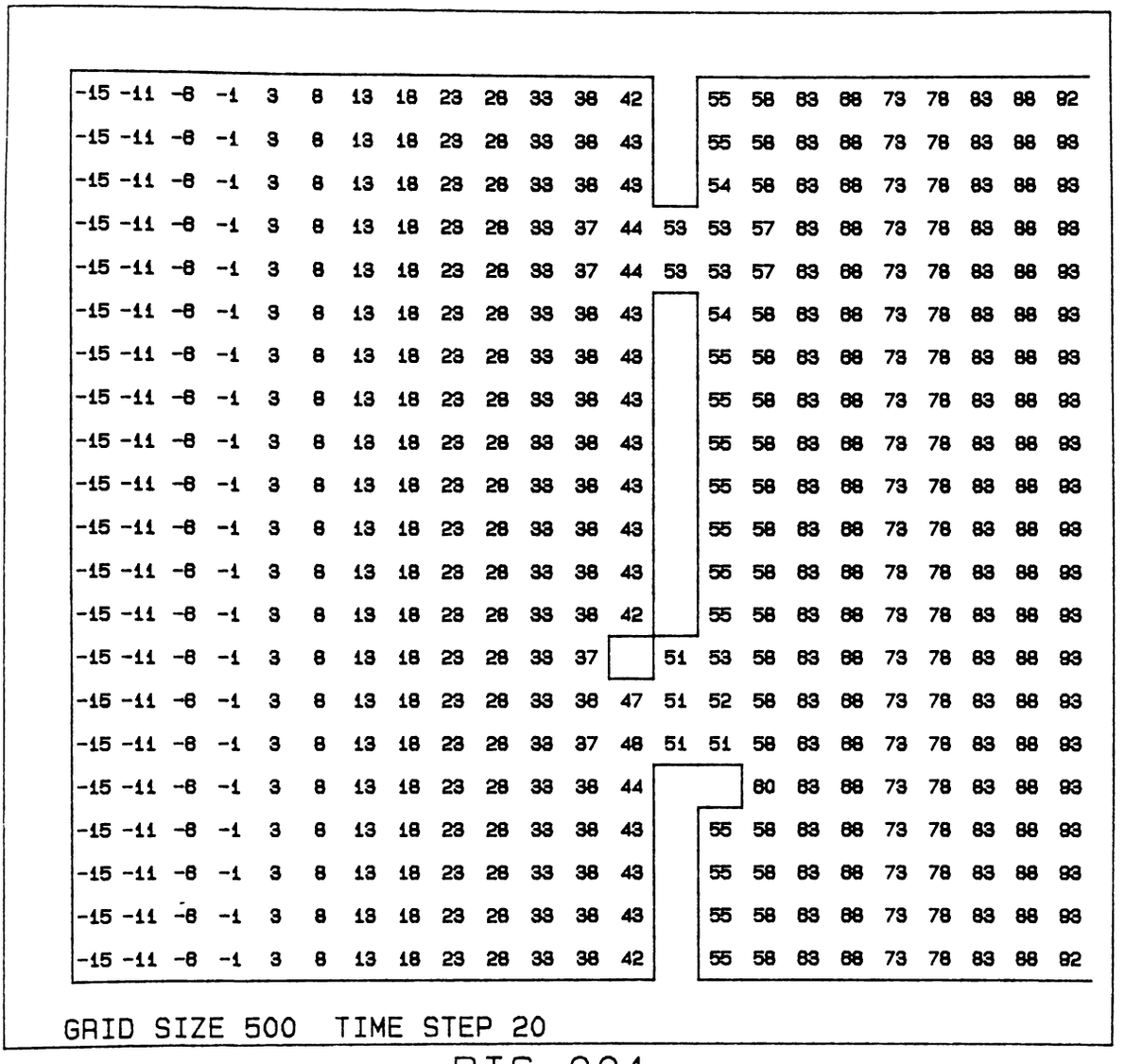

Figure 11.7: Initial configuration of a schematised inlet with a symmetrical and offset entrance both 1000m wide at the narrowest point. The sea bed gradient is rectilinear. Depths are in metres times 10 and vary from 9.3m at the open boundary to -1.5m up-harbour. Cells are 500m-square.

Figure 11.8: Tauranga Entrance to Tauranga Harbour (NZ 5411, 1975).

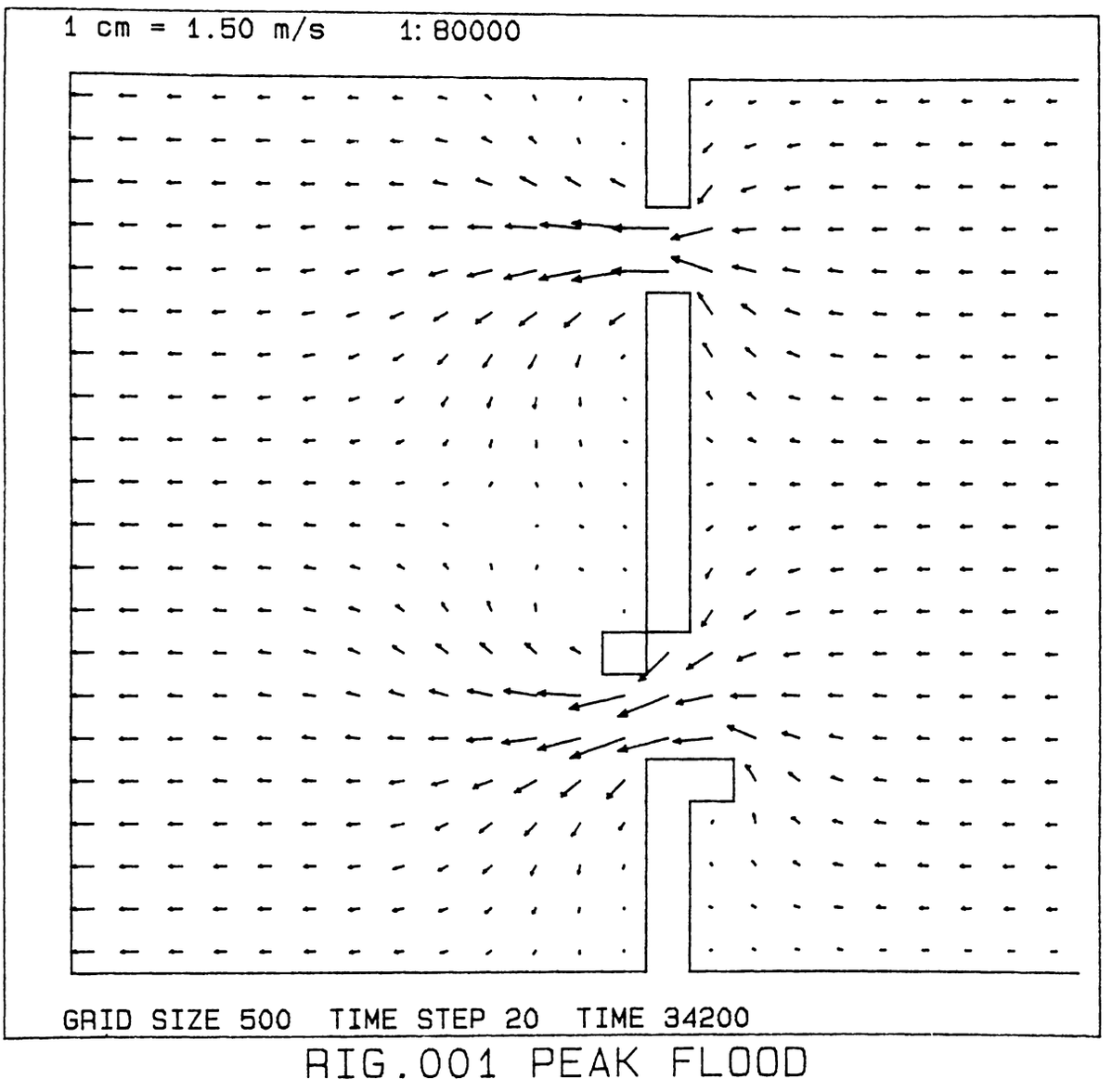

Figure 11.9: Flow pattern at peak flood in the schematised inlet for the initial bathymetry. Tides are summarised at the open boundary with range of 3m and MSL of 1.5m above datum.

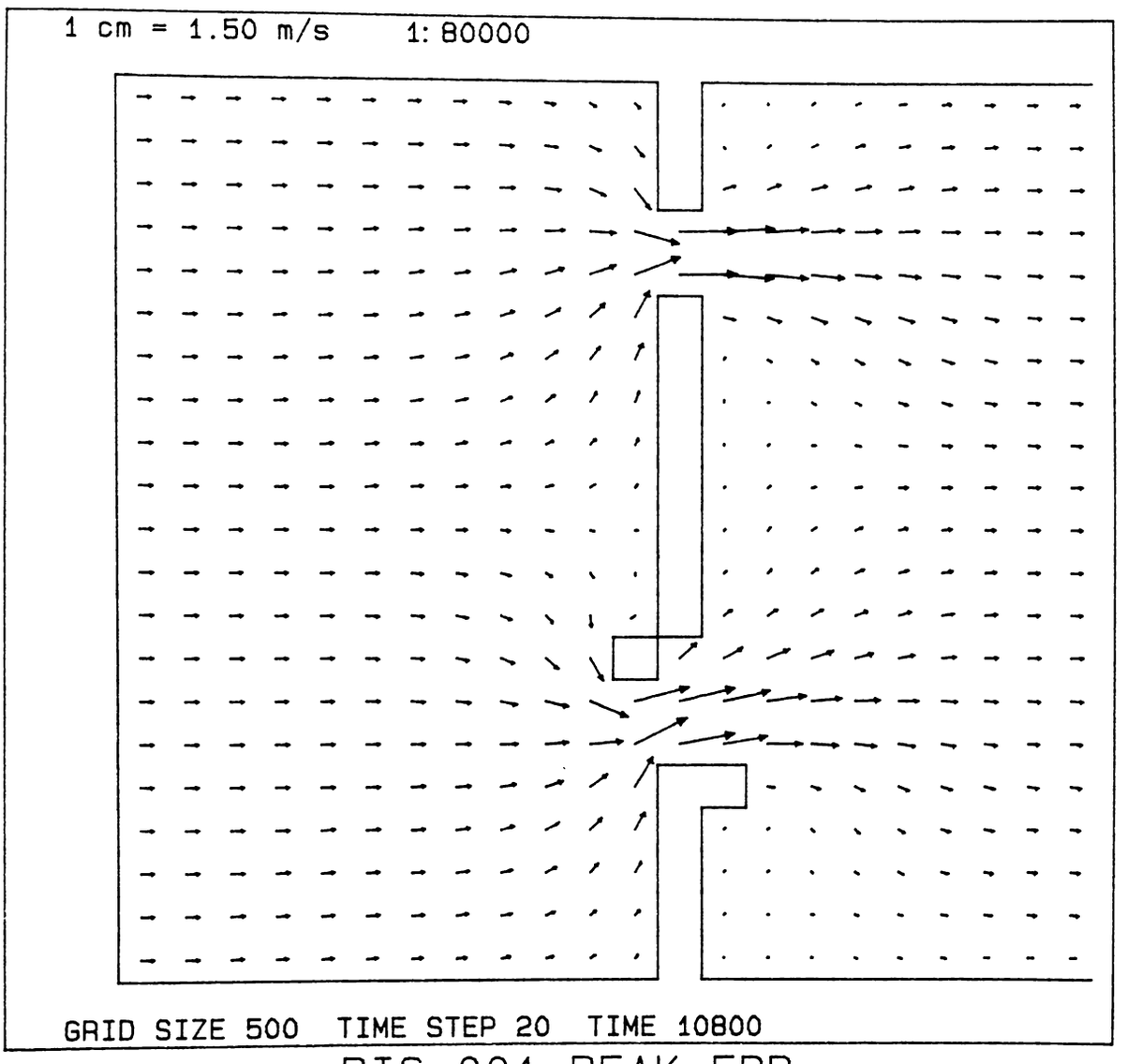

Figure 11.10: Flow pattern at peak ebb in the schematised inlet for the initial bathymetry. Tides are sinusoidal at the open boundary with range of 3m and MSL of 1.5m above datum.

MATAKANA ISLAND
MOUNT MAUNGANUI
231 m
OTUMOETAI
TAURANGA
37°40'
37°39'
37°38'S
176°10'E
176°09'E
N
0
500
1000m
5m Contour
Stations
LEGEND
>10⁴
10³-10⁴
0-10³

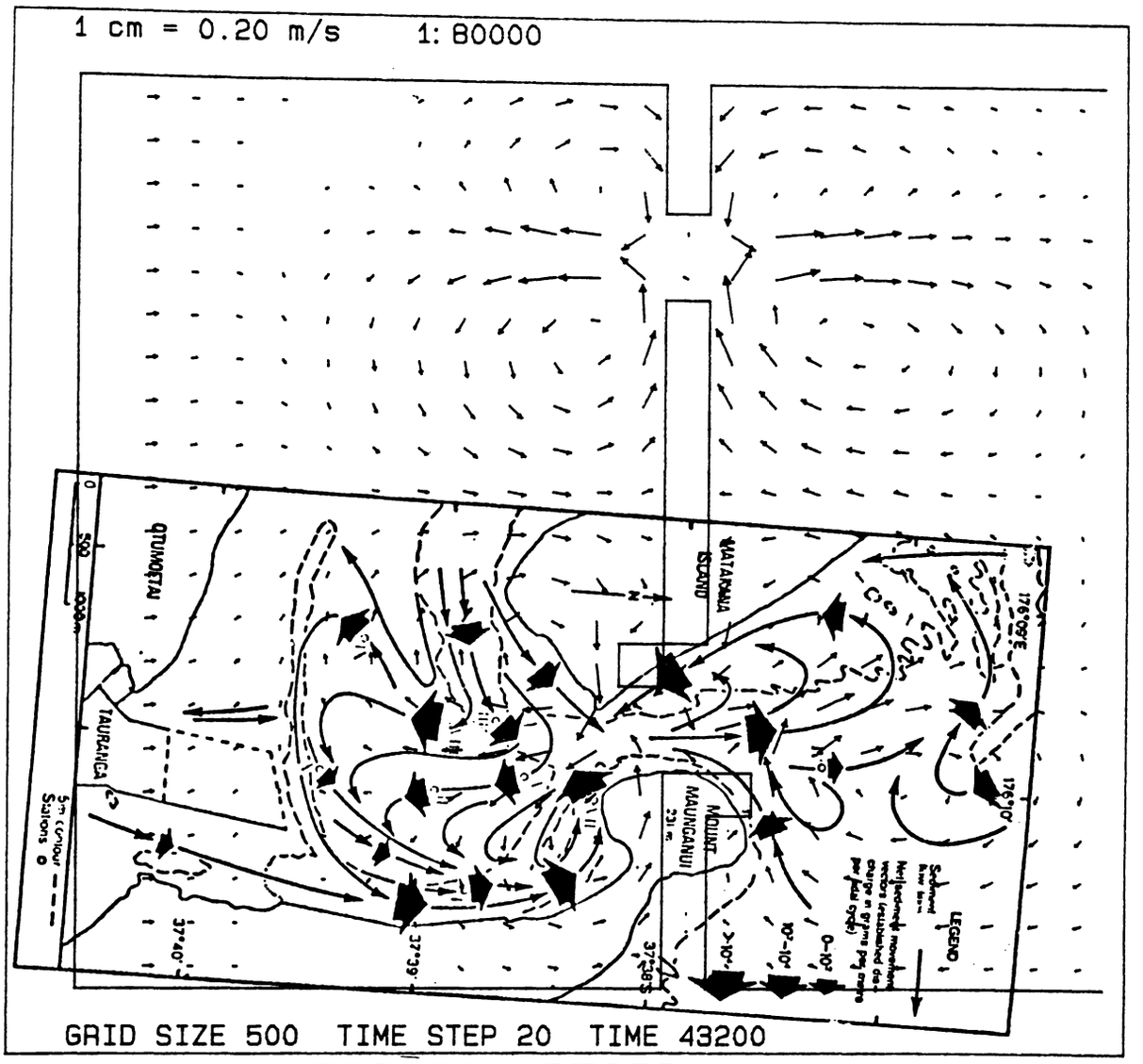

Figure 11.11: Tidal cycle residual velocity vectors in the schematised tidal inlet for the initial bathymetry. Tides are sinusoidal at the open boundary with range of 3m and MSL at 1.5m above datum. The overlay shows residual transport directions and current vectors after Davies-Colley and Healy (1978) for Tauranga Harbour.

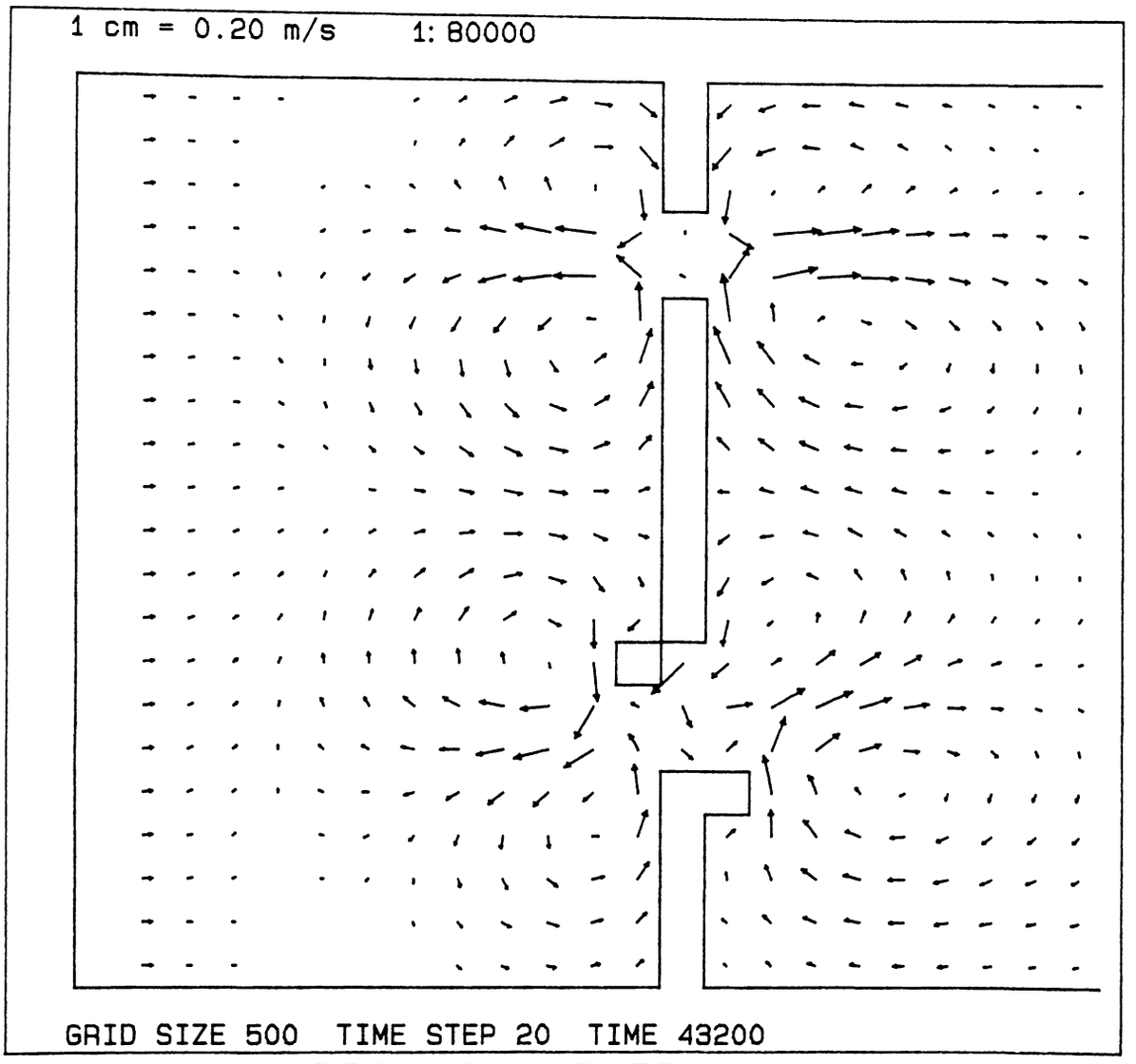

Figure 11.11: Tidal cycle residual velocity vectors in the schematised tidal inlet for the initial bathymetry. Tides are sinusoidal at the open boundary with range of 3m and MSL at 1.5m above datum. The overlay shows residual transport directions and current vectors after Davies-Colley and Healy (1978) for Tauranga Harbour.

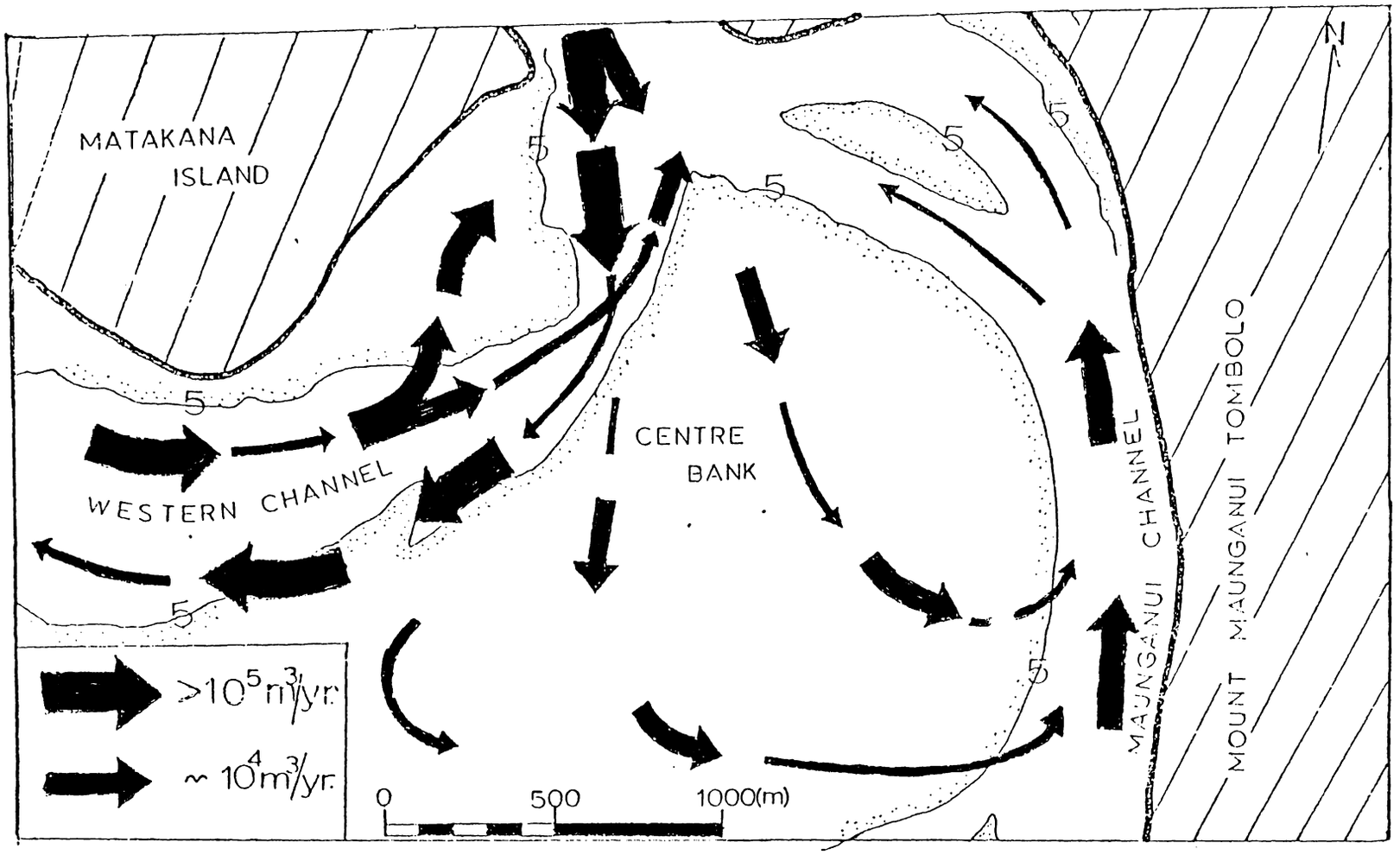

Figure 11.12: Nett sediment transport for Tauranga Harbour proposed by Dahm (1983). Note that the arrows represent sediment transport directions and not residual tidal cycle flow vectors.

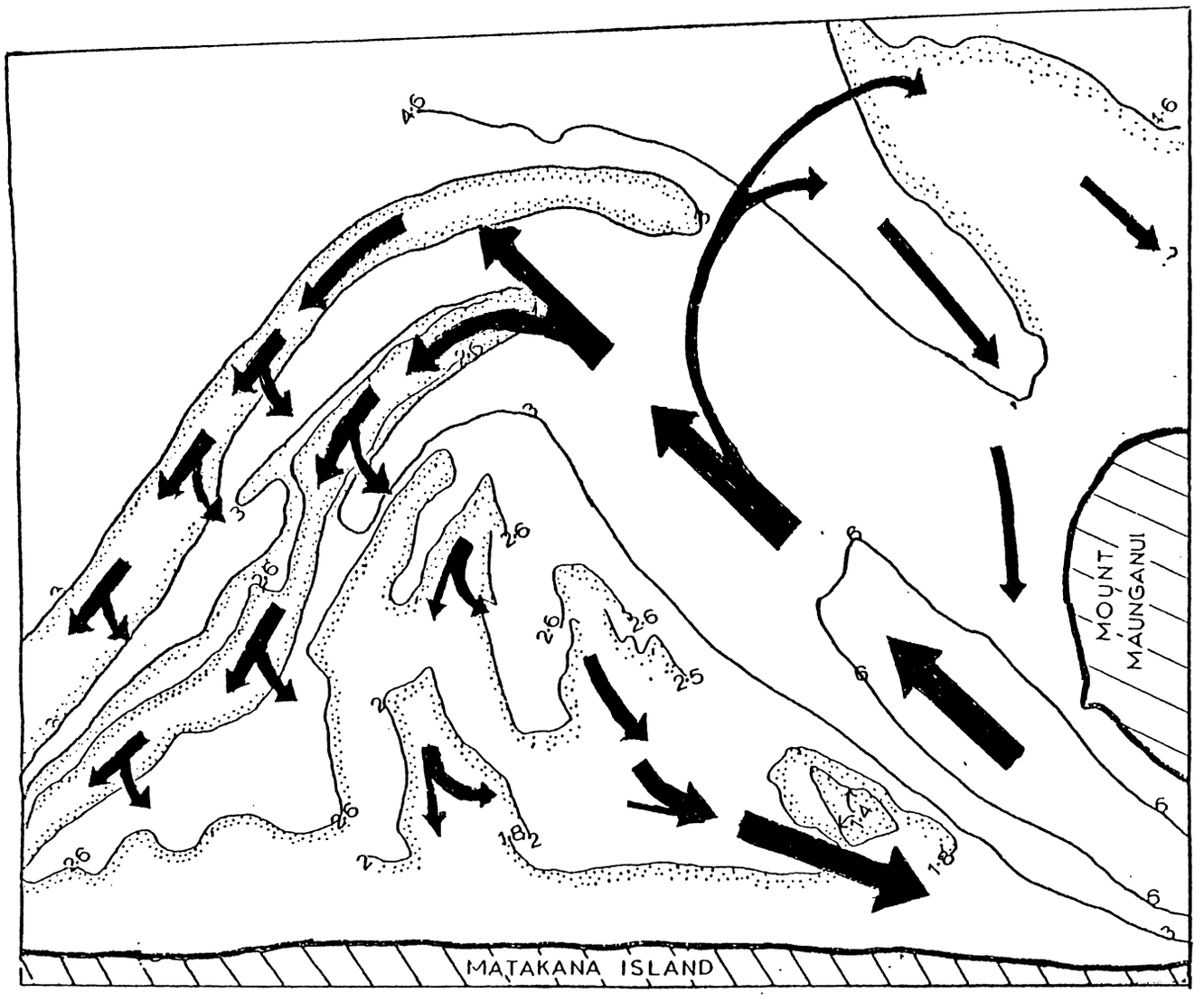

Figure 11.13: Nett sediment transport outside the entrance to Tauranga Harbour after Dahm (1983). Note that the arrows represent sediment transport directions and are not residual tidal cycle flow vectors.

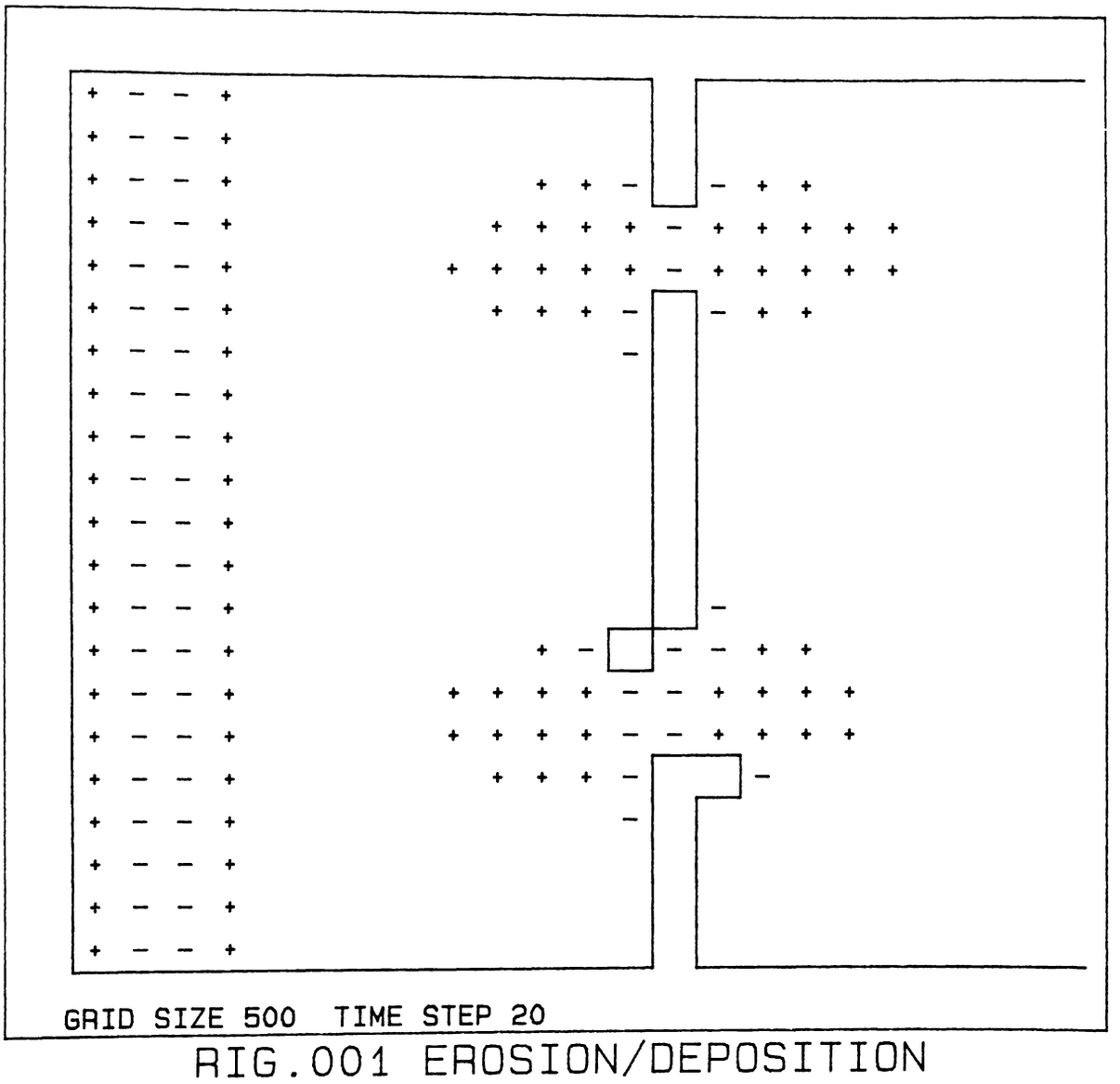

Figure 11.14: Erosion/deposition pattern obtained with SAND2d in the schematised tidal inlet for the initial bathymetry.

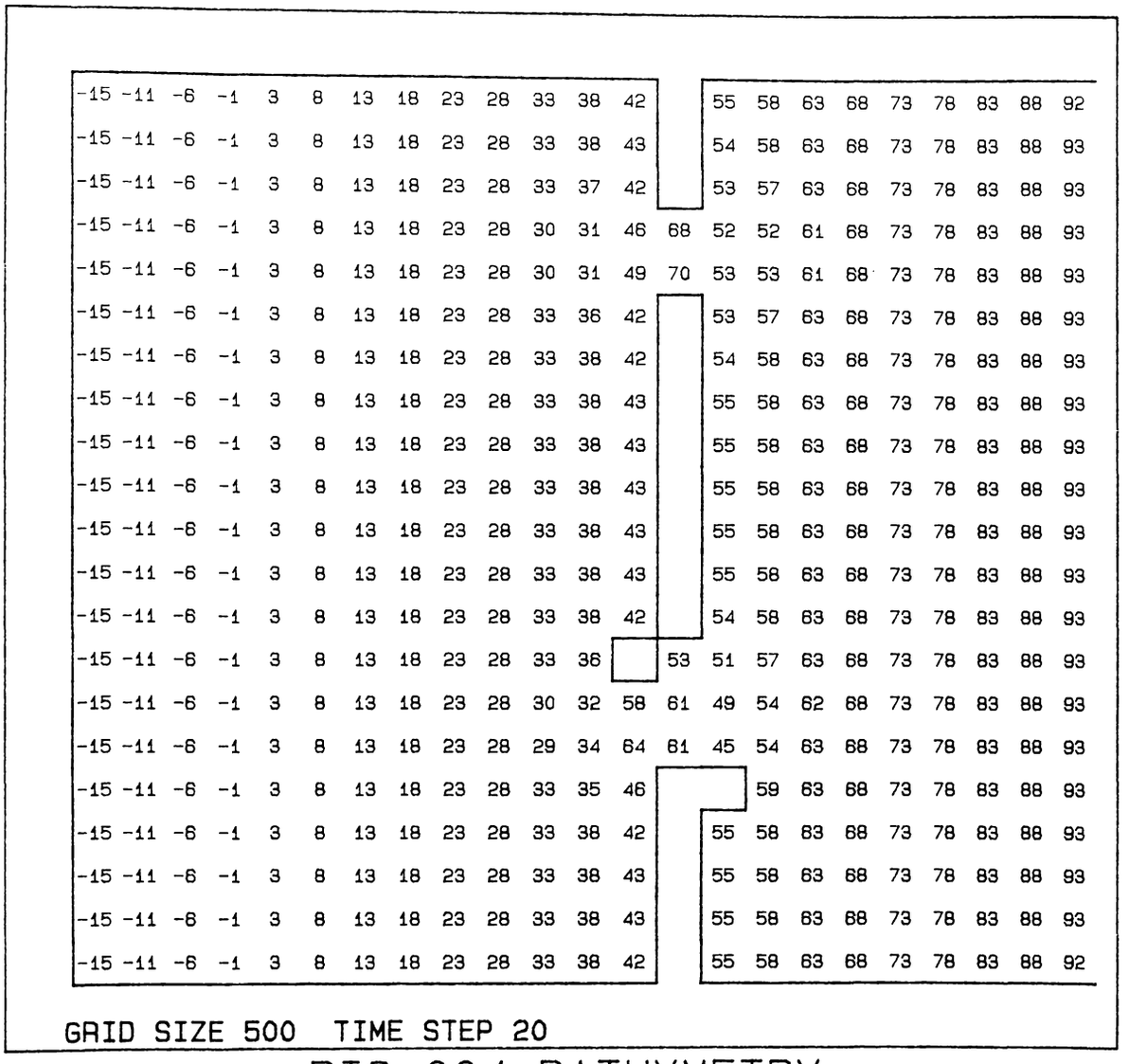

RIG.004 BATHYMETRY

Figure 11.15: Bathymetry after 4 coupled iterations in the schematised tidal inlet. Depths are in metres times 10 and vary from 9.3m at the open boundary to -1.5m up harbour. Tides are sinusoidal at the open boundary with range of 3m and MSL at 1.5m above datum.

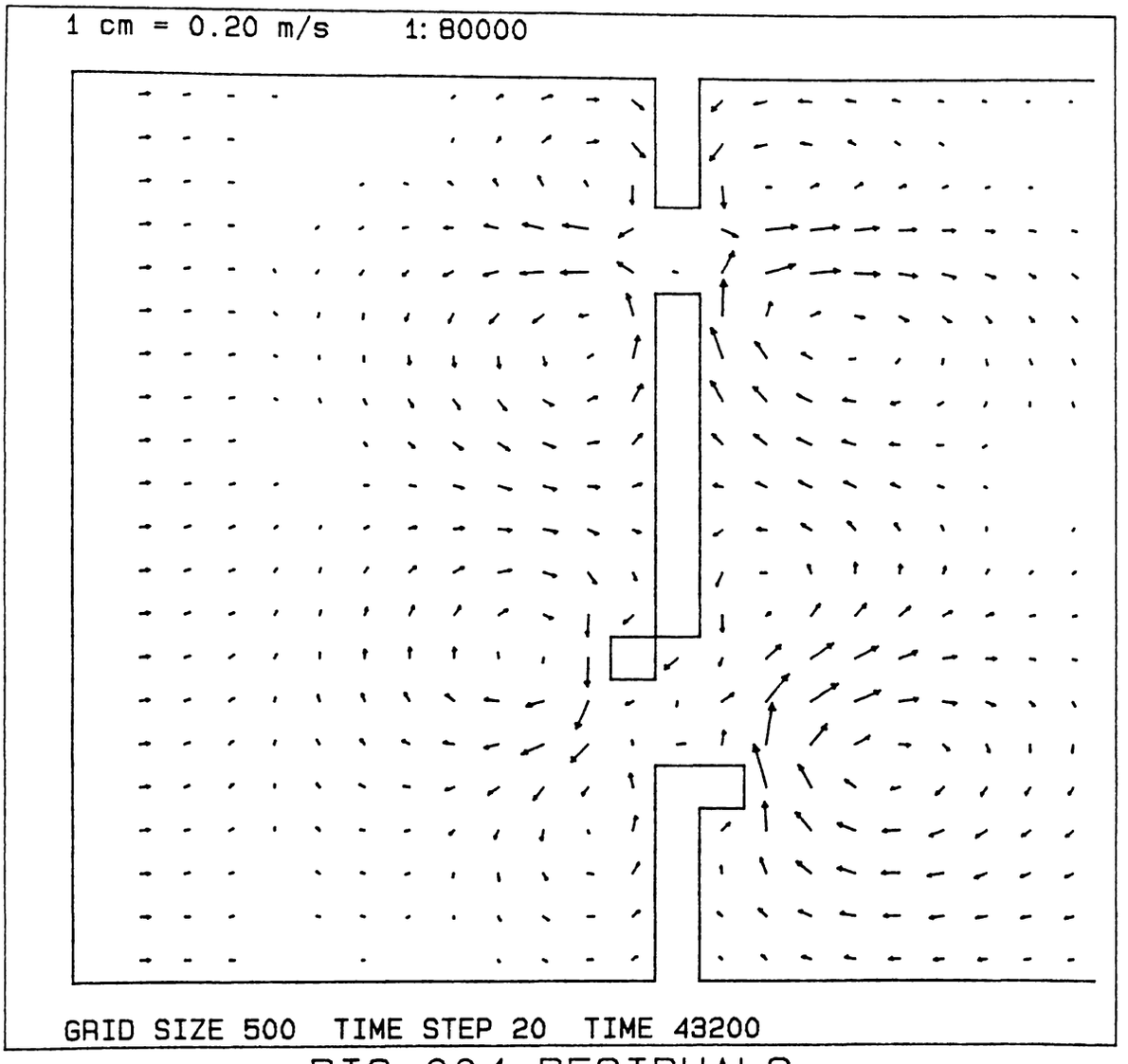

Figure 11.16: Tidal cycle residual velocity vectors in the schematised tidal inlet after 4 coupled iterations.

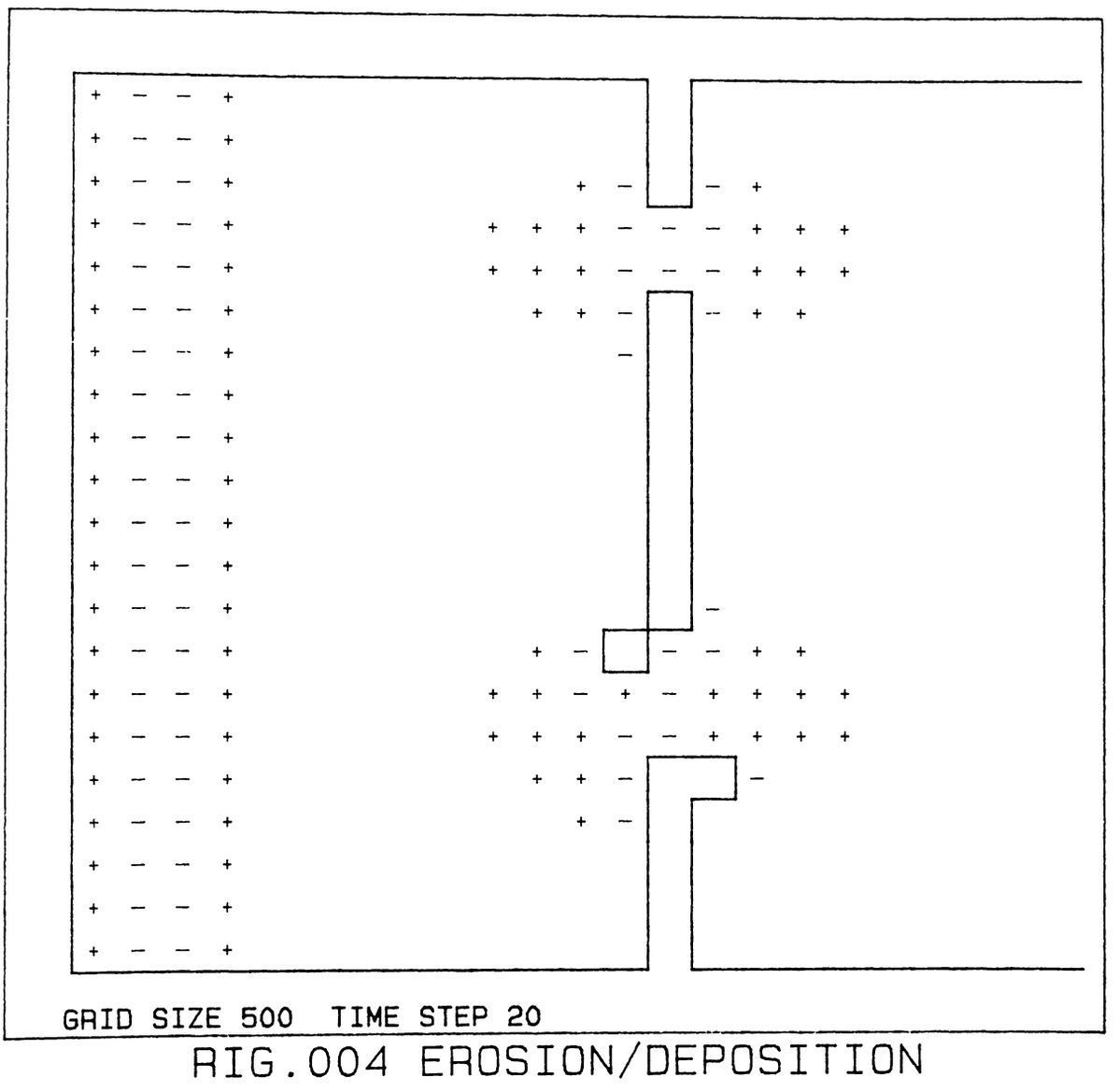

Figure 11.17: Erosion/deposition pattern in the schematised tidal inlet after 4 coupled iterations.

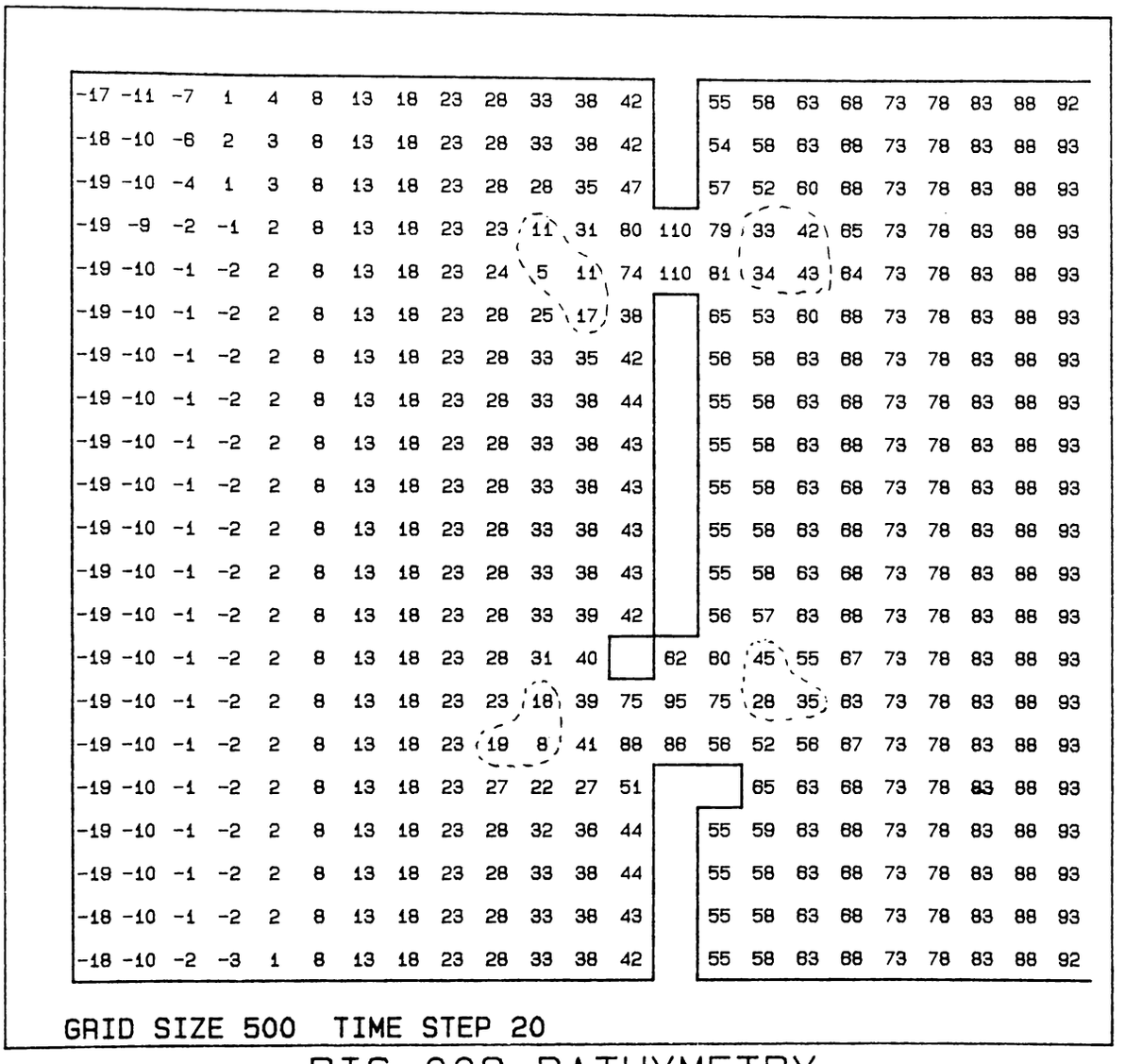

Figure 11.18: Bathymetry after 8 iterations in the schematised tidal inlet. Depths are in metres times 10 and vary from 9.3m at the open boundary to -1.9m up-harbour. Tides are sinusoidal at the open boundary with range of 3m and MSL at 1.5m above datum.

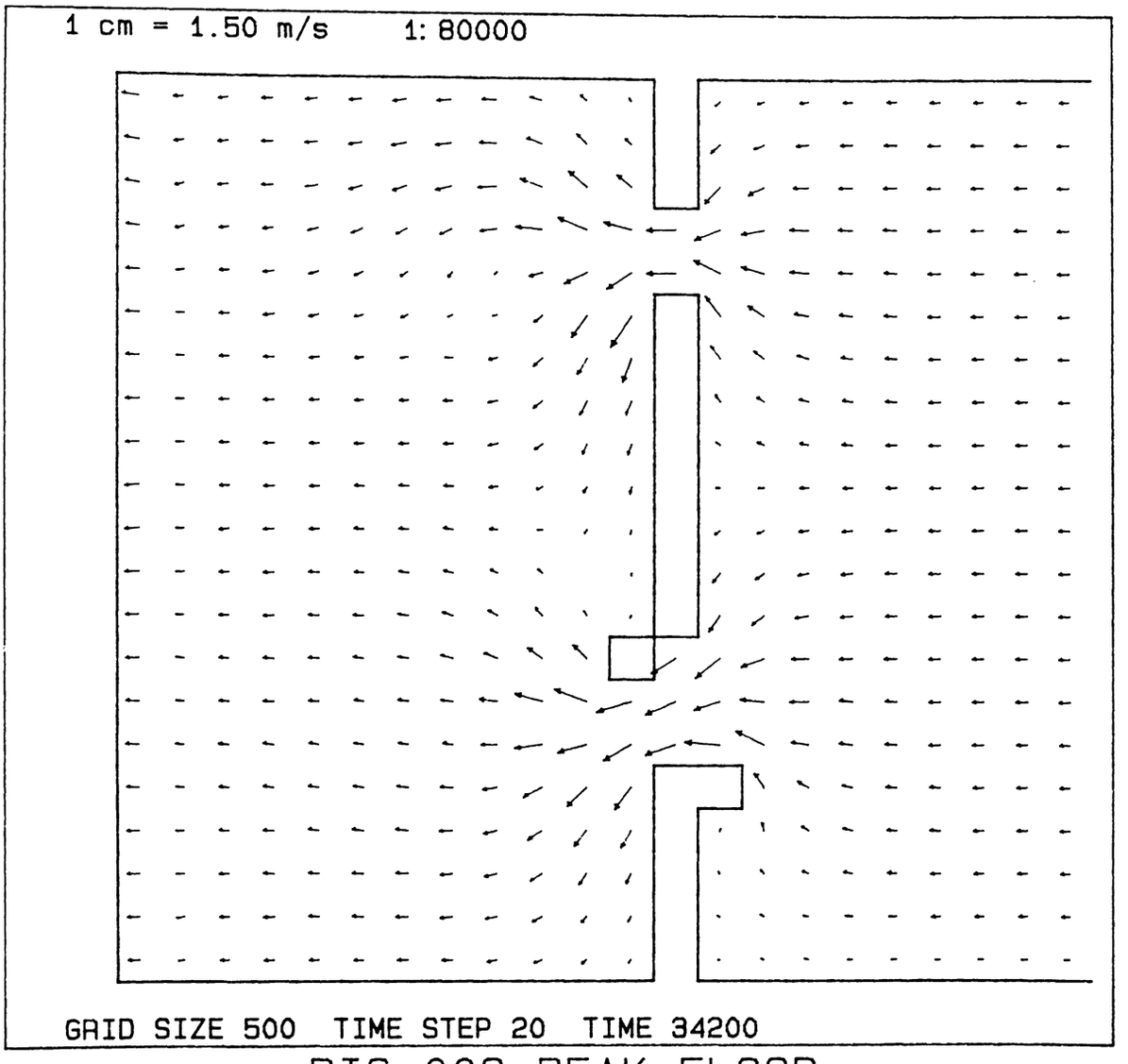

Figure 11.19: Flow pattern at peak flood in the schematised tidal inlet after 8 coupled iterations. Tides are sinusoidal at the open boundary with range of 3m and MSL at 1.5m above datum.

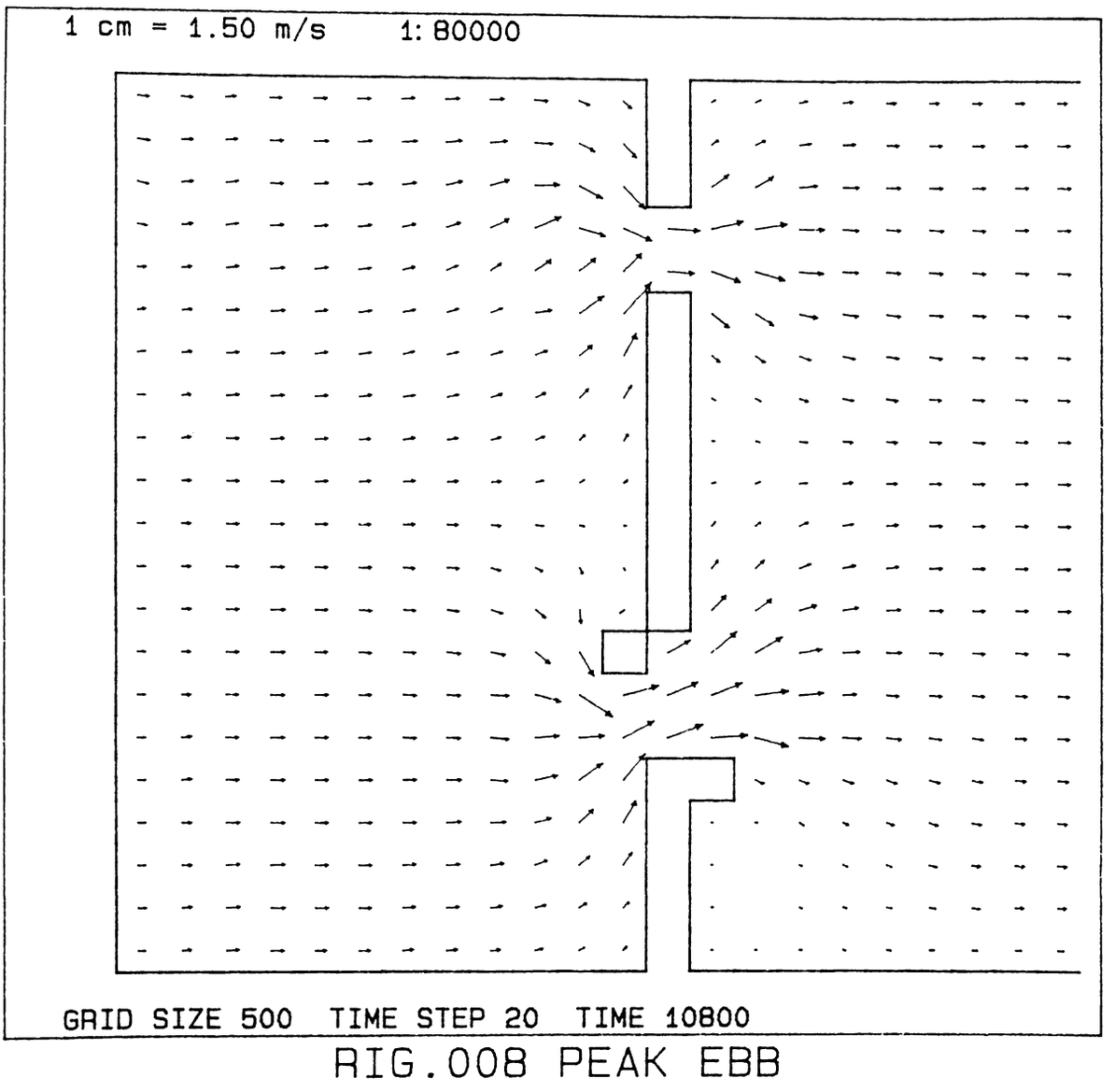

Figure 11.20: Flow pattern at peak ebb in the schematised tidal inlet after 8 coupled iterations. Tides are sinusoidal at the open boundary with range of 3m and MSL at 1.5m above datum.

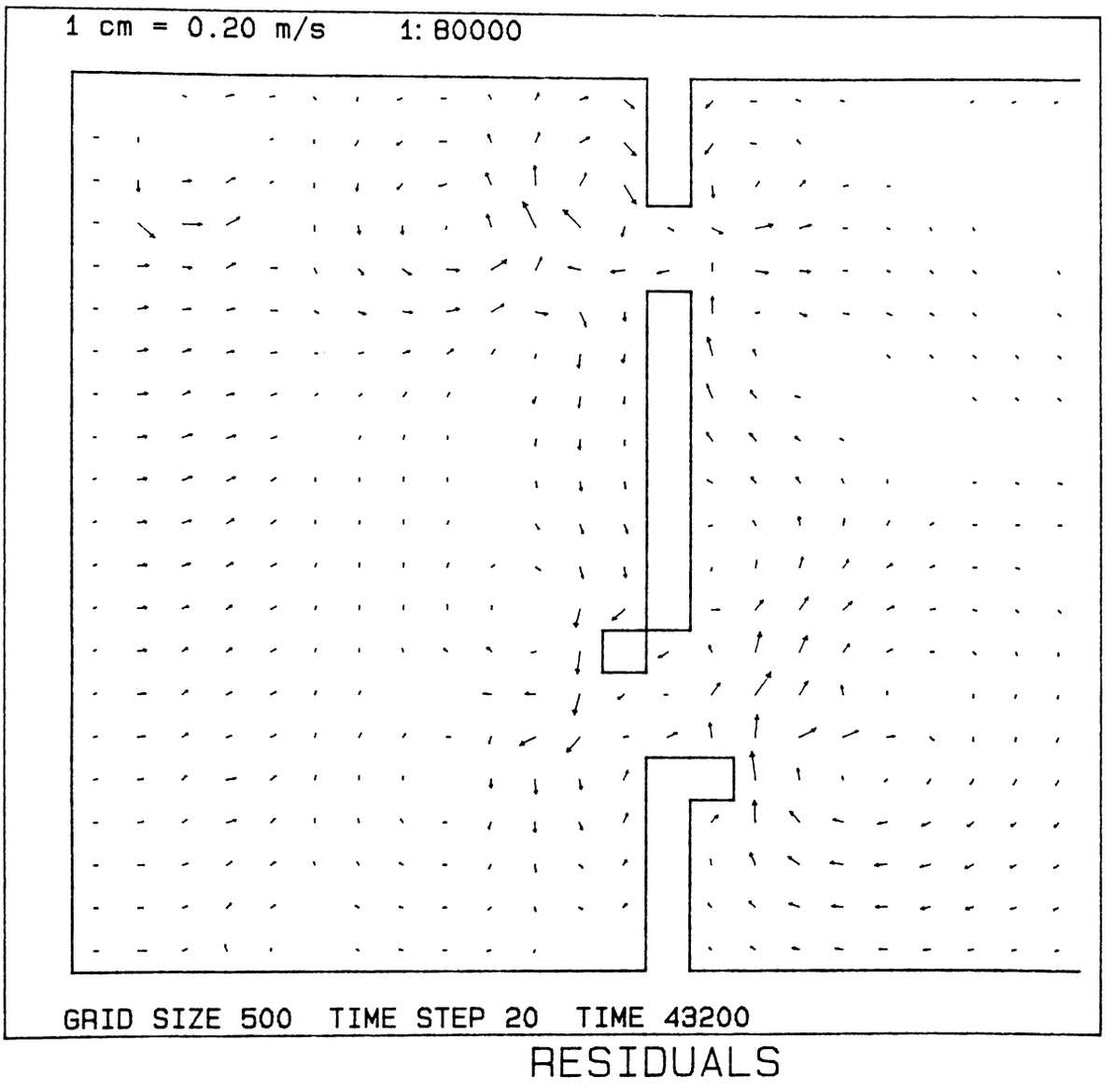

Figure 11.21: Tidal cycle residual velocity vectors in the schematised tidal inlet after 8 iterations.

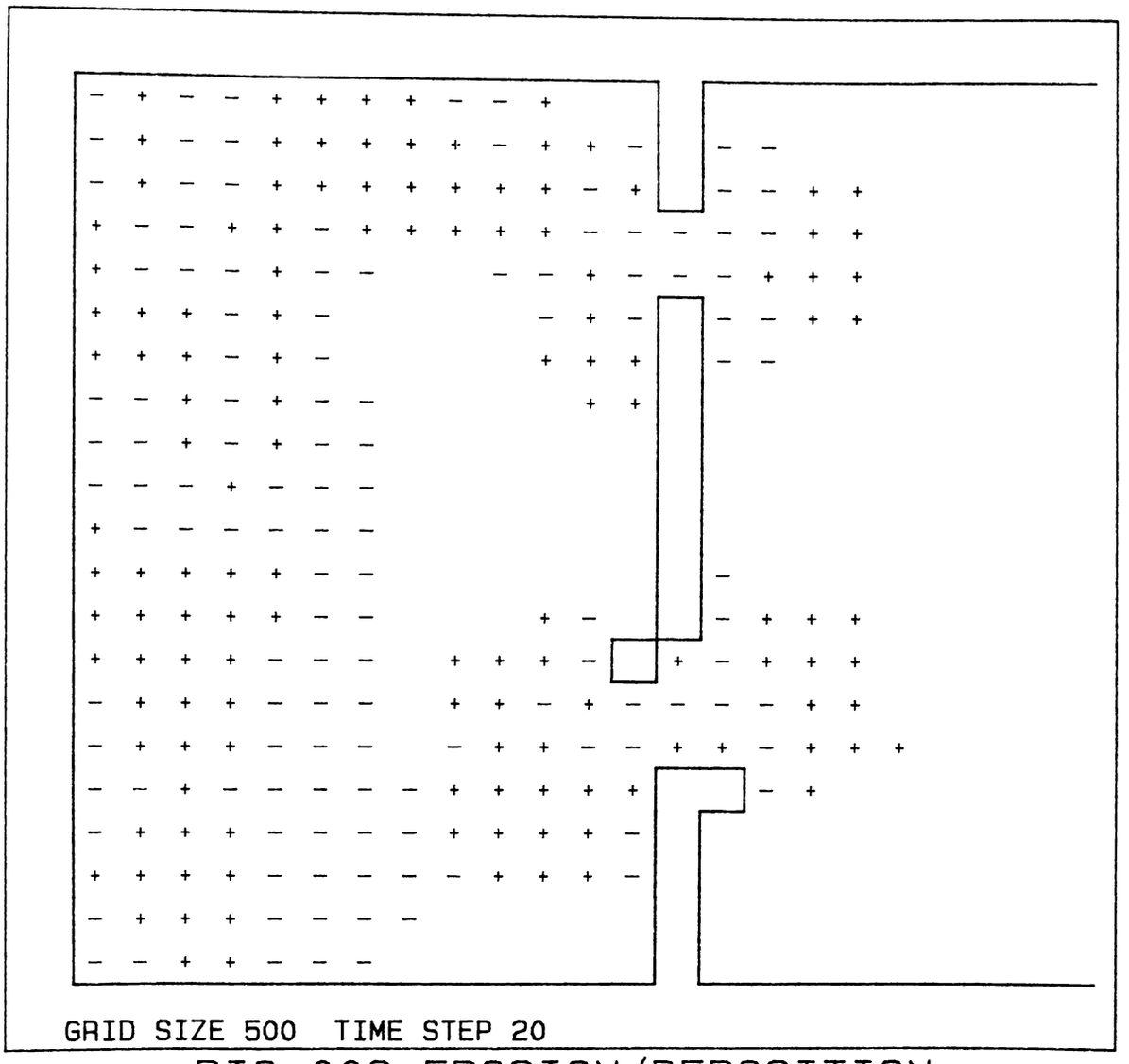

Figure 11.22: Erosion/deposition pattern in the schematised tidal inlet after 8 coupled iterations.

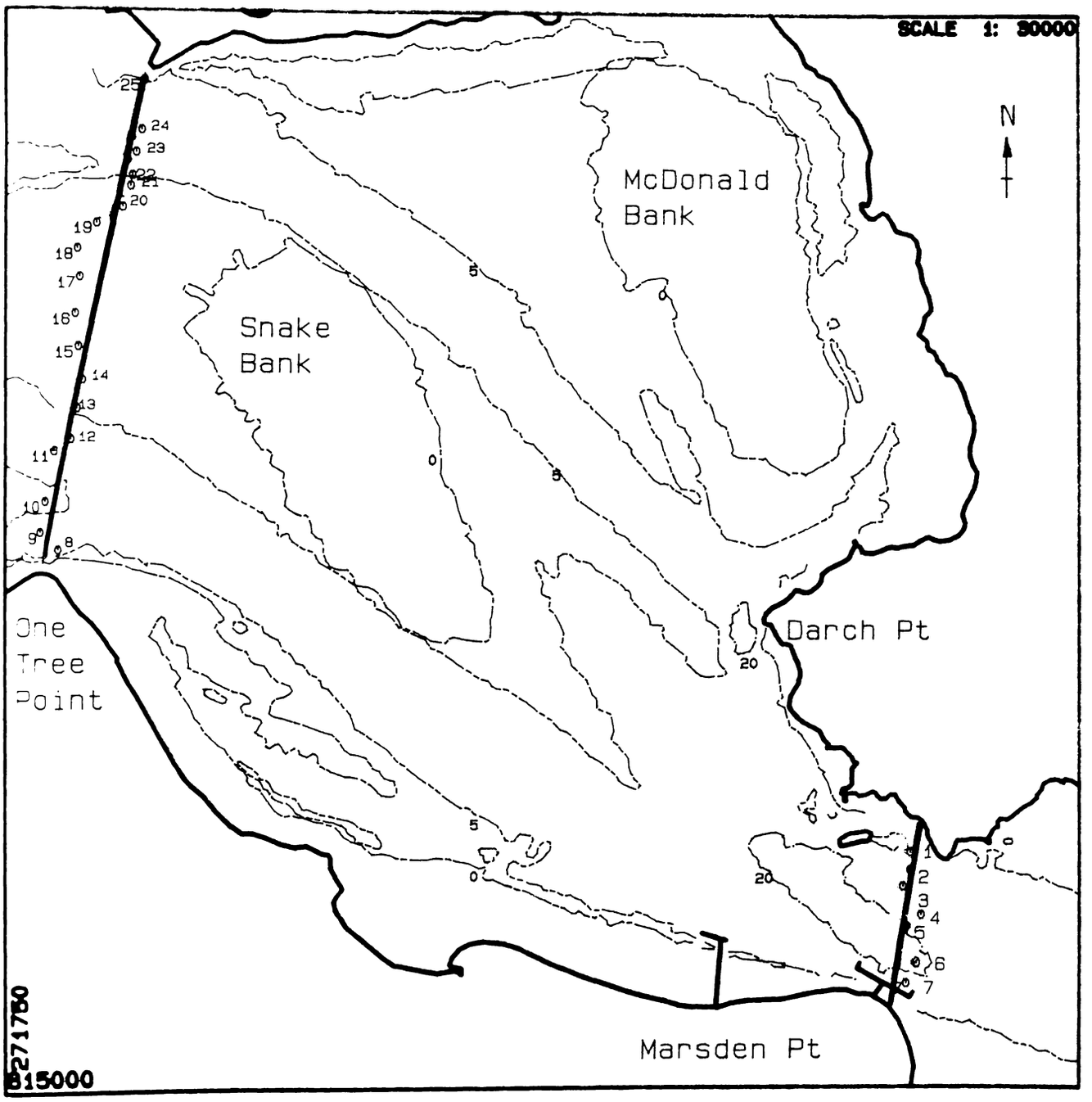

Figure 11.23: Locations of photograph sites used for determination of Availabilities at the open boundaries for the Iterative Mode.

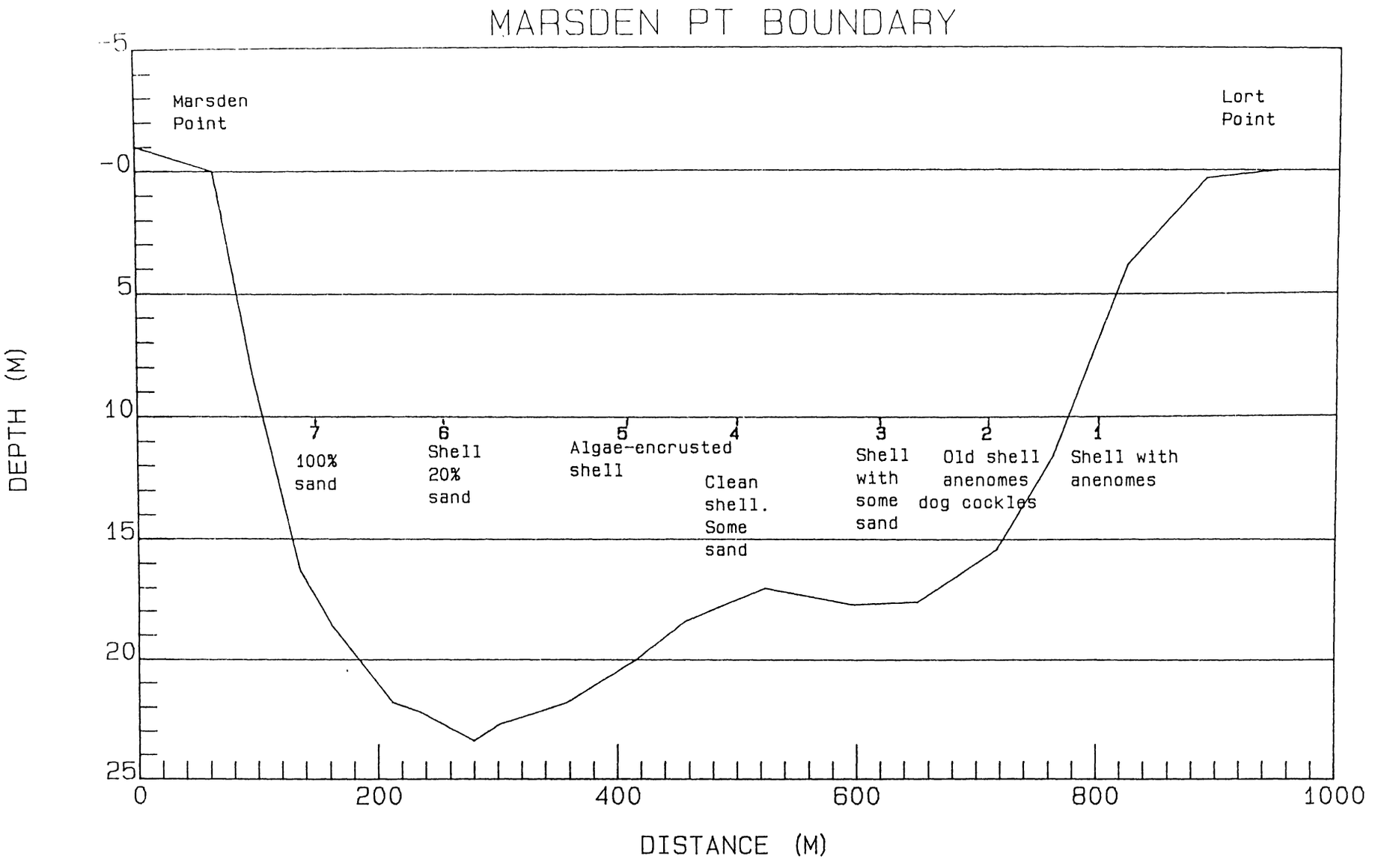

Figure 11.24: Marsden Point to Lort Point cross-section showing photograph locations with a brief summary of the type of sea bed.

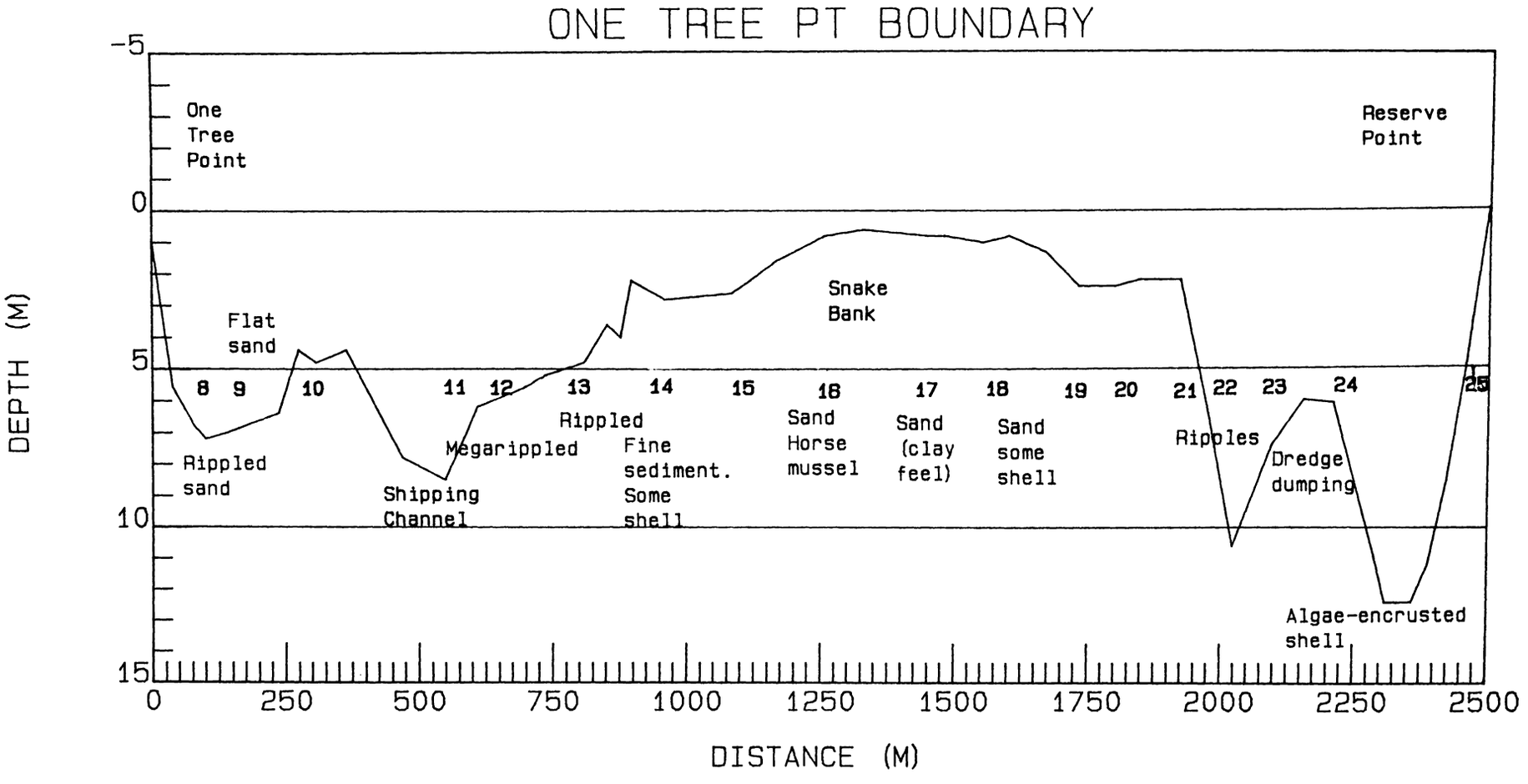

Figure 11.25: One Tree Point to Reserve Point cross-section showing photograph locations with a brief summary of bed facies.

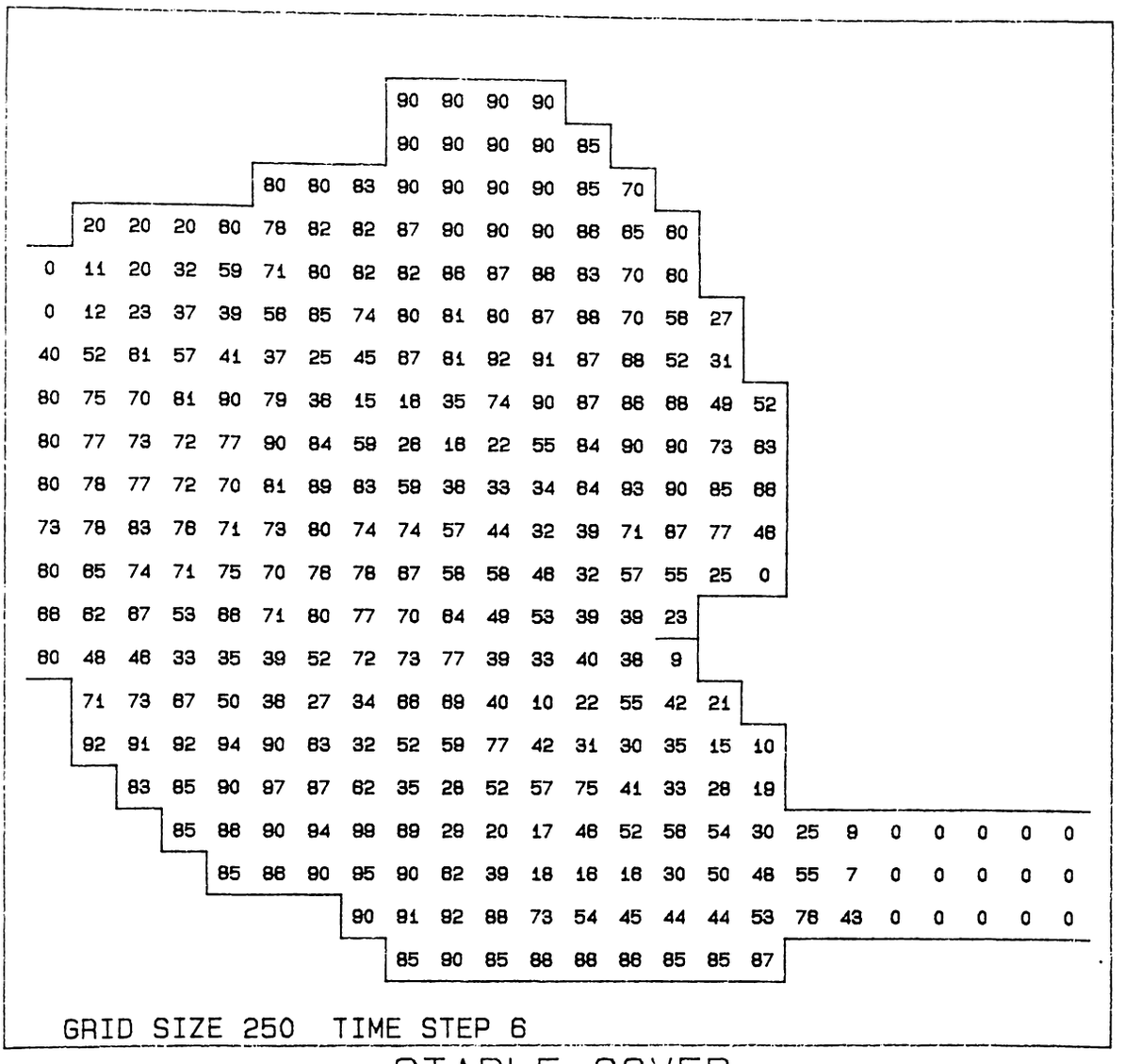

Figure 11.26: Stable harbour Availabilities showing the percentage sand cover in each cell determined using underwater photography, grain size analyses and side-scan sonar results in Whangarei Harbour. Optimisation was performed with 10 iterations.

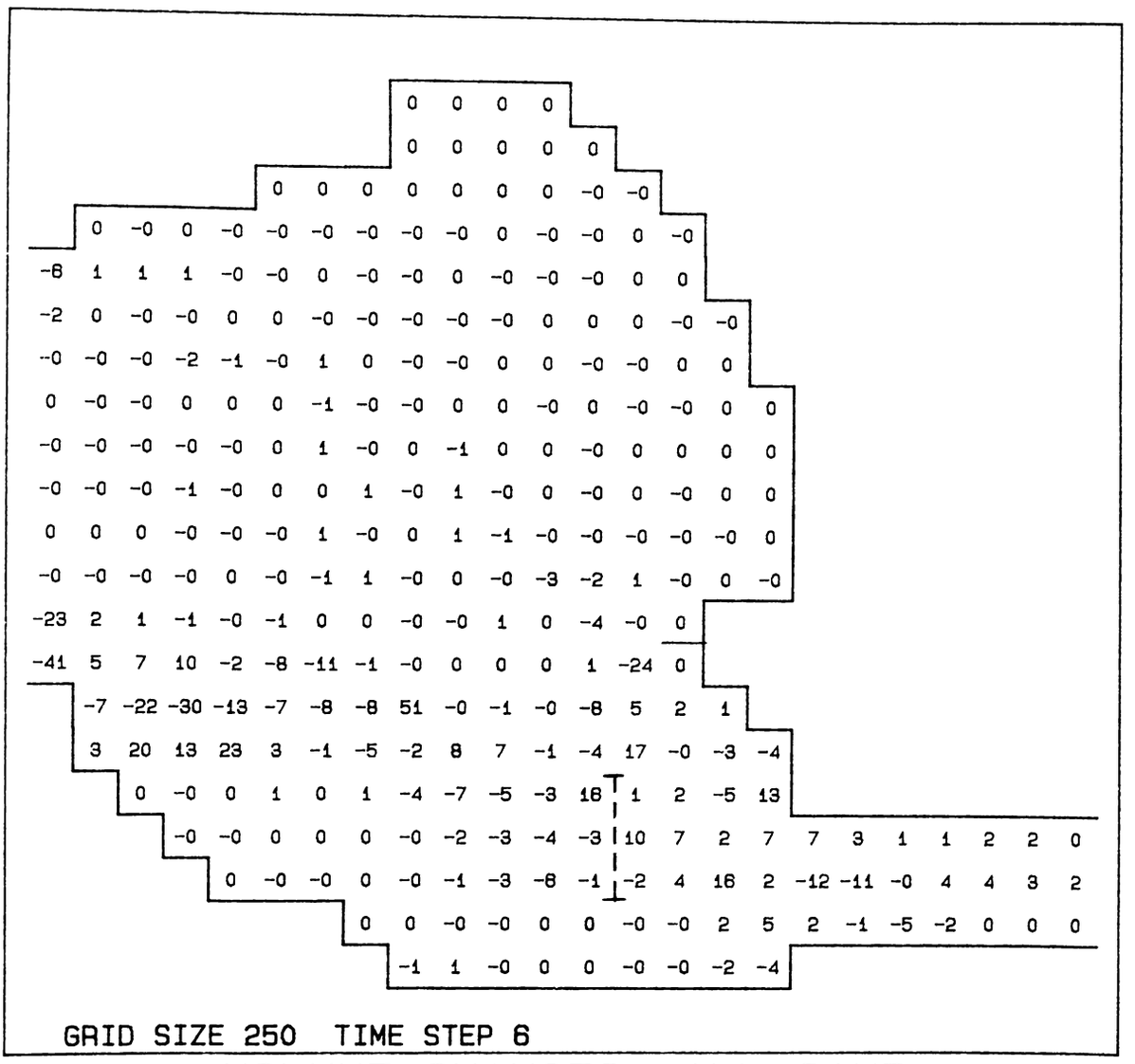

Figure 11.27: Annual volume changes in 1000's of m^3 in 250m-square cells, for Whangarei Harbour floored by non-cohesive sand. $D_{50} = 0.0003m$, $D_{65} = 0.00035$, $P = 0.45$, $\rho_s = 2650\ kg.m^{-3}$. The channel cross-section shown was used to find nett discharges through the port site.

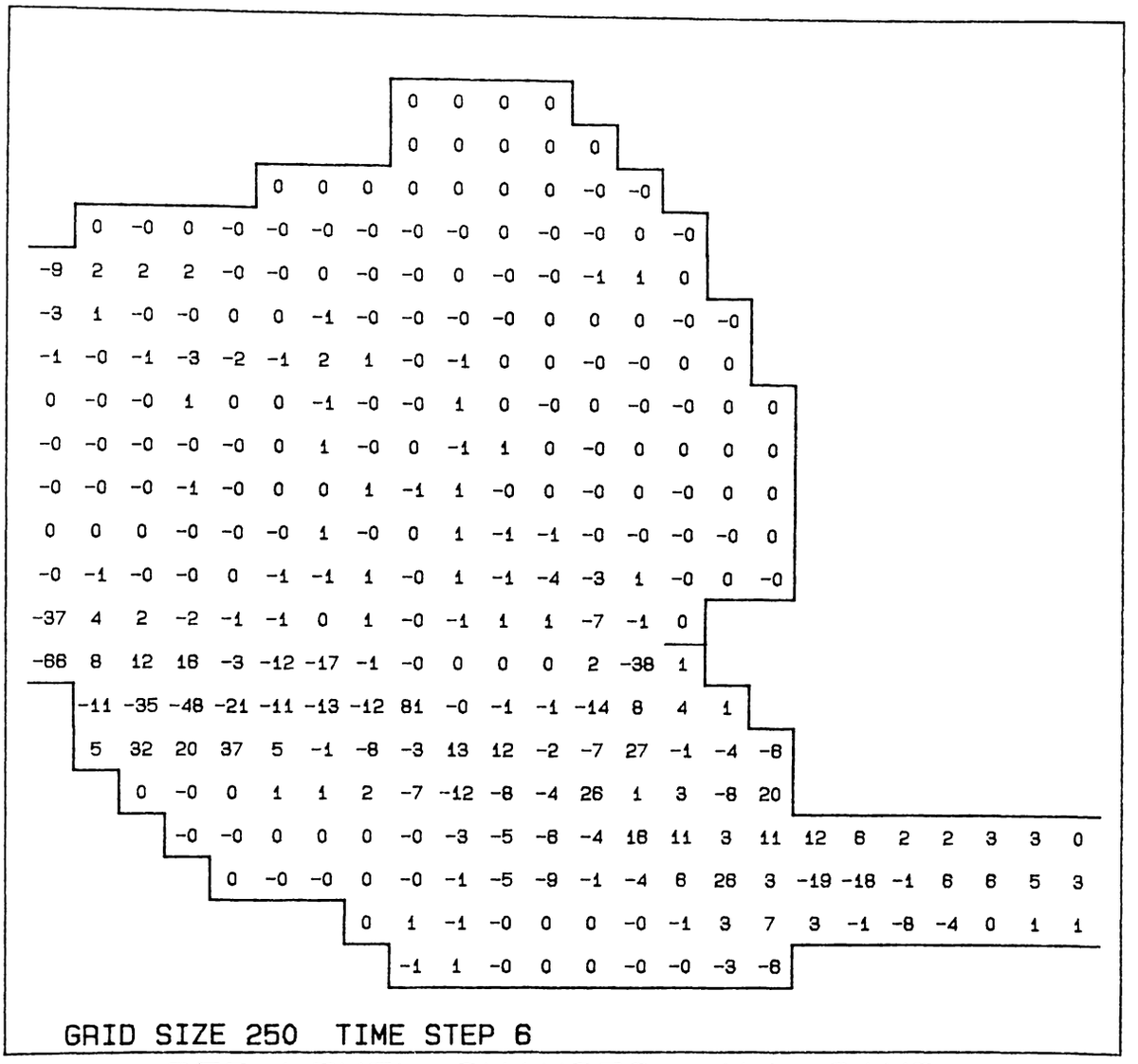

Figure 11.28: Annual bed level changes in centimetres (m x 100) in 250m-square cells for Whangarei Harbour floored by non-cohesive sand. $D_{50} = 0.0003m$, $D_{65} = 0.00035m$, $P = 0.45$, $\rho_s = 2650\ kg.m^{-3}$.

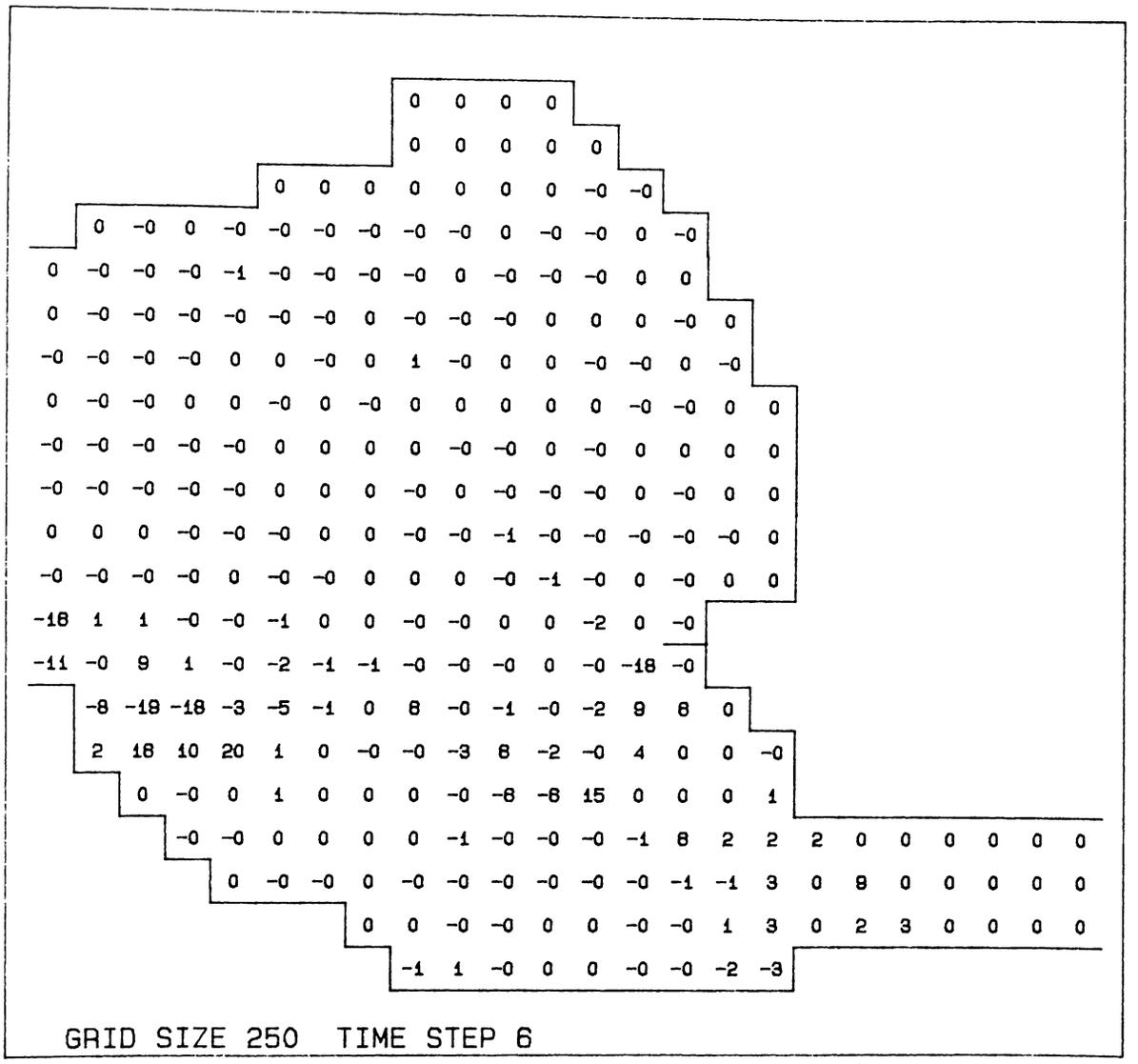

Figure 11.29: Annual volume changes in 1000's of m^3 in 250m-square cells for the stable harbour Availabilities. $D_{50} = 0.0003m$, $D_{65} = 0.00035m$, $P = 0.45$, $\rho_s = 2650\ kg.m^{-3}$.

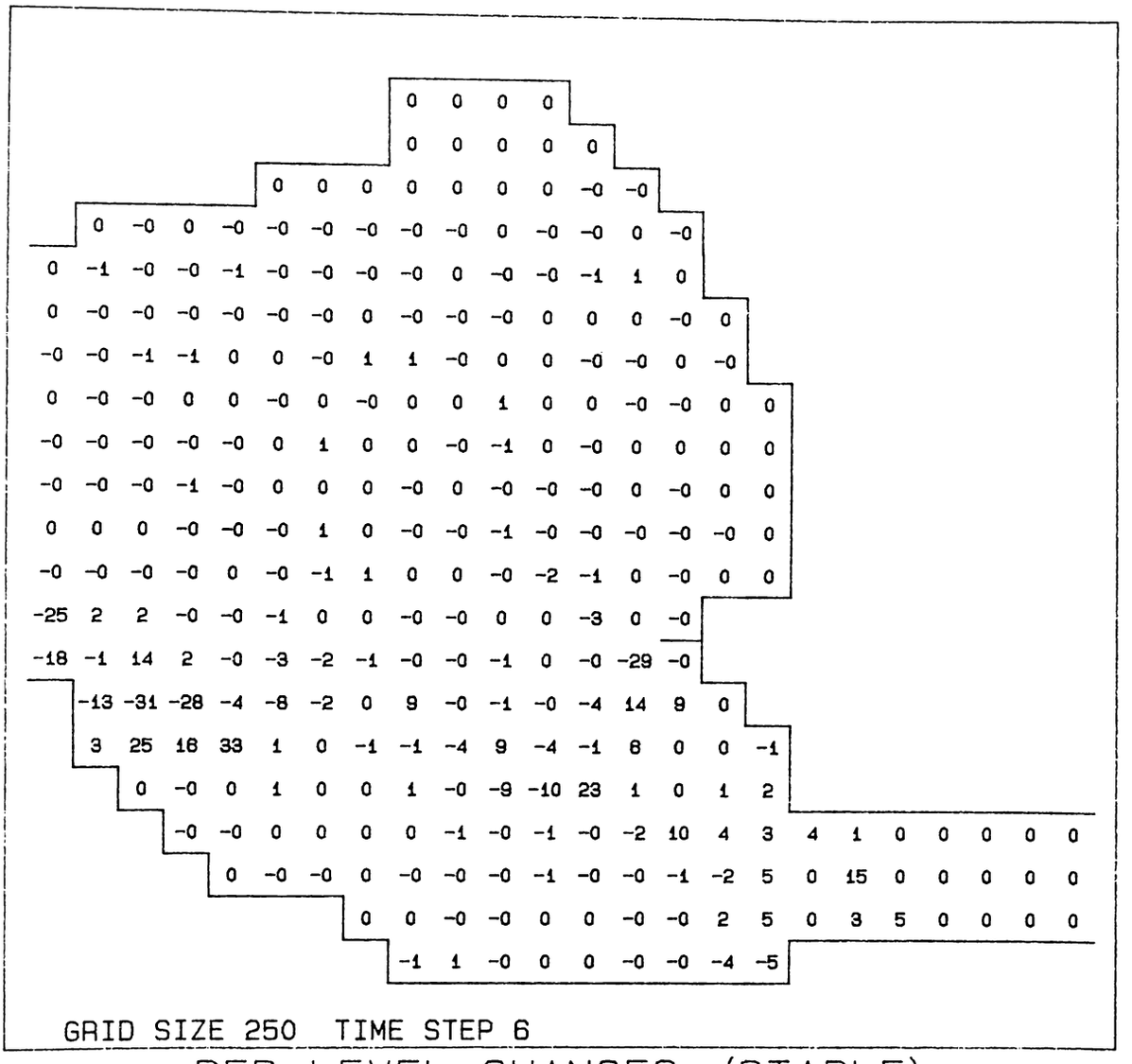

BED LEVEL CHANGES (STABLE)

Figure 11.30: Annual bed level changes in centimetres (m x 100) 250m-square cells for the stable harbour Availabilities. $D_{50} = 0.0003m$, $D_{65} = 0.00035m$, $P = 0.45$, $\rho_s = 2650\ kg.m^{-3}$.

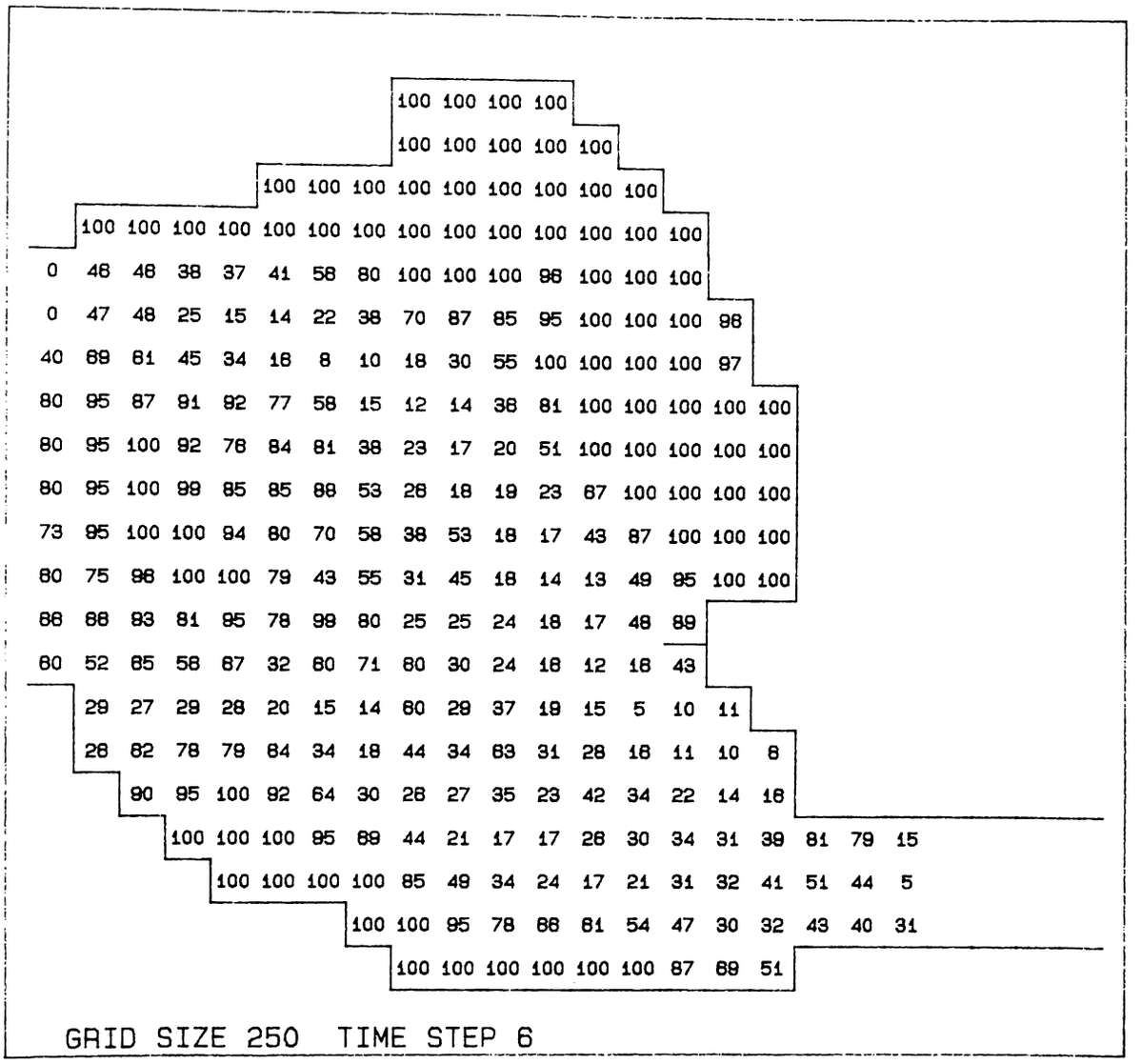

Figure 11.31: Stable harbour Availabilities showing the percentage sand cover in each cell and determined by Iteration using the Spring tide flow pattern with flux cut-off of 10 kg/m/tidal cycle.

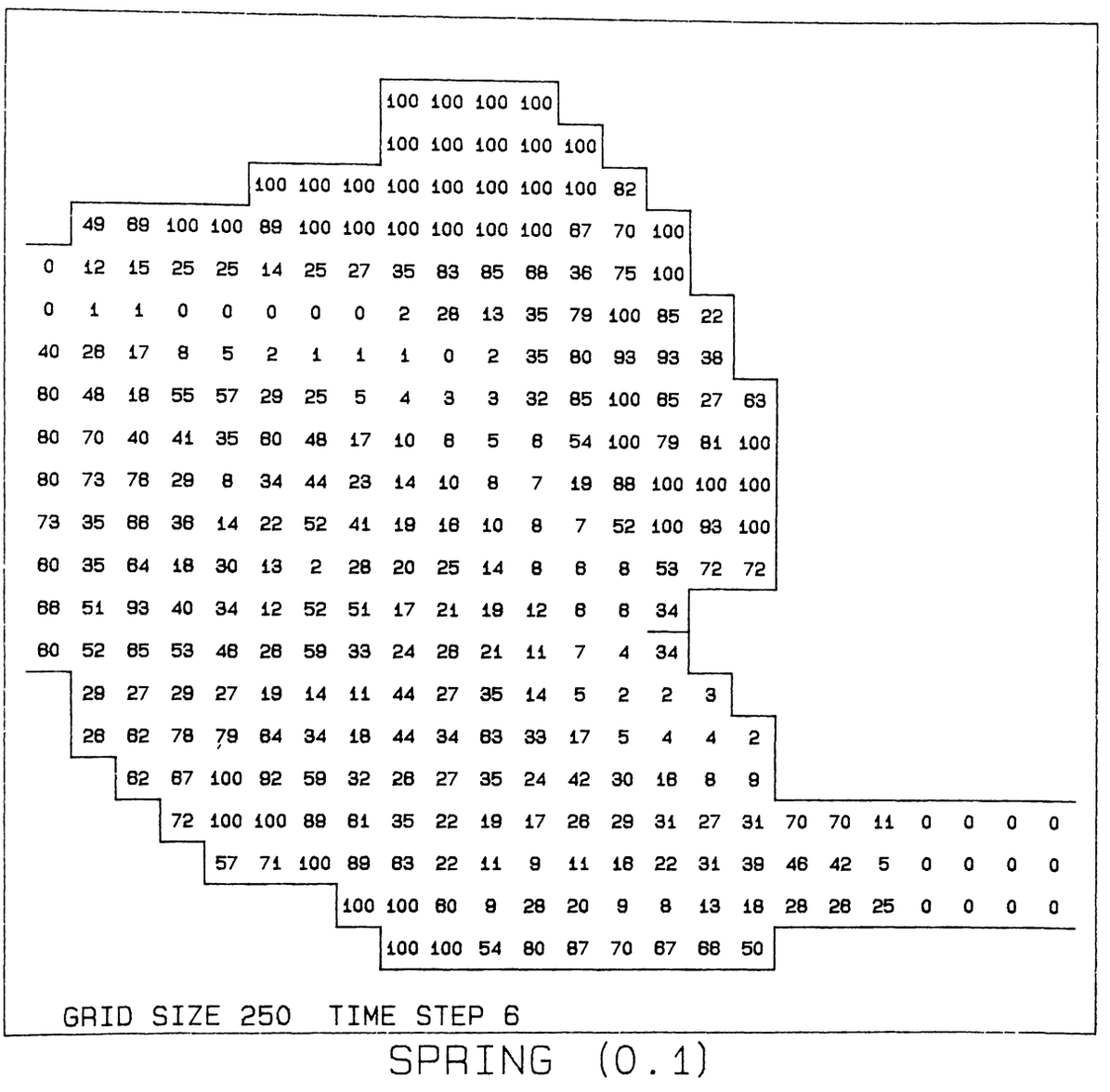

SPRING (0.1)

Figure 11.32: Stable harbour Availabilities showing the percentage sand cover in each cell and determined by Iteration using the Spring tide flow pattern with flux cut-off of 0.4 kg/m/tidal cycle.

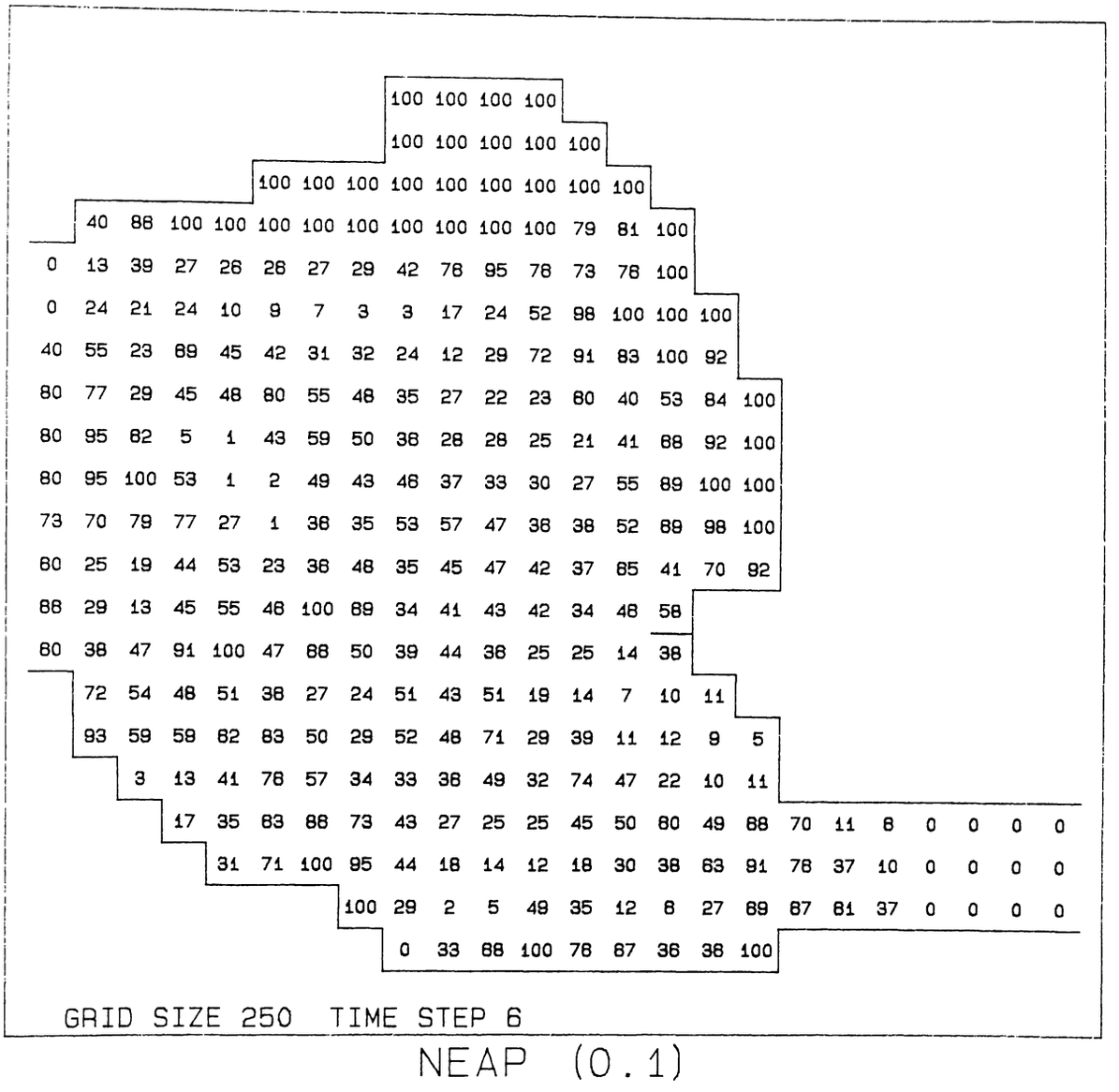

Figure 11.33: Stable harbour Availabilities showing the percentage sand cover in each cell and determined by Iteration using the Neap tide flow pattern scaled to a Spring range with flux cut-off of 0.4 kg/m/tidal cycle.

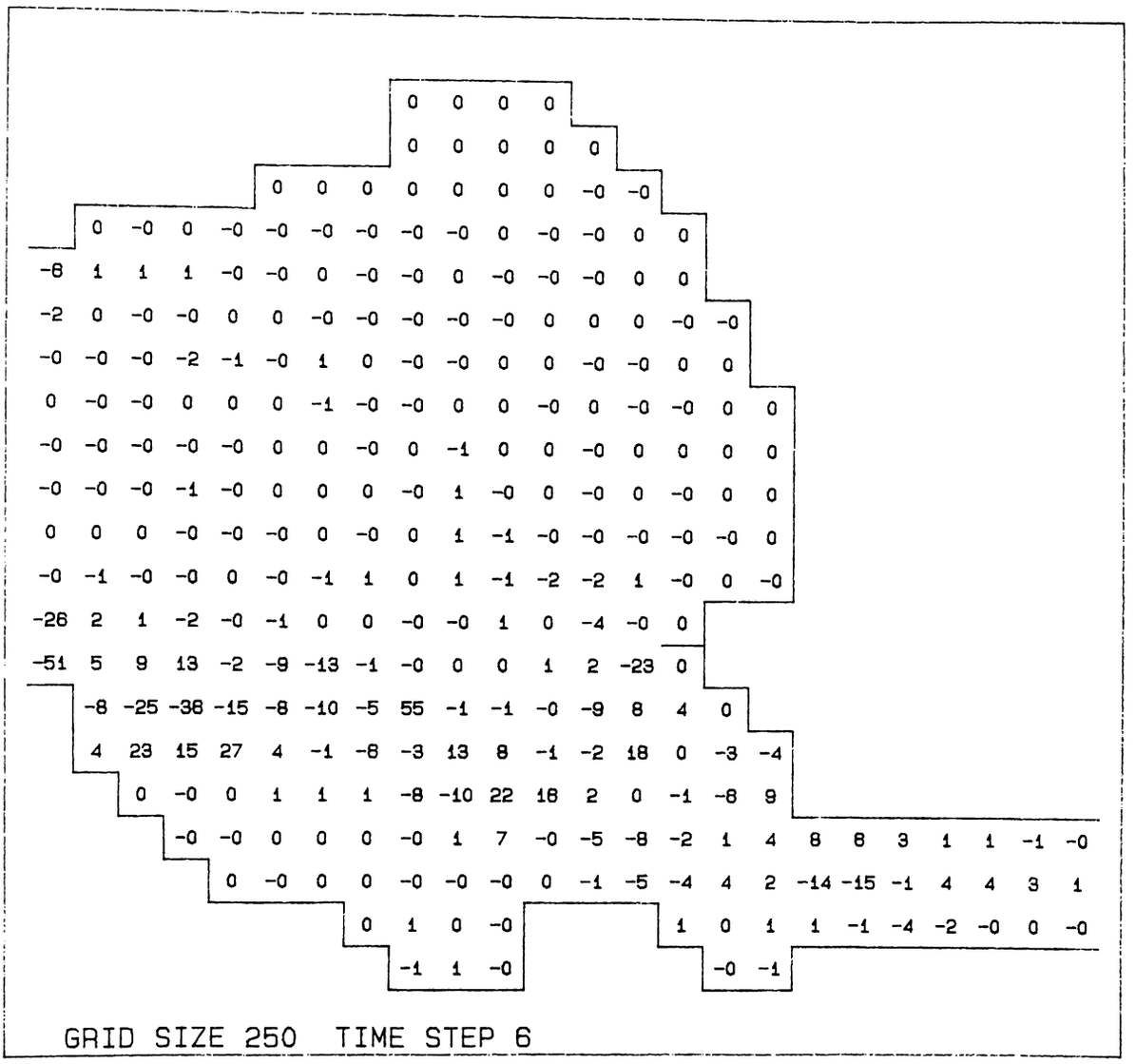

Figure 11.34: Annual volume changes after port construction in 1000's of m^3 in 250m-square cells for a harbour floored by non-cohesive sand. $D_{50} = 0.0003m$, $D_{65} = 0.00035m$, $P = 0.45$, $\rho_s = 2650\ kg.m^{-3}$.

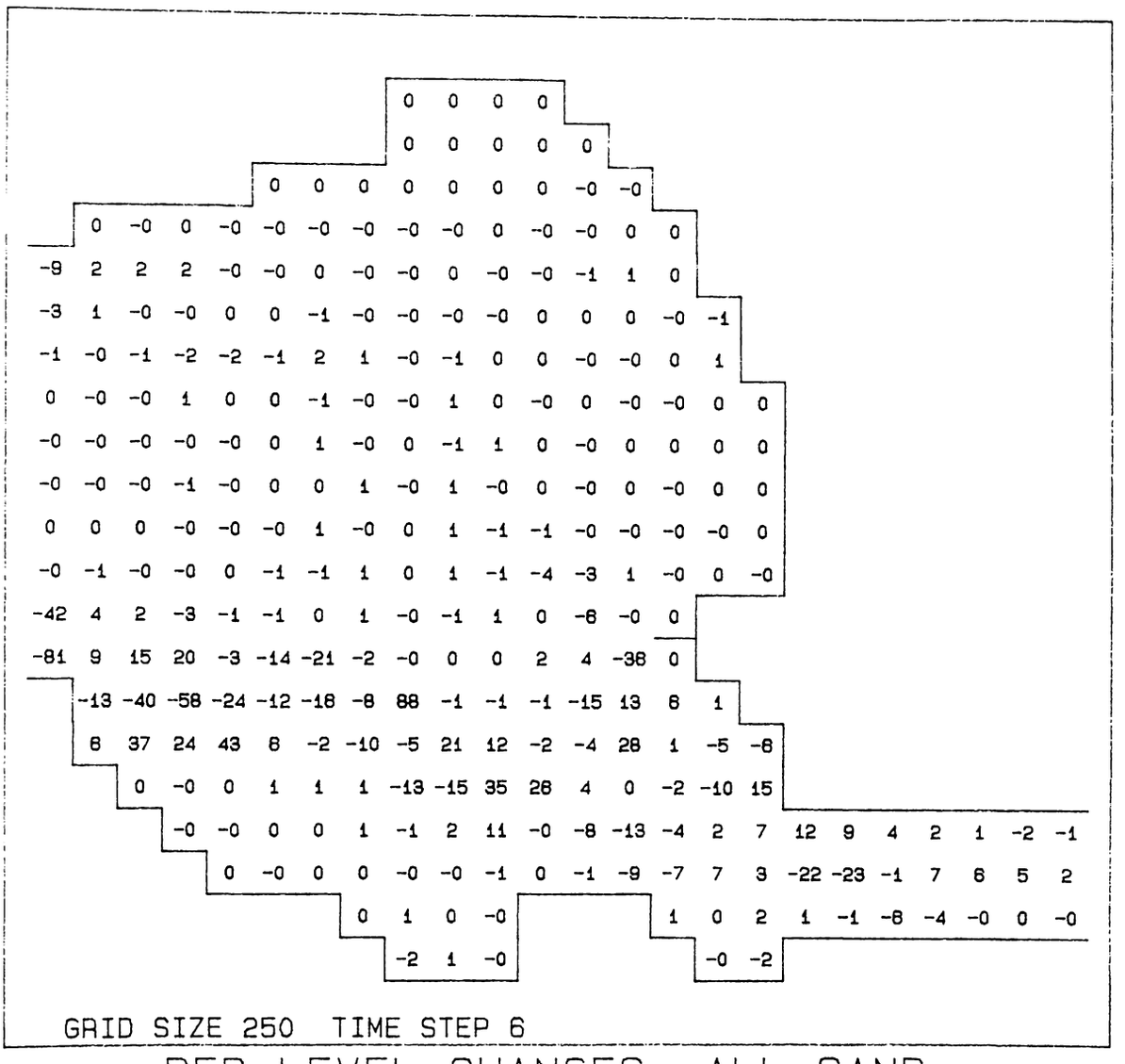

Figure 11.35: Annual bed level changes after port construction in centimetres (m x 100) in 250m-square cells for a harbour floored by non-cohesive sand. $D_{50} = 0.0003m$, $D_{65} = 0.00035m$, $P = 0.45$, $\rho_s = 2650\ kg.m^{-3}$.

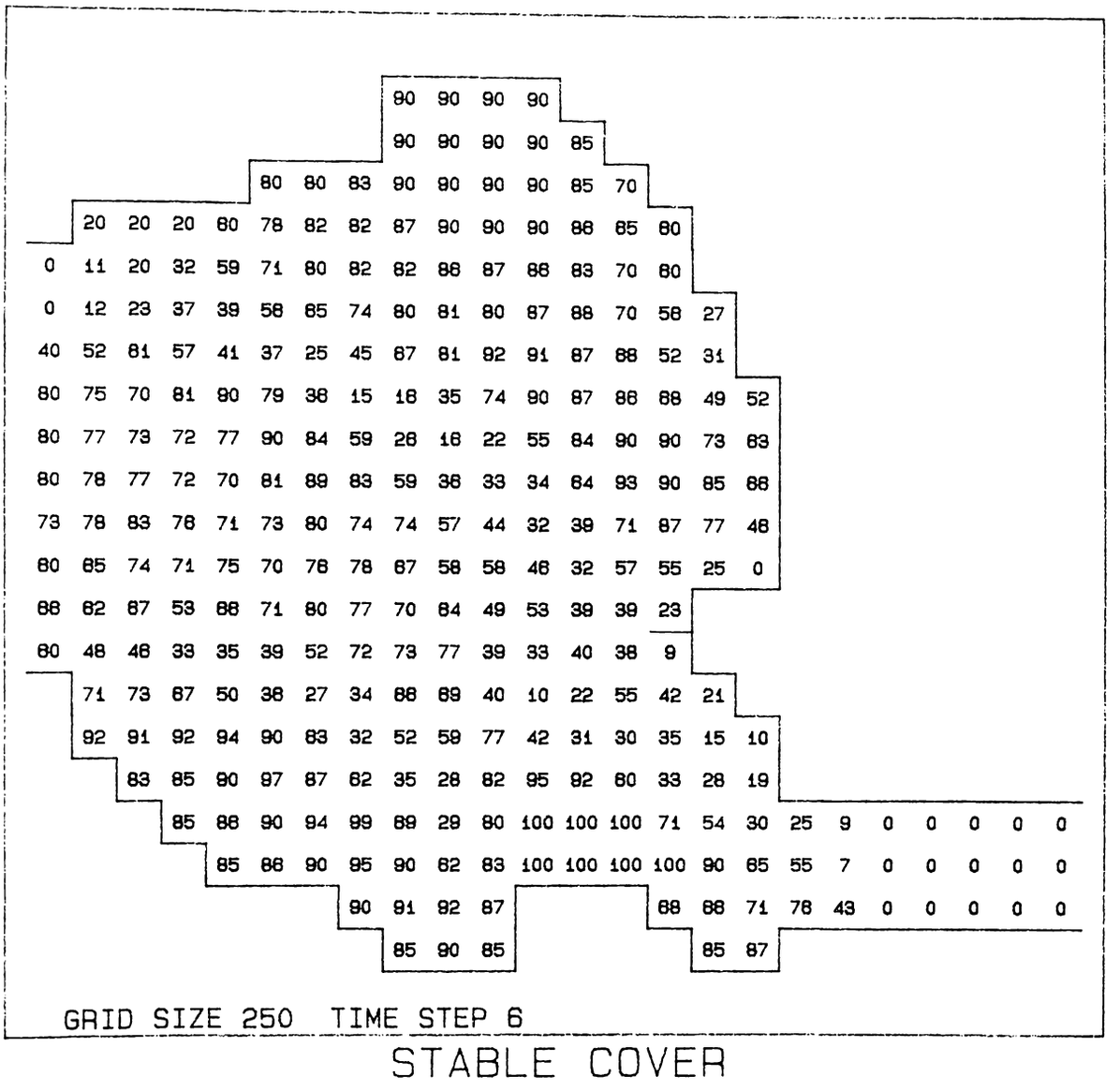

Figure 11.36: Stable harbour Availabilities after port construction assuming the dredge zone is entirely sandy. Other Availabilities were obtained after analysis of bed photographs, grain size samples and side-scan sonar results.

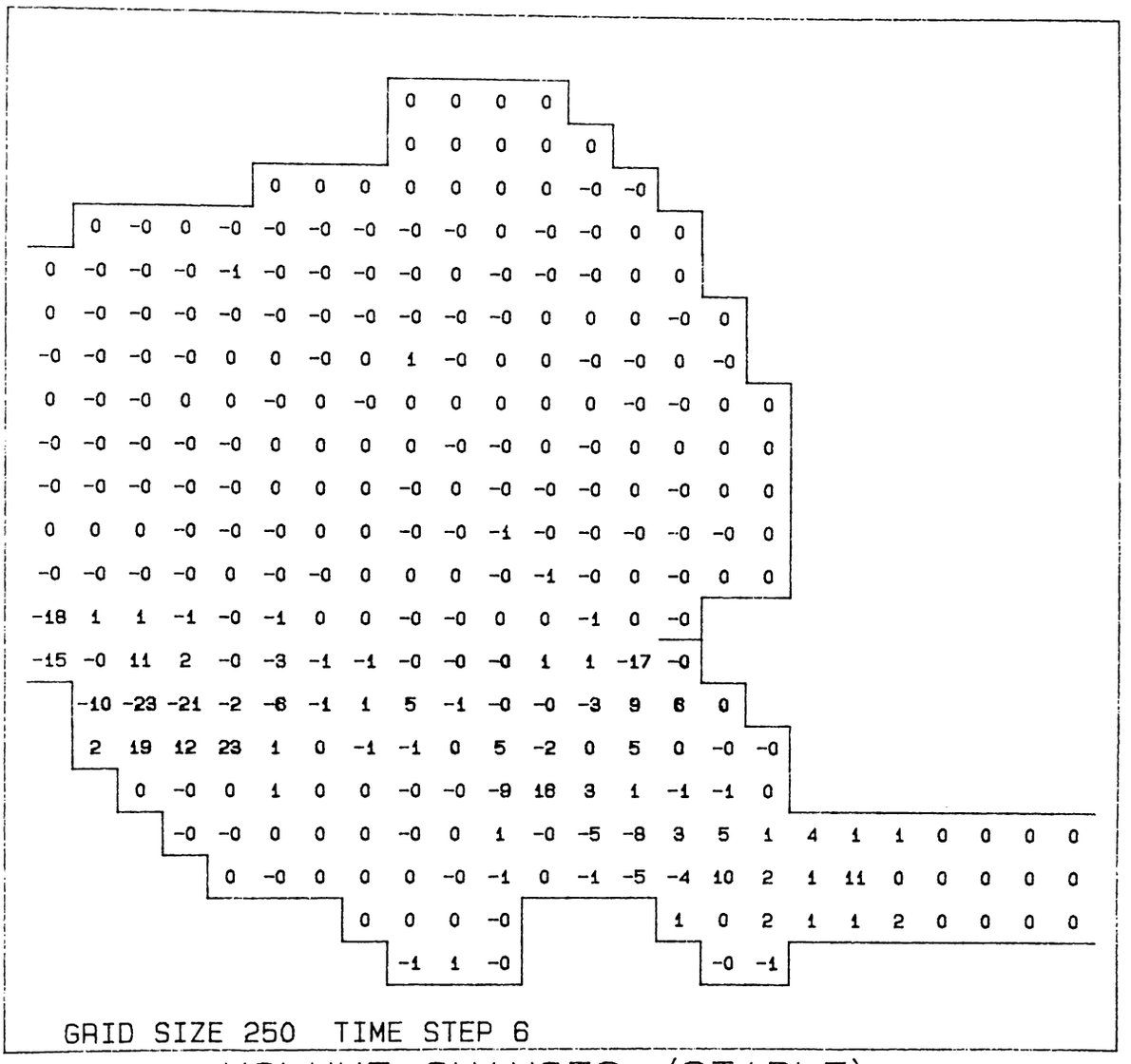

Figure 11.37: Annual volume changes after port construction in 1000's of m^3 in 250m-square cells with proper representation of the bed facies (Figure 11.35). $D_{50} = 0.0003m$, $D_{65} = 0.00035m$, $P = 0.45$, $\rho_s = 2650\ kg.m^{-3}$.

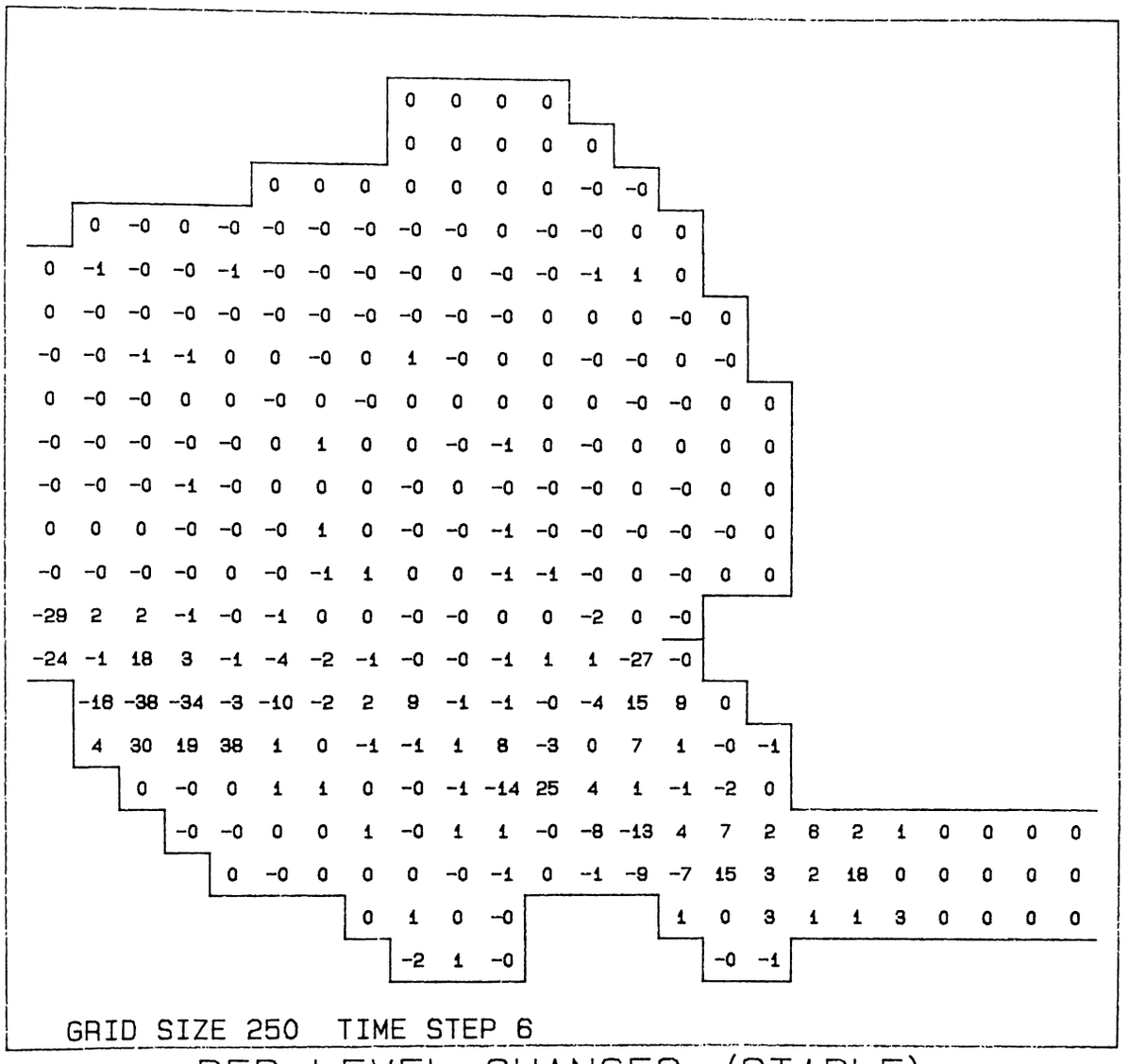

BED LEVEL CHANGES (STABLE)

Figure 11.38: Annual bed level changes after port construction in centimetres (m x 100) in 250m-square cells with proper representation of the bed facies (Figure 11.35). $D_{50} = 0.0003$m, $D_{65} = 0.00035$m, $P = 0.45$, $\rho_s = 2650$ kg.m^{-3}.

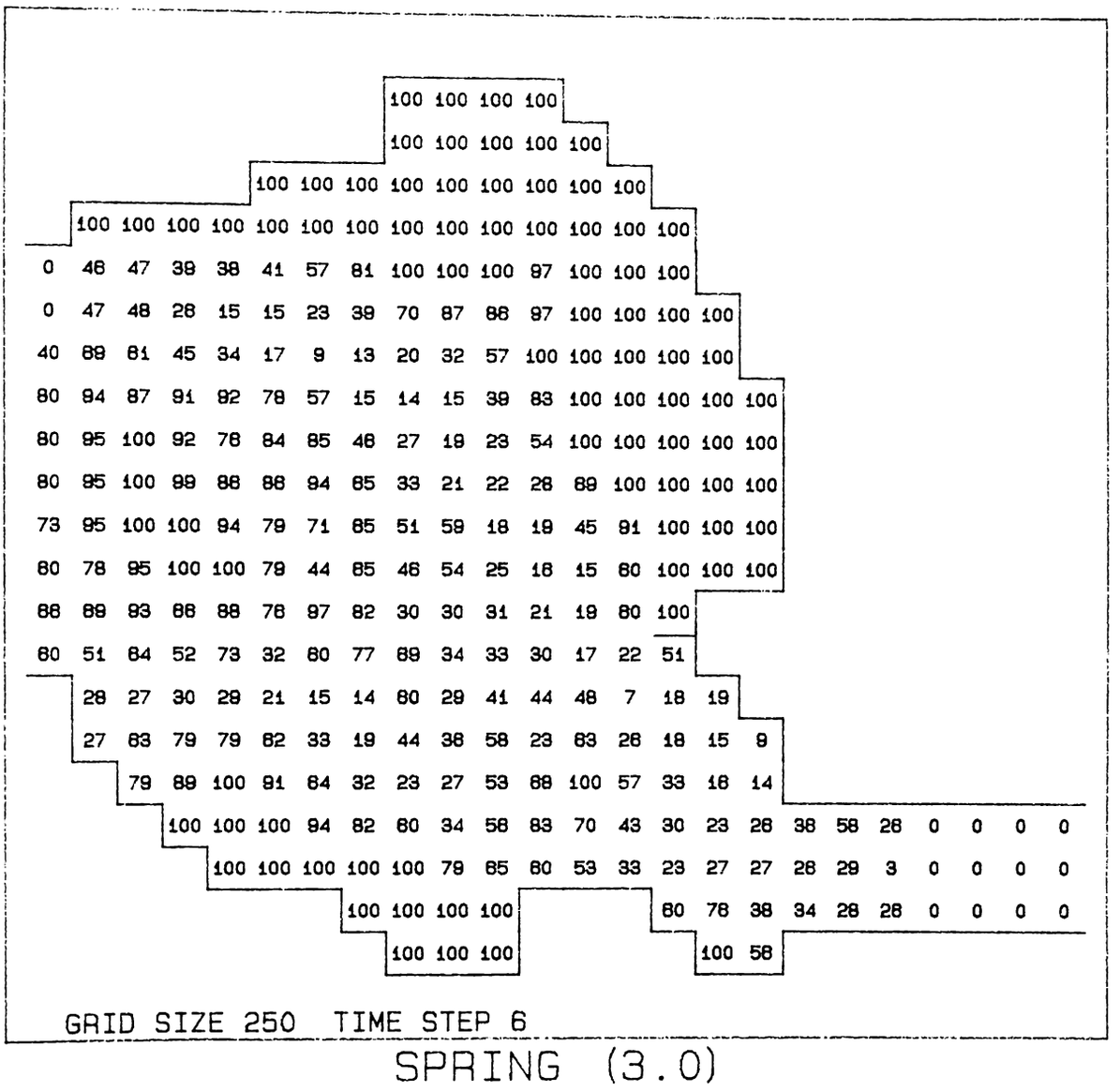

SPRING (3.0)

Figure 11.39: Stable harbour Availabilities after port construction showing the percentage sand cover in each cell determined by Iteration. Spring tide flow pattern with a flux cut-off of 10 kg/m/tidal cycle.

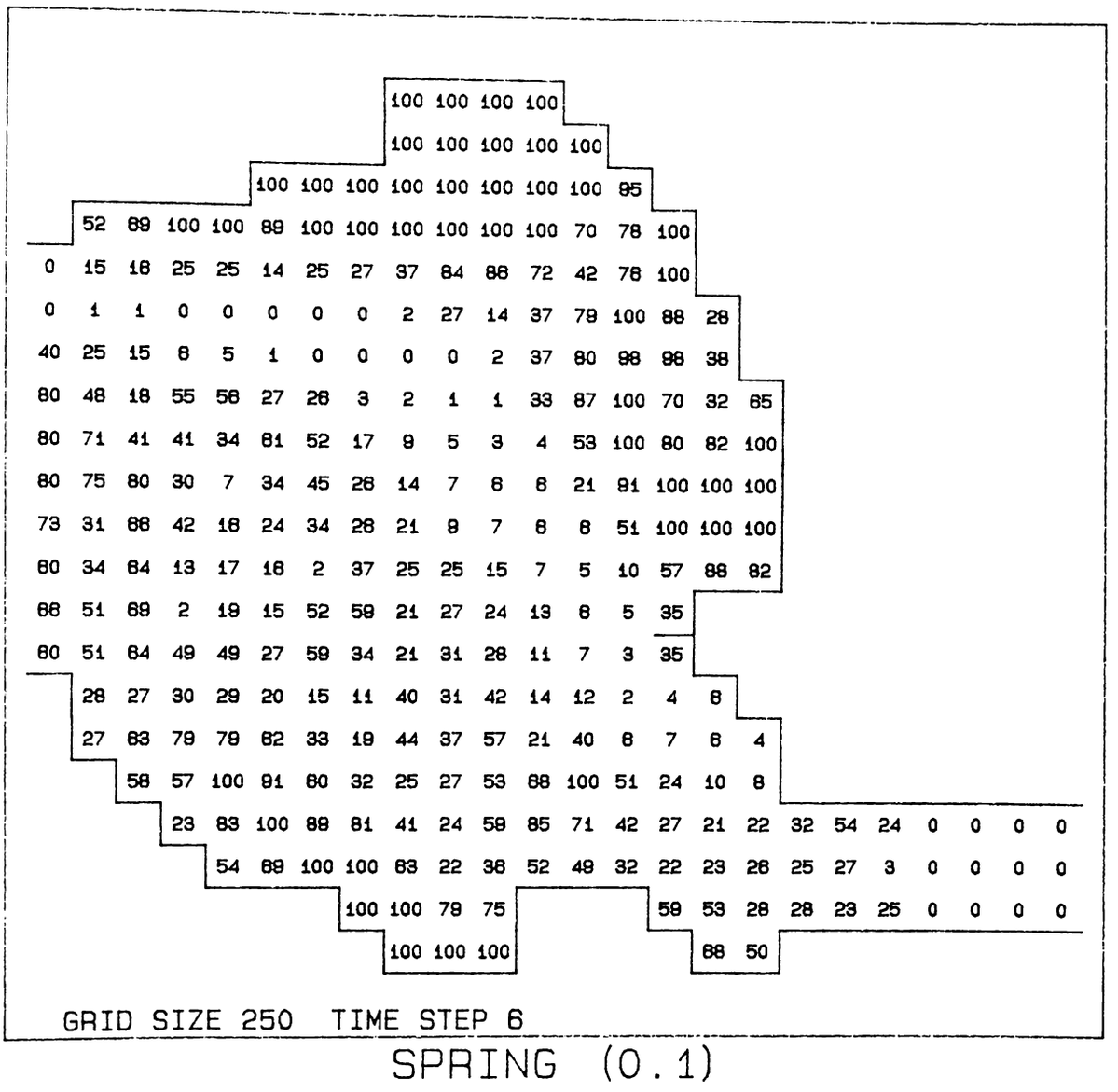

Figure 11.40: Stable harbour Availabilities after port construction showing the percentage sand cover in each cell determined by Iteration. Spring tide flow pattern with a flux cut-off of 0.4 kg/m/tidal cycle.

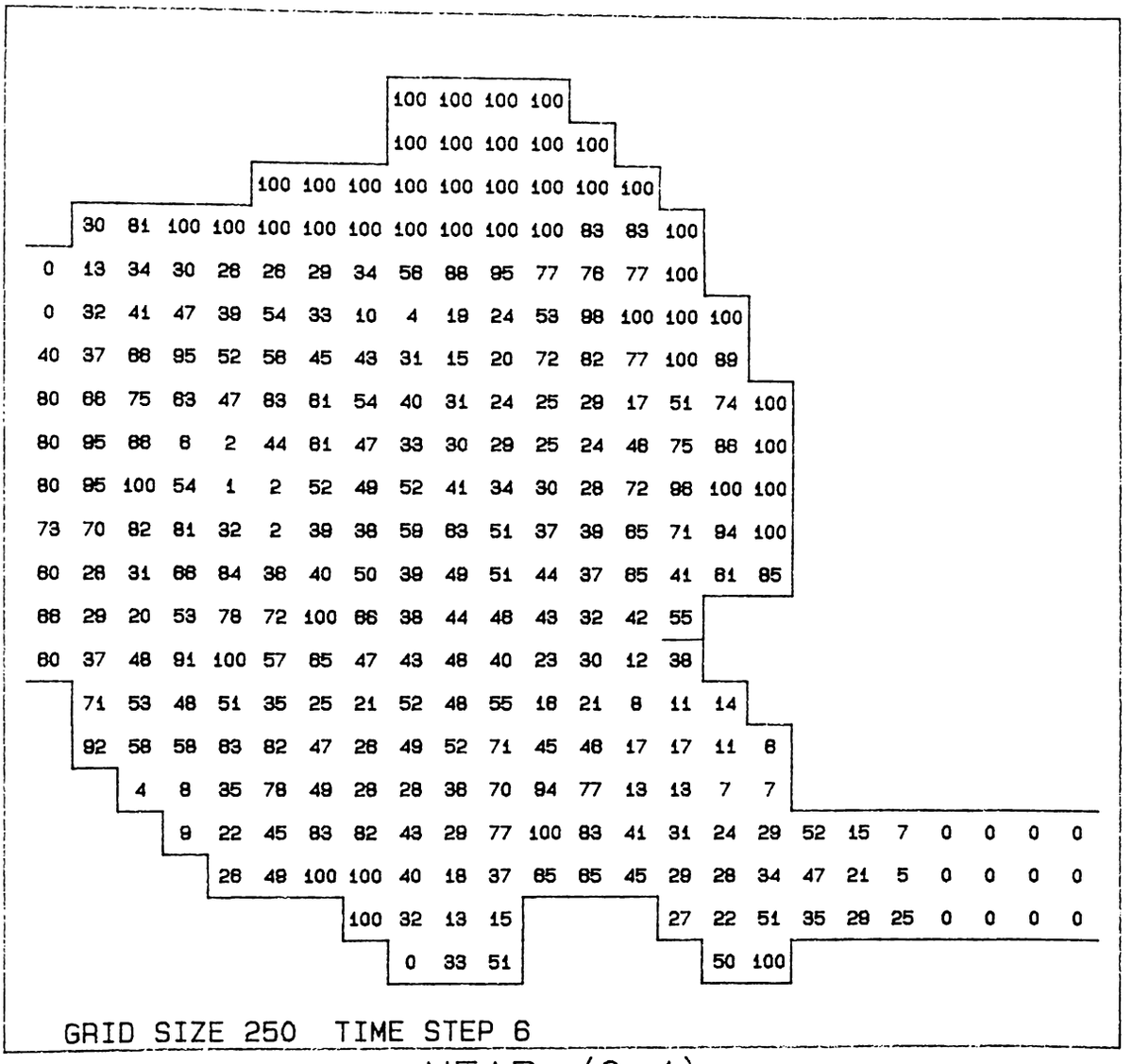

Figure 11.41: Stable harbour Availabilities after port construction showing the percentage sand cover in each cell determined by Iteration. Neap tide flow pattern scaled to a Spring range with a flux cut-off of 0.4 kg/m/tidal cycle.

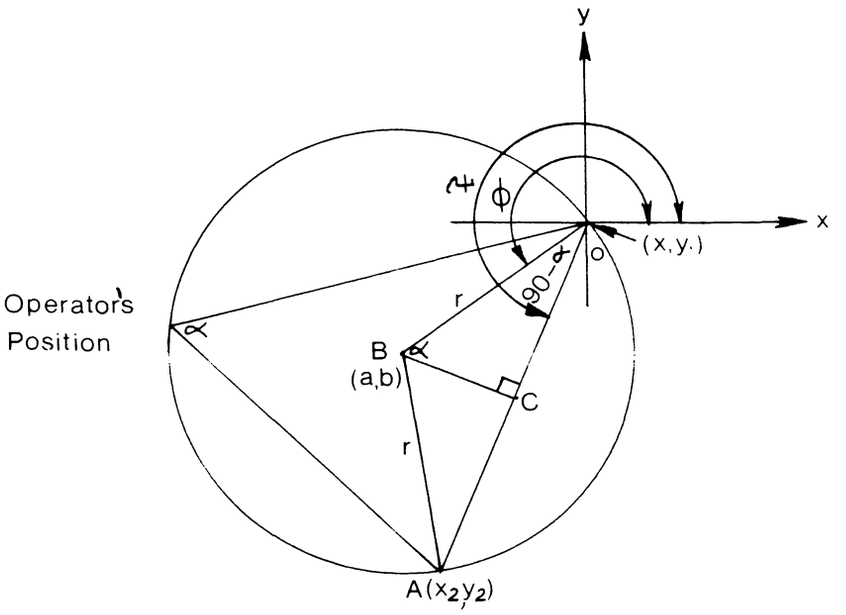

Figure A1.1: Construction and definition of terms for sextant position fixing solution.

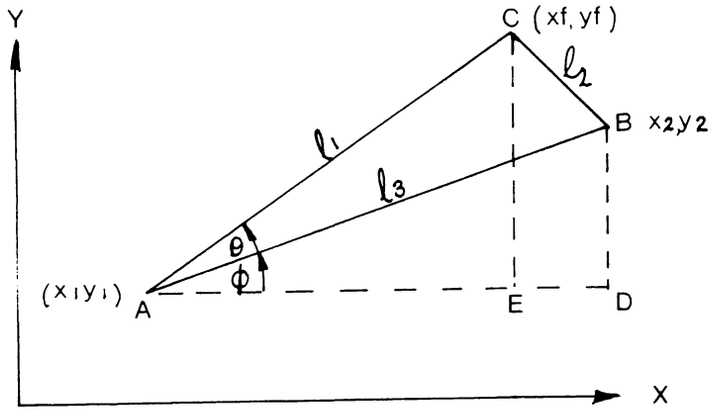

Figure A1.2: Construction and definition of terms for Electronic Distance Measuring Equipment position fixing solution.

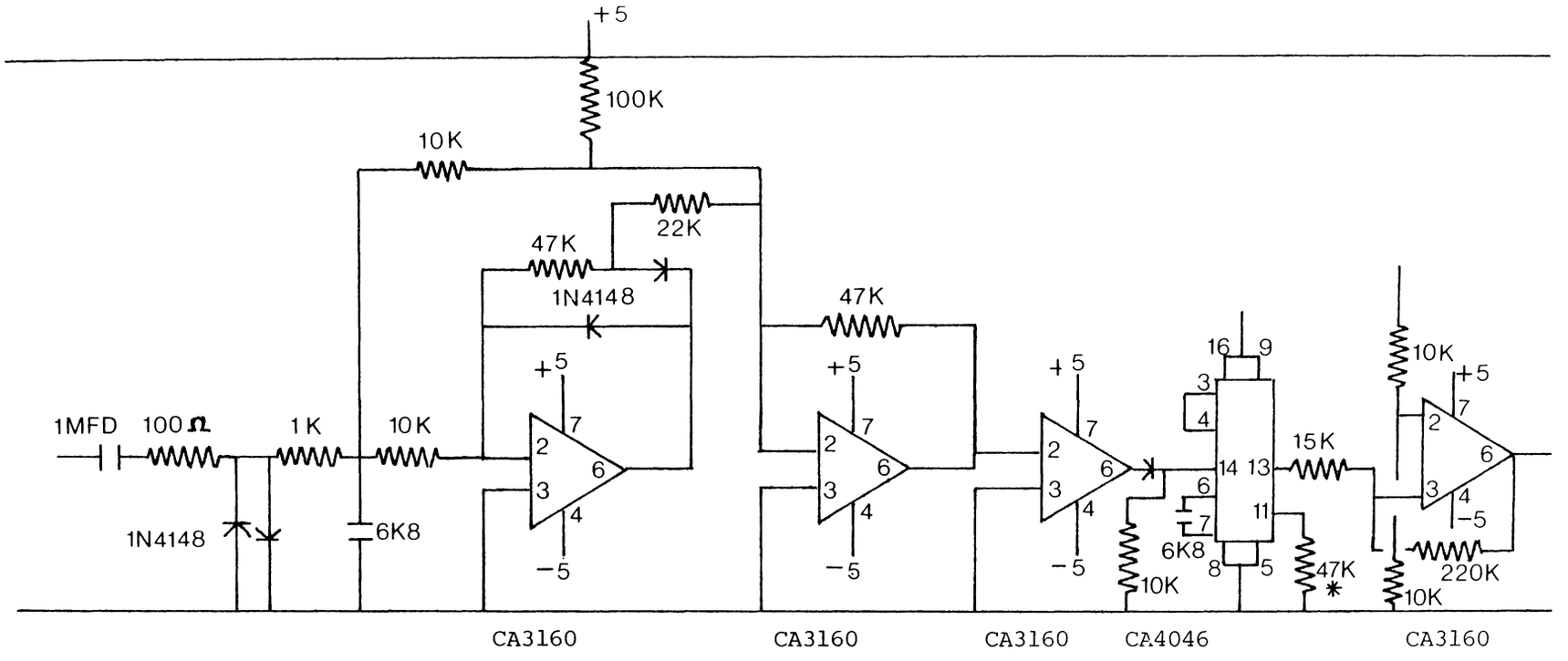

Figure A4.1: Circuit diagram for the frequency to voltage converter of the data acquisition system, SUBTLE. High and low frequency shift key (FSK) tones from a cassette tape input are converted to voltages for computer recognition (±5 volts).

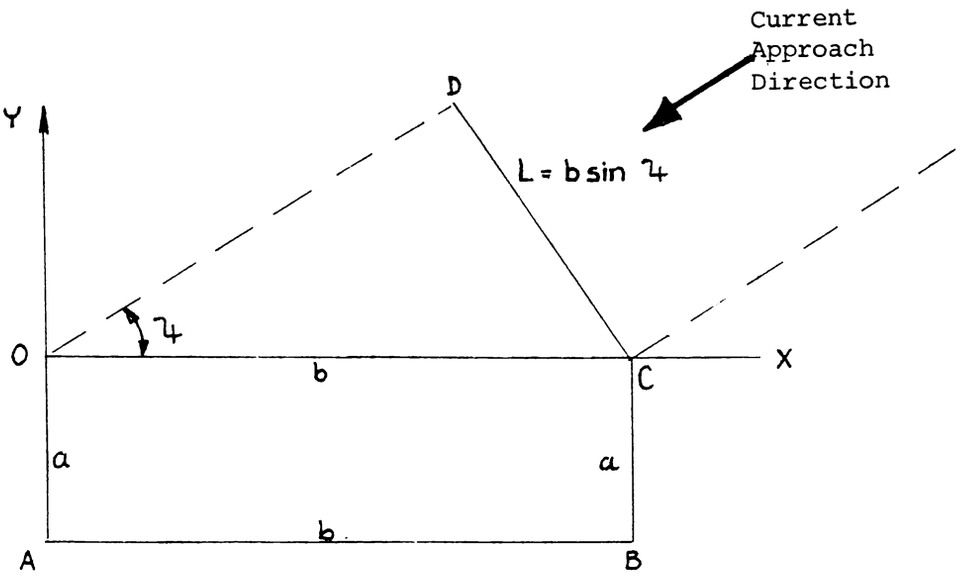

FIGURE A6.1: Rectangular Trap OABC with Sides of Length a and b

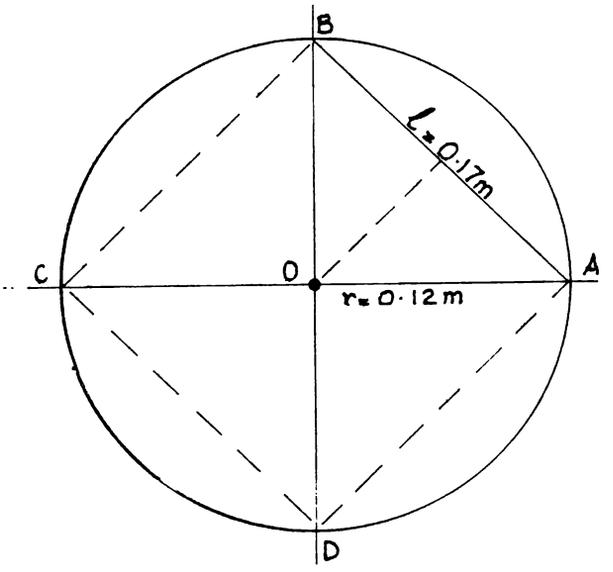

FIGURE A6.2: Embedded circular trap with 4 compartments.

```
 **  EACH SITE IS CODED WITH AN INTEGER NUMBER  **
1   NZRC CHIMNEY    275566.4    815089.7
2   NZRC FLARE STACK    275572.5    815246.4
3   NZRC OIL TOWER ON JETTY (WESTERN END)    275909.9    815636.1
4   NZRC OIL TOWER ON JETTY (EASTERN END)    276162.4    815490.0
5   NZRC EXTREME END OF JETTY (WESTERN END)    275876.3    815657.9
6   NZRC EXTREME END OF JETTY (EASTERN END)    276198.9    815471.0
7   NZRC WESTERN-MOST DOLPHIN    275701.9    815699.9
8   NZRC EASTERN-MOST DOLPHIN    276321.6    815343.7
9   BACK LEAD ON MARSDEN POINT (ORANGE BEACON)    276060.2    815262.9
10  MARSDEN B POWER STATION CHIMNEY (NORTHERN)    273334.7    811320.3
11  MARSDEN A POWER STATION CHIMNEY (SOUTHERN)    273261.8    811102.1
12  FRENCHMAN'S ISLAND    278605.2    812860.4
13  LEADING LIGHTS FRONT LEAD (ORANGE BEACON)    277135.2    813960.9
14  MT. MANAIA    277633.8    817554.3
15  MT. ABOVE HOME PT. (121M)    278670.0    813895.0
16  CASTLE POINT    277277.8    816297.7
17  LORT POINT    276319.2    816145.9
18  PASSAGE ISLAND    275812.2    816211.0
19  NHB JETTY (WESTERN END)    275127.9    815775.1
20  NHB JETTY (EASTERN END)    275259.1    815742.2
21  NHB HOLIDAY HOME (CENTRE)    274730.0    815440.0
22  POINT SINCLAIR    272472.8    816879.0
23  SINCLAIR FRONT LEAD    272970.7    816726.6
24  CABLE BCN 700M NE OF SINCLAIR BCN (11 SEC)    272766.2    817493.9
25  SHELL CUT REACH FRONT LEAD (NEON)    273557.5    817444.1
26  S1 BEACON    273159.5    817751.1
27  S2 BEACON    272254.8    817999.4
28  S3 BEACON    271809.2    818331.5
29  S4 BEACON    271774.1    818232.5
30  S6 BEACON    270482.5    818836.5
31  ONE TREE POINT BOAT RAMP PILE    271944.6    817636.0
32  MANGANESE POINT    271205.0    820200.0
33  POST SW OF MOTUKIORE ISLAND    271495.0    820350.0
34  RESERVE POINT    272165.0    820370.0
35  POINT 300M SE OF RESERVE POINT    272446.7    820089.3
36  MUNRO BAY WEST POINT    274361.3    820353.3
37  MC DONALD ISLAND    274990.3    819504.4
38  RED BEACON ON SE CORNER OF MC DONALD BANK    275820.3    818474.4
39  DARCH POINT    275427.0    817350.2
40  SP1H    273471.3    817585.9
41  SP2H    273107.4    818341.8
42  SP3H    272057.6    819004.9
43  SP4H    273688.2    818727.9
44  SP5H    273874.4    817876.4
45  SP6H    275080.7    818738.7
46  SP1M    276648.0    815136.3
47  SP2M    276350.6    814715.8
48  SP3M    275874.5    814036.2
49  SP4M    276356.1    814007.6
50  SP5M    277537.3    814630.0
51  SP6M    278167.7    815682.5
52  TAURIKURA    278543.6    815913.7
53  ONE TREE POINT IRON BAR    272013.7    817493.4
54  PORTLAND PIPE    258970.5    818773.1
55  TRIG F    259134.9    823261.9
56  LIMESTONE TRIG    263208.9    821142.0
57  STEVENS PT    264589.7    823061.8
58  RMG    275136.3    813955.8
59  TURF    272742.1    809445.9
60  PAPICH RD    274492.4    815557.2
61 ONE TREE PT REAR LEAD    271559.7    817137.0
62  SHELL BANK WEST FRONT LEAD    267050.5    820505.3
63  SHELL BANK WEST REAR LEAD    264782.9    821571.6
64  MCKENZIE AT LAINGS BEACH    279554.1    792135.9
```

Table 1.1: Numbered landmarks and their Mt Eden Geodetic Metric Coordinates (East then North). Locations are shown in Figure 1.2.

Table 2.1: Characteristics of lower-flow regime bedforms (modified after Harms, et al., 1975).

	Ripples	Megaripples	Sandwaves
Spacing	60 cm	60 cm – 6 m	6 m
Height/spacing ratio	variable	relatively large	relatively small
Geometry	highly variable	sinuous to highly three-dimensional, prominent scour pits in troughs	straight to sinuous, uniform scour in troughs
Characteristic flow velocity	low (>25–30 cm/sec, < 40–50 cm/sec)	high (>70–80 cm/sec, < 100–150 cm/sec)	moderate (>30–40 cm/sec, < 70–80 cm/sec)
Velocity asymmetry	negligible to substantial	negligible to substantial	usually substantial

From Boothroyd (1978)

Line (1)	5.8	3.4	3.4	5.8	6.8	5.5	6.8	5.5	4.6	5.5	5.2	4.6
Mean 5.00±1.28	6.5	4.9	2.8	2.8	4.9							
Line (2)	5.8	4.6	4.0	5.2	7.1	4.3	7.4	4.9	3.4	4.3		
Mean 5.15±1.17	3.7	5.8	7.1	5.5	5.2	5.2	4.0	4.2				
Line (3)	6.8	4.6	3.1	3.7	7.1	6.8	5.8	5.5	5.8	4.3		
Mean 5.53±1.20	5.5	5.2	5.8	4.9	5.8	7.4						

Table 2.2: Consecutive megaripple wavelengths (m) at Fix 102.

4.0	3.6	5.3	4.0	8.3	3.0	4.3	6.8	7.0	7.0
3.3	6.0	3.0	5.0	7.0	5.3	4.0	7.0	4.6	3.6
3.3	3.6	2.0	3.3	9.3	1.3	3.6	3.3	2.7	5.6
4.3	4.3	4.3	5.6	6.3	3.3	6.0	3.3	3.0	4.6
5.3	3.3	3.3	3.0	5.3	4.3	4.0	3.0		

Table 2.3: Consecutive megaripple wavelengths (m) measured at Fix 589.

Sounding Line Identification	North Metric Co-ordinate	East Metric Co-ordinate
L1H	817636.0	271944.6
L2H	817636.0	271944.6
L3H	816879.0	272472.8
L4H	815643.3	274743.4
L5H	815600.0	275055.5
L6H	815540.0	275341.5
L7H	815550.0	275739.9
L1M	814036.2	275874.5
L2M	814737.6	276050.0
L3M	813960.9	277135.2
L4M	814950.2	276130.0
L5M	814007.6	276356.1
L6M	814065.2	275389.2

TABLE 3.1: DEFINED SOUNDING LINE ORIGINS IN MT EDEN GEODETIC METRIC CO-ORDINATES

Sounding Line Identification	Gradient	Intercept (c)
L1H	12.40472	2555760.3
L2H	0.664922	636746.67
L3H	0.7131233	622572.3
L4H	2.71617	69393.3
L5H	2.48668	131624.9
L6H	2.102772	236559.7
L7H	2.364255	163580.6
L1M	1.422211	421684.5
L2M	-0.0723447	834708.3
L3M	1.667483	351842.5
L4M	0.359436	715699.1
L5M	3.8670641	-254679.3
L6M	-0.05973665	830516.0

TABLE 3.2: SOUNDING LINE EQUATIONS IN MT EDEN GEODETIC METRIC CO-ORDINATE SYSTEM

$N = mE + c$ where N is the North co-ordinate, and E is the East co-ordinate

Contour (m)	Volume above Contour x 10^6 m^3		Change x $10^6 m^3$	Change/year m^3
	1959	1981		
-1	0.66	0.85	+0.20	+9090
-2	2.06	2.10	+0.04	+1820
-3	4.25	4.27	+0.02	+910
-4	7.6	8.05	+0.45	+20500
-5	12.6	13.7	+1.1	+50000
-6	19.5	21.8	+2.3	+105000
-7	28.8	31.9	+3.1	+141000
-8	40.7	43.2	+2.5	+114000
-10	65.7	68.7	+3.0	+136000

Table 3.3: Mair Bank volume changes (after DHI, 1982).

SECTION	MAXIMUM DEPTH (M)	WIDTH AT C.D. (M)	AREA BELOW C.D. (M)	AREA BELOW M.S.L. (M)	HYDRAULIC RADIUS AT C.D.
1	26.2	791	13410	14608	16.91
2	28.2	945	13382	14843	14.13
3	30.6	930	13344	14794	14.25
4	28.0	1015	13098	14641	12.88
5	24.0	1138	12728	14525	11.16
6	19.6	1233	12990	14984	10.53
7	16.8	1269	12973	15061	10.22
8	14.6	1453	13283	15607	9.14
9	15.6	1616	14295	16876	8.84
10	22.2	1758	14945	17695	8.49

TABLE 3.4: Statistics of the 10 Entrance Gorge Cross-Sections Digitised from the 1981 Navy Bathymetric Survey

Wind Speed ($m.s^{-1}$)	Significant Wave Height (m)			Period of Spectrum Peak(s)		Significant Period(s)
	J	L	SMB	J	L	SMB
10	1.11	1.27	1.15	4.7	5.1	3.8
20	2.22	3.68	2.60	6.0	7.5	5.4
30	3.33	6.83	3.85	6.8	9.4	6.1

Table 4.1: JONSWAP (J), Liu (L) and Sverdrup-Munk-Bretschneider (SMB) wave heights and periods for 10, 20 and 30 $m.s^{-1}$ wind speeds and 47km fetch.

	Mean M_z (mm)	D_{35} (mm)	D_{50} (mm)	D_{65} (mm)
Megaripple Crests	.58	.41	.47	.57
Megaripple Troughs	1.52	.84	1.82	2.76
Site 51	.23	.20	.22	.24
Site 53	.18	.16	.18	.19

Table 4.2: Grain sizes by the Moments method for the finger megaripple. site (Figure 2.8) and at RNZN Sites 51 and 53 (NZ5213, Serials 3a and 4a).

Survey	1	2	3	4	5	6
Onshore	9.2	.6	3.6	74.9	12.3	2.0
Offshore	4.2	11.5	8.4	1.4	8.2	10.0

Table 4.3: Onshore and offshore total wave potentials for the 15-day period prior to surveys 1-6. All figures were divided by 10^5.

Experiment	Description Of Release	Time	Time After Slack Water of First Release	Time of High or Low Tide	Date	Tidal Range (m)	Wind Speed $m.s^{-1}$	Wind Direction (^{o} True)	Experiment Type
1	South of Mair Bank and in Shipping Channel	16:12-17:52	1:37	14:30	20.5.81	1.80	11.0	320	Flood
2	Between Reserve and One Tree Points	09:57-14:00	1:02	08:55	21.5.81	1.73	5.6	330	Ebb
3	Entrance Gorge near Lort Point	10:27 12:13	0:37	09:50	12.6.81	1.53	Calm	-	Flood
4	Mouth of Parua Bay	09:11 10:47	3:34	05:37	15.6.81	1.60	Calm	-	Ebb
5	Entrance Gorge near Lort Point	08:08-10:14	1:46	06:22	16.6.81	1.63	1.7	330	Ebb
6	Between One Tree Point and Beacon S2	08:27-10:14	1:27	07:00	17.6.81	1.72	2.8	270	Ebb
7	Off Munro Point	08:53-10:44	1:08	07:45	18.6.81	1.75	2.8	290	Ebb
8	Off Blacksmith's Creek	10:17-12:49	1:05	09:12	4.7.81	2.41	10.0	280	Ebb
9	Off Marsden Point	14:24-16:06	1:34	12:50	16.7.81	1.73	5.6	260	Flood

TABLE 5.1: DROGUE EXPERIMENTS - STATISTICS

080282 DRGDRM.DAT DROGUES OUT OF HARBOUR INTO BREAM BAY

EAST	NORTH	TIME	DROGUE	EXPT	EAST	NORTH	TIME	DROGUE	EXPT
275150.	815960.	9.4800	2	1	277651.	814771.	10.2007	2	1
278526.	812714.	10.5729	2	1	279970.	811628.	11.4258	2	1
280558.	812164.	12.3702	2	1	279156.	811644.	13.5724	2	1
278828.	809933.	15.1645	2	1	278747.	809080.	16.1548	2	1
278754.	808508.	17.0630	2	1	276400.	815340.	10.3153	3	1
276428.	813846.	11.2454	3	1	276219.	813378.	13.4257	3	1
276879.	814166.	15.4113	3	1	277081.	814310.	15.5141	3	1
277800.	814600.	0.0000	3	1	275800.	816110.	0.0000	3	1
273750.	819500.	18.0000	3	1	275170.	816150.	9.4900	4	1
277667.	815063.	10.3652	4	1	278184.	814034.	10.5338	4	1
278226.	813195.	11.0234	4	1	279965.	811449.	11.4450	4	1
280827.	812044.	12.3544	4	1	279411.	812005.	13.5939	4	1
278575.	810651.	15.2010	4	1	278109.	809896.	16.1144	4	1
277639.	809295.	17.1500	4	1	275395.	816170.	9.4947	5	1
277731.	815169.	10.3722	5	1	278232.	814253.	10.5255	5	1
278234.	813365.	11.0338	5	1	279529.	811559.	11.4108	5	1
280558.	812085.	12.3756	5	1	279168.	811123.	12.4610	5	1
281269.	808908.	14.1949	5	1	282341.	808017.	16.3025	5	1
282439.	807926.	16.4822	5	1	275810.	816170.	9.5020	6	1
276840.	815817.	10.1740	6	1	277830.	815477.	10.4014	6	1
278077.	815344.	10.4903	6	1	278409.	815121.	11.1309	6	1
276998.	814065.	11.2221	6	1	276654.	814207.	13.3830	6	1
277111.	814530.	15.3754	6	1	277318.	815213.	17.4102	6	1
275800.	816090.	0.0000	6	1	275141.	817060.	18.2000	6	1

Table 5.1: Drogue positions and times for the ebb full-tidal cycle experiment on 8-Feb-82.

010382 DRFOLL.DAT RELEASED OFF NHB WHART AT LOW TIDE

EAST	NORTH	TIME	DROGUE	EXPT	EAST	NORTH	TIME	DROGUE	EXPT
275110.	815810.	7.0200	1	1	274677.	815833.	7.4400	1	1
274613.	817649.	8.0700	1	1	273708.	818965.	9.0238	1	1
271958.	819005.	10.4000	1	1	270761.	818556.	11.5100	1	1
269980.	818460.	12.2300	1	1	270947.	818198.	13.5200	1	1
272716.	817702.	14.4600	1	1	274071.	817024.	15.1000	1	1
275326.	816291.	15.3442	1	1	278120.	813441.	16.3000	1	1
278340.	812740.	16.4200	1	1	278764.	811967.	16.5100	1	1
279609.	810509.	17.1700	1	1	275150.	816010.	7.0300	2	1
274346.	816070.	7.4800	2	1	273927.	816134.	8.2129	2	1
273594.	816602.	8.2811	2	1	273074.	816942.	9.2224	2	1
270520.	818910.	11.4700	2	1	270364.	818816.	12.2000	2	1
270506.	818252.	13.4800	2	1	272402.	817801.	14.5100	2	1
273770.	817270.	15.1400	2	1	274794.	816759.	15.3830	2	1
275687.	816007.	15.5856	2	1	277220.	815148.	16.2200	2	1
278305.	812778.	17.0000	2	1	279069.	811364.	17.2400	2	1
275150.	816180.	7.0400	3	1	274187.	816565.	7.5100	3	1
273660.	817360.	7.5500	3	1	272270.	818090.	8.4231	3	1
275150.	816290.	7.0500	4	1	274187.	816555.	7.5100	4	1
272730.	817650.	8.3435	4	1	270827.	818142.	9.3700	4	1
269977.	817957.	10.2600	4	1	269292.	817962.	11.0800	4	1
268237.	817064.	11.3400	4	1	268600.	817670.	12.3000	4	1
269530.	817640.	13.4000	4	1	270760.	817420.	14.3700	4	1
271237.	817740.	14.5900	4	1	272046.	817755.	15.2252	4	1
273421.	817338.	15.4722	4	1	274617.	816725.	16.0706	4	1
274917.	816559.	16.1314	4	1	278320.	814350.	17.4400	4	1
275290.	816380.	7.0500	5	1	274240.	817047.	7.5800	5	1
272795.	817700.	8.3653	5	1	275370.	816520.	7.0700	6	1
274860.	817798.	8.1100	6	1	273757.	818914.	9.0600	6	1
271470.	819150.	10.4400	6	1	269696.	818343.	14.0300	6	1
271642.	818386.	14.5529	6	1	272236.	817899.	15.2139	6	1
273594.	817354.	15.4553	6	1	274278.	817086.	16.0952	6	1
277622.	815682.	17.5400	6	1					

Figure 5.3: Drogue positions and times for the flood full-tidal cycle experiment on 1-Mar-82.

010382 DRFOLL.DAT RELEASED OFF NHB WHARF AT LOW TIME

EAST	NORTH	TIME	DROGUE	EXPT	EAST	NORTH	TIME	DROGUE	EXPT
275110.	815810.	7.0200	1	1	274677.	815833.	7.4400	1	1
274613.	817649.	8.0700	1	1	273708.	818965.	9.0238	1	1
271958.	819005.	10.4000	1	1	270761.	818556.	11.5100	1	1
269980.	818460.	12.2300	1	1	270947.	818198.	13.5200	1	1
272716.	817702.	14.4600	1	1	274071.	817024.	15.1000	1	1
275326.	816291.	15.3442	1	1	278120.	813441.	16.3000	1	1
278340.	812740.	16.4200	1	1	278764.	811967.	16.5100	1	1
279609.	810509.	17.1700	1	1	275150.	816010.	7.0300	2	1
274346.	816070.	7.4800	2	1	273927.	816134.	8.2129	2	1
273594.	816602.	8.2811	2	1	273074.	816942.	9.2224	2	1
270520.	818910.	11.4700	2	1	270364.	818816.	12.2000	2	1
270506.	818252.	13.4800	2	1	272402.	817801.	14.5100	2	1
273770.	817270.	15.1400	2	1	274794.	816759.	15.3830	2	1
275687.	816007.	15.5856	2	1	277220.	815148.	16.2200	2	1
278305.	812778.	17.0000	2	1	279069.	811364.	17.2400	2	1
275150.	816180.	7.0400	3	1	274187.	816565.	7.5100	3	1
273660.	817360.	7.5500	3	1	272270.	818090.	8.4231	3	1
275150.	816290.	7.0500	4	1	274187.	816555.	7.5100	4	1
272730.	817650.	8.3435	4	1	270827.	818142.	9.3700	4	1
269977.	817957.	10.2600	4	1	269292.	817962.	11.0800	4	1
268237.	817064.	11.3400	4	1	268600.	817670.	12.3000	4	1
269530.	817640.	13.4000	4	1	270760.	817420.	14.3700	4	1
271237.	817740.	14.5900	4	1	272046.	817755.	15.2252	4	1
273421.	817338.	15.4722	4	1	274617.	816725.	16.0706	4	1
274917.	816559.	16.1314	4	1	278320.	814350.	17.4400	4	1
275290.	816380.	7.0500	5	1	274240.	817047.	7.5800	5	1
272795.	817700.	8.3653	5	1	275370.	816520.	7.0700	6	1
274860.	817798.	8.1100	6	1	273757.	818914.	9.0600	6	1
271470.	819150.	10.4400	6	1	269696.	818343.	14.0300	6	1
271642.	818386.	14.5529	6	1	272236.	817879.	15.2139	6	1
273594.	817354.	15.4553	6	1	274278.	817086.	16.0952	6	1
277622.	815682.	17.5400	6	1					

Figure 5.3: Drogue positions and times for the flood full-tidal cycle experiment on 1-Mar-82.

LOCATION	EBB ($m.s^{-1}$)		FLOOD ($m.s^{-1}$)	
	1	2	1	2
Shoal Bay	.66	.69	.53	.57
Shipping Channel (Inside)	.44	.91	.54	.77
Main Channel (Outside)	.96	1.02	.65	.79
Behind Calliope Bank	.32	-	.48	-
Marsden Point Distributary Channel	.16	-	.29	-

TABLE 5.4: Mean water speeds from drogue releases. (after Black et. al., 1982)

High Water		Low Water		$\Delta H/\Delta T$ (m/hr)
Time	Amplitude	Time	Amplitude	
0015	2.47	0630	0.36	Flood: 0.31
1245	2.30	1900	0.48	Ebb: 0.29

TABLE 5.5: TIDES OF 24/7/81 MEASURED AT MARSDEN POINT N.H.B. WHARF

FLOOD: The range of tide from 0630 low water to 1245 high water is 1.94

EBB: The range of tide from 1245 high water to 1900 low water is 1.82

Site	Sounding Pole I	Sounding Pole II	120m Shoreward of Sounding Pole II	Marsden Point	Mair Bank
East Bearing	226648	276351	276256	276354	276724
North Bearing	815136	814716	814793	815065	814823

TABLE 5.6: METRIC CO-ORDINATES OF SITES

Time	Time After High Tide (mins)	Count	Velocity ($m.s^{-1}$)	Direction (° True)	Depth of meter (m)	Water Depth (m)	Date
0901	241	7	.04	158	.5	-	14/7/81
1316	-264	87	.22	329	.5	.62	14/7/81
1442	-178	105	.26	335	.5	1.08	14/7/81
1544	-116	54	.15	335	.5	1.48	14/7/81
1546	-114	68	.18	335	.5	1.48	14/7/81
1549	-111	75	.20	335	1.0	1.48	14/7/81
1634	-66	45	.13	335	.5	1.7	14/7/81
1636	-64	46	.13	335	1.0	1.7	14/7/81
0854	149	145	.35	197	.5	1.3	16/7/81
1002	217	29	.09	158	.5	.85	16/7/81
		SOUNDING POST 1 (SP1H)					
0912	252	101	.25	85	.5	1.2	14/7/81
0916	256	99	.25	93	1.0	1.15	14/7/81
1330	-250	28	.09	323	0.5	1.12	14/7/81
1332	-248	33	.10	323	1.0	1.12	14/7/81
1353	-227	27	.09	305	0.5	1.12	14/7/81
1505	-155	63	.17	295	1.0	1.7	14/7/81
1508	-152	49	.14	295	0.5	1.7	14/7/81
1600	-100	62	.17	307	1.0	1.98	14/7/81
1602	-98	55	.15	307	0.5	1.98	14/7/81
0908	163	127	.31	113	0.5	1.55	16/7/81
0910	165	128	.31	108	1.0	1.55	16/7/81
1029	244	98	.25	105	0.5	1.10	16/7/81
		SOUNDING POST 2 (SP2H)					
0936	276	110	.27	86	1.0	2.06	14/7/81
1340	-240	49	.14	285	1.0	2.16	14/7/81
1343	-237	44	.13	285	0.5	2.16	14/7/81
0914	169	130	.32	85	1.0	2.52	16/7/81
0916	171	107	.27	86	0.5	2.52	16/7/81
1037	252	138	.34	86	0.5	2.00	16/7/81
1039	254	148	.36	86	1.0	2.0	16/7/81
		SOUNDING POST 3 (SP3H)					
0951	291	122	.30	58	0.5	.61	14/7/81
1409	-211	155	.38	302	0.5	.98	14/7/81
1516	-144	168	.40	314	0.5	1.4	14/7/81
1518	-142	196	.47	314	1.0	1.4	14/7/81
1612	-88	137	.33	314	0.5	1.68	14/7/81
1614	-86	187	.45	314	1.0	1.68	14/7/81
0924	179	114	.28	63	0.5	1.32	16/7/81
1050	265	82	.21	58	0.2	0.8	16/7/81
1052	267	87	.22	58	0.2	0.8	16/7/81
		SOUNDING POST 4 (SP4H)					
1001	301	41	.12	215	0.5	0.9	14/7/81
1425	-195	92	.23	341	0.5	1.08	14/7/81
1526	-134	122	.30	310	1.0	1.45	14/7/81
1528	-132	93	0.24	310	0.5	1.45	14/7/81
1624	-76	100	0.25	329	1.0	1.72	14/7/81
1626	-74	101	0.25	329	0.5	1.72	14/7/81
0931	186	58	.16	102	0.5	1.03	16/7/81
1111	286	34	.10	36	0.2	0.45	16/7/81
		SOUNDING POST 5 (SP5H)					
1321	-259	243	.57	317	Surface	-	14/7/81
1459	-161	185	.44	317	Surface	-	14/7/81
1555	-105	111	.28	317	Surface	-	14/7/81
0855	150	174	.42	120	Surface	-	16/7/81
1019	234	238	.56	158	Surface	-	16/7/81
1021	236	241	.57	137	Surface	-	16/7/81
		BEACON S1					
1436	-184	62	.17	319	.5	2.75	14/7/81
1438	-182	66	.18	319	1.0	2.75	14/7/81
1537	-123	36	.11	158	1 metre below Surface	-	14/7/81
0846	141	117	.29	113	1.0	2.08	16/7/81
0848	143	69	.18	113	0.5	2.08	16/7/81
0953	208	32	.10	138	1.0	1.48	16/7/81
0955	210	27	.09	138	0.5	1.57	16/7/81
		SHELL CUT REACH LEADING LIGHT					
1450	-170	85	.22	306	0.5	2.13	14/7/81
1452	-168	90	.23	316	1.0	2.13	14/7/81
1010	225	31	.10	141	0.5	1.7	16/7/81
1012	227	33	0.10	141	1.0	1.65	16/7/81
		POINT SINCLAIR FRONT LEAD					
0939	194	108	0.27	110	0.5	1.4	16/7/81
0941	196	116	0.29	110	1.0	1.4	16/7/81
1100	275	43	0.12	234	0.2	0.9	16/7/81
		SOUNDING POST 6 (SP6H)					

TABLE 5.7: Velocity measurements around Snake Bank made with an Ott Impellor Meter.

Location	SP1H	SP2H	SP3H	SP4H	SP5H	Sinclair Front Lead	S1	Shell Cut
Angle ^{o}True	158	101	86	311	323	317	Neutral	Neutral

TABLE 5.8: Directions of flow at peak speed during the tidal cycle at sites around Snake Bank and at the Point Sinclair Front Lead.

Site	Date	Coordinates (Metrics)	Location	Bed Type	Depth Below CD (m)	Tidal Range (m)		Temperature °C		Salinity (‰)	
						Ebb	Flood	High	Low	High	Low
A	4/12/79	815892N 274790E	450 WNW of NHB Wharf	Old Shell	8.0	2.24	2.14	-	-	-	-
B	5/12/79	816082N 274110E	1200m WNW of NHB Wharf	Possibly Sand	4.8	2.22	2.15	-	-	-	-
	30/9 /80	815730N 275360E	140m East of NHB Wharf	Old Shell	8.7	2.29	2.39	-	-	-	-
	29/9 /80	815670N 275660E	440m East of NHB Wharf	Shell and Sand	9.7	2.53	2.59	-	-	-	-
E	14/10/80	815992N 274460E	800m WNW of NHB Wharf	Megaripples	6.8	1.70	1.83	-	-	-	-
F	10/2 /81	816222N 275035E	Near No. 19 Buoy	Megaripples	7.5	2.36	2.34	-	-	-	-
I	12/2 /81	815822N 275610E	400m ENE of NHB Wharf	Flat Sandy	11.2	2.15	2.01	-	-	-	-
	19/1 /81	816532N 274892	800m NNW of NHB Wharf	Megaripples	7.5	2.08	1.99	-	-	-	-
M	13/2 /81	815712N 275840E	Off Western NZRC Dolphin	Megaripples	14.8 -18.5	1.97	1.84	-	-	-	-
	11/2 /81	815013N 276920E	Northern Mair Bank	Shell	1.1	2.26	2.20	-	-	-	-
S	30/6 /81	816955N 273815E	Channel Near SCRFL	Old Shell (Some Sand)	10.2	2.28	2.33	14.1	13.0	34.2	32.0
S	30/6 /81	817609N 273213E	Near S1	-	10.0	2.28	2.33	14.5	13.0	33.7	31.6
	30/6 /81	817987N 272297E	Near S2	Probably Megaripples	6.9	2.28	2.33	14.5	13.0	33.7	31.3
T	30/6 /81	819888N 272458E	South of Reserve Pt	Old Shell	12.1	2.28	2.33	14.2	12.8	33.3	31.4
	2/7 /81	814703N 276271E	Channel off Marsden Pt	Old Shell (Some Sand)	1.6	2.40	2.60	14.5	14.0	34.2	33.0
	2/7 /81	815275N 277664E	Channel Nth Mair Bank	Old Shell	16.0	2.40	2.60	15.0	14.0	33.9	33.3
U	2/7 /81	814233N 278256E	Urquharts Bay Mouth	Shell (Some Sand)	20.0	2.40	2.60	14.9	14.0	33.6	33.5
V	2/7 /81	814365N 277340E	South of Mair Bank	Shell	2.3	2.40	2.60	14.4	14.4	33.8	33.7
	20/7 /81	815756N 276030E	Off NZRC Wharf	Shell	26.0	1.97	2.07	12.5	11.8	34.4	33.4
A1 (1)	29/10/81	815870N	Port Site	Rippled	5.5	1.93	2.02	13.3	14.4	34.2	34.0
A1 (2)	16/12/81	274723E	(South)	Sand	-8.0		2.49		18.1		33.8
A2 (1)	29/10/81	816058N	Port Site	Possibly	7.5	1.93	2.02	13.1	14.2	34.2	34.0
A2 (2)	16/12/81	274770E		Shell			2.49		18.3		33.6
A3 (1)	29/10/81	816168N	Port Site	Old Shell	9.8	1.93	2.02	13.2	14.0	34.2	34.1
A3 (2)	16/12/81	274772E					2.49		18.3		33.7
A4 (1)	29/10/81	816391N	Port Site	-		1.93	2.02	13.2	14.0	34.2	33.9
A4 (2)	16/10/81	274770E	(North)				2.49		18.2		33.8
B1 (1)	12/11/81	815601N	Entrance	Rippled	2.9	2.36	2.42	14.8	15.7	34.0	34.0
B1 (2)	14/11/81	275543E	Gorge (Sth)	Sand	-5.6	2.60	2.50	14.9	16.2	34.0	33.6
B2 (1)	12/11/81	815836N	Entrance	Sand Waves	10.5-	2.36	2.42	14.6	15.5	34.2	33.9
B2 (2)	14/11/81	275635E	Gorge		15.2	2.60	2.50	14.8	15.8	34.1	33.8
B3 (1)	12/11/81	815981N	Entrance	Old Shell	20.2-	2.36	2.42	14.5	15.4	34.1	34.0
B3 (2)	14/11/81	275840E	Gorge		31.8	2.60	2.50	14.7	16.1	34.1	33.8
B4 (1)	12/11/81	816355N	Entrance	-	3.1-	2.36	2.42	14.8	15.6	34.1	33.8
B4 (2)	14/11/81	275798E	Gorge (Nth)		8.5	2.60	2.50	14.9	15.8	34.1	33.8
C1 (1)	13/11/81	817527N	Shipping	Megaripples	3.9-	2.06	2.22	14.6	15.4	33.9	32.7
C1 (2)	14/12/81	272689E	Channel (Sth)		6.4	2.51	2.77	16.3	18.7	34.3	33.4
C2 (1)	18/11/81	817696N	Shipping	Sand Waves	11.7-	2.06	2.22	14.2	15.4	34.0	33.0
C2 (2)	14/12/81	272806E	Channel	Old Shell	15.2	2.51	2.77	16.0	18.5	34.3	33.2
C3 (1)	13/11/81	817818N	Shipping	Old Shell	9.4-	2.06	2.22	14.4	15.2	34.0	33.3
C3 (2)	14/12/81	272876E	Channel		12.6	2.51	2.77	16.0	18.1	34.3	33.2
C4 (1)	13/11/81	817894N	Shipping	-	4.4-	2.06	2.22	14.4	15.8	34.0	32.3
C4 (2)	14/12/81	272974E	Channel (Nth)		6.7	2.51	2.77	16.4	18.0	34.4	33.3
C5	12/12/81	819742N 273980E	Shoal Bay (North)	-	2.0-2.4	2.49	2.40	15.6	18.2	34.0	32.8
C2	12/12/81	819573N 273767E	Shoal Bay	Shell and Algae	3.7	2.49	2.40	15.6	18.4	34.0	32.8
C3	12/12/81	819408N 273542E	Shoal Bay	Shell and Algae	3.8	2.49	2.40	15.6	17.8	34.1	32.7
C4	12/12/81	819228N 273429E	Shoal Bay (South)	Sand Waves	3.0	2.49	2.40	15.6	17.6	34.2	33.2
S1	18/1 /82	816300N 275039E	Near 19 Buoy	Megaripples	7.8	1.65	1.57	20.3	20.8	34.6	34.5
S2	20/1 /82	816339N 274915E	Near 19 Buoy & S3	Megaripples	6.5	1.48	1.27	20.3	20.9	34.6	34.6
S3	9/2 /82	816316N 274928E	Near 19 Buoy & S2	Megaripples	7.1	2.36	2.22	19.6	20.6	34.4	34.5
S4	2/3 /82	816873N 274457E	Snake Bank Extn. SE	Megaripples	1.9	2.14	2.05	19.5	21.3	34.2	32.4
S5	29/3 /82	817988N 274534E	Shoal Bay	Megaripples	6.9	2.41	2.34	19.0	19.2	34.6	33.7

TABLE 5.9: Information for the Braystoke velocity profile measurement sites including temperature and salinity at high and low tide.

Site	Date	Coordinates (Metrics)	Location	Bed Type	Depth Below CD (m)	Tidal Range (m)		Temperature °C		Salinity (‰)	
						Ebb	Flood	High	Low	High	Low
A	4/12/79	815892N 274790E	450 WNW of NHB Wharf	Old Shell	8.0	2.24	2.14	-	-	-	-
B	5/12/79	816082N 274110E	1200m WNW of NHB Wharf	Possibly Sand	4.8	2.22	2.15	-	-	-	-
C	30/9 /80	815730N 275360E	140m East of NHB Wharf	Old Shell	8.7	2.29	2.39	-	-	-	-
D	29/9 /80	815670N 275660E	440m East of NHB Wharf	Shell and Sand	9.7	2.53	2.59	-	-	-	-
E	14/10/80	815992N 274460E	800m WNW of NHB Wharf	Megaripples	6.8	1.70	1.83	-	-	-	-
F	10/2 /81	816222N 275035E	Near No. 19 Buoy	Megaripples	7.5	2.36	2.34	-	-	-	-
I	12/2 /81	815822N 275610E	400m ENE of NHB Wharf	Flat Sandy	11.2	2.15	2.01	-	-	-	-
K	19/1 /81	816532N 274892	800m NNW of NHB Wharf	Megaripples	7.5	2.08	1.99	-	-	-	-
M	13/2 /81	815712N 275840E	Off Western NZRC Dolphin	Megaripples	14.8 -18.5	1.97	1.84	-	-	-	-
N	11/2 /81	815013N 276920E	Northern Mair Bank	Shell	1.1	2.26	2.20	-	-	-	-
1	30/6 /81	816955N 273815E	Channel Near SCRFL	Old Shell (Some Sand)	10.2	2.28	2.33	14.1	13.0	34.2	32.0
2	30/6 /81	817609N 273213E	Near S1	-	10.0	2.28	2.33	14.5	13.0	33.7	31.6
3	30/6 /81	817987N 272297E	Near S2	Probably Megaripples	6.9	2.28	2.33	14.5	13.0	33.7	31.3
4	30/6 /81	819888N 272458E	South of Reserve Pt	Old Shell	12.1	2.28	2.33	14.2	12.8	33.3	31.4
5	2/7 /81	814703N 276271E	Channel off Marsden Pt	Old Shell (Some Sand)	1.6	2.40	2.60	14.5	14.0	34.2	33.0
6	2/7 /81	815275N 277664E	Channel Nth Mair Bank	Old Shell	16.0	2.40	2.60	15.0	14.0	33.9	33.3
7	2/7 /81	814233N 278256E	Urquharts Bay Mouth	Shell (Some Sand)	20.0	2.40	2.60	14.9	14.0	33.6	33.5
8	2/7 /81	814365N 277340E	South of Mair Bank	Shell	2.3	2.40	2.60	14.4	14.4	33.8	33.7
9	20/7 /81	815756N 276030E	Off NZRC Wharf	Shell	26.0	1.97	2.07	12.5	11.8	34.4	33.4
A1(1)	29/10/81	815870N	Port Site	Rippled	5.5	1.93	2.02	13.3	14.4	34.2	34.0
A1(2)	16/12/81	274723E	(South)	Sand	-8.0		2.49		18.1		33.8
A2(1)	29/10/81	816058N	Port Site	Possibly	7.5	1.93	2.02	13.1	14.2	34.2	34.0
A2(2)	16/12/81	274770E		Shell			2.49		18.3		33.6
A3(1)	29/10/81	816168N	Port Site	Old Shell	9.8	1.93	2.02	13.2	14.0	34.2	34.1
A3(2)	16/12/81	274772E					2.49		18.3		33.7
A4(1)	29/10/81	816391N	Port Site	-		1.93	2.02	13.2	14.0	34.2	33.9
A4(2)	16/10/81	274770E	(North)				2.49		18.2		33.8
B1(1)	12/11/81	815601N	Entrance	Rippled	2.9	2.36	2.42	14.8	15.7	34.0	34.0
B1(2)	14/11/81	275543E	Gorge (Sth)	Sand	-5.6	2.60	2.50	14.9	16.2	34.0	33.6
B2(1)	12/11/81	815836N	Entrance	Sand Waves	10.5-	2.36	2.42	14.6	15.5	34.2	33.9
B2(2)	14/11/81	275635E	Gorge		15.2	2.60	2.50	14.8	15.8	34.1	33.8
B3(1)	12/11/81	815981N	Entrance	Old Shell	20.2-	2.36	2.42	14.5	15.4	34.1	34.0
B3(2)	14/11/81	275840E	Gorge		31.8	2.60	2.50	14.7	16.1	34.1	33.8
B4(1)	12/11/81	816355N	Entrance	-	3.1-	2.36	2.42	14.8	15.6	34.1	33.8
B4(2)	14/11/81	275798E	Gorge (Nth)		8.5	2.60	2.50	14.9	15.8	34.1	33.8
C1(1)	18/11/81	817527N	Shipping	Megaripples	3.9-	2.06	2.22	14.6	15.4	33.9	32.7
C1(2)	14/12/81	272689E	Channel (Sth)		6.4	2.51	2.77	16.3	18.7	34.3	33.4
C2(1)	18/11/81	817696N	Shipping	Sand Waves	11.7-	2.06	2.22	14.2	15.4	34.0	33.0
C2(2)	14/12/81	272806E	Channel	Old Shell	15.2	2.51	2.77	16.0	18.5	34.3	33.2
C3(1)	18/11/81	817818N	Shipping	Old Shell	9.4-	2.06	2.22	14.4	15.2	34.0	33.3
C3(2)	14/12/81	272876E	Channel		12.6	2.51	2.77	16.0	18.1	34.3	33.2
C4(1)	18/11/81	817894N	Shipping	-	4.4-	2.06	2.22	14.4	15.8	34.0	32.3
C4(2)	14/12/81	272974E	Channel (Nth)		6.7	2.51	2.77	16.4	18.0	34.4	33.3
D1	12/12/81	819742N 273980E	Shoal Bay (North)	-	2.0-2.4	2.49	2.40	15.6	18.2	34.0	32.8
D2	12/12/81	819573N 273767E	Shoal Bay	Shell and Algae	3.7	2.49	2.40	15.6	18.4	34.0	32.8
D3	12/12/81	819408N 273542E	Shoal Bay	Shell and Algae	8.8	2.49	2.40	15.6	17.8	34.1	32.7
D4	12/12/81	819228N 273429E	Shoal Bay (South)	Sand Waves	8.0	2.49	2.40	15.6	17.6	34.2	33.2
S1	18/1 /82	816300N 275039E	Near 19 Buoy	Megaripples	7.8	1.65	1.57	20.3	20.8	34.6	34.5
S2	20/1 /82	816339N 274915E	Near 19 Buoy & S3	Megaripples	6.5	1.48	1.27	20.3	20.9	34.6	34.6
S3	9/2 /82	816316N 274928E	Near 19 Buoy & S2	Megaripples	7.1	2.36	2.22	19.6	20.6	34.4	34.5
S4	2/3 /82	816873N 274457E	Snake Bank Extn. SE	Megaripples	1.9	2.14	2.05	19.5	21.3	34.2	32.4
S5	29/3 /82	817988N 274534E	Shoal Bay	Megaripples	6.9	2.41	2.34	19.0	19.2	34.6	33.7

TABLE 5.9: Information for the Braystoke velocity profile measurement sites including temperature and salinity at high and low tide.

	EBB				FLOOD			
	Mean ($m.s^{-1}$)	Maximum ($m.s^{-1}$)	Minimum ($m.s^{-1}$)	Coefficient of Variation	Mean ($m.s^{-1}$)	Maximum ($m.s^{-1}$)	Minimum ($m.s^{-1}$)	Coefficient of Variation
Blacksmith	0.82	1.17	0.50	21%	0.62	0.83	0.40	16%
NHB	0.86	1.21	0.56	18%	0.51	0.66	0.38	12%
OTP	0.79	1.17	0.48	22%	0.75	1.07	0.50	17%
Shoal	0.62	0.99	0.46	19%	0.61	0.91	0.45	15%

TABLE 5.10: Statistics of the maximum velocities recorded during half tidal cycles on the Aanderaa current meters.

	EBB			FLOOD			
	a	b	r_{12}	a	b	r_{12}	Equation Type
Blacksmith N = 78	0.0	41.68	-	0.0	31.56	-	y=bx
	4.77	39.26	.96	21.16	20.82	.91	y=bx+a
	43.39	0.94	.96	39.16	.69	.91	$y=ax^b$
	31.50	0.48	.95	31.53	.34	.90	$y=ae^{bx}$
N.H.B. N = 102	0.0	44.94	-	0.0	26.82	-	y=bx
	15.01	37.11	.92	27.54	12.44	.80	y=bx+a
	49.79	.84	.91	37.67	.48	.81	$y=ax^b$
	37.43	.43	.90	32.16	.24	.80	$y=ae^{bx}$
O.T.P. N = 102	0.0	41.41	-	0.0	39.36	-	y=bx
	-3.35	43.15	.97	15.47	31.28	.95	y=bx+a
	39.66	1.06	.97	45.08	.79	.94	$y=ax^b$
	27.74	.54	.96	34.41	.40	.94	$y=ae^{bx}$
Shoal N = 65	0.0	34.04	-	0.0	33.34	-	y=bx
	5.57	31.01	.91	18.85	22.98	.90	y=bx+a
	36.15	.90	.91	40.51	.68	.89	$y=ax^b$
	26.29	.46	.91	31.53	.35	.90	$y=ae^{bx}$

TABLE 5.11: Best fit curves (linear, power and exponential) of maximum water speed ($m.s^{-1}$ x 100) attained on the Aanderaa current meters in a half tidal cycle versus the half tidal range (m). N is number of points involved in the fitting. r_{12} is the correlation coefficient.

	EBB					FLOOD					
Site	$\bar{U}_1$	U_1 Max Unscaled	U_1 Max ΔH=2.2	$\bar{U}$ Max Unscaled	$\bar{U}$ Max ΔH=2.2	$\bar{U}_1$	U_1 Max Unscaled	U_1 Max ΔH=2.2	$\bar{U}$ Max Unscaled	$\bar{U}$ Max ΔH=2.2	V_2
A	.40	.67	.66	.74	.73	.32	.46	.47	.49	.48	-.17
B	.36	.51	.51	.57	.57	.30	.41	.42	.48	.48	-.10
C	.45	.77	.74	.90	.86	.25	.38	.33	.39	.36	-.38
D	.44	.69	.60	.85	.74	.22	.36	.33	.45	.38	-.29
E	.25	.39	.54	.50	.65	.24	.33	.44	.43	.52	-.10
F	.55	.79	.74	1.14	1.06	.41	.61	.57	.84	.79	-.13
I	.40	.69	.71	.94	.96	.33	.51	.56	.60	.66	-.12
K	.33	.54	.57	.66	.70	.57	.90	1.00	1.00	1.11	.27
M	.34	.61	.68	.83	.93	.23	.41	.49	.41	.49	-.16
N	.41	.50	.49	.51	.50	.31	.41	.41	.44	.44	-.09
1	.60	.70	.66	.97	.94	.46	.61	.58	.86	.81	-.06
2	.59	.82	.79	.98	.95	.46	.71	.67	.94	.89	-.08
3	.49	.59	.57	.76	.73	.51	.76	.72	.89	.84	.12
4	.22	.39	.38	-	-	.30	.37	.35	-	-	-.04
5	.40	.55	.50	.52	.48	.59	.87	.74	.92	.78	.19
6	.32	.79	.72	-	-	.63	.79	.67	-	-	-.04
7	.52	.70	.64	-	-	.36	.47	.40	-	-	-.23
8	.22	.36	.33	.36	.33	.57	.70	.59	.68	.62	.28
9	.37	.63	.70	.76	.85	.42	.62	.66	.85	.90	-.31
A1(1)	.34	.56	.64	.66	.75	.25	.29	.34	.42	.46	-.31
A2(1)	.37	.50	.57	.68	.77	.41	.56	.65	.56	.61	.07
A3(1)	.58	.69	.79	.81	.92	.36	.51	.56	.63	.69	-.17
A4(1)	.49	.99	1.13	.83	.95	.52	.69	.75	.76	.83	-.20
B1(1)	.31	.51	.48	.49	.46	.21	.27	.25	.34	.31	-.32
B1(2)	.32	.36	.31	.41	.35	.21	.27	.32	.27	.24	.02
B2(1)	.68	.76	.71	.97	.90	.41	.56	.51	.58	.53	-.16
B2(2)	.62	.86	.73	1.15	.97	.43	.59	.52	.55	.48	-.17
B3(1)	-	-	-	1.19	1.11	-	-	-	1.21	1.10	-
B3(1)	-	-	-	1.03	.87	-	-	-	-	.84	-
B4(1)	-	-	-	.69	.64	.44	.69	.63	.66	.60	-
B4(2)	.27	.52	.44	.54	.46	.38	.59	.52	.62	.55	.08
C1(1)	.50	.59	.63	.68	.73	.36	.44	.44	.44	.44	-.18
C1(2)	.56	.68	.60	.81	.71	.41	.55	.44	.55	.44	-.15
C2(1)	-	0.74	.79	.81	.86	.51	.61	.61	.77	.76	-.13
C2(2)	.73	.83	.73	1.05	.92	.56	.74	.59	.83	.66	-.11
C3(1)	-	.56	.60	.81	.86	.67	.70	.69	.80	.79	.07
C3(2)	.59	.72	.63	.97	.85	.58	.70	.62	.92	.73	-.01
C4(1)	.47	.66	.71	.73	.78	.38	.51	.51	.55	.55	-.16
C4(2)	.64	.72	.63	.87	.76	.43	.53	.43	.60	.48	-.19
D1	.34	.41	.36	.46	.41	.31	.35	.32	.31	.28	-.06
D2	.36	.49	.43	.59	.52	.27	.33	.30	.33	.30	-.18
D3	.37	.61	.54	.81	.72	.41	.47	.42	.58	.53	-.13
D4	.31	.43	.38	.71	.63	.49	.61	.56	.67	.61	.19
S1	.47	.60	.80	.69	.92	.44	.73	1.02	.71	1.00	.12
S2	.48	.63	.94	.63	.93	.37	.53	.92	.57	.99	-.01
S3	.57	.83	.79	.99	.92	.51	.63	.62	.87	.86	-.12
S4	.55	.78	.80	.76	.78	.50	.67	.73	.74	.79	-.05
S5	.51	.71	.65	.79	.72	.41	.58	.54	.71	.67	-.09

TABLE 5.12 : Velocity Statistics at the Braystoke Sites. Velocities are in ms^{-1}. V_2 is the Velocity Asymmetry Index.

Site	ΔH=1.6, q=1								ΔH=2.2, q=1							
	Ebb		Flood		Residual		Time (Secs) Above Threshold		Ebb		Flood		Residual		Time (secs) Above Theshold	
	U_1	Dirn	U_1	Dirn	U_r	Dirn	Ebb	Flood	U_1	Dirn	U_1	Dirn	U_1	Dirn	Ebb	Flood
A	.41	119	.34	289	.28	121	127	26	.49	116	.41	290	.05	146	227	230
B	.36	122	.00	-	.36	122	61	0	.43	118	.38	304	.02	57	199	215
C	.42	103	.00	-	.42	103	166	0	.54	106	.34	318	.46	104	213	23
D	.40	94	.00	-	.40	94	142	0	.49	96	.34	295	.42	95	214	21
E	.36	122	.34	300	.30	123	136	12	.47	122	.37	299	.04	136	189	194
F	.46	113	.36	292	.11	115	236	179	.61	113	.47	293	.08	111	268	258
I	.41	114	.36	283	.09	132	201	149	.52	115	.46	284	.06	164	257	255
K	.37	128	.55	305	.27	304	118	275	.46	129	.72	305	.24	301	210	302
M	.43	104	.34	254	.27	112	157	44	.52	103	.39	269	.20	113	249	133
N	-	-	-	-	-	-	-	-								
1	.43	139	.40	306	.11	155	248	159	.56	138	.49	309	.09	161	286	243
2	.48	129	.41	318	.13	119	210	141	.61	129	.50	318	.09	107	261	239
3	.39	109	.45	297	.07	320	168	198	.50	110	.55	298	.08	323	235	279
4	.00	-	.00	-	.00	-	0	0	.37	111	.34	310	.11	88	87	54
5	.37	195	.44	31	.28	35	64	259	.44	200	.53	36	.21	48	161	315
6	.48	133	.44	316	.04	331	195	250	.63	134	.57	317	.06	330	225	304
7	.41	185	.00	-	.41	185	199	0	.54	186	.37	16	.32	183	232	77
8	.00	-	.40	50	.40	50	0	248	.00	-	.52	53	.52	53	0	314
9	.49	94	.42	286	.11	73	223	169	.63	94	.53	290	.12	59	260	228
A1(1)	.42	99	.00	-	.42	99	197	0	.57	99	.00	-	.57	99	245	0
A2(1)	.39	107	.41	298	.04	8	173	172	.49	108	.54	300	.06	50	248	205
A3(1)	.52	123	.35	295	.09	138	219	212	.66	122	.46	296	.08	142	257	288
A4(1)	.61	108	.46	291	.05	96	232	253	.66	108	.60	291	.03	327	243	290
B1(1)	.35	107	.00	-	.35	107	73	0	.44	104	.00	-	.44	104	157	0
B1(2)	.00	-	.00	-	.00	-	0	0	.00	-	.00	-	.00	-	0	0
B2(1)	.47	118	.35	268	.30	125	243	68	.61	118	.42	273	.17	148	281	251
B2(2)	.45	110	.41	266	.16	132	172	101	.56	110	.49	270	.15	138	231	169
B4(1)	.33	152	.36	257	.29	246	27	131	.42	150	.45	262	.26	228	134	213
B4(2)	.00	-	.36	297	.36	297	0	69	.40	153	.42	286	.17	237	130	165
C1(1)	.43	117	.00	-	.43	117	182	0	.55	116	.40	307	.15	104	233	176
C1(2)	.40	126	.00	-	.40	126	193	0	.51	125	.38	300	.14	131	258	185
C2(1)	.48	125	.38	305	.07	126	233	209	.61	125	.49	304	.06	128	279	276
C2(2)	.47	128	.38	297	.06	169	237	246	.61	128	.49	297	.06	178	280	302
C3(1)	.41	130	.46	312	.10	315	174	246	.51	135	.59	312	.11	308	230	292
C3(2)	.40	128	.40	309	.00	-	205	207	.51	128	.50	309	.03	319	265	300
C4(1)	.45	128	.36	318	.15	119	204	118	.56	128	.44	318	.10	108	265	233
C4(2)	.40	141	.00	-	.40	141	216	0	.52	140	.40	320	.09	139	270	237
D1	.00	-	.00	-	.00	-	0	0	.36	118	.00	-	.36	118	104	0
D2	.00	-	.00	-	.00	-	0	0	.38	124	.33	318	.27	122	129	23
D3	.37	121	.40	305	.03	336	53	55	.42	125	.44	306	.05	312	165	200
D4	.00	-	.44	297	.44	297	0	100	.37	125	.49	297	.17	290	134	227
S1	.48	111	.51	301	.02	336	217	253	.61	112	.66	301	.07	338	264	294
S2	.55	112	.51	291	.03	12	221	246	.68	112	.67	298	.04	47	282	277
S3	.44	105	.41	288	.02	72	223	220	.58	104	.53	289	.03	52	255	263
S4	.44	107	.44	294	.03	349	226	243	.56	106	.56	293	.04	359	283	295
S5	.41	?	.36	?	.17	?	166	81	.52	?	.43	?	-	-	234	242

TABLE 5.13: Residual Vectors at 1m above the bottom
Speeds are in ms^{-1} and direction is ^{o}True

Site	ΔH=2.2, q=3								ΔH=1.6, q=3											
	Ebb		Flood		Residual		Time (Secs) Above Threshold		Ebb		Flood		Residual		Time (Secs) Above Threshold		Spring		Neap	
	U_1	Dirn	U_1	Dirn	U_1	Dirn	Ebb	Flood	U_1	Dirn	U_1	Dirn	U_1	Dirn	Ebb	Flood	ϕ_{pot}	Dirn	ϕ_{pot}	Dirn
A	.51	118	.41	290	.31	126	227	230	.41	119	.34	289	.37	120	127	26	1.21	119	0.065	119
B	.44	119	.38	304	.23	107	199	215	.36	122	.00	-	.36	122	61	0	0.24	118	0.002	122
C	.57	103	.35	318	.54	102	213	23	.44	101	.00	-	.44	101	166	0	2.94	103	0.221	101
D	.51	95	.34	295	.49	95	214	21	.40	94	.00	-	.40	94	142	0	1.25	95	0.049	94
E	.48	122	.38	298	.30	126	189	194	.36	123	.34	300	.34	123	136	12	0.61	122	0.003	123
F	.64	113	.48	293	.42	113	266	258	.48	113	.37	292	.34	114	236	179	7.05	113	0.785	113
I	.55	117	.47	284	.33	134	257	255	.42	116	.36	284	.29	126	201	149	2.06	121	0.143	116
K	.47	129	.75	304	.60	303	210	332	.38	128	.58	304	.49	303	118	275	24.02	304	4.282	304
M	.54	103	.41	265	.43	109	249	133	.44	104	.35	254	.39	109	157	44	2.24	104	0.209	104
N																	-	-	-	-
1	.59	138	.51	307	.37	150	286	242	.44	138	.40	306	.31	149	248	159	3.65	142	0.277	140
2	.64	129	.52	317	.41	122	261	239	.49	129	.42	317	.35	124	210	141	6.16	127	0.759	128
3	.51	109	.58	298	.35	310	235	279	.40	110	.46	298	.29	308	168	198	3.01	302	0.378	299
4	.37	111	.34	310	.26	94	87	54	.00	-	.00	-	.00	-	0	0	0.01	111	0.000	-
5	.44	199	.60	30	.48	33	161	315	.37	195	.46	28	.41	30	64	259	5.99	30	0.565	28
6	.65	133	.59	316	.19	29	225	304	.49	133	.45	316	.14	54	195	250	2.06	125	0.368	129
7	.57	187	.37	16	.50	186	232	77	.43	186	.00	-	.43	186	199	0	3.20	187	0.199	186
8	.00	-	.53	51	.53	51	0	317	.00	-	.41	50	.41	50	0	248	2.54	51	0.127	50
9	.66	94	.55	287	.43	80	260	228	.50	94	.43	285	.34	83	223	169	7.00	90	0.930	92
A1(1)	.59	99	.00	-	.59	99	245	0	.45	99	.00	-	.45	99	197	0	4.31	99	0.340	99
A2(1)	.51	107	.56	298	.26	354	248	205	.40	106	.43	297	.21	333	173	172	1.11	312	0.114	303
A3(1)	.70	123	.48	295	.47	128	257	288	.53	123	.36	294	.38	127	219	212	12.06	124	1.746	123
A4(1)	.77	107	.62	291	.42	101	243	290	.63	107	.47	290	.33	101	155	248	13.65	105	3.506	106
B1(1)	.44	104	.00	-	.44	104	157	0	.35	107	.00	-	.35	107	73	0	0.21	104	0.001	107
B1(2)	.00	-	.00	-	.00	-	0	0	.00	-	.00	-	.00	-	0	0	0.00	-	0.000	-
B2(1)	.63	118	.43	272	.47	127	281	251	.48	118	.35	268	.43	122	243	68	7.31	119	0.820	118
B2(2)	.59	109	.51	268	.41	126	231	169	.46	109	.41	266	.34	124	172	101	3.16	115	0.331	113
B4(1)	.42	150	.48	259	.40	234	134	213	.33	152	.37	255	.35	247	27	131	0.69	251	0.008	255
B4(2)	.41	153	.44	289	.32	250	130	165	.00	-	.36	297	.36	297	0	69	0.18	274	0.002	297
C1(1)	.57	117	.40	306	.42	114	233	176	.43	117	.00	-	.43	117	182	0	3.16	117	0.182	117
C1(2)	.52	126	.39	300	.38	128	258	185	.40	126	.00	-	.40	126	193	0	1.73	126	0.066	126
C2(1)	.65	126	.51	305	.42	126	279	276	.50	126	.39	306	.33	126	233	209	7.53	126	1.100	126
C2(2)	.63	128	.50	297	.39	141	280	302	.48	129	.38	297	.30	140	237	246	6.11	131	0.770	129
C3(1)	.53	132	.61	312	.40	312	230	292	.41	129	.47	311	.31	314	174	246	4.57	312	0.586	311
C3(2)	.52	128	.51	309	.16	324	265	300	.40	128	.40	309	.09	99	205	207	0.07	104	0.001	9
C4(1)	.59	128	.45	318	.40	122	265	233	.45	128	.36	318	.35	124	204	118	4.26	127	0.349	128
C4(2)	.54	140	.40	321	.37	140	270	237	.41	141	.00	-	.41	141	216	0	2.42	140	0.111	141
D1	.36	118	.00	-	.36	118	104	0	.00	-	.00	-	.00	-	0	0	0.003	118	0.00	-
D2	.39	123	.33	318	.35	122	129	23	.00	-	.00	-	.00	-	0	0	0.03	123	0.00	-
D3	.43	123	.45	306	.24	312	165	200	.38	120	.41	305	.21	319	53	55	0.18	309	0.022	307
D4	.38	126	.52	297	.41	294	134	227	.00	-	.46	298	.46	298	0	100	1.54	297	0.220	298
S1	.64	111	.70	301	.39	322	264	294	.49	111	.53	301	.30	321	217	253	7.28	312	1.159	309
S2	.73	113	.70	299	.33	82	282	277	.57	113	.52	299	.25	79	221	246	4.35	93	1.390	106
S3	.60	105	.54	289	.30	92	255	263	.45	105	.41	288	.23	94	223	220	2.60	101	0.273	104
S4	.59	108	.59	294	.23	1	283	295	.45	108	.45	294	.18	358	226	243	0.57	359	0.052	346
S5	.53	?	.43	?	-	-	234	242	.42	?	.36	?	-	-	166	81	1.63	ebb	0.112	ebb

TABLE 5.14 : Residual Vectors at 1m above the bottom. Speeds are in $m.s^{-1}$ and directions in ^{o}True.

Site	Date	Lower levels fitted to K-P	Upper levels fitted to UVDL	All data fitted to K-P	All data fitted to UVDL
4	18/1/82 N = 20	.026	.023	.029	.019
2	20/1/82 N = 17	.018	.018	.021	.014
3	9/2/82 N = 20	.042	.042	.052	.035
1	29/3/82 N = 20	.027	.028	.034	.023
	Mean $\overline{X}$	.028	.028	.034	.023

Table 6.1: Mean friction velocity $\overline{u_*}$ over a tidal cycle obtained by fitting velocity profiles to the Karman-Prandtl and Universal Velocity Defect Laws. The lower level includes speeds measured within 20% of the water depth from the sea bed, usually at 0.5, 1.0 and 2.0m. The upper level covers from 15% of the depth to the surface, usually at 2.0, 4.0 and 6.0m. N is the number of values in the average. Data were obtained from 4 complete tidal cycle gaugings each at a different location within Whangarei Harbour as indicated on Fig. 1.

SITE		U_1 ($m.s^{-1}$)			u_* ($m.s^{-1} \times 100$)			C_1 (10^{-3})			z_o ($m \times 100$)			r		
		EBB	FLOOD	BOTH	EBB	FLOOD	BOTH	EBB	FLOOD	BOTH	EBB	FLOOD	BOTH	EBB	FLOOD	BOTH
A	MIN.	0.31	0.31	0.31	2.78	-1.66	-1.66	2.38	0.00	0.00	0.03	0.00	0.00	0.92	-0.92	-0.92
	MEAN	0.47	0.38	0.43	3.92	0.09	2.22	8.73	0.84	5.22	1.74	0.00	0.97	0.98	-0.01	0.54
	S.D.	0.11	0.05	0.10	1.05	1.25	2.25	6.44	0.86	6.21	2.25	0.01	1.86	0.03	0.77	0.71
	MEDN	0.46	0.39	0.41	3.62	0.19	2.78	7.23	0.56	2.43	0.93	0.00	0.03	0.99	0.12	0.93
	MAX.	0.67	0.46	0.67	6.16	1.88	6.16	22.54	2.10	22.54	6.94	0.02	6.94	1.00	0.92	1.00
B	MIN.	0.31	0.31	0.31	1.32	0.87	0.87	1.43	0.45	0.45	0.00	0.00	0.00	0.83	0.74	0.74
	MEAN	0.41	0.36	0.38	2.19	1.68	1.92	3.43	2.53	2.95	0.34	0.10	0.21	0.94	0.93	0.94
	S.D.	0.08	0.04	0.06	0.99	0.43	0.77	3.28	1.67	2.51	0.71	0.22	0.51	0.05	0.07	0.06
	MEDN	0.41	0.36	0.36	1.83	1.79	1.79	1.66	2.46	2.46	0.01	0.03	0.03	0.96	0.95	0.95
	MAX.	0.51	0.41	0.51	4.21	2.50	4.21	10.54	6.50	10.54	2.02	0.70	2.02	0.98	1.00	1.00
C	MIN.	0.32	0.30	0.30	0.46	-1.27	-1.27	0.07	0.47	0.07	0.00	0.00	0.00	0.34	-0.77	-0.77
	MEAN	0.54	0.33	0.47	2.30	-0.48	1.37	2.73	1.35	2.27	0.21	0.00	0.14	0.69	-0.37	0.34
	S.D.	0.15	0.03	0.16	1.35	1.25	1.86	2.79	0.61	2.35	0.45	0.00	0.37	0.21	0.79	0.69
	MEDN	0.54	0.33	0.43	2.08	-1.02	1.54	2.13	1.56	1.57	0.03	0.00	0.00	0.71	-0.76	0.67
	MAX.	0.77	0.38	0.77	4.98	1.37	4.98	8.50	1.83	8.50	1.30	0.01	1.30	0.96	0.81	0.96
E	MIN.	0.32	0.31	0.31	-2.70	-0.74	-2.70	0.01	0.00	0.00	0.00	0.00	0.00	-0.91	-0.39	-0.91
	MEAN	0.36	0.32	0.35	0.58	0.06	0.39	3.08	0.49	2.11	0.29	0.00	0.18	0.40	0.20	0.32
	S.D.	0.03	0.01	0.03	2.12	0.85	1.68	3.24	0.45	2.81	0.45	0.00	0.37	0.81	0.72	0.73
	MEDN	0.37	0.32	0.34	1.19	-0.03	0.54	1.38	0.57	0.98	0.00	0.00	0.00	0.91	-0.01	0.51
	MAX.	0.39	0.33	0.39	3.06	0.96	3.06	7.64	0.89	7.64	1.02	0.00	1.02	0.94	1.00	1.00
F	MIN.	0.46	0.32	0.32	2.87	-2.92	-2.92	1.96	5.05	1.96	0.01	0.36	0.01	0.76	-0.66	-0.66
	MEAN	0.67	0.46	0.56	7.10	4.29	5.55	14.84	11.74	13.14	3.62	2.66	3.10	0.92	0.81	0.86
	S.D.	0.12	0.10	0.15	5.14	2.68	4.12	22.96	5.92	15.59	7.44	2.26	5.12	0.08	0.49	0.36
	MEDN	0.71	0.50	0.52	5.15	4.71	4.90	6.20	9.63	9.12	0.62	1.69	1.51	0.94	0.98	0.96
	MAX.	0.79	0.61	0.79	19.46	7.55	19.46	75.15	21.00	75.15	23.21	6.31	23.21	1.00	1.00	1.00
I	MIN.	0.31	0.30	0.30	2.14	-2.54	-2.54	4.75	0.01	0.01	0.30	0.00	0.00	0.85	-0.76	-0.76
	MEAN	0.52	0.41	0.46	5.42	0.32	2.87	11.58	2.24	6.91	2.53	0.13	1.33	0.95	0.06	0.51
	S.D.	0.12	0.07	0.11	1.44	1.82	3.07	5.68	2.30	6.39	2.22	0.19	1.97	0.05	0.63	0.63
	MEDN	0.55	0.41	0.44	5.81	0.53	2.63	9.71	1.28	5.45	1.72	0.00	0.44	0.98	0.23	0.86
	MAX.	0.69	0.51	0.69	6.77	2.99	6.77	25.16	5.59	25.16	8.01	0.47	8.01	0.99	0.88	0.99
K	MIN.	0.33	0.36	0.33	1.39	-3.59	-3.59	1.15	0.17	0.17	0.00	0.00	0.00	0.64	-0.83	-0.83
	MEAN	0.44	0.63	0.56	3.26	2.99	3.10	6.25	5.14	5.57	1.08	0.88	0.95	0.92	0.70	0.79
	S.D.	0.07	0.20	0.18	1.84	2.75	2.38	5.66	5.79	5.60	1.69	1.75	1.68	0.13	0.52	0.42
	MEDN	0.44	0.62	0.50	3.22	3.53	3.38	5.61	3.00	3.41	0.48	0.07	0.11	0.97	0.87	0.96
	MAX.	0.54	0.90	0.90	6.15	6.61	6.61	17.13	19.44	19.44	4.69	5.66	5.66	1.00	1.00	1.00
M	MIN.	0.33	0.31	0.31	1.55	-2.91	-2.91	1.66	0.29	0.29	0.01	0.00	0.00	0.70	-0.84	-0.84
	MEAN	0.46	0.36	0.43	3.59	-2.01	1.87	7.22	3.94	6.21	1.30	0.40	1.02	0.91	-0.66	0.43
	S.D.	0.11	0.05	0.10	1.31	1.03	2.94	5.82	3.56	5.32	1.92	0.67	1.66	0.09	0.20	0.77
	MEDN	0.41	0.36	0.38	4.31	-2.28	2.35	5.61	3.34	4.01	0.48	0.10	0.18	0.94	-0.71	0.89
	MAX.	0.61	0.41	0.61	4.94	-0.56	4.94	17.09	8.79	17.09	4.67	1.40	4.67	0.99	-0.38	0.99
N	MIN.	0.31	0.31	0.31	2.77	2.15	2.15	7.97	2.76	2.76	1.13	0.05	0.05	0.92	0.69	0.69
	MEAN	0.41	0.37	0.38	3.63	3.23	3.39	8.01	9.14	8.69	1.14	1.88	1.58	0.95	0.83	0.88
	S.D.	0.13	0.05	0.08	1.21	0.95	0.93	0.05	6.71	4.78	0.02	2.17	1.59	0.05	0.12	0.11
	MEDN	0.41	0.39	0.39	3.63	3.60	3.60	8.01	8.53	8.05	1.14	1.31	1.15	0.95	0.87	0.91
	MAX.	0.50	0.41	0.50	4.49	3.94	4.49	8.05	16.14	16.14	1.15	4.27	4.27	0.99	0.91	0.99
O	MIN.	0.40	0.34	0.34	0.16	0.91	0.16	0.02	0.53	0.02	0.00	0.00	0.00	0.12	0.70	0.12
	MEAN	0.60	0.50	0.54	1.66	1.85	1.77	0.88	1.45	1.20	0.00	0.02	0.01	0.67	0.87	0.78
	S.D.	0.14	0.11	0.13	1.18	1.00	1.02	0.82	1.14	1.00	0.00	0.04	0.03	0.40	0.14	0.29
	MEDN	0.65	0.47	0.61	1.87	1.58	1.58	0.95	1.13	1.13	0.00	0.00	0.00	0.78	0.95	0.95
	MAX.	0.70	0.61	0.70	2.73	3.54	3.54	1.61	3.37	3.37	0.00	0.10	0.10	0.99	1.00	1.00
P	MIN.	0.60	0.33	0.33	2.16	1.99	1.99	1.30	0.78	0.78	0.00	0.00	0.00	0.98	0.73	0.73
	MEAN	0.70	0.50	0.58	3.13	2.88	2.97	1.99	4.24	3.40	0.03	0.41	0.27	0.99	0.91	0.94
	S.D.	0.11	0.14	0.16	1.37	1.11	1.12	1.12	3.12	2.70	0.05	0.58	0.48	0.01	0.11	0.10
	MEDN	0.68	0.51	0.56	2.54	2.58	2.56	1.39	3.02	2.83	0.00	0.07	0.05	1.00	0.98	0.98
	MAX.	0.82	0.71	0.82	4.70	4.75	4.75	3.28	8.66	8.66	0.09	1.35	1.35	1.00	0.99	1.00
Q	MIN.	0.40	0.30	0.30	0.38	-11.17	-11.17	0.08	0.16	0.08	0.00	0.00	0.00	0.60	-0.93	-0.93
	MEAN	0.49	0.51	0.50	2.42	0.66	1.30	2.77	24.14	16.37	0.14	5.69	3.67	0.88	0.61	0.71
	S.D.	0.09	0.18	0.15	1.66	5.40	4.37	2.26	50.75	40.78	0.22	12.62	10.17	0.19	0.69	0.56
	MEDN	0.49	0.50	0.50	2.45	2.62	2.62	2.72	2.75	2.75	0.05	0.05	0.05	0.95	0.80	0.91
	MAX.	0.59	0.76	0.76	4.41	4.87	4.87	5.57	138.53	138.53	0.47	34.10	34.10	1.00	1.00	1.00
R	MIN.	0.33	0.30	0.30	0.97	1.20	0.97	0.61	1.18	0.61	0.00	0.00	0.00	0.33	0.50	0.33
	MEAN	0.36	0.34	0.35	3.14	1.43	2.12	13.29	1.88	6.44	4.17	0.02	1.68	0.66	0.67	0.67
	S.D.	0.04	0.04	0.03	3.08	0.20	1.81	17.93	0.83	10.95	5.89	0.03	3.72	0.47	0.22	0.28
	MEDN	0.36	0.35	0.35	3.14	1.50	1.50	13.29	1.65	1.65	4.17	0.01	0.01	0.66	0.60	0.60
	MAX.	0.39	0.37	0.39	5.32	1.59	5.32	25.98	2.80	25.98	8.34	0.05	8.34	1.00	0.92	1.00

SITE		U_1 ($m.s^{-1}$)			u_* ($m.s^{-1} \times 100$)			C_1 (10^{-3})			z_o ($m \times 100$)			r		
		EBB	FLOOD	BOTH	EBB	FLOOD	BOTH	EBB	FLOOD	BOTH	EBB	FLOOD	BOTH	EBB	FLOOD	BOTH
5	MIN.	0.40	0.52	0.40	1.12	4.46	1.12	0.41	3.14	0.41	0.00	0.08	0.00	0.76	0.97	0.76
	MEAN	0.48	0.73	0.63	2.25	4.81	3.78	3.77	4.80	4.39	0.44	0.39	0.41	0.88	0.97	0.94
	S.D.	0.11	0.19	0.20	1.60	0.53	1.66	4.75	2.26	2.92	0.62	0.48	0.46	0.17	0.00	0.10
	MEDN	0.48	0.81	0.55	2.25	4.54	4.46	3.77	3.88	3.88	0.44	0.16	0.16	0.88	0.97	0.97
	MAX.	0.55	0.87	0.87	3.38	5.42	5.42	7.13	7.37	7.37	0.87	0.94	0.94	1.00	0.98	1.00
6	MIN.	0.43	0.41	0.41	0.26	0.21	0.21	0.01	0.01	0.01	0.00	0.00	0.00	0.12	0.12	0.12
	MEAN	0.61	0.63	0.62	2.05	1.74	1.88	2.28	1.61	1.91	0.16	0.03	0.09	0.65	0.62	0.63
	S.D.	0.16	0.17	0.16	1.34	1.42	1.31	2.76	1.55	2.04	0.29	0.04	0.19	0.41	0.39	0.37
	MEDN	0.62	0.68	0.68	2.29	2.07	2.07	1.50	1.87	1.87	0.02	0.01	0.01	0.75	0.86	0.86
	MAX.	0.79	0.79	0.79	3.36	3.62	3.62	6.12	3.33	6.12	0.60	0.10	0.60	0.99	0.95	0.99
7	MIN.	0.53	0.32	0.32	2.82	-7.81	-7.81	2.53	1.06	1.06	0.03	0.00	0.00	0.70	-1.00	-1.00
	MEAN	0.60	0.39	0.51	3.55	-2.94	0.77	3.70	10.54	6.63	0.18	3.02	1.40	0.78	-0.16	0.37
	S.D.	0.07	0.08	0.13	0.51	4.49	4.35	1.47	14.82	9.36	0.22	5.17	3.35	0.10	0.90	0.73
	MEDN	0.58	0.38	0.53	3.68	-2.06	2.82	3.25	2.93	2.93	0.10	0.06	0.06	0.74	-0.29	0.72
	MAX.	0.70	0.47	0.70	4.02	1.04	4.02	5.75	27.62	27.62	0.51	8.99	8.99	0.92	0.80	0.92
8	MIN.	0.36	0.54	0.36	0.91	-0.65	-0.65	0.63	0.14	0.14	0.00	0.00	0.00	0.98	-0.16	-0.16
	MEAN	0.00	0.64	0.58	0.00	2.16	1.91	0.00	1.62	1.42	0.00	0.01	0.01	0.00	0.69	0.75
	S.D.	0.00	0.08	0.14	0.00	1.91	1.75	0.00	1.02	0.99	0.00	0.01	0.01	0.00	0.57	0.51
	MEDN	0.36	0.66	0.62	0.91	2.95	2.60	0.63	1.99	1.76	0.00	0.01	0.01	0.98	0.97	0.97
	MAX.	0.36	0.70	0.70	0.91	3.41	3.41	0.63	2.37	2.37	0.00	0.03	0.03	0.98	0.98	0.98
9	MIN.	0.43	0.34	0.34	0.54	-0.84	-0.84	0.16	0.01	0.01	0.00	0.00	0.00	0.56	-0.44	-0.44
	MEAN	0.51	0.47	0.48	0.91	3.73	3.02	0.41	13.42	10.17	0.00	3.92	2.94	0.67	0.66	0.66
	S.D.	0.11	0.10	0.10	0.42	3.37	3.14	0.42	17.36	15.93	0.00	6.13	5.52	0.14	0.54	0.46
	MEDN	0.46	0.43	0.45	0.83	3.29	2.53	0.17	4.83	2.35	0.00	0.31	0.06	0.63	0.90	0.86
	MAX.	0.63	0.62	0.63	1.37	9.53	9.53	0.89	42.90	42.90	0.00	14.47	14.47	0.83	0.99	0.99
A1	MIN.	0.37	0.00	0.37	2.26	0.00	2.26	1.85	0.00	1.85	0.01	0.00	0.01	0.62	0.00	0.62
	MEAN	0.47	0.00	0.47	2.33	0.00	2.33	2.80	0.00	2.80	0.08	0.00	0.08	0.79	0.00	0.79
	S.D.	0.13	0.10	0.13	0.10	3.37	0.10	1.34	17.36	1.34	0.10	6.13	0.10	0.24	0.54	0.24
	MEDN	0.47	0.00	0.47	2.33	0.00	2.33	2.80	0.00	2.80	0.08	0.00	0.08	0.79	0.00	0.79
	MAX.	0.56	0.00	0.56	2.41	0.00	2.41	3.75	0.00	3.75	0.14	0.00	0.14	0.96	0.00	0.96
A2	MIN.	0.37	0.32	0.32	3.04	-4.08	-4.08	4.19	1.10	1.10	0.21	0.00	0.00	0.98	-0.51	-0.51
	MEAN	0.44	0.45	0.44	3.41	0.45	1.72	6.20	3.85	4.86	0.67	0.38	0.50	0.99	0.48	0.70
	S.D.	0.07	0.10	0.08	0.47	3.08	2.70	1.80	3.32	2.86	0.42	0.52	0.46	0.01	0.67	0.55
	MEDN	0.45	0.46	0.45	3.24	1.52	2.84	6.76	3.21	5.30	0.77	0.20	0.41	1.00	0.76	0.91
	MAX.	0.50	0.56	0.56	3.94	2.84	3.94	7.66	7.86	7.86	1.03	1.09	1.09	1.00	0.91	1.00
A3	MIN.	0.36	0.40	0.36	4.65	0.87	0.87	4.55	0.29	0.29	0.26	0.00	0.00	0.91	-0.01	-0.01
	MEAN	0.58	0.44	0.51	5.08	2.58	3.83	10.20	4.78	7.49	2.22	0.57	1.40	0.94	0.63	0.79
	S.D.	0.19	0.06	0.15	0.45	1.48	1.69	8.17	3.97	6.47	3.03	0.54	2.15	0.03	0.56	0.39
	MEDN	0.69	0.42	0.47	5.04	3.32	4.09	6.48	6.25	6.37	0.69	0.63	0.66	0.92	0.94	0.93
	MAX.	0.69	0.51	0.69	5.55	3.53	5.55	19.57	7.81	19.57	5.71	1.08	5.71	0.97	0.97	0.97
A4	MIN.	0.39	0.32	0.32	2.93	1.97	1.97	0.87	1.34	0.87	0.00	0.00	0.00	0.56	0.77	0.56
	MEAN	0.60	0.52	0.56	3.87	3.36	3.58	7.75	4.96	6.16	1.51	0.52	0.95	0.72	0.86	0.80
	S.D.	0.34	0.15	0.23	0.84	1.17	0.99	5.95	3.08	4.33	1.31	0.55	1.00	0.16	0.10	0.14
	MEDN	0.43	0.54	0.54	4.12	3.48	4.10	11.15	5.28	7.02	2.25	0.48	0.84	0.71	0.83	0.81
	MAX.	0.99	0.69	0.99	4.55	4.52	4.55	11.22	7.96	11.22	2.28	1.12	2.28	0.88	1.00	1.00
R1	MIN.	0.34	0.00	0.34	-0.51	0.00	-0.51	0.10	0.00	0.10	0.00	0.00	0.00	-0.53	0.00	-0.53
	MEAN	0.43	0.00	0.43	0.13	0.00	0.13	0.31	0.00	0.31	0.00	0.00	0.00	0.24	0.00	0.24
	S.D.	0.12	0.15	0.12	0.91	1.17	0.91	0.29	3.08	0.29	0.00	0.55	0.00	1.08	0.10	1.08
	MEDN	0.43	0.00	0.43	0.13	0.00	0.13	0.31	0.00	0.31	0.00	0.00	0.00	0.24	0.00	0.24
	MAX.	0.51	0.00	0.51	0.77	0.00	0.77	0.52	0.00	0.52	0.00	0.00	0.00	1.00	0.00	1.00
R1	MIN.	0.30	0.00	0.30	1.74	0.00	1.74	2.33	0.00	2.33	0.03	0.00	0.03	0.81	0.00	0.81
	MEAN	0.33	0.00	0.33	2.41	0.00	2.41	6.47	0.00	6.47	1.04	0.00	1.04	0.84	0.00	0.84
	S.D.	0.04	0.15	0.04	0.96	1.17	0.96	5.85	3.08	5.85	1.43	0.55	1.43	0.04	0.10	0.04
	MEDN	0.33	0.00	0.33	2.41	0.00	2.41	6.47	0.00	6.47	1.04	0.00	1.04	0.84	0.00	0.84
	MAX.	0.36	0.00	0.36	3.09	0.00	3.09	10.61	0.00	10.61	2.05	0.00	2.05	0.87	0.00	0.87
R2	MIN.	0.63	0.41	0.41	3.48	0.57	0.57	2.70	0.17	0.17	0.04	0.00	0.00	0.91	0.04	0.04
	MEAN	0.68	0.47	0.58	4.25	2.86	3.55	4.14	5.98	5.06	0.29	1.27	0.78	0.95	0.40	0.67
	S.D.	0.07	0.08	0.13	0.95	2.22	1.70	2.19	7.81	5.23	0.39	2.14	1.48	0.04	0.48	0.43
	MEDN	0.65	0.44	0.60	3.95	3.03	3.71	3.05	2.93	2.99	0.07	0.06	0.07	0.96	0.22	0.92
	MAX.	0.76	0.56	0.76	5.31	5.00	5.31	6.66	14.85	14.85	0.74	3.74	3.74	0.97	0.94	0.97
R2	MIN.	0.46	0.37	0.37	2.15	1.03	1.03	1.52	0.30	0.30	0.00	0.00	0.00	0.07	0.31	0.07
	MEAN	0.62	0.50	0.56	3.97	2.40	3.18	4.57	4.81	4.69	0.44	0.97	0.70	0.63	0.56	0.59
	S.D.	0.21	0.12	0.17	1.78	1.62	1.75	3.14	6.93	4.81	0.56	1.67	1.15	0.49	0.31	0.37
	MEDN	0.55	0.54	0.55	4.06	1.98	3.10	4.40	1.34	2.96	0.24	0.00	0.12	0.89	0.45	0.67
	MAX.	0.86	0.59	0.86	5.70	4.18	5.70	7.80	12.78	12.78	1.07	2.90	2.90	0.92	0.91	0.92
R4	MIN.	0.00	0.37	0.37	0.00	0.58	0.58	0.00	0.15	0.15	0.00	0.00	0.00	0.00	0.01	0.01
	MEAN	0.00	0.51	0.51	0.00	2.66	2.66	0.00	4.38	4.38	0.00	0.65	0.65	0.00	0.46	0.46
	S.D.	0.21	0.16	0.16	1.78	1.80	1.80	3.14	5.19	5.19	0.56	1.07	1.07	0.49	0.48	0.48
	MEDN	0.00	0.47	0.47	0.00	3.66	3.66	0.00	2.82	2.82	0.00	0.05	0.05	0.00	0.40	0.40
	MAX.	0.00	0.69	0.69	0.00	3.73	3.73	0.00	10.17	10.17	0.00	1.88	1.88	0.00	0.96	0.96
R4	MIN.	0.52	0.31	0.31	3.92	-0.51	-0.51	5.67	0.09	0.09	0.49	0.00	0.00	0.30	-0.16	-0.16
	MEAN	0.00	0.48	0.49	0.00	3.01	3.23	0.00	7.42	6.98	0.00	1.49	1.24	0.00	0.28	0.29
	S.D.	0.00	0.15	0.12	0.00	3.42	2.83	0.00	6.36	5.27	0.00	1.30	1.17	0.00	0.47	0.39
	MEDN	0.52	0.55	0.54	3.92	3.21	3.56	5.67	10.71	8.19	0.49	2.09	1.29	0.30	0.23	0.26
	MAX.	0.52	0.59	0.59	3.92	6.32	6.32	5.67	11.47	11.47	0.49	2.38	2.38	0.30	0.78	0.78

SITE		U_1 ($m.s^{-1}$)			u_* ($m.s^{-1} \times 100$)			C_1 (10^{-3})			z_0 ($m \times 100$)			r		
		EBB	FLOOD	BOTH	EBB	FLOOD	BOTH	EBB	FLOOD	BOTH	EBB	FLOOD	BOTH	EBB	FLOOD	BOTH
	MIN.	0.32	0.37	0.32	1.25	-1.91	-1.91	1.53	0.13	0.13	0.00	0.00	0.00	0.70	-0.93	-0.93
	MEAN	0.50	0.40	0.45	2.44	-0.62	0.91	2.32	1.00	1.66	0.03	0.01	0.02	0.89	-0.30	0.29
	S.D.	0.15	0.04	0.11	1.06	1.23	1.97	0.80	1.43	1.27	0.04	0.02	0.03	0.17	0.76	0.82
	MEDN	0.58	0.39	0.41	2.78	-0.51	0.90	2.30	0.20	1.92	0.02	0.00	0.01	0.97	-0.53	0.62
	MAX.	0.59	0.44	0.59	3.30	0.56	3.30	3.13	2.65	3.13	0.08	0.04	0.08	1.00	0.55	1.00
C1	MIN.	0.37	0.32	0.32	2.12	-1.16	-1.16	3.30	0.20	0.20	0.09	0.00	0.00	0.96	-0.98	-0.98
	MEAN	0.56	0.41	0.47	3.43	0.76	1.83	3.72	4.53	4.20	0.14	1.25	0.81	0.98	0.16	0.49
	S.D.	0.14	0.10	0.13	0.95	2.26	2.25	0.39	9.48	7.08	0.05	3.05	2.34	0.02	0.84	0.75
	MEDN	0.60	0.39	0.46	3.63	0.09	1.69	3.74	0.74	2.36	0.15	0.00	0.05	0.98	0.22	0.94
	MAX.	0.68	0.55	0.68	4.36	4.94	4.94	4.10	23.84	23.84	0.19	7.48	7.48	1.00	0.97	1.00
C2	MIN.	0.00	0.45	0.45	0.00	0.79	0.79	0.00	0.31	0.31	0.00	0.00	0.00	0.00	0.17	0.17
	MEAN	0.00	0.51	0.51	0.00	1.85	1.85	0.00	1.82	1.82	0.00	0.09	0.09	0.00	0.42	0.42
	S.D.	0.14	0.07	0.07	0.95	1.05	1.05	0.39	2.23	2.23	0.05	0.18	0.18	0.02	0.20	0.20
	MEDN	0.00	0.49	0.49	0.00	1.66	1.66	0.00	0.93	0.93	0.00	0.00	0.00	0.00	0.45	0.45
	MAX.	0.00	0.61	0.61	0.00	3.29	3.29	0.00	5.11	5.11	0.00	0.37	0.37	0.00	0.60	0.60
C2	MIN.	0.56	0.40	0.40	2.92	1.72	1.72	2.31	0.54	0.54	0.02	0.00	0.00	0.14	0.15	0.14
	MEAN	0.73	0.56	0.64	3.97	2.98	3.42	2.93	3.51	3.25	0.07	0.28	0.19	0.63	0.67	0.66
	S.D.	0.13	0.12	0.15	0.95	1.21	1.16	0.56	2.83	2.06	0.05	0.52	0.38	0.35	0.30	0.30
	MEDN	0.77	0.54	0.61	4.01	2.84	3.46	2.87	2.76	2.76	0.06	0.05	0.05	0.74	0.78	0.78
	MAX.	0.83	0.74	0.83	4.95	4.71	4.95	3.65	8.19	8.19	0.13	1.20	1.20	0.91	0.92	0.92
C3	MIN.	0.00	0.64	0.64	0.00	1.74	1.74	0.00	0.62	0.62	0.00	0.00	0.00	0.00	0.77	0.77
	MEAN	0.00	0.68	0.68	0.00	3.02	3.02	0.00	2.28	2.28	0.00	0.08	0.08	0.00	0.83	0.83
	S.D.	0.13	0.03	0.03	0.95	1.45	1.45	0.56	1.96	1.96	0.05	0.14	0.14	0.35	0.08	0.08
	MEDN	0.00	0.69	0.69	0.00	2.71	2.71	0.00	1.79	1.79	0.00	0.01	0.01	0.00	0.79	0.79
	MAX.	0.00	0.70	0.70	0.00	4.60	4.60	0.00	4.44	4.44	0.00	0.25	0.25	0.00	0.92	0.92
C3	MIN.	0.50	0.36	0.36	4.17	0.80	0.80	6.20	0.15	0.15	0.62	0.00	0.00	0.89	-0.04	-0.04
	MEAN	0.59	0.58	0.58	5.10	1.90	3.32	7.58	1.64	4.28	1.04	0.05	0.49	0.94	0.46	0.68
	S.D.	0.10	0.14	0.12	0.93	1.41	2.04	1.79	1.84	3.56	0.56	0.07	0.63	0.05	0.44	0.40
	MEDN	0.57	0.65	0.61	5.07	1.15	4.17	7.08	0.46	3.68	0.87	0.00	0.14	0.95	0.44	0.89
	MAX.	0.72	0.70	0.72	6.09	4.25	6.09	9.97	3.68	9.97	1.81	0.14	1.81	0.99	0.96	0.99
C4	MIN.	0.31	0.32	0.31	0.63	1.31	0.63	0.35	0.88	0.35	0.00	0.00	0.00	0.48	0.85	0.48
	MEAN	0.47	0.41	0.44	1.84	1.64	1.76	1.70	1.72	1.71	0.03	0.02	0.03	0.71	0.92	0.80
	S.D.	0.17	0.10	0.13	1.14	0.41	0.85	1.39	0.87	1.10	0.06	0.02	0.05	0.22	0.05	0.19
	MEDN	0.45	0.41	0.41	1.73	1.51	1.51	1.44	1.67	1.67	0.00	0.01	0.01	0.71	0.94	0.85
	MAX.	0.66	0.51	0.66	3.28	2.10	3.28	3.57	2.61	3.57	0.12	0.04	0.12	0.95	0.95	0.95
C4	MIN.	0.58	0.39	0.39	2.59	1.35	1.35	2.00	0.86	0.86	0.01	0.00	0.00	0.97	0.87	0.87
	MEAN	0.64	0.47	0.55	3.56	1.68	2.48	3.13	1.32	2.09	0.11	0.00	0.05	0.99	0.93	0.96
	S.D.	0.07	0.06	0.11	0.86	0.31	1.14	1.31	0.52	1.28	0.14	0.01	0.10	0.01	0.05	0.05
	MEDN	0.63	0.49	0.53	3.82	1.63	2.08	2.82	1.23	1.96	0.05	0.00	0.01	0.99	0.94	0.97
	MAX.	0.72	0.53	0.72	4.26	2.08	4.26	4.57	1.96	4.57	0.27	0.01	0.27	1.00	0.99	1.00
D1	MIN.	0.30	0.33	0.30	1.82	-1.03	-1.03	2.07	0.87	0.87	0.01	0.00	0.00	0.93	-0.30	-0.30
	MEAN	0.37	0.34	0.36	2.41	0.26	1.55	4.48	1.53	3.30	0.37	0.01	0.23	0.98	0.34	0.72
	S.D.	0.06	0.01	0.05	0.93	1.82	1.63	2.59	0.93	2.49	0.47	0.01	0.38	0.04	0.91	0.57
	MEDN	0.40	0.34	0.35	1.93	0.26	1.82	4.14	1.53	2.19	0.20	0.01	0.02	0.99	0.34	0.99
	MAX.	0.41	0.35	0.41	3.48	1.55	3.48	7.22	2.19	7.22	0.90	0.02	0.90	1.00	0.99	1.00
D2	MIN.	0.37	0.31	0.31	2.32	0.77	0.77	3.92	0.55	0.55	0.17	0.00	0.00	0.76	0.60	0.60
	MEAN	0.42	0.32	0.38	3.48	0.97	2.47	6.85	0.97	4.50	0.90	0.00	0.54	0.92	0.78	0.86
	S.D.	0.06	0.01	0.07	1.00	0.27	1.55	2.93	0.60	3.84	0.79	0.00	0.75	0.14	0.26	0.18
	MEDN	0.41	0.32	0.37	4.06	0.97	2.32	6.85	0.97	3.92	0.79	0.00	0.17	1.00	0.78	0.96
	MAX.	0.49	0.33	0.49	4.06	1.16	4.06	9.79	1.40	9.79	1.75	0.00	1.75	1.00	0.96	1.00
D3	MIN.	0.42	0.31	0.31	4.23	2.28	2.28	4.81	2.46	2.46	0.31	0.03	0.03	0.89	0.75	0.75
	MEAN	0.50	0.41	0.44	5.71	2.73	3.84	15.98	4.98	9.11	4.41	0.47	1.95	0.95	0.89	0.92
	S.D.	0.10	0.07	0.09	2.24	0.33	1.97	13.57	2.59	9.43	5.24	0.62	3.50	0.05	0.09	0.08
	MEDN	0.47	0.42	0.44	4.61	2.78	3.03	12.06	4.39	5.10	2.61	0.24	0.37	0.96	0.92	0.93
	MAX.	0.61	0.47	0.61	8.29	3.08	8.29	31.09	9.20	31.09	10.32	1.54	10.32	1.00	0.99	1.00
D4	MIN.	0.43	0.38	0.38	3.69	2.47	2.47	7.36	1.63	1.63	0.94	0.00	0.00	0.87	0.89	0.87
	MEAN	0.43	0.49	0.47	3.82	2.96	3.21	7.92	4.49	5.47	1.12	0.39	0.60	0.93	0.95	0.95
	S.D.	0.00	0.11	0.10	0.19	0.39	0.53	0.79	2.54	2.69	0.25	0.41	0.50	0.08	0.05	0.05
	MEDN	0.43	0.42	0.43	3.82	2.94	3.02	7.92	4.89	6.30	1.12	0.33	0.64	0.93	0.98	0.98
	MAX.	0.43	0.61	0.61	3.96	3.54	3.96	8.47	7.45	8.47	1.29	0.97	1.29	0.98	0.99	0.99

SITE		u_1 (m.s^{-1})			u_* (m.s^{-1} x 100)			C_1 (10^{-3})			z_o (m x 100)			r		
		EBB	FLOOD	BOTH	EBB	FLOOD	BOTH	EBB	FLOOD	BOTH	EBB	FLOOD	BOTH	EBB	FLOOD	BOTH
S1	MIN.	0.40	0.31	0.31	1.74	1.90	1.74	1.00	0.68	0.68	0.00	0.00	0.00	0.73	0.53	0.53
	MEAN	0.50	0.50	0.50	2.46	2.70	2.59	2.59	4.01	3.39	0.07	0.40	0.25	0.87	0.88	0.88
	S.D.	0.07	0.13	0.10	0.65	0.63	0.63	1.16	3.27	2.60	0.08	0.76	0.58	0.10	0.16	0.13
	MEDN	0.52	0.53	0.52	2.32	2.71	2.39	2.93	2.69	2.81	0.06	0.04	0.05	0.90	0.96	0.93
	MAX.	0.59	0.73	0.73	3.39	3.95	3.95	4.24	11.41	11.41	0.21	2.36	2.36	0.98	1.00	1.00
S2	MIN.	0.35	0.34	0.34	0.51	1.56	0.51	0.08	1.33	0.08	0.00	0.00	0.00	0.76	0.86	0.76
	MEAN	0.52	0.42	0.47	1.49	2.39	1.94	0.94	3.80	2.37	0.00	0.44	0.22	0.80	0.94	0.87
	S.D.	0.09	0.06	0.09	0.65	1.09	0.98	0.63	3.99	3.12	0.01	1.08	0.77	0.03	0.06	0.09
	MEDN	0.56	0.41	0.47	1.34	1.80	1.79	1.01	2.38	1.65	0.00	0.03	0.01	0.81	0.97	0.85
	MAX.	0.61	0.53	0.61	2.28	4.63	4.63	2.08	12.75	12.75	0.02	2.88	2.88	0.84	1.00	1.00
S3	MIN.	0.36	0.30	0.30	2.12	2.55	2.12	1.60	3.16	1.60	0.00	0.08	0.00	0.65	0.71	0.65
	MEAN	0.61	0.51	0.55	4.66	4.13	4.38	6.53	6.89	6.72	0.90	0.91	0.90	0.89	0.93	0.91
	S.D.	0.14	0.10	0.13	1.51	1.13	1.32	3.27	2.46	2.80	0.80	0.68	0.71	0.11	0.08	0.10
	MEDN	0.62	0.55	0.55	4.60	4.21	4.24	6.50	6.90	6.60	0.70	0.81	0.72	0.92	0.95	0.94
	MAX.	0.85	0.61	0.85	6.90	5.56	6.90	10.97	11.15	11.15	2.19	2.25	2.25	1.00	0.99	1.00
S4	MIN.	0.32	0.31	0.31	1.43	0.77	0.77	0.44	0.55	0.44	0.00	0.00	0.00	0.92	0.76	0.76
	MEAN	0.55	0.50	0.52	2.95	3.26	3.11	3.63	4.94	4.32	0.27	0.54	0.41	0.97	0.94	0.95
	S.D.	0.14	0.13	0.13	0.97	1.14	1.05	2.39	3.20	2.85	0.30	0.73	0.57	0.02	0.09	0.06
	MEDN	0.54	0.49	0.53	3.28	3.19	3.28	2.73	4.44	3.88	0.05	0.25	0.16	0.97	0.98	0.97
	MAX.	0.72	0.68	0.72	4.07	5.23	5.23	6.41	11.23	11.23	0.67	2.28	2.28	1.00	1.00	1.00
S5	MIN.	0.34	0.32	0.32	2.48	1.56	1.56	1.33	2.38	1.33	0.00	0.03	0.00	0.82	0.07	0.07
	MEAN	0.55	0.45	0.50	3.23	2.82	3.01	4.26	4.03	4.14	0.36	0.24	0.30	0.94	0.79	0.86
	S.D.	0.15	0.08	0.13	0.62	0.86	0.76	2.49	1.62	2.01	0.44	0.32	0.37	0.06	0.29	0.22
	MEDN	0.56	0.46	0.48	3.13	2.62	2.99	3.26	3.94	3.90	0.10	0.17	0.16	0.95	0.92	0.92
	MAX.	0.71	0.58	0.71	4.50	4.69	4.69	7.77	7.82	7.82	1.07	1.08	1.08	0.99	1.00	1.00

Table 6.2: Minimum, mean, standard deviation, median and maximum values of velocity at 1m above the bed u_1 (m.s^{-1}); friction velocity, u_* (m.s^{-1} x 100); Drag Coefficient, C_1 (x 10^3) ; roughness length, z_o (m x 100); and the correlation coefficient representing the goodness of fit to the logarithmic profile, r, for all Braystoke vertical profile velocity measurement sites.

SITE		u_1 ($m.s^{-1}$)			u_* ($m.s^{-1} \times 100$)			C_1 (10^{-3})			z_o ($m \times 100$)			r		
		EBB	FLOOD	BOTH	EBB	FLOOD	BOTH	EBB	FLOOD	BOTH	EBB	FLOOD	BOTH	EBB	FLOOD	BOTH
AL	MIN.	0.30	0.30	0.30	-9.72	-11.17	-11.17	0.00	0.00	0.00	0.00	0.00	0.00	-0.91	-1.00	-1.00
	MEAN	0.52	0.47	0.50	3.22	2.07	2.61	5.50	5.09	5.28	0.89	0.85	0.87	0.83	0.59	0.70
	S.D.	0.14	0.13	0.14	2.29	2.39	2.41	7.11	10.67	9.17	2.22	2.89	2.60	0.28	0.57	0.47
	MEDN	0.52	0.45	0.47	3.23	2.27	2.73	3.69	2.69	3.03	0.14	0.04	0.07	0.94	0.87	0.91
	MAX.	0.99	0.90	0.99	19.46	9.53	19.46	75.15	138.53	138.53	23.21	34.10	34.10	1.00	1.00	1.00
SN	MIN.	0.32	0.30	0.30	-2.70	-3.59	-3.59	0.01	0.00	0.00	0.00	0.00	0.00	-0.91	-0.98	-0.98
	MEAN	0.54	0.48	0.51	3.50	2.61	3.03	5.55	5.37	5.46	0.85	0.85	0.85	0.87	0.67	0.76
	S.D.	0.14	0.13	0.14	2.51	2.21	2.39	8.53	5.12	6.93	2.65	1.53	2.13	0.25	0.55	0.44
	MEDN	0.54	0.46	0.50	3.30	2.91	3.06	3.90	3.82	3.82	0.16	0.15	0.15	0.94	0.93	0.93
	MAX.	0.86	0.90	0.90	19.46	7.55	19.46	75.15	23.84	75.15	23.21	7.48	23.21	1.00	1.00	1.00
SH	MIN.	0.31	0.30	0.30	-9.72	-7.81	-9.72	0.00	0.00	0.00	0.00	0.00	0.00	-0.57	-1.00	-1.00
	MEAN	0.52	0.48	0.50	2.90	1.71	2.25	5.83	4.20	4.94	1.07	0.74	0.89	0.78	0.51	0.63
	S.D.	0.13	0.14	0.14	2.35	2.45	2.47	6.54	7.51	7.11	2.12	2.54	2.36	0.32	0.62	0.52
	MEDN	0.50	0.46	0.47	3.24	1.83	2.53	4.16	2.14	2.52	0.20	0.02	0.03	0.92	0.84	0.87
	MAX.	0.79	0.87	0.87	8.29	9.53	9.53	31.09	42.90	42.90	10.32	14.47	14.47	1.00	1.00	1.00
AC	MIN.	0.31	0.30	0.30	-2.70	-11.17	-11.17	0.08	0.11	0.08	0.00	0.00	0.00	-0.91	-0.93	-0.93
	MEAN	0.48	0.44	0.46	3.39	2.07	2.61	6.57	6.66	6.62	1.13	1.23	1.19	0.82	0.59	0.69
	S.D.	0.12	0.12	0.12	2.82	2.57	2.74	10.02	15.79	13.68	3.16	4.14	3.76	0.33	0.60	0.52
	MEDN	0.46	0.41	0.43	3.06	2.46	2.74	5.32	2.88	3.75	0.41	0.06	0.15	0.92	0.89	0.92
	MAX.	0.77	0.81	0.81	19.46	9.53	19.46	75.15	138.53	138.53	23.21	34.10	34.10	1.00	1.00	1.00
DE	MIN.	0.30	0.30	0.30	-9.72	-3.59	-9.72	0.00	0.00	0.00	0.00	0.00	0.00	-0.57	-0.83	-0.83
	MEAN	0.48	0.47	0.48	2.77	2.26	2.54	5.37	4.72	5.08	0.93	0.76	0.85	0.81	0.65	0.74
	S.D.	0.12	0.13	0.12	2.22	2.11	2.18	6.25	6.24	6.24	2.04	2.00	2.01	0.30	0.49	0.40
	MEDN	0.46	0.44	0.45	2.70	2.45	2.53	3.30	2.93	3.14	0.09	0.06	0.08	0.93	0.87	0.91
	MAX.	0.82	0.90	0.90	8.29	7.36	8.29	31.09	41.79	41.79	10.32	14.10	14.10	1.00	1.00	1.00

Table 6.3: Minimum, mean, standard deviation, median and maximum values of velocity at 1m above the bed, u_1 ($m.s^{-1}$); friction velocity, u_* ($m.s^{-1} \times 100$); Drag Coefficient, C_1 ($\times 10^3$); roughness length, z_o ($m \times 100$); and the correlation coefficient representing the goodness of fit to the logarithmic profile, r, for vertical velocity profile measurement sites. Data has been broken into 5 subsets: (i) all sites; (ii) sites with sand beds; (iii) sites with shell beds; (iv) profiles during accelerating currents; and (v) profiles during decelerating currents.

n	r α = 0.5	r α = .10
3	.99	.95
4	.91	.80
5	.81	.69
6	.73	.61
7	.67	.55

Table 6.4: Correlation coefficient to be exceeded for the profile to be logarithmic at the α = 0.05 and α = 0.10 levels of significance. n is number of velocities fitted.

Site	Ebb			Flood			Both			Site	Ebb			Flood			Both		
	n	N	%	n	N	%	n	N	%		n	N	%	n	N	%	n	N	%
A	10	10	100	3	8	38	13	18	72	A3	3	3	100	2	3	67	5	6	83
B	2	8	25	2	9	22	4	17	24	A4	0	3	0	1	3	33	1	6	17
C	3	8	38	0	4	0	3	12	25	B1	1	2	50	-	-	-	1	2	50
D	2	9	22	1	3	33	3	12	25	B1	0	2	0	-	-	-	0	2	0
E	2	4	50	1	3	33	3	7	43	B2	2	3	67	1	3	33	3	6	50
F	6	13	46	8	10	80	14	23	61	B2	0	3	0	0	3	0	0	6	0
I	9	9	100	1	9		10	18	56	B3(2)	-	-	-	0	1	0	0	1	0
K	5	7	71	2	11	7	7	18	39	B4	-	-	-	0	3	0	0	3	0
M	9	9	100	2	4	50	11	13	85	B4	0	3	0	0	3	0	0	6	0
N	1	2	50	0	3	0	1	5	20	C1	2	3	67	0	3	0	2	6	33
1	0	4	0	1	5	20	1	9	11	C1	1	3	33	0	6	0	1	9	11
2	2	3	67	0	5	0	2	8	25	C2	-	-	-	0	4	0	0	4	0
3	2	4	50	1	7	14	3	11	27	C2	1	4	25	1	5	20	2	9	22
4	1	2	50	0	3	0	1	5	20	C3	0	1	0	1	3	33	1	4	25
5	1	2	50	0	3	0	1	5	20	C3	3	4	75	1	5	20	4	9	44
6	1	4	25	0	5	0	1	9	11	C4	1	4	25	2	3	67	3	7	43
7	0	4	0	0	3	0	0	7	0	C4	3	3	100	3	5	60	6	8	75
8	1	2	50	1	5	20	2	7	29	D1	2	3	67	1	2	50	3	5	60
9	0	3	0	2	9	22	2	12	17	D2	2	3	67	1	3	33	3	6	50
A1	1	2	50	-	-	-	1	2	50	D3	2	4	50	3	5	60	5	9	56
A2	3	4	75	0	3	0	3	7	43	D4	1	3	33	4	5	80	5	8	68

Table 6.5 (a): The number of vertical velocity profiles (n) out of a total of N at each site which exhibit a logarithmic shape at the α = 0.05 level of significance, separately for ebb and flood and with both combined. The % columns show the percentage of logarithmic profiles.

Site	α = .05									α = .10								
	Ebb			Flood			Both			Ebb			Flood			Both		
	n	N	%	n	N	%	n	N	%	n	N	%	n	N	%	n	N	%
S1	1	7	14	2	9	22	3	16	19	4	7	57	5	9	56	9	16	56
S2	0	7	0	2	8	25	2	15	13	0	7	0	5	8	63	5	15	33
S3	1	9	11	0	10	0	1	19	5	4	9	44	5	10	50	9	19	47
S4	2	9	22	5	10	50	7	19	37	8	9	89	7	10	70	15	19	79
S5	1	8	13	3	9	33	4	17	24	4	8	50	6	9	67	10	17	59
All Sites	90	207	43	58	226	26	148	433	34	-	-	-	-	-	-	-	-	-
S-series	5	40	13	12	46	26	17	86	20	20	40	50	28	46	61	48	86	56

Figure 6.5 (b): The number of logarithmic velocity profiles (n) out of N profiles at the S-series sites for the α = 0.05 and α = 0.10 levels of significance. The statistics for all sites combined including those in Table 6.4 (a) are given.

Site	(i) C_1	(ii) $\bar{C}_1$	(iii) C_1
S1	4.1	3.4	2.8
S3	7.0	6.7	6.6
S4	4.4	4.3	3.9
S5	4.6	4.1	3.9

Table 6.6: The Drag Coefficient (x 10^3) (i) calculated using the bedform geometry (Table 7.2); (ii) the mean value averaged over the tidal cycle found using the measured vertical velocity profiles and; (iii) the median value from the velocity profiles.

	(i)	(ii)	(iii)	(iv)	(v)	(vi)		
Site	Median c	c" V&H	c' KP	c' MS	c (KP,V&H)	c (MS,V&H)	Deviations (%) (v)	(vi)
S1	21.4	25.0	29.9	42.2	19.2	21.5	-10	0
S3	17.5	18.7	29.4	40.8	15.8	17.0	-10	-3
S4	17.2	20.0	27.4	35.7	16.2	17.4	- 6	1
S5	19.8	22.8	30.2	43.0	18.2	20.1	- 8	2

Table 6.7: (i) the median friction factor ($c = \bar{u}/u_*$) obtained by curve fitting the measured vertical velocities to logarithmic profile; (ii) the form drag friction factor obtained using the Vanoni and Hwang equation and bed geometry (Table 7.2) (iii) skin friction factor using the Karman Prandtl equation (iv) the skin friction factor using the Manning-Strickler equation (v) combined friction factor using the Vanoni and Hwang and Karman Prandtl friction factors (vi) combined friction factor using the Vanoni and Hwang and Manning-Strickler friction factors. Deviations of columns (v) and (vi) from column (i) are given.

	S3 Low Tide	S3 Peak Flow	S3 High Tide	S6 High Tide	S6 Low Tide	S4 High Tide	S4 Low Tide	S5 Low Tide
Megaripple Height (m)	0.20	0.10	0.17	0.10	0.11	.15	.15	.16
Angle of Repose	27°	20°	27.5°	34°	27°	30°	29°	32°
Ripple Height (m)	.02	.04	.01	.01	.01	.03	.03	-
Ripple Wavelength (m)	.18	.20	.12	.08	.15	.20	.20	-

Table 7.1: Summary of bedform geometry from 90 underwater photographs. Note that the same features were not necessarily photographed at different tidal stages.

Site	D_{35} (mm)	D_{50} (mm)	D_{65} (mm)	D_{90} (mm)	Mean Depth (m)	Temp. (°C)	$\bar{\Delta}$ (m)	$\bar{\Lambda}$ (m)
S1	.28	.30	.32	.39	9.3	21	.17	7.5
S3	.32	.34	.37	.48	8.6	20	.25	3.7
S4	.30	.32	.34	.41	3.4	20	.15	4.6
S5	.20	.24	.27	.44	8.4	19	.16	4.2

Table 7.2: Grain sizes from sediment traps emptied after peak flow, mean depth at the site, temperature and mean bedform height ($\bar{\Delta}$) and wavelength ($\bar{\Lambda}$). The bedform geometry for S1 relies on only one measurement of Δ and Λ.

Site	Region	Mean M_Z (mm)	Standard Deviation (ø)	Skewness (ø)	Kurtosis (ø)	D_{50} (mm)	Description
S1	Crest	.31	.33	-1.41	15.52	.31	Very Well Sorted
	Sediment Trap	.32	.68	-4.08	23.14	.30	Moderately Well Sorted
	Trough	.35	1.22	-3.68	16.36	.29	Poorly Sorted
S3	Diver Sample	.44	.90	-2.84	12.51	.38	Moderately Sorted
	Sediment Trap	.39	.95	-4.00	21.31	.34	Moderately Sorted
S4	Crest	.31	.57	-4.02	25.42	.29	Moderately Well Sorted
	Sediment Trap	.32	.52	-2.49	21.76	.32	Moderately Well Sorted
	Trough	.31	.32	-5.09	46.43	.31	Very Well Sorted
S5	Crest	.44	.73	-1.80	8.55	.40	Moderately Sorted
	Sediment Trap	.25	.71	-1.83	9.45	.25	Moderately Sorted
	Trough	1.18	2.4	-1.74	2.13	.60	Very Poorly Sorted

Table 7.3: Grain Sizes for the S Series, obtained by the moments method. Verbal classification of sorting is after Folk (1968).

z_o (m)	D = .0001m u'_{*cr} = .0104 5m	10m	D = .0002m u'_{*cr} = .0128 5m	10m	D = .0005m u'_{*cr} = .0164 5m	10m	D = .0010m u'_{*cr} = .0223 5m	10m	
.0001	.0148	.0147	.0182	.0181	.0234	.0231	.0318	.0315	Friction Velocity ($m.s^{-1}$)
.0005	.0153	.0151	.0189	.0186	.0242	.0238	.0329	.0323	
.0010	.0157	.0153	.0193	.0189	.0247	.0242	.0336	.0329	
.0050	.0171	.0163	.0211	.0201	.0270	.0257	.0367	.0350	
.0001	.34	.34	.42	.42	.54	.54	.73	.72	Velocity at 1m ($m.s^{-1}$)
.0005	.29	.29	.36	.35	.46	.45	.62	.61	
.0010	.27	.26	.33	.33	.43	.42	.58	.57	
.0050	.23	.22	.28	.27	.36	.34	.49	.46	
	.30		.35		.44		.52		Critical Speed from Bedload Formula

Table 7.4: Critical friction velocity (u_*), and 1m speed, (u_1), for selected grain sizes (D) and roughness lengths (z_o) for water depths of 5m and 10m. Critical skin friction velocity (u'_{*cr}) was obtained from the Yalin Threshold curve using the corresponding grain sizes. Critical 1m speed derived from the Karman Prandtl skin friction equation for bedload transport calculations is given. (ρ_s = 2650 $kg.m^{-3}$).

Site	Bedforms z_o			Median Profile z_o			Mean Profile z_o			u'_{*cr} (Yalin Curve)	θ'_{cr} (Yalin Curve)	u''_{*cr} / $\bar{u}_{cr}$ = 0.4	u_{*cr} / $\bar{u}_{cr}$ = 0.4	$\bar{u}_{1cr}$
	z_o (m)	u_{1cr}	u_{*cr}	z_o (m)	u_{1cr}	u_{*cr}	z_o (m)	u_{1cr}	u_{*cr}					
S1	.0019	.33	.0211	.0005	.39	.0203	.0025	.32	.0213	.0140	.042	.0160	.0213	.35
S2	-	-	-	.0001	.45	.0198	.0022	.32	.0212	(.0140)	(.042)	-	-	.39
S3	.0084	.28	.0238	.0072	.29	.0235	.0090	.28	.0239	.0146	.040	.0213	.0258	.28
S4	.0024	.33	.0217	.0016	.34	.0214	.0044	.31	.0223	.0143	.041	.0198	.0244	.33
S5	.0033	.30	.0204	.0016	.32	.0199	.0030	.30	.0204	.0133	.048	.0170	.0216	.31

Table 7.5: Critical friction and 1m velocities ($m.s^{-1}$) for the S-series obtained with z_o from the bedform geometry and the median and mean values from curve fitting the vertical velocity profiles. The average of the three is shown in the last column, $\bar{u}_{1cr}$. Critical skin friction from the Yalin Threshold Curve with the D_{50} grain size, and the corresponding Shields Entrainment Function are given. The second and third last columns give critical form drag and total friction velocities obtained with the Vanoni and Hwang equation with $\bar{u}_{cr}$=0.4 $m.s^{-1}$. Grain size at S1 was not measured and is assumed to be D_{50} = 0.0003m.

SITE	DEPTH (m)	GRAIN SIZE (mm)	BED GEOMETRY (m)	OBSERVED THRESHOLD		EXTRAPOLATED THRESHOLD		PREDICTED THRESHOLD	
				u_*	u_1	u_*	u_1	u_*	u_1
Pickering Passage	20	.42	Ripples Δ = .015 - .024 Λ = .16	.0224	.39	.0180	.37	.0225	.38
Salmon Bank	20	.38	Ripples Δ = .02 - .035 Λ = .10 - .30	.0235	.38	.0150	.32	.0220	.34

Table 7.6: Comparison of Sternberg's (1971) observed and extrapolated thresholds with the predicted value from the bed geometry.

S3		S4		S5	
TIME	MASS/m	TIME	MASS/m	TIME	MASS/m
EBB		FLOOD		EBB	
930-1045	15.0	705- 845	13.37	1140-1255	4.37
1055-1235	79.58	855-1015	30.26	1300-1420	9.25
1115-1245	75.50				
1250-1410	2.92	1022-1215	6.62	1425-1615	2.93
1240-1420	36.54				
FLOOD		EBB		FLOOD	
1540-1713	2.97	1330-1445	9.61	1730-1940	3.05
1715-1848	19.41	1455-1620	19.58	1935-2130	12.92
1848-2030	2.82	1625-1800	18.03	2130-2300	5.51

Table 7.7: VUV trapped masses of sediment per unit width of bed (kg/m) with the trapping periods. Transport rates calculated later vary according to the time above the velocity threshold in each trapping period. At S3, the two data pairs were averaged after transport rates had been determined.

Site	$\frac{\Delta}{\Lambda}$	K	Average Nett Megaripple Advance (m)	Megaripple Advance Rate kg/m/tidal cycle	Bedload Equation Prediction kg/m/tidal cycle
S1	.023	1.68	-	-	-
S2	.050	1.43	-	-	-
S3	.068	1.23	.70	78.0	77.2
S4	.033	1.58	.18	15.5	18.9
S5	.038	1.55	.26	23.5	33.4

Table 7.8: Megaripple steepness (Δ/Λ); K from Engel and Lau (1981); average measured megaripple advance over the tidal cycle; mass transport rate from the megaripple advance with the Engel and Lau equation; and the mass transport rate using the bedload equation in the Chaper.

		Megaripple Number							
		1	2	3	4	5	6	Average	Time
S3	Wavelength (m)	4.2	4.6	4.7	3.0	2.7	3.3	3.7	09.00 (High Tide)
	Advance During Ebb (m)	-3.5	-3.8	-4.2	-3.7	-2.9	-3.1	-3.5	15.40 (Low Tide)
	Advance During Flood (m)	2.9	3.8	3.1	2.9	2.2	2.3	2.9	21.30 (High Tide)
	Nett Advance Over Tidal Cycle (m)	-0.6	0.0	-1.1	-0.8	-0.7	-0.8	-0.7	
S4	Wavelength	4.25	6.85	5.9	4.35	2.60	-	4.8	07.00 (Low Tide)
	Advance (m)	1.6	1.65	2.0	1.8	2.2	1.25	1.75	10.25 (Peak Flood)
	Slipface Length (m)	.20	.20	.20	.15	.15	.30	.20	10.25 (Peak Flood)
	Wavelength (m)	-	4.45	6.15	6.0	3.3	3.0	4.63	12.00 (High Tide)
	Advance (m)	2.1	1.9	2.25	2.05	2.55	1.45	2.05	12.00 (High Tide)
	Wavelength (m)	4.9	6.7	6.1	3.9	2.8	1.9	4.38	18.00 (Low Tide)
	Height (m)	.12	.15	.18	.16	.15	-	.15	18.00 (Low Tide)
	Advance (m)	-1.85	-2.3	-2.5	-2.5	-2.55	-1.65	-2.23	18.00 (Low Tide)
	Slipface Length (m)	.2	.25	.3	.3	.3	.2	.26	18.00 (Low Tide)
	Nett Advance Over Tidal Cycle (m)	.25	-.4	-.25	-.45	0.0	-.20	-.18	
S5	Wavelength (m)	-	4.0	4.6	4.5	3.2	4.0	4.06	10.00 (High Tide)
	Slipface Length (m)	-	.30	.30	.30	.40	.30	.32	10.00 (High Tide)
	Advance (m)	-1.6	-1.9	-1.85	-1.5	-2.1	-2.0	-1.83	1540 (Low Tide)
	Wavelength (m)	-	4.0	4.9	4.8	3.6	3.9	4.24	22.30 (High Tide)
	Height (m)	.10	.15	.15	-	.20	.12	.14	22.30 (High Tide)
	Slipface (m)	-	.30	.30	.20	.70	.25	.35	22.30 (High Tide)
	Advance (m)	1.35	1.60	1.65	1.35	1.60	1.85	1.57	22.30 (High Tide)
	Nett Advance Over Tidal Cycle (m)	-.25	-.30	-.20	-.15	-.50	-.15	-.26	22.30 (High Tide)

Table 7.9: Megaripple geometry and advance measurements by Divers, Sites S3-S5.

Site	Time	Concentrations (mg/l)			Depth (m)	u_1 ($m.s^{-1}$)	u_* ($m.s^{-1}$)	$\bar{u}$ ($m.s^{-1}$)	Z	Z_m	x	β	$q_{ss} \times 10^3$ ($kg\ m^{-1}s^{-1}$)
		0.1m	0.3m	1.0m									
S3	10:35	47.39	12.98	8.52	9.0	.77	.0610	.94	1.38	.70	1.20	1.97	29.6
	12:06	37.85	38.05	17.51	8.4	.68	.0554	.94	1.53	.33	1.46	4.70	54.6
	17:20	3.82	2.39	0.91	8.7	.57	.0557	.80	1.52	.60	1.28	2.54	2.5
	18:37	2.04	3.08	2.52	9.1	.61	.0497	.79	1.71	-.08	-	-	5.8
S4	9:19	32.7	4.19	2.63	3.6	.65	.0394	.73	2.00	.94	1.21	2.12	4.8
	11:12	28.3	3.14	4.62	4.4	.60	.0346	.61	2.28	.68	1.35	2.36	5.3
	15:09	123.7	35.68	13.81	3.7	.78	.0326	.72	2.42	.84	1.31	2.89	29.2
S5	13:20	33.01	31.65	6.95	8.2	.71	.0348	.78	1.47	.66	1.20	2.22	27.1
	15:11	6.23	8.01	3.60	7.4	.62	.0309	.56	1.65	.24	1.50	7.00	8.0
	21:31	22.08	12.03	4.64	9.3	.47	.0295	.66	1.73	.65	1.25	2.66	11.1

Table 7.10: Suspended sediment data from megaripple sites, giving sand concentrations at 0.1m, 0.3m and 1.0m above the bed; velocity at 1m (u_1); friction velocity (u_*); mean vertically-averaged velocity ($\bar{u}$); Rouse Number (z); Rouse Number obtained by linear regression (z_m), exponent of the fall velocity (x); Rouse Number correction (β); and the suspended sediment transport rate (q_{ss}).

		Mean	Standard Deviation	Maximum	Minimum	Coefficient of Variation (%)	Number of pts in average
Period (hrs)	Ebb	6.15	0.24	7.00	5.17	3.92	384
	Flood	6.28	0.27	7.25	5.50	4.29	391
	All	6.21	0.26	7.25	5.17	4.24	775
Range (m)	Ebb	1.87	0.34	2.67	1.17	18.35	384
	Flood	1.87	0.35	2.80	1.19	18.73	391
	All	1.87	0.35	2.80	1.17	18.53	775
Range/ Periods ($m.hr^{-1}$)	Ebb	0.31	.06	0.45	0.18	18.52	384
	Flood	0.30	.06	0.44	0.18	18.71	391

Table 7.11: Tidal statistics, half tidal period, range and range/period, for the inclusive period from June to December 1982.

TIDE RANGES CORRESPONDING WITH DATA ARE:
1.40 1.90 2.40
MEAN AND STANDARD DEVIATION OF NORMAL CURVE 1.870 0.347
TIDAL PERIOD 12.420 SEDIMENT DENSITY 2650.0 POROSITY 0.450

SITE	ΔH=1.4	ΔH=1.9	ΔH=2.4	MASS/TIDE	VOLUME/YEAR	DIRN (°T)
A	0.932	15.317	85.683	24.0855	11.66	121.
B	0.000	2.197	15.077	3.6037	1.75	119.
C	2.851	38.216	206.975	59.1784	28.66	98.
D	0.715	12.054	76.321	20.6370	9.99	94.
E	0.146	4.034	30.626	7.7910	3.77	124.
F	6.595	81.152	409.078	120.2030	58.21	112.
I	2.311	30.695	158.802	46.1217	22.33	127.
K	42.320	543.440	2815.900	830.7137	402.27	303.
M	2.122	31.943	172.540	49.1886	23.82	106.
1	2.656	39.025	203.199	58.6864	28.42	144.
2	8.420	87.404	439.467	130.0896	63.00	127.
3	3.415	42.698	215.045	63.1711	30.59	302.
4	0.000	0.139	0.896	0.2171	0.11	104.
5	6.988	85.920	444.077	129.3720	62.65	26.
6	3.753	31.859	150.332	45.9233	22.24	123.
7	1.904	31.710	178.910	50.1346	24.28	188.
8	1.439	27.113	162.990	44.6265	21.61	50.
9	9.796	99.574	497.700	147.7598	71.55	89.
A1	6.540	41.847	242.677	69.8242	33.81	100.
A2	0.886	12.892	64.797	18.9465	9.17	312.
A3	19.720	189.560	947.830	282.0016	136.56	125.
A4						
B1	0.000	1.796	16.258	3.6949	1.79	106.
B1	0.000	0.000	0.143	0.0587	0.03	100.
B2	7.280	90.351	466.356	135.8787	65.80	120.
B2	3.597	43.856	225.485	65.8281	31.88	116.
B4	0.391	8.051	53.103	14.1171	6.84	243.
B4	0.053	1.990	15.265	3.8517	1.87	276.
C1	2.040	32.384	178.321	50.4343	24.42	117.
C1	0.894	15.993	98.409	26.7933	12.97	127.
C2	11.020	114.600	569.880	169.3403	82.00	127.
C2	7.385	84.811	421.090	124.7113	60.39	132.
C3	4.459	55.853	283.660	83.0813	40.23	312.
C3	0.082	2.736	11.410	3.4748	1.68	121.
C4	4.371	54.082	278.440	81.2067	39.32	127.
C4	1.335	22.515	131.860	36.5061	17.68	140.
D1	0.000	0.000	1.018	0.4178	0.20	117.
D2	0.000	0.391	4.032	0.8987	0.44	121.
D3	0.148	3.415	18.850	5.2708	2.55	210.
D4	2.453	31.148	164.390	47.4981	23.00	298.
S1	18.035	153.861	801.164	236.1649	114.36	307.
S2	15.730	127.013	646.092	192.4911	93.21	102.
S3	3.214	38.150	192.130	56.5488	27.38	101.
S4	1.528	10.680	51.794	15.8074	7.65	75.
S5	1.338	18.914	102.340	29.2186	14.15	131.
F	7.049	95.253	515.212	147.3333	71.35	112.
K	62.918	555.750	2902.900	853.5200	413.32	303.
A4	14.567	171.420	898.212	260.8683	126.33	90.
S1	36.331	362.056	1887.600	552.6412	267.62	307.
S2	58.522	548.697	2813.600	830.5599	402.20	101.
S3	6.645	81.692	467.110	131.5955	63.73	101.
S4	10.288	129.356	688.599	198.4549	96.10	75.

Figure 7.12: Nett sediment transport fluxes including suspended load at the Braystoke vertical profile velocity measurement sites for a sandy bed. The first 3 columns provide dry mass rates (kg/m/tidal cycle) for a neap ($\Delta H = 1.4m$), mean ($\Delta H = 1.9m$) and spring ($\Delta H = 2.4m$) tidal range. The mass/tide (kg/m/tidal cycle) is an average weighted by the probability of tidal range occurrence. The volumn/year ($m^3/m/year$) is the weighted annual volume fluxes for a density of 2650 $kg.m^{-3}$ and porosity of 0.45. The sites repeated at the bottom of the table provide total fluxes (ebb and flood summed) over the tidal cycle instead of nett fluxes.

Time/Date	Mins After High Tide	Meter Elevation Above Sea Bed (m)	Velocity ($m.s^{-1}$)	Direction (^{o} True)	Water Depth (m)	Position and Site Codes
0802/177	42	1.0	0.21	80	1.7	White post in front of house (WP1)
0804/177	44	.5	0.21	98	1.7	
0935/177	135	.2	0.19	108	1.27	
0937/177	137	.5	0.21	108	1.25	
0840/137	-190	.5	0.06	264	.8	
0920/237	-150	.2	0.06	274	1.05	
1003/237	-107	.2	0.08	268	1.40	
1005/237	-105	.5	0.05	268	1.40	
1110/237	-40		NO CURRENT AT ANY LEVEL			
1308/237	78	.2	0.20	111	1.62	
1310/237	80	.5	0.23	111	1.62	
1413/237	143	.5	0.20	101	1.17	
1449/237	179	.2	0.13	102	.82	
1415/237	145	.2	0.16	101	1.17	
0813/177	53	.5	10.3	102	1.14	On Sand Flat Pontoon Near Boat Ramp
0821/177	61	.2	0.15	94	.58	Sediment Trap I (TP1)
1100/237	-50	NO CURRENT				
1258/237	68	.2	0.14	105	.57	
0955/237	-115		Negligible		.33	Sediment Trap II (TP2)
1105/237	-45		Negligible		.60	
1301/237	71	.2	0.14	105	.60	
0832/177	72	.2	0.15	93	.52	Buoy in front of house (BOY)
0910/237	-160	.5	0.14	278	1.14	White post west of house (800m) (WP2)
0912/237	-158	.2	0.14	272	1.14	
1115/237	-35	NO CURRENT				
1314/237	84	.5	0.28	111	1.7	
1316/237	86	.2	0.24	111	1.7	
1421/237	151	.2	0.12	108	1.26	
1423/237	153	.5	0.15	108	1.26	
0839/177	79	.2	0.16	67	.5	Pylon 10 NHB Wharf (P10)
0845/177	85	.2	0.25	65	.55	Pylon 14 NHB Wharf (P14)
1038/237	-72	.2	NO CURRENT		.55	
1322/237	92	.2	0.20	62	.67	
0852/177	92	.2	0.29	63	.64	Pylon 18 NHB Wharf (P18)
1032/237	-78	.5	0.12	244	.66	
1035/237	-75	.2	0.10	264	.66	
1326/237	96	.2	0.25	53	.7	
0858/177	98	.2	0.33	65	1.0	Pylon 22 NHB Wharf (P22)
0900/177	100	.5	0.38	65	1.0	
1026/237	-84	.2	0.11	272	.98	
1028/237	-82	.5	0.13	243	1.0	
1333/237	103	.2	0.31	49	.95	
1332/237	102	.5	0.37	49	.92	
0847/237	-183	.5	0.20	266	.9	Pylon 24 NHB Wharf (P24)
0849/237	-181	.2	0.20	266	.9	
1012/237	-98	.5	0.12	246	1.57	
1016/237	-94	.2	0.14	268	1.55	
1343/237	113	.5	0.36	53	1.37	Ripples Aligned with flow
1344/237	114	.2	0.25	53	1.37	
1431/237	161	.5	0.40	46	.87	"
1433/237	163	.2	0.27	46	.81	"
0947/177	147	.5	Negligible Current	111	.95	Midway B/N NHB & NZRC Wharves (posn.I)
0855/237	-175	.2	0.09	295	1.24	Midway B/N NHB & NZRC Wharves (posn. II) (MID)
0857/237	-173	.5	0.12	265	1.24	
1044/237	-66	.2	0.07	247	1.93	
1046/237	-64	.5	0.07	268	2.18	
1352/237	122	.2	0.07	90	1.66	
1354/237	124	.5	0.07	90	1.56	
1437/237	167	.2	0.13	122	1.15	
1439/237	169	.5	0.18	109	1.18	

Table 8.1: Ott Current Meter Measurements on the Inter-Tidal Zone at Marsden

Date	New Trap Number	New Traps (kg/m/tidal cycle)				VUV Traps (kg/m/tidal cycle)				
		Off	On	Left	Right	1 (F1)	2 (F3)	3 (F3)	4 (F4)	5 (F4)
21-Jul-81	F1	8.8	8.8	7.5	7.1					
22-Jul-81	F2	23.3	32.1	21.0	20.8					
28-Jul-81						38.9	39.2	38.5	47.5	55.3
30-Jul-81						70.6	59.4	57.0	56.1	30.1
31-Jul-81	F2	10.3	10.0	7.6	8.8	14.6	6.6	4.7	15.5	22.8
1-Aug-81	F2	3.7	4.5	3.0	3.0	7.0	4.2	5.4	17.6	20.4
	F3	1.3	2.0	1.8	2.0					
2-Aug-81	F2	8.4	12.0	8.1	7.5	17.6	15.9	15.9	41.7	34.2
	F3	3.2	4.3	3.5	3.7					
	F4	8.4	9.3	7.1	7.9					
	F5	8.1	8.2	7.9	8.8					
3-Aug-81	F2	1.3	1.6	1.5	1.7	2.4	3.5	3.8	7.8	6.2
	F3	0.4	1.3	1.0	0.9					
	F4	1.5	0.9	1.7	1.7					
	F5	1.1	0.9	0.8	0.9					
4-Aug-81	F2	0.0	0.0	0.0	0.0	2.2	3.0	3.4	15.1	18.9
	F3	0.3	0.4	0.5	0.3					
	F4	2.2	1.7	1.3	1.8					
	F5	1.3	1.0	0.9	0.9					
5-Aug-81	F2	0.0	0.0	0.0	0.0	0.43	-	-	-	-
	F3	0.0	0.42	0.0	0.0					
	F4	0.0	0.0	0.0	0.0					
	F5	0.0	0.0	0.0	0.0					
6-Aug-81 (am, 1 cycle)	F3	6.8	5.2	7.5	5.8	29.9	34.8	26.2	-	-
6-Aug-81 (pm, 1 cycle)	2,3,4,5 (all full)	55.0	55.0	55.0	55.0	228.4	349.4	379.5	201.4	253.0
7-Aug-81 (am, 1 cycle)	F3	43.0	41.5	41.7	45.0	176.4	85.2	211.7	68.9	62.3
8-Aug-81 (am)	F2	3.4	5.4	3.0	3.3	4.5	6.0	6.1	3.4	1.2
	F3	1.3	0.9	1.3	1.3					
9-Aug-81 (am)	F2	9.2	12.1	7.4	8.3	37.4	25.5	18.1	9.9	15.0
	F3	1.5	2.1	1.3	2.1					
9-Aug-81 (pm)	F2	25.8	31.7	22.8	24.5	112.6	119.1	71.9	209.0	114.5
	F3	6.7	7.7	5.8	8.8					
12-Aug-81 (am, 5 cycles)	F2	5.5	5.6	5.3	4.9					
	F3	1.2	1.2	1.3	1.2					
14-Aug-81 (am, 4 cycles)	F2	1.2	2.4	1.1	1.2	3.1	4.7	8.2	48.8	33.6
	F3	0.6	0.8	0.9	0.8					
15-Aug-81 (noon)	F2	2.5	4.3	2.6	3.0	12.8	10.3	19.8	37.4	40.0
	F3	0.9	1.7	1.3	0.8					
	F4	7.1	4.8	3.8	7.8					
	F5	1.7	1.0	1.3	2.3					
16-Aug-81 (noon)	F2	0.0	0.6	0.4	0.4	2.9	5.7	12.7	5.9	5.0
	F3	0.0	0.0	0.0	0.0					
	F4	0.0	0.0	0.0	0.0					
	F5	0.0	0.0	0.0	0.0					
19-Aug-81 (pm, 7 cycles)	F2	1.3	2.3	1.7	1.6					
	F3	0.6	0.9	0.9	0.8					
	F4	1.7	1.7	1.3	1.9					
	F5	1.1	0.8	1.1	1.2					

Table 8.2: Sediment trap catches for the August series in rates of kg/m/tidal cycle, for the new circular embedded traps (F1-F5) and neighbouring VUV traps (1-5). Traps were deployed in the inter-tidal zone at the proposed port site.

Collection Time	Trap	Average Catch (kg/m/tidal cycle)	Resultant (kg/m/tidal cycle) Magnitude	Resultant (kg/m/tidal cycle) Direction ($^{o}_{T}$)	Number of Tidal Cycles
21-Jul-81 at 16.00	F1	8.0	0.2	106	2
22-Jul-81 at 17.00	F2	24.3	4.4	200	2
28-Jul-81	2-3 (F3)	38.8	0.3	112	2
at 10.00	4-5 (F4)	51.4	3.9	292	2
31-Jul-81	F2	9.2	0.6	303	2
at 13.00	2-3 (F3)	5.7	1.0	112	2
	4-5 (F4)	19.2	3.7	292	2
1-Aug-81	F2	3.5	0.4	202	2
at 14.00	F3	1.8	0.4	223	2
	2-3 (F3)	4.8	0.6	292	2
	4-5 (F4)	19.0	1.4	292	2
2-Aug-81	F2	9.0	1.8	193	2
at 15.00	F3	3.7	0.6	211	2
	F4	8.2	0.6	244	2
	F5	8.3	0.5	287	2
	2-3 (F3)	15.9	0.0	-	2
	4-5 (F4)	37.9	3.8	112	2
3-Aug-81	F2	1.5	0.2	229	2
at 16.00	F3	0.9	0.5	197	2
	F4	1.4	0.3	22	2
	F5	0.9	0.1	357	2
	2-3 (F3)	3.7	0.1	292	2
	4-5 (F4)	7.0	0.8	112	2
4-Aug-81	F2	0.0	0.0	-	2
at 16.00	F3	0.4	0.1	130	2
	F4	1.8	0.4	337	2
	F5	1.0	0.1	22	2
	2-3 (F3)	3.2	0.2	292	2
	4-5 (F4)	17.0	1.9	292	2
5-Aug-81	F2	0.0	0.0	-	2
at 17.00	F3	0.1	0.21	202	2
	F4	0.0	0.0	-	2
	F5	0.0	0.0	-	2
6-Aug-81	F3	6.3	1.2	67	1
at 06.00	2-3 (F3)	30.5	4.3	112	1
6-Aug-81	2-3 (F3)	364.5	15.1	292	1
at 18.00	4-5 (F4)	227.2	25.8	292	1
7-Aug-81	F3	42.8	1.8	216	1
at 06.00	2-3 (F3)	148.5	63.3	292	1
	4-5 (F4)	65.6	3.3	112	1
8-Aug-81	F2	3.8	1.0	211	2
at 07.00	F3	1.2	0.2	22	2
	2-3 (F3)	6.1	0.1	292	2
	4-5 (F4)	2.3	1.1	112	2
9-Aug-81	F2	9.3	1.5	219	2
at 08.00	F3	1.7	0.5	252	2
	2-3 (F3)	21.8	3.7	112	2
	4-5 (F4)	12.4	2.5	292	2
9-Aug-81	F2	26.2	3.0	218	1
at 20.00	F3	7.3	1.6	274	1
	2-3 (F3)	95.5	23.6	112	1
	4-5 (F4)	161.7	47.3	112	1
12-Aug-81	F2	5.4	0.3	162	5
at 11.00	F3	1.2	0.1	112	5
14-Aug-81	F1	1.5	0.6	196	4
at 12.00	F3	0.8	0.1	135	4
	2-3 (F3)	3.9	0.8	292	4
	4-5 (F4)	41.2	7.6	112	4
15-Aug-81	F2	3.1	0.9	216	2
at 13.00	F3	1.2	0.4	173	2
	F4	5.9	2.3	321	2
	F5	1.5	0.6	326	2
	2-3 (F3)	11.6	1.3	112	2
	4-5 (F4)	38.7	1.3	292	2
16-Aug-81	F2	0.4	0.3	202	2
at 14.00	F3, F4, F5	0.0	0.0	-	2
	2-3 (F3)	4.3	1.4	292	2
	4-5 (F4)	5.5	0.5	112	2
19-Aug-81	F2	1.7	0.5	200	7
at 16.00	F3	0.8	0.2	193	7
	F4	1.6	0.3	296	7
	F5	1.0	0.1	352	7

Table 8.3: Average and resultant sediment trap transport rates (kg/m/tical cycle) for the embedded new traps (F1 - F5) and VUV traps (2 - 3, 4 - 5) for the August series. Traps were deployed in the inter-tidal zone at the proposed port site.

Trap	kg/m/tidal cycle	m^3/m/year	Direction (^oT)
F1	0.19	0.09	106
F2	0.89	0.43	207
F3	0.19	0.09	264
F4	0.64	0.31	314
F5	0.25	0.12	325
2-3 (F3)	3.38	1.64	292
4-5 (F4)	2.02	0.98	112

Table 8.4: Overall sediment transport resultants for the August series. Traps were deployed in the intertidal zone at the proposed port site.

DAY	TIME	NO. OF WAVES	$H_{z,max}$	$H_{z,\frac{1}{3}}$	$\bar{H}_z$	$T_{z,max}$	$T_{Hz,\frac{1}{3}}$	$\bar{T}_z$	$T_{z,\frac{1}{3}}$	TIDES M ABOVE CD	TIDES TYPE	WINDS DIRN (°T)	WINDS SPEED ($m.s^{-1}$)
18-Aug-83	13.48	70	.08	.05	.05	60.0	5.4	3.6	8.5	1.86	Flood	100	2
	19.48	67	.05	.05	.05	20.3	2.0	1.8	3.6	1.10	Ebb	30	0
19-Aug-83	1.48	37	.08	.05	.05	11.0	2.0	2.3	4.1	1.75	Flood	325	4
	7.48	0	-	-	-	-	-	-	-	1.10	Ebb	330	2
	13.48	34	.12	.06	.05	66.8	13.1	7.0	16.9	1.55	Flood	60	3
	19.48	55	.05	.05	.05	33.3	5.5	3.5	8.9	1.39	Ebb	35	3
20-Aug-83	1.48	29	.08	.06	.05	24.0	7.3	5.5	13.8	1.46	Flood	35	2
	7.48	59	.32	.17	.11	27.6	6.3	4.3	9.4	1.40	Ebb	50	8
	13.48	23	.35	.21	.12	39.8	13.9	10.1	23.3	1.27	Flood	30	8
	19.48	21	.44	.29	.16	35.6	16.4	11.7	23.2	1.74	Ebb	30	13
21-Aug-83	1.48	50	.09	.08	.05	45.0	9.0	4.5	10.4	1.24	Flood	50	5
	7.48	79	.05	.05	.05	10.5	1.6	1.3	2.7	1.75	Ebb	30	0
	13.48	14	.05	.05	.05	25.5	2.3	4.1	9.9	1.04	Flood	270	6
	19.48	65	.05	.05	.05	61.0	2.0	3.5	8.0	2.10	Ebb	310	3
22-Aug-83	1.48	64	.05	.05	.05	6.3	1.3	1.7	2.7	0.98	Flood	310	3
	7.48	71	.05	.05	.03	2.3	0.7	0.7	1.0	2.04	Ebb	15	1
	13.48	35	.12	.06	.05	36.9	4.5	3.7	9.6	-	-	10	5
	19.48	55	.08	.05	.05	32.0	4.7	4.3	8.9	-	-	320	1
23-Aug-83	1.48	76	.05	.05	.05	4.8	1.3	1.1	2.1	-	-	330	0
	7.48	29	.08	.05	.05	112.5	14.9	6.4	17.5	-	-	305	3
	13.48	3	.05	.05	.05	49.8	49.8	17.5	49.8	-	-	250	7
	19.48	16	.08	.05	.05	78.8	21.0	14.9	42.0	-	-	300	1
24-Aug-83	1.48	0	-	-	-	-	-	-	-	-	-	300	1
	7.48	16	.08	.08	.05	50.75	20.4	13.2	28.6	-	-	300	2
	13.48	54	.05	.05	.05	10.5	1.9	1.2	2.3	-	-	0	4
	19.48	72	.12	.06	.05	31.0	4.7	3.3	6.4	-	-	270	4
25-Aug-83	1.48	11	.05	.05	.05	14.0	3.9	5.3	11.0	-	-	325	4
	11.53	28	.09	.05	.05	149.0	18.6	7.7	19.9	1.28	Ebb	160	6
	17.53	78	.05	.05	.05	42.5	1.0	1.6	3.3	1.48	Flood	150	5
	23.53	117	.05	.05	.05	46.5	2.2	1.8	4.1	1.53	Ebb	90	1
26-Aug-83	5.53	122	.05	.05	.05	30.5	1.07	1.4	2.8	1.29	Flood	150	7
	11.53	76	.05	.05	.05	79.5	4.6	2.5	6.2	1.55	Ebb	170	8
	17.53	31	.17	.14	.09	29.8	5.8	4.1	9.8	1.23	Flood	130	8
	23.53	33	.20	.12	.09	31.6	12.1	7.4	15.8	1.84	Ebb	135	8
27-Aug-83	5.53	11	.05	.05	.05	19.3	12.3	5.8	12.3	1.04	Flood	150	8
	11.53	46	.05	.05	.05	26.5	3.3	3.2	8.0	1.84	Ebb	170	6
	17.53	17	.05	.05	.05	26.5	10.6	7.7	18.6	1.00	Flood	140	7
	23.53	51	.05	.05	.05	7.3	1.5	1.6	2.3	2.12	Ebb	115	6
28-Aug-83	5.53	20	.05	.05	.05	7.8	2.4	2.7	5.5	0.86	Flood	145	5
	11.53	49	.05	.05	.05	10.3	2.5	2.2	3.9	2.14	Ebb	150	5
	17.53	48	.09	.06	.05	55.8	10.5	5.2	13.8	0.85	Flood	125	6
	23.53	123	.20	.12	.09	9.4	2.4	2.1	3.2	2.35	Ebb	120	6
29-Aug-83	5.53	4	.08	.08	.06	5.5	?	2.9	5.5	0.70	Flood	100	2
	11.53	119	.30	.18	.14	6.5	2.5	2.1	3.1	2.35	Ebb	115	8
	17.53	29	.12	.08	.06	51.5	15.0	7.7	19.2	0.80	Flood	140	6
	23.53	161	.26	.06	.05	17.8	2.2	1.6	3.1	2.50	High	140	9
30-Aug-83	5.53	0	-	-	-	-	-	-	-	0.74	Low	180	7
	11.53	62	.07	.03	.03	88.8	8.6	4.1	10.1	2.47	Flood	190	7
	17.53	177	.03	.03	.03	14.8	1.8	1.9	3.7	0.85	Ebb	235	4
	23.53	70	.05	.04	.03	46.2	6.7	3.5	7.2	2.47	Flood	290	2
31-Aug-83	5.53	0	-	-	-	-	-	-	-	0.72	Ebb	320	0
	11.53	107	.14	.09	.08	11.8	3.2	2.4	4.1	2.30	Flood	260	8
	17.53	59	.09	.06	.05	27.8	6.7	3.9	8.7	0.93	Ebb	260	3
	23.53	26	.05	.05	.04	24.5	3.8	1.6	3.9	2.21	Flood	300	1
01-Sep-83	17.15	71	.05	.05	.05	30.5	2.1	2.2	4.7	1.30	Ebb	280	4
	23.15	16	.05	.05	.05	109.8	109.8	14.1	37.6	1.65	Flood	310	2
02-Sep-83	11.15	24	.14	.09	.06	41.8	18.7	8.5	19.0	1.32	Flood	290	8
	17.15	111	.05	.05	.05	34.5	1.2	2.1	4.8	1.62	Ebb	290	6
	23.15	114	.12	.08	.05	28.0	3.0	2.2	3.7	1.23	Flood	300	5
03-Sep-83	5.15	188	.05	.05	.05	5.0	1.0	0.8	1.3	1.68	Ebb	320	3
	11.15	24	.08	.06	.05	46.5	14.8	8.4	18.2	0.95	Flood	270	9
	17.15	112	.05	.05	.05	19.0	2.2	2.3	4.0	2.03	Ebb	280	6
04-Sep-83	5.15	0	-	-	-	-	-	-	-	2.12	Ebb	310	0
	11.15	11	.05	.05	.05	2.8	2.0	1.4	2.3	0.58	Flood	260	2
	17.15	111	.15	.11	.08	2.8	2.8	2.2	3.7	2.37	High	240	6
05-Sep-83	5.15	157	.05	.05	.05	5.5	2.0	1.6	2.7	2.33	Flood	300	0
	11.15	15	.05	.05	.05	2.3	1.1	1.2	1.6	0.35	Ebb	180	2
	17.15	39	.14	.09	.06	37.3	12.3	6.1	14.0	2.46	Flood	260	3
06-Sep-83	5.15	112	.08	.05	.05	18.8	2.8	2.3	4.4	2.26	Flood	310	1
	11.15	38	.05	.05	.05	29.0	1.0	2.5	5.9	0.41	Ebb	80	1
	17.15	3	.05	.05	.05	9.0	3.3	4.8	9.0	2.25	Flood	90	2
07-Sep-83	5.15	14	.08	.05	.05	30.0	2.6	4.4	11.3	2.01	Flood	320	0
	11.15	2	.05	-	.05	88.3	-	46.6	-	0.77	Ebb	40	2
	17.15	103	.15	.09	.06	8.7	3.1	2.4	4.2	1.89	Flood	30	4
	23.15	55	.17	.11	.08	31.8	9.1	4.3	9.9	1.19	Ebb	20	8
	5.15	0	-	-	-	-	-	-	-	1.60	Flood		

Table 8.5: Wave height (m) and period (s) statistics obtained after a zero up-crossing analysis of sea level measurements made at Marsden Point on a capacitance-type wave height probe. Tides and winds were recorded on the NHB Marsden Point wharf. All heights have been scaled by a 50% calibration correction. 1024 sea levels were recorded at 0.25 Hz for each record.

DAY	TIME	NO. OF WAVES	$H_{z,max}$	$H_{z,\frac{1}{3}}$	$\bar{H}_z$	$T_{z,max}$	$T_{Hz,\frac{1}{3}}$	$\bar{T}_z$	$T_{z,\frac{1}{3}}$	TIDES		WINDS	
										M ABOVE CD	TYPE	DIRN (^oT)	SPEED ($m.s^{-1}$)
09-Sep-83	11.48	107	.06	.04	.04	24.5	2.2	1.5	3.4	1.56	Ebb	30	1
	17.48	2	.07	-	.07	100.3	-	52.3	-	1.27	Flood	35	7
	23.48	81	.08	.04	.04	9.5	2.0	1.7	3.6	1.94	Ebb	340	12
10-Sep-83	5.48	90	.07	.04	.04	10.0	3.5	2.7	5.2	0.94	Flood	10	6
	11.48	88	.36	.23	.15	10.8	3.7	2.9	5.0	2.16	Ebb	340	13
	17.48	51	.06	.04	.04	41.8	8.1	4.4	9.7	0.84	Flood	320	12
	23.48	114	.16	.09	.06	19.5	3.6	2.1	4.1	2.36	Ebb		
11-Sep-83	11.48	46	.09	.04	.04	67.0	6.2	2.8	7.2	2.49	Ebb	300	9
	17.48	10	.04	.04	.04	2.25	1.25	1.4	1.8	0.58	Flood	305	6
	23.48	57	.04	.04	.04	27.5	8.8	4.2	9.6	2.56	Ebb	10	2
12-Sep-83	11.48	18	.06	.04	.04	44.5	18.4	10.7	25.5	2.56	High	40	8
	17.48	25	.04	.04	.04	12.25	1.2	1.8	3.8	0.48	Ebb	320	11
	23.48	7	.04	.04	.04	16.8	5.5	6.9	11.8	2.52	Flood	340	6
13-Sep-83	11.48	19	.07	.05	.04	112.1	34.8	12.2	36.7	2.42	Flood	325	6
	17.48	36	.04	.04	.04	87.5	1.9	4.1	10.3	0.64	Ebb	295	4
	23.48	118	.08	.07	.06	8.0	2.6	2.1	3.2	2.25	Flood	330	5
14-Sep-83	11.52	68	.24	.12	.07	21.8	4.2	3.7	7.0	2.15	Flood	270	9
	17.52	143	.10	.07	.05	10.3	1.9	1.7	2.6	0.87	Ebb	260	0
	23.52	24	.14	.11	.07	35.3	14.8	10.0	20.1	2.04	Flood	0	8
15-Sep-83	5.52	104	.54	.36	.25	9.5	2.6	2.4	3.6	0.9	Ebb	330	14
	11.52	35	.24	.16	.10	26.7	12.8	6.7	13.7	1.85	Flood	280	10
	17.52	70	.04	.04	.04	4.5	1.2	1.4	2.7	1.20	Ebb	240	7
	23.52	119	.04	.04	.04	13.3	1.7	1.9	2.8	1.67	Flood	270	2
16-Sep-83	5.52	55	.04	.04	.04	21.8	2.6	3.1	6.7	1.24	Ebb	270	1
	11.52	98	.06	.04	.04	19.5	2.1	2.1	4.5	1.48	Flood	220	6
	17.52	52	.04	.04	.04	10.5	2.4	2.6	5.4	1.52	Ebb	250	5
	23.52	89	.04	.04	.04	11.8	2.8	2.8	5.0	1.32	Flood	305	2
17-Sep-83	5.52	133	.04	.04	.04	10.5	1.6	1.8	3.2	1.52	Ebb	260	1
	11.52	65	.04	.04	.04	13.0	1.7	1.7	3.2	1.16	Flood	270	7
	17.52	34	.06	.04	.03	76.3	13.1	6.0	16.4	1.83	Ebb	250	4
	23.52	116	.04	.04	.04	19.3	0.8	1.3	2.7	1.07	Flood	310	0
18-Sep-83	5.52	12	.04	.04	.04	43.0	15.7	13.3	27.4	1.83	Ebb	290	0
	11.52	0	-	-	-	-	-	-	-	0.94	Flood	190	5
	17.52	306	.04	.04	.04	2.8	0.5	0.7	1.0	2.08	Ebb	250	2
26-Sep-83	10.28	67	.10	.07	.05	19.0	6.6	3.7	7.2	2.43	High	330	8
	16.28	123	.16	.08	.05	12.8	2.5	2.1	3.2	0.59	Low	320	13
	22.28	84	.16	.07	.05	16.8	4.9	2.9	5.4	2.43	High	10	7
27-Sep-83	10.28	33	.22	.14	.08	50.8	14.9	6.9	15.8	2.44	Flood	300	9
	16.28	149	.06	.04	.04	13.3	1.9	1.7	2.8	0.63	Ebb	250	8
	22.28	70	.22	.10	.06	16.7	4.4	3.6	6.4	2.38	Flood	250	6
28-Sep-83	10.28	91	.14	.07	.06	24.0	3.9	2.8	5.2	2.31	Flood	230	7
	16.28	43	.05	.05	.04	37.3	6.7	3.5	8.4	0.78	Ebb	260	7
	22.28	32	.06	.05	.04	55.0	14.8	7.7	22.0	2.15	Flood	270	3
29-Sep-83	10.28	63	.06	.04	.04	31.3	4.3	3.1	6.8	2.01	Flood	255	7
	16.28	92	.10	.05	.05	24.3	4.6	2.7	5.8	1.05	Ebb	250	8
30-Sep-83	4.28	87	.05	.04	.04	20.5	2.5	2.6	5.1	1.07	Ebb	320	2
	16.28	144	.10	.06	.05	10.0	2.6	1.8	3.0	1.42	Ebb	270	9
01-Oct-83	4.28	78	.05	.06	.04	10.8	3.2	3.1	5.7	1.52	Ebb	-	-
	16.28	29	.07	.05	.04	45.0	16.8	8.3	20.7	1.87	Ebb	-	-
	22.28	134	.04	.04	.04	13.5	1.4	1.3	2.7	1.12	Flood	-	-
02-Oct-83	4.28	62	.04	.04	.04	35.3	2.0	2.8	5.7	1.93	Ebb	-	-
	10.28	65	.06	.05	.04	42.0	6.1	3.5	8.0	0.85	Flood	-	-
	16.28	157	.13	.08	.06	9.8	2.0	1.6	2.7	2.25	Ebb	-	-
03-Oct-83	4.28	113	.06	.04	.04	17.5	2.5	2.2	4.6	2.23	Flood	-	-

Table 8.6: Wave height (m) and periods(s) statistic obtained after a zero up-crossing analysis of sea level measurements made at Marsden Point on a capacitance-type wave height probe. Tides and winds were recorded on the NHB Marsden Point wharf. All heights have been scaled by a 20% calibration correction. 1024 sea levels were recorded at 0.25 H_z for each record.

DATE	20/8	20/8	20/8	26/8	29/8	10/9	14/9	15/9	15/9	27/9
Time	7:48	13:48	19:48	17:53	11:53	11:48	11:52	5:52	11:52	10:28
Wind Speed	8	8	13	8	8	13	9	14	10	9
Wind Direction	50	30	30	130	115	340	270	330	280	300
$H_{z,\frac{1}{3}}$	.17	.21	.29	.14	.18	.23	.12	.36	.16	.14
Tide Level	1.40	1.27	1.74	1.23	2.35	2.16	2.15	0.90	1.85	2.44
Tide Type	Ebb	Flood	Ebb	Flood	Ebb	Ebb	Flood	Ebb	Flood	Flood

Table 8.7: The ten largest wave events during the 6-week recording period at Marsden Point from 18-Aug-82 to 3-Oct-82.

DATE	26/8	26/8	27/8	29/8	31/8	2/9	3/9	7/9	9/9	10/9
Time	11:53	11:53	5:53	23:53	11:53	11:15	11:15	23:15	23:48	17:48
Wind Speed	8	8	8	9	8	8	9	8	12	12
Wind Direction	170	135	150	140	260	290	270	20	340	320
$H_{z,\frac{1}{3}}$	.05	.12	.05	.06	.09	.09	.06	.11	.04	.04
Tide Level	1.55	1.84	1.04	2.50	2.30	1.32	0.95	1.19	1.94	0.84
Tide Type	Ebb	Flood	Flood	High	Flood	Flood	Flood	Ebb	Ebb	Flood

DATE	11/9	12/9	12/9	14/9	26/9	26/9	27/9	29/9	30/9
Time	11:48	11:48	17:48	23:52	10:28	16:28	16:28	16:28	16:28
Wind Speed	9	8	11	8	8	13	8	8	9
Wind Direction	300	40	320	0	330	320	250	250	270
$H_{z,\frac{1}{3}}$	.04	.04	.04	.11	.07	.08	.04	.06	.06
Tide Level	2.49	2.56	0.48	2.04	2.43	0.59	0.63	1.05	1.42
Tide Type	Ebb	High	Ebb	Flood	High	Low	Ebb	Ebb	Ebb

Table 8.8: Wave height measurements made at Marsden Point when wind strengths exceeding 7 $m.s^{-1}$ in the measurement period from 18-Aug-82 to 3-Dec-82.

DATE		10/9	14/9	14/9	15/9	15/9
Time		11:48	11:52	23:52	5:52	11:52
Fetch (m)		4600	1480	5200	2000	2200
Actual	H	.23	.12	.11	.36	.16
	T	3.7	4.2	14.8	2.6	12.8
JONSWAP	H	.45	.18	.30	.32	.24
	T	2.4	1.5	2.1	1.9	1.7
SMB	H	.57	.25	.36	.46	.33
	T	2.4	1.7	2.0	2.2	1.9

Table 8.9: Comparison of measured wave height and periods with the semi-empirical JONSWAP and Sverdrup-Munk-Bretschneider relationship.

DATE	$\frac{H_{z,\frac{1}{10}}}{H_{z,\frac{1}{3}}}$	$\frac{H_{z,\frac{1}{3}}}{\bar{H}_z}$	$\frac{H_{z,max}}{H_{z,\frac{1}{3}}}$	$\frac{H_{z,\frac{1}{10}}}{\bar{H}_z}$	$\frac{T_{Hz,\frac{1}{3}}}{\bar{T}_{z,\frac{1}{3}}}$	$\frac{T_{Hz,\frac{1}{3}}}{\bar{T}_z}$	$\frac{T_{z,\frac{1}{3}}}{\bar{T}_z}$	$\frac{T_{z,max}}{T_{Hz,\frac{1}{3}}}$	β_H (r)	β_T (r)
10-Sep-83 11:48	1.31	1.50	1.59	1.98	0.73	1.30	1.77	2.93	2.71 (.98)	1.70 (.97)
14-Sep-83 11:52	1.42	1.59	2.01	2.27	0.69	1.40	2.01	4.51	1.62 (.97)	0.85 (.92)
14-Sep-83 23:52	1.24	1.62	1.26	2.00	0.77	1.47	1.90	2.14	1.95 (.95)	1.24 (.99)
15-Sep-83 5:52	1.28	1.41	1.61	1.79	0.74	1.04	1.40	2.97	3.17 (.98)	2.64 (.95)
15-Sep-83 11:52	1.23	1.48	1.33	1.82	0.93	1.71	1.84	1.86	2.49 (.99)	1.47 (.99)
Average	1.30	1.52	1.56	1.97	0.77	1.38	1.78	2.88	2.39	1.58
Hawaii Offshore		1.72	1.80		0.90	1.56				
Hawaii Reef		1.70	1.60		0.74	1.30			1.77	1.67
Rayleigh		1.60	1.74	2.03	-	-				

Table 8.10: Zero up-crossing height and period ratios for five selected sea level records made at Marsden Point with a capacitance-type wave probe. β_H and β_T are the peakedness of the height and period distributions respectively.

DATE	SKEWNESS	KURTOSIS	ξ_s^2	Q_p	$\frac{T_{Hz,\frac{1}{3}}}{T_{mo1}}$	$\frac{\bar{T}_z}{T_{mo2}}$
10-Sep-83 11:48	1.17	4.48	0.84	0.54	1.23	1.42
14-Sep-83 11:52	1.24	5.80	0.88	0.37	1.06	1.68
14-Sep-83 23:52	1.02	3.69	0.93	0.41	2.32	3.56
15-Sep-83 5:52	0.92	3.88	0.75	1.22	.98	1.15
15-Sep-83 11:52	0.35	3.16	0.94	0.46	1.84	2.08
Average	0.94	4.20	0.87	0.6	1.49	1.98
Hawaii Offshore	0	>3.0	-	1.5	1.29	1.20
Hawaii Reef	1.0	>3.0	-	0.75-1.0	1.47	1.62
Goda (1974)					1.30	1.20
Haring et. al. (1976)					1.33	1.15

Table 8.11: Skewness and Kurtosis of 1024 sea level elevations for 5 selected records made at Marsden Point with a capacitance-type wave probe. Also included is the spectral width ξ_s^2; Goda's spectral peakedness parameter, Q_p.

Date \ Time	0000	0600	1200	1800
11/11/81	2.6 150	.00	2.6 230	3.6 220
12/11/81	.00	.00	6.2 260	3.1 340
13/11/81	5.1 350	2.6 350	5.1 310	2.6 080
14/11/81	2.6 330	3.6 360	8.2 360	9.3 360
2/12/81	2.6 070	2.6 010	.00	.00
3/12/81	.00	.00	.00	.00

Table 9.1: Wind strengths ($m.s^{-1}$) and directions (^{o}True) recorded at the Marsden Point anenometer at 13m above MSL.

November	5	6	7	8	9	10	11	12	13	14	27	28	29	30
Rainfall (mm)	-	-	-	12	-	6	0.5	1	1.2	32	-	8	66	10
December	1	2	3											
Rainfall (mm)	-	4	-											

Table 9.2: Rainfall in each preceeding 24 hr period for one week prior to each of the model tide simulations. Measured at NHB Marsden Point control tower.

14/11/81					12/11/81				3/12/81		
Type	LINMOD	Smith-McNaught	Currents	DHI	Type	LINMOD	Smith-McNaught	Currents	Type	LINMOD	Smith-McNaught
Ebb	194	199	-	186	Flood	184	185	-	Flood	-	-
Flood	207	204	161	202	Ebb	182	175	195	Ebb	119	115
Ebb	205	197	203	199	Flood	186	185	162	Flood	130	125

Table 9.3: Prisms ($m^3 \times 10^6$) for the modelling periods comparing LINMOD with Smith-McNaught planimeter results, averaged current measurements across the entrance throat, and with S21 (DHI, 1982).

14/11/81			12/11/81			3-Dec-81		
Time	Tide (m)	Volume (m^3)	Time	Tide (m)	Volume (m^3)	Time	Tide (m)	Volume (m^3)
2.30	0.14	196	1.00	0.24	200	1.00	-	-
9.00	3.10	400	7.50	2.91	385	6.00	2.42	340
15.00	0.31	203	13.50	0.39	210	12.00	0.77	225
21.30	3.00	395	19.50	2.97	395	18.5	2.59	350

Table 9.4: Harbour water volumes calculated from Figure 9.11 with tide levels being the average of the tides at Port Whangarei and Marsden Point at low or high water.

Site		Marsden Point	B1	B2	B3	Passage Island	B4	Near Lort Pt
Distance Across Profile (m)		0	220	500	775	990	1090	1250
EBB	12/11/81	.00	.28	.64	.81	.00	.17	.00
	14/11/81	.00	.27	.67	.84	.00	.22	.00
FLOOD	12/11/81	.00	.20	.37	.78	.00	.43	.00
	14/11/81	.00	.22	.41	.73	.00	.41	.00

Table 9.5: Mean Speeds Averaged Vertically and Over Each Half Tidal cycle from measured velocity profiles across the entrance throat (Chapter 5, B-series). Distances along the cross-section of the sites are shown.

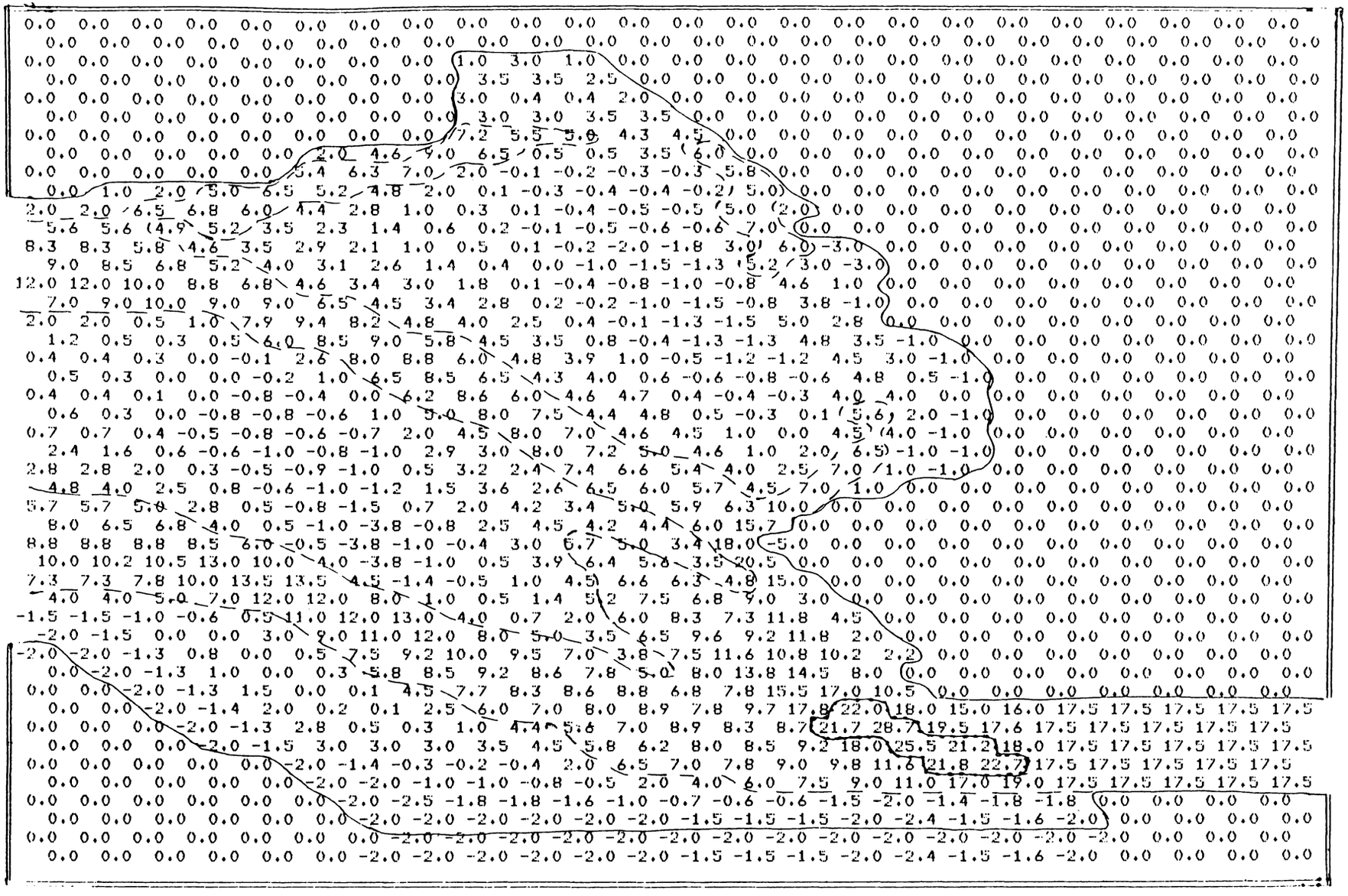

Table 10.1: Bathymetry for fine grid model showing depths in metres.

SPRING TIDE SIMULATION, 14-NOV-81.

TIME	MARSDEN POINT TIDE	ONE TREE POINT TIDE	MARSDEN POINT GRADIENT	ONE TREE POINT GRADIENT
8.7500	0.1200	-0.0047	0.0000E-01	-1.6000E-06
9.2500	0.1900	0.0424	0.0000E-01	-1.5585E-06
9.7500	0.3500	0.2283	0.0000E-01	1.0886E-07
10.2500	0.5900	0.4876	0.0000E-01	1.3572E-06
10.7500	0.8700	0.7837	0.0000E-01	1.1488E-06
11.2500	1.1800	1.0867	0.0000E-01	1.1053E-06
11.7500	1.4900	1.3738	0.0000E-01	1.1610E-06
12.2500	1.7900	1.6847	0.0000E-01	1.1684E-06
12.7500	2.0900	1.9953	0.0000E-01	1.0243E-06
13.2500	2.3500	2.2859	0.0000E-01	1.0671E-06
13.7500	2.5800	2.5469	0.0000E-01	8.1105E-07
14.2500	2.7500	2.7692	0.0000E-01	6.9066E-07
14.7500	2.8700	2.9364	0.0000E-01	4.0628E-07
15.2500	2.9100	3.0292	0.0000E-01	3.0352E-07
15.7500	2.8200	3.0187	0.0000E-01	9.5444E-06
16.2500	2.6300	2.8563	0.0000E-07	1.4969E-05
16.7500	2.3900	2.5988	0.0000E-07	1.7320E-05
17.2500	2.1000	2.2962	0.0000E-07	1.0552E-05
17.7500	1.7600	1.9617	0.0000E-07	1.5309E-05
18.2500	1.4500	1.6115	0.0000E-07	1.3208E-05
18.7500	1.1700	1.2934	0.0000E-07	1.0694E-05
19.2500	0.8900	0.9952	0.0000E-07	8.3801E-06
19.7500	0.6600	0.7131	0.0000E-07	6.2962E-06
20.2500	0.4800	0.4783	0.0000E-01	3.2989E-06
20.7500	0.3200	0.2964	0.0000E-01	-1.2489E-06
21.2500	0.3100	0.1887	0.0000E-01	-9.6435E-07
21.7500	0.3600	0.2369	0.0000E-01	-2.8102E-06

NEAP TIDE SIMULATION, 3-DEC-81.

TIME	MARSDEN POINT TIDE	ONE TREE POINT TIDE	MARSDEN POINT GRADIENT	ONE TREE POINT GRADIENT
1.0000	2.2000	2.2893	0.0000E-06	7.0002E-06
1.5000	2.1200	2.2131	0.0000E-06	5.3534E-06
2.0000	1.9900	2.0731	0.0000E-06	2.4143E-06
2.5000	1.7900	1.8731	0.0000E-06	2.5542E-06
3.0000	1.6100	1.6731	0.0000E-06	2.8470E-06
3.5000	1.4300	1.4759	0.0000E-06	2.8265E-06
4.0000	1.2400	1.2847	0.0000E-06	2.8252E-06
4.5000	1.0800	1.0955	0.0000E-06	2.5166E-06
5.0000	0.9200	0.9370	0.0000E-06	1.3595E-06
5.5000	0.7900	0.7822	0.0000E-07	8.1957E-07
6.0000	0.7000	0.6634	0.0000E-08	7.8424E-07
6.5000	0.6700	0.6084	0.0000E-06	9.6896E-07
7.0000	0.7000	0.6231	0.0000E-07	1.7749E-06
7.5000	0.7700	0.6978	0.0000E-06	2.3205E-06
8.0000	0.9000	0.8334	0.0000E-06	2.4801E-06
8.5000	1.0500	1.0187	0.0000E-06	2.6909E-06
9.0000	1.2400	1.1983	0.0000E-06	1.6949E-06
9.5000	1.4400	1.3909	0.0000E-06	4.7232E-07
10.0000	1.6400	1.5968	0.0000E-07	3.5599E-07
10.5000	1.8300	1.7968	0.0000E-07	2.8503E-07
11.0000	2.0000	1.9840	0.0000E-07	1.4876E-07
11.5000	2.1400	2.1531	0.0000E-08	1.0799E-07
12.0000	2.2600	2.2838	0.0000E-07	1.1702E-07
12.5000	2.3400	2.3836	0.0000E-07	-1.3810E-07
13.0000	2.3800	2.4473	0.0000E-07	-4.8519E-07
13.5000	2.3300	2.4356	0.0000E-07	7.2159E-07

Tables 10.2 (left) and 10.3: Open boundary tides and transverse gradients for the Spring (14-Nov-81) and Neap (3-Dec-81) tide simulations of Whangarei Harbour.

SITE	GRID COORDINATES		SPRING				NEAP			
			EBB		FLOOD		EBB		FLOOD	
	J	K	MODEL	FIELD	MODEL	FIELD	MODEL	FIELD	MODEL	FIELD
A	14.1	3.85	.89	.86	.65	.61	.48	.52	.40	.37
B	11.35	4.1	.63	.67	.49	.61	.37	.40	.29	.37
C	16.45	3.8	.97	1.02	.71	.46	.51	.61	.44	.28
E	12.6	3.9	.78	.77	.61	.66	.44	.46	.37	.40
F	14.75	5.3	1.22	1.25	1.03	1.00	.64	.75	.60	.61
I	17.4	4.2	1.10	1.13	.84	.86	.58	.68	.50	.51
K	13.95	6.4	1.15	0.83	1.06	1.41	.61	.50	.61	.86
M	18.4	4.0	1.12	1.10	.86	.62	.59	.66	.49	.38
1	9.3	7.1	1.14	1.11	.88	1.03	.62	.67	.53	.61
2	6.45	9.0	1.13	1.12	.93	1.13	.64	.67	.56	.69
3	2.1	10.1	1.10	0.86	.90	1.07	.61	.52	.54	.65
9	19.0	4.3	1.21	1.00	.98	1.14	.63	.60	.54	.70
S1	14.7	5.6	1.20	1.09	1.09	1.27	.63	.65	.63	.78
S2	14.25	5.7	1.19	1.10	1.07	1.26	.62	.66	.62	.77
S3	14.35	5.65	1.20	1.09	1.07	1.09	.63	.65	.62	.67
S4	12.0	7.5	.93	.92	.95	1.00	.51	.55	.55	.61
S5	11.4	11.75	.84	.85	.78	.85	.45	.51	.47	.52

Table 10.4: Comparison of maximum ebb and flood mean vertically-averaged water velocities, from 2DD and after scaling field measurements according to tidal range. Model grid coordinates of each measurement site are given.

NUMBER	TIDAL RANGE (M)	WITH PORT?	COMMENTS
190	2.6	No	Effectively same as 219
191	1.6	No	Effectively same as 221
192	2.6	No	Coriolis f = 0
195	2.6	No	Wind 10 $m.s^{-1}$ from 101° T
204	2.6	No	Wind 10 $m.s^{-1}$ from 110° T
213	2.6	Yes	Effectively same as 220
214	2.6	No	Wind 10 $m.s^{-1}$ from 236° T
219	2.6	No	
220	2.6	Yes	13m depths
221	1.6	No	
222	1.6	Yes	13m depths
223	2.6	Yes	14m depths
224	2.6	Yes	Unchanged open bounds. 13m depths
226	2.6	No	Convective momenta terms set to zero
227	2.6	No	Constant depths of 5m and 10m.

Table 10.5: Summary of model runs.

depth (m)	0.5	1.0	2.0	5.0	10.0	20.0	30.0
$\frac{u_1}{u_{1old}}$	1.0	.97	.94	0.9	0.91	0.91	0.92

Table 11.1: Ratio of the 1m velocities obtained from the mean velocity by accounting for the change of velocity profile gradient (u_1) and by assuming that the Karman Prandtl is valid throughout the water volumn (u_{1old}), for $z_o = 0.001$m.

	FACTOR	z_o	d	FACTOR
(i)	To find u_1: $\frac{1}{1 - \frac{\log_{10}(0.38d)}{\log_{10}(z_o)}}$	0.001	10	0.84
		0.005	10	0.80
		0.0005	10	0.85
		0.001	2	1.04
		0.001	5	0.91
		0.001	10	0.84
		0.001	20	0.77
(ii)	To find u_*: $5.75 \log_{10}(\frac{0.37d}{z_o})$	0.001	10	20.6
		0.005	10	16.6
		0.0005	10	22.3
		0.001	2	16.6
		0.001	20	22.3

Table 11.2: Conversion factors to relate the mean flow speed to (i) the speed at 1m above the bed; and (ii) the friction velocity. A typical range of roughness lengths, z_o, and flow depths, d, is presented.

SITE	D_{95}	D_{65}	D_{50}	D_{35}	P(1φ)	SITE	D_{95}	D_{65}	D_{50}	D_{35}	P(1φ)
1	1.22	1.77	2.01	2.23	98	64	-1.72	0.37	0.92	1.44	48
2	1.01	1.60	1.78	2.01	95	65	-0.79	1.69	2.01	2.31	87
3	0.79	1.56	1.78	2.04	90	66	-3.93	-1.74	0.45	1.53	46
4	0.78	1.49	1.74	2.03	91	67	-4.44	-4.06	-3.82	-3.19	11
5	1.39	2.13	2.40	2.59	99	68	-4.63	-3.91	-3.80	-3.55	7
6	1.45	2.27	2.51	2.62	99	71	1.24	1.92	2.11	2.30	97
7	1.36	2.44	2.59	2.70	98	72	-4.15	1.52	1.99	2.30	69
8	-5.90	-2.49	0.36	1.44	44	73	1.11	1.95	2.37	2.59	96
9	-5.68	-3.32	-1.74	0.34	27	76	-1.82	1.33	1.76	2.18	72
10	-3.90	-3.32	-3.03	-2.76	3	77	-3.82	1.07	1.54	1.86	66
14	-5.71	-3.50	-1.29	0.86	22	78	-1.47	1.54	1.83	2.15	81
16	-0.01	2.42	2.59	2.71	94	79	-3.92	1.33	1.85	2.20	69
18	-3.65	0.79	1.40	1.71	61	88	0.89	2.87	3.06	3.27	95
19	-4.58	-2.28	-0.87	0.98	34	90	-2.18	1.99	2.35	2.58	83
20	-1.50	1.29	1.48	1.65	75	91	-4.14	-3.25	-1.99	1.21	36
21	-3.87	-1.53	-0.60	0.48	25	92	-3.37	2.01	2.29	2.53	85
22	-5.63	-2.69	-1.70	-0.13	25	94	2.00	2.34	2.45	2.56	99
23	-2.75	1.85	1.97	2.09	91	95	1.31	2.24	2.36	2.46	95
24	-5.11	-1.55	0.89	1.55	48	96	-4.10	-3.32	-2.75	-1.64	25
25	-5.70	-2.61	0.46	1.25	41	98	-5.11	-4.44	-3.94	-3.80	8
26	-4.57	-3.91	-3.63	-2.80	20	99	-2.38	1.67	1.92	2.10	74
27	-4.07	2.33	2.45	2.56	88	100	-4.73	-4.61	-4.54	2.14	39
28	-3.93	2.39	2.60	2.74	91	102	-4.75	-4.65	-4.61	-4.56	0
29	1.73	2.48	2.60	2.71	98	103	-4.73	-4.60	-4.54	-3.89	0
30	-3.60	2.41	2.57	2.67	87	104	-4.72	-4.54	-4.26	-3.95	22
31	1.25	2.51	2.60	2.68	96	105	-5.05	-4.37	2.22	2.54	54
32	0.77	1.68	1.91	2.16	93	106	-5.18	-4.63	-4.52	-3.86	13
33	-5.22	-5.07	-4.70	-4.26	5	107	-5.18	-4.04	-3.79	-1.50	34
35	1.28	2.13	2.39	2.59	97	108	-4.00	2.21	2.47	2.60	85
37	0.77	1.40	1.60	1.86	88	109	1.49	2.26	2.39	2.53	98
38	1.41	2.12	2.37	2.56	99	110	-4.53	1.82	2.23	2.50	78
39	1.42	2.30	2.51	2.63	98	111	-4.25	0.79	1.17	1.44	57
40	1.69	2.51	2.61	2.71	99	112	1.79	2.13	2.21	2.31	99
41	-2.65	-0.14	0.69	1.10	38	113	-3.95	-3.55	-3.28	-2.77	5
42	-3.96	2.09	2.30	2.46	81	114	-3.71	-1.76	0.44	1.58	42
43	1.27	1.85	2.02	2.17	97	115	-4.48	-4.38	-4.33	-4.28	19
44	1.52	2.01	2.13	2.25	99	117	1.50	2.00	2.12	2.23	97
45	1.63	2.41	2.53	2.63	97	118	-4.59	-3.93	-3.73	-3.43	4
46	1.77	2.37	2.51	2.61	100	119	-4.05	-1.96	-0.94	0.61	27
47	1.93	2.43	2.54	2.63	99	120	-2.94	1.04	1.35	1.55	66
48	1.77	2.46	2.56	2.64	99	121	-1.30	1.30	1.52	1.70	76
49	-1.81	2.13	2.33	2.48	91	122	-5.61	-0.96	1.22	1.64	54
50	-0.61	1.42	1.68	1.98	85	123	-3.56	1.94	2.11	2.24	84
51	1.29	2.07	2.18	2.29	97	124	-3.79	-0.10	1.25	1.81	53
52	1.86	2.32	2.44	2.56	99	125	-2.99	-2.90	-2.86	-2.82	0
53	1.97	2.37	2.50	2.60	99	126	-1.68	1.37	1.59	1.79	79
55	1.57	1.96	2.20	2.39	100	127	-5.66	-0.54	0.97	1.68	51
56	-4.16	-1.11	0.06	0.70	24	128	-2.00	0.19	0.82	1.34	45
57	1.79	2.27	2.40	2.53	99	129	-2.95	1.43	1.83	2.20	75
58	-0.08	1.76	1.89	2.05	88	130	1.46	2.55	2.67	2.80	96
59	1.27	2.34	2.48	2.58	96	131			2.27		85
60	-5.19	-4.00	-3.87	-3.71	0	132			1.24		53
62	2.03	2.60	2.74	2.89	99	134			1.42		65
63	-4.52	-0.46	1.01	1.84	50	135			1.41		61

Table 11.3: Grain sizes after a textural analysis of bed sediment samples taken by the RNZN in Whangarei Harbour and over Mair Bank. Site locations are shown in Figure 2.9. Percentile sizes correspond with the grain size which is exceeded by 95%, 65%, 50% or 35% of the grain size distribution by weight. P(1φ) gives the percentage of weight exceeding 1 phi.

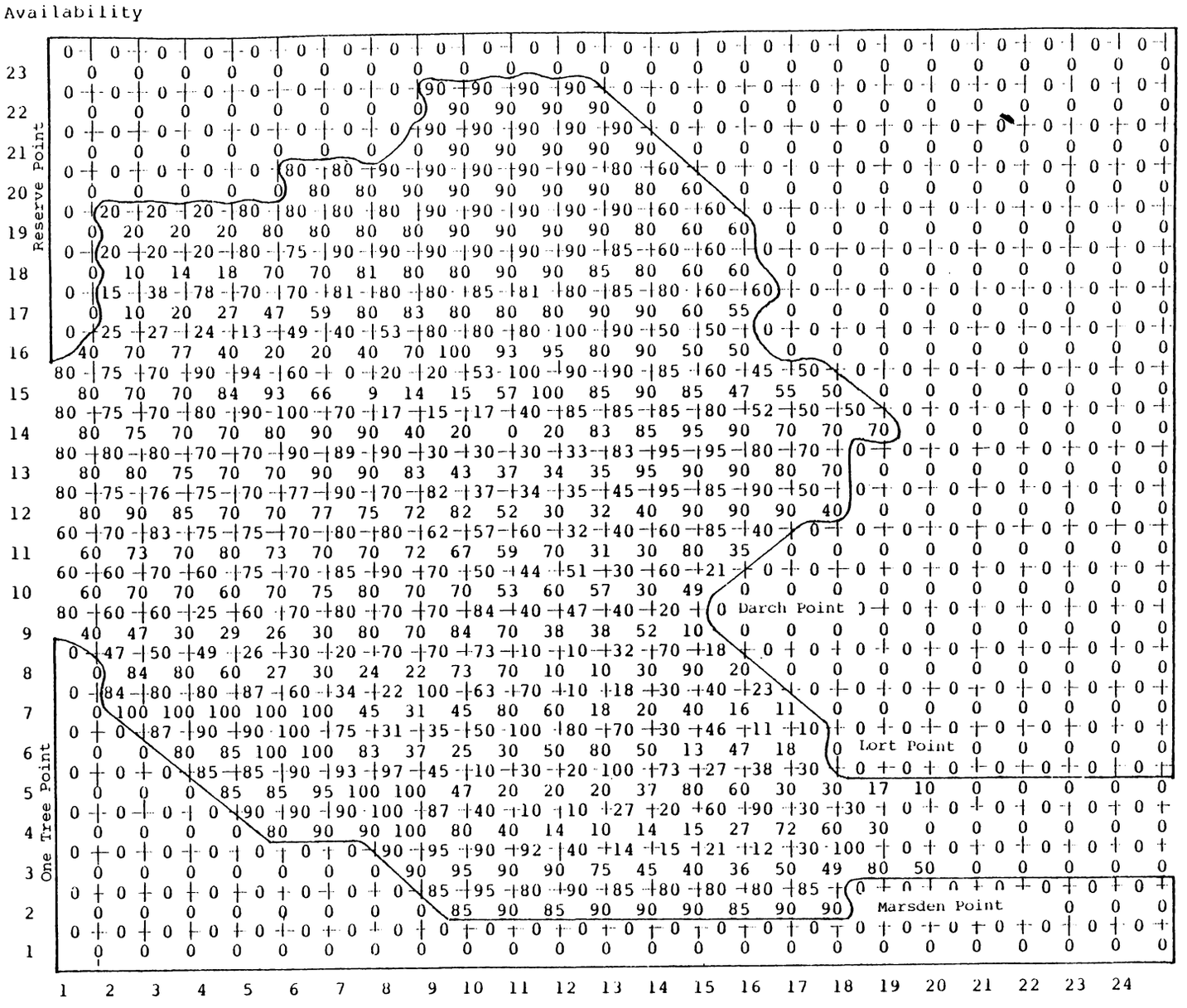

Table 11.4: Availabilities in Whangarei Harbour on each of the 2-dimensional model cell walls. The cells are numbered J = 1 to 24 across the page and K = 1 to 23 up the page, and can be located in Figure 11.26.

Fix Marks	Sextant Angle	Theodolite Angle	Calculated Angle	Code Number
11 second Beacon to Shell Cut Reach Front Lead	15° 24'	15° 23'	15° 21'	1
Shell Cut Reach Front Lead to Darch Pt	53° 52'	53° 53'	53° 53'	2
Darch Pt to Passage Is.	36° 8'	36° 7'	35° 58'	3
Passage Is. to Lort Pt	8° 32'	8° 31'	8° 39'	4
Lort Pt to Flare Stack	33° 54'	33° 53'	33° 55'	5
Flare Stack to NZRC Chimney	7° 31'	7° 30'	7° 28'	6
S1 Beacon to McDonald Is.	38° 30'	-	38° 28'	7
Sinclair Beacon to S1	25° 33'	25° 31'	25° 31'	8
Passage Is. to NZRC Chimney	49° 54'	49° 53'	50° 01'	9

TABLE A1.1: Comparison of Sextant, Theodolite and Calculated Angles

	METRIC TO YARDS				YARDS TO METRIC			
NUMBER	GEOGRAPHIC		YARDS(YARDS)		GEOGRAPHIC		METRIC(M)	
	LATITUDE	LONGITUDE	NORTH	EAST	LATITUDE	LONGITUDE	NORTH	EAST
1	.00035	.00008	.01	.00	.00022	.00002	.00	.00
2	.00009	.00010	.00	.01	.00006	.00010	.00	.00
3	.00000	.00009	.00	.01	-.00002	.00007	.01	.00
4	-.00004	.00016	.00	.00	-.0009	-.00007	.00	.00

TABLE A1.2: Computer accuracy test. Showing conversions from metric through geographic to national yards and vice versa. The numbers quoted are the differences between the actual and calculated values in seconds for latitude and longitude, and metres and yards.